



International Journal of Advanced Computer Science and Applications

Volume 7 Issue 8

August 2016



ISSN 2156-5570(Online)

ISSN 2158-107X(Print)



www.ijacsa.thesai.org

Editorial Preface

From the Desk of Managing Editor...

It may be difficult to imagine that almost half a century ago we used computers far less sophisticated than current home desktop computers to put a man on the moon. In that 50 year span, the field of computer science has exploded.

Computer science has opened new avenues for thought and experimentation. What began as a way to simplify the calculation process has given birth to technology once only imagined by the human mind. The ability to communicate and share ideas even though collaborators are half a world away and exploration of not just the stars above but the internal workings of the human genome are some of the ways that this field has moved at an exponential pace.

At the International Journal of Advanced Computer Science and Applications it is our mission to provide an outlet for quality research. We want to promote universal access and opportunities for the international scientific community to share and disseminate scientific and technical information.

We believe in spreading knowledge of computer science and its applications to all classes of audiences. That is why we deliver up-to-date, authoritative coverage and offer open access of all our articles. Our archives have served as a place to provoke philosophical, theoretical, and empirical ideas from some of the finest minds in the field.

We utilize the talents and experience of editor and reviewers working at Universities and Institutions from around the world. We would like to express our gratitude to all authors, whose research results have been published in our journal, as well as our referees for their in-depth evaluations. Our high standards are maintained through a double blind review process.

We hope that this edition of IJACSA inspires and entices you to submit your own contributions in upcoming issues. Thank you for sharing wisdom.

Thank you for Sharing Wisdom!

Managing Editor
IJACSA
Volume 7 Issue 8 August 2016
ISSN 2156-5570 (Online)
ISSN 2158-107X (Print)
©2013 The Science and Information (SAI) Organization

Editorial Board

Editor-in-Chief

Dr. Kohei Arai - Saga University

Domains of Research: Technology Trends, Computer Vision, Decision Making, Information Retrieval, Networking, Simulation

Associate Editors

Chao-Tung Yang

Department of Computer Science, Tunghai University, Taiwan

Domain of Research: Software Engineering and Quality, High Performance Computing, Parallel and Distributed Computing, Parallel Computing

Elena SCUTELNICU

"Dunarea de Jos" University of Galati, Romania

Domain of Research: e-Learning, e-Learning Tools, Simulation

Krassen Stefanov

Professor at Sofia University St. Kliment Ohridski, Bulgaria

Domains of Research: e-Learning, Agents and Multi-agent Systems, Artificial Intelligence, Big Data, Cloud Computing, Data Retrieval and Data Mining, Distributed Systems, e-Learning Organisational Issues, e-Learning Tools, Educational Systems Design, Human Computer Interaction, Internet Security, Knowledge Engineering and Mining, Knowledge Representation, Ontology Engineering, Social Computing, Web-based Learning Communities, Wireless/ Mobile Applications

Maria-Angeles Grado-Caffaro

Scientific Consultant, Italy

Domain of Research: Electronics, Sensing and Sensor Networks

Mohd Helmy Abd Wahab

Universiti Tun Hussein Onn Malaysia

Domain of Research: Intelligent Systems, Data Mining, Databases

T. V. Prasad

Lingaya's University, India

Domain of Research: Intelligent Systems, Bioinformatics, Image Processing, Knowledge Representation, Natural Language Processing, Robotics

Reviewer Board Members

- **Aamir Shaikh**
- **Abbas Al-Ghaili**
Mendeley
- **Abbas Karimi**
Islamic Azad University Arak Branch
- **Abdelghni Lakehal**
Université Abdelmalek Essaadi Faculté
Polydisciplinaire de Larache Route de Rabat, Km 2 -
Larache BP. 745 - Larache 92004. Maroc.
- **Abdul Razak**
- **Abdul Karim ABED**
- **Abdur Rashid Khan**
Gomal University
- **Abeer ELkorany**
Faculty of computers and information, Cairo
- **ADEMOLA ADESINA**
University of the Western Cape
- **Aderemi A. Atayero**
Covenant University
- **Adi Maaita**
ISRA UNIVERSITY
- **Adnan Ahmad**
- **Adrian Branga**
Department of Mathematics and Informatics,
Lucian Blaga University of Sibiu
- **agana Becejski-Vujaklija**
University of Belgrade, Faculty of organizational
- **Ahmad Saifan**
yarmouk university
- **Ahmed Boutejdar**
- **Ahmed AL-Jumaily**
Ahlia University
- **Ahmed Nabih Zaki Rashed**
Menoufia University
- **Ajantha Herath**
Stockton University Galloway
- **Akbar Hossain**
- **Akram Belghith**
University Of California, San Diego
- **Albert S**
Kongu Engineering College
- **Alcinia Zita Sampaio**
Technical University of Lisbon
- **Alexane Bouënard**
Sensopia
- **ALI ALWAN**
International Islamic University Malaysia
- **Ali Ismail Awad**
Luleå University of Technology
- **Alicia Valdez**
- **Amin Shaqrah**
Taibah University
- **Amirrudin Kamsin**
- **Amitava Biswas**
Cisco Systems
- **Anand Nayyar**
KCL Institute of Management and Technology,
Jalandhar
- **Andi Wahyu Rahardjo Emanuel**
Maranatha Christian University
- **Anews Samraj**
Mahendra Engineering College
- **Anirban Sarkar**
National Institute of Technology, Durgapur
- **Anthony Isizoh**
Nnamdi Azikiwe University, Awka, Nigeria
- **Antonio Formisano**
University of Naples Federico II
- **Anuj Gupta**
IKG Punjab Technical University
- **Anuranjan misra**
Bhagwant Institute of Technology, Ghaziabad, India
- **Appasami Govindasamy**
- **Arash Habibi Lashkari**
University Technology Malaysia(UTM)
- **Aree Mohammed**
Directorate of IT/ University of Sulaimani
- **ARINDAM SARKAR**
University of Kalyani, DST INSPIRE Fellow
- **Aris Skander**
Constantine 1 University
- **Ashok Matani**
Government College of Engg, Amravati
- **Ashraf Owis**
Cairo University
- **Asoke Nath**

St. Xaviers College(Autonomous), 30 Park Street,
Kolkata-700 016

- **Athanasios Koutras**
- **Ayad Ismaeel**
Department of Information Systems Engineering-
Technical Engineering College-Erbil Polytechnic
University, Erbil-Kurdistan Region- IRAQ
- **Ayman Shehata**
Department of Mathematics, Faculty of Science,
Assiut University, Assiut 71516, Egypt.
- **Ayman EL-SAYED**
Computer Science and Eng. Dept., Faculty of
Electronic Engineering, Menofia University
- **Babatunde Opeoluwa Akinkunmi**
University of Ibadan
- **Bae Bossoufi**
University of Liege
- **BALAMURUGAN RAJAMANICKAM**
Anna university
- **Balasubramanie Palanisamy**
- **BASANT VERMA**
RAJEEV GANDHI MEMORIAL COLLEGE, HYDERABAD
- **Basil Hamed**
Islamic University of Gaza
- **Basil Hamed**
Islamic University of Gaza
- **Bhanu Prasad Pinnamaneni**
Rajalakshmi Engineering College; Matrix Vision
GmbH
- **Bharti Waman Gawali**
Department of Computer Science & information T
- **Bilian Song**
LinkedIn
- **Binod Kumar**
JSPM's Jayawant Technical Campus, Pune, India
- **Bogdan Belean**
- **Bohumil Brtnik**
University of Pardubice, Department of Electrical
Engineering
- **Bouchaib CHERRADI**
CRMEF
- **Brahim Raouyane**
FSAC
- **Branko Karan**
- **Bright Keswani**
Department of Computer Applications, Suresh Gyan
Vihar University, Jaipur (Rajasthan) INDIA
- **Brij Gupta**

University of New Brunswick

- **C Venkateswarlu Sonagiri**
JNTU
- **Chanashekhhar Meshram**
Chhattisgarh Swami Vivekananda Technical
University
- **Chao Wang**
- **Chao-Tung Yang**
Department of Computer Science, Tunghai
University
- **Charlie Obimbo**
University of Guelph
- **Chee Hon Lew**
- **Chien-Peng Ho**
Information and Communications Research
Laboratories, Industrial Technology Research
Institute of Taiwan
- **Chun-Kit (Ben) Ngan**
The Pennsylvania State University
- **Ciprian Dobre**
University Politehnica of Bucharest
- **Constantin POPESCU**
Department of Mathematics and Computer
Science, University of Oradea
- **Constantin Filote**
Stefan cel Mare University of Suceava
- **CORNELIA AURORA Gyorödi**
University of Oradea
- **Cosmina Ivan**
- **Cristina Turcu**
- **Dana PETCU**
West University of Timisoara
- **Daniel Albuquerque**
- **Dariusz Jakóbczak**
Technical University of Koszalin
- **Deepak Garg**
Thapar University
- **Devena Prasad**
- **DHAYA R**
- **Dheyaa Kadhim**
University of Baghdad
- **Djilali IDOUGH**
University A.. Mira of Bejaia
- **Dong-Han Ham**
Chonnam National University
- **Dr. Arvind Sharma**

Aryan College of Technology, Rajasthan Technology
University, Kota

- **Duck Hee Lee**
Medical Engineering R&D Center/Asan Institute for
Life Sciences/Asan Medical Center
- **Elena SCUTELNICU**
"Dunarea de Jos" University of Galati
- **Elena Camossi**
Joint Research Centre
- **Eui Lee**
Sangmyung University
- **Evgeny Nikulchev**
Moscow Technological Institute
- **Ezekiel OKIKE**
UNIVERSITY OF BOTSWANA, GABORONE
- **Fahim Akhter**
King Saud University
- **FANGYONG HOU**
School of IT, Deakin University
- **Faris Al-Salem**
GCET
- **Firkhan Ali Hamid Ali**
UTHM
- **Fokrul Alom Mazarbhuiya**
King Khalid University
- **Frank Ibikunle**
Botswana Int'l University of Science & Technology
(BIUST), Botswana
- **Fu-Chien Kao**
Da-Y eh University
- **Gamil Abdel Azim**
Suez Canal University
- **Ganesh Sahoo**
RMRIMS
- **Gaurav Kumar**
Manav Bharti University, Solan Himachal Pradesh
- **George Pecherle**
University of Oradea
- **George Mastorakis**
Technological Educational Institute of Crete
- **Georgios Galatas**
The University of Texas at Arlington
- **Gerard Dumancas**
Oklahoma Baptist University
- **Ghalem Belalem**
University of Oran 1, Ahmed Ben Bella
- **gherabi noreddine**

- **Giacomo Veneri**
University of Siena
- **Giri Babu**
Indian Space Research Organisation
- **Govindarajulu Salendra**
- **Grebenisan Gavril**
University of Oradea
- **Gufan Ahmad Ansari**
Qassim University
- **Gunaseelan Devaraj**
Jazan University, Kingdom of Saudi Arabia
- **GYÖRÖDI ROBERT STEFAN**
University of Oradea
- **Hadj Tadjine**
IAV GmbH
- **Haewon Byeon**
Nambu University
- **Haiguang Chen**
ShangHai Normal University
- **Hamid Alinejad-Rokny**
The University of New South Wales
- **Hamid AL-Asadi**
Department of Computer Science, Faculty of
Education for Pure Science, Basra University
- **Hamid Mukhtar**
National University of Sciences and Technology
- **Hany Hassan**
EPF
- **Harco Leslie Henic SPITS WARNARS**
Bina Nusantara University
- **Hariharan Shanmugasundaram**
Associate Professor, SRM
- **Harish Garg**
Thapar University Patiala
- **Hazem I. El Shekh Ahmed**
Pure mathematics
- **Hemalatha SenthilMahesh**
- **Hesham Ibrahim**
Faculty of Marine Resources, Al-Mergheb
University
- **Himanshu Aggarwal**
Department of Computer Engineering
- **Hongda Mao**
Hossam Faris
- **Huda K. AL-Jobori**
Ahlia University
- **Imed JABRI**

- **iss EL OUADGHIRI**
- **Iwan Setyawan**
Satya Wacana Christian University
- **Jacek M. Czerniak**
Casimir the Great University in Bydgoszcz
- **Jai Singh W**
- **JAMAIAH HAJI YAHAYA**
NORTHERN UNIVERSITY OF MALAYSIA (UUM)
- **James Coleman**
Edge Hill University
- **Jatinderkumar Saini**
Narmada College of Computer Application, Bharuch
- **Javed Sheikh**
University of Lahore, Pakistan
- **Jayaram A**
Siddaganga Institute of Technology
- **Ji Zhu**
University of Illinois at Urbana Champaign
- **Jia Uddin Jia**
Assistant Professor
- **Jim Wang**
The State University of New York at Buffalo,
Buffalo, NY
- **John Sahlin**
George Washington University
- **JOHN MANOHAR**
VTU, Belgaum
- **JOSE PASTRANA**
University of Malaga
- **Jui-Pin Yang**
Shih Chien University
- **Jyoti Chaudhary**
high performance computing research lab
- **K V.L.N.Acharyulu**
Bapatla Engineering college
- **Ka-Chun Wong**
- **Kamatchi R**
- **Kamran Kowsari**
The George Washington University
- **KANNADHASAN SURIYAN**
- **Kashif Nisar**
Universiti Utara Malaysia
- **Kato Mivule**
- **Kayhan Zrar Ghafoor**
University Technology Malaysia
- **Kennedy Okafor**
Federal University of Technology, Owerri
- **Khalid Mahmood**
IEEE
- **Khalid Sattar Abdul**
Assistant Professor
- **Khin Wee Lai**
Biomedical Engineering Department, University
Malaya
- **Khurram Khurshid**
Institute of Space Technology
- **KIRAN SREE POKKULURI**
Professor, Sri Vishnu Engineering College for
Women
- **KITIMAPORN CHOOCHOTE**
Prince of Songkla University, Phuket Campus
- **Krasimir Yordzhev**
South-West University, Faculty of Mathematics and
Natural Sciences, Blagoevgrad, Bulgaria
- **Krassen Stefanov**
Professor at Sofia University St. Kliment Ohridski
- **Labib Gergis**
Misr Academy for Engineering and Technology
- **LATHA RAJAGOPAL**
- **Lazar Stošić**
College for professional studies educators
Aleksinac, Serbia
- **Leanos Maglaras**
De Montfort University
- **Leon Abdillah**
Bina Darma University
- **Lijian Sun**
Chinese Academy of Surveying and
- **Ljubomir Jerinic**
University of Novi Sad, Faculty of Sciences,
Department of Mathematics and Computer Science
- **Lokesh Sharma**
Indian Council of Medical Research
- **Long Chen**
Qualcomm Incorporated
- **M. Reza Mashinchi**
Research Fellow
- **M. Tariq Banday**
University of Kashmir
- **madjid khalilian**
- **majzoob omer**
- **Mallikarjuna Doodipala**
Department of Engineering Mathematics, GITAM
University, Hyderabad Campus, Telangana, INDIA

- **Manas deep**
Masters in Cyber Law & Information Security
- **Manju Kaushik**
- **Manoharan P.S.**
Associate Professor
- **Manoj Wadhwa**
Echelon Institute of Technology Faridabad
- **Manpreet Manna**
Director, All India Council for Technical Education,
Ministry of HRD, Govt. of India
- **Manuj Darbari**
BBD University
- **Marcellin Julius Nkenlifack**
University of Dschang
- **Maria-Angeles Grado-Caffaro**
Scientific Consultant
- **Marwan Alseid**
Applied Science Private University
- **Mazin Al-Hakeem**
LFU (Lebanese French University) - Erbil, IRAQ
- **Md Islam**
sikkim manipal university
- **Md. Bhuiyan**
King Faisal University
- **Md. Zia Ur Rahman**
Narasaraopeta Engg. College, Narasaraopeta
- **Mehdi Bahrami**
University of California, Merced
- **Messaouda AZZOUZI**
Ziane Achour University of Djelfa
- **Milena Bogdanovic**
University of Nis, Teacher Training Faculty in Vranje
- **Miriampally Venkata Raghavendra**
Adama Science & Technology University, Ethiopia
- **Mirjana Popovic**
School of Electrical Engineering, Belgrade University
- **Miroslav Baca**
University of Zagreb, Faculty of organization and
informatics / Center for biometrics
- **Moeiz Miraoui**
University of Gafsa
- **Mohamed Eldosoky**
- **Mohamed Ali Mahjoub**
Preparatory Institute of Engineer of Monastir
- **Mohamed Kaloup**
- **Mohamed El-Sayed**
Faculty of Science, Fayoum University, Egypt
- **Mohamed Najeh LAKHOUA**
ESTI, University of Carthage
- **Mohammad Ali Badamchizadeh**
University of Tabriz
- **Mohammad Jannati**
- **Mohammad Alomari**
Applied Science University
- **Mohammad Haghighat**
University of Miami
- **Mohammad Azzeh**
Applied Science university
- **Mohammed Akour**
Yarmouk University
- **Mohammed Sadgal**
Cadi Ayyad University
- **Mohammed Al-shabi**
Associate Professor
- **Mohammed Hussein**
- **Mohammed Kaiser**
Institute of Information Technology
- **Mohammed Ali Hussain**
Sri Sai Madhavi Institute of Science & Technology
- **Mohd Helmy Abd Wahab**
University Tun Hussein Onn Malaysia
- **Mokhtar Beldjehem**
University of Ottawa
- **Mona Elshinawy**
Howard University
- **Mostafa Ezziyani**
FSTT
- **Mouhammd sharari alkasassbeh**
- **Mourad Amad**
Laboratory LAMOS, Bejaia University
- **Mueen Uddin**
University Malaysia Pahang
- **MUNTASIR AL-ASFOOR**
University of Al-Qadisiyah
- **Murphy Choy**
- **Murthy Dasika**
Geethanjali College of Engineering & Technology
- **Mustapha OUJAOURA**
Faculty of Science and Technology Béni-Mellal
- **MUTHUKUMAR SUBRAMANYAM**
DGCT, ANNA UNIVERSITY
- **N.Ch. Iyengar**
VIT University
- **Nagy Darwish**

Department of Computer and Information Sciences,
Institute of Statistical Studies and Researches, Cairo
University

- **Najib Kofahi**
Yarmouk University
- **Nan Wang**
LinkedIn
- **Natarajan Subramanyam**
PES Institute of Technology
- **Natheer Gharaibeh**
College of Computer Science & Engineering at
Yanbu - Taibah University
- **Nazeeh Ghatasheh**
The University of Jordan
- **Nazeeruddin Mohammad**
Prince Mohammad Bin Fahd University
- **NEERAJ SHUKLA**
ITM UNiversity, Gurgaon, (Haryana) Inida
- **Neeraj Tiwari**
- **Nestor Velasco-Bermeo**
UPFIM, Mexican Society of Artificial Intelligence
- **Nidhi Arora**
M.C.A. Institute, Ganpat University
- **Nilanjan Dey**
- **Ning Cai**
Northwest University for Nationalities
- **Nithyanandam Subramanian**
Professor & Dean
- **Noura Aknin**
University Abdelamlek Essaadi
- **Obaida Al-Hazaimeh**
Al- Balqa' Applied University (BAU)
- **Oliviu Matei**
Technical University of Cluj-Napoca
- **Om Sangwan**
- **Omaima Al-Allaf**
Asesstant Professor
- **Osama Omer**
Aswan University
- **Ouchtati Salim**
- **Ousmane THIARE**
Associate Professor University Gaston Berger of
Saint-Louis SENEGAL
- **Paresh V Virparia**
Sardar Patel University
- **Peng Xia**
Microsoft

- **Ping Zhang**
IBM
- **Poonam Garg**
Institute of Management Technology, Ghaziabad
- **Prabhat K Mahanti**
UNIVERSITY OF NEW BRUNSWICK
- **PROF DURGA SHARMA (PHD)**
AMUIT, MOEFDRE & External Consultant (IT) &
Technology Tansfer Research under ILO & UNDP,
Academic Ambassador for Cloud Offering IBM-USA
- **Purwanto Purwanto**
Faculty of Computer Science, Dian Nuswantoro
University
- **Qifeng Qiao**
University of Virginia
- **Rachid Saadane**
EE departement EHTP
- **Radwan Tahboub**
Palestine Polytechnic University
- **raed Kanaan**
Amman Arab University
- **Raghuraj Singh**
Harcourt Butler Technological Institute
- **Rahul Malik**
- **raja boddu**
LENORA COLLEGE OF ENGINEERNG
- **Raja Ramachandran**
- **Rajesh Kumar**
National University of Singapore
- **Rakesh Dr.**
Madan Mohan Malviya University of Technology
- **Rakesh Balabantaray**
IIIT Bhubaneswar
- **Ramani Kannan**
Universiti Teknologi PETRONAS, Bandar Seri
Iskandar, 31750, Tronoh, Perak, Malaysia
- **Rashad Al-Jawfi**
Ibb university
- **Rashid Sheikh**
Shri Aurobindo Institute of Technology, Indore
- **Ravi Prakash**
University of Mumbai
- **RAVINA CHANGALA**
- **Ravisankar Hari**
CENTRAL TOBACCO RESEARCH INSTITUE
- **Rawya Rizk**
Port Said University

- **Reshmy Krishnan**
Muscat College affiliated to Stirling University.U
- **Ricardo Vardasca**
Faculty of Engineering of University of Porto
- **Ritaban Dutta**
ISSL, CSIRO, Tasmania, Australia
- **Rowayda Sadek**
- **Ruchika Malhotra**
Delhi Technological University
- **Rutvij Jhaveri**
Gujarat
- **SAADI Slami**
University of Djelfa
- **Sachin Kumar Agrawal**
University of Limerick
- **Sagarmay Deb**
Central Queensland University, Australia
- **Said Ghoniemy**
Taif University
- **Sandeep Reddivari**
University of North Florida
- **Sanskriti Patel**
Charotar University of Science & Technology,
Changa, Gujarat, India
- **Santosh Kumar**
Graphic Era University, Dehradun (UK)
- **Sasan Adibi**
Research In Motion (RIM)
- **Satyena Singh**
Professor
- **Sebastian Marius Rosu**
Special Telecommunications Service
- **Seema Shah**
Vidyalankar Institute of Technology Mumbai
- **Seifedine Kadry**
American University of the Middle East
- **Selem Charfi**
HD Technology
- **SENGOTTUVELAN P**
Anna University, Chennai
- **Senol Piskin**
Istanbul Technical University, Informatics Institute
- **Sérgio Ferreira**
School of Education and Psychology, Portuguese
Catholic University
- **Seyed Hamidreza Mohades Kasaei**
University of Isfahan
- **Shafiqul Abidin**
HMR Institute of Technology & Management
(Affiliated to GGS Indraprastha University), Hamidpur, Delhi -
110036
- **Shahanawaj Ahamad**
The University of Al-Kharj
- **Shaidah Jusoh**
- **Shaiful Bakri Ismail**
- **Shakir Khan**
Al-Imam Muhammad Ibn Saud Islamic University
- **Shawki Al-Dubae**
Assistant Professor
- **Sherif Hussein**
Mansoura University
- **Shriram Vasudevan**
Amrita University
- **Siddhartha Jonnalagadda**
Mayo Clinic
- **Sim-Hui Tee**
Multimedia University
- **Simon Ewedafe**
The University of the West Indies
- **Siniša Opic**
University of Zagreb, Faculty of Teacher Education
- **Sivakumar Poruran**
SKP ENGINEERING COLLEGE
- **Slim BEN SAOUD**
National Institute of Applied Sciences and
Technology
- **Sofien Mhatli**
- **sofyan Hayajneh**
- **Sohail Jabbar**
Bahria University
- **Sri Devi Ravana**
University of Malaya
- **Sudarson Jena**
GITAM University, Hyderabad
- **Suhail Sami Owais Owais**
- **Suhas J Manangi**
Microsoft
- **SUKUMAR SENTHILKUMAR**
Universiti Sains Malaysia
- **Süleyman Eken**
Kocaeli University
- **Sumazly Sulaiman**
Institute of Space Science (ANGKASA), Universiti
Kebangsaan Malaysia

- **Sumit Goyal**
National Dairy Research Institute
- **Suparek Janjarasjitt**
Ubon Ratchathani University
- **Suresh Sankaranarayanan**
Institut Teknologi Brunei
- **Susarla Sastry**
JNTUK, Kakinada
- **Suseendran G**
Vels University, Chennai
- **Suxing Liu**
Arkansas State University
- **Syed Ali**
SMI University Karachi Pakistan
- **T C.Manjunath**
HKBK College of Engg
- **T V Narayana rao Rao**
SNIST
- **T. V. Prasad**
Lingaya's University
- **Taiwo Ayodele**
Infonetmedia/University of Portsmouth
- **Talal Bonny**
Department of Electrical and Computer Engineering, Sharjah University, UAE
- **Tamara Zhukabayeva**
- **Tarek Gharib**
Ain Shams University
- **thabet slimani**
College of Computer Science and Information Technology
- **Totok Biyanto**
Engineering Physics, ITS Surabaya
- **Touati Youcef**
Computer sce Lab LIASD - University of Paris 8
- **Tran Sang**
IT Faculty - Vinh University - Vietnam
- **Tsvetanka Georgieva-Trifonova**
University of Veliko Tarnovo
- **Uchechukwu Awada**
Dalian University of Technology
- **Udai Pratap Rao**
- **Urmila Shrawankar**
GHRCE, Nagpur, India
- **Vaka MOHAN**
TRR COLLEGE OF ENGINEERING
- **VENKATESH JAGANATHAN**
- **ANNA UNIVERSITY**
- **Vinayak Bairagi**
AISSMS Institute of Information Technology, Pune
- **Vishnu Mishra**
SVNIT, Surat
- **Vitus Lam**
The University of Hong Kong
- **VUDA SREENIVASARAO**
PROFESSOR AND DEAN, St.Mary's Integrated Campus, Hyderabad
- **Wali Mashwani**
Kohat University of Science & Technology (KUST)
- **Wei Wei**
Xi'an Univ. of Tech.
- **Wenbin Chen**
360Fly
- **Xi Zhang**
illinois Institute of Technology
- **Xiaojing Xiang**
AT&T Labs
- **Xiaolong Wang**
University of Delaware
- **Yanping Huang**
- **Yao-Chin Wang**
- **Yasser Albagory**
College of Computers and Information Technology, Taif University, Saudi Arabia
- **Yasser Alginahi**
- **Yi Fei Wang**
The University of British Columbia
- **Yihong Yuan**
University of California Santa Barbara
- **Yilun Shang**
Tongji University
- **Yu Qi**
Mesh Capital LLC
- **Zacchaeus Omogbadegun**
Covenant University
- **Zairi Rizman**
Universiti Teknologi MARA
- **Zarul Zaaba**
Universiti Sains Malaysia
- **Zenzo Ncube**
North West University
- **Zhao Zhang**
Deptment of EE, City University of Hong Kong
- **Zhihan Lv**

Chinese Academy of Science

- **Zhixin Chen**
ILX Lightwave Corporation
- **Ziyue Xu**
National Institutes of Health, Bethesda, MD

- **Zlatko Stacic**
University of Zagreb, Faculty of Organization and
Informatics Varazdin
- **Zuraini Ismail**
Universiti Teknologi Malaysia

CONTENTS

Paper 1: Encoding a T-RBAC Model for E-Learning Platform on ORBAC Model

Authors: Kassid Asmaa, Elkamoun Najib

PAGE 1 – 9

Paper 2: Simulation of Building Evacuation: Performance Analysis and Simplified Model

Authors: Yasser M. Alginahi, Muhammad N. Kabir

PAGE 10 – 17

Paper 3: Towards Enhancing Supportive E-Learning Courses using Smart Tags

Authors: Hayel Khafajeh, Heider Wahsheh, Ahmad Alhaishi, Mofareh Alqahtani

PAGE 18 – 23

Paper 4: A Novel Cylindrical DRA for C-Band Applications

Authors: Hamed Gharsallah, Lotfi Osman, Lassaad Latrach

PAGE 24 – 28

Paper 5: Adaptive Threshold for Background Subtraction in Moving Object Detection using Stationary Wavelet Transforms 2D

Authors: Oussama Boufares, Nouredine Aloui, Adnene Cherif

PAGE 29 – 36

Paper 6: Optimization of OADM DWDM Ring Optical Network using Various Modulation Formats

Authors: Vikrant Sharma, Dalveer Kaur

PAGE 37 – 41

Paper 7: Performance Analysis & Comparison of Optimal Economic Load Dispatch using Soft Computing Techniques

Authors: Vijay Kumar, Dr. Jagdev Singh, Dr. Yaduvir Singh, Dr. Sanjay Prakash Sood

PAGE 42 – 48

Paper 8: A New DTC Scheme using Second Order Sliding Mode and Fuzzy Logic of a DFIG for Wind Turbine System

Authors: Zinelaabidine BOUDJEMA, Rachid TALEB, Adil YAHDOU

PAGE 49 – 56

Paper 9: FPGA Implementation of Parallel Particle Swarm Optimization Algorithm and Compared with Genetic Algorithm

Authors: BEN AMEUR Mohamed sadek, SAKLY Anis

PAGE 57 – 64

Paper 10: Simulation of Shunt Active Power Filter Controlled by SVPWM Connected to a Photovoltaic Generator

Authors: Ismail BOUYAKOUB, Abedelkader DJAHBAR, Benyounes MAZARI,

PAGE 65 – 71

Paper 11: PSIM and MATLAB Co-Simulation of Photovoltaic System using “P and O” and “Incremental Conductance” MPPT

Authors: ANAS EL FILALI, EL MEHDI LAADISSI, MALIKA ZAZI

PAGE 72 – 76

Paper 12: Implementing and Comparison between Two Algorithms to Make a Decision in a Wireless Sensors Network

Authors: Fouad Essahlaoui, Ahmed El Abbassi,

PAGE 77 – 83

Paper 13: Emotion Recognition from Speech using Prosodic and Linguistic Features

Authors: Mahwish Pervaiz, Tamim Ahmed Khan

PAGE 84 – 90

Paper 14: Medical Image Inpainting with RBF Interpolation Technique

Authors: Mashail Alsalamah, Saad Amin

PAGE 91 – 99

Paper 15: Content based Video Retrieval Systems Performance based on Multiple Features and Multiple Frames using SVM

Authors: Mohd Aasif Ansari, Hemlata Vasishtha

PAGE 100 – 105

Paper 16: Finite Elements Modeling of Linear Motor for Automatic Sliding Door Application

Authors: Aymen Lachheb, Lilia El Amraoui, Jalel Khedhiri

PAGE 106 – 112

Paper 17: A Review of Solutions for SDN-Exclusive Security Issues

Authors: Jakob Spooner, Dr Shao Ying Zhu

PAGE 113 – 122

Paper 18: Optimized Voting Scheme for Efficient Vanishing Point Detection in General Road Images

Authors: Vipul H.Mistry, Ramji Makwana

PAGE 123 – 130

Paper 19: Automated Simulation P2P Botnets Signature Detection by Rule-based Approach

Authors: Raihana Syahirah Abdullah, Faizal M.A., Zul Azri Muhamad Noh, Nurulhuda Ahmad

PAGE 131 – 135

Paper 20: A Survey on Case-based Reasoning in Medicine

Authors: Nabanita Choudhury, Shahin Ara Begum

PAGE 136 – 144

Paper 21: MRPPSim: A Multi-Robot Path Planning Simulation

Authors: Ebtehal Turki Saho Alotaibi, Hisham Al-Rawi

PAGE 145 – 155

Paper 22: Software Design Principles to Enhance SDN Architecture

Authors: Iyad Alazzam, Izzat Alsmadi, Khalid M.O Nahar

PAGE 156 – 163

Paper 23: Evaluating the Usability of Optimizing Text-based CAPTCHA Generation

Authors: Suliman A. Alsuhibany

PAGE 164 – 169

Paper 24: Performance Optimization of the Multi-Pumped Raman Optical Amplifier using MOICA

Authors: Mohsen Katebi Jahromi, Seyed Mojtaba Saif, Masoud Jabbari

PAGE 170 – 180

Paper 25: Influence of Adopting a Text-Free User Interface on the Usability of a Web-based Government System with Illiterate and Semi-Literate People

Authors: Ms. Ghadam Alduhailan, Dr. Majed Alshamari

PAGE 181 – 188

Paper 26: Chemical Reaction Optimization for Max Flow Problem

Authors: Reham Barham, Ahmad Sharieh, Azzam Sliet

PAGE 189 – 196

Paper 27: Factors Influencing Patients' Attitudes to Exchange Electronic Health Information in Saudi Arabia: An Exploratory Study

Authors: Mariam Al-Khalifa, Shaheen Khatoon, Azhar Mahmood, Iram Fatima

PAGE 197 – 204

Paper 28: Efficient Load Balancing Algorithm for the Arrangement-Star Network

Authors: Ahmad M. Awwad, Jehad A. Al-Sadi

PAGE 205 – 213

Paper 29: Analytical Performance Evaluation of Ipv6 and Ipv4 Over 10 Gigabit Ethernet and Infiniband using Ipoib

Authors: Eric Gamess, Humberto Ortiz-Zuazaga

PAGE 214 – 222

Paper 30: Ontology-based Query Expansion for Arabic Text Retrieval

Authors: Waseem Alromima, Ibrahim F. Moawad, Rania Elgohary, Mostafa Aref

PAGE 223 – 230

Paper 31: A Hybrid Approach for Measuring Semantic Similarity between Documents and its Application in Mining the Knowledge Repositories

Authors: Ms. K. L. Sumathy, Dr. Chidambaram

PAGE 231 – 237

Paper 32: A Novel Approach for Submission of Tasks to a Data Center in a Virtualized Cloud Computing Environment

Authors: B.Santhosh Kumar, Dr. Latha Parthiban

PAGE 238 – 242

Paper 33: Evaluation of Wellness Detection Techniques using Complex Activities Association for Smart Home Ambient

Authors: Farhan Sabir Ujager, Azhar Mahmood, Shaheen Khatoon, Muhammad Imran, Umair Abdullah

PAGE 243 – 253

Paper 34: A Study of Resilient Architecture for Critical Software-Intensive System-of-Systems (Sisos)

Authors: Nadeem Akhtar, Malik Muhammad Saad Missen, Nadeem Salamat, Amnah Firdous, Mujtaba Husnain

PAGE 254 – 258

Paper 35: Speech Impairments in Intellectual Disability: An Acoustic Study

Authors: Sumanlata Gautam, Latika Singh

PAGE 259 – 264

Paper 36: Urdu Text Classification using Majority Voting

Authors: Muhammad Usman, Zunaira Shafique, Saba Ayub, Kamran Malik

PAGE 265 – 273

Paper 37: An Item-based Multi-Criteria Collaborative Filtering Algorithm for Personalized Recommender Systems

Authors: Qusai Shambour, Mou'ath Hourani, Salam Fraihat

PAGE 274 – 279

Paper 38: Pattern Recognition Approach in Multidimensional Databases: Application to the Global Terrorism Database

Authors: Semeh BEN SALEM, Sami NAOUALI

PAGE 280 – 286

Paper 39: An Improved Pulmonary Nodule Detection Scheme based on Multi-Layered Filtering and 3d Distance Metrics

Authors: Baber Jahangir, Muhammad Imran, Qamar Abbas, Shahina Rabeel, Ayyaz Hussain

PAGE 287 – 291

Paper 40: Autonomous Vehicle-to-Vehicle (V2V) Decision Making in Roundabout using Game Theory

Authors: Lejla Banjanovic-Mehmedovic, Edin Halilovic, Ivan Bosankic, Mehmed Kantardzic, Suad Kasapovic

PAGE 292 – 298

Paper 41: Analytical and Numerical Study of the Onset of Electroconvection in a Dielectric Nanofluid Saturated a Rotating Darcy Porous Medium

Authors: Abderrahim Wakif, Zoubair Boulahia, Rachid Sehaqui

PAGE 299 – 311

Paper 42: BRIQA: Framework for the Blind and Referenced Visual Image Quality Assessment

Authors: Jaime Moreno, Oswaldo Morales, Ricardo Tejeida, Eduardo Garc´ıa, Yasser S´anchez

PAGE 312 – 319

Paper 43: Cohesion Based Personalized Community Recommendation System

Authors: Md Mamunur Rashid, Kazi Wasif Ahmed, Hasan Mahmud, Md. Kamrul Hasan, Husne Ara Rubaiyeat

PAGE 320 – 326

Paper 44: Face Recognition in Uncontrolled Environment

Authors: Radhey Shyam, Yogendra Narain Singh

PAGE 327 – 333

Paper 45: Architecture Considerations for Big Data Management

Authors: Khalim Amjad Meerja, Khaled Almustafa

PAGE 334 – 342

Paper 46: An Improved Approach for Text-Independent Speaker Recognition

Authors: Rania Chakroun, Leila Beltaïfa Zouari, Mondher Frikha

PAGE 343 – 348

Paper 47: Using Persuasive Recommendations in Wellness Applications based upon User Activities

Authors: Hamid Mukhtar

PAGE 349 – 356

Paper 48: Using Persuasive Recommendations in Wellness Applications based upon User Activities

Authors: Maaz Bin Ahmad, Muhammad Fahad, Abdul Wahab Khan, Muhammad Asif

PAGE 357 – 360

Encoding a T-RBAC Model for E-Learning Platform on ORBAC Model

Kassid Asmaa
STIC Laboratory
Chouaib Doukkali University
El Jadida, Morocco

Elkamoun Najib
STIC Laboratory
Chouaib Doukkali University
El Jadida, Morocco

Abstract—with rapid development and increase in the amount of available resources in E-learning platforms, the need to design new architecture for such systems has become inevitable to improve the search quality and simplifying ways to take online courses. The integration of multi-agent systems has played a very important role in developing open, interactive and distributed learning systems. A lot of research in E-learning and multi-agent system have been put into developing infrastructure and providing content, security and trust issues have hardly ever been considered worth knowing that security issues may endanger the success of these platforms.

The application of a control access policy, as one of the most important aspects of security, in E-learning platform based on multi agent systems , plays an important role to secure interaction with agents/users and reinforcing it with the integration of trust level .The work of this paper is to encode a new access control model developed in previous works based on “ role based access control model “ and trust level, on “Organization based access control model” to improve the security level in E-learning platforms based on multi-agent systems.

The encoded model is implemented and evaluated by “MotOrbac” tool, in order to define its validity context and limitations for a large and extended deployment.

Keywords—Security policies; Access control; Rbac model; Orbac model; e-learning platforms; trust; multi-agent systems

I. INTRODUCTION

The definition of E-Learning is understood simply as a means of teaching throughout the online internet technology , it is a convenient and inexpensive way to gain knowledge and learn ; It has become the need of the hour since more and more people are taking online courses; With the development of Information Technology, E-learning is developing rapidly; It is does not only support teaching and learning, but also some Intelligence interaction among the collaborative team members[1], to design such complex platform, designers use one of the emerging technologies in distributed Environment: Agent based technology ,

Multi agent system in E-learning system makes a great change in the society because the conventional education system need the presence of the student and the instructor at the same time, same place and at the same interval of time, which is somehow difficult to manage every time . This technology is helping in developing interactive and better E-learning system. In agent-based systems, agents try to get information from other or gain access to remote service

provider agents in order to achieve their goals. We have seen considerable effort being put into development of the content and infrastructure for the e-learning system, yet there is hardly any effort being put into these system for making them secure, especially, in open environments where agents are able to freely move around, many activities would be unsafe and unreliable because it is hard to know which agents are trustworthy and which external accesses are not harmful. Worth knowing that the integration of security concerns could help towards the development of more secure multi agent systems.

A lot of models how are found in the literature consider the integration of trust in multi agent systems as the key to protect it, and as a basis for building a satisfactory model of security based on access control policies, one of the most developed security methods, it is expressed by identifying the restriction of access rights an entity has over system resources. Access controls are the concrete mechanisms that are put in place to assert whether or not the current user can perform a given action on a given resource.

As we know to achieve a satisfactory level of security, it is necessary to define a security policy that meets the needs of the application, several formalisms have been proposed and developed during last years to overcome the limitations of the models above depending on the nature of systems and their development witch make the management of the different levels of access rights to multiple types of resources by different and distributed users more complex : DAC [4], MAC[5], RBAC [6], TBAC[7] or TMAC[8] . In these models we find a lot of extensions of role based access control (RBAC) which make this one as the standard of access control models. The concept of RBAC had begun with multi-users and multi-applications on-line systems pioneered in the 1970s. The difference between RBAC and the other access control models is the ease of security administration which is manifested by linking permissions with roles, while the users are assigned to definite role. In spite of that Rbac model and its extensions, must take into consideration the new demands:

- Every organization has the opportunity to have their own policies.
- Rules in access policies, with the integration of context concept, become dynamic.
- Rules in access policies must be self-adaptive to the temporal conditions, the location of the user and the previous user behavior.

Hence the appearance of OrBAC model (Organisation-Based Access Control) who is more oriented security policy. It is a model allowing abstract notions of users, action and object, expressing rights context, obligations or recommendations not only the permission like traditional models. It contributes to define abstractions which allow us to relate managed objects to one another or which allow us to relate users, or groups of users, to groups of objects.

In this paper, the work is to encode a new model that we developed in previous work [9] based on the two access control model "TrustBAC model" [10] and "Dynamic RBAC with trust- satisfaction and reputation for multi-agent systems" [11]; the main goal of this model is to incorporate the advantages of both to improve the highest degree of security in E-learning platforms based on multi-agent systems.

Having given an initial introduction and motivation of the proposed work, the rest of this paper is structured as follows: In Section 2 an overview of some of the related works on access control. There is a plethora of works in access control mechanisms. Here we present some of the works that are related to trust, e-learning platforms and multi-agent systems access control model. The proposed model, its components and an example of how our new model works in E-learning platform are presented in Section 3 including the trust evaluation method; Section 4 presents the main concepts and components of orbac model Section 5 is dedicated to present the encoded model. The basic concept of e-learning platform oriented spatial metaphor based on Multi-agent systems, with a use case of the model in a concrete e-learning scenario for educational purpose will be presented in section 6. Finally, we conclude the paper with some perspectives in section 7.

II. RELATED WORK

Since security has become an essential asset in numerous application areas such as e-learning platforms, the integration of security policies has become a major issue in the design of security architectures.

Much work has been done in the area of e-learning, since it covers a broad category of applications and processes, such as education via the Internet / computer (web based learning/ computer based learning), virtual classrooms and digital collaboration [14]. In this section we would briefly discuss the research works related of security requirements for e-learning and multi-agent platforms.

To achieve a good level of security, there are many important elements that must be taken into account, and this has been discussed in a good way and can be reached in [11]. In [12], proposals for Security of e-learning Systems and security requirements for Multi-agent systems have been discussed; Security case modeling has been taken into account with emphasis on use cases.

Security has already proved an important requirement for the success of MAS, so there are already some works in this research area cited in [13], showing the concern of multi-agent community with security.

Access control model it is an important method of grant the three security Principles of computing: confidentiality,

integrity and availability, the control of how resources are accessed it is very important in the protection of the e-learning platforms based on Multi-agent technology, preventing unauthorized modification or disclosure of resources. A lot of access control models have been developed ,a relevant work is provided by Xiao et al. – an authorization mechanism based in RBAC model [6], the authors consider that using policies based on roles is possible to build a security architecture that automatically adapts to system changes.. However it is still not enough for open and decentralized multi-centric systems in terms of dynamic and unknown users, to overcome the limitations of RBAC for this kind of systems, authors have proposed credential-based access control models [15, 16]. This model implement a concept of binary trust which mean that a user has to produce a predetermined set of credentials (proofs) to gain some determined access privileges. It's provides information about the rights, qualifications, responsibilities and other characteristics attributable to its bearer by one or more trusted authorities also it provides trust information about the authorities themselves. The combination between credential based access control and role-based access control make the security administration more flexible [17, 18]. even though the credential based models solve the problem of access control in open systems ,still not enough in terms of given information about the behavior or action of the user, the credential model shows its limits to achieve a satisfy level of security , that why a lot of research has been done to improve the evaluation of trust on integrating the mechanism of history and context information (context awareness takes an important part which identifies the user's needs by analyzing the context information of user environment) of the user [19, 20, 21].

The TrustBAC model, enhance the binary trust paradigm with multi-level trust which make the model much richer : trust levels in the users can be determined not only by using the credentials presented by the user but also from the results of past interactions with the user, from recommendations about the user and/or knowledge about other characteristics of the user.

To highlight the dynamic changes of the environment and the roles assigned to users , researchers develop a new access control model for multi-agent systems based on the RBAC model with the integration of trust concept : "Dynamic RBAC with trust-satisfaction and reputation for multi-agent systems"[9] because In multi agent systems the context information collected from diverse sensor agents needs to be protected from unauthorized access and properly shared by many agents depending on the types of information and roles of user agents. For efficient access control to these resources, this model updates dynamically the roles and permissions according to the continuously changing environment. The proposed model employs the notion of trust evaluated with the measure of satisfaction and reputation.

The incorporation of the advantages of both latest models cited above gives birth to a more efficient new model that we developed in previous works and to improve the highest level of security in E-learning platforms based on multi-agent systems: The notion of trust in multi-agent system which can be used, is to put the relationship into the dynamic multi-agent system to control the access to the resources and services , so,

if an agent wants to request a service, as first step , it needs to pass the permission test checking on whether it is authorized or not, then it must solve the problem of security.

As we know ORBAC model produce a rich and modular (the designer can define a policy security independently of the implementation), but with the integration of the concept of trust make it more dynamic (rules can be activated or deactivated based on trust levels of the user or the organization) and more interactive (the recent behaviors of the trustee are used to control the access of resources). In the literature two different model of TRUS T-ORBAC are proposed for two different platform the first is ‘A Trust Access Control Model in Multi-Organization Environments’ [19] and ‘A Trust-Orbac Control is a new model dedicated to the security of Cloud Computing Systems’ [2]. The difference between these two models is in the fact to evaluate the trust; knowing that this later change from one to another system.

III. THE PROPOSED MODEL

This model allows to us an *access control management* more dynamic and precise, with the help of three modules that build the access control structure of our approach:

- The “*Trust Evaluation Module*” it’s the principal; it receives access requests, analyzes, collection of context values and other parameters, and sends the trust value of the user to the Access Control System module.
- The “*Access Control System*” makes decisions for each application based on the value of trust of the user provided by the *trust evaluation* module; The “Trust evaluation module” plays a key role in the proposed model. It calculates the values of trust based on the reputation, satisfaction and context values.
- The “*context module*” is responsible for collecting user and environment information’s.

A. Evaluation of a trust value

Before exploring the parameters to evaluate trust value, we first define trust in the context of this paper. Trust is defined in a variety of ways. Many authors examine the various definitions of trust and then provide a working definition of trust for internet applications: “Trust is the firm belief in the competence of an entity to act dependably, securely, and reliably within a specified context”. However, in our model we adopt the definition of Mui et al. , because the definition of trust is based on reputation which both are strongly related to evaluate trust in Multi agent systems: “Trust is a subjective expectation an agent has about another’s future behavior based on the history of their encounters”.

The trust value in a practical system is calculated **Satisfaction** which represents the confidence of the services and resources the agents provide, and **Reputation** which represents the recent behavior and past history of requesting agent.

We compute the trust value of an agent as

$$\text{Trust} = \alpha_1 * \text{SD} + \alpha_2 * \text{R} \quad (1)$$

$$\alpha_1 + \alpha_2 = 1 \text{ and } \alpha_1, \alpha_2 > 0$$

Where α_1 and α_2 are the weight coefficients defined by the System according to the application.

- **Satisfaction degree SDi** is between 0 and 1. If it is close to 0, it means that agent-i is untrustworthy. On the contrary, if it is close to 1, agent-i is trustworthy.

- **Reputation** is evaluated by calculating local and *global* reputation. Local reputation is the quotient of number of honest transactions and the sum of honest and malicious transactions between agent-i and agent-j. The global reputation is the average value of the local reputation values of an agent evaluated by other agents; more details are explained in [9].

B. Basic concept of the new model

The components of this model can be treated as an agent ; they are cited as follow:

- **User agent** : is the user how carries to access the resources according to the user’s role (same as user in RBAC model)
- **Trust-levels agent** : responsible for checking the trust value of the agents and classifying it in different levels
- **Role Agent**: responsible for keeping the list of the roles and managing the their hierarchy.
- **Permission Agent** : its role is keep the list of permissions
- **Sensor Agents**: its role is collects the context information and sends it to the ‘Context-Aware Agent’.
- **Session Agent**: its role is register the rules in ‘Context-Aware Agent’ besides connecting ‘User Agent’ and ‘Permission Agent. It is dynamically updates the user’s role according to the context.
- **Context-Aware Agent**: its role is infers the context using diverse context information and reports the result when the rule is fired.

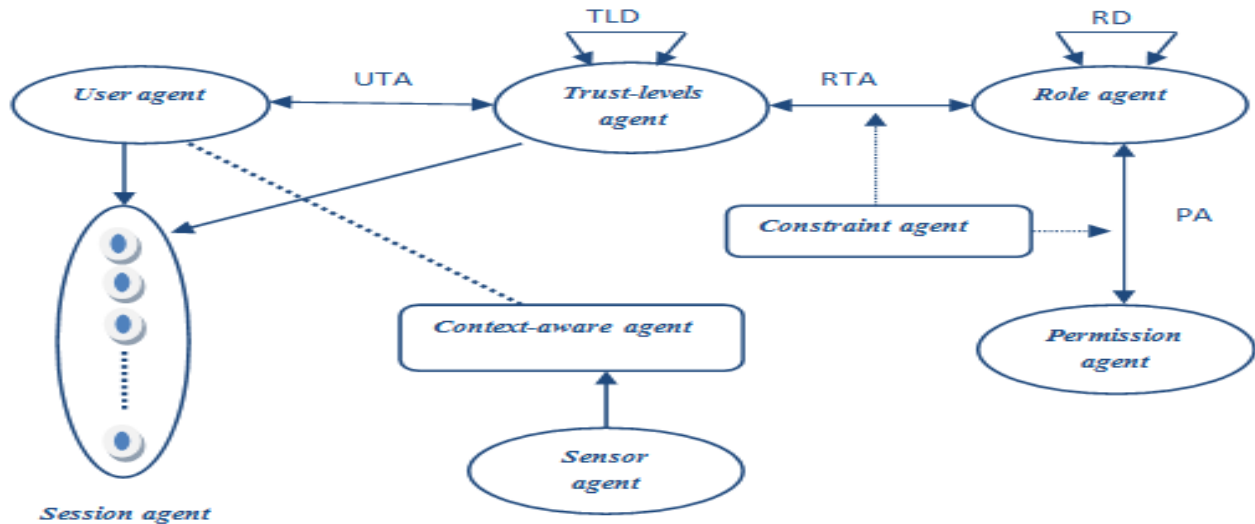


Fig. 1. The new model

The structure of the new model is presented in Figure 1.

The difference between trust-role-based dynamic access control mechanisms and the other access control models is that the user's role can control policy by its trust level.

C. The process of access authorization

The access authorization process is illustrated in the Figure 2 as following:

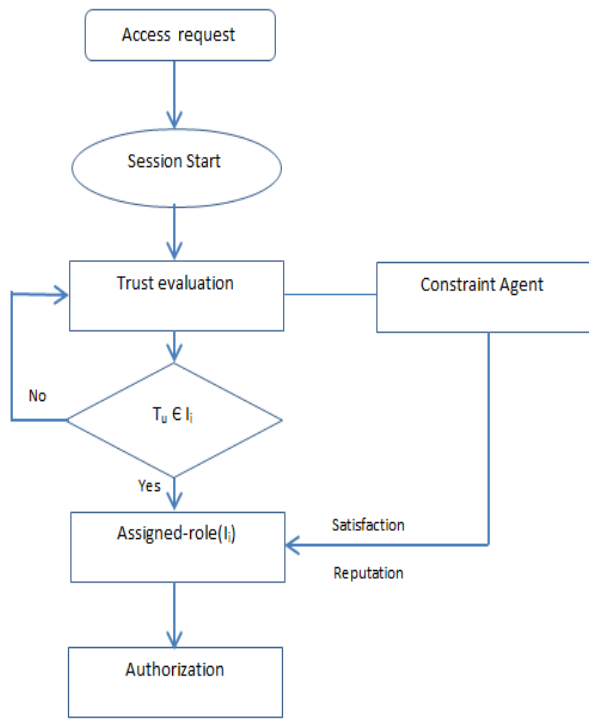


Fig. 2. access authorization process

The access authorization process is summarized:

Step 1: After a request for access is made, a session is started.

Step 2: Once the session is established, the trust evaluation module which is based on reputation and trust gives a value of the requester (user).

Step 3: If the user confidence value T_u , belongs to the interval defined by the administrator, specific roles are assigned to the user depending this interval and constraint agent, after that the authorization is granted. Alternatively, we recalculate the confidence value if there is an unexpected error.

IV. PRESENTATION OF ORBAC MODEL

Organisation Base Access Control, is an access model that took over the cited above models by adding the concept of abstract entities. In the beginning, OrBAC was proposed in [10] to meet security policy requirements in the health care fields.

The application of OrBAC model in different platforms confirms its expressive power, adding to these, OrBAC includes contextual rules based not only on permissions but also prohibitions, obligations and recommendation which make the security policy rich, modular and dynamic.

A. Basic concepts of OrBAC model

The central entity in Or-BAC is the Organization. An organization can be seen as an organized group of subjects playing a role or another. Worth knowing a group of subjects does not necessarily correspond to an organization. More specifically, the fact that each object plays a role in the organization is an agreement between the materials to form an organization.

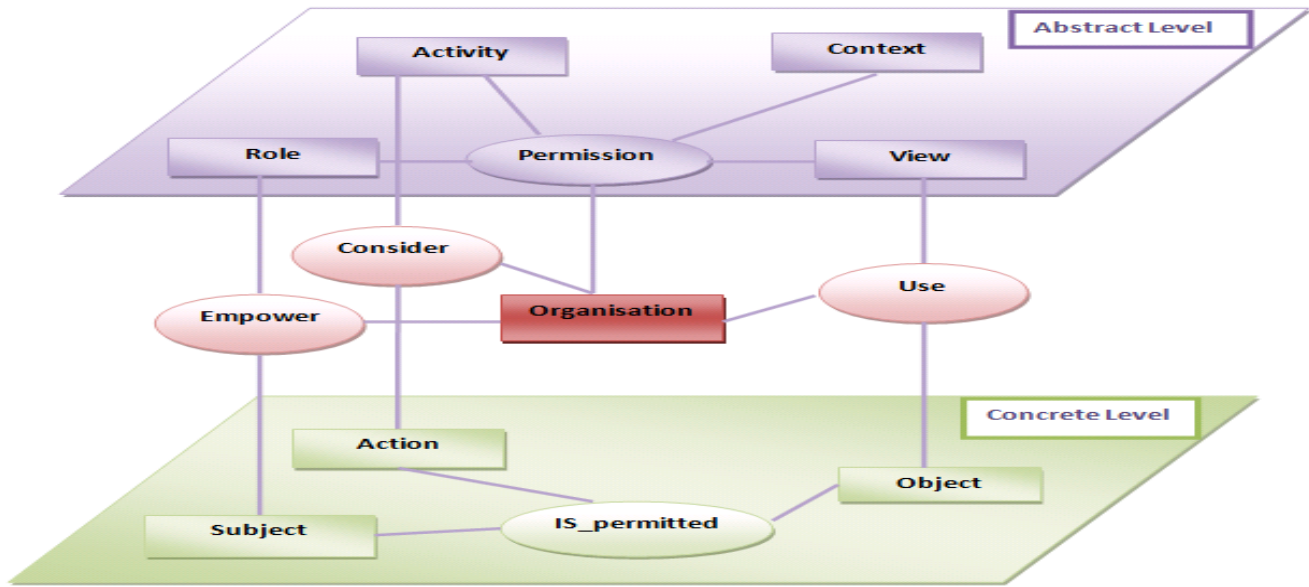


Fig. 3. The ORBAC model

As the Figure 3, the introduction of an abstract level where the role, activity and view concepts abstract the subject, action and object concepts [8] allow to the designer the possibility to define a policy security policy independently of the implementation .A view is a set of objects that satisfy a common property. An activity includes actions involved the same principles and privileges apply only in the specific context.

Each organization *org* specifies its own security rules, some *role* may have the *permission*, *prohibition*, and *obligation* or *recommendation* to do some *activity* on some *view* given an associated *context* is true:

- permission*(org, role, activity, view, context).
- prohibition* (org, role, activity, view, context).
- obligation* (org, role, activity, view, context).
- recommendation* (org, role, activity, view, context).

B. The new Concepts characterizing the model

In ORBAC model, new concepts have been added in a developed way, and which have characterized as the most developed access control model, in the following table you found these concepts with their explanation.

Notion	In ORBAC model an organization can be divided in sub-organization, a role in sub-role, activity in sub-activity, and a view in sub-view. These decompositions generate hierarchical relationships between the parent entity (generalization) and the Child entity (specialization).
Of hierarchy	In order to express this hierarchy OrBAC introduces the predicates <i>sub_role</i> (org, R1, R2) which means that in organization org, role R1 is a sub-role of the role R2, same thing with <i>sub-activity</i> (org, A1, A2) and <i>sub-view</i> (org, V1, V2).

Notion of Context	Express different types of constraints that control the activation of the rules expressed in the access control policy. OrBAC model represents the contextual constraints allocation rights, brings together the different contexts by type, to acceptance a request an evaluation of the context must be done , this evaluation is based on some information in order to test the activation of the context.
Notion Of Conflict	Since Or-BAC model specifies at the same time permissions and prohibitions the appearance of conflict became remarkable, especially when a user is permitted and prohibited to perform an action on object a conflicts can occur. To model such a situation, we introduce a predicate called <i>conflict</i> () used in rules as follow: <div style="border: 1px solid black; padding: 5px; width: fit-content; margin: 10px auto;"> $Is_permitted(s, \alpha, o) \wedge Is_prohibited(s, \alpha, o) \rightarrow conflict ()$ </div>

V. ENCODING THE PROPOSED MODEL ON ORBAC MODEL

This section provide an encoding of the proposed model, which is based on RBAC model with trust level, on OrBAC organizational model. For each concept (role, type, context ...) used in the model, we provide its counterpart in the OrBAC model to confirm the expressive power of this later.

Two concepts of ORBAC model are not directly used in the proposed model:

- **The concept context** which is not exploited in a larger and varied manner, so with the use of context OrBAC model, we can express different types of extra conditions or constraints that control activation of rules.
- **The concept of organization:** in this case the OrBAC model is supposed to have a fixed value, we assume here that we have only one organization we simply call "learn-organization".

A. Subject / role

As we said in the previous section, in the ORBAC model, a subject may be either an active entity: a user / agent, an organization STIC laboratory or department of IT In our platform, the **entity subject** lists the UID (User Identifier) of this system, each UID is related to specific username. The **entity Role** is used to structure the relationship between subjects and organizations. In our case, like the table show, the roles «Privilege-student », «administrator», are played by users specially students.

TABLE I. SUBJECTS / ROLE

Role	Subject
Privilege-student	{Mr Najib}
basic-student	{Mlle Fatima , Mr Khalid}
Public-Student	{Asmaa,zahira,hind...}
administrator	{Imad}

B. objects / view

In our model, the entity subject primarily represents non-active entities such as files, emails, printed forms ..., in e-learning platform, we consider objects as courses, exams, practical work.... The **entity views** like role is used to structure the relationship between objects and organizations. The following table summarize some of view/object used in e-learning platform.

TABLE II. OBJECTS / VIEW

View	Objects
course	Course-X.doc/html/pdf/ppt
Resource-sup	- video/-shéma.jpg / ...
Resource-Test	-Quiz.doc/-Exam-modul-x.doc
Doc-team	- Doc-team 1/2/3
training	-Training-BD

C. Activities / Action

Security policies specify allowed access to passive entities by active entities and regulate the actions performed on the system. In ORBAC model, the Action entity includes IT actions like "read", "write", "send", etc. The activities will be "consult", "edit", "transmit", etc. Each organization may consider the same action used in the realization of different activities. You find in the following table some Activity/Actions used in E-learning.

TABLE III. ACTIVITY / ACTIONS

Activity	Actions
Creation	- writing courses / exercises -filed courses / exercises
Update	-Modification /Suppression(courses / exercises)
Follow	-Explain-course/project – Answer-questions
download	-Download (course/Exam)
Answer	-Answer (questions/exam)
Register	-Registration

D. Trust context

We recall that a context is a condition over the environment, to control the activation context, the systems has to give some information to check if the condition is satisfied or not worth knowing that there is many type of context in ORBAC model, the following figure resume and presents the taxonomy of contexts and describes all the information necessary that the system should be able to provide for their evaluating [25].

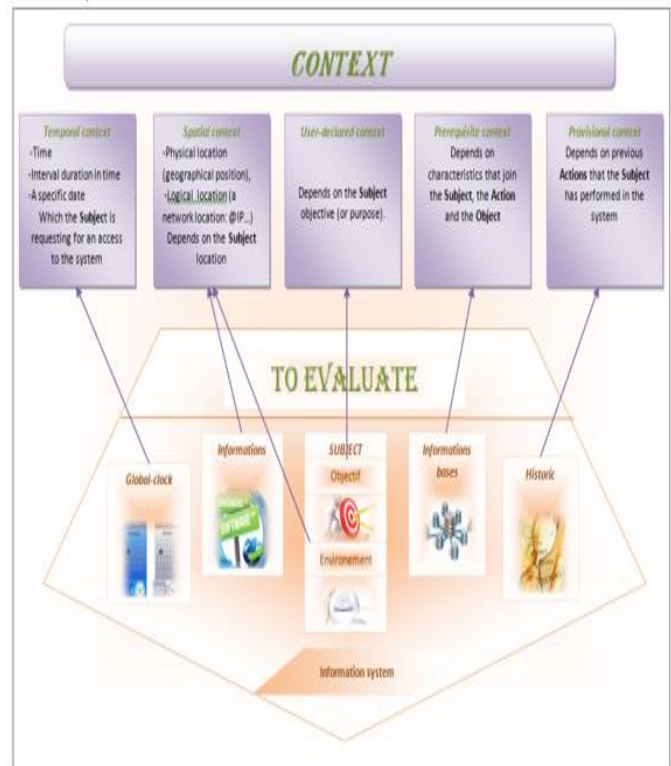


Fig. 4. Context taxonomy and required data

In this model we need to add a novel type of context (TRUST-CONTEXT), the role of this latest is to check if the trust levels of the user/agent respect the administrator levels or not .

As you can see n figure 4, our encoded model TRUST-ORBAC model for E-learning platform based on multi agent system, give birth of a new level witch named *trust level*, adding to abstract and concert levels.

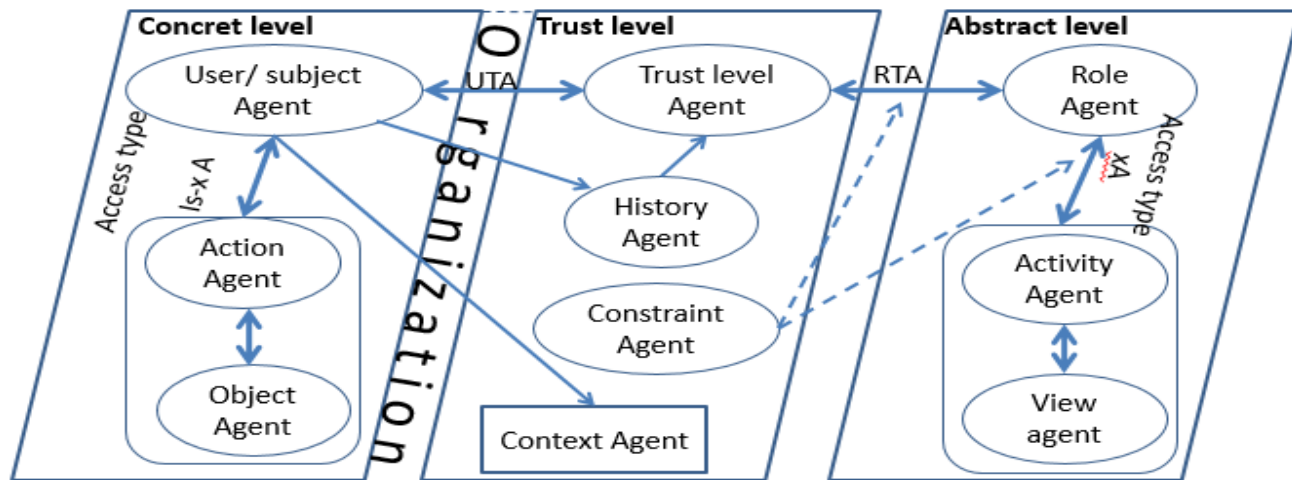


Fig. 5. New Trust-ORBAC model for e-learning platform based on multi-agent systems

VI. THE EVALUATION OF SECURITY POLICY OF THE PROPOSED MODEL

A. Presentation of the platform

For this purpose we assume that the E-learning platform is manipulated by different actors: tutors, learners, and teachers where each actor plays a specific role in the learning process.

- The teacher sets its pedagogical scenario through the learning platform, using some tools and resources offered by the platform.
- The tutor supports the students in their learning activity, in order to help them, and evaluate their progress.
- The student use the pedagogical scenario proposed by the teacher, in order to achieve some educational goals like understanding the course content.

So each actors in the platform has a specific security levels associated with a level of his trust for example we have here some levels which identify the nature of student: *privilege*, *basic*, *public*. This concept keep to the user/agent possibility to enter with *public* policy which is the lower limit applied to the platform.

B. Example of access authorization process

Here we present an example to explain how the present model works:

Let ‘*public student*’, ‘*basic student*’ and ‘*privilege student*’ be three roles in the ROLES set of the platform. We specify the following: Assigned Roles ([0.38, 0.7]) = *privilege student*, Assigned Roles ([0.06, 0.3]) = *public student* and Assigned Roles ([0.16, 0.5]) = *basic student*. In general as first step a student must log in to the system by its credentials. Then the

system verify and evaluate its trust value for example 0.45, therefore, according to Assigned Roles the user at this stage is allowed to act as a *privilege student* as well as a *basic* and *public student*. Let the privilege users of the platform be allowed to write comment about the courses presented in the database of the platform as well as the uploading copies of courses that are not presented in the database we consider that Abusive/irrelevant comments and upload of an inauthentic file as negatives events.

During the session, we consider that the student writes some bad comments and upload a several inauthentic documents. Each of these activities get reported in the session, Let T evaluates trust periodically within a session. At some evaluation point we have $v=0.345$. This means that the student is not ‘trustworthy’ to the platform as a *privilege student*. That is why the system automatically refuses the role of *privilege student* for the student. During the remaining time in this session, he can no longer acts as a *privilege student*. So if there is a section of articles in the database which is only available to *privilege student* then he cannot access those articles anymore. However, he can continue to act as a *basic/public student* who will keep it for its next login, except if the confidence level increases with the good actions and is reached to 0.35. It can again act as a *privilege student*.

C. Simulation with motorbac tool

Designers of the Or-BAC model have developed MotOrBAC [23][24] a security policy tool which can be used to specify, simulate, evaluate and administrate the security policies not only based OR-BAC model but also RBAC model, This is partly due to the fact that its GUI is independent of its API and RBAC has common entities of the OrBAC model.

Security policies expressed by MotOrBAC have a declaration section which provides useful information on

security policy like: the date of the last version of the policy, creation date, version, We can also use this declaration part to inform the access control model used to express in this tool, In fact, when the security policy is expressed from RBAC, certain parts of MotOrBAC will be disabled: views, activities, prohibitions, obligations[25].

In this simulation we considered that the trust value is an attribute of the subject, it's already calculated with an independent program.

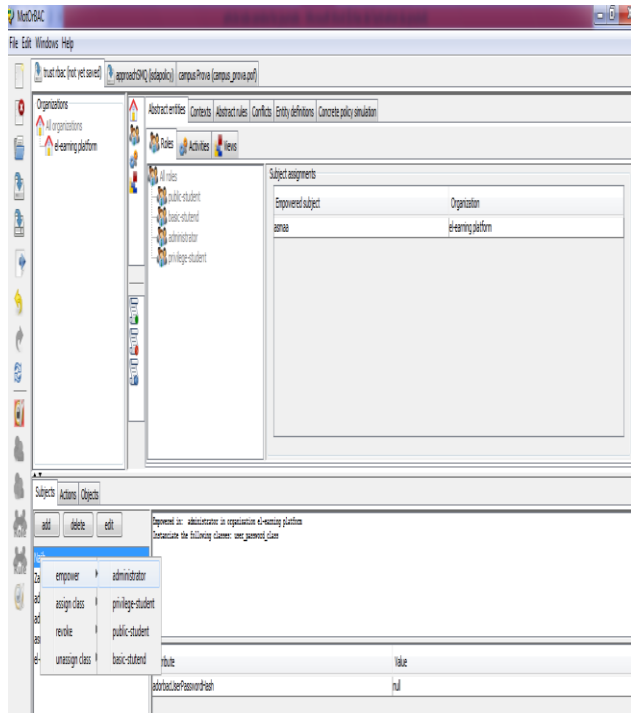


Fig. 6. role/subjects entities

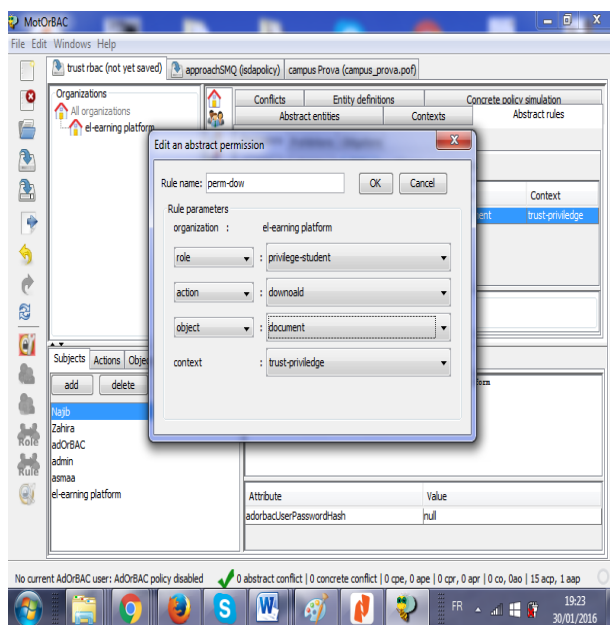


Fig. 7. The creation of the rules

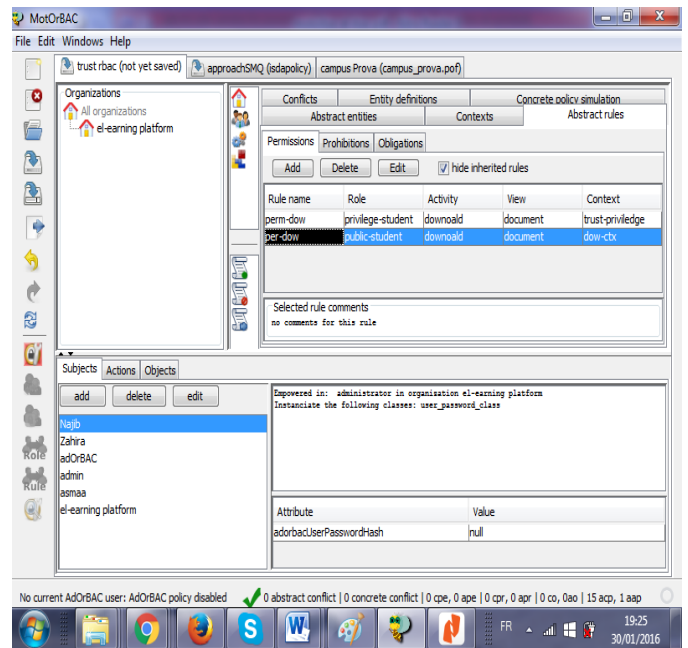


Fig. 8. Set of permission rules

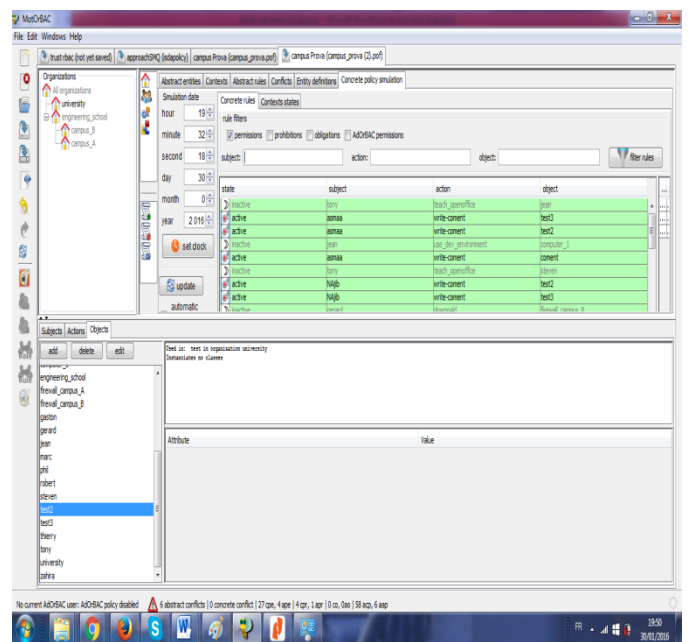


Fig. 9. Simulation of the policy

VII. CONCLUSION AND PERSPECTIVES

The main goal of this paper, is to provide a new model based on ORBAC model, adapted to e-learning platform based on multi agent systems in order to have a satisfactory level of its security, taking into consideration the different interactions of these actors/agents and the integration of context and trust level. It allows to set certain conditions for the application of safety rules. This improvement may reside on richness as modularity of ORBAC model

This new model is implemented and evaluated by "MotOrbac": a simulation tool, to define its validity context

and limitations for an extended deployment .how ever this approach still not enough and rich so as future work , we encode the proposed model on Orbac model, in order to make it more rich and modular, and to prove how the expressive power and flexibility of ORBAC model work.

This work can be extended to a new TRUST-ORBAC model that analyzes the risks before making a decision to accept or deny access while taking account of the context information to determine trust levels of the subjects, the level of trust required by each role and the environmental risk threshold: The evaluation of risk should be done dynamically and in real time.

REFERENCES

- [1] S. Ahmad, & M.U. Bokhari, "A New Approach to Multi Agent Based Architecture for Secure and Effective E-learning" International Journal of Computer Applications, 46. 2012
- [2] Bokhari, M.U., Ahmad, S. and Alam, S. 2011. Modern Tools and Technologies for Interactive Learning. In Proceedings of the Computing For Nation Development, Bharati Vidyapeeth's Institute of Computer Applications and Management, New Delhi
- [3] Asmaa,K, Najib E,' A Comparative approach of different Or-BAC extensions: Application and limits'.In Proceedings of the 5thWorkshop on Codes, Cryptography and Communication Systems (WCCCS), El Jadida ,Morocco, 2014,pp. 67 – 72.
- [4]] B. Lampson. "Protection", 5th Princeton Symposium on Information Sciences and Systems, pp. 437-443, Mars 1971.
- [5] D. Bell et L. LaPadula. "Secure computer systems:Unified exposition and multics interpretation", Technical Report ESD TR73-306, The MITRE Corporation, Mars 1976.
- [6] R. Sandhu, E. Coyne, H. Feinstein et C.E.Youman. "Role-based access control models". IEEE Computer, 29(2), pp. 38-47, 1996.
- [7] R. Thomas et R. Sandhu. "Task-based Authorization Controls (TBAC): A Family of Models for Active and Enterprise-oriented Authorization Management". 11th IFIP WorkingConference on Database Security, Lake Tahoe, California, USA, pp. 166-181, 1997.
- [8] R. Thomas. "TMAC: A primitive for Applying RBAC in collaborative environment". 2nd ACM, Workshop on RBAC, Fairfax, Virginia, USA, pp . 13-19, Novembre 1997.
- [9] A.Kassid,N.El kamoun "Towards a new access control model based on Trust-level for E-learning platform" international journal of information assurance and security.
- [10] S. Chakraborty, I. Ray, "TrustBAC: Integrating Trust Relationships into the RBAC Model for Access Control in Open Systems," In Proc. of the 11th ACM Symposium on Access Control Models and Technologies, Lake Tahoe, California, USA, 2006, pp. 49-58.
- [11] J. W.Woo, M. J. Hwang, C. G. Lee, and H. Y. Youn. Dynamic role-based access control with trust-satisfaction and reputation for multi-agent system. International Conference on Advanced Information Networking and Applications Workshops, 0:1121-1126, 2010.
- [12] Kambourakis G, Security and Privacy in m-Learning and Beyond: Challenges and stae-of-the-art. International Journal of u- and e-Service, Science and Technology, Vol. 6, No. 3, June 2013.
- [13] S. H. Hasan, D. M. Alghazzawi, and A. Zafar "E-Learning systems and their Security" BRIS Journal of Adv. S & T (ISSN. 0971-9563) vol.2, no 3, pp. 83-92, 2014
- [14] Rodolfo Carneiro Cavalcante , Ig Ibert Bittencourt , Alan Pedro da Silva , Marlos Silva , Evandro Costa , Robério Santos, A survey of security in multi-agent systems, Expert Systems with Applications: An International Journal, v.39 n.5, p.4835-4846, April, 2012 [doi>10.1016/j.eswa.2011.09.130]
- [15] T. Kuhlmann. "Why E-Learning is So Effective," 19 April, 2013].
- [16] M. Blaze, J. Feigenbaum, and J. Ioannidis. The KeyNote Trust Management System Version 2. Internet Society, Network Working Group. RFC 2704,1999.
- [17] M. Blaze, J. Feigenbaum, and J. Lacy. Decentralized Trust Management. In Proceedings of 17th IEEE Symposium on Security and Privacy, pages 164–173, Oakland, California, USA, May 1996.
- [18] N. Li and J. Mitchell. Datalog with Constraints: A Foundation for Trust-management Languages. In Proceedings of the 5th International Symposium on Practical Aspects of Declarative Languages, New Orleans, Louisiana, January 2003.
- [19] N. Li and J. Mitchell. RT: A Role-based Trust Management Framework. In Proceedings of the 3rd DARPA Information Survivability Conference and Exposition, Washington D.C., April 2003.
- [20] M. Abadi and C. Fournet. History-based Access Control for Mobile Code. In Proceedings of the 10th Annual Network and Distributed System Security Symposium, pages 107–121, San Diego, California, USA, February 2003.
- [21] G. Edjlali, A. Acharya, and V. Chaudhary. History-based Access Control for Mobile Code. In Proceedings of the 5th ACM Conference on Computer and Communication Security (CCS'98), pages 38–48, San Francisco, California, USA, November 1998
- [22] F. Feng, C. Lin, D. Peng et J. Li, «A Trust and Context Based Access Control Model for Distributed Systems,» Proc. of the 2008 10th IEEE International Conference on High Performance Computing and Communications, pp. 629-634, 2008
- [23] I. Ray and S. Chakraborty. A Vector Model of Trust for Developing Trustworthy Systems. In Proceedings of the 9th European Symposium of Research in Computer Security (ESORICS 2004), volume 3193 of Lecture Notes in Computer Science, pages 260–275, Sophia Antipolis, France, September 2004
- [24] Autrel, F., Cuppens, F., Cuppens-Boulahia, N., Coma, C.: MotOrBAC 2: a security policytool. In: 3rd Conference on Security in Network Architectures and Information Systems (SAR-SSI 2008), Loctudy, France, pp. 273–288 (2008).
- [25] A.kassid, N.El kamoun "Evaluation of a Security Policy Based on OrBAC Model Using MotOrBAC: Application E-learning' on Advances in Ubiquitous Networking: Proceedings of the UNet'15,PP.129-139.

Simulation of Building Evacuation: Performance Analysis and Simplified Model

Yasser M. Alginahi

Dept. of Computer Science
Deanship of Academic Services
Taibah University, P.O. Box 344
Madinah, Saudi Arabia

Muhammad N. Kabir

Faculty of Computer Systems and Software Engineering,
University Malaysia Pahang,
26300 Gambang,
Pahang, Malaysia

Abstract—Crowd evacuation from industrial buildings, factories, theatres, protest areas, festivals, exhibitions and religious/sports gatherings is very crucial in many dangerous scenarios, such as fire, earthquakes, threat and attacks. Simulation of crowd evacuation is an integral part of planning for emergency situations and training staff for crowd management. In this paper, simulation of crowd evacuation for a large building-hall is studied using a popular crowd-simulation software BuildingEXODUS. Evacuation of the fully occupied hall is simulated with eleven test cases using the different experimental setups in the software. The results of the different evacuation scenarios are analysed to check the effect of various parameters involved in the evacuation performance. Finally, using the evacuation test results, simplified models are developed. It is found that the model outputs are in good agreement with the simulation results. Therefore, the models can readily be used for fast computation of the evacuation results without running the actual simulation.

Keywords—Crowd Evacuation; BuildingEXODUS; Modelling & Simulation; Least squares method

I. INTRODUCTION

The issue of crowd behaviour and movement has been a concern for researchers over the last few decades. Crowd evacuation from confined areas e.g., industry building, theatres, protest areas, festivals, exhibitions and religious/sports gatherings is utmost important in many dangerous events, such as fire, earthquakes, threat and attacks. Increasing the crowd density during the evacuation can lead to hazardous scenarios including crushing, being struck, violent acts, stampedes, etc. Simulation of crowd evacuation is integral part for planning to avoid such hazardous situations and to make efficient crowd management during the normal situation. Evacuation simulation is essential for designing (the number, widths and locations of) the exits of the confined area for safe evacuation of the occupants. Three approaches are used to simulate crowd, which are fluids, cellular automata and particles.

Most of the work in the area of crowd simulation uses the particle approach [1]. Many studies have been performed on crowd simulation with different structures and situations. A recent survey done by Wang and Sun [2] addresses the current research of large-scale crowd evacuation with four principal aspects: evacuation theories, evacuation modelling, evacuation decision-making and evacuation risk evaluation. The authors

concluded that more research is required to be done on large-scale evacuation since existing evacuation models have not fully considered the uncertain factors in the evacuation process. Thalmann et al [3] modelled virtual humans according to perception, emotion and behavior; Helbing et al. [4] produced a social force model for simulation of building escape panic; Braun et al. [5] modified the work of Helbing et al. by incorporating the concept of a group of pedestrians to the social force model. Bouvier et al. [6] simulated pedestrians and airbags deployment; and the work of Musse et al. [7] was based on decision-making and movement.

The work of Kiyona et al. [8] used the numerical analysis method, Distinct Element Method (DEM), to simulate emergency evacuation behaviour from a confined underground shopping center passageways during an earthquake. Chunmiao et al. [9] presented a study of evacuation process in buildings using BuildingExodus. They investigated the effect of number of exits and population and concluded that there was a linear relationship between the number of population and the evacuation time. Kiyono and Mori [10] considered an elliptic shape for human body to simulate emergency evacuation from a confined area. They used Distinct Element Method (DEM) with modified strength of the spring for high-density crowd to model the evacuation process and validated the model by comparing the simulation results with a real pedestrian flow.

Alighadr et al. [11] presented a case study on emergency evacuation of a populated marketplace called Timche Muzaffariyye using distinct element method DEM. They used two different numbers of exits for evacuation simulation in order to evaluate the performance. In addition, some research on guided evacuation techniques include: Onorati et al. [12] discussed modelling of accessible evacuation routes for different types of people, Yang et al. 2014 developed a modified social force model for pedestrian dynamics to better reflect pedestrians' behavioural characteristics. Abdelghany et al. [14] described an optimization model based on genetic algorithm for the evacuation of large-scale pedestrian facilities with multiple exit gates. Haron et al. [15] presents a study on fifty-five crowd simulation software and recommends the suitable crowd simulation software for studying crowd at large complexes. Alginahi et al. [1] presents a crowd simulation for the multi-storey washroom facilities using Discrete Event Simulation. Nassar and Bayyoumi, [16], which presents a discrete-event simulation model to assess the effect of mosque

This work is sponsored by the deanship of Scientific Research at Taibah University, Saudi Arabia.

prayer hall configuration with different exit locations on the egress times of the occupants in the prayer hall.

From the above research works available in literature, it is very clear that crowd simulation research is an interesting area of research and much work is needed to address all different aspects and related parameters of crowd behaviour, building structures, characteristics of crowds, social behaviours etc.

In this work we simulate the crowd evacuation of a large building-hall considering different parameters involved in crowd simulation. The hall has eight doors each of which is approximately three meters in width. Figure 1 shows the layout of the hall used in this study. Three doors are located in the left side and five, in the right side of the figure. The dimension of the hall is approximately 87m × 58m, while each door is three meters wide. The purpose of simulating this building is to evaluate the evacuation performances with different test cases. Eleven tests cases generated by different experimental setups are simulated. Test results are analysed to scrutinize the influence of various parameters on the evacuation scenarios. Test results are analyzed to scrutinize the influence of various parameters on the evacuation performance. Furthermore, with the evacuation test results, simplified models are developed which are in excellent agreement with the test results. Therefore, instead of running the expensive simulation, one can readily use the simplified models for fast computation of the evacuation results.

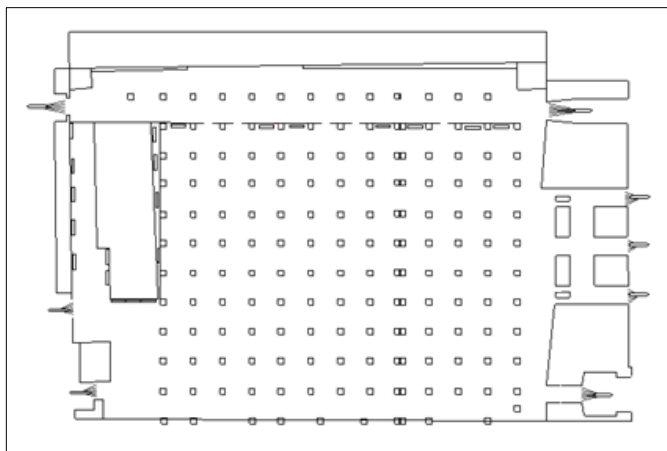


Fig. 1. Approximate layout for the Worshipping Hall (Area of study)

The rest of the paper is organized as follows. Following this introduction, section 2 provides the methodology and experimental setup. Section 3 presents the simulation results and analysis. The simplified evacuation model is formulated in section 4 and section 5 concludes this paper.

II. METHODOLOGY AND EXPERIMENTAL SETUP

The authors in this study decided to use BuildingEXODUS [17] in order to carry normal and emergency simulations for the large building-hall. The main reason for using

BuildingEXODUS is its popularity and affordable price. According to the crowd evacuation software evaluation by Haron et al., [15], BuildingEXODUS is considered one of the most popular crowd evacuation software developed at the University of Greenwich. BuildingEXODUS is a suite of software tools designed to simulate the evacuation and movement of people within complex structures. BuildingEXODUS is one of the evacuation models contained in this software package. BuildingEXODUS can be used to demonstrate compliance with building codes, evaluate the evacuation capabilities of all types of structures and investigate population movement efficiencies within structures. The system is able to simulate the evacuation of large number of people from different types of buildings such as multi-floor buildings. BuildingEXODUS adopts fluid dynamic models coupled with discrete virtual reality simulation techniques.

Eleven experiments (test cases) were conducted to evaluate the evacuation performances. The test cases with their description are provided in Table 1. The number of occupants in the hall is 4100 which is the estimated maximum capacity before the evacuation begins. Now the experimental setup of parameters, initial values and other considerations for simulation using BuildingEXODUS manual are discussed for each test case.

TABLE I. DESCRIPTION OF THE DIFFERENT EXPERIMENTAL SCENARIOS

Case	Description
1	Using default settings of BuildingEXODUS
2	With altered potential map
3	With full local familiarity
4	With 50% attractiveness for all doors
5	With 5% of the population in wheelchairs and using travel speeds as specified in the Exodus manual
6	With response time (0-1 seconds) and potential map in test case 2
7	With response time (0-5 seconds) and potential map in test case 2
8	With response time (0-10 seconds) and potential map in test case 2
9	With extreme behavior enabled and potential map test case 2
10	Avoid congestion and potential map in test case 2
11	Combination of test cases 2, 5, 6, 9 and 10

In test case 1, default values as specified in the user manual are considered for objects i.e., doors, nodes, arcs and occupants with exception of ages of individuals. Occupants follow the potential map of the geometry given in Figure 2. Potential is a measure of a node distance from the nearest door. The occupants move from the nodes of higher potential to the nodes of lower potential which brings them closer to the nearest door. Occupants do not make decisions that take them to nodes of higher potential, but prefer to wait until an alternative of lower potential is offered. For this test case, the behaviour of the population is normal indicating that they conform to the potential map at all times and do not redirect unless they fall under the potential influence of a nearby exit [17].

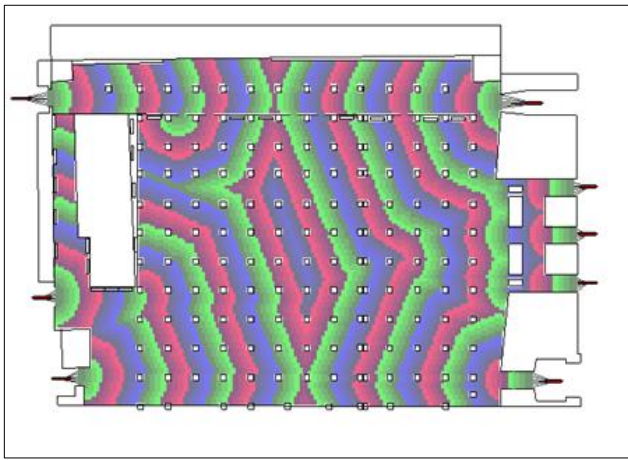


Fig. 2. Default potential map

In test case 2, internal exits are inserted with potential values as specified in Table 2. The corresponding potential map is displayed in Figure 3. In test case 3, the occupants do not follow the potential map. All the occupants are assumed to be familiar with all exits. Occupants behaviour is normal indicating that the occupant knowledge of exits is prioritized according to the initial distance of the exits from the occupant and usages of the doors.

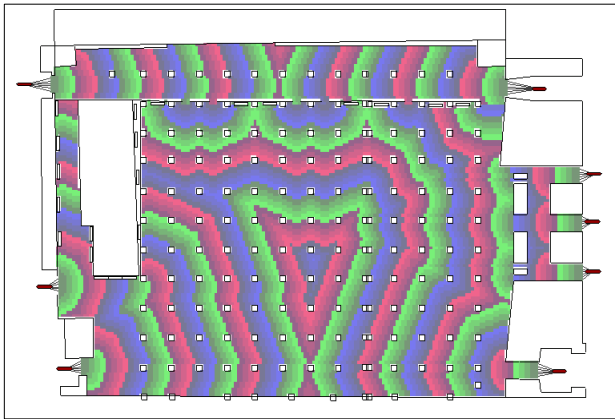


Fig. 3. Potential map for Test Case 2

TABLE II. INTERNAL EXITS WITH POTENTIAL VALUES

Door No.	Potential	Door No.	Potential
D1	100.000	InDoor_1	100.000
D2	100.000	InDoor_2	100.000
D3	100.000	InDoor_3	100.000
D4	100.000	InDoor_4	100.000
D5	100.000	InDoor_5	100.000
D6	100.000	InDoor_6	100.000
D7	100.000		
D8	100.000		

Test case 4 is similar to the previous test case 3 with the exception that the occupants knowledge of a certain doors is automatically determined by a probability value supplied as the attractiveness of the door. We consider that for each door, 50% of the population are familiar with it (by probability). Occupants exit from one of the doors which they are familiar with. As in the previous case, the occupants exit list is ordered

according to initial distance and the usage of the door. In test case 5, with wheelchairs and travel speeds according to the evacuation model data presented in Table 3.

TABLE III. TRAVEL SPEEDS FOR TEST CASE 5

Panel	Age	Percentage	Speed (min-max)
1	3-16	10	0.78- 1.578
2	17-29	25	1.586-1.49
3	30-55	37.5	1.48- 1.255
4	56-80	22.5	1.246-1.03
5 (Wheel chair)	30-80	5	0.69

Test cases 6-11 use the altered potential map of test case 2 given in Figure 3. Test cases 6-8 use different response time as shown in Table 1. In test case 6, response time ranges between zero and one second for the entire population. In test case 7, response time is increased to be between zero and five seconds. Test case 8 has the maximum response time range i.e., between zero and ten seconds for the entire population.

Test case 9 uses extreme behaviour where the occupant movement only relies on the distance from the exits. In this case, the population moves according to the altered potential map. However, they are given the additional option of moving to locations of higher potential when their wait time exceeds their patience limit which ranges from 0-5 minutes. In test case 10, a sign was associated with each door enabling the occupants to observe the area around the door and assess the congestion around it. The occupants can then make the decision to avoid the congestion by redirecting to another door. The visibility catchment area of signs given in Figure 4 is the area which it is visible by the occupants. Only occupants within this area are able to view the sign and the congestion around it. Test case 11 is produced with the combination of test cases 2, 5, 6, 9 and 10.

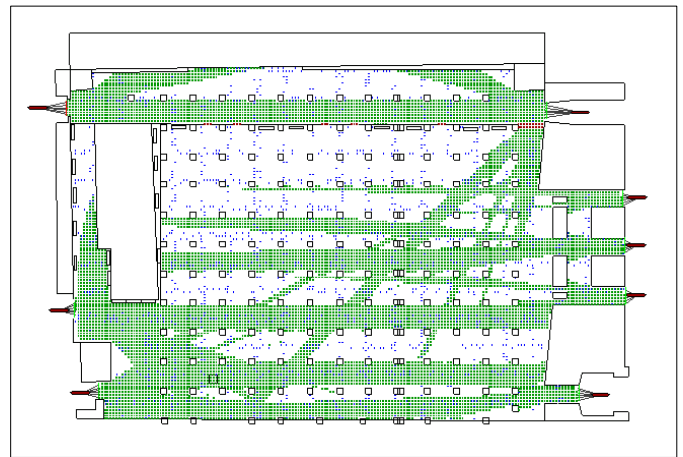


Fig. 4. Visibility catchment area of the signs

III. RESULTS AND ANALYSIS

The results of the test cases described in the previous section are explained and analysed. The complete graphical results from test case 1 are provided to demonstrate the capability of the software. The complete results of other test cases are provide in Tables 4 – 5 for all test cases. However, results of all the test cases which are required for the comparison and analysis are presented. Figures 5-7 and

Tables 4-5 present the results of test case 1. Figures 5a-5b plots the flow rate of the people through D1 to D8 doors while Figure 5c displays the total flow rate from all the doors. It can be observed that the flow rate is initially zero and increases to some value (average maximum flow rate) and continues to fluctuate around the value before sharply reducing to zero. Note that the average maximum flow rate is about 16 for all 8 doors. The maximum flow rate in Figure 5c with all doors is about 128 ($16 \times 8 = 128$). The evacuation time is the longest with door D8 that equalled 338 seconds; Table 5 verifies this.

Table 5 provides the total and average evacuation time for all the doors, average response time and average cumulative

wait time, average distance and optimal performance statistics (OPS). Note that OPS is measured from 0.0 to 1.0, where the lower values indicate more efficient evacuation [17]. Table 4 shows the door usage i.e., how many evacuees exit through each door. Figure 6 shows the total number of evacuee over time for the doors corresponding to the doors in Figure 5. Note that the general trends of the total number of evacuee are almost linear with time i.e., increase gradually and then they become constant after the evacuation is over. Figure 7 shows the areas of congestion for test case 1 where the duration of congestion exceeds 10% of the evacuation time.

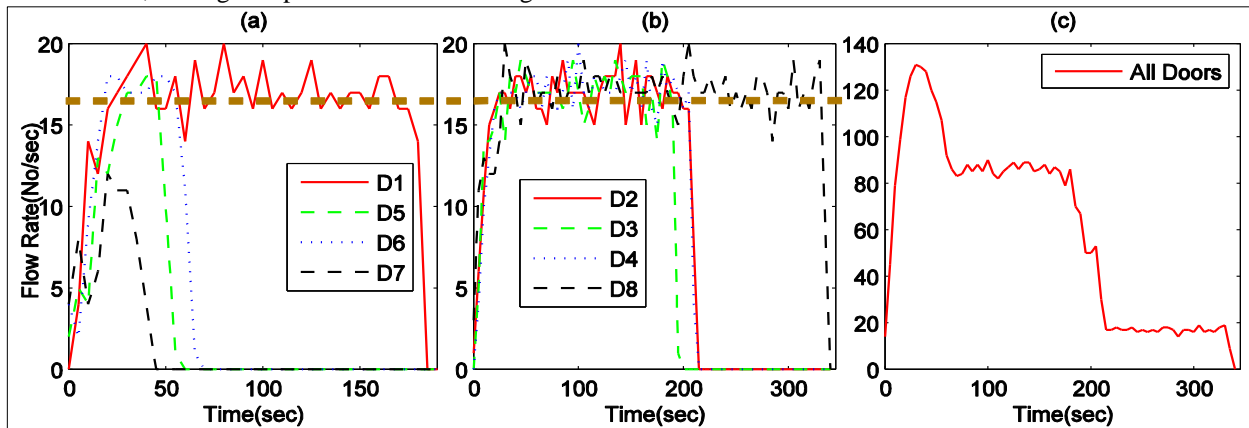


Fig. 5. Evacuation flow rate over time with different doors in test case 1

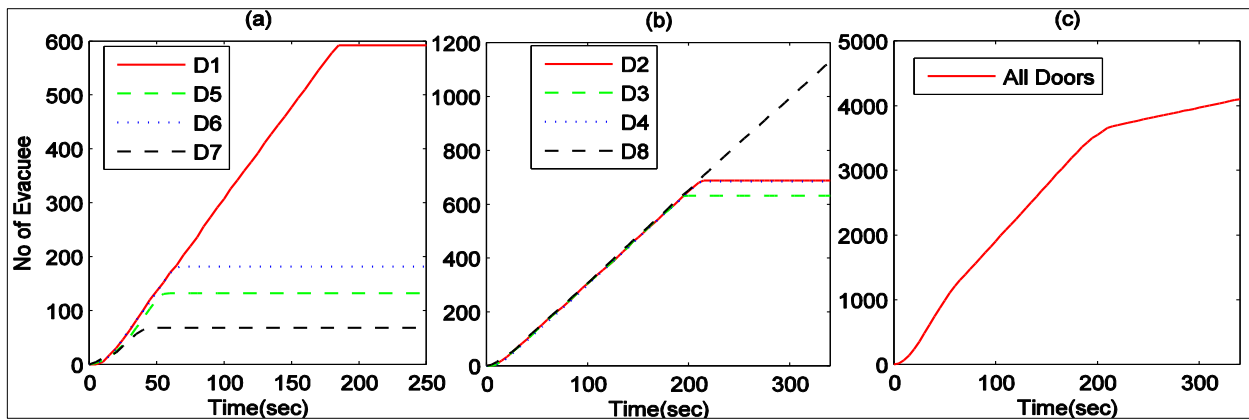


Fig. 6. Total number of evacuees over time with different doors in test case 1

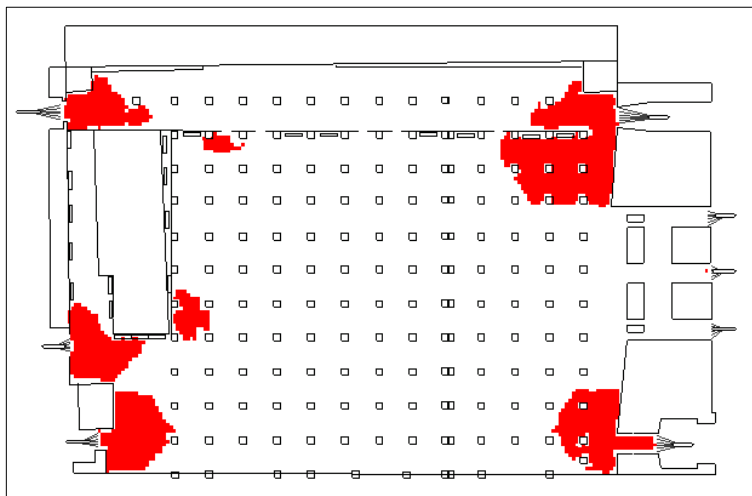


Fig. 7. Areas of congestion for test case 1

TABLE IV. DOOR USAGE FOR ALL TEST CASES

Door No	Test Cases										
	1	2	3	4	5	6	7	8	9	10	11
D1	1124	1004	1091	739	1001	983	1053	1051	1003	892	750
D2	132	151	155	362	136	125	135	139	152	247	360
D3	181	240	165	368	256	251	233	251	238	224	370
D4	68	157	73	348	141	150	144	136	160	293	361
D5	684	713	690	517	753	796	726	731	712	625	522
D6	631	638	602	605	616	599	561	611	601	727	599
D7	688	604	733	694	582	638	665	640	641	557	659
D8	592	593	591	467	615	558	583	541	593	535	479

TABLE V. SUMMARY OF EVACUATION ESTIMATES FOR ALL TEST CASES WITH THE INITIAL POPULATION OF 4100 INSIDE THE BUILDING

Test Cases	Total Elapsed Time		OPS	Average Total Elapsed Time (Sec)	Average Response Time (Sec)	Average Cumulative Wait Time (Sec)	Average Distance
	Sec	Min					
1	338.25	5.6375	0.591	117.92	14.90	77.87	31.68
2	300.07	5.00117	0.525	107.83	15.16	65.95	33.35
3	329.47	5.49117	0.575	116.40	15.16	75.76	31.67
4	232.32	3.872	0.230	98.51	15.16	49.70	41.03
5	301.09	5.018	0.513	110.30	14.99	66.61	33.64
6	305.49	5.0915	0.491	116.15	29.66	60.19	32.73
7	352.74	5.879	0.078	177.59	149.07	5.02	29.09
8	642.29	10.7048	0.032	323.16	297.95	2.06	28.58
9	304.92	5.082	0.534	107.90	15.16	61.27	39.65
10	273.75	4.562	0.362	101.42	14.99	57.15	35.99
11	390.62	6.51	0.065	187.39	152.34	2.47	38.50

Figure 8 shows the total and average elapsed (evacuation) time for all doors, average response time, average cumulative wait time and the average distance for the different test cases. Figure 9 shows a bar graph depicting the optimal performance statistics (OPS) for the test cases. We observe that the average evacuation time follows the trend of total evacuation time. The evacuation time is the minimum with test case 4 and highest

with test case 8. Average wait time mostly makes the opposite behaviour of evacuation time. OPS follows the similar behaviour of average wait time. It reveals that if the response time increases, the evacuation time and response time increase, but the wait time and the OPS decrease. Test cases 4 and 10 have the smallest evacuation time since case 4 uses 50% attractiveness for all doors and test case 10 uses sign to

signal the occupants of the congestion. However, wait time for test case 10 is higher than that of test case 4. Test case 5 where some 5% occupants use wheelchairs does not make much difference with the default setting or altered potential map in test case 2. The same behaviour is also observed with test case 9 which represents the extreme behaviour. Variation of average distance is very small for different cases.

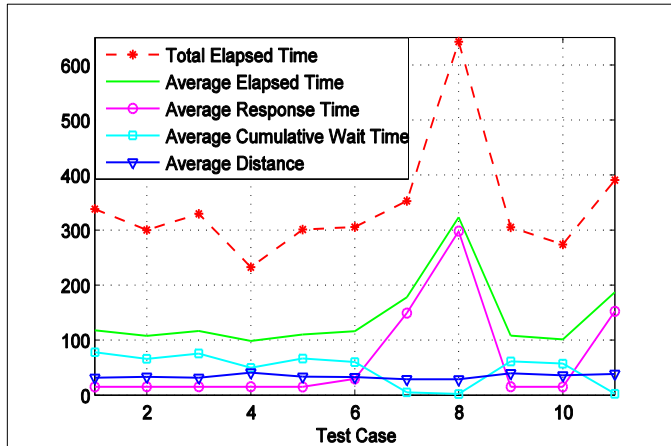


Fig. 8. Evacuation estimates with different test cases

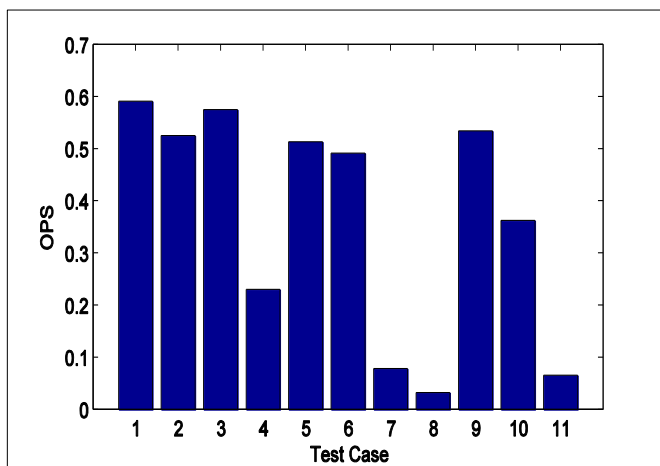


Fig. 9. Optimal Performance Statistics for all test cases

IV. SIMPLIFIED EVACUATION MODEL

The evacuation results through all the doors presents well-behaved trajectories without any fluctuation. Therefore, the trajectories can be fitted with some functions so that the result can be readily obtained from the functions without running the simulation repeatedly. Besides the computational time is much cheaper for the evacuation if we can build such functions.

First, we try to find the different evacuation patterns. In Figure 10, the number of evacuees through all the doors is plotted over time for different test cases. It is observed that in the figure, the plots with almost identical behaviours are grouped. It is apparent in Figure 10 (a) that the evacuation behaviours with the test cases 1, 2, 3, 5, 6 are similar. This similarity can also be observed for test cases 4 and 9; and 7 and 11 as shown in Figures 10 (b) and 10 (c) respectively. Notice that the evacuation with the test case 8 is different from the others. The average number of evacuees over time for the test cases with similar evacuation behaviour is referred to as the evacuation pattern. These evacuation patterns are plotted in Figure 11. The goal here is fit the evacuation pattern by a model function.

The Matlab cftool is used to find the most appropriate functions to fit the evacuation patterns. Figure 11 plots the number of evacuee over time and their fitting functions for different evacuation patterns. Each plot can be identified by different line properties presented in the legends. Different types of functions were tried to fit these data. Finally, the function produces the best fit was chosen and was used for the plots in Figure 11.

The function is presented as follows

$$f(t) = p_0 + p_1t + p_2t^2 + p_3t^3 + \dots + p_6t^6 \quad (1)$$

Equation (1) which is a function of order 6. This function is used for fitting the simulation data of number of people over time t . The fitting is performed using least squares method which generates the values of p_0, p_1, \dots, p_6 . Once these values are determined, the plot of number of people over time can be accomplished. The values of p_0, p_1, \dots, p_6 obtained from the least squares method are listed in Table 6 below. Table 6 provides the values and root mean square error (RMSE) values of $f(t)$ for different evacuation patterns. The values of p_0, p_1, \dots, p_6 are different for different patterns due to their different evacuation data. For a specific pattern, the values will be constant. Thus using these constants, the function $f(t)$ can be used for evaluating associated output for any value of time t . The last row in Table 6 provides RMSE with which errors with the data fitting can be readily checked i.e., how closely the function fits with the data. Since the simulation uses assumptions and approximations, the functions can never fit perfectly with the simulation results. As mentioned earlier, that we tried a number of functions to fit with the data and the best and most reasonable function given in equation (1) was considered for fitting the data. Figure 11 demonstrates how closely the function fits the data. We observe that the function and the data are in a good agreement. Hence, it can be concluded that the functions can be used to evaluate the associated values.

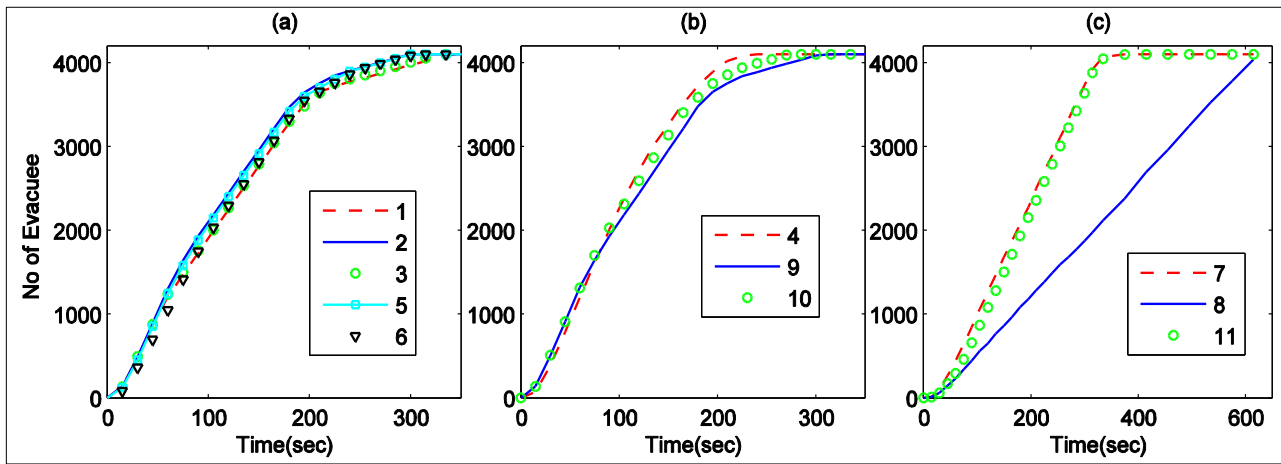


Fig. 10. Evacuation with time for different test cases

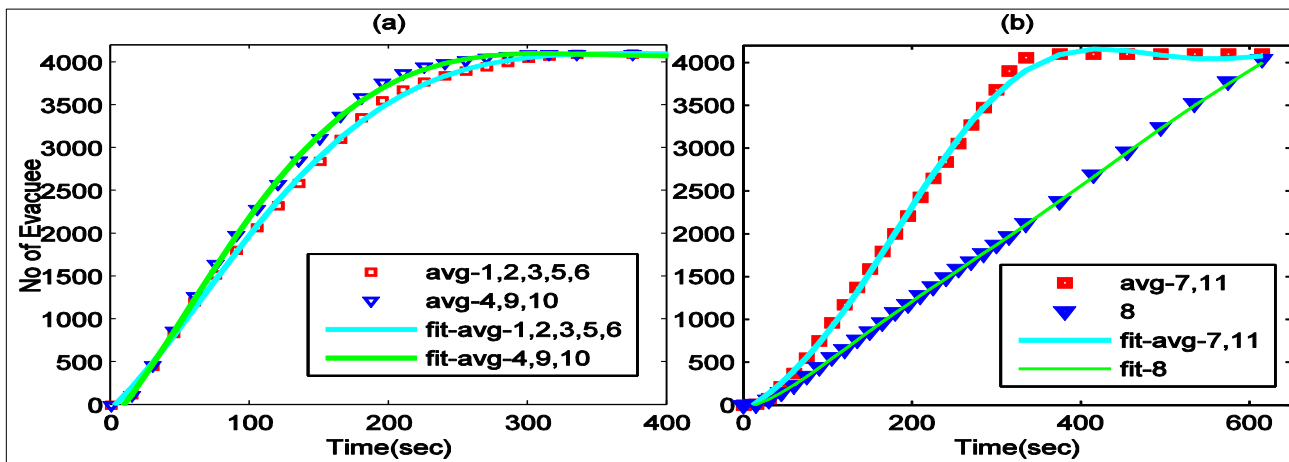


Fig. 11. Evacuation model and average evacuation of nearest test cases

TABLE VI. VALUES OF p_0, p_1, \dots, p_6 FOR DIFFERENT SCENARIOS

Properties	Avg. of Test Cases 1,2,3,5,6	Avg. of Test Cases 4,9,10	Avg. of Test Cases 7,11	Test Case 8
p_0	-46.7	-53.15	-73.43	-37.85
p_1	15.05	13.7	7.034	2.053
p_2	0.1252	0.2055	-0.003988	0.05817
p_3	-0.0009205	-0.001558	0.000415	-0.0003113
p_4	2.303e-006	4.288e-006	-1.878e-006	8.105e-007
p_5	-2.583e-009	-5.333e-009	2.919e-009	-1.007e-009
p_6	1.099e-012	2.515e-012	-1.539e-012	4.774e-013
RMSE for $f(t)$	44.09	36.5	64.26	8.638

V. CONCLUSION

In this work, crowd evacuation for a building-hall is investigated using a popular crowd-simulation software BuildingEXODUS. Eleven evacuation test cases generated using the different experimental setups in the software are simulated. The simulation results are scrutinized to check the effect of various parameters involved in the evacuation performance. It is noted that with higher response time, the response time increases, the evacuation time and response time increase, but the wait time decreases. Evacuation time is small with 50% attractiveness for all doors (case 4) and with using sign to signal the occupants of the congestion (case 10). It was found that test case 10 has higher wait time than test

case 4. Test case 5 where 5% occupants use wheelchairs does not differ much on the evacuation characteristics with the normal evacuation (case 1, 2). Test case 9 with the extreme behaviour representing emergency evacuation follows the same trend of case 5. This behaviour of case 5 and 9 is due to the almost constant egress of the people from the confined area through fixed width doors.

Furthermore, simplified evacuation models are developed which are in excellent agreement with the evacuation test results. These models are computationally inexpensive and thus they can immediately compute the evacuation results.

ACKNOWLEDGEMENT

The authors would like to thank the Deanship of Scientific Research at Taibah University for their support to conduct this research work.

REFERENCES

- [1] Alginahi, Yasser M., Muhammad N. Kabir, and Ali I. Mohamed. (2013) "Optimization of High-Crowd-Density Facilities Based on Discrete Event Simulation." *Malaysian Journal of Computer Science* 26: 4.
- [2] Wang, J. H., & Sun, J. H. (2014), "Principal Aspects Regarding to the Emergency Evacuation of Large-scale Crowds: A Brief Review of Literatures Until 2010." *Procedia Engineering*, 71, 1-6.
- [3] Thalmann, D., Musse, S., Kallmann, M., (1999) "Virtual Humans' Behaviour: Individuals, Groups and Crowds," *Proc. International Conference on Digital Media Futures, British Computer Society, Bradford, UK*, pp. 13 –15.
- [4] Helbing D. et al., (2000) "Simulating Dynamical Features of Escape Panic." *Nature*, 407, pp. :487-490.
- [5] Braun, A. Musse, S., de Oliveira, L., Bodmann, B., (2003) "Modelling Individual Behaviours in Crowd simulation." *Proc. of Computer Animation and Social Agents*, pp. 143-148.
- [6] Bouvier, E., (1997) "From Crowd Simulation to Airbag Deployment: Particle Systems, a New Paradigm of Simulation." *J. Electronic Imaging*. Vol. 6, No. 1, pp. 94-107.
- [7] Musse, S. et al., (1998) "Crowd Modelling in Collaborative Virtual environments." *Proc. ACM Symposium on Virtual Reality Software and Technology*. pp. 115-123.
- [8] Kiyono, Junji, Kenzo Toki, and Fusanori Miura. (2000) "Simulation of evacuation behavior from an underground passageway during an earthquake." *In 12th world conference on earthquake engineering*. Paper, no. 1800.
- [9] Chunmiao, Y., Chang, L., Gang, L., & Peihong, Z. (2012). "Safety evacuation in building engineering design by using BuildingExodus." *Systems Engineering Procedia*, 5, 87-92.
- [10] Kiyono, J., & Mori, N. (2004), "Simulation of emergency evacuation behavior during a disaster by Use of elliptic distinct elements." *13th world conference on earthquake engineering*, No. 134, pp. 1-6.
- [11] Alighadr, S., Fallahi, A., Kiyono, J., Fitrasha, N. R., & Miyajima, M. (2012) "Emergency Evacuation during a Disaster, Study Case: "Timche Muzaffariyye-Tabriz Bazaar" Iran." *Conference proceeding of 15 WCEE*, Lisbon.
- [12] Onorati, T., Malizia, A., Diaz, P., & Aedo, I. (2014). "Modeling an ontology on accessible evacuation routes for emergencies." *Expert Systems with Applications*, 41(16), 7124-7134.
- [13] Yang, X., Dong, H., Wang, Q., Chen, Y., & Hu, X. (2014), "Guided crowd dynamics via modified social force model." *Physica A: Statistical Mechanics and its Applications*, 411, pp. 63-73.
- [14] Abdelghany, A., Abdelghany, K., Mahmassani, H., & Alhalabi, W. (2014), "Modeling framework for optimal evacuation of large-scale crowded pedestrian facilities." *European Journal of Operational Research*, 237(3), pp. 1105-1118.
- [15] Haron, Fazilah, Yasser M. Alginahi, Muhammad N. Kabir, and Ali I. Mohamed. (2012) "Software Evaluation for Crowd Evacuation Software Evaluation for Crowd Evacuation-Case Study," *International Journal on Computer Science Issues*. Vol. 9, Issue 6, No. 2.
- [16] Nassar, K., & Bayyoumi, A. (2012), A simulation study of the effect of mosque design on egress times, *Proceedings of the Winter Simulation Conference*, Berlin, p. 110.
- [17] Galea, E. R., Gwynne, S., Lawrence, P. J., Filippidis, L. and Blackshields D., (2011) "buildingEXODUS V5.0 User Guide and Technical Manual," *Fire Safety Engineering Group*, University of Greenwich, UK.

Towards Enhancing Supportive E-Learning Courses using Smart Tags

Hayel Khafajeh
Computer Information Systems
Zarqa University
Zarqa, Jordan

Heider Wahsheh
Computer Science Department
King Khaled University
Abha, Saudi Arabia

Ahmad Albhaishi
Computer Science Department
King Khaled University
Abha, Saudi Arabia

Mofareh Alqahtani
Computer Science Department
King Khaled University
Abha, Saudi Arabia

Abstract—E-learning management systems have emerged as a method of education development in many universities in the Arab world. E-learning management system tools provide a basic environment for interaction between faculty members and students, and these tools require information technology to obtain the most benefit. This paper proposes a method for enhancing the delivery of supportive e-learning courses using smart tags, such as NFC technique. The study sample comprises students at a supportive E-learning course in King Khaled University. This study aims to propose a technique to enhance the delivery of E-learning courses using these tags, which enable teachers and students to interact with the educational material and track their academic performance. The conducted experiments used receiver operating characteristic (ROC) prediction quality measurements to evaluate the proposed technique.

Keywords—*Learning Management System (LMS); Supportive courses; Blended courses; Online Courses; Quality Matters*

I. INTRODUCTION

Educational technology is a necessity to ensure the success of educational systems. Hence, educators always take advantage of new technologies that could enhance teaching and learning processes that increase performance efficiency.

The number of creative people in a community is not attributable to distinguished mental capabilities or educational systems. Traditional education systems do not evolve creative minds, but the creative student in the framework of the traditional education system is considered creative when he/she overcomes the limitations and determinants of the traditional education system. Modern education systems drive the evolution of the brain and motivate authors by establishing the principle that the primary goal of education is to raise the ability of students to think, innovate, and search for information until they acquire knowledge [1].

Universities in the Kingdom of Saudi Arabia have experienced outstanding achievements in the use of E-learning by adopting the “Blackboard” E-learning management system. E-learning is one of the modes of education that use the

Internet and other technologies to provide scientific technology courses to students and provide communication and interaction between them as well as the faculty and the learning resources.

Usually, E-learning systems offer three main levels using blackboard system, which are as follows:

- Supportive E-learning (traditional): At this level, the educational process applies in a classroom, and the E-learning systems and tools facilitate and support the learning process [1].
- Blended or hybrid E-learning: This method replaces the face-to-face classroom sessions with electronic activities on the site and use tools of the E-learning system [1].
- Online (Full) E-learning: This method replaces all the courses and face-to-face classroom sessions with electronic activities on the course site by using the tools of an E-learning system, with the exception of the final exam and limited face-to-face sessions decided by the faculty members [1].

The NFC tag is a wireless smart technology used to transfer data, such as text or numbers between two NFC enabled devices. One of them is an NFC tag, such as a sticker. The tag contains small microchips and an antenna, which store a small amount of information, such as URL. The second is the NFC device, such as a smartphone [2].

In this paper, the authors propose a method to enhance supportive E-learning courses at the King Khalid University through the use of NFC smart tags. The proposed method has been applied on a sample of 1000 students in the Introduction to Computer course (Hal 101). The practical part of the course uses E-learning. The next section discusses related studies to this paper. The third section presents detailed information on the adopted dataset. The fourth section explains the structure of the proposed methodology, and fifth section presents the experiments and results. Finally, the sixth section presents the conclusions.

This research is funded by the Deanship of Research and Graduate Studies in Zarqa University /Jordan

II. RELATED WORK

Saparkhojayev and Guvercin [3] proposed the use of the radio-frequency identification (RFID) system based on RFID Tags to identify automatically the presence or absence of students in Suleyman Demirel University, Kazakhstan. All classes are provided with personal computers (PC) connected to a web camera and RFID reader. These PCs and their peripherals are connected to the main server. The system uses a database. The instructor has to input his/her ID and password to the system to start verifying whether the students who had attended the lecture are the enrolled students in the course. This manual verification is considered one of the main flaws in their system [3]. Nainan, Parekh, and Shah [4] presented the components of RFID systems, emphasized scalability and security of the systems, and tested the feasibility and practicality. Soliman and Guizan [5] investigated the enhancement of E-learning system usage of learner profiles through mobile learning. They argued that proper understanding of the learner is crucial and achieved through the availability of learner profiles for mobile learning environments. Therefore, they applied RFID with smart tags to identify and extract the data/profile of learners. Their study concluded that learner profiles are personalization-enablers for e-learning systems and identification cards for learners to explore different learning environments. The system also provides the context and location-awareness services to learners [5].

Hamid [6] presents two major problems facing universities. The first one is wasting time in recording attendance for students and the second is losing part of the power for the operation of devices with little or no educational institutional benefit. HANISAH was introduced as solution to these problems through the use of RFID technology. Frequency identification radio (FIR), which is an automatic identification method, relies on storing and retrieving data using devices that deal with posting and reception from a distance. The system has been building applications using the Internet to monitor attendance records of students. Information technology through existing attendance management system on the computer RFID aims to solve everyday problems and assist faculty members in accessing the system easily via the Internet. The system could be equipped to create reports and provide valuable information on student commitments to attend lectures in real time [6].

Riahi [7] describes the ways to benefit from the environment of cloud computing to build sustainable and widely used E-learning systems. Cloud computing is considered by Riahi [7] as a suitable infrastructure for building large-scale E-learning systems. He presents five main layers of E-learning, namely, hardware and software resource layers, resource management, server, and business application.

According to Dominikus and Schmidt [8], "The Internet of Things (IoT) is an upcoming topic as things are getting smarter and are able to connect themselves with each other." The study describes a method that applies concepts from Mobile Internet Protocol (MPI v6) to enable a two-way end-to-end communication with passive RFID tags into the Internet. Furthermore, they apply concepts from MIPv6 where tags do not require IPv6 functionality themselves, but communicate

with readers using their standard RFID communication protocol. The readers provide MIPv6 functionality and act as a gateway between the Internet and the tags. They concluded that MIPv6 allows full integration of passive RFID tags via the IoT [8].

The study of [9] highlights the omitting factors in E-learning environment, which reflects the illegal behavior of students. The authors studied a sample of 150 students and 15 instructors for several online courses by using questionnaires. The experiment results indicated that the Learning Management System (LMS) supported academic institutions, but issues are missing legal development. The study recommended the use of a new model that could integrate society members in the LMS of an academic institution. The proposed model was evaluated based on statistical measurements. The results showed the effectiveness of the proposed model.

Peters [10] explained that mobile technology is implicitly used in formal education. Millions of sites are linked with mobiles used by students because they all search for information even though they may not be in the official records of the training course.

Many educational institutes recognize the importance and benefits of using mobile learning, but these benefits are limited by several factors. The most important limitations include age of teachers and trainers, their ability, cost of providing mobile devices, and infrastructure necessary for operation and connectivity.

The increasing growth of the functionality of mobiles as smart devices appears to have a clear place in training and education. Management of m-learning is very important for learners as they shift teachers from indoctrination process to guidance, as well as help learners to get instantly limited skills for the knowledge economy. The proposed system enhances the interaction among three main partners, including students, teachers, and parents of students, in one account [10].

III. DATASET OF THE STUDY SAMPLE: SUPPORTIVE E-LEARNING

King Khalid University applies supportive E-learning for all courses that students should attend in the classrooms. The curriculum should be presented by using the learning management system (Blackboard), and the lecturer assigns the subject area, assignments, and forum discussions [11].

Each supportive E-learning course must contain

- platform of the curriculum and information on the lecturer,
- scientific material of the course (not required to cover all course materials, but is preferable),
- link to course-related announcements, and
- link to hold discussions with the students.

The practical component of the Introduction to Computer course (Hal 101) is regularly taught at King Khalid University under the direct supervision of the Department of Computer

Science at the Faculty of Computer Science, and the component uses supporting E-learning level [12]. The study sample consists of 1000 students from the main university campus, includes supportive e-learning requirements, and considers international quality standards. Quality Matters (QM) was applied after obtaining approval from the Deanship of E-learning at the University of King Khalid for the two courses [13].

The respondents were asked if they have smart phones and internet connections. Approximately 95% of the respondents have this technology, and this figure sufficiently covers the limitation of 5% of the author sample. King Khalid University provides Internet services over wireless networks to all students and faculty members. As for the students who do not have smart phones, the Deanship of E-learning at the King Khalid University provided iPad devices to support the activities of E-learning at the university [11].

IV. METHODOLOGY

The proposed methodology consists of the following phases:

1) The authors developed a mobile application utilizing the NFC technique.

2) The lecturer is responsible for creating various related links available to students on the E-learning system and controlling accessibility by using the secure browser (LockDown Browser) [14].

3) Authors have two main types of NFC tags. The first type is used for student attendance system, in which every student has a tag containing the students' information (student ID). Once the student enters the classroom, a special reader attached to the main door will read the student's information and register students who attend the lecture.

4) The second type of NFC tag is a sticker found on the worksheet given once during the semester.

5) The lecturer includes these links in the class worksheets using tiny URL, which is stored in the second NFC tag in the worksheet as a sticker. The advantage of using tiny URL is to use the same NFC during the whole semester. Moreover, the lecturer could change the content of the tiny URL without changing the NFC sticker. The students use their smartphones as an NFC tag scanner to search for the specific URL.

6) The technique features (variables) are then extracted.

7) The hypotheses are stated.

8) The proposed technique using receiver operating characteristic (ROC) prediction quality measurements is evaluated.

V. EXPERIMENTS AND RESULTS

The proposed method was tested on 1000 students in the Introduction to Computer course (practical) at the supportive E-learning level. The authors prepared the links using the LockDown Browser in the blackboard system [14].

The Secure Browser (LockDown Browser) refers to an application designed to open various tests and links over the Internet and can be integrated easily with E-learning management systems, such as Blackboard [14].

The LockDown Browser application prevents the student from copying or pasting answers to questions or taking screen shots, as well as from opening other browser windows. Hence, the system guarantees specific academic use.

The Eighth General Standards of Quality Matters must consider special needs, accessibility to links, and different manners [13]. In the proposed technique, blind students could point their smart phones to the NFC tags, which will identify the blind student and link them directly to the audio lectures. In the Hal 101 course, the authors used the link of the course in the Blackboard system with one link or divided the activities to generate many NFC tags. The authors followed the guidelines below for their supportive E-learning courses:

1) They established NFC tags (Figure (1)) for the attendance activity. The reader at the main door reads the student tags. The NFC reader will retrieve the student name and ID, and send the data to the registration database in the university server. This step will save time because checking of the attendance has been done. Hence, classroom time is fully utilized for the lecture.

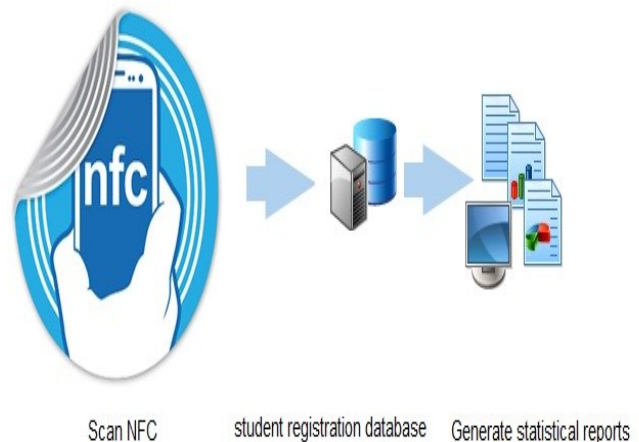


Fig. 1. NFC for student attendance

2) Another tag will be in the hard copy (course sheet), which contains a link to the lectures on the Blackboard system. Thus, students could review lectures as a type of asynchronous learning, as shown in Figure 2.

3) The lecturers placed another tag for the quizzes and discussion boards in the last part of the worksheet. Appropriate links using NFC tags would enable the students to participate in the forum, and students could avoid the barriers of fear through e-participation.



Fig. 2. NFC on student worksheets

To evaluate the proposed method, a questionnaire was designed for 1000 students. The questionnaire asked about the benefits of the proposed method and the authors extracted possible features (variables).

The authors have two types of variables (i.e., dependent and independent). Dependent variables refer to variable results computed in reference to other variables, whereas independent variables are not based on other variables [15].

In this study, independent variables are as follows:

- 1) Student Academic Level (SAL)
- 2) Field of studies (FS)

TABLE I. DEPENDENT VARIABLES

Variable	Description
FT	Flexible Technique
IT	Inexpensive Technique
ST	Safe Technique
QT	Quick Technique

The null hypothesis indicates that the independent variables did not participate in computing the dependent variables. The alternate hypothesis explores the relation between dependent and independent variables [15]. The hypotheses are presented in Table 2.

TABLE II. HYPOTHESES

1. The proposed technique explores inexpensive environment of learning delivery.
2. The proposed technique prevents copy/paste and cheating cases and offers a safe environment.
3. The proposed technique presents flexible learning environment and saves the time for feedback, assessment, and monitoring.
4. The proposed technique enhances student results.
H_0 : Independent variables do not participate.
H_1 : Independent variables participate.

The authors used Statistical Package for the Social Sciences (SPSS) [16] to accept or reject the alternative hypothesis. Alternative hypotheses are acceptable when P value < 0.05.

Table 3 presents the decision results for the hypothesis.

TABLE III. HYPOTHESIS RESULTS

Hypothesis	P-value	Result
First Hypothesis	0.0011	Accept the alternative.
Second Hypothesis	0.0020	Accept the alternative.
Third Hypothesis	0.0084	Accept the alternative.
Fourth Hypothesis	0.0091	Accept the alternative.

The following Receiver Operating Characteristic (ROC) prediction quality measurements were used to evaluate the proposed method: Accuracy, Precision, Recall, and F-measure (F-M) [17]

$$Accuracy_i = \frac{TP + TN}{TP + FP + TN + FN} \dots\dots\dots (1)$$

$$Recall_i = \frac{TP}{TP + FN} \dots\dots\dots (2)$$

$$Precision_i = \frac{TP}{TP + FP} \dots\dots\dots (3)$$

$$F - measure = \frac{(2 \times TP)}{(2 \times TP) + FP + FN} \dots\dots\dots (4)$$

where TP is True Positive, TN is True Negative, FP is False Positive, and FN is False Negative.

1) Accuracy: This characteristic indicates the closeness of computations to the true values.

2) Kappa statistic (KS): This value finds the error reduction percent, which is compared to all errors in the sample. Kappa values are between 0 and 1. A KS value close to 1 presents better value than 1 near 0 [12].

3) Mean Absolute Error (MAE): MAE computes the average of errors that appear in the set of the estimation, which explores the relative values to the actual outcomes [13].

Table 4 summarizes the evaluation results.

TABLE IV. EVALUATION RESULTS

Accuracy	Precision	Recall	F-measure
80.4%	0.805	0.804	0.823

The proposed application has an accuracy of 80.4%. The effectiveness measurement results of the application are KS, MAE, Root Mean Squared Error (RMSE), Relative Absolute Error (RAE), and Root Relative Squared Error (RRSE). The calculated values are shown in Table 5.

TABLE V. EFFECTIVENESS MEASURE RESULTS OF SVM CLASSIFIER

Author's application	KS	MAE	RMSE	RAE	RRSE
	0.6493	0.2679	0.346	71.71%	80.07%

Table 5 shows the effectiveness of the proposed application with probability of occurrence of several error rates.

Table 6 summarizes the results of the comparison between the present study and previous studies using different measurements.

TABLE VI. COMPARISON OF DIFFERENT TECHNIQUES

Study	Technique	Purpose	Covered range	Evaluation
Present study	NFC	1. Allow secured tests 2. Facilitate access of blind students to audio lectures 3. Automate student attendance record 4. Interact easily with E-learning materials	1. Short range (up to 10 cm). 2. Sufficient for the target of this study	1. Effective by saving time 2. Enhances student results 3. Prevents cheating 4. Flexible learning environment for feedback, assessment, and monitoring 5. Low possibility of error occurrence in reading proposed tags
Study [3]	RFID	Automate student attendance	Longer distance (several meters)	Flexible, which may be extended by adding more modules
Study [4]	RFID	1. Identify individual students based on their unique tag identifiers 2. Generate reports 3. Detect errors in tag 4. Integrates data storage	Longer distance (10–100 meters)	Saves the time and improves operation efficiency
Study [5]	RFID	1. Automate student attendance 2. Get education resources	N/A	Proposed implementation without evaluation
Study [6]	RFID	Automate student attendance.	Longer distance (10–100 meters).	Provide context-awareness for educational process

VI. CONCLUSION

E-learning in universities in Saudi Arabia has become the most important source of knowledge for application. The wide environment that contains a huge amount of digital information is ranked and seeded reliably and accurately in line with the needs of learners of different courses at the university. In the supportive E-learning courses, information technologies are necessary to activate learning management system tools in this type of course.

This paper proposed a method for the development of supportive E-learning courses at the King Khalid University using NFC. The study sample consisted of 1000 students in a supportive E-learning course. The main results are as follows.

First, the technology must apply main quality standards, which refer to e-learning being accessible to all students without any considerations. Second, the technology must be safe and inexpensive, as well as contribute to relieving the burdens of the curriculum through the use of electronic tools to access lectures, assignments, and discussions. The proposed technique should enable students to receive educational resources and monitor their academic performance (such as registering to attend classes and running tests). The manner should be commensurate with the abilities of students and provide access to the student community and interactive product. The experiments were evaluated using SPSS, and the results showed that the proposed technique is safe, flexible, inexpensive, and enhances student grades. The proposed method was evaluated using ROC prediction quality measurements. The conducted results indicate the effectiveness of the proposed technique.

ACKNOWLEDGMENT

This research is funded by the Deanship of Research and Graduate Studies of Zarqa University, Jordan.

REFERENCES

- [1] E. Galy, C. Downey, J. Johnson, "The Effect of Using E-Learning Tools in Online and Campus-based Classrooms on Student Performance," *Journal of Information Technology Education*, vol. 10, pp. 1-22, 2011.
- [2] ISO/IEC 18092:2004 Information technology -- "Telecommunications and information exchange between systems -- Near Field Communication -- Interface and Protocol (NFCIP-1) ," ISO. Retrieved 25 December 2015.
- [3] N. Saparkhojayev, S. Guvercin, "Attendance Control System based on RFID technology," *IJCSI International Journal of Computer Science Issues*, vol. 9, pp.1694-0814, May 2012.
- [4] S. Nainan, R. Parekh, T. Shah, "RFID Technology Based Attendance Management System," *International Journal of Computer Science Issues (IJCSI)*, vol. 10, pp. 516-521, January 2013.
- [5] M. Soliman, S. Guizan, "Investigating RFID Enabled Devices In Smart Electronic Learning Environments," *Conference ICL2009, Villach, Austria*, pp 963-968, September 2009.
- [6] H. Hamid, "RFID based systematic students attendance management system," thesis submitted as partial fulfillment of the requirement for the award of the Bachelor of Electrical Engineering (Electronics), November, 2010.
- [7] G. Riahi, "E-learning Systems based on Cloud Computing: A Review," *Proceedings of the 2015 International Conference on Soft Computing and Software Engineering (SCSE'15)*, pp. 352–359, 2015.
- [8] S. Dominikus and J. Schmidt, "Connecting Passive RFID Tags to the Internet of Things," *Interconnecting Smart Objects with the Internet Workshop*, pp.1-3, 2001.
- [9] A. Muhammad, H. Wahsheh, A. Shah, F. Ahmad, "Ethical perspective of learning management system a model to support moral character of online learner," *The 5th International Conference on Information and Communication Technology for The Muslim World (ICT4M)*, pp. 1-6, 2014.
- [10] K. Peters, "m-Learning: Positioning educators for a mobile, connected future," *International Review of Research in Open and Distance Learning*, vol.8, pp. 1-17, 2007.
- [11] The deanship of e-learning in King Khalid University, accessed on September, 2014, available at: <http://elc.kku.edu.sa/>
- [12] Course Description in the college of Computer Science, accessed on September, 2014, available at: <http://cs.kku.edu.sa/>
- [13] Quality Matters in King Khalid University (Arabic version), accessed on September, 2014, available at: http://elc.kku.edu.sa/sites/default/files/CourseQualityRubric_0810_Ar.pdf

- [14] Lockdown-browser, accessed September, 2015, available at: <http://www.respondus.com/products/lockdown-browser/>
- [15] R. N. Cardinal, "Graduate-level statistics for psychology and neuroscience ANOVA in practice, and complex ANOVA designs," 2004, from http://egret.psychol.cam.ac.uk/psychology/graduate/Guide_to_ANOVA.pdf
- [16] SPSS software, accessed on September, 2015, at: <http://www01.ibm.com/software/analytics/spss/>
- [17] I. Witten, E. Frank, "Data Mining: Practical Machine Learning Tools and Techniques", Morgan Kaufmann Series in Data Management Systems, 2005.

AUTHOR PROFILE



Assistant Professor HAYEL KHAFAJEH obtained his Ph.D. in Computer Information Systems in 2008 in Jordan. He joined Zarqa University, Jordan in 2009. In 2010, he served as Head of the CIS Department for two years. Since academic year 2014/2015, he has served as the Vice Dean of the IT College at Zarqa. Professor Hayel Khafajeh has worked for 23 years in the educational field as programmer, teacher, head of IT division, and manager of ICDL Center. He has published many educational computer books for the Ministry of Education in Jordan. In 2013, he published

his JAVA PROGRAMMING book for university students. His research interests include information retrieval and E-learning. He is the author of several publications on these topics.

His teaching interests focus on information retrieval, C++ programming, Java programming, and DBMS (ORACLE & MS Access).



Heider Wahsheh obtained his Master's degree in Computer Information Systems from Yarmouk University, Jordan, in 2012. Between 2013 and 2015, he was a Lecturer in the College of Computer Science at King Khalid University, Saudi Arabia. He is the author of many articles in IR, big data, sentiment analysis, NLP, data mining, and mobile agent systems.



Ahmad Albhaishi obtained his Master's degree in Computer Science from California Lutheran University, USA, 2012–2013. He is a lecturer at the College of Computer Science at King Khalid University, Saudi Arabia. His research interests include information retrieval, data mining, and E-learning.



Mofareh Alqahtani obtained his Master's degree in Computer Science from George Washington University, USA. He is a Lecturer in the College of Computer Science at King Khalid University, Saudi Arabia. His research interests include information retrieval, data mining, and E-learning.

A Novel Cylindrical DRA for C-Band Applications

Hamed Gharsallah, Lotfi Osman and Lassaad Latrach

Department of Physics
UR "CSEHF" 13ES37

Faculty of Sciences of Tunis, University of Tunis El Manar, 2092 Tunisia

Abstract—In this paper, we study a Dielectric Resonator Antenna of cylindrical shape with circular polarization for applications in the C band. The proposed antenna is composed of two different layers. The first is Polyflon Polyguide with relative permittivity $\epsilon_{r1} = 2.32$ and a loss tangent $\tan\delta = 0.002$ as a lower layer. The second is Rogers RO3010 with relative permittivity $\epsilon_{r2} = 10.2$ and a loss tangent $\tan\delta = 0.0035$ as an upper layer which is excited by dual probe feed. The 90° phase shift of two probes feed can create a circular polarization. In this study, we focused on the effect of the variations in the height of the Polyflon Polyguide as well as the probe feed. Simulations under HFSS software have led to bandwidth values of about 2.2 GHz and 2.6 GHz for the proposed antenna with one probe and dual probe, respectively. The obtained gains are higher than 5.4 dB and can range up 8.1 dB.

Keywords—Dielectric Resonator Antenna; gain; reflection coefficient; circular polarization; axial ratio

I. INTRODUCTION

Nowadays, many researchers are interested in the dielectric resonators. This theme is introduced in 1983 [1], and widely studied and used over the last two decades owing to their attractive properties like for examples the small size, the simplicity of feeding by classical methods and the very high radiation efficiency compared to microstrip antennas [2]. The Dielectric Resonator Antenna (DRA) has characteristics that can be modified according to an appropriate choice of dimensions of the resonator as well as its dielectric constant.

Let us note that the production of dielectric resonators (DR) don't add additional constraints and can also easily adjust the quality factor and the resonant frequency [3]-[4]. A cylindrical DRA is simple to design allowing an easy control of the resonant frequency and the Q-factor by the ratio radius/height and the permittivity ϵ_r . It would be necessary to know that it is possible to excite the different modes of this type of DRA by adjusting the position and the type of excitation, thereby obtaining an omnidirectional or broadside radiation pattern [5].

The circular polarization (CP) is preferred in the antenna applications because this system gives a wide flexibility in the orientation of the antennas in transmission mode as well as in reception mode [6], and can increase the bandwidth [7]-[8]. The broadband CP antenna applications include many areas such as radar, RFID and satellite. In satellite applications, a CP is preferred in order to overmaster the consequences of the rotation of polarization due to the atmosphere. In the case of radar applications, the CP signals are used so as to obtain a maximum of information about the target [9].

The CP is a combined excitation of two degenerate orthogonal modes. The vector of the electric describes a circle over time and a helical motion along the propagation direction. The DRA is used for many reasons among which the very broad bandwidth. For a single DRA, the use of a cylindrical or a conical shape can increase this bandwidth. A dielectric constant of low value can reduce the quality factor Q and thereafter increases the width of the bandwidth [10]. In order to obtain best results, we will focus on another technique using a multilayer configuration for different permittivities ϵ_r [11]-[12].

In this paper, a cylindrical dual layer dielectric resonator circularly polarized antenna excited by a dual coaxial probe feed is proposed for C-band applications. To achieve a wideband performance, we need to stack two dielectric layers one over the other. Therefore, the lower layer is of type Polyflon Polyguide with relative permittivity $\epsilon_{r1}=2.32$ and a loss tangent $\tan\delta=0.002$, and the upper layer is of type Rogers RO3010 of dielectric constant $\epsilon_{r2}=10.2$ and a loss tangent $\tan\delta=0.0035$. To make sure to get good impedance matching and ensure at the same time wideband performance, it is necessary to use a coaxial probe feed excitation. It should also be known that a dual coaxial probe feed inclined by 90° can create the circular polarization.

The best advantage of the use of a coaxial probe feed excitation is the direct coupling into a $50\text{-}\Omega$ system without the need of a matching network [13]. The effects of the probe and the Polyflon Polyguide heights will be studied through the use of the HFSS commercial software [14].

We present in this paper the simulation results of the return loss, gain and axial ratio of the cylindrical dielectric resonator antenna (CDRA) that we propose with dual layer and that works in the C-band.

II. ANTENNA DESIGN

Fig.1 shows the geometry of the proposed cylindrical dielectric resonator antenna. The shape of the DRA, the type and the location of the excitation are responsible of the antenna characteristics.

The cylindrical shape of the dielectric resonator gives a large degree of freedom. Thereby, the coaxial probe feed located adjacent to a CDRA offers a large coupling and thereafter a high gain and a symmetric radiation pattern. The mode excited with this location is the $HEM_{11\delta}$ mode.

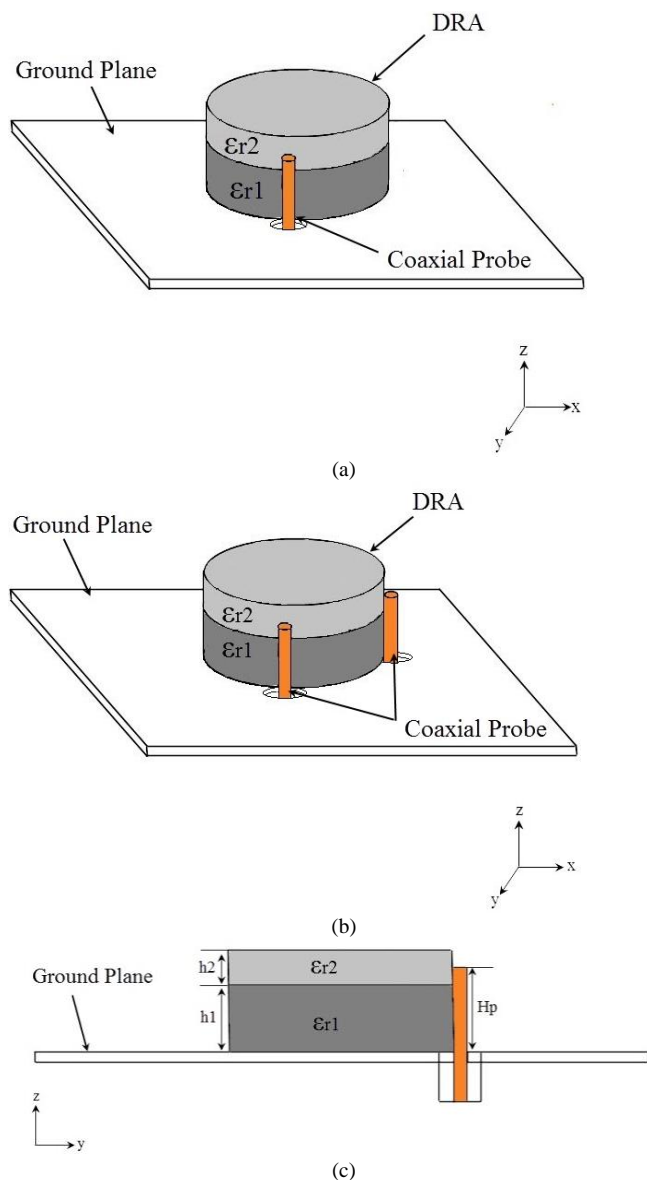


Fig. 1. Cylindrical DRA design, (a) with only one probe feed, (b) with two probes feed, (c) cut-view (y-z plane)

The relation (1) gives the formula of the resonance frequency of a CDRA corresponding to the case of HEM₁₁₆ mode [15].

$$f = \frac{6.324c}{2\pi\sqrt{2+\epsilon_r}} \left\{ 0.27 + 0.36 \frac{a}{2h} + 0.02 \left(\frac{a}{2h} \right)^2 \right\} \quad (1)$$

where ϵ_r is the permittivity, a is the radius and h is the height of the antenna. Its quality factor is expressed by the following relation (2).

$$Q = 0.01007 (\epsilon_r)^{1.3} \left(\frac{a}{h} \right) \left[1 + 100e^{-[2.05 \left(\frac{a}{2h} \right) \frac{1}{80 \left(\frac{a}{h} \right)^2]} \right] \quad (2)$$

The percentage bandwidth is given by

$$\% BW = \frac{\Delta f}{f_r} * 100 = \frac{s-1}{Q\sqrt{s}} * 100 \quad (3)$$

where Δf and f_r are the bandwidth and the resonant frequency, respectively. The VSWR is the voltage standing wave ratio of the antenna.

Equation (4) shows the relation between h and ϵ_r .

$$\epsilon_{r\text{eff}} = \frac{h_{\text{eff}}}{h_1/\epsilon_{r1} + h_2/\epsilon_{r2}} \quad \text{with} \quad h_{\text{eff}} = h_1 + h_2 \quad (4)$$

where h_1 and h_2 are the heights of Rogers RO3010 (upper layer) and Polyflon Polyguide (lower layer), respectively.

This equation indicates the influence of the couple thickness-permittivity on the resonance frequency and the Q-factor, and thereby the bandwidth for the dual layer dielectric resonator antenna [14]. The parameters $\epsilon_{r\text{eff}}$ and h_{eff} replace ϵ_r and h in (1) and (2) so that $\epsilon_{r\text{eff}}$ becomes the effective permittivity and h_{eff} the effective height. Fig. 1(a) and Fig. 1(b) exhibit the 3-D view of the dual layer cylindrical dielectric resonator antenna with one probe feed and dual probe feed, respectively. Fig. 1 (c) represents the cut-view (y-z plane) of this structure. It is composed of a Polyflon Polyguide characterized by $\epsilon_{r1}=2.32$ as lower layer and a Rogers RO3010 with $\epsilon_{r2}=10.2$ as upper layer. The proposed antenna is located in the middle of the ground plane with dimensions equal to $L_g \times W_g \times H_g$. The radii of the lower and upper layers of the antenna are identical but with different heights.

The use of a coaxial probe has no effect on the matching of the antenna and the circular polarization is generated from the 90° phase shift. The optimized value of the height H_p is 8.2 mm thus obtaining a good reflection coefficient at the resonant frequency.

Table I below shows the optimized parameters of the proposed antenna.

TABLE I. OPTIMIZED PARAMETERS OF THE PROPOSED ANTENNA

Dimension	Value (mm)
L_g	60
H_g	1
h_1	6.67
H_p	8.2
W_g	60
a	11
h_2	3.33

III. RESULTS AND DISCUSSION

A. Parametric Results

The results are obtained for the reflection coefficient versus frequency. We achieved a wide bandwidth for the antenna double layer where the top layer has a higher permittivity and the inferior layer has a lower permittivity. The upper layer is made of Rogers RO3010 with $\epsilon_{r2} = 10.2$, whereas the lower layer is made of Polyflon Polyguide with $\epsilon_{r1} = 2.32$.

The simulation results of the S11 parameter for different values of h_1 and H_p are shown in Fig. 2. We can confirm that an interesting impedance bandwidth of about 38% is obtained in the [4.6 – 6.8] GHz frequency range for both $h_1 = 6.67$ mm (Fig. 2a) than for $H_p = 8.2$ mm (Fig. 2b).

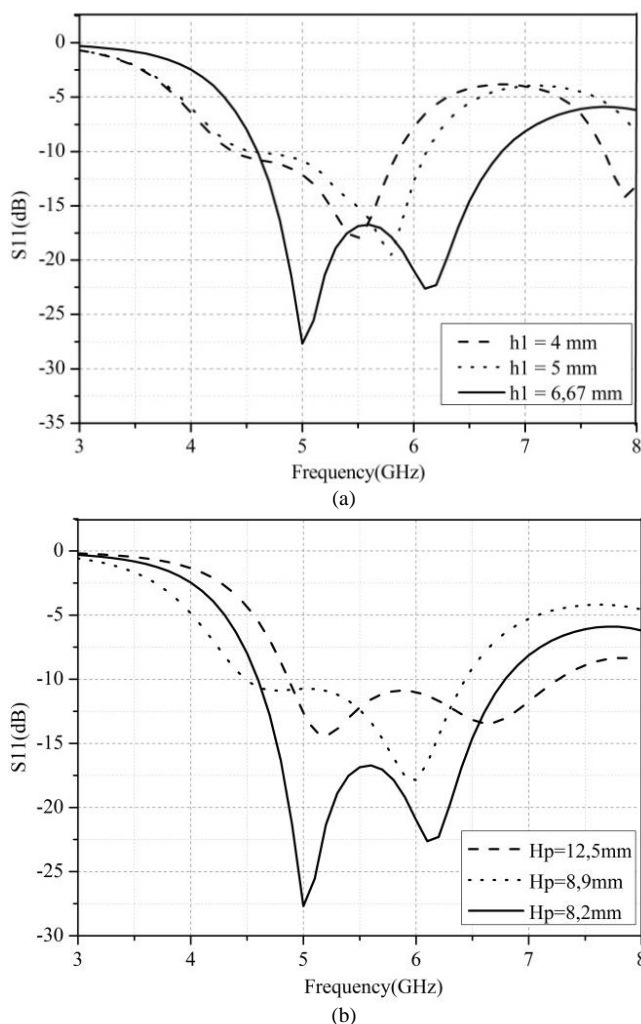


Fig. 2. Reflection coefficient of the proposed dual segment cylindrical DRA with one probe feed: (a) for different values of h_1 , (b) for different values of H_p

Fig. 3 shows the simulation result of the S11 parameter in the case of two probes feed shifted 90° degree. It is this inclination that creates the circular polarization.

We notice that the impedance bandwidth is around 44% in the frequency band [4.5-7.1] GHz. Therefore, we can deduce that the circular polarization is able to increase the bandwidth and that the latter is larger in the case of dual probe feed than in that of only one probe feed.

This increase of the bandwidth can range from 37.9 % up to 44 % in the [4.5-7.2] GHz frequency band.

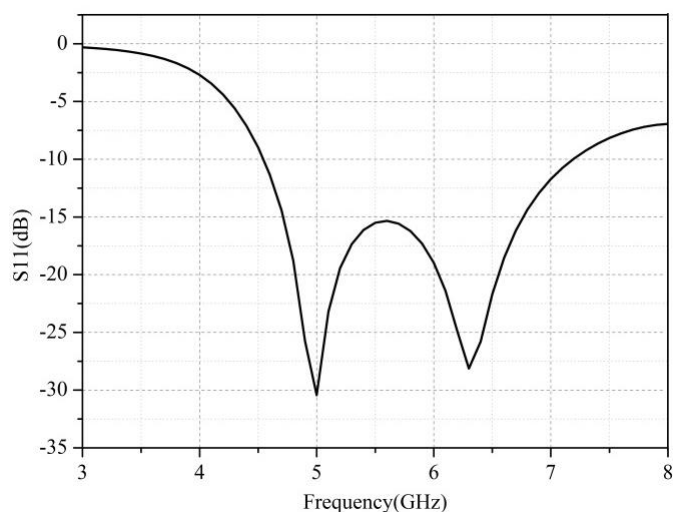


Fig. 3. Reflection coefficient of the proposed dual layer cylindrical DRA with two probes feed

Fig. 4 shows a comparison of the simulation results of the S11 parameter carried out under Ansoft HFSS and CST studio softwares.

The difference observed between the two curves is due to different calculation methods of these two commercial tools.

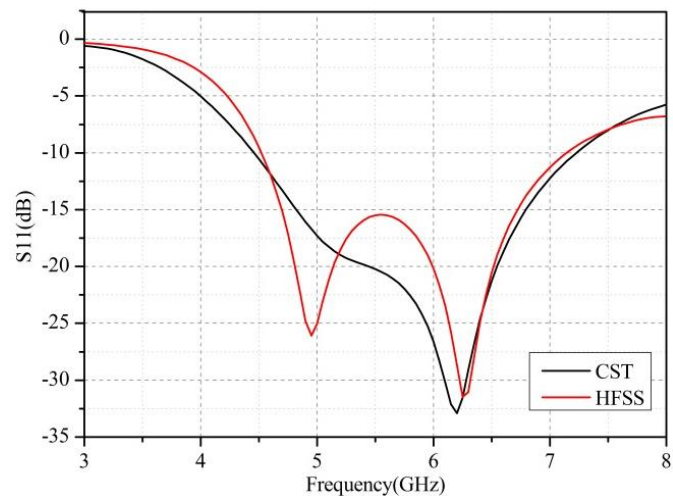


Fig. 4. Comparison of the S11 results performed with Ansoft HFSS and CST studio softwares

B. Axial Ratio

Fig. 5 exhibits the result of the simulated axial ratio of the proposed antenna with two probes feed. It generates the circular polarization in all the bandwidth.

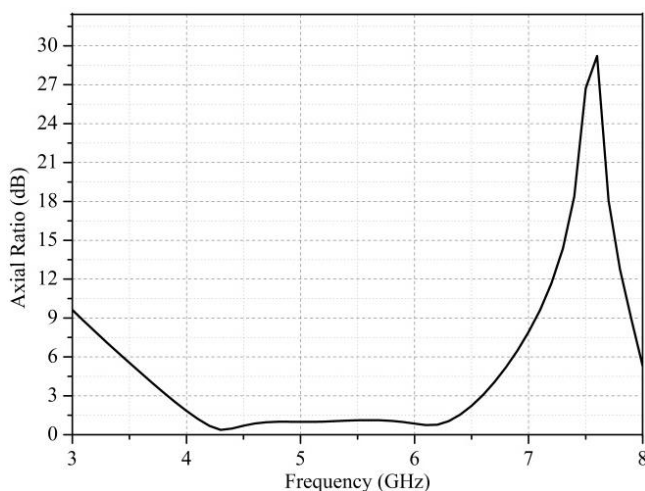


Fig. 5. Simulated axial ratio of the proposed dual layers cylindrical DRA with dual probe feed

C. Gain

Fig. 6 shows the simulation results of the gain over a frequency range from 4.5 GHz to 7.1 GHz.

The proposed dual layer cylindrical DRA with two probes feed offers simulated values of gain reaching 8.1 dB and no less than 5.4 dB in the frequency range from 4.5 GHz to 7.1 GHz.

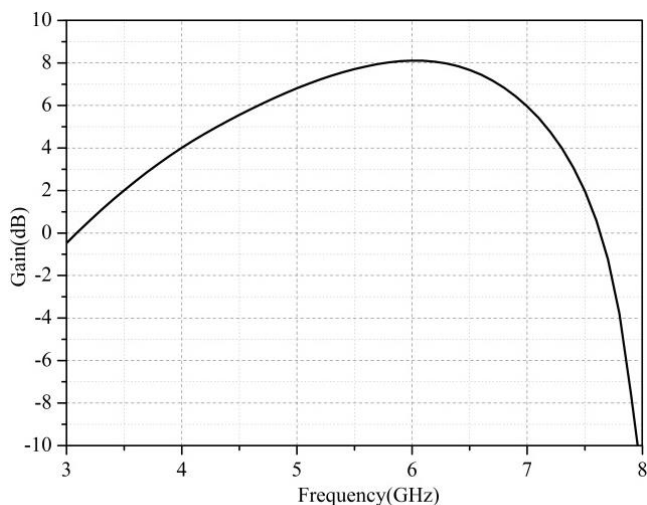


Fig. 6. Gain of the proposed dual layer cylindrical DRA with dual probe feed

Fig. 7 shows that the simulated gain in 3D at 5 GHz, 5.8 GHz and 6.4 GHz frequencies are 7 dB, 8 dB and 7.9 dB, respectively. We denote that the antenna gain is constant throughout the bandwidth.

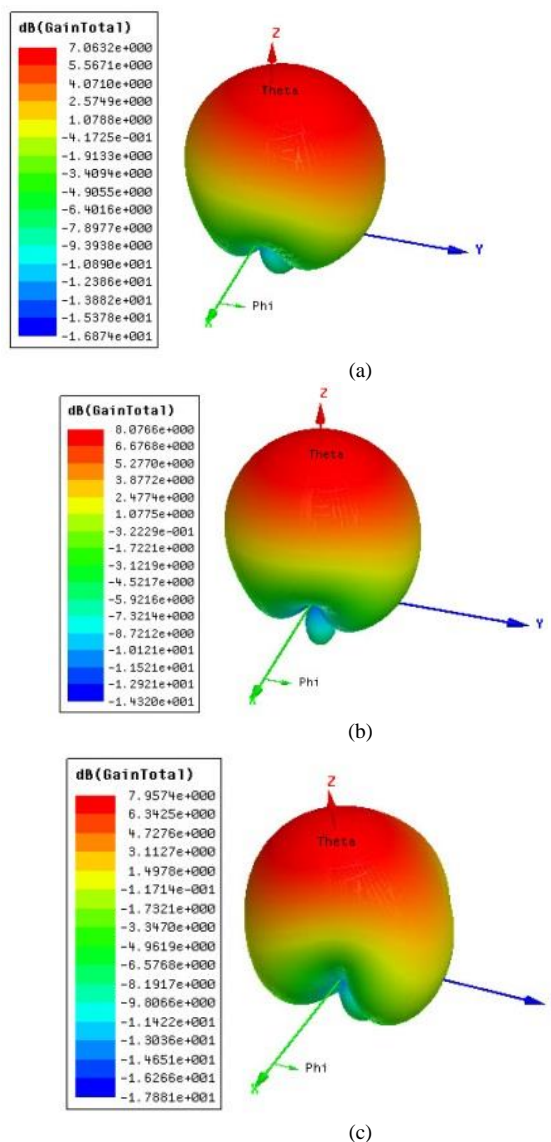


Fig. 7. Gain of the proposed antenna: (a) 5 GHz, (b) 5.8 GHz and (c) 6.4 GHz

D. Radiation Patterns

Fig. 8 shows the polar representation of the radiation patterns obtained in the E-plane (x-z plane) and the H-plane (y-z plane), respectively with $\phi=0^\circ$ and $\phi=90^\circ$ at the resonant frequency of 5.8 GHz. The radiation pattern is broadside in the two planes.

REFERENCES

- [1] S. A. Long, M.W. McAllister, and L. C. Shen, "The resonant cylindrical dielectric cavity antenna," IEEE Transactions on Antennas and Propagation, Vol. 43, AP-31, No.3, May 1983.
- [2] Petosa Aldo, Dielectric Resonator Antennas Handbook, Artech House, 2007.
- [3] A. A. Kishk and A. W. Glisson, "Bandwidth Enhancement For Split Cylindrical Dielectric Resonator Antennas," Progress In Electromagnetics Research, PIER 33, 97–118, 2001.
- [4] H. Y. Huang, J. Y. Wu, and K. L. Wong, "Cross-Slot-Coupled Microstrip Antenna and Dielectric Resonator Antenna for Circular Polarization," IEEE Transactions on Antennas and Propagation, Vol. 47, No. 4, April 1999.
- [5] A. W. Glisson, D. Kajfez, and J. James, "Evaluation of modes in dielectric resonators using a surface integral equation formulation," IEEE Trans. Microwave Theory Tech., vol. ATT-31, no.12, December 1983.
- [6] L. C. Y. Chu, D. Guha, and Y.M.M. Ontario, "Comb-shaped circularly polarized dielectric resonator antenna," Electronics Letters, Vol. 42 No. 14, 6th July 2006.
- [7] H. Gharsallah, L. Latrach, and L. Osman, "Development of a Novel Wideband Conical Dielectric Resonator Antenna," IEEE 15th Mediterranean Microwave Symposium (MMS), Lecce, Italy, Nov. 30 2015-Dec. 2 2015.
- [8] Y. D. Zhou, Y. C. Jiao, Z. B. Weng, and T. Ni, "A Novel Single-Fed Wide Dual-Band Circularly Polarized Dielectric Resonator Antenna," IEEE Antennas and Wireless Propagation, Vol. 15, 2016.
- [9] R. Y. Sun, "Bandwidth Enhancement of Circularly Polarized Dielectric Resonator Antenna," ETRI Journal, Volume 37, Number 1, February 2015.
- [10] R. K. Chaudhary, K. V. Srivastava, and A. Biswas, "Three-Element Multilayer Multipermittivity Cylindrical Dielectric Resonator Antenna For Wideband Applications With Omnidirectional Radiation Pattern And Low Cross-Polarization," Microwave and Optical Technology Letters, Vol. 54, No. 9, September 2012.
- [11] Y. Geand and K. P. Esselle, "A Dielectric Resonator Antenna for UWB Applications," IEEE Transactions on Antennas and Propagation, 2009.
- [12] R. K. Chaudhary, K. V. Srivastava, and A. Biswas, "Four Element Multilayer Cylindrical Dielectric Resonator Antenna Excited by a Coaxial Probe for Wideband Applications," Communications (NCC), National Conference on Bangalore, 2011.
- [13] Z. N. Chen., et al., "Effect of Parasitic Disk on a Coaxial Probe-Fed Dielectric Resonator Antenna," Microwave and Optical Technology Letters," Vol. 15, No. 3, June 1997, pp. 166-168.
- [14] "Ansoft Corporation", High Frequency Structure Simulator, v 15.
- [15] A. Rashidian, K. Forooraghi, and M. R. Tayefeh, "A New Method For Calculating The Resonant Frequency of Multisegment Dielectric Resonator Antennas," Microwave & Telecommunication Technology, 2003.

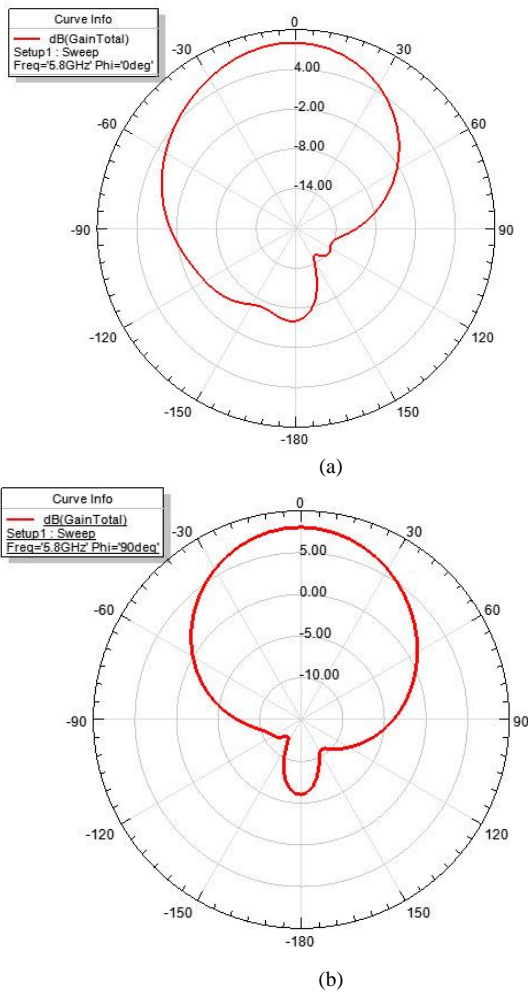


Fig. 8. Radiation patterns of the antenna at 5.8 GHz. (a) in the E-plane (x-y plane), (b) in the H-plane (y-z plane)

IV. CONCLUSION

A dual layer cylindrical dielectric resonator antenna with circular polarization functioning in C-band has been studied in this paper. The obtained results of this proposed antenna showed an increase of the bandwidth of up to 44% in the [4.5-7.2] GHz frequency band with two probes feed, and the gain is able to reach 8.1 dB in this frequency band. Finally, we remind that this antenna is designed for WLAN/WIMAX communication systems operating in the C-band.

Adaptive Threshold for Background Subtraction in Moving Object Detection using Stationary Wavelet Transforms 2D

Oussama Boufares

Physics department
Innov'Com laboratory, Sciences
Faculty of Tunis, University of Tunis
El-Manar
Tunis, Tunisia

Noureddine Aloui

Centre for Research on
Microelectronics & Nanotechnology,
Sousse Technology Park,
Sousse, Tunisia

Adnene Cherif

Physics department
Innov'Com laboratory, Sciences
Faculty of Tunis, University of Tunis
El-Manar
Tunis, Tunisia

Abstract—Both detection and tracking objects are challenging problems because of the type of the objects and even their presence in the scene. Generally, object detection is a prerequisite for target tracking, and tracking has no effect on object detection. In this paper, we propose an algorithm to detect and track moving objects automatically of a video sequence analysis, taken with a fixed camera. In the detection steps we perform a background subtraction algorithm, the obtained results are decomposed using discrete stationary wavelet transform 2D and the coefficients are thresholded using Birge-Massart strategy. The tracking step is based on the classical Kalman filter algorithm. This later uses the Kalman filter as many as the number of the moving objects in the image frame. The tests evaluation proved the efficiency of our algorithm for motion detection using adaptive threshold. The comparison results show that the proposed algorithm gives a better performance of detection and tracking than the other methods.

Keywords—moving object detection; SWT; background subtraction; adaptive threshold; kalman filter

I. INTRODUCTION

It is easy for a human being to recognize images or other objects around him, but it is a very complex problem for an automated system. Nevertheless, many systems need to have information on the presence or the absence of objects in their environment. In other terms, object detection and tracking in a video sequences have been one of many important problems in computer vision and have attracted more and more researchers working on it. Furthermore, moving object detection has been used for many computer vision applications, including recognition of traffic scenarios [1], supervision traffic flow [2], collision prediction of pedestrians [3], face detection [4], human-machine interaction [5], etc. While detecting and tracking, we need to analyze video sequences to detect and track target in each frame, to achieve monitoring and to master the dynamic variation of the moving objects in order to confirm their exact position. In general, there are lots of methods which can be classified into three categories: optical flow [15, 37], [16], temporal difference [13], [14] and background subtraction. The algorithms of temporal difference quickly adapt to sudden changes in the environment, but the resulting shapes of target are frequently incomplete. In general,

optical flow methods present the projected motion on the image plane to high approximation based on the feature of flow vectors. Unfortunately, flow vectors of moving objects only indicate streams of moving objects, thus detecting a sparse form of object regions. Moreover, the computational complexity of optical flow methods is usually too high to easily implement the motion task in the general video surveillance system. Usually, background subtraction is the operation that logically follows the background modeling to obtain a motion detection. If the background model is an image, an absolute difference between this model and each incoming video frame is performed to obtain motion detection. When there is a statistical model, we calculate the probability that each pixel belong to the background by testing the value observed in the model, the importance of the observed movement varies in the opposite direction to the calculated probability.

Many algorithms have been proposed for the moving objects detection. Yumiba et al. [10] proposed an algorithm called ST-Patch for motion detection to cover dynamic changes in background. Authors in [30] proposed a method to evaluate the quality of stereoscopic images that are afflicted by symmetric distortions. Edward J. Delp and Ka Ki Ng [11] invented an approach to calculate the threshold automatically and dynamically relating to the pixels' intensities in the present frame and a method to update the background model based on learning the rate relating to the differences between the background model and the last image. Elham Kermani and Davud Asemani [12] proposed new method based on adaptive structure firstly detects the edges of motion objects, then, Bayesian algorithm corrects the shape of detected objects.

Many studies have been used subband adaptive thresholding for denoising image using discrete wavelet transform (DWT) [13, 14]. For us, our contribution consists to integrated this technique in video sequences to detect moving objects with stationary wavelet transforms 2D. According to the difficulty of motion detection in video surveillance, the most used techniques deal with a fixed camera [15, 16] or closed world representations [17] which rely on a fixed background or a specific knowledge on the type of actions taking place, where various difficult cases are not perfectly

solved and must be improved such as identification, occlusion, tracking of object, localization and removing shadows of objects.

In this paper, we have developed a novel approach for motion detection based on discrete stationary wavelet transform. The rest of this paper is organized as follow. In Section 2, the adaptive background subtraction algorithm detects all the moving objects to get the whole moving area. In this step, the different objects obtained by calculating the result of the difference between the background frame and the present frame image, and then thresholding by discrete stationary wavelet transforms SWT[18]. In Section 3, once a target is detected the tracking phase starts. Therefore, we adopt the Kalman filter for more effective monitoring of targets. Section 4, experimental results and some discussion are presented. Finally, Section 5 concludes this paper with a discussion and the imagination of our future work.

This figure shows the flowchart of the background subtraction.

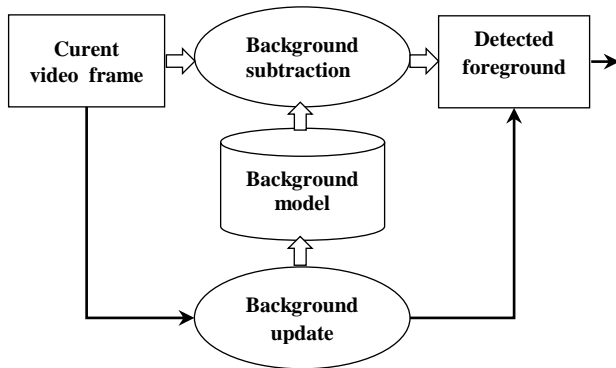


Fig. 1. System block diagram of the background subtraction. [20]

II. PROPOSED ADAPTIVE THRESHOLD USING SWT FOR DETECTION OF MOVING OBJECTS

In this section, an adaptive threshold technique based on SWT is applied on the obtained image using background subtraction, to detect moving objects of each frame in a video scene. For better follow up the concept of proposed algorithm, the basic idea of detection using background subtraction is firstly described. Then, it will be combined with the stationary wavelet SWT. As a result, an integrated background subtraction-SWT algorithm is obtained for optimally detecting moving objects.

Motion detection methods are basically a process which detects the object in the surveillance area [19]. The following diagram summarizes the proposed algorithm for motion detection with background subtraction based on an adaptive threshold. The following figure 4 involves a number of different steps, each of them are discussed below:

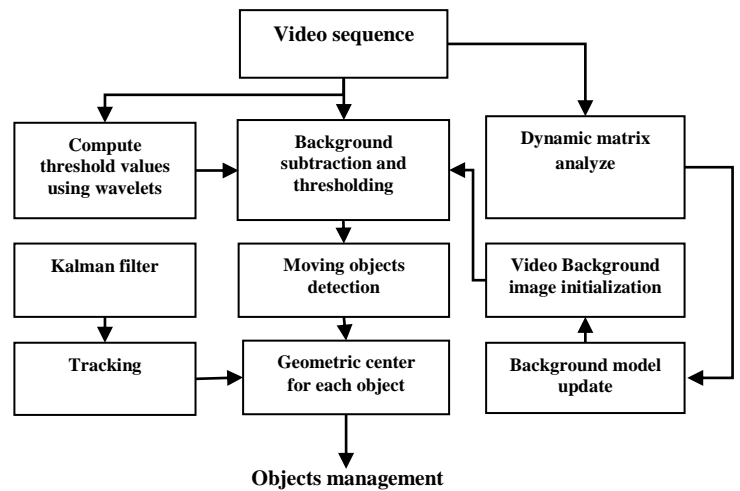


Fig. 2. Block diagram of the proposed algorithm

A. Background frame initialization

For video analysis, the background initialization is highly important after the pre-processing is done on each frame. When the background image is initialized it will be presented as the reference image. There are many techniques to obtain the initial background frame. For example, calculate the background image by averaging the first images, or take the first frame as the background directly or using a background image sequences without the prospect of moving objects to estimate the background model parameters.

In this part, we consider that the video begins with the background in the absence of moving objects. We use the selective averaging method [21] to obtain the initial background model as:

$$B(s) = \frac{\sum_{m=1}^N I_m(s)}{N} \quad (1)$$

Where $B(s)$ and $I_m(s)$ are respectively the intensity of pixel of the background model and the intensity of pixel s of the m^{th} frame, and N is the number of frames used to construct the background model.

B. Background subtraction

After obtaining the initial background model, the subtraction between the current frame and the reference frame is done for the moving object detected. The subtraction will be done pixel by pixel of the both frames. The simple version of this scheme, where a pixel at location s in the current frame f_s , is indicated as foreground if:

$$|f_s - B_s| > \delta \quad (2)$$

B_s is The background image δ is the adaptive threshold calculated by stationary wavelet.

The Background subtraction is used to recognize the pixel intensity of foreground which is obtained by the difference between the current image and the background image. Let consider that $Diff_s$ is the binary foreground of an image.

$$Diff_s(k) = \begin{cases} 1 & \text{for } |f_s(k) - B_{(s)(k-1)}(k-\gamma)| > \delta \\ 0 & \text{for others} \end{cases} \quad (3)$$

Where γ represents the interval time between the current frame and the old one. The threshold adaptive δ that classifies between foreground and background can be determined by our proposed algorithm using stationary wavelet.

C. Image Analysis using wavelet stationary

In this subsection, the thresholding step is based on stationary wavelet transform. First, the foreground result is decomposed into different sub-bands using SWT. Then, the obtained coefficients are thresholded. These sub-bands are shown in the table below:

TABLE I. DECOMPOSITION OF FRAME INTO FOUR SUB-BANDS EXPLOITING SWT

Diagonal (HH)	Approximation (LL)
Vertical (LH)	Horizontal (HL)

H and L present respectively the low and the high-pass filters. The LL sub-band is the low resolution residual composed of low frequency elements and this sub-band which is further split at higher levels of decomposition. After decomposition, the obtained coefficients in the detailed sub-bands are thresholded to reduce the noise and also the thresholded frame is reconstructed from the thresholded sub-bands [22], [23]. The steps of wavelet thresholding are described as follows:

- i. Decompose the frame exploiting SWT.
- ii. Threshold the coefficients of wavelet exploiting the chosen threshold algorithm.
- iii. Reconstruct the frame exploiting ISWT for the threshold frame.

1) Universal threshold

The universal threshold (Visu Shrink) δ has been proposed by Donoho [24]. It is described as:

$$\delta = \sigma \sqrt{2 \ln(N)} \quad (4)$$

Where N is the number of the wavelet coefficients and σ is the noise variance in that frame which is computed from the diagonal sub-band (HH) as:

$$\sigma = MAD(HH) / 0.6745 \quad (5)$$

To predict the noise level σ , authors in [29] proved that the Median Absolute Deviation is presented as:

$MAD(X) = |X - Median(X)|$ converges to 0.6745 times σ as the sample size.

2) Proposed adaptive threshold

The universal threshold exploits a threshold value that is directly depends on the standard deviation of the interfering signal and tracks the hard threshold rule. It is changed

exploiting weighted median and golden ratio. Fig.3 depicts the block diagram of the suggested algorithm.

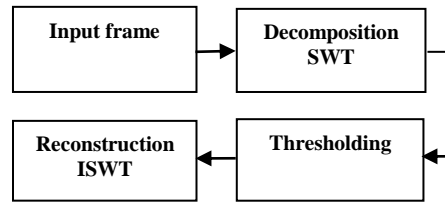


Fig. 3. Block diagram of the suggested algorithm

In this part, replacing the value '2' with the golden ratio value '1.68' is suggested to use and the threshold δ is computed as:

$$\delta = \sigma \sqrt{1.68 \ln(N)} \quad (6)$$

Instead of the conventional median given in (5), we use the weighted median to calculate the median value of the high pass party of the frame. This method opts the classical weight function (W) [25] for calculating the weighted coefficient of the diagonal sub-band (HH) which is given by the following:

$$w(s) = \frac{1}{e^{|\text{HH}(s)|}} \quad (7)$$

Here's is the coordinate of the HH sub-band. The diagonal sub-band HH will be multiplied with the weight W to get the weighted diagonal sub-ban HH1.

$$HH_1 = w(s) * HH(s) \quad (8)$$

The noise variance σ is then determined from the weighted diagonal sub-band (HH1) as follow:

$$\sigma = Median(HH) / 0.6745 \quad (9)$$

After calculating the noise variance, the modified universal threshold is applied to the frame and the process is treated in the suggested algorithm.

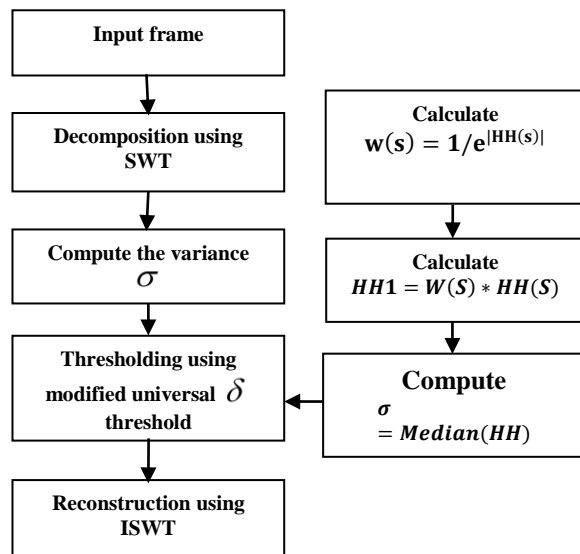


Fig. 4. Algorithm describing thresholding method of modified universal threshold exploiting weighted median and golden ratio

After the background subtraction step, we use hard thresholding given as follow:

$$Diff_k = \begin{cases} 1 & \text{for } |f_k(s) - B_{k-1}(s)| > \delta \\ 0 & \text{for others} \end{cases} \quad (10)$$

The hard threshold eliminates coefficients underneath a threshold value (δ) that is obtained by the proposed algorithm of thresholding.

The last equation describes the segmentation after the differentiation of the present and the background frame. That subtracted image obtains the subtracted value of each pixel, that pixel value is compared with the threshold value. If the subtracted pixel value is greater than the threshold value so, it will take 1 else it will take 0.

The value of 1 presents the black color and the value of 0 presents the white color. So the segmented image obtains the moving target in white with a black background, as result, the moving object is detected.

D. Background update

Now, we present a short introduction to the background update approach suggested by authors in [26] that is based on a dynamic matrix. First, a dynamic matrix $D(k)$ is analyzed in order to have a decision whether this pixel appertains to the foreground or not. Supposing that $I(k)$ is the input image at time k that is the index for the pixel position $I_s(k)$. The expression (4) of the dynamic matrix $D(k)$ at time k is given by:

$$D_s = \begin{cases} D_s(k-1)Diff_s(t) = 0, & D_s(k-1) \neq 0 \\ \rho & Diff_s(t) = 0 \end{cases} \quad (11)$$

Where λ presents the time length to record the pixel's moving state. When $D_s(k)$ corresponds to zero, the pixel will be updated into the background with a linear model.

$$B_s(k) = \alpha I_s(k) + (1 - \alpha)I_s(k) \quad (12)$$

B_s is the background frame at time k and α is the weight of input image.

III. OBJECT TRACKING USING KALMAN FILTER

The Kalman filter is usually applied in investigations of dynamic systems, prediction, analysis, processing and control. Kalman filter is an optimal filter for the discrete data linear filtering issue. It's an ensemble of equations that offers a good solution to sequential systems. As such, two equations describe the kalman filter which are: the time update equations and the measurement update equations. Time update equations, from time step K to step $K+1$, are in charge of projecting forward the current step and error covariance predicts to get the priori predictions for the upcoming time state. The measurement update equations are accountable for the feedback that means to incorporate a novel measurement into a priori estimation to get better posteriori estimation.

The time update equations can be also accounted as predictive equations and the measurement update equations as corrector equations. Indeed the final prediction algorithm looks

like an estimator-corrector algorithm that giving solutions for numerical problems as presented below in Fig.5.

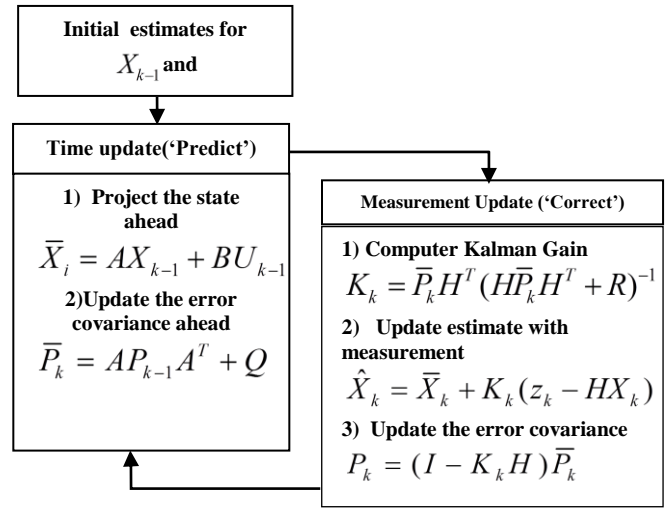


Fig. 5. The whole operation of the Kalmanfilter

Where, P is the estimation error covariance. Q presents the process noise covariance, R depicts the measurement error covariance and K presents the Kalman gain. We assume a discrete-time linear system state equation and an observation model, as follow:

The state equation and measurement model are:

$$\begin{cases} X_k = AX_{k-1} + BW_k \\ Z_k = HX_k + V_k \end{cases} \quad (13)$$

Where A , B and H are the model matrices. w_k and v_k depict respectively the process and the measurement noise.

In this paper, the state vector is defined as $x_k = [x_{0,k}, y_{0,k}, l_k, h_k, v_{x,k}, v_{y,k}, v_{l,k}, v_{h,k}]^T$,

$(x_{0,k}, y_{0,k})$ are the horizontal and vertical centroid coordinate, (l_k, h_k) depict half-width and half-height of the tracking window,

$(v_{x,k}, v_{y,k}, v_{l,k}, v_{h,k})$ represent their speed respectively.

In the following, A is the transition matrix and H is the measurement one of our tracking systems with the Gaussian process w_k and measurement v_k . These noise values are entirely dependent on the system that is being tracked and adjusted experimentally.

$$A = \begin{bmatrix} 1 & 0 & 0 & 0 & t & 0 & 0 & 0 \\ 0 & 1 & 0 & 0 & 0 & t & 0 & 0 \\ 0 & 0 & 1 & 0 & 0 & 0 & t & 0 \\ 0 & 0 & 0 & 1 & 0 & 0 & 0 & t \\ 0 & 0 & 0 & 0 & 1 & 0 & 0 & 0 \\ 0 & 0 & 0 & 0 & 0 & 1 & 0 & 0 \\ 0 & 0 & 0 & 0 & 0 & 0 & 1 & 0 \\ 0 & 0 & 0 & 0 & 0 & 0 & 0 & 1 \end{bmatrix}$$

Observation matrix H can be described as:

$$H = \begin{bmatrix} 1 & 0 & 0 & 0 & 0 & 0 & 0 & 0 \\ 0 & 1 & 0 & 0 & 0 & 0 & 0 & 0 \\ 0 & 0 & 1 & 0 & 0 & 0 & 0 & 0 \\ 0 & 0 & 0 & 1 & 0 & 0 & 0 & 0 \end{bmatrix}$$

The introduction of Kalman filter can be used to estimate the object's location, size in a small range and to gain trajectories of moving objects.

IV. EXPERIMENTAL RESULTS

At present, many motion detection approaches have been developed that execute well in some types of videos but not in others. There is a list of challenging problems in the video surveillance applications addressed including shadows, repeated motions of background and illumination changes. To show the ability of the proposed algorithm to handle key challenges of real-world videos, it has been applied to several sequences with different frame rates and detection challenges. In order to better understand the performance of the algorithm, we use seven real video sequences, which are "traffic" "campus" "intelligent room" "hall monitor" "laboratory" "people" and "traffic2", to test each method by results simulation and qualitative evaluation. Concerning each motion detection challenge, one or more videos have been selected.

A. Simulation results

This part presents the experimental result comparison between our algorithm for moving objects and other motion detection methods, including the Mixture of Gaussian algorithm MOG [27] and multiple $\Sigma-\Delta$ estimation MDE method [28]. The first comparison is made with MOG being a widely exploited adaptive background subtraction algorithm. It has good performance for the stationary and the nonstationary backgrounds. The second compared algorithm is the robust method of (MDE) being done by estimating the static background. Detection results have been compared for the case where competitor methods exhibit the best possible performance as the results of other methods have been collected from [27,28] (figures 7, 8 and 9 of [27,28] and figure 6 of method exploiting fixed threshold).

The figure 6 describes the obtained results of "video sequences people" by applying an adaptive thresholding based on SWT techniques. Where 6.a' depicts the original frames and 6.b' stands for detection results of our algorithm. 6.c' and 6.d' are the detection results of foreground while the threshold value is set at 33 and 80. In this video, it may be observed that the approach exploited set thresholds fails to generate good results in the presence of diverse frames, for a high threshold value, noise positions will be wrongfully detected as foreground objects. It may be seen that our algorithm can detect and separate the moving objects of walking persons almost perfectly.

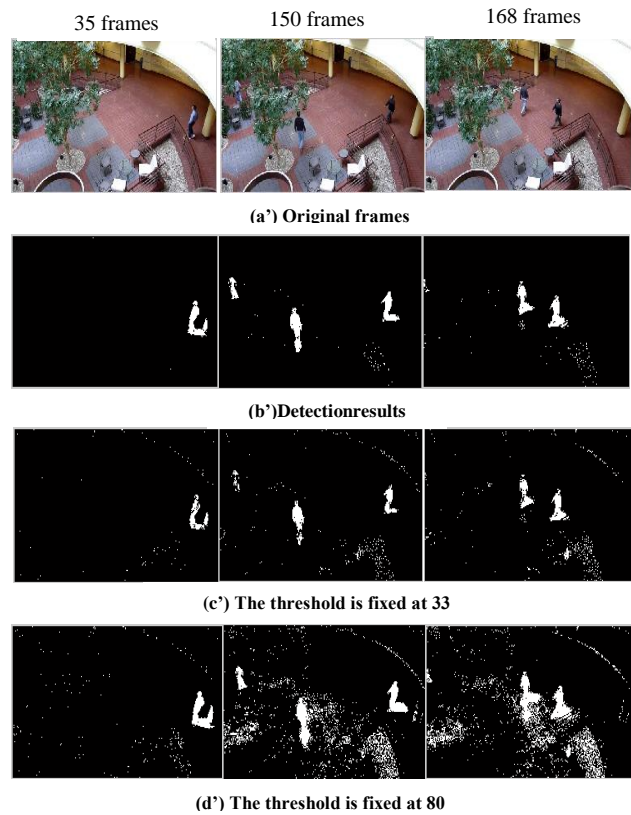
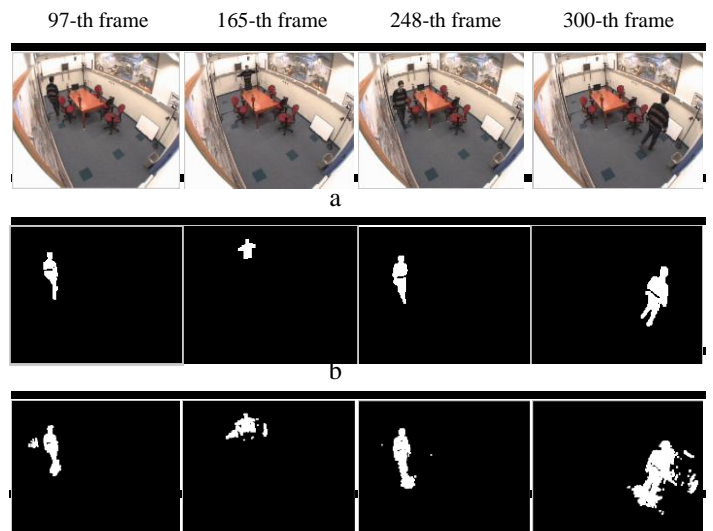


Fig. 6. Detection results of proposed algorithm compared with the method using fixed threshold

In Fig. 7(a), a man is walking in a room. Some system noises are present in this video sequence due to the low quality of the camera. As presented in Fig 7(c) and 7(d), both MOG and MDE methods produce serious noise by the noisy systems. Our approach applies after subtracting the background frame and the current frame image, an adaptive threshold using stationary wavelet transforms 2D to compute the characteristic for the probabilities of the background and the foreground. Therefore, the proposed algorithm can detect the moving objects and remove the shadows of walking persons, as shown in Fig. 7(b).



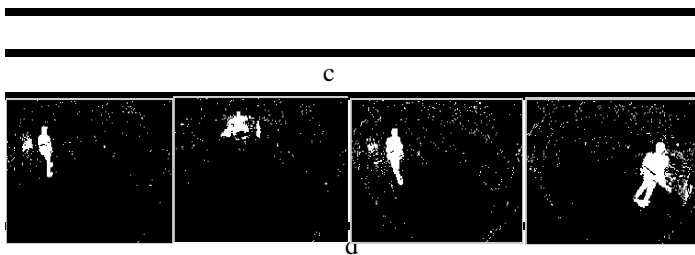


Fig. 7. Detection results of our algorithm compared with indoor sequence with shadows

In Fig. 8(a'), a set surveillance camera takes a scene with different vehicles from one direction. As presented in Fig. 8(c'), the MOG algorithm exploits many Gaussian kernels to produce a mixture background model, thus producing the motion challenging problems. Compared with the MOG, the MDE algorithm also produces a mixture background model by constant sign computation. Moreover, constant sign computation is also applied to compute the threshold parameter in terms of motion detection. Regrettably, the threshold value is still changed when the novel pixel presents the background, thus detecting the false object pixels, as presented in Fig. 8(d'). The suggested algorithm detects the moving object by comparing the background values and the foreground values that are computed by adaptive threshold using SWT. Hence, noise artifacts with sudden illumination changes caused on off lights are reduced in the detection results described in Fig. 8(b').

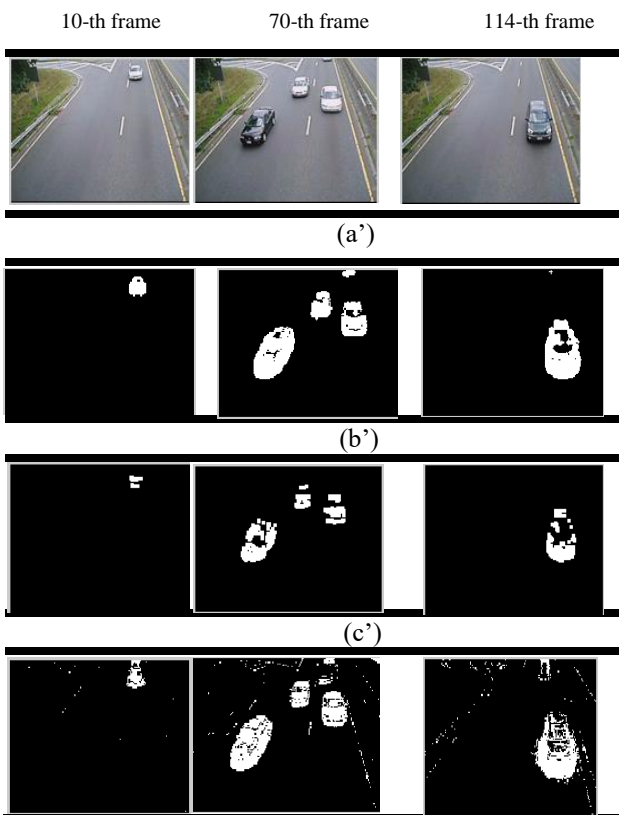


Fig. 8. Detection results of the suggested algorithm compared with sequence with varying illumination

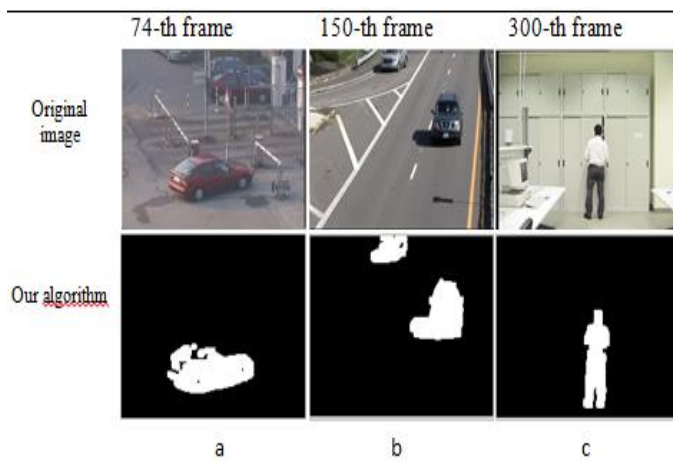


Fig. 9. Detection results of the proposed method on different Scene

Figure 9 depicts the performance of the proposed algorithm on three other videos with the same challenges discussed above.

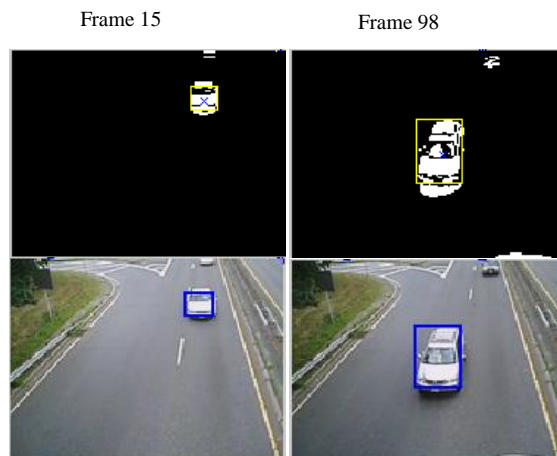


Fig. 10. Tracking results of the traffic video

Figure 10 presents the tracking results for a video traffic of moving cars in an indoor sequence. The experiments affected the tracking of moving object exploiting the adaptive background subtraction based on stationary wavelet transforms and Kalman filtering. The moving target may be detected and tracked effectively with our algorithm at frames 98 and 15. Row 1 is the detection results and row 2 is the tracking results.

TABLE II. THE RESULTS OF OBJECTS DETECTION AND TRACKING

Video		c	d	e	Proposed algorithm
traffic	detection	10	7	5	10
	tracking	7	5	3	9
Correction Rate (%)		70	50	30	90

The table.2 shows the comparison of performance between the suggested method and the algorithm using different fixed

thresholds, the best performance of detection and tracking was obtained by our adaptive threshold algorithm.

B. Quantitative evaluation

To evaluate the effectiveness of the suggested algorithm, we exploited the parameters (precision and recall) for compare the proposed method to the other algorithms the parameters are defined as follows:

$$recall = \frac{Tp}{Tp + Fn}$$
$$precision = \frac{Tp}{Tp + Fp}$$
$$F - measure = \frac{2 * recall * precision}{recall + precision}$$

Where Tp is total number of true positive pixels, Fn presents the number of false negative pixels, Fp presents the number of false positive pixels. The Table 1 describes the results of accuracy values for Traffic sequence.

TABLE III. COMPARISON OF DIFFERENT METHODS FOR THE OBJECT DETECTION EXPERIMENT

	Hall monitor			Intelligent room		
	Recall	precision	F-measure	Recall	precision	F-measure
MDE[28]	0.53	0.83	0.64	0.83	0.2	0.32
MOG[27]	0.78	0.83	0.8	0.82	0.72	0.76
Proposed algorithm	0.76	0.87	0.8	0.79	0.86	0.82

Table 3 shows the average f_measure rate of each algorithm for "Hall monitor, intelligent room" test scenes. As a result, the suggested algorithm attains the biggest f_measure values compared to other mentioned methods. In particular, we can easily show that the proposed method attains better accuracy rates of all metrics than 85% concerned to motion detection.

V. CONCLUSION

This paper used a background subtraction to detect the objects moving through an adaptive threshold technique based on SWT in order to improve our algorithm to detect and track the moving targets. The suggested algorithm does not only outperform the drawbacks of high complex calculation and slow speed for the background subtraction, but also preserves the wavelet characteristics of the flexible multi-resolution image and the capacity for processing with noises and wrong motion such as moving leaves of trees. Compared to other algorithms, the experimental results prove that the proposed approach can detect and track the moving objects efficiently and with robustness. Moreover, the simplicity of the proposed method indicates that the approach can be implemented in different intelligent systems.

REFERENCES

[1] M. Haag and H. H. Nagel, "Incremental recognition of traffic situations from video image sequences," *Image Vis. Comput.*, vol. 18, no. 2, pp. 137–153, Jan. 2000.

[2] G. Ginesu, D. D. Giusto, and V. Margner, "Detection of foreign bodies in food by thermal image processing," *IEEE Trans. Ind. Electron.*, vol. 51, no. 2, pp. 480–490, Apr. 2004.

[3] S. Park and J. Aggarwal, "A hierarchical Bayesian network for event recognition of human actions and interactions," *Multimedia Syst.*, vol. 10, no. 2, pp. 164–179, Aug. 2004.

[4] A. C. Shastri and R. A. Schowengerdt, "Airborne video registration and traffic-flow parameter estimation," *IEEE Trans. Intell. Transp. Syst.*, vol. 6, no. 4, pp. 391–405, Dec. 2005.

[5] J. Melo, A. Naftel, A. Bernardino, and J. Santos-Victor, "Detection and classification of highway lanes using vehicle motion trajectories," *IEEE Trans. Intell. Transp. Syst.*, vol. 7, no. 2, pp. 188–200, Jun. 2006.

[6] H. Cheng, N. Zheng, X. Zhang, J. Qin, and H. Wetering, "Interactive road situation analysis for driver assistance and safety warning systems: Framework and algorithms," *IEEE Trans. Intell. Transp. Syst.*, vol. 8, no. 1, pp. 157–167, Mar. 2007.

[7] M. Castrillon, O. Deniz, C. Guerra, and M. Hernandez, "ENCARA2: Real-time detection of multiple faces at different resolutions in video streams," *J. Vis. Commun. Image R.*, vol. 18, no. 2, pp. 130–140, Apr. 2007.

[8] S. Cherng, C.-Y. Fang, C.-P. Chen, and S.-W. Chen, "Critical motion detection of nearby moving vehicles in a vision-based driver-assistance system," *IEEE Trans. Intell. Transp. Syst.*, vol. 10, no. 1, pp. 70–82, Mar. 2009.

[9] A. Licsar, T. Sziranyi, and L. Czuni, "Trainable blotch detection on high resolution archive films minimizing the human interaction," *Mach. Vis. Appl.*, vol. 21, no. 5, pp. 767–777, Aug. 2010.

[10] A. Amditis, E. Bertolazzi, M. Bimpas, F. Biral, P. Bosetti, M. Da Lio, L. Danielsson, A. Gallione, H. Lind, A. Saroldi, and A. Sjögren, "A holistic approach to the integration of safety applications: The INSAFES subproject within the European framework programme 6 integrating project PReVENT," *IEEE Trans. Intell. Transp. Syst.*, vol. 11, no. 3, pp. 554–566, Sep. 2010.

[11] M. Ding, Z. Tian, Z. Jin, M. Xu, and C. Cao, "Registration using robust kernel principal component for object-based change detection," *IEEE Geosci. Remote Sens. Lett.*, vol. 7, no. 4, pp. 761–765, Oct. 2010.

[12] J. L. Castro, M. Delgado, J. Medina, and M. D. Ruiz-Lozano, "An expert fuzzy system for predicting object collisions. Its application for avoiding pedestrian accidents," *Expert Syst. Appl.*, vol. 38, no. 1, pp. 486–494, Jan. 2011.

[13] C.-C. Chang, T.-L. Chia, and C.-K. Yang, "Modified temporal difference method for change detection," *Opt. Eng.*, vol. 44, no. 2, pp. 1–10, Feb. 2005.

[14] J.-E. Ha and W.-H. Lee, "Foreground objects detection using multiple difference images," *Opt. Eng.*, vol. 49, no. 4, p. 047 201, Apr. 2010.

[15] F. Barranco, J. Diaz, E. Ros, and B. Pino, "Visual system based on artificial retina for motion detection," *IEEE Trans. Syst., Man, Cybern. B, Cybern.*, vol. 39, no. 3, pp. 752–762, Jun. 2009.

[16] A. Doshi and A. G. Bors, "Smoothing of optical flow using robustified diffusion kernels," *Image Vis. Comput.*, vol. 28, no. 12, pp. 1575–1589, Dec. 2010.

[17] Yumiba, M. Miyoshi, and H. Fujiyoshi, "Moving Object Detection with Background Model based on Spatio-Temporal Texture," *IEEE Workshop on Applications of Computer Vision (WACV)*, 2011.

[18] K. K. Ng and E. J. Delp, "Object Tracking Initialization Using Automatic Moving Object Detection," in *Proc. of SPIE/IS&T Conference on Visual Information Processing and Communication*, vol. 7543, San Jose, CA, January 2010.

[19] ElhamKermani and DavudAsemani, "A robust adaptive algorithm of moving object detection for video surveillance" *EURASIP Journal on Image and Video Processing* 2014, 2014:27

[20] Chang S. G. (2000): Adaptive Wavelet Thresholding for Image Denoising and Compression, *IEEE transactions on Image processing*, Vol.9, No.9.

[21] Chang S.G.; Yu B.; Martin Vetterli (2000): Spatially Adaptive Wavelet Thresholding with Context Modeling for Image Denoising, *IEEE.trans.on image proc.*, VOL.9, no.9, PP.1522-1531.

- [22] W.E.L. Grimson, L. Lee, R. Romano, and C. Stauffer. Using adaptive tracking to classify and monitor activities in a site. In CVPR98, pages 22–31, 1998.
- [23] I. Haritaoglu, D. Harwood, and L.S. Davis. W4S: A real-time system for detecting and tracking people in 2 1/2-d. In ECCV98, 1998.
- [24] M. Isard and A. Blake. A mixed-state condensation tracker with automatic model-switching. In ICCV98, pages 107–112, 1998.
- [25] S. Mallat (1999). “A Wavelet Tour of Signal Processing”. Academic Press.
- [26] M. Kalpana Chowdary , S. Suparshya Babu , S. Susrutha Babu , Dr. Habibulla Khan“FPGA Implementation of Moving Object Detection in Frames by Using Background Subtraction Algorithm” International conference on Comm.unication and Signal Processing, April 3-5, 2013.
- [27] Ahmed Elgammal “Background Subtraction theory and practice” Morgan & cLaypool publishers.
- [28] S.-K. Wang, B. Qin, Z.-H. Fang, and Z.-S. Ma, “Fast shadow detection according to the moving region,” Proceedings of the International Conference on Machine Learning and Cybernetics, vol. 3, August 2007, pp. 1590–1595.
- [29] www.mors.org/UserFiles/file/.../Wavelet_Denoising.pdf.
- [30] Liu, Y., Yang, J., Meng, Q., Lv, Z., Song, Z., & Gao, Z. (2016). “Stereoscopic image quality assessment method based on binocular combination saliency model”. *Signal Processing*, 125, 237-248.
- [31] Li, W., Cosker, D., Lv, Z., & Brown, M. (2016). “Dense nonrigid ground truth for optical flow in real-world scenes”. arXiv preprint arXiv:1603.08120

Optimization of OADM DWDM Ring Optical Network using Various Modulation Formats

Vikrant Sharma

ECE Department

I.K.G. Punjab Technical University
Jalandhar (Punjab), India

Dalveer Kaur

ECE Department

I.K.G. Punjab Technical University
Jalandhar (Punjab), India

Abstract—In this paper, the performance of the ring optical network is analyzed at bit rate 2.5 Gbps and 5 Gbps for various modulation formats such as NRZ rectangular, NRZ raised cosine, RZ soliton, RZ super Gaussian, RZ raised cosine and RZ rectangular. The effect of insertion losses is analyzed. It is observed that RZ Soliton performs better than all other formats and using this scheme system can exist up to 95 dB insertion loss. It has been observed that there is a rise in the system performance for NRZ rectangular and RZ soliton formats after 10 GHz bandwidth.

Keywords—NRZ; RZ; OADM; WDM; ADM; ROADM; PRBS

I. INTRODUCTION

With the increasing requirement of bandwidth expansion & higher data rates, the network providers are moving towards the Optical Communication. Therefore, DWDM technology is developed to support tremendous bandwidth. An OADM drops one or more pre-selected wavelengths from the multi-wavelength signal entering the input fiber followed by adding of one or more pre-selected wavelengths into the multi-wavelength signal that exits from an output fiber. An optical add-drop multiplexer can be referred as certain kind of optical cross-connect [1,2].

In WDM ring network, the devices are connected in a circularly manner. Each node in this network works as a repeater and works under same protocol. The rings formed can be unidirectional or bidirectional depending upon the flow of data. In case of a unidirectional ring, a failure may occur due to breaking of cable or other damages in cable and thus may disrupt the signal flow. In case of bidirectional ring, no such failure occurs and the signal continues to travel even if cable breakdown occurs [3,4]. The most widely used fiber optical ring network is SONET (Synchronous optical network) which consists of bidirectional ring. Wavelength Division Multiplexing (WDM) is used in SONET ring. Even with the increase in online users, the data transfer rate does not get affected in WDM [5,6].

Add Drop Multiplexers (ADMs) are network elements that are used to bypass traffic through different nodes. Electronic ADMs indeed are very costly; thus, Optical Add-Drop Multiplexers (OADM) was introduced to cut down the cost. OADM can also be referred as wavelength add-drop multiplexers (WADM). With the use of OADMs, cost of network can be decreased as number of ADMs needed in the network decreases [7,8]. The WDM ring is presented in Fig. 1.

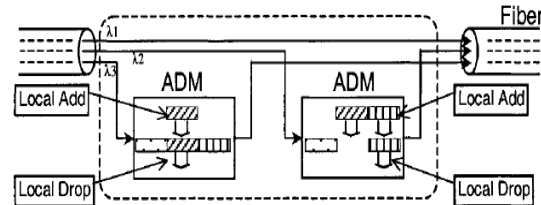


Fig. 1. WDM ring network

An OADM is a device which is employed to be used in WDM systems. OADMs are used for selecting the paths for different light channels entering or exiting a single mode fiber. “Add” here means to add new wavelength channels to the WDM signal and “Drop” means to remove the channels [9,10,11]. The internal structure of OADM system is presented in Fig. 2.

There are three stages in OADM. These are de-multiplexer, multiplexer and path between them used for adding or dropping signals. The de-multiplexer is used to separate the input signal in different wavelengths. The multiplexer is used to multiplex the wavelength from de-multiplexer and add port [12,13].

In Reconfigurable Optical Add-Drop Multiplexer (ROADM), Wavelength selective switching module is used to switch traffic from a WDM system at the wavelength layer. ROADM allows adding and dropping of channels in fiber without the need of converting it to electronic signal and then to optical signal [14,15].

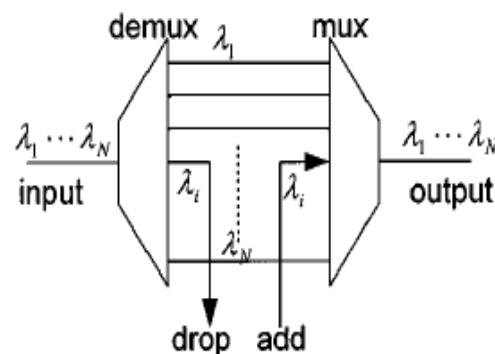


Fig. 2. Internal structure of OADM [1]

II. RELATED WORK

R.Randhawa et al. [16] investigated and compared the various network topologies. Analysis is done with the signal, as it passes through each node in each of the network topology. It was found that in case of ring topology, there was no detectable signal degradation in the ring network. An increase in quality factor was found in a ring network. In the case of bus topology, it was observed that with the increased number of nodes, the quality of signal decreases and the power penalty increases. For the star topology, it was observed that the received power values of each node at a same distance from the hub are same and performance was also same. The performance of tree topology was almost indistinguishable to the performance of the ring topology.

A.Sheetal et al. [17] presented the simulation analysis of 40 Gbps long haul DWDM System with enormous capacity up to 1.28Tb/s. The simulations were done for Carrier-Suppressed Return-to-Zero (CSRZ), Duobinary Return to-Zero (DRZ) and Modified Duobinary Return-to-Zero (MDRZ) modulation formats. A modified modulation format MDRZ was presented in the paper. A maximum transmission distance of 1450 km for 32 channels DWDM system was obtained with MDRZ modulation format using symmetric compensation.

Dhiman et al. [18] investigated different modulation formats for four-channel WDM CATV system with OADM. The impact of wavelength and frequency on eye opening and Q-value was observed for added & dropped channels at various length spans.

Sharma et al. [19] studied 16 wavelengths with channel spacing of 0.4 nm on unidirectional non-linear single mode fiber for 10 Gbps. The evaluation of the system was observed using different modulation formats such as RZ, NRZ, DPSK and CRZ using design parameters, namely, BER, eye diagram and Q²dB. It was observed that CRZ modulation capable of achieving BER of e^{-27} and Q factor in the range of 20.3.

S. Bang et al. [20] demonstrated the Q factor performance resulting from CPM and FWM effects for the signaling formats like NRZ, RZ, DPSK and the RZ-Soliton. It was found that RZ-Soliton was most efficient among all data formats used for 16 channel DWDM systems. It was also determined from the simulation results that DPSK signal is least affected by the generated FWM. It was concluded that DPSK signaling format was reliable for transmission of fiber.

III. MODULATION FORMATS

Various modulation formats are discussed as follows:

1) *NRZ Rectangular*: Depending upon the transmitted bit, an electrical output signal is obtained. When the input bit is '1', the output signal remains at the low level during the entire bit time and when input bit is '0', the output signal remains at high level during entire bit time.

2) *NRZ Raised Cosine*: It is same as NRZ rectangular, the only difference is that in this case the signal is forced to return to zero level at the end of each bit even if the two consecutive bits are '1'.

3) *RZ Rectangular*: In this case, the output signal has two electrical levels. When '1' is applied as input signal, a high is obtained at output for time period with the value of bit time multiplied with duty cycle and for the remaining time the output goes low. When '0' is applied as input signal the output remains low for the entire bit time.

4) *RZ Raised Cosine*: This is same as RZ rectangular modulation, the only difference is that the switching between the two levels i.e. high and low is not instantaneous. It has a raised cosine shape.

5) *RZ Super gaussian*: When '1' is applied as input, a super gaussian shaped pulse is obtained at the output and when '0' is applied as input, a low level signal is obtained at the output.

6) *RZ Soliton*: When '1' is applied as input a soliton shaped pulse is obtained at the output and when '0' is applied as input, a low level signal is obtained at the output.

IV. SIMULATION ENVIRONMENT

The block diagram of simulation setup is presented in Fig. 3. It is a 36-node ring network with one channel being added or dropped at each node. In order to analyze the network; performance parameters namely Q-factor, BER, and optical spectrum analyzer is provided at each node. The input source is low noise signal which is further connected to OADM. OADM is used to add and drop frequency at each node. The two nodes are connected by a fiber channel. A Single mode fiber of 100 km span having dispersion of 16 ps/nm/km and dispersion compensation fiber of 20 km span having dispersion of 80 ps/nm/km is utilized in the simulation. A semiconductor optical amplifier is used to boost the signal. Here the saturation power of SOA is set to 9.14 mw and the insertion loss at input and output is 3 dB. Since it is a ring network, all the frequencies are connected circularly such that frequency f_1 of node 1 is added and frequency f_{36} of node 36 is dropped and at next node f_3 is added and f_1 is dropped. The reference frequency is 193 and simulation is done at this frequency at bit rate 10 Gbps. The laser power for OADM is 0 dBm. PRBS sequence degree is 7, crosstalk is fixed at -90 dB and bandwidth of filter is 8 GHz.

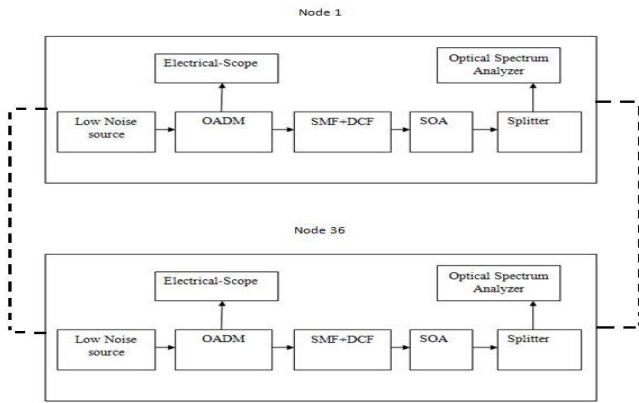


Fig. 3. Block diagram of simulation setup

V. SIMULATION RESULTS

The simulation setup is analyzed at four different bandwidths of OADM such as 5, 10, 15 & 20 GHz. The results are analyzed for different modulation formats such as NRZ raised cosine, NRZ rectangular, RZ soliton, RZ super Gaussian, RZ raised cosine and RZ rectangular. The simulation results are presented in Fig. 4 to Fig. 11.

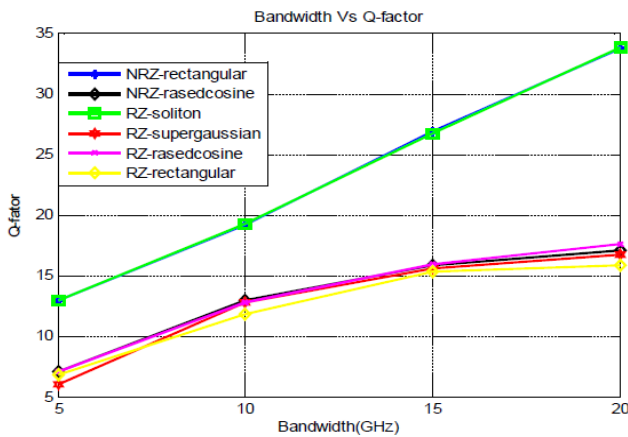


Fig. 4. Bandwidth versus Q-factor for 2.5 Gbps

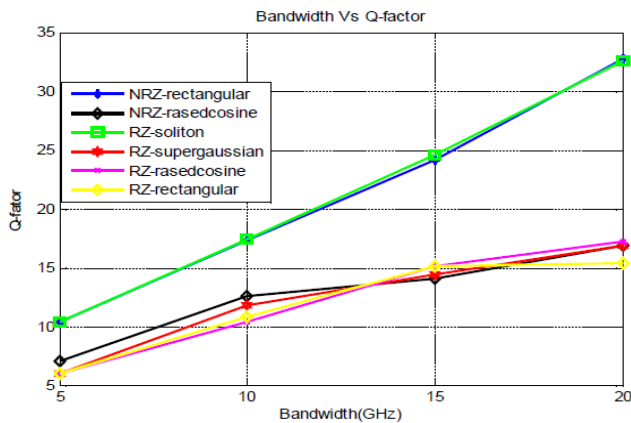


Fig. 5. Bandwidth versus Q-factor for 5 Gbps

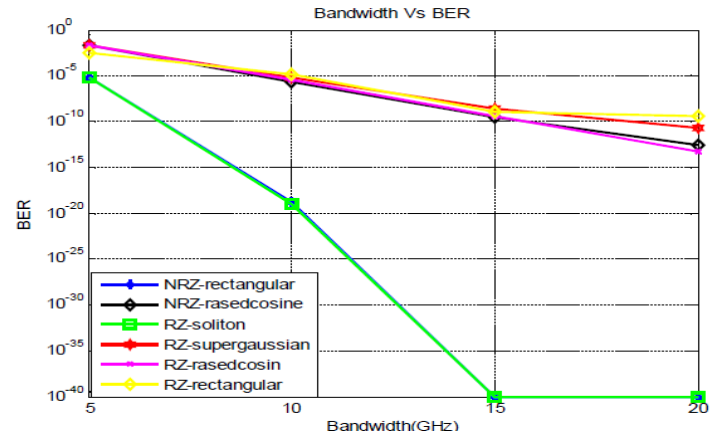


Fig. 6. Bandwidth versus BER for 2.5 Gbps

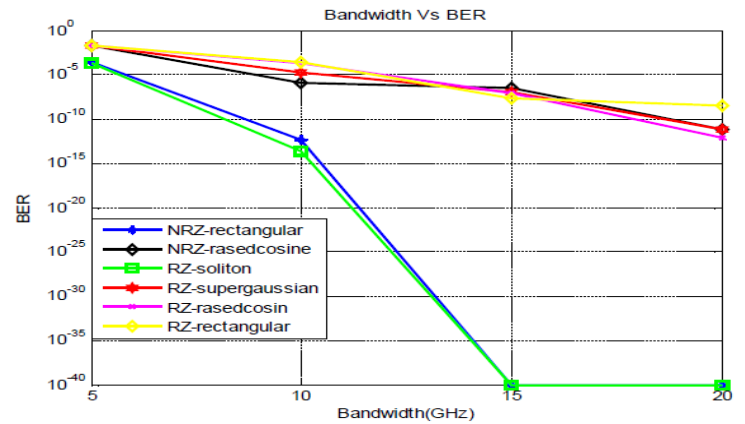


Fig. 7. Bandwidth versus BER for 5 Gbps

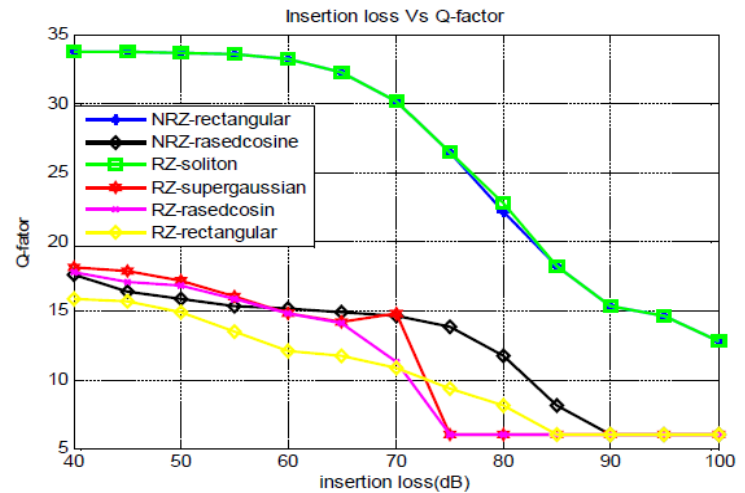


Fig. 8. Insertion loss versus Q-factor for 2.5 Gbps

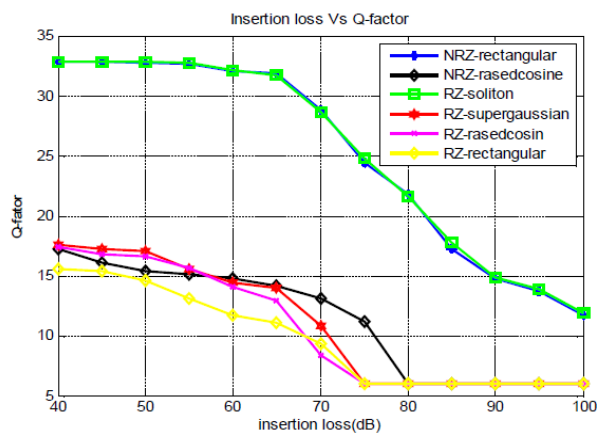


Fig. 9. Insertion loss versus Q-factor for 5 Gbps

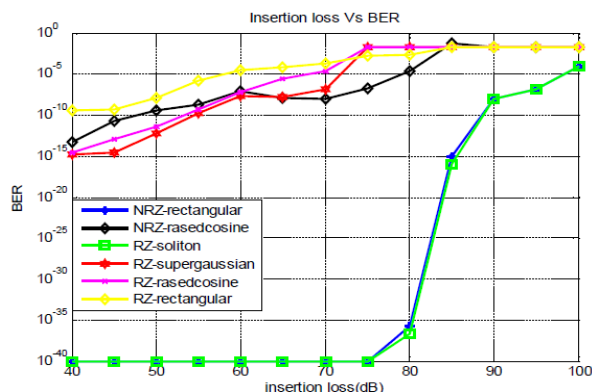


Fig. 10. Insertion loss versus BER for 2.5 Gbps

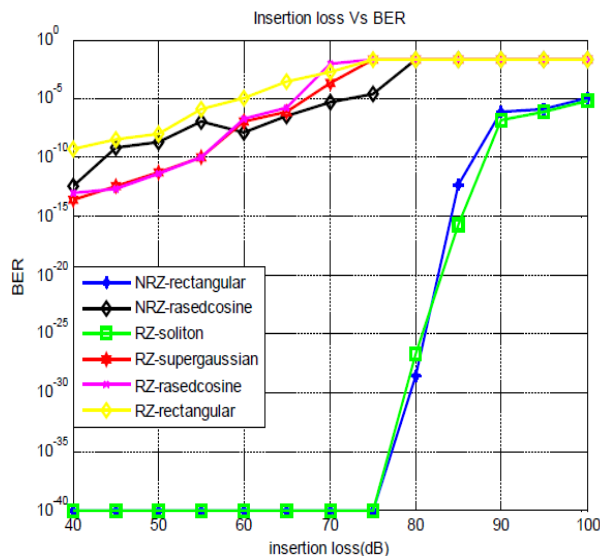


Fig. 11. Insertion loss versus BER for 5 Gbps

VI. DISCUSSION

The simulation results at 2.5 Gbps & 5 Gbps for Q-factor versus Bandwidth at different modulation formats are presented in Fig. 4 to Fig. 5 and Bandwidth versus BER are presented in Fig.6 and Fig. 7. NRZ rectangular and RZ soliton were observed to be better as compared to other modulation

formats. Q-factor of 33.6 dB was observed for NRZ rectangular modulation format and was observed to be 33.56 Db for RZ soliton modulation format for 20 GHz. The value of BER (bit rate error) for NRZ rectangular and RZ soliton is $1.6e^{-19}$ and $2.1e^{-14}$ respectively. It is observed from Fig. 5 that the Q factor reduces with increase in bit rate from 2.5 Gbps to 5 Gbps. Reduced Q factor value was observed to be 31.79 dB for NRZ rectangular modulation format and was observed to be 32.55 dB for RZ soliton modulation format for 20 GHz bandwidth. The value of BER for NRZ rectangular and RZ soliton is $4.2 e^{-13}$ and $2.1e^{-12}$ respectively. The simulation results at 2.5 Gbps & 5 Gbps comparison of Insertion Loss versus Q-factor for different modulation formats are presented in Fig.8 to Fig. 9 and Insertion Loss v/s BER are presented in Fig.10 and Fig. 11. It is observed from Fig. 8 and Fig. 9 that the value of Q factor for NRZ rectangular format and RZ soliton is 33.69 dB for insertion loss of 40 dB and these modulation formats have survivable BER up to insertion loss of 90 dB. It is observed from Fig. 10 and Fig. 11 that the Q factor is 32.79 and 32.82 for NRZ rectangular and RZ soliton modulation format respectively for insertion loss of 40 dB and these modulation formats have survival BER up to 85 dB.

VII. CONCLUSION

The performance of the ring optical network was analyzed at bit rate of 2.5 Gbps and 5 Gbps for various modulation formats. It was observed that the system could exist for 2.5 Gbps and 5 Gbps for RZ soliton and NRZ rectangular format at bandwidth less than 10 GHz. It was observed from the results that the quality of the signal was degraded as the frequency increased from 10 GHz, also, the value of Q factor and BER increases for RZ soliton and NRZ rectangular formats. Also, it was observed that 90 dB of insertion loss can be achieved for a system.

REFERENCES

- [1] S. Tibuleac and M. Filer, "Transmission Impairments in DWDM Networks with Reconfigurable Optical Add-Drop Multiplexers," Journal of Lightwave Technology, vol. 28, pp. 143-148, 2010.
- [2] A. Willner and S. Hwang, "Transmission of Many WDM Channels Through a Cascade of EDFAs in Long-Distance Links and Ring Networks", Journal of Lightwave Technology, Vol.13, No. 5, pp. 802-811, 1995.
- [3] S. Singh, "Investigation of Wavelength division multiplexed ring network topology to enhance the system capacity", International Journal of Light and Electron Optics, Vol. 125, No. 21, pp. 6527-6529, 2010.
- [4] K. Singh, N. Singh and G.Dhaliwal, "Performance Analysis of different WDM systems", International Journal of Engineering Science and Technology, Vol. 4, No. 3, pp. 1140-1144, 2012.
- [5] A. Borsali, H. Badaoudi, M. Aichi and W. Aichi, "Effect of Wavelength Spacing For WDM system on the Quality of Transmission", International Journal of Computer Science, Vol. 9, No. 2, pp. 441-443, 2012.
- [6] A. Aloisio, F. Ameli, A. Amico, R. Giordano, G.Giovanetti and V.Izzo, "Performance Analysis of a DWDM Optical Transmission System", IEEE transactions on Nuclear Science, Vol. 59, No. 2, pp. 251-255, 2010.
- [7] I. Trifonovs, V. Bobrovs and G. Ivanovs, "Optimization of a Bidirectional DWDM solution", Journal of Electronics and Electrical Engineering, Vol. 115, No. 9, pp. 37-40, 2010.
- [8] R. Goyal and R. Kaler, "A novel architecture of hybrid (WDM/TDM) passive optical networks with suitable modulation format", Optical Fiber Technology, Vol. 18, No. 6, pp. 518-522, 2012.

- [9] X. Liu, "Can 40-Gb/s Duobinary Signals be Carried Over Transparent DWDM Systems With 50-GHz Channel Spacing?", IEEE Photonics Technology Letter, Vol.16, No.6, pp. 1328-1330, 2005.
- [10] Q. Liu, N. Ghani and T. Frangieh, "Topology Abstraction Schemes in Multi-Domain Full Wavelength Conversion DWDM Networks", IEEE International Symposium on High capacity Optical Networks and enabling technology, Dubai, pp. 1-6, 2007.
- [11] S. Ghoniemy, K. George, and L. MacEachern, "Performance Evaluation and Enhancements of 42.7 Gbps DWDM Transmission System using Different Modulation Formats," Ninth Annual Communication Networks and Services Research Conference, pp. 189-194, 2011.
- [12] V. Sharma, A. Sharma, and D. Kaur, "Observation and Mitigation of power transients in 160 Gbps optical backhaul networks," European Scientific Journal, vol.9, pp. 327-332, 2013.
- [13] R. Randhawa, " Optimum performance and analysis of Ring Optical networks," Optik-International Journal for Light and Electron Optics, vol. 120, pp. 934-940, 2009.
- [14] M.Jazayerfar, S. Warm, R. Elschner, I.Sackey, C.Meuer, C. Schubert and K.Petermann, "Performance Evaluation of DWDM communications systems with Fiber Optical Parametric Amplifier", Journal of Lightwave Technology, Vol. 31, No. 9, pp. 1454-1461, 2013.
- [15] S. Singh and L. Kumar, "Performance Investigations on DWDM-OADM Optical Ring Network for CRZ Data Format at Different Fiber Length," International Journal of Scientific & Engineering Research, vol 2, pp. 186-191, 2011.
- [16] R.Randhawa and J. Sohal, "Comparison of optical network topologies for wavelength division multiplexed transport networks", International Journal For light and Electron Optics, Vol. 121, No. 12, pp. 1096-1110, 2010.
- [17] A.Sheetal, A. Sharma and R.Kaler, " Simulation of high capacity 40 Gb/s long haul DWDM system using different modulation formats and dispersion compensation schemes in presence of Kerr's effect", International Journal For light and Electron Optics, Vol. 13, No. 8, pp. 739-749, 2010.
- [18] A. Dhiman, T. Kaur, K. Singh, and K. Singh, " Performance analysis of different modulation formats in 4-channel CATV transmission system using OADM," Optik - International Journal for Light and Electron Optics, vol. 124, pp. 68101-6814, 2013.
- [19] A. Sharma and J. Malhotra, "Performance Optimization of Multichannel, High Speed DWDM OADM Ring," CiiT International Journal of Signal Processing, vol. 6, pp. 134-138, 2012.
- [20] S. Bang and D. Daut, "Analysis of CPM and FWM Phenomena for various signaling formats in 16 Channel DWDM", International Conference on Internet, Bishkek, Kyrgyzstan, pp. 37-41, 2005.

Performance Analysis & Comparison of Optimal Economic Load Dispatch using Soft Computing Techniques

Vijay Kumar, Associate Professor,
Adesh Institute of Technology,
Kharar (Mohali), India

Dr. Yaduvir Singh,
Harcourt Butler Technological Institute,
Kanpur, India

Dr. Jagdev Singh, Associate Professor,
Beant College of Engineering & Technology,
Gurdaspur, India

Dr. Sanjay Prakash Sood, Associate Professor,
Centre for development & advanced computing,
Mohali, India

Abstract—Power plants not situated at similar space from center of loads and their fuel prices are dissimilar. In this paper, ELD of actual power generation measured. ELD is preparation of generators to reduce total functioning price of generator units exposed to equality constraint of power balance within minimum and maximum working limits of producing units. In this paper FL, GAs & hybridization of GA-FL is utilized to find optimal solution of ELD systems. ELD resolutions found by resolving conservative load flow equations though at same time reducing fuel prices. Performance of results is analyzed by comparing the data values obtained with the help of soft computing techniques in ELD.

Keywords—ELD; FL; GA; FCGA

I. INTRODUCTION

ED is small term fortitude of optimal output of a lot of electricity generation amenities & to meet system load at nethermost probable cost subject to transmission and working restraints. ELD is resolved by particular computer software which honor operational and system restraints of existing possessions and consistent transmission abilities. In electrical power systems, a incessant equilibrium must be preserved among electrical generation and fluctuating load mandate, though system frequency, voltage stages and security too reserved constant. Besides, it is required that price of such generation be less. In addition, separation of load in producing plant develops a vital operation in addition to an economic matter which resolved at each load change (1%) or each 2-3 minutes. Research methods effectively castoff to resolve optimum load flow difficulties by using direct or non-linear encoding but these algorithms usually restricted to systematic functions. Numerous tasks are multi-modal, intermittent. Stochastic selection approaches used to improve these functions. Although customary resolution methods use features of problem to govern following sampling point, stochastic resolution methods make no such conventions. In its place, subsequent sampled point resolute centered on stochastic sampling or decision rules than a set of deterministic conclusion rules. GAs used to resolve tough difficulties with objective functions that not retain possessions such as

continuity, differentiability. These algorithms preserve and operate a set of answers and implement a existence of the fittest approach in their hunt for a improved solution.

The process of generation services to harvest energy at deepest price to constantly assist clients by identifying any working limits of generation and transmission services. Planning and process of power systems under prevailing circumstances, its growth and future growth requires load flow educations, short circuit studies and constancy studies. Though load flow studies are very important for planning, control and processes of prevailing & future growth as acceptable operation of the system be contingent upon knowing belongings of inter connection, new loads, new producing stations or new transmission lines afore they are installed.

II. LITERATURE SURVEY

G.Sahu et.al (2014) grants the presentation of GA to resolve ELD problem of power system. Planned algorithm verified on two dissimilar test systems seeing transmission damages. The chief cause of cutting total fuel cost and preserve power flows within safety range. **B. Hosamani et.al (2014)** addresses planning and operation of power systems and introduced an approach to provide consumers with reliable and quality power at an economical cost. The main intent of this paper is to develop efficient and fast Fuzzified Particle Swarm Optimization (FPSO) procedure to attain the optimum results of multi-constrained dynamic ED, OPF. This paper focuses on the multi- constrained dynamic economic dispatch problem and introduces the Fuzzified particle swam optimization to solve it. **S. H.Elyas et.al (2014)** introduces a proficient approach for comprehending problem of ELD with effect of valve point by utilizing a novel hybrid procedure for optimization. The fundamental goal for discovery resolution of problem of ELD is to plan the output of committed units of generator so as to fulfill the load of system under numerous operating imperatives. **B.Sahu (2013)** explains GA and quadratic programming ideas in resolving economic load dispatch (ELD) in which entire price of producing power is reduced with a valve point loading outcome though satisfying load request regardless of transmission line losses. **V. Karthikeyan (2013)**

explains that price competence is utmost significant problem of power system operations and makes an attempt to catch out the least price by using Particle Swarm Optimization Procedure considering statistics of three generating units. The paper involves the use of damage coefficients with maximum power limit and cost function. PSO and Simulated Annealing smeared to find out the least price for diverse power request. **F. Farheen et.al (2013)** presented operation of PSO for dynamic problem of ELD. The economic operation of the systems which are generating has constantly involved an imperative position in an industry of electric power. **A. Gharegozi et.al (2013)** presents a novel method to solve the issue of best planning using Cuckoo Search Algorithm. The proposed approach provides the most appropriate convergence in the response, high computational speed and high accuracy. **L. Chopra et.al (2012)** shows simple GA and refined GA technique applicable to ELD which books for reduction of price for operational constraints. Lambda iteration technique needs precise alteration of lambda which not provide global optimum resolution. **A. Hasan Zade et.al (2011)** describes ELD problem as a constrained optimization problem and hence efficient method needed to explain this problematic. The paper involves use of a particular variant of Evolutionary Algorithm namely DE to address ELD problem. Fuzzy logic controller designed to control the amplification factor vector of DE dynamically during the process of optimization. **S.C. Swain et.al (2010)** introduces the utilizations of techniques of computational intelligence to problems of ELD. The equation of fuel price of thermal plant is normally communicated a quadratic equation which is continuous. In conditions of real world, the equations of fuel cost occur discontinuous. In perspective of above, both cost equations which are continuous or discontinuous are considered in the present paper. **Bakirtzis. A (1994)** presented two GAs results to ELD. Benefit of GA resulting not enforce any convexity limitations on generator price function. Additional benefit for GAs for efficiently coded to effort on parallel machines. **A.G. Bakirtzis et.al (2002)** introduces an enhanced genetic algorithm for finding the solution of optimal power flow (OPF) with control variables which are both discrete and continuous. **H. Jagabondhu et.al (2009)** grants a relative learning of four diverse evolutionary algorithms i.e. GA bacteria foraging optimization, ant colony optimization and PSO for solving ELD. Concert of every algorithm for resolving ED problem analysed and simulation consequences are shown for precision, consistency and finishing time. **Altun H et.al (2008)** highlighted execution issues of soft computing methods for an effective solicitation to solve ED problem for inhibited optimization problem in power systems. The paper presents review of fundamentals of the methods and includes discussion of the implementation of methods in ED problematic. **A. Kandari et.al (2007)** grants a novel and precise technique for assessing input-output curve limits of power plants. These limits are very imperative for execution economic dispatch values. The greater the precision of projected coefficients, extra precise consequences attained from calculations of economic dispatch. **J. Nanda (2001)** resolves ELD problematic with Line flow limits over operative application of GA since losses of system transmission, power balance equation as equality constraint, active power generations of units and current limits in different lines for

inequality constraints. **Palanichamy et.al (1991)** offered a direct and computationally effective technique for ELD. The accustomed B coefficients used for calculation of transmission losses, incremental transmission losses and penalty factors.

III. ECONOMIC LOAD DISPATCH

ELD is one of substantial functions in automatic generation control. The Economic Load Dispatch of power production units is an important issue in electric utility industry. Schedule of individual units production which reduces total functioning price of a power system while meeting total load plus transmission losses in generator parameters. This is implication to save energy and tumbling emission.

The problematic goes more compound in great scale system henceforth problematic to find out optimum result due to nonlinear function which comprises number of local optimum. Therefore, importance to resolve this problematic precisely. For financial operation of system total ultimatum must be optimally collective between all generating units reducing total production rate though sustaining operative limits on system.

The fuel rate for all power generation unit explained firstly. Hence total production cost function of ELD problem is distinct as the whole sum of the fuel prices for all generating plant units as stated below:

$$F_T = \sum_{i=1}^{NG} \{a_i P_i^2 + b_i P_i + c_i |d_i \sin e_i (P_i^{\min} - P_i)|\},$$

Where, NG is total number of producing units

F_T is total generating price

P_i is the power output of producing unit i

P_i^{\min} is lowest output of producing unit i

a_i, b_i, c_i, d_i, e_i are fuel rate coefficients of unit i

Above equation calculates total generating rate of producing plant.

A. The Lambda –Iteration Method (LIM)

This is utmost prevalent technique to contract with ELD problematic. Here, variable introduced for solving constraint optimization problem which is said to be as Lagrange multiplier. Lambda explained by unraveling systems of equation. All inequality constraints gratified equations resolved by iterative technique

1) Let a appropriate value λ (0) & this value must be greater than prevalent capture of incremental rate distinctive of the numerous generators.

2) Calculate the separate generations

3) Check the equality

$$P_d = \sum_{n=1}^n P_n$$

B. Langrangian multiplier

Significant and simplest technique of stating economic dispatch load method as a transmission loss of generator power output is B- coefficients. The general formulae of loss formulae as:

$$P_L = \sum_{i=1}^k \sum_{j=1}^k P_i B_{ij} P_j$$

B_{ij} are loss coefficients or B-coefficients, P_i, P_j are real power injection of i th, j th buses.

Above inhibited optimization problematic changed into unrestricted optimization problem. Lagrangian multiplier is a method applied to minimize or maximize in equality constraints form. An augmented function is as:

$$L = C_t + \lambda (P_D + P_L - \sum_{i=1}^k P_i)$$

C_t is total fuel cost for all generating units and λ is said as Lagrangian multiplier. For minimizing the cost, L with P_i equal to zero.

C. Fuzzy Logic in ELD

The characteristic of fuzzy logic to deal with fuzzy or crisp values without much concern for precise input and continuous operation in case of feedback sensor failure makes it be called as robust and reliable method. Despite of wide variation in the inputs output control is smooth control function. The fuzzy logic controller operates on user-defined rules hence it adapted modify system performance. By the generation of appropriate governing rules the system can be incorporated with new sensors. Fuzzy logic is not limited one or two control outputs, and it is not essential to calculate rate-of-change of limits in order for implementation. The sensor data is sufficient because that provides some signal of system action.

The fuzzy modeling control system starts with deciding input and output variables of fuzzy logic. Mamdani fuzzy inference system used for this. This method used for fuzzy modeling process to acquire information about a data set to calculate the membership function limits which greatest permit the related fuzzy inference system to trail the specified input-output data. This FIS system intended for MISO system. MISO system comprises two inputs and one output.

D. Linguistic variables

These are variables stated in plain language words. These show an significant role in demonstrating crisp information such that it accurately suitable for the problem. Since usage of linguistic variables detected to decrease whole computation complication in many applications & mainly valuable in representing composite non-linear applications. Linguistic variables are fundamental to fuzzy logic operations, however they are frequently flouted in the arguments on the virtues of fuzzy logic. In fuzzy logic applications, non-numeric linguistic variables frequently applied relative to arithmetical values.

IV. RESEARCH METHODOLOGY

A. Algorithm for ELD Using GA

The numerous stages included in solution of GA Algorithm are:

- 1) Select Population extent, amount of generations, sub-strings length and quantity of trials.
- 2) Produce primary arbitrarily coded strings as population associates in the first generation.
- 3) Decipher population to acquire power generation of units in strings.

4) Implement load flow reflecting the unit generation excluding for the slack bus. To assess the system transmission losses, slack bus generation, line flows.

5) Calculate fitness of population members.

6) Execute selection centered on Reproduction executing. Roulette Wheel process with embedded Elitism trailed by crossover with embedded Mutation to produce the novel population for the subsequent generation.

B. Algorithm for ELD Using GA

Lambda iteration method decent loom to determine ELD due to which generator parameters easily controlled. The penalty factors applied to reflect the impact of losses. Fuzzy with ELD system is applicable to optimization problems. System will obtain optimum resolution to complications with fuzzy constrictions and fuzzy variables. The values of power which is obtained from ELD is then adjusted by fuzzy practical rules and gives more appropriate and approximate results for power of each unit.

- Compute optimal dispatch and entire rate ignoring losses λ .
- Use dispatch and loss formula, compute system losses. It explained by using MATLAB script and function file that use solve MATLAB function to resolve system of equations.
- Discover optimal dispatch for a entire generation of PD by coordination equations and loss formula.
- Economic dispatch problematic containing transmission losses computed for effect of transmission losses to represent total transmission loss as a quadratic function of generator power outputs.
- For minimum cost derivative of L (penalty factor) is required with each P_i equal to zero.
- For generating unit outputs P_1, P_2 and P_3 are power units of 1, 2 and 3 for better approximation. It can be designed as a flowchart as:

if $P_3 < P_{3min}$ $P_3 = P_{3min}$; else

if $P_3 > P_{3max}$ $P_3 = P_{3max}$; end end if $P_2 < P_{2min}$ $P_2 = P_{2min}$; else if $P_2 > P_{2max}$ $P_2 = P_{2max}$; end end if $P_1 < P_{1min}$ $P_1 = P_{1min}$; else if $P_1 > P_{1max}$ $P_1 = P_{1max}$;

- Units are ranked according to their full load production cost rate and committed accordingly.
- The system obtain optimal solution to problems with fuzzy constraints and fuzzy variables.

C. Algorithm for ELD Using Fuzzy-GA

- 1) First of all, adjust all limits population size, number of generations, sub-strings length.
- 2) Initial arbitrary population of individuals produced where the entities coded string of binary numerals.
- 3) Assessment of fitness population members accomplished on the basis of a fitness function.

- 4) When optimization benchmark happened, nominated population members more accepted on for diverse processes.
- 5) The assortment procedure is achieved.
- 6) Afterward, fuzzy logic originates into play with fuzzy crossover regulator.
- 7) The random member first associated with the crossover probability value and if benchmark gratified, border achieved.
- 8) Likewise for mutation, arbitrary member equated beside mutation probability value.

V. EXPERIMENTAL ANALYSIS & RESULTS

A. Results obtained for ELD using Genetic Algorithm

1) Power Generated

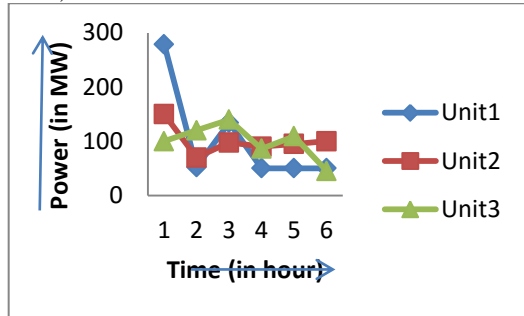


Fig. 1. Power generated

Figure 1 shows power generation for three units which varying according to time/hour. In unit-1 range of powers are 278.912, 52.260, 134.305, 50, 50 & 50 for different ranges which shown by blue lines in figure. In unit-2, power ranges are 150, 70, 97.77, 90, 95 & 100 for power ranges shown by red lines. In unit -3, power ranges are 100, 120, 140, 86.23, 109.30 & 45 for different maximum & minimum power ranges & shown by green lines in figure. All power are in MW.

2) Fuel Cost

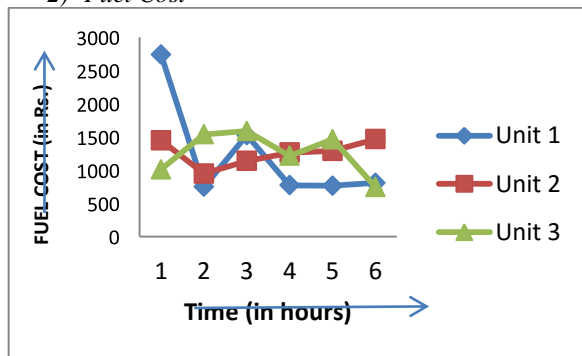


Fig. 2. Fuel Cost

Figure 2 describes fuel cost for three units & cost is according to time per hour. For unit 1 fuel costs are 748.55 to 2736.93 & shown by blue lines. For unit 2, fuel costs are 946.55 to 1465 for power intervals & shown by red lines. For unit 3, fuel costs are 745.18 to 1536.83 for power ranges & shown by green lines.

B. Results obtained for ELD using FL

Figure 5.2.1 shows fuzzy input membership functions. Membership function referred as “gaussmf” used for three linguistic variables low, medium, high for input variables. Figure shows input variable as high with a range of 0 to 150.

1) Fuzzy input (power) membership function

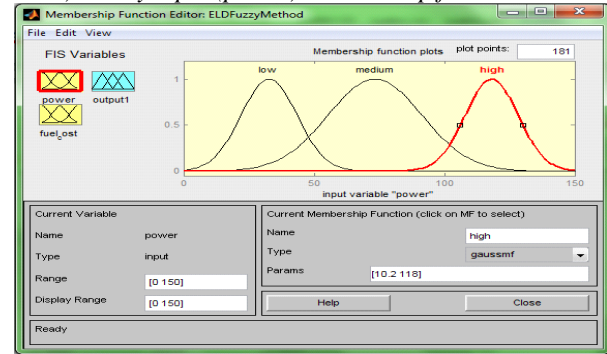


Fig. 3. Fuzzy input (power) membership function

2) Fuzzy output membership function

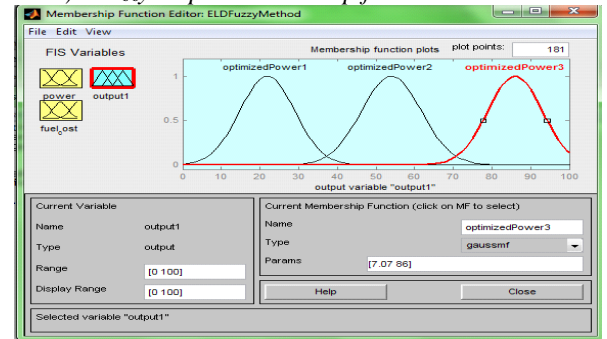


Fig. 4. Fuzzy output membership function

3) Linguistic Variables

TABLE I. LINGUISTIC LEVELS OF POWER INPUT

Input Parameters	Low	Medium	High
P(Power) in MW	0-60	30-130	80-150
Fuel cost (in Rs)	0-50	30-70	60-100

Three membership functions generated for input variable in fuzzy system. The low, medium and high are linguistic levels of power input. For input parameter of power low range is 0 to 60, medium range is 30 to 130 & high range is 80 to 150. For fuel cost low range is 0 to 50, medium range is 30 to 70 & high range is 60 to 100.

TABLE II. LINGUISTIC LEVELS OF OUTPUT VARIABLES

Output Parameters	Optimized Power1	Optimized Power2	Optimized Power3
Optimized Power (in MW)	0-42	30-80	65-100

Table no.2 shows linguistic levels for output variables. Here, Optimizedpower1, optimizedpower2 and optimizedpower3 are linguistic levels. Optimized power1 computed from 0 to 42, optimized power 2 computed is 30 to 80 & optimized power 3 computed as 65 to 100.

4) Surface Viewer

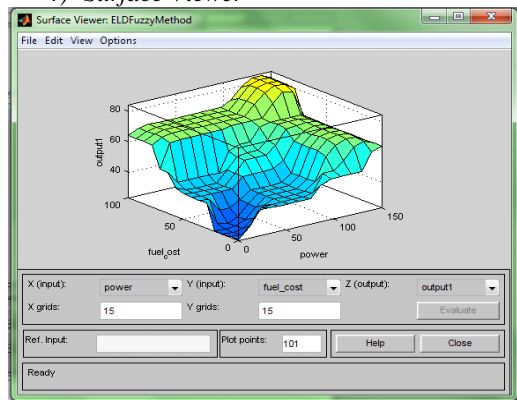


Fig. 5. Surface Viewer

Figure no.5 shows surface viewer is a GUI tool used for examine output surface of a FIS which is stored in a file for any inputs. It selects the two input variables to allot two input axes Y & X, this output value allotted to Z-axis. For a smoother plot creation, Plot point field is used to state number points so that membership functions calculated in input/output sort. Here, 101 is a default value which utilized to observe reliance of outputs for any input. Here, input axis shows as power & fuel cost & output axis as optimized power.

C. Results obtained for ELD using Genetic Algorithm infused with Fuzzy Logic

TABLE III. OPTIMAL RESULT OBTAINED USING GA

Pmin (PW)	Pmax (MW)	Power generated (MW)	Fuel cost (Rs)	Error (%)
50	150	50	772.5	0.1450
75	200	61.932	997.3	0.2131

TABLE IV. OPTIMAL RESULT OBTAINED USING FL

Pmi (MW)	Pmax (MW)	Power generated (MW)	Fuel cost (Rs)	Error (%)
50	150	69.24	779	0.105
75	200	81.321	1009	0.167

TABLE V. OPTIMAL RESULT OBTAINED USING FCGA

Pmin (M)	Pmax (MW)	Power generated (MW)	Fuel cost (Rs)	Error (%)
50	150	93.23	669.5	0.087
75	200	117.324	869.2	0.102

To acquire optimal solution for ELD system, comparison of all results done using minimum & maximum power limits. Here, generated power, cost of fuel & transmission errors

compared to achieve optimal solution. For powers of 50 MW to 150 MW, following observations obtained:

1) In GA, generated power is 50 MW for a fuel cost of Rs.772.5 & an error of 0.14501. In FL method, generated power is 69.24 MW with a fuel cost of Rs.779 & an error of 0.10501. In FCGA method, generated power is 93.23 with a fuel cost of 669.5 & an error of 0.00871. By comparing three parameters (as shown in figures nos.6,7 & 8) it is found that FCGA method generates more power with less fuel rates & transmission errors as compared to GA & FL methods.

2) For minimum power of 75 MW & maximum power of 200 MW, by comparing values in figure nos.6,7 & 8, it is again found that FCGA methods generates more power with less cost & transmission errors as compared to GA & FL methods.

D. Comparisons of soft computing methods to obtain optimal solution for ELD system

Comparison of power generation, fuel cost & errors depicted in figures for three methods.

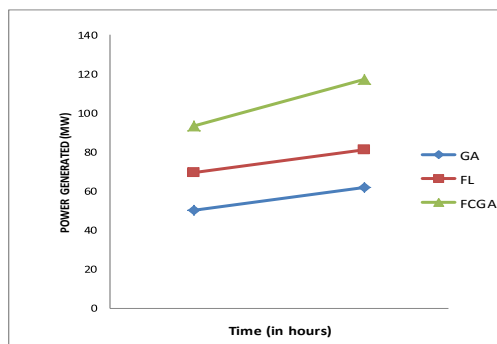


Fig. 6. Comparison of power generation

Figure shows that FCGA produces higher power levels as compared to FL & GA methods.

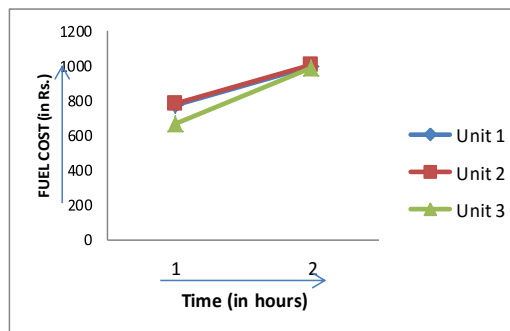


Fig. 7. Comparison of Fuel Costs

Fig.7. shows that FCGA has less fuel cost for power generation as compared to FL & GA methods.

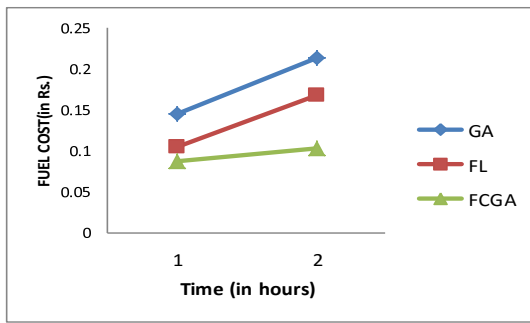


Fig. 8. Comparison of transmission errors

Figure no.8 shows, FCGA has less transmission errors for power generation as compared to FL & GA methods.

VI. CONCLUSION

Simulation results using GA, FL & GA infused fuzzy shows performance improvement between these algorithms. Results shows that GA infused fuzzy shows has better performance as compared to GA & FL techniques since FCGA considers average fitness, change in fitness, optimized crossover probability & optimized mutation probability variables. It observed that performance improvement of ELD increased as required minimum & maximum power ranges increased, resulting cost of power generation reduces with an increase of power generation using soft computing techniques. Transmission errors reduced to -0.0579 which is 39.93% less than GA method & -0.0179 which is 17.04% less as compared to FL method. So, performance improvement of ELD system is able to increase subsequently by reducing transmission error during generation of power. FCGA proved best for optimal solution of power generation with minimum cost & transmission errors as compared to GA & FL methods.

REFERENCES

- [1] Sarat Kumar Mishra, Sudhansu Kumar Mishra, "A Comparative Study of Solution of Economic Load Dispatch Problem in Power Systems in the Environmental Perspective", International Conference on Intelligent Computing, Communication & Convergence (ICCC-2014), Procedia Computer Science 48 (2015) 96 – 100, ELSEVIER
- [2] Bin XU, Ping-an ZHONG, Yun-fa ZHAO, Yu-zuo ZHU, Gao-qi ZHANG, "Comparison between dynamic programming and genetic algorithm for hydro unit economic load dispatch", Water Science and Engineering, 2014, 7(4): 420-432 doi:10.3882/j.issn.1674-2370.2014.04.007
- [3] R. Gopalakrishnan and A. Krishnan, "An efficient technique to solve combined economic and emission dispatch problem using modified Ant colony optimization", Sadhana Vol. 38, Part 4, August 2013, pp. 545–556, Indian Academy of Sciences
- [4] Sunil Kumar Singh, Lobzang Phunchok, Khwairakpam Chaoba Singh, Y R Sood, "Genetic Algorithm a Noble Approach For Economic Load Dispatch", International Journal of Engineering Research and Applications (IJERA) ISSN: 2248-9622, National Conference on Emerging Trends in Engineering & Technology (VNCET-30 Mar'12)
- [5] Nagendra Singh and Yogendra Kumar, "Multiobjective Economic Load Dispatch Problem Solved by New PSO", Hindawi Publishing Corporation Advances in Electrical Engineering Volume 2015, Article ID 536040, 6 pages, 10.1155/2015/536040
- [6] V.Karthikeyan, S.Senthilkumar & Vijayalakshmi, "A New Approach to the Solution Of Economic Dispatch Using Particle Swarm Optimization With Simulated Annealing", International Journal on Computational Sciences & Applications (IJCSA) Vol.3, No.3, June 2013
- [7] Ali Hasan Zade, Sayyed Mohammad Ali Mohammadi, Ali Akbar Gharaveisi, "Fuzzy logic controlled differential evolution to solve economic load dispatch problems", Received: 2011/08/07; Accepted: 2011/09/15 Pages: 29-40
- [8] Er. Mukesh Garg, Er. Manjeet Singh, Er. Vineet Girdher, "Comparative Study of Economic Load Dispatch (ELD) Using Modified Hopfield Neural Network", Proceedings of 'I-Society 2012' at GKU, Talwandi Sabo Bathinda (Punjab), International Journal of Computing & Business Research ISSN (Online): 2229-6166,
- [9] Paolo Dadone, "Design Optimization of Fuzzy Logic Systems", Dissertation submitted to the Faculty of the Virginia Polytechnic Institute and State University
- [10] S. H. Elyas, P. Mandal, A. U. Haque, A. Giani, Tseng Tzu-Liang, "A new hybrid optimization algorithm for solving economic load dispatch problem with valve-point effect", North American Power Symposium (NAPS), pp. 1-6, 2014.
- [11] François Chevre, François Guely, "Fuzzy Logic", Groupe Schneider, "Technical series"
- [12] Harpreet Singh, Madan M. Gupta, Thomas Meitzler, Zeng-Guang Hou, Kum Kum Garg, Ashu M. G. Solo, and Lotfi A. Zadeh, "Real-Life Applications of Fuzzy Logic", Advances in Fuzzy Systems, Volume 2013 (2013), Article ID 581879, 3 pages, 10.1155/2013/581879
- [13] Bhagyashree Hosamani, C R Sharada Prasad, "Analysis of Economic Load Dispatch Using Fuzzified PSO", IJRET : International Journal of Research in Engineering and Technology eISSN: 2319-1163 | pISSN: 2321-7308
- [14] Bishnu Sahu, Soumya Das, T. Manoj Patra, "Economic Load Dispatch in Power System using Genetic Algorithm", International Journal of Computer Applications (0975 – 8887) Volume 67– No.7, April 2013
- [15] Gajendra Sahu, Kuldeep Swarnkar, "Economic Load Dispatch by Genetic Algorithm in Power System", International Journal of Science, Engineering and Technology Research (IJSETR), Volume 3, Issue 8, August 2014 ISSN: 2278 – 7798
- [16] A. Bhattacharya and P. K. Chattopadhyay, "Solving complex economic load dispatch problems using biogeography-based optimization," Expert Systems with Applications, vol. 37, no. 5, pp. 3605–3615, 2010.
- [17] X. Xia, A.M. Elaiw, "Optimal dynamic economic dispatch of generation: A review", Electric Power Systems Research, (Elsevier), pp.975–986, 2010
- [18] S.C. Swain, S. Panda, A.K. Mohanty, C. Ardil, "Application of Computational Intelligence Techniques for Economic Load Dispatch" World Academy of Science, Engineering and Technology pp 63-69, 2010.
- [19] F. Farheen, M. A. Ansari, M. Kardam, "Implementation of particle swarm optimization for dynamic economic load dispatch problem", International Conference on Energy Efficient Technologies for Sustainability (ICEETS), pp. 1273-1278, April 2013.
- [20] Dubey Manisha, Dubey Aalok, "Genetic Algorithm Based Design of Fuzzy Logic Power System Stabilizers in Multimachine Power System", World Academy of Science, Engineering and Technology vol.66, pp.975-982.
- [21] Cho Sung-Bae, 2002 "Fusion of neural networks with fuzzy logic and genetic algorithm", Department of Computer Science, Yonsei University, pp.363–372.
- [22] Guo-Li Zhang ; Hai-Yan Lu ; Geng-Yin Li ; "Guang-Quan Zhang Dynamic economic load dispatch using hybrid genetic algorithm and the method of fuzzy number ranking", Machine Learning and Cybernetics, 2005. Proceedings of 2005 International Conference on (Volume:4) , 18-21 Aug. 2005, Page(s): 2472 - 2477 Vol. 4, IEEE
- [23] T. Yalcinoz, H. Altun, and M. Uzam, "Economic Dispatch Solution Using A Genetic Algorithm Based on Arithmetic Crossover", IEEE
- [24] Prof. Vikrant Sharma, Navpreet Singh Tung, Rashmi Rana and Vivek Guleria, "Fuzzy Logic Controller Modelling for Economic Dispatch and Unit Commitment in Electrical Power System", International Journal of Emerging Research in Management & Technology ISSN: 2278-9359 (Volume-2, Issue-10)
- [25] J. Nanda, R. Badri Narayanan, "Application of genetic algorithm to economic load dispatch with Lineflow constraints", Electrical Power and Energy Systems 24 (2002) 723-729

- [26] Bouktir.T, Mahdad.B, and Srairi.K., "Fuzzy Controlled Genetic Algorithm For Environmental/Economic Dispatch with Shunt FACTS Devices", IEEE press, pp.201, 2003
- [27] Benasla.L, Belmadant.A and Rahli M., "Hooke-Jeeves' Method Applied to a New Economic Dispatch Problem Formulation" journal of information science and engineering 24, 907-917 (2008)
- [28] Song Y.H., Wang G.S., Wang P.Y. and Johns A.T., "Environmental economic dispatch using fuzzy logic controlled genetic algorithms," IEE Proc. Generation Transmission Distribution, vol. 144, pp. 377-382, July 1997.
- [29] Lily Chopra, Raghuwinder Kaur, "Economic Load Dispatch Using Simple And Refined Genetic Algorithm", International Journal of Advances in Engineering & Technology, ISSN: 2231-1963, Nov. 2012
- [30] Farooqi M.R., Jain P. and Niazi K.R., "Using Hopfield Neural Network for Economic Dispatch of Power Systems" , IEEE Power Engineering Conference, 2003. PECon 2003, Proceedings, Bangi, Malaysia, pp. 5-10, 15-16 Dec. 2003.
- [31] Park J.H., Kim Y.S., Eom I.K. and Lee K.Y., "Economic Load Dispatch for piecewise Quadratic Cost Function Using Hopfield Neural Network", IEEE Transactions on Power Systems, vol. 8, no. 3, pp. 1030-1038, Aug.1993.
- [32] AL-Kandari A.M. and El-Naggar K.M., "A genetic-based algorithm for optimal estimation of input-output curve parameters of thermal power plants," Springer Berlin / Heidelberg Journal of Electrical Engineering, vol. 89, no. 8, pp. 585- 590, Sept., 2007.
- [33] Roa C.A-Sepulveda, Herrera M., Pavez-Lazo. B, Knight U.G., Coonick A.H., "Economic Dispatch using fuzzy decision trees", Electric Power Systems Research 66 (2003) 115_/122, Dec 2002
- [34] King T.D., El-Hawary M.E. and El-Hawary F., "Optimal environmental dispatching of electric power systems via an improved hopfield neural network model." IEEE Transactions on Power Systems, vol. 10, no. 3, pp.1559-1565, Aug. 1995.
- [35] M. Sailaja Kumari1, M.Sydulu, "A Fast Computational Genetic Algorithm for Economic Load Dispatch", International Journal of Recent Trends in Engineering Vol. 1, No. 1, May 2009
- [36] Y. Labbi, D. Ben Attous, "A Hybrid GA-PS Method To Solve The Economic Load Dispatch Problem", Journal of Theoretical and Applied Information Technology, 2005 – 2010
- [37] R. Ouiddir, M. Rahli and L. Abdelhakem-Koridak, "Economic Dispatch using a Genetic Algorithm: Application to Western Algeria's Electrical Power Network", Journal Of Information Science And Engineering 21, 659-668 (2005)
- [38] Leandro dos Santos Coelho, Chu-Sheng Lee, "Solving economic load dispatch problems in power systems using chaotic and Gaussian particle swarm optimization approaches", Electrical Power and Energy Systems 30 (2008) 297–307, ELSEVIER
- [39] Hesham K. Alfares and Mohammad Nazeeruddin, "Electric load forecasting: literature survey and classification of methods", International Journal of Systems Science, 2002, volume 33, number 1, pages 23-34
- [40] Altun H. and Yalcinoz T, 2008 "Implementing soft computing techniques to solve economic dispatch problem in power systems," Expert Systems with Applications, vol. 35, pp. 1668–1678
- [41] Brar Y.S et.al, 2004 "Interactive fuzzy satisfying multi-objective generation scheduling", Asian Journal of Information Technology, Vol. 3, pp. 973-982.
- [42] Casillas Jorge et.al,2007 "Fuzzy-XCS: A Michigan Genetic Fuzzy System", IEEE Transactions on fuzzy systems, vol.15,pp97-107
- [43] Chang Y.C et.al,2005 "Optimal chiller loading by genetic algorithm for reducing energy consumption", Energy and Buildings (Elsevier), Vo.37, pp.147-155.
- [44] Chawla Gaganpreet et.al,2005 "Artificial Neural Network Applications for Power System Protection", Proceedings of IEEE Canadian Conference on Electrical and Computer Engineering, Saskatoon, Canada, pp. 1954-1957
- [45] Mahdad Belkacem et.al,2008"Optimal power Flow of the Algerian Network using Genetic Algorithm/Fuzzy Rules," Power and Energy Society General Meeting - Conversion and Delivery of Electrical Energy in the 21st Century, IEEE, pp. 1-8, 20-24.
- [46] Nanda J et.al, 1994 "Economic emission load dispatch with line flow constraints using a classical technique," IET Generation, Transmission and Distribution, vol. 141, no. 1, pp. 1–10
- [47] Ozansoy et.al, 2007 "The Real-Time Publisher/Subscriber Communication Model for Distributed Substation Systems", IEEE Transactions on Power Delivery, vol. 22, pp.1411-1423.
- [48] Phan Phi Anh and Gale Tim ,2007 "Two-Mode Adaptive Fuzzy Control With Approximation Error Estimator", IEEE Transactions on fuzzy system, vol.15pp. 943-955
- [49] Pothiya S et.al ,2008,"Application of multiple tabu search algorithm to solve dynamic Economic Dispatch considering generator constraints", Energy Conservation and Management vol. 49, no. 4, pp. 506-516.
- [50] Rabbani M.G et.al ,2004"Application of fuzzy controlled SMES unit in automatic generation control", Department of Electrical and Electronic Engineering Rajshahi University of Engineering & Technology 3rd International Conference on Electrical & Computer Engineering ICECE 2004, pp.28-30
- [51] Sayah Samir, Zehar Khaled ,2008 "Using Evolutionary Computation to Solve the Economic Load Dispatch Problem, Department of Electrical Engineering, vol. 12, p. 67-78
- [52] Coelho L.d.S, Mariani V.C,2009"Chaotic artificial immune approach applied to economic dispatch of electric energy using thermal units,"International Journal of Chaos, Solitons and Fractals(Elsevier) , pp 2376–2383.
- [53] Alireza Gharegozi and Rozbeh Jahani, "A New Approach for Solving the Unit Commitment Problem by Cuckoo Search Algorithm", Indian Journal of Science and Technology | Print ISSN: 0974-6846 | Online ISSN: 0974-5645, Vol 6 (9) | September 2013
- [54] Bakirtzis. A, Petridis.V, and Kazarlis.S, July 1904 "Genetic Algorithm solution to the Economic Dispatch problem", IEE Proc-Gener, vol.141, No.4
- [55] A. G. Bakirtzis, P.N. Biskas, C. E. Zoumas, V. Petridis, "Optimal power flow by enhanced genetic algorithm, IEEE Trans. On Power Systems, Vol. 17, pp. 229-236, May 2002.
- [56] Palanichamy C. and Shrikrishna K. (1991), "Simple algorithm for economic power dispatch" electrical power syst. Res, Vol.21 pp 174-153.

A New DTC Scheme using Second Order Sliding Mode and Fuzzy Logic of a DFIG for Wind Turbine System

^{1,*} Zinelaabidine BOUDJEMA

Department of Electrical Engineering
Laboratoire Génie Electrique et
Energies Renouvelables (LGEER),
University of Chlef, Hay Salem
02000, Algeria

² Rachid TALEB

Department of Electrical Engineering
Laboratoire Génie Electrique et
Energies Renouvelables (LGEER),
University of Chlef, Hay Salem
02000, Algeria

³ Adil YAHDOU

Department of Electrical Engineering
Laboratoire Génie Electrique et
Energies Renouvelables
(LGEER), University of Chlef, Hay
Salem 02000, Algeria

Abstract—This article present a novel direct torque control (DTC) scheme using high order sliding mode (HOSM) and fuzzy logic of a doubly fed induction generator (DFIG) incorporated in a wind turbine system. Conventional direct torque control strategy (C-DTC) using hysteresis controllers presents considerable flux and torque undulations at steady state period. In order to ensure a robust DTC method for the DFIG-rotor side converter and reduce flux and torque ripples, a second order sliding mode (SOSM) technique based on super twisting algorithm and fuzzy logic is used in this paper. Simulation results show the efficiency of the proposed method of control especially on the quality of the provided power comparatively to a C-DTC.

Keywords—DFIG; wind turbine; DTC; SOSM; super twisting; fuzzy logic

I. INTRODUCTION

Among all kinds of renewable energy sources that are being developed recently in the world, wind energy source is the fastest growing one [1]. Currently, variable speed wind turbine system (WTS) employing DFIG is the most popular technology in presently installed wind turbines [2]. This is because DFIG presents many advantages compared to other generators used in WTSs such as reduced converter size, improved efficiency, and economic benefits [3].

Stator vector control with proportional-integral (PI) regulators is the usual strategy employed currently for WTS based on DFIG [4,5]. This strategy presents a good decoupling between the two current axes (d and q), therefore the model of the DFIG becomes simple and PI regulators can be employed. However, this method of control is highly depends on the accuracy of the machine parameters, employs diverse loops and needs a big regulation strength in order to ensures stability during the whole speed domain [6].

To avoid the disadvantages of the field oriented control method, a novel DTC scheme has been discussed in this paper [7,4]. In the C-DTC strategy, torque and flux are directly regulated through switching table plus hysteresis regulators. However, some drawbacks brake the employ of these regulators, for example variable switching frequency and torque ripple [8,9]. In several research articles realized on DTC scheme, these undesirable problems are decreased by

employing space vector modulation (SVM) technique, but the control robustness was immolated [10,11].

In recent years, sliding mode control (SMC) based on the theory of variable structure systems (VSS) has been extensively employed for nonlinear systems. It uses a particular version of on-off control, or discontinuous signal across the sliding surface, satisfying the sliding mode condition, to achieve a robust control. However, the SMC has a major inconvenience which is the chattering effect created by the discontinuous part of control. In order to resolve this problem, various adjustments to the usual control law have been discussed. The approach based on boundary layer is applied in almost all cases [12]. Another efficiency solution consists to substitute the discontinuous control signal by fuzzy logic one has also been used recently in some research works [13-15]. For the same goal the notion of HOSM control has also proven its competence in [16,17] for different applications.

Some useful solutions for sliding mode DTC with small torque and flux undulations, applied for induction motor (IM) controls are presented in [18,19]. In [20], the authors suggest the using of a DTC with SOSM controllers employed to IM drive.

In the aim to design an advanced DTC with very small torque and flux undulations and without chattering effect, in our article we suggest to employ a new DTC scheme based on SOSM and fuzzy logic functions for a DFIG-based wind turbine. This is for essential objects, including reducing mechanical stresses and improving power quality provided to the grid. The SOSM technique generalizes the basic SMC design by integrating second order derivatives of the sliding variable [21]. A few of such controllers have been discussed in the literature [22-25].

The rest of the paper is arranged as follows. In section 2, the modeling of the DFIG-based WTS is presented. Section 3 provides the application of the SOSM-DTC scheme to the DFIG. In section 4 the novel SOSM-DTC strategy using on fuzzy logic algorithm is applied to the DFIG control. Section 5 discusses the simulation results to demonstrate the effectiveness of the proposed control strategy.

II. MODEL OF THE DFIG-BASED WTS

A. The WTS model

Equation (1) gives the expression of the power captured by a WTS:

$$P_t = \frac{1}{2} C_p(\lambda, \beta) R^2 \rho v^3 \quad (1)$$

Where, R , ρ , v , C_p , λ and β are respectively: radius of the turbine (m), air density (kg/m^3), wind speed (m/s), the power coefficient, the tip speed ratio and blade pitch angle (deg).

The power coefficient C_p is given as follows [26]:

$$C_p = (0.5 - 0.167)(\beta - 2) \sin \left[\frac{\pi(\lambda + 0.1)}{18.5 - 0.3(\beta - 2)} \right] - 0.0018(\lambda - 3)(\beta - 2) \quad (2)$$

With:

$$\lambda = \frac{\Omega_r R}{v} \quad (3)$$

Where, Ω_r is the wind turbine speed.

B. Model of the DFIG

The DFIG model in Park reference frame is given by [27,28]:

$$\begin{cases} V_{ds} = R_s I_{ds} + \frac{d}{dt} \psi_{ds} - \omega_s \psi_{qs} \\ V_{qs} = R_s I_{qs} + \frac{d}{dt} \psi_{qs} + \omega_s \psi_{ds} \\ V_{dr} = R_r I_{dr} + \frac{d}{dt} \psi_{dr} - \omega_r \psi_{qr} \\ V_{qr} = R_r I_{qr} + \frac{d}{dt} \psi_{qr} + \omega_r \psi_{dr} \end{cases}, \begin{cases} \psi_{ds} = L_s I_{ds} + M I_{dr} \\ \psi_{qs} = L_s I_{qs} + M I_{qr} \\ \psi_{dr} = L_r I_{dr} + M I_{ds} \\ \psi_{qr} = L_r I_{qr} + M I_{qs} \end{cases} \quad (4)$$

Where $(V_{ds}, V_{qs}, V_{dr}, V_{qr})$, $(I_{ds}, I_{qs}, I_{dr}, I_{qr})$, $(\psi_{ds}, \psi_{qs}, \psi_{dr}, \psi_{qr})$ are respectively the stator and rotor voltages, currents and fluxes, R_s and R_r are the resistances of the rotor and stator respectively, L_s , L_r and M are the inductance own stator, rotor, and the mutual inductance between two coils respectively.

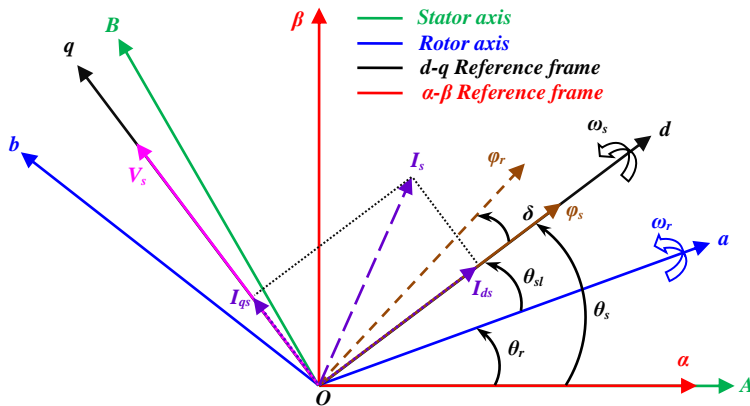


Fig. 1. Field oriented control technique

The stator and rotor pulsations and rotor speed are interconnected by the following equation: $\omega_s = \omega + \omega_r$.

Where ω_s and ω_r are respectively the stator and rotor electrical pulsations, while ω is the mechanical one.

The mechanical equation of the DFIG is:

$$C_{em} = C_r + J \cdot \frac{d\Omega}{dt} + F_r \cdot \Omega \quad (5)$$

Where we can express the electromagnetic torque C_{em} as follows:

$$C_{em} = \frac{3}{2} n_p \frac{M}{L_s} (\psi_{qs} I_{dr} - \psi_{ds} I_{qr}) \quad (6)$$

Where C_r , Ω , J , F_r and n_p are respectively: the load torque (Nm), mechanical rotor speed (rad/s), the inertia (kg.m^2), the viscous friction (Nm/s) and the number of pole pairs.

The stator powers of the DFIG are defined as:

$$\begin{cases} P_s = \frac{3}{2} (V_{ds} I_{ds} + V_{qs} I_{qs}) \\ Q_s = \frac{3}{2} (V_{qs} I_{ds} - V_{ds} I_{qs}) \end{cases} \quad (7)$$

To obtain a decoupled control between the stator active and reactive powers, we use a dq reference frame linked to the stator flux as shown in figure 1. Basing on equation (4) and supposing that the stator resistance can be neglected we can write:

$$\psi_{ds} = \psi_s \quad \text{and} \quad \psi_{qs} = 0 \quad (8)$$

$$\begin{cases} V_{ds} = 0 \\ V_{qs} = \omega_s \psi_s \end{cases} \quad (9)$$

$$\begin{cases} I_{ds} = -\frac{M}{L_s} I_{dr} + \frac{\psi_s}{L_s} \\ I_{qs} = -\frac{M}{L_s} I_{qr} \end{cases} \quad (10)$$

By using (9) and (10), equations (6) and (7) can be written as follows:

$$\begin{cases} P_s = -\frac{3}{2} \frac{\omega_s \psi_s M}{L_s} I_{qr} \\ Q_s = -\frac{3}{2} \left(\frac{\omega_s \psi_s M}{L_s} I_{dr} - \frac{\omega_s \psi_s^2}{L_s} \right) \end{cases} \quad (11)$$

$$C_{em} = -\frac{3}{2} n_p \frac{M}{L_s} I_{qr} \psi_{ds} \quad (12)$$

III. SOSM-DTC OF DFIG

The main objective of using SOSM-DTC is to develop a robust control of torque and rotor flux of the DFIG. In our system, the electromagnetic torque and flux are respectively controlled by V_{dr} and V_{qr} .

Chattering effect which is a serious problem that exists in the conventional SMC can be very hurtful for the DFIG because it can create some undesirable phenomenon such as torque pulsation, current harmonics and acoustic noise, etc [29]. To relieve the influence of this problem, various solutions have been proposed [30, 31]. HOSM is one of the solutions proposed recently to eliminate the effect of this problem. This control method can ensure eradication of this undesirable phenomenon because it can acts on the sliding surface and its 1st derivative ($S = \dot{S} = 0$) [17, 32]. On the other hand, to retain the main advantages of the usual method, they debate the chattering phenomenon and offer advanced precision in practice. In the last decade many research works have applied this type of control [22, 23].

The big problem that accompanies the HOSM control executions is the increased required information. Indeed, it's

necessary to know the derivatives of the surface $\dot{S}, \ddot{S}, \dots, S^{(n-1)}$ for performing an nth-order controller. Amid all algorithms used recently for the HOSM control, the super-twisting one is an exclusion. Indeed, this kind of algorithms needs just the information about S [24]. Therefore, the super twisting algorithm has been employed in this paper. As presented in [25], for all SOSM controllers stability can be easily verified with this algorithm.

The bloc diagram of the DFIG control using SOSM-DTC is shown in figure 2.

The SOSM controllers of rotor flux and electromagnetic torque are used to act successively on the two rotor voltage components as in (13) and (14) [20,33].

$$V_{dr} = K_1 |S_{\varphi_r}|^r \text{sign}(S_{\varphi_r}) + V_{dr1} \quad (13)$$

$$\dot{V}_{dr1} = K_1 \text{sign}(S_{\varphi_r})$$

$$V_{qr} = K_1 |S_{C_{em}}|^r \text{sign}(S_{C_{em}}) + V_{qr1} \quad (14)$$

$$\dot{V}_{qr1} = K_2 \text{sign}(S_{C_{em}})$$

Where the sliding mode variables are the flux magnitude error $S_{\varphi_r} = \varphi_r - \varphi_r^*$ and the torque error $S_{C_{em}} = C_{em}^* - C_{em}$, and the control gains K_1 and K_2 should verify the terms of stability.

A. Controller synthesis

Suppose a dynamic system defined as follows:

$$\frac{dx}{dt} = a(x,t) + b(x,t)u, \quad y = c(x,t) \quad (15)$$

where u is the input, x is the variable state and y is the output.

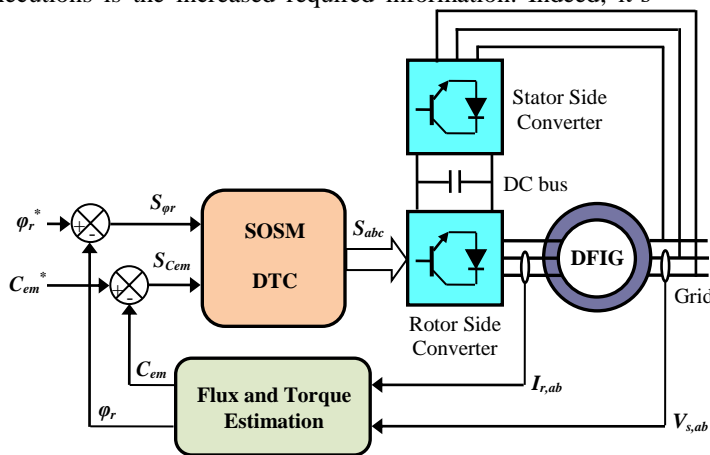


Fig. 2. Bloc diagram of the DFIG with SOSM-DTC

The main object of the control is to find an expression of the input $u = f(y, \dot{y})$ that be able to forces the trajectories of the system toward the beginning dot of the phase plane represented by $y = \dot{y} = 0$, if feasible in restricted period of time. Input u is supposed a new state variable, where the switching control is appended to its derived \dot{u} . Output y is regulated by a SOSM controller.

$$u = K_1 |S|^r \text{sign}(S) + u_1 \quad (16)$$

$$\dot{u}_1 = K_2 \text{sign}(S)$$

Where $S = y^* - y$ is the sliding surface.

As indicated by expressions (16), the appropriate stipulation for convergence to S that can verify stability is for the gains to be large sufficient [20].

$$K_1 > \frac{A_M}{B_m}, K_2 \geq \frac{4A_M}{B_m^2} \cdot \frac{B_M(K_1 + A_M)}{B_m(K_1 - A_M)} \quad (17)$$

Where $A_M \geq |A|$ and $B_M \geq B \geq B_m$ are the bigger and lower limits of A and B in the 2nd derivative of the output y .

$$\frac{d^2y}{dt^2} = A(x,t) + B(x,t) \frac{du}{dt} \quad (18)$$

IV. FUZZY SECOND ORDER SLIDING MODE DIRECT TORQUE CONTROL (FSOSM-DTC)

SOSM control has proven in several studies and research applications its effectiveness in minimizing chattering effect which is mainly caused by the presence of a discontinuous control term containing the *sign* function [13-15]. To ameliorate the SOSM-DTC of the DFIG and more and more decrease the adverse effect caused by the *sign* function, in this work we suggest to employ a hybrid approach of second order sliding mode and fuzzy logic by replacing this function by an inference fuzzy system.

For the proposed FSOSM-DTC, the universes of discourses are first divided into the seven linguistic variables NB, NM, NS, EZ, PS, PM, PB, triangular and trapezoidal membership functions are chosen to represent the linguistic variables for the inputs and outputs of the controllers.

The fuzzy labels used in this study are negative big (NB), negative medium (NM), negative small (NS), equal zero (EZ), positive small (PS), positive medium (PM) and positive big (PB).

Figure 3 describes these choices.

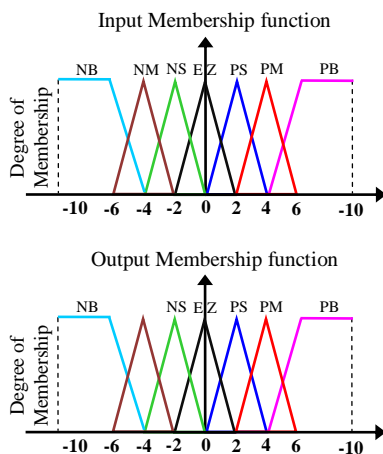


Fig. 3. Fuzzy sets and its memberships functions

V. SIMULATION RESULTS

In order to evaluate the proposed DTC strategy of the DFIG, simulation tests using MATLAB Software have been realized and discussed in this section. The DFIG parameters used in simulations are as follows: nominal stator power $P_{sn} = 1.5$ MW, $n_p = 2$, $R_s = 0.012 \Omega$, $R_r = 0.021 \Omega$, $L_s = 0.0137$ H, $L_r = 0.0136$ H, $M = 0.0135$ H, $F_r = 0.0024$ Nm/s, $J = 1000$ kg.m². C-DTC, SOSM-DTC and FSOSM-DTC are evaluated by simulations regarding tracking performances, total harmonic

distortion (THD) of stator current and robustness versus variation of machine parameters.

A. Tracking performances

This test has the goal to analyze and compare the behavior of the three used DTC control methods regarding tracking performances. The obtained simulation results are shown by figures 4-7. As it's shown by figures 4-6, electromagnetic torque and rotor flux curves for the three used DTC methods follows excellently their references. Furthermore, we observe that the FSOSM-DTC and SOSM-DTC strategies guarantee the decoupling between the d and q axes contrary to the C-DTC where the coupling trace between them is somewhat clear. Otherwise, figure 7 illustrates the harmonic spectrums of the stator current for the three DTC control methods. Through this figure, it can be noticed that the total harmonic distortion (THD) is minimized for the SOSM-DTC method (THD = 1.31%) when compared to the C-DTC one (THD = 2.22%) and the THD is more and more reduced by using fuzzy logic (THD = 1.15%). Based on the results above, it can be said that the FSOSM-DTC has proven its efficiency in reducing chattering phenomenon in addition to keeping the same advantages of the SOSM-DTC scheme.

B. Test of Robustness

In order to examine the performances of the three DTC control methods regarding robustness against variation of machine parameters, these last have been deliberately modified as follows: the values of R_s and R_r are multiplied by 2 while the values of L_s , L_r and M are divided by 2. The DFIG speed was kept equal to its face value. Figures 8-10 illustrate the obtained simulation results. These results show clearly that parametric variations test augment somewhat the time-response of the results obtained with C-DTC method. In addition, these results demonstrate that the parametric variations generate a visible influence on electromagnetic torque and rotor flux curves and that the influence seems more significant for the C-DTC compared to the other DTC schemes. Therefore, it can be concluded that the new proposed FSOSM-DTC scheme and in addition to its efficiency in reducing chattering phenomenon has kept the most important advantage of the SMC approach which is the robustness.

VI. CONCLUSION

In this paper, a new DTC scheme of a doubly fed induction generator attached to the electric network through the stator part and fed by a back to back inverter by the rotor part has been discussed. Firstly, a modeling of a DFIG-based wind turbine has been presented. Frequently used in the WTSs, this generator presents several benefits such as variable speed function and the ability to work in the four quadrants. Secondly, a new DTC scheme using SOSM and fuzzy logic is synthesized and compared to both C-DTC and SOSM-DTC. In term of tracking performances electromagnetic torque and rotor flux curves for the three used DTC methods follows excellently their references, however a problem of coupling is emerged in the C-DTC curves that is removed with the other SOSM-DTC methods. Furthermore, the obtained results have approved that the FSOSM-DTC works with a lesser chattering effect. A test of robustness has also been elaborated in this paper where the machine parameters have been deliberately changed. After

these variations, a few ripples have been induced on the curves of electromagnetic torque and rotor flux but with a significant influence with the C-DTC strategy compared to the other DTC

methods. In light of the obtained results, one can conclude that the proposed FSOSM-DTC scheme represents an important tool for systems using DFIG such as WTSs.

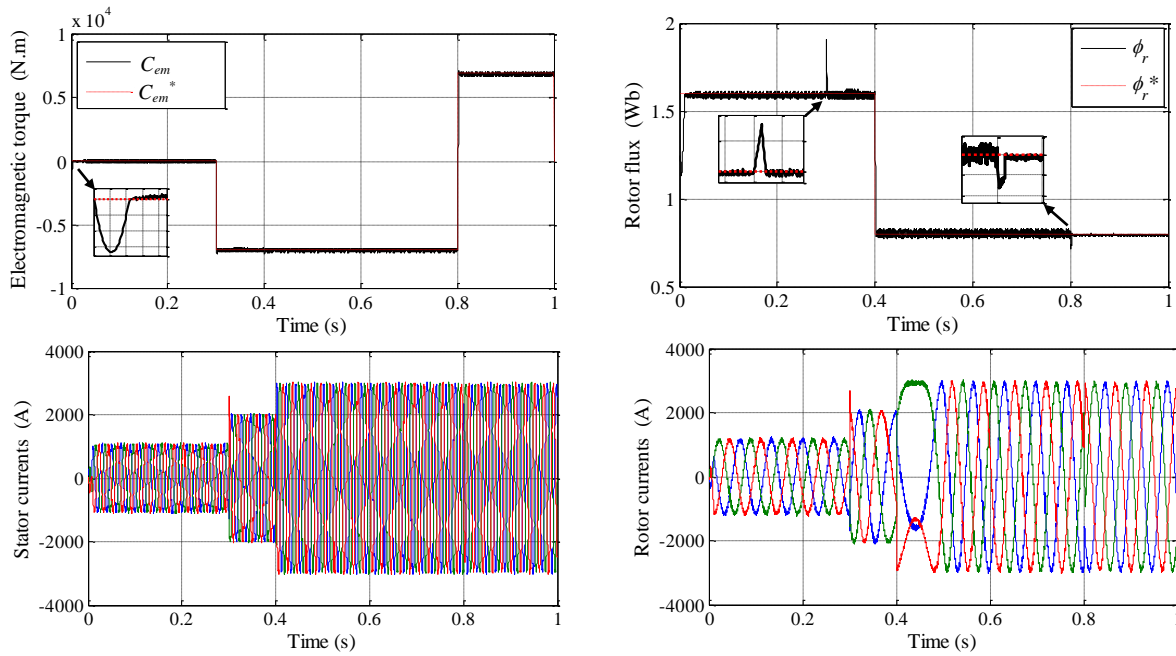


Fig. 4. C-DTC strategy responses (reference tracking test)

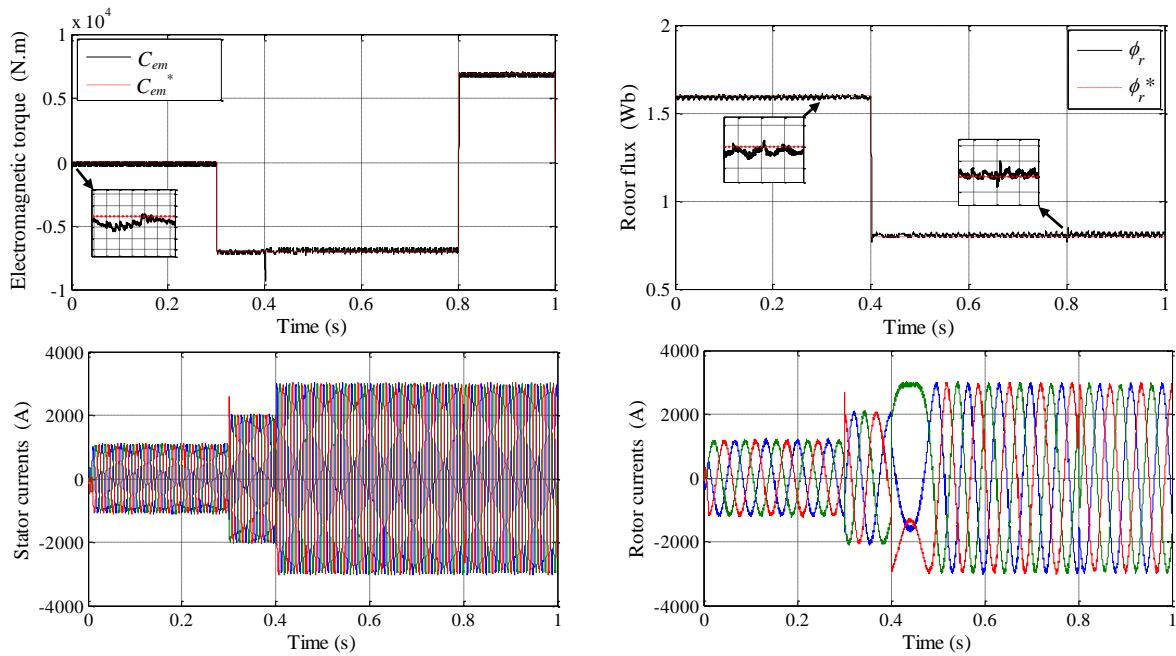


Fig. 5. SOSM-DTC strategy responses (reference tracking test)

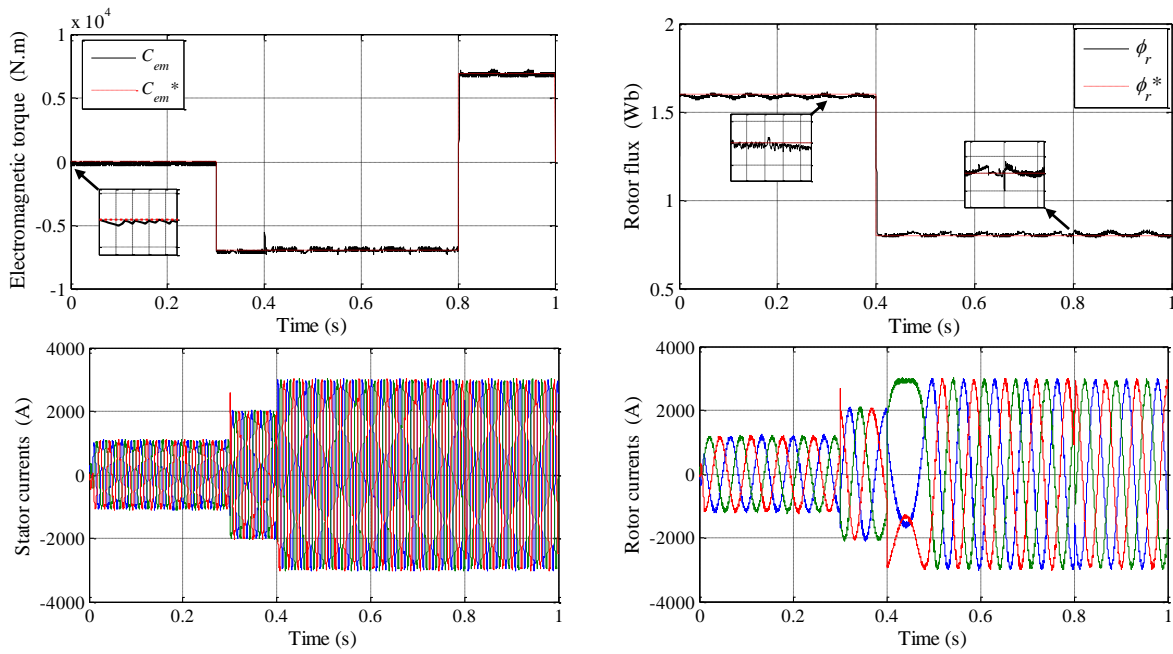


Fig. 6. FSOSM-DTC strategy responses (reference tracking test)

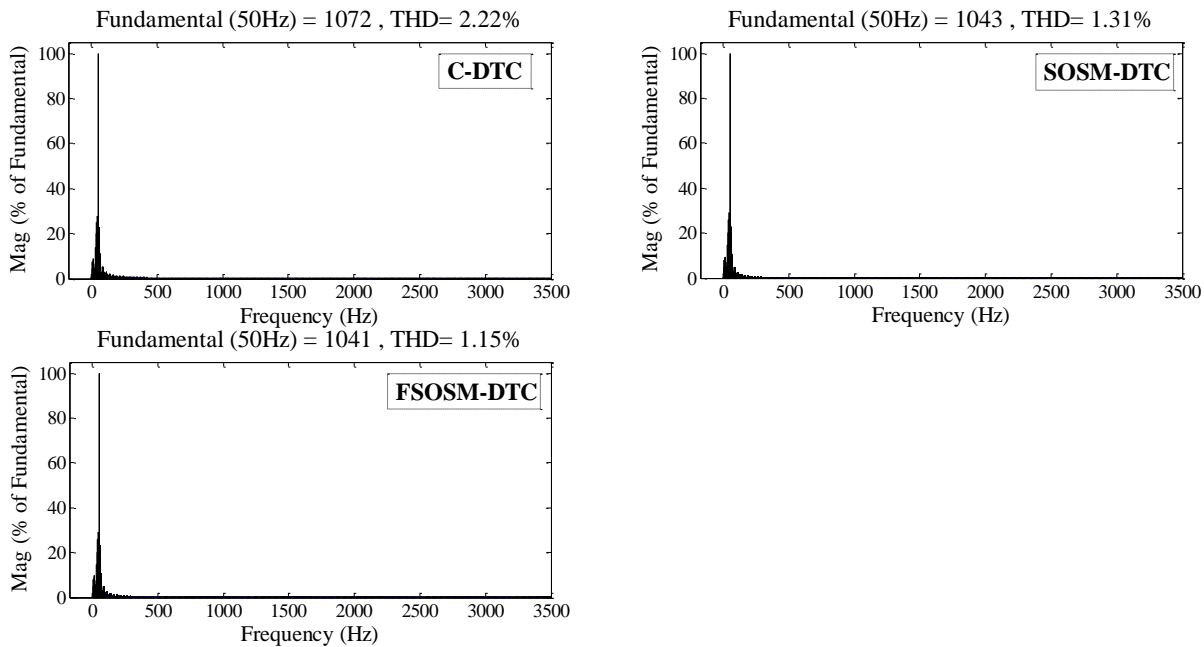


Fig. 7. THD of one phase stator current for a DFIG

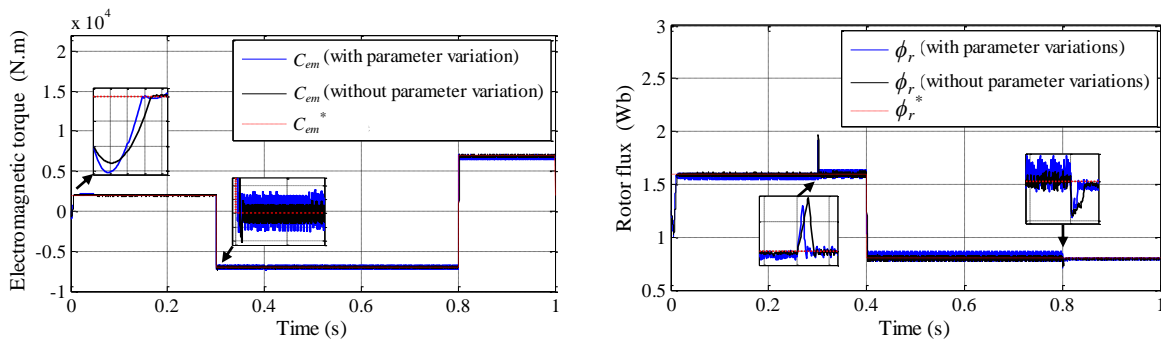


Fig. 8. C-DTC strategy responses (robustness test)

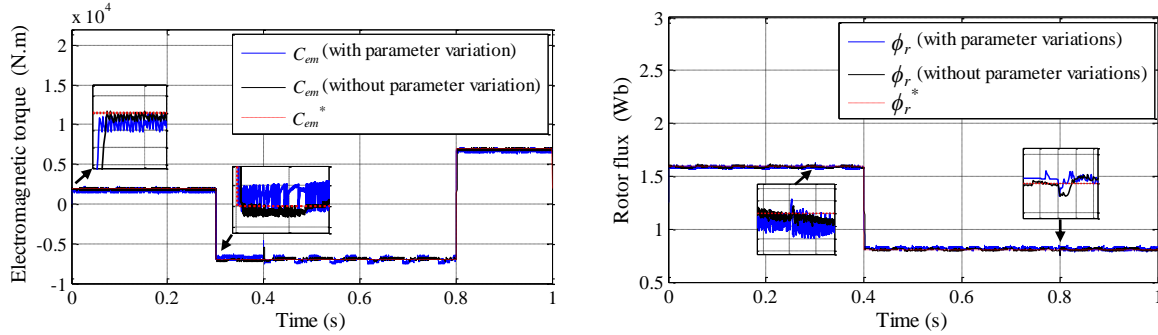


Fig. 9. SOSM-DTC strategy responses (robustness test)

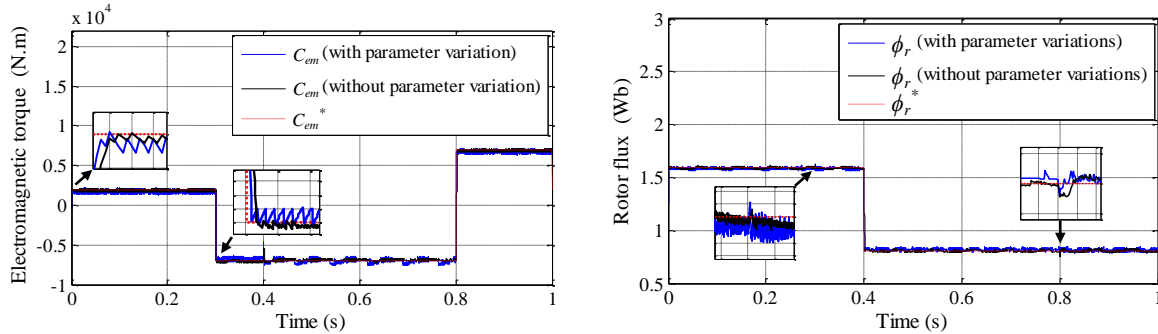


Fig. 10. FSOSM-DTC strategy responses (robustness test)

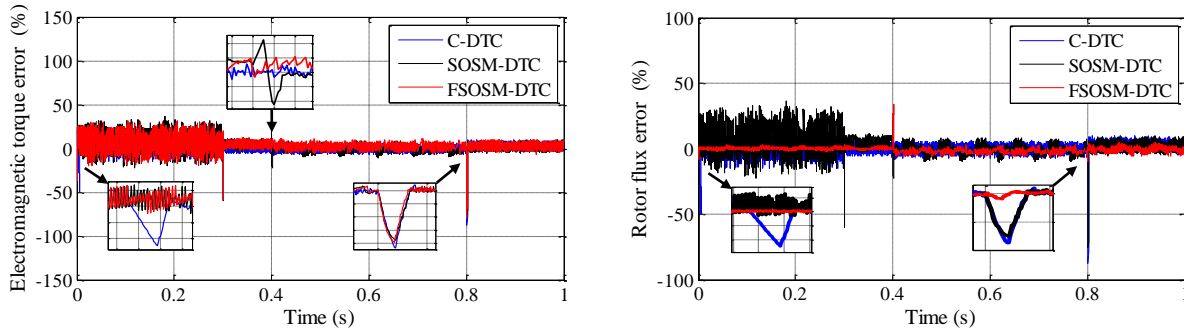


Fig. 11. Error curves (robustness test)

REFERENCES

- [1] Lakhoua M.N., "Systemic Analysis of a Wind Power Station in Tunisia", Journal of Electrical and Electronics Engineering, ISSN: 1844-6035, University of Oradea Publisher, Vol. 4, N°1, 2011.
- [2] M. Edrah, L.K. Lo, O. Anaya-Lara, "Impacts of high penetration of DFIG wind turbines on rotor angle stability of power systems," IEEE T Sustain Energ, Vol. 6, 2015, pp. 759-766.
- [3] A.B. Ataji, Y. Miura, T. Ise, H. Tanaka "Direct Voltage Control With Slip Angle Estimation to Extend the Range of Supported Asymmetric Loads for Stand-Alone DFIG," IEEE T Power Electr, Vol. 31, No. 2, February 2016, pp. 1015-1025.
- [4] A.M. Rao, N.K. Kumar, K. Sivakumar, "A multi-level inverter configuration for 4n pole induction motor drive by using conventional two-level inverters," In: IEEE 2015 International Conference on Industry Technology, 17-19 March 2015, Seville, Spain: IEEE. pp. 592-597.
- [5] Y. Zhang, Z. Li, T. Wangy, W. Xuy, J. Zhuy, "Evaluation of a class of improved DTC method applied in DFIG for wind energy applications," In: IEEE 2011 International Conference on Electrical Machines and Systems, 20-23 August 2011, Beijing, China: IEEE. pp. 2037-2042.
- [6] S.E. Ardjoun, M. Abid, "Fuzzy sliding mode control applied to a doubly fed induction generator for wind turbines," Turk J Elec Eng & Comp Sci, Vlo. 23, 2015, pp. 1673-1686.
- [7] X. Yao, Y. Jing, Z. Xing, "Direct torque control of a doubly-fed wind generator based on grey-fuzzy logic," In: International Conference on Mechatronics and Automation, Harbin, China, 2007. pp. 3587-3592.
- [8] G.S. Buja, M.P. Kazmierkowski, "Direct torque control of PWM inverter-fed AC motors - a survey," IEEE T Ind Electron, Vol. 51, 2004, pp. 744-757.
- [9] J. Holtz, "Pulse width modulation for electronic power conversion," P IEEE, Vol. 82, 1994, pp. 1194-1214.
- [10] S.Z. Chen, N.C. Cheung, K.C. Wong, J. Wu, "Integral sliding-mode direct torque control of doubly-fed induction generators under unbalanced grid voltage," IEEE T Energy Conver, Vol. 25, 2010, pp. 356-368.
- [11] X. Zhu, S. Liu, Y. Wang, "Second-order sliding-mode control of DFIG-based wind turbines," In: IEEE 2014 3rd Renewable Power Generation Conference, 24-25 September 2014, Naples, Italy: IEEE. pp. 1-6.
- [12] M.A.A Morsy, M. Said, A. Moteleb, H.T. Dorrah, "Design and implementation of fuzzy sliding mode controller for switched reluctance

- motor,” In: IEEE 2008 International Conference on Industrial Technology, 21-24 April 2008, Chengdu, China: IEEE. pp. 1367-1372.
- [13] X. Yuan, Z. Chen, Y. Yuan, Y. Huang, “Design of fuzzy sliding mode controller for hydraulic turbine regulating system via input state feedback linearization method,” *Energy*, Vol. 93, 2015, pp. 173-187.
- [14] H.U. Rehman, R. Dhaouadi, “A fuzzy learning-sliding mode controller for direct field-oriented induction machines,” *Neurocomputing*, Vol. 71, 2008, pp. 2693-2701.
- [15] N. Ullah, W. Shaoping, M.I. Khattak, M. Shafi, “Fractional order adaptive fuzzy sliding mode controller for a position servo system subjected to aerodynamic loading and nonlinearities,” *Aerosp Sci Technol*, Vol. 43, 2015, pp. 381-387.
- [16] M. Van, H.J. Kang, Y.S. Suh, “A novel fuzzy second-order sliding mode observer controller for a T-S fuzzy system with an application for robot control,” *Int J Precis Eng Man*, Vol. 14, 2013, pp.1703-1711.
- [17] S. Mefoued, “A second order sliding mode control and a neural network to drive a knee joint actuated orthosis,” *Neurocomputing*, Vol. 155, 2015, pp. 71-79.
- [18] Z. Yan Z, C. Jin, V.I. Utkin, “Sensorless sliding-mode control of induction motors,” *IEEE T Ind Electron*, Vol. 47, 2000, pp. 1286-1297.
- [19] C. Lascu, I. Boldea, F. Blaabjerg, “Variable-structure direct torque control – A class of fast and robust controllers for induction machine drives,” *IEEE T Ind Electron*, Vol. 51, 2004, pp. 785-792.
- [20] C. Lascu, F. Blaabjerg, “Super-twisting sliding mode direct torque control of induction machine drives,” In: IEEE 2014 Energy Conversion Congress and Exposition, 14-18 September 2014, Pittsburgh, PA: IEEE. pp. 5116-5122.
- [21] S. Benelghali, “On multiphysics modeling and control of marine current turbine systems,” PHD, Bretagne Occidentale University, France, 2009.
- [22] G. Bartolini, A. Ferrara, E. Usani, “Applications of a sub-optimal discontinuous control algorithm for uncertain second order systems,” *Int J Robust Nonlin*, Vol. 7, 1997, pp. 299-310.
- [23] G. Bartolini, A. Ferrara, E. Usani, “Chattering avoidance by second-order sliding mode control,” *IEEE T Automat Contr*, Vol. 43, 1998, pp. 241-246.
- [24] A. Levant, L. Alelishvili, “Integral high-order sliding modes,” *IEEE T Automat Contr*, Vol. 52, 2007, pp. 1278-1282.
- [25] A. Levant, “Higher-order sliding modes, differentiation and output feedback control,” *Int J Control*, Vol. 76, 2003, pp. 924-941.
- [26] S. Elaimani, “Modélisation de différentes technologies d'éoliennes intégrées dans un réseau de moyenne tension,” PhD, University of Lille, France, 2009.
- [27] F. Poitier, T. Bouaouiche, M. Machoum, “Advanced control of a doubly-fed induction generator for wind energy conversion,” *Electr Pow Syst Res*, Vol. 79, 2009, pp. 1085-1096.
- [28] A. Bakouri, A. Abbou, H. Mahmoudi, K. Elyalaoui, “Direct torque control of a doubly fed induction generator of wind turbine for maximum power extraction,” In: IEEE 2014 International Renewable and Sustainable Energy Conference, 17-19 October 2014; Ouarzazate, Morocco: IEEE. pp. 334-339.
- [29] W.J. Wang, J.Y. Chen, “Passivity-based sliding mode position control for induction motor drives,” *IEEE T Energy Conver*, Vol. 20, 2005, pp. 316-321.
- [30] J.J.E. Slotine, “Sliding controller design for nonlinear systems,” *Int J Control*, Vol. 40, 1984, pp. 421-434.
- [31] B. Beltran, M.E.H. Benbouzid, T. Ahmed-Ali, “High-order sliding mode control of a DFIG-based wind turbine for power maximization and grid fault tolerance,” In: IEEE 2009 International Electric Machines and Drives Conference, May 2009; Miami, Florida, USA: IEEE. pp. 183-189.
- [32] B. Beltran, M.H. Benbouzid, T. Ahmed-Ali, “Second-order sliding mode control of a doubly fed induction generator driven wind turbine,” *IEEE T Energy Conver*, Vol. 27, 2012, pp. 261-269.
- [33] S. Benelghali, M.E.H. Benbouzid, J.F. Charpentier, T. Ahmed-Ali, I. Munteanu, “Experimental validation of a marine current turbine simulator: Application to a PMSG-based system second-order sliding mode control,” *IEEE T Ind Electron*, Vol. 58, 2011, pp. 118-126.

FPGA Implementation of Parallel Particle Swarm Optimization Algorithm and Compared with Genetic Algorithm

BEN AMEUR Mohamed sadek

Laboratory of Microelectronic, university of Monastir,
Monastir, Tunisia

SAKLY Anis

National Engineering School of Monastir,
Monastir, Tunisia

Abstract—In this paper, a digital implementation of Particle Swarm Optimization algorithm (PSO) is developed for implementation on Field Programmable Gate Array (FPGA). PSO is a recent intelligent heuristic search method in which the mechanism of algorithm is inspired by the swarming of biological populations. PSO is similar to the Genetic Algorithm (GA). In fact, both of them use a combination of deterministic and probabilistic rules. The experimental results of this algorithm are effective to evaluate the performance of the PSO compared to GA and other PSO algorithm. New digital solutions are available to generate a hardware implementation of PSO Algorithms. Thus, we developed a hardware architecture based on Finite state machine (FSM) and implemented into FPGA to solve some dispatch computing problems over other circuits based on swarm intelligence. Moreover, the inherent parallelism of these new hardware solutions with a large computational capacity makes the running time negligible regardless the complexity of the processing.

Keywords—PSO algorithm; GA; FPGA; Finite state machine; hardware

I. INTRODUCTION

Over the last decade, several meta-heuristic algorithms are proposed to solve hard and complex optimization problems. The effectiveness of this algorithm give satisfaction to solve the most difficult problems for many algorithms related for various optimization problems. The proposed architecture is tested on some benchmarks functions. We have also analyzed the operators of GAs to describe how the performance of each one can be enhanced by incorporating some features of the other. We used standard benchmarks functions to make comparison between the two algorithms. In fact, PSO algorithm use the technique [1] that explores all the search space to fix parameters that minimizes or maximizes a problem. So, the ability and the simplicity to solve complex problems make the studies active in this area compared with many others optimization techniques [2] [3].

This research attempts to present that PSO has a good effectiveness to find the best global optimal solution as the GA but with a better computing efficiency (less using of resource hardware and execution time). The main objective of this paper is to compare the computational efficiency of our optimized PSO with GA and other PSO algorithms using a set of benchmark test problems. The results of this optimization algorithm could prove to be important for the future study of

PSO. The organization of the paper is described as follow: The first chapter briefly introduces the general steps performing the mechanism of PSO. Especially, a brief introduction of pseudo random number generator [4]. The next section describes the background functional architecture which performs the GA and PSO algorithm. In chapter 3, a description of the architecture used in the hardware implementation of PSO and genetic algorithm; the second part illustrates the experimental results of some benchmarks functions applied into the PSO algorithm and compared with GA and others PSO algorithms. Finally, we conclude our work and we make some implications and directions for future studies.

II. PARTICLE SWARM OPTIMIZATION

In Particle Swarm Optimization algorithm we can say that each « bird » may be a solution through a search space. Birds are called particles and to explore all the search space, each particle is evaluated by the fitness function and to manage the flying of the swarm to the prey, they use velocities module. Each particle flies around the solution by following the optimum position of particles [5][6]. All particles are associated with points in the search space and their positions are depending on their own solution and of their neighbors. Some particles come into play randomly in every iteration through this environment; they look the assessment of themselves and their neighbors [7]. Then, they follow successful particles of the given problem. PSO algorithm give satisfactory results in solving many dispatch problems related to biology medical, finance, 3d graphics, image processing and others. [8], but it is hard to choose the setting parameters because it is too complicated to find the best setting of a desired application. So, we have to set first, several parameters of the PSO algorithm: [9] [10]:

- Position and velocity equations of particles
- Number of particles in the search space
- The Gbest fitness achieved.
- Positions of particles having the best solution of all.
- Number of iteration

In the beginning we generate a random population after that we search for the best solution after each iteration. Then, the particles update their positions using two best solutions. The first one is the best solution towards the problem and it is

named « lbest ». The other optimal solution is followed by the PSO algorithm and obtained by any particles from the population and it is named « Gbest ».

A. The random number generator

Programming PSO algorithms requires the use of random generator; there are several methods to generate a random numbers. In fact it is impossible to generate a random number based on algorithms that’s why they are called pseudo random number. The random generators programs are particularly suitable for implementation and effective. Most pseudo random algorithms try to produce outputs that are uniformly distributed. A common class generator uses a linear congruence. Others are inspired by the Fibonacci sequence by adding the two previous values. Most popular and fast algorithms were created in 1948 D. H. Lehmer introduced linear generators congruents and will eventually become extremely popular.

In our algorithm we used the bloc of the pseudo random generator [13] at the initial position of particles and in the velocity vector. We choose the frequently used pseudo-random generator called the linear congruent of Lehmer:

$$F_{n+1} = (A * F_n + B) \text{ mod } C \tag{1}$$

Where: - F_{n+1} : is the random number obtained from the function F

- F_n : is the previous number obtained
- A and B : are multiplicative and additive value, respectively
- C : the modulo number

B. Position and velocity equations

Velocity equation allows changing the position of a desired particle and generally, the objective of using PSO algorithm is to indicate by their positions the distance to the best particle. So, these equations are updated throughout the race of iterations using the equations below:

$$V_i(t + 1) = W_{moy} + c_1 r_1 (lbest_i - x_i(t)) + c_2 r_2 (Gbest - x_i(t)) \tag{2}$$

$$X_i(t) = X_i(t) + V_i(t) \tag{3}$$

$x_i(t)$ is the particle position at time t and v_i is the velocity of particle at the instant t(i), w is parameters, c_1 and c_2 are constant coefficients, r_1 and r_2 are random numbers at each iteration, « Gbest » is the optimal solution found until now and « lbest » is the best solution found by the particle i. So, generally the velocity vector allows directing the research process and reflects the sociability of the particles.

The convergence to the optimum solution can be fixed by a number of iterations depending on the fitness or when the variation tends to zero (like sphere function) or when it tends to the best minimized solution. Here some parameters that comes into play:

- The number of population.
- The size of the neighborhood.
- The dimension of the search space.
- The values of the coefficients.
- The maximum speed.

Each iteration allows the particles to move as a function of three components:

- Its current speed
- Its local best solution
- The global best solution in its neighborhood.

TABLE I. EXAMPLE OF SOME SELECTED PARTICLES

Particles	iteration			
	1	2	3	n
X_1	001001111110010	001001111110001	001001111110000	...
X_2	0010011111100011	0010011111100011	0010011111100011	...
X_3	0010011111000001	0010011111000001	0010011111000001	...
X_n	X_{n1}	X_{n2}	X_{n3}	...

In this table we present a sample from the sphere function, we can easily see that the “lbest” of particle x_1 is located in it_3 and the “lbest” of particle x_2 and x_3 are located in it_2 but the “gbest” is x_3 and located in it_2 .

The global minimum for the sphere function is clearly located at $x_i = 0$, in each iteration we pick the “lbest” and we save the results into memory in order to compare its value with the new position of particles in the next iteration.

III. ARCHITECTURE OF GA AND PSO ALGORITHMS

A. GA architecture

To optimize a problem in GA, we have to explore all the searching state in order to maximize (or minimize) a chosen function. So, the use of genetic algorithm is suitable for a quick exploration of an area. The organizational chart that describes the architecture of GA is shown by the following figure.

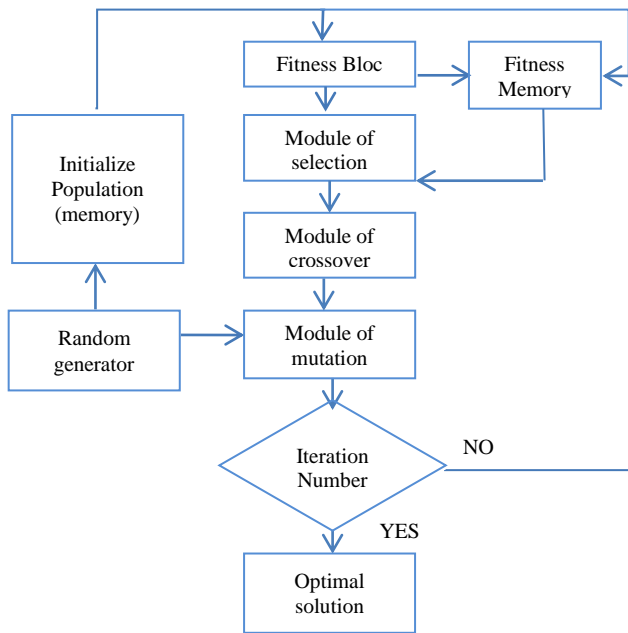


Fig. 1. Architecture Of The GA

B. PSO architecture

The architecture of our optimized PSO algorithm is presented in the following figure:

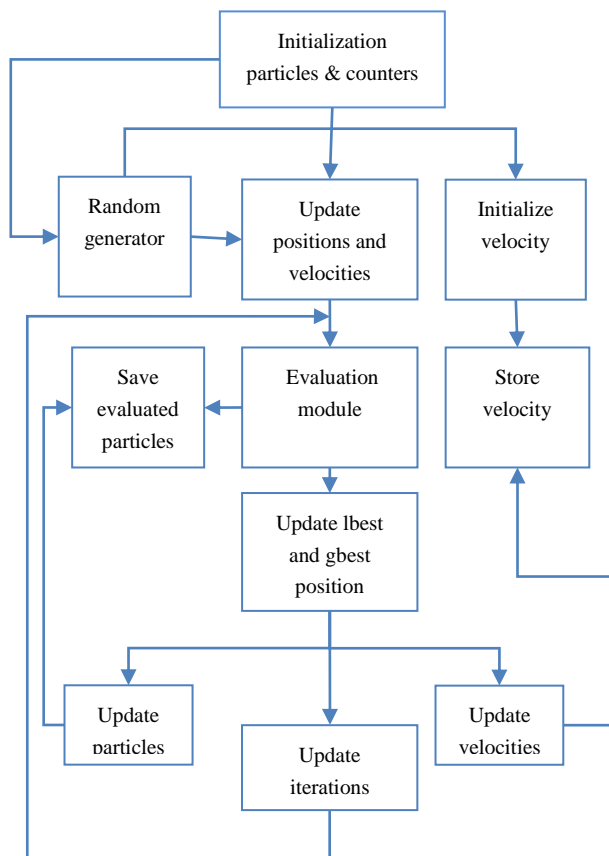


Fig. 2. Internal architecture of the PSO algorithm

For hardware implementation of PSO algorithm, the architecture is decomposed into five operations that are performed on each particle: update the position, evaluate the fitness, update the particle's best position, update the global best position and update the velocity.

We can demonstrate from the two architectures that the two algorithms share some common points. In fact the two algorithms begin with a random population in the search space and both of them use fitness module to evaluate the generation.

Both of them update the generation and search for an optimal value using the pseudo random number but the two of them does not guarantee the success. However, the Particle Swarm Optimization doesn't have crossover and mutation operators. Indeed, PSO update its particles using the velocity module.

C. The FSM

In our paper a dynamic parallel PSO is implemented to be applied into large optimization problem and compared with GA and others PSO algorithms. The FSM is used to exploit all type of parallelism to find the optimum solution in a reduced portion of times. The dynamical process of FSM is represented in figure 3, in fact every state may have at every time a position of many possible finite states. Firstly, we must propose a number of fixed states; every transition may have one or more around states. In this way, states which have only one state and have no possible transitions we named the final states.

The algorithm performs the updating of the optimum fitness number after the evaluations for all the particles. Here, when we update their positions and velocities we can obtain a good convergence rates after evaluating each particle. In a dynamic parallel computing, the main factor of performance is the communication latency after each transition between states. The goal of parallel dynamic computing is to produce optimal results even when we use multiple processors to reduce the running time. In this architecture we used pair memory modules to compound the bandwidth and thus, we can ameliorate the capabilities of our algorithm and we cannot do this only if we use Dual Channel bloc RAM. In that way we can access to the data memory in two modes write or read at the same frequency. There are problems with the dual RAM. In fact, the reading time of the content of memory is delayed by one clock comparative to the last reading. The description of the 8 states is presented in the sequel:

- S0: Initialize parameters, signals and counters of PSO algorithm and goto S1
- S1: Generate initial population and their velocities using random generator and goto S2 or S3
- S2: Save positions and velocities value into memory (RAM)
- S3: Evaluate particles using fitness module and goto S4 or S5
- S4: Save evaluated value into Bloc RAM and goto S6

- S5: Test gbest If fit(i) <Global-best(i) then update Global-best and if the number of iteration is achieved then go to final state else go to State S7
- S6: Test lbest If fit(i) < local-best(i) then update local-best(i) then, go to S2 and return to state S4
- S7: Update particles positions and velocities
- S8: Update the number of iteration if iteration not achieved then go to state S3 else go to final state (SF)
- SF: Display the optimum solution.

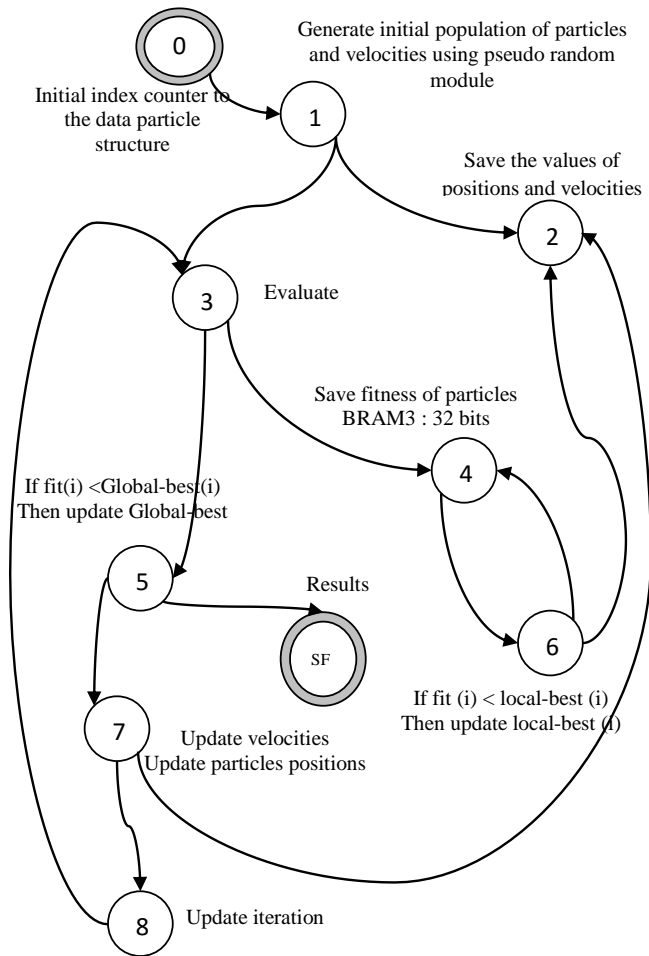


Fig. 3. The finite state machine of the PSO algorithm

Luckily, new advances in processor technology are capable and available to compute a complex program and use low cost power beyond clusters of mid-range performance computers. So, the dynamic process implemented in the particle swarm optimization could be separated in two states which update position and velocity of each particle using dynamic process with the goal to reduce the processing time.

In our paper, the soul of the parallel processing was used to generate a dynamic PSO algorithm and the aim of using parallel computing to the PSO algorithm, is to speed up the algorithm processing using a uniform distribution method to achieve optimum solutions with a significant execution time.

Figure 3 present the finite state machine of the global control module; especially, it presents step by step the code of the PSO in order to keep the algorithm more practical.

D. Benchmark test functions

The Most researchers use a number of population size between 10 to 50 for the performance comparison between algorithms, here we fixed the population at 20 chromosome for the GA and the same for PSO algorithm. To test the PSO and to compare its performance with other algorithm, we used some standard benchmark functions which are described as below:

- Sphere function
- Rosen-brock function
- Rastrigin function
- Zakharov function

Some well-known benchmark functions have been selected for comparing the two implementations. So, to test and compare the performance of our proposed PSO algorithm we used unimodal and multimodal functions. These functions are described as below:

$$f_1(x) = \sum_{i=1}^n x_i \quad (4)$$

$$f_2(x, y) = \sum_{i=1}^{n-1} (x_i^2 + y_i^2) \quad (5)$$

$$f_3(x, y) = \sum_{i=1}^{n-1} [(1 - x_i)^2 + 100(y_i - x_i^2)^2] \quad (6)$$

$$f_4(x) = 10n - \sum_{i=1}^n (x_i^2 - 10\cos(2\pi x_i)) \quad (7)$$

$$f_5(x) = x_i^2 + (0.5ix_i)^2 + (0.5ix_i)^4 \quad (8)$$

IV. VALIDATION EXAMPLES

Most researchers use a number of population size between 10 to 50 for the performance comparison of GA and PSO, the swarm size used for the PSO is the same as the population size used in GA and is fixed at 20 particles in the PSO swarm and 20 chromosomes in GA population. In the GA all variables of each individual are represented with binary strings of '0' and '1' that are referred to as chromosomes. Like genetic algorithm, PSO begins with a random population and to perform its exploration, GA use three operators (crossover, selection and mutation) to propagate its population from iteration to another.

A. The sphere function

$$f_1(x) = \sum_{i=1}^n x_i \quad (9)$$

Sphere function is useful to evaluate the characteristics of our optimization algorithms, such as the robustness and the convergence velocity. This function has a local minimum and it is unimodal and continuous. The interval of search space is between [-1,1]. Figure 4 present the results of simulation using modelsim of the sphere function.

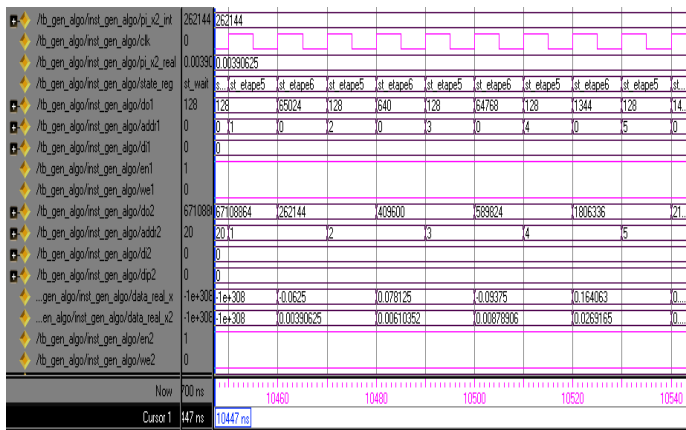


Fig. 4. Simulation results of function f1

The detailed results describe that our solution converges to zero from iteration to another.

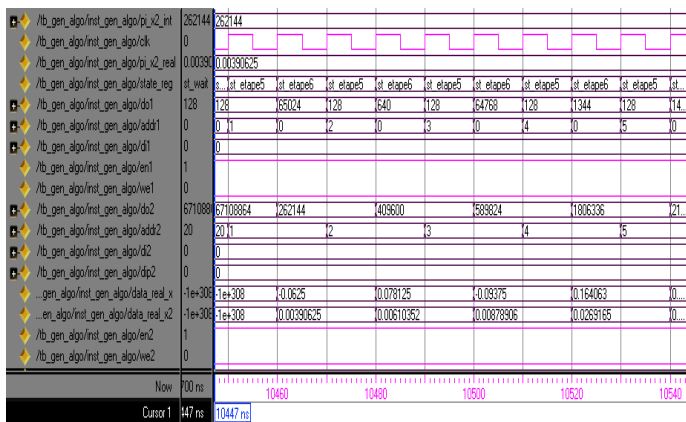


Fig. 5. Simulation results of function f2

These particles work together in a parallel dynamic state to get the best solution of any function. They update position and velocity even if the algorithm has a lot of particles and this cannot make a hard impact on the global execution time speed. Indeed, the number of particles in this algorithm is limited by the size of embedded features of FPGA. The following tables present the number of LUT (Look up Table), bloc RAM and all the resource materials used in this function.

TABLE II. DEVICE UTILIZATION SUMMARY OF PSO

(PSO) Sphere function			
logic	used	available	utilisation
slices	225	1920	11%
flip flops	214	3840	5%
4 inputs	354	3840	9%
IOBs	10	173	5%
BRAM	5	12	41%
multiplexers	4	12	33%
GCLKS	3	8	37%

TABLE III. DEVICE UTILIZATION SUMMARY OF GA

(GA) Sphere function			
logic	used	available	utilisation
slices	581	1920	30%
flip flops	600	3840	15%
4 inputs	864	3840	22%
IOBs	23	173	13%
BRAM	2	12	16%
multiplexers	8	12	66%
GCLKS	5	8	62%

In the following figure, we can easily see the difference between the two algorithms, here the PSO algorithm give better optimization in the use of hardware resources than the Genetic Algorithm.

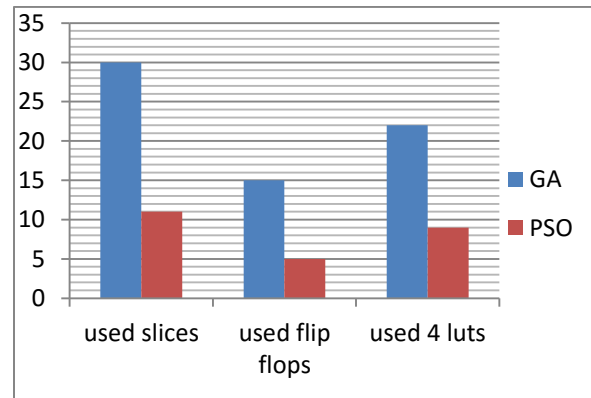


Fig. 6. Comparison of hardware resource between PSO and GA

We implemented the sphere function with two algorithms, GA and PSO using Spartan 3 from Xilinx, and then we can realize that the processing time of one iteration of PSO algorithm gives higher operation speed for optimization problems rather than genetic algorithm. The following table describes this.

TABLE IV. PROCESSING TIME OF ONE ITERATION

algorithm	psa	genetic
Execution of one Iteration (clock cycle)	1180	9740

B. The rastrigin function

This function is described below:

$$f_4(x) = 10n - \sum_{i=1}^n (x_i^2 - 10\cos(2\pi x_i)) \quad (10)$$

The Rastrigin function contains several local minima. But it has just one global minimum and it is highly multimodal and the location of the minima is distributed regular.

- 4,320 logic cell and equivalents
- 12 x 18K of bit block RAMs (216K bits)
- 12 of hardware multipliers (18x18)
- 4 Digital extern clock (DCMs)
- A lot of I/O signals and it is up to 173
- Three “40” pin expansion connectors
- PS/2 mouse/keyboard port, VGA port and serial port.

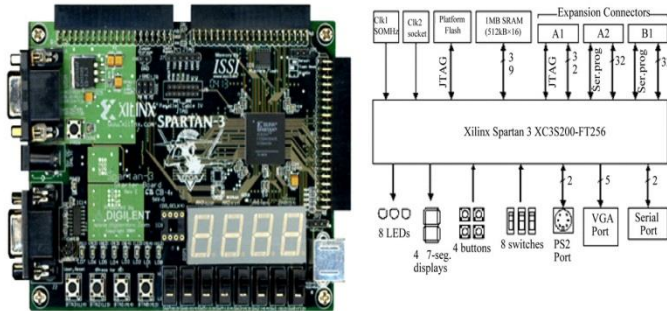


Fig. 11. The Block Diagram of SPARTAN-3

To make a comparison of this algorithm to deliver better solution in a significant time especially, its robustness and speed, we have tested it against other meta-heuristic algorithms, like genetic algorithms and another PSO algorithm. For GA, we used the basic model with elitism method and a probability of mutation equal 5%. The simulations have been carried out using spartran-3 of Xilinx with 50MHz. We have also fixed the population $n = 20$ for all simulations. The results are favorable and proved that Real BAT can be effective for many problems related to any algorithms used. The experiment results was carried out at minimum 5 % which allow judging whether the results of the PSO are acceptable and optimized in execution time compared to the best results of other algorithms.



Fig. 12. Display of the number of iteration to achieve the optimal solution

VI. RELATED WORK

Since its invention, many researchers have worked on the PSO algorithm [11] and how to accelerate its performance to give a good convergence and to reduce the use of hardware resource for embedded applications. In this section we will

present some works lean on parallelization algorithms proposed by other researches. In fact, there are many interesting improvements using PSO algorithm for several applications; al.Reynolds [12] suggested a smart technique for modified PSO algorithm using neural networks. His technique is based on a deterministic approach while the particles update their positions to simplify the hardware implementation because the standard PSO algorithm has been implemented to use random generators only for the operations of update and to reduce the hardware resource Upegui and Peña [13] use a discrete recombination of PSO algorithm called (PSODR), that’s allow to decrease the time of computing of the velocity module. It is clear that these modified PSO algorithm allows generating competitive results compared to those of the basic PSO algorithm [14]. Moreover another works on the PSODR algorithm are proposed by Bratton and Blackwell with simplified models of the PSODR algorithm are analyzed and proposed by Blackwell and Bratton [15] with effective results and promising.

Many researches presented a modified variant of PSO either to reduce the materials resource or to eliminate explicit problem related directly on the architecture of PSO. That’s why we developed a modified architecture using finite state machine to program a parallel algorithm that could give effective results to solve several problems [16]. Thus, we fixed the representations of the data by 20 particles to bearing several purpose of applications.

A comparison performance of PSO algorithms on some processors platforms are represented in the following table. We choose two different processors platforms, the Xilinx xc3s500 [17] and the Xilinx Micro-Blaze soft processor core for the Sphere test function.

TABLE VII. COMPARISON OF OTHER PLATFORMS

Plat_ form	Xilinx xc3S500		Xilinx microblaze		Spartran xc3S200	
	Average nb. Iter. (st.dev)	Average .Exe. time (s) (st.dev)	Average .nb. iter. (st.dev)	Average .Exe. time(s)(st.dev)	Average. iter.(st.d ev)	Averag e.Exe. time(s) (st.dev)
Spher e functi on	338 (30.9)	0.28 (0.03)	382 (27.0)	10.4 (0.65)	420 (88.9)	0,024 (0.001)

The random number generator plays a big role in the implementation of the two algorithms. That’s why we can obtain some difference in the number of iterations even we use the same equation of random generator and the same initial seed used for the three tests. In order to evaluate the performance of our proposed PSO algorithm, we consider and compare two implementations of the PSO process: the first one is our algorithm and the second use the processor Xilinx MicroBlaze [18].

TABLE VIII. DEVICE UTILIZATION SUMMARY OF THE PSO ALGORITHM ON SPARTAN XC3S200 AND XC3S500

	Tested function (sphere)	Number of slices	Block BRAM	MULT18x18s
Other PSO algorithm [18]	Xilinx xc3s500	1523 (32.7%)	7 (35%)	8 (40%)
proposed algorithm	Xilinx xc3s200	225 (11%)	5 (41%)	3 (37%)

VII. CONCLUSION

In this work, we developed a hardware implementation on FPGA of a Particle Swarm Optimization algorithm. The effectiveness of our PSO algorithm has been tested on several benchmark functions for many degrees of parallelism. This architecture exploits all the parallelism to allow updating the particle positions and velocities to get a good performance of the fitness function using a finite state machine and implemented as hardware on Xilinx spartan 3 (xc3s200). In this algorithm we used a FSM to exploit all the parallelisms that make the program converge very quickly. The FSM allow updating the positions and velocities of particles and after that we can take independently the result of the better optimized fitness from the position of particles. In this paper the simulation results demonstrate that all the states and modules can be executed at the same time and the execution time can be reduced a lot.

The proposed PSO algorithm proves that it has a favorable convergence speed compared to the other meta-heuristic algorithms and the complexity of the algorithm depends on the size of design space, it means the number of allocated particles and the complexity of the problem. So, the PSO's robustness is attached to its enhanced ability to achieve a satisfaction between two requirements, the numbers of used memory and the processing time of algorithm to solve complex problems.

REFERENCES

[1] P.K. Tripathi, S. Bandyopadhyay, K.S. Pal, Multi-objective particle swarm optimization with time variant inertia and acceleration coefficients, *Information Sciences* 177 (22) (2007) 5033–5049.
[2] A.S. Mohais, R. Mohais, C. Ward, Earthquake classifying neural networks trained with dynamic neighborhood PSOs, in: *Proceedings of the 9th Annual Conference on Genetic and, Evolutionary Computation (GECCO'07)*, pp. 110–117.

[3] G.S. Tewolde, D.M. Hanna, R.E. Haskell, and Multi-swarm parallel PSO: hardware implementation, in: *Proceedings of the 2009 IEEE Symposium on Swarm* (2009).
[4] D.H. Lehmer, *Mathematical methods in large-scale computing units*, Ann. Computing Lab. Harvard Univ. 141-146, 1951.
[5] R.M. Calazan, N. Nedjah, L.M. Mourelle, Parallel coprocessor for PSO, *International Journal of High Performance Systems Architecture* (4) (2011) 233–240.
[6] EDA Industry Working Groups, *VHDL – Very High Speed Integrated Circuits Hardware Description Language*, September 201
[7] N. Nedjah, L.S. Coelho, L.M. Mourelle, *Multi-Objective Swarm Intelligent Systems – Theory & Experiences*, vol. 261, Springer, Berlin, (2010).
[8] A. Ratnaweera, S.K. Halgamuge, H.C. Watson, Self-organizing hierarchical particle swarm optimizer with time-varying acceleration coefficients, *IEEE Transaction on System, Man and Cybernetics* 8 (3) (2004) 240–255.
[9] Hardware/software co-design for particle swarm optimization algorithm Shih-An Li, Chen-Chien Hsu b, Ching-Chang Wong, Chia-Jun Yu, *Information Sciences* 181, Elsevier (2011) 4582–4596
[10] A hardware accelerator for Particle Swarm Optimization, Rogério M. Calazan, Nadia Nedjah, Luiza M. Mourelle, *Applied Soft Computing*, Elsevier (2013)
[11] A hardware accelerator for Particle Swarm Optimization Rogério M. Calazan, Nadia Nedjah, Luiza M. Mourelle *Applied Soft Computing* xxx (2013).
[12] P.D. Reynolds, R.W. Duren, M.L. Trumbo, R.J. Marks, II, FPGA Implementation of Particle swarm optimization for inversion of large neural networks, in: *Proceedings 2005 IEEE Swarm Intelligence Symposium* (2005).
[13] J. Peña, A. Upegui, A population-oriented architecture for particle swarms, in: *Second NASA/ESA Conference on Adaptive Hardware and Systems*, (AHS 2007), pp. 563–570.
[14] J. Peña, A. Upegui, E. Sanchez, Particle swarm optimization with discrete recombination: an online optimizer for evolvable hardware, in: *First NASA/ESA Conference on Adaptive Hardware and Systems*, (AHS 2006), pp. 163–170.
[15] D. Bratton, T. Blackwell, Understanding particle swarms through simplification: a study of recombinant PSO, in: *Proceedings of the 9th 1013 Annual Conference on Genetic and, Evolutionary Computation (GECCO'07)*, pp. 2621–2627.
[16] Y. Maeda, N. Matsushita, Simultaneous perturbation particle swarm 1035 optimization using FPGA, in: *Proceedings of International Joint Conference 1036 on Neural Networks (IJCNN 2007)*, pp. 2695–2700.
[17] G.S. Tewolde, D.M. Hanna, R.E. Haskell, Multi-swarm parallel PSO: hardware 1054 implementation, in: *Proceedings of the 2009 IEEE Symposium on Swarm Intelligence (SIS09)*, Nashville, TN, pp. 60–66.
[18] A modular and efficient hardware architecture for particle swarm, optimization algorithm Girma S. Tewolde Q1, Darrin M. Hanna, Richard E. Haskell *Microprocessors and Microsystems* xxx, Elsevier (2012).

Simulation of Shunt Active Power Filter Controlled by SVPWM Connected to a Photovoltaic Generator

Ismail BOUYAKOUB

Laboratory of Electrical Drives,
University of Sciences & Technology of Oran
Oran, Algeria

Benyounes MAZARI

Laboratory of Electrical Drives,
University of Sciences & Technology of Oran
Oran, Algeria

Abedelkader DJAHBAR

Electrical Engineering Department,
Hassiba Benbouali University,
Chlef, Algeria

Omar MAAROUF

Electrical Engineering Department,
Hassiba Benbouali University,
Chlef, Algeria

Abstract—In this paper we study the shunt active power filter. This filter contains a voltage three-level inverter controlled by the SVPWM strategy supplied by a the DC bus powered by a solar array to improve the quality of electric energy and eliminate harmonics currents generated by non-linear loads, the latter identified by the method of multivariable filter. The objective of this study is to obtain an unpolluted source into the power grid where all the simulation results are obtained by using MATLAB Environment.

Keywords—shunt active power filter; harmonic currents; MVF; SVPWM; three level inverter; GPV

I. INTRODUCTION

The Sources of Energy are divided into two categories. The Renewable sources and the Petrol and Gas energies. The Renewable are divided into many types such as: Solar, Wind and Hydraulic energies. These energies were used from the foundation of humans which means its usage was from long ages throughout history until the out-break of the industrial Revolution.

In this period of time, Petrol's prices were very sheep as a consequence, renewable sources were excluded. In contrary, during recent years and due to the increase of fuel's prices and the environmental problems caused by the use of conventional fuels we come back to use renewable sources of energy.

Renewable sources are inexhaustible, clean. These sources can be used in a decentralized way that makes it so easy to work with. It also had the additional advantage of being complimentary wherein the integration between them is favorable.

The two-level voltage source inverter has been very popular in drives for many years due to its ease of

implementation and control. However, two-level inverters can be limited by the voltage ratings of the semiconductor devices, particularly in high power applications [1]. Multilevel inverters were developed to help address this concern as well as other limitations of two-level inverters. In particular, three-level inverters have been popular due to their improvement in output waveforms without overly complicating the design and control of the inverter[2].

The Multi- variable filter is proposed to extract harmonic currents instead of classical harmonics extraction based on High Pass Filters, the Three Phase Currents/Voltages are detected by using current/voltage sensors. The inverter currents had been controlled by using SVPWM. This paper is presented in order to analyze the simulation of a PV interactive Shunt Active Power Filter topology that simultaneously achieves Harmonic Current damping. To reference the Shunt Active Filter Current Computation we should use the "Multi-variable filter" method and apply the carrier-based SVPWM to get a signal generation.

II. THE STUDIED CONFIGURATION

The proposed configuration consists of a PV solar generator connected to a DC bus to a three -phase voltage inverter, coupled in parallel to a network through an inductor. This electrical system supplies a non-linear receiver consisting of a rectifier having as a load resistor in series with an inductor. The block diagram in Figure 1 illustrate this configuration. The photovoltaic installation connected to the network with an active filter to improve the quality of energy on the network connection point. It is therefore the voltage inverter control algorithm which is adopted to simultaneously ensure at the electrical network compensation harmonic pollution.

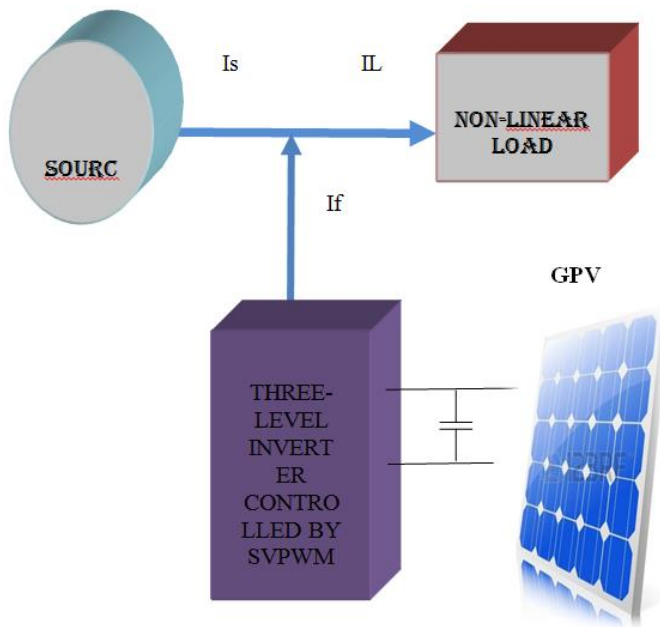


Fig. 1. Configurations of photovoltaic interactive Shunt Active Filter system

III. PV MODEL

The Photovoltaic cell is mainly a p-n junction made in a slender plate semiconductor, a solar energy sent an electromagnetic radiation, and this radiation is converted into electricity by the photovoltaic panel when it is exposed to the Sun rays, the Photons, which have an energy higher than the Band-Gap Energy of the semiconductor, create some pairs Electron-Hole proportional to the incident rays, if we want to build a model of the PV generator, we have to start by the identification of the equivalent electrical circuit to the source. Several Mathematical models have been designed to represent their highly non-linear characteristics given by semiconductor junctions that are the most important components in PV modules. Most models of photovoltaic generators that have some numbers of concerned parameters in the compute of output voltage and current, the model of single diodes in this paper is shown on (Fig.2). [3]

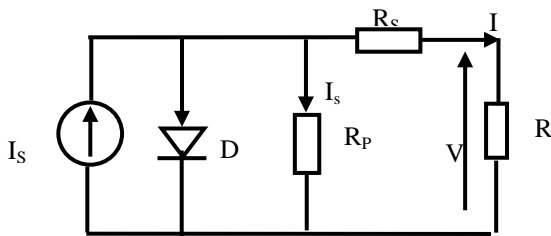


Fig. 2. Equivalent circuit model

The above model can be extended to represent PV array with Np cells in parallel and Ns cell in series so we have here and.

$$I \left(1 + \frac{R_{sT}}{R_{shT}} \right) = n_p I_{SC} - n_p I_S \left(\exp \left[\frac{q \left(\frac{V}{n_s} + IR_{sT} \right)}{AkT_c} \right] - 1 \right) - \frac{V / n_s}{R_{shT}}$$

here $R_{shT} = \frac{n_p}{n_s} \times R_p$ and $R_{sT} = \frac{n_s}{n_p} \times R_s$.

The above model shows that an array of PV cells is nonlinear device having its characteristics depending on the solar irradiance and ambient temperature. The temperature. The following figure (Fig.3) represents the evolution of a DC bus voltage.

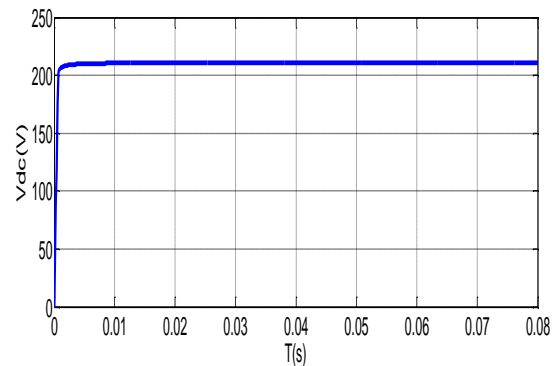


Fig. 3. Evolution of a Dc bus voltage

IV. THREE LEVEL INVERTER (NPC)

Currently, Multilevel inverters are being investigated. Moreover, these are being used in various industrial applications. A three level inverter is one of the most popular converters employed in medium and high power applications. Their advantages include the capability to reduce the harmonic content and decrease the voltage or current ratings of the semiconductors. As shown in Figure 1. The studied system is constituted of a DC supply, and a three level inverter bridge, we start by defining the Fij connection function of switch. It is "1" if the switch closed and "0" otherwise.

In controllable mode, the connection functions are related to the relation (1).

Fij in the following manner:

$$F_{ij} = \begin{cases} 1 & \text{if } S_{ij} \text{ is closed} \\ 0 & \text{if } S_{ij} \text{ is open} \end{cases} \quad (2)$$

The switches of each leg are complementary pairs:

$$F_{ij} = 1 - F_{(i-2)j}; i=3; j=1,2,3$$

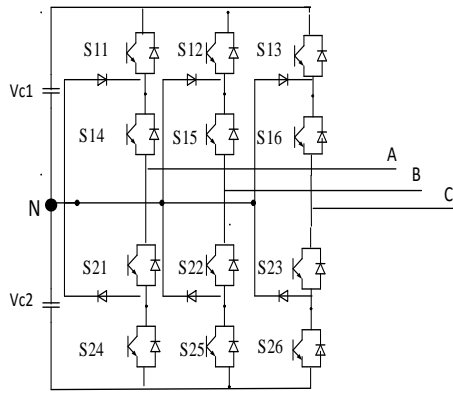


Fig. 4. Three level inverter

1) Space Vector PWM for a Three Level Inverter

There are altogether 27 switching states (table 1) that correspond to 19 voltage vectors whose positions are fixed. These space voltage vectors can be classified into four groups, where the first group corresponds 3 zero vectors or null vectors (V0, V7, V14), the second group consists of large voltage vectors (V15-V20), the third group consists of medium voltage vectors (V8-V13), and finally the fourth group consists of small voltage vectors (V1-V6). The last three groups can be distinguished by three hexagons illustrated in Figure 5.

TABLE I. THE SWITCHING STATES OF A THREE-LEVEL INVERTER

Switching States	S11	S12	S13	Vector
1	0	0	0	V0
2	1	1	1	V7
3	2	2	2	V14
4	1	0	0	V1
5	1	1	0	V2
6	0	1	0	V3
7	0	1	1	V4
8	0	0	1	V5
9	1	0	1	V6
10	2	1	1	V1
11	2	2	1	V2
12	1	2	1	V3
13	1	2	2	V4
14	1	1	2	V5
15	2	1	2	V6
16	2	1	0	V8
17	1	2	0	V9
18	0	2	1	V10
19	0	1	2	V11
20	1	0	2	V12
21	2	0	1	V13
22	2	0	0	V15
23	2	2	0	V16
24	0	2	0	V17
25	0	2	2	V18
26	0	0	2	V19
27	2	0	2	V20

The figure 5.shows the different switching state

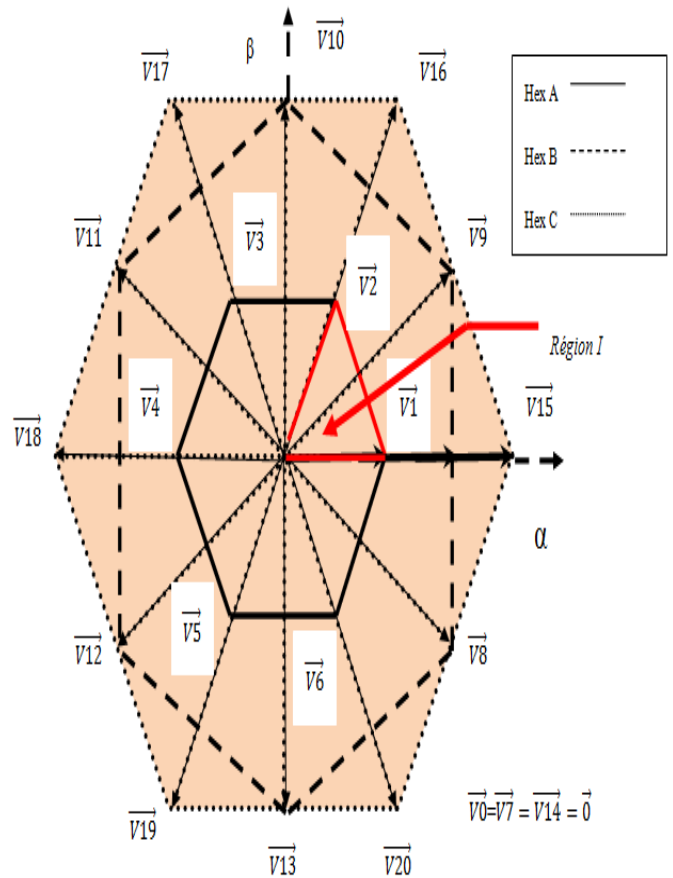


Fig. 5. A Three-level voltage inverter vectors in the (α-β) frame

2) Hexagon Identification

The small hexagon, we now called Hex A, bounded by the vectors, identical amplitude equal to 0.408.Vdc, The average hexagon, be called Hex. B, defined by the vectors, identical amplitude equal to 0.612.Vdc, The large hexagon, be called Hex. C, delimited by the vectors, identical amplitude equal to 0.816.Vdc.[5]

Each hexagon contains six sectors.

3) Sectors Identification

$$sector = \begin{cases} 1 & \text{if } 0 \leq \theta < \pi/3 \\ 2 & \text{if } \pi/3 \leq \theta < 2\pi/3 \\ 3 & \text{if } 2\pi/3 \leq \theta < \pi \\ 4 & \text{if } \pi \leq \theta < 4\pi/3 \\ 5 & \text{if } 4\pi/3 \leq \theta < 5\pi/3 \\ 6 & \text{if } 5\pi/3 \leq \theta < 2\pi \end{cases} \quad (3)$$

4) Calculating the period of Application of the control Vector

As mentioned before, we separate between 03 hexagons Figure 5. When each one is founded by 06 areas. Therefore, we have 18 areas; the computing of their switching time is carried out, respectively. To make this ask easy, and for goal

of the resemblance between the 06 areas of a hexagon on one side, and the similitude between hexagons “a” and “c” on the other side, and similitude between hexagons ‘a’ and ‘c’ on the other side (the biggest magnitude in hexagon ‘a’ ($E/\sqrt{6}$) is the half of the biggest magnitude in hexagon ‘c’ ($E\sqrt{2}/\sqrt{3}$)), due to all these causes, the procedure for the switching times calculation, is by taking only two areas of the hexagon ‘a’ and hexagon ‘b’, corresponds to the positive component of V_{ref} will take into account. Then the other switching times will be counted from the others four areas. Do not forget that the limiting vectors (V_1 to V_20) magnitudes will take the values below [5]

- Region I switching times calculation:

$$T_s = T_k + T_{k+1} + nT \tag{4}$$

Region I for $k=0$

$$\begin{cases} T_1 = T_s \cdot \frac{\sqrt{6}V_\alpha^* - \sqrt{2}V_\beta^*}{V_{dc}} \\ T_2 = T_s \cdot 2\sqrt{2} \frac{V_\beta^*}{V_{dc}} \\ T_0 = (T_s - T_1 - T_2) / 6 \end{cases} \tag{5}$$

The strategy of vector PWM consists of five steps diagrammed by the flowchart Figure 6.

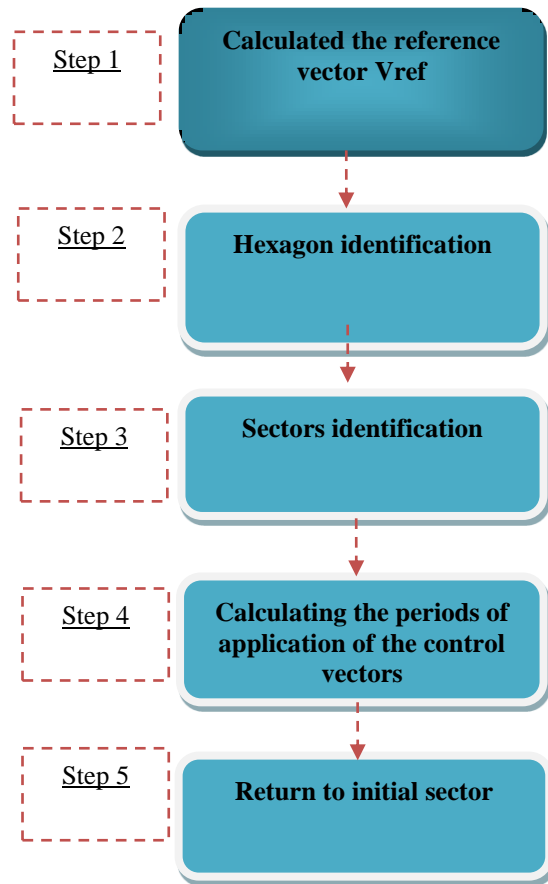


Fig. 6. Steps in SVPWM

VI. IDENTIFYING HARMONIC CURRENT

1) Identifying Harmonic Current by the Method of MVF

MVF is a filter has been produced by M.Benhabibe [6]. Its operating principle is based on the work of the Song Hong-Scok basing on the extraction of the fundamental signals from the axes. However, is practically used to isolate the direct particular order of harmonics even for the inverse [7].

The equivalent transfer function of integration in the synchronous reference "SRF" is given by:

$$i_{\alpha\beta}(s) = e^{j\omega_c t} \int e^{-j\omega_c t} i_{\alpha\beta}(t) dt \quad (6)$$

Once we apply the Laplace transformation, we get:

$$H(s) = \frac{\hat{i}_{\alpha\beta}(s)}{i_{\alpha\beta}(s)} = \frac{s + j\omega_c}{s^2 + \omega_c^2} \quad (7)$$

When developing this equation, we get the expressions:

$$\hat{i}_\alpha = \frac{k}{s} [i_\alpha(s) - \hat{i}_\alpha(s)] - \frac{\omega_c}{s} \hat{i}_\beta(s) \quad (8)$$

$$\hat{i}_\beta = \frac{k}{s} [i_\beta(s) - \hat{i}_\beta(s)] - \frac{\omega_c}{s} \hat{i}_\alpha(s) \quad (9)$$

Figure 7 illustrates the multi variable filter's scheme.

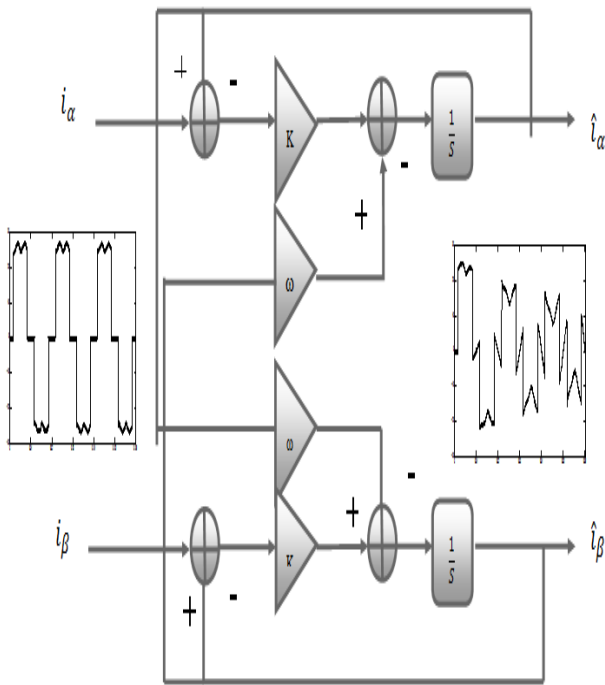


Fig. 7. Multi-Variable Filter

VII. SHUNT ACTIVE FILTER

In power distribution network, active power filters are widely used to reduce harmonics caused by nonlinear loads. This paper describes a shunt active power filter with a control system based on the multi-level inverter (PWM). The wide spread of power electronics equipment in modern electrical systems and power converter units causes the increase of the harmonics disturbance in the AC mains currents which became a major concern due to the adverse effects on all equipment and distribution network [4].

The circuit configuration of the studied active filter is shown in Figure 8. The configuration is designed to cancel current harmonics on the AC side and make the source current in phase with the voltage source. The source current, after compensation, becomes sinusoidal and in phase with the voltage source.

A. Control Scheme

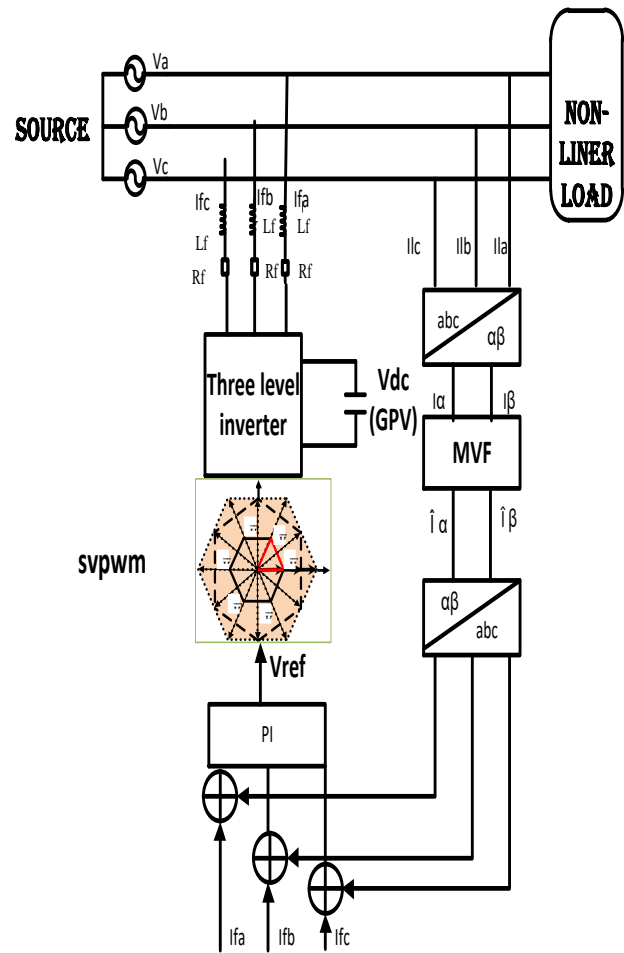


Fig. 8. the block diagram of a Shunt Active Power Filter control scheme

VIII. SIMULATION RESULT

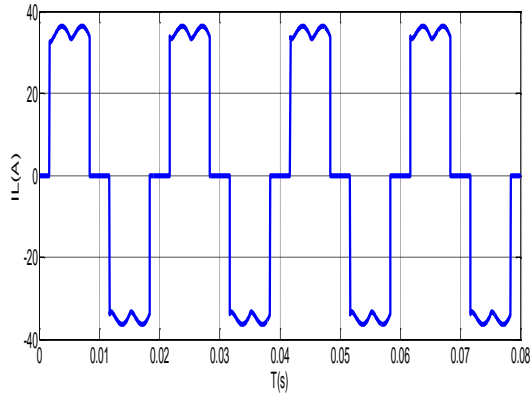


Fig. 9. The current to be terminal of non-linear load

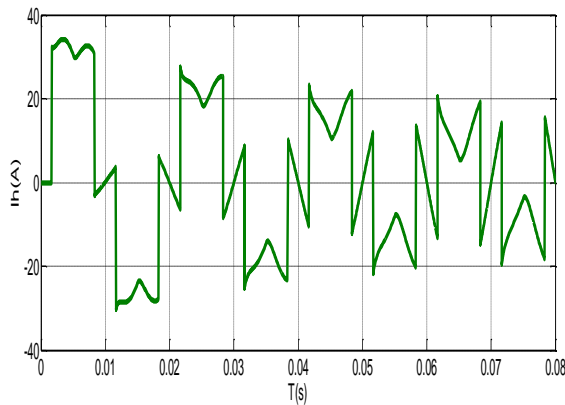


Fig. 10. harmonic current identifying by MVF

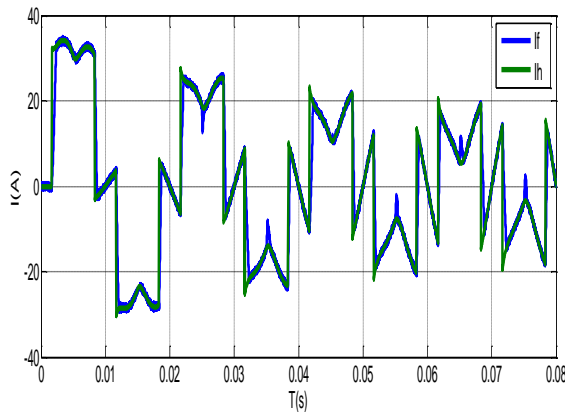


Fig. 11. The output current of the inverter and the harmonic current

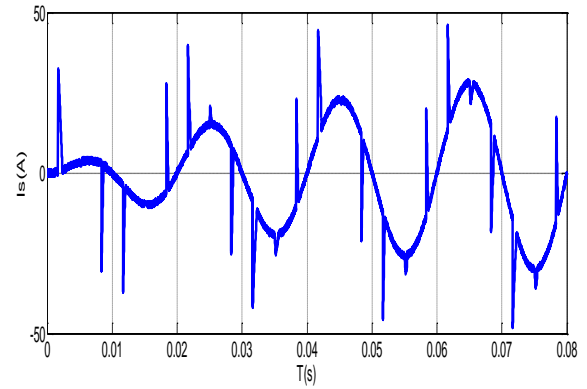


Fig. 12. The filter current

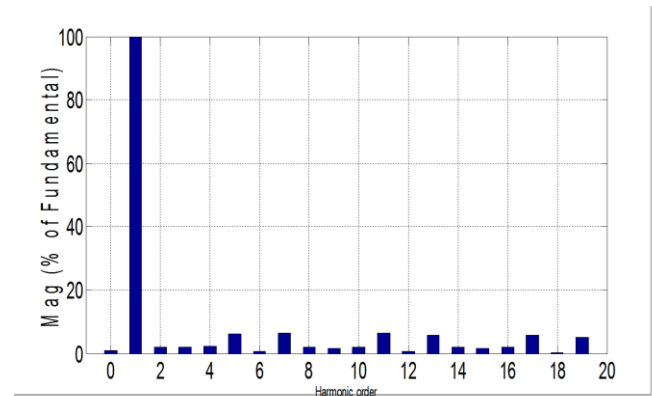


Fig. 13. harmonic current spectrum filtered

IX. CONCLUSION

The purpose of this article is focused on improving the power quality of the network based on the compensation of harmonic currents using a shunt active power filter.

The control of SVPWM take an essential part in improving the performance of APF and Produces good filtering quality, which has been obtained by the used of Matlab simulation environment, Show us that some self-charging current source stay close to a sinusoidal wave. Note that other techniques can also be used to enhance the system response.

The work that will be continued in this context is the development of the experimental applications of these proposed strategies, to confirm the effectiveness of the achieved Results.

REFERENCES

- [1] Saleh, S. , Azizur Rahman, M., “An Introduction to Wavelet Modulated Inverters”, IEEE Press, 2011.
- [2] Strandt, Rebecca, A .,“ Comparison of Three Space Vector PWM Methods for a Three-Level Inverter with a Permanent Magnet Machine Load”, *Master's Theses (2009 -)*. Paper 234.
- [3] Srinivas, K., Srinivas, G., Narasihma Rao,Dr.K., “Simulation of Shunt Active Power Filter Connected to a Photovoltaic Array for compensating Current Harmonics in Single Phase System ”, *International Journal of Advanced Research in Electrical,Electronics and Instrumentation Engineering* Vol. 3, Issue 12, December 2014
- [4] Sandeep kumar, D.,Venu madhav, G, “power quality improvement with a shunt active power filters using matlab / simulink, international journal of innovative research in electrical, electronics, instrumentation and control engineering” ,(IJRITCC)vol. 3, issue 1, january 2015.
- [5] Djeghloud, H., Benalla ,H., “ Space Vector Pulse Width Modulation Applied to the Three-Level Voltage Inverter”,5th International Conference on Technology and automation, Thessaloniki,(ICTA'05) Greece, October 15-16, 2005.
- [6] Benhabib, M. C., Jacquot ,E., Saadate, S. , “An Advanced Control Approach for a Shunt Active Power Filter”, *International Conference on Renewable Energy and power Quality*, (2003) April 9-11, Vigo, Spain.
- [7] Laib, H. , Kouara ,H., Chaghi ,A. , “ A New Approach of Modular Active Power Filtering”, *International Journal of Advanced Science and Technology* Vol. 50, January, 2013

PSIM and MATLAB Co-Simulation of Photovoltaic System using “P and O” and “Incremental Conductance” MPPT

ANAS EL FILALI

Laboratory LM2PI, ENSET,
Mohamed V University
Rabat, Morocco

EL MEHDI LAADISSI

Laboratory LM2PI, ENSET,
Mohamed V University
Rabat, Morocco

MALIKA ZAZI

Laboratory LM2PI, ENSET,
Mohamed V University
Rabat, Morocco

Abstract—The photovoltaic (PV) generator shows a nonlinear current-voltage (I-V) characteristic that its maximum power point (MPP) differs with irradiance and temperature. by employing simple maximum power point tracking algorithms, we can track this MPP and increase the efficiency of our photovoltaic system. Two methods for the maximum power point tracking (MPPT) of a photovoltaic system under variable temperature and insolation conditions are discussed in this work: Incremental Conductance compared to conventional tracking algorithm (P&O).

In this paper, a new modeling solution is presented, using co-simulation between a specialist modeling tool called PSIM and the popular Matlab software using simcoupler module. Co-simulation is carried out by implementing the MPPT command circuits in PSIM and PV panel, boost DC-DC converter and battery in MATLAB/Simulink.

Keywords—Photovoltaic; Boost; PWM; MPPT; P and O; Incremental Conductance; co-simulation

I. INTRODUCTION

Photovoltaic power generation is nonpolluting, wide-distribution and promising renewable energy. But there are many problems to be solved in the development process, and the energy efficiency is one of the key points. PV panel is a nonlinear source that converts visible light into direct current (DC), it is influenced by irradiation and temperature in its operation. The PV panel characteristic presents an optimal operation point called the maximum power point (MPP) that allows the panel to generate maximum power. Maximum power point tracking (MPPT) is the process of finding this point and keeping the operation there.]

There are different techniques used to track the maximum power point: Constant Voltage (CV) method, Constant Current (CC) method Perturb & Observe (P&O), Incremental Conductance (InC) etc. In this paper, performances of two most preferably used MPPT algorithms are compared: Perturb & observe and Incremental Conductance.

Co-simulation tool is a very important tendency in electronic simulation, that allows to rely on the merits of two powerful environments in complementary way to improve the efficiency of a stand-alone photovoltaic system: Simulink as a powerful environment for system modeling and simulation and PSIM as a widely used software in many areas, and it is

characterized by a friendly simulation environment and powerful waveform processing.

The rest of the paper is sorted out as follows: Section 2 presents a description of modeling the PV panel and covers theory of boost dc-dc converter of the PV system. Section 3 discuss on two MPPT algorithms P&O and InC in term of their structures and improvements. Simulation work including the results are discussed in Section 4. Finally, a simple conclusion is given in Section 5.

II. MODELING OF PV SYSTEM USING SIMULINK

A photovoltaic cell that absorbs solar energy and converts it into electricity, is basically a photoactive semiconductor P-N junction diode. To increase the power obtained by the PV cell, we interconnect several PV cells, so that we get a PV panel.

Different configurations can be used to model PV cell such as single diode model, two diode model [1], and R_s - R_p model. the single diode configuration of PV module has been selected for this work due to degree of precision and simplicity, and the majority of previous works used single diode model [2].

A. Mathematical Equations Related to PV Modeling

The basic solar cell equation is given by :

$$I = I_{ph} - I_d - I_p \quad (1)$$

Where I_d is the diode internal diffusion current which is defined by:

$$I_d = I_0 \exp((V + R_s I)/V_t - 1) \quad (2)$$

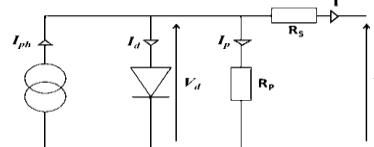


Fig. 1. The equivalent circuit of PV cell

The I_0 in the equation represents the dark saturation current or diode saturation current:

$$I_0 = \frac{I_{scn} + K_i \Delta T}{\exp\left(V_{ocn} + \frac{K_v \Delta T}{V_t}\right) - 1} \quad (3)$$

B. Modeling the PV Panel

specifications of PV panel, made by Green light energy company, are presented in Table 1.

TABLE I. PV PANEL SPECIFICATIONS

Parameters	Values
Open Circuit Voltage (Voc)	21.67 Volt
Short Circuit Current (Isc)	3.14 Amp
Voltage at Pmax (Vmpp)	17.47 Volt
Current at Pmax (Impp)	2.86 Amp
Maximum Power (Pmpp)	50 Watt
Number of Cell	36

Based on mathematical equations related to PV modeling, a complete Simulink block diagram of PV panel is demonstrated in Fig 2.

To test the validity of the PV model, we must have nonlinear characteristics. The figures below present the PV panel characteristics under changing climatic conditions.

Fig 3 shows the variation in the characteristics at various temperature when temperature shifts from 0°C to 75°C and the irradiance is kept steady at 1000w/m², Then the temperature is kept constant at 25°C while irradiance values varies from 400w/m² to 1000w/m². The variation in characteristics of the chose PV panel are presented in Fig 4.

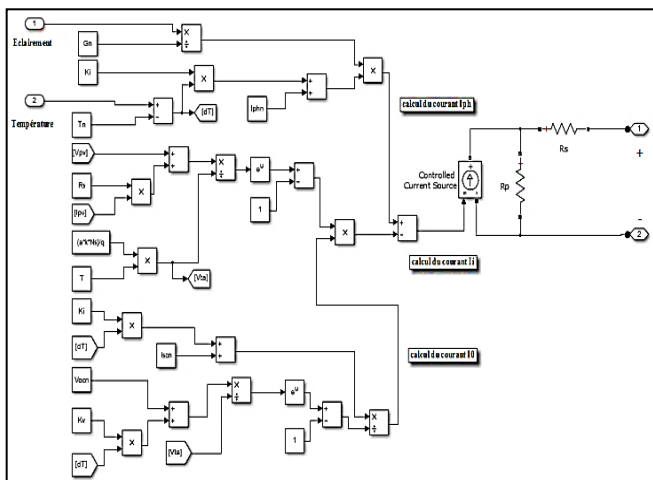


Fig. 2. simulation model of PV panel

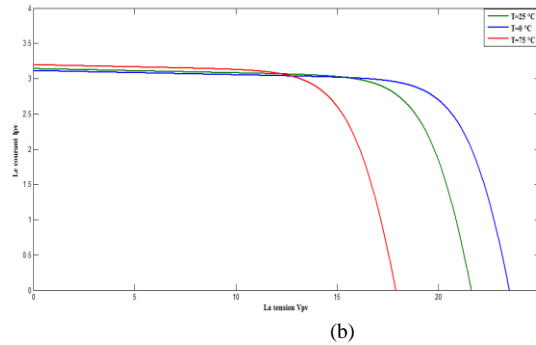
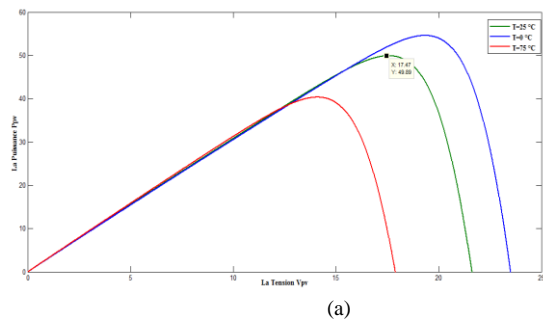


Fig. 3. (a) P-V characteristic of a PV panel (b) I-V characteristic of a PV panel for changed temperature

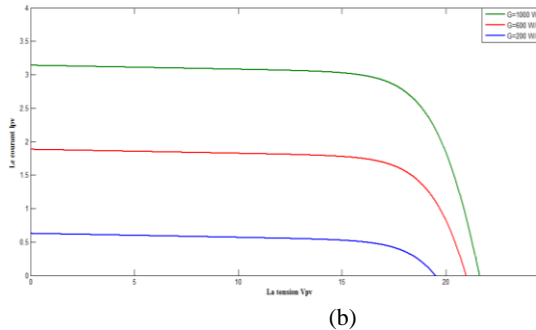
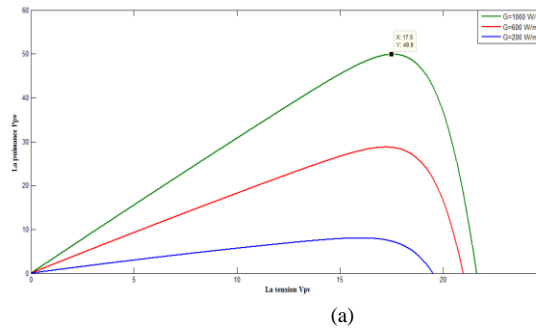


Fig. 4. (a) P-V characteristic of a PV panel (b) I-V characteristic of a PV panel for changed irradiance

C. DC-DC Boost Converter

DC-DC converters are employed for the transmission of the power of PV panel to battery side guaranteeing that maximum power has been transmitted which make use of MPPT [3]. The regulation is typically accomplished by pulse width modulation (PWM) that attacks the switching device which can be Bipolar power transistor or MOSFET; it depends on switching speed, voltage and current. The used battery has a nominal voltage of 24V, thus we use Boost dc-dc converter to increase dc voltage. Fig 5 shows the structure of boost converter in the PV system.

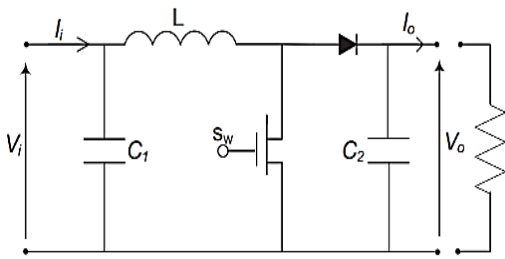


Fig. 5. Basic circuit of the boost converter

The main role of the MPPT is to regulate the duty cycle of the boost converter to achieve maximum power.

III. MAXIMUM POWER POINT TRACKING ALGORITHM

A. Perturb and Observe Method

P&O method is commonly used in PV systems. Based on the P-V characteristic, when PV power and voltage are expanding, a perturbation will add a step size ΔD with the duty cycle D , so as to create next cycle of perturbation and to drive the operating point moving toward the MPP. On the off chance that the PV power drops and PV voltage rises, the algorithm will work in the opposite way, until the algorithm reaches the MPP. This algorithm is not appropriate in high variation of the solar irradiation. The voltage oscillates around the maximum power point (MPP) and never reaches a precise value.

The biggest advantage of P&O method is the easy implementation and simple to code it using cheap digital devices besides ensuring high robustness. However, this method presents oscillations around the MPP and it suffers when subjected to rapid irradiation change. [4] [5] [6] [7] [8].

Fig 6 and Fig 7 present the flowchart and the main circuit for P&O algorithm developed in PSIM environment

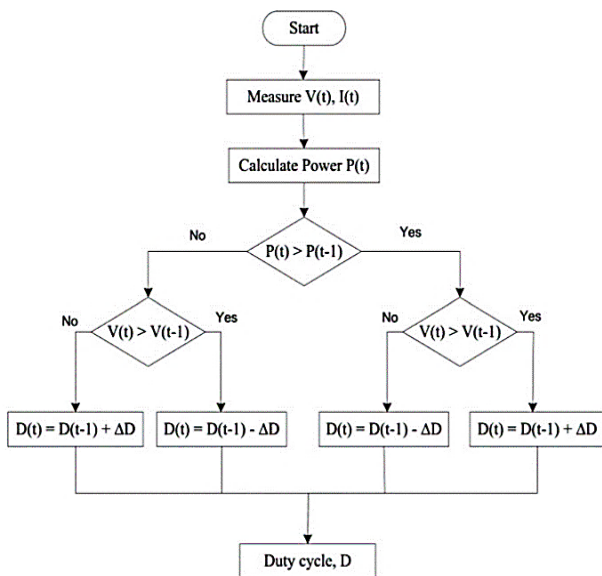


Fig. 6. flowchart of P&O algorithm

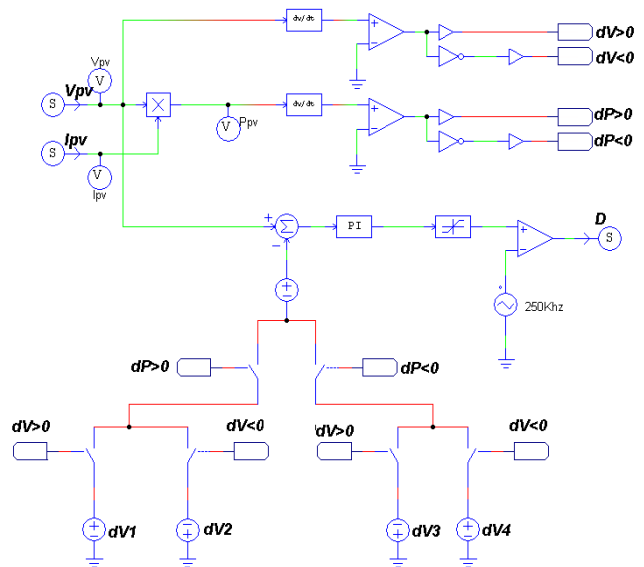


Fig. 7. model of P&O MPPT in PSIM

B. Incremental conductance method

This algorithm perturbs the voltage in one direction. If the sign of the derivative of the power dP/dV is positive, the algorithm will increase the voltage; else, it will decrease the voltage [9].

InC method is concluded from the differentiation of power with respect to voltage, due to this fact that this value in maximum power point is equal to zero.

$$\frac{dP_{pv}}{dV_{pv}} = \frac{d(I_{pv} \times V_{pv})}{dV_{pv}} \quad (4)$$

$$\frac{dP_{pv}}{dV_{pv}} = I_{pv} \frac{dV_{pv}}{dV_{pv}} + V_{pv} \frac{dI_{pv}}{dV_{pv}} = 0 \quad (5)$$

$$\frac{dI_{pv}}{dV_{pv}} = -\frac{I_{pv}}{V_{pv}} \quad (6)$$

Besides, $\frac{I_{pv}}{V_{pv}}$ is called instantaneous conductance and $\frac{dI_{pv}}{dV_{pv}}$ is incremental conductance, the place where these two values are equal the MPP will be there.

Figures below show the flowchart of Incremental Conductance algorithm (Fig 8) and the mains circuit developed in PSIM environment (Fig 9)

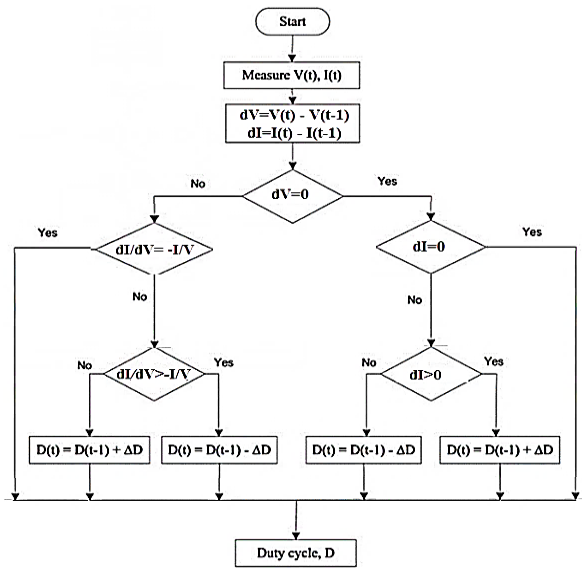


Fig. 8. flowchart of Incremental Conductance algorithm

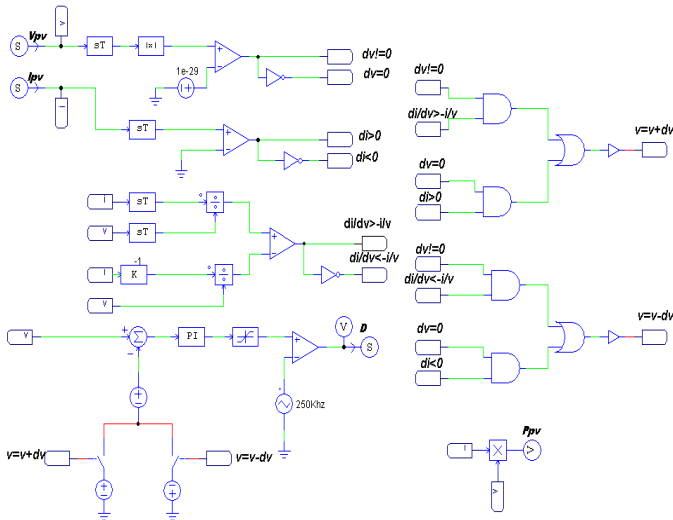


Fig. 9. model of InC MPPT in PSIM

IV. SIMULATION RESULTS

In this paper, an additional module to the PSIM software called Simcoupler, will be used, permitting for co-simulation between PSIM and SIMULINK. This module is easy to use and gives a quick simulation and waveform display in both PSIM and SIMULINK as shown in Fig 12 and Fig14.

To achieve this co-simulation, there are three modules as shown in Fig10. In PSIM, SLINK_IN module gets signal from SIMULINK and SLINK_OUT yield signal to SIMULINK. In SIMULINK, SimCoupler model block, interconnects with other part through input and output port. So that we can use the capability of two powerful softwares in complementary way.

PI controller is used to eliminate the steady state error obtained as a result of comparison between the PV panel voltage and the varied voltage value. a limiter placed at the output of PI controller to avoid over saturation.

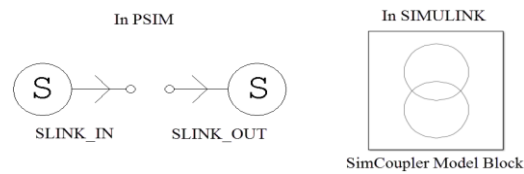


Fig. 10. Simcoupler block

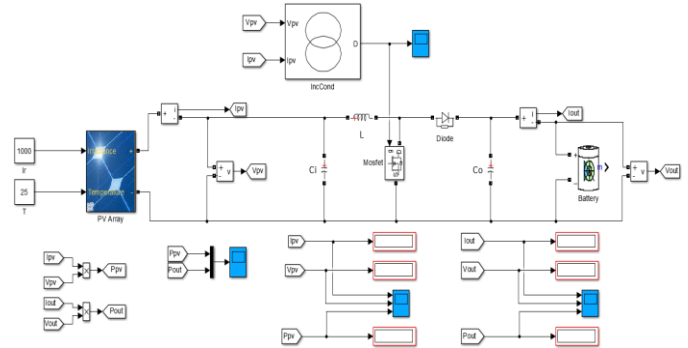


Fig. 11. Model of PV System

To generate pulse for controlled switch Mosfet of DC/DC boost converter, the output of PI controller is compared with carrier wave (Fig 7 and Fig 9)

Simulink Model of PV System with MPPT that is used for simulations is depicted in Fig 11

The figures below present the variation of the power of the module with P&O and InC controllers in standard atmospheric conditions (1000W/m², 25°C) using waveforms provided by SIMULINK and PSIM software.

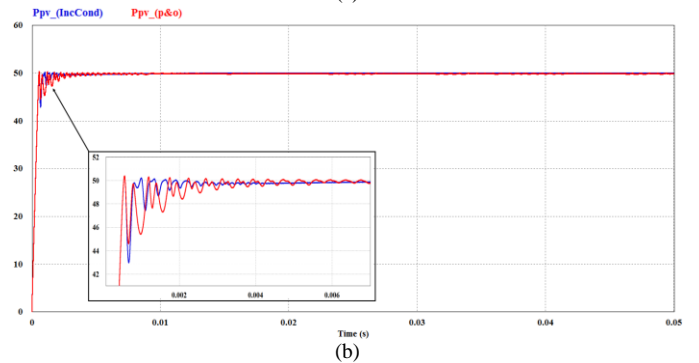
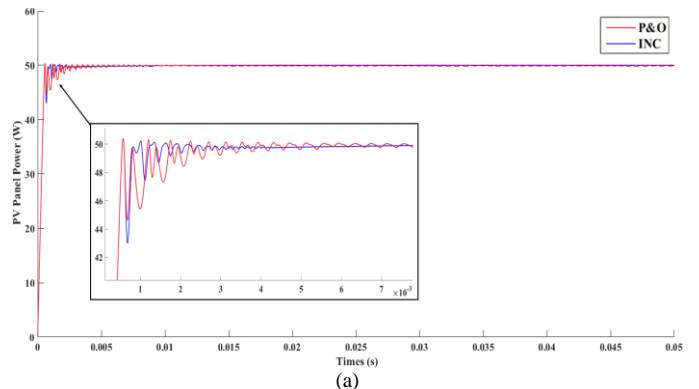


Fig. 12. Performances of P&O and InC under standard atmospheric conditions (a) Simulink (b) PSIM

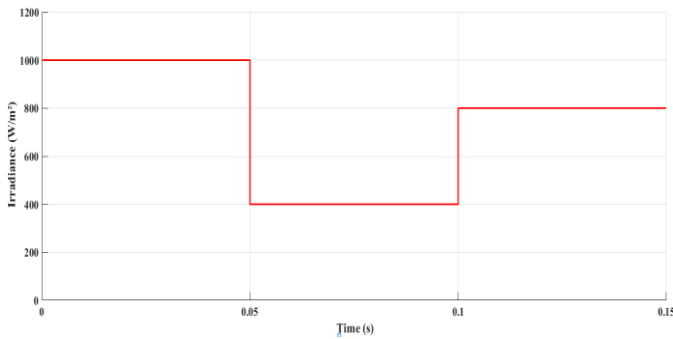


Fig. 13. Step variation of irradiance

To evaluate and compare the performances of the P&O and InC MPPT algorithms, we did a simulation test in which the PV panel is exposed to a variation in irradiance as shown in Fig 13.

The first level is set at $G = 1000 \text{ w/m}^2$. At $t = 0.05 \text{ sec}$, the irradiance is rapidly stepped down to $G = 400 \text{ w/m}^2$, and then it is stepped up to 800 w/m^2 at $t=0.1 \text{ sec}$. The temperature is kept constant at 25°C all along diverse irradiance levels.

The output power of the PV panel using the two algorithms is presented in Fig 14.

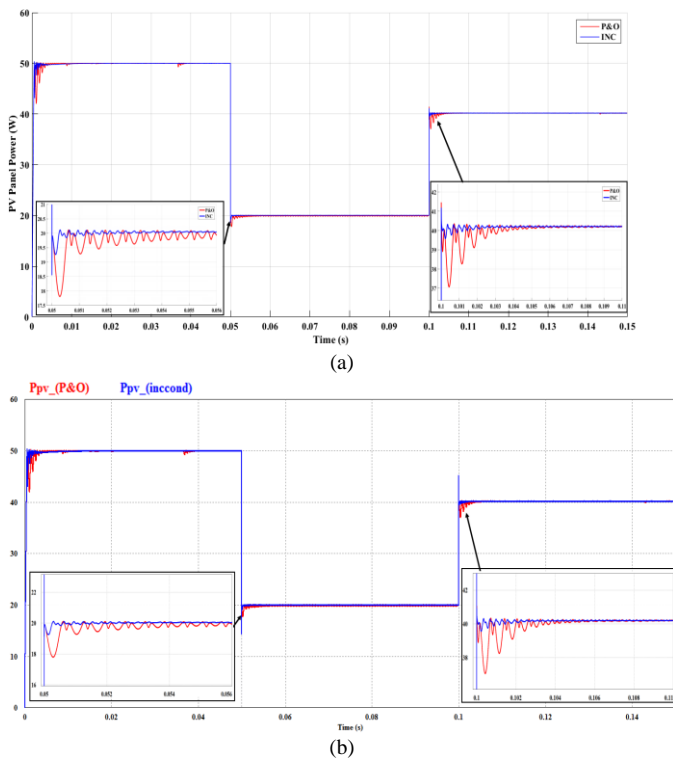


Fig. 14. Performances of P&O and InC under a rapid change in climatic conditions (a) Simulink (b) PSIM

By analyzing the figure, we can conclude that the InC starts to track the MPP little more quickly than P&O. The zoomed in window shows that P&O oscillates all over the

MPP's line which causes waste of power while in the InC there is no such oscillations.

Finally, despite of the general better performances of the InC algorithm presented in this paper, the simplicity of the P&O MPPT makes it largely used according to the facility to implement in most applications.

V. CONCLUSION

The simulation results demonstrate that the P&O and the Incremental Conductance MPPTs reach the expected MPP.

P&O and InC algorithms are both concluded from the derivative of power with voltage, however, results show some differences in the tracking performances of the two algorithms under both stagnant and variable conditions. It has observed that the Incremental Conductance reaches at the MPP little faster than P&O in all cases and shows better performance for fast irradiance changes and a better steadiness when the MPP is attained. It has observed that P&O oscillates all over the MPP's line which causes waste of power while in the InC there is no such oscillations.

REFERENCES

- [1] Ishaque, K., Salam, Z., Amjad, M., & Mekhilef, S. (2012). An improved particle swarm optimization (PSO)-based MPPT for PV with reduced steady-state oscillation. *IEEE transactions on Power Electronics*, 27(8), 3627-3638.
- [2] Huan-Liang Tsai, Ci-Siang Tu, and Yi-Jie Su "Development of Generalized Photovoltaic Model Using MATLAB/SIMULINK" *Proceedings of the World Congress on Engineering and Computer Science 2008 WCECS 2008*, October 22 - 24, 2008, San Francisco, USA
- [3] Bennett, T., Zilouchian, A., Messenger, R.: 'Photovoltaic model and converter topology considerations for MPPT purposes', *Sol. Energy*, 2012, 86, pp. 2029–2040.
- [4] Sera, D.; Kerekes, T.; Teodorescu, R.; Blaabjerg, F. Improved MPPT Algorithms for Rapidly Changing Environmental Conditions. In *Proceedings of Power Electronics and Motion Control*, Portoroz, Slovenia, 30 August–1 September 2006; pp. 1614–1619
- [5] Katherine A. Kim and Philip T. Krein, "Photovoltaic Converter Module Configurations for Maximum Power Point Operation", University of Illinois Urbana-Champaign Urbana, IL 61801 USA.
- [6] Liu X., Lopes L.A.C.: "An improved perturbation and observation maximum power point tracking algorithm for PV panels" *Power Electronics Specialists Conference, 2004. PESC 04. 2004 IEEE 35th Annual Volume 3*, 20-25 June 2004 Pages: 2005 - 2010 Vol.3
- [7] Femia N., Petrone G., Spagnuolo G., Vitelli M.: "Optimizing sampling rate of P&O MPPT technique" *Power Electronics Specialists Conference, 2004. PESC 04. 2004 IEEE 35th Annual Volume 3*, 20-25 June 2004 Pages: 1945 - 1949 Vol.3
- [8] Lian, K.L.; Jhang, J.H.; Tian, IS., "A Maximum Power Point Tracking Method Based on Perturb-and-Observe Combined With Particle Swarm Optimization," *Photovoltaics*, *IEEE Journal of*, vol.4, no.2,pp.626,633, March 2014
- [9] Kjaer, S. B. (2012). Evaluation of the "hill climbing" and the "incremental conductance" maximum power point trackers for photovoltaic power systems. *Energy Conversion*, *IEEE Transactions on*, 27(4), 922-929
- [10] M. A. Elgendy, B. Zahawi, and David J. Atkinson, "Assessment of the Incremental Conductance Maximum Power Point Tracking Algorithm", *IEEE Trans*, vol. 4, no. 1, jan 2013

Implementing and Comparison between Two Algorithms to Make a Decision in a Wireless Sensors Network

Fouad Essahlaoui

Team Science and Materials
Engineering Dept. of Physics, FST,
B.P. 509, Boutalamine, Errachidia,
My Ismail University, Morocco

Ahmed El Abbassi

Laboratory of Electronics, Physical
Instrumentation and Measurements,
Dept. of Physics, FST, B.P. 509,
Boutalamine, Errachidia, My Ismail
University, Morocco

Rachid Skouri

Team Science and Materials
Engineering Dept. of Physics,
FST, B.P. 509, Boutalamine,
Errachidia, My Ismail University,
Morocco

Abstract—The clinical presentation of acute CO poisoning and hydrocarbon gas (Butane CAS 106-97-8) varies depending on terrain, humidity, temperature, duration of exposure and the concentration of gas toxic:

From then consciousness disorders (100 ppm or 15%) rapidly limiting miners to ambient air and under oxygen until sudden coma (300 ppm or 45%) required hospitalization monitoring unit, if not the result in few minutes it's death in the poisoning site [1].

Leakage of the filling butane gas in the plant and very close to the latter position at the Faculty and under gas detection project. Has met a set of sensors to warn of possible leak, which can affect students, teachers and staff of the institution.

Therefore, this document describes the implementation of two methods: the first is Average filter and the second as Cusum algorithm, to make a warning decision swished a signal given by the wireless sensors [9] [14-15]. Which installed in the inner side of Faculty of Science and Technology in Errachidia.

Keywords—Wireless Network; Sensors; Stationary; Filter; CUSUM; Average; Arduino; Butane

I. INTRODUCTION

A. Background

This work falls within the framework of a project of gas leak detection of propane from a company that is close to the Faculty of Sciences and Techniques Errachidia. As a result the interaction of gas temperature and humidity may causes damage and infection to students, teachers and staff of the institution [3-7].

The minors consciousness disorders (drowsiness, lethargy, confusion) and behavioral disorders evoke a toxic neurotropic and require monitoring unit because they can evolve rapidly a toxic coma Fig(1).

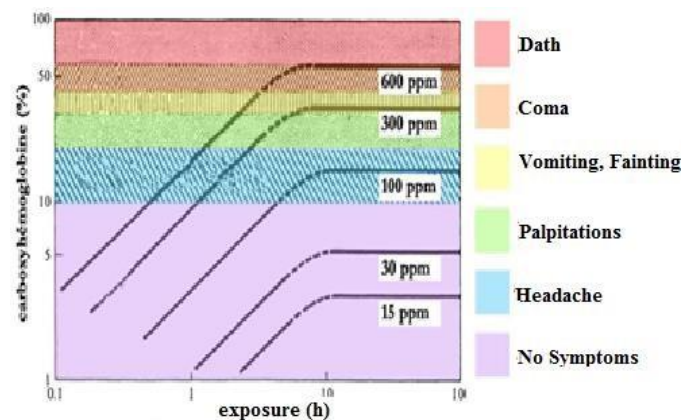


Fig. 1. Symptoms of CO poisoning according to exposure and concentration HBCO [2]

A signal with stationary ruptures or not fast-matter is a step in the treatment or the probabilistic diagnosis, to the other random of real signals appearance of several sensors and merged for a decision.

This approach considers that the signal is a succession of homogeneous segments of constant or slowly varying features, separated by sharp transitions where the signal characteristics change rapidly. A non-stationary transition or fast rupture is a short signal from the observation period it is necessary to decide in which interval a transition occurs: Hypothesis 1 or hypothesis 2 [16-17].

This amount assumes that the observed signal is stationary or non-stationary. Those techniques are used in telecommunications, radar, sonar signals and in biomedical treatments and they are manifested as powerful tools to interpret signals.

B. Overview

The idea is to compare two signal-processing techniques from several sensors. One is based on the cumulative sum algorithm CUSUM [18] the other one is based on the use of averaging filter-rolling average. Many researchers have worked on the decision-making based on pressing ie tool.

However, the optimal algorithm is what gives the average value and standard deviation parameters describing the rupture with much precision avoiding as possible a false alarm [10].

The first break detection approach is based on the use of digital filters average to estimate the mean and variance. Indeed, it is based on the moving average over an observation window and beyond a certain threshold before.

The second approach is based on the CUSUM algorithm often used for making decision in many phenomena to following failure detection signals [11]. In this work, we have treatments signals from gas sensors, temperature and humidity...?

II. THEORETICAL APPROACH'S

A. Approach based on Filters Average:

This method is based on the variance's estimation of the moment first order sliding [11-12]. The main feature of this filter is his nonlinearity, which is an outputs value close to zero in the stationary signal, and in the presence of a rupture represents a high amplitude response. The figure below fig. 2 shows the block diagram of the filter used.

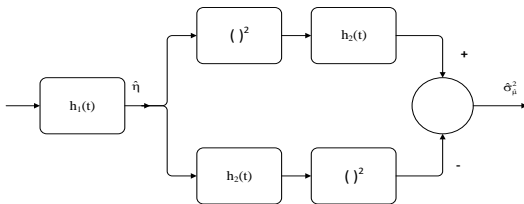


Fig. 2. Average estimator followed by variance estimator

The algorithm of this first approach presented as followed

Algorithm 1: Average filter

- Step 1: capture the data
- Step 2: estimate the mind of data
- Step 3: estimate the variance of mind
- Step 4: detection the rupture in data
- Step 5: loopback to Step 1 if (estimate the variance < S)
- Step 6 if (no)
- Step 6: alarm (estimate the variance > S)

(S : determinated threshold)

The impulse response h1 (t) satisfied:

$$\int_{-\infty}^{+\infty} h_1(t)dt = H_1(0) \quad (1)$$

Where H1 (f) is the Fourier transform of h1 (t). The output of this filter is given by:

$$\hat{\mu}(t) = (h_1 * x)(t) \quad (2)$$

Where h1(t) is an estimator of average value $\hat{\mu}$. The variance is given by:

$$\text{Var}[\hat{\mu}(t)] = \sigma^2 \int_{-\infty}^{+\infty} h_1(t)^2 dt \quad (3)$$

Where σ^2 is the variance of the input process. It is proposed to estimate this variance of $\hat{\mu}(t)$ on a time horizon:

$$\hat{\sigma}_{\hat{\mu}}^2(t) = h_2(t) * [\hat{\mu}(t)]^2 - [h_2(t) * \hat{\mu}(t)]^2 \quad (4)$$

Where h is impulse response of a linear filter and invariant.

For not involving average in (4) one requires the normalization condition:

$$\int_{-\infty}^{+\infty} h_2(t)dt = 1 \quad (5)$$

The goal is to choose filters $h_1(t)$ and $h_2(t)$ as for a stationary input $x(t)$, $\hat{\mu}$ assumes a substantially constant value.

Accordingly, $\hat{\sigma}_{\hat{\mu}}^2(t)$ will have a positive value close to zero. For an input having a mean change, $\hat{\mu}$ has a transition and $\hat{\sigma}_{\hat{\mu}}^2(t)$ locally increases, Operate the variation of $\hat{\sigma}_{\hat{\mu}}^2(t)$ indicating a poor local estimate of $\hat{\mu}$, to highlight the searched transition responsible for this state of affairs.

Made filters h_1 and h_2 minimize (3) and are given by:

$$h_1(t) = \frac{1}{T_1} \text{rect}\left(\frac{t}{T_1}\right) \quad (6)$$

Where T_1 denotes the filter length and $\text{rect}(t)$ the normalized rect angular function. is defined in the same manner h_2 the impulse response of the second filter that minimizes noise by:

$$h_2(t) = \frac{1}{T_2} \text{rect}\left(\frac{t}{T_2}\right) \quad (7)$$

For validate the performance of this filter experimentally and break detection power by implementing it on an embedded system basic Arduino board, for melting of stationary signals from various sensors in real time. Next, we examine these signals representing the random and stationary physical quantities such as propane gas, Temperature or humidity simultaneously.

B. Approach based on CUSUM algorithm:

To compare these experimental results found with those based on the CUSUM algorithm by comparing the statistical values. Where $x[n]$ is a discrete random signal, supposed sample independent and identically distribute. The samples follow a probability density functions $p(x[t_n], \theta)$ that depends on deterministic parameter θ . This parameter can be the mean μ_x or the variance σ_x^2 of $x[n]$.

The randomly feature of the signal can contain one or many abrupt occurring at the time. t_{nc} This threshold is modeled by

an instantaneous modification of the value of θ occurring at rupture time t_{nc} . Therefore, $\theta = \theta_0$ before t_{nc} and $\theta = \theta_1$ from t_{nc} to the current sample.

According to these assumptions, the whole probability density function of the signal p_x observed between the first sample $x[0]$ and the current one $x[k]$ can take two different forms.

While no change occurs hypothesis H_0 , the probability density function of $X[t_n]$ is given by:

$$P_x/H_0 = \prod_{t_n=0}^k p(x[t_n], \theta_0) \quad (8)$$

While the one change occurs hypothesis H_1 , this probability density functions becomes:

$$P_x/H_1 = \prod_{t_n=0}^{t_{nc}-1} p(x[t_n], \theta_0) \prod_{t_n=t_{nc}}^k p(x[t_n], \theta_1) \quad (9)$$

Supposed the abrupt change to be known. The unknowns to be determined are:

The occurrence of an abrupt change between $t_n = 0$ and $t_k = k$.

The value of the possible change time t_{nc} .

The approach followed here is to develop an algorithm in order to detect the signal sample after sample. However, at each new sample, one of the two previous hypotheses H_0 or H_1 has first to be decoded. In this case, a change can be detected (H_1 decided), the change is here which is approximated by an estimator \hat{t}_{nc} .

The log-likelihood ratio [Kay 98] is used. It is defined by:

$$L_x = \ln\left(\frac{P_x/H_1}{P_x/H_0}\right) \quad (10)$$

Then, decide H_1 if $L_x > h$ (else H_0), where h is threshold set by user.

Reporting (1) and (2) in (3) we obtained:

$$L_x[k, t_{nc}] = \ln\left(\frac{P_x/H_1[k, t_{nc}]}{P_x/H_0[k]}\right) = \sum_{t_n=t_{nc}}^{t_k} \ln\left(\frac{p(x[t_{nc}], \theta_1)}{p(x[t_n], \theta_0)}\right) \quad (11)$$

Estimation step: the change time \hat{t}_{nc} .

Once use the maximum likelihood estimate, we obtain \hat{t}_{nc} as:

$$\hat{t}_{nc} = \arg \max_{1 \leq t_{nc} \leq t_k} p_x/H_1[t_k, t_{nc}] = \arg \max_{1 \leq t_{nc} \leq t_k} L_x[t_k, t_{nc}] \quad (12)$$

$$t_{nc} = \arg \max_{1 < t_{nc} \leq t_k} \sum_{t_n=t_{nc}}^{t_k} \ln\left(\frac{p(x[t_n], \theta_1)}{p(x[t_n], \theta_0)}\right) \quad (13)$$

The CUSUM algorithm is traduced as following:

Algorithm 2: Cusum Algorithm

- Step 1:** set the threshold value
- Step 2:** measure the current data
- Step 3:** decide between H_0 (no change) and H_1 (one change)
- Step 4:** if H_1 do Step 5 to Step 7 else returned to Step 2
- Step 5:** store the detection time $t_{change} = t_{comet}$
- Step 6:** Estimate the change time
- Step 7:** reset the algorithm from Step 2

III. EXPERIMENTAL AND RESULTS

A. The operating model

In this project, the simulation and implementation are on Arduino Mega type, the acquisition of several random signals from sensors and, applying filters initially for the detection of abrupt change threshold that gave good results since it detects breakage and filters the signal at the same time. Each signal is able to determine the break after treatment threshold, the mean and variance were in normal state i.e. before the break and after the break. All results are reported in graphs of real signal random nature. near processing, by these two algorithms implemented on the embedded system called Arduino device and it calculates the deferred statistical parameters determined experimentally on table below.

TABLE I. CAPTURED SIGNALS AND DATA ACQUISITION OF DIFFERENT SENSORS BEFORE TREATMENT

Hour	Sensors		
	DHT 11 Humidity	MQ 6 Gas	LM 35 Temperature
0.9302662	22	146	29.3
0.93096065	22	144	29.3
0.93165509	22	145	29.3
0.93234954	22	146	29.3
0.93304398	22	146	29.79
0.93375	22	146	29.3
0.93444444	22	146	29.3
0.93513889	22	146	29.3
0.93583333	22	146	29.3
0.93652778	22	145	29.79
0.93722222	22	147	29.3
0.93791667	22	147	29.3
0.93861111	22	147	29.3
0.93931713	22	147	29.3

0.94001157	22	148	29.79
0.94070602	22	149	29.79
0.94140046	22	149	29.79
0.94209491	22	148	29.3
0.94278935	22	149	29.79

These data has been measured every minute they reached different sensors installed outdoor of the laboratory, they represented respectively, the humidity moisture sensor, the gas sensor and the temperature sensor.

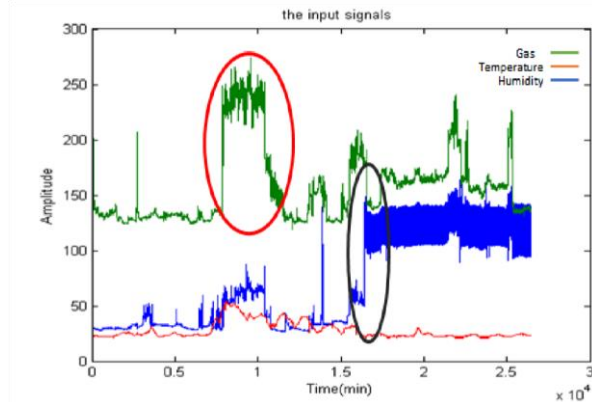


Fig. 3. The randomize original signals captured from different sensors

In these measurements of the humidity signal was almost constant, while the temperature signal was around 29 °C and had a break near 8 mn up to 10 minutes this rupture is very pronounced for gas signal on Fig 3.

Also on this graph, a rupture of the gas signal appears. This means that there is a leak gas period corresponding to a phase of discharging and charging on the factory, which is located near the lab.

B. The Experimental Equipment

The Equipment used in this project are embedded system type Arduino Mega card, three sensors for temperature, gas and humidity simultaneously of types: LM35, MQ6 and DHT11. a laptop, Breadboards, RF module and Jumper wires figure 4.

The signal from sensors goes to Arduino card for the processing [19-20], then the results pass through an USB serial port to the laptop. These data is exploited by Matlab software program to plot the result for showing alarms [8].

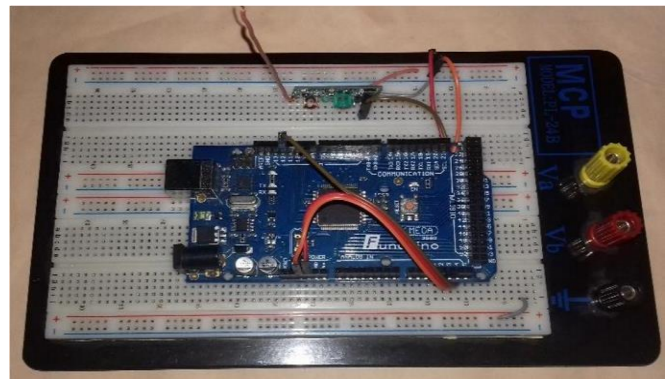
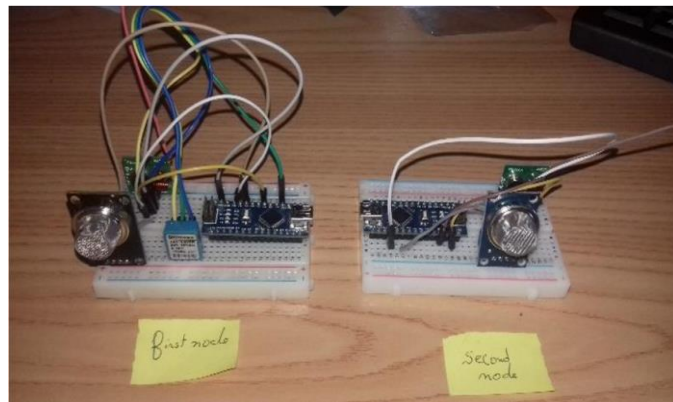


Fig. 4. Experimental Equipment (a- Two of second level Node b- principal level Node)

C. Experimental Results

The results given by the two processing algorithms implemented on the card are

1) Average filter:

The Given results at the output of the first filter using the following parameters (14) are

$$h_1(t) = \text{rect}(t)$$

$$h_2(t) = \frac{1}{15} \text{rect}\left(\frac{t}{15}\right) \tag{14}$$

The observations of the two windows have been carefully selected in order to get the best results.

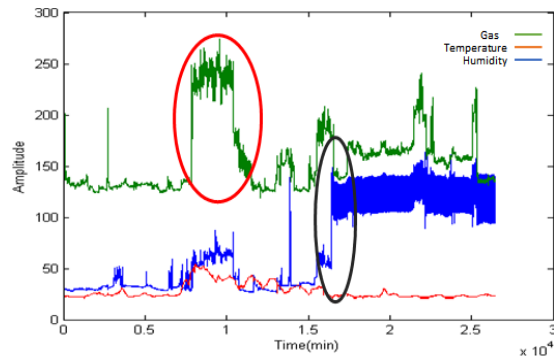


Fig. 5. Three randomize signals from different sensors before treatment by average filtering

Figure 5 shows the signals detected by the various sensors. the gas sensor is clearly shown by a rupture between 0.7 and 1,2mn about two days. this range represents the gas leak period during the charging and discharging of the stock at the gas factory. This takes about two days ($\mu_{1g} = 240\text{ppm}$) before returning to normal ($\mu_{0g} = 140\text{ppm}$) the signal representing the temperature under normal conditions is around ($\mu_{0T} = 37^\circ\text{C}$) and subsequently forced to amplitude transition ($\mu_{1T} = 120^\circ\text{C}$).

The humidity signal varies little and has a slight variation around the mean value especially at night.

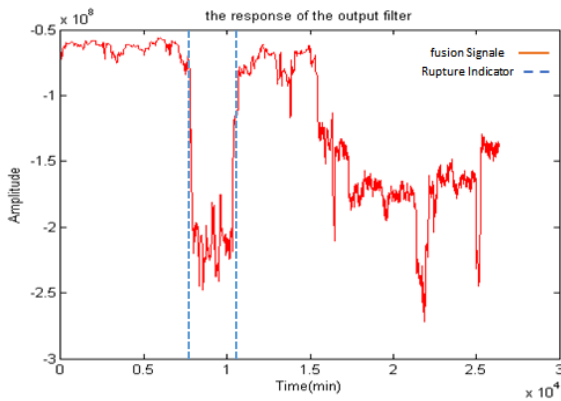


Fig. 6. The fusion processing signals using the filtering operation

Figure 6 shows the signal merged in solid lines and the various breaks threshold marked by dotted lines. In the signal of gas leakage representative rupture threshold is preponderant is always lasts about two days.

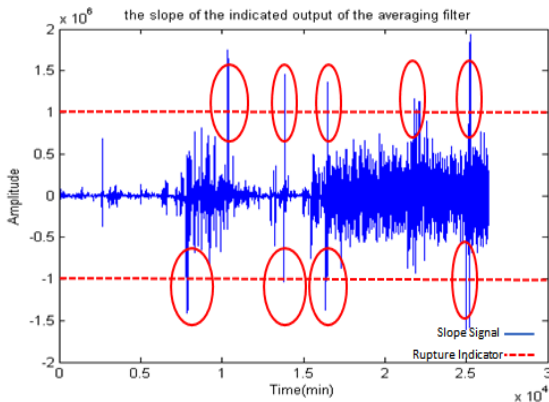


Fig. 7. The derivative of fusional signal with thresholds for the average filter

Figure 7 shows the derivative of the merged signal where repetitive peaks with an average around zero mark thresholds of the overall signal.

TABLE II. DIFFERENT EXPERIMENTAL PARAMETERS EXTRACTED USING THE AVERAGE FILTER

Average filter					
σ_{fs}	$(\sigma_{fs})^2$	μ_{fs}	$S\sigma_{fs}$	$(S\sigma_{fs})^2$	$S\mu_{fs}$
3.3766	3.3766	-1.2358	1.2541	1.2541	-276.7339

Where:

- σ_{fs} : Variance of the fusion signal with the average filter
- $(\sigma_{fs})^2$: Covariance of the fusion signal with The average filter
- μ_{fs} : Average of the fusion signal with The average filter
- $S\sigma_{fs}$: Variance of the slope signal fusion with The average filter
- $(S\sigma_{fs})^2$: Covariance of the slope signal fusion with The average filter
- $S\mu_{fs}$: Average of the slope signal fusion with The average

filter

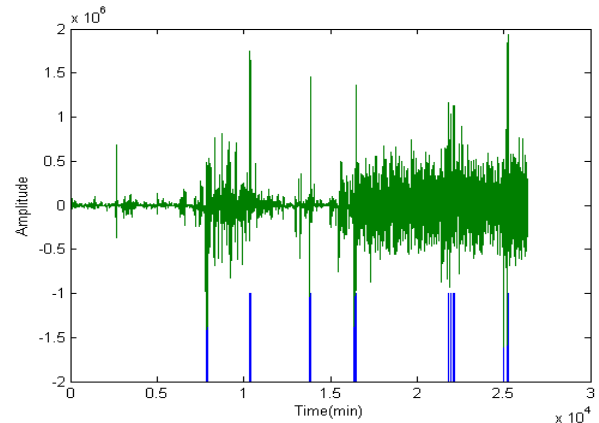


Fig. 8. Fusional signal with thresholds for many ruptures after average filter processing

Figure 8 shows the different extracts statistical parameters of the merged global signal.

2) CUSUM Algorithms:

The Implementation of this second algorithm gives the following results for the same data as in TABLE I.

The output of CUSUM Algorithm is:

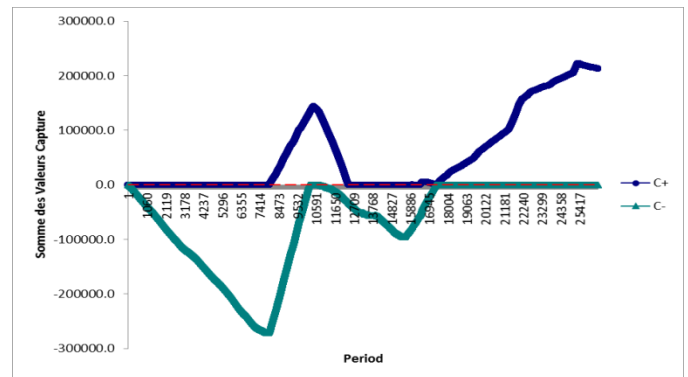


Fig. 9. The result fusional signal after CUSUM algorithm processing

Figure 9 characterizes the rupture of the signal after processing by the CUSUM algorithm. After derivation of the signal 9, the gas leakage protester breaking point is very clear is predominant.

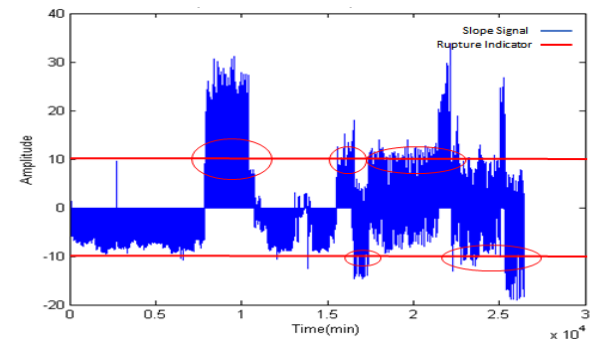


Fig. 10. The derivative of fusional signal with thresholds for the CUSUM algorithm

Figure 10 shows the rupture positions and the corresponding time duration. Note here that the second algorithms determine the breaking point is the threshold of the gas leak in the amplitude and time.

TABLE III. DIFFERENT EXPERIMENTAL PARAMETERS EXTRACTED USING THE CUSUM ALGORITHM

CUSUM Algorithm					
σ_{fs}	$(\sigma_{fs})^2$	μ_{fs}	$S\sigma_{fs}$	$(S\sigma_{fs})^2$	$S\mu_{fs}$
1.0591	1.0591	-3.1701	25.0089	25.0089	-0.0157

Table III shows the statistical parameters determined by the Cusum algorithm operated on the merged signal.

The different extracted parameters are defined as:

- σ_{fs} : Variance of the fusion signal with CUSUM algorithm
- $(\sigma_{fs})^2$: Covariance of the fusion signal with CUSUM algorithm
- μ_{fs} : Average of the fusion signal with CUSUM algorithm
- $S\sigma_{fs}$: Variance of the slope signal fusion with CUSUM algorithm
- $(S\sigma_{fs})^2$: Covariance of the slope signal fusion with CUSUM algorithm
- $S\mu_{fs}$: Average of the slope signal fusion with CUSUM algorithm

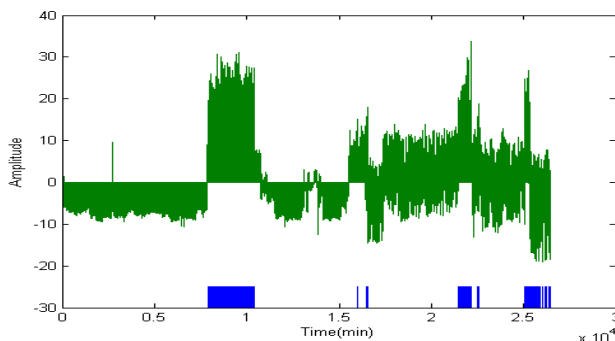


Fig. 11. Signal with marquees of position rupture for CUSUM filter

IV. CONCLUSION

In this work, we have implemented two methods of decision making following the detection of failure in these real and random signals outcome from multiple wireless sensors.

The first is based on the Averaging filter and the second is on the CUSUM algorithm. after melting of signals by statistical methods and determining the mean value and the variance of the resulting signal, an alarm can be triggered after fusion signals by statistical methods and determination of the average value and the variance of the resulting signal. Otherwise, an alarm can be triggered to prevent or alert management against a possible catastrophe example: a fire, a gas leak or take security measurement.

The results are translated into graphs plotted in real time and the defined parameters are reported in the tables for both techniques implemented on the embedded system, which is Arduino Mega card. The filter method is better than the CUSUM since it detects and at the same time filter if ever there

is noise in addition. Our results are in good agreement with those found in the literature by other techniques.

REFERENCE

- [1] DE, TWA, SÉ DE, and WRA DE. "FICHE TECHNIQUE SANTÉ-SÉCURITÉ," 2011. [http://microbertfuels.com.previewyoursite.com/msds-data/Propane%20avec%20Odorant%20\(French\)%20-%20Provident%20Energy%20Ltd%20.pdf](http://microbertfuels.com.previewyoursite.com/msds-data/Propane%20avec%20Odorant%20(French)%20-%20Provident%20Energy%20Ltd%20.pdf).
- [2] de Calais, APPA Nord-Pas. "Intoxications Au Monoxyde de Carbone." Accessed August 9, 2016. http://www.intoxco-ndpc.fr/files/PDF/Dossier_CO.pdf.
- [3] Utilisateur, Super. "Recherchez Un Antidote En Ligne." : : : : E Formation En Médecine D'urgence: : : : : Accessed August 9, 2016. <http://www.efurgences.net/index.php/seformer/toxicologie/231-antidotecanada>.
- [4] B. W. de S. Arruda, R. P. Guimaraes Lima, and C. P. D. Souza, "An artificial immune system-based anomaly detection method applied on a temperature control system," International Journal of Industrial Electronics and Drives, vol. 1, no. 3, p. 145, 2014.
- [5] M. L. Sampson, V. Gounden, H. E. van Deventer, and A. T. Remaley, "CUSUM-Logistic Regression analysis for the rapid detection of errors in clinical laboratory test results," Clinical Biochemistry, Oct. 2015.
- [6] Z. Wu, M. Yang, M. B. C. Khoo, and F.-J. Yu, "Optimization designs and performance comparison of two CUSUM schemes for monitoring process shifts in mean and variance," European Journal of Operational Research, vol. 205, no. 1, pp. 136–150, Aug. 2010.
- [7] Carbon monoxide poisoning CO folder created in 2005 has put jor in 2010 appa (Association for the Prevention of Air Pollution)
- [8] Ingle, Vinay K., and John G. Proakis. *Digital Signal Processing Using MATLAB*. 3rd ed. Stamford, Conn: Cengage Learning, 2012.
- [9] Krishnamachari, Bhaskar. "An Introduction to Wireless Sensor Networks." USC Viterbi School of Engineering, 2005. <http://www.wsncs.zjut.edu.cn/download/20100130213026563.pdf>.
- [10] Wu, Yanhong. *Inference for Change-Point and Post-Change Means after a CUSUM Test*. Lecture Notes in Statistics 180. New York, NY: Springer, 2005.
- [11] Reboul, Serge. "Estimation et Détection Conjointe Pour La Fusion D'informations." Université du Littoral Côte d'Opale, 2014. <https://tel.archives-ouvertes.fr/tel-01067478/>.
- [12] Mohindru, Parul, Vikshant Khanna, and Rajdeep Singh. "Forest Fire Detection: Various Approaches." *International Journal of Emerging Science and Engineering (IJESE) ISSN*, 2013, 2319–6378.
- [13] Sekkas, Odysseas, Stathes Hadjiefthymiades, and Evangelos Zervas. "A Multi-Level Data Fusion Approach for Early Fire Detection." In *Intelligent Networking and Collaborative Systems (INCOS), 2010 2nd International Conference on*, 479–483. IEEE, 2010. http://ieeexplore.ieee.org/xpls/abs_all.jsp?arnumber=5702146.
- [14] Ferdoush, Sheikh, and Xinrong Li. "Wireless Sensor Network System Design Using Raspberry Pi and Arduino for Environmental Monitoring Applications." *Procedia Computer Science* 34 (2014): 103–10. doi:10.1016/j.procs.2014.07.059.
- [15] Souissi, Rachid, and Mohsen Ben-Ammar. "An Intelligent Wireless Sensor Network Temperature Acquisition System with an FPGA." *Wireless Sensor Network* 6, no. 1 (2014): 1–7. doi:10.4236/wsn.2014.61001.
- [16] Callegari, C., S. Giordano, M. Pagano, and T. Pepe. "WAVE-CUSUM: Improving CUSUM Performance in Network Anomaly Detection by Means of Wavelet Analysis." *Computers & Security* 31, no. 5 (July 2012): 727–35. doi:10.1016/j.cose.2012.05.001.
- [17] Castagliola, Philippe, and Petros E. Maravelakis. "A CUSUM Control Chart for Monitoring the Variance When Parameters Are Estimated." *Journal of Statistical Planning and Inference* 141, no. 4 (April 2011): 1463–78. doi:10.1016/j.jspi.2010.10.013.
- [18] Severo, Milton, and Joao Gama. "Change Detection with Kalman Filter and Cusum." In *Discovery Science*, 243–254. Springer, 2006. http://link.springer.com/chapter/10.1007/11893318_25.

- [19] S. Kay. Fundamentals of statistical signal processing, volume 1: Estimation theory. Prentice Hall, 1_{st} edition, 1993.
- [20] S. Kay. Fundamentals of statistical signal processing, volume 2: Detection theory. Prentice Hall PTR, 1998.

Emotion Recognition from Speech using Prosodic and Linguistic Features

Mahwish Pervaiz
Computer Sciences Department
Bahria University, Islamabad
Pakistan

Tamim Ahmed Khan
Department of Software Engineering
Bahria University, Islamabad
Pakistan

Abstract—Speech signal can be used to extract emotions. However, it is pertinent to note that variability in speech signal can make emotion extraction a challenging task. There are a number of factors that indicate presence of emotions. Prosodic and temporal features have been used previously for the purpose of identifying emotions. Separately, prosodic/temporal and linguistic features of speech do not provide results with adequate accuracy. We can also find out emotions from linguistic features if we can identify contents. Therefore, We consider prosodic as well as temporal or linguistic features which help increasing accuracy of emotion recognition, which is our first contribution reported in this paper. We propose a two-step model for emotion recognition; we extract emotions based on prosodic features in the first step. We extract emotions from word segmentation combined with linguistic features in the second step. While performing our experiments, we prove that the classification mechanisms, if trained without considering age factor, do not help improving accuracy. We argue that the classifier should be based on the age group on which the actual emotion extraction be required, and this becomes our second contribution submitted in this paper.

Keywords—Emotion Extraction; Prosodic Features; Temporal Features; Dynamic Time Wrapping; Segmentation

I. INTRODUCTION

User interfaces are becoming increasingly complicated as the requirements, standards and de-facto standards are improving day by day. User interfaces are also providing speech processing systems to help users give commands without physically interacting through a keyboard. Speech is an important means of human to human (and machines) communications, and it carries additional information as well. We can find out the underlying emotional and psychological aspects as well. Speech processing provides a list of various features and characteristics of sound that can be further analyzed to reveal valuable information.

Although research work is done and various applications are developed but emotion recognition from speech is still a challenging task. Main reason for this is variability of expression even for the same emotion. According to representation of emotions in two-dimensional space, joy and anger both have common acoustic attributes like amplitude of voice, pitch, number of times their speech meets zero axis. In the same manner, fear and sad have some common attributes. Therefore, problem occurs between recognition of these two sets of emotions due to the fact that we extract emotion directly and only from speech signal or text and due to the feature set

we use for recognition of emotion. Acoustic features of speech like pitch, energy or volume are also somewhat misleading if considered alone e.g., if a person is angry, he might speak in normal tone using harsh words to express his anger. Similarly, people may shout in anger while some don't. Some people speak loudly when they are happy or excited while other may not. Therefore, we can say that people use speech signal's features and speech semantics to present their emotions in our everyday life. This makes it clear that we need to extract emotions from acoustic as well as from semantic features to arrive at a conclusive result regarding the hidden emotions in a speech signal.

Therefore, we present an approach to consider prosodic and linguistic features to improve emotions extraction from speech. Our motivation for this research is an expected use in an e-learning system which does an offline emotions analysis of kindergarten students and reports their emotional changes throughout the day. The rest of the paper is organized as follows; we explain our emotions extraction approach in Section 2 and we introduce our two stages of our proposed model in Section 3 and Section 4 respectively. We discuss our experiments for evaluation in Section 5 and discuss our results in Section 6. We finally present related work in Section 7 and conclusion in Section 8.

II. EMOTION EXTRACTION FROM SPEECH

We implement a two-staged model where we extract emotions from speech signal using prosodic and temporal features in the first stage. We extract emotions from words with semantic orientation in the second stage. We present an overview of our proposal is given in Figure 1.

While considering prosodic features, we consider pitch, energy and Zero Crossing Rate (ZCR), where temporal features including Mel Frequency Cepstral Coefficients (MFCC) and Linear Prediction Coefficient (LPC) are considered in Stage-1. We use Support Vector Machine (SVM) classifier for classification of speech based on temporal and prosodic features. While extracting linguistic features in the second stage, we extract words by segmenting speech signal using pause between words. We then use dynamic time wrapping (DTW) with MFCC for matching signal for recognition of that word. Finally, we compare extracted words with our dictionary which contains words with class labels to see if a word or its synonym is used to express an emotion in word under consideration. Our reason to consider MFCC and LPC in stage-1 is the fact that we are extracting emotions at segment

level and according to [21] spectral features specially MFCC and LPC are very beneficial to identify emotions of short

length segment [21]. This helps us to get better performance of our system.

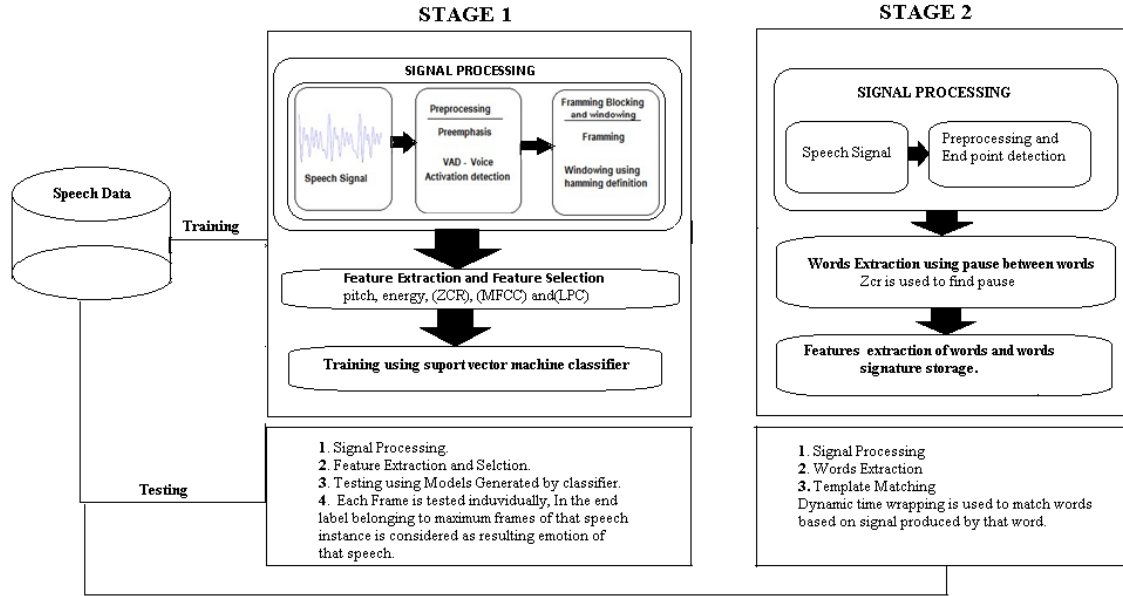


Fig. 1. Emotion Recognition from Speech

III. STAGE-I: EMOTION EXTRACTION FROM SPEECH WITH PROSODIC & TEMPORAL FEATURES

In this stage, emotions are extracted from speech signal using prosodic and temporal features as discussed in above section. This stage comprises of three steps, Signal processing, features extraction and calculation and training of the classifier. We explain of these steps in detail.

A. Signal Processing

As speech signal contains noise that can increase error rate so it is important to minimize noise as possible. Signal processing is performed on speech signal to improve the correctness and efficiency of the extraction process. The following steps are involved in signal processing.

- Pre-Emphasize
- Voice Activity Detection
- Framing and Windowing

Speech signal suffers from additive noise because of its high dynamic range. We apply Pre-Emphasize to spectrally flatten speech signal and removal of low frequency noise. We first remove DC components by extracting mean value from all samples value and then filtering is applied on it. Pre-Emphasizer are often represented by first order high pass filter. The configuration of this filter in time domain is given by Eq. 1. Sample of original signal and pre-emphasize signal is shown in Figure 2.

$$h(n) = 1, -0.9375 \quad (1)$$

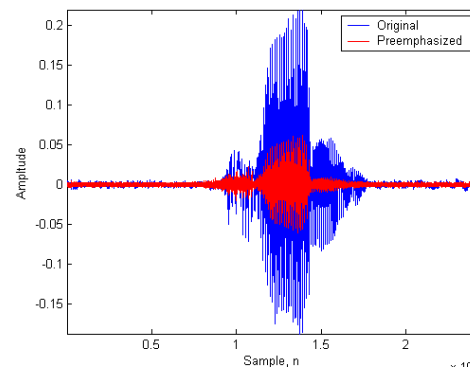


Fig. 2. Pre-emphasized signal

We use voice activity detection to detect start and end point of speech. It is pertinent to note that VAD could be applied in time domain as well as frequency domain. In Time domain volume and ZCR with high order difference are used and in frequency domain variance and entropy of spectrum is used for end point detection. We then select features threshold and then any frame with high values than threshold is considered as positive and negative otherwise [18]. There are four intuitive way to select threshold, as shown by the following four equations:

$$\begin{aligned} Vth &= v_{max} * \alpha, \\ Vth &= v_{median} * \beta, \\ Vth &= v_{min} * \gamma, \\ Vth &= v_1 * \delta \end{aligned} \quad (2)$$

We use the algorithm presented in [16] to detect end points. After detection if end points we segment speech signal into blocks. Speech signal after voice activity detection is presented in Figure 3. Classification accuracy is proportion to the length of utterance [2] where spectral analysis of speech signal at sub

utterance with small size of frame level gave good classification rate. Instead of taking whole speech utterance as a single block, we divide speech signals into small matrix with appropriate length of each frame. We use frame length of 40ms and sample size of 16000Hz and then we calculate total number of points in wav file by multiplying sample rate with frame size. After dividing into frame, we apply windowing on each frame. Hamming window reduces signal discontinuity on end of frames [11]. The coefficients of a Hamming window are computed from the following equation. The window length is $L=N+1$.

$$w(k) = 0.54 - 0.46\cos(2\pi k / K - 1) \quad (3)$$

B. Feature Calculation and Feature Selection

After preprocessing is done framing and windowing is applied. Features are extracted from each frame for parameterization of feature vector. Features we have extracted are pitch, MFCC, and LPC. Pitch related statistics convey considerable information in speech about emotions status in a speech segment [1] and Yu et al [23]. We calculate pitch for each frame using correlation function.

Human ear hearing uses nonlinear frequency units [12]. Therefore for each utterance with original frequency another subjective pitch is measured on Mel scale. Mel scale offers linear frequency spacing below 1000h and logarithmic frequency spacing above 1000Hz. As given in literature spectral features gave more classification accuracy at frame level than prosodic features. Kim et al. argued that statistics relating to MFCCs also carry emotional information [10]. In this research we extracted First 13 coefficient of MFCC. Next, we convert signal from time domain to frequency domain using Fast Fourier Transform (FFT). Spectral Analysis showed that in speech signal different timbre correspond differently over frequency with different energy distribution. We apply FFT for converting signal to frequency domain in order to find out the magnitude frequency for each frame. We then measure step Mel frequency wrapping subjective pitch on Mel scale and spectrum is simulated with the use of filter bank. One filter is used for each component. Finally, we convert Log Mel spectrum back to time domain which results in MFCC as real numbers and we use discrete cosine transform to convert back into time domain. Basic idea of linear predictive coding is to predict current frame from linear sequences of past frames.

We use signal processing tool box for computing LPC coefficients of each frame. We use the following equation to compute LPC as:

$$lpc(x, p) \quad (4)$$

Where p is the p^{th} order linear predictor (FIR Filter) that is used to predict current frame x .

$$x(n) = -a(2)x(n-1) - a(3)x(n-2) \dots - a(p+1)x(n-p)$$

We compute 13 LPC coefficient and extract zero crossing rate of the signal by calculating how many time a signal meet with zero axes. Next, we compute energy for each frame using log energy equation defined in [3] as:

$$E = 10 * \log_{10}(e + s 2n) \quad (5)$$

Here, "e" is a small positive constant added to prevent the computing of log of zero. It is important to note that e is much less than the mean-squared value of the speech samples. We use configuration for Energy as given by Eq. 6 below.

$$E1 = 10 * \log_{10}(eps + \frac{sum(FRAME, 2)}{size(FRAME, 2)}) \quad (6)$$

We then use forward selection algorithm for selection of features after extraction of features. We begin with basic values of energy, volume, MFCC and LPCC and in each iteration, we add one feature and their statistics like mean, median, standard deviation and variance. We compare performance accuracy with the previous iteration at the end of each iteration.

C. Classification through SVM

We use a classifier to predict emotional labels using selected set of features. We use static classifier Support Vector Machines (SVM) that is inherently two class problem for linearly separable data. In our case, we have multidimensional data that is not linearly separable because some classes share same features that could not be linearly separable. We use SVM with One Versus All (OVA) for classification and we perform classification for every single frame of the speech signal and then for whole speech signal emotion with the maximum number of frames is finalized as an emotional label of that speech signal. We train SVM classifier with three data sets. We use 70% of data for training, and we use 30 percent data for testing. The number of models generated by SVM is the same number of emotion classes they have for each data set. Algorithms of emotion extraction with speech spectral and prosodic features is given in Algorithm 1.

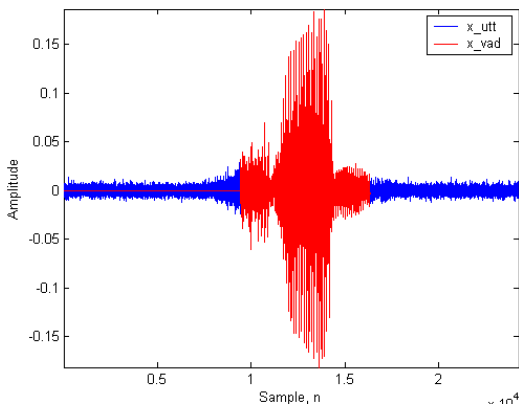


Fig. 3. Speech sample after voice activity detection

```
Algorithm 1 Emotion Extraction using speech prosodic and spectral Features
Let F be the set of speech files
For each f in F
{
P=Preprocessing(f)
V=VAD(P)
S=Segmentation(V)
for each s in S
{
[M]=Mfcc(s)
[L]=Lpcc(s)
P=Pitch(s)
Vol=Volume(s)
Z=Zcr(s)
meanMfcc=Mean(M)
medianMfcc=Median(M)
stdMfcc= Std(M)
meanLpcc=Mean(L)
medianLpcc=Median(L)
stdLpcc= Std(L)
Features=[P,Vol,Z,meanMfcc,MedianMfcc,stdMfcc,meanLpcc,MedianLpcc,stdLpcc,
ClassLabel]
TrainSvm(Features);
}
}
```

IV. STAGE - II: SPEECH CONTENT PROCESSING

In the second stage, we extract emotions based on linguistic features (words and semantics). We use same data sets for training and testing of this system. We perform signal processing as we do in Stage 1 but we do segmentation based on words using ZCR. ZCR is helpful in depicting pause between words and we extract features of each segment (word). We then store these words and features in a file which we treat as the dictionary with labels. We match words with dictionary we created earlier in testing phase, and extract emotions. We extract words by parsing speech signal and then detect segments based on pause between words. We compute Zero-crossing rate to segment speech and consider each segment as a single word.

We extract Mel Frequency Cepstrum Coefficient (Mfcc) and Zero Crossing Rate (ZCR) of each word. We store and use MFCC and ZCR for word recognition later and we generate signal for each word uttered and we store in dictionary as discussed earlier. In case we recognize a word, we use corresponding label of that words as their corresponding emotion. We use Dynamic Time Wrapping (DTW) to recognize words uttered by speaker with words stored in our dictionary. We recognize corresponding label of those words and consider it as resulting label of speech.

V. EXPERIMENTAL SETUP

We use three datasets for training and testing our model. These are Surrey Audio-Visual Expressed Emotions (SAVEE), Polish Emotional speech database (POLISH) and a locally developed dataset of Sky School Kindergarten students' dataset (KSD). Researchers of Technical University of Lodz, Poland develop Polish Emotional speech database and it contains recordings from four male and four female actors in a single session. Each actor utters five different sentences in 6 different emotions. Emotions are joy, boredom, fear, anger, sadness, and neutral. Sentences do not contain any emotional semantic. There are a total of 240 utterance in the database. The database contains 16 bit, 44 kHz recordings under studio noise environment.

University of Surrey develops SAVEE database [5] where the database comprises audio and visual data of four actors. Age of actors is between 27 to 31 years with average age 30 years. The database comprises of seven emotions i.e., anger, disgust, fear, happiness, sadness, surprise and neutral. Each participant utters fifteen sentences in seven emotions. There are four actors used where two possessing English accent; one possessing southern and one possessing Scottish accent.

We develop a dataset considering students between ages six to eight years. We record speech data for speech recognition and emotion recognition. For speech recognition, we select different emotional keywords mostly used by children and tag them with emotion classes like if there is word "disappointed" we tag it with class sad. If the word is "Wow", we tag it with class happy or excited. In case, a word belongs to two classes, we tag it to class that contain most probability of having that word. We given students different words and sentences containing emotional keywords and ask them to speak that sentences three to four times for speech recognition module. We record student voices depicting different emotions for emotion extraction from speech signal. We then manipulate speech data at word level, we use five labelers for listening the data in successive order and annotate each sound independently as belonging to one of five classes. We label data at word level and sentence level. We give an emotional keyword and sentence where we find a label with maximum vote by labeler. We give label based on the prosodic and temporal features at sentence level but we do word level labeling based that word solely at the word level. We call our database Kindergarten Students Database (KSD).

VI. RESULTS AND DISCUSSION

We present our results considering three speech data sets such that we run both stages separately as well as in conjunction to report overall improvements. We consider SAVEE dataset, Polish dataset and KSD datasets as discussed earlier. Our results for Stage 1 and Stage 2 for SAVEE dataset are displayed in Figure 4 and in Figure 5. Similarly results of polish emotional speech datasets with prosodic and temporal features (stage 1) are demonstrated in Figure 6 and with linguistic features (stage 2) are demonstrated in Figure 7. Figure 8 present results of stage 1 with our own developed dataset (KSD) and stage 2 results for the same dataset are presented in Figure 9. We report our combined results in Figures 10, 11 and 12. It is straightforward to conclude that results of prosodic and temporal features are better than linguistic features with SAVEE and POLISH data sets where linguistic features are proven to be better parameters than prosodic in case of KSD dataset.

The reason behind these result is the variability of speaker's accent, tone, age, fluency and ability to express emotions. SAVEE and POLISH data contains speech of adults while our data set contains voices of students from KG level. Adults can better express their emotions than KG students and their speech's tone varies with their emotion. Another important aspect of SAVEE and Polish datasets is that the recordings are from actors who can better differentiate emotions with their expression and style.

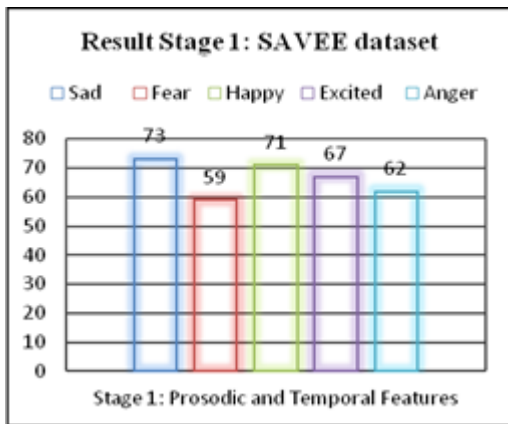


Fig. 4. Result Stage-1, SAVEE dataset

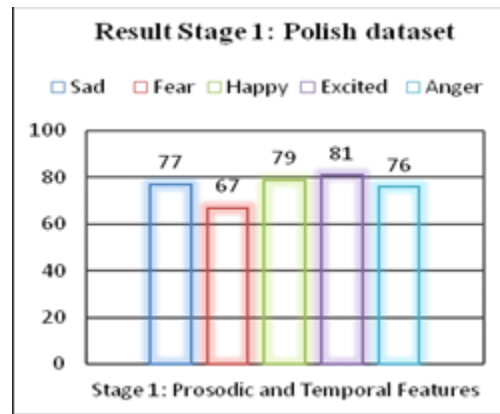


Fig. 6. Result stage 1 with Polish dataset

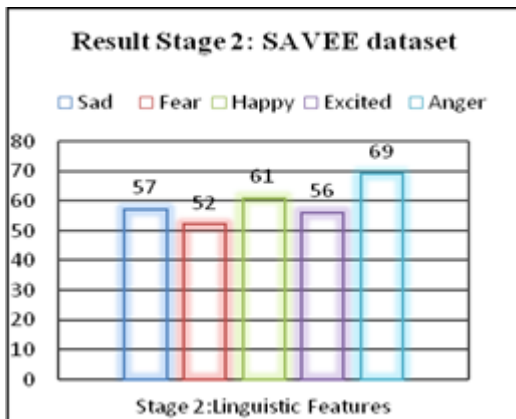


Fig. 5. Result Stage 2, SAVEE dataset

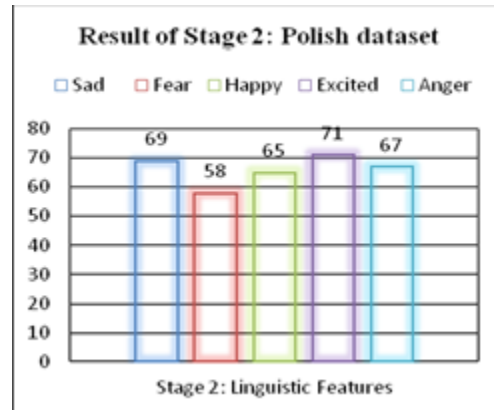


Fig. 7. Result stage 2 with Polish dataset

However, adults speak more fluently, and their speech has no clear pause between words and hence words segmentation is difficult for adults in SAVEE and POLISH datasets. Therefore, prosodic and temporal features extraction gives a better result for these datasets. Second reason for our first result because KG students are not able to express emotions more clearly with their voice. We noted that most KG students speak in the same volume in a happy and angry mood while they have the same tone in fear and in sad emotion. However, they (KG students) speak slower than adults in case of SAVEE and POLISH datasets and hence, word segmentation with KG students' speech gives more accurate results as compared to young people's speech. After concluding reasons for the fact that stage 1 is displaying an overall better performance than the outcome of stage-2, we focus on the overall results presented in Figures 10 - 12 where we present combination of both stages and extract emotion based on combine features. Although we could not segment all words of a speaker but with words that we could extract we used their semantic plus prosodic and temporal features of speech and then concluded emotion of speaker. Here we clearly find out an overall gain in almost each case.

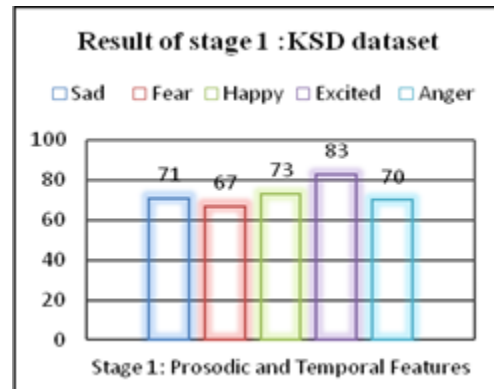


Fig. 8. Result stage-1 with KSD dataset

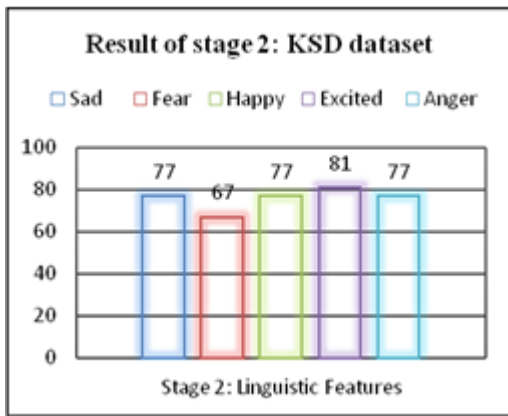


Fig. 9. Result stage-2 with KSD dataset

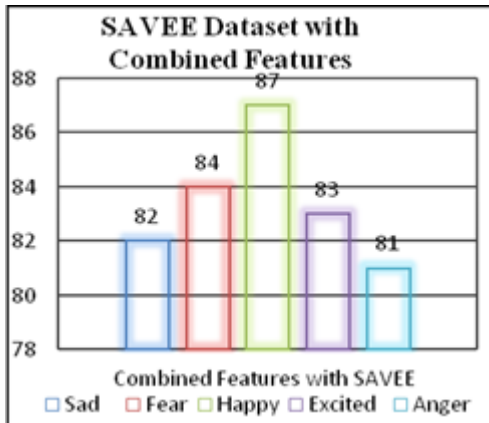


Fig. 10. Result of SAVEE dataset with combined features

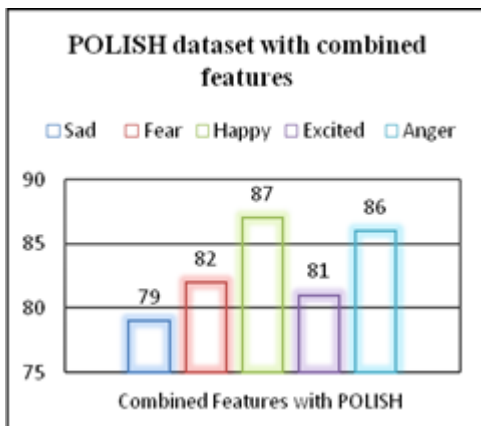


Fig. 11. Result of POLISH dataset with combined features

We also report overall complexity of the algorithm, and we calculate the overall time taken in case of running Stage-1, Stage-2 and both the stages combined. We find out that the time taken for all cases remains minutely less than the total time taken for each stage separately, and none of the cases is posing any serious constraints neither the data nor computation time is expanding drastically. This is mainly because we have performed same steps twice extracted - once during stage - 1 where we perform segmentation to divide speech signals into small segments with the help of ZCR and calculated spectral feature (MFCC) of speech segments to get information's of

human's emotion and second time in stage - 2 when we performed segmentation using ZCR to segment words uttered by speaker and extracted MFCC to recognize words.

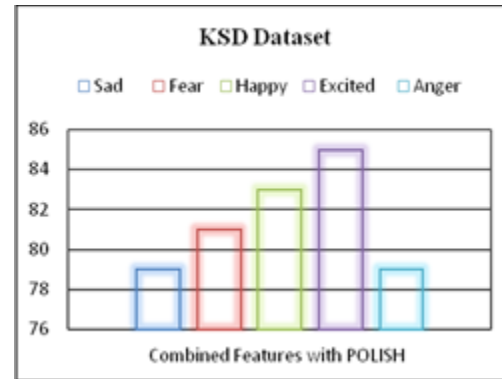


Fig. 12. Result of KSD dataset with combined features

VII. RELATED WORK

Researcher have implemented various models for recognition of emotions from speech using different sets of features. Yildirim [22] conducts a study aimed to analyze how speech is modulated with the change in speaker emotional state. They measure vowel articulation, spectral energy and acoustic parameters of speech to find acoustic similarity and difference between different states of emotions. They also perform discriminant analysis to check the acoustic separability of emotion at utterance level. The author conclude that some emotions have similar acoustic properties and they mentioned happiness/anger and sadness/neutral in this category. Author of [3] present speech signal driven approach to deal with two class similarity problem. They use HMM based features with combination of prosodic and spectral features and achieved accuracy of 47.83% with two class similarity problem [3]. Alexander [6] present a new method to identify emotions using parameters of glottal airflow signal. The effectiveness of their system is tested with Artificial Neural Network (ANN), SVM, Hidden Markov Model (HMM), K Nearest neighbour (KNN), Bayesian classifier, Gaussian Mixture Model (GMM), decision tree and a new optimum path classifier (OPF). They find best results of glottal features with SVM and OPF. MFCC are extracted from data for classification of emotion [6], [9]. Spectral and prosodic features are identified in[13] and experiment are conducted after implementing three classifiers to identify emotions. The authors build Gaussian Mixture Model with prosodic features, SVM with prosodic features and Gaussian Mixture Model with Prosodic features. The authors calculate features and then apply algorithm to select most relevant features and show that prosodic features are more helpful in detection of emotion than spectral features. Another framework in which they extracted 133 speech features and aimed to identify feature set that would be appropriate to discriminate between seven emotions based on speech processing [7]. They use Neural network classifier with 35 input vectors and tested their model using Berlin dataset that include speaker dependant and speaker independent instances.

Zhu [25] identified emotions deficiencies in an E-Learning environment and proposed emotion recognition system for them. They build speech corpus from various subjects belongs

to different languages and extracted prosodic features. They use Sequential Forward Selection (SFS) approach to select most appropriate feature set and used to classify emotions with General Regression Neural Network (GRNN). Considering emotion recognition a challenging task, Zhang performs an experiment with SVM is used for classification of 4 emotions and feature set of prosodic and speech quality features. He proposes that combination of prosodic and speech quality features increase 10% recognition rate [24]. The researchers in [14] extract quality Quality and prosodic features that overlap and complement each other in identification of emotions. Wang [20] combines these two stages and used optimal searching properties of Genetic algorithm considering personal characters of emotions. They achieve 86% recognition accuracy with this searching algorithm [20]. The author of [2] extend their research of 2009 and extract spectral features at stressed vowels, unstressed vowels and at consonant. They find that these levels contain more rich information's about emotions than utterance level. Their results show higher accuracy at segment level than at utterance level [2].

We present a new model where we extract emotions at two stages and then combine both stages result. Our results are 83.4 % with SAVEE 83% with polish 68% with KSD dataset. The results are better in the sense that when we have speech that has no clear words our stage1 with prosodic and temporal features help in identification of emotions. In case these features don't help to identify emotion correctly, words semantics help in identifying emotions of speaker. So this hybrid system of prosodic, spectral and words semantic features perform better than other system.

VIII. CONCLUSION

We have considered prosodic, temporal as well as linguistic features which has been helpful in increasing accuracy of emotion recognition. For the purpose of elaborating our results, we have used a two-staged model for emotion recognition. We have used the results by each stage separately and in a combined manner to present that our approach works better and produced significant results. We conclude from our results that considering prosodic as well as linguistic features together helps improving overall results without degrading performance. We propose algorithm where we extract emotions based on prosodic and temporal features in the first step and we extract emotions from word segmentation combined with linguistic features in the second step. While performing our experiments, we prove that the classification mechanisms, if trained without considering age factor, do not help improving accuracy. We provide our argument that the classifier should be based on the age group on which the actual emotion extraction be required and this becomes our second contribution submitted in this paper

REFERENCES

- [1] Baenziger, T. a. (2005). The role of intonation in emotional expressions. *Speech communication*, 3.
- [2] Bitouk, D. a. (2012). Class-level spectral features for emotion recognition. *Speech communication*.
- [3] Bozkurt, E. a. (2009). Improving automatic emotion recognition from speech signals. In *NTERSPEECH* (pp. 324-327).
- [4] Dellaert, F. a. (1996). Recognizing emotion in speech. In *Spoken Language, 1996. ICSLP 96. Proceedings., Fourth International Conference on* (pp. 1970-1973).
- [5] Hoque, M. E. (2006). Robust recognition of emotion from speech. In *Intelligent Virtual Agents* (pp. 42-53). Springer.
- [6] Iliiev, A. I. (2010). Spoken emotion recognition through optimum-path forest classification using glottal features. *Computer Speech & Language*, 3.
- [7] Iliou, T. a.-N. (2009). Statistical evaluation of speech features for emotion recognition. In *Digital Telecommunications, 2009. ICDT'09. Fourth International Conference on* (pp. 121-126).
- [8] K Sreenivasa and Koolagudi, S. G. (2012). *Emotion Recognition Using Speech Features*. Springer Science & Business Media.
- [9] Kao, Y.-h. a.-s. (2006). Feature analysis for emotion recognition from Mandarin speech considering. In *InterSpeech*.
- [10] Kim, D.-S. a.-Y. (1999). Auditory processing of speech signals for robust speech recognition in real-world noisy environments. *Speech and Audio Processing, IEEE Transactions on*, 55-69.
- [11] Koolagudi, S. G. (2012). Emotion recognition from speech: a review. *International journal of speech technology*, 99-117.
- [12] Lopez-Poveda, E. A. (2001). A human nonlinear cochlear filterbank. *The Journal of the Acoustical Society of America*, 3107-3118.
- [13] Luengo, I. a. (2005). Automatic emotion recognition using prosodic parameters. In *Interspeech* (pp. 493-496).
- [14] Lugger, M. a. (2007). The relevance of voice quality features in speaker independent emotion . In *Acoustics, Speech and Signal Processing, 2007.* (pp. 13-17).
- [15] Petrushin, V. (1999). Emotion in speech: Recognition and application to call centers. In *Proceedings of Artificial Neural Networks in Engineering* (pp. 7-10).
- [16] Rabiner, L. R. (1975). An algorithm for determining the endpoints of isolated utterances. *Bell System Technical Journal*, 297-315.
- [17] Rabiner, L. R. (1975). *Theory and application of digital signal processing*. Englewood Cliffs, NJ, Prentice-Hall, Inc., 1975. .
- [18] Shen, J.-l. a.-w.-s. (1998). Robust entropy-based endpoint detection for speech recognition in noisy environments. In *ICSLP* (pp. 232-235).
- [19] Ververidis, D. a. (2006). Emotional speech recognition: Resources, features, and methods. *Speech communication*, 1162-1181.
- [20] Wang, Y. a. (2008). Adaptive and optimal classification of speech emotion recognition. In *Natural Computation, 2008. ICNC'08. Fourth International Conference on* (pp. 407-411).
- [21] Wu, S. a.-Y. (2011). Automatic speech emotion recognition using modulation spectral features. *Speech Communication*, 768-785.
- [22] Yildirim, S. a. (2004). An acoustic study of emotions expressed in speech. In *INTERSPEECH*.
- [23] Yu, F. a.-Y. (2001). Emotion detection from speech to enrich multimedia content. In *Proceedings of the second IEEE pacific rim conference on multimedia*: (pp. 550-557).
- [24] Zhang, S. (2008). Emotion recognition in Chinese natural speech by combining prosody and voice quality features. In *Advances in Neural Networks-ISNN 2008* (pp. 457-464).
- [25] Zhu, A. a. (2007). Study on speech emotion recognition system in E-learning. In *Human-Computer Interaction. HCI Intelligent Multimodal Interaction Environments* (pp. 544-55)

Medical Image Inpainting with RBF Interpolation Technique

Mashail Alsalamah*, Saad Amin

Faculty of Engineering and Computing, Coventry University, Priory St, Coventry CV1 5FB, United Kingdom

Abstract—Inpainting is a method for repairing damaged images or to remove unwanted parts of an image. While this process has been performed by professional artists in the past, today, the use of this technology is emerging in the medical area – especially in the medical imaging realm. In this study, the proposed inpainting method uses a radial basis function (RBF) interpolation technique. We first explain radial basis functions and then, the RBF interpolation system. This technique generally depends on matrix processes. Thus, matrix operations are executed after the interpolation and form a main part of the process. This interpolation matrix has a known value used for interpolating n values and we need to find $M - 1$ for the $n + 1$ values of the original and inserted data. Implementation of an inpainting operation is carried out in an object-oriented programming (OOP) language. This is where the process is completed. The algorithm used in this study has a graphical user interface. Further, several skin images are used for testing this system. The obtained output represents a high level of accuracy that can support the validity of the proposed method.

Keywords—Inpainting; interpolate; texture synthesis; exemplar texture inpainting; Radial Basis Function

I. INTRODUCTION

One of the most interesting problems in image processing is reconstructing damaged or incomplete images as much as possible. This problem is referred to in many papers [1,2]. The main question in reconstructing damaged images is, “What value was in a corrupted position and how can this be restored?”. One of the conditions for solving this problem is to have as much information as possible from the original image. Then, appropriate existing methods can use this information and try to reconstruct the missing information [1]. The amount of information retained from the original image is very important as the quality of the result depends on it. The radial basis function (RBF) method is based on the principle of variational implicit functions and can be used for the interpolation of scattered data, see data. The possibility of missing data restoration (image inpainting) by the RBF method was mentioned in [3]. The method was used for surface retouching and marginally for image inpainting [3].

Inpainting is a method to repair damaged images or to remove unwanted parts of an image. While this process has been performed by professional artists in the past, today the use of technology is emerging in the medical imaging realm.

Several mathematical algorithms are used for inpainting, such as Laplace’s equations [4], isoline [5], texture synthesis [6] and interpolation [7]. The popular graphics program Adobe Photoshop [2] has a feature called content-aware fill in

its CS5 version. This feature performs a type of inpainting with high efficiency and low latency. Another graphics program, GIMP [8] which is an open-source project, contains an inpainting plugin called Resynthesizer [1]. This plugin uses a texture synthesis method to perform the inpainting operation.

There are other software programs available for video inpainting, these programs in general provide object removal. Adobe After Effect [2] and Apple Final Cut Pro [8] software provides such a feature. The problem with Adobe After Effects is that it is prone to unnecessary crashing, which makes it difficult to operate or deal with as it needs to be reset frequently.

The RBF interpolation-based inpainting method performs interpolation instead of texture matching, just like the texture synthesis method [9]. Therefore, the focus of this paper is to explore the effective usage of inter-polation based RBF inpainting.

The objectives of this paper are as follows: first, inpainting with an RBF interpolation method, and not pattern matching; second, rapid completion of an inpainting process. Further, the developed method should yield a satisfactory or relatively high-quality result.

Moreover, the speed factor can be changed by finding new ways to complete the same task with a quicker implementation. Quality depends on how the calculation results are used and can be improved by combining them with other information from the source image.

II. INTERPOLATION

In mathematics, interpolation is carried out to find the missing parts of a number series. This number series is either simple or complex mathematical series.

To find the missing numbers of a series, if the mathematical function is known, by setting the appropriate parameters, we can find the missing parts along with their exact values. For example, assume that function $f(x) = x^2$ is known and some values are missing in the following series: 0, 1, 4, a , b , 25, c , 49. For $x = 1$, the result is 1; $x = 3$ would give 9. Therefore, $a = 3$. Similarly, by substituting x with 4 and 6, we obtain $b = 16$ and $c = 36$, and thus, the interpolation is completed.

However, sometimes, it is almost impossible to figure out the function of a number series [10].

In this situation, missing values can only be found by using certain known values. The RBF interpolation method is used in such a case. RBF interpolation uses values in series and the distances between these values to create a base function structure. All missing parts can be found one by one by using the base function as in [11].

In digital imagery, each pixel is defined by a mixture of red, green, and blue colors. The RBF interpolation method is completely compatible with the RGB structure shown in [9]. Therefore, the problem with the interpolation system is that it is not perfect. It cannot ultimately find exact values; only estimated ones. Because of this reason, this method cannot yield perfect inpainting results. However, using interpolated values in a different way can enhance the quality of the results.

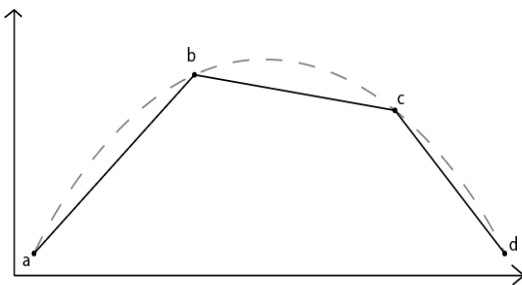


Fig. 1. Curve fitting

III. IMAGE INPAINTING

Inpainting is the process of reconstructing lost or deteriorated parts of images and videos. For instance, in the case of a valuable painting, this task will be carried out by a skilled image restoration artist. In the digital world, inpainting (also known as image interpolation or video interpolation) refers to the application of sophisticated algorithms to replace lost or corrupted parts of the image data (mainly small regions) or to remove small defects [11].

In Figure 2, an inpainting process is shown on an old photo. The output is very good, and almost all the lost parts are repaired.



Fig. 2. Old photo inpainting

However, not all inpainting processes are successful. One of the reasons for this is not having a sufficient number of known points on the input picture, or sometimes, the algorithm used for the inpainting. One example for such a case is as follows:



Fig. 3. Unsuccessful inpainting

Here, the text “Meow!!” has not been inpainted properly; thus, at the end, we obtain an unsuccessful result. Different techniques can be used for improving the inpainting quality, such as selecting, iterative inpainting in small portions, and inpainting of an area more than once as stated in [12]. Some of these techniques can be performed automatically, and the others need a more intelligent system [11].

IV. INPAINTING METHODS

There are different inpainting methods designed to provide good solutions for specific situations. These methods can be divided into two groups. One group of methods can be used on texture-based images, and the other on non-texture-based images.



Fig. 4. Seamless brick wall texture

A. Texture Synthesis

One of best texture inpainting methods is texture synthesis. Texture synthesis is the process of algorithmically constructing a large digital image from a small digital sample image by taking advantage of its structural content [13]. This method can be used for digital image editing, three-dimensional (3D) computing, and inpainting.

Texture synthesis searches through the whole picture and tries to find the best matching points to fill the holes in the image. Because texture images generally have repeating parts,

at the end, a seamless image is generated as demonstrated in [2].

B. Exemplar-Based Inpainting

Another method is exemplar-based inpainting. This method uses a texture synthesis algorithm and gives a higher priority to linear structures. Therefore, this is perceived that it gives better results: Linear structures are preserved, and no blurring occurs as shown in [12]. In the study, the RBF interpolation technique is used. RBF functions are also used for artificial intelligence systems as discussed in [11]. This shows that in a way this project uses an intelligent system to do inpainting. Inpainting with RBF is not used for texture-based or detailed images because of its blurry output.

The easiest way to explain interpolation is to find an unknown number in a series of numbers.

$$X = \{1, 2, 3, a, 5, 6, b, 8, 9\}$$

In this number series, numbers are in an ascending order, and the values of a and b are unknown. Interpolation is used for finding these unknown values by using the known numbers.

A more complicated example is to find more detailed points in a curve.

C. Convolution-based image inpainting algorithm

Convolution-based image inpainting algorithms as discussed in [5] are very fast. However, in many cases, they do not provide adequate results with respect to sharp details such as edges. In this method, the mask coefficients are calculated using the gradient of the image to be inpainted. The algorithm is fast, iterative, and simple to implement, and provides adequate results.

V. RADIAL BASIS FUNCTIONS (RBF)

An RBF is a real-valued function whose value depends only on the distance from the origin. RBFs are generally represented by the Φ (phi) symbol.

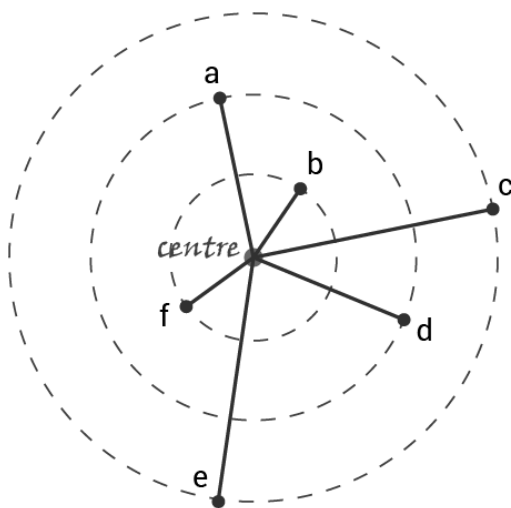


Fig. 5. Radial distances

In the above Figure 5, a center point and six other points connected to the center with a line are shown. An RBF takes the distance between any of these six points and the center and calculates a value.

Φ (distance) = Value of RBF. Distances from each point to the center are shown in table 1 below:

TABLE I. RBF POINTS AND DISTANCES

Point	Distance to center	Point	Distance to center
Point a	2	Point d	2
Point b	1	Point e	3
Point c	3	Point f	1

Irrespective of where the points are located in the space, as long as their distances to the center are equal, the results of the RBF are the same.

Thus, RBF (distance from point a to center) = RBF (distance from point d to center)

RBF (distance from point b to center) = RBF (distance from point f to center)

RBF (distance from point c to center) = RBF (distance from point e to center)

There are a number of functions that provide the attributes of an RBF.

Most simply, a linear RBF is $\Phi(r) = r$ [14]. Note: r denotes distance and thus, cannot be negative.

Another RBF is called Gaussian (GA). Its function is denoted as $\Phi(r) = e^{-(\epsilon r)^2}$. This function is generally used in RBF networks for artificial intelligence systems. Further, this function will be implemented in this study to observe its effect on the inpainting process.

VI. RBF INTERPOLATION

RBF interpolation is matrix-based linear equation solving.

$$[K][L]=[M]$$

In this matrix equation, K denotes an $n \times n$ matrix, L represents an $n \times 1$ matrix, and M indicates another $n \times 1$ matrix.

The variable n denotes (number of known points + 3). The number 3 comes from (number of dimensions + 1). In this study, the considered image is two dimensional. Therefore, each point has only x and y coordinates. This implies that RBF interpolation can be applied to images that have more than two dimensions, as demonstrated in [12].

The definition of a point in RBF interpolation is given as a function as follows:

$$f(p) = q(p) + \sum_{j=0}^n \lambda_j \Phi(|p - p_j|)$$

This formula will be generated for each known point. In this formula, p denotes the current point in the list of known points, $f(p)$ represents the color of point p , and $q(p)$ denotes a polynomial. Because this project uses 2D images, $q(p) = c_0 * x + c_1 * y + c_2 * 1$, where x and y represent the position of a point

on the surface; and c_0 , c_1 , and c_2 represent the unknown multipliers.

λ_j denotes a real-valued weight, which is unknown at first, $|p - p_j|$ represents a Euclid norm distance between two points, $\Phi(|p - p_j|)$ indicates an RBF that takes distance as a parameter.

One important point here is that in digital imaging, colors are represented by a combination of red, green, and blue. Further, in image formats such as PNG and TIFF, there is an alpha layer that changes the color transparency. The abovementioned RBF interpolation function is used for each of the alpha, red, green, and blue layers shown in [15].

To be able to explain this function better, an example will be given with three different points as shown in table 2.

Colors will be chosen only once, not for each different color. At the end, linear equations will be formulated.

TABLE II. POINTS WITH COLORS

Point	X	Y	Color
p_0	1	1	240
p_1	2	3	245
p_2	4	2	255

The equation for p_0 is

$$240 = c_0*1 + c_1*1 + c_2*1 + \lambda_0*\Phi(|p_0 - p_0|) + \lambda_1*\Phi(|p_0 - p_1|) + \lambda_2*\Phi(|p_0 - p_2|)$$

The equation for p_1 is

$$245 = c_0*2 + c_1*3 + c_2*1 + \lambda_0*\Phi(|p_1 - p_0|) + \lambda_1*\Phi(|p_1 - p_1|) + \lambda_2*\Phi(|p_1 - p_2|)$$

The equation for p_2 is

$$250 = c_0*4 + c_1*2 + c_2*1 + \lambda_0*\Phi(|p_2 - p_0|) + \lambda_1*\Phi(|p_2 - p_1|) + \lambda_2*\Phi(|p_2 - p_2|)$$

The distance between two points can be calculated by using the Pythagorean theorem.

$$|p_0 - p_0| = 0$$

$$|p_0 - p_1| = |p_1 - p_0| = \sqrt{(1 - 2)^2 + (1 - 3)^2} = \sqrt{5}$$

$$|p_0 - p_2| = |p_2 - p_0| = \sqrt{(1 - 4)^2 + (1 - 2)^2} = \sqrt{10}$$

$$|p_1 - p_2| = |p_2 - p_1| = \sqrt{(2 - 4)^2 + (3 - 2)^2} = \sqrt{5}$$

After deciding which RBF to use, we find that in the given equations, only c_0 , c_1 , c_2 , λ_0 , λ_1 , and λ_2 will be left as unknown.

Apart from color values, all other known values will be kept in matrix K. The unknown variables will be in matrix L. Finally, the color values will be in matrix M.

The following RBF interpolation matrix is created using the above equations:

$$\begin{bmatrix} x_0^n & x_0^{n-1} & x_0^{n-2} & \dots & x_0 & 1 \\ x_1^n & x_1^{n-1} & x_1^{n-2} & \dots & x_1 & 1 \\ \vdots & \vdots & \vdots & & \vdots & \vdots \\ x_n^n & x_n^{n-1} & x_n^{n-2} & \dots & x_n & 1 \end{bmatrix} \begin{bmatrix} a_n \\ a_{n-1} \\ \vdots \\ a_0 \end{bmatrix} = \begin{bmatrix} y_0 \\ y_1 \\ \vdots \\ y_n \end{bmatrix}$$

To be able to solve this matrix equation, the matrix K must be a square matrix. Further, to be able to decrease the number of calculations performed by the processor, the matrix has to be mirrored.

When the matrix is solved, the values of all unknown variables will be found. At this point, any unknown point put into matrix K will generate color values in matrix M with basic matrix multiplication. Thus, RBF interpolation will be completed

VII. DESIGN

The task is based on a model-view-controller (MVC) pattern. The graphical user interface solution of Visual C# is used as the view. Each view, which is called a form in Visual C#, has its own class for coding. This coding class is the controller of the project. The model of the project is all classes written for the inpainting process.

Because of the complexity of the inpainting process, more than one class needs to be written for the model part. The structure of these classes and their relation to each other are determined on the basis of different concerns. The following figure 6 shows the structure of the whole system.

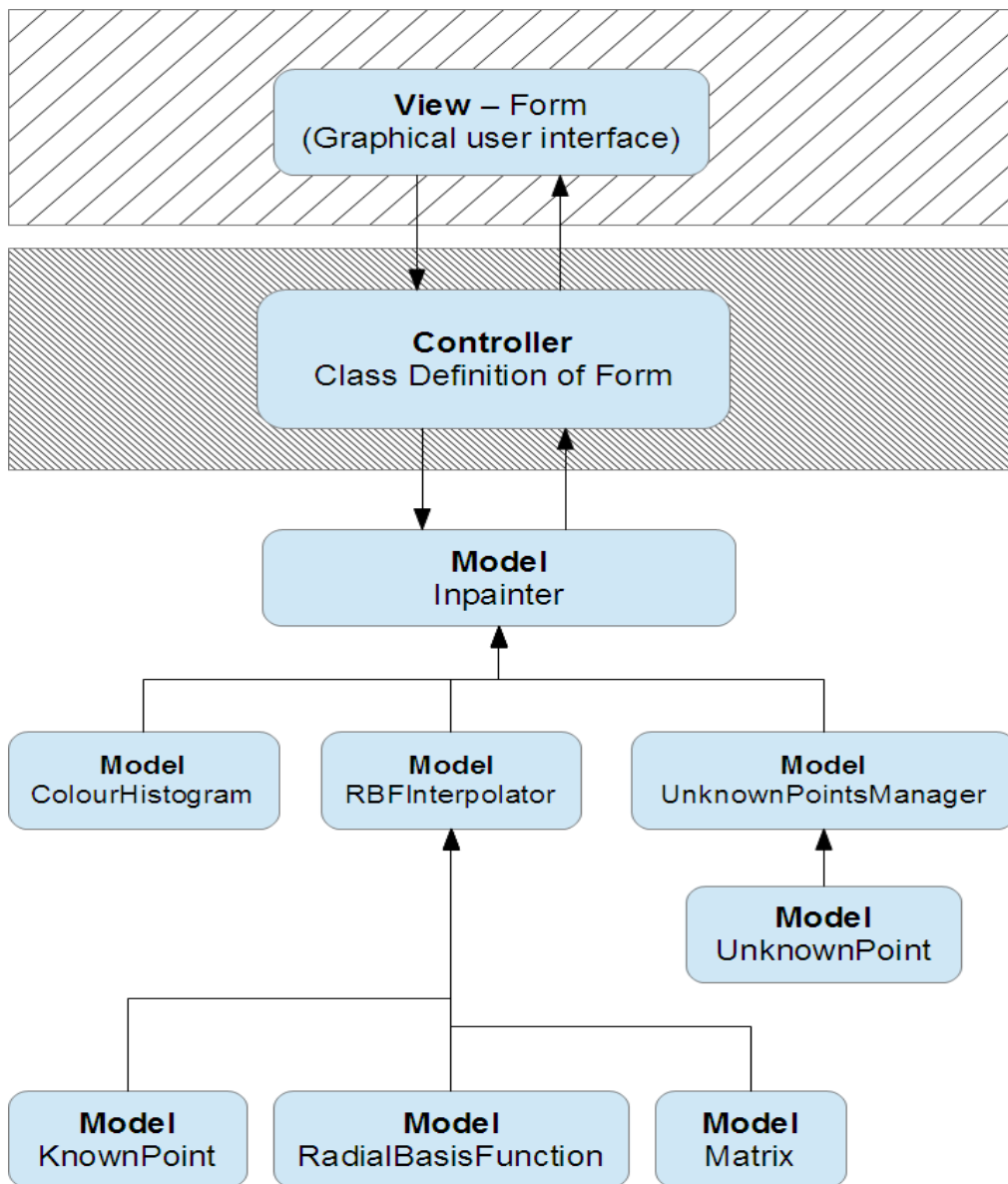


Fig. 6. System structure

The top part is used for presenting the view, the next row is the controller, and the rest contains the model classes. In this presentation, connections are drawn to show links between classes. These links are based on the usage of each other. Further, details increase from the top to the bottom and decrease from the bottom to the top, but in the latter case, the bindings increase as shown in [15].

In the fields of image processing and photography, a color histogram is a representation of the distribution of colors in an image. For digital images, a color histogram represents the number of pixels that have colors in each range of a fixed list of color ranges that span the image's color space, the set of all possible colors.

The color histogram can be built for any type of color space, although the term is more often used for 3D spaces such as RGB and HSV. For monochromatic images, the term intensity histogram may be used instead. For multispectral images, where each pixel is represented by an arbitrary number of measurements (for example, beyond the three measurements in RGB), the color histogram is N-dimensional, with N being the number of measurements taken. Each measurement has its own wavelength range of the light spectrum, some of which may be outside the visible spectrum.

In the following Figure 7, all model classes are shown with their attributes and models. The details of each class are explained in the implementation part.



Fig. 7. Class diagram

VIII. METHODOLOGY

This study is based on a graphical user interface. The inpainting operation is performed in three steps. First, the user loads the image file.

After this step, the area of the image where the inpainting process will take effect must be selected. Next, a selection process is carried out by drawing onto the image. Selection does not end when the mouse button is released. Before the inpainting operation, as many different points of the image as possible can be completed, the inpainting operation starts by user's click on the inpaint button on the main menu. A new thread is created for the inpainting process. This new thread prevents the locking of the graphical user interface. The progress of the inpainting operation is displayed on a new form window. Each selected pixel on the image passes

through the inpainting operation. When all pixels have passed through, a new image is displayed on the form window. There is no limit on the number of times the user can perform the inpainting operation. Further, in case unwanted points of the image are selected, the selected area can be cleaned up with one mouse-click on the main menu. This is discussed in greater detail by [16].

In general, the process involves the following:

- The global picture determines how to fill in the gap. The purpose of inpainting is to restore the unity of the work.
- The structure of the gap surroundings is supposed to be continued into the gap. Contour lines that arrive at the gap boundary are prolonged into the gap.

- The different regions inside a gap, as defined by the contour lines, are filled with colors matching those of the gap boundary.
- The small details are painted; i.e., “texture” is added.

IX. IMPLEMENTATION

In this study, we used Microsoft Visual Studio 2010. The steps for the implementation are such as starting a new project for a C# based .Net application.

A. Implementation of knownpoint class

The known points are the pixels that are not marked to be inpainted as shown in figure 8. These pixels are available for use in the inpainting process while creating a coefficient matrix.

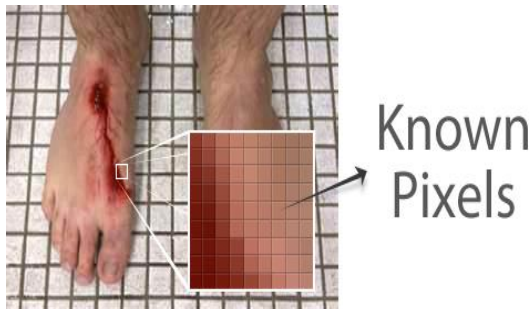


Fig. 8. Display of Pixels

As already explained, the distance of one pixel from another is very important for the RBF interpolation technique. The distance between two points is calculated using the x and y coordinates of these points.

Another crucial attribute for the interpolation process is the value of each known pixel. These three attributes of each known pixel are stored in a class, and their getters are defined; these are needed to read the values of the abovementioned attributes while performing a calculation in the interpolator.

B. Implementation of rbf interpolator

This is the class where all interpolation calculations are performed. Matrix operations are heavily reliant on the methods of this class. Because of the complexity of these methods, explanations will be provided by using the following equation:

$$\begin{bmatrix} \text{Coefficient} \\ \text{Matrix} \end{bmatrix} = \begin{bmatrix} \text{Variables} \\ \text{Matrix} \end{bmatrix} \begin{bmatrix} \text{Product} \\ \text{Matrix} \end{bmatrix}$$

In fact, here, the methods are defined to divide the whole into small pieces. Therefore, in general, one method uses the output of another method. Therefore, the interpolation process is carried out by calling the related methods one after another.

C. Implementation of unknownpoint class

The term “unknown point” refers to the pixels when the source image is marked. An inpainter system sees the unmarked points as the known points. As explained in “What

is Interpolation?,” interpolation creates new points on the basis of the already known points. Therefore, the system first creates a unique UnknownPoint class for each marked pixel, and while performing inpainting, fills these classes with the interpolated values.

Because each marked pixel has its own UnknownPoint class instance, this class must retain the position of this pixel. Further, as will be discussed later, in order to be able to enhance the quality of the inpainting process, each UnknownPoint class keeps a count of the known points around it. This will be used to select the unknown point to be interpolated first.

D. Implementation of unknownpoint manager class

The UnknownPoint class holds an unknown point’s information as an object. This class is used for maintaining a list of all the unknown points under control. Further, by providing extra functionality, it decreases the complexity of inpainting. Further, it is used for enhancing the quality of the result. During the inpainting operation, it is important to start with the unknown point that has the maximum number of known points around it. A larger number of known points imply a better interpolation calculation. However, if a program continues using the adjacent unknown points because they come in order and have the maximum number of known pixels around them, the result quality may deteriorate. To prevent such deterioration, it is a good practice to randomize the list of unknown points. Thus, even if there are many unknown points with the same number of known points, instead of the adjacent best ones, randomly selected unknown points will be used in the next step. This method also improves the quality of inpainting.

E. Implementation of inpainter class

This class is the managing director of the entire inpainting process. At first sight, there are not many methods or attributes in it, but it gains its importance from the usage of the other implemented classes.

This class has some constant definitions for the unknown point window frame. Padding values are defined as constants to decrease future complexity on an event such as a requirement for a change in a padding value. Therefore, it needs only one constant attribute’s value to change; the rest of the program still stays the same and works in the same way.

Other attributes are used for maintaining the progress values. These values are used for passing the progress of the inpainting process to another thread in order to show the percentage of the process completed. The total number of unknown points is stored as the maximum progress value. The number of inpainted points is stored as the progress value. By using two of these values, the program calculates and displays the percentage of the entire inpainting process completed. The figure 9 shows the inpainting process.

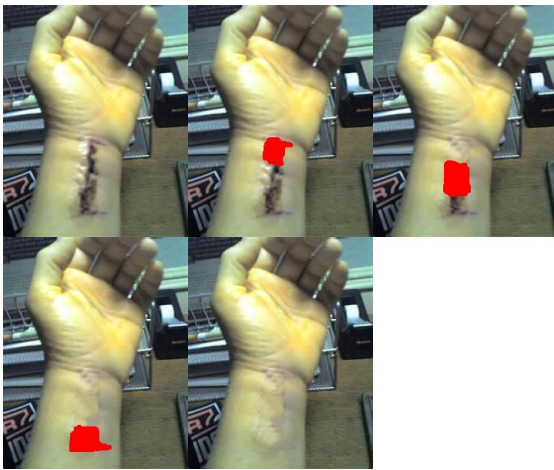


Fig. 9. Inpainting process

X. OUTCOME AND EVALUATION

Considering the methods of performing inpainting and the views presented by various authors, we need to consider conducting many tests of these methods in order to identify a seamless inpainting method.

This method takes two versions of the original image and an improved image and looks at similarities of all pixels one by one. To measure the accuracy of the system, the average of all the similarities is calculated.

The similarity calculation is based on the power of 2 in mathematics and the distance between two colors.

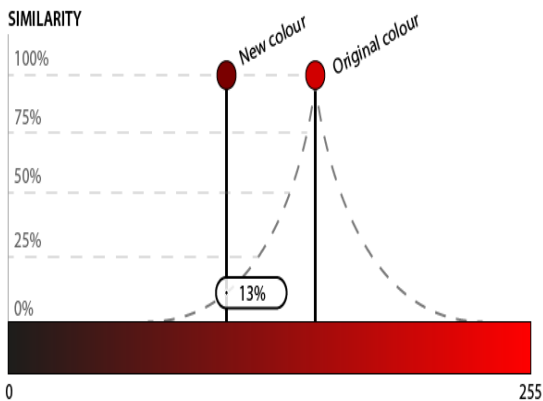


Fig. 10. Accuracy graph

The graph used for this operation is shown on both sides of the original color's values in the above image. According to the new color's value, the similarity is calculated on the basis of that curve. This is because accuracy measurement is carried out within the system and is part of the C# program as shown in figure 10.

The tests and results of some of the outputs have been provided in the figures below, which show some of the images used for the system. Figure 11a shows the original image, and Figure 11b shows the improved image. The accuracy between the affected areas for the two images is measured, and the accuracy of the system is 99.59%



Fig. 11. (a) Scared (b) Clear Accuracy: 99.5%

The following two figures, namely Figures 12 and 13, show the same images as Figure 13 wherein both Figure 12a and Figure 13a show the original images, and Figures 12b and 13b show the improved images obtained using the proposed system; the accuracy is 99.88% and 99.68%, respectively.



Fig. 12. (a) Bleeding (b) Clear Accuracy: 99.8%



Fig. 13. (a) Bleeding (b) Clear Accuracy: 99.68%

The following table represents some of the data used for the system; the range of accuracy is 99.13 to 99.91, and the average accuracy of the system is 99.56% for all the data used for testing the proposed system.

TABLE III. IMAGE AND SIMILARITY

No.	Image	Similarity (%)
1	Leg abrasion	99.51
2	Back bleed	99.13
3	Stitch	99.63
4	Arm bleed	98.88
5	Wrist cut	99.68
6	Leg cut	99.68
7	Face stitch	99.59
8	Face cut	99.84
9	Wrist stitch	99.91
10	Neck boils	99.75

The results obtained have high accuracy and show that the methods used are effective in meeting the objectives of this research.

Different types of implementations have been identified: Implementation of KnownPoint Class, Implementation of

RBF Interpolator, Implementation of Unknown Point class, Implementation of Inpainter Class, and Implementation of Unknown Points Manager class. All these techniques suggest disparate methods and thus, different levels of quality of the outcome. The need for a seamless technique arises from the need to identify the best aspects of all the above mentioned methods and ensure that these are used with an interface that allows for easy manipulation by the user.

On the basis of the above results, we concluded the following:

- This research met the set objectives including inpainting with an RBF interpolation method and not pattern matching.
- The inpainting process was completed as quickly as possible.
- A satisfactory or relatively high-quality result was obtained.

XI. CONCLUSION

In this study, we examined the RBF interpolation technique for inpainting images. It has been found that this technique is good for gradient-like images. It can form good connections between colors and edges. Thus, RBF interpolation is a good method for skin inpainting operations. The algorithm that has been used has a graphical user interface. Several skin images have been used for testing the proposed system. In the testing part, the inpainting operation is used for wound images. The results revealed high performance of the proposed method. A considerable number of the improved images were studied, and in some of these images, the damage was almost unnoticeable. Further, repeating the operation led to an increase in the accuracy and the quality of the improved image. However, matrix calculations are very time consuming, and RBF interpolation is directly based on large matrices.

REFERENCES

- [1] Bertalmio M, Sapiro G, Caselles, Ballester C. "Image inpainting." *Proceedings of SIGGRAPH 2000*, New Orleans, 2000, pp. 417-424.
- [2] Kozhokin N, et al. "An approach to surface retouching and mesh smoothing." *International Journal: The Visual Computer* 2003; 19(7-8):549-564.
- [3] Kojekine N, Savchenko V. "Using CSRBFs for surface retouching." *Proceedings of The 2nd IASTED International Conference Visualization, Imaging and Image Processing VIIP 2002*, Malaga, Spain, 2002.
- [4] Bertalmio, Marcelo, Andrea L. Bertozzi, and Guillermo Sapiro. "Navier-stokes, fluid dynamics, and image and video inpainting." In *Computer Vision and Pattern Recognition, 2001. CVPR 2001. Proceedings of the 2001 IEEE Computer Society Conference on*, vol. 1, pp. 1-355. IEEE, 2001.
- [5] Nauta, Jelle, and Sander Feringa. "Qualitative Comparison of 2D Digital Inpainting Techniques." *10th SC@ RUG 2012-2013*: 18.
- [6] Bertalmio, Marcelo, Luminita Vese, Guillermo Sapiro, and Stanley Osher. "Simultaneous structure and texture image inpainting." *Image Processing, IEEE Transactions on* 12, no. 8 (2003): 882-889.

- [7] Chan, Tony F., and Jianhong Shen. "Nontexture inpainting by curvature-driven diffusions." *Journal of Visual Communication and Image Representation* 12, no. 4 (2001): 436-449.
- [8] Powell M J D. "A new iterative algorithm for thin plate spline interpolation in two dimensions." *Annals of Numerical Mathematics* 1997;4:519-527.
- [9] Iske A. "Multiresolution methods in scattered data modelling." *Lecture notes in computational science and engineering*. Berlin: Springer Verlag; 2004, p. 37.
- [10] Wendland H. "Scattered data approximation", *Cambridge monographs on applied and computational mathematics*, Vol. 17. Cambridge: Cambridge University Press; 2005.
- [11] Uhler K, Skala V. "Radial basis function use for the restoration of damaged images." In: *Computer vision and graphics*, Dordrecht: Springer; 2006, p. 839-844.
- [12] Shu C, Ding H, Yeo KS. "Local radial basis function-based differential quadrature method and its application to solve two-dimensional incompressible Navier-Stokes equations." *Computer Methods in Applied Mechanics and Engineering* 2003;192(7):941-954.
- [13] Golitschek M, Light W. "Interpolation by polynomials and radial basis functions on spheres." *Constructive Approximation* 2000;17:1-18.
- [14] Wright, Grady Barrett. "Radial basis function interpolation: numerical and analytical developments." (2003).
- [15] Genton MC. Classes of kernels for machine learning: A statistics perspective. *J. Machine Learning Research*, 2001;2:299-312.
- [16] Shen M, Chen J, Li B. Image piecewise inpainting based on radial basis function. "International Journal of Intelligent Computing and Cybernetics" 2008;1(4):537-548.

AUTHOR PROFILE

Mashail Alsalamah

Current position, grades:PhD research student
University studies:Coventry University
Scientific interest: Artificial Neural Network,Algorithm.
Publications <3>:
Experience:a lecture at Qassim University .
Bachelor in Computer science from Qassim University.
Diploma in acadmic English and Computer science from Essex University
Msc in Computing from Coventry University.
PhD student in Health Informatics at Coventry University.

Saad Amin



Current position, grades:PhD Principal Lecture
University studies:Coventry University
Scientific interest:Artificial Intelligence,Algorithm,Information System.
Publications <79>:
Experience: Post-graduate Programme Manager and Principal Lecturer in Network Computing in the Faculty of Engineering and Computing.

Involved with a European Community project at the Parallel Algorithms Research Centre, Loughborough University. The main objectives of the project were to establish a European standard platform for the exploration of biocomputational, nanotechnological and holographic algorithms.

The principal investigator of several funded projects. He has supervised eight completed PhD students and has eight current PhD students. He has published more than 70 papers in peer-reviewed journals, reputable conferences and books chapters on many aspects of this research. He has organised international conferences and workshops, as well as acted as Session Chair and on program committees for many international conferences.

Served on the IEEE Committee for Signal Processing Chapter for the UK and Ireland and Vice-Chairman of the British Computer Society/Middle East section.

Content based Video Retrieval Systems Performance based on Multiple Features and Multiple Frames using SVM

Mohd.Aasif Ansari, Hemlata Vasishtha
Engineering & Technology,
Shri Venkateshwara University,
Gajraula, India

Abstract—In this paper, Content Based Video Retrieval Systems performance is analysed and compared for three different types of feature vectors. These types of features are generated using three different algorithms; Block Truncation Coding (BTC) extended for colors, Kekre's Fast Codebook Generation (KFCG) algorithm and Gabor filters. The feature vectors are extracted from multiple frames instead of using only key frames or all frames from the videos. The performance of each type of feature is analysed by comparing the results obtained by two different techniques; Euclidean Distance and Support Vector Machine (SVM). Although a significant number of researchers have expressed dissatisfaction to use image as a query for video retrieval systems, the techniques and features used here provide enhanced and higher retrieval results while using images from the videos. Apart from higher efficiency, complexity has also been reduced as it is not required to find key frames for all the shots. The system is evaluated using a database of 1000 videos consisting of 20 different categories. Performance achieved using BTC features calculated from color components is compared with that achieved using Gabor features and with KFCG features. These performances are compared again with the performances obtained from systems using SVM and the systems without using SVM.

Keywords—CBVR; KFCG; Multiple Frames; SVM; BTC; Gabor filter

I. LITERATURE REVIEW AND RELATED WORK

Researchers have developed a number of techniques, methods and systems in the field of content based video retrieval systems. They are required to effectively search, index and retrieve videos from databases but the reliable and effective systems are still awaited for huge databases [6]. For this reason, text based searches are still in practice for the video retrieval systems [5]. A content based retrieval system was developed for commercial use [15]. Face detection method was used for image and video searches in this system. But this method also proved to be very poorly performing [8] by the automatic systems participated in the video retrieval track [16]. A hope emerged when low level features were utilized. Comparison of low level features extracted from key frames of the query and the videos from database provide better results for video retrieval systems [6]. Other useful and much more important information from videos can bring performance of the video retrieval systems to a great level of success. Researchers still face a challenge to utilize important

information such as sequence of shots, temporal and motion information [5]. To compensate this problem and to get better retrieval performance, a video retrieval system [2] utilized all frames of a shot instead of only the key frames so that more visual features are extracted. Another system [12] integrated color and motion features for better utilization of spatio-temporal information but a fact is still relevant that an efficient image retrieval technique results in an efficient video retrieval technique where image from the query video is used as a query [8]. The system proposed here utilizes visual features from multiple frames instead of a single frame, key frames of the shot or all of its frames. The proposed system provides the much required solutions to the problems mentioned above which are, lower efficiency when only a single image is used, high computational cost when key frames are used and unavailability of proper tools for clustering algorithm. This system provides reasonable efficiency along with low computation cost.

In section II, features extraction algorithms and classification are discussed; section III discusses about similarity measure; section IV shows the methodology to calculate result parameters in the proposed CBVR system, while the proposed CBVR system is elaborated in section V. Result analysis is presented in section VI; problems and challenges faced by the CBVR system are discussed in section VII and it is concluded by section VIII.

II. FEATURES EXTRACTION AND CLASSIFICATION

Color, texture and motion features are the most useful features for classification and retrieval of videos. Color histogram proves to be useful to represent color content while extraction of Gabor features is a popular way to represent texture features [4].

A. Extraction of BTC Features

Block truncation coding (BTC) is basically a compression technique for images [14]. BTC features are calculated for small blocks formed by dividing an image instead of calculating for each pixel [17], [18]. BTC is used to obtain features from color information of pixels belonging to the small blocks. BTC features from multiple frames are employed to obtain very high precision and recall values. These features can also be used for image classification and retrieval purpose. The BTC technique can be extended to RGB

images by considering each color component (red, green and blue) as a separate plane [14]. BTC features are obtained as shown in the equations (1-5).

- An inter band average image (IBAI) is formed as shown in (1)

$$I_{avg}(x, y) = I_R(x, y) + I_G(x, y) + I_B(x, y) \quad (1)$$

- Threshold values for the three color components are calculated as shown in (2) for one of the components (red).

$$R_{threshold} = \frac{\sum_{r=0}^x \sum_{c=0}^y I_R(r, c)}{x * y} \quad (2)$$

- Binary bitmaps are created for each of the three components as shown in (3) for the red component

$$R_{bm}(r, c) = \begin{cases} 1, & I_R(r, c) \geq R_{threshold} \\ 0, & otherwise \end{cases} \quad (3)$$

- m_1 and m_2 are the mean values found for the three components as shown in (4) and (5) for the red components.

$$m_{R1} = \frac{\sum_{r=0}^x \sum_{c=0}^y R_{bm}(r, c) I_R(r, c)}{\sum_{r=0}^x \sum_{c=0}^y R_{bm}(r, c)} \quad (4)$$

$$m_{R2} = \frac{\sum_{r=0}^x \sum_{c=0}^y (1 - R_{bm}(r, c)) I_R(r, c)}{x * y - \sum_{r=0}^x \sum_{c=0}^y R_{bm}(r, c)} \quad (5)$$

where, $m_1 = \{m_{R1}, m_{G1}, m_{B1}\}$ and $m_2 = \{m_{R2}, m_{G2}, m_{B2}\}$

m_1 and m_2 represent the entire block. Mean values of all the blocks considered together represent the entire image.

B. Extraction of Gabor Features

Gabor features provide good representation of edge and texture features for objects and texts and help to distinguish them effectively from the background [7]. Gabor filters are capable of extracting features from edges or regions of different objects inside an image directed towards desired orientations with different frequencies [22].

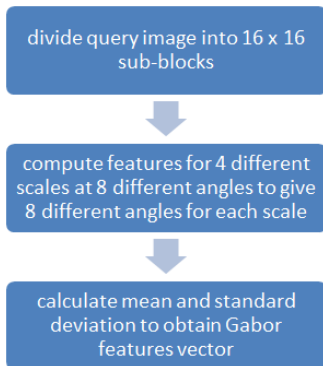


Fig. 1. Gabor Filter Algorithm

Method to extract Gabor features is shown in Fig. 1 while the mathematical expressions are given from equation 6 to equation 11 [20].

For a given image, discrete Gabor wavelet transform is given by a convolution using equation (6) for an image $I(r, c)$ where, $r = 0, 1, 2, \dots, R$ and $c = 0, 1, 2, \dots, C$.

$$W_{uv} = \sum_p \sum_q I(r - p, c - q) G_{uv}^*(p, q) \quad (6)$$

Where, G_{uv}^* is complex conjugate of G_{uv} . G_{uv} is generated by some morphological operations on mother wavelet. $p * q$ is the size of filter mask, u and v are scale and orientations.

Gabor filters are applied on the image with different orientations and different scales to find a set of magnitudes $E(u, v)$ containing the energy distribution in the image in different orientations and scales as shown in (7).

$$E(u, v) = \sum_r \sum_c |W_{uv}(r, c)| \quad (7)$$

To obtain texture features Standard deviation σ and mean are required and calculated as shown in equations (8) and (9) respectively

$$\text{Standard Deviation, } \sigma_{uv} = \sqrt{\frac{\sum_r \sum_c (|W_{uv}(r, c)| - \mu_{uv})^2}{R * C}} \quad (8)$$

$$\text{Mean, } \mu_{uv} = \frac{E(u, v)}{R * C} \quad (9)$$

Texture features vector F is formed by a set of feature components [25], [26] i.e., different values of σ_{uv} and μ_{uv} calculated by varying u and v as shown in equation (10).

$$f = [\sigma_{u_0v_0}, \sigma_{u_1v_1} \dots \sigma_{u_{uv}v}] \quad (10)$$

$$f_{Gabor} = \frac{f - \mu}{\sigma} \quad (11)$$

C. Extraction of KFCG Features

Compression is achieved in vector quantization by using some bits to represent a closest codeword for small blocks formed by dividing an entire image [27]. Linde-Buzo-Gray (LBG) is most commonly used algorithm to generate codebook [28]. In LBG algorithm, vectors found in the blocks are training vectors which are separated to form different clusters. They are divided again and again by process of iteration. Codebook vectors are centroid of these clusters [29]. A training vector is represented by codebook vector closest to it [30]. Codebook vectors are represented by a set of codewords which are used to encode and decode the images [31]. Kekre's Fast Codebook Generation (KFCG) Algorithm is basically used for image compression [32] [23]. It requires less time to generate the codebook through vector quantization method. The codebook generated is used in the proposed system as a feature vector for video retrieval purpose [20].

D. Classification of Features using Support Vector Machine

Support Vector Machine (SVM) improves performance of content based image retrieval (CBIR) significantly [11]. It is the inspiration to use SVM for CBVR too. SVM can utilize the features representing a video similarly it does for CBIR. Here, the feature vector can be the features extracted from frames, shots, scenes or events. Features from known categories of videos are labeled to train the svm. Similar features extracted from other videos are used by SVM for classification of videos. Use of SVM is a milestone in automatic classification of videos [19] with better efficiency.

III. SIMILARITY MEASURE

Features extracted from the images provide most convenient method for similarity measurement [1]. The query video is retrieved by finding similarity between its feature

vector [9], [10] and feature vector of the videos stored in database. Video similarity is measured at different resolution [13]. So the selection of features becomes relevant for calculating similarity. Similar videos can also be obtained by using SVM. The videos classified by SVM to form one category show greater similarity among them. The most similar video can be obtained by finding euclidean distance between the query video and the videos classified to form that category. Again, the feature vector is used to calculate the euclidean distance.

The equation for Euclidean distance between a query frame q and a database frame d is shown in (12)

$$\text{Euclidean Distance} = \sqrt{\sum_{n=1}^N (V_{dn} - V_{qn}) \cdot (V_{dn} - V_{qn})} \quad (12)$$

Where V_{dn} are the feature vectors of database frame d and V_{qn} are the feature vectors of query frame q each having size N [20].

IV. RESULT EVALUATION METHOD

The performance of video retrieval is evaluated with the same parameters as it is evaluated in image retrieval [11]. Recall and precision are the two parameters [2] as given in (13) and (14).

$$\text{Recall} = \frac{DC}{DB} \quad (13)$$

$$\text{Precision} = \frac{DC}{DT} \quad (14)$$

DC = number of similar clips detected correctly

DB = number of similar clips in the database

DT = total number of detected clips

V. PROPOSED CBVR SYSTEM

A CBVR system is proposed in this paper in which multiple frames are obtained for the query videos and the videos' database instead of using single frame or key frames or all frames [2]. BTC, Gabor and KFCG features are obtained as mentioned above in features extraction section. The similar and most relevant videos are obtained from the output directory containing videos of that category. Significantly higher results have been obtained using this system. A typical methodology is used in this system where a video is retrieved from its category. Here, database is processed offline. The videos are represented by feature vectors formed from any one or a combination of more than one from three types of features extracted from their multiple frames. Feature vectors are then labelled and stored in the features database. An SVM is trained for the categories registered in the system using labelled feature vectors stored in the database. Variables are obtained from the trained SVM. Feature vectors from the query videos are used for classification using SVM variables already saved. Videos obtained in the output folder are the videos of the desired category. For a query clip, videos stored in the given category can be ranked according to the distance measures and most similar videos are retrieved. Euclidean distance is used to measure similarity [20]. Retrieval system without using SVM is shown in Fig. 2 [20]. Most similar

videos are obtained based on minimum distance between feature vectors stored in the database and feature vectors of the query image. As mentioned above, multiple frames based classification and retrieval yields acceptable results without the complexity of finding key frames to represent a shot.

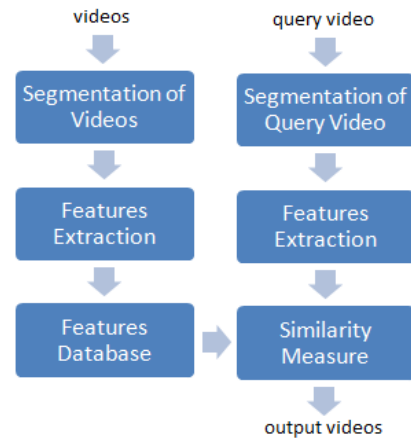


Fig. 2. Proposed CBVR system

A process flow of the CBVR system using SVM is shown in Fig. 3. Multiple frames are obtained during segmentation. Features are then extracted for each of those frames and stored in feature vectors database. Feature vectors are labelled for the pre-decided categories.

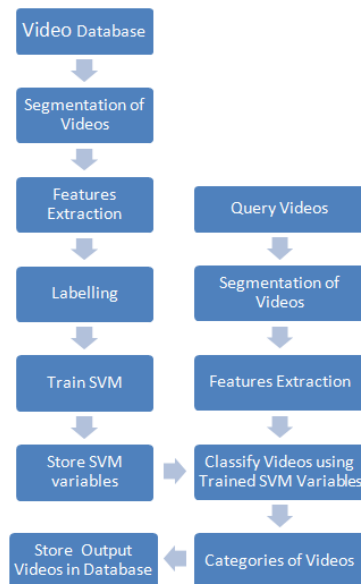


Fig. 3. Proposed CBVR system

SVM is trained and its variables are stored. This process is done offline. The query videos are separated into the categories based on stored SVM variables using feature vectors of the query videos. Videos obtained for different categories are stored with different categories in the output database. The query video can be retrieved by exact similarity matching from the classified videos using Euclidean distance method.

VI. RESULTS

A. Database

The technique using multiple frames with one or multiple features using SVM is applied to a video database having 1000 videos with 20 categories of 50 videos each as shown in Fig. 4. Videos similar to the query video are stored in output folder after classification using SVM classifier. The precision and recall values are computed by grouping the number of classified videos belonging to the category of query video and then finding minimum distance between them and the query video.

B. Analysis of Results

The charts shown from Fig. 5 to Fig. 10 for different features represent the retrieval results obtained for retrieving and classification of video clips from different categories. These categories are among the 20 categories of video clips from the video database of 1000 videos. The results obtained are highly appreciable for all the categories. The results are obtained using SVM based on Gabor features extracted from multiple frames of the video clips. Similarly, results are also obtained using block truncation coding method extended for color images [24] and KFCG algorithm. The charts compare the performance obtained by the system using SVM with the performance obtained from system based on same features without using SVM [21]. Comparison of systems performance is also done using three different features without using SVM and while using SVM.



Fig. 4. Sample video database of 1000 videos with 20 categories

1) Results for video clips using Gabor features

Fig. 5 shows results (precision values) obtained by CBVR system based on Gabor features extracted from multiple frames using SVM. There is a significant improvement in results using SVM as compared to results obtained without using SVM except for one case.

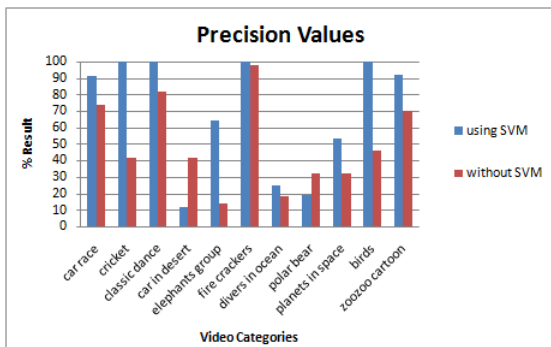


Fig. 5. Comparison of Precision values shown for given categories of videos using SVM and without using SVM using Gabor features

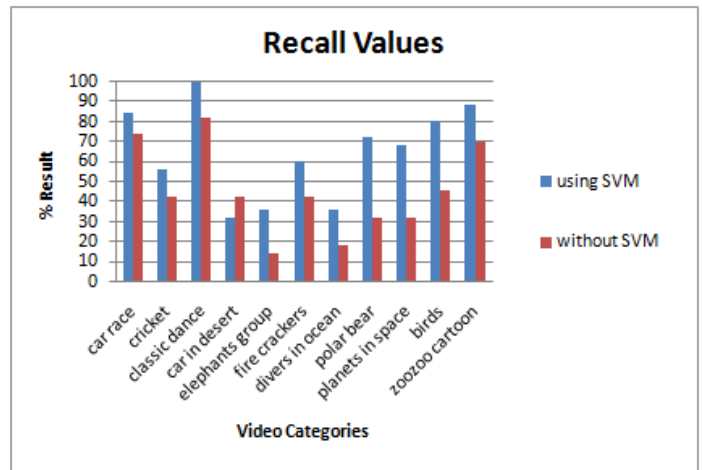


Fig. 6. Comparison of Recall values shown for given categories of videos using SVM and without using SVM using Gabor features

Fig. 6 shows results (recall values) obtained by CBVR system based on Gabor features extracted from multiple frames using SVM. There is significant improvement in results using SVM as compared to results obtained without using SVM except for one case.

2) Results for video clips using KFCG features

Fig. 7 shows results (precision values) obtained by CBVR system based on KFCG features extracted from multiple frames using SVM. There is significant improvement in results using SVM as compared to results obtained without using SVM except for one case.

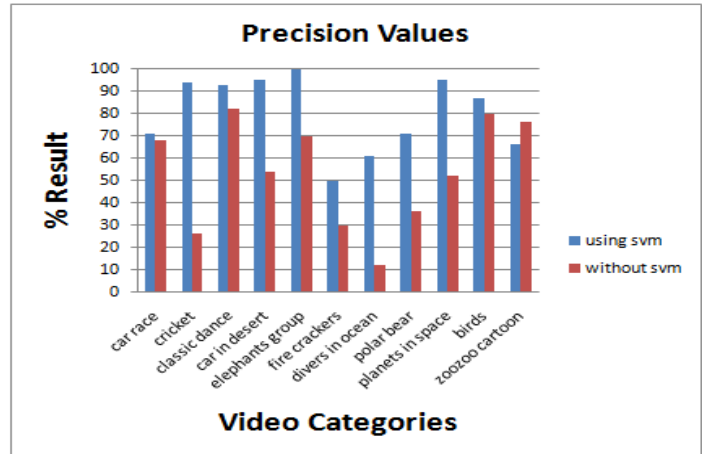


Fig. 7. Comparison of Precision values shown for given categories of videos using SVM and without using SVM using KFCG features

Fig. 8 shows results (recall values) obtained by CBVR system based on KFCG features extracted from multiple frames using SVM. There is significant improvement in results using SVM as compared to results obtained without using SVM except for one case.

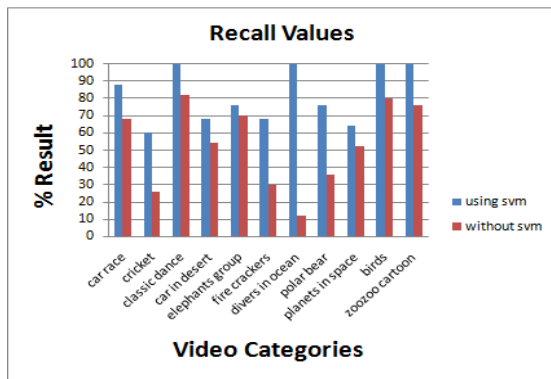


Fig. 8. Comparison of Recall values shown for given categories of videos using SVM and without using SVM using KFCG features

3) Results for video clips using BTC features

Fig. 9 shows results (precision values) obtained by CBVR system based on BTC features extracted from multiple frames using SVM. There is significant improvement in results using SVM as compared to results obtained without using SVM.

Fig. 10 shows results (recall values) obtained by CBVR system based on BTC features extracted from multiple frames using SVM. There is significant improvement in results using SVM as compared to results obtained without using SVM.

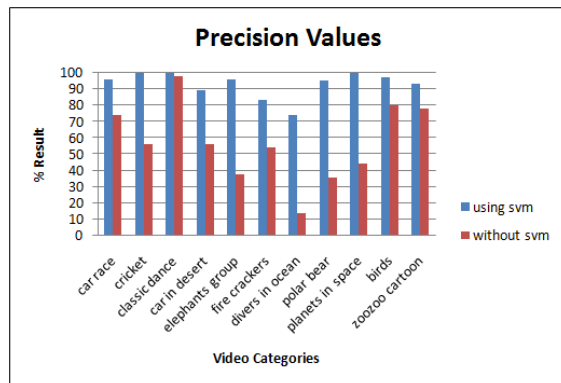


Fig. 9. Comparison of Precision values shown for given categories of videos using SVM and without using SVM using BTC features

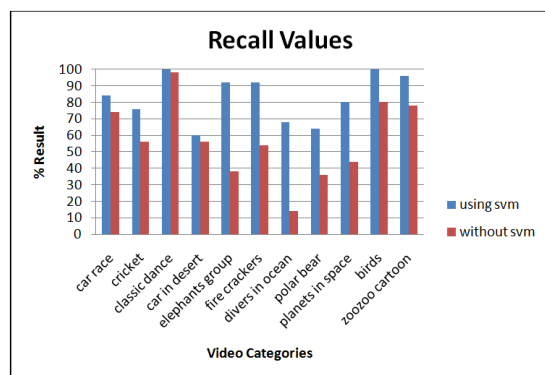


Fig. 10. Comparison of Recall values shown for given categories of videos using SVM and without using SVM using BTC features

VII. PROBLEMS AND CHALLENGES

Low level features representing the frames are used in implementation of CBVR systems using query by image or query by clips like the one shown in the proposed system. These low level features extracted from frames are used to measure similarity between different videos. Due to this, different types of videos containing distinct objects but with similar backgrounds may produce false retrievals. For example, videos showing players playing football may be retrieved along with videos showing players playing cricket due to similar background of the field or a video showing a person delivering speech may be retrieved with videos showing a different person delivering speech with a similar background of the stage. Low level features are utilised for content based image retrieval when query is done by example image. Performance and efficiency of such systems searching video is quite acceptable when non-identical features are present in them but the performance is very poor when low level features belonging to different videos are identical. This is due to the fact that they are unable to utilise the semantic features e.g., different videos having different electronic equipments but with distinct low level features.

VIII. CONCLUSION

The proposed system shows better classification and enhanced video retrieval results. The higher efficiency has become possible due to utilization of distinct features representing distribution of color information (BTC method), inclination of edges in multiple directions (Gabor algorithm), codewords representing blocks (KFCG algorithm). Though, the result is appreciable for all the three types of features but the Precision and Recall values are much higher for BTC and KFCG features as compared to Gabor features. The performance is boosted further due to use of features from multiple frames instead of using single key frame representing a shot. Additional improvement is achieved by the use of SVM which makes the system highly efficient.

IX. FUTURE SCOPE

Computational cost of the proposed system is better as there is no requirement to find the key frames for each shot. Though we have enhanced classification and retrieval of videos, an attention and focus is required to eliminate the drawback of producing false result when videos have similar backgrounds. Another scope of future research is the recognition and grouping of videos belonging to same category but having different low level features.

REFERENCES

- [1] Weiming Hu, Nianhua Xie, Li Li, Xianglin Zeng, Maybank S., "A Survey on Visual Content-Based Video Indexing and Retrieval", IEEE Transactions on Systems, Man, and Cybernetics, Part C (Applications and Reviews), 41-6,797-819, 11/2011
- [2] Liang-Hua Chen, Kuo-Hao Chin, Hong-Yuan Liao, "An integrated approach to video retrieval", Proceedings of the nineteenth conference on Australasian database-Volume 75, 49-55, 2008
- [3] Dengsheng Zhang, Aylwin Wong, Maria Indrawan, Guojun Lu, "Content-based Image Retrieval Using Gabor Texture Features", IEEE Transactions PAMI, pages 13-15, vol. 12.
- [4] Yining Deng, B.S. Manjunath, "Content-based Search of Video Using Color, Texture, and Motion", IEEE, pg 534-537, 1997

- [5] Ja-Hwung Su, Yu-Ting Huang, Hsin-Ho Yeh, Vincent S. Tseng, "Expert Systems with Applications", 37, pg 5068-5085, 2010
- [6] Nicu Sebe, Michael S. Lew, Arnold W.M. Smeulders, "Video retrieval and summarization", Computer Vision and Image Understanding, vol. 92, no. 2-3, pg 141-146, 2003
- [7] C. V. Jawahar, Balakrishna Chennupati, Balamanoahar Paluri, Nataraj Jammalamadaka, "Video Retrieval Based on Textual Queries", Proceedings of the Thirteenth International Conference on Advanced Computing and Communications, Coimbatore, Citeseer, 2005
- [8] Alexander G. Hauptmann, Rong Jin, and Tobun D. Ng, "Video Retrieval using Speech and Image Information", Electronic Imaging Conference (EI'03), Storage Retrieval for Multimedia Databases, Santa Clara, CA, January 20-24, 2003.
- [9] Swain M.J. and Ballard, B.H. "Color Indexing," Int'l J. Computer Vision, vol. 7, no. 1, pp. 11-32, 1991.
- [10] Hafner, J. Sawhney, H.S. Equitz, W. Flickner, M. and Niblack, W. "Efficient Color Histogram Indexing for Quadratic Form Distance," IEEE Trans. Pattern Analysis and Machine Intelligence, 17(7), pp. 729-736, July, 1995.
- [11] Aljahdali, S., Ansari, A., Hundewale, N., "Classification of Image Database Using SVM With Gabor Magnitude", International Conference on Multimedia Computing and Systems (ICMCS), Tangier, Morocco, 2012, vol., no., pp.126,132, 10-12 May 2012
- [12] Mohd. Aasif Ansari, Hemlata Vasishtha, "CBVR and Classification of Video Database-Latest Trends, Methods, Effective Techniques, Problems and Challenges", International Journal of Computer Applications (ISSN : 0975 - 8887), Volume 125 - No. 6, September 2015
- [13] R. Lienhart, "A System For Effortless Content Annotation To Unfold The Semantics In Videos," in Proc. IEEE Workshop Content-Based Access Image Video Libraries, pp. 45-49, Jun. 2000.
- [14] Guoping Qiu, "Colour Image Indexing Using BTC", IEEE Transaction on Image Processing, Vol. 12, January 2003.
- [15] Visionics Corporate Web Site, FaceIt Developer Kit Software, <http://www.visionics.com>, 2002.
- [16] The TREC Video Retrieval Track Home Page, <http://www.nlpir.nist.gov/projects/trecvid/>
- [17] Edward J. Delp, Martha Saenz, and Paul Salama, "BLOCK TRUNCATION CODING (BTC)", Handbook of Image and Video Processing: BTC, Video and Image Processing Laboratory, School of Electrical and Computer Engineering, Purdue University, West Lafayette, Indiana.
- [18] Delp, E.J., "Image Compression Using Block Truncation Coding", IEEE Transactions on Communication, ISSN : 0090-6778, Volume:27, Issue:9, pg 1335-1342, Sep 1979,.
- [19] Markos Zampoglou, Theophilos Papadimitriou, IEEE Member, and Konstantinos I. Diamantaras, IEEE Member, "Support Vector Machines Content-Based Video Retrieval based solely on Motion Information", IEEE, ISSN : 1551-2541, Print ISBN: 978-1-4244-1566-3, 2007.
- [20] Mohd. Aasif Ansari, Hemlata Vasishtha, "Enhanced Video Retrieval and Classification of Video Database Using Multiple Frames Based on Texture Information", International Journal of Computer Science and Information Technologies (ISSN : 0975 - 9646), Volume 6 (2), pg 1740 - 1745, April 2015
- [21] Mohd. Aasif Ansari, Hemlata Vasishtha, "Enhanced Video Retrieval and Classification of Video Database Using Multiple Frames Based on MBTC features", International Journal of Advances in Electronics and Computer Science (ISSN : 2393 - 2835), Volume 2 (12), pg 32 - 39, Dec 2015
- [22] Arti Khaparde, B. L. Deekshatulu, M. Madhavilath, Zakira Farheen, Sandhya Kumari V, "Content Based Image Retrieval Using Independent Component Analysis", IJCSNS International Journal of Computer Science and Network Security, VOL.8 No.4, April 2000.
- [23] H. B. Kekre, Tanuja K. Sarode, "Fast Codebook Generation Algorithm for Color Images using Vector Quantization," International Journal of Computer Science and Information Technology, Vol. 1, No. 1, pp.: 7-12, Jan 2009.
- [24] Mohd. Aasif Ansari, Hemlata Vasishtha, "CBVR and Classification of Videos based on BTC Color Features using SVM", Proceedings of the International Conference on Emerging Research Trends in Applied Engineering and Technology, KGCE, Karjat, ISBN: 978-93-5258-409-3, 1-2 April, 2016.
- [25] Flickner M. et al, "Query by image and video content: the QBIC system", IEEE Computer 1995, Volume 28, Number 9, pp 23-32, 1995.
- [26] C. Faloutsos, R. Barber, M. Flicker, J. Hafner, W. Niblack, D. Petkovic and W. Equitz, "Efficient and effective querying by image content", J. Intell. Inf. Systems 3, 231-262, 1994.
- [27] Mukesh Mittal, Ruchika Lamba, "Image Compression Using Vector Quantization Algorithms: A Review", International Journal of Advanced Research in Computer Science and Software Engineering (ISSN: 2277 128X), Volume 3, Issue 6, June 2013.
- [28] Manoj Kumar, Poonam Saini, "Image Compression With Efficient Codebook Initialization Using LBG algorithm", International Journal of Advanced Computer Technology (IJACT), ISSN:2319-7900, vol. 2, no. 2
- [29] Jari Kangas, "Increasing the Error Tolerance in Transmission of Vector Quantized Images by Self-Organizing Map", Helsinki University of Technology, Finland.
- [30] Yu-chen, Hu, Bing-Hwang, Su Chih-Chiang Tsou, "Fast VQ codebook search algorithm for grayscale image coding", Science Direct Image and vision computing 26(2008) 657-666.
- [31] Asmita A. Bardekar, Mr. P.A. Tijare, (IJCSIT) International Journal of Computer Science and Information Technologies, Vol. 2 (6), 2011, 2584-2589. ISSN:0975-9646
- [32] H. B. Kekre, Tanuja K. Sarode, "New Fast Improved Codebook Generation Algorithm for Color Images using Vector Quantization," International Journal of Engineering and Technology, vol.1, No.1, pp.: 67-77, September 2008.

Finite Elements Modeling of Linear Motor for Automatic Sliding Door Application

Aymen Lachheb

Research Unit of Mechatronic
Systems and Signals
National Engineering School of
Carthage
Rue des entrepreneurs, 2035, Tunis

Jalel Khedhiri

Unit Signal, Image and Intelligent
Control of Industrial
System (SICISI)
National Engineering School of
Tunis

Lilia El Amraoui

Research Unit of Mechatronic
Systems and Signals
National Engineering School of
Carthage
Rue des entrepreneurs, 2035, Tunis

Abstract—In this paper, a linear switched reluctance motor is designed and investigated to be used as a sliding door drive system. A non linear two dimensions finite model is built to predict the performance of the designed motor. Thus, the static electromagnetic characteristics are investigated and analyzed. The inductance and the electromagnetic force are determined for different translator position and current intensities with consideration of magnetic saturation effects. The results of analysis prove that the magnetic behavior of this motor is non linear. Furthermore, an important asymmetry of the static and dynamic characteristics between the extreme phases and the central phase is observed in high excitation levels.

Keywords—linear motor; sliding door; 2D-finite-element analysis; switched reluctance

I. INTRODUCTION

Recently, linear motors are widely used in a large number of applications and have become more and more used in many areas, particularly in industries such as transportation, manufacturing, and robotics [1-3]. Contrary to the conventional systems where the linear movement is obtained by coupling a rotary motor to a ball screw system, the linear motor allows a direct linear drive without using rotary to linear transmission system. Then, it has fewer moving parts so low inertia. Furthermore, the use of linear motors is recommended for applications which require high speed and accuracy [4], with this technology the load is connected directly to the motor due to the absence of transmission systems which results in high performance capabilities and excellent dynamic characteristic. Because of these merits and benefits, linear motor has been increasingly studied in recent years [3], [5], [6], [7].

In reference [6], a vertical propulsion actuator system of a ship elevator with Linear Switched Reluctance Machine (LSRM) is designed and compared to traditional systems.

The design of electromechanical devices requires accurate prediction of the developed forces. In fact, these forces are derived from field solutions obtained by numerical computational methods. Several methods are in use, but some of them seem to be able to produce consistently accurate results. The advantages and disadvantages of each method are discussed in [8], [9].

Various methods have been reported in many work to predict the distribution of the magnetic field of electromagnetic

structures, as the method of reluctance networks, the analytical method [5-6], 2D finite element [7], and 3D finite elements [8]. In this paper, a 2D finite element method is used to study the performances of switched reluctance linear motor.

Generally the classic automatic door opening is equipped with rotary motor and transmission systems. In such systems, the number of moving parts is important that can increase the possibilities of failures and has negative effects on the system dynamic and reliability [10].

To improve the performances and reduce the cost of the sliding door systems, a linear motor is proposed to compete the classical systems.

The first part of this paper is dedicated to the sizing of switched reluctance linear motor suitable for sliding door application. In fact, the main dimension and motor specifications are described.

Part II is reserved for the modeling of the linear motor using analytical method. This model can express the principles of electromechanical conversion governing the operation of a linear actuator with switched reluctance, as analytical relation with the assumption of the non-linearity of the used materials.

In part III, a 2D finite element (FE) model was developed to study the electromagnetic characteristics, the 2D FE model used to analyze and investigate the static behavior of the linear motor. The numerical solution of the developed model leads to compute the magnetic vector potential at each step displacement and to predict the magnetic field density and the magnetic force.

The developed mechanical model given by the classical motion equation is solved by using a numerical transient solver to obtain the dynamic characteristics. Then, the results obtained by the two dimensions finite element method analysis are presented. Finally, part V describes the conclusion of the work.

II. SIZING OF THE SWITCHED RELUCTANCE LINEAR MOTOR

The device to be studied in this work for sliding door application is a linear planar structure with three phases (A, B, C). It is composed of two ferromagnetic parts, the stator is an equidistant toothed bar and the translator which is the moving part of the motor.

The proposed motor has an active translator (with a coil), it's composed of three modules separated by a nonmagnetic part, and each module represents a phase and contain two coils in series.

The design of the linear motor required careful analysis of the required specifications, the studied motor provide a bidirectional force that moves a sliding door which have a weight of 20 Kg.

Fig.1 shows the structure and winding diagram of the designed motor.

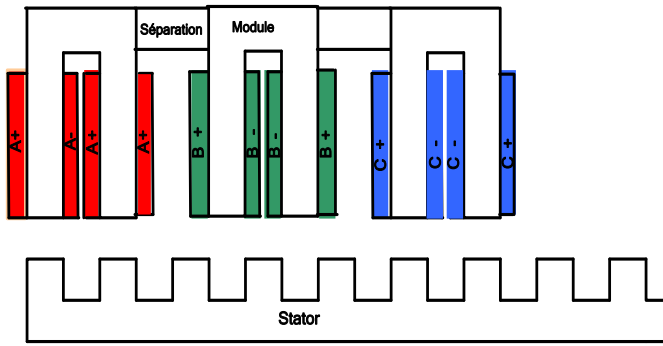


Fig. 1. Linear motor configuration and winding diagram

The choice of the width of the teeth of the motor as well as at the translator and stator must absolutely ensure the reversibility and regularity of motion.

This is guaranteed by the choice of pole pitch equal on the translator and the stator. Furthermore, the widths of teeth and slots for the translator and the stator should be equal, [5].

Indeed, the inequality of widths of teeth and pole pitch at the stator and mobile modules creates steps permeance around the equilibrium position, which induce a dead zone on the static force characteristics on which the movable part can move freely, Fig.2.

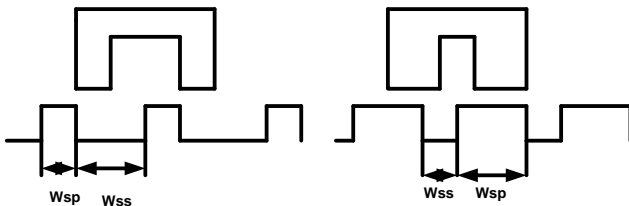


Fig. 2. Two elementary module configuration

The pole width and slot width are related to the pole pitch by the following equation:

$$\lambda = w_{ts} + w_{tp} \quad (1)$$

Where w_{ts} is translator slot width, w_{tp} is translator pole width.

The mover part includes three similar module shifted by a non magnetic separation has a width determinate by (2), [8].

$$c = c_0 + k\lambda \quad (2)$$

The mechanical step δ_m is related to the pole pitch and the number of phases by (3).

$$\delta_m = |c_0 - w_{ss}| = \frac{\lambda}{n} \quad (3)$$

The yoke thickness in the stator and in the translator is choosing equal to the slot width.

$$C_{sy} = C_{ty} = w_{ts} \quad (4)$$

The Fig.3 present a half cross of the studied motor

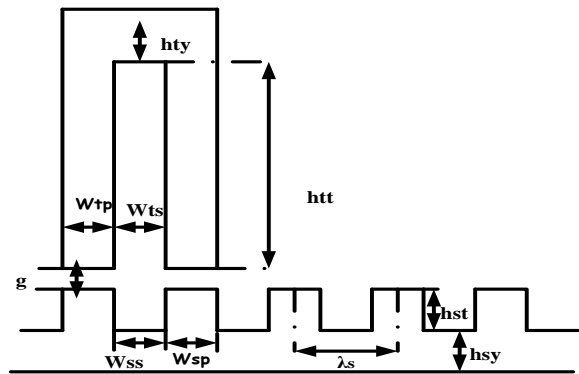


Fig. 3. Half Cross Section of the motor

The most significant geometry of the translator and stator are cited in the Table I:

TABLE I. SPECIFICATIONS OF DESIGNED MOTOR

	Parameters	Symbols	Values
Stator	Teeth width	w_{sp}	30mm
	Slots width	w_{ss}	30 mm
	Teeth high	h_{st}	30 mm
	Yoke thickness	C_{sy}	30 mm
Translator	Teeth width	w_{tp}	30 mm
	Slots width	w_{ts}	30 mm
	Teeth high	h_{tt}	150 mm
	Yoke thickness	C_{ty}	30 mm
Coil	Number of turn	N	450
	Section of copper	S_c	0.5 mm ²
Separation	Width of separation	C	50 mm
	Air gap	g	0.5mm

III. LINEAR MOTOR MODELING

The linear motor model is done in two stages, the first stage describes the electromagnetic equations, in the second stage the mechanical equations is developed.

A. Electromagnetic Equations

By neglecting the phase mutual effect, the phase voltage of the linear motor is related to the flux linked in the winding by Faraday's law as :

$$U = Ri + \frac{d\phi(x,i)}{dt} \quad (5)$$

Where i is the phase current, U is the terminal voltage, R is the phase winding resistance and ϕ is the flux linkage.

The flux linkage in a linear motor phase varies as a function of the phase current and translator position, thus

$$U = Ri + \frac{\partial\phi}{\partial i} \cdot \frac{\partial i}{\partial t} + \frac{\partial\phi}{\partial x} \cdot \frac{\partial x}{\partial t} \quad (6)$$

The relation between flux and inductance is defined as follows:

$$\phi(x,i) = L(x,i) i \quad (7)$$

The characteristics of flux and inductance are determined by the 2D finite element method which will be presented subsequently.

In general, the thrust force produced by the linear motors, derived from coenergy.

When one phase is excited the electromagnetic force is written as follows:

$$F_x = \frac{\partial W_c(i,x)}{\partial x} \Big|_{i=cte} \quad (8)$$

The coenergy of each phase can be calculated in terms of flux linkage.

$$W_c(i,x) = \int_0^i \phi(i,x) di \quad (9)$$

B. Mechanical Equation

The mechanical equation of the drive system is obtained by the Newton equation given by the following equation:

$$m \frac{d^2x}{dt^2} = F_x - F_c - f_0 \text{sign}\left(\frac{dx}{dt}\right) - \xi \frac{dx}{dt} \quad (10)$$

Where:

F_x : electromagnetic force (N)

$\frac{dx}{dt}$: linear speed (m/s)

m : moving part and load weight (Kg),

F_c : the load force (N)

f_0 : the dray coefficient

ξ : viscosity coefficient (N.s/m)

IV. 2-D FINITE ELEMENT ANALYSIS (FEA)

FEA is widely used to determine the performance of designed machine and allows to provide an accurate characteristic prediction.

In this work, a 2D FEA is used to predict the static and the dynamic response of the studied motor.

A. Static characterization

A FE model is developed to study the static behavior of the proposed motor. In fact, a complete configuration of the FE model obtained by using motor specification is shown in Fig.4.

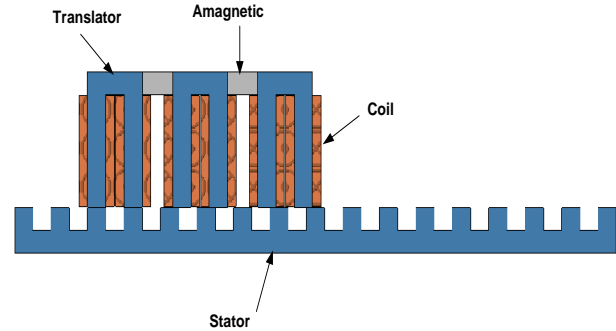


Fig. 4. Linear planner motor with modular configuration

The proposed structure of three phase motor, having a movable armature suspended over a fixed stator. The translator consists of three similar modules with six poles having command coils, and each module has two poles and has the same pole pitch.

The three modules are spaced so that only two poles at a time can be aligned with the poles of the stator. Non-magnetic separations are necessary between the various modules in order to impose a regular shift.

The windings of the electric circuit are laminated with copper and they are concentrated around the pole of each module, the coils of a same phase are connected in series.

The used material to manufacture the stator and translator is a 1010 steel, the corresponding magnetization curve of the last material is shown in Fig.5.

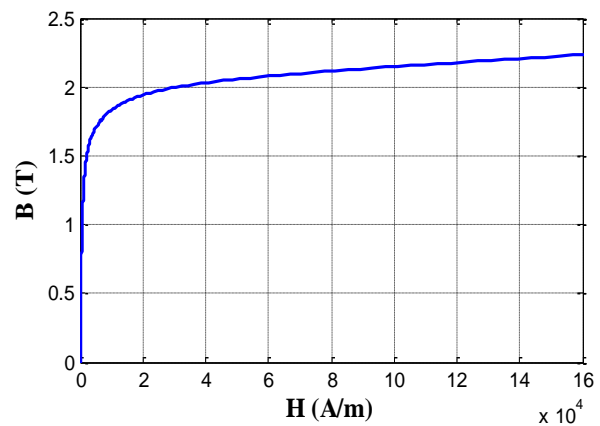


Fig. 5. The B-H curve of ferromagnetic material (1010 Steel)

This curve has three distinct regions, the steep initial part of the curve where a small increase in H produces a large increase in B , the knee of the curve and the saturated region beyond the knee where a large increase in H implies a small increase in B .

It can be observed from Fig. 5, that a flux density about 2 T marks the onset of saturation in the used material.

The design of many electromechanical devices requires the accurate prediction of the developed force.

In fact, the designed structure of the proposed linear motor was analyzed by use of 2D non linear FEA, then, a series of simulations is done by a 2D static solver in order to compute the electromagnetic force and flux linkage values for different translation position over one electric period. The obtained computed force as function of the translator positions is presented in Fig. 6 and Fig.7 for two case phases excitations of 1200AT, 3000AT respectively.

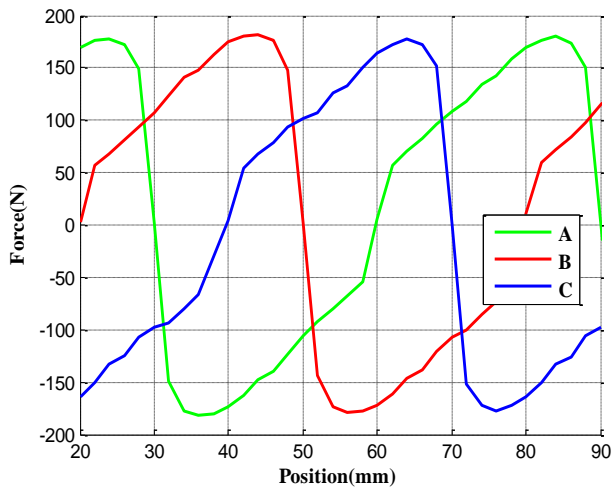


Fig. 6. Developed forces phases excited by 1200AT

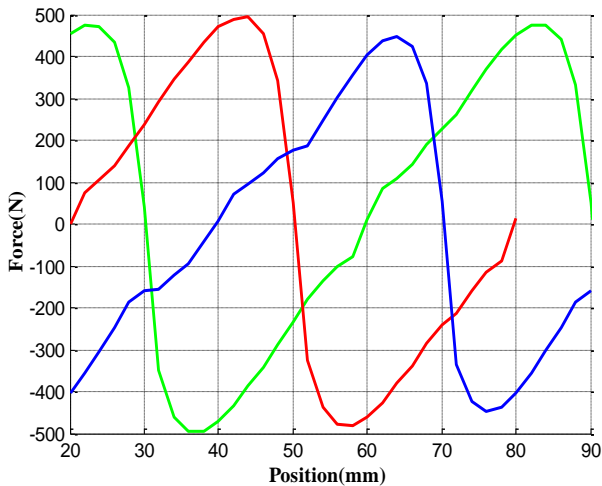
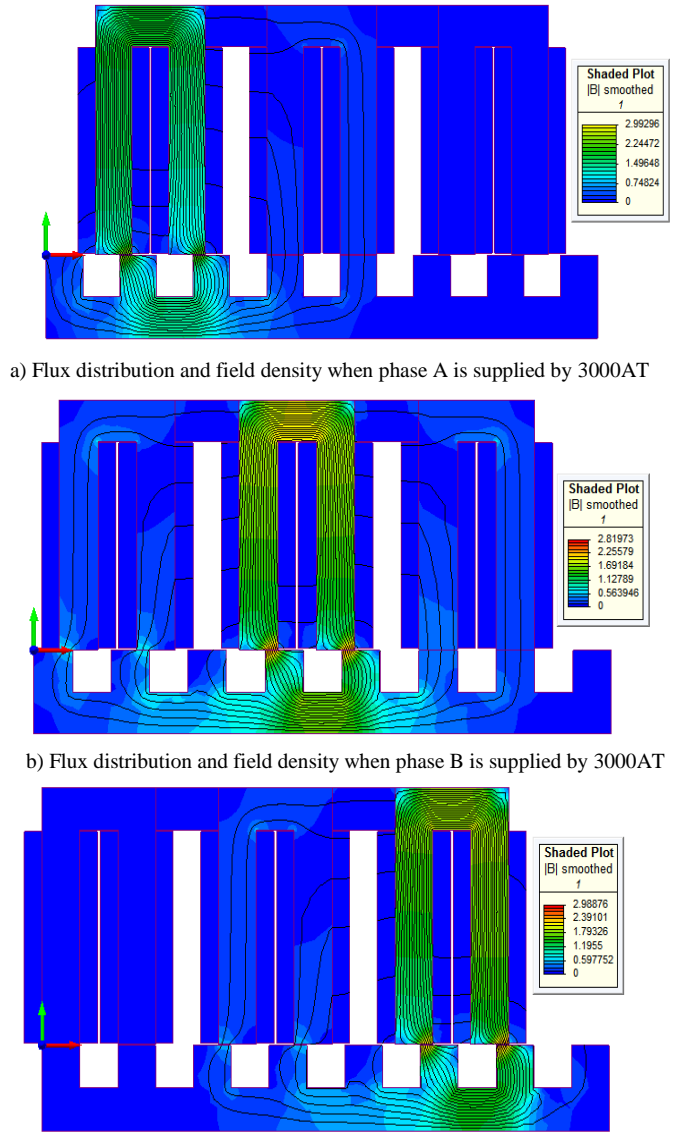


Fig. 7. Developed forces phases excited by 3000AT

The developed forces showed in Fig.6 and Fig.7 indicates that there is significant dissymmetry between the extremes and the central phase. At a current excitation about 3000Atrs, the extrem phase generates a maximum force of 500N, while the central phase develops a maximum force not exceeding 450 N. It's clear that the end effect occurs for high values of excitation.

The magnetic flux path and magnetic field density are presented in the figures below when the three phases A,B,C

successively excited by 3000AT. The distribution of the flux in the motor allows us to specify the degree of magnetic saturation in the different parts of a machine as well as the ratio of useful to leakage flux throughout the magnetic circuits.



a) Flux distribution and field density when phase A is supplied by 3000AT

b) Flux distribution and field density when phase B is supplied by 3000AT

c) Flux distribution and field density when phase C is supplied by 3000 AT

Fig. 8. Distribution of line flux through different phases

The analysis of the magnetic flux distribution for the same supplied current, confirm that a magnetic dissymmetries between the extreme phases and the phase in the center due to magnetic leakages.

The magnetic leakage in the central phase is more important than the extrem phases due to the leakage flux circulating through neighboring modules despite that there is a non-magnetic separator between them. Therefore, this magnetic losses creates a parasitic forces that affect the performance of the machine.

It can be seen from Fig.8, that when the field current is 3000AT, the magnetic saturation arises in the pole tips of the

stator and the translator. However, the pole bodies are not saturated.

The static characteristics of the linear machine are represented by the flux linkage variation with phase ampere turn and translator position.

Figure 9 illustrates a magnetization curve which is a plot of a flux linkage versus Ampere-turn at three positions. These curves correspond respectively to the aligned, intermediaries, and unaligned position. The obtained flux curves as a function of the ampere turn are non linear and confirm the saturation of the used material for high values of current excitation.

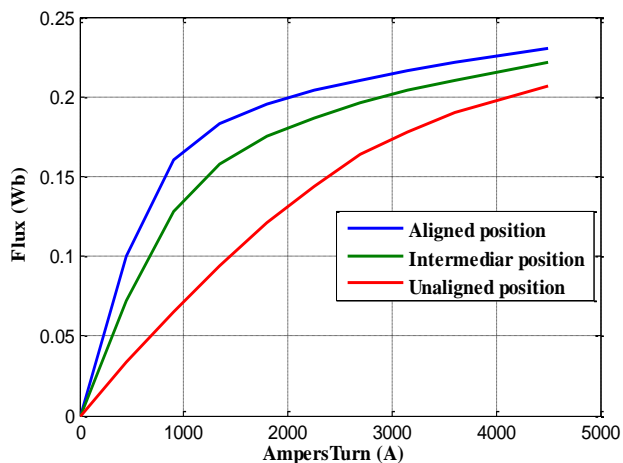


Fig. 9. Flux linkage as a function of ampere turn and translator position

In order to determine the profile of the inductance resorted the flux linkage equation given by (7).

The graphic in figure 10 shows the curves of inductance with the translator position for different magneto-motive force values between 600AT to 3000AT, where the translator is moved from an aligned position to an unaligned position.

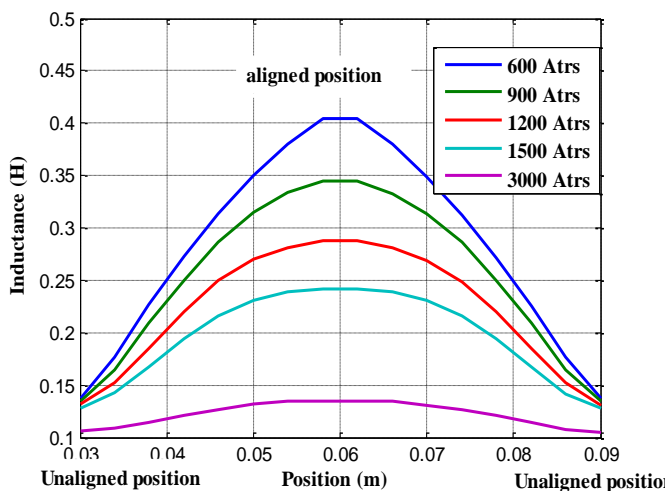


Fig. 10. Inductance-ampere turn characteristics

The obtained results show that the phase inductance in a LSRM is a periodic function of the translator position, the

inductances curves are characterised by a maximum and a minimum value, these two values correspond in fact to the aligned and unaligned positions.

The results show at a given translator position, the phase inductance decreases with the applied phase current because of magnetic saturation.

The phase inductance at the aligned position varies considerably with the supplied current. However, the unaligned inductance does not very much changed, mainly because of the large reluctance that characterizes wide air gap in the flux path.

B. Dynamic response

The proposed linear motor is designed for direct drive system. Thus, it's important to study the dynamic behavior. In this topic, a model was developed by FE method and was used to predict the dynamic behavior of the proposed motor.

In this work, a coupled electromagnetic-mechanical model for transient analysis of linear motor has been described, the mechanical parameters of the proposed structure are: $m = 20 \text{ Kg}$, $\xi = 65 \text{ N.s / m}$, $f_0 = 0.1 \text{ N}$.

The simulation of the dynamic of the motor is done according to the synopsis schema bellow.

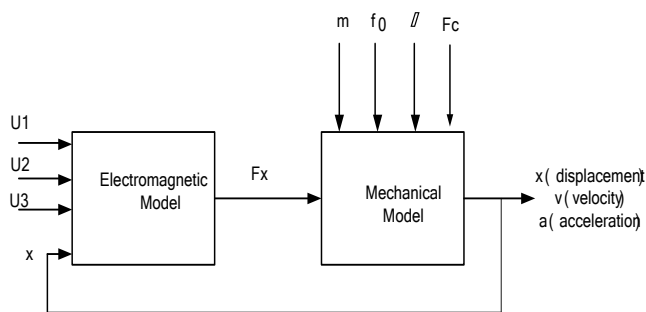


Fig. 11. Synopsis diagram

In the following, we present the performances of the motor obtained by transient analysis FEM. The dynamic responses obtained are shown in Fig12-15.

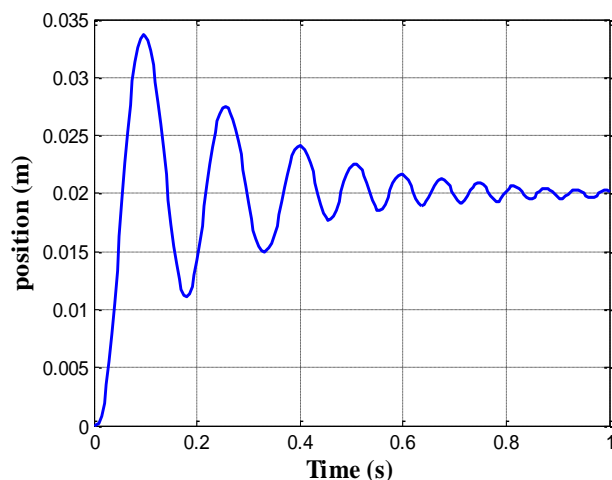


Fig. 12. Displacement versus time

The computed displacement versus time is obtained when the coil is excited by 900Atrs, the movable part being initially shifted from -20mm relative to the aligned position, when a single phase is excited, the translator should move one step and stop at the position (stable equilibrium position).

The characteristic of displacement presents some oscillations around its balance position which is equal to 20mm corresponding to the elementary step displacement of the designed motor.

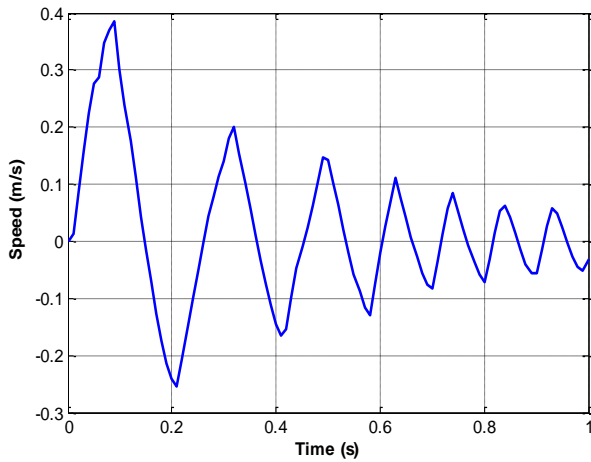
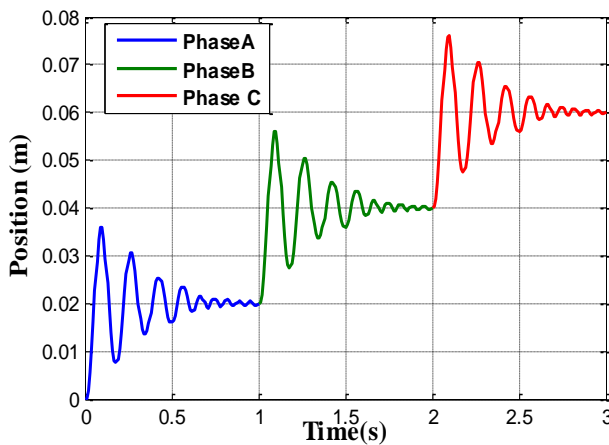


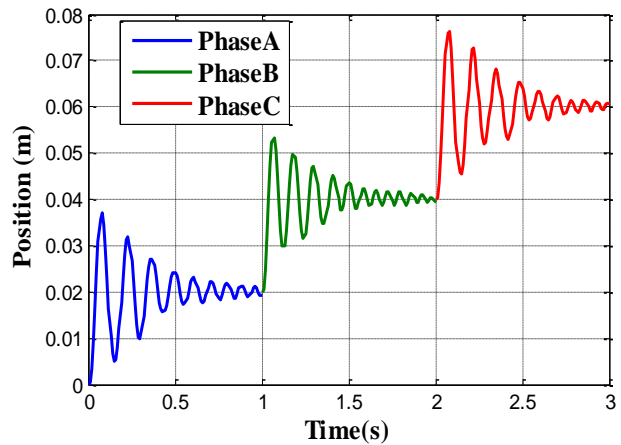
Fig. 13. Velocity versus time

In Fig.13 the moving part starts from the zero velocity to reach a maximum of 0.38 m/s then it tends to the zero value at 1s where the translator reaching the rest position.

One can observe from Fig. 13 that the velocity of the motor is characterized by a strong oscillation and great over shoot.



a) Supplied current 900 Atrs



b) Supplied current 3000 Atrs

Fig. 14. Dynamic response of motor on three steps for two different currents

The displacement curve showed in Fig. 14 is obtained for two excitations current values corresponding to a linear region of magnetization curve and saturation region.

The obtained results indicate that the working in 3 successive mechanical steps without a load when only one phase is excited for a constant period. The period of each step is 1 second.

Also, the presented result shows at the first time phase A was excited allowing moving the translator on the first equilibrium position corresponding to 20 mm after that the phase B, and C must be excited successively to obtain the other equilibrium position.

Fig 14.b show that the overshoots and the response of the system is increasing with the increase of the current excitation and an asymmetry appears between the external phases and central phase responses.

Fig.15 illustrate the characteristic of displacement when the phase A is excited with taking into account the effect of the load. When a load force is applied to the system, the equilibrium position of the linear motor is affected an error, it is shown that the displacement is accompanied by a great error with high value of load force.

These phenomena affect the position accuracy may cause loss of synchronization at high speed. To overcome such problems a logic control technique is necessary.

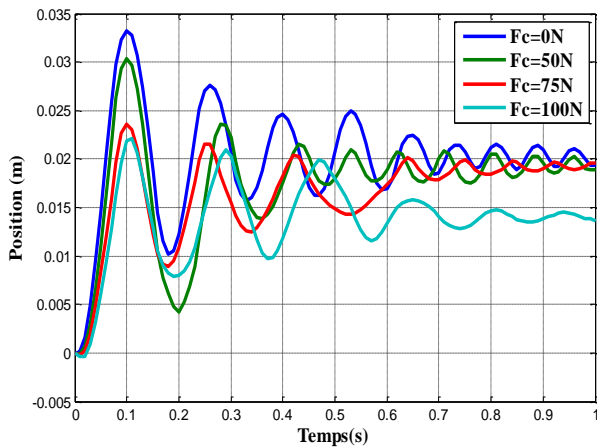


Fig. 15. Displacements versus time for different loads force

V. CONCLUSION

In order to improve the performance of the classical sliding door systems, a linear motor has been proposed. In this paper, an approach for linear switched reluctance sizing and design has been presented. For that reason, a model is developed by finite element method to calculate the static field and electromagnetic force produced by the chosen structure.

In addition, a FE analysis was performed on a basic pattern using nonlinear magnetic materials taking into account the saturation effects. The flux linkage and inductance characteristics are presented and discussed according to translator position and current. The obtained results show the presence of an important asymmetry and magnetic leakage between the motor phases in high excitation levels.

Based on the finite element method, the dynamic characteristics such as the displacement and the velocity are obtained. Then, the effect of the load in position is analysed, it was found that the variation of these parameters affects the positioning accuracy of the linear motor.

In the future research an optimal control strategy must be elaborated to reduce the significant oscillation of the motor and to improve its performance.

REFERENCES

- [1] N.S.Lobo, Hong Sun Lim R.Krishnan, "Comparison of linear switched reluctance machines for vertical propulsion application: Analysis, design, and experimental correlation," IEEE Transactions on industry applications, Vol.44, No.4, August 2008.
- [2] Lorand Szabo,Dan-Cristian Popa,Vasile Iancu "Compact double sided modular linear motor for narrow industria appications,"Power Electronics and Motion, Conference IEEE,2006.
- [3] F.Daldaban, N.Ustkoyuncu ,"A novel linear switched reluctance motor for railway transportation systems, " Energy Conversation and Management,2010.
- [4] Lilia El Amraoui, " Conception electromagnétique d'une gamme d'actionneur Linéaire Tubulaire à Réductance variable, " Thèse Doctorat en Génie Electrique, Ecole Centrale de Lille, 2002.

- [5] L. El Amraoui ,F.Gillon ,,"Performance estimation of linear tubular actuator, " Conferences maglev, 2002.
- [6] Hong Sun Lim , Hong Sun Lim , "Design and Control of a Linear Propulsion System for an Elevator Using Linear Switched Reluctance Motor Drives, " IEEE transactions on industrial electronics, Vol. 55, No. 2, February 2008.
- [7] Byeong Seok Lee, Han Kyundg Bae, Praveen Vijayraghavan,R.krishnan, "Design of a linear Switched Reluctance Machine, " IEEE Transaction on industry application ,1999.
- [8] El Amraoui, GILLON F, Brochet P,BENREJEB M, "Design of a linear tubular step motor, " Electromotion01,4th International symposium on Advanced Elecromechanical Motion Systems,vol.1 pp.223-228.
- [9] Mokrani Lakhdar ,Contribution à la CAO optimisee des machines electriques , application au moteur linéaire à induction, " thèse doctorat en Electrotechnique, Faculté des sciences de l'ingénieur de Batna ,2005.
- [10] M. Dursum, F. Koc, H.Ozbay, "Determination of geometric dimensions of a double sided linear switched reluctance motor, " World Academy of Science Engineering and Technology, 46,2010.
- [11] Zaafrane Wajdi , khediri Jalel, Rehaoulia Habib , "Comparative design and modeling study of single sided linear planner switched reluctance motor, " Wseas transactions on circuit and systems ,volume 13,2014.
- [12] J. G. Amoros , P. Andrada , "Sensitivity Analysis of Geometrical Parameters on a Double-Sided Linear Switched Reluctance Motor, " IEEE Transactions on Industrial Electronics, VOL. 57, NO. 1, January 2010.
- [13] Khidiri Jalel , "Alimentation et commande d'un actionnaire linéaire triphasé à flux transversale, " Thèse de Docteur Ingénieur en Génie Electrique,Université des Science et Technique de Lille Flandres-Artois,1986.
- [14] Zaafrane Wajdi , Khidiri Jalel, Rehaoulia Habib, "2-D finite element design of a single sided linear planner switched reluctance motor," World Applied Sciences Journal , 25 (3): 494-499, 2013.
- [15] Ge Baoming , Anibal T.de Almeida, "Design of Transverse Flux Linear Switched Reluctance Motor , " IEEE transaction on magnetics , Vol. 45, No. 1, January 2009 .
- [16] Ruiwu Cao, Ming Cheng, Chris Mi, "A linear doubly salient permanent magnet motor with modular and complementary structure, " IEEE transaction on magnetics, Vol.47,No.12,December 2011.
- [17] S.Taghipour Boroujeni, J.Milimonfared,"Design prototyping and analysis of a novel tubular permanent magnet linear machine, " IEEE transaction on magnetics, Vol.45,No.12,December 2009.
- [18] M. Jufer, " Traité d'électricité, électromécanique," traité d'électricité, électromécanique", Presses Polytechniques et Universitaires romndes, Lausanne 1995.
- [19] T.J.E.Miller, "Optimal design of switched reluctance Motos, " IEEE Trans.Ind, Electron, Vol.49, no.1,pp.15-27,Feb.2002.
- [20] R.Krishnan,R.Arumugam, and J.F.Lindsay, "Design procedure for switched reluctance motors," IEEE Trans. Ind. Appl, Vol.24,no.3, pp.456-461, May/June.1988.
- [21] H.S.Lim and R. krishnan, " Ropless elevator with linear switched reluctance motor drive actuation systems," IEEE Trans, Ind , Elecron , Vol .55 no.2,pp.534-542, Feb.2008.
- [22] N.S. Lobo, H.S.Lim, a,d R.krishnan, "Comparaison of linear switched reluctance machines for vertical propulsion application Analysis, design and experimental correlation," IEEE Trans. Appl, Vol.44, no.4,pp.1134-1142, Jul/Aug.2008.
- [23] P.K ,Budig, "The application of linear motors ,," In Proc.3rd IEEE Int.Power Electron.and Motion Contorl Conf.Aug. 2000,vol.3,pp 1336-1341.

A Review of Solutions for SDN-Exclusive Security Issues

Jakob Spooner

Department of Computing and Mathematics
University of Derby
Derby, England

Dr Shao Ying Zhu

Department of Computing and Mathematics
University of Derby
Derby, England

Abstract—Software Defined Networking is a paradigm still in its emergent stages in the realm of production-scale networks. Centralisation of network control introduces a new level of flexibility for network administrators and programmers. Security is a huge factor contributing to consumer resistance to implementation of SDN architecture. Without addressing the issues inherent from SDNs centralised nature, the benefits in performance and network configurative flexibility cannot be harnessed. This paper explores key threats posed to SDN environments and comparatively analyses some of the mechanisms proposed as mitigations against these threats – it also provides some insight into the future works which would enable a securer SDN architecture.

Keywords—SDN; software; security; OpenFlow; networking; network security; NFV

I. INTRODUCTION

Software Defined Networking is a paradigm that emerged in around 1995 with the introduction of Active Networking – programmable functions integrated within network architecture, enabling programmers to innovate the way in which they function [1]. Whilst the roots of SDN lay in technologies first introduced over 20 years ago, the concept is still extremely relevant to this day and is considered by many to be the new face of networking [2]. Historically, packetised data-networks have consisted of hardware-based networking devices operating at Layers 2 and 3 of the OSI model. Software is then implemented on top of these layers, to provide other pieces of vital network functionality, i.e. transport control for the network, e-mail applications, file transfer etc.

In traditional networks, network hardware such as routers and switches can be logically divided into two individual planes; the data plane and the control plane. The data plane is concerned with the forwarding of data-packets, whilst the control plane makes packet-forwarding decisions based on the routing protocols configured on the device. The tightly bundled nature of these two planes introduces a level of rigidity – network operators cannot easily manipulate forwarding decisions on a per flow basis. SDN aims to challenge this by separating the control and data planes. This segregation allows network programmers to develop their own controllers, pieces of software with a global view of the network [2]. This allows for a level of control that was not possible without a great deal of work in traditional network architectures due to the tightly bundled nature of data-plane and control-plane. In SDN, rules, known as flows, based on a set of conditions (e.g. all HTTP

packets over a particular size) are created centrally by network admins, installed on the controller and then pushed out to network devices in the data plane. Devices store the flows in their local cache, and in the event that they receive a packet, they check the currently stored flows for one matching the received packet. These flows govern the way in which packets should traverse the network [3], leading to a network which is easier to manage due to a centralisation of control.

SDN gives network administrators the ability to collect traffic statistics from the network devices and pass these onto the control plane for processing. This allows for in depth security-analysis without any negative effects on the performance of the data-plane [4]. SDN makes it possible to configure security policies centrally at the controller and push them out network wide. This is in stark contrast to the painstaking process of individually configuring access control lists and security policies on every router or switch in the network [5]. SDN allows easy integration of third-party software into the environment via the SDN framework, meaning that plugin-like applications can be deployed to aid certain security & non-security related tasks [4]. As SDN controllers hold a global view of the network, they introduce the possibility of network-wide intrusion detection systems, which utilize the traffic statistics they receive from the network devices. As devices are required to communicate back to the controller at regular intervals, it ensures that compromised devices are found quickly and reduces the chances of false positives, an issue that is still yet to be solved in the context of traditional networks [3].

Whilst some of the benefits of an SDN-based infrastructure are clear, there are also some apparent shortcomings, which need to be addressed before implementation of the paradigm can become widespread. Programmers are able to leverage the centralised control in SDN architectures to build reactive, self-healing mechanisms to mitigate against traditional network attacks [6]. However, the fact that SDN changes the way that networks operate entirely is likely to bring about new attack methods that can be used to exploit the individual components of an SDN architecture, and the ways in which they interact (i.e. devices-to-controller, controller-to-controller and controller-to-application). For example, an attacker successfully compromising the controller of a network is particularly lethal, as this single-point of failure can render the entire network inaccessible [4].

The introduction of a centralised controller completely changes a networks architecture. This is what makes SDN so

unique in comparison to traditional networks. With the centralised point of control, all other layers need to maintain an interface over which they can exchange important information. Commonly, the interface utilised by the data-plane and control-plane to communicate with one-another is known as the Control-Data-Plane interface, or the Southbound Interface. SDN Applications also reside in a conceptual application layer, and communicate with the controller through the 'Northbound Interface' or Control-Application-Plane interface. Applications residing on this layer have the ability to solicit directly with the controller and obtain useful information about the networks logical/physical state. This is advantageous to programmers writing SDN applications, as their programs can access large quantities of meaningful, real-time data. With this, however, comes great risk – adversaries may be able to program their applications to utilise this useful information to form attacks, and compromise the availability, integrity and confidentiality of data travelling within the network.

This change in network architecture brings around juxtaposition. On one hand, the increased flexibility and ability to innovate with network applications and network control, gives programmers the ability to better protect against traditional network attacks i.e. TCP-based DoS attacks, eavesdropping, man-in-the-middle attacks. On the other hand, the links between control-plane, data-plane and application-plane bring about new attack platforms for adversaries attempting to illegitimately use network services. Much research has been carried out over the years on traditional security attacks, however this paper focuses on attacks which are exclusive to SDN due to changes in the architecture. The solutions covered below attempt to mitigate attacks targeting these SDN-exclusive attack platforms, and ensure that adversaries cannot utilise the change in architecture to their own advantage.

The remainder of this paper is structured as follows: section II explores some of the security threats aimed at SDN environments; section III discusses some of the currently proposed mitigations and provides a comparative analysis of them; section IV discusses the current gaps in security and how these can be filled going forward, and section V concludes the paper, with an insight into future direction

II. THREATS TO SECURITY IN SDN ENVIRONMENTS

Networks running under the SDN paradigm still have the same security requirements as traditional network settings, as it is likely that they will be carrying at times, private and confidential information [7]. SDN completely changes the architecture and the inter-communicative aspects of the components in the network - from this arises a completely new platform for attackers looking to perform security-breaching attacks. This leads to a need for similar levels of security as traditional networks, but to defend against threats of a different nature [8]. This section of the paper examines some of these key threats and aims to justify their importance.

A. DDoS/DoS Attacks (Flow-decision Requests)

1) *DDoS (Flow-decision Requests)*: Numerous types of conventional DDoS attacks can be carried out in an SDN environment, but it is a variation utilising forged flow entries

which can be harnessed by an adversary in order to target a controller and compromise its availability. By flooding the controller with requests for a flow-decision, the controllers compute resources could become overwhelmed, and the controller would be rendered unable to deal with any legitimate requests it receives [2]. By targeting the centralised point of control (i.e. the controller) it renders the entire network largely unusable. Whilst data-paths currently in the network may be able to function temporarily with a downed controller, once the hard timeout of rules in their table has expired they will be required to solicit with the controller again, which will be unable to deal with requests. If an attacker(s) is able to be persistent with their flooding, this will eventually cause the unavailability of all network functionality.

2) *DoS Attacks (Switch flow-table entry flooding)*: At the data plane level, falsely created flow-entries can be flooded to other devices in order to consume the space in their flow entry tables. This leaves the forwarding devices unable to add any legitimate flow entries to their tables [3]. This results in devices being unable to incorporate subsequent flow-updates, leaving the network in a broken, disparate state. One of the key issues with the data-plane devices within Software Defined architectures is that of the switches inability to differentiate between legitimate flow requests and illegitimate ones. This flaw allows for attackers to perform successful DoS attacks at the Data plane level by filling the switches flow-buffer with false requests [4].

Whilst it would be possible for an adversary to target an individual data-path and attempt to halt its availability, it is far more likely that the controller would be targeted, effectively creating and spreading a system-wide lapse in availability. The prospect of this can be potentially devastating, particularly in production settings where services seeing high usage will be unusable to clients and employees. Furthermore, with availability for all clients removed, an adversary can plan and carry out further attacks which may aim to compromise the integrity and confidentiality of sensitive data on the network. For these reasons the above DDoS/DoS attacks have been mentioned in this paper and are considered amongst the most important attack types.

B. Hijacked/Rogue Controller

The controller can be thought of as the centralized 'brain' of an SDN. It controls the whole network from one point, making it arguably the most vital component of SDN architecture. An attacker that manages to compromise the controller essentially has control over the whole network [9]. Ability to control the actions of the controller would allow the attacker to manipulate flow entries in any way that he/she choose, e.g. stopping certain packet types reaching their destination, re-directing packets to malicious nodes in the infrastructure. In conjunction with this, the attacker could aim to compromise a particular forwarding-device in the network and enable it to operate as a 'man-in-the-middle' or black-hole/grey-hole node. This would allow the attacker to potentially drop, alter or inspect the contents of any packet it receives [10]. Another possibility is that an attacker

successfully registers a 'rogue' controller in the control plane of the network. With this rogue controller in place the adversary may be able to influence/halt the availability of other controllers, change rules installed in data-paths caches and effectively halt/manipulate the workings of applications in the applications layer.

Any attack that targets the controller/controllers in SDN architecture can have potentially devastating effects. Whilst the centralised nature and ability to collate information at one point can be massively advantageous to network administrators/programmers, in the wrong hands it could be utilised to spearhead attacks on the integrity of control messages/sensitive application information, the availability of important services to a systems users, and the confidentiality of sensitive user information utilised by applications in the application layer. Any approach attempting to successfully halt hijacked/rogue controllers should focus on ensuring the authenticity of the controller, before allowing it to make any changes to the network.

C. Malicious Applications

Due to the allowance of the SDN framework for integration of third-party applications, the issue of malicious applications arises. Applications exhibiting malicious behavior within an SDN environment can have catastrophic consequences, similar to that of a compromised controller [2]. Authentication and authorization of an application to operate within an SDN environment is difficult to enforce. Applications relying on deep packet-inspection techniques to operate can pose potential risks to the network – they may be able to indirectly control the entire network through the information they have collected during packet-inspection [11].

The increased amount of data, and the way in which it is centrally located is what gives malicious applications the ability to threaten the integrity and confidentiality of user/network information that they have access to. Securing the northbound interface is a difficult task, as each application utilising it may require access to a unique subset of information from the controller. In order to successfully monitor this, some kind of strict, information-access policy need to be enforced. This ensures that an application declares which information it will need and is only able to access these. This could ensure that applications are not covertly stealing or using information from other applications. Authenticity must also be ensured, before an application is able to communicate with the controller.

D. Control-Data Plane Link Attacks

Another key area in SDNs which presents opportunities for attackers would be the link between the control plane and the data plane. The OpenFlow specification defines use of TLS (Transport Layer Security) as optional [12], making this a weak-point and clearly susceptible to various attacks, i.e. man-in-the-middle attacks, black-hole attacks.

1) *Man-in-the-middle Attack:* A man-in-the-middle type attack takes place when a malicious node establishes itself between the controller and the data-paths residing on the data plane. Instead of directly forwarding the messages straight to

the controller (or vice-versa), the 'man-in-the-middle' node is able to manipulate/ or inspect the contents of packets [13].

2) *Black-hole Attack:* A black-hole type attack could also be performed, in which a node establishes itself in between a targeted device and the controller, and simply drops any packets it receives without forwarding them to the controller. This results in a breakdown of network communications and renders the services unavailable to legitimate users [3].

If an attacker does manage to establish itself as an intermediary between the control plane and data plane, it can potentially be devastating to the entire network. The man-in-the-middle type attack is a direct attack on the integrity of control messages between network devices in the data plane and the controller. An adversary can change control messages and shape the way the network is formed to a way advantageous to them. On the other hand, the black-hole type attack is a direct attack on the availability of the networks services. If all messages between network devices and the controller are not being forwarded by the malicious node, it will inevitably result in a breakdown in communication, with devices in the data plane unable to solicit the controller when necessary. This link between control and data plane is clearly a weak-point, and acts as a ripe attack platform for adversaries. It is therefore extremely important that it is secure before SDNs see widespread usage in production settings.

E. Eavesdropping Attacks

Adversaries attempting to gain illegitimate access to SDN networks or halt service availability may find it advantageous to eavesdrop (the act of illegitimately capturing and inspecting the packets flowing over a connection) on certain connections in the network [14]. This may allow them to gather meaningful information which can then be used to carry out more intrusive attacks. Eavesdropping attacks have long been carried out in traditional network settings – wireless architectures are particularly weak due to their over-the-air transmissions. However, in the context of SDN, eavesdropping can be carried out to inspect the packets traversing the link between control-data plane, and also exclusively at the data plane. At the data plane, [15] discusses a ease-of-use 'listening' mode integrated into OpenFlow switches can be utilized by a malicious adversary (that has been able to compromise the switch) in order to inspect the packets transmitted by surrounding switches, allowing attackers to learn important control information. In a sense, eavesdropping carried out at the control and data plane is more of a passive attack and does not directly affect the availability, confidentiality or integrity of data. It does, however, empower attackers to carry out further attacks which compromise these security aspects.

In the context of eavesdropping carried out at the Application-Control Plane link, however, the confidentiality of sensitive information can be directly compromised. A malicious adversary can learn information pertaining to a particular user if they manage to eavesdrop on a connection transmitting sensitive application data. This makes eavesdropping a particularly serious attack – confidentiality must be ensured before critical applications carrying sensitive information can be deployed in an SDN-environment.

F. Side by Side Comparison of Attacks

The following table summarises the above investigation and allows us to see the layers of abstraction that each attack affects in the SDN-architecture, and the specific security aspects that they could potentially compromise.

TABLE I. COMPARISON OF SDN ATTACK TYPES

Attack	Targeted SDN Layer	Affected Security Aspect		
		Availability	Confidentiality	Integrity
Distributed Denial of Service	Control, Data	x		
Denial of Service	Control, Data	x		
Hijacked/Rogue Controller	Control, Data, App	x	x	x
Malicious Applications	App		x	x
Man-in-the-middle	Control, Data, Control-data link		x	x
Black-hole	Control, Data, Control-data link	x	x	
Eavesdropping	Control, Data, App		x	

Each attack investigated in this section has been, or still is, fairly common in the realm of traditional networks. The interesting part is, that with the introduction of new attack-platforms inherent from SDNs architectural changes, comes variations of the attack which are then exclusive to SDNs. Whilst the traditional variations of each of these attacks can be dealt with in a more appropriate, effective manner due to the centralised nature of SDN, it is these SDN-exclusive variations which pose the largest challenge and that need to be given attention when moving forward with SDN security. The following section aims to look at currently proposed solutions to the above attacks and evaluates their effectiveness.

III. MITIGATIONS AGAINST SECURITY CHALLENGES IN SDN

The previous section defined some of the key threats to both the control and data planes in the context of SDN environments. The separation of these planes leads to highly configurable networks; however it also introduces the possibility of a number of security threats. This section explores some of the mitigations proposed for these individual threats, and then introduces some network-wide solutions which aim to secure both the control and data plane [2].

A. DDoS/DoS Attack Mitigations

DoS Attacks on SDN networks can be carried out at both the control and data plane levels. Below are a number of solutions; some specifically aim to defend the control plane, some the data plane, and others provide protection to both of these planes.

Seungwon Shin et al. [16] introduce a solution for TCP based control plane DoS attacks – AVANT-GUARD. This solution consists of two components; a Connection Migration mechanism used in establishing useful TCP sessions from failed ones, and Actuating Triggers which enable data plane devices to activate flow rules under certain pre-defined conditions. Connection Migration proxies the TCP handshake that takes place when nodes initiate a TCP connection, and ensures that the handshake is successfully completed and the session established before allowing any flow entries pertaining to this session to be forwarded to the controller. This reduces the possibility of TCP-SYN packet flooding attacks on the controller as the handshake will not have been completed for these sessions. The Actuating Triggers mechanism introduced in [16] also reduces the computational load incurred by the controller, by allowing devices to activate certain flow rules in their tables under predefined conditions. This reduces the number of transmitted flow-requests. Evaluative tests prove that in the presence of a TCP-SYN based DDoS attack, the response time of the controller to legitimate flow requests increases by a negligible amount in the order of milliseconds, along with the percentage of overhead incurred [16]. Whilst the performance of AVANT-GUARD is desirable, the approach is generally limited due to the fact that it targets one particular variation of the DDoS attack (TCP-SYN based attacks). An option would be to deploy this solution alongside other DDoS prevention mechanisms targeting other attack variations, however this configuration could become cumbersome and resource intensive. Instead, a solution defending the control plane from a wide variety of DDoS attack types would be more desirable.

Paulo Fonseca et al. [17] present a novel mechanism to prevent control plane based DoS attacks - CPRcovery. This replication based component allows for the handing-over of control from one controller, failing due to the presence of a saturation attack, to a secondary controller. To achieve this, switches check for the presence of a properly operating controller by sending an inactivity probe. If this probe determines inactivity in the controller, a connection is made to a secondary controller which assumes the role of the failed one. To ensure this process is seamless, the initial primary controller sends state update messages to the secondary controllers in the network [17]. This multi-layer approach does provide resilience, and unlike AVANT-GUARD [16], it provides the control plane with protection from a wide variety of attacks. It is, however, noted in [17] that once the secondary controller assumes a primary role, it is then susceptible to DoS attacks itself. One further downside to CPRcovery is its performance. Due to the overhead incurred from the instantiation and connection of recovery controllers, CPRcovery can be quite slow [17], with response times far higher than that of AVANT-GUARD. It would appear that this is a trade-off for the more thorough protection offered in [17].

Presented in [18] is FlowRanger, a proposal described as a request prioritizing algorithm for control plane-based DoS attacks. At a fundamental level, FlowRanger implements a priority-based scheduling system, with its key metric being that of trust-values held by each node in a network. Controllers implementing FlowRanger are able to evaluate the trust values

of each node they are receiving requests from and buffer them in separate priority queues [18]. Other proposals ([16], [17]) implement a rate-limiter for the amount of requests which can be sent to the controller, however this results in the dropping of some legitimate requests. This is clearly an issue; in production environments it is not acceptable for legitimate flow-requests to be dropped. FlowRanger challenges this with its priority queueing mechanism; suspected attacking requests will still be served, albeit at a lower priority than others. This works well, for example, if a legitimate switch is having issues and is having to retransmit flow-requests to the controller. It will be initially buffered in a lower priority queue, but eventually the request will be served. This means that once the switch has established itself and replenished its flow-cache with correct rules, its trust value will increase and its requests will return to higher priority queues. FlowRanger differs from previous implementation in that its priority queues are implemented at the controller, instead of in a distributed manner. This provides a further layer of protection (as long as the controller is not compromised). Simulation results also show that the centralised nature of this mechanism make it a higher performer than previously proposed solutions [18]. Reference [19] introduces a method utilizing user-behaviour analysis. Whilst this sounds effective in premise, the adoption of strong assumptions regarding the number of flow-requests generated by users leaves a lot to be desired. The source IPs of requests is tracked by the controller and if the profile of packets received from that IP fall into a certain category, the IP is marked as malicious. The controller then subsequently drops requests from that IP. This suffers from similar issues to AVANT-GUARD [16], in which genuine requests from non-malicious users may be ignored.

References [16], [17], [18] and [19] all focus on control plane-based DoS/DDoS attacks. Whilst it is arguably more vital that the control plane is protected, data-plane based attacks do exist and require ample protection. In [20] a data-plane oriented DoS mitigation known as Virtual source Address Validation Edge mechanism (VAVE) is proposed. VAVE is pre-emptive as it attempts to detect the presence of a node using IP-spoofing techniques to mask its real identity – this type of behaviour often leads to DoS attacks. By checking incoming packets against entries in the flow-table, the VAVE interface in the network determines if the packet is a recognised type – if not, the validity of the packet is checked against a list of pre-defined rules [20]. This could potentially cause issues, as if the pre-defined list of rules is not thorough, certain legitimate packets could be dropped, causing availability issues for genuine clients. As this mitigation only defends against data plane attacks, it would leave the controller susceptible to DoS attacks. To provide thorough protection against all types of DoS, parallel implementation of VAVE alongside AVANT-GUARD or CPRecovery would be more appropriate. This parallel implementation does however come with the downside of high computational cost and a chance of conflicting configurations.

One major issue with the currently proposed solutions for DoS/DDoS attacks is that they wait for the adversary to strike, and then attempt to deal with the aftermath. In the case of [16], [17] and [21], it is possible for the network to be rendered

temporarily unavailable before any attempt to mitigate is made. FlowRanger [18] challenges this to a degree, and in general appears to be the strongest solution from the selection reviewed above. One solution which does put emphasis on early DDoS detection is presented in [22]. The scheme utilises a measure of entropy variation in the attack packets destination IP field. The method claims to stop the attack within the first 500 transmitted attack packets. Whilst this is early, it is likely that a reasonable amount of damage will have been done during this period of time. It seems clear that defending against attacks in the control plane are two entirely separating things. Networks would benefit greatly from a solution which simultaneously protects both of these planes, whilst still achieving a reasonable level of performance.

B. Hijacked/Rogue Controller Mitigations

Unauthorised access to the controller in an SDN environment has been identified as one of the most potent threats. Various approaches towards protecting an SDN from unauthorised access at the control plane level have been proposed. The authors in [9] suggest multiple-controller architecture coupled with a ‘Byzantine Fault-Tolerance’ mechanism, in which a number of controllers dictate to the switches in the environment. Each switch in the network is connected to a set of controllers, and when one controller fails due to a successful attack, another controller takes over and connection with the failing one is severed. This particular proposal utilises a high level of resources; however an algorithm is introduced to reduce resource consumption by determining the optimal amount of controllers connected to each switch based on latency requirements and the tolerance of the switch to faulty controllers. Simulation results presented in [9] suggest that the method achieves reasonable levels of performance when the size of the data plane is small; however, as the number of switches grows the amount of controllers needed also increases, resulting in lower performance in larger-scale environments. It could be said that the proposal in [9] suffers from the same flaws as CPRecovery, in that even though a replacement controller gains control of the network, once it has taken control it is then subject to the same attacks as the previous controller. It would appear that the most effective solutions provide defense against the occurrence of an attack, and not just provide fault-tolerance and resilience should the attack occur.

In contrast to the above proposal, the authors of [23] introduce a mechanism aiming to secure SDNs by forcing them to operate in a distributed manner. An earlier work, [24], presented by the same authors defines the workings of this hybrid, distributed SDN system, in which the controller continues to centrally define flow rules, but puts algorithms in place to enable switches to spread flows to other devices in the network. In [23], a number of mechanisms are proposed which work cooperatively to provide security in this distributed environment. The use of a Trust Manager System is introduced. This is an actively maintained list containing ID’s for all of the devices currently operating in the network. This is then coupled with encrypted transmissions of all flow entries occurring between controller- data plane device and data plane device– data plane device. An authentication mechanism is put in place to allow each data plane device in the network to

check the authenticity and validity of the node that a flow originated from. This approach is in stark contrast to [9] which relies simply on a fault-tolerance mechanism. As mentioned in section II.C.2 of this paper, [23] enforces the use of TLS in all of its controller-to-equipment transmissions, making these communications inherently secure. One inherent issue with the distributed nature of [23] would be the difficult process of configuring and debugging issues with it. Since the overall proposal consists of a number of linked mechanisms, a fault in one place would bring down the entire system, or at least leave it partially operating and open to attacks. The process of accurately pinpointing the point of failure could be a difficult process. Since the nature of SDN forces networks to operate in a centralised manner, it would seem logical to develop centralised security mechanisms to complement it.

No simulation results are presented in [23] leading to the assumption that the method may not have been subject to adequate testing as of yet - this would make [9] seem more reliable – however, the lower computational overhead incurred in [23] would make it more desirable in the network setting. The distributed architecture presented also appears to be more efficient, and its generic nature allows the use of any encryption method to be used as part of its implementation, making it a more flexible option [23]. One similarity between these two solutions is the fact that they both provide protection only to communications existing on the control plane and the control-data plane link. Presented in [25] is a method which provides protection for both the Control Plane and the Data Plane. AuthFlow prevents the access of unauthorised hosts to the network, and ensures that they are properly authenticated through the use of a RADIUS server. Extensible Authentication Protocol (EAP) is used to encapsulate any messages that hosts send to the RADIUS server, requesting authentication. An intercepting authenticator relays these messages to the controller, which then adds the host sending the packets to its list of authorised hosts. A particular strength of this proposal is that packets containing flow entry updates for other devices are not transmitted until both devices are successfully authenticated [25]. Whilst this approach provides strong protection and authorisation for legitimate hosts on the data plane, its weakness lies in its underlying technologies. EAP is generally considered as weak in the realm of authentication [26], and whilst it does allow the configurators to select their own authentication and encryption methods, any hacker with knowledge in traditional attacks should be able to force an entry into the network as a rogue data-path.

Compared to the Byzantine Fault Tolerance mechanism described in [9] and the distributed security model in [23], AuthFlow appears to offer a more thorough solution, providing authentication and authorisation at both the control and data planes of an SDN environment. Test results presented in the AuthFlow paper suggest that the method successfully prevents unauthorised access of both data-plane hosts and controllers to the network, and does so in an efficient manner - with low computational and communicational overhead incurred, due to the low amount of controller input [25]. The AuthFlow mechanism also appears to be more scalable than the other two proposals in that it does not require more controllers to be added as the data plane increases its size; new devices can

simply authenticate with the RADIUS server and be added to the trusted-device list stored at the controller.

One further proposal which appears to offer strong authenticity, validity and integrity in terms of the flow rules installed in switches is PERM-GUARD [27]. Offering protection to at all layers of the SDN model (Control, Data, Application, and the links in between them), PERM-GUARD employs a scheme that manages the flow-rule production permissions of controllers and applications in an SDN infrastructure. If a controller or application wishes to push flow-rules out to data-paths on the network, they are required to authenticate themselves to a centralised authority by means of an identity based signature. Each legitimate controller or application will hold one of these signatures, and appropriate flow-production permissions will be set on authentication [27]. If one of these signatures cannot be presented, then the controller/application in question will be considered illegitimate. Whilst this does not necessarily stop attackers from attempting to hijack controllers or create rogue controllers and connect them to the network, it will deny them the ability to make malicious changes to the network structure by pushing rules out to data-paths in the network.

It would appear that PERM-GUARD is the strongest of all the solutions covered in the above section – it provides protection for not only controllers but also applications. It is a great strength of any solution when it is able to provide cross-layer protection from a common attack. In general it appears that it is not the task of stopping an already-identified hijacked/rogue controller that is difficult - it seems detecting them in the first place is the hard part. Preemptive mechanisms which prevent hijackers and rogue controllers from ever gaining access to the network would need to be developed in order to ensure that there is little to no chance of compromise.

C. Malicious Application Mitigations

Malicious applications are another dangerous threat in the context of SDNs. A compromised application or an application that has been programmed with malicious intent can allow an attacker to leverage control of the entire network [28]. Similarly, an application with buggy code can introduce vulnerabilities that attackers could exploit to gain unauthorised access to the network. The authors in [21] propose ‘FortNOX’ – a mechanism which monitors the insertion of flow-rules from security applications to devices in the network. New flow-rules are first checked against all other existing flow rules on a receiving device, and in the presence of a conflict, the new flow is discarded and not added to the local cache. This mechanism allows admins to enforce a set of hard-coded rules which override any dynamically-created rules. This ensures false flows added to the network by malicious applications to direct traffic to compromised nodes will not be permitted [21]. One particular downfall of this approach is the fact that legitimate security-applications that rely on dynamic modification of flows within the network will not operate properly in the presence of admin-created hardcoded rules. The authors in [21] do not explore this scenario, so future work could relate to this area and introduce a permissions-based mechanism to allow certain dynamic flows to take precedence.

An alternative to the previous proposal, the authors in [28] present Rosemary - a small network operating system (NOS) which is ran in multiple instances on top of the control plane of an SDN. Each application running in the environment is executed within an individual instance of Rosemary, effectively isolating each application. This allows for close monitoring of every application deployed on the network in terms of the resources it uses and the packets it transmits or receives. As well as providing a platform for monitoring malicious activities of individual network applications, Rosemary provides a level of resilience in that if one application fails or crashes, others will continue to run inside their isolated instance of the NOS [28]. Rosemary's description as a 'robust, secure and high-performance NOS' would concur with the results of evaluative test. Tests show that successful attack rates are very low in the presence of Rosemary, with high levels of performance achieved in terms of the throughput achieved and latency observed. This, however, comes with the downside of a high computational overhead, especially when compared to FortNOX which incurs relatively low levels of overhead [21].

Another proposal, LegoSDN [29] is conceptually similar to Rosemary in that it provides a layer of isolation between the controller and the application layer of an SDN environment. The key difference is that all applications are bundled together in one plane, whereas Rosemary implements a single container for each individual application. Whilst LegoSDN isn't designed specifically for combatting attacks, it isolates applications that are identified as failing - a failing application being one of the key signs of the beginnings of an application-based attack [29]. In this sense, LegoSDN provides a pre-emptive mechanism - isolating potentially malicious apps from the network before they are able to cause damage. In comparison to FortNOX and Rosemary, LegoSDN does not provide a thorough enough mitigation against attacks. A parallel implementation of LegoSDN and FortNOX may be more appropriate, providing a type of first line and second line defence, respectively.

OperationCheckpoint is introduced in [10] as an SDN application control system, taking into account both the information that an SDN application reads from the underlying network, and the rules and policies it pushes out to data-paths in the network. OperationCheckpoint employs a thorough set of user-defined permissions, covering all OpenFlow related tasks. Each application that then needs to be used will be mapped to a specific subset of these permissions. Applications will then be unable to perform any actions that lie outside the set of permissions it has been mapped to (unless a change is authorised by administrators/operators) [10]. This effectively stops applications created by malicious adversaries from capturing sensitive data or executing malicious commands in the data plane, because these actions need to be declared first. By enforcing this declaration of necessary functionality, it allows network operators to build bespoke permission sets and ensure they know precisely how each application is behaving.

OperationCheckpoint seems to be the most thorough method of protecting an SDN infrastructure from malicious applications. In comparison to other solutions, it seems to perform better due to the simplistic nature of its permissions

system. This is in contrast to certain solutions such as Rosemary, which in terms of its performance is lacking due to the fact that every application is ran in its own environment. This has the tendency to incur high levels of overhead. One feature of SDN is the fact that there are a set of common APIs that can be used at the northbound interface between applications and the controller. This is advantageous in the sense that it removes the possibility of cross platform vulnerabilities arising through poor configuration/coding of middleware.

D. Control Plane and Data Plane Link Attack Mitigations

The link between the control plane and data plane carries transmissions of flow-entries down to the data plane for devices to add to their local cache [28]. The specification for OpenFlow, the most widely used and supported protocol for SDN operations [2], specifies an optional implementation of Transport Layer Security (TLS) for this link, however as this is optional, many of the available controller APIs don't enforce or support this option. For this connection to be completely secure, controller specifications would need to enforce this usage of TLS - providing secure encrypted transmissions and the authentication of entities at each end of the link.

In addition to this, IDS style systems could be implemented to thwart man-in-the-middle and black-hole type attacks occurring on this particular link. The authors in [30] present a methodology in which the Bro IDS system is integrated with a Ryu-based Python controller. On reception of a packet the IDS utilises deep packet inspection techniques to inspect the packet and determine its source, destination, payload among other things. Acting as a signature based IDS, bad-traffic and malicious activities are pre-configured into the controller, and unknown packets are then checked against these signatures to identify the presence of malicious packets [30]. Evaluative tests carried out in [30] suggest that the response times of this mechanism are quite slow. This is due to the additional load incurred on the controller from integration of the IDS system.

Due to the fact that the majority of attacks that take place within this link are variations on the traditional man-in-the-middle and black-hole attacks, it may be possible to protect the Control-Data plane link via traditional means. That is not to say that this would be a thorough solution. As explored above, employing an IDS system to identify potentially malicious nodes forwarding messages across this link would ensure that falsified messages are not forwarded between data-paths and controllers, confidential data is not extracted, and that availability is not compromised by means of a black-hole attack.

E. Eavesdropping Attack Mitigations

Defending against eavesdropping in any environment can be a particularly difficult task. This is due to the passive nature of the attack; attackers can simply establish themselves as a node in the network and activate a listening mode. This enables them to view the stream of packets that traverses them. Since eavesdropping nodes will often appear to have similar behavioural characteristics to legitimate clients, it can be difficult to detect them. In an SDN environment, this difficulty is exacerbated with the introduction of new attack platforms stemming from the centralised nature. An example of this

would be the control-data plane link and the control-application plane link.

A passive approach to defending against eavesdropping in the data plane and the control-data plane link is presented in [26] as Random Route Mutation. Its premise lies in randomly changing the course of packet flow, such that the destination IP stays the same. By changing this flow it aims to obfuscate the packet traces collected by adversarial clients. Such a method has been implemented in traditional network settings with moderate success. Authors in [26] claim that simulation results prove the RRM mechanism to be both efficient and effective in reducing the number of successfully eavesdropped packets. The approach has also been implemented in a NOX controller, suggesting that it is applicable to SDN environments as well. One particular downfall of this approach is it does not consider the intelligence of the adversaries it attempts to defend against. Whilst the technique may instantly see considerable reduction in the amount of eavesdropped packets, should adversaries learn of the algorithms utilized for randomizing packet flows, they may be able to reverse the affects by applying the reverse algorithm to their packet captures. Whilst this passive approach provides some mitigation, it is clear that its effect is limited and a more thorough solution would be necessary should SDN see widespread usage in production settings.

In [15], Combat-Sniff is introduced. Combat-Sniff implements both an active-detection mechanism which actively scans for eavesdropping nodes, and a pro-active defense method which aims to prevent malicious adversaries from being able to sniff packets in the first place. An attacker is able

to force a switch into storing an illegitimate flow entry in its cache that forwards all packets to itself. Combat-Sniff combats this by taking random samples of the flow entries installed in each of the switches tables and checking their integrity [15]. Should a flow be identified as illegitimate, the appropriate port on the switch is shut down and packets are no longer transmitted through it. Combat-Sniff also aims to retain the confidentiality of information on packets travelling through a switch by ensuring that the switch is partially blind. This means that the switch is intelligent enough to know how to forward the packet, but is unaware of the packets contents. Whilst, in premise, this solution seems technically sound, and evaluative tests prove it to be a reasonable performer with a fair level of effectiveness, it would be important to ensure that the weight of the random flow-entry sampling is ample enough to ensure illegitimate flows are identified.

It appears that eavesdropping is generally a very difficult attack to defend against, with not many solutions existing solely to defend against it. Intrusion Detection Systems and Intrusion Protection Systems can potentially be configured to detect eavesdropping nodes, however the passive nature of the attack makes it inherently difficult to detect. It appears that the two existent solutions ([26], [15]) are both more geared towards reducing the damage of any eavesdropping attacks. A more effective solution would attempt to prevent any sort of eavesdropping taking place. This could be achieved by employing some strong encryption method, and giving only authenticated data-paths and controllers the correct key to unencrypt packets.

TABLE II. SUMMARY OF ATTACK MITIGATION

Targeted Attack	Affected Security Aspects	Proposed Solution	SDN Layer				
			Data	Control-Data link	Control	Control-App link	Application
DoS/DDoS	Availability	AVANT-GUARD [16]			x		
		CPRcovery [17]			x		
		FlowRanger [18]			x		
		VAVE [20]	x				
		Entropy-based detection [22]	x		x		
Hijacked/Rogue Controller	Availability, Confidentiality, Integrity	Byzantine Fault Tolerance [9]			x		
		Trust Management System [23]	x		x		
		AuthFlow [25]		x	x	x	x
		PERM-GUARD [27]	x		x		x
Malicious Applications	Confidentiality, Integrity	FortNOX [21]		x	x	x	x
		Rosemary [28]			x		x
		LegoSDN [29]			x	x	x
		OperationCheckpoint [10]			x	x	x
Control-Data Link Plane Attacks (MITM, Black-hole)	Availability, Confidentiality, Integrity	BroIDS [2]	x	x	x	x	x
Eavesdropping	Confidentiality	Random Route Mutation	x	x			
		Combat-Sniff [26]	x	x			

REFERENCES

F. Summarising solutions

Each of the attack solutions explored above have been evaluated in terms of their strengths and weaknesses. Solutions have been comparatively analysed in order to identify the gaps that are yet to be filled in terms of SDN security. In order to summarise the evaluative exercise above, a table has been produced, showing each of the solutions, the attack type they aim to defend against, the logical SDN layer they operate at and the security aspects they aim to maintain (table 2).

IV. DISCUSSION AND CONCLUSION

SDN is a promising platform which has been extensively used in research settings due to its highly configurable nature, allowing researchers and experimenters to create bespoke forwarding rules in their environments. It is yet to have made much of an impact in large-scale production settings, due to inherent security issues introduced through the separation of the control and data planes. This paper explored a number of key threats unique to the SDN platform and discusses for each a number of mitigations that have been proposed. It appears that currently one of the weaker areas of SDN security is the link between the application layer, and the network that lies underneath it. Ensuring that this is secure is vital – not only does this link carry sensitive information about the network state, but in production settings, it could potentially carry sensitive client data. By developing robust application frameworks, it would help for a standardised method of developing and deploying applications. This reduces the chance for poor configuration/development and makes it easier to create generic security applications which can be applied to a large majority of SDN deployments.

A general theme which can be observed from the suggested solutions is that they aim to defend against just one particular type of attack, and do not provide overall protection in the network setting. To ensure a secure software-defined network, parallel implementation of combinations of the proposed schemes would have to be considered. This could achieve larger amounts of computational overhead and creates chances of conflicting configurations. These issues lead to the possible introduction of further vulnerabilities to the environment and the chance of false positives when scanning the network for attacks. To provide more thorough and well-rounded security the integration of an intrusion detection system in the controller of the network which identifies and prevents attacks based on pre-defined attack signatures could be implemented. The fact that traffic data is collected in the data plane and passed onto the controller for analysis provides a natural environment to implement IDS. It is clear, however, that with adding security mechanisms such as IDS to the controller, more overhead will be generated and performance of the network in terms of its throughput and the latency achieved could be negatively affected. To improve security in SDN infrastructures, it would be important to find a balance in the trade-off between security and performance by implementing a thorough, network-wide security regime whilst achieving desirable levels of performance. Before implementation of SDN can become wide spread this would need to be researched and developed further.

- [1] N. Feamster, J. Rexford and E. Zegura, "The Road to SDN: An Intellectual History of Programmable Networks", ACM SIGCOMM Computer Communication Review, vol. 44, no. 2, pp. 87-98, 2014.
- [2] S. Scott-Hayward, G. O'Callaghan and S. Sezer, "SDN Security: A Survey" in "Future Networks and Services", November 2013.
- [3] M. Dabbagh, B. Hamdaoui, M. Guizani and A. Rayes, 'Software-defined networking security: pros and cons', IEEE Communications Magazine, vol. 53, no. 6, pp. 73-79, 2015.
- [4] I. Ahmad, S. Namal, M. Ylianttila and A. Gurtov, 'Security in Software Defined Networks: A Survey', Communications Surveys & Tutorials, 2015.
- [5] D. Kreutz, F. Ramos, P. Esteves Verissimo and C. Esteve Rothenberg, 'Software-Defined Networking: A Comprehensive Survey', Proceedings of the IEEE, vol. 103, no. 1, pp. 14-76, 2015.
- [6] Z. Hu, M. Wang, X. Yan, Y. Yin and Z. Luo, 'A Comprehensive Security Architecture for SDN', 18th International Conference on Intelligence in Next Generation Networks, pp. 30-37, 2015.
- [7] L. Schehlmann, S. Abt and H. Baier, 'Blessing or curse? Revisiting security aspects of Software-Defined Networking', International Conference on Network and Service Management (CNSM), pp. 382-387, 2014.
- [8] D. Kreutz, F. M. Ramos, and P. Verissimo, "Towards Secure and Dependable Software-Defined Networks," in Proceedings of the Second ACM SIGCOMM Workshop on Hot Topics in Software Defined Networking, ser. HotSDN '13. ACM, August 2013, pp. 55–60.
- [9] H. Li, P. Li, S. Guo, and S. Yu, "Byzantine-resilient secure software-defined networks with multiple controllers," in Communications (ICC), 2014 IEEE International Conference on. IEEE, 2014, pp. 695–700.
- [10] S. Scott-Hayward, C. Kane, and S. Sezer, "OperationCheckpoint: SDN Application Control," in 22nd IEEE International Conference on Network Protocols (ICNP). IEEE, 2014, pp. 618–623.
- [11] J. Hizver, 'Taxonomic Modelling of Security Threats in Software Defined Networking', BlackHat Conference, pp. 1-16, 2015.
- [12] S. Sezer, S. Scott-Hayward, P. Chouhan, B. Fraser, D. Lake, J. Finnegan, N. Viljoen, M. Miller, and N. Rao, "Are we ready for SDN? Implementation challenges for software-defined networks," Communications Magazine, IEEE, vol. 51, no. 7, 2013
- [13] E. de la Hoz, R. Paez-Reyes, G. Cochrane, I. Marsa-Maestre, J. Moreira Lemus and B. Alarcos, "Detecting and Defeating Advanced Man-In-The-Middle Attacks against TLS", International Conference on Cyber Conflict, pp. 209-221, 2014.
- [14] H. Dai, Q. Wang, D. Li and R. Chi-Wing Wong, "On Eavesdropping Attacks in Wireless Sensor Networks with Directional Antennas", International Journal of Distributed Sensor Networks, pp. 1-13
- [15] F. Jiang, C. Song, H. Xun and Z. Xu, "Combat-Sniff: A Comprehensive Countermeasure to Resist Data Plane Eavesdropping in Software-Defined Networks", American Journal of Networks and Communications, vol. 5, no. 2, pp. 27-34, 2016.
- [16] S. Shin, V. Yegneswaran, P. Porras, and G. Gu, "AVANT-GUARD: scalable and vigilant switch flow management in software-defined networks," in Proceedings of the 2013 ACM SIGSAC conference on Computer & Communications Security. ACM, 2013, pp. 413–424.
- [17] P. Fonseca, R. Bennessby, E. Mota, and A. Passito, "A replication component for resilient OpenFlow-based networking," in Network Operations and Management Symposium (NOMS), 2012 IEEE. IEEE, 2012, pp. 933–939.
- [18] L. Wei and C. Fung, "FlowRanger: A Request Prioritizing Algorithm for Controller DoS Attacks in Software Defined Networks", Next Generation Networking Symposium, pp. 5254-5259, 2015.
- [19] N. Dao, J. Park, M. Park and S. Cho, "A feasible method to combat against DDoS attack in SDN Network", International Conference on Information Networking, pp. 309-311, 2015.
- [20] G. Yao, J. Bi, and P. Xiao, "Source address validation solution with OpenFlow/NOX architecture," in 19th IEEE International Conference on Network Protocols (ICNP). IEEE, 2011, pp. 7–12.

- [21] P. Porras, S. Shin, V. Yegneswaran, M. Fong, M. Tyson, and G. Gu, "A security enforcement kernel for OpenFlow networks," in Proceedings of the first workshop on Hot topics in software defined networks. ACM, 2012, pp. 121–126.
- [22] S. Mousavi and M. St-Hilaire, "Early Detection of DDoS Attacks against SDN Controllers", International Conference on Computing, Networking and Communications, pp. 77-81, 2015.
- [23] O. O. MM and K. Okamura, "Securing Distributed Control of Software Defined Networks," in International Journal of Computer Science & Network Security, vol. 13, no. 9, 2013.
- [24] O. M. Othman and K. Okamura, "Hybrid Control Model for Flow-Based Networks," in the international conference COMPSAC 2013 - The First IEEE International Workshop on Future Internet Technologies, Kyoto, Japan, 2013.
- [25] D. M. F. Mattos, L. H. G. Ferraz, and O. C. M. B. Duarte, "AuthFlow: Authentication and Access Control Mechanism for Software Defined Networking," pp. 1-7.
- [26] Q. Duan, E. Al-Shaer and H. Jafarian, "Efficient Random Route Mutation considering flow and network constraints", Conference on Communications and Network Security (CNS), pp. 260-268, 2013.
- [27] M. Wang, J. Liu, J. Chen, X. Liu and J. Mao, "PERM-GUARD: Authenticating the Validity of Flow Rules in Software Defined Networking", International Conference on Cyber Security and Cloud Computing, pp. 127-133, 2015.
- [28] S. Shin, Y. Song, T. Lee, S. Lee, J. Chung, P. Porras, V. Yegneswaran, J. Noh, and B. B. Kang, "Rosemary: A Robust, Secure, and HighPerformance Network Operating System," in Proceedings of the 2014 ACM SIGSAC Conference on Computer and Communications Security. ACM, 2014, pp. 78–89.
- [29] B. Chandrasekaran and T. Benson, "Tolerating SDN application failures with LegoSDN," in Proceedings of the 13th ACM Workshop on Hot Topics in Networks. ACM, 2014, p. 22.
- [30] P. Zanna, B. O'Neill, P. Radcliffe, S. Hosseini and S. Ul Hoque, 'Adaptive threat management through the integration of IDS into Software Defined Networks', 2014 International Conference and Workshop on the Network of the Future, pp. 1-5, 2014.

Optimized Voting Scheme for Efficient Vanishing Point Detection in General Road Images

Vipul H.Mistry

Ph.D. student, Electronics & Communication Engineering
Department,
Uka Tarsadia University, Surat, India

Ramji Makwana

Professor & Head, Department of Information Technology,
V.V.P. Engineering College,
Rajkot, India

Abstract—Next generation automobile industries are aiming for development of vision-based driver assistance system and driver-less vehicle system. In the context of this application, a major challenge lies in the identification of efficient road region segmentation from captured image frames. Recent research work suggests that use of a global feature like vanishing point makes the road detection algorithm more robust and general for all types of roads. The goal of this research work is the reduction of computational complexity involved with voting process for identification of vanishing point. This paper presents an efficient and optimized voter selection strategy to identify vanishing point in general road images. The major outcome of this algorithm is the reduction in computational complexity as well as improvement in efficiency of vanishing point detection algorithm for all types of road images. The key attributes of the methodology are dominant orientation selection, voter selection based on voter location and modified voting scheme, combining dominant orientation and distance based soft voting process. Results of a number of qualitative and quantitative experiments clearly demonstrate the efficiency of proposed algorithm.

Keywords—Road Detection; Vanishing Point; Gabor Filter; voting scheme; general road segmentation

I. INTRODUCTION

Vision-based autonomous navigation is the future of automobile industry. Some companies have already incorporated features like driver assistance system based on GPS and various sensors. The future of this advancement is vision based driverless vehicle car. One of the major constraint in the development vision based driverless car is the efficient detection of road area. With advancements in proximity sensors, it is possible to detect roads but still vision based approach is one which can enhance the usefulness of the system to a great extent. With proximity sensors, one cannot understand nearby environment and recognize various properties of the surface on which vehicle is moving. The only solution is a vision based approach where a car can recognize the road surface with the help of the camera mounted on it. This camera will work like the human eye and provide the scene information regarding images. The task is now reduced to understand this 2-D image and extract information required as per various applications. In last decade researchers have done considerable work in this area and suggested some good approaches for identification of road surface from a given image. These approaches mainly focus on extraction of features that can help to distinguish between the road and off-road regions.

All road segmentation algorithms are mainly classified into two categories: region properties based approaches [1-7] and boundary based approaches [8-11]. Various road types i.e. structured, unstructured, rural roads and highways along with various surrounding environments and day light conditions make the task more challenging for both previously suggested methods. The solution is a use of vanishing point. The vanishing point of an image provides a strong cue for road identification and makes the algorithm general for all types of roads with various surrounding environments. The goal of this research paper is to suggest optimized voter selection strategy based voting process that will reduce the computational complexity of existing vanishing point detection algorithm and enhance the accuracy of the same. Rest of the paper is organized as follows: Section II highlights major contributions by various researchers in vanishing point detection and draws concluding remarks to motivate further scope of research work. Section III describes proposed optimum voter selection strategy. Section IV describes modified voting process for vanishing point detection. Section V demonstrates the efficiency and effectiveness of the algorithm based on various qualitative and quantitative experiments.

II. LITERATURE SURVEY

To overcome the challenges introduced by semi-structured and unstructured roads, the concept of vanishing point detection came into existence. The majority of vanishing point detection methods rely on line segments in the image. The task of detecting those vanishing points, which correspond to the dominant directions of a scene, is traditionally solved in two steps. Firstly, line segments are clustered together and then vanishing point is selected under the condition that a cluster of line segments share a common vanishing point. A different approach for reducing the computational complexity of the accumulation step is to apply the Hough transformation, by mapping the parameters of the line segments into a bounded Hough space [9, 11]. Tuytelaars *et al.* [11] applied the Hough transformation three times (Cascade Hough transformation). At different levels of the Cascade Hough transformation a peak in the Hough space corresponds to a vanishing point and a vanishing line respectively.

Rasmussen *et al.* [14-15] replaced edge detection step with dominant orientation identification using texture properties. This method greatly influenced the research work towards identification of vanishing point estimation. Most of the existing vanishing point detection methods rely on three

steps: extraction of dominant orientations, identification of any line segments in the image and voting procedure for vanishing point estimation [14-17]. To achieve precise orientation estimation, one needs to apply a large number of orientation filters in all possible directions from 0° to 180°. Designing and applying a bank of differently rotated filters is computationally expensive. To address this problem Freeman and Adelson [13] proposed a steerable filter in which each arbitrarily oriented filter can be formed by a linear combination of a fixed set of basis-oriented filters. But it still requires steering the basis-oriented filters in all directions with a precision of 1°. In 2010, Hui Kong *et. al.* [17] came up with a general road detection method from a single image using Vanishing point detection approach. He suggested 36 orientations Gabor Filters for extraction of orientation information at each edge pixel. Distance based soft voting procedure suggested in this paper also made the detection process more robust and increased the efficiency in vanishing point detection.

In 2012, Peyman Moghadam *et. al.* [18] proposed a novel methodology based on image texture analysis for the fast estimation of the vanishing point detection in the challenging environments. The key attributes of the methodology consist of the optimal local dominant orientation method that uses joint activity of four Gabor filters followed by an efficient and robust voting scheme for real-time detection of the vanishing point. Estimation of vanishing point greatly enhances the robustness and effectiveness of road detection for all type of roads, irrespective to structured roads with lane markings, semi- structured roads without lane markings and unstructured roads with improper road regions. Combining the efficiency of edge-based methods and the orientation coherence concept of texture-based methods Xin Lu [20] proposed a more efficient method for vanishing point detection in 2012. In 2014, Cheng Xu *et. al.* [21] introduced a concept of dominant road orientation based voting in place of soft voting methods used by Hui Kong *et. al.* [16-17] and Peyman Moghadam *et al* [18].

The accuracy of vanishing point detection methods discussed so far mainly depends on three parameters: efficiency of orientation extraction, effective voter selection and candidate selection for vanishing point to be used during voting process. The motivation of this research work is to suggest an optimum method for voter selection and use of only most effective voters during the voting process. This will enhance the speed of the algorithm, and it will also increase the efficiency of the existing algorithm. Major contributions of this research paper are listed as follows:

- Optimum voter selection based on dominant orientations of an image.
- Removal of outliers based on edge map and horizon line detection.
- Strategy for voter selection and candidate vanishing point selection.
- Modified locally adaptive soft voting scheme with dominant orientation information.

Next section describes the fundamental steps for vanishing point detection and also highlights the ways to make the algorithm more efficient and fast.

III. PROPOSED OPTIMUM VANISHING POINT AND VOTER CANDIDATE SELECTION

The vanishing point plays an important role as a global constraint for detecting road direction, since all parallel border road lines and road edges converge into a single vanishing point [14]. The basic steps for vanishing point detection are orientation extraction, selection of candidate pixels as vanishing point candidates and voting process.

A. Selection of Dominant Orientations

In this paper, 36 Gabor orientation Filters are used to extract orientation information at each pixel. A Gabor filter can be viewed as a sinusoidal plane of particular frequency and orientation, modulated by a Gaussian envelope. The kernels of the Gabor filters are similar to the 2-D receptive field profiles of the mammalian cortical simple cells and exhibit desirable characteristics of spatial locality and orientation selectivity. For an orientation of ϕ and a scale ω , the Gabor wavelets are defined by [19].

$$\psi_{\omega,\phi}(x,y) = \frac{\omega}{\sqrt{2\pi c}} e^{-\omega^2(4a^2+b^2)/(8c^2)} (e^{ia\omega} - e^{-c^2/2}) \quad (1)$$

Where, $a = x \cos \phi + y \sin \phi$, $b = -x \sin \phi + y \cos \phi$, $c = 2.2$

$$\omega = \omega_0 \times 2^k, \omega_0 = 2.1, k = 0, 1, 2, 3, 4 \dots \quad (2)$$

To best characterize local texture properties including step and roof edge elements at an image pixel $I(x, y)$, we examine the standard “complex response” of the Gabor filter given by equation 3 for n evenly spaced Gabor filter orientations.

$$I_{\text{complex}}(x,y) = (\text{godd} * I)(x,y)^2 + (\text{geven} * I)(x,y)^2 \quad (3)$$

The response image for an orientation is defined as the average of the responses at the different scales. The dominant orientation is selected as the filter orientation which elicits the maximum complex response at that location.

The orientations of road texture pixels are consistence in nature. Considering the fact that road region in a given image frame consists of more than 50% of the image area, there will be very few orientations which are consistence in the nature and they can provide a very useful cue for effective voter selection. For the selection of the dominant orientations we calculate normalized histogram of orientations and consider only those orientations whose normalized score is more than or equal to a threshold value of $\text{Th}_{\text{orient}} \geq 0.6$. Figure 1 shows a normalized histogram of orientations for road image. In our experiment, we discard all the pixels whose orientations are other than selected dominant orientations. The optimal value of $\text{Th}_{\text{orient}}$ is selected by tuning on our test image set, where $\text{Th}_{\text{orient}}=0.6$ gives maximum detection accuracy of a vanishing point.

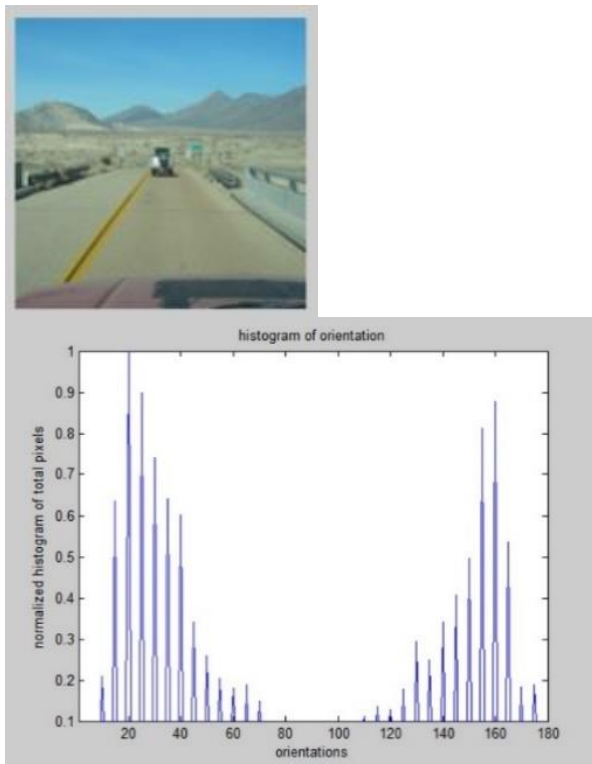


Fig. 1. Normalized Histogram of Orientation for given Road Image

Figure 2 demonstrates the accuracy of the vanishing point over different Th_{orient} values. Here accurate vanishing point means the results for which Euclidean distance between

detected vanishing point and manually selected ground truth vanishing point is less than or equal to 10 pixels.

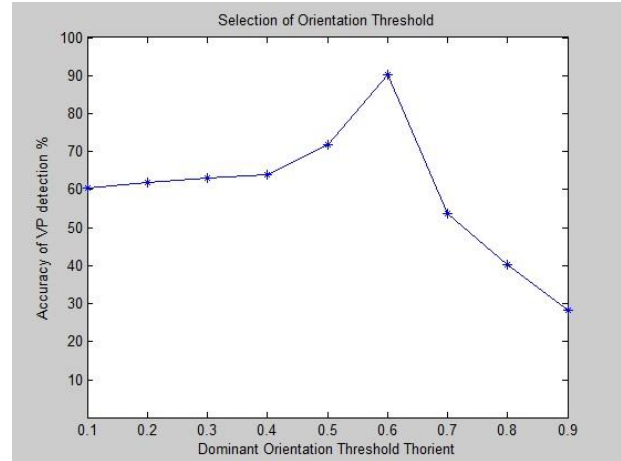


Fig. 2. Effect of Th_{orient} on accuracy of Vanishing Point Detection

B. Selection of Candidate Pixels for Voting Process

Accuracy and speed of a vanishing point detection process depend on no of effective voters and total no of pixels used for the voting process. Figure 3 demonstrates proposed voter selection strategy.

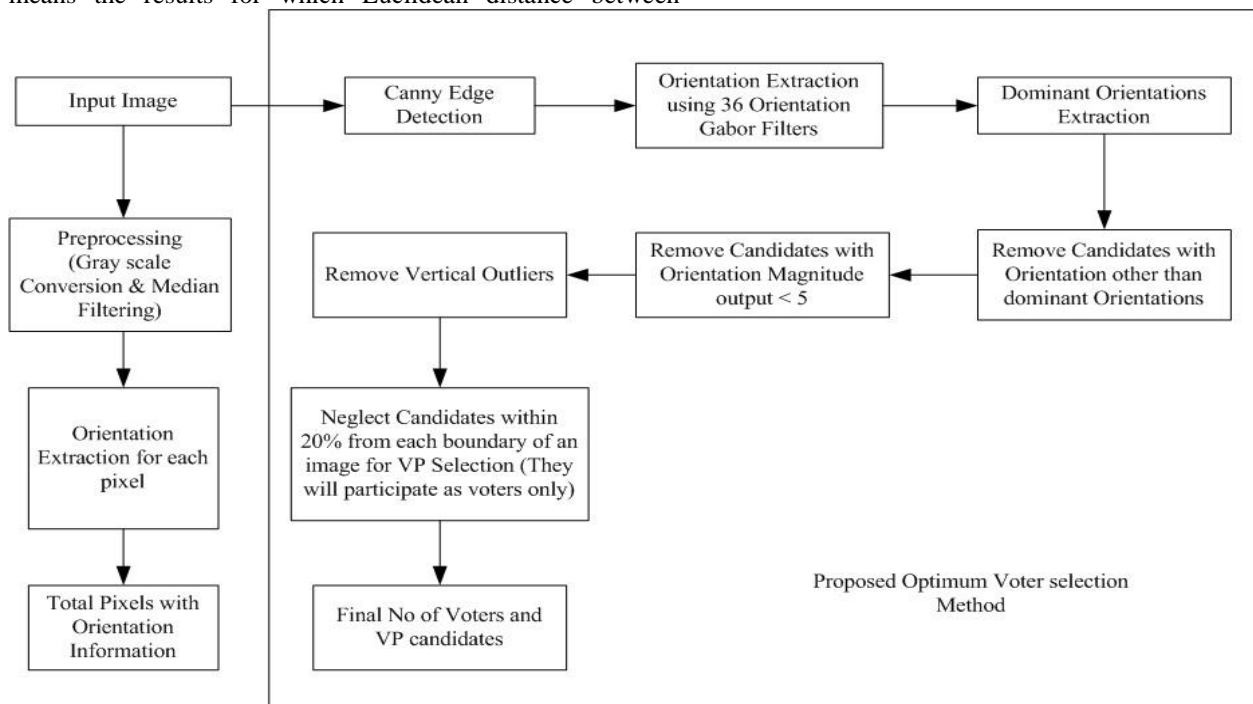


Fig. 3. Proposed Optimum Voter and Candidate Vanishing Point Selection Strategy

In proposed approach, candidate pixels are selected based on following steps:

Step I: Candidate should be an edge pixel.

Step II: Orientation of candidate pixel should be one of the dominant orientations.

Step III: Insufficient number of voters in road images, where vanishing point is lying in bottom part of an image and major portion of an image contains sky regions, an accuracy of vanishing point decreases.

1) To address this problem we propose to identify horizon line in an image. First, the sobel horizontal filter is used to get the horizontal edge points in an image.

2) Scan all the rows from the top of an edge image and calculate a total number of horizontal edge pixels in the same row.

3) The Row which contains maximum no of edge points is selected as horizon line.

Step IV: Selection of Edge Pixels within 25% from the Horizon Line.

1) Edge pixels above horizon line effectively do not play many roles in efficient selection of vanishing point. That's why removal of all the pixels lying within 25% portion of image from top to horizon line will not affect much on overall detection accuracy.

Step V: Removal of Outliers based on Orientation Confidence Score.

1) The confidence value is normalized magnitude response of Gabor filter with dominant orientation out of 36 orientations at that pixel.

2) Remove all outliers whose orientation confidence value is less than 2% of maximum confidence value.

Step VI: Removal of Vertical Outlier.

1) Pixels which belongs to vertical structures around the road like trees lead to the wrong erroneous detection of the vanishing point.

2) Remove pixels with orientation 90 degree in vertical length of 25% of image height are more than 20 then those pixels are considered as off road pixels due to surrounding vertical structures.

Step VII: Modification in voting area as well as Vanishing point Candidates Selection Strategy.

1) Pixels which belongs to the road surface or near road boundaries play a pivot role in true vanishing point detection. We propose to select vanishing point from selected candidates only.

2) Figure 4 shows the eligibility criteria for voter and vanishing point candidate based on location. Considering the

region of interest, we neglect all the candidate pixels which belong to 20% of the portion from either side of the image.

3) As shown in figure 4, only those pixels are eligible vanishing candidates who belongs to the white portion of an image.

4) A Similar strategy is adopted for voter selection. Rather than considering semicircular region for voter selection as proposed in [17], we allow those pixels to vote which are within rectangle region of 25% of image height and 40% of image width from vanishing point candidate, as shown by a yellow portion in figure 4 which is overlapped on white image portion.

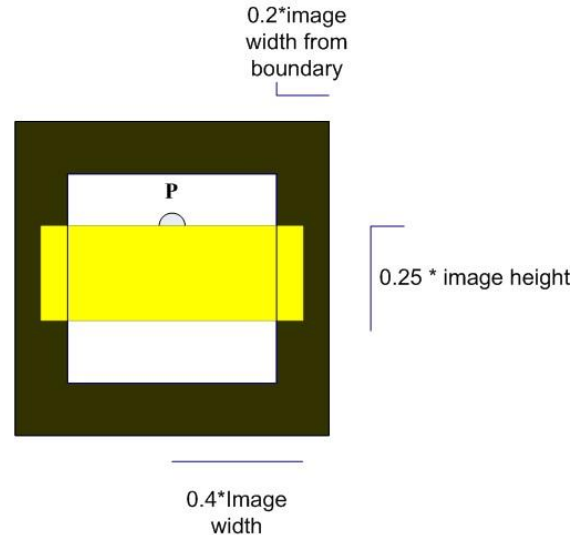


Fig. 4. Voter and Vanishing Point eligibility based on Location

As shown in figure 4 for a pixel P to be valid vanishing point candidate it has to be within an inner white square region, eliminating all candidates within 20% of the portion from image boundaries. Voter pixel can vote for pixel P if it is within the yellow rectangle. The goal of the modifying voting area is to allow maximum pixels below candidate pixel from the road surface and near road boundaries to vote for vanishing point. Remaining pixels after all above mentioned steps are considered as eligible candidates for vanishing point voting process.

Figure 5 demonstrates the selection of effective voters which will take part during the voting process.

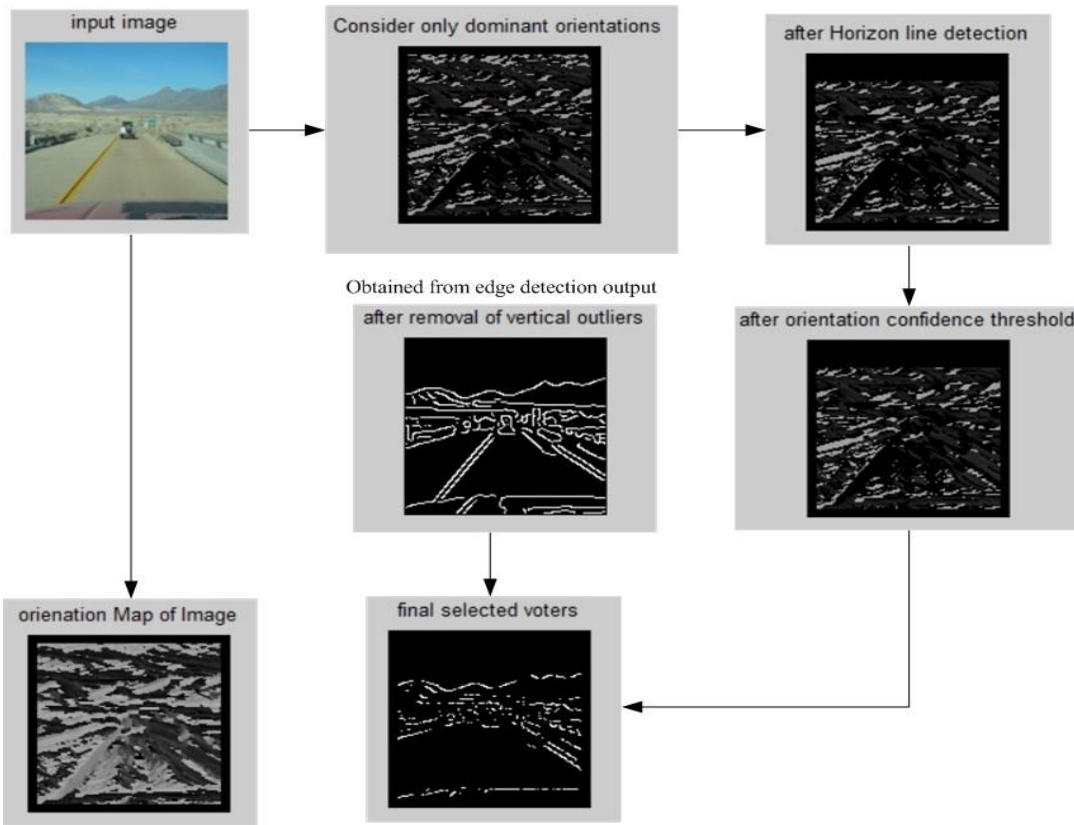


Fig. 5. Optimized Selected Voter and Candidate Pixels used for Voting Process

IV. MODIFIED VOTING PROCESS

The voting procedure is most important and critical stage of vanishing point estimation problem. Once we have computed the texture orientation at each pixel of the image, one can make these pixels vote to obtain the vanishing point. Precisely, a pixel P for which the texture orientation is the vector \vec{P} can vote for all the pixels V above P such that the angle $\gamma = \angle((PV), \vec{P}) < 5^\circ$ between the direction (PV) . Here 5° is the angle between two consecutive Gabor orientation filters used to extract orientations in an image. This type of voting process is referred as hard voting scheme. The only problem with this scheme is, it tends to favor points that are located in the upper portion in the image. The said problem was overcome by distance based soft voting scheme proposed by Hui Kong et al. [16-17]. Equation 4 demonstrates the voting score calculation using distance based soft voting process [16].

$$\text{Vote}(P, V) = \begin{cases} \frac{1}{1 + [\gamma d(P, V)]^2}; & \text{if } \gamma \leq \frac{1}{1 + 2d(P, V)} \\ 0; & \text{otherwise} \end{cases} \quad (4)$$

In distance based soft voting process the major drawback is pixels in line with road direction but having angle $\gamma > 5$ degrees are omitted from voting score calculation process which may lead to an incorrect vanishing point. In our experiments, we propose to use equation 5 for voting score calculation.

$$\text{Vote}(P, V) = e^{\left(\frac{-d(P, V) * (\gamma - \text{DominantOrientation})}{\text{DiagonalDistance}}\right)} \quad (5)$$

Where,

DominantOrientation = dominant orientation with which orientation of pixel voter orientation matches.

DiagonalDistance = Diagonal distance of image

The key advantages of modified equation are:

- We allow all pixels to vote whose orientation is consistent with dominant orientations. The basic idea behind proposed modification is to remove all the voters whose orientations are not consistent with dominant orientations. This will increase the efficiency of the voting process as voters for which $\gamma > 5$ degrees but their orientation is consistent with dominant orientation can take part in the voting process. All erroneous voters for which $\gamma < 5$ but their orientations are not consistent with dominant orientations are neglected from voting process.
- DominantOrientation will act as a weighting parameter for voting score. If voter's orientation is one of the dominant orientation but angle $\gamma > 5$ degrees, then voting score will be weighted by a value of γ . This will further enhance the effectiveness of orientation based soft voting process.

V. RESULT AND ANALYSIS

Vanishing point detection algorithm is tested on standard image dataset consists of structured, semi-structured and unstructured images used by researchers in [22]. The dataset consists of images with varying intensity variations, color and texture variations and surrounding environment variations. Some image samples are shown in figure 6. All the images are resized to 128x128.

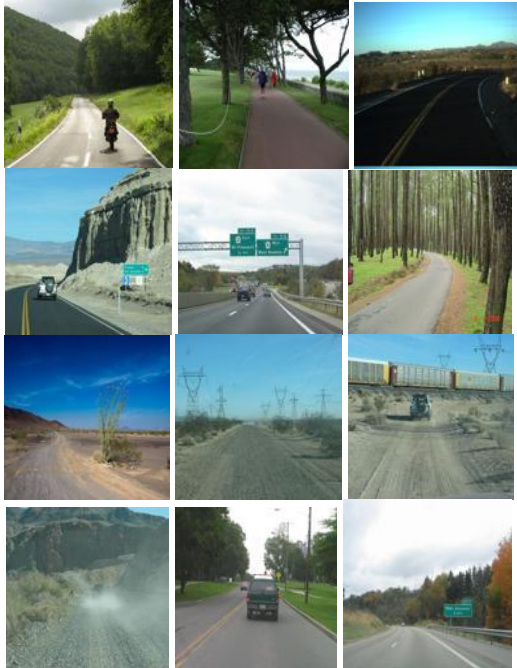


Fig. 6. Sample images from Image Database (128x 128 size)

To demonstrate the performance of proposed algorithm we generated five sets of the dataset with manually marked vanishing point by five different persons. The median filter is used to find out the final ground truth location by finding median in x and y coordinates of all marked vanishing points by different users. Figure 7 shows the results of detected vanishing point along with manually marked vanishing point as ground truth.



Fig. 7. Vanishing Point Detection results in yellow color with Ground Truth Positions marked with black color

Further to measure the error in vanishing point detection we have used a normalized Euclidean distance where a Euclidean distance between measured vanishing point and ground truth location is divided by the diagonal distance of the image [18].

$$NormError = \frac{||P-P0||}{D} \tag{6}$$

Where,

P = Detected location of vanishing point

P0=Ground Truth location of vanishing point

D= Diagonal distance of image

Euclidean Distance of more than 10 pixels is considered as invalid vanishing point detection in our experiments. Image database consists of images with different road types and surroundings. Figure 8 shows the distance between detected vanishing point and ground truth positions against all images used. Average distance comes out to be 5.96 pixels for all test images.

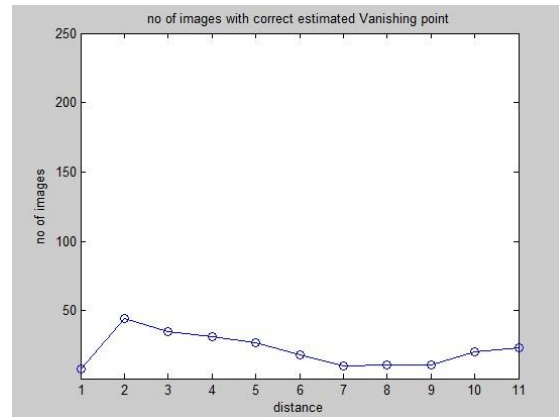


Fig. 8. Distance between detected Vanishing point and Ground Truth Position of Vanishing point for no of images

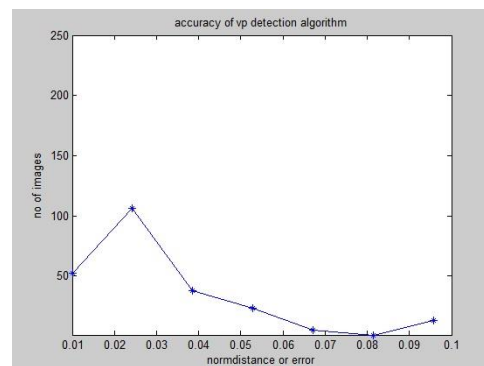


Fig. 9. Norm Distance Error for No of Images used in Experimentation

The efficiency of proposed algorithm is demonstrated in Figure 9. It shows the histogram of error in vanishing point detection against all test images. Distance error more than 0.06 is considered as the wrong detection of a vanishing point. Results are presented for 250 road images which include

structured, semi-structured and unstructured road types. Average NormError for the proposed method is 0.033. The accuracy of proposed system is compared with previously suggested methods. Table 1 illustrates the accuracy with modifications suggested in voter and vanishing point selection strategy as well as voting score calculation process.

TABLE I. QUANTITATIVE EVALUATION OF VANISHING POINT DETECTION ALGORITHM

VP Detection Results	Quantitative Evaluation Parameters		
	Average Euclidean Distance	Average Accuracy %	Average Norm Error
Proposed Method	5.964	90.33	0.033
Without horizon line Detection	7.2351	86.97	0.04
Without modification in Voting score calculation (use of only distance based soft voting)	7.34	82.77	0.0405

Quantitative comparison of proposed vanishing point detection algorithm with previously proposed methods for vanishing point detection based on Gabor filter orientation extraction is shown in table 2.

TABLE II. ACCURACY COMPARISON WITH PREVIOUSLY PROPOSED METHODS FOR VANISHING POINT DETECTION

	Edge-Based Method [12]	Rasmussen [15]	Kong et. al [17]	Peyman et. al[18]	Proposed Method with optimized voter selection strategy
Norm Error	0.171	0.0903	0.052	0.036	0.033

VI. CONCLUSION

Less computational cost and speed are the two major concerns in existing vanishing point detection algorithms [14-18, 20, 21]. Speed and computational cost of vanishing point detection algorithm mainly depend on total no of pixels used during voting process. If we can optimize the no of pixels and select only most efficient pixels during the voting process the performance can be improved. With this motivation, we presented an optimized strategy to select most effective candidates for the vanishing point detection process. Selection strategy of efficient voter depends on the efficient selection of dominant orientation and removal of outlier pixels which may lead to inaccurate results. Once efficient pixels are selected, second modification suggested here is location based eligible candidate selection for vanishing point and voter. Finally, the use of combined soft voting and dominant orientation based voting score calculation increases the accuracy of vanishing point detection. Error in vanishing point occurs when vanishing points are located in the bottom part of an image, and large portion of an image contains sky region. To overcome this problem we suggest a very simple and fast horizon line detection based outlier removal method to reject the outliers which may lead to inaccurate results. Furthermore, a series of qualitative and quantitative results are presented to

validate the accuracy of proposed algorithm. The proposed algorithm outperforms previously suggested methods regarding accuracy using only 2.36% of total image pixels i.e. average 360 pixels from 128x128 images.

REFERENCES

- [1] Y. He, H. Wang and B. Zhang, "Color-based road detection in urban traffic scene." IEEE Trans. Intell. Transp. Syst., Vol. 5(4), pp.309-318, 2004.
- [2] G. Finlayson, S. Hordley, C. Lu and M. Drew, "On the removal of shadows from images." IEEE Trans. Pattern Anal. Mach. Intell., Vol. 28, pp. 59-68, 2006.
- [3] C. Tan, T. Hong, T. Chang and M. Shneier, "Color model-based real-time learning for road following." Proc. IEEE Intell. Transp. Syst. The conference, pp. 939-944, 2006.
- [4] Tsung-Ying Sun, Shang-Jeng Tsai and Chan V, "HSI color model based lane-marking detection." Proc. Intelligent Transportation Systems Conference, pp. 1168-1172, September 2006.
- [5] D. Puig and M. A. Garcia, "Automatic Texture Feature Selection for Image Pixel Classification. Pattern Recognition." Vol. 39, pp.1996 - 2009, 2006.
- [6] D. Puig, M. A. Garcia and J. Melende, "Application- Independent Feature Selection for Texture Classification." Pattern Recognition, Vol. 43, pp. 3282-3297, 2010
- [7] Alvarez J. and López A. M. Road Detection Based on Illuminant Invariance. IEEE Trans. Intelligent Transportation Systems, Vol. 12, pp. 184-193, 2011.
- [8] K. H. Chen and W. H. Tsai, "Vision-Based Autonomous Land Vehicle Guidance in Outdoor Road Environments Using Combined Line and Road Following Techniques." Journal of Robotic Systems, Vol. 14(10), pp. 711-728, 1997.
- [9] B. Yu and A. K. Jain, "Lane boundary detection using a multiresolution Hough transform." Proc. IEEE Int. Conf. Image Processing, vol. 2, pp. 748-751, 1997.
- [10] Dezhi Gao, Wei Li, Jianmin Duan and Banggui Zheng, "A practical method of road detection for intelligent vehicle." Proc. IEEE International Conference on Automation and Logistics, pp. 980,985, 5-7 Aug. 2009.
- [11] Tuytelaars T., Van Gool L., Proesmans M. and Moons, T, "The cascaded Hough transform as an aid in aerial image interpretation." Proc. International Conference on Computer Vision, Vol. 4, pp. 67-72, Jan 1998.
- [12] Y.Wang, E. K. Teoh and D. Shen, "Lane detection and tracking using B-Snake." Image Vis. Comput., Vol 22(4), pp. 269-280, 2004.
- [13] W. T. Freeman and E. H. Adelson, " The design and use of steerable filters." IEEE Trans Pattern Anal. Mach. Intell. Vol. 13(9), pp. 891-906, 1991.
- [14] C. Rasmussen, "Grouping dominant orientations for ill-structured road following." Proc. IEEE Conf. Comput. Vis. Pattern Recog., pp. 470-477, 2004.
- [15] C. Rasmussen, "Texture-based vanishing point voting for road shape estimation." Proc. British Machine Vision Conf., 2004.
- [16] H. Kong, J.Y. Audibert and J. Ponce. Vanishing point detection for road detection. Proc. IEEE Conf. Computer Vision Pattern Recognition, 2009, 96-103.
- [17] H. Kong, J.Y. Audibert and J. Ponce, "General road detection from a single image." IEEE Trans. On Image Processing, Vol. 19(8), pp. 2211-2220, 2010.
- [18] Moghadam, P. Starzyk J.A. and Wijesoma W.S., "Fast Vanishing-Point Detection in Unstructured Environments." IEEE Trans. On Image Processing, Vol. 21(1), pp. 425-430, 2012.
- [19] T. Lee, "Image representation using 2d Gabor wavelets." IEEE Trans. Pattern Anal. Mach. Intell., Vol. 18(10), pp. 959-971, 1996.
- [20] Xiqun Lu, "A new efficient vanishing point detection from single image." Proc. ICASSP, pp. 901-904, 2012.
- [21] Cheng Xu, Youqi Cai, Zheng Tian, Tao Li and Yan Liu, "Principal Orientation and generalized vanishing point based road detection." Proc.

International Conference on Computer Science and Service System, pp.
394-397, 2014.

[22] http://web.mit.edu/huikong/www/Road_Detection_files/roadImgs_final.rar

Automated Simulation P2P Botnets Signature Detection by Rule-based Approach

Raihana Syahirah Abdullah

Faculty of Information and Communication Technology
Universiti Teknikal Malaysia Melaka (UTeM)
Hang Tuah Jaya, 76100 Durian Tunggal, Melaka

Faizal M.A.

Faculty of Information and Communication Technology
Universiti Teknikal Malaysia Melaka (UTeM)
Hang Tuah Jaya, 76100 Durian Tunggal, Melaka

Zul Azri Muhamad Noh

Faculty of Information and Communication Technology
Universiti Teknikal Malaysia Melaka (UTeM)
Hang Tuah Jaya, 76100 Durian Tunggal, Melaka

Nurulhuda Ahmad

Faculty of Engineering and Built Environment Universiti
Kebangsaan Malaysia (UKM)
43600 Bangi, Selangor

Abstract—Internet is a most salient services in communication. Thus, companies take this opportunity by putting critical resources online for effective business organization. This has given rise to activities of cyber criminals actuated by botnets. P2P networks had gained popularity through distributed applications such as file-sharing, web caching and network storage whereby it is not easy to guarantee that the file exchanged not the malicious in non-centralized authority of P2P networks. For this reason, these networks become the suitable venue for malicious software to spread. It is straightforward for attackers to target the vulnerable hosts in existing P2P networks as bot candidates and build their zombie army. They can be used to compromise a host and make it become a P2P bot. In order to detect these botnets, a complete flow analysis is necessary. In this paper, we proposed an automated P2P botnets through rule-based detection approach which currently focuses on P2P signature illumination. We consider both of synchronisation within a botnets and the malicious behaviour each bot exhibits at the host or network level to recognize the signature and activities in P2P botnets traffic. The rule-based approach have high detection accuracy and low false positive.

Keywords—Botnets; P2P Botnets; Signature; Rule-based

I. INTRODUCTION

The botnets population are rapidly growing and they become a huge threat on the Internet. Botnets has been declared as Advanced Malware (AM) and Advanced Persistent Threat (APT) listed attacks which able to manipulate advanced technology where the intricacy of threats need for continuous detection and protection as stated by [1] [2] [3]. These attack will be almost exclusively for financial gain as claimed by [4]. The chronology of botnets attack disclosed the evidence on the seriousness and sophisticated nature in the recent cyber-attack. The growth of Internet itself had reflected to the growth of incidents in security environment. The numerous of security incidents that occurred will cause major loss for the organizations. From a survey conducted by American Society for Industrial Security and Pricewaterhouse-Cooper, there was a loss of USD45 million for 1000 companies due to the security breach [5].

According to marketing networking group Chief Marketing Officer (CMO) Council, a data breach could cost an average of US Dollar14 million on a recovery cost [6]. A survey made by [7], Computer Security Institute (CSI), Computer Crime and Security reported that the lost due to security breach was US Dollar 288 by 618 per respondent. This shows a multiple costs also needed to clean up the botnets infections. Significantly, this research bridged important relationship with botnets technology as depicted in Figure 1 where early emergence of P2P botnets existence in year 2002 and rapidly growth until now with more robust, complicated and flexible P2P botnets. This fact has motivated research communities to do further research on P2P botnets issue.

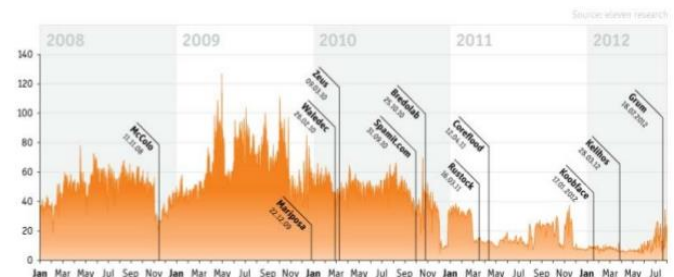


Fig. 1. Evolution of P2P Botnets Technology [8]

So, it was important to build a security mechanism which designed to prevent intrusion from hacker so that it can take action and improves the system security [9]. This research field is known as intrusion detection. Intrusion Detection System (IDS) is a system that continually monitors the dynamic behaviour of the computer system to warn against actions that compromise the integrity, security, and availability [10]. In the real environment practice, IDS focused on detecting known threats or detecting the volume of the traffic generated by bot host after it has been activated [11]. An important problem in the field of intrusion detection is the management alerts [12] as IDS tends to produce high number of false positive alerts as claimed by [13] [14] [15]. Most of the botnets has generating low-volume periodic communication to botmaster which increased false alarm rate and make it harder to be detected as mentioned by [11] [16].

The increment of the traffic volume can cause the IDS to produce large number of alarms as discussed by [17]. Reducing false alarms is a serious problem needs an attention in ensuring the IDS efficiency as mentioned by [14] [18].

As the botnets and advance malware evolve rapidly, the approaches and techniques for detecting botnets need to be improvised. Previous researchers have contributed lots of efforts and works to address the botnets issues. Most of the approaches have developed for detecting Internet Relay Chat (IRC)-based or Hypertext Transfer Protocol (HTTP)-based botnets. These approaches only operate at the network level that focused for traffic signatures on flow patterns [19]. Unfortunately, the detection approaches designed for IRC-based and HTTP-based botnets may become inefficient against the new P2P based botnets as it focused only on the specific protocol [1]. Basically, P2P botnets detector tool is also identified as intrusion detection tool. The exponential growth of P2P botnets and the new distribution channels available to cyber criminals identify that the need for good protection is crucial. So that, it would be feasible to detect P2P botnets through P2P traffic signatures and behaviors [20].

The rest of paper is organized as follows. In Section II, we provides details background on the signature-based detection concept. Section III will describes the methodology of overall process. Next, Section IV will elaborates details on detection module of our proposed P2P botnets automated rule-based detection. While, the results and discussion are also discuss in this section. At last, our paper is concluded in Section V.

II. BACKGROUND

Generally, signature-based is a supervised learning method where it develop the capability on detecting malicious behaviours on the basis of previously seen malicious events [21]. The signature-based detection modelled the known attack behaviour that learned from attack pattern [22]. By recognizing known attack methods, signature detection is able to recognize when the intrusive patterns occurred. As claimed by [23] during the process of inspection, when the suspicious behaviours partially corresponded with the records of intrusive knowledge base, it automatically can be judged as the intrusion.

The main selection of Java also because it can provides the IF-ELSE statement that referring to the basic of rule-based declaration in terms of generating the signature. All of these benefits are needed in developing the P2P botnets signature detection. Due to the P2P botnets detection have their own signatures and behaviours, therefore a NetBeans IDE version 7.4 are the best selection and option in order to implement the rule-based signature in this research. Generally, NetBeans is an open source and free software that address the needs of developers, users and businesses particularly to enable them to develop the products quickly, efficiently and easily by leveraging the strengths of Java platform [24]. This statement is fully supported by [25] where they were stated that the NetBeans platform provides a reliable and flexible modular architecture to application developers. Conveniently, it also helpful for develop Java desktop, mobile and web application. The strength of Netbeans's offered the best support for latest technologies, fast and smart coding, rapid user interface

development and rich set of community provided plugins. Previously, [25] declared the latest version of NetBeans IDE and platform certainly keeping the rhythm, introducing new high-impact features and revamping traditional functionality at full throttle.

Another concern of this paper is how to determine the P2P botnets. This paper highlights the need of analyzing the behaviors and parameters of botnets to determine the anomalous in P2P botnets. Through the prediction of P2P network traffic will define several behaviors and parameters that helped to distinguish between P2P normal and P2P botnets. Otherwise, proposed detection module for P2P botnets will help to solve the issue of limited detection technique in order to detect anomalous P2P botnets. The propose detection module for P2P botnets will improvise the network security. So, the details process flow for P2P botnets detection module will be discovered in next section.

III. METHODOLOGY

This section discusses in detail the process involved for the P2P botnets detection as depicted in Figure 2. The process started with input the data from raw of P2P botnet file. Then, the system will be do automated process by show the analysis result in short time. The unknown behavior or signature that has been detected will send to anomaly stage for further action.

Generally, signature-based is a supervised learning method in detecting the malicious behaviour on the basis of previously seen malicious events. The second stage of P2P Botnets Detection Module is the signature-based detection that make detection on known attack. The detection signature has been composed through analysis part. The P2P botnets detection technique has been developed as signature module. This technique has the capability to analyse the malicious activities described as variant behaviours, make classification on P2P variant types and sub-attack types and generate the conclusion either the submitted files is a P2P normal or P2P botnets indeed. This technique also able to produce the report on activities performed by P2P botnets.

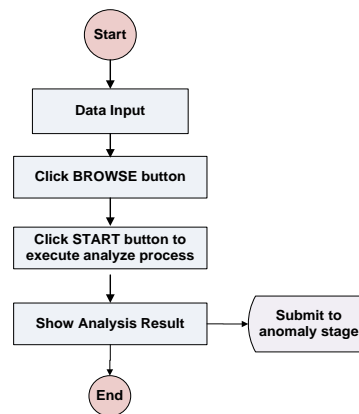


Fig. 2. Process Flow of Signature Module

The signature-based in this detection technique is involved three layer detections as indicated in Figure 3. The three layer detections in signature-based technique consist of:

- Detection only scenario - Mainly decide whether the logs or packets are normal or abnormal
- Detection and classification - Detect the logs or packets by classify them into six main attack types/variants
- Detection and detailed classification - Make classification of sub-attack types based on their attributes and behaviours for every variant

```

The rule-based method role as a signature-based technique to detect
known P2P botnets
[1] Load captured packet and host log (Input= S1, S2)
[2] Initialize S with Si=normal/abnormal, Sii=classification
attack types, Siii=classification sub attack types
[3] If Si=abnormal then Si=abnormal;
[4] Else Si=normal
[5] End
[6] If Sii=classification attack types then Sii=classification attack
types;
[7] Else Sii=none;
[8] End
[9] If Siii=classification sub attack types then Siii=classification
sub attack types
[10] Else Siii=none;
[11] End
[12] If Si=abnormal or If Sii=classification attack types or
Siii=classification sub attack
types then Detected, d=1
[13] Else if Si=normal then Detected, d=0 (proceed with
statistical test on anomaly-
based section )
[14] End
    
```

Fig. 3. Rule-based detection

The principal step in signature-based has the ability to immediate detection and impossibility of false positives. But signature-based is only capable to be used for detection of well-known botnets. More important, very similar bots with slightly different signature may be missed-out to be detected. However, the anomaly-based technique faced with the problem of detecting unknown botnets through show existence of bots in the network. Anomaly-based technique also has the extra capabilities in terms of reducing false negative alert and detecting multistep attack. Nevertheless, it cannot reduce the false positive alert which can only be reduced by using signature-based technique. Hence, this has given an implication that there are complement each other weaknesses. The fully results are briefly discusses in the next section.

IV. RESULT AND DISCUSSION

Generally, NetBeans has been chosen as its supports java as the main language in its application. As claimed by software programmer and designer that java is simple, free, easy to design, easy to write, easy to compile, debug, and able to learn rather than others programming languages. Besides that, Java is a platform-independent, portable and flexible in nature where a program easily to run from one computer system to another. The most significant feature of Java that appropriate for this research because its support host log and network packet in Packet Capture (PCAP) format and

Comma-Separated Values (CSV) format. It also supported by Graphical User Interface (GUI) with integration of network libraries too. Reasonably, the selection of Java also because it can provides the IF-ELSE statement that referring to the basic of rule-based declaration in terms of developing the P2P botnets signature detection. Thus, the NetBeans IDE version 7.4 are the best option in order to implement the rule-based signature. In the signature-based stage, these research requires a PCs to develop and test the system.

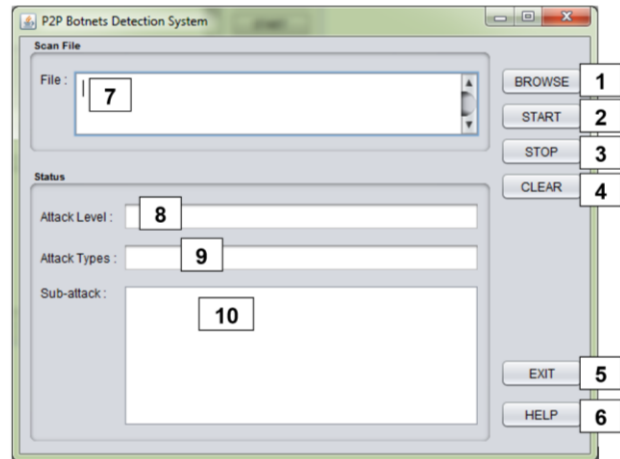


Fig. 4. Design of Signature-based Module

The signature-based system that will be developed here will have an interface that possible to be used by users towards the convenience of designing usage. By designing the interface, it offers the opportunity for the users to perform the detection process, tailored to their needs. The interface is illustrates in Figure 4. Then, the description of each control which marked by number will be discussed in the following table. The explanation about each button and text area are describes in Table 1.

TABLE I. DESCRIPTION OF CAPTION IN SIGNATURE-BASED MODULE

No.	Control Caption	Processing	Description
1.	BROWSE	User: Click the BROWSE button. System: Go to BROWSE file window.	This button is used to open the Browse File window, to choose the file that want to be submitted.
2.	START	User: Click the START button. System: Begin the analysis process.	This button is clicked if user wants to start the process.
3.	STOP	User: Click the STOP button. System: Stop the analysis process.	This button is clicked if user wants to stop the process.
4.	CLEAR	User: Click the CLEAR button. System: Clear all the current process.	This button is clicked if user wants to clear the text area.
5.	EXIT	User: Click the EXIT button. System: Exit the whole system.	This button is clicked if user wants to exit the system.
6.	HELP	User: Click the HELP	This button is

No.	Control Caption	Processing	Description
		button. System: Go to HELP file window.	clicked if user wants to get the related info about this system.
7.	File Text Area	User: Choose a file by clicking BROWSE button first. System: Show the path of chosen file.	Showing the file path of the selected or browsed file.
8.	Attack Level Text Area	User: Click the START button. System: Automatically generate the level of analysis.	Showing the attack level whether the host-level or network-level.
9.	Attack Types Text Area	User: Click the START button. System: Automatically show the types of variants.	Showing the types of variants.
10.	Sub-attack Text Area	User: Click the START button. System: Show the signature for detected variant.	Showing the list of attributes and behaviours for each of detected variant.

The result from Table 2 showed that the signature-based detection has the capabilities to predict 100% correctly for the overall detection rate with 0% of false alarm rate of the P2P network traffic. The improvement of overall detections in the signature-based module from classification table in data mining module are indicated that this signature-based system technically effective for outcome attack detection. Therefore, it can be summarized that this signature-based detection has better prediction and capabilities to distinguish between the normal and attack events reached for thousands of dataset for each variant.

TABLE II. SIGNATURE-BASED MODULE DETECTION RESULT

Variante	False Negative (FN)	Accuracy (A)	Detection Rate (DR)	False Alarm Rate (FAR)
Invalid Hash	0	100%	100%	0%
Allapple.L	2	99.99%	100%	0%
RBOT	6	99.98%	100%	0%
Palevo	3	100.00%	100%	0%
Srvcp	2	99.99%	100%	0%
Tnnbtib	0	100%	100%	0%

Inclusively, this signature-based detection system in this research promises the better enhancement in P2P botnets detection technique. The entire six variants have fully detected as the P2P botnets based on the detection result. But, Table 2 shows the detail of the result where the False Negative (FN) emphasize some of the undetectable attributes or undetectable P2P botnets values as the attack declares as normal. Alternately, this problem can be tackled by conducting the anomaly-based detection. In the next of detection stage, the chi-square statistical test with multivariate process has been perform. The tabulated of false negative that indicates undetectable P2P botnets has been proves can be successfully detected through the statistical approach. The

detail steps on detecting P2P botnets through anomaly statistical test has been explaining in the next sub-section.

V. CONCLUSION

Currently, the signature that has been analyse by most of researchers are not updated enough. This study presents a new signature and behaviours in detecting P2P botnets. The proposed detection module is based on rule-based approach. The result show that the proposed detection module have high detection accuracy with ability to detect known P2P botnets and produce a high detection rate with low false alarm rate. Hence, the developing detection module based on automated signature-based approach with updated dataset has been the most promising approach to fight against botnets threat in real P2P botnets files. The further work will be done on the developed of automated P2P botnets signature in different attack type and platform.

ACKNOWLEDGMENT

The authors would like to express the appreciation to Inforsnet Group Research of Universiti Teknikal Malaysia Melaka (UTeM) and MyBrain15 Programme by Ministry of Higher Education Malaysia (MoHE) in encouraging the authors to publish this paper. This work was supported by the MoE of Malaysia under Grants FRGS/1/2014/ICT04/FTMK/02/ F00212.

REFERENCES

- Zeidanloo, H. R. a. A., A.B. (2010), "Botnet Detection by Monitoring Similar Communication Patterns", (IJCSIS) *International Journal of Computer Science and Information Security* Vol. 7(No. 3): 36-45
- Deerman, J. 2012, Advanced Malware Detection through Attack Life Cycle Analysis: The Evolution of Malware, *ISC8 Secure*.
- Patrick, T., 2013. Advanced Malware Detection Through Attack Lifecycle Analysis, *ISC8 Secure*.
- Husin, J. 2009. ICT, Youth and Terrorism. International Conference on Youth and Terrorism Kuala Lumpur.
- Conovan, Q., Ye, N., Emran, S.M., Li, X. and Chen, Q. 2001. Statistical Process Control for Computer Intrusion Detection. *Proceedings of DARPA Information Survivability Conference and Amp; Exposition II DISCEX, IEEE*.
- Boonbox, 2009. Types of IT Security Threats and Their Consequences: White Paper Report. *Pacific Coast Information System PCIS*.
- Robert Richardson 2007. CSI Computer Crime and Security Survey, The 12th Annual Computer Crime and Security Survey.
- Charles, L. 2013. *Malware Threats in our Cyber Infrastructure*, Yogyakarta: Swiss German University.
- Sundaram, A. 1996. An Introduction to Intrusion Detection. *ACM Digital Library*.
- Razak, S., Zhou, M. and Lang, S. D. 2002. Network Intrusion Simulation Using OPNET. *Proceedings of the OPNETWORK2002*, pp. 1-5.
- Chandrashekar, J., Orrin, S., et al. (2009), "The Dark Cloud: Understanding and Defending against Botnets and Stealthy Malware", *Intel Technology Journal* Vol. 13 (Issues 2).
- Moon, S. S. and Kyeong, J. J., 2006. Alert Correlation Analysis in Intrusion Detection. *Proceedings of the 2nd International Conference Advanced Data Mining and Applications ADMA 2006*, pp. 1049-1056.
- Emmanuel, H., 2006. Experimental Validation and Analysis of an Intelligent Detection and Response Strategy to False Positives and Network Attacks. *Proceedings of the IEEE Intelligence and Security Informatics Conference*, pp. 711-714.
- Tjhai, G. C., Furnell, S. M., Papadaki, M. and Clarke, N. L., 2010. A Preliminary Two-Stage Alarm Correlation and Filtering System Using

- SOM Neural Network and K-Means Algorithm. *Journal of Computers and Security*, Vol. 29, pp. 712-723.
- [15] Subbulakshmi, T., Mathew, G. and Shalinie, D. S. M. 2010. Real Time Classification and Clustering of IDS Alerts Using Machine Learning Algorithms. *International Journal of Artificial Intelligence & Applications IJAIA*, Vol. 1, No.1, pp. 1-9.
- [16] Song, J., Takakura, H., Okabe, Y. and Kwon, Y., 2011. Correlation Analysis Between Honeypot Data and IDS Alerts Using One-class SVM. In *Intrusion Detection Systems*, pp. 173-192. InTech Open Access Publisher.
- [17] Cheung, S., Fong W. M. and Lindqvist, U. 2010. Modelling Multistep Cyber Attacks for Scenario Recognition. *Proceedings of the 3rd DARPA Information Survivability Conference and Exposition DISCEX III*, Vol. 1, pp. 284-292.
- [18] Lin, H. H., Mao, C. H. and Lee, H. M. 2009. False Alarm Reduction by Weighted Score-Based Rule Adaptation Through Expert Feedback. *Proceedings of the 2nd International Conference on Computer Science and its Applications 2009 CSA 2009*, pp. 1-8.
- [19] Yuanyuan, Z., H. Xin, et al. (2010), "Detection of Botnet using Combined Host-and Network-Level Information". *IEEE/IFIP International Conference on Dependable Systems and Networks (DSN)*
- [20] He, J., Yang, Y., Wang X., and Zeng, Y., 2014. Peer Sorter: Classifying Generic P2P Traffic in Real-Time. *IEEE International Conference on Computational Science and Engineering*. pp. 605-613
- [21] Ferragut, E.,M., Laska, J. and Bridges, R.A. 2012. A New, Principled Approach to Anomaly Detection, *11th International Conference on Machine Learning and Applications, IEEE*.
- [22] Ngadi, M., A., Yazid, M. I., and Hanan, A., 2005. A Study on Advanced Statistical Analysis for Network Anomaly Detection. *Project Report, Faculty of Computer Science and Information System, Skudai, Johor*.
- [23] Bao, X., Xu, T. and Hou, H. (2009), "Network Intrusion Detection Based on Support Vector Machine," International Conference on Management and Service Science (MASS).
- [24] NetBeans Community, 2013. Welcome to the NetBeans Community. Available at: <https://netbeans.org/about/> [Accessed on 14 March 2014]
- [25] Leonardo, G. 2007, Reach Out with the IDE and Platform. *NetBeans Magazines*.
- [26] He, J., Yang, Y., Wang X., and Zeng, Y., 2014. Peer Sorter: Classifying Generic P2P Traffic in Real-Time. *IEEE International Conference on Computational Science and Engineering*. pp. 605-613
- [27] Karuppayah S., Fischer M., Rossow, C., and Max, M. 2014. On Advanced Monitoring in Resilient and Unstructured P2P Botnets. *IEEE ICC - Communication and Information Systems Security Symposium*. pp. 871-877

A Survey on Case-based Reasoning in Medicine

Nabanita Choudhury
Department of Computer Science
Assam University
Silchar, India

Shahin Ara Begum
Department of Computer Science
Assam University
Silchar, India

Abstract—Case-based reasoning (CBR) based on the memory-centered cognitive model is a strategy that focuses on how people learn a new skill or how they generate hypothesis on new situations based on their past experiences. Among various Artificial Intelligence tracks, CBR, due to its intrinsic similarity with the human reasoning process has been very promising in the utilization of intelligent systems in various domains, in particular in the domain of medicine. In this paper, we extensively survey the literature on CBR systems that are used in the medical domain over the past few decades. We also discuss the difficulties of implementing CBR in medicine and outline opportunities for future work.

Keywords—case-based reasoning; medicine; artificial intelligence; soft computing

I. INTRODUCTION

Case-Based Reasoning (CBR) is an area of machine learning research based on the memory-centered cognitive model [1]. CBR arose out of the research in cognitive science. It is defined as a model of reasoning that integrates problem solving, understanding and learning, and incorporates all of them with memory processes. It involves adapting earlier solutions to meet new demands, using old cases to explain or justify new solutions, and reasoning from past events to interpret a new situation. In CBR terminology, a case usually denotes a problem situation [2]. CBR can be considered as a form of similarity-based or analogical reasoning since the basic principle that is implicitly assumed to be applied in problem solving methodology is that similar problems have similar solutions [3].

CBR as a problem solving paradigm, is essentially different from other major Artificial Intelligence (AI) approaches in many aspects. Unlike other approaches which rely solely on the general knowledge of a problem domain, or which associate along inferred relationships between problem descriptors and conclusions, CBR utilizes the specific knowledge of previously experienced problem situations [2]. CBR can be applied as ‘reasoning by experience in AI’ as compared to rule-based reasoning which is applied as ‘reasoning by logic in AI’ [4]. The intuitive appeal of CBR comes due to its similarity to human problem solving behavior. Just as people draw on past experiences while solving a new problem, which often does not require in-depth analysis of the problem domain, CBR can be based on shallow knowledge and does not require significant effort in knowledge engineering as required by other AI fields like rule-based reasoning [5].

Medical reasoning on the other hand, involves processes ‘that can be systematically analyzed, as well as those

characterized as intangible’ [6]. In medicine, the experts not only use rules to diagnose a problem, but they also use a mixture of textbook knowledge and experience. The experience consists of cases, typical and exceptional ones, and the physicians take them into account for reasoning. So, case-oriented methods should be very efficient in the domain of medical diagnosis, mainly because reasoning with cases corresponds with the typical decision making process of physicians. Also, incorporating new cases means automatically updating parts of the changeable knowledge [7]. Despite these, CBR has not become as successful in the medical domain, as it is in other fields for building intelligent systems [8].

The present paper surveys the available literature on systems developed using CBR for solving various problems in medicine. We begin in Section 2 by describing the basic notions of CBR and its models, with a brief description of the phases in CBR life cycle. Section 3 gives a brief description of medical reasoning. Section 4 surveys various CBR based systems developed over past few decades in the domain of medicine. In Section 5, we point out certain issues of using CBR in the field of medicine. Section 6 concludes the paper with a discussion on future directions of research.

II. INSIDE CASE-BASED REASONING

CBR is an analogical reasoning method, which means that it reasons from old cases or experiences to solve problems or interpret anomalous situations [9]. But the major difference between CBR and analogy is that analogy reasons across domains, whereas CBR reasons inside one domain [10]. In CBR, the reasoning is based on remembering past experiences, as explained by Althoff et al. [11] - ‘To solve a problem, remember a similar problem you have solved in the past and adapt the old solution to solve the new problem.’ CBR can be interpreted in many ways [12] by different groups of people. For example, for cognitive scientists, it is a plausible high-level model for cognitive processing; for artificial intelligence researchers, it is a computational paradigm for solving problems; and for expert system practitioners, it is a design model.

CBR arose out of the research in cognitive science. The earliest contributions in this area were from Roger Schank and his colleagues at Yale University [2]. During the period 1977–1993, CBR research was regarded as a plausible high-level model for cognitive processing. Three CBR workshops were organized in 1988, 1989, and 1991 by the U.S. Defense Advanced Research Projects Agency (DARPA), which officially marked the birth of the discipline of CBR. In 1993, the first European workshop on CBR (EWCBR-93) was held

in Kaiserslautern, Germany; and the first International Conference on CBR (ICCB-95) was held in Sesimbra, Portugal. Many international workshops and conferences on CBR have been held in different parts of the world since then. Medical applications have been a part of the CBR community from the very beginning and are included in almost every international conference on CBR [13].

A. CBR Models

To understand the working of CBR, various models have been proposed in the literature. These include Hunt's model, Allen's model, Kolodner and Leake's model [14], and R⁴ model, developed by Aamodt & Plaza [2]. Of these, the most widely used model and at the highest level of generality is the R⁴ model [15]. The process involved this model can be represented by a schematic cycle comprising of the four R's, as illustrated in Figure 1.

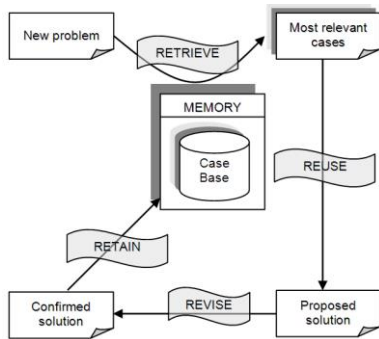


Fig. 1. The R4 Cycle [2]

- Retrieve the most similar case (s)
- Reuse the information and knowledge from retrieved case (s) to solve the problem
- Revise the proposed solution
- Retain the parts of this solution likely to be useful in future.

B. CBR Life Cycle

The problem solving life cycle of CBR essentially consists of retrieval, adaptation, and maintenance. Each of these has its own importance in the successful working of the CBR system.

1) Retrieval

Retrieval is often considered the most important phase of CBR since it lays the foundation for overall working of the CBR system [16]. Retrieval includes the process of finding those cases within a case base, which are most similar to the current case. The most commonly investigated retrieval techniques include nearest neighbor retrieval, inductive approaches, knowledge guided approaches, and validated retrieval [5], [17]. Some hybrid algorithms have also been proposed e.g. Discretised Highest Similarity with Pattern Solution Re-use algorithm [18].

2) Adaptation

The next two phases of the CBR cycle, viz. reuse and revise are often difficult to distinguish in many practical applications, as a result of which many researchers replace and combine

them into a single stage called adaptation [5]. In the early 90's the CBR community focused on retrieval only. Investigations of the various aspects of adaptation started after that [19]. Most of the advances also have been achieved at the retrieval and retain phase of CBR [20]. In the reuse phase, advances have been obtained depending on the system purpose viz. diagnosis, classification, tutoring and planning (such as therapy support). Regarding diagnosis and classification, most of the systems rely on adaptation methods that consist of copying the solution of the most similar case or a combination of them, i.e. reusing the solution [21].

3) Maintenance

After reusing and revising the retrieved case, the next step in CBR cycle is to retain the case (s). There are many approaches to achieve this. Many systems store only the solution of the previous problem, whereas some systems store the solving process [16]. In many cases, this process of retaining leads to an uncontrolled growth in the case base, which in turn leads to a poorer performance of the system in terms of speed [22]. So, the need of maintaining a case base arises.

III. MEDICAL REASONING

Medical reasoning is divided into diagnostic reasoning, planning, and patient management [23]. This reasoning is carried out in terms of physiological states, complaints, symptoms and so forth [24]. Diagnostic reasoning includes cognitive activities like gathering information, recognition of patterns, solving problems and decision making [25]. Diagnostic investigations are quite complex and error prone [26]. Table 1 outlines the diagnostic process.

TABLE I. DIAGNOSTIC CYCLE [27]

Step	Decision
1	Select a diagnostic test (or question)
2	Carry out the selected test and observe its outcome
3	Either (i) select a further diagnostic test and so return to step 1; or (ii) make a diagnosis in the light of the outcomes so far obtained

This diagnosis process may become easier and more reliable if equipped with an expert system that provides past diagnosis of cases, thereby helping the physician to arrive at a solution based on the past experiences [28].

IV. CBR SYSTEMS IN MEDICINE

CBR used in medical reasoning literature is termed as 'instance-based recognition' [29]. Unlike other knowledge domains, cases have to be professionally documented in medical domain [30]. The very fact that the methodology of CBR systems closely resembles the thought process of a physician suggests a successful use of CBR in medicine [31]. Koton pointed out while introducing CASEY - 'A physician's problem-solving performance improves with experience. The performance of most medical expert systems does not' [32]. The experts in the medical domain do not use rules for diagnosis. What they use is the knowledge they obtain from books, as well as experiences just the way in which CBR works [7].

The main advantage of CBR systems in medicine is the automatic formation of a facility adapted knowledge base [33], which is a very important aspect in medical decision making. Also, the continuously changing nature of medical knowledge base, presence of more than one solution, and complexity in modeling also make CBR applicable in medical domain [34]. As a result, CBR has been used for building intelligent computer-aided decision support systems in the medical domain in the past few decades [35].

CBR decision support systems can be classified [20] as planning, classification, tutoring, and diagnostic systems based on their purpose oriented properties. Table 2 lists in chronological order, some of the CBR systems developed in the field of medical reasoning over the years. Also, it classifies these systems according to their objectives and attempts to find out the extent to which adaptation phase of CBR is used in these systems.

TABLE II. CBR SYSTEMS IN MEDICINE

Author(s)	System	Ref.	Objective	Technique(s) used	Area of Application	Adaptation (if any)
Koton	CASEY	[32]	Diagnosis	CBR, Rule-based domain theory, and Model-based reasoning	Coronary disease	Adaptation with rules attempted
Bareiss, Porter & Wier	Protos	[36]	Classification and Diagnosis	CBR	Hearing disorders	No adaptation
Gierl & Stengel-Rutkowski	GS.52	[37]	Diagnosis	CBR	Dysmorphic syndromes	Adaptation performed with the application of constraints (contradictions)
Macura & Macura	MacRad	[38]	Classification	CBR	Radiology Images	No adaptation
Haddad, Moertl & Porenta	SCINA	[39]	Image Interpretation	CBR and Rule-based reasoning	Myocardial Perfusion Scintigrams	Adaptation performed with Rule-base
Reategui, Campbell, & Leao	--	[40]	Diagnosis	CBR and Neural networks	Congenital heart diseases	No adaptation
Hsu & Ho	--	[28]	Diagnosis	CBR, Fuzzy logic, Neural networks, Induction, and Knowledge-based technology	General	Adaptation performed with Rule-base
Bichindaritz, Kansu & Sullivan	CARE-PARTNER	[41]	Knowledge-support assistance	CBR, Rule-based reasoning, and Information retrieval	General	Adaptation performed with rules, cases and pathways
LeBozec et al.	IDEM	[42]	Classification	CBR	Radiology Images	No Adaptation
Gierl, Bull, & Schmidt	TeCoMED	[30]	Classification (forecasting)	CBR, Rule-based reasoning, and Model-based reasoning	Epidemics	Compositional Adaptation
Perner	--	[43]	Classification, Knowledge acquisition/management	CBR, Image processing, and Data mining	Medical image analysis	No Adaptation
Schmidt, Pollwein, & Gierl	COSYL	[44]	Classification	CBR	Liver transplantation	No Adaptation
Goodridge, Peter, & Abayomi	MED2000	[45]	Diagnosis	CBR and Neural networks	Hematological diseases	No Adaptation
Phuong, Thang, & Hirota	--	[46]	Diagnosis	CBR and Fuzzy logic	Lung diseases	No Adaptation
Marling & Whitehouse	Auguste	[47]	Planning	CBR and Rule-based reasoning	Alzheimer's disease	No Adaptation
Golobardes et al.	CaB-CS	[48]	Classification	CBR	Breast cancer	No Adaptation
Montani et al.	--	[49]	Planning	CBR, Rule-based reasoning, and Model-based reasoning	Type 1 diabetes	Adaptation performed with rules
Vorobieva, Gierl, & Schmidt	--	[50]	Planning	CBR	Endocrinology	Adaptation performed and task oriented adaptation model developed
Hsu & Ho	--	[51]	Diagnosis	CBR, Neural networks, Fuzzy theory, Induction, Utility theory, and Knowledge-based planning technology	Multiple diseases	Adaptation performed with knowledge-based planning
Nilsson & Funk	--	[52]	Classification	CBR and Rule-based reasoning	Respiratory sinus arrhythmia	No Adaptation
Kwiatkowska & Atkins	Somnus	[53]	Diagnosis	CBR, Fuzzy logic, and Semiotics	Obstructive sleep apnea	No Adaptation
Perner et al.	--	[54]	Classification, Knowledge acquisition/management	CBR and Image processing	Recognition of Airborne Fungi Spores	No Adaptation

Brien, Glasgow & Munoz	--	[55]	Classification	CBR	Attention-deficit hyperactivity disorder	No Specific Adaptation
Chang	--	[56]	Diagnosis	CBR	Development delay in children	Adaptation performed with the help of human experts
Shi & Barnden	--	[57]	Diagnosis	CBR and Induction	Multiple disorders	Abductive Adaptation with rules
Montani & Portinale	RHENE	[58]	Classification, planning, knowledge acquisition/management	CBR and Temporal Abstractions	Hemodialysis	No Adaptation
d'Aquin, Lieber & Napoli	KASIMIR	[59]	Diagnosis, classification, knowledge acquisition/management	CBR, Semantic web, Belief revision theory, Fuzzy logic, and Ergonomy	Breast cancer	Adaptation Performed (Adaptation Guided Retrieval)
Díaz, Fdez-Riverola & Corchado	geneCBR	[60]	Diagnosis and classification	CBR and Fuzzy Logic	Cancer	Adaptation Performed with the help of human expert
Park, Kim & Chun	--	[61]	Classification and diagnosis	CBR and Probability	General	No Adaptation
Töpel, Neumann & Hofstadt	--	[62]	Diagnosis and planning therapy information	CBR	Inborn metabolic disease	No Adaptation
Quellec et al.	--	[63]	Classification	CBR and Decision trees	Diabetic retinopathy	No Adaptation
Cordier et al.	FrakaS	[64]	Diagnosis, Knowledge acquisition/management	CBR	Oncology	Conservative adaptation performed
Marling, Shubrook & Schwartz	--	[65]	Planning	CBR	Type 1 diabetes	No adaptation
Little, Salvetti & Perner	ProtoClass	[66]	Classification	CBR	General	No adaptation
Ahmed et al.	--	[67]	Diagnosis	CBR and Fuzzy logic	Stress	No adaptation
Rodríguez et al.	SAPRIM	[68]	Prediction	CBR, Neural networks, and Fuzzy Logic	Pediatric risk	No adaptation
Corchado, Bajo & Abraham	GerAmi	[69]	Planning, Knowledge acquisition/management	CBR and Variational calculus	Alzheimer's disease	Adaptation performed
De Paz et al.	--	[70]	Diagnosis and classification	CBR, Neural networks, and Statistics	Leukemia	Adaptation performed with Classification Tree
Obot & Uzoka	--	[71]	Diagnosis	CBR, Rule-based reasoning, and Neural networks	Hepatitis	Adaptation performed with the help of rules and neural network
Lin	--	[72]	Diagnosis	CBR and Classification and regression tree (CART)	Liver diseases	No adaptation
Ahn & Kim	GOCBR	[73]	Diagnosis	CBR and Genetic algorithms	Breast Cancer	No adaptation
Begum et al.	--	[74]	Diagnosis	CBR and Fuzzy logic	Stress	No adaptation
Yao & Li	ANMM4CBR	[75]	Classification	CBR	Gene expression data	No adaptation
Gu et al.	CBR-DENT	[76]	Knowledge management	CBR and Fuzzy Logic	Odontology	Adaptation performed
Lin & Chuang	--	[77]	Diagnosis	CBR, Analytic hierarchy process, and Neural networks	Liver diseases	No adaptation
Jagannathan et al.	--	[78]	Planning	CBR and Fuzzy logic	Brain cancer radiotherapy	Adaptation suggested, but not performed
Ahmed et al.	--	[79]	Planning	CBR and Fuzzy logic	Stress	Adaptation performed
Douali et al.	--	[80]	Diagnosis	Case-based Fuzzy cognitive maps	Urinary tract infection	No adaptation
Chuang	--	[81]	Diagnosis	CBR and Neural networks (Back propagation network)	Liver disease	No adaptation
Petrovic, Mishra & Sundar	--	[82]	Planning	CBR and Dempster-Shafer theory	Prostate Cancer	Adaptation performed
van den Branden et al.	Excelicare CBR	[83]	Classification	CBR and Genetic Algorithm	Electronic patient record	No adaptation

López et al.	eXiT*CBR	[84], [85]	Diagnosis	CBR, Pedigree tools, and Genetic algorithms	Breast cancer	Adaptation performed
Ahmed, Begum & Funk	--	[86]	Diagnosis	CBR, Fuzzy logic, Rule-based reasoning, and Textual information retrieval	Stress	No adaptation
Montani et al.	--	[87]	Classification and planning	CBR	Hemodialysis	No adaptation
Khelassi et al.	--	[88]	Diagnosis	CBR, Rule-based reasoning, Distributed reasoning, and Fuzzy logic	Cardiac arrhythmia	No adaptation
Marling et al.	4DSS	[89]	Planning	CBR and Rule-based reasoning	Type 1 diabetes	Adaptation performed
Juarez et al.	GRACE	[90]	Supporting protocol design	CBR	Frontotemporal dementia	Adaptation performed with rule-base
Ahmed, Begum, & Funk	--	[91]	Diagnosis, classification and planning	CBR, Fuzzy logic, Rule-based reasoning, and Textual information retrieval	Stress Management	No adaptation
Ahmed, Islam, & Loutfi	--	[92]	Patient identification	CBR	General	No adaptation
Begum, Ahmed, & Barua	--	[93]	Classification	CBR and Fuzzy logic	Physiological sensor signals	No adaptation
Ekong, Inyang, & Onibere	--	[94]	Diagnosis	CBR, Neural networks, and Fuzzy logic	Depression disorder	No adaptation
Huang et al.	--	[95]	Classification and diagnosis	CBR, Neural networks, and Adaptive Neuro-Fuzzy Inference System	Breast cancer	No adaptation
Montani et al.	--	[96]	Classification (retrieval)	CBR	Comparative genomics	No adaptation
Chattopadhyay et al.	--	[97]	Diagnosis	CBR	Premenstrual syndrome	Adaptation
Pla et al.	eXiT*CBR. v2	[98]	Diagnosis	CBR, Genetic algorithms, and Cooperative multi agent system technology	General	Adaptation performed
Leal et al.	--	[99]	Planning	CBR and Principal component analysis	Continuous glucose monitoring systems in intensive care unit	No adaptation
Teodorović, Šelmić, & Mijatović-Teodorović	--	[100]	Planning	CBR and Bee colony optimization	Thyroid cancer	No adaptation
Henriet et al.	EquiVox	[101]	Representations of human organs	CBR and Neural networks	Numerical representation of human organs	Adaptation performed with ANN
Sharaf-El-Deen	--	[102]	Diagnosis	CBR and Rule-based reasoning	Breast Cancer and Thyroid disease	Adaptation performed with rules
Yin et al.	--	[103]	Diagnosis	CBR	Headache	No adaptation
Tyagi & Singh	--	[104]	Classification	CBR	Asthma	No adaptation
Khussainova, Petrovic, & Jagannathan	--	[105]	Planning	CBR and Clustering	Radiotherapy (Brain Cancer)	No adaptation
Saraiva et al.	--	[106]	Diagnosis	CBR and Rule-based reasoning	Four types of gastrointestinal cancer	No adaptation
Chakraborty et al.	CEDS	[107]	Diagnosis	CBR	Cholera	No adaptation
Nasiri, Zenkert, & Fathi	DePicT	[108]	Diagnosis and recommendation	CBR		No adaptation
Banerjee & Chowdhury	--	[109]	Diagnosis	CBR, Fuzzy clustering, and Decision trees	Retinal Abnormalities	No adaptation

From our study, it was observed that CBR in the medical domain has a wide range of application. Most of the systems are developed specifically to deal with a particular disease. Secondly, most of the systems act as prototypes, and not as final products, as mentioned by Blanco [110]. These systems require a human expert to interpret the final result. Another visible trend was the successful hybridization of CBR with soft

computing methods. 32 out of 76 systems studied by us have used some or the other soft computing techniques in addition to CBR. Moreover, among the 76 systems, 51 systems completely avoid automatic adaptation and mainly work as retrieval only systems. The other systems do have the adaptation phase in them, but often the reasoning mechanism in those is coupled with rule-based reasoning, or various soft computing methods.

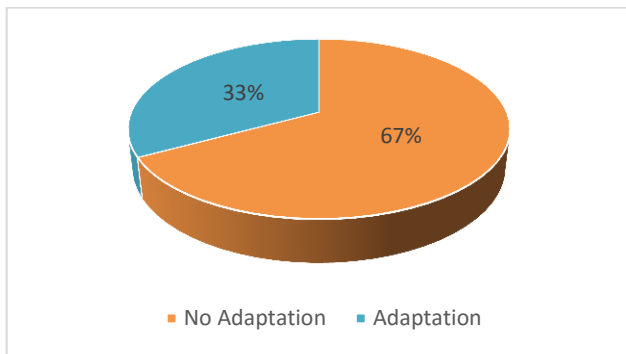


Fig. 2. Percentage of systems in terms of adaptation performed

V. PROBLEMS IN MEDICAL CBR SYSTEMS

Though the above discussion reflects the successful use of CBR in medicine, there are some limitations which restrict the use of CBR in medicine. In a medical case, the number of features is often extremely large, thereby making the generalization and adaptation quite difficult [20]. At the same time, reliability cannot be guaranteed in medical CBR systems [111]. The limited number of reference cases aids to the problem of implementing a medical CBR system [35]. But the most important concern in the successful implementation of medical CBR systems is the adaptation problem. As our study suggests, so far, the number of systems in the medical domain that apply the complete CBR method is very less. Most of the systems use no adaptation at all, and the task of adaptation is left to the human expert.

d'Aquin et al. [59] remark that adaptation in medicine is quite a complex procedure, as it needs to deal with the lack of relevant information about a patient, the applicability and consequences of the decision, the closeness to the decision thresholds and the necessity to consider patients according to different viewpoints. Schmidt et al. [7] also point out that giving autonomy to the adaptation step of CBR has been a difficult step in Medicine. Due to these challenges, most of the advances made in medical CBR systems focus on the retrieval phase. The adaptation phase is limited to planning tasks [21]. No general models have been developed for adaptation as it largely depends on the domain and application characteristics.

Our study reveals that medical CBR systems deal with the adaptation problem in two ways. Most of the systems avoid the adaptation problem by applying only retrieval phase of CBR cycle [19] while some others attempt to solve it. One of the earliest medical expert systems, CASEY [32] makes an attempt to solve the adaptation task. In this, the creation of a complete rule base for adaptation is time consuming, as a result of which a few general operators are used for adaptation. And when no similar case can be found or if adaptation fails, CASEY uses a rule-based domain theory. But since knowledge acquisition is the bottleneck for the development of rule-based medical expert systems, the development of complete adaptation rule bases have never become a successful technique to solve the adaptation problem in medical CBR systems [7]. The application of constraints leads to a better solution, as in the GS.52 project [37] but only for specific situations. KASIMIR [59] uses similarity paths and reformulation to support the adaptation, but adaptation knowledge in the form of rules is

still required. Some of the more recent systems perform adaptation successfully, with the help of soft computing techniques, e.g. eXiT*CBR.v2 [98] revises and reuses the cases using genetic algorithms; EquiVox developed by Henriet et al. [101] performs adaptation using artificial neural networks. So, the inclusion of soft computing techniques suggests improved automatic adaptation in medical CBR systems.

VI. CONCLUSIONS AND FUTURE SCOPE

A fundamental part of the CBR system is learning by remembering cases. CBR systems, cognitively similar to human beings, take into account previous experiences for solving new problems, consider both subjective and objective knowledge unlike other expert systems, and can incrementally acquire knowledge automatically, but still, these are not as successful in medicine as in other domains. The main reason for this is the adaptation problem. The retrieval and maintenance phases have gained a lot of attention of the researchers, while the adaptation phase is still in its infancy. The adaptation phase involves multifarious problems which include dealing with the closeness to the decision threshold used to determine similar cases, among other issues. The majority of the medical CBR systems avoid the adaptation problem, and act as retrieval only systems and leave case adaptation and case update to be performed by human experts. A solution to adaptation problem is the integration of CBR with other methodologies. The synergism of these methodologies leads to the development of new sophisticated and hybridized systems.

It was observed in our survey that a majority of successful medical CBR systems are built around a combination of CBR and other artificial intelligence methods. From the very beginning, hybrid systems came into existence for medical CBR systems; Koton's CASEY [32] being an example which hybridizes CBR and RBR. Soft computing techniques viz. fuzzy logic, artificial neural networks, in particular back-propagation neural networks and Bayesian models, and evolutionary strategies have proved to be very efficient in enhancing the capabilities of CBR systems. With the use of these techniques, adaptation knowledge can be determined automatically from the cases, which leads to more robustness of this knowledge [5]. Schmidt, Vorobieva, & Gierl [8] have mentioned that the application of adaptation rules or operators, though general seems to be the only technique which can solve medical adaptation problems. We suggest the use of fuzzy decision trees for this; wherein fuzzy decision rules can be generated, and rough set techniques can be used to simplify these rules.

In the domain of medicine, where clear domain knowledge is often not available, automatic adaptation is difficult to develop. So, hybrid combinations of soft computing techniques may be explored and implemented in greater details in the adaptation phase of CBR to move forward the success story of CBR in the otherwise difficult domain of medicine.

REFERENCES

- [1] L. D. Xu, "Case based reasoning," *Potentials*, IEEE, vol. 13, no. 5, pp. 10-13, 1994.

- [2] A. Aamodt and E. Plaza, "Case-based reasoning: Foundational issues, methodological variations, and system approaches," *AI communications*, vol. 7, no. 1, pp. 39-59, 1994.
- [3] E. Armengol, F. Esteva, L. Godo, and Torra, "On learning similarity relations in fuzzy case-based reasoning," *Transactions on Rough Sets II, Lecture Notes in Computer Science*, vol. 3135, pp. 14-32, 2004.
- [4] M. Ahmed, S. Begum, and P. Funk, "The 3 CDSSs: An overview and application in case-based reasoning," in *Proceedings of the 27th annual workshop of the Swedish artificial intelligence society*, pp. 25-32, 2012.
- [5] S. K. Pal and S. C. Shiu, *Foundations of soft case-based reasoning*, John Wiley & Sons, 2004.
- [6] R. S. Ledley and L. B. Lusted, "Reasoning Foundations of Medical Diagnosis Symbolic logic, probability, and value theory aid our understanding of how physicians reason," *Science*, vol. 130, no. 3366, pp. 9-21, 1959.
- [7] R. Schmidt, S. Montani, R. Bellazzi, L. Portinale, and L. Gierl, "Case-based reasoning for medical knowledge-based systems," *International Journal of Medical Informatics*, vol. 64, no. 2, pp. 355-367, 2001.
- [8] R. Schmidt, O. Vorobieva, and L. Gierl, "Case-based adaptation problems in medicine," in *Proceedings of WM2003: Professionelles Wissensmanagement*, Kollen-Verlag Bonn, 2003.
- [9] J. L. Kolodner, "Improving human decision making through case-based decision aiding. *AI magazine*", vol. 12, no. 2, pp. 52, 1991.
- [10] M. M. Richter and A. Aamodt, "Case-based reasoning foundations," *The Knowledge Engineering Review*, vol. 20, no. 03, pp. 203-207, 2005.
- [11] K. D. Althoff, R. Barletta, M. Manago, and E. Auriol, "A Review of Industrial Case-Based Reasoning Tools," *AI Intelligence*, Oxford, 1995.
- [12] D. W. Aha, "The omnipresence of case-based reasoning in science and application," *Knowledge-based systems*, vol. 11, no. 5, pp. 261-273, 1998.
- [13] R. Schmidt, "Case-Based Reasoning in Medicine Especially an Obituary on Lothar Gierl," *Advanced Computational Intelligence Paradigms in Healthcare-1*, pp. 63-87, 2007.
- [14] D. B. Leake, *Case-Based Reasoning: Experiences, lessons and future directions*. MIT press, 1996.
- [15] G. Finnie and Z. Sun, "A logical foundation for the case-based reasoning cycle," *International journal of intelligent systems*, vol. 18, no. 4, pp. 367-382, 2003.
- [16] R. L. De Mantaras et al., "Retrieval, reuse, revision and retention in case-based reasoning," *The Knowledge Engineering Review*, vol. 20, no. 03, pp. 215-240, 2005.
- [17] E. Simoudis and J. Miller, "Validated retrieval in case-based reasoning," in *Proceedings of AAAI*, pp. 310-315, 1990.
- [18] D. W. Patterson, N. Rooney, and M. Galushka, "Efficient Retrieval for Case-Based Reasoning," in *Proceedings of FLAIRS Conference*, pp. 144-149, 2003.
- [19] R. Schmidt and O. Vorobieva, "The Adaptation Problem in Medical Case-Based Reasoning Systems," *Successful Case-based Reasoning Applications-I*, pp. 117-141, 2010.
- [20] M. Nilsson and M. Sollenborn, "Advancements and Trends in Medical Case-Based Reasoning: An Overview of Systems and System Development," in *Proceedings of FLAIRS Conference*, pp. 178-183, 2004.
- [21] C. Pous et al., "Modeling reuse on case-based reasoning with application to breast cancer diagnosis," *Artificial Intelligence: Methodology, Systems, and Applications, Lecture Notes in Computer Science*, vol. 5253, pp. 322-332, 2008.
- [22] A. Lawanna and J. Daengdej, "Methods for case maintenance in case-based reasoning," *Int. J. Comput. Inform. Eng.*, vol. 4, pp. 10-18, 2010.
- [23] W. J. Long, "Medical informatics: reasoning methods," *Artificial Intelligence in Medicine*, vol. 23, no. 1, pp. 71-87, 2001.
- [24] P. Lucas, "The representation of medical reasoning models in resolution-based theorem provers," *Artificial intelligence in medicine*, vol. 5, no. 5, pp. 395-414, 1993.
- [25] R. A. Miller and A. Geissbuhler, "Diagnostic decision support systems," in *Clinical Decision Support Systems*, Springer New York, pp. 99-125, 2007.
- [26] R. Seising, "From vagueness in medical thought to the foundations of fuzzy reasoning in medical diagnosis," *Artificial Intelligence in Medicine*, vol. 38, no. 3, pp. 237-256, 2006.
- [27] T. R. Taylor, J. Aitchison, E. M. McGirr, "Doctors as decision-makers: a computer-assisted study of diagnosis as a cognitive skill," *British medical journal*, vol. 3, no. 5765, pp. 35-40, 1971.
- [28] C. C. Hsu and C. S. Ho, "A hybrid case-based medical diagnosis system," in *Proceedings Tenth IEEE International Conference on Tools with Artificial Intelligence*, 1998, pp. 359-366, 1998.
- [29] H. Eshach and H. Bitterman, "From Case-based Reasoning to Problem-based Learning," *Academic Medicine*, vol. 78, no. 5, pp. 491-496, 2003.
- [30] L. Gierl, M. Bull, and R. Schmidt, "CBR in Medicine," *Case-Based Reasoning Technology, Lecture Notes in Computer Science*, vol. 1400, pp. 273-297, 1998.
- [31] R. T. Macura and K. Macura, "Case-based reasoning: opportunities and applications in health care," *Artificial Intelligence in Medicine*, vol. 9, no. 1, pp. 1-4, 1997.
- [32] P. Koton, "A medical reasoning program that improves with experience," *Computer methods and programs in biomedicine*, vol. 30, no. 2, pp. 177-184, 1989.
- [33] R. Schmidt, B. Pollwein, and L. Gierl, "Experiences with case-based reasoning methods and prototypes for medical knowledge-based systems," *Artificial Intelligence in Medicine, Lecture Notes in Computer Science*, vol. 1620, pp. 124-132, 1999.
- [34] A. Holt, I. Bichindaritz, R. Schmidt, and P. Perner, "Medical applications in case-based reasoning," *The Knowledge Engineering Review*, vol. 20, no. 03, pp. 289-292, 2005.
- [35] M. U. Ahmed, S. Begum, E. Olsson, N. Xiong, P. Funk, "Case-Based Reasoning for Medical and Industrial Decision Support Systems," in *Successful Case-based Reasoning Applications-I*, pp. 7-52, 2010.
- [36] E. R. Bareiss, B. W. Porter, and C. C. Wier, "Protos: An exemplar-based learning apprentice," in *Proceedings of the fourth international workshop on machine learning*, pp. 12-23, August 1987.
- [37] L. Gierl and S. Stengel-Rutkowski, "Integrating consultation and semi-automatic knowledge acquisition in a prototype-based architecture: Experiences with dysmorphic syndromes," *Artificial Intelligence in Medicine*, vol. 6, no. 1, pp. 29-49, 1994.
- [38] R. T. Macura and K. J. Macura, "MacRad: Case-based retrieval system for radiology image resource," *AAAI Technical Report FS-95-03*, 1995.
- [39] M. Haddad, D. Moertl, and G. Porenta, "SCINA: A case-based reasoning system for the interpretation of myocardial perfusion scintigrams," *Computers in Cardiology*, pp. 761-764, 1995.
- [40] E. B. Reategui, J. A. Campbell, and B. F. Leao, "Combining a neural network with case-based reasoning in a diagnostic system," *Artificial Intelligence in Medicine*, vol. 9, no. 1, pp. 5-27, 1997.
- [41] I. Bichindaritz, E. Kansu, and K. M. Sullivan, "Case-based reasoning in care-partner: Gathering evidence for evidence-based medical practice," *Advances in case-based reasoning, Lecture Notes in Computer Science*, vol. 1488, pp. 334-345, 1998.
- [42] C. LeBozoc, M. C. Jaulent, E. Zapletal, and P. Degoulet, "Unified modeling language and design of a case-based retrieval system in medical imaging," in *Proceedings of the AMIA Symposium*, pp. 887-891, 1998.
- [43] P. Perner, "An architecture for a CBR image segmentation system," *Engineering Applications of Artificial Intelligence*, vol. 12, no. 6, pp. 749-759, 1999.
- [44] R. Schmidt, B. Pollwein, and L. Gierl, "Medical multiparametric time course prognoses applied to kidney function assessments," *International journal of medical informatics*, vol. 53, no. 2, pp. 253-263, 1999.
- [45] W. Goodridge, H. Peter, and A. Abayomi, "The Case-Based Neural Network Model and its use in medical expert systems," *Artificial Intelligence in Medicine, Lecture Notes in Computer Science*, vol. 1620, pp. 232-236, 1999.
- [46] N. H. Phuong, V. V. Thang, and K. Hirota, "Case based reasoning for medical diagnosis using fuzzy set theory," *Biomedical fuzzy and human sciences: the official journal of the Biomedical Fuzzy Systems Association*, vol. 5, no. 2, pp. 1-7, 2000.

- [47] C. Marling and P. Whitehouse, "Case-based reasoning in the care of Alzheimer's disease patients," Case-based reasoning research and development, Lecture Notes in Computer Science, vol. 2080, pp. 702-715, 2001.
- [48] E. Golobardes, X. Llorà, M. Salamó, and J. Martí, "Computer aided diagnosis with case-based reasoning and genetic algorithms," Knowledge-Based Systems, vol. 15, no. 1, pp. 45-52, 2002.
- [49] S. Montani et al., "Integrating model-based decision support in a multi-modal reasoning system for managing type 1 diabetic patients," Artificial Intelligence in Medicine, vol. 29, no. 1, pp. 131-151, 2003.
- [50] O. Vorobieva, L. Gierl, and R. Schmidt, "Adaptation methods in an endocrine therapy support system," in Workshop Proceedings of the Fifth International Conference on Case-Based Reasoning, NTNU, Trondheim, Norway, pp. 80-88, 2003.
- [51] C. C. Hsu and C. S. Ho, "A new hybrid case-based architecture for medical diagnosis," Information Sciences, vol. 166, no. 1, pp. 231-247, 2004.
- [52] M. Nilsson and P. Funk, "A case-based classification of respiratory sinus arrhythmia," Advances in Case-Based Reasoning, Lecture Notes in Computer Science, vol. 3155, pp. 673-685, 2004.
- [53] M. Kwiatkowska and M. S. Atkins, "Case representation and retrieval in the diagnosis and treatment of obstructive sleep apnea: a semio-fuzzy approach," in Proceedings of the 7th European Conference on Case-Based Reasoning, pp. 25-35, 2004.
- [54] P. Perner, H. Perner, S. Jänichen, and A. Bühring, "Recognition of airborne fungi spores in digital microscopic images," in Proceedings of the 17th International Conference on Pattern Recognition, 2004, vol. 3, pp. 566-569.
- [55] D. Brien, J. Glasgow, and D. Munoz, "The application of a case-based reasoning system to attention-deficit hyperactivity disorder," Case-Based Reasoning Research and Development, Lecture Notes in Computer Science, vol. 3620, pp. 122-136, 2005.
- [56] C. L. Chang, "Using case-based reasoning to diagnostic screening of children with developmental delay," Expert Systems with Applications, vol. 28, no. 2, pp. 237-247, 2005.
- [57] W. Shi and J. A. Barnden, "Using inductive rules in medical case-based reasoning system," in MICAI 2005: Advances in Artificial Intelligence, Lecture Notes in Computer Science, pp. 3789, pp. 900-909, 2005.
- [58] S. Montani and L. Portinale, "Accounting for the Temporal Dimension in Case-based Retrieval: A Framework for Medical Applications," Computational Intelligence, vol. 22, no. 3-4, pp. 208-223, 2006.
- [59] M. d'Aquin, J. Lieber, J., and A. Napoli, "Adaptation knowledge acquisition: A case study for case-based decision support in oncology," Computational Intelligence, vol. 22, no. 3-4, pp. 161-176, 2006.
- [60] F. Díaz, F. Fdez-Riverola, and J. M. Corchado, "GENE-CBR: A case-based reasoning tool for cancer diagnosis using microarray data sets," Computational Intelligence, vol. 22, no. 3-4, pp. 254-268, 2006.
- [61] Y. J. Park, B. C. Kim, and S. H. Chun, "New knowledge extraction technique using probability for case-based reasoning: application to medical diagnosis," Expert Systems, vol. 23, no. 1, pp. 2-20, 2006.
- [62] T. Töpel, J. Neumann, and R. Hofestädt, "A medical case-based reasoning component for the rare metabolic diseases database RAMEDIS," in Twentieth IEEE International Symposium on Computer-Based Medical Systems, pp. 7-11, June 2007.
- [63] G. Quéllec et al., "Multimedia medical case retrieval using decision trees," Proceedings of the 29th Annual International Conference of the IEEE EMBS, pp. 4536-4539, 2007.
- [64] A. Cordier, B. Fuchs, J. Lieber, and A. Mille, "On-line domain knowledge management for case-based medical recommendation," in 5th workshop on CBR in the Health Sciences, a workshop of the seventh International Conference on Case-Based Reasoning (ICCBR-07), pp. 285-294, 2007.
- [65] C. Marling, J. Shubrook, and F. Schwartz, "Case-based decision support for patients with type 1 diabetes on insulin pump therapy," Advances in Case-Based Reasoning, Lecture Notes in Computer Science, vol. 5239, pp. 325-339, 2008.
- [66] S. Little, O. Salvetti, and P. Perner, "Evaluating a Case-Based Classifier for Biomedical Applications," in 21st IEEE International Symposium on Computer-Based Medical Systems, pp. 584-586, 2008.
- [67] M. U. Ahmed, S. Begum, P. Funk, N. Xiong, and B. Von Schéele, "Case-based reasoning for diagnosis of stress using enhanced cosine and fuzzy similarity," Transactions on Case-Based Reasoning for Multimedia Data, vol. 1, no. 1, pp. 3-19, 2008.
- [68] Y. Rodríguez et al., "Prediction of Pediatric Risk Using a Hybrid Model Based on Soft Computing Techniques," in MICAI 2008: Advances in Artificial Intelligence, pp. 472-481, 2008.
- [69] J. M. Corchado, J. Bajo, and A. Abraham, "GerAmi: Improving healthcare delivery in geriatric residences," Intelligent Systems, vol. 23, no. 2, pp. 19-25, 2008.
- [70] J. F. De Paz, S. Rodríguez, J. Bajo, and J. M. Corchado, "Case-based reasoning as a decision support system for cancer diagnosis: A case study," International Journal of Hybrid Intelligent Systems, vol. 6, no. 2, pp. 97-110, 2009.
- [71] O. U. Obot and F. M. E. Uzoka, "A framework for application of neuro-case-rule base hybridization in medical diagnosis," Applied Soft Computing, vol. 9, no. 1, pp. 245-253, 2009.
- [72] R. H. Lin, "An intelligent model for liver disease diagnosis," Artificial Intelligence in Medicine, vol. 47, no. 1, pp. 53-62, 2009.
- [73] H. Ahn and K. J. Kim, "Global optimization of case-based reasoning for breast cytology diagnosis," Expert Systems with Applications, vol. 36, no. 1, pp. 724-734, 2009.
- [74] S. Begum, M. U. Ahmed, P. Funk, N. Xiong, and B. Von Schéele, "A case-based decision support system for individual stress diagnosis using fuzzy similarity matching," Computational Intelligence, vol. 25, no. 3, pp. 180-195, 2009.
- [75] B. Yao and S. Li, "ANMM4CBR: a case-based reasoning method for gene expression data classification," Algorithms for Molecular Biology, vol. 5, no. 1, pp. 5-14, 2010.
- [76] D. X. Gu, C. Y. Liang, X. G. Li, S. L. Yang, and P. Zhang, "Intelligent technique for knowledge reuse of dental medical records based on case-based reasoning," Journal of medical systems, vol. 34, no. 2, pp. 213-222, 2010.
- [77] R. H. Lin and C. L. Chuang, "A hybrid diagnosis model for determining the types of the liver disease," Computers in Biology and Medicine, vol. 40, no. 7, pp. 665-670, 2010.
- [78] R. Jagannathan, S. Petrovic, A. McKenna, and L. Newton, "A fuzzy non-linear similarity measure for case-based reasoning systems for radiotherapy treatment planning," in Artificial Intelligence Applications and Innovations, IFIP Advances in Information and Communication Technology, vol. 339, pp. 112-119, 2010.
- [79] M. U. Ahmed, S. Begum, P. Funk, N. Xiong, and B. Von Schéele, "A multi-module case-based biofeedback system for stress treatment," Artificial Intelligence in Medicine, vol. 51, no. 2, pp. 107-115, 2011.
- [80] N. Douali, J. De Roo, E. I. Papageorgiou, and M. C. Jaulent, "Case Based Fuzzy Cognitive Maps (CBFCM): new method for medical reasoning: comparison study between CBFCM/FCM," in 2011 IEEE International Conference on Fuzzy Systems (FUZZ), pp. 844-850, 2011.
- [81] C. L. Chuang, "Case-based reasoning support for liver disease diagnosis," Artificial intelligence in medicine, vol. 53, no. 1, pp. 15-23, 2011.
- [82] S. Petrovic, N. Mishra, and S. Sundar, "A novel case based reasoning approach to radiotherapy planning," Expert Systems with Applications, vol. 38, no. 9, pp. 10759-10769, 2011.
- [83] M. van den Branden, N. Wiratunga, D. Burton, and S. Craw, "Integrating case-based reasoning with an electronic patient record system," Artificial Intelligence in Medicine, vol. 51, no. 2, pp. 117-123, 2011.
- [84] B. López et al., "eXiT* CBR: A framework for case-based medical diagnosis development and experimentation," Artificial intelligence in medicine, vol. 51, no. 2, pp. 81-91, 2011.
- [85] B. López et al., "System overview: Breast cancer prognosis through CBR," CBR in the Health Sciences, Workshop at the Twentieth

- International Conference on Case-Based Reasoning (ICCBR 2012), pp. 105-110, 2012.
- [86] M. U. Ahmed, S. Begum, and P. Funk, "A hybrid case-based system in clinical diagnosis and treatment," in 2012 IEEE-EMBS International Conference on Biomedical and Health Informatics (BHI), pp. 699-704, 2012.
- [87] S. Montani, G. Leonardi, A. Bottrighi, L. Portinale, and P. Terenziani, "Extending a time series retrieval tool to deal with sub-series matching: an application to the hemodialysis domain," in CBR in the Health Sciences, Workshop at the Twentieth International Conference on Case-Based Reasoning (ICCBR 2012), pp. 59-68, 2012.
- [88] A. Khelassi, and M. A. Chikh, "Cognitive Amalgam with a Fuzzy sets and case based reasoning for accurate cardiac arrhythmias diagnosis," in CBR in the Health Sciences, Workshop at the Twentieth International Conference on Case-Based Reasoning (ICCBR 2012), pp. 69-79, 2012.
- [89] C. Marling, R. Bunescu, J. Shubrook, and F. Schwartz, "System Overview: The 4 Diabetes Support System," in CBR in the Health Sciences, Workshop at the Twentieth International Conference on Case-Based Reasoning (ICCBR 2012), pp. 81-86, 2012.
- [90] J. M. Juarez et al., "Supporting Frontotemporal Dementia Protocols by CBR Graph Models," in Workshop Proceedings of the 20th International Conference on Case-Based Reasoning (ICCBR 2012), pp. 87-99, 2012.
- [91] M. U. Ahmed, S. Begum, and P. Funk, "System Overview on the Clinical Decision Support System for Stress Management," in Proceedings of the ICCBR 2012 Workshop on CBR in the Health Sciences, pp. 111-116, 2012.
- [92] M. U. Ahmed, A. M. Islam, and A. Loutfi, "A case-based patient identification system using pulseoximeter and a personalized health profile," in Proceedings of the ICCBR 2012 Workshop on CBR in the Health Sciences, pp. 117-127, 2012.
- [93] S. Begum, M. U. Ahmed, and S. Barua, "Multi-scale entropy analysis and case-based reasoning to classify physiological sensor signals," in Proceedings of the ICCBR 2012 Workshop on CBR in the Health Sciences, pp. 129-138, 2012.
- [94] V. E. Ekong, U. G. Inyang, and E. A. Onibere, "Intelligent decision support system for depression diagnosis based on neuro-fuzzy-CBR hybrid," Modern Applied Science, vol. 6, no. 7, pp. 79-88, 2012.
- [95] M. L. Huang, Y. H. Hung, W. M. Lee, R. K. Li, and T. H. Wang, "Usage of case-based reasoning, neural network and adaptive neuro-fuzzy inference system classification techniques in breast cancer dataset classification diagnosis," Journal of medical systems, vol. 36, no. 2, pp. 407-414, 2012.
- [96] S. Montani, G. Leonardi, S. Ghignone, and L. Lanfranco, "Flexible case-based retrieval for comparative genomics," Applied intelligence, vol. 39, no. 1, pp. 144-152, 2013.
- [97] S. Chattopadhyay, S. Banerjee, F. A. Rabhi, and U. R. Acharya, "A Case-Based Reasoning system for complex medical diagnosis," Expert Systems, vol. 30, no. 1, pp. 12-20, 2013.
- [98] A. Pla, B. López, P. Gay, and C. Pous, "eXiT* CBR. v2: Distributed case-based reasoning tool for medical prognosis," Decision Support Systems, vol. 54, no. 3, pp. 1499-1510, 2013.
- [99] Y. Leal et al., "Principal component analysis in combination with case-based reasoning for detecting therapeutically correct and incorrect measurements in continuous glucose monitoring systems," Biomedical Signal Processing and Control, vol. 8, no. 6, pp. 603-614, 2013.
- [100] D. Teodorović, M. Šelmić, and L. Mijatović-Teodorović, "Combining case-based reasoning with Bee Colony Optimization for dose planning in well differentiated thyroid cancer treatment," Expert Systems with Applications, vol. 40, no. 6, pp. 2147-2155, 2013.
- [101] J. Henriët, P. E. Leni, R. Laurent, and M. Salomon, "Case-Based Reasoning adaptation of numerical representations of human organs by interpolation," Expert Systems with Applications, vol. 41, no. 2, pp. 260-266, 2014.
- [102] D. A. Sharaf-El-Deen, I. F. Moawad, and M. E. Khalifa, "A new hybrid case-based reasoning approach for medical diagnosis systems," Journal of medical systems, vol. 38, no. 2, pp. 1-11, 2014.
- [103] Z. Yin et al., "A clinical decision support system for the diagnosis of probable migraine and probable tension-type headache based on case-based reasoning," The journal of headache and pain, vol. 16, no. 1, pp. 29, 2015.
- [104] A. Tyagi and P. Singh, "ACS: Asthma Care Services with the Help of Case Based Reasoning Technique," Procedia Computer Science, vol. 48, pp. 561-567, 2015.
- [105] G. Khussainova, S. Petrovic, and R. Jagannathan, "Retrieval with Clustering in a Case-Based Reasoning System for Radiotherapy Treatment Planning, 2015. (<http://dx.doi.org/10.1088/1742-6596/616/1/012013>).
- [106] R. M. Saraiva, J. Bezerra, M. Perkusich, H. Almeida, and C. Siebra, "A Hybrid Approach Using Case-Based Reasoning and Rule-Based Reasoning to Support Cancer Diagnosis: A Pilot Study," Studies in health technology and informatics, vol. 216, pp. 862-866, 2015.
- [107] S. Chakraborty, C. Pal, S. Chatterjee, B. Chakraborty, and N. Ghoshal, "Knowledge-Based System Architecture on CBR for Detection of Cholera Disease," Intelligent Computing and Applications, Advances in Intelligent Systems and Computing, vol. 343, pp. 155-165, 2015.
- [108] S. Nasiri, J. Zenkert, and M. Fathi, "A Medical Case-Based Reasoning Approach Using Image Classification and Text Information for Recommendation," Advances in Computational Intelligence, Lecture Notes in Computer Science, vol. 9095, pp. 43-55, 2015.
- [109] S. Banerjee and A. R. Chowdhury, "Case Based Reasoning in the Detection of Retinal Abnormalities Using Decision Trees," Procedia Computer Science, vol. 46, pp. 402-408, 2015.
- [110] X. Blanco, S. Rodríguez, J. M. Corchado, and C. Zato, "Case-based reasoning applied to medical diagnosis and treatment," Distributed Computing and Artificial Intelligence, Advances in Intelligent Systems and Computing, vol. 217, pp. 137-146, 2013.
- [111] I. Bichindaritz, "Solving safety implications in a case based decision-support system in medicine," in Proceedings of the Fifth International Conference on Case-based Reasoning Workshop on Case-Based Reasoning in the Health Sciences, pp. 178-183, 2003.

MRPPSim: A Multi-Robot Path Planning Simulation

Ebtehal Turki Saho Alotaibi, Hisham Al-Rawi

Computer Science Department, Al Imam Muhammad Ibn Saud Islamic University
Riyadh, SA

Abstract—Multi-robot path planning problem is an interesting problem of research having great potential for several optimization problems in the world. In multi-robot path planning problem domain (MRPP), robots must move from their start locations to their goal locations avoiding collisions with each other. MRPP is a relevant problem in several domains, including; automatic packages inside a warehouse, automated guided vehicles, planetary exploration, robotics mining, and video games. This work introduces MRPPSim; a new modeling, evaluation and simulation tool for multi-robot path planning algorithms and its applications. In doing so, it handles all the aspects related to the multi-robot path planning algorithms. Through its working, MRPPSim unifies the representation for the input. This algorithm provides researchers with a set of evaluation models with each of them serving a set of objectives. It provides a comprehensive method to evaluate and compare the algorithm's performance to the ones that solve public benchmark problems inas shown in literature. The work presented in this paper also provides a complete tool to reformat and control user input, critical small benchmark, biconnected, random and grid problems. Once all of this is performed, it calculates the common performance measurements of multi-robot path planning algorithms in a unified way. The work presented in this paper animates the results so the researchers can follow their algorithms' executions. In addition, MRPPSim is designed as set of models, each is dedicated to a specific function, this allows new algorithm, evaluation model, or performance measurements to be easily plugged into the simulator.

Keywords—component; simulation; modeling; evaluation; multi-robot path planning problem; performance measurements

I. INTRODUCTION

Formally, Multi-robot path planning problem (MRPP) consists of a graph and a set of robots. In such problems, each robot has to reach its destination in the minimum time with minimum number of moves. MPP is a relevant problem in a wide range of domains, including; automatic packages inside a warehouse [2], automated guided vehicles [3], planetary exploration [4], robotics mining [5], and video games [6].

There are several variants of MRPP algorithms in the literature with their specialized strengths. However, to have clear vision about these algorithms' performance, these need to be evaluated on a unified robust tool. The multi-robot path planning simulation (MRPPSim) is a modeling, evaluation and simulation tool for multi-robot path planning algorithms and its applications. It handles all the aspects related to the multi-robot path planning algorithms. Hence, the researchers need only to worry about their algorithms. MRPPSim aims to provide the researcher set of evaluation models, each of them serves one of the following objectives;

Objective.1: Test and track the algorithm's behavior for specific cases in fully controlled problems.

Objective.2: Track the algorithm's behavior and compare its performance with the algorithms that are already evaluated on predefined small critical problems in [7].

Objective.3: Test the algorithm's behavior on very large graphs when the occupying ratio (robots number/vertices count) increases.

Objective.4: Compare the algorithm's performance to the performance of the algorithms already tested in publically available large scale problems [1] such as [7-9].

Objective.5: Compare the algorithm's performance to the performance of the algorithms solves biconnected graphs [10], [7, 8]

Objective.6: Test the algorithm's behavior on fixed biconnected graph's size when the occupying ratio increases.

Objective.7: Evaluate the algorithm's performance against the algorithms that solve random graphs.

Objective.8: Track the algorithm's behavior on fixed random graph's size when the occupying ratio increases.

Objective.9: Compare the algorithm's performance to the algorithms that solve grid graphs [7, 8, 10].

Objective.10: Test the algorithm behavior on fixed grid graph's size when the occupying ratio increases.

Objective.11: Evaluate the algorithm's performance on biconnected graphs of fixed occupying ratio when the graph's size increases.

Objective.12: Evaluate the algorithm's performance on random graphs of fixed occupying ratio when the graph's size increases.

Objective.13: Evaluate the algorithm's performance on grid graphs of fixed occupying ratio when the graph's size increases.

This paper is organized as follows; after this introduction, the problem is defined in Section II. In Section III, the multi-robot path planning simulation MRPPSim is introduced. In Section IV, MRPPSim objectives are discussed in details. Finally, conclusions and future works are presented in Section V.

II. PROBLEM STATEMENT

Going through the literature related to MRPP algorithm, we found an urgent need of having a graph-based multi-robot path

planning simulator that can cover different types of scenarios and problems. The study of all available algorithms implementations and its performance measurements calculations as well as essential. The simulation is to provide a ready implementation of state-of-art algorithms in the field. During this study, the work started by looking into iRRT simulator [11]. iRRT is a simple Java program for simulating that is widely used for robotics path planning algorithm known as Rapidly-exploring Random Tree or RRT. This algorithm was developed by Sertac Karaman et al. [12] and it works for a single-robot configuration. During the process, several extensions were implemented to fit multi-robot RRT requirements. However, the representation of the robots environment was limited to being continuous environment, while we were also interested in graph-based algorithms. This would enable working with problem scenarios and variations that have not been catered for previously.

III. METHODOLOGY

The proposed work, i.e. MRPPSim is written as an open source C++ code¹ designed to be fully modularized so that researchers can have the ability to plug any modifications.

A. Input

The input parameter for MRPPSim can be classified based on the simulation model which will be described in the next section. In our implementation, the user is initially required to select the simulation model and the algorithm to be used. Based on that, the user can enter or select the main two input for any algorithm. These inputs include; the representation of the environment in the form of undirected graph; $G(V,E)$, whatever the simulation model or the algorithm, the graph that would be sent to the algorithm in XML format representation describing numbered vertices V , and the linking edges E (Fig.1). The second input is the instance; $I(R, Locations)$, which is the representation of the number of robots; R , and robots' configuration within the environment; $Locations$, the robots configuration is the definition of the robots start and goal locations in graph's vertices term. (Fig.2).

```
<?xml version="1.0" encoding="UTF-8"?>
<graphml xmlns="http://graphml.graphdrawing.org/xmlns"
xmlns:xsi="http://www.w3.org/2001/XMLSchema-instance"
xsi:schemaLocation="http://graphml.graphdrawing.org/xmlns
http://graphml.graphdrawing.org/xmlns/1.0/graphml.xsd">
<key id="key0" for="node" attr.name="Coordinate"
attr.type="string" />
<key id="key1" for="edge" attr.name="Weight"
attr.type="double" />
<graph id="G" edgedefault="undirected"
parse.nodeids="canonical" parse.edgeids="canonical"
parse.order="nodesfirst">
<node id="n0">
<data key="key0">0.0 0.0 0.0</data>
</node>
<node id="n1">
<data key="key0">1.0 0.0 0.0</data>
</node>
<node id="n2">
<data key="key0">2.0 0.0 0.0</data>
</node>
<edge id="e0" source="n0" target="n1">
<data key="key1">1</data>
</edge>
<edge id="e2" source="n1" target="n2">
<data key="key1">1</data>
</edge>
```

```
</edge>
<edge id="e3 source="n2" target="n0">
<data key="key1">1</data>
</edge>
</graph>
</graphml>
```

Fig. 1. The environment representation is a graph in xml format

```
graph =//Graph.xml
agent: start = 0, goal = 2
agent: start = 2, goal = 3
```

Fig. 2. The robots (agents) start and goal locations (instance) representation is a text file in specific format

B. Simulation models

As already mentioned, MRPPSim is written as a C++ code that offers a set of simulation models, Each of these can serve as set of objectives in our problem definition. This section will present an overview of each simulation model in detail starting with the user input until the algorithm inputs which is the graph and the instance, described earlier, in the following form;

AlgorithmX (G, I)

1) Fully controlled model

In this selection, the user will be able to set the attributes of both graph and the instance to be tested. Once the user enters the graph G (user defined, user defined) attributes and the instance I (user defined) descriptions, MRPPSim then converts the input to the form defined in the subsection A, and send these inputs to the selected algorithm as;

AlgorithmX (G (user defined), I (user defined)).

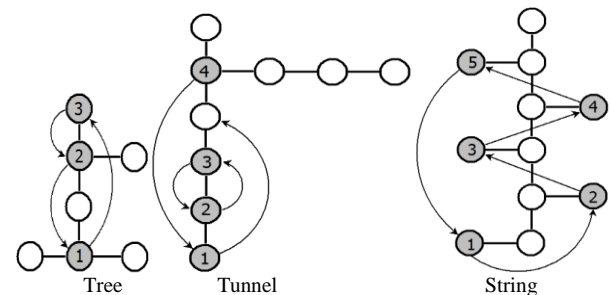
The aim of this model is to provide the user with the ability to track specific cases in fully controlled problem (Objective.1).

2) Small benchmark model

In order to cater for a wider class of instances, MRPPSim has defined six benchmark problems evaluated in [7], a tree with cycle leaves problem evaluated in [11] and a biconnected graph in [10](Fig.3). It is noteworthy that besides the graph G (ready V , ready E), the instance is also defined in these problems as I (ready R , ready $locations$). Therefore, the algorithm input would be;

AlgorithmX(G (ready V , ready E), I (ready R , ready $locations$)).

The aim of this model is to get the user with the ability to compare the algorithm with already evaluated algorithm on these problems (Objective.2).



¹ <https://pushandspin.wordpress.com/source-code/>

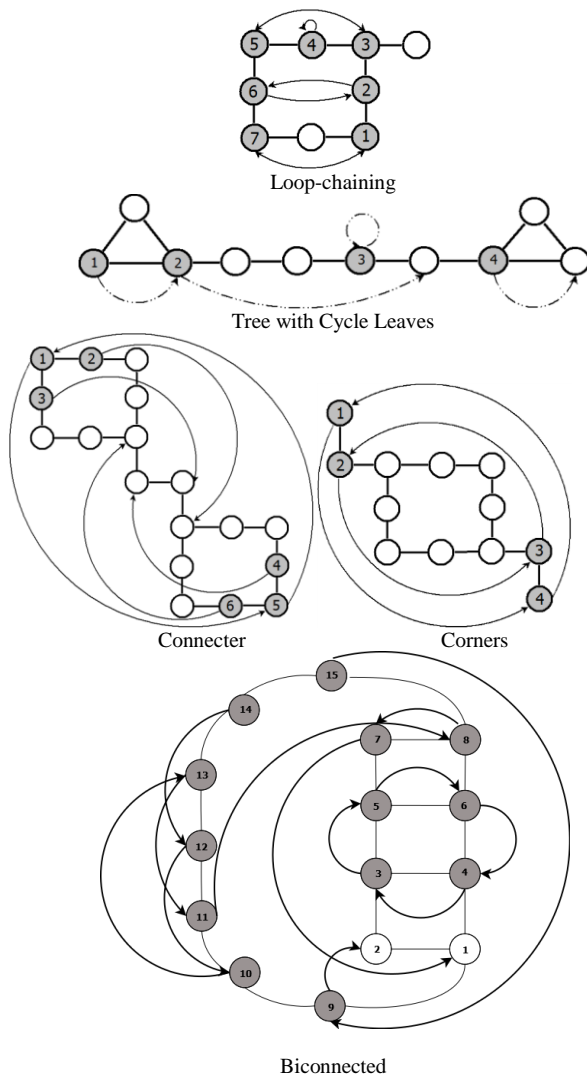


Fig. 3. Small benchmark problems

3) Public benchmark model

Sturtevant in his paper [1] has presented a new repository that has been placed online² to improve the evaluation of grid-based problems. The repository allows researchers to use the same problems and test sets, thereby increasing the reproducibility of published results. In the repository, two main sets are described; Commercial Game Benchmarks and Artificial Benchmarks. Each map has been coded in a way to be parsed. The maps are attached with a set of scenarios describing the instances. However, this repository requires a little modification in order to be applicable to the chosen problem domain. This is due to the fact that in some scenarios, there would be multiple robots on the same start and/or goal position. Consequently, instead of using attached scenarios, we have designed random generator. It is used to generate any number of robots for the given graph randomly. The procedures for generating random instances is;

1. Parameter: n : the number of vertices, r : the number of robots.

² <http://movingai.com/benchmarks/>

2. For each r ;
 1. Select random node s such that $s \notin \text{start set}$
 2. Set s as starting vertex of r .
 3. $\text{start set} = \text{start set} \cup s$
 4. Select random vertex g such that $s \notin \text{goal set}$
 5. Set s as goal vertex of r .
 6. $\text{goal set} = \text{goal set} \cup g$.

In the Commercial Game Benchmarks, the maps contain areas of land or water and the robots can only move on water. (Fig.4,5). Moreover, in the Artificial Benchmarks, the maps contain areas of passageways and walls. We have designed a parser to read the coded maps and transform them into graphs with each element in the map converted to vertex if it not obstacles (lands/walls). This results in graphs that are characterized by a large set of connected vertices. The parser generates a fixed graph representation; $G(\text{coded } V, \text{coded } E)$, for every coded map. In addition set of instances describing the start and goal locations would also be generated for each graph randomly by the generator given the number of robots R , minimum number of robots, maximum number of robots and the step size; $I(R, \sum_{i=0}^{\max} \text{min} + (i * \text{StepSize})$, random locations). Hence, The algorithms input would be;

AlgorithmX ($G(\text{coded } V, \text{coded } E)$,

$I(R, \sum_{i=0}^{\max} \text{min} + (i * \text{StepSize}), \text{random locations})$).

The aim of this model is to test the algorithm behavior on very large graphs when the occupying ratio (robots number/vertices count) increases (Objective.3) and to compare the algorithm's performance to the performance of the algorithms already tested in these public problems (Objective.4).

4) One-Factor controlled model

While studying Multi-Robot Path Planning problem, we came across two critical factors affecting the algorithms' performance. These are the size of the graph and the occupying ratio (number of robots/ number of vertices). In this section we will overview two type of models; each type controlling one of these critical factor and randomize the other in order to generate graphs and instance files.

a) Fixed-Graph with Variable-Robot model

In this model, number of instances are to be generated for the same graph size. After setting the graph size, the user can set the minimum number of robots, maximum number of robots and the step size to generate required number of instances varying in the occupying ratio.

BICONNECTED GRAPH

The biconnected graph is a connected graph on two or more vertices having no articulation vertices. MRPPSim provides Biconnected graph generator representing $G(V, E_{bi})$ with the number of vertices; V . The generator will generate the biconnected topology by inserting edges E_{bi} between these vertices. In this version of MRPPSim we have used the same biconnected graph generator in [10]. It generates random biconnected graphs conforming to three parameters; h the number of handles, C_0 the size of the initial cycle, and l the maximum handle length (Fig.6).



Fig. 4. AR0306SR map of Baldurs Gate II (left), its coded map (right)



Fig. 5. AR0603SR map of Baldurs Gate II (left), its coded map (right)

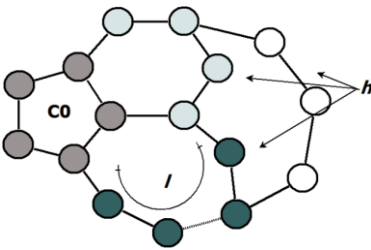


Fig. 6. initial cycle (C0), maximum handle length (l) and number off handles (h) in Surynek grap

Since this model is FG-VR model, the instances I need to be generated randomly. The user can set the minimum number of robots, maximum number of robots and the step size to generate a number of instances varying in the occupying ratio; $\sum_{i=0}^{max} min + (i * StepSize)$. However, the robots location; $locations$ need to be randomized totally. Furthermore, The algorithm input would be;

AlgorithmX ($G(h, C_0, l)$,

$I(\sum_{i=0}^{max} min + (i * StepSize), random\ locations)$).

The aim of this model is to provide the researcher with the ability to compare the algorithm's performance to the performance of the algorithms thereby meeting objective 5 and 6 mentioned in earlier sections.

RANDOM GRAPH

MRPPSim provides random graph generator; $G(V,E)$ given the number of vertices; V , the generator would generate the random topology by inserting edges E_{rand} between these vertices. Since this model is FG-VR model, the instances I will be generated randomly. As has been described earlier, the user can set the minimum number of robots, maximum number of robots and the step size to generate number instances varying in the occupying ratio; $\sum_{i=0}^{max} min + (i * StepSize)$, the robots location; $locations$ will be randomized totally. Therefore, the algorithm input would be;

AlgorithmX ($G(V,E_{rand})$,

$I(\sum_{i=0}^{max} min + (i * StepSize), random\ locations)$)

The aim of this model is to provide the researcher with the ability to evaluate the algorithm performance against the performance of algorithms already existing that solve random graphs (Objective.7) and to track algorithm behavior on fixed random graph's size when the occupying ratio increases. (Objective.8).

GRID GRAPH

MRPPSim provides random graph generator; $G(V,E)$ given the number of vertices; V , the generator would generate the random topology by inserting edges E_{grid} between these vertices. In this version of MRPPSim, We have used the same generator in [10] to generate grid instances of $n \times n$ size with a constant value of the parameter $(h, C_0, l) = G((n-1)^2-1, 4, 4)$. Since this model is FG-VR model, the instances I would be generated randomly. On the other hand, the user can set the minimum number of robots, maximum number of robots and the step size to generate a number of instances varying in the occupying ratio; $\sum_{i=0}^{max} min + (i * StepSize)$, the robots location; $locations$ will be randomized totally. The algorithm input thus would be;

AlgorithmX ($G((n-1)^2-1, 4, 4)$,

$I(\sum_{i=0}^{max} min + (i * StepSize), random\ locations)$).

The aim of this model is to get the researcher with the ability to compare the algorithm's performance to the performance of the algorithms that solve grid graphs, [8], [7]. (Objective.9) and to evaluate the grid graphs when the occupying ratio increase (Objective.10).

b) Fixed-Robot with Variable-Graph model

In this model, a number of graphs will be generated for the same occupying ratio (number of robots/number of vertices). After setting the robot number, the user can set the minimum number of vertices, maximum number of vertices and the step size to generate a number of graphs varying in their size.

BICONNECTED GRAPH

Since we have used the same biconnected graph generator as presented in [10], the graph would be generated according to a single variable x that can range from the given minimum number of vertices to the given maximum number of vertices by the given step size. The variable x would be used for all three parameters (number of handles; h , initial cycle size; C_0 , and maximum handle length; l). The graph size V hence would be C_0+h*l . The number of empty vertices would be kept fixed to the given occupying ratio. Hence, the instance would be $I(occupying\ ratio * V, random\ location)$. The algorithm input will be:

AlgorithmX ($G(x, x, x)$, $I(occupying\ ratio *(x+x*x), random\ location)$),

such that, $x = \sum_{i=0}^{max} min + (i * StepSize)$.

The aim of this model is to get the researcher with the ability to evaluate algorithm's performance on biconnected graphs of fixed occupying ratio when the graph's size increases. (Objective.11).

RANDOM GRAPH

After the researcher has set the occupying ratio, minimum number of vertices, maximum number of vertices and the step size, the random generator would automatically generate graph $G (V_i = \sum_{i=0}^{max} min + (i * StepSize), E_{rand})$. The instance would be $I (V_i * occupying\ ratio, random\ locations)$. Hence, the algorithm input would be:

AlgorithmX (G($V_i = \sum_{i=0}^{max} min + (i * StepSize)$, E_{rand}),
 $I (V_i * occupying\ ratio, random\ locations)$).

The aim of this model is to get the researcher with the ability to evaluate the algorithm performance on random graphs of fixed occupying ratio when the graph's size increases. (Objective.12).

GRID GRAPH

After the researcher has set the occupying ratio, the minimum number of vertices, maximum number of vertices and the step size. MRPPSim would automatically generate different grids $G (V_i = \sum_{i=0}^{max} min + (i - 1)^2 - 1, 4, 4)$, E_{grid} with the same occupying ratio. The instances would be $I (V_i * occupying\ ratio, random\ locations)$. Therefore, the algorithm input would be;

AlgorithmX (G($\sum_{i=0}^{max} min + (i - 1)^2 - 1, 4, 4$), E_{grid}),
 $I(V_i * occupying\ ratio, random\ locations)$).

The aim of this model is to evaluate the algorithm performance on grid graphs of fixed occupying ratio when the graph's size increases (Objective.13).

C. Output

The most common performance measurements of multi-robot path planning algorithms in [7, 8, 10] are;

1) The path length

Objective.1: We will track the execution of Push and Swap algorithm³ on Θ -shape graph with $G(7,8)$ and two robots where the goal location of each one is the start location of the other $I(2,(2,5),(5,2))$

Even though some algorithms in literature have implemented parallel implementation, our contribution in this work is to unify the performance parameters allowing the researchers to calculate the path length as the total number of sequential moves.

2) The CPU time

The execution time has been calculated as the real time between the algorithm start time to the end time. In addition, we have ignored the execution time of the preprocess of the algorithms.

3) The makespan

Makespan is the number of time steps required to get all robots to their destination.

4) The optimized path length

These measurements carry any improvement of path length on the original algorithm.

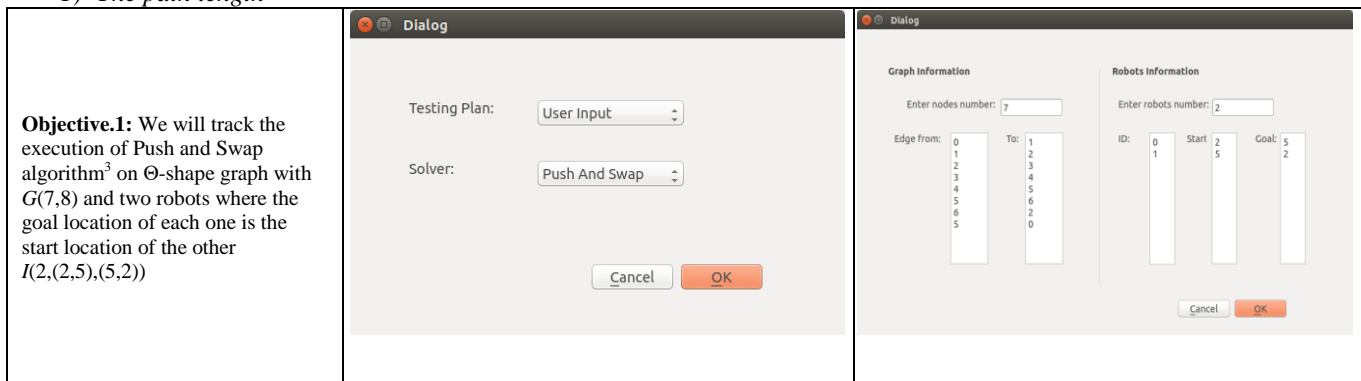
5) The optimized makespan

These measurements carry any improvement of makespan on the original algorithm.

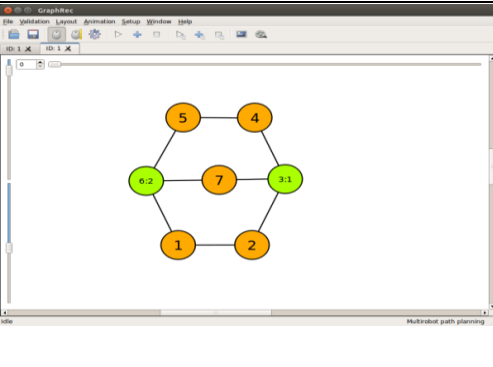
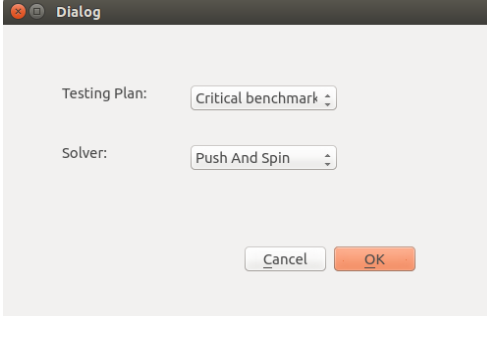
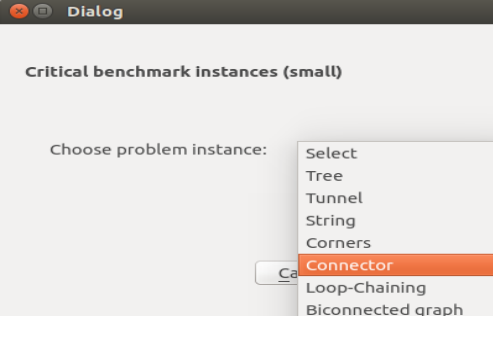
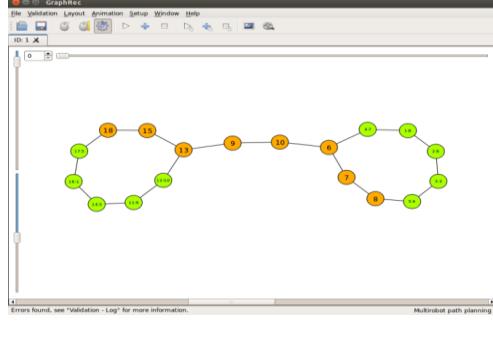
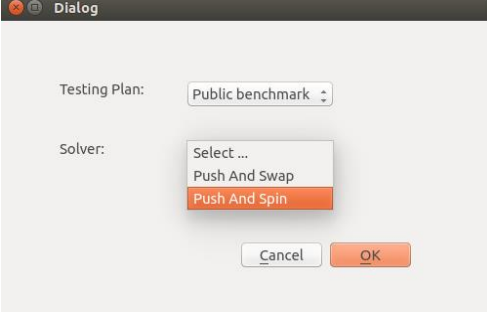
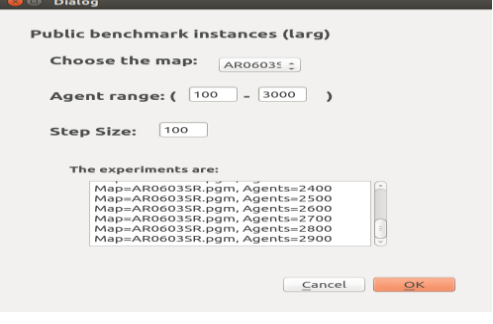
The animation results would be written in the format readable to GraphRec simulator [14]. On its completion, all these results would be stored in the experiment folder. The researchers can then track the movement and the execution of the algorithm by running the animation results in GraphRec.

IV. RESULTS

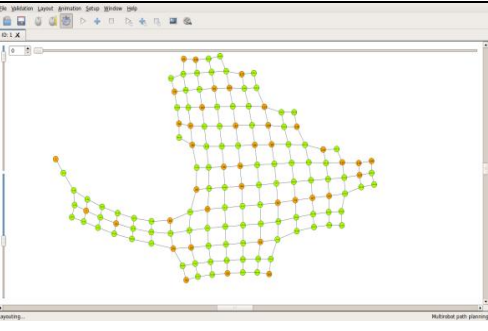
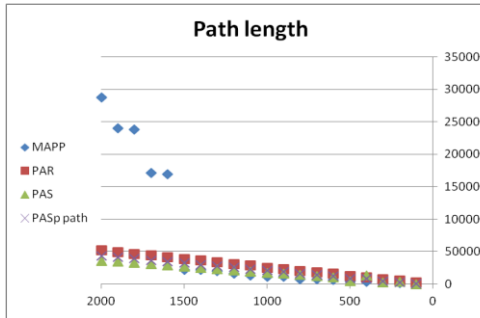
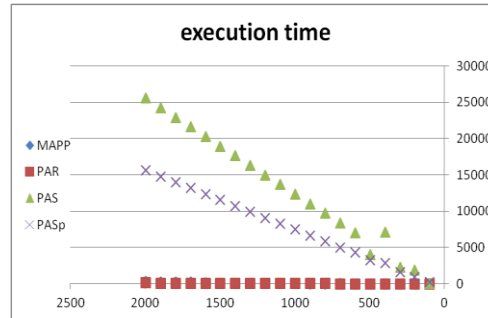
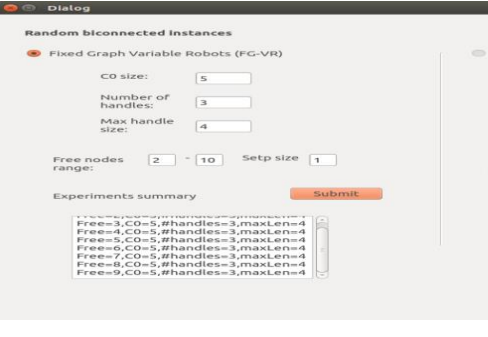
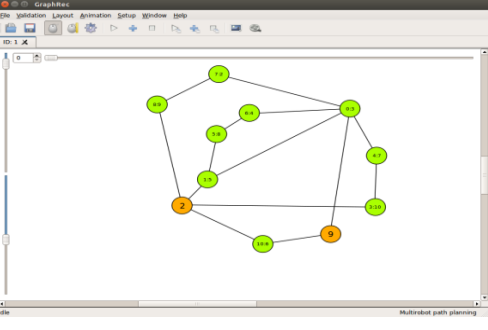
The results of this work are aimed to verify whether the objectives described earlier are satisfied or not. In this section, we will recall every objective and show the ability of MRPPSim to achieve it.

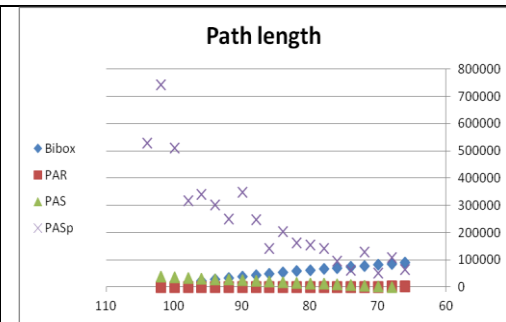
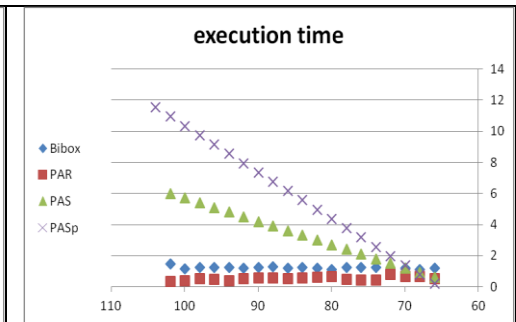
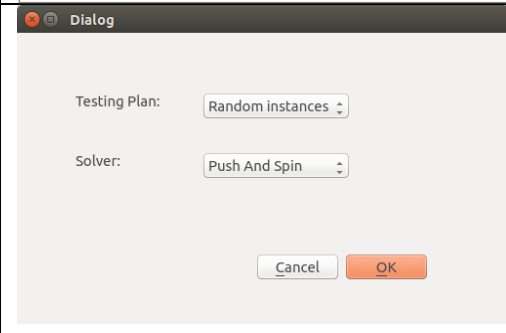
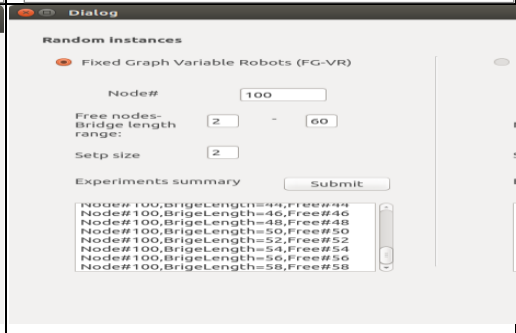
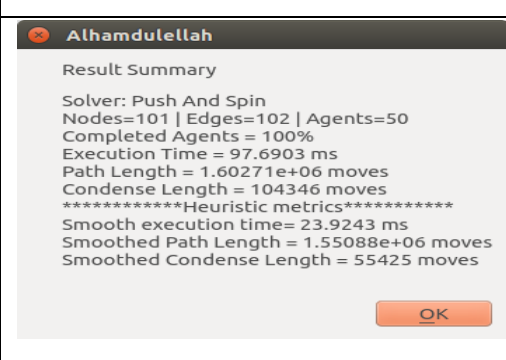
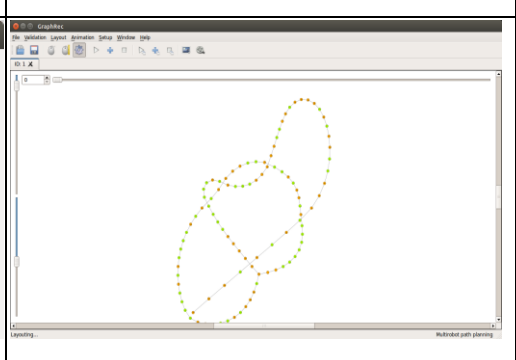
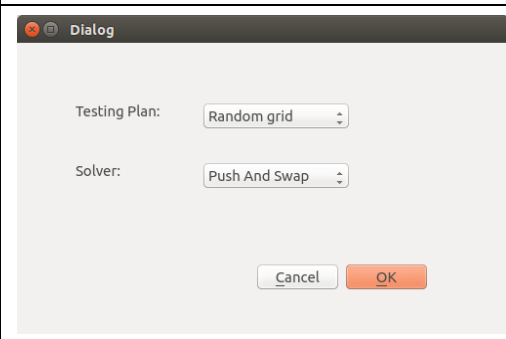
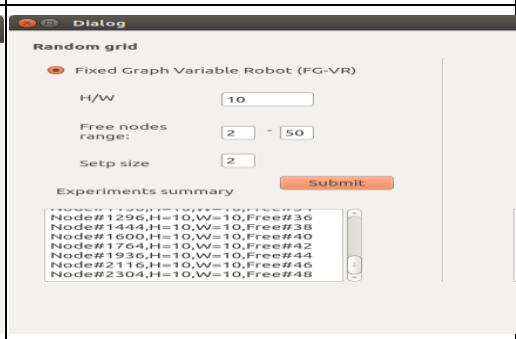
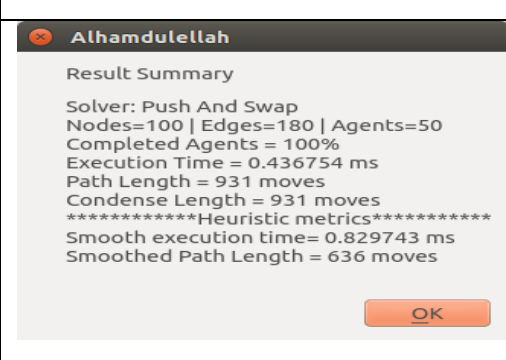
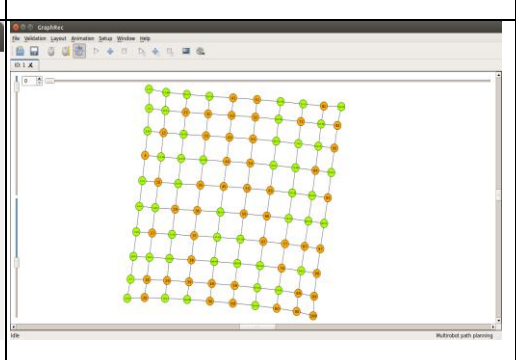


³ One of the implemented algorithm in MRPPSim

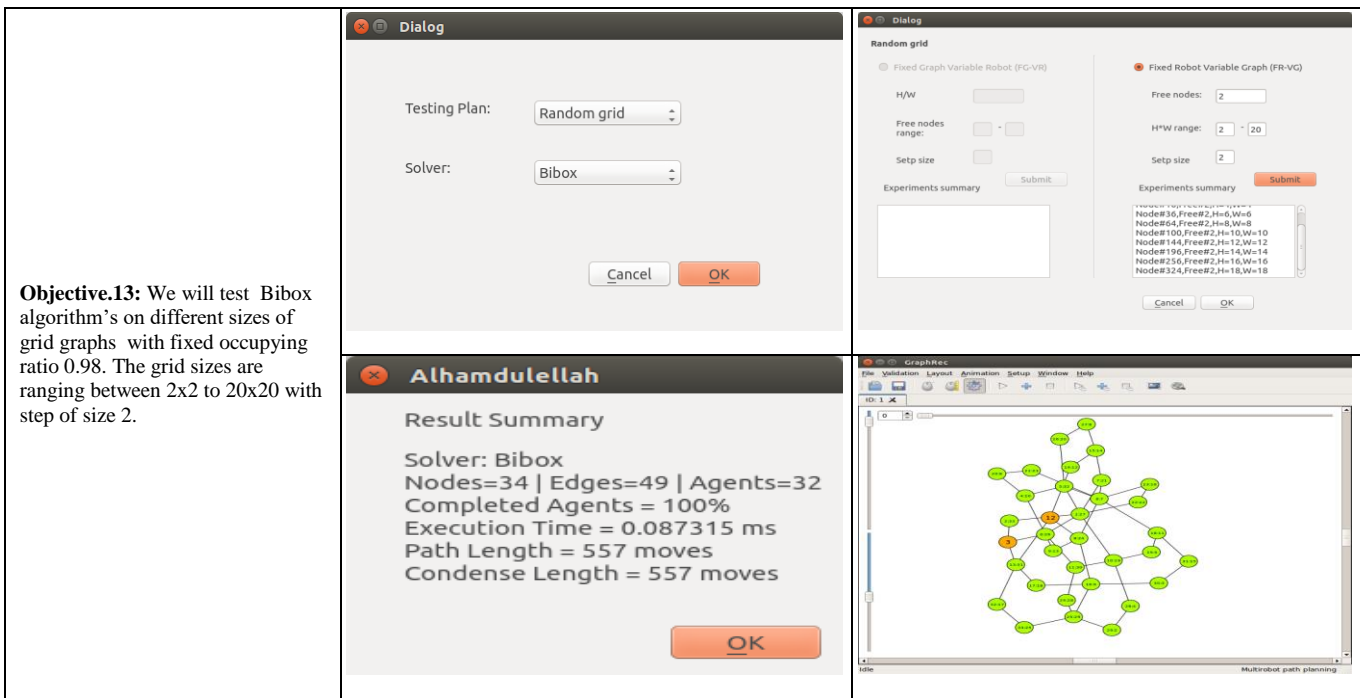
		
<p>Objective.2: We will track the execution of Push and Swap algorithm⁴ on Connector problem.</p>		
		
<p>Objective.3: We will evaluate the performance of Push and Spin algorithm on public Commercial game benchmark problem AR0603SR with 57873 vertices and number of robots ranging between 100 to 3000 with step size 100.</p>		

⁴ One of the implemented algorithm in MRPPSim

	 <p>Alhamdulillah</p> <p>Result Summary</p> <p>Solver: Push And Spin Nodes=57873 Edges=103204 Agents=600 Completed Agents = 100% Execution Time = 4300.87 ms Path Length = 122812 moves Condense Length = 69592 moves *****Heuristic metrics***** Smooth execution time= 2.56794 ms Smoothed Path Length = 120118 moves Smoothed Condense Length = 66948 moves</p> <p>OK</p>	
<p>Objective.4: We will compare the performance of Push and Spin algorithm to the performance of Push and Swap, Push and Rotate and MAPP algorithms on public Commercial game benchmark problem AR0307SR with a number of robots ranging from 200 to 2000 with step size 100</p>	 <p>path length</p> <p>Y-axis: 0 to 900,000 X-axis: 2500 to 0</p> <p>Legend: path (blue diamonds)</p>	 <p>execution time</p> <p>Y-axis: 0 to 8,000 X-axis: 2500 to 0</p> <p>Legend: time (blue diamonds)</p>
<p>Objective.5,6: Bibox is the complete algorithm for biconnected graphs. We will track the behavior of Bibox algorithm on a biconnected graph with initial cycle=5, number of handles=4 and maximum handle length=3 when the number of free vertices ranging between 2 to 10 with a step of size 1. Then, we will compare that results to the results of Push and Swap, Push and Rotate and Push and Spin algorithms on the same experiments settings.</p>	 <p>Dialog</p> <p>Testing Plan: Random biconnect</p> <p>Solver: Bibox</p> <p>Cancel OK</p>	 <p>Dialog</p> <p>Random biconnected Instances</p> <p>Fixed Graph Variable Robots (FG-VR)</p> <p>CO size: 5 Number of handles: 3 Max handle size: 4</p> <p>Free nodes range: 2 - 10 Setp size 1</p> <p>Submit</p> <p>Experiments summary</p> <p>Free=3,CO=5,#handles=3,maxLen=4 Free=4,CO=5,#handles=3,maxLen=4 Free=5,CO=5,#handles=3,maxLen=4 Free=6,CO=5,#handles=3,maxLen=4 Free=7,CO=5,#handles=3,maxLen=4 Free=8,CO=5,#handles=3,maxLen=4 Free=9,CO=5,#handles=3,maxLen=4</p>
	 <p>Alhamdulillah</p> <p>Result Summary</p> <p>Solver: Bibox Nodes=11 Edges=14 Agents=9 Completed Agents = 100% Execution Time = 0.01234 ms Path Length = 127 moves Condense Length = 127 moves</p> <p>OK</p>	

	 <p>Path length</p> <p>Legend: Bibox (blue diamond), PAR (red square), PAS (green triangle), PASp (purple cross)</p>	 <p>execution time</p> <p>Legend: Bibox (blue diamond), PAR (red square), PAS (green triangle), PASp (purple cross)</p>
<p>Objective.7,8: Push and Spin algorithm assumes to solve any random solvable graph, where the solvable graphs are any graph with a number of empty vertices equal the longest bridge. Since Push and Spin algorithm is the one which able to solve such instances, we will track its execution on a graph with 100 vertices and the number of free vertices ranging between 2 to 60 with step of size 2.</p>	 <p>Dialog</p> <p>Testing Plan: Random instances</p> <p>Solver: Push And Spin</p> <p>Buttons: Cancel, OK</p>	 <p>Dialog</p> <p>Random Instances</p> <p>Fixed Graph Variable Robots (FG-VR)</p> <p>Node#: 100</p> <p>Free nodes-Bridge length range: 2 - 60</p> <p>Setp size: 2</p> <p>Submit</p> <p>Experiments summary</p> <pre> Node# 100, BridgeLength=46, Free#46 Node# 100, BridgeLength=48, Free#48 Node# 100, BridgeLength=50, Free#50 Node# 100, BridgeLength=52, Free#52 Node# 100, BridgeLength=54, Free#54 Node# 100, BridgeLength=56, Free#56 Node# 100, BridgeLength=58, Free#58 </pre>
	 <p>Alhamdulellah</p> <p>Result Summary</p> <p>Solver: Push And Spin Nodes=101 Edges=102 Agents=50 Completed Agents = 100% Execution Time = 97.6903 ms Path Length = 1.60271e+06 moves Condense Length = 104346 moves *****Heuristic metrics***** Smooth execution time= 23.9243 ms Smoothed Path Length = 1.55088e+06 moves Smoothed Condense Length = 55425 moves</p> <p>OK</p>	 <p>Graphical visualization of a path on a graph.</p>
<p>Objective.9,10: We will track Push and Swap algorithm execution on a graph of size 10x10 and number of free vertices ranging between 2 to 50 with a step of size 2. Then, we will compare that results to the results of Push and Rotate, Push and Spin and Bibox algorithms on the same experiments settings.</p>	 <p>Dialog</p> <p>Testing Plan: Random grid</p> <p>Solver: Push And Swap</p> <p>Buttons: Cancel, OK</p>	 <p>Dialog</p> <p>Random grid</p> <p>Fixed Graph Variable Robot (FG-VR)</p> <p>H/W: 10</p> <p>Free nodes range: 2 - 50</p> <p>Setp size: 2</p> <p>Submit</p> <p>Experiments summary</p> <pre> Node# 1296, H=10, W=10, Free#36 Node# 1444, H=10, W=10, Free#38 Node# 1600, H=10, W=10, Free#40 Node# 1764, H=10, W=10, Free#42 Node# 1936, H=10, W=10, Free#44 Node# 2116, H=10, W=10, Free#46 Node# 2304, H=10, W=10, Free#48 </pre>
	 <p>Alhamdulellah</p> <p>Result Summary</p> <p>Solver: Push And Swap Nodes=100 Edges=180 Agents=50 Completed Agents = 100% Execution Time = 0.436754 ms Path Length = 931 moves Condense Length = 931 moves *****Heuristic metrics***** Smooth execution time= 0.829743 ms Smoothed Path Length = 636 moves</p> <p>OK</p>	 <p>Graphical visualization of a path on a 10x10 grid.</p>

<p>Objective.11: We will test Push and Spin algorithm's on different sizes of biconnected graphs with a fixed occupying ratio 0.98. The graphs sizes are ranging between (initial cycle, number of handles, maximum handle length)=(4,4,4) to (100,100,100) with step of size 4.</p>		
<p>Objective.12: We will track the execution of Push and Spin algorithm's on different sizes of random graphs with a fixed occupying ratio, 0.98. The graphs sizes is ranging between 5 to 100 with step of size 5.</p>		



Objective.13: We will test Bibox algorithm's on different sizes of grid graphs with fixed occupying ratio 0.98. The grid sizes are ranging between 2x2 to 20x20 with step of size 2.

V. CONCLUSION AND FUTURE WORKS

As can be observed, the MRPP simulator provides complete simulation/evaluation tool for offline multi-robot path planning. Its major strength is its ability to provide the algorithms imposed graph representation for its environment. MRPP allows the researchers to;

- Test and track the algorithm's behavior for specific cases in fully controlled instances.
- Track the algorithm's behavior and compare its performance with the algorithms that already evaluated on predefined small critical instances in [7].
- Test the algorithm behavior on very large graphs when the occupying ratio (robots number/vertices count) increases.
- Compare the algorithm performance to the algorithms already tested in public large problems [1] such as [7-9].
- Compare the algorithm's performance to the performance of algorithms solves biconnected graphs [10], [7, 8].
- Test the algorithm behavior on fixed biconnected graph's size when the occupying ratio increases.
- Evaluate the algorithm performance against the algorithms solves random graphs.
- Track the algorithm behavior on fixed random graph's size when the occupying ratio increases.
- Compare the algorithm's performance to the performance of algorithms solves grid graphs [7, 8, 10].

- Test the algorithm behavior on fixed grid graph's size when the occupying ratio increases.
- Evaluate the algorithm performance on biconnected graphs of fixed occupying ratio when the graph's size increases.
- Evaluate the algorithm performance on random graphs of fixed occupying ratio when the graph's size increases.
- Evaluate the algorithm performance on grid graphs of fixed occupying ratio when the graph's size increases.
- Plug new simulation model, MRPP algorithm implementation or performance measurement calculation.

Future work may include designing secure database, reporting set of experiments using different types of diagrams and adding new evaluation algorithms.

REFERENCES

- [1] N. R. Sturtevant, "Benchmarks for grid-based pathfinding," Computational Intelligence and AI in Games, IEEE Transactions on, vol. 4, pp. 144-148, 2012.
- [2] E. Guizzo, "Three Engineers, Hundreds of Robots, One Warehouse," IEEE Spectr., vol. 45, pp. 26-34, 2008.
- [3] K. Dresner and P. Stone, "A multiagent approach to autonomous intersection management," Journal of Artificial Intelligence Research, pp. 591-656, 2008.
- [4] J. Leitner, "Multi-robot cooperation in space: A survey," in Advanced Technologies for Enhanced Quality of Life, 2009. AT-EQUAL'09., 2009, pp. 144-151.
- [5] J. M. Roberts, E. S. Duff, and P. I. Corke, "Reactive navigation and opportunistic localization for autonomous underground mining vehicles," Information Sciences, vol. 145, pp. 127-146, 2002.
- [6] D. Nieuwenhuisen, A. Kamphuis, and M. H. Overmars, "High quality navigation in computer games," Science of Computer Programming, vol. 67, pp. 91-104, 2007.

- [7] R. Luna and K. E. Bekris, "Push and swap: Fast cooperative path-finding with completeness guarantees," in IJCAI, 2011, pp. 294-300.
- [8] B. d. Wilde, A. W. ter Mors, and C. Witteveen, "Push and Rotate: a Complete Multi-agent Pathfinding Algorithm," Journal of Artificial Intelligence Research, pp. 443-492, 2014.
- [9] K.-H. C. Wang and A. Botea, "Mapp: a scalable multi-agent path planning algorithm with tractability and completeness guarantees," Journal of Artificial Intelligence Research, pp. 55-90, 2011.
- [10] P. Surynek, "A novel approach to path planning for multiple robots in bi-connected graphs," in Robotics and Automation, 2009. ICRA'09. IEEE International Conference on, 2009, pp. 3613-3619.
- [11] E. T. S. Alotaibi and H. Al-Rawi, "Multi-Robot Path-Planning Problem for a Heavy Traffic Control Application: A Survey International Journal of Advanced Computer Science and Applications(IJACSA),", International Journal of Advanced Computer Science and Applications(IJACSA), vol. 7, p. 10, 1,7,2016 2016.
- [12] S. Karaman and E. Frazzoli, "Sampling-based algorithms for optimal motion planning," The International Journal of Robotics Research, vol. 30, pp. 846-894, 2011.
- [13] D. Kornhauser, G. Miller, and P. Spirakis, Coordinating pebble motion on graphs, the diameter of permutation groups, and applications: IEEE, 1984.
- [14] P. Koupy, "Visualization of problems of motion on a graph," BSc, Department of Theoretical Computer Science and Mathematical Logic, Charles University in Prague, Faculty of Mathematics and Physics, Prague, 2010.

Software Design Principles to Enhance SDN Architecture

Iyad Alazzam

Department of Computer
Information Systems
Yarmouk University, Irbid, Jordan

Izzat Alsmadi

Department of Computer Science,
University of New Haven, West
Haven, CT, USA

Khalid M.O Nahar

Department of Computer Science
Yarmouk University,
Irbid, Jordan

Abstract—SDN as a network architecture emerged on top of existing technologies and knowledge. Through defining the controller as a software program, SDN made a strong connection between networking and software engineering. Traditionally, network programs were vendor specific and embedded in hardware switches and routers. SDN focuses on isolation between control and forwarding or data planes. However, in the complete SDN network, there are many other areas (i.e. CPU, memory, hardware, bandwidth and software). In this paper, we propose extending SDN architecture and propose isolation layers with the goal of improving the overall network design. Such flexible architecture can support future evolution and changes without the need to significantly change original components or modules.

Keywords—component; SDN; OpenFlo; Software design; SDN architecture; Design principles; Design patterns

I. INTRODUCTION

Software Defined Networking (SDN) has recently evolved as an alternative flexible network architecture to traditional network systems. The flexibility that software programs offer over the hardware is one major SDN feature.

Traditional network switches and routers that route data from and to local networks include two in-cohesive functional components; data plane that includes information about traffic, and how to deal with it and control plane for control and management functionalities. SDN proposes to decouple those two in-cohesive planes and include in new switches the data plane only. Control plane is moved to a separate software-based module. A new protocol, OpenFlow is designed to handle communication between the newly separated modules or planes. As the main protocol used in SDN, OpenFlow is used in many research and technical documentations as a synonym to SDN. We will also follow this acronym in this paper and use the two terms interchangeably.

Through such separation, developers and network administrators can have now full control over their networks. Routing algorithms that were closed and vendor specific are not any more. Applications can be developed on top of the controller to communicate and interact with the controller. Those applications, also called middle-boxes can be provided, through the controller, with customized flow-based information.

As a new architecture or technology, SDN comes with both challenges and opportunities. In this paper we will focus on the rise of software roles in SDN in comparison with traditional

network. In software engineering, software design principles and patterns proposed how we can design software products that are easy to use, reuse, update and maintain. Modularity is a core software design concept related to developing a program with different software modules. Those modules should be highly cohesive from the inside (i.e. the inner components of modules) and at the same time coupling between the different modules should be minimized. Interfaces are software components that exist to support modularity goals. Different modules should interact with each other only through well-defined interfaces.

Many network appliances such as: Firewalls, IDS, traffic optimizers, load balancers, etc. are going to be developed to communicate with SDN controller. Without proper well-defined interfaces between each one of those applications and the controller, intruders can easily have back doors through those applications to access security sensitive controller resources. Using well-defined interfaces, controller and its modules can then provide very specific services to those applications. In addition, those specific services should be called after fulfilling several pre-conditions from the application side including pre-conditions related to self-identity and authorization proof. Currently, those applications can be defined and can expose controller modules or resources directly.

Specification and design should be separated from implementation which shows one way to fulfill those specifications. While in those SDN goals implementation was referring to physical configuration in switches, we believe that this can also be applied to code concrete implementation that should be isolated from network high level configuration that can exist in policies. Currently, many software controllers include mixed functionalities between core controller modules, quality assurance, monitoring, management, policies, or security modules, etc.

We will focus here on software design principles. Abstraction is one of the software design concepts that is heavily investigated in the software engineering field. Abstraction is about focusing on relevant information and ignoring irrelevant information suitable or relevant to the problem domain or to the level of the current system details. In software construction and implementation, abstract classes or interfaces are always proposed at the top of a library or a hierarchy to make the structure more stable and able to cope with changes or modifications. This is to acknowledge that software programs and their requirements are very volatile and

change rapidly. Consequently a good software design should allow and accommodate such changes without the need to restructure the software or the system.

SDN architecture facilitates tasks' delegation. In traditional networks, network administration cannot be delegated and it has to be controlled from network devices. Three SDN features together (centrality, ability to monitor all network components from one location and programmability) can make it possible for network administrators to delegate different administration tasks to different users without losing the ability to manage or monitor them.

In this paper, we will revisit SDN architecture based on software design principles and patterns and show how such architecture can be improved. We believe that SDN separation of control and data plane is not enough. We will focus on abstraction layers in software parts.

The rest of the paper is organized as the following: In section two we will introduce several research papers that are relevant to the paper subject. In section three we will present goals and approaches for an enhanced SDN architecture. Paper is then concluded with a summary section.

II. LITERATURE REVIEW

Software engineering can bring several advantages to SDN. For example, Software engineering has mature knowledge, tools and experience in software design, development and testing. Bringing those to SDN can be a very important beneficial joint venture.

Modularity is about developing software or system components that can be easily used, reused, modified, updated or maintained. It is very important to build an SDN architecture that allows developers to easily add new applications or middle-boxes without the need to significantly cause a system configuration/reconfiguration. Monsanto et al 2013 acknowledge that current OpenFlow architecture has limited support for creating modular applications[1].

Reitblatt et al 2012 [2] discussed one problem related to SDN configuration updates. This is since current networks continuously change and evolve. Therefore it is very important for a good SDN design to cope with those frequent changes. Authors presented mechanisms to handle packet or flow level updates' consistency checking. In other words, a mechanism should exist to check whether a recent flow or packet update is consistent with the network state and its flow rules in flow tables. Authors proposed an abstract interface to offer solid mechanisms for handling configuration updates. Authors showed also several case studies of why such updates should to be investigated.

In the subject of policies' isolation, Monsanto et al 2013 discussed the ability of SDN architecture or its flows to accept commands from different policies. A policy orchestration abstraction is a possible a solution to orchestrate the process of handling several policies that may come from different applications or departments (e.g. security policies, business process policies, financial policies, audit or monitoring policies). Pyretic or other policy programming languages are proposed as tools to allow users to define policies in a common

language. However, in addition to policy language, an abstraction or orchestration layer is still necessary and should not be mixed with policy languages that should be used to describe policies. Network slicing is another layer of abstraction or isolation. However, slicing is performed to isolate logical networks from each other and not policies from each other. In other words, in one slice, we expect to see several policies that need to interact with each other or need to enforce different aspects on the same flows. Different slices deal with different flows and consequently the slice isolation itself should guarantee that policies from different slices should be isolated from each other.

Casado et al 2012 [3] report can be considered as a reassessment of SDN proposed separating the network into three layers or interfaces in terms of control transformation: Hosts, operators and packets. Each one of those layers should have their own control on packets while they traverse the network. Authors argued that traditional Internet has no differentiation among all those interfaces. On the other hand, MPLS has distinguished two of them: Host and packet interfaces. SDN tackled requirements for network operators that were not acknowledged by Internet or MPLS networks. However, SDN did not distinguish between host-network and packet-switch interfaces. Authors proposed a hybrid approach of SDN-MPLS to get the advantages of both and have those three as clearly defined and separated interfaces. Rather than having one controller in original SDN, authors proposed two controllers: A fabric controller to provide basic packet transport (Host-network interface) and an edge controller responsible for complex network services (Operator network interface). Authors here focused on the design of the network and the interfaces related to traffic transportation. In other words, authors focused on the carrier and ignored the fact that the data or the content can have the same problem. Specifically, information is only considered from the network port and on. However, information is created and controlled before that (in the middle-box or the controller). Network control is separated between Fabric and edge controllers. On the other hand, software components that are using the network should be also functionally decomposed. The key idea here is that if two things are functionally not cohesive or that they solve different problems then they should be separated from each other. The edge controller still has several functions that are not cohesive.

In addition to the fact that SDN has different modules that are not functionally cohesive, there is another issue related to the levels of abstractions. A policy that users or administrators understand is at a very different level of abstraction from a policy, or rule, that a firewall or a switch can understand. For example, existing research discussed the challenge between dealing with high level policies at the application level and having to write very low level flow rules in switches or firewalls. The gap between those two can be very large. In addition, low level flow rules should be allowed to change easily and dynamically. On the other hand, high level policies are expected to be more stable and change infrequently. Approaches that tried to give more details to policies suffer from building policies that are network dependent. This makes those policies very complex to reuse or to be able to

accommodate network changes. On the other hand, designing policies with that are very abstract can make them very hard to implement or be interpreted in terms of flow or firewall rules. Some papers already proposes an abstraction or adaptor layer between high level policies and flow or firewall rules to isolate them from each other and allow each one to change without impacting the other (e.g. Pan et al 2013 [4], Kang et al 2013 [5], and Moshref et al 2013 [6]).

Abstraction (i.e. network virtualization) was the main reason to bring networking to software programmability. Abstraction in SDN tries to extract simplicity from the control plane (Shenker et al 2011 [7]). It can produce a design that is modular; easy to change, evolve, reconfigure, etc. Authors claimed that network layers include abstraction in the data plane. However, control plane lacks having such layering or abstraction. Authors' report in SDN defined three abstractions: Distribution (controller), forwarding (network virtualization and switches) and configuration (NOS). Distribution of control allows a global view of the network. Forwarding abstraction separates the functionalities in switches between management and forwarding and takes the management task to the controller. The key idea was that those two functions are not cohesive and consequently there is a need to separate or isolate them from each other.

Existing papers or technical reports discussed also abstraction in network or hardware parts of OpenFlow networks (e.g. Danilewicz et al 2014 [9]).

Kind et al 2012 proposed an enhanced SDN architecture where several new splits should be introduced in addition to the split between control and data plane originally proposed in SDN. This includes the split between the control plane and the NOS, which is a modified version of hypervisors' architecture where a basic filter layer can be an alternative to a hypervisor. They also proposed a split between forwarding (network edge) that requires only basic functionalities and processing entities (network core) that requires more intelligent processing and analysis. They focused on applying this SDN modified architecture in carrier grade networks.

Software Defined Internet Architecture (SDIA) is proposed based on SDN to solve the problem of Internet evolution and the need for a flexible architecture (Raghavan et al 2012 [10]). The main idea is to decouple the architecture from the infrastructure so that changes on one will not affect the other. Architecture refers to the current IP based model or any other alternative; while infrastructure refers to physical network resources and equipment. Authors claimed that SDN by its current architecture can help but to a limited range.

Pan et al 2013 proposed FlowAdapter as a middle layer between OpenFlow data plane in switches and the controller [4]. Authors described the goal of such adapter which is to support having flexible rules that can be handled by "inflexible" hardware. In other words, this layer shields both data and control plane from each other and allows changing one of them without a significant overhead on the other. In software design, this is a recommended design principle "Find what is varying and encapsulate it" (Shalloway and Trott 2005 [11])

Sugiki 2013 [8] proposed an integrated management framework to standardize SDN development. This can also contribute to making the development in SDN programming mature. However, our focus in this paper is SDN programming design and not implementation.

Design patterns concepts are also used in traditional networks for network architecture to best layer network components based on some quality aspects (e.g. Dart et al 2013 [12]). Smith et al 2014 proposed policy-controlled management patterns in SDN [21]. This is a framework to provide abstraction for orchestrating different services implemented in SDN and that require policy information or interaction. While one of the major goals of SDN was to make the architecture open and vendor independent, however, the fact that currently the area is premature and the effort to develop controllers and applications is not formalized, this may take SDN development to another problem of lacking united or standard architecture. In software engineering, formal methods suffered from such problem for years and this problem is considered one of the main reasons why formal methods are struggling to gain more popularity as it was sought.

III. GOALS AND APPROACHES

The goal of good software design patterns and principles is to improve the quality of the developed product. Good design can help the software applications now and in future. This is since a well-designed software should have high qualities such as performance, security, usability that are important for the current usage. In addition for future software maintenance and expansion, good software design can help in maintenance, reusability, testing, etc.

The controller or one of its modules should be able to orchestrate the communication between the different application that are built on top of the SDN network and those applications should be able to share the information without coupling those modules with each other or without security problems.

The applications need not to be aware of each other or communicate directly with each other. The key mechanisms to achieve this are isolation and abstraction. Ideas from software design principles and patterns can be utilized in this aspect. Design principles in general focus on the following main design quality aspects: Abstraction, encapsulation and reusability. Isolation can be also a major benefit to security as it limits the expansion of security intrusions. Figure 1 shows a recent SDN architecture (Alsmadi and Xu 2015).

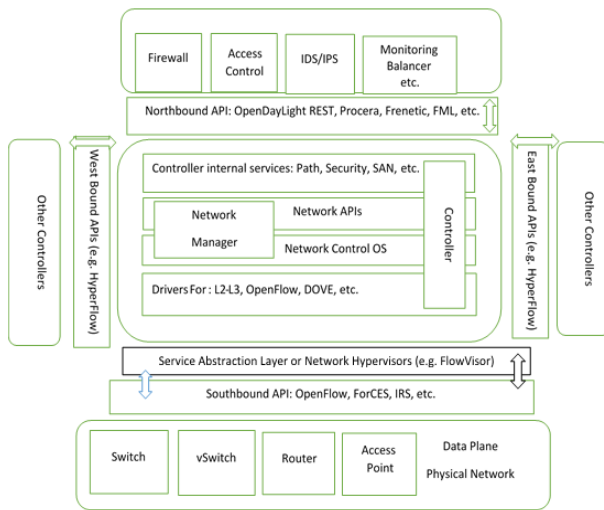


Fig. 1. SDN architecture (Alsmadi and Xu 2015)

In comparison with early SDN architectures, Figure 1 shows that interfaces and isolations between the different layers are already in evaluation and development. For example, Service Abstraction Layer (SAL) exists to isolate south bound APIs from the controller. It can help integrating the same controller with more than one south bound API or protocol.

Many researchers and domain experts acknowledge that SDN architecture itself is recent and premature. On the other hand, SDN came with no new technologies or inventions. Rather, it came to clarify, accumulate, and coin findings in the networking field over the past years. From the software engineering or programming side, similarly, SDN does not need to start everything from scratch and can learn from areas where there have been accumulated knowledge and experience over the years. Software design in particular is considered a matured field and concepts related to: Object Oriented Design (OOD), software construction, testing, design principles and patterns have a rich inventory of: tools, methods, etc. that can be utilized.

OpenFlow protocol itself can be considered, in a very simple manner, an abstraction layer or adapter to allow software programs to interact with switches. This is since for commercial or business, not technical reasons, vendors of switches and routers don't allow developers to program or interact with traditional switches. In that sense, OpenFlow protocol provides that well-defined interface to program or communicate with switches. This communication or programming can be conducted through the controller.

We will present all areas in SDN architecture that should include separate software communication adaptors. Those adaptors should include interfaces to facilitate communication between their edge modules. In some cases where communication is two-ways, two different interfaces should be designed. We also showed some contributions already in some areas to indicate that research is already going in this direction.

South Bound Interface: An abstraction layer or adapter should exist between controller and its switches. A well-defined interface or public methods should be defined on switches to allow the controller to access switches only through

those public interfaces. The interface that switches should expose depends on the type of services that they provide. For example, controller should be able to read flow rules, add new flows, delete or update flow rules (i.e. CRUD on flow rules). As software classes, there should be two main classes for the interaction between controller and switches: Flows and flow rules. Controller should be allowed to change some of those classes' attributes through setters and getters.

From a software design perspective, in the flow rules insertion process, the controller, as a client should fulfill all flow insertion constraints or network invariants before being allowed to insert a new flow rule. Controller can then have a separate monitoring module that will be queried to retrieve those invariants. However, some of those constraints such as rules-conflict can be only judged after adding the flow to the switch flow tables. Abstraction layer module should then orchestrate the process and start a roll-back process where after the insertion if a rule-conflict case occurs between the new added rule and existing ones, the addition process is reversed with all related activities.

Existing research already proposed a software abstraction layer between SDN controller and switches for several different purposes. For example, Khurshid et al 2013 proposed VeriFlow as a verification layer between controller and switches [13]. The goal of this layer to verify that flow rules inserted in the switches from the controller do not violate certain network wide invariants (e.g. reachability, loop freeness, consistency).

Policies should be isolated from flow rules. Policies should include high level information about resources (e.g. user, host, application, etc.). They should not include information that are low level dependent (e.g. IP address, port, MAC address, etc.). In networking terminologies, L1-L3 information are considered low level information, L4-L7 information are considered high level information. An abstraction layer should exist to separate and isolate those two layers from each other.

Policies in network security serve three different levels:

Application level policies: At the application level, users write policies to regulate users-applications-systems interactions. They can specify who can do what, when and how. However, at this level, users are not identified as individuals but as groups. Network, systems and applications are only identified by general names without any technical terms. Typically, at this level, we expect policies such as:

Employees should not be able to access accounting services remotely.

Students should not be allowed to use smart devices during exams.

Users can have unlimited Internet download speed only after working hours.

In those examples, we showed that at this level, policies or policy sets should be for groups and not individuals (as individuals represent instances of their groups which can be specified in level2 policies). Similarly, applications and devices are known by general categories that can have several instance examples (e.g. accounting, smart devices, Internet).

For simplicity we will call them at the first level as policy sets, at the second level as policies and at the third level as rules. Policy sets include policies and policies include rules.

Middle level policies: Level two should include information typically included in Access Control Lists (ACLs). This is an intermediate stage between high level policy sets and low level rules. Every authorized person, application, or service should have an entry in this access control system. There are currently several examples of ACLs such as those that exist in operating systems, databases or websites active directory or user management, ACLs in firewalls, port control, and routers.

Low level policies: Rules in flow tables and firewalls in particular. Those should have the same attributes exist in flows so that checking and matching those rules with flows can be simple, dynamic and direct. Since those rules will talk to and direct low level network components, for performance issues, they need to be simple and straightforward. Unlike, high level policies, those rules and location dependent and include network level information (e.g. IP, MAC addresses, port number, etc.).

Two-way communication should be orchestrated between each two consecutive layers. From top to bottom, special tools should be developed to allow automatic translation from high to low level terminologies. On the other hand, information from bottom up should be used to improve policies. ACLs in the middle layer provide constraints on flows at the low level. On the other hand, a special module should be developed to support a feedback control where information from network flows can be used to trigger future rules in ACL. Data mining, Artificial Intelligence (AI) and patterns' recognition methods can be used to analyze network traffic and make rules' recommendations. Those can be triggered for security purposes such as breaches or attacks or they can be triggered for QA purposes (e.g. performance). Between ACLs and high level policies, modules should be developed to allow automatic translation of policies to ACLs. On the other hand, feedback control is also recommended to reevaluate existing policies or trigger adding new ones based on network traffic and environment.

In this specific category, Qazi et al 2013 proposed SIMPLE as a layer between security policies and flow rules [15]. This layer is required to isolate L2-L3 low level layers' required information from L4-L7 policies' information.

Controller Internal Interfaces: Controller and its internal modules should be separated from high level middle-boxes and applications (e.g. firewall, IDS, load balancer, etc.). Controller can provide services to those applications through well-defined interfaces.

This is currently the most important abstraction layer to provide. This abstraction should exist between the controller as a complete module and any other applications that should be developed and that will interact with the controller. In other words, those are not built-in modules in the controller OpenDaylight and many other controllers are currently using REST API for this specific purpose.

Existing research proposed several examples of either security or other types of applications that should be developed on this top level or also called southbound section (e.g. load balancer, monitoring tools, etc.). Existing research also discussed security concerns when developing such applications and showed that there is a need to make interactions between the controllers and those applications in such manners that guarantee isolation in terms of security, configuration, reconfiguration, reuse, etc.

In the controller itself also, Network Operating System (NOS) should be isolated from the controller. Those are two different units with two different functionalities or responsibilities. Network hypervisors already exist to isolate those two components from each other and allow the communication between them. In this section in particular terms such as (network APIs) are used to refer to this abstraction or isolation layer between controller services and NOS.

Existing research already proposed different structures for such layer. For example (Porras et al 2012 [16] and Shin et al 2013 [17]) proposed a security control or interface between controller and security applications to allow deploying composable security services. Fayazbakhsh et al 2013 proposed FlowTag to tag flows in middle-boxes so that controller can know which application originates a particular flow [18].

Controller internally includes several functions that are not cohesive with each other and consequently should be isolated from each other. Those can be largely divided into: Control and security, administration and management, flow management and communication with switches, monitoring, and load balancing. A high level application which needs only one of those components to communicate with should not be coupled with all other components. In addition for security purposes, isolating those components from each other can limit the spread of attacks and help detecting them. As an example, let's assume we have the monitoring and control separated in two different modules, if control module is compromised, monitoring can help administrators see the details and take counter actions. Separating those modules can be logical only or it can be also physical (i.e. on different controllers or slices).

Logical or Functional Interfaces: Isolation or virtualization already exists in SDN in several other popular areas. The first one is the isolation between the different VMs where they are logically isolated from each other but may run in the same tenant or physical resources. Tenants are isolated from each other where each tenant in a cloud datacenter represents a different company that should be completely isolated from other tenants. Each tenant can have one or more VMs based on demand or requirement. For scalability and load balancing issues, controller tasks can be divided into different functional or logical slices. In this case, we want the different slices to communicate with each other. However, again such interaction should be conducted through well-defined interfaces and data or control from each slice should not interfere with those of the others.

Controller Distributed Architecture Interfaces: A single controller is not a realistic approach for production networks.

Consequently a cluster of controllers should exist to support each other and coordinate tasks' distribution. However, current OpenFlow standard does not allow inter-domain information exchange between the different controllers. Nonetheless, there are many use cases that justify the need for those different controllers to communicate with each other. Needless to say, that such communication between the different controllers should be performed through well-defined interfaces. Different controllers should not interfere with each other or violate others' security regulations. The exchange interface should consequently orchestrate such communication.

A virtualization layer such as FlowVisor (Sherwood et al 2009 [19]) is proposed to isolate the controller or a cluster of controllers from the underlying physical and networking elements. This logical layer intercepts all messages between controllers and switches. From the virtual world perspective, FlowVisor acts as VMWare or Virtual Box that logically isolates operating system from physical components. Consequently, different operating systems can work on the same machine or physical resources.

An adaptor should exist in the data plane between forwarding functions (network edge) and processing functions (network core) (Kind et al 2012[20], Raghavan et al 2012[10]).

Design patterns

The controller is the central control and management module in SDN. Even in controller distributed architecture, each switch is expected to communicate security with only one controller or controller slice. In design pattern a singleton pattern is proposed in such cases to enforce communicating with only one single instance. A singleton pattern should mediate communication between controller and switches from one side and controller and applications from the other side. From software design patterns, a singleton class or pattern is needed when we want a class to be available to the whole application and also that the whole application should have one and only one instance. This seems to be the same usage profile of the controller.

Design patterns' assessment

The usage of design patterns in software programs showed a mature level of experience from the software development team. In order to evaluate the usage of design patterns in SDN, we conducted several experiments using Java controllers (e.g. Floodlight, Beacon, FlowVisor, IRIS, and Maestro). We used tools that can perform automatic design patterns' detection (e.g. Pattern4, PDE, Pinot, etc.). Preliminary results showed few instances of usage of design patterns in those SDN or controller programs.

OpenFlow Software version

SDN separates and isolates control from data planes. Control plane (i.e. the controller) is completely a software application. OpenFlow protocol is developed to control communication between the controller and the data plane or the switches. However, we argue that OpenFlow focused on defining how controller should communicate with the switches from a networking or communication perspective. OpenFlow should be extended to specify how controller should

communicate with the switches from a software perspective. This is since controller is completely a software and switches include also embedded software elements. In this section, we will focus from a high level perspective on what should OpenFlow software version (OpenFlowS) should include.

In SDN, controllers add flows to switches. A separate software module should exist to orchestrate and handle communication between controller and switches. Part of the functions that this orchestrator or adaptor module should handle is checking preconditions or constraints before allowing controller to add, delete or update a flow rule. This module should be responsible for tracking all network state related attributes. For example, through the flow-addition process, inconsistency can occur where the network state is changing while the controller is adding the flow rule based on expired information. This is usually referred to as "race condition". Proactive controllers may eventually notice and fix such inconsistencies. However, this will add complexity and overhead over the controller and the network (Peresini et al 2013 [14]).

From a software perspective, controller and switches are two modules or packages that need to interact with each other and provide services to each other. In this specific architecture, in most cases the controller is the client and the switches play the software service provider role. For example, the controller needs to CRUD (i.e. Create, Read, Update and Delete) rules from switch flow table(s). Those should be represented by public services in the switch. A switch should include a software interface with those four as public services. The inputs that controller will provide when calling those services depend on the specific method and will include flow rule attributes as well as other possible attributes related to programming or design (e.g. rule ID, group, etc.).

OpenFlowS adaptor should typically include abstract classes or interfaces. Those should regulate how controller and switches interact with each other. For example, they should include the, high level, public services that should be provided along with their headers and signatures. They should also provide pre-conditions and post-conditions for those public services.

The organization behind SDN and OpenFlow (Open Networking Foundation, ONF) in a report in 2012, identified four major goals for SDN. Those four goals are related to software design and principles:

SDN aims at decoupling switch management and control plane from data plane. Coupling and cohesion are widely popular software design metrics upon which good design quality is evaluated. Internal modules should be highly related and interconnected to each other from functional perspectives (i.e. high cohesion). On the other hand, different modules should be lightly coupled with each other and only through well-defined interfaces.

A centralized controller to manage one to many switches. Different switches are controlled by same functionalities. They are only different in low level details that should be handled by switches themselves. High level functions that are similar

should be centralized in one location. Low level details are distributed across the different switches.

We described this goal from two perspectives. The first one is related to policies in which global policies should be centralized, location independent and express the general design goals of the network. However, each switch or security control can have their own rules that are location dependent and that interpret high level policies from a small local scope perspective.

The other perspective is related to modules' isolation through the different adaptors. Communication through the different modules in such case can be formalized. One of the ambitious goals of SDN is to achieve automating different policy activities: Implementation, enforcement, configuration, orchestration, etc. A modular design is a key toward achieving such goal.

SDN should support the ability to manage network behavior through well- defined interfaces and modules. In other words, the "what part" should be separated from the "how part" and well-defined interface should exist and isolate them from each other. Although control in SDN can add or delete switch flow rules in the flow tables, however, this should not mean to allow controller to tamper internal switch architecture.

Using well-defined interfaces between controller and switches makes it possible for one controller to interact smoothly with switches from different vendors. A software open adaptor with well-defined interface should be designed between controller and different switches to shield both of them from each other and to formalize communication between them.

Deign Patterns Evaluation

In order to assess the level of using design patterns in SDN, we evaluated three open source controllers written in Java: Floodlight (www.projectfloodlight.org/floodlight), IRIS (openirisproject.tumblr.com) and Maestro (code.google.com/p/maestro-platform). The goal is to evaluate which such relatively large software applications are developed based on mature design perspectives. We should acknowledge however the debate on whether the usage of design patterns indicate a mature good design or not.

Evaluating Floodlight with Pattern4 design pattern detection tool, results showed only using one design pattern (Singleton) with 53 instances. No other design pattern is shown to be used in Floodlight.

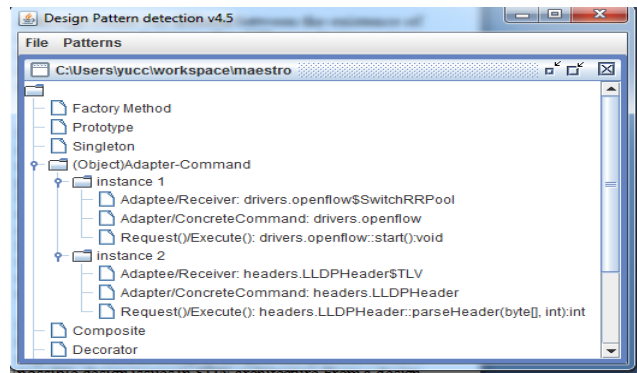


Fig. 2. Design pattern detection tool: Pattern4

Table 1 shows design patterns' instances in Maestro based on Pattern4 tool.

TABLE I. PATTERN4 ON MAESTRO CONTROLLER

pattern/class	Singleton	Adapter	State/Strategy	Visitor
	1	2	3	7

Table 2 shows design patterns' instances in IRIS based on two design pattern detection tools; Pattern4 and Web Of Patterns (WOP). Results showed the wide variation between the two tools in detecting the occurrence of design patterns usage.

TABLE II. PATTERN4 Vs WOP ON IRIS CONTROLLER

abstract factory	bridge	Proxy	Template Method	State /Strategy	Decorator	Adapter	Singleton	Pattern Tool
0	0	2	3	23	1	28	20	pattern4
2	1874	62	96	0	0	478	0	WebOfPatterns (WOP)

TABLE III. PATTERN4 Vs WOP ON OPENFLOWJ CONTROLLER

abstract factory	bridge	Prototype	Proxy	Template Method	State /Strategy	Decorator	Adapter	Singleton	Pattern Tool
0	0	4	0	0	13	0	5	22	pattern4
0	0	0	0	0	0	0	12	0	WebOfPatterns (WOP)

TABLE IV. PATTERN4 ON OPENFLOWJAVA-MASTER AND LACP-MASTER CONTROLLERS

Controller	Singleton	State/Strategy
openflowjava-master	6	4
lACP-master	12	0

Although results was different between the existence of design patterns between the different design pattern detection tools, however, results showed that such relatively large and

important software applications are not considering the usage of design patterns.

IV. CONCLUSION

SDN is an emerging architecture for designing networks and distributing their functionalities. This new architecture took into consideration some of the problems and challenges in traditional networks. Two features in SDN can be considered as core and differentiate SDN from traditional networks. The first one is splitting control from data plane and moving it from switches to a new software program called the controller. The second one is in making this controller open as a vendor independent and to be programmed and extended by developers and users.

SDN is about programmable networks and consequently it makes sense to use some of the mature software experience such as design principles and patterns to solve possible design issues in SDN architecture. From a design perspective, those can make the network design easier to use, reuse, update, maintain and interact with. Software in SDN has a major role and this role is expected to continuously grow. From a software design perspective, SDN architecture is not mature enough. This explains why recent implementations of open controller should as Opendaylight extend the architecture to include new abstraction layers such as: Service Abstraction Layer (SAL) and REST API in two different locations of the architecture.

SDN focuses on the networking perspective when control is isolated from data. From a software perspective, there are many components in the SDN architecture that are not cohesive and that should be decoupled from each other. We showed also that there are already research proposals and progresses toward that goal. This will continue to evolve and we presented here a picture of the possible abstraction layers that SDN architecture may end up having. Those abstraction layers are necessary to allow different components that are not cohesive and that should be decoupled to communicate with each other through well-defined interfaces. This will allow those different modules to be used and evolve aside from each other.

REFERENCES

- [1] C. Monsanto, J. Reich, N. Foster, J. Rexford, and D. Walker, "Composing software-defined networks," in Proceedings of the 10th USENIX conference on Networked Systems Design and Implementation, ser. nsdi'13. Berkeley, CA, USA: USENIX Association, 2013, pp. 1–14.
- [2] Mark Reitblatt, Nate Foster, Jennifer Rexford, Cole Schlesinger, David Walker: Abstractions for network update. SIGCOMM 2012: 323-334
- [3] M. Casado, T. Koponen, S. Shenker, A. Tootoonchian, "Fabric: A Retrospective on Evolving SDN," in Proc. of the first workshop on Hot topics in software defined networks, Helsinki, Finland, Aug. 2012, pp. 8 5-90.
- [4] Heng Pan, Hongtao Guan, Junjie Liu, Wanfu Ding, Chengyong Lin, GaogangXie: The FlowAdapter: enable flexible multi-table processing on legacy hardware. HotSDN 2013: 85-90
- [5] Nanxi Kang, Zhenming Liu, Jennifer Rexford, and David Walker, Optimizing the "One Big Switch" Abstraction in Software-Defined Networks CoNEXT'13, December 9–12, 2013, Santa Barbara, California, USA.
- [6] M. Moshref, M. Yu, A. Sharma, and R. Govindan, "VCRIB: Virtualized rule management in the cloud," in NSDI, Apr 2013
- [7] Scott Shenker, Martin Casado, TeemuKoponen, and Nick McKeown, The future of networking and the past of protocols, A presentation, June, 2011
- [8] Akiyoshi Sugiki: An integrated management framework for virtual machines, switches, and their SDNs. ICON 2013: 1-6
- [9] G. Danilewicz, M. Dziuba, J. Kleban, M. Michalski, R. Rajewski, M. Grief: Project ALIEN - abstraction layer for devices non-OpenFlow SDN networks. Telecommunication Review September 2014
- [10] BarathRaghavan, Martin Casado, TeemuKoponen, Sylvia Ratnasamy, Ali Ghodsi, Scott Shenker: Software-defined internet architecture: decoupling architecture from infrastructure. HotNets 2012: 43-48
- [11] Alan Shalloway and James Trott, Design Patterns Explained, A new perspective on object oriented design, second edition, Addison-Wesley, 2005.
- [12] Eli Dart , Lauren Rotman , Brian Tierney , Mary Hester , Jason Zurawski, The Science DMZ: a network design pattern for data-intensive science, Proceedings of SC13: International Conference for High Performance Computing, Networking, Storage and Analysis, November 17-21, 2013, Denver, Colorado [doi>10.1145/2503210.2503245]
- [13] A. Khurshid, W. Zhou, M. Caesar, and P. Godfrey, "VeriFlow: Verifying network-wide invariants in real time," ACM SIGCOMM Computer Communication Review, vol. 42, no. 4, pp. 467–472, 2012, 10th USENIX Symposium on Networked Systems Design and Implementation (NSDI), April 2013.
- [14] Peter Peresíni, MaciejKuzniar, DejanKostic: OpenFlow Needs You! A Call for a Discussion about a Cleaner OpenFlow API. EWSDN 2013: 44-49
- [15] Z. A. Qazi, C.-C. Tu, L. Chiang, R. Miao, V. Sekar, and M. Yu, "SIMPLE-fyingMiddlebox Policy Enforcement Using SDN." ACM SIGCOMM, August 2013
- [16] Phillip Porras , Seungwon Shin , Vinod Yegneswaran , Martin Fong , Mabry Tyson , GuofeiGu, A Security Enforcement Kernel for OpenFlow Networks, HOTSDN 2012.
- [17] S. Shin, V. Yegneswaran, P. Porras, and G. Gu, "AVANT-GUARD: Scalable and Vigilant Switch Flow Management in Software-Defined Networks," in Proceedings of the 2013 ACM conference on Computer and communications security, ser. CCS '13. ACM, 2013
- [18] S. Fayazbakhsh, V. Sekar, M. Yu, and J. Mogul, "FlowTags: Enforcing Network-Wide Policies in the Presence of Dynamic Middlebox Actions," in Proceedings of the second workshop on Hot topics in software defined networks. ACM, 2013.
- [19] R. Sherwood, G. Gibb, K. Yap, G. Appenzeller, M. Casado, N. McKeown, and G. Parulkar. Flowvisor: A network virtualization layer. OpenFlow Switch Consortium, Tech. Rep, 2009.
- [20] Kind, M., Westphal, F.J., Gladisch, A., Topp, S.: SplitArchitecture: applying the software defined networking concept to carrier networks. In: IEEE World Telecommunications Congress (WTC) (2012)
- [21] Paul Smith, Alberto E. Schaeffer Filho, David Hutchison, AndreasMauthe: Management patterns: SDN-enabled network resilience management. NOMS 2014:1-9
- [22] Alsmadi, Izzat, Dianxiang Xu, Security of Software Defined Networks: A Survey, Computer and Security Journal, Elsevier, Volume 53, 09/2015.

Evaluating the Usability of Optimizing Text-based CAPTCHA Generation

Suliman A. Alsubibany
Computer Science Department
College of Computer, Qassim University
Buridah, Saudi Arabia

Abstract—A CAPTCHA is a test that can, automatically, tell human and computer programs apart. It is a mechanism widely used nowadays for protecting web applications, interfaces, and services from malicious users and automated spammers. Usability and robustness are two fundamental aspects with CAPTCHA, where the usability aspect is the ease with which humans pass its challenges, while the robustness is the strength of its segmentation-resistance mechanism. The collapsing mechanism, which is removing the space between characters to prevent segmentation, has been shown to be reasonably resistant to known attacks. On the other hand, this mechanism drops considerably the human-solvability of text-based CAPTCHAs. Accordingly, an optimizer has previously been proposed that automatically enhances the usability of a CAPTCHA generation without sacrificing its robustness level. However, this optimizer has not yet been evaluated in terms of improving the usability. This paper, therefore, evaluates the usability of this optimizer by conducting an experimental study. The results of this evaluation showed that a statistically significant enhancement is found in the usability of text-based CAPTCHA generation.

Keywords—text-based CAPTCHA; usability; security; optimization; experimentation; evaluation

I. INTRODUCTION

Nowadays, several studies have been conducted for web-based services that may be exposed by some attacks using such tools. In particular, researchers tend to make some of the theoretical and practical methods not only to prevent these attacks, but also to distinguish bots from humans. One of these methods is called Human Interactive Proofs (HIPs). Where from these endeavours, a captcha 1 has been developed to resist these attacks and improve the robustness level of such systems [7].

A captcha (Completely Automated Public Turing test to tell Computer and Human Apart) has been proposed to improve the security of services and verify that a client request is submitted by individual users from online operations rather than by malicious software. It is a program that generates and grades tests that humans can pass easily, whereas computers cannot [13]. A good captcha should satisfy two main requirements: robustness and usability. The robustness aspect is its strength to defend against adversarial attacks; the usability aspect is the ease with which humans pass its challenges [5]. These aspects have attracted considerable

attention in the research community (e.g. [2, 11, 10, 8, 9]). The text-based captcha is the most commonly deployed type in websites, such as *Gmail*, *eBay*, and *Facebook*, to date, with many advantages [2].

Over the past decade, the generation of captcha uses combinations of distorted characters and obfuscation techniques that humans can recognise, whereas they may be difficult for automated scripts. Recently, collapsing or Crowding Characters Together (CCT) technique has been recommended in several studies, such as in [1, 2], as the main anti-segmentation technique. Although of this, a number of character confusions that lead to unsolvable schemes by humans have been recognised in [3] which are expanded in our previous work [4]. Additionally, the accuracy and response time of solving the captcha drop drastically the human-solvability for websites that utilise this technique such as Google and Recaptcha [4, 5, 6, 8]. To overcome this concern, an optimizer that can optimise the generated text of captchas to keep the same level of security while improving the usability level for a varied character set has been proposed in [4].

In particular, the optimizer is designed to be embedded in a text-based captcha generator, and the generated text is optimised based on a set of rules which are empirically derived. These rules are then fed into a developed captcha generator with different fonts and size. Afterwards, the optimizer checks if there is any confusion for character or combination of characters, and then replaced with a set of non-confusing characters based on its position [4], and more details will be given in Section 2. However, the usability of this proposed optimizer has not yet been evaluated. Thus, this paper evaluates the usability of this optimizer and the main hypothesis H_1 is that “*The human-solvability of text-based captchas is significantly improved after using the optimizer.*”

To validate this hypothesis, an experimental study is conducted in which a text-based captcha generator that contains the optimizer is developed. The experiment focuses on the effect of collapsing mechanism on the usability of a generated scheme. A within-subject design (i.e. *prepost-test design*) experiment was used in which fifty-three subjects are participated. The results of the experiment showed that there is a statistically significant improvement after using the optimizer in terms of the accuracy and response time. So, this result supported our hypothesis.

The rest of this paper is organized as follows. Section 2 presents an overview of the optimizer. Section 3 explains the

¹ For the sake of readability, the acronym is written here in lowercase throughout this article as it is normally written in capitals

methods. Section 4 presents the results. The results are discussed in Section 5. Section 6 concludes the paper with future works.

II. AN OVERVIEW OF THE OPTIMIZER

This section highlights the optimizer that has been proposed in [4]. That is, the optimizer aims to improve the usability of text-based captcha without interfering with their robustness level. In particular, there are three important characteristics that the optimizer can exhibit. These are: optimising the generated text based on a set of rules; refining the optimised text; and positioning the optimised character [4]. Fig. 1 shows the proposed design of the optimizer. Each of the optimizer's characteristics is explained below.

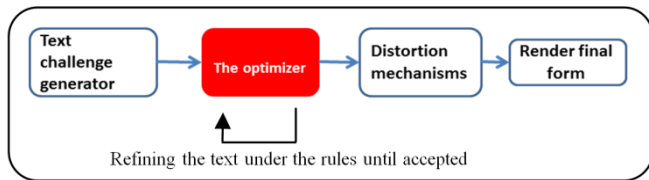


Fig. 1. The design of the optimizer [4]

1) *The optimization rules:* To make the captcha more robust against attacks, different distortion methods have been deployed, for example, CCT, random arcs, overlapping characters and random angled connected line. Specifically, for CCT, captchas appear to be more difficult even for the human. By increasing the level of distortion, a number of confusing letters such as “bl” can resemble “lol” or “ld”. Furthermore, a captcha generator is built that can produce these confusing character, for example, when the characters touch or overlap with each other. By analysing these, the optimization rules are constructed. Hence, the optimization rules are collected empirically. Moreover, as will be seen later, the confusing character is replaced with a suitable non-confusing character based on its position [4].

The non-confusing characters are a set of characters that are developed empirically by both the confusion matrix and the generator. As shown in Fig. 2, the substitution process is accomplished by replacing a confusing character with one of a series of non-confusing characters. However, the position of the confusing character is considered where replacing confusion characters with a random character from non-confusion characters set can result in another confusion character [4]. More details are in the next section.

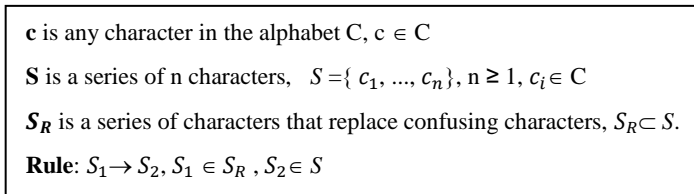


Fig. 2. The general rule of replacing [4]

2) *Refining the optimised text:* As shown, optimising the generated text operates by replacing a character or combination of characters that caused the confusion with non-

confusing characters. This, however, may cause a new character confusion. For example, in the case of the “cl” rule, replacing “l” with “m” can resemble “am”. Thus, the step of refining the optimised text can simply reduce the possibility of a new character confusion that may occur depending on the position of the character as shown in Fig. 3. It is important to note that the algorithm will be terminated when replacing the confusing character with a non-confusing character that will not effect the remaining characters (*Refine= True* in Fig. 3). In other words, the termination of the refining step occurs when generated text is free from all possible confusing characters [4]. The position of the optimised character is detailed in the next section.

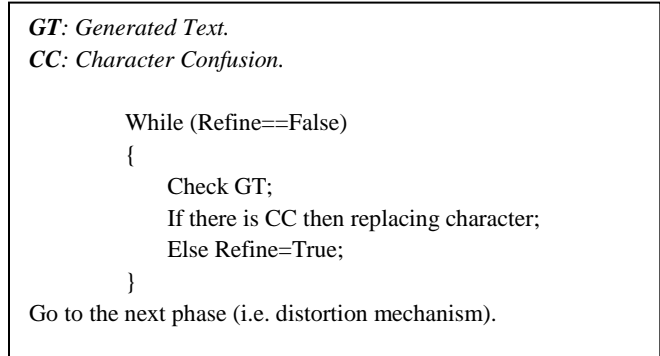


Fig. 3. Illustration of the optimizer's algorithm [4]

3) *The position of the optimised character:* The position of the replaced character is important in the process of optimization. There are three possible positions in the process of replacing characters. Firstly, the optimised character is the first character of the text, so it should only check the effect of the second character on the optimised character. Secondly, the optimised character is in the middle. Therefore, it should check both the effect of the right character and the left character on the optimised character. Finally, the optimised character is the last character, and it should check only the effect of the previous character to the last character. The rules of these positions are presented in Fig. 4 [4].

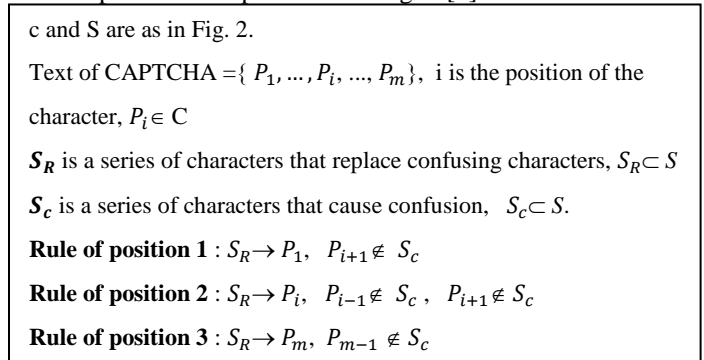


Fig. 4. Rules of the positions [4]

III. METHODS

A controlled laboratory experiment in which participants were asked to solve a set of generated captchas after and before

using the optimizer is conducted. The aim of this experiment is to evaluate the usability of the proposed optimizer in [4] and has been highlighted in the previous section. The following sections present the setup and the procedure of the experiment.

A. Experiment Setup

The experiment involves subjects to solve a set of captchas that are generated by the developed generator. The experiment design, participants, system, variables, and materials are explained in this section.

1) *Experiment Design:* We use a within-subject design, which means that each participant is assigned to all of the following experimental sessions. Session 1 represents *solving captchas before using the optimizer*, while Session 2 represents *solving captchas after using the optimizer*.

2) *Users:* Fifty-three participants were recruited for this experiment, 40 male and 13 female. The mean age of the participants was approximately 25 years. More than half of participants came from technical background (31), whereas the remaining came from non-technical backgrounds. Participants from technical category included university students from science and engineering, while the non-technical category came from social science disciplines.

3) *System:* A captcha generator is developed by using a Java programming language that embeds the proposed optimizer. This generator produces challenges with different types of text which includes all the confusion characters that presented in [4]. In addition to these confusion characters, we discovered a new set of confusion characters as shown in Table 1.

TABLE I. A NEW SET OF CONFUSION CHARACTERS AND THEIR OPTIMIZATION RULES

Characters	Problem	Enhancement
“ck”	It can resemble “ok” or “ak”	Replace character “c” with character “w”
“cn”	It can resemble “on”	Replace character “c” with character “z”
“cp”	It can resemble “op” or “qo”	Replace character “c” with character “z”
“lo”	It can resemble “b” or “p”	Replace character “l” with character “z”
“pl”	It can resemble “ld” or “lq”	Replace character “l” with character “w”
“rl”	It can resemble “nl”	Replace character “l” with character “g”
“rp”	It can resemble “np”	Replace character “r” with character “w”
“ol”	It can resemble “d” or “q”	Replace character “o” with character “w”

Furthermore, in order to enable the users to solve the generated captcha schemes, a Graphical User Interface (GUI)

is developed by using a Java Applet, as shown in Fig. 5. The main goal is that the participants are asked to recognise the letters that are generated by the developed generator, and submit them by pressing on the submit bottom. In case a participant presses the submit bottom before writing the presented letters or leaves the box of the letters, which enables the user to write the recognised letters in, empty, then a warning message is appeared.



Fig. 5. The developed GUI

4) *Variable:* The main independent variable of this experiment is the optimization technique. The accuracy of solving the generated captcha and the response time (i.e. the time consumed) to solve the generated captcha are the dependent variables.

5) *Materials: stimulus and rational:* The stimulus material provided to participants consisted of a set of generated schemes before and after applying the optimization algorithm. The subjects were asked to solve this set sequentially. The same set was assigned to all subjects, rather than generating different sets. There were several reasons for this. First, different sets may be of different schemes, making the measurement and comparison of participant’s answer a difficult task. Second, different sets might be applied because the generator is developed by the author. This would again introduce biases that are difficult to control. Finally, using the same set of captchas for everyone affected experimental control over unanticipated biases.

B. Procedure

In this section, the way the experiment was run is explained, i.e. instructions to participants, tasks, and the data collected.

1) *Instruction:* Subjects were instructed to solve the presented captchas by writing their letters as they are appeared. The subjects were instructed that there are two

sessions, and 20 minutes break between these sessions². Subjects were instructed that there are 37 captchas that will be presented in each session, sequentially. These 37 captchas were chosen in order to reflect all possible confusion characters that mentioned in [4] as well as the discovered set in Table 1. Subjects were told that if they needed a break during a session, they were to do so after they had solved all sessions' captchas. Subjects were able to gauge their progress by looking at a counter at the middle of the screen which showed how many captcha had been solved so far and how many yet remained. Subjects were admonished to focus on the task and to avoid distractions, such as talking with the experimenter, while the task was in progress.

2) *Takes*: The experiment was conducted in a controlled laboratory environment to avoid any distractions and collect the desired data without any biases. After every captcha sent by the participant, the system is not giving information about the recognition made whether the submit letters of a generated captcha are correct or not³, and once all captchas are solved, a notice message that the task is done and thank you for the participation is shown. Finally, the participant was asked to fill a short survey/questionnaire about his or her experience.

3) *Collected data*: The letters of each submitted captcha and the time taken to solve it are recorded by the system.

IV. RESULTS

In the experimental study, all participants successfully completed their tasks. The following discusses the hypothesis regarding the accuracy of solving captchas before and after using the optimization algorithm, the response time, the accuracy vs. response time and solvability of captchas.

A. Testing Hypothesis: Does the solvability of text-based captcha improved?

The average accuracy of solving the presented captchas before and after using the optimization algorithm is shown in Fig. 6. It can be seen that the accuracy of solving captchas in session 2 had significantly enhanced compared with session 1. This indicates that there are implications of applying the optimization algorithm. In particular, in session 1, the accuracy was less than 60%, and was more than 90% in session 2. This signifies that the accuracy in session 1 was far less than in session 2, possibly because eliminating the confusion characters, which are presented in session 1's samples. The statistical significance of this will now be discussed.

Table 2 compares the solvability in two sessions, with respect to the accuracy before applying the optimizer (left column) as well as after applying the optimizer (right column). For both, average (Avg.), standard deviation (SD), minimum (Min) and maximum (Max) values are provided. It was found that the average accuracy before using the optimizer was %57.54, while it was %95.7 after using the optimizer. A t-test yields a result of $t=-23.37$, $p<0.0001$, indicating that the

difference between session 1 and session 2 is indeed statistically significant.

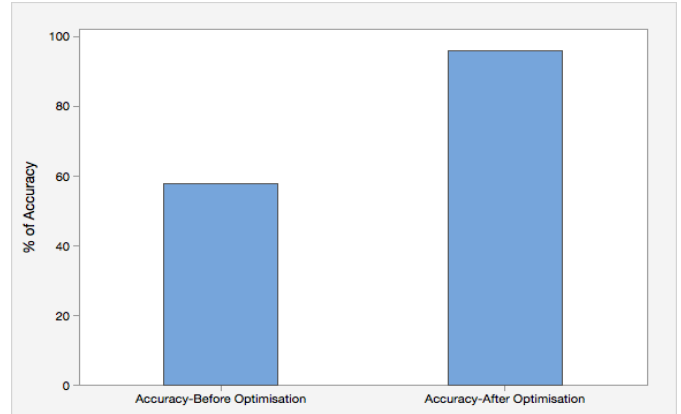


Fig. 6. The average accuracy of solving captchas before and after using the optimization algorithm

TABLE II. ACCURACY OF BOTH BEFORE AND AFTER USING THE OPTIMIZER

Accuracy before using the optimizer (Session 1)					Accuracy after using the optimizer (Session 2)				
N	Avg.	SD	Min	Max	N	Avg.	SD	Min	Max
53	%57.5	10.8	34.0	77	53	%95.7	4.8	83.0	100

This result validates the hypothesis H₁ that the human-solvability of text-based captcha is significantly improved after using the optimizer.

B. Response Time

With respect to the response time, there was found to be a significant difference as shown in Table 3. That is, the average response time before using the optimization algorithm was 8.72 minutes, while it was 5.20 minutes in session 2. A t-test yields a result of $t=6.42$, $p<0.0001$, indicating that the time consumed for responding in session 1 is significantly higher than that in session 2. In other words, a statistically significant difference is found in the response time variable.

TABLE III. RESPONSE TIME OF BOTH BEFORE AND AFTER USING THE OPTIMIZER

Response Time (min) before using the optimizer (Session 1)					Response Time (min) after using the optimizer (Session 2)				
N	Avg.	SD	Min	Max	N	Avg.	SD	Min	Max
53	8.72	3.6	4.2	18.0	53	5.20	1.5	2.80	8.98

C. Accuracy vs. Response Time

In this section, we would like to see whether there is an inverse relationship between the accuracy and response time. In particular, a correlation between the accuracy and response time in which an increase in the value of the accuracy results in a decrease in the value of response time or vice versa. Therefore, by looking at users' performance, an obvious trade-off between the accuracy and the response time can be observed. For example, before using the optimization

² This is to avoid any unnecessary confounding factor biasing the results (at the cost of starting the next session immediately).
³ This is to evaluate the accuracy of each participant's respond by comparing it with the generated one.

algorithm, presenting captchas that include some character confusions lead to decreasing the accuracy, and this directs to increase the response time, as shown in Fig. 7 and Fig.8.

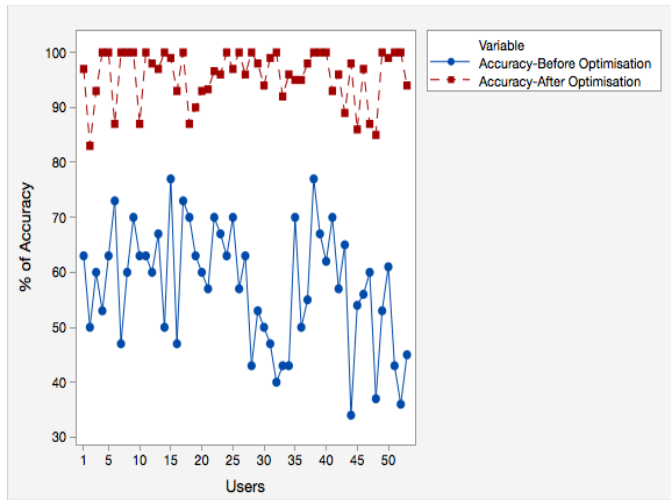


Fig. 7. The accuracy of solving captchas before and after using the optimization algorithm by all users

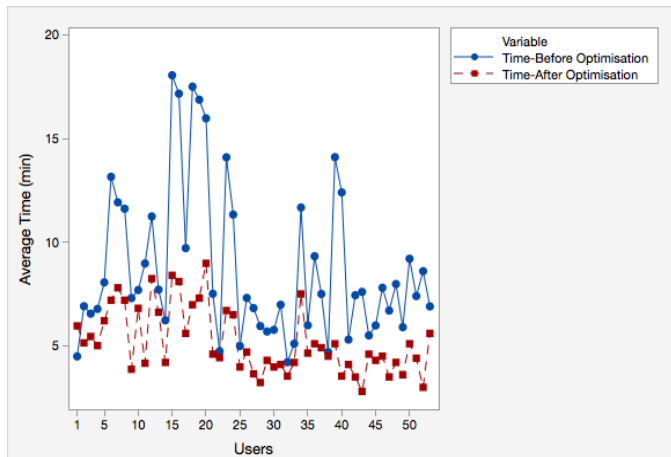


Fig. 8. The average response time of solving captchas before and after using the optimization algorithm by all users

D. Solvability of captchas

Qualitative data were collected, in the form of a survey, to get such feedback about the generated captchas for both before (i.e. session 1) and after (i.e. session 2) using the optimization algorithm. In particular, we were looking for the difficulty level of the generated captchas regarding the solvability.

In session 1, most of the participants, 89% (47 out of 53), stated that the generated captchas were annoying due to the confusion of some characters, for example, “o” and “c.” On the other hand, 11% (6 out of 53) indicated that the generated captchas were not easy but solvable.

In session 2, 93% (49 out of 53) pointed out that the generated captchas were usable; the remaining 4 participants (7%) found that the generated captchas were not easy but solvable.

V. DISCUSSION

The experimental study provides statistically significant evidence that the human-solvability of text-based captcha is significantly improved after using the optimizer. In particular, Table 2 shows that the accuracy of solving captchas in session 2 was significantly higher than in session 1. Accordingly, the main objective of this experiment, namely “solvability improved” is established. In other words, the result of the experiment does support the hypothesis.

Interestingly, the experimental study also gives statistically significant indication that the response time before using the optimization algorithm was higher than after using the optimization algorithm, as shown in Table 3. This result shows an inverse correlation between the accuracy and response time, as demonstrated in Fig. 7 and Fig. 8. However, by looking at Fig. 8, several users took almost the same response time in both sessions, and this also is confirmed by the survey’s results. The possible explanation can be that users may solve presented captchas as fast as possible, but without taking care of their level of typing accuracy. This can be shown obviously in the accuracy results in Fig. 7.

Since a good captcha should satisfy the robustness and usability aspects, our paper is evaluated only the usability aspect. However, evaluating the robustness is beyond the scope of this paper. For this, a future work is required to achieve the key point of the proposed optimizer in [4] which is that the usability of captchas is improved without sacrificing their robustness level. Furthermore, the results of our paper may contribute towards the recently introduced benchmark in [12] that the generation of usable-secure text-based captcha can be improved.

VI. CONCLUSION AND FUTURE WORK

This paper evaluates the usability of optimising captchas through a controlled experimental study. The hypothesis behind this evaluation is that the human-solvability of text-based captcha is significantly improved after using the optimizer. The rationale of this hypothesis is based on the observation that applying such distortion mechanisms that act as a defence approach against segmentation attack increases character confusions. The results of this evaluation showed that the optimization algorithm is significantly enhanced the solvability of generated captchas. Not only this, but also the optimization algorithm is significantly improved the response time of solving captchas.

Our ongoing work would be to conduct a security experiment to validate that the optimizer keeps the same level of security while improving the usability level. Furthermore, as some current approaches are using a combination of different types of characters (e.g., numbers and letters) to avoid human’s recognition confusion on text-based captchas, we would compare the results of the optimizer with this kind of settings.

ACKNOWLEDGMENT

We would like to thank all participants of our experiment. The author gratefully acknowledges Qassim University, represented by the Deanship of Scientific Research, on the

material support for this research under the number (3233) during the academic year 1436 AH / 2015 AD.

REFERENCES

- [1] J. Yan and A. S. E. Ahmad, "A low-cost attack on a Microsoft captcha," *Proceedings of the 15th ACM conference on Computer and communications security - CCS '08*, 2008.
- [2] E. Bursztein, M. Martin, and J. Mitchell, "Text-based CAPTCHA strengths and weaknesses," *Proceedings of the 18th ACM conference on Computer and communications security - CCS '11*, 2011.
- [3] J. Yan and A. S. E. Ahmad, "Usability of CAPTCHAs or usability issues in CAPTCHA design," *Proceedings of the 4th symposium on Usable privacy and security - SOUPS '08*, 2008.
- [4] S. A. Alsuhbany, "Optimising CAPTCHA Generation," 2011 Sixth International Conference on Availability, Reliability and Security, 2011.
- [5] E. Bursztein, S. Bethard, C. Fabry, J. C. Mitchell, and D. Jurafsky, "How Good Are Humans at Solving CAPTCHAs? A Large Scale Evaluation," *2010 IEEE Symposium on Security and Privacy*, 2010.
- [6] M. Motoyama, K. Levchenko, C. Kanich, D. McCoy, G. M. Voelker, and S. Savage, "Re: CAPTCHAs-Understanding CAPTCHA-Solving Services in an Economic Context," *USENIX Security Symposium*, Vol. 10, 2010, pp. 3.
- [7] C. J. Hernandez-Castro, M. D. R-Moreno, and D. F. Barrero, "Using JPEG to Measure Image Continuity and Break Copy and Other Puzzle CAPTCHAs," *IEEE Internet Computing IEEE Internet Comput.*, vol. 19, no. 6, pp. 46–53, 2015.
- [8] E. Bursztein, A. Moscicki, C. Fabry, S. Bethard, J. C. Mitchell, and D. Jurafsky, "Easy does it: More usable captchas," *Proceedings of the 32nd annual ACM conference on Human factors in computing systems - CHI '14*, 2014.
- [9] Y.-L. Lee and C.-H. Hsu, "Usability study of text-based CAPTCHAs," *Displays*, vol. 32, no. 2, pp. 81–86, 2011.
- [10] S.-Y. Huang, Y.-K. Lee, G. Bell, and Z.-H. Ou, "An efficient segmentation algorithm for CAPTCHAs with line cluttering and character warping," *Multimed Tools Appl Multimedia Tools and Applications*, vol. 48, no. 2, pp. 267–289, Jan 2009.
- [11] G. Mori and J. Malik, "Recognizing objects in adversarial clutter: breaking a visual CAPTCHA," *2003 IEEE Computer Society Conference on Computer Vision and Pattern Recognition, 2003. Proceedings.*
- [12] S. A. Alsuhbany, "A Benchmark for Designing Usable and Secure Text-Based Captchas," *International Journal of Network Security & Its Applications*, vol.8, no 4, pp. 41–54, July 2016.
- [13] L. Von Ahn, M. Blum, J. and Langford, "Telling humans and computers apart automatically," *Communications of the ACM*, vol. 47, no 2, pp.56–60, 2004.

Performance Optimization of the Multi-Pumped Raman Optical Amplifier using MOICA

Mohsen Katebi Jahromi

Department of Electronic
Safashahr branch, Islamic Azad
University
Safashahr, Iran

Seyed Mojtaba Saif

Department of Computer
Safashahr branch, Islamic Azad
University
Safashahr, Iran

Masoud Jabbari

Department of Electronic
Marvdasht branch, Islamic Azad
University
Marvdasht, Iran

Abstract—In order to achieve the best gain profile for multi pump distributed Raman amplifiers in Wavelength Division Multiplexing (WDM) transmission systems, the power and wavelength of pumps, the type of pumping configuration and the number of pump signals are the most important factors. In this paper, using a Multi-Objective Imperialist Competition Optimization Algorithm (MOICA) with lowest power consumption and lowest number of pumps, we propose the most uniform gain profile for two types of pumping configurations in S- band and compare the results. Considering the design conditions including the type of pumping configuration, fiber length, fiber type and number of pump signals and using the multi-objective algorithm, we propose a method which can be used to achieve a gain level in which the amplifier has the lowest power consumption and lowest gain ripple. According to this, we can design a powerful WDM transmission system by Distributed Raman Amplifier (DRA) with a good performance and efficiency.

Keywords—Raman amplifier; ICA; WDM System; Optical fiber; Multi-objective Optimization

I. INTRODUCTION

Distributed Raman fiber amplifier is a powerful and hopeful technology for telecommunication systems with high capacity and long path line. It uses the transmission line as a medium to create the Raman gain. Especially in WDM systems in which the simultaneous strengthen of multi-channel light wave signals is required, it yields a magnificent increase in the extent and capacity of the light wave systems. [1-3].

Raman amplification is based on stimulated Raman scattering (SRS), which is a non-linear effect in signal transmission through optical fiber. It results in an amplification of the optical signal, assuming that the pump signal enters the fiber with a correct wavelength and power [2-4].

One of the most recent improvements in the Raman systems is the multi-pump distributed Raman amplifier. It causes the bandwidth extent and gain profile uniformity at the desired bandwidth, which is very important in WDM systems.

In this paper, a backward pump structure in S-band is used. In this structure, the noise sources have the least impact on the amplifier performance. Furthermore, although it can be used in C & L -bands, in the S-band, the Raman amplifier gives the superior results compared to the other optical amplifiers. The structure of a forward pump and seven backward pumps are

also used in implementing the optimization algorithm to emerge the effect of pump configuration. Various methods, such as Genetic Algorithm (GA), multi-population genetic algorithm and firefly algorithm are employed to optimize the performance of distributed Raman fiber amplifier [5]. However, the Imperialist Competition Algorithm (ICA) is a stronger tool compare to the other designing methods. The results of four optimization methods for reducing the gain ripple with the same number of iterations are reported in Table 1. As seen in this table, the result of ICA method has the lowest value. It is worth mentioning that according to the random nature of the algorithms used in Table 1, they are applied five times and then the average of results is compared in Table 1.

In this paper a multi-objective imperialist competition optimization algorithm is used to have a uniform gain profile with lowest gain ripple and minimum consumption power of pumps .the results are compared with other optimization algorithms that are used in other works in this field.

In most of related works only the gain ripple is optimized and a multi-objective optimization algorithm is not used, but in this paper the number and power of pumps are optimized to achieve the best gain profile in a determined gain level with minimum consumption of power .and also by using the suggested method in this paper the best gain level with minimum of gain ripple and consumption of power can be found for a Raman amplifier with a specified configuration of pumps. So the recommended method is very useful in designing of multi-pump distributed raman amplifier.

The rest of this paper is organized as follow: in Section 2, the mathematical model of Raman amplifier used in numerical simulation is presented. In Section 3, the MOICA method used in this article to optimize the designing process is explained. The result of numerical simulation is then in Section 4 and finally, Section 5 concludes the paper.

II. THE MATHEMATICAL MODEL OF A RAMAN AMPLIFIER

A simple scheme of a Distributed Raman Amplifier (DRA) is depicted in Figure 1. As seen in this figure, it is composed of an optical fiber having the length L as a medium gain and forward (co) and backward (counter) pumps.

$$\frac{dP_v^\pm}{dz} = \mp \alpha_v P_v^\pm + P_v^\pm \sum_{\mu > \nu} \frac{g_{\mu\nu}}{A_{eff}} (P_\mu^+ + P_\mu^-) - P_v^\pm \sum_{\mu < \nu} \frac{g_{\mu\nu}}{A_{eff}} (P_\mu^+ + P_\mu^-) \quad (1)$$

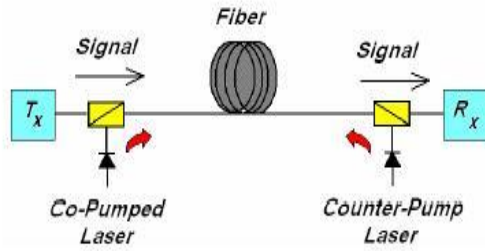


Fig. 1. Scheme of a DRA used in optical communication system [6]

TABLE I. THE RESULT OF DIFFERENT OPTIMIZATION ALGORITHM IN BACKWARD PUMPING CONFIGURATION

Algorithm	Gain Ripple in Run1	Gain Ripple in Run2	Gain Ripple in Run3	Gain Ripple in Run4	Gain Ripple in Run5	Mean
GA	0.4272	0.3670	0.5025	0.2906	0.6828	0.4540
Firefly	1.0203	0.6879	1.0802	1.2400	1.3978	0.9449
multi population -GA	0.2532	0.7295	0.3323	0.4372	0.5344	0.4573
ICA	0.4553	0.1989	0.2384	0.3048	0.3046	0.3004

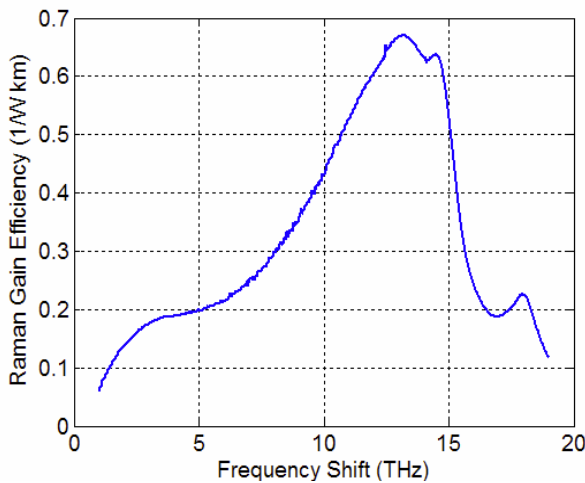


Fig. 2. Measured Raman gain efficiency curve($\lambda_p=1420\text{nm}$) [8]

$$G_{on-off} = \frac{p_s(L) \text{ with pumps on}}{p_s(L) \text{ with pumps off}} \quad (2) = \exp(C_R L_{eff} [P_p^+(0) + P_p^-(L)])$$

In which L_{eff} is the fiber effective length in which most of the Raman gain is created

where ν and μ indexes indicate the light frequencies and + and - indexes show the backward and forward signal propagation. P_ν and α_ν represent the optical power and attenuation coefficient, respectively and $g_{\mu\nu}$ is the Raman gain at the frequency ν caused by the pump at frequency μ . A_{eff} is also the effective cross section of optical fiber. The related diagram is shown in Figure 2 [8].

The equation 1 includes the signal-signal, signal-pump and pump-pump interactions. However, the interactions such as amplified spontaneous emission (ASE) and temperature dependence are neglected because they do not have a significant effect on the optimization process.

In this paper, we use the “true wave reach low water peak” fiber because it has a low loss compare to the other types of optical fibers in water peak area. This limitation is used for choosing the pump wave length. The corresponding Raman gain diagram is shown in Figure 2.

Using solutions of Equation 1, a quantity named on-off Raman gain is often achieved for every signal channel at the desired frequency band. This quantity is defined as the signal power increase at the amplifier output when the pumps are turned on. Therefore, for small signals we have:

$$L_{eff} = \frac{[1 - \exp(-\alpha_p L)]}{\alpha_p} \quad (3)$$

These equations can be used to estimate the appropriate pump power to achieve a given gain with acceptable fluctuations. For transmission of WDM systems, the Raman amplifiers should be designed so that a uniformed and wide gain spectrum is created, having the conditions and limitations such as the number of pumps, the signal band range and the type of fiber used. Thus, in designing the configuration of Raman amplifiers pumps, the role of optimization algorithms is very important.

The multiple-objective optimization algorithm used in this paper, improves the on-off Raman gain fluctuations with the least pump power consumption.

III. MULTI-OBJECTIVE OPTIMIZATION

The multi-objective optimization consists of some different and even contradictory aims that should be, minimized or maximized at the same time. Some equal or unequal constraints should be considered by the solutions. A multi-objective optimization can be expressed by the following formulas [9, 10]:

$$\text{Minimize } \vec{f}(\vec{x}) = [f_1(\vec{x}), f_2(\vec{x}), \dots, f_K(\vec{x})]$$

Subject to:

$$g_i(\vec{x}) \leq 0 \quad i = 1, 2, \dots, m$$

$$h_i(\vec{x}) \leq 0 \quad i = 1, 2, \dots, p$$

In the above equations \vec{x} is the n dimensional decision vector, $f(i) : \mathbb{R}^n \rightarrow \mathbb{R} \quad i=1,2,\dots,k$ are the objective functions and $g_i, h_j : \mathbb{R}^n \rightarrow \mathbb{R} \quad i=1,2,\dots,m \quad j=1,2,\dots,p$ are limitations and constraints.

A solution vector is called a Pareto optimal vector if a better solution cannot be found which is more optimal in an objective function and operates appropriately in the other objective functions.

In this concept, instead of finding an optimal solution, a set of optimal solutions is found which is called the Pareto optimal set or Pareto optimal solutions. A vector corresponding to an optimal Pareto solution is mentioned as a non-dominated vector. To draw the aim function, a set of all solutions which are non-dominated are used that are called the Pareto forefronts [11, 12, 13].

At single-objective optimization, there is only one search space while in multi-objective optimization, there are two search spaces including the variables and the objectives search space. There-fore, diversity can be defined in either space. In multi-objective optimization, those solutions that are not close to Pareto forefront are not suitable. If the objective functions are not in the conflict, the Pareto optimal set will have a member. Therefore, the optimal Pareto forefront set exists only if the objective functions are in conflict with each other.

The solution s_1 dominates s_2 if and only if the two following conditions are satisfied:

- 1) Considering all the objectives, the s_1 solution is better or the same as s_2 solution.
- 2) Solution s_1 , is strongly better than s_2 at least in one objective.

If s_1 dominates s_2 according to the above mentioned conditions, it is considered as a better solution. The theory space includes a set of all solutions which do or do not dominate each other. A set of all solutions which do not dominate each other is called the Pareto forefront solutions. These non-dominant solutions are connected by a curve which is called the Pareto forefront optimal set. Figure 3 represents the Pareto forefront solutions for a problem with two opposite objective functions.

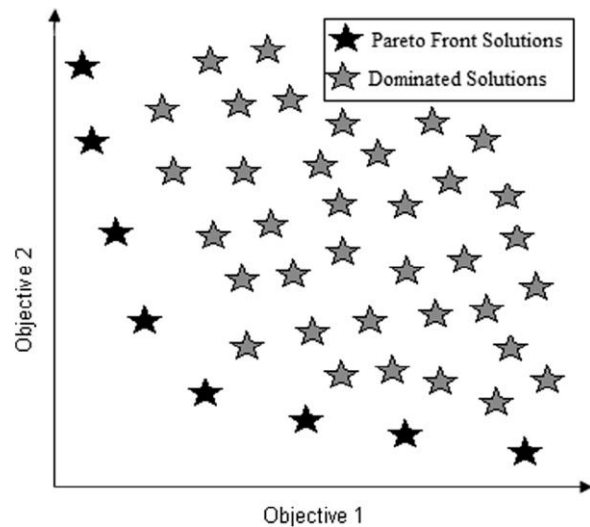


Fig. 3. Pareto-front solutions[14]

B. Fast sorting of non-dominants

The NSGA-II and MOPSO algorithms are two predominant multi-objective evolutionary methods in which the individual evolution is performed using the fast sorting of non-dominants and crowded distance.

The fast sorting of non-dominants is a strategy which ranks the solutions according to the objective function. If the crowded distance increases, the algorithm can distinguish between the two per-sons with the same rank. Those solutions with grade one are called the Pareto forefront and no solution can dominate them. Those solutions with the grade two will be defeated by only one solution. This process is performed on all solutions and all solution ranks are determined.

This sorting is done in two steps. At the first step, some solutions with grade one are identified. At the second step, the other solutions are identified (see Figure 4). Every solution is compared with the other solutions and if there is any solution which dominates it the corresponding counter variable is increased by one unit. In addition, all of the solutions which are defeated by this solution are saved in an array named Sp . Thus, at the end of the first step, the Pareto forefront set is identified. The number of times that one solution is defeated is saved in variable n_p . Therefore, there is a solution, with $n_p=0$ in forefront Pareto F1. At the second phase, rank of the other solutions is achieved using the information from the first step.

C. Imperialist competition algorithm

The imperialist competition algorithm begins with producing an initial population of possible solutions each of which called a country. Based on its value, every country can be a colony or an imperialist (an emperor). The strong countries are considered as imperialists who control some weaker countries as emperors. This algorithm is based on the competition among the emperors. The weak emperors would finally collapse and hand over their colonies to the stronger emperors. Finally, the algorithm converges to a single emperor. In this case the best solution of the optimization problem is achieved.

At the first step of the imperialist competition algorithm, the emperors are created. Every imperialist receives some colonies according to its power. This process is done according to the equations 4 and 5 which is shown in Figure 5. The more powerful imperialists would have a higher number of colonies while the less powerful imperialists would have a less number of colonies.

$$P_i = \left(\max_{1 \leq j \leq N_{imp}} \{C_j\} \right) - C_i \quad (4)$$

$$NC_i = \text{round} \left(\left\lfloor \frac{P_i}{\sum_{j=1}^{N_{imp}} P_j} \right\rfloor \times [N - N_{imp}] \right) \quad (5)$$

Where C_i is the cost of the i th emperor, P_i is the power of the i th imperialist and NC_i shows the number of colonies belong to the i th imperialist.

After initializing the empires, the absorption process starts. Figure 6 represents how countries move toward the corresponding empire. This movement is according to Equation 6. In the process of movement of colonies toward the imperialists, there is always a possibility that a colony reaches to a better condition compared to the emperor. In such cases the colony would be replaced by the emperor and would be converted to an imperialist. The process continues with the new empire and the colonies which are under the control of the previous empire would move toward the new empire.

$$X_{\text{new}} = X_{\text{old}} + \beta d \quad (6)$$

After the process of power absorption, every empire would be calculated based on the total power of that empire and its dependent colonies. However the effect of colonies is negligible. The power is calculated as follow:

$$T.C_n = \text{Cost}(\text{imperialist}_n) + \xi \text{ mean} \{ \text{Cost}(\text{colonies of empire}_n) \} \quad (7)$$

where ξ is a constant in the open range of zero to one.

The competition between the empires is the most important challenge in which each of them tries to take the other's colonies. While the weaker empires are trying to survive, the stronger ones are expanding their territory. The competition between the empires is stimulated by separating colonies from the weaker empires and giving them to the stronger ones. The probability of ownership of every emperor is proportional to its power. When an empire loses all of its colonies, it would fall and be eliminated. Finally, a single empire would remain which controls all of the countries. When all of the countries and even the emperor have the same situation, this is the sign of reaching to the answer of optimizations problem.

D. multi-objective imperialist competition algorithm

There are two fundamental issues in development of a MOEA:

- 1) The competence of each individual based on all of the goals
- 2) Maintaining the diversity of the final solution

In order to determine the competence of each individual in this algorithm, the method of fast sorting of non-dominants and

a new initiative method named sigmoid method is used. In previous MOEAs, the crowded distance was used for comparing the individuals which did not provide a quantitative measurement. In the algorithm used in this design, a quantitative measurement is provided. This measurement is important in determining the empire countries and the power of imperialist countries and estimating the total power of empires for competition of imperialist.

Firstly, rank of the countries is defined by non-dominant rapid sorting method according to all goals. All of the countries situated in the Pareto optimal front have the rank one and the emperors are selected from this collection which has a strong effect on convergence and diversity of solutions. The more the number of goals is, the more this effect would be.

After identifying the rank of each country the sigmoid function is applied and the competence of every individual is estimated. In the main ICA, each country is assigned on the basis of objective function power. In this method, the power of each country is based on all the targets (or in the other words on the multi-objective). Therefore the following assumptions should be considered:

Assumption 1: the power of every country is related to its rank. According to this, the weaker countries have the higher ranks and the stronger ones have the smaller ranks.

Assumption 2: those countries with the same ranks are compared by the sigmoid method.

After applying the non-dominant rapid ranking method if a country has the rank C its power is calculated as follow

$$\text{Fitness}_c = \sum_{j=1}^D \left[\frac{F_j(C)}{\sum_{i=1}^{N_{\text{Rank}(C)}} F_j(i)} \right] (\text{Rank}(C) - 1) \times D$$
$$\text{Power}_c = \frac{1}{\text{Fitness}_c} \quad (8)$$

In the equations (8), D is the number of goals, $f(i)$ is the value of the i th object and $N_{\text{Rank}(c)}$ is the number of the countries with the rank C. The power of the c th country is shown by Power_c and after calculation; the related amount of fitness is achieved. The fitness amount of a function is the all target values and rank of the individual. At the first part of equation (8), amount of all objectives is normalized based on the related amounts of objectives of all of individuals having the same rank. The normalization is done according to the rank in which the solution is located not according to the total space of the search. The second part of that equation highlights the role of the rank in amount of fitness and even the best solutions in higher ranks (the weaker solutions) have more fitness (of course, in the minimization problems) compare to the bad solutions that are in the lower ranks. Therefore, the normalization according to the rank leads to a more reliable and effective quantitative comparison of the solutions with the same rank. The normalized amount of all goals is reported as fitness.

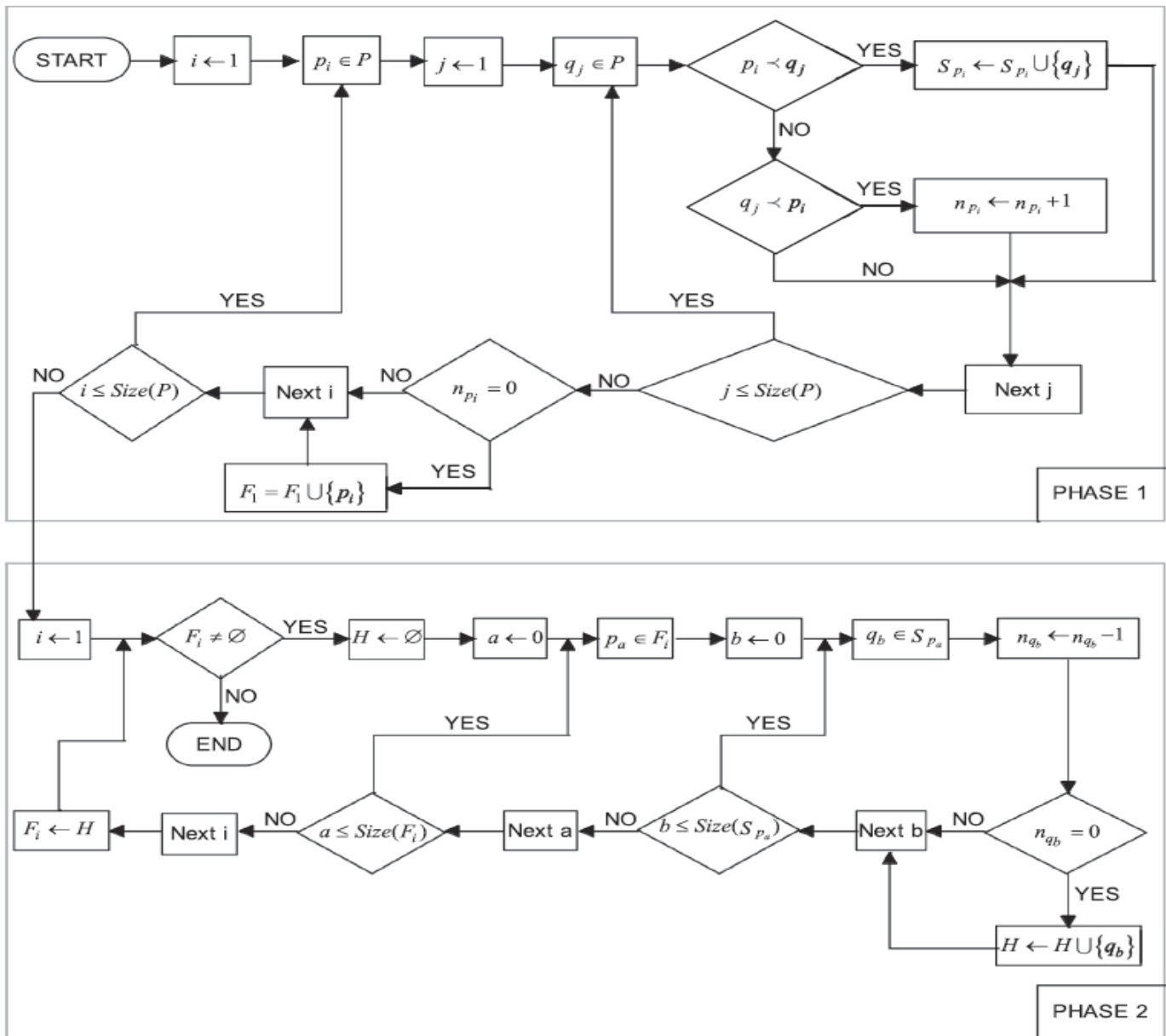


Fig. 4. Fast non-dominated sorting[14]

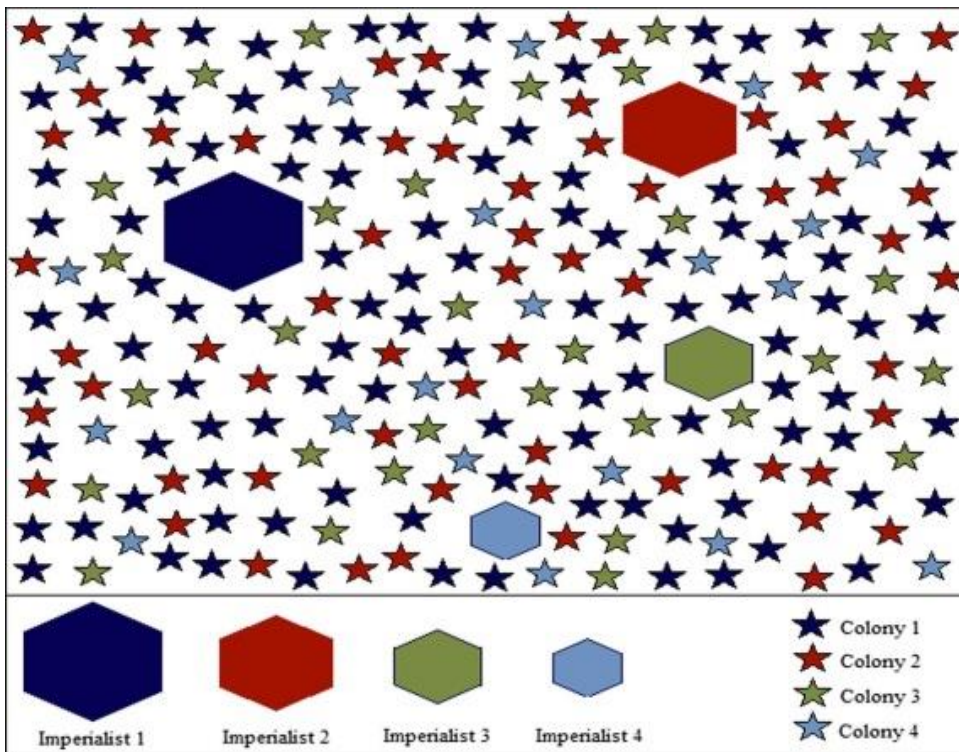


Fig. 5. Creation of Imperialist

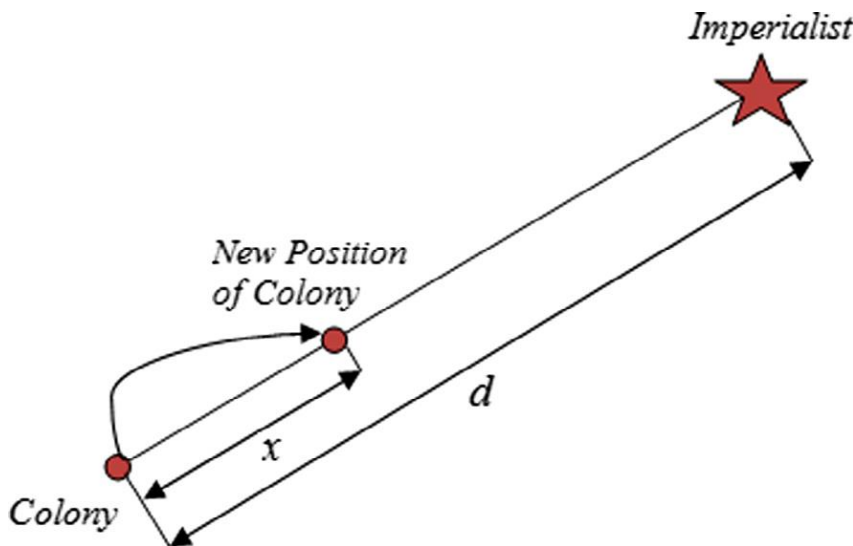


Fig. 6. the method of movement of countries toward the related empire

After estimating the power of all countries the multi-objective imperialist competition algorithm acts similar to its single objective version. For example, N_{imp} of the most powerful countries are selected as emperors. The rest of the countries are divided between the empires based on their powers. The share of empire from colonies will be calculated by the following equation

$$P_n = \left| \frac{Power_n}{\sum_{i=1}^{N_{imp}} Power_i} \right| \quad (9)$$

It should be noticed that to calculate the power, all of the countries are collected in a set and their ranks are calculated according to the objectives and using the non-dominant rapid ranking method. Then, their corresponding power is calculated using the sigmoid method. After calculating the power, the countries are divided again based on their previous situation among the emperors.

The flowchart of the multi-objective imperialist competition algorithm is shown in figure 7

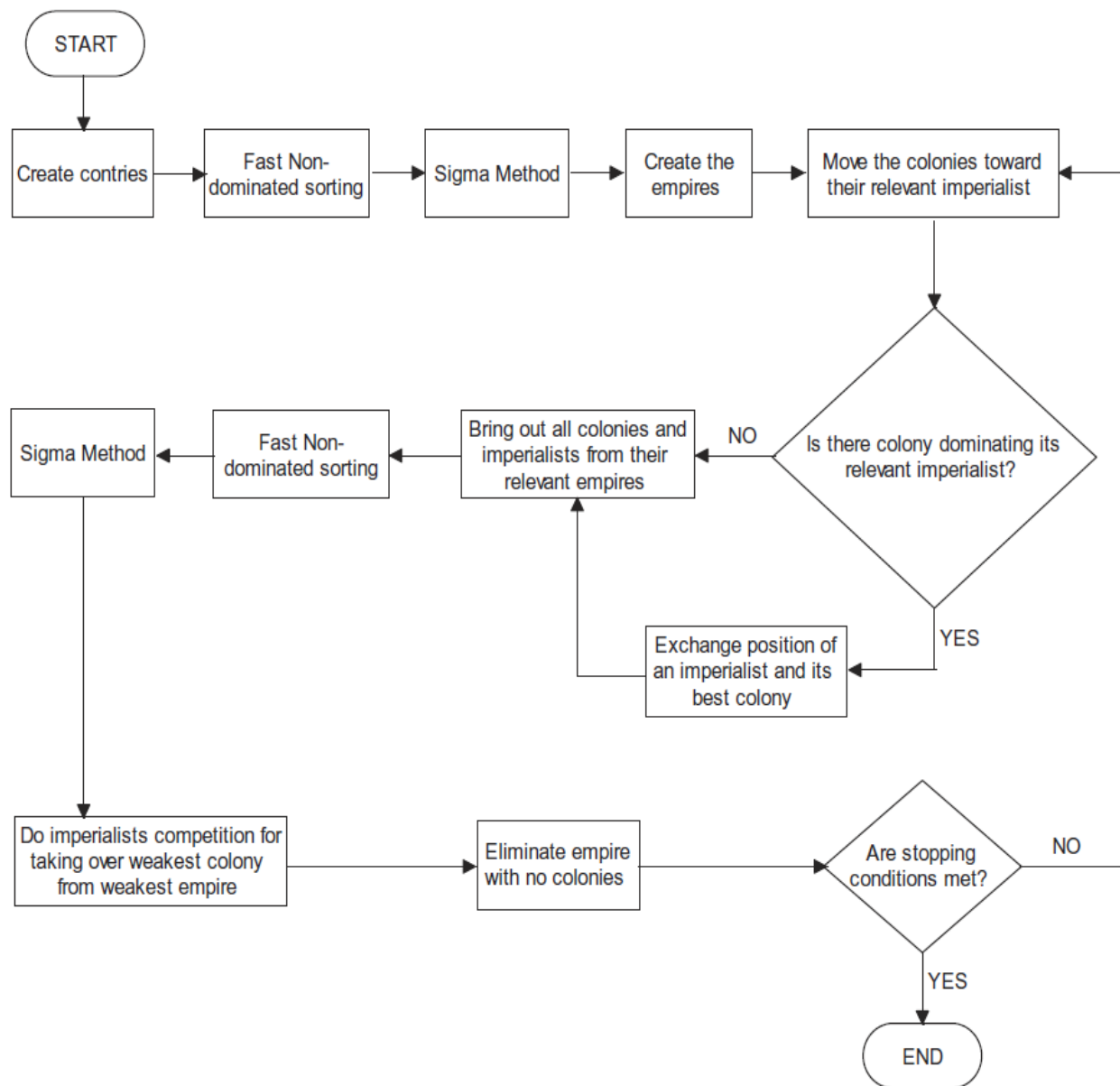


Fig. 7. flowchart of multi-objective Imperialist competition algorithm

IV. SIMULATION AND RESULTS

In this study, the equation (1) is firstly obtained for each signal wavelength and pump and for simulation of Raman Effect it is solved using the numerical methods as coupled equations. Then, using the multi-objective imperialist competition algorithm [14], suitable values for power and wave length of pumps are found so that the value of gain ripple and the total using power of r pumps in S-band with bandwidth of 80nm are both minimized at the same time.

The input signal channels are selected from 1460nm to 1530nm with spaces of 5nm. The power of each input signal channel is 10mW and the fiber length is 100 kilometers.

The gain optimization is done around a constant and given number. This number is also considered as one of the variables

that the optimization algorithm should find its appropriate size. Thus, the calculation formula of gain ripple is considered as one of the goal functions in the optimization algorithm in the form of equation 10. The second objective function in this multi-objective optimization is equal to the set of pumps powers.

$$\text{Max } \{ \text{Abs} [\text{gain} (\lambda_{s1}) - g_0, \text{gain} (\lambda_{s2}) - g_0, \dots, \text{gain} (\lambda_{s16}) - g_0] \} \quad (10)$$

As mentioned in the optimization section, using the multi-objective optimization algorithms we finally reach to a set of suitable answers called the Pareto optimized forefront. Figure 8, shows the Pareto diagram for the final case. The optimized gain level (g_0) of 3dB is achieved and the fluctuations around it have been reported in Table 2. In Figure 8, two goals are considered as two dimensions which are independent from

each other. In the other words one of our theory spaces is two dimensional.

This algorithm is considered for optimization with limitation for pump signal which is used as follow:

$$p_1-p_8(0-70\text{mw}) \quad \text{و} \quad \lambda_1-\lambda_8(1359-1450\text{nm})$$

The results are reported in Table 2. The number of iterations of algorithm for finding the optimum answer was 1150. The initial number of countries was 400 and among them, 20 countries were selected as emperors. 5 imperialist were finally remained. The number of Pareto forefront members was 180 at the last iteration. Among them, the information of 5 selected imperialist is shown in the Table 2. The number of algorithm iterations was determined by trial and error according to the hardware limits for test. Verifying the information related to the locations of 180 members of Pareto fore front members, the similarity and vicinity of their locations reveal that the algorithm has converged and found the optimal solution.

As seen in Table 2 and Fig. 9, in imperialist 1, the ripple of 0.09402 dB around the gain level of 3db is achieved with total pump power of 255.2 mw which is the minimum amount of gain ripple among five of the best algorithm answers. In imperialist 4, the gain ripple of 0.24708 dB is achieved with total pump power of 244.44213 mw which is the minimum amount of the used pump power among the selected answers. In this case, the pump power rate is decreased compared to the

previous structure while the gain ripple is increasing. Now, according to the design requirements and importance of each parameter, one of the available pump structures in Table 2 is selected to implement the desired Raman amplifier. By comparing the results of Table 2 in which the least value is 0.09402 with that of [15] which has the same condition as this paper for simulation except that it uses the PSO optimization algorithm, it is concluded that the gain ripple is decreased compared to the reported rate of 0.136. Furthermore, as seen in Table 2, since the power of the 8th pump is zero, the number of pump signals in all of five imperialist is decreased to seven signals. It means that in ICA algorithm, the desired ideal answer could be achieved using a fewer number of pump signals which is an advantage of the employed method. Assuming that the noise effect is negligible and in the desired amplifier design, the pump configuration is selected as one forward pump and 7 backward pumps, the obtained results are reported in Table 3.

According to Table 3 and Figure 10, it is obvious that in this configuration, more uniformed gain profile can be achieved with fewer pump power. For example, the second answer in Table 2 which is related to the configuration of 8 backward pumps has approximately the same gain ripple compared to the second answer in Table 3.

Even in the second case, the rate of fluctuations is lesser. However, the rate of consumed power in the second case is 32.5 mW lesser.

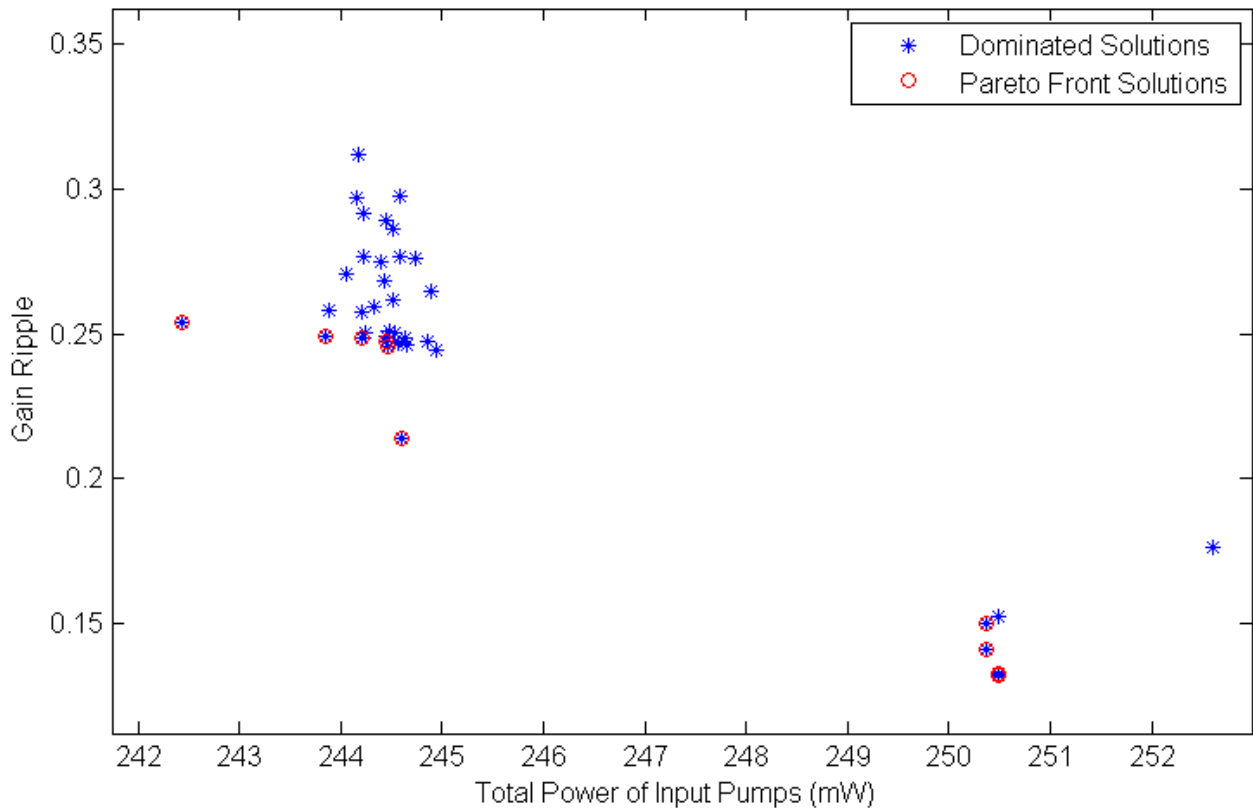


Fig. 8. Pareto diagram for final case

TABLE II. THE RESULT OF OPTIMIZATION WITH MULTI-OBJECTIVE ICA ALGORITHM IN BACKWARD PUMPING STRUCTURE

8 pump powers P_j (mW) and their Frequencies λ_j (THz)									total power of input pumps (mW)	gain ripple (dB)	
Imp		1	2	3	4	5	6	7			8
1	P	39.3061	30.02521	0.696911	54.74846	16.50323	56.01128	57.91191	0	255.2031	0.09402
	λ	218.8645	217.0124	220.4194	208.8315	219.7974	214.3313	210.7513	0		
2	P	62.39576	54.53276	20.88627	45.83234	49.01956	4.996665	12.826	0	250.4893	0.13247
	λ	209.4038	210.9225	219.0399	215.9991	217.7805	206.8966	213.4935	0		
3	P	68.26442	36.63109	7.186206	53.70375	19.24751	36.95877	22.60885	0	244.6006	0.2136
	λ	210.9862	218.6084	206.9732	216.408	218.6216	210.0791	210.6517	0		
4	P	37.5164	39.02661	0	67.81045	1.769148	33.67335	64.64617	0	244.44213	0.24708
	λ	217.9719	219.6433	220.3698	210.4618	218.092	209.53	213.9637	0		
5	P	50.04193	29.57433	21.50764	63.78989	43.73134	41.72416	0	0	250.3693	0.14998
	λ	216.8354	208.0884	210.9685	209.8689	218.7318	214.2194	211.1866	0		

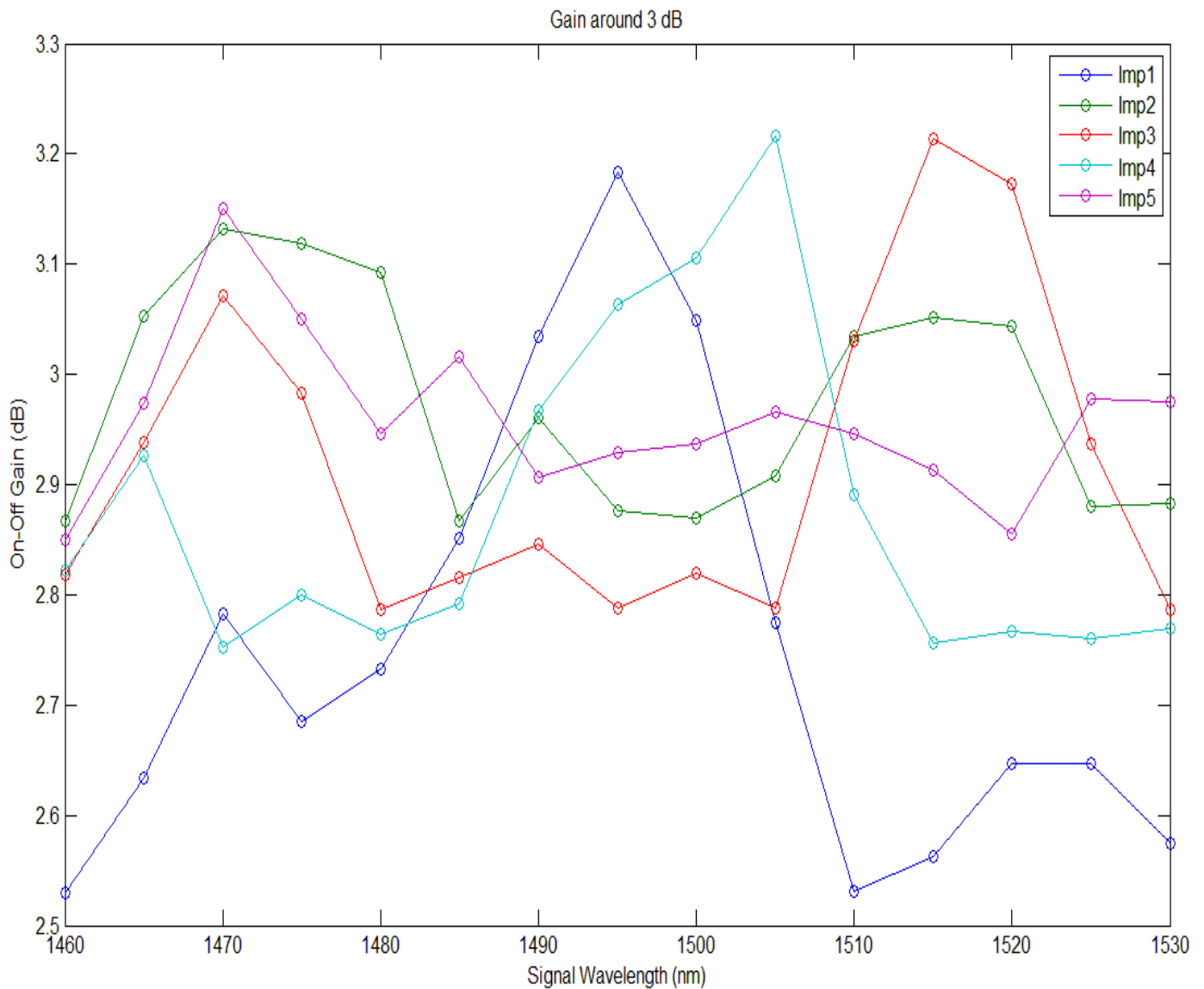


Fig. 9. The spectrum of Raman gain that achieved with multi-objective ICA algorithm in backward pumping structure

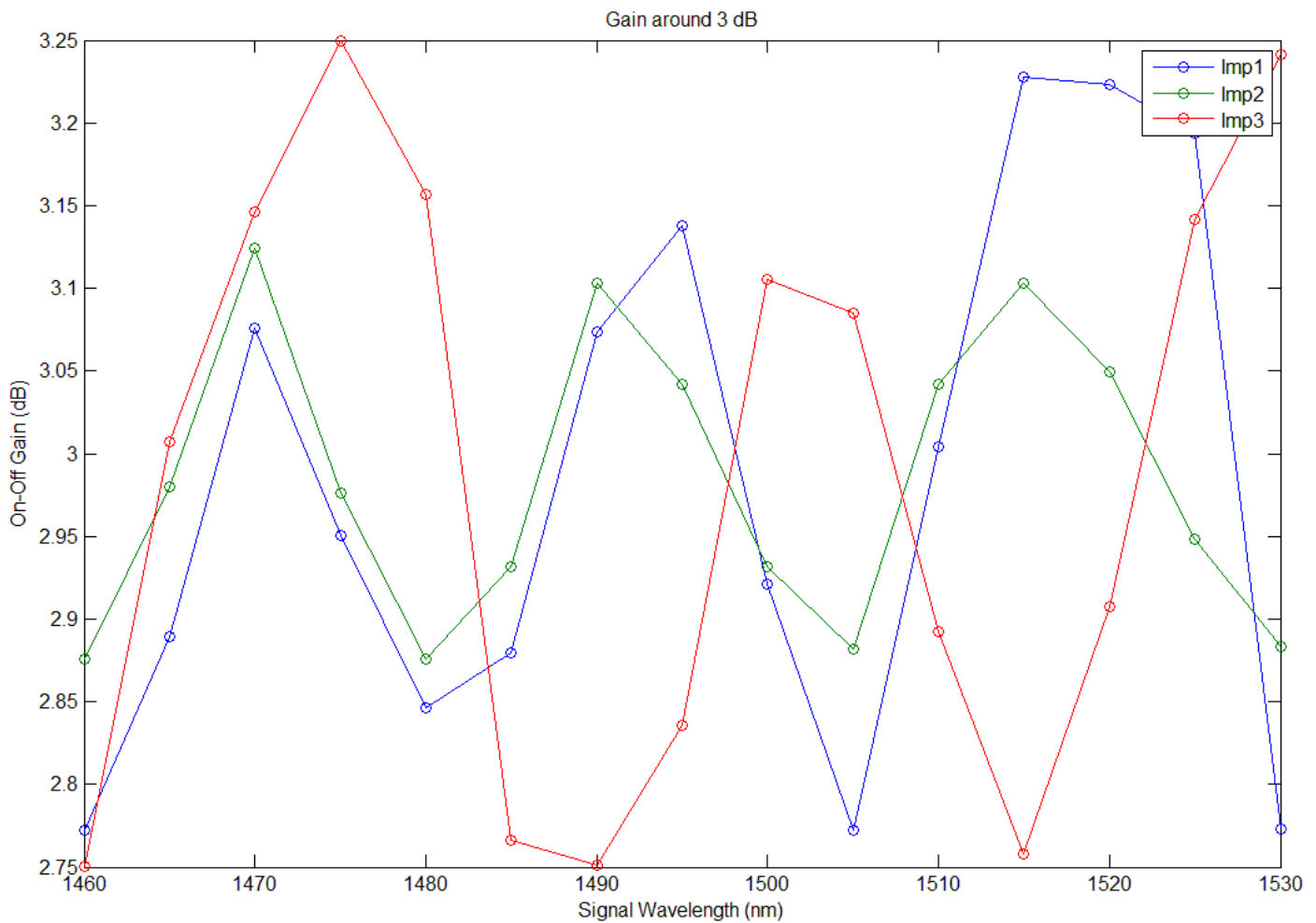


Fig. 10. The spectrum of Raman gain that achieved with multi-objective ICA algorithm in 1 forward and 7 backward pumping structure

TABLE III. THE RESULT OF OPTIMIZATION WITH MULTI-OBJECTIVE ICA ALGORITHM IN 1 FORWARD AND 7 BACKWARD PUMPING STRUCTURE

8 pump powers P_j (mW) and their Frequencies λ_j (THz) 1 Forward 7 backward									total power of input pumps (mW)	gain ripple(d B)	
	1	2	3	4	5	6	7	8			
$P_{1\text{ forward}}$	P	41.80618	0	66.53483	2.145349	0	0.619079	51.58809	43.10304	205.7966	0.2277
	λ	218.7108	206.8973	211.1566	206.8966	219.7067	220.5882	215.8289	209.4899		
$P_{7\text{ backward}}$	P	36.84844	21.75133	25.25959	69.79903	6.913643	0.456617	7.666741	43.20697	211.902	0.1246
	λ	218.7592	211.0864	213.7549	209.6391	219.1319	220.472	210.7508	216.1991		
$P_{3\text{ backward}}$	P	70	9.024821	0	38.15369	1.623326	59.97018	0.620729	25.17374	204.5665	0.2498
	λ	217.7616	213.0262	219.9269	214.5634	216.166	209.2603	207.571	208.4559		

V. CONCLUSION

In this paper, using the multi-objective optimization algorithm with the least consumed power of pump, the most uniform gain profile in S-band was achieved. The effect of pump configuration on Raman amplifier performance in optimal case was also verified. The simulation results reveal that if the noise does not interfere, the structure of one forward pump and seven backward pumps is a better design for achieving the best performance with the lowest pump power. However, in most of the researches in this field, only the gain

profile is uniformed without considering any limit for the consumed power and only the backward pump structure is used. The employed optimization algorithm in this paper is a multi-objective ICA which as shown in this paper, has a high performance in optimization of Raman amplifier compared to the other algorithms in this field.

For future work the recommended algorithm can be applied in a Raman optical fiber amplifier that uses a new class of optical fiber such as a photonic crystal fiber (PCF) as a medium gain, and also MOICA can be potentially applicable to

the swarm dynamics such as [16] to increase the performance of optimization.

REFERENCES

- [1] Fiuza, J., Mizutani, F., Martinez, M. A. G., Pontes, M. J., & Giraldi, M. R. Analysis of distributed Raman amplification in the S-band over a 100 km fiber span. *Journal of Microwave and Optoelectronics*, . (2007). 6, 323-334.
- [2] Jahromi, M. K., & Emami, F. Simulation of Distributed Multi-Pump Raman Amplifiers in Different Transmission Media. *International Journal of Communications*, . (2008) 2(4), 205-212.
- [3] Bromage, J. Raman amplification for fiber communications systems. *Journal of Lightwave Technology*, . (2004). 22(1), 79
- [4] Islam, M. N. Raman amplifiers for telecommunications. *Selected Topics in Quantum Electronics, IEEE Journal of*, . (2002). 8(3), 548-559
- [5] Mohsen katebi jahromi ,seyed mojtaba saif, Farzin Emami Application of imperialist competitive algorithm for distributed fiber raman amplifier . *Indian J.Sci.Res.* (2014) 7 (1): 1154-1161.
- [6] Liu, X., Chen, J., Lu, C., & Zhou, X. Optimizing gain profile and noise performance for distributed fiber Raman amplifiers. *Optics express*(2004).. 12(24), 6053-6066.
- [7] Jiang, H. M., Xie, K., & Wang, Y. F. Flat gain spectrum design of Raman fiber amplifiers based on particle swarm optimization and average power analysis technique. *Optics and Lasers in Engineering*(2012).. 50(2), 226-230
- [8] Fiuza, J., Mizutani, F., Martinez, M. A. G., Pontes, M. J., & Giraldi, M. R. Analysis of distributed Raman amplification in the S-band over a 100 km fiber span. *Journal of Microwave and Optoelectronics*, . (2007). 6, 323-334.
- [9] Li, X., & Wong, H. S. Logic optimality for multi-objective optimization. *Applied Mathematics and Computation*, . (2009). 215(8), 3045-3056.
- [10] Ashry, G. A.. On globally convergent multi-objective optimization. *Applied mathematics and computation*(2006), 183(1), 209-216.
- [11] Deb, K., Pratap, A., Agarwal, S., & Meyarivan, T. A. M. T.. A fast and elitist multiobjective genetic algorithm: NSGA-II. *Evolutionary Computation, IEEE Transactions on*(2002), 6(2), 182-197.
- [12] Coello Coello, C. A., & Lechuga, M. S. MOPSO: A proposal for multiple objective particle swarm optimization. In *Evolutionary Computation, (2002).. CEC'02. Proceedings of the 2002 Congress on* (Vol. 2, pp. 1051-1056). IEEE.
- [13] Ali, H., Shahzad, W., & Khan, F. A. Energy-efficient clustering in mobile ad-hoc networks using multi-objective particle swarm optimization. *Applied Soft Computing*, (2012). 12(7), 1913-1928.
- [14] Enayatifar, R., Yousefi, M., Abdullah, A. H., & Darus, A. N. MOICA: A novel multi-objective approach based on imperialist competitive algorithm. *Applied Mathematics and Computation*. (2013), 219(17), 8829-8841.
- [15] Emami, F., & Akhlaghi, M. Gain Ripple Decrement of S-Band Raman Amplifiers. *Photonics Technology Letters, IEEE*, (2012). 24(15), 1349-1352.
- [16] Shang, Yilun, and Roland Bouffanais. "Consensus reaching in swarms ruled by a hybrid metric-topological distance." *The European Physical Journal B* 87.12 (2014): 1-7.

Influence of Adopting a Text-Free User Interface on the Usability of a Web-based Government System with Illiterate and Semi-Literate People

Ms. Ghadam Alduhailan

Department of Information Systems
College of Computer Sciences and Information Technology
King Faisal University, Hofuf P.O. Box 380 Al-Ahsa
31982 Kingdom of Saudi Arabia

Dr. Majed Alshamari

Department of Information Systems
College of Computer Sciences and Information Technology
King Faisal University, Hofuf P.O. Box 380 Al-Ahsa
31982 Kingdom of Saudi Arabia

Abstract—Illiterate and semi-literate people usually face different types of difficulties when they use the Internet, such as reading and recognising text. This research aims to develop and examine the influence of adopting a text-free user interface on the usability of a web-based government system with illiterate and semi-literate people. A number of steps have been followed in order to achieve this research goal. An extensive literature review has been carried out to explore the adoption of different concepts or representations of content to help illiterate/semi-literate people in Information and Communication Technology (ICT) projects. Then a consolidated framework is proposed and adopted in order to develop a text-free user interface. This can help in building a text-free user interface for a certain service here in Saudi Arabia. Cultural factors, education level, text-free icons, and usability guidelines have been considered in the above-mentioned framework. A prototype of a web-based government system after taking into account the above framework has been designed and developed. Usability testing and heuristic evaluation have been used as usability assessment methods in order to evaluate the system usability and its impact on the usability for illiterate people in Saudi Arabia. The results are encouraging as the achieved results of usability measures imply that adopting the consolidated framework has influenced the usability in this research.

Keywords—text-free interface; web-based system; usability; e-services; government; consolidated framework

I. INTRODUCTION

Information and communication technology (ICT) has improved societies in different ways. Actually, people consider technology to be a tool that can help them to perform their daily functions efficiently and effectively. E-governments use the World Wide Web (WWW) as a tool to deliver their services to all citizens.

Most e-government websites provide e-services that rely on textual interface conjunction with little use of graphics and icons that describe the content of websites. Therefore, a group of users can easily use and interact with governments' websites and take advantage of available services. However, there are groups of users in society who are not able to access and benefit from e-government services. Users who are unable to read and write struggle with the accessibility of available services due to the heavy use of text on most governmental

websites. Different ways have been proposed in order to assess the usage of these users' categories, such as accessibility tools, usability evaluation methods, and other technologies.

Success in implementing and developing e-government is the goal of many government organisations. This process requires a good understanding of the needs of users and system requirements. Thus, such requirements are expected to be considered including illiterate or semi-literate, and even people who suffer from computer illiteracy.

The rest of the paper is organized as follows. Background and related work is discussed in section II. Section III presents the research questions and the used methodology in this research. It includes how the website was selected and the justifications. Participants recruitment and tasks' selections are also explained in this section. Data analysis and discussion is presented in section IV. The paper concludes with its general findings, recommendation and conclusion.

II. BACKGROUND AND RELATED WORK

Many studies have investigated factors, challenges and obstacles that have an influence on adopting e-government in many countries, e.g. Jordan, Bahrain, Qatar, Egypt, Pakistan, Taiwan, Germany and Saudi Arabia such as [4][2][13][1][28][27][30][31][32]. These studies have introduced to which extent such factors impact on adopting e-government from the perspective of users or governments. The studies have found that most countries lack considering factors and addressing challenges and obstacles which have an influence on adopting e-government and providing it to the fullest. Furthermore, the results have provided only general recommendations for countries' governments to focus attention on all or some of these factors or obstacles without proposing specific solutions. Table 1 shows most factors, challenges and obstacles found in adopting e-government in many countries.

E-government acceptance should highly consider a number of factors which are related to users' needs, e.g. culture, education, usability and accessibility, and not just interest in implementing good infrastructure for ministries, e.g. availability of hardware, networks and servers [4][2][13][1]. In Saudi Arabia, [2][4] have studied challenges and obstacles affecting e-government adoption. The main obstacles have

been found: availability, education level, trust, accessibility and usability [2][4].

TABLE I. CHALLENGES AND OBSTACLES IN E-GOVERNMENT

Factors	Explanation	References
Infrastructure, e-readiness, availability	To what extent the major IT infrastructure facilities, e.g. hardware, software and skills, are ready and available to all users and government sectors	[2], [4], [27], [30]
Privacy, security, trust	To what extent the government provides a secure e-transaction and ensures user information privacy.	[1], [2], [4], [30], [31]
Service complexity, ease of use, accessibility	To what extent the e-service design is usable, accessible and understandable by different citizens.	[1], [2], [27], [30], [32]
Service quality, website quality, compatibility	To what extent the information and content of the e-government websites satisfy different citizens and are compatible with a unified design framework.	[27], [30], [32]
Culture, education, Internet and computer skills	Country culture, religion, education level of different citizens, and computer skills all have an impact as social factors in adopting e-government	[1], [2], [4], [31]
Awareness	To what extent a country's government spreads the awareness	[30]

The ability to read and write is one of the important factors which allow individuals to integrate in society and digital society, and exchange knowledge and information. The United Nations Educational, Scientific and Cultural Organization (UNESCO) has defined literacy as “the ability to read, write and understand short written sentences in everyday life”. Being unable, or finding it difficult, to read or write is a kind of disability which mediates e-inclusion and accessibility of e-government websites [15].

UNESCO provides great effort and many programmes to eliminate illiteracy in many countries. UNESCO considers literacy to be very important, especially in rapid development and usage of technology in most of our lives [15]. However, still there are groups of illiterate people in many countries according to statistics. According to UNESCO Day 2014, “there are still 781 million adults and 126 million youths who cannot read or write a simple sentence” [15].

Recently, an article was published in Al Eqtisadiah newspaper in Saudi Arabia which states that the number of illiterate people in Saudi Arabia amounted to 1.2 million of the population by the end of 2013; this number forms 5.6% of the population [8]. The highest rate of illiteracy was in elderly people between 50 and 75 years of age, with the rate at about 40% regarding total illiterate people who are aged above 15 years [8]. This group of users need to utilise e-services. However, there are only a few studies that have addressed and developed a suitable interface for illiterate and semi-literate users to improve their ICT projects in developing countries such as [3][5][7][9][11][14]. Addressing a problem related to people who have difficulty in accessing ICT projects is not just

a hardware problem, but needs to consider other factors, e.g. how to design and provide information presented in ICT projects [7].

Medhi et al. defined a text-free interface as the “liberal use of graphics and photographs for visual information, and voice for providing information normally provided via text” [11]. Thus, a text-free interface is a replacement for textual content with expressive photographs, drawing images, and audio. It has been shown that an interface without text can be useful and preferable by users unable to read text (illiterate) and with a low level of education (semi-literate) [11][9][16]. Nevertheless, most illiterate people used mobile phones, were familiar with number pads, and were able to identify numbers [11][9]. This implies that a text-free user interface can be usable by illiterate users when containing numerical text.

The process of developing an interface for illiterate and semi-literate users includes observing and understanding users in specific contexts, as well as analysing and gathering information, and includes these perspectives in the design [11]. Medhi et al. and other studies have proven that involving and understanding illiterate users' needs in a design process can help to recognise problems during interface development and selecting the more effective and expressive types of pictures and other types of media [11][6][3][5]. Due to illiterate people often having a different system of thinking, some pictures may be interpreted completely differently, depending on the level of education of the person and culture [7].

Thatcher et al. have developed an ATM icon-based interface in respect of helping illiterate bank customers [16]. Choosing the best icons and pictures to translate the intended meaning of content depends on the community culture, psychology and religion of illiterate users [7][3]. However, Goetze et al. and Thatcher et al. have found that most of the pictures have the same interpretation in different countries, whereas native language is understandable by only a specific country or region [7][16]. This led to concluding that an icon-based interface is better than a speech-based interface for illiterate people, especially in countries with many different languages, dialects and accents [16]. In addition, the human mind responds to images and it is very easy for a user to understand a particular text in the form of pictures [7].

Ávila et al. and Medhi et al. have shown that illiterate people can interpret both realistic pictures and drawing (cartoon) images [7][3]. Choosing between these two types of icons depends on the context of the task and system [3]. Designers can use realistic pictures when focusing on the credibility or creating a direct connection with a particular concept in the real world [3]. However, they can use drawing images when focusing on representing a general concept or they need to take advantage of the flexibility to draw concepts rather than realistic pictures [3]. Insertion of expressive pictures and icons in conjunction with text can be beneficial for functionality and lowly literate people. Friscira et al. have shown that keeping text with pictures will be better for low illiteracy, due to removing text not allowing low literates to discover and encourage them to learn reading and writing [6].

The VideoKheti mobile system project has shown the benefits of using multimodal interaction when designing a text-

free interface [5]. Multimodal systems can offer a flexible, efficient and usable environment for lowly literate users [5]. Therefore, it provides many ways for lowly literate users to interact through input modalities, such as speech and touch, in addition to receiving information through the system through output modalities, such as speech synthesis, smart graphics and other modalities, opportunely combined [9]. This method of HCI allows lowly literate and novice users to choose their preferred style of interaction [9]. VideoKheti has been built on multimodal interfaces and the first system is targeted at lowly literate users, which combines touch, graphics, and speech input on a mobile interface and is completely text-free [5]. However, it has examined this kind of interface with semi-literate people and applied the project to mobile phones only.

Sherwani et al. have developed a telephony system to help illiterate people by using speech recognition technology and comparing it with touch technology to access information in a healthcare system [14]. However, the adoption of a speech recognition interface for illiterate users' needs considerable effort and to be well designed in order to be better and more effective than a touch interface for both low-literacy and higher-literacy users [14].

Earlier studies have been focused on an innovative way to address illiteracy constraints through designing a user interface suitable for the illiterate and semi-literate population [3][5][6][11][14]. It will adopt and use icons and images only in designing the text-free interface [16]. As mentioned before, the advantage of icons and images is that they are more understandable by different countries and regions with a variety of languages and dialects, whereas the disadvantage is how to refine and select the best icons and images to reflect the intended meaning of instructions or tasks in a specific system. Medhi et al. have suggested using voice feedback as help instructions in order to explain some instructions or tasks [11], designing a user interface using text with icons and images in order to encourage semi-literate users to learn reading or guess written content with the help of icons [6][3]. Nevertheless, the text will not help illiterate people as they never read or write. A speech-based user interface will be designed as an interaction method for lowly literate people [14]. However, it needs to be well designed due to different dialects and accents, particularly in larger countries.

III. RESEARCH QUESTION AND METHODOLOGY

This research aims to examine the impact of text-free user interface on usability while illiterate and semi-illiterate use e-services. This can be achieved after proposing a consolidated framework, which will adopt culture, users' needs and usability guidelines, to develop text-free user interface for a local e-service. A prototype will be developed taking into account the proposed consolidated framework. The proposed prototype will be evaluated in terms of its usability with illiterate and semi-illiterate users through proper usability evaluation methods.

A. selection and Development of text-free web-based system:

An e-government web-based system has been chosen for this research where it has to be used by the all citizen her in Saudi Arabia so illiterate and semi illiterate people have to use such a system. In order to develop the prototype; three steps

have to be considered: images and icons development, images' should meet usability guidelines and cultural and users' needs should be also considered. Firstly, all images and icons have been designed for the purpose of the project and to fit with the selected e-service functions except the common icons and images such as cancellation icons and others. Secondly, images usability guidelines have been taken into considerations such as meaningfulness, styling quality, localability, message quality and metaphor. Thirdly, culture and users' needs have been also considered such as the images should be acceptable with Saudi culture. It will also reflect users' needs while using the proposed system. The prototype of the selected system has been developed taking into consideration the aforementioned steps consulting 2 experts to ensure a professional development has been taken into account.

Usability evaluation is expected to be carried out after ensuring the prototype has been developed and its ready for evaluation to answer the research question. Two usability evaluation methods have been used in this research; usability testing and heuristic evaluation. the UT method needs users participation where heuristic evaluation needs experts to be conducted. Therefore, both methods have been chosen for this research in order to eliminate any risk of ignoring any type of "user" or "expert" point of view.

Usability testing aimed at gathering qualitative and quantitative data by observing the users' performance and user satisfaction after finishing the test session, as well as finding usability problems potentially encountered by illiterate/semi-literate users. This method needs representative users to perform predefined tasks. Participants recruitment, task selection, test environment and measures will be discussed.

B. Participants recruitment:

Saudi illiterate/semi-literate users were the targeted audience of both genders. Neilson found that five users are enough for user testing through formative usability evaluation; however, 15 users help to identify more problems at the first evaluation [20]. Dumas and Redish have pointed out that 6–12 users are sufficient to conduct user testing [21]. Thus, in this testing, 15 participants have been recruited. Moreover, user consent was taken from users. The pre-test questionnaire was filled out by the users.

C. Task selection:

The tasks have been selected based on the four selected services which have been designed for the purpose of the project. Each service is represented as a user task, as recommended by [34] [21].

D. Test environment:

An appropriate location has been prepared and organised to conduct an effective test session. The selected location should be quiet and comfortable for every participant. The observer sat away from the participant as not to interrupt his/her attention while performing the given tasks as its recommended by [34][21].

E. Usability measurements:

The usability of a software, website or product is measured by to what extent it is easy to use for the targeted users [19].

Five metrics have been identified by Jakob Nielsen to evaluate the ease of use or usability: learnability, efficiency, memorability, errors and satisfaction [19]. Memorability is measured by how users become proficient when facing the design after a period of time. Thus, it has been excluded due to the long time needed for the evaluation. Learnability is calculated by task completion when the user performs the task the first time [19]. Task completion has been determined by monitoring the user during the task using three rates proposed by Jakob Nielsen (S = Success, F = Failure, P = Partial success) [22]. Success indicates the user terminating the task without errors, Partial success means the user succeeding in performing the task with error(s), and Failure means the user giving up finishing the task [22]. The efficiency is checked by the time the user takes to complete the task after learning the design [19]. For that, the test has been recorded using Screen Recorder software, which helps to measure the efficiency (time on completion of task). The errors measure is calculated by the number and frequency of errors encountered by the users during the test [19]. Also, Screen Recorder software was used to identify user errors through performing each task. Satisfaction is evaluated by to what extent the user enjoyed and was interested in using the design [19]. User satisfaction has been measured by asking the user orally after finishing the tasks using a 5-point Likert scale (very satisfied, satisfied, neutral, dissatisfied, and very dissatisfied).

Heuristics evaluation was organised and prepared to ensure effective inspection and results. Preparing the procedure included selection of evaluators, guidelines with detailed checklists, stating evaluation materials and instructions, and piloting the guidelines and checklists to ensure its compatibility with the text-free web-based system before starting the real evaluation.

F. Selection of heuristics evaluation guidelines:

The most frequent set of heuristics used in evaluating a user interface has been proposed by Nielsen [24]. It consists of 10 heuristics which are used in text-free user interface evaluation [3]. Nevertheless, a new text-free interface needs additional principles or guidelines in conjunction with Nielsen's heuristics. For this reason, Nielsen's 10 heuristics have been extended with text-free principles proposed by Medhi et al. during her field study [11]. These principles have developed as guidelines for a text-free user interface. Furthermore, Flexibility and Minimalist Design principles in Nielsen heuristics have been excluded because it intended to evaluate the ability of expert users to accelerate his interaction with the interface by using shortcuts or an alternative way of interaction. This heuristic is not suitable for illiterate/semi-literate users because they need a few steps and settings in order to reduce the potential user errors. In addition, there is little knowledge and experience of illiterate/semi-literate users in using a computer; thus, there is no room for adjusting interface settings. The following list has been used which is a combination of Nielsen heuristics [24] and Medhi text-free principles [11]:

- 1) Visibility of System Status
- 2) Match Between System and the Real World
- 3) User Control and Freedom

- 4) Consistency and Standards
- 5) Help Users to Recognise, Diagnose, and Recover from Errors
- 6) Error Prevention
- 7) Recognition Rather Than Recall
- 8) Aesthetic and Minimalist Design
- 9) Help and Documentation
- 10) Avoid text (but using numbers may be okay).
- 11) Use semi-abstracted graphics, photorealism with deeper interaction
- 12) Pay attention to subtle graphical cues. User response may depend on psychological, cultural or religious biases.
- 13) Provide voice feedback for all functional units

G. Selection of evaluators:

Five evaluators were recruited (two female and three male) after taking their consent as recommended by [17]. The evaluators have studied a usability analysis and testing course and have little experience in using a text-based website version.

H. Evaluation materials and steps:

Afterwards, a heuristics evaluation sheet was prepared with 13 selected heuristics. A number of checklists have been listed in order to help the evaluator to assess the interface against every heuristic. The evaluation sheet was submitted by e-mail to everyone in order to ensure conducting the evaluation independently to guarantee unbiased results [25]. The evaluation sheet included the goal and objectives of assessment and the website tasks without providing any guide or aid as to how to use the design. Furthermore, it was requested from each evaluator to spend some minutes exploring the interface and then review it to fill out the sheet, find problems and provide their comments. The problems found during heuristics evaluation have integrated with user testing problems in a single table (in the next section).

I. Piloting the experiment:

A pilot experiment of heuristics checklists has been done by an independent evaluator. The importance of piloting the heuristics checklists is to guarantee that it is adequately clear and appropriate to the text-free interface [25]. In the pilot experiment, the evaluator has achieved all heuristics evaluation steps and procedures. The results of this evaluation are excluded from findings due to there being discussion and clarification with the evaluator.

J. Severity rating:

Problem severity helps to rank the seriousness of the problem to the targeted users during using the website. Using Jakob Nielsen's severity rating, all problems gathered and observed by two usability methods have been returned to the five heuristics evaluators to rank the severity of each problem [26]. The severity rating scale from 0 to 4 is as follows: 0 = I don't agree that this is a usability problem at all; 1 = Cosmetic problem only: need not be fixed unless extra time is available on the project; 2 = Minor usability problem: fixing this should be given low priority; 3 = Major usability problem: important to fix, so should be given high priority; 4 = Usability catastrophe: imperative to fix this before the product can be

released [26]. Each evaluator did the rating alone and then computed the average of rates for each problem [26].

IV. DATA ANALYSIS AND DISCUSSIONS

This section includes analysis of data collected from two usability evaluation methods which have been selected in this project. Starting with finding all problems from these methods, a comparison between types of problems has been discovered by each method. Thereafter, analysis data was gathered from usability testing in order to assess and find the overall user usability of the text-free web-based system.

A. User Testing and Heuristics Evaluation Problems:

After running user testing and heuristics evaluation, this section discusses what problems have been detected, the number and frequency of problems found by each method, common problems discovered by both, and the types of problems in terms of the impact of the problem on user usability. The following table (Table 3) shows the number of problems discovered by heuristics evaluation and usability testing and the number of common problems:

TABLE II. NUMBER OF PROBLEMS

Evaluation Method	No. of Problems	No. of Common Problems
Heuristics Evaluation	17	4
Usability Testing	9	
Total no. of problems	22	

Overall, 22 distinct problems have been discovered from both usability testing and heuristics evaluation. Usability testing has revealed five distinct problems, heuristics evaluation has found 13 distinct problems, and four problems were common.

B. Discovered problems based on frequency:

From the extracted problems, the number of observations have been discovered. The evaluation found that the highest frequency was in problems which related to skills needed in using a computer (using a dropdown menu and check boxes). Most of the illiterate/semi-literate users do not use a computer. The usability tester observed that illiterate/semi-literate users tend to click on-based tasks.

Regarding the images and icons design problems were in second place with less frequency. This was according to the images and icons feature which was assumed before in the consolidated framework. Notice that only images and icons belong (some concepts or website functions need help in conjunction with images such as a voice or video, as there is no agreement to interpret the same exactly intended meaning by all people), e.g. the image of the Reporting Missing Documents service has a problem. Although there is help in the form of a voice with the image, it may need to add the voice when the mouse is over an image instead of a separate icon for a voice under the image. That is easier for illiterate/semi-literate users, as observed in the map during the evaluation.

The other images and icons which belong to other features have been recognised by users. However, regarding the feature that is assumed (illiterate/semi-literate users can recognise numbers), only two users out of 15 can't read numbers.

C. Discovered problems based on severity:

Heuristics evaluation found a usability catastrophe and mostly major and cosmetic problems. It revealed the problems related to different aspects in overall web design, e.g. validation problems, error prevention problems, page title, and space between icons which are not detected or overlooked by real users. The major problems by heuristics may have an effect on users' usability after a period of time of interaction with the design. Usability testing discovered major and minor problems frequented by users. This leads to heuristics evaluation considered a complement to usability testing and these two usability methods can provide exhaustive usability evaluation [33]. Table 3 shows the discovered problems based on severity.

TABLE III. TYPE OF PROBLEMS BASED ON SEVERITY

Type of Problem	# of HE Problems	# of UT Problems	# of common Problems	Total
catastrophe	1	-	-	1
Major	5	1	2	8
Minor	1	2	2	5
Cosmetic	6	2	-	8

D. Usability Testing:

The data collected from usability testing have been used to assess the text-free web-based usability according to usability metrics: learnability, efficacy and user errors. As mentioned before, the testing was carried out on 15 (seven male and eight female) participants. They have the following profile characteristics as shown in Table 4:

TABLE IV. PARTICIPANTS' PROFILE CHARACTERISTICS

Characteristics	Response	Male (Percentage)	Female (Percentage)	Total
Age	20-30	0 (0%)	1 (12.5%)	1 (6.6%)
	31-40	2 (28.6%)	2 (25%)	4 (26.6%)
	41-50	4 (57.1%)	3 (37.5%)	7 (46.6%)
	51 or more	1 (14.3%)	2 (25%)	3 (20%)
Educational Level	Illiterate	4 (57.1%)	3 (37.5%)	7 (46.6%)
	Semi-literate	3 (42.9%)	5 (62.5%)	8 (53.3%)
Computer Skills	Excellent	0 (0%)	0 (0%)	0 (0%)
	Good	2 (28.6%)	1 (12.5%)	3 (20%)
	Bad	3 (42.9%)	4 (50%)	7 (46.6%)
	No skills	2 (28.6%)	3 (37.5%)	5 (33.3%)

E. Learnability (Task Completion):

As observed in the success level chart, two users failed in completing Task #1, as they were unable to identify the way of selecting the services (small check box). These users were aged 51 and above; moreover, they did not have experience with a computer and bad experience skills in using a smart phone.

In Task #2, four users failed in performing the task on account of the Reporting Missing Documents icon on the home page not translating the intended meaning. They have clicked on booking an appointment at Civil Affairs, and their commentary does this service in the government office. They also did not try to click on voice icons. Furthermore, they performed Task #2 as a first or second task according to the assigned task order.

Furthermore, four users failed in Task #4 because they failed in how to enter the date using the dropdown menu. Note that all of these users did not have or have bad computer skills.

The success rate was calculated as Jakob Nielsen suggested. Partial success (p) took 50% of success, was added to the success (S) case, and then divided the value over the overall attempts as follows $(S + (p*0.5)/\text{No. of attempts})$ [22]. The overall success rate of the design from 60 attempts is 75%. Jakob Nielsen found that most website success rate scores are less than 50% if the user is dealing with design the first time [22]. Additionally, Jeff Sauro pointed out 78% as a measurement for the success rate. This percentage was an average success rate found in 1200 different areas and the design of software and website tasks with expert and novice users [29]. Ismail has assessed the usability of educational computer games for children which have the same characteristics of our design in respect of using images and children not proficient in reading. Their system achieved a 73.18% success rate [28]. The result of 75% is considered reasonable and good due to a score above 50% compared with Nielsen, as the users interact with the system the first time, which is close to Ismail, finding 73.18% when compared to a similar design and characteristics. It is also close to Jeff Sauro's success rate measurement, although his results are from different types of users and software domains.

F. Efficiency (Time on Task):

During the usability testing session, the observed efficiency of the success completion task increases based on the task order. The time of every task decreases if the task has been performed by a user as the third or fourth task in order regardless of the user profile or characteristics. This is due to the user becoming more familiar with the design and the design becoming learnable after performing more than two tasks [19]. In these results, Task #1 has been excluded because only one success case happened.

The geometric means have been considered in computing the average time for each task, as recommend by Jeff Sauro and Jakob Nielsen [23]. The geometric mean is better in order. A very big value can skew the result in an arithmetic mean, especially if the sample size is less than 20 [23]. As mentioned before, excluding Task #1, Task #4 has the highest geometric mean due to having the highest number of steps to perform it relative to other tasks. Table 5 displays the geometric mean for Task #2, Task #3 and Task #4:

TABLE V. GEOMETRIC MEAN OF TASK TIME

Task	Geometric Mean (sec.)
Task #2	69 sec.
Task #3	84 sec.
Task #4	117 sec.

G. Number of errors:

Most problems have been frequented in Task #1 (roughly 45% (19 user errors from 42) of the total frequency rate during usability testing). This problem related to computer skill (selecting from check boxes). Meanwhile, Task #3 has recorded the lowest frequency rate of 2% (one user error from 42) during usability testing due to no computer skills needed (depending on click or touch). Moreover, Task #2 and Task #

contain a dropdown menu that needs some skills in using a computer. The only user error with the most frequency related to image and icon design was the Reporting Missing Documents icon. The non-understandable meaning of this icon while using a dropdown menu error in Task #2 has influenced an increase in the number of errors in Task #2 after Task #1 is in place.

H. Satisfaction:

The satisfaction was measured by one question to assess the overall user experience and pleased after using the text-free interface. Single Ease Questions (SEQs) have been used to measure the overall user experience and satisfaction with the design (as recommended by Jeff Sauro) being easy to answer and collect, particularly for illiterate/semi-literate users [34]. We used a 5-point Likert scale in the form, and explained each point scale to the user to select one of them. The answer was taken orally by the observer after the test session. Although some of the users succeeded and some had errors, all of the users had a positive response and a willingness to use the text-free interface if available on government websites.

V. MOST IMPORTANT FINDINGS AND PROJECT CONTRIBUTION

Conducting such research offers different findings and contributions. These can be divided into different categories, such as research findings, recommendations, and contributions.

A. Research Findings:

As discussed in the beginning of this project, adoption of e-government requires decision makers to pay more attention to users' needs. It can be noticed that previous literature in many countries, particularly in Saudi Arabia, has not considered some of the factors which would help them to achieve success in implementing e-government. These factors are related to users, such as availability, accessibility, usability and different education levels.

Furthermore, it can be also noticed that a few researchers have conducted and proposed solutions for illiterate/semi-literate users in different developing countries, such as India, Brazil and Switzerland [7][6][3]. To the best knowledge of the author's knowledge, there are no proposed solutions related to user interfaces which have been introduced in Saudi Arabia for people with a low level of education; in addition, the user interfaces proposed in other countries have different representations, such as using icons only [16], icons with text for semi-literate users [6][3], speech [14] or multimodal representations on a mobile phone for semi-literate users only [5].

Thus, this project can be considered proposing a solution to help governments and other organisations in solving availability, accessibility and usability of web-based system content for low education level problems. This solution adopts a text-free user interface by using a combination of icons, images and audio, proposing a consolidated framework in order to accelerate the development process of appropriate and understandable icons and images.

This project has found that text-free interfaces have influences on user performance and satisfaction when illiterate

and semi-literate people use the system. The users' performance has increased users' learnability and efficiency. The design success rate has achieved 75%, which can be considered positive as illiterate/semi-literate users have encountered the interface the first time when compared with the achieved results of [22] and [29]. This group of users cannot be considered expert users. Additionally, users' learnability has been affected positively where users did not need more time after they performed the first task. This concludes that the text-free interface is easy to learn and illiterate/semi-literate users became familiar with the interface after performing one or two tasks. It has been observed that illiterate/semi-literate users are willing to accept and use e-government web-based systems if they consider their needs and become text-free interfaces. This result is in line with [16] and [11].

B. Recommendations:

It can be recommended that adoption of text-free user interfaces can positively influence the usability of e-government systems while illiterate/semi-literate users use them. Moreover, it can be also recommended that user interface design should be as simple as possible in respect of interaction methods, avoiding complex task actions, small images, icons and interface controls, and adopting click- or touch-based tasks as suggested by references [5] and [6] and mouse-over actions as pointed out by Medhi [11].

Furthermore, it is highly recommended that designers and developers use the consolidated framework as it helps in the design of images and icons and in developing effective and efficient images and icons for different websites, cultures and countries. Image usability guidelines, countries' culture, and proposed image features during usability evaluation methods have shown their adequacy to accelerate reaching or closing understandable images and icons without iterative design with real users which happened with Thatcher and Medhi [16] [11]. Moreover, image features were based on using truthfulness and clear and visible images and icons, e.g. real objects in life, globally known things and countries' environment and culture. The images do not matter if represented in a photographic or abstraction way, but they should be credible and intelligible and have a direct meaning to the intended concept as found by Ávila [3]. Additionally, using voices can be helpful in conjunction with concepts which do not have agreement representation or images. In [16], it has been mentioned that during his experiments to develop comprehensible icons for all users, it was not necessary for all icons to be 100% understandable by all users, as users could understand them after continuing using the interface [16].

C. Conclusion and Future Work:

Current and relevant literature has been reviewed in respect of developing a text-free interface for illiterate and semi-literate people in many countries. Moreover, the literature review covered discount usability evaluation methods and compared these methods. The project has developed a web-based system for government services in Saudi Arabia. The project suggests a consolidated framework which is expected to include users' needs, cultural factors, and usability guidelines which can be used for developing any text-free

interface. Therefore, all of the selected e-services will be developed to be text-free interfaces, applying usability testing and heuristic evaluation on a developed design in order to answer the research question. The project found that the text-free interface has an influence on improving illiterate/semi-literate usability of e-government systems. The text-free interface should be designed in such a way as to be simple and understandable by these kinds of users according to their country, culture and website domain.

For future work, this project can be extended to redesign the interface to solve the problems which were discovered as major problems during usability evaluation. Furthermore, transfer another service on the Ministry of Interior websites. The following table contains major problems discovered during usability evaluation and recommendations for a future design. This research can be applied to different domains, e.g. healthcare, or different countries and cultures when using the same proposed image features or adding new features based on the user's needs who they targeted. It can be also compared with the traditional e-services. It can also be extended to target different groups of users such as disabled people.

ACKNOWLEDGMENT

Thanks to Dr. Qazi Mudassar Ilyas and Dr. Amna Asif Khan for their valuable feedback while conducting this research.

REFERENCES

- [1] Alomari, M., Sandhu, K., & Woods, P. (2010). Measuring social factors in e-government adoption in the Hashemite Kingdom of Jordan. *International Journal of Digital Society (IJDS)*, 1(2), 163–172.
- [2] Alshehri, M., Drew, S., & Alfarraj, O. (2012). A comprehensive analysis of e-government services adoption in Saudi Arabia: Obstacles and challenges. *Higher education*, 6, 8-2. LITERACY DATA SHOW PERSISTENT GENDER GAP.
- [3] Ávila, I., & Gudwin, R. (2009). Icons as helpers in the interaction of illiterate users with computers. *Proc. of the Interfaces and Human Computer Interaction*, 20–22.
- [4] Basamh, S. S., Qudaih, H. A., & Suhaimi, M. A. (2014). E-Government Implementation in the Kingdom of Saudi Arabia: An Exploratory Study on Current Practices, Obstacles & Challenges. *International Journal of Humanities and Social Science*, 4(2), 296–300.
- [5] Cuendet, S., Medhi, I., Bali, K., & Cutrell, E. (April 2013). VideoKheti: Making video content accessible to low-literate and novice users. In *Proceedings of the SIGCHI Conference on Human Factors in Computing Systems* (pp. 2833–2842). ACM.
- [6] Friscira, E., Knoche, H., & Huang, J. (March 2012). Getting in touch with text: Designing a mobile phone application for illiterate users to harness SMS. In *Proceedings of the 2nd ACM Symposium on Computing for Development* (p. 5). ACM.
- [7] Goetze, M., & Strothotte, T. (2001). An approach to help functionally illiterate people with graphical reading aids. In *Smart Graphics Symposium UK* (pp. 21–23).
- [8] http://www.aleqt.com/2015/02/10/article_929782.html, viewed on 15/02/2015
- [9] Kumar, R. (2011/2012). Graphical User Interface: A GUI based application for illiterate/semi-literate Indian construction laborers, in University of Leeds.
- [10] Kumar, S., Karyamsetti, R., Ratala, R., Kaur, A., & Tejosh, S., Human Computer Interaction for Illiterate and Semi-illiterate Users to Access E-government Application.
- [11] Medhi, I., Sagar, A., & Toyama, K. (2007c). Text-Free User Interfaces for Illiterate and Semiliterate Users, *Information Technology for International Development*, 4(1), 37–50.

- [12] Nordberg, C. (2010). Exploring the text free interface for illiterate users: Designing an icon-based prototype for mobile phones.
- [13] Ovais Ahmad, M., Markkula, J., & Oivo, M. (2013). Factors affecting e-government adoption in Pakistan: a citizen's perspective. *Transforming Government: People, Process and Policy*, 7(2), 225–239.
- [14] Sherwani, J., Palijo, S., Mirza, S., Ahmed, T., Ali, N., & Rosenfeld, R. (April 2009). Speech vs. touch-tone: Telephony interfaces for information access by low literate users. In *Information and Communication Technologies and Development (ICTD)*, 2009 International Conference (pp. 447–457). IEEE.
- [15] UNESCO Institute for Statistics, <http://www.uis.unesco.org/literacy/Pages/literacy-day-2014.aspx>, 2014.
- [16] Thatcher, A., Mahlangu, S., & Zimmerman, C. (2006). Accessibility of ATMs for the functionally illiterate through icon-based interfaces. *Behaviour & Information Technology*, 25(1), 65–81.
- [17] Hertzum, M., & Nielsen, J. (2001). The Evaluator Effect: A Chilling Fact About Usability Evaluation Methods. *International Journal of Human-Computer Interaction*, 15(1), pp. 183–204.
- [18] Rubin, J., & Chisnell, D. (2006). *Handbook of Usability Testing*, Second Edition: How to Plan, Design and Conduct Effective Tests: Wiley Publishing, Inc.
- [19] Nielsen, J. (2003). Usability 101: Introduction to usability.
- [20] Nielsen, J. (2000). Why you only need to test with 5 users.
- [21] Dumas, J. S., & Redish, J. (1999). *A practical guide to usability testing*. Intellect Books.
- [22] Nielsen, J. (2001). Success rate: The simplest usability metric. *Jakob Nielsen's Alertbox*, 18.
- [23] Measuringu, "Average Task Times In Usability Tests: What To Report?", [Online], <http://www.measuringu.com/average-times.php>, Jeff Sauro, April 21, 2010.
- [24] Nielsen, J. 10 Usability Heuristics for User Interface Design, 1995, accessed: November 12, 2014. [Online]. Available: <http://www.nngroup.com/articles/ten-usability-heuristics/>
- [25] Nielsen, J., & Molich, R. (March 1990). Heuristic evaluation of user interfaces. In *Proceedings of the SIGCHI Conference on Human Factors in Computing Systems* (pp. 249–256). ACM.
- [26] Nielsen, J. (1995). Severity ratings for usability problems. *Papers and Essays*, 54.
- [27] Mariam Rehman, Vatcharaporn Esichaikul, & Muhammad Kamal (2012). "Factors influencing e - government adoption in Pakistan", *Transforming Government: People, Process and Policy*, Vol. 6, Iss: 3, pp. 258-282.
- [28] Ismail, M., Diah, N. M., Ahmad, S., Kamal, N. A. M., & Dahari, M. K. M. (June 2011). Measuring usability of educational computer games based on the user success rate. In *Humanities, Science & Engineering Research (SHUSER)*, 2011 International Symposium (pp. 56–60). IEEE.
- [29] Measuringu, "10 Essential Usability Metrics", [Online], <http://www.measuringu.com/average-times.php>, Jeff Sauro, November 30, 2011.
- [30] Abdel-Fattah, M. A. K. (June 2014). Factors Influencing Adoption and Diffusion of e-Government Services. In *European Conference on e-Government* (p. 1). Academic Conferences International Limited.
- [31] Meftah, M., Gharleghi, B., & Samadi, B. (2015). Adoption of E-Government among Bahraini Citizens. *Asian Social Science*, 11(4), p. 141.
- [32] Liang, S. W., & Lu, H. P. (2013). Adoption of e-government services: An empirical study of the online tax filing system in Taiwan. *Online Information Review*, 37(3), 424–442.
- [33] Paz, F., Paz, F. A., Villanueva, D., & Pow-Sang, J. A. (April 2015). Heuristic Evaluation as a Complement to Usability Testing: A Case Study in Web Domain. In *Information Technology-New Generations (ITNG)*, 2015 12th International Conference (pp. 546–551). IEEE.
- [34] Measuringu, "If You Could Only Ask One Question, Use This One", [Online], <http://www.measuringu.com/blog/single-question.php>, Jeff Sauro, March 2, 2010.

Chemical Reaction Optimization for Max Flow Problem

Reham Barham

Department of Computer Science
King Abdulla II School for
Information and Technology
The University of Jordan
Amman, Jordan

Ahmad Sharieh

Department of Computer Science
King Abdulla II School for
Information and Technology
The University of Jordan
Amman, Jordan

Azzam Sliet

Department of Computer Science
King Abdulla II School for
Information and Technology
The University of Jordan
Amman, Jordan

Abstract—This study presents an algorithm for MaxFlow problem using "Chemical Reaction Optimization algorithm (CRO)". CRO is a recently established meta-heuristics algorithm for optimization, inspired by the nature of chemical reactions. The main concern is to find the best maximum flow value at which the flow can be shipped from the source node to the sink node in a flow network without violating any capacity constraints in which the flow of each edge remains within the upper bound value of the capacity. The proposed MaxFlow-CRO algorithm is presented, analyzed asymptotically and experimental test is conducted. Asymptotic runtime is derived theoretically. The algorithm is implemented using JAVA programming language. Results show a good performance with a complexity of $O(I E^2)$, for I iterations and E edges. The number of iterations I in the algorithm, is an important factor that will affect the results obtained. As number of iterations is increased, best possible max-Flow value is obtained.

Keywords—Chemical reaction optimization(CRO); Decomposition; Heuristic; Max Flow problem; Molecule; Optimization; Reactions; Synthesis

I. INTRODUCTION

Imagine a material traveling without obstruction through a system from a source, where the material is produced, to a destination, where it is consumed. The flow of the material at any point in the system is the rate at which the material moves [1]. We can interpret the weighted directed graph as a flow networks. Flow networks can represent many real life situations like petrol flowing through conduits, and parts through assembly lines [1]. The maximum flow problem becomes one of the most well known problems for combinatorial optimization in the weighted directed graph [2]. This problem can be applied in many areas of applications such as networks, engineering, and transportations [2].

Related to its important, many researches solved this problem using different methods and techniques [1]. In the maximum flow problem, the goal is to get the greatest rate at which we can ship the material from the produced point to the consumed one without violating any capacity constraint in which the flow of each edge remains within the upper bound value of the capacity [1].

Toshinori et al. in [2] define the max flow problem as: "The problem is to determine an optimal solution for a given directed, integer weighted graph. The weight at each edge

represents the flow capacity of the edge. Under these constraints, we want to maximize the total flow from the source to the sink". In [3] they define it as " In deterministic networks, the maximum-flow problem asks to send as much flow (information or goods) from a source to a destination, without exceeding the capacity of any of the used links. Solving maximum-flow problems is for instance important to avoid congestion and improve network utilization in computer networks or data centers or to improve fault tolerance".

In this study, a potential solution to the maximum flow problem using a recent algorithm which is called "Chemical Reaction Optimization (CRO)" is investigated. This algorithm, as it is reported in [4]: "CRO is a recently established meta-heuristics for optimization, inspired by the nature of chemical reactions. A chemical reaction is a natural process of transforming the unstable substances to the stable ones. The molecules interact with each other through a sequence of elementary reactions. At the end, they are converted to those with minimum energy to support their existence. This property is embedded in CRO to solve optimization problem".

Furthermore, CRO is a technique which loosely couples chemical reactions with optimization. It does not attempt to capture every detail of chemical reactions [4]. In general, the principles of chemical reactions are governed by the first two laws of thermodynamics. The first law (conservation of energy) says that energy cannot be created or destroyed; energy can transform from one form to another and transfer from one entity to another. The second law says that the entropy of a system tends to increase, where entropy is the measure of the degree of disorder [4]. Potential energy is the energy stored in a molecule with respect to its molecular configuration [4].

The rest of this study is organized as follow. Section II will present the literature review. Section III will illustrate the maximum flow problem. Section IV will show how chemical reaction optimization works. Section V presents the proposed algorithm. Section VI shows the analysis of the algorithm. An illustrated example is presented in section VII. The experimental results are presented in section VIII. Section IX is the conclusion and future work.

II. LITERATURE REVIEW

The maximum flow problem has been widely studied by many researchers using several methods. The first pseudo-polynomial algorithm for the maximum flow problem is the augmenting path algorithm of Ford and Fulkerson (1956) [5, 6]. Dinic [7] and Edmonds and Karp [8] independently obtained polynomial versions of the augmenting path algorithm. Edmonds and Karp (1972) and Dinic (1970) independently proved that if each augmenting path is shortest one, the algorithm will perform $O(nm)$ augmentation steps, where n is the number of vertices, and m is the number of edges in the graph. The shortest path (length of each edge is equal to one) can be found with the help of breadth-first search (BFS) algorithm. Since then, several more-efficient algorithms have been developed. Ahuja and Orlin improved the shortest augmenting path algorithm in 1987 [12]. The push and re-label method is introduced by Goldberg [9] and Goldberg and Tarjan [10], along with some of its more efficient variants. It maintains a preflow and updates it through push operations. It introduces the relabel operation to perform fine-grain updates of the vertex distances. Orlin [14] presents improved polynomial time algorithms for the max flow problem defined on a network with n nodes and m arcs, and shows how to solve the max flow problem in $O(nm)$ time, improving upon the best previous algorithm due to King, Rao, and Tarjan [15] who solved the max flow problem in $O(nm \log m / (n \log n))$ time.

Genetic algorithm (GA), which is considered as evolutionary algorithm, has been also applied to solve max flow optimization problems such as in [2]. In [2], each solution is represented by a flow matrix. The fitness function is defined to reflect two characteristics: balancing vertices and the saturation rate of the flow. Starting with a population of randomized solutions, better and better solutions are sought through the genetic algorithm. Optimal or near optimal solutions are determined with a reasonable number of iterations compared to other previous GA applications.

CRO is a recently proposed general-purpose meta-heuristic, which has been developed intensely in the past few years [11]. The CRO was proposed by Lam et al. in 2010, and was originally designed for solving combinatorial optimization problems. They solved some classical problems, e.g., quadratic assignment problem and channel assignment problem. It could also provide solutions to some applications solved by other evolutionary algorithms such as genetic algorithm. As in [13], they use genetic algorithm to deal with optimization of parameters of constructive cost model. Therefore, CRO can be used for these types of applications. In this study, we proposed to use chemical reaction optimization algorithm to solve the maximum flow problem.

III. MAXIMUM FLOW PROBLEM

Suppose there is a directed network $G = (V, E)$ defined by a set V of nodes (or vertices) and a set E of arcs (or edges). Each arc (i, j) in E has an associated nonnegative capacity u_{ij} where i, j are nodes in V . Also, there are two distinguished special nodes in G : a *source* (or start) node s and a *sink* (or a target) node t [1]. For each i in V , denote by $E(i)$ all the arcs emanating from node i . Let $U = \max \{u_{ij} \mid (i, j) \in E\}$. Denote the number of vertices by n and the number of edges by m [1].

The goal is to find the maximum flow from the source node s to the sink node t that satisfies the arc capacities and mass balance constraints at all nodes [2]. Representing the flow on arc (i, j) in E by x_{ij} , an optimization model for the maximum flow problem can be obtained as in (1) [1]:

$$\begin{aligned} \text{Maximize } f(x) &= \sum_{(i,j) \in E(s)} x_{ij} \text{ subject to } \dots (1) \\ \sum_{\{j:(i,j) \in E\}} x_{ij} - \sum_{\{j:(j,i) \in E\}} x_{ji} &= 0 \quad \forall i \in V \setminus \{s, t\} \\ 0 \leq x_{ij} &\leq u_{ij} \quad \forall (i, j) \in E \end{aligned}$$

IV. CHEMICAL REACTION OPTIMIZATION (CRO)

The CRO algorithm as described in [4]: "is a multi-agent algorithm and the manipulated agents are molecules. Each molecule has several attributes, some of which are essential to the basic operations of CRO. The essential attributes include: (a) the molecular structure (ω); (b) the potential energy (PE); and (c) the kinetic energy (KE). Other attributes depend on the algorithm operators and they are utilized to construct different CRO variants for particular problems provided that their implementations satisfy the characteristics of the elementary reactions. Molecular structure ω captures a solution of the problem. It is not required to be in any specific format: it can be a number, a vector, or even a matrix. Potential energy PE is defined as the objective function value of the corresponding solution represented by ω . If f denotes the objective function, then $PE(\omega) = f(\omega)$. Kinetic energy KE is a non-negative number and it quantifies the tolerance of the system accepting a worse solution than the existing one".

There are four types of elementary reactions in CRO, each of which takes place in each iteration of CRO. They are employed to manipulate solutions (i.e. explore the solution space) and to redistribute energy among the molecules [4]. Assume that molecules are in a container, one of the following four reactions will be possible to occur in each of CRO iteration.

A. On-wall ineffective collision

An on-wall ineffective collision represents the situation when a molecule collides with a wall of the container and then bounces away remaining in one single unit but with new structure due to collision with wall. In this collision, ω produces ω' , i.e., $\omega \rightarrow \omega'$ [4].

B. Decomposition

Decomposition refers to the situation when a molecule hits a wall of the container and then breaks into several parts. Assume that ω produces ω_1 and ω_2 , i.e., $\omega \rightarrow \omega_1 + \omega_2$ [4].

C. Inter-molecular ineffective collision

Inter-molecular ineffective collision takes place when two molecules collide with each other and then bounce away. Assume that ω_1 and ω_2 , after collision with each other, produce ω_1' and ω_2' , i.e., $\omega_1 + \omega_2 \rightarrow \omega_1' + \omega_2'$. This reaction could be similar to on-wall ineffective collision but with two molecules to collide rather than one [4].

D. Synthesis

Synthesis does the opposite of decomposition. A synthesis happens when multiple (assume two) molecules hit against each other and fuse together, i.e., $\omega_1 + \omega_2 \rightarrow \omega'$ [4].

In order to find the maximum flow using CRO, there is a need to explore the search space. To achieve that, number of solutions, which are called Molecules in CRO, need to be generated. Each of these solutions or 'molecules' has its own potential energy which is the objective function value for that solution, and a kinetic energy which helps in making decision; if the generated solution is better than its parent or not. Now imagine that these molecules are in a container and due to their high kinetic energy, they move inside the container in arbitrary directions. This situation, leads to perform collisions between these molecules in different forms. These collisions are known as chemical reactions. Chemical reactions take different shapes and conditions [4].

CRO mimics these reactions and use them as operators to help moving the molecules from local optimum into global optimum as possible [4]. CRO, as mentioned before, has four types of reactions. These types differ from each other based on the nature of the reaction and the numbers of molecules participate in the reaction [4]. If one molecule is selected, and an ineffective collision is occurred, then it is on-wall ineffective reaction. If an effective reaction occurs, then the decomposition reaction will happen. In the other hand, if two molecules are selected, then there are possibilities of occurrence of synthesis reaction which is effective reaction, or inter-molecular reaction which is ineffective reaction [4].

Through these reactions, some of good solutions will be generated and some of bad ones will be destroyed. After particular number of iterations or stop criteria is met, the best solution among available solutions in the container will be selected and considered.

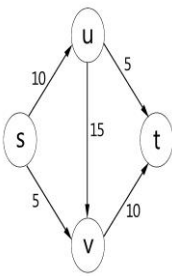
V. ALGORITHM: "MAXFLOW-CRO"

Now let us apply CRO to find the possible solution for Maximum Flow Problem. Figures 1 through 6, present the pseudo-code for the proposed "MaxFlow_CRO" algorithm. TABLE 1 shows the main attributes and their meaning related to the proposed algorithm "MaxFlow_CRO" for the molecules, in comparison with chemical meaning in CRO.

A. MaxFlow-CRO initialization stage

As in [4], CRO has three main stages: the initialization, the iterations, and the final stage. The MaxFlow-CRO algorithm, as shown in Figure1: lines1, 11 and 31, presents these three stages. First, the initialization stage can be shown in Figure1 as in lines 1-10. From Section III, maximum flow problem has a graph of nodes and edges; each edge is a directed and weighted edge. These weights represent the capacity for those edges. This graph can be represented as a capacity matrix $C[i][j]$, and used as a basis to generate number of flow matrices, Figure1:lines2 and 10, which are called parents. There are number of generated parents based on the value setting for parentSize variable (Figure1: line3). S is the source node, and t is the sink. Iteration number variable is important here, it is used as a stop criterion (Figure1:line3).

TABLE I. PROFILE FOR CRO-MAXFLOW MOLECULE

Profile: Flow network	Chemical meaning	CRO-MaxFlow meaning
	Molecular structure	Candidate solution: flow matrix
	Potential energy	Value of maximum flow for such candidate solution
	Kinetic energy	Measure of tolerance of having worse solution
	Number of hits	Current total number of iterations
	Minimum structure	Current optimal max flow solution

After that, a number of parents based on the specified value of the parentSize variable (Figure1: line10), will be generated. The generated parents are represented by a flow matrix $F[i][j]$. Parent, solution and molecule are used interchangeably. These parents represent the first generation in the population. Generating parents had been a challenge because in order to consider them as max flow solutions, they should obey the constraints as mentioned in formula (1). Max flow problem has two common constraints. The first one says the generated flow must not exceed the identified capacity for any edge. The second says that for each node in the graph, the incoming flow must equal to the outgoing flow. The first constraint could be controlled by specifying the upper range of the generated flow based on the capacity on an edge. Generating the flow randomly will make second constraint hard to satisfy. So, MaxFlow-CRO use a function called objectiveFunction() to repair the flow and compute the current max flow value. Therefore, a feasible solution meets the constraints can be obtained. The details of parent generating function can be shown in Figure 2.

The objective function (Figure2: line5) can be computed using the known shortest augmenting path algorithm as in [8]. The max flow value, computed by the objective function, represents the current maximum flow value, and as the iterations and reactions proceed, this value will be improved gradually. Note that, objective function and PE are used interchangeably.

In Figure1, lines 6 and 7, α is a decomposition threshold, β is a synthesis threshold, and both of them are initially assigned by dividing parentSize variable value by 2. The reason from computing α and β like that, to make sure that synthesis and intermolecular reactions will be possibly happened after number of on-wall and decomposition reactions are triggered. The goal is to degrade the chance of synthesis reaction occurrence. Both of decomposition and on-wall reactions help to save or increase the number of parents, but synthesis reactions tend to decrease number of parents.

B. MaxFlow-CRO Iteration stage

The goal from CRO reactions is to increase the ability to improve the resulted value of max flow. As iterations operate,

the max flow value will be improved gradually until reach the best max flow. Iteration stage is shown in Figure 1: lines 11-31. After generating the required parents, PE for each of them will be computed. Then one or two molecules will be picked randomly based on the value of the variable "b". The variable b is generated randomly between 0 and 1 (Figure1: line12). If the value of b is larger than the value of the variable "molecule", which is a predefined variable used as a threshold for the variable b, then one molecule will be selected; but if not, then two molecules will be selected. Also, the value of the molecule variable will be generated randomly between 0 and 1 (Figure1:line9).

If one molecule is selected, there is a possibility to on-wall ineffective or decomposition reactions to happen. So, to be more accurate, CRO as in [4] puts a criteria, which is $HIT > \alpha$ (Figure1: line15), where HIT is a variable counts the number of times the specific molecule participate in a reaction and initialized to 0 (Figure1: line5 and 29). If this criterion has been met, then decomposition reaction will be occurred (Figure1: line16). Else, the on-wall ineffective collision will be occurred (Figure1: line18).

The same will happen if two molecules are selected but here the reactions are different. In this case, the possibility is for synthesis and inter-molecular reactions to be happened. There are some conditions that must be satisfied, which are $KE \leq \beta$ [4] (where KE is kinetic energy) and the number of parents is not less than 2. This is to be sure that synthesis and inter-molecular reactions can be occurred correctly (Figure1: line23). If the criterion in line 23 has been met, then synthesis reaction will occur (Figure1: line24). Else, the inter-molecule ineffective reaction will occur (Figure1: line26). Each time the reaction happens, the KE will be decremented by one (Figure1: line30).

In the final stage and after finishing the specific number of iterations, which was the stop criterion, the best molecule which has the largest maximum flow value obtained will be selected and its maximum flow value will be returned (Figure1: lines 31-33).

C. Reactions

When on-wall ineffective function is called (Figure3), the chosen molecule will be changed by regenerating randomly the flow of its first half, (Figure3: lines1-3). Then, the objective function will be computed and the max flow value is compared with that for the original molecule. If it is greater than the original, then it will be confirmed and the original solution will be destroyed; else the generated molecule will be destroyed.

The same will be happened when intermolecular ineffective collision is called (Figure4), but in this case, there are two molecules instead of one. Apply the same procedure used for on-wall function for each molecule separately and test the resulted molecules if they have max flow greater than the original molecules or not. Figure4: lines 1-13 are for the first molecule. Lines 14-26 are for the second one. In synthesis function (Figure6), the molecules with large max flow value will be returned and the other ones will be destroyed (Figure6: lines 1-7).

Algorithm: MaxFlow-CRO

```
1 //initialization phase
2 Set flow_network_size, C[i][j]: maximum capacity
3 parentSize, iterationNumber, s: source node, t:
4 sink node
5 HIT= 0
6  $\beta = \text{parentSize}/2$ 
7  $\alpha = \text{parentSize}/2$ 
8  $KE = \text{parentSize}/1.5$ 
9 Generate molecule  $\in [0, 1]$ 
10 parentGenerating(C[i][j] , parentSize )
11 for (int i=1 to iterationNumber) // Iteration phase
12   Generate b  $\in [0, 1]$ 
13   if b > Molecule then
14     Randomly select one parent
15     if (HIT >  $\alpha$ ) then
16       Decomposition( )
17     else
18       OnWallIneffectiveCollision( )
19   end if
20
21 else
22   Randomly select two molecules
23   if ( $KE \leq \beta$  && parentSize  $\geq 2$  ) then
24     Synthesis( )
25   else if (parentSize  $\geq 2$ )
26     IntermolecularIneffectiveCollision( )
27   end if
28 end if
29 HIT++
30 KE--
31 Check for any new maximum solution
32 end for-loop // final stage
33 return the best solution found
```

Fig. 1. Pseudo-code for "MaxFlow-CRO" algorithm

Function: parentGenerating()
Input: C[i][j]: maximum capacity, parentSize
Output: F_i: flow matrices

```
1 for ( int i=1 to popSizs )
2   for (int j=1 to no. of edges in the graph)
3     randomly generate Fi[i][j]
4     // where  $0 \leq F_i[i][j] \leq C[i][j]$ 
5     PEi = objectiveFunction(Fi)
6     return Fi, PEi
7   end for-loop
8 end for-loop
```

Fig. 2. Pseudo-code for parent initialization function

Function: onWallIneffectiveCollision()
Input: F_i //one molecule
Output: F_i' // new molecule

```
1 for (j=1 to flow_network_size/2)
2   F1'=generate new flow randomly
3 end for-loop
4 //Compute objective function for the new molecule
5 PE' = objectiveFunction(F1')
6 //confirm the new solution or dismiss
7 if (PE'> PE ) then
8   destroy Fi
9   return F1'
10 else
11   dismiss F1'
12 End if
```

Fig. 3. Pseudo-code for on-wall ineffective collision function

Function: IntermolecularIneffectiveCollision()
Input: F₁, F₂ // two molecules
Output: F₁', F₂' //two new molecules

```
1 // for F1
2 for (j=1 to flow_network_size/2)
3   F1'= generate new flow randomly
4 end for-loop
5 PE1' = objectiveFunction(F1')
6 //Compute PE' objective function for the
7 new molecule
8 if (PE1'> PE1 ) then // solution confirmed
9   destroy F1
10  return F1'
11 else
12  dismiss F1'
13 end if
14 // for F2
15 for (j=1 to flow_network_size/2)
16   F2'= generate new flow randomly
17 end for-loop
18 PE2' = objectiveFunction(F2')
19 //Compute PE' objective function for the
20 new molecule
21 if (PE2'> PE2 ) then // solution confirmed
22   destroy F2
23   return F2'
24 else
25   dismiss F2'
26 end if
```

Fig. 4. Pseudo-code for inter-molecule ineffective collision function

Figure5 shows the decomposition function. In this function one molecule is used to produce two molecules. First, two copies, for the original molecule, are produced (Figure 5: lines 2 and 15). For the first copy, take the first half of flows and randomly regenerate them (Figure5: lines 3-5), then compute the objective function (Figure5: lines7) and compare it with that for the original (Figure5: lines 8-13). In order to confirm the new molecule, it should have max flow greater than that for the original. The same occurs for the second copy but regenerate the second half of flows in order to produce a molecule different from the first one (Figure5: lines 15-18). Then compute the objective function and compare the result

with that for original to confirm or destroy the second new molecule (Figure5: lines19-27).

Function: Decomposition()
Input: F₁ // one molecule
Output: F₁', F₂' // two new molecules

```
1 // generate the first solution F1'
2 Copy the original solution Fi into F1
3 for (i=1 to network_flow_size/2)
4   F1'= Randomly generate new flow
5 end for-loop
6 // objective function for the new molecule
7 PE1'=objectiveFunction(F1')
8 if (PE1'> PEi ) then // solution confirmed
9   destroy Fi
10  return F1'
11 else
12  dismiss F1'
13 end if
14 // generate the second solution F2'
15 Copy the original solution Fi into F2
16 for (i= network_flow_size/2 to network_flow_size)
17   F2'= Randomly generate new flow
18 end for-loop
19 // objective function for the new molecule
20 PE2'=objectiveFunction(F2')
21 //confirm the new solution or dismiss
22 if (PE2'> PEi ) then // solution confirmed
23   destroy Fi
24   return F2'
25 else
26   dismiss F2'
27 end if
```

Fig. 5. Pseudo-code for Decomposition function

VI. ANALYSIS OF MAXFLOW-CRO ALGORITHM

A. Time complexity

For initial max flow of the first parent generation, the run time complexity can be approximated by $O(N E f)$, where N is the number of parent nodes, E is the number of edges in flow network and f is the maximum flow in the flow network graph. The Random Number between 0-1 is approximated by $O(1)$; which can be ignored since it has a constant value.

Starting the optimization algorithm: the run time complexity can be approximated by $O(I X)$, where I is the number of iterations and X is the complexity for each method (depends on random selection). Below is the complexity calculation for each reaction, so we will be able to find the worst case.

- 1) Decomposition function: $O(E^2)$, where E is number of edges in the graph.
- 2) On-Wall ineffective collision function: $O(E^2)$, where E is number of edges in the graph.
- 3) Synthesis function: $O(C)$, where C: constant, synthesis function contains If and assignment statements, see Figure6.

4) Inter-Molecular function: $O(E^2+E+E)=O(E^2)$, where E is number of edges in the graph.

The worst case is when randomization leads to $O(E^2)$, so replace X with $O(E^2)$. Therefore the time complexity for the optimization algorithm is $O(I E^2)$.

Max flow calculation for the results: This is similar to the initial $O(R E f)$, where R is the remaining items in the input array, E is the number of edges in the graph, f is the maximum flow in the graph. Thus, the final Time complexity will be: $O(N E f) + O(I E^2) = O(I E^2)$.

B. Space complexity:

The initial input needs $O(N E^2)$, where E is the number of edges in the graph, and N is the number of nodes. For the four methods in the optimization algorithm:

- 1) Intermolecular function: $O(2E^2) = O(E^2)$.
- 2) On-Wall ineffective collision function: $O(E^2)$.
- 3) Synthesis function: $O(1)$, the size of the used graph already calculated in input so no need to include it again.
- 4) Decomposition function: $O(2E^2)$. Additional graph for swapping is needed, so it is $O(E^2)$. The worst case will be $O(2E^2) + O(E^2) = O(E^2)$.

Function: synthesis()

Input: F_1, F_2, PE_1, PE_2 // two molecules

Output: F_3 : solution has greater value of flow

- ```

1 If (PE1>PE2) then
2 F3 = F1
3 destroy F2
4 else
5 F3 = F2
6 destroy F1
7 return F3

```

Fig. 6. Pseudo-code for Synthesis function

Therefore, the final space complexity will be:  $O(N E^2) + O(E^2) = O(N E^2)$ .

## VII. EXAMPLE FOR MAXFLOW-CRO ALGORITHM

To understand how this study uses CRO to optimize maximum flow problem, refer to TABLE1 again. It shows a profile for a directed graph of four nodes and five edges, each edge has its own directed capacity, which will be used in this example and called molecule. The goal from this capacity matrix is to use it as a basis for producing flow matrices within their edges capacity. This example represents the capacity and the possible flow on the edge as flow/ capacity, as shown in Figures 7 through 10.

### A. On-wall ineffective reaction

On-wall ineffective reaction uses total-half change method [4]. First, take the molecule that picked randomly from the population of parents, as one shown in Figure 7. Then, regenerate the first half part of its flows. After that, objective function will be applied to compute the new flow. This max

flow value will be compared with the original max flow value. If it is larger than before, the new value will be confirmed; else it will be dismissed and the parent molecule will be remained. Figure7 shows that the new molecule has max flow value better than that for original one, so it will be confirmed.

### B. Decomposition reaction

In decomposition reaction, the molecule will be copied into other two molecules. For each of these resulted molecules, half values will be selected and regenerated randomly. For the first copy, select the first half, while second half is selected for the second copy. So, a new two molecules will be produced. After that, objective function will be applied, as shown in Figure8. This operation is called total-half change operator [4].

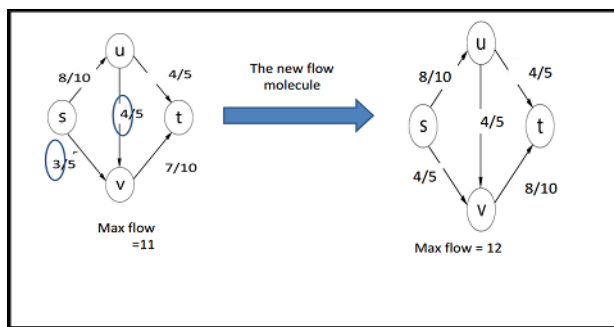


Fig. 7. On-wall ineffective collision reaction example

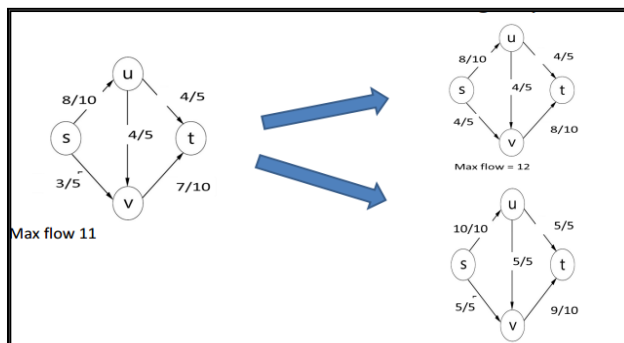


Fig. 8. Decomposition reaction example

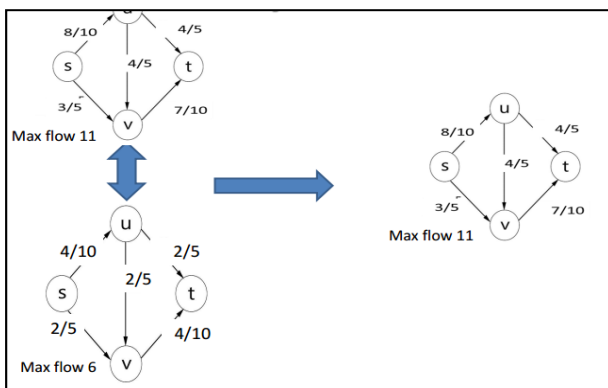


Fig. 9. Synthesis reaction example

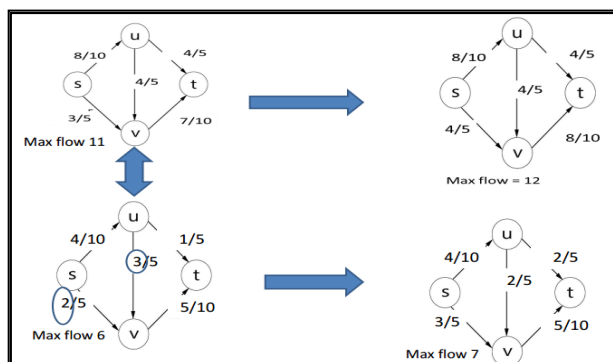


Fig. 10. Inter-molecular reaction example

C. Synthesis reaction

In the synthesis reaction, simply select the molecule which has greater flow value than the other molecule, as shown in Figure 9.

D. Inter-molecular reaction

Inter-molecular reaction is the same as on-wall reaction, but the procedure will be applied on two molecules rather than one, as shown in Figure 10.

VIII. RESULTS

The MaxFlow-CRO program was implemented and executed using a dataset of different flow\_network\_size: number of nodes in the graph. These dataset sizes are ranging from 50 to 1000 nodes as shown in TABLE2. Datasets with further sizes were unable to be tested on the test PC due to memory limitations. The algorithm was tested using Intel-core™ i5-2450M CPU with 2.50 GHz, 4 GB RAM (2.5 GB usable), and windows7 32-bit operating system. The application program is written using Java and executed in Net-Beans IDE 7.1.2, using ten structured classes. Each dataset is experimented 10 times, runtime in seconds is recorded, and an average runtime is calculated. Figure11 shows the experimental runtimes depicted from TABLE2. Figure11 represents how execution time behaves with increasing size of the graph. From this Figure, we can conclude that the algorithm has a quadratic polynomial time complexity, which is possibly a good performance. The experiments show that, as initial parent size and number of iterations increase, better results for max flow will be obtained. Runtimes in TABLE2 are recorded when the highest possible value for max flow is reached by the application program.

TABLE II. RUN TIMES (IN SECONDS) FOR DIFFERENT NETWORK SIZES

| Network Size | Average runtimes(sec) | Network Size | Average runtimes(sec) |
|--------------|-----------------------|--------------|-----------------------|
| 50           | 0.109                 | 550          | 114.198               |
| 100          | 0.625                 | 600          | 149.497               |
| 150          | 2.429                 | 650          | 178.372               |
| 200          | 4.449                 | 700          | 230.718               |
| 250          | 11.278                | 750          | 278.584               |
| 300          | 18.694                | 800          | 301.045               |
| 350          | 24.45                 | 850          | 396.915               |
| 400          | 43.233                | 900          | 425.62                |
| 450          | 54.37                 | 950          | 459.185               |
| 500          | 80.142                | 1000         | 506.103               |

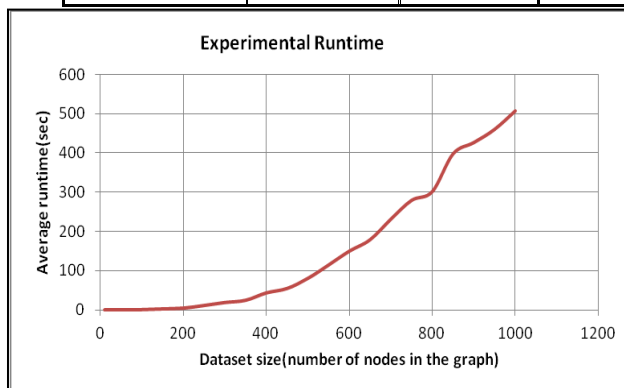


Fig. 11. Runtime graph for experimental results

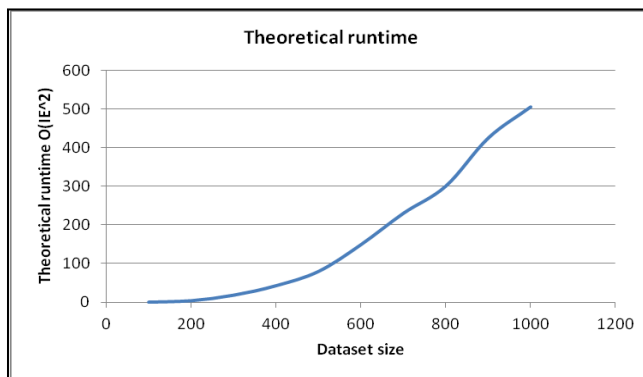


Fig. 12. Theoretical runtime graph for  $O(IE^2)$  complexity

Figure 12 shows the chart for the asymptotic notation ( $IE^2$ ), such that  $I = 75$  and  $E = 100$ . It is clear from both Figure11 and Figure12 that experimental and theoretical results converge. Many terms are removed from the asymptotic notation of the runtime complexity when calculated theoretically, and that explains the slight difference in shape between the two Figures.

## IX. CONCLUSION AND FUTURE WORK

This study proposes a potential solution to maximum flow problem through using chemical reaction optimization algorithm. The proposed MaxFlow-CRO algorithm is presented, analyzed asymptotically and experimental test is conducted. Asymptotically, the algorithm runtime is  $O(I E^2)$ . Asymptotic runtime is proved theoretically. The experiments show that, as initial value of parent\_size variable and numbers of iterations are increased, better results for max flow will be obtained. Initial parent\_size variable didn't affect the run time, because initialization operations, in general, are out of runtimes consideration. In other hand, iterations number is an important factor that can affect the value of max flow and run time duration. As a future work, the algorithm could be improved to reach the possible highest max-flow value using less number of iterations by implementing the algorithm on supercomputer to evaluate its performance in parallel. In addition, we can conduct a comparison between this proposed algorithm and other heuristic, meta-heuristic or evolutionary algorithms used to solve maximum flow problem in terms of their performance.

### REFERENCES

- [1] T. H. Cormen, C. E. Leiserson, R. L. Rivest and C. Stein, Introduction to Algorithms, 3rd ed., The MIT Press, 2009.
- [2] Munakata, T. and Hashier, D.J. "A genetic algorithm applied to the maximum flow problem", Proc. 5th Int. Conf. Genetic Algorithms, 1993, pp. 488-493
- [3] Kuipers, S. Yang, and S. Trajanovski, "Constrained Maximum Flow in Stochastic Networks", IEEE 22nd International Conference on Network Protocols, 2014, pp. 397-408.
- [4] A.Y.S. Lam, V.O.K. Li, "Chemical reaction optimization: a tutorial", Memetic Computing 4, 2012, pp. 3-17.
- [5] Ford jr., L.R., Fulkerson, D.R., Flows in networks. Princeton University Press, Princeton, 1962
- [6] Ford jr., L.R., Fulkerson, D.R., "Maximal flow through a network". Can. J. Math. 8(3), 1956, pp. 399-404.
- [7] Dinic, E.A., "Algorithm for solution of a problem of maximum flow in networks with power estimation". Sov. Math. Doklady. 11(8), 1970, pp. 1277-1280.
- [8] Edmonds, J., Karp, R.M., "Theoretical improvements in algorithmic efficiency for network flow problems". J. Assoc. Comput. Machinery 19(2), 1972, pp. 248-264.
- [9] Goldberg, A.V., "A new max-flow algorithm". Technical Report MIT/LCS/ TM-291, Laboratory for Computer Science, M.I.T, 1985.
- [10] Goldberg, A.V., Tarjan, R.E., "A new approach to the maximum flow problem". Proc. 18th ACM STOC, 1986, pp. 136-146.
- [11] Y. S. Lam and V. O. K. Li, "Chemical-reaction-inspired metaheuristic for optimization", IEEE Trans Evol Comput vol. 14, no. 3, 2010, pp. 381- 399.
- [12] R. K. Ahuja, T. L. Magnanti, and J. B. Orlin., Network Flows: Theory, Algorithms, and Applications, Prentice Hall, 1993.
- [13] Sheta, A. F. "Estimation of the COCOMO Model Parameters Using Genetic Algorithms for NASA Software Projects". Journal of Computer Science 2 (2), 2006, pp. 118-123.
- [14] J. B. Orlin. Max flows in  $o(nm)$  time, or better. In STOC'13: Proceedings of the 45th Annual ACM Symposium on the Theory of Computing, 2013, pp.765-774.
- [15] V. King, S. Rao, and R. Tarjan, "A faster deterministic maximum flow algorithm", In Proceedings of the 8th Annual ACM-SIAM Symposium on Discrete Algorithms, 1992, pp. 157-164.

# Factors Influencing Patients' Attitudes to Exchange Electronic Health Information in Saudi Arabia: An Exploratory Study

<sup>1</sup>Mariam Al-Khalifa, <sup>1\*</sup>Shaheen Khatoon, <sup>2</sup>Azhar Mahmood, <sup>1</sup>Iram Fatima

<sup>1</sup>College of Computer Science and Information Technology, Department of Information System  
King Faisal University, Al- Ahsa, Saudi Arabia

<sup>2</sup>Shaheed Zulfiqar Ali Bhutto Institute of Science and Technology, Islamabad, Pakistan

**Abstract**—Health Information Exchange (HIE) systems electronically transfer patients' clinical, demographic, and health-related information between different care providers. These exchanges offer improved health care quality, reduced medical errors and health care costs, increase patient safety and organizational efficiency. However, technologies cannot bring such improvements if patients are reluctant to share personal health information which could impede the success of HIE system. The purpose of this study is to identify different factors that determine patients' acceptance for sharing their medical information among different care provider. Based preliminary on the Theory of Planned Behavior (TPB) and Technology Acceptance Model (TAM) combined with patients' perspective an integrated model is proposed. A questionnaire survey is conducted to measure the proportion of respondents' willingness to share their information with the residence of the eastern province of Kingdom of Saudi Arabia. A sample of 300 respondents over 18 years of age is collected. Basic descriptive statistical analysis, reliability and validity assessment is conducted to analyze data and measure the goodness of model. Furthermore, Structural Equation Modelling is used to test research hypothesis. The finding shows that perceived benefit, perceived risk, subjective norms and attitude are the main predictors of patients' willingness or unwillingness to share their health information. The study revealed that more attention should be directed to these factors during the design and implementation of future HIE system to avoid expected barriers.

**Keywords**—Health Information Exchange; Electronic Medical Record; TAM; Theoretical Model Introduction

## I. INTRODUCTION

Saudi Arabia government is consuming billions to enhance quality of healthcare and to extends its coverage over the last three decades [1]. This lead to increase in number of care providers, out of them, 60 % of healthcare services are provided by the ministry of health, the remaining services are provided by others governments bodies such as National Guard, Ministry of Defense and Aviation, Ministry of Interior, University Hospitals and private sector. Different care providers are managing and accomplishing health care services with significant variation in the information system used. Many of them using Electronic Medical Record (EMR) systems for rendering health care services. As a result, patient information has scattered in various healthcare providers, and hospital staff is unable to review the medical history of patients who have

visited other hospitals. It leads to redundant diagnostic tests or prescription of medications, which would compromise the quality of patient care. There is a need of integrated EMR among different hospitals to improve quality of care provided to patients, and improve efficiency of health care sector [2, 3].

Studies have shown despite the benefits of electronic Health Information Exchange (HIE) systems there is a potential threat to the confidentiality of information and their implication on patients' privacy. Due to these threats HIE system are either not available or underutilized. One of the classical examples is Care. Data [4] launched by NHS England 2013 where they took an initiative to integrate patient records stored in the machines of general practitioners with information from social services and hospitals to make one centralized data archive. Unfortunately, this data share project failed due to risk of privacy it posed between patient and practitioners. Another example is doctor boycott to use inter organizational network with in British National Health service design to improve exchange of information on the ground of potential threat to information confidentiality [5]. Therefore, without balancing patient's preferences for spreading their information over potential benefit that occurred to society the successful implementation of such system is challenging task. This issue is of particularly importance in context of Saudi Arabia where impact of social norms is relatively high as compare to western world. Unless patients are sure that personal information will not be distributed against their wish they may be reluctant to disclose sensitive information that is crucial to their correct treatment.

Although patient interests are at the core of medical confidentiality policy their understanding and view of possible information usage is at the margin of scholarly attention. In order to implement HIE system understanding patients' perceived need for HIE, their preference, acceptance of technology, perceived benefit and concerns about information exchange technology is essential. Thus, this study explored the antecedent factors of patients' intentions to accept HIE system from the perspective of information system adoption. It investigates the direct and indirect effect of various factors such as privacy, trust, social norms and patient involvement respectively on their intention and attitude towards sharing health information. Based on Technology Acceptance Model (TAM) [6] and Theory of Planned Behavior (TPB) [7] combined with patients' attitude and concerns, a conceptual

model is proposed to explain the intention of patients' to share their sensitive health information. The main goal is to study patients' preferences that affect the acceptance of HIE. These preferences should be considered when developing and implementing systems, standards and policies to eliminate the expected barriers.

Rest of paper is organized as follow: Literature related to health information system and its acceptance is presented in Section II. The proposed model and research method is presented in section III and IV. Research results and research implications are discussed in section V. Finally, section VI concludes the paper.

## II. LITERATURE REVIEW

Prior studies have identified HIE related privacy and security concerns [8] and public attitude toward adoption of HIE system [9, 10]. Some studies discussed attitude of doctors [11-14] and nurses [3] toward the usage of EMR and few of them discussed patient's acceptance of Health information system [15, 16]. However, these studies mainly focus on consumers' reluctance to use new technology.

There are very few studies which exclusively focus on patient attitudes toward sharing their health information. E.g. Whiddett, et al. [17] conducted a study of primary care patients in New Zealand and found that patient would like to be consulted about type of information before being released. Simon, et al. [18] surveyed Massachusetts community of northeastern United States to collect patient opinions about distribution of their information. The study found that patients are more concerned about privacy over HIE benefits. A proportion of respondent shows willingness to share information if they are consulted prior to sharing their information. Dhopeswarkar et al. [19] conducted a survey to understand consumer preferences regarding the privacy and security of HIE. The study explored that patients prefer to view and permit the portion of information being shared with other parties. All these studies are exclusively validated in context of western culture, whereas in Saudi Arabia the impact of subjective norms on individual to share information is markedly different. Furthermore, previous studies based on general perception of consumers' behavior by considering privacy and security concerns.

Compared to previous studies, this study highlighting the factors driving patients' intention by developing a theoretical model adopted from psychological and social science theories describing user attitude and behavior toward specified behavior. These theories include Theory of Reasoned Action (TRA) [20], Theory of Planned Behavior (TPB) [7] to describe user behavior and attitude and Technology Acceptance Model

(TAM) [6] that predict and explain health IT acceptance and use.

TRA is a general social-psychological/behavioral theory that had been proven useful for understanding a variety of behaviors. It suggests that a person's behavior is determined by persons' attitude and subjective norm [20]. TPB [7] is an extension of TRA, suggesting that in addition to attitude and subjective norm, a person's perceived behavioral control (PBC) also influences behavioral intention. It refers to a person's behavior based on past experience (such as privacy protection and invasion) and the anticipated abilities to carry out the behavior. Although TPB is adopted by many researchers to explain the behavior of persons toward certain action, however, it does not specify belief set that is relevant to specific behavior of IT usage and acceptance. Since the major antecedent to IT use is behavioral intention (BI) to use it, hence TPB is extended to Technology Acceptance Model (TAM). TAM determines that the intention to use a system is effected by individual's attitude towards using the system. Perceived usefulness is influenced directly by behavioral intention (BI) [21]. Furthermore, perceived usefulness and perceived ease of use are two factors influenced by additional external variables and determines users' attitude and perceived ease of use i.e. the easier it is to use the more useful it can be.

Based upon these three theories combined with general consumers' perception of health care literature a theoretical model is proposed in next section to identify antecedent factor to determine patient attitude towards sharing their health information.

## III. PROPOSED MODEL AND HYPOTHESIS

Technology Acceptance Model (TAM) and Theory of Planned Behavior (TPB) are selected as the reference to develop theoretical model for determining patients' intention to accept Health Information Exchange system. Proposed model is shown in Fig. 1. It consists of eight external variable (constructs) based on theoretical arguments from HIE acceptance perspective. The selection of these constructs is supported by previous studies from Health Information System and Technology acceptance literature [6, 8, 12, 21, 22]. Behavior Intention is adopted from original TAM model as the primary predictor of actual usage behavior [21]. Subjective Norms and external variables such as Age, gender and background are adopted from TPB. Furthermore, we extended the model with other constructs such as Perceived Benefits of HIE, Perceived Risk, Trust, Privacy Concerns and Patients' Involvement to provide precise understanding of patients' behavioral antecedents based upon theoretical arguments from HIE perspective [11, 16, 23, 24]. Description of constructs adopted in proposed model is shown in Table I.

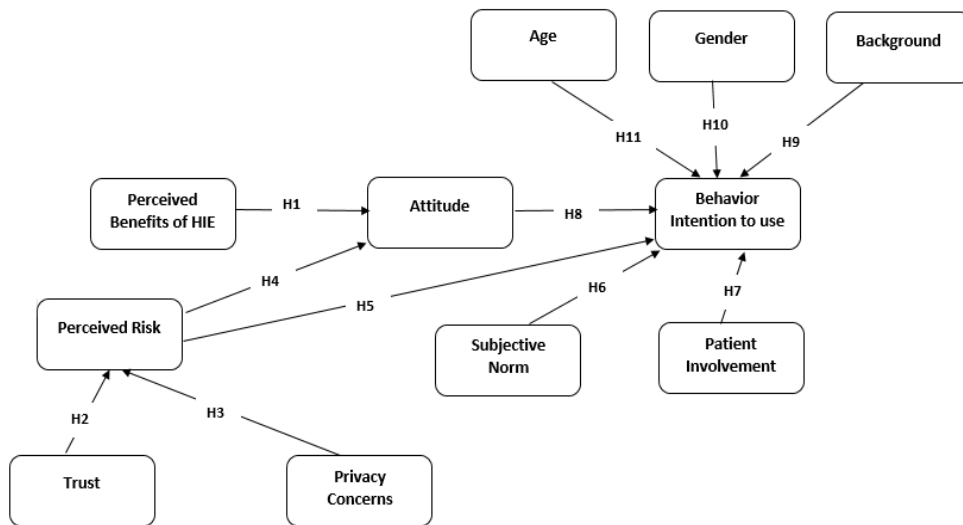


Fig. 1. Proposed Model of Health Information Exchange

TABLE I. THEORETICAL CONSTRUCTS WITH DESCRIPTION

| Construct                | Description                                                                                                              |
|--------------------------|--------------------------------------------------------------------------------------------------------------------------|
| Behavior Intention (BI)  | Measure the strength of person’s formulated conscious plan to perform or not perform some specified future behavior [15] |
| Perceived Benefits (PB)  | Degree of persons understanding for the efficacy of HIE system.                                                          |
| Perceived Risk (PRisk)   | Level of patient’s uncertainty in use of Health information system                                                       |
| Subjective Norms (SN)    | Refer to the persons’ perception of performing some action based upon other people expectations [20].                    |
| Trust                    | Measures the level of patients’ perception about the legality, standard and technology adopted by HIE system.            |
| Privacy Concerns (PC)    | Patients concern who will access and how to use their information.                                                       |
| Attitude (ATT)           | Refers to persons’ behavior which directly influence the strength of that behavior.                                      |
| Patient Involvement (PI) | Measures the degree of patient involvement in process of information sharing and usage.                                  |

Following eleven hypotheses are constructed to examine proposed model.

**H1:** Higher level of perceived benefits of HIE leads to more positive attitude to share health information.

**H2:** Higher level of trust leads to low perceived risk to share their health information.

**H3:** High level of privacy concerns lead to high perceived risk to share health information

**H4:** Higher level of perceived risk lead to more negative attitude to share health information.

**H5:** Patient’s perceived risk has a negative effect on their behavior intention.

**H6:** A higher level of subjective norms leads to more positive behavior intention to share health information.

**H7:** Patient involvement has a positive effect on their behavior intention to share their health information.

**H8:** A positive attitude leads to more positive behavior intention to share health information.

**H9:** Patients’ higher level of HIE related background has a positive effect on behavior intention.

**H10:** Gender will positively influence on behavior intention to share health information more for men.

**H11:** Age will positively influence on behavioral intention to share health information more for younger than elderly.

In this study, we considered the patients’ age above 18 years because the patients younger than 18 could not have their own account or respond the survey [16]. Furthermore, they will influence negatively since they are unable to take a decision about their health information and most of them rely on their parents.

#### IV. RESEARCH METHODOLOGY

##### A. Survey Instrument Development

Data is collected from surveys administered through structured questionnaire. Survey items used to operationalize the construct investigated in proposed model are adopted from previous studies as shown in Table II. To adopt them for Saudi culture, items were first drafted in English and test for clarity and face validity by team of two professors. To get the maximum response, items were also translated into Arabic language. A backward translation method was used where items were translated back and forth to English and Arabic language by team of two bilinguals’ professors. The Arabic and English version were subject to three patients for content clarity and completion time estimation. All items were measured using a five-point Likert-type scale, with anchors ranging from “strongly agree” to “strongly disagree.” Survey

was distributed via email, WhatsApp, tweeter, Facebook as well as conducted online.

TABLE II. THEORETICAL CONSTRUCTS WITH SURVEY ITEMS

| Constructs     | Survey Items                                                                                                                      |
|----------------|-----------------------------------------------------------------------------------------------------------------------------------|
| BI [12, 22]    | BI1: I intend to share my health information when it becomes available with my physician.                                         |
|                | BI2: I intend to share my health information with other caregivers as often as needed.                                            |
|                | BI3: To the extent possible, I would share my health information with others providers frequently.                                |
| ATT [12, 24]   | ATT1: Sharing my health information would be a good idea.                                                                         |
|                | ATT2: Sharing my health information is unpleasant.                                                                                |
|                | ATT3: Sharing my health information is beneficial for my health care.                                                             |
| PB[14, 25]     | PB1: Sharing my health information save time and decrease cost.                                                                   |
|                | PB2: Sharing my health information reduce duplication in medication, reports and lab tests.                                       |
|                | PB3: Sharing my health information help physician to accurately diagnosis                                                         |
| SN[24, 26]     | SN1: People who are important to me would think that I should share my health information with other organizations.               |
|                | SN2: People who influence me would think that I should share my health information.                                               |
|                | SN3: People whose opinions are valued to me would prefer that I should share my health information with other organizations [26]. |
| PI[27]         | PI1: I prefer to sign a consent before my information being released.                                                             |
|                | PI2: I prefer to approve which information that I agree to share.                                                                 |
|                | PI3: I want to receive notification before sharing my information.                                                                |
| PRisk [13, 24] | PRisk1: Sharing my health information lead to breach of privacy because my information could be used without my knowledge.        |
|                | PRisk2: Sharing my health information would pose risks to my treatments and diagnoses.                                            |
| Trust [13, 15] | Trust1: I can trust health care providers to share my information.                                                                |
|                | Trust2: I cannot trust on information technology used due to potential threats                                                    |
| PC [28, 29]    | PC1: I am concerned that another care provider could misuse my health information.                                                |
|                | PC2: I am concerned about sharing my health information because of what others might do with them.                                |
|                | PC3: I am concerned about sharing my health information because it could be sold to third parties.                                |

**B. Tool and Techniques**

Data is analyzed using SPSS V24.0 and WarpPLS 5.0 [30]. SPSS is a well-known and commonly used program for statistical analysis and used to compute descriptive statistics, frequencies, and percentages of collected data. WarpPLS 5.0 is used to assess the reliability, validity as well as hypothesis testing. Structural Equation Modeling (SEM) is used for hypothesis testing. SEM is most commonly used multivariate technique [31] for instrument validation and model testing to identify series of relationship constitutes in large-scale model or an entire theory.

**C. Demographic Characteristics**

A total number of 300 responses from Saudis and non-Saudis residence in Eastern province is collected. Table III presents the sample distribution of gender, age and background. Results show that the most respondents were female (59.3%). The majority of the respondents (58%) indicate that the respondents do not have previous background about health information exchange. Statistics also shows that the majority of the respondents (38.7%) were between 18 to 30 years of age group.

TABLE III. RESPONDENTS' CHARACTERISTICS (N=300)

| Measure    | Item               | Frequency | Percentage |
|------------|--------------------|-----------|------------|
| Gender     | Female             | 178       | 59.3       |
|            | Male               | 122       | 40.7       |
| Age        | 18 to 30 years     | 116       | 38.7       |
|            | 31 to 40 years     | 93        | 31         |
|            | 41 to 50 years     | 51        | 17         |
|            | 51 years and above | 40        | 13.3       |
| Background | Yes                | 126       | 42         |
|            | No                 | 174       | 58         |

**V. DATA ANALYSIS AND RESULTS**

The analysis of data from the 300 samples is conducted in two stages. At first stage, the model is estimated using Confirmatory Factor Analysis (CFA) to test whether constructed variable possesses sufficient reliability and validity. Based upon CFA, constructed variable and measuring items that best fitted the data are identified. Constructs and items that do not best fit the data are removed from model. In second stage structural relationships among the model constructs identified to test whether proposed hypothesis are supported by data or not.

**A. Assessment of the Measurement Model**

Model reliability, Convergent and Discriminant validity [32] is examined to identify the adequacy of measurement model. Cronbach's Alpha is used to assess reliability. Its values varies between 0 and 1, the higher the values the more reliable and desirable are the measuring items pertaining to given construct [33]. According to C. E. Lunneborg [34] values should be more than 0.70, however, 0.60 or 0.50 is also acceptable [35, 36]. It can be observed from the Table IV, the range of the Cronbach Alpha varies -0.023–0.831 where, *Attitude* and *Trust* has negative values. The items with value less than recommended are dropped from model. The item dropped are *Trust* construct and item-2 (*ATT2*) from the *Attitude* construct to achieve recommended value of Cronbach's Alpha as shown in Table V. Convergent validity is assessed by using Composite Reliability and Average Variance Extracted (AVE). It can also be observed from Table VI composite reliability and AVE are greater than recommended value of 0.70 and 0.50 [36, 37]. Discriminant Validity is measured to identify that one construct is truly distinct from all other construct in research model [32, 38]. It is measured by examining AVE to ensure that each construct share large variance with the other constructs. Hair et al. [39] stated that the discriminant validity is supported when the square root of individual construct is higher than the variance shared between the constructs. Table VII shows square roots of AVEs

(diagonal cells) greater than the correlations between constructs.

TABLE IV. RELIABILITY TESTING

| Construct | No. of Items | Mean | Std. Dev. | Cronbach's Alpha |
|-----------|--------------|------|-----------|------------------|
| BI        | 3            | 4.09 | 0.75      | 0.744            |
| ATT       | 3            | 3.58 | 0.93      | -0.386           |
| PB        | 3            | 4.35 | 0.79      | 0.767            |
| SN        | 3            | 3.76 | 0.93      | 0.831            |
| PI        | 3            | 4.06 | 0.97      | 0.687            |
| PRisk     | 2            | 2.97 | 1.14      | 0.535            |
| Trust     | 2            | 3.44 | 0.98      | -0.023           |
| PC        | 3            | 3.19 | 1.11      | 0.803            |

TABLE V. RELIABILITY TESTING AFTER DROPPING TRUST AND ATT2

| Constructs | No. of Items | Mean | Std. Dev. | Cronbach's Alpha |
|------------|--------------|------|-----------|------------------|
| BI         | 3            | 4.09 | 0.75      | 0.744            |
| ATT        | 2            | 4.16 | 0.87      | 0.677            |
| PB         | 3            | 4.35 | 0.79      | 0.767            |
| SN         | 3            | 3.76 | 0.93      | 0.831            |
| PI         | 3            | 4.06 | 0.97      | 0.687            |
| PRisk      | 2            | 2.97 | 1.14      | 0.535            |
| PC         | 3            | 3.19 | 1.11      | 0.803            |

TABLE VI. CONVERGENT VALIDITY

| Constructs | Comp. Rel. | AVE  |
|------------|------------|------|
| BI         | .855       | .663 |
| ATT        | .861       | .631 |
| PB         | .866       | .684 |
| SN         | .899       | .747 |
| PI         | .827       | .615 |
| PRisk      | .811       | .682 |
| PC         | .884       | .717 |

TABLE VII. DISCRIMINANT VALIDITY

| Constructs | BI           | ATT          | PB           | SN           | PI           | PRisk        | PC           |
|------------|--------------|--------------|--------------|--------------|--------------|--------------|--------------|
| BI         | <b>0.814</b> |              |              |              |              |              |              |
| ATT        | 0.618        | <b>0.794</b> |              |              |              |              |              |
| PB         | 0.471        | 0.592        | <b>0.827</b> |              |              |              |              |
| SN         | 0.486        | 0.438        | 0.432        | <b>0.864</b> |              |              |              |
| PI         | -0.046       | -0.005       | 0.103        | 0.070        | <b>0.784</b> |              |              |
| PRisk      | -0.207       | -0.430       | -0.166       | -0.113       | 0.310        | <b>0.826</b> |              |
| PC         | -0.159       | -0.263       | -0.105       | -0.076       | 0.360        | 0.434        | <b>0.847</b> |

B. Assessment of Structural Model

The structural model is evaluated and hypothesis are tested after establishing adequacy of measurement model. Structural Equation Model (SEM) is built to indicates the path relationship among the construct. It is done by determining the predictive power of model and by analyzing the hypothesized relationship among the constructs. Firstly, the coefficient of determination R-Square ( $R^2$ ) for each of three endogenous constructs is calculated to determine the predictive power of research model. It can be observed from Fig. 2. that model has high predictive power since it shows 42% variance in Behavior

Intention (BI) and 45% variance in Attitude (ATT) which is supported by meta-analysis of research on TRA and TPB [40] where average variance in intention is 40–50%. The Perceived Risk (PRisk) account for 19 % variance. Secondly, direct effect of each exogenous construct on the endogenous construct to estimates the standardized path coefficients (*beta*) between constructs. It is indicated by  $\beta$  value with p significance level presented numerically on solid line leading from the exogenous construct to the endogenous construct in Fig. 2.

C. Hypothesis Testing

Result of hypothesis testing are summarized in Table VIII. The ‘Findings’ column indicates whether that hypothesis was supported or not supported depending on the path coefficients  $\beta$  and *p*-value. The result shows that five hypotheses were significantly supported and five hypotheses are not empirically supported by the data.

Following is the summary of hypothesis test:

- **H1:** A higher level of Perceived Benefits (PB) of HIE lead to more positive attitude (ATT) to share health information. PB achieved a strong positive direct influence on ATT (beta = 0.585,  $p < 0.001$ ). Hence, H1 is supported.
- **H2:** Higher level of Trust leads to low perceived risk to share their health information. H2 is removed due to removal of Trust construct during testing for constructs’ reliability.
- **H3:** High level of Privacy Concerns (PC) lead to high perceived risk (PRisk) to share health information. PC achieved a strong positive direct influence on PRisk (beta = 0.435,  $p < 0.001$ ). Hence, H3 is supported.
- **H4:** higher level of PRisk lead to more negative Attitude (ATT) to share health information. PRisk achieved a strong negative direct influence on ATT (beta = -0.228,  $p < 0.001$ ). Hence, H4 is supported

The result shows that H1 has more effect in this study than H4. This mean PB effect on patient’s ATT with beta coefficient = 0.585 is higher than the effect of PRisk on ATT (beta coefficient = -0.228). Perceived benefits and perceived risk are considered as two factors that influence the attitude of patients to share their health information.

- **H5:** Patient’s Perceived Risk (PRisk) has a negative effect on their Behavior Intention (BI) to share their health information. PRisk achieved a strong positive direct influence on BI (beta = 0.149,  $p = 0.004$ ). Hence, H5 is not supported.
- **H6:** A higher level of Subjective Norms (SN) leads to more positive Behavior Intention (BI) to share health information. SN achieved a strong positive direct influence on BI (beta = 0.203,  $p < 0.001$ ). Hence, H6 is supported.

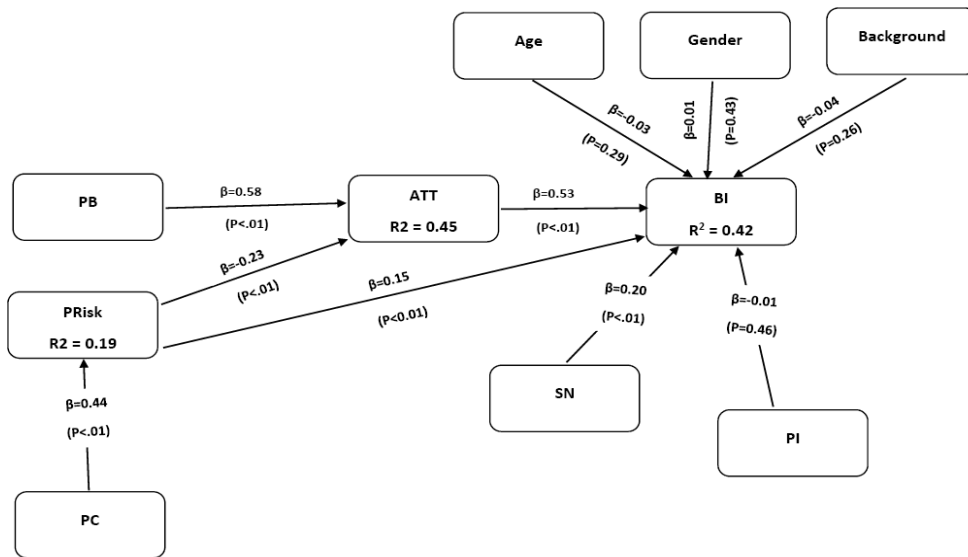


Fig. 2. Structural Model Results (Denotes significance at the  $p<0.01$  level)

- **H7:** Patient Involvement (*PI*) has a positive effect on their Behavior Intention (*BI*) to share their health information. *PI* achieved a strong negative direct influence on *BI* (beta = -0.006,  $p = 0.461$ ). Hence, H7 is not supported.
- **H8:** A positive Attitude (*ATT*) leads to more positive Behavior Intention (*BI*) to share health information. *ATT* achieved a strong positive direct influence on *BI* (beta = 0.534,  $p < 0.001$ ). Hence, H8 is supported.

The result shows that H8 has more effect than H6. This mean patients' attitude effect on behavior intention with beta coefficient = 0.534 is higher than the effect of subjective norm on intention behavior (beta coefficient = 0.203). These findings are supported by another IS acceptance studies [13] in which the attitude positively effect on behavior intention. Accordingly, attitude explained 42% of the variance in patients' intention to share their information. Similar to our study the outcomes [41] indicate that attitude of patients and subjective norm are the main determinants to share health information. Patients' decisions about HIE system acceptance could be strongly effected by their peers and friends.

- **H9:** Patients' higher level of HIE related background has a positive effect on behavior Intention (*BI*) to share their health information. Background achieved a strong negative direct influence on *BI* (beta = -0.037,  $p = 0.261$ ). Hence, H10 is not supported.
- **H10:** Gender will positively influence on *BI* to share health information more for men. Gender did not display significant interactions with behavior intention (beta = 0.010,  $p = 0.428$ ). Hence, H11 is not supported.
- **H11:** Age will positively influence on *BI* to share health information more for younger than elderly. Age did not show significant interactions with behavior intention (beta = -0.032,  $p = 0.290$ ). Hence, H12 is not supported.

TABLE VIII. SUMMARY OF RESEARCH FINDINGS

| Hypothesis / Path   | Beta value | P value | Finding       | R <sup>2</sup> |
|---------------------|------------|---------|---------------|----------------|
| H1: PB → ATT        | 0.585      | <0.001  | Supported     | .45            |
| H3: PC → PRisk      | 0.435      | <0.001  | Supported     | .19            |
| H4: PRisk → ATT     | 0.228      | <0.001  | Supported     | .45            |
| H5: PRisk → BI      | 0.149      | 0.004   | Not Supported | .42            |
| H6: SN → BI         | 0.203      | <0.001  | Supported     | .42            |
| H7: PI → BI         | 0.006      | 0.461   | Not Supported | .42            |
| H8: ATT → BI        | 0.534      | <0.001  | Supported     | .42            |
| H9: Background → BI | 0.037      | 0.261   | Not Supported | .42            |
| H10: Gender → BI    | 0.010      | 0.428   | Not Supported | .42            |
| H11: Age → BI       | 0.032      | 0.290   | Not Supported | .42            |

## VI. CONCLUSION

Governments in developing countries are spending huge amounts of money in implementing and exchanging EMR which is becoming progressively complex and leads to implementation failures. In addition, low acceptance of such system has been a major problem for health care providers.

This study developed the understanding of the determinant of HIE system acceptance. It identifies the patients concerns and their preferences to share their sensitive health information disseminated among different health care providers through such systems. The result of the analysis indicated that *Perceived Benefits* and *Perceived Risks* are the two factors influence the attitude of patients to share their health information. Moreover, *Attitude* and *Subjective Norms* have significant effects on *Behavior Intention* to share health information. Based on these findings this study revealed that more attention should be directed toward ensuring that patient is fully informed about the benefits of HIE and they have high level of trust on HIE legality, standard, policies and

technology. Furthermore, they should be trained and educate time to time to maximize HIE acceptance and usage. The findings also imply that the design and development of future systems should also incorporate sophisticated and flexible access control policies that can be adapted to meet the preferences of individual patients to reduce expected barriers.

#### ACKNOWLEDGEMENTS

We would like to thank **Dr. Mohammad Elhassan, Assistant Professor, King Faisal University** for his expert opinion on design, development and validation of proposed model as well as instrument clarity and face validity.

#### REFERENCES

- [1] M. M. Altuwajiri, "Electronic-health in Saudi Arabia. Just around the corner?," Saudi medical journal, vol. 29, no. 2, pp. 171-178, 2008.
- [2] S. Bah, H. Alharthi, and A. A. El Mahalli, "Annual survey on the level and extent of usage of electronic health records in government-related hospitals in Eastern Province, Saudi Arabia," Perspectives in Health Information Management, vol. 8, no. 1, pp. 102-153, 2011.
- [3] H. Asiri, B. AlDosari, and B. Saddik, "Nurses' attitude, acceptance and use of Electronic Medical Records (EMR) in King AbdulAziz Medical City (KAMC) in Riyadh, Saudi Arabia," 2014.
- [4] L. Presser, M. Hruskova, H. Rowbottom et al., "Care. data and access to UK health records: patient privacy and public trust," Tecnology Science. August, vol. 11.
- [5] S. Davies, "Dystopia on the health superhighway," The Information Society, vol. 12, no. 1, pp. 89-94, 1996.
- [6] R. J. Holden, and B.-T. Karsh, "The technology acceptance model: its past and its future in health care," Journal of biomedical informatics, vol. 43, no. 1, pp. 159-172, 2010.
- [7] Ajzen, "The theory of planned behavior," Organizational behavior and human decision processes, vol. 50, no. 2, pp. 179-211, 1991.
- [8] L. Dimitropoulos, and S. Rizk, "A state-based approach to privacy and security for interoperable health information exchange," Health Affairs, vol. 28, no. 2, pp. 428-434, 2009.
- [9] L. Dimitropoulos, V. Patel, S. A. Scheffler et al., "Public attitudes toward health information exchange: perceived benefits and concerns," The American journal of managed care, vol. 17, no. 12 Spec No., pp. SP111-6, 2011.
- [10] Hoerbst, C. D. Kohl, P. Knaup et al., "Attitudes and behaviors related to the introduction of electronic health records among Austrian and German citizens," International journal of medical informatics, vol. 79, no. 2, pp. 81-89, 2010.
- [11] J. S. Shapiro, J. Kannry, A. W. Kushniruk et al., "Emergency physicians' perceptions of health information exchange," Journal of the American Medical Informatics Association, vol. 14, no. 6, pp. 700-705, 2007.
- [12] P. J. Hu, P. Y. Chau, O. R. L. Sheng et al., "Examining the technology acceptance model using physician acceptance of telemedicine technology," Journal of management information systems, vol. 16, no. 2, pp. 91-112, 1999.
- [13] J. M. O. Egea, and M. V. R. González, "Explaining physicians' acceptance of EHCR systems: An extension of TAM with trust and risk factors," Computers in Human Behavior, vol. 27, no. 1, pp. 319-332, 2011.
- [14] H. C. O'Donnell, V. Patel, L. M. Kern et al., "Healthcare consumers' attitudes towards physician and personal use of health information exchange," Journal of general internal medicine, vol. 26, no. 9, pp. 1019-1026, 2011.
- [15] R. Ahlan, and B. I. e. Ahmad, "An overview of patient acceptance of Health Information Technology in developing countries: a review and conceptual model," SciKA-Association for Promotion and Dissemination of Scientific Knowledge, 2015.
- [16] Hassol, J. M. Walker, D. Kidder et al., "Patient experiences and attitudes about access to a patient electronic health care record and linked web messaging," Journal of the American Medical Informatics Association, vol. 11, no. 6, pp. 505-513, 2004.
- [17] R. Whiddett, I. Hunter, J. Engelbrecht et al., "Patients' attitudes towards sharing their health information," International journal of medical informatics, vol. 75, no. 7, pp. 530-541, 2006.
- [18] S. Simon, J. S. Evans, A. Benjamin et al., "Patients' attitudes toward electronic health information exchange: qualitative study," Journal of medical Internet research, vol. 11, no. 3, pp. e30, 2009.
- [19] R. V. Dhopeswarkar, L. M. Kern, H. C. O'Donnell et al., "Health care consumers' preferences around health information exchange," The Annals of Family Medicine, vol. 10, no. 5, pp. 428-434, 2012.
- [20] Ajzen, and M. Fishbein, "Understanding attitudes and predicting social behaviour," Prentice-Hall, Englewood-Cliffs, NJ., 1980.
- [21] F. D. Davis, "Perceived usefulness, perceived ease of use, and user acceptance of information technology," MIS quarterly, pp. 319-340, 1989.
- [22] F. D. Davis, R. P. Bagozzi, and P. R. Warshaw, "User acceptance of computer technology: a comparison of two theoretical models," Management science, vol. 35, no. 8, pp. 982-1003, 1989.
- [23] E. D. M. Nour, "Physicians' use of and attitudes toward electronic medical record system implemented at a teaching hospital in Saudi Arabia," The Journal of the Egyptian Public Health Association, vol. 82, no. 5-6, pp. 347-364, 2006.
- [24] P.-J. Hsieh, "Physicians' acceptance of electronic medical records exchange: An extension of the decomposed TPB model with institutional trust and perceived risk," International journal of medical informatics, vol. 84, no. 1, pp. 1-14, 2015.
- [25] S.-i. Lee, H. Park, J.-W. Kim et al., "Physicians' perceptions and use of a health information exchange: a pilot program in South Korea," TELEMEDICINE and e-HEALTH, vol. 18, no. 8, pp. 604-612, 2012.
- [26] L. Wu, J.-Y. Li, and C.-Y. Fu, "The adoption of mobile healthcare by hospital's professionals: An integrative perspective," Decision Support Systems, vol. 51, no. 3, pp. 587-596, 2011.
- [27] Turan, A. Ö. Tunç, and C. Zehir, "A Theoretical Model Proposal: Personal Innovativeness and User Involvement as Antecedents of Unified Theory of Acceptance and Use of Technology," Procedia-Social and Behavioral Sciences, vol. 210, pp. 43-51, 2015.
- [28] L. Miltgen, and H. J. Smith, "Exploring information privacy regulation, risks, trust, and behavior," Information & Management, vol. 52, no. 6, pp. 741-759, 2015.
- [29] S. Bandyopadhyay, "Consumers' online privacy concerns: causes and effects," 2012.
- [30] N. Kock, "WarpPLS 5.0 user manual," Laredo, TX: ScriptWarp Systems, 2015.
- [31] Fornell, and D. F. Larcker, "Evaluating structural equation models with unobservable variables and measurement error," Journal of marketing research, pp. 39-50, 1981.
- [32] T. Campbell, and D. W. Fiske, "Convergent and discriminant validation by the multitrait-multimethod matrix," Psychological bulletin, vol. 56, no. 2, pp. 81, 1959.
- [33] R. R. Gliem, and J. A. Gliem, "Calculating, interpreting, and reporting Cronbach's alpha reliability coefficient for Likert-type scales," in Midwest Research-to-Practice Conference in Adult, Continuing, and Community Education, 2003.
- [34] E. Lunneborg, "Book Review: Psychometric Theory: Second Edition Jum C. Nunnally New York: McGraw-Hill, 1978, 701 pages," Applied Psychological Measurement, vol. 3, no. 2, pp. 279-280, 1979.
- [35] J. C. Nunnally, I. H. Bernstein, and J. M. t. Berge, Psychometric theory: JSTOR, 1967.
- [36] J. F. Hair, W. C. Black, B. J. Babin et al., Multivariate data analysis: Pearson Prentice Hall Upper Saddle River, NJ, 2006.
- [37] Fornell, and D. F. Larcker, "Structural equation models with unobservable variables and measurement error: Algebra and statistics," Journal of marketing research, pp. 382-388, 1981.
- [38] J. C. Anderson, and D. W. Gerbing, "Structural equation modeling in practice: A review and recommended two-step approach," Psychological bulletin, vol. 103, no. 3, pp. 411, 1988.

- [39] J. Hair, R. Anderson, R. Tatham et al., "Multivariate Data Analysis. New Jersey: Prentivce-Hall International," Inc, 1998.
- [40] S. Sutton, "Predicting and explaining intentions and behavior: How well are we doing?," *Journal of applied social psychology*, vol. 28, no. 15, pp. 1317-1338, 1998.
- [41] Bhattacharjee, "Acceptance of e-commerce services: the case of electronic brokerages," *Systems, Man and Cybernetics, Part A: Systems and Humans*, IEEE Transactions on, vol. 30, no. 4, pp. 411-420, 2000.

# Efficient Load Balancing Algorithm for the Arrangement-Star Network

Ahmad M. Awwad  
Computer Science Department  
Petra University  
Amman, Jordan

Jehad A. Al-Sadi  
Information Technology and Computing Department  
Arab Open University  
Amman, Jordan

**Abstract**—The Arrangement-Star is a well-known network in the literature and it is one of the promising interconnection networks in the area of super computing, it is expected to be one of the attractive alternatives in the future for High Speed Parallel Computers. The Arrangement-Star network has many attractive topological properties such as small diameter, low degree, good connectivity, low broadcasting cost and flexibility in choosing the desired network size. Although, some of the research work has been done on Arrangement-Star network, it still needs more investigation and research efforts to explore these attractive topologies and utilize it to solve some real life applications. In this paper we attempt to fill this gap by proposing an efficient algorithm for load balancing among different processors of the Arrangement-Star network. The proposed algorithm is named as Arrangement Star Clustered Dimension Exchange Method ASCDEM presented and implemented on the Arrangement-Star network. The algorithm is based on the Clustered Dimension Exchange Method (CDEM). The ASCDEM algorithm is shown to be efficient in redistributing the load balancing among all different processors of the network as evenly as possible. A complete detail of this algorithm in addition to examples and discussions to explore the benefits of applying this distributed algorithm is presented in this paper. Furthermore an analytical study on the algorithm is presented and discussed to explore the attractive performance of the proposed algorithm.

**Keywords**—Interconnection Networks; Topological Properties; Arrangement-Star; Load balancing

## I. INTRODUCTION

The Arrangement-Star network as a case of study on vertex product networks [1, 2, 3, 4], it is constructed from the cross product of the Star and Arrangement graphs. It has shown to have superior topological properties over its constituents: the Star and Arrangement graphs [5, 6, 7]. Besides having a smaller diameter, node degree, and number of links, it has a lower broadcasting cost and more flexibility in choosing the desired network size.

Although some algorithms proposed for the Arrangement-Star graph such as distributed fault-tolerant routing algorithm [5], some of the important problems that the Arrangement-Star network still needs more efforts and researchers is the issue of load balancing among different processors of this network. Since there is no enough research work in literature for proposing efficient algorithms for load balancing on the Arrangement-Star network. In this research effort we move one more step in filling this gap by investigating and proposing the ASCDEM algorithm on the Arrangement-Star

network, the proposed algorithm is based on the CDEM algorithm which was able to redistribute the load balance among all node of the networks on OTIS-Hypercube network as evenly as possible [8]. A reasonable and efficient implementation of the ASCDEM algorithm on the Arrangement-Star network will make it more attractive for the solving real life applications problem.

This paper is organized as follows: In the next section we present the related work on load balancing, section III introduces the necessary basic notations and definitions, section IV presents the implementation of the ASCDEM algorithm on the Arrangement-Star network, furthermore we present examples on SCDEM algorithm to explain and explore detailed transactions of the algorithm on different Arrangement-Star network sizes, section V presents an analytical study of the ASCDEM algorithm, finally section VI concludes this research work.

## II. BACKGROUND AND RELATED WORK

Many attractive properties for the Arrangement-Star graph have been shown in the literature enabled it to be one of the candidate's networks for the High Speed Parallel Computers (HSPC) and a reasonable choice for any real life applications [5]. This outcome about Arrangement-Star network has motivated us to spend more time and do some research on it for some important class of algorithms such as: the load balancing because still this networks suffers from shortening in number of algorithms for the load balancing problem in general and for load balancing problem in specific. This algorithm has been studied and proposed for many HSPC infrastructures ranging from electronic networks [5] and also for Optoelectronic networks [9, 10].

The Load balancing algorithm is a famous type of problems that is needed by all HSPC infrastructures. The load balancing problem have been investigated from many angles and point views. As an example on the literature work this problem was investigated by the researchers Ranka, Won, and Sahni [11], As conclusion of their work they come out with an efficient algorithm to be implemented on HSPC called the Dimension Exchange Method (DEM) on the hypercube topology. This algorithm (DEM) constructed and developed by issuing and getting the average load of neighbors' nodes, where the symmetric degree of the hypercube is  $n$ , All adjacent nodes which are connected on the  $n^{\text{th}}$  dimension they will exchange their task loads to redistribute the task load and as evenly as possible, the processor with extra load will share

any extra amount of the load to its adjacent neighbor node. The DEM algorithm main advantage that it was able to redistribute the load balances of processors among all neighbors as evenly as possible. Furthermore Ranka and *et al* have enhance the load balance in the DEM algorithm in its worst case to achieve  $\log 2n$  on the cube network [11].

Zaho, Xiao, and Qin have investigated and proposed hybrid structure of diffusion and dimension exchange called DED-X which worked in a perfect manner for the load balancing algorithm on Optoelectronic networks [12]. The DED-X problem main task was to redistribute the load balancing between different nodes of the network to three different phases. The achieved outcome on Optical Transpose Interconnection System networks proved that the redistribution of load balance between all nodes of the topology was efficient and mostly even. Furthermore the reached outcome and the issued results of the simulation from Zaho et al of the proposed algorithms on load balancing has shown a considerably big improvements in enhancement in redistribution the load balancing of the processors of the topology [12]. In a different literature and research done by Zaho and Xiao they investigated a different algorithm named t DED-X for load balancing on homogeneous optoelectronic technology and they proposed new algorithm framework, Generalized Diffusion-Exchange- Diffusion Method, this framework was efficient for the load balancing distribution on the Heterogeneous optoelectronic technology [11, 13, 14].

On the other hand Zaho, Xiao, and Qin have investigated and proved that the efficiency of the new investigated load balancing algorithms to be more effective than the X old load balancing algorithm [12].

The target of this research effort is to investigate a new algorithm for the load balancing among the nodes of the Arrangement-Star networks named Arrangement Star Clustered Dimension Exchange Method (ASCDEM). The algorithm is based on the Clustered Dimension Exchange Method (CDEM) [13].

### III. DEFINITIONS AND TOPOLOGICAL PROPERTIES

During the last two decades a big number of interconnection networks for High Speed Parallel Computers (HSPC) investigations are proposed in literature [6, 13, 15]. As an example one of these networks was the hypercube interconnection network [8, 13]. Also a well know example is the Star network [6]. Some properties of this network have been studied in the literature including its basic topological properties, parallel path classification, node connectivity and embedding [17, 18, 19, 20]. The authors Akers and Krishnamurthy have proved that the Star graph has several advantages over the hypercube network including a lower degree for a fixed network size of the comparable network sizes, a smaller diameter, and smaller average diameter. Furthermore they showed that the Star graph is maximally fault tolerant edge, and vertex symmetric [6].

The major drawback of the Star network is related to its scalability problem [21]. The size of the Star network increases as a factorial function, and thus grows widely very rapidly; for example, the value of  $5!$  is equal to 120 while the

value of  $6!$  is 720. Until today despite its attractive topological properties, the Star graph has not been used in practical systems yet because of this problem.

In an attempt to address this problem in the Star network, Day and Tripathi [7] have proposed the Arrangement graph as a generalization of the Star graph. The Arrangement graph is a family of undirected graphs that contains the Star graph family. It slightly brings a solution to the problem of the scalability, which the Star graph suffers from (i.e. the problem of growth of the number  $n!$  of nodes in the  $n$ -Star). It also preserves all the nice qualities of the Star graph topology including, hierarchical structure, vertex and edge symmetric, simple shortest path routing and many fault tolerance properties [7]. Still a common drawback of the Star and Arrangement graphs is the restriction on the number of nodes:  $n!$  for the Star graph and  $m!/(m-k)!$  for the Arrangement graph. The set of values of  $n!$  (or  $m!/(m-k)!$ ) is spread widely over the set of integers; so, one will be faced with the choice of too few or too many available nodes.

However, there has been relatively a limited research efforts have been dedicated to design efficient algorithms for the Arrangement-Star graph including broadcasting [19], selection and sorting [20, 22], Fast Fourier Transform [23], and Matrix Multiplications [24] and load balancing. In an attempt to overcome the load balancing problem we present an efficient algorithm for load balancing problem on Arrangement-Star graph to redistribute the load balancing among all processors of the network as evenly as possible.

An Arrangement graph is specified by two parameters  $m$  and  $k$ , satisfying  $1 \leq k \leq m$ . For simplicity let  $\langle m \rangle = \{1, 2, \dots, m\}$  and  $\langle k \rangle = \{1, 2, \dots, k\}$ .

**Definition 1:** The  $(m, k)$ -Arrangement graph  $A_{m,k} = (V_1, E_1)$ ,  $1 \leq k \leq m-1$  is defined as follows [7]:

$$V_1 = \{p_1 p_2 \dots p_k \mid p_i \in \langle m \rangle \text{ and } p_i \neq p_j \text{ for } i \neq j\} = P_k^m, \text{ and}$$

$$E_1 = (p, q) \mid p \text{ and } q \text{ in } V_1 \text{ and for some } i \text{ in } \langle k \rangle, p_i \neq q_i \text{ and } p_j = q_j \text{ for } j \neq i\}.$$

That is, the nodes of  $A_{m,k}$  labelled with a unique Arrangements of  $k$  elements out of  $m$  symbols  $\langle m \rangle$ , and the edges of  $A_{m,k}$  connect Arrangements which differ in exactly one of their  $k$  positions. An edge of  $A_{m,k}$  connecting two Arrangements which differ only in position  $i$  called an  $i$ -edge. In this case,  $p$  and  $q$  are  $i$ -adjacent and  $q$  is called  $(i, q_i)$ -neighbour of  $p$ . The  $(m, k)$ -Arrangement graph  $A_{m,k}$  is regular of degree  $k(m-k)$  and of size  $m!/(m-k)!$ , and diameter  $\lfloor 3k/2 \rfloor$ . The  $(m, m-1)$ -Arrangement graph  $A_{m,m-1}$  is isomorphic to  $n$ -Star graph  $S_n$  [3, 7], and the  $(m, 1)$ -Arrangement graph is isomorphic to the complete graph with  $m$  nodes [7].

**Definition 2:** The  $n$ -Star graph, denoted by  $S_n$ , has  $n!$  nodes each labelled with a unique permutation on  $\langle n \rangle = \{1, \dots, n\}$ . Any two nodes are connected if, and only if, their corresponding permutations differ exactly in the first and one other position.

The diameter,  $\delta$ , and the degree,  $\alpha$ , of the Star graph are as follows [6]:

$\delta$ , of  $n$ -Star graph =  $\lfloor 1.5(n-1) \rfloor$

$\alpha$ , of the  $n$ -Star graph =  $n-1$ , where  $n > 1$ .

**Definition 3:** The Arrangement-Star graph is the cross product of the  $n$ -Star graph and the  $(m, k)$ -Arrangement graph, and is given by  $AS_{n,m,k} = A_{m,k} \otimes S_n$  such that  $n > 1$  and  $1 \leq k \leq m$ .

Note that if  $G_1$  and  $G_2$  are two undirected graphs then for any node  $X = \langle x_1, x_2 \rangle$  in the cross product graph,  $G = G_1 \otimes G_2$ , has an address consisting of two parts, one coming from  $G_1$  and the other coming from  $G_2$ . We will denote the earlier part by  $lp(X) = x_1$  and the later part by  $rp(X) = x_2$ .

Figure 1 shows the topology of  $AS_{2,3,2}$  that is obtained from the graph product of  $S_2$  and  $A_{3,2}$  networks. A node  $X = \langle u, v \rangle$  in  $AS_{2,3,2}$  consisting of two parts, left part coming from the Star graph and the right part coming from the Arrangement graph ( $lp$  and  $rp$ ). Two nodes  $X = \langle u, v \rangle$  and  $Y = \langle u', v' \rangle$  are connected if,  $lp(X) = lp(Y)$  and  $rp(X)$  is connected  $rp(Y)$  in  $A_{m,k}$  (in this case  $X$  and  $Y$  are said Arrangement-connected) or  $rp(X) = rp(Y)$  and  $lp(X)$  is connected  $lp(Y)$  in  $S_n$  (in this case  $X$  and  $Y$  are said Star-connected). For instance in Figure 1 the node  $ab13$  is connected to the node  $ab12$ , and the node  $ab23$  is connected to the node  $ba23$ .

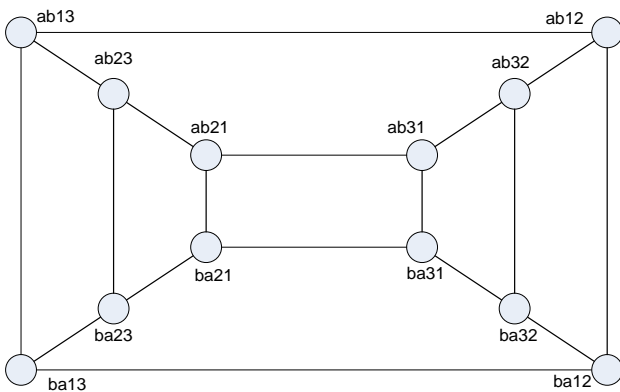


Fig. 1. Arrangement-Star graph,  $AS_{2,3,2}$

#### IV. THE IMPLEMENTATION OF THE ASCDEM ALGORITHM ON THE ARRANGEMENT-STAR NETWORK

The algorithm we present in this paper ASCDEM is based on the Clustered Dimension Exchange Method CDEM for load balancing for the Arrangement-Star Interconnection networks [8].

The main achievement of the new presented ASCDEM is to obtain even load balancing for the  $AS_{n,m,k}$  network by redistributing the load size to reach an equal load size at each node within the whole network. The structure of the  $AS_{n,m,k}$  network consists of  $S_n$  network as a first level structure of the hierarchal  $AS_{n,m,k}$  network, the first level of  $S_n$  consists of  $n!$  Sub-graphs, each sub-graph represented by an  $A_{m,k}$  Arrangement graph. The links and edges between the nodes of the whole graph have been identified and described in the above section.

The ASCDEM load balancing algorithm is based on the following two phases:

• Phase 1: Distributing the load balancing among all sub-graphs of the first level hierarchal  $S_n$  graph, we Start by balancing the load of every two nodes via the edges that connect these sub-graphs within the Star topology structure. By the end of this phase we guarantee that all sub-graphs will have almost the same total number of loads since each sub-graph is represented as if it is a single node of the Star network structure in the first level hierarchy. It worth to mention here, that the load within each sub-graph is not sorted at this stage. To complete this phase we need to make  $n!/2$  parallel redistribution steps of load among every two nodes via a Star structure edge. But at each of these parallel steps, there will be an  $n-1$  sequential exchanges for each node with its  $n-1$  neighbors within the Star structure.

• Phase 2: Distributing the load size within each sub-graph, this will the second level of the hierarchal  $AS_{n,m,k}$  network, where each sub-graph is an Arrangement graph representation, by the end of the phase 1, all sub-graphs will have the same load size, then by redistributing the load sizes among these Arrangement graphs, the whole  $AS_{n,m,k}$  network will have almost equal load sizes at each node. This phase requires  $m!/2(m-k)!$  parallel redistribution steps of load among every two nodes via an Arrangement structure edge. But at each of these parallel steps, there will be a  $k*(m-k)$  sequential exchanges for each node with its  $k*(m-k)$  neighbors within the Arrangement structure. By the end of this phase, all nodes will have almost the same load size, the following algorithm in Fig 2 describe the ASCDEM method of load balancing.

ASCDEM algorithm works on redistributing load balancing among all processors of the network, phase 1 is done in parallel among all nodes via the Star topological connections. Then Phase 2 is also done in parallel among all nodes via the Arrangement topological connections.

• Phase 1: The load balancing between the processors; sub-graphs; of  $S_n$  based on ASCDEM algorithm is exchanged as in steps 1 to 14 in parallel, at first step the load exchange will be between all the processors in which they differ in 1<sup>st</sup> position and 2<sup>nd</sup> position for all the factor networks of  $S_n$  i.e.  $S_{n-1}$ . Then the same process will be repeated continually until it reach the neighbours  $p_j$  that are  $n$  positions far away from  $p_i$ . By the end of this phase all sub-graphs will have almost the same total number of load sizes.

Note that  $n-1$  is the number of neighbors of any processor in  $S_n$ :

1. for  $p = 2; p \leq n; p++$  // Start of phase#1
- 2.
3. for all neighbour nodes  $p_i$  and  $p_j$  which they differ in 1<sup>st</sup> and  $p$  position of  $S_n$  do in parallel
4. Give-and-take  $p_i$  and  $p_j$  total load sizes of the two nodes
5.  $TheAverageLoad_{p_i,j} = \text{Floor} (Load_{p_i} + Load_{p_j})/2$
6. if (  $Totalload_{p_i} \geq \text{excess } AverageLoad_{p_i,j}$  )
7. Send excess load  $p_i$  to the neighbour node  $p_j$
8.  $Load_{p_i} = Load_{p_i} - \text{extra load}$
9.  $Load_{p_j} = Load_{p_j} + \text{extra load}$
10. else

11. Receive extra load from neighbour  $p_j$
12. Load  $p_i = \text{Load } p_i + \text{extra load}$
13. Load  $p_j = \text{Load } p_j - \text{extra load}$
14. Repeat steps (1 to 13)  $\left\lfloor \frac{3}{2}(n-1) \right\rfloor$  times // diameter of the Star Topology -End of phase#1
15. for  $p = 1; p \leq k; p // \text{the } k^{\text{th}} \text{ positions- Start of phase\#2}$
16. for  $d = 1; d < k*(m-k+1); d++ // \text{differ of } k^{\text{th}} \text{ position}$
17. for all neighbor nodes  $p_{ki}$  and  $p_{kj}$  which they differ in exactly one  $k$  position of  $A_{m,k}$  do in parallel
18. Give-and-take  $p_{ki}$  and  $p_{kj}$  total load sizes of the every two neighbor nodes where there are differ in exactly  $d$  in their  $k^{\text{th}}$  position //  $|k_i - k_j| = d$  excluding the fixed positions
19.  $\text{TheAverageLoad } p_{ki,kj} = \text{Floor}(\text{Load } p_{ki} + \text{Load } p_{kj})/2$
20. if (  $\text{Totalload } p_{ki} > \text{excess AverageLoad } p_{ki,kj}$  )
21. Send excess load  $p_{ki}$  to the neighbour node  $p_{kj}$
22. Load  $p_{ki} = \text{Load } p_{ki} - \text{extra load}$
23. Load  $p_{kj} = \text{Load } p_{kj} + \text{extra load}$
24. else
25. Receive extra load from neighbour  $p_{kj}$
26. Load  $p_{ki} = \text{Load } p_{ki} + \text{extra load}$
27. Load  $p_{kj} = \text{Load } p_{kj} - \text{extra load}$
28. Repeat steps (15 to 27)  $\left\lfloor \frac{3}{2}k \right\rfloor$  times // diameter of the Arrangement topology -End of phase#2

Fig. 2. The ASCDEM load balancing Algorithm

Phase 2: The load balancing within the processors of each sub-graph where each sub-graph is an  $A_{m,k}$  network. The ASCDEM algorithm in steps 15 to 28 performed in parallel, at first step the load exchange will be between all the processors in which they differ in exactly one  $k$  position for any two neighboring nodes, which means they are connected via an Arrangement structure. Then the same process will be repeated continually all of the  $\left\lfloor \frac{3}{2}k \right\rfloor$  neighbors. By the end of this phase all nodes of the network will have almost the same load size.

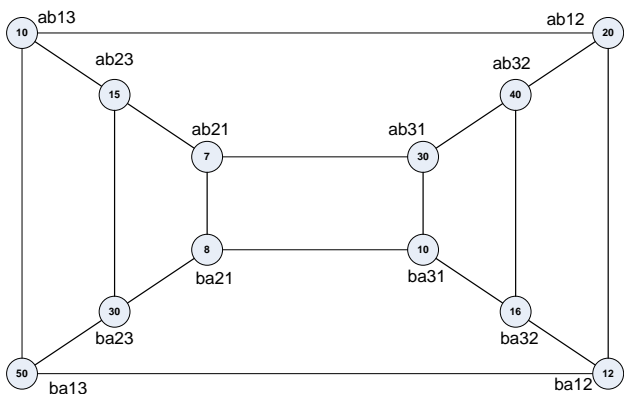


Fig. 3. Arrangement-Star graph,  $AS_{2,3,2}$  with initial loads

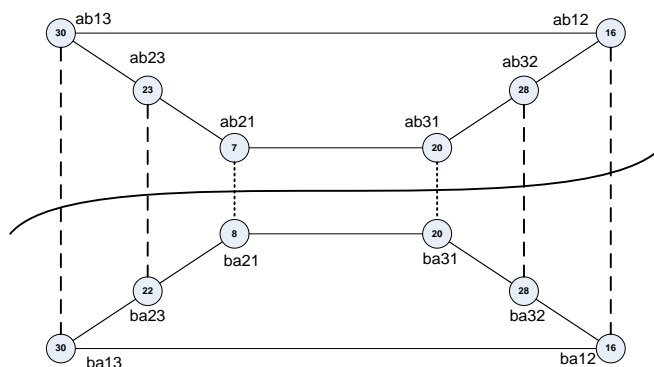


Fig. 4. Arrangement-Star graph,  $AS_{2,3,2}$  after performing ASCDEM phase 1

**Example 1:** - To explain the ASCDEM algorithm presented in Fig. 2, the following example implements the load balancing algorithm on a  $AS_{n,m,k}$  network where  $n=2$ ,  $m=3$ , and  $k=2$ .

Fig. 3 shows the  $AS_{2,3,2}$  network, it consists of two sub-graphs connected to each other via a Star structure, each sub-graph is represented as an Arrangement graph;  $A_{3,2}$  which has 6 processors. The total number of processors in the  $AS_{2,3,2}$  network is twelve. Each node has an original load size assigned to it and it is represented in the figure inside every node. Since the degree of  $AS_{2,3,2}$  is 3, it follows that each node connected to three other direct nodes, two of nodes via the Arrangement graph edges, and one node via the Star graph edge.

First we Start by implanting phase 1 of the algorithm by following the steps 2-12. Fig. 4 shows the new load size for each node after completing the first phase, edges in bold and dash lines represent the Star graph structure links, the curve line is to distinguish between the two Arrangement graphs in the figure. By the end of this phase, the total load sizes for each of the two sub-graphs are almost equal.

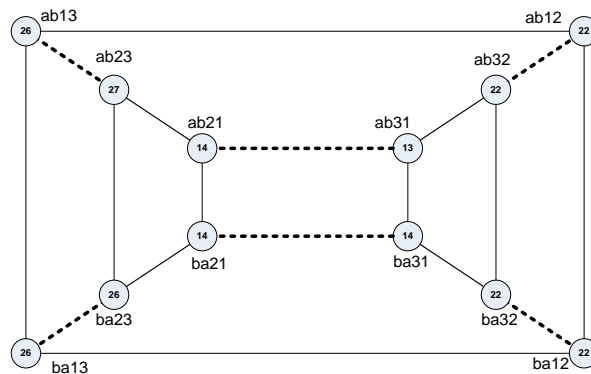


Fig. 5. Arrangement-Star graph,  $AS_{2,3,2}$  after performing phase 2 where  $k=1$

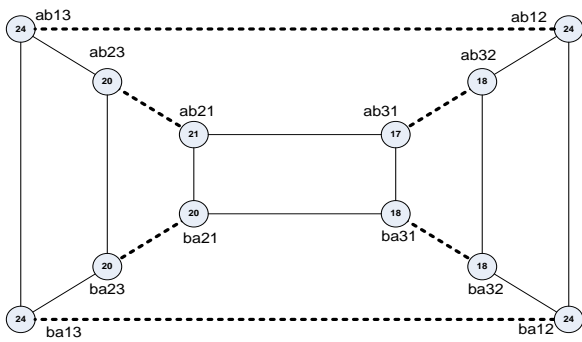


Fig. 6. Arrangement-Star graph,  $AS_{2,3,2}$  after performing phase 2 where  $k=2$

In phase 2 of the algorithm all adjacent nodes which differ in one and only one of their  $k$  position will redistribute their load balancing equally, this phase is done for each sub-graph separately and in parallel, at each parallel step, each node do this redistribution with its neighbors via an Arrangement graph edges. Figure 5 shows the parallel redistribution of loads within each Arrangement sub-graph for the first position where  $k=1$ , the dashed lines represent these exchanges between every two pair of nodes. Figure 6, shows the results for the  $k$  position=2. Figure 7 shows the final redistributed load size of every node, noting that the second phase of the algorithm is repeated 3 times;  $m!/2(m-k)!$ ; to guarantee that equal distribution is done across the whole network to reach nodes at diameter distance from each other. Furthermore, all node exchanges at the same  $k$  position are done in parallel. The final results prove the efficiency of our algorithm where all nodes' loads are almost equal.

To present the Arrangement-Star network clearly, figure 8 is an example of this network where we refer to it as  $AS_{3,3,2}$ . The size of the Star is 6 and the each node of the Star is presented by an Arrangement network of  $A_{3,2}$ . The size of each Arrangement network is also 6 nodes. The total size of the whole network is 36 nodes as it is obvious from the figure below that each node is connected other neighboring nodes based of the properties of the Star and the Arrangement networks. For example the node abc13 is connected to the two neighboring nodes; abc12 and abc23; via the Arrangement graph properties and also it is connected to the two neighboring nodes; bac13 and cba13; via the Star network properties.

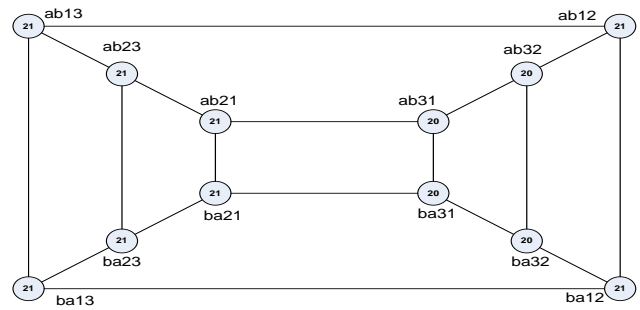


Fig. 7. Arrangement-Star graph,  $AS_{2,3,2}$  after performing the ASCDEM algorithm

In the following example we will present the ASCDEM algorithm behavior on  $AS_{3,3,2}$  described above to give more details about this algorithm:

**Example 2:** - To explore the ASCDEM algorithm presented in Fig. 2 in more details, we present another Arrangement-Star network to implement the load balancing algorithm on it. This network is denoted as  $AS_{n,m,k}$  network where  $n=3$ ,  $m=3$ , and  $k=2$ .

Fig. 9 shows the Arrangement-Star graph of  $AS_{3,3,2}$  interconnection network, where each node in of the 6 nodes Star graph is represented by a complete Arrangement network of  $A_{3,2}$ , which consists of 6 nodes. Since the degree of  $AS_{3,3,2}$  is  $n-1 + k(m-k)$  which is equal to 4, it follows that each node connected to four other direct nodes, two of nodes via the Arrangement graph edges, and two nodes via the Star graph edge.

First we Start by implanting phase 1 of the algorithm by following the steps 2-12. Fig. 10 shows the new load size for each node after completing the first phase. By the end of this phase, the total load sizes for each of the six sub-graphs are almost equal. Where each sub-graph is represented by an Arrangement network of  $A_{3,2}$ .

Fig. 11 shows the final load size for each node after completing the second phase which is also the final phase of the algorithm. By the end of this phase, the total load size for each node is almost equal. This proves that our algorithm works properly and performs the load balancing accurately.

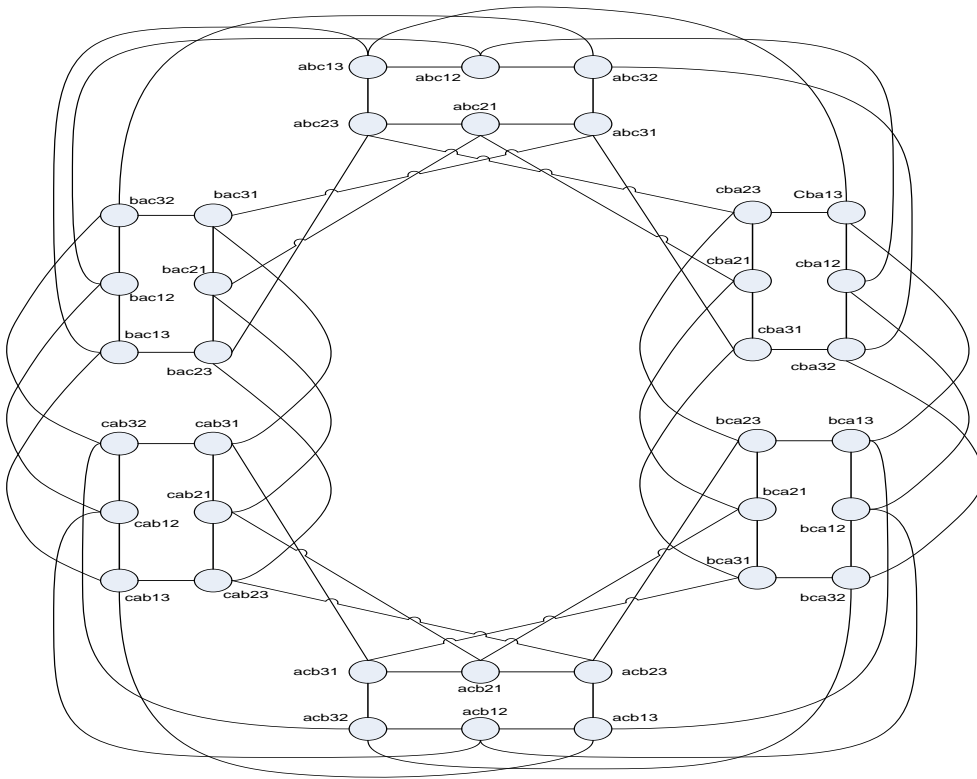


Fig. 8. Arrangement-Star graph,  $AS_{3,3,2}$

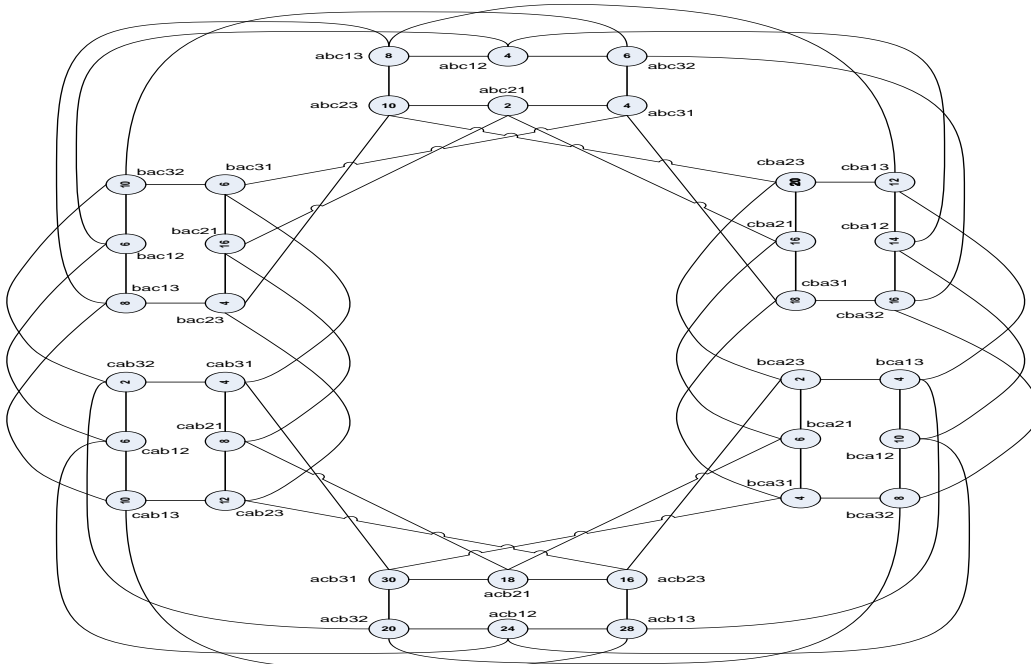


Fig. 9. Arrangement-Star graph,  $AS_{3,3,2}$  -Initial state

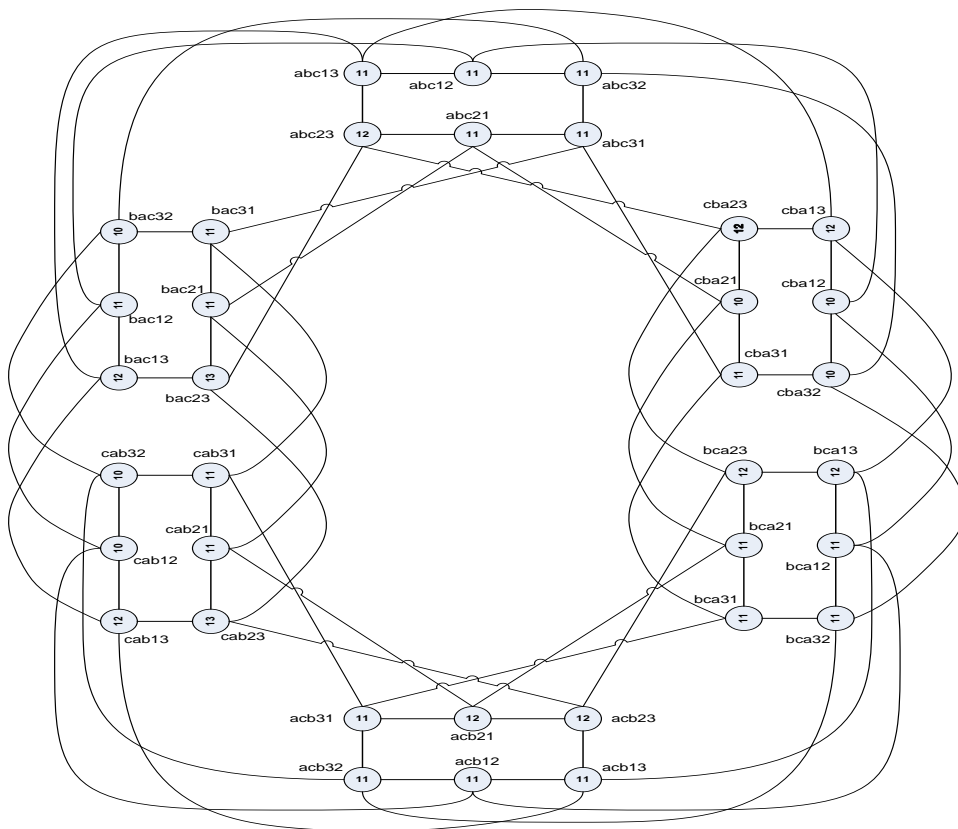


Fig. 10. Arrangement-Star graph,  $AS_{3,3,2}$  – End of phase 1

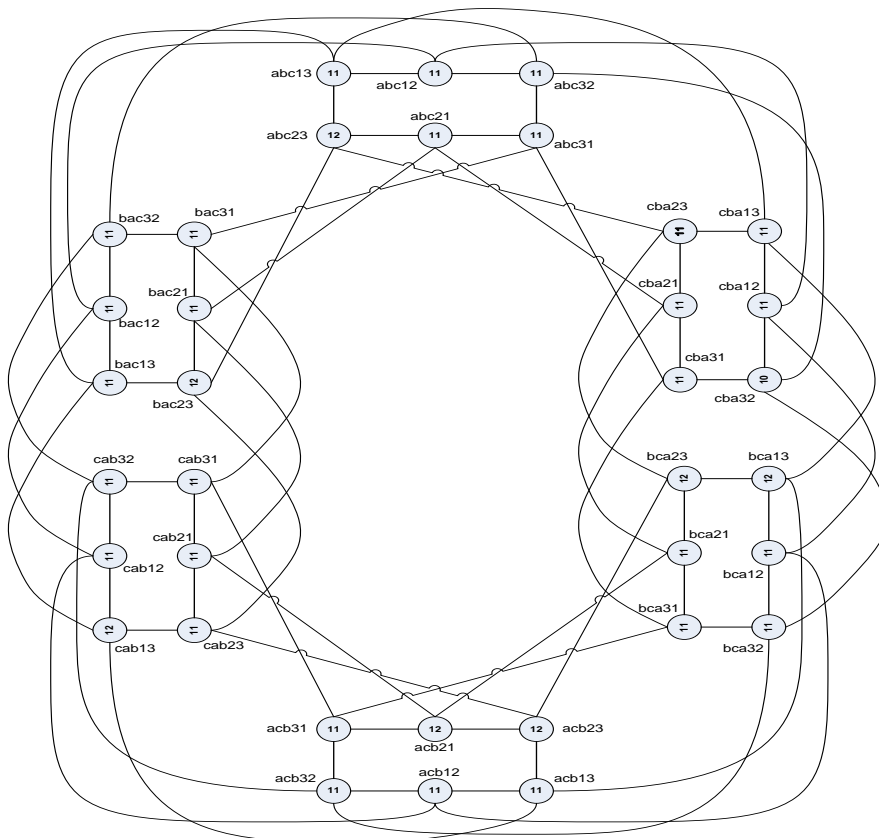


Fig. 11. Arrangement-Star graph,  $AS_{3,3,2}$  End of phase 2

## V. ANALYTICAL STUDY

In this section we introduce analytical results of the ASCDEM load balancing algorithm behavior on the Arrangement-Star network. The following propositions are summarizing the outcome of this analytical study.

**Proposition #1:** By performing the first phase of ASCDEM algorithm, the total number of sequential steps is equal to the diameter of the Star network which is  $\left\lceil \frac{3}{2}(n-1) \right\rceil$ .

Since the structure of the Arrangement-Star graph is based on representing an Arrangement graph as a node within the Star graph with parallel connectivity within the nodes of the whole network, ASCDEM algorithm utilizes this feature to distribute the load sizes among the sub-graphs of the graph; Arrangement networks; by utilizing the properties of the Star graph to distribute the loads where the longest length between any two sub-graphs is equal to the diameter of the Star graph.

**Proposition #2:** The total number of sequential steps performed by ASCDEM algorithm in the second phase is equal to the diameter of the Arrangement network which is  $\left\lceil \frac{3}{2}(K) \right\rceil$ .

As mentioned earlier, the structure of the Arrangement-Star graph is based on representing an Arrangement graph as a node within the Star graph. By the Start of phase 2 of the ASCDEM algorithm, each sub-graph which is represented by an Arrangement graph will distribute the load sizes among its nodes distantly from other sub-graphs of the whole graph. To do this redistribution we need to perform a diameter sequentially steps to reach the farthest two nodes of the Arrangement graph.

**Proposition #3:** To perform the two phases of ASCDEM algorithm, the total number of sequential steps is equal to:

$\left\lceil \frac{3}{2}(K) \right\rceil + \left\lceil \frac{3}{2}(n-1) \right\rceil$  where  $\left\lceil \frac{3}{2}(K) \right\rceil$  is the diameter of the Arrangement graph and  $\left\lceil \frac{3}{2}(n-1) \right\rceil$  is the diameter of the Star graph.

Propositions number 1 and 2 justifies the outcome presented in proposition number 3.

**Proposition #4:** By the end of the first phase of ASCDEM algorithm, the total number of load sizes at each sub-graph of the whole network is almost equal.

After the  $\left\lceil \frac{3}{2}(n-1) \right\rceil$  exchanges of load sizes which represent the diameter of the Star graph, every node of the Star structure will has almost an equal size of load. Furthermore since each node of the Star structure is represented by a sub-graph of Arrangement graph structure, then each sub-graph will have an almost the same size of load. These exchanges are performed in the first phase of the ASCDEM algorithm.

**Proposition #5:** By the end of phase 2 of ASCDEM algorithm, the total number of load sizes at each node of the whole network is almost equal.

Since phase 1 guarantees equal redistribution of load sizes among the sub-graphs of the network and by the end of second

phase every sub-graph will redistribute the load size among its nodes, then each node will have an almost the same size of load. These exchanges are performed in the second phase of the ASCDEM algorithm.

**Proposition #6:** At each sequential step of phase 1 of ASCDEM algorithm, the total number of parallel exchanges is:

$\frac{n!}{2} * \frac{m!}{(m-k)!}$  where  $n$  denotes the  $n$ -Star network and  $m, k$  denotes the Arrangement  $A_{m,k}$  network.

Since every two nodes of the Star graph exchanges their load sized at once and the number of nodes of the Star graph is  $n!$ , then there are  $\frac{n!}{2}$  exchanges done in parallel. Also since every node in the Star graph is represented as an Arrangement graph, then these exchanges are actually performed within the nodes of every 2 Arrangement sub-graphs, where the size of each sub-graph is equal to  $\frac{m!}{(m-k)!}$ .

**Proposition #7:** The total number of exchanges performed by phase 1 of ASCDEM algorithm is equal to  $\frac{n!}{2} * \frac{m!}{(m-k)!} * \left\lceil \frac{3}{2}(n-1) \right\rceil$  where  $n$  denotes the  $n$ -Star network and  $m, k$  denotes the Arrangement  $A_{m,k}$  network.

By referring to proposition number 6 which explain the number of parallel exchanges at each sequential step and also by referring to proposition number 1 which explains the number of sequential steps of the first phase, it gives a clear justification of the outcome of this proposition.

**Proposition #8:** At each sequential step of phase 2 of ASCDEM algorithm, the total number of parallel exchanges is:

$n! * \frac{m! * (m-k)!}{2}$  where  $n$  denotes the  $n$ -Star network and  $m, k$  denotes the Arrangement  $A_{m,k}$  network.

Since every two nodes of the arrangement graph exchanges their load sized at once and the number of nodes of the Arrangement graph is  $\frac{m!}{(m-k)!}$ , then there are  $\frac{m! * (m-k)!}{2}$  exchanges done in parallel. Also since this occurs at every representation of a node in the Star graph, then these exchanges are actually performed  $n!$  in parallel, where the Star graph has  $n!$  number of nodes.

**Proposition #9:** The total number of exchanges performed by phase 2 of ASCDEM algorithm is equal to  $\frac{m! * (m-k)!}{2} * n! * \left\lceil \frac{3}{2}(k) \right\rceil$  where  $n$  denotes the  $n$ -Star network and  $m, k$  denotes the Arrangement  $A_{m,k}$  network

By referring to proposition number 8 which explain the number of parallel exchanges at each sequential step and also by referring to proposition number 2 which explains the number of sequential steps of the second phase, it gives a clear justification of the outcome of this proposition.

**Proposition #10:** The total number of exchanges performed by the whole algorithm of ASCDEM is equal to

$\frac{m*n!}{2}((m-k)! * \left\lfloor \frac{3}{2}(k) \right\rfloor + \frac{1}{(m-k)!} * \left\lfloor \frac{3}{2}(n-1) \right\rfloor)$  where  $n$  denotes the  $n$ -Star network and  $m,k$  denotes the Arrangement  $A_{m,k}$  network

The above equation represents the total summation of proposition number 7 and proposition number 9.

By utilizing the above propositions to the well known general equations of latency time, communication cost, throughput, and processors speed we can extend our study to present real outcomes and results based on the specifications of the machines that could be built on the above network and utilizes the ASCEDM algorithm. We think this will be open ideas for any future work based on our algorithm.

## VI. CONCLUSION

In this research we have investigated and proposed an algorithm named Arrangement-Star Clustered Dimension Exchange Method (ASCDEM), the proposed algorithm in based on the well-known efficient algorithm SCDEM which was proposed by Mahafza and et al named (CDEM).The main target of the ASCDEM algorithm is to redistribute the load balancing among all the processors of the Arrangement-Star network as evenly as possible. As shown above the algorithm was able to redistribute the load balance among all the nodes of the  $AS_{n,m,k}$  in an efficient approach.

Furthermore, two detailed examples were conducted and discussed to explore and explain the two phases of the ASCDEM algorithm. Also an analytical study was performed on this algorithm which presents the quantities specifications of the algorithm. This analytical study could be utilized for any future work to propose a further performance study on the proposed algorithm such as: total execution time, efficient load balancing accuracy, latency, number of communication moves and complexity speed of the ASCDEM.

## REFERENCES

- [1] K. Day and A. Al-Ayyoub, "The Cross Product of Interconnection Networks", *IEEE Trans. Parallel and Distributed Systems*, vol. 8, no. 2, Feb. 1997, pp. 109-118.
- [2] S. B. Akers, and B. Krishnamurthy, "A Group Theoretic Model for Symmetric Interconnection Networks," *Proc. Intl. Conf. Parallel Proc.*, 1986, pp. 216-223.
- [3] Ayyoub, "The Cross Product of Interconnection Networks", *IEEE Trans. Parallel and Distributed Systems*, vol. 8, no. 2, Feb. 1997, pp. 109-118.
- [4] A. Al-Ayyoub and K. Day, "A Comparative Study of Cartesian Product Networks", *Proc. of the Intl. Conf. on Parallel and Distributed Processing: Techniques and Applications*, vol. I, August 9-11, 1996, Sunnyvale, CA, USA, pp. 387-390.
- [5] Ahmad Awwad, "vertex Product networks", University of Glasgow, Computer Science Dept. thesis, 2001.
- [6] S. B. Akers, D. Harel and B. Krishnamurthy, "The Star Graph: An Attractive Alternative to the n-Cube" *Proc. Intl. Conf. Parallel Processing*, 1987, pp. 393-400.
- [7] K. Day and A. Tripathi, "Arrangement Graphs: A Class of Generalised Star Graphs," *Information Processing Letters*, vol. 42, 1992, pp. 235-241.
- [8] Jehad Al-Sadi, "Implementing FEFOM Load Balancing Algorithm on the Enhanced OTIS-n-Cube Topology", *Proc. of the Second Intl. Conf. on Advances in Electronic Devices and Circuits - EDC 2013*, 47-5.
- [9] G. Marsden, P. Marchand, P. Harvey, and S. Esener, "Optical Transpose Interconnection System Architecture," *Optics Letters*, 18(13), 1993, pp. 1083-1085.
- [10] Qin Y, Xiao W, Zhao C (2007), "GDED-X schemes for load balancing on heterogeneous OTIS networks", In: ICA3PP, pp 482-492.
- [11] Ranka, Y. Won, S. Sahni, "Programming a Hypercube Multicomputer", *IEEE Software*, 5 (5): 69 - 77, 1998.
- [12] Zhao C, Xiao W, Qin Y (2007), "Hybrid diffusion schemes for load balancing on OTIS networks", In: ICA3PP, pp 421-432
- [13] B.A. Mahafzah and B.A. Jaradat, "The Load Balancing problem in OTIS-Hypercube Interconnection Network", *J. of Supercomputing* (2008) 46, 276-297.
- [14] N. Imani et al, "Perfect load balancing on Star interconnection network", *J. of supercomputers*, Volume 41 Issue 3, September 2007. pp. 269 - 286.
- [15] K. Day and A. Tripathi, "A Comparative Study of Topological Properties of Hypercubes and Star Graphs", *IEEE Trans. Parallel & Distributed Systems*, vol. 5.
- [16] Kaled Day and Abdel-Elah Al-Ayyoub, "Node-ranking schemes for the Star networks", *Journal of parallel and Distributed Computing*, Vol. 63 issue 3, March 2003, pp 239-250.
- [17] I. Jung and J. Chang, "Embedding Complete Binary Trees in Star Graphs," *Journal of the Korea Information Science Society*, vol. 21, no. 2, 1994, pp. 407-415.
- [18] Berthome, P., A. Ferreira, and S. Perennes, "Optimal Information Dissemination in Star and Pancake Networks," *IEEE Trans. Parallel and Distributed Systems*, vol. 7, no. 12, Aug. 1996, pp. 1292-1300.
- [19] Mendia V. and D. Sarkar, "Optimal Broadcasting on the Star Graph," *IEEE Trans. Parallel and Distributed Systems*, Vo.: 3, No. 4, 1992, pp. 389-396.
- [20] S. Rajasekaran and D. Wei, "Selection, Routing, and Sorting on the Star Graph," *J. Parallel & Distributed Computing*, vol. 41, 1997, pp. 225-33.
- [21] A. Al-Ayyoub and K. Day, "The HyperStar Interconnection Network," *J. Parallel & Distributed Computing*, vol. 48, no. 2, 1998, pp. 175-199.
- [22] A. Menn and A.K. Somani, "An Efficient Sorting Algorithm for the Star Graph Interconnection Network," *Proc. Intl. Conf. on Parallel Processing*, 1990, pp.1-8.
- [23] P. Fragopoulou and S. Akl, "A Parallel Algorithm for Computing Fourier Transforms on the Star Graph," *IEEE Trans. Parallel & Distributed Systems*, vol. 5, no. 5, 1994, pp. 525-31.
- [24] S. Lakshminarayanan, and S.K. Dhall, "Analysis and Design of Parallel Algorithms Arithmetic and Matrix Problems," McGraw-Hill Publishing Company, 1990.

# Analytical Performance Evaluation of IPv6 and IPv4 Over 10 Gigabit Ethernet and InfiniBand using IPoIB

Eric Gamess

School of Computer Science  
Central University of Venezuela  
Caracas, Venezuela

Humberto Ortiz-Zuazaga

Department of Computer Science  
University of Puerto Rico  
San Juan, Puerto Rico

**Abstract**—IPv6 is the response to the shortage of IPv4 addresses. It was defined almost twenty years ago by the IETF as a replacement of IPv4, and little by little, it is becoming more preponderant as the Internet protocol. The growth of Internet has led to the development of high performance networks. On one hand, Ethernet has evolved significantly and today it is common to find 10 Gigabit Ethernet networks in LANs. On the other hand, another approach for high performance networking is based on RDMA (Remote Direct Memory Access) which offers innovative features such as kernel bypass, zero copy, offload of splitting and assembly of messages in packets to the CAs (Channel Adapters), etc. InfiniBand is currently the most popular technology that implements RDMA. It uses verbs instead of sockets and a big effort of the community is required to port TCP/IP software to InfiniBand, to take advantage of its benefits. Meanwhile, IPoIB (IP over InfiniBand) is a protocol that has been proposed and permits the execution of socket-based applications on top of InfiniBand, without any change, at the expense of performance. In this paper, we make a performance evaluation of IPv6 and IPv4 over 10 Gigabit Ethernet and IPoIB. Our results show that 10 Gigabit Ethernet has a better throughput than IPoIB, especially for small and medium payload sizes. However, as the payload size increases, the advantage of 10 Gigabit Ethernet is reduced in comparison to IPoIB/FDR. With respect to latency, IPoIB did much better than 10 Gigabit Ethernet. Finally, our research also indicates that in a controlled environment, IPv4 has a better performance than IPv6.

**Keywords**—IPv4; IPv6; Performance Evaluation; InfiniBand; IP over InfiniBand; 10 Gigabit Ethernet; Benchmarking Tools

## I. INTRODUCTION

Internet Protocol version 6 (IPv6) [1][2][3][4] is around for some years now. It is a solution to the unexpected dramatic growth of the Internet, which is facing the exhaustion of available IPv4 addresses. This new version of IP has 128-bit addresses, while IPv4 is limited to 32-bit addresses. Furthermore, IPv6 adds many improvements in areas such as routing, multicasting, security, mobility, and network auto-configuration. According to IPv6 statistics made by Google [5], more than 10% of the users that require services from this company do it with an IPv6 connection. Cisco Systems [6] is gathering and publishing information about IPv6 deployment in the world. As reported by the recollected data, Belgium is the country with the highest IPv6 deployment in the world, with more than 55%. In the USA, the deployment is around 44%.

RDMA (Remote Direct Memory Access) communications differ from normal IP communications because they bypass kernel intervention in the communication process. That is with RDMA, the CA (Channel Adapter) directly places the application's buffer into packets on sending, and the content of the packets into the application's buffer on reception, without any intervention of the CPU. This allows a much better communication system with zero copy. Moreover, the CA also manages the splitting and assembly of messages into packets in RDMA, while IP fragmentation and TCP segmentation are in charge of the CPU in typical IP communications. As a result, RDMA provides high throughput and low latency while incurring a minimal amount of CPU load.

Recently, three major RDMA fabric technologies have emerged: InfiniBand [7][8][9], RoCE [10][11] (RDMA over Converged Ethernet), and iWARP [12][13] (internet Wide Area RDMA Protocol). InfiniBand seems to have the major acceptance of these three technologies, hence many manufacturers are offering a wide variety of products (CAs and switches), especially for the fields of HPC (High Performance Computing) and Data Centers. InfiniBand defines its own stack of protocols. Moreover, it does not use sockets as TCP/IP applications do, and is based on "verbs". To date, just few applications have been ported to verbs to work on top of InfiniBand. It is more than likely that it will take time to adapt popular socket-oriented applications to verbs. Hence, the IETF (Internet Engineering Task Force) has proposed a new protocol called IP over InfiniBand (IPoIB) [14][15][16] to run existing TCP/IP applications in an InfiniBand network without any changes.

In this work, we make a performance evaluation of 10 Gigabit Ethernet and IP over InfiniBand, where the former is the new de facto technology for local area network. We report the throughput and latency obtained at the level of UDP and TCP, for IPv6 and IPv4, when varying the payload size. To do so, we use famous benchmarking tools of the field of networking.

The rest of this paper is organized as follows: we discuss related work in Section II. A survey of InfiniBand and IPoIB is made in Section III. Section IV presents the testbed for our experiments, and some benchmarking tools for point-to-point network evaluation are introduced in Section V. The results of our network performance evaluation is presented and discussed in Section VI. Finally, Section VII concludes the paper and gives directions for future work in this area.

## II. RELATED WORK

In the field of the assessment of the performance of IPv6 and IPv4, there are several studies that evaluate their capacities based on benchmarking tools, with different operating systems and network technologies. Narayan, Shang, and Fan [17][18] studied the performance of TCP and UDP traffic with IPv6 and IPv4 on a Fast Ethernet LAN, using various distributions of Windows and Linux. A similar study was conducted by Kolahi et al. [19], where the TCP throughput of Windows Vista and Windows XP was compared using IPv6 and IPv4, also on a Fast Ethernet LAN. A comparison of the network performance between Windows XP, Windows Vista, and Windows 7 was conducted by Balen, Martinovic, and Hocenski [20], under IPv6 and IPv4. Their testbed consisted of two computers connected through a point-to-point link with Gigabit Ethernet. The authors of [21] assessed the throughput of UDP and TCP over IPv6 and IPv4 for Windows XP and Windows 7 in a point-to-point network, where the two end-nodes were connected by a Gigabit Ethernet link. Soorty and Sarkar [22][23] evaluated UDP over IPv6 and IPv4, using different modern operating systems. In [22], the computers of the testbed were running Windows 7, Windows Server 2008, Ubuntu Server 10.04, and Red Hat Enterprise Server 5.5. In [23], they used Ubuntu Server 10.04 and Red Hat Enterprise Server 5.5. For both cases [22][23], the network between the end-nodes also consisted of a back-to-back Gigabit Ethernet connection. The performance of the IP protocols has also been compared in wireless networks [24].

Some other efforts are more focused on modeling the performance of IPv6 and IPv4. An upper bound model to compute TCP and UDP throughput for IPv6 and IPv4 in Ethernet networks was presented by Gamess and Surós [25]. They compared the performance of various operating systems (Windows XP, Solaris 10, and Debian 3.1) with this upper bound, using a point-to-point network with Ethernet and Fast Ethernet technologies. Gamess and Morales [26] developed models to compute the throughput and latency of IPv6 and IPv4 in Ethernet LANs. They validated the proposed models doing experiments in Ethernet and Fast Ethernet networks, where the end-nodes were connected through a chain of routers (from 0 to 5 routers).

As far of InfiniBand is concerned, just a few works have been done. Cohen [27] did a low-level evaluation of InfiniBand (Send/Receive and RDMA operations) in a back-to-back connection between two end-nodes, i.e. a fabric without InfiniBand switches. Latency, throughput, and CPU load were reported by the author. In [28], Rashti and Afsahi evaluated three network technologies (10-Gigabit iWARP, 4X SDR InfiniBand, and Myrinet-10G) at the user-level and MPI [29] (Message Passing Interface) layer. The authors of [30] evaluated 4X FDR InfiniBand and 40GigE RoCE on HPC and cloud computing systems. They did some basic network level characterizations of performance, but most of the work is done with MPI point-to-point and collective communication benchmarks. In [31], Sur, Koop, Chai, and Panda did a network-level performance evaluation of the Mellanox ConnectX architecture on multi-core platforms. They evaluated low-level operations such as RDMA Write and RDMA Read, as well as high level applications as a whole.

As discussed in this section, many works have been done to evaluate the performance of IPv6 and IPv4 over Ethernet, Fast Ethernet, and Gigabit Ethernet. InfiniBand has also been assessed in a few studies, at low-level (Send/Receive, RDMA Read, and RDMA Write operations) and MPI level. To the best of our knowledge, this effort is the first one that compares the performance of IPv6 and IPv4 over 10 Gigabit Ethernet and InfiniBand using IPOIB.

## III. A SURVEY OF INFINIBAND AND IPOIB

In this section, we briefly introduce InfiniBand and IPOIB. We describe key concepts that can significantly help for the understanding of this research work.

### A. Introduction to InfiniBand

InfiniBand [7][8][9] defines the notion of QPs (Queue Pairs) which consists of two queues: a SQ (Send Queue) and a RQ (Receive Queue). At the transport layer of the OSI model, InfiniBand offers several transport services which include: RC (Reliable Connection) and UD (Unreliable Datagram). In the RC transport service, a QP-to-QP connection must be established between the two RC QPs before transmission. It is a point-to-point connection, hence the involved QPs can only send packets to each other and receive packets from each other. An Ack/Nak mechanism permits the requester logic (QP SQ) to verify that all the packets are delivered to the responder (QP RQ). In the UD transport service, there is no initial connection setup with the remote QP prior to sending or receiving messages. It is not a QP-to-QP connection, hence the QPs can send and receive packets to and from any potential remote QPs.

InfiniBand has several speed grades known as: SDR (Simple Data Rate), DDR (Double Data Rate), QDR (Quadruple Data Rate), FDR (Fourteen Data Rate), and EDR (Enhanced Data Rate). SDR, DDR, and QDR use 8B/10B encoding, i.e., 10 bits carry 8 bits of data. In other words, the data rate is 80% of the signal rate. FDR and EDR use the more efficient 64B/66B encoding. Table I shows the signal rate and data rate achieved by InfiniBand, depending on the width of the link (1X, 4X, 8X, or 12X). The non-shaded rows represent the signal rate, while the shaded rows correspond to the data rate.

TABLE I. SIGNAL AND DATA RATES ACHIEVED BY INFINIBAND IN GBPS

|     | SDR  | DDR  | QDR   | FDR     | EDR      |
|-----|------|------|-------|---------|----------|
| 1X  | 2.5  | 5.0  | 10.0  | 14.0625 | 25.78125 |
|     | 2.0  | 4.0  | 8.0   | 13.64   | 25.0     |
| 4X  | 10.0 | 20.0 | 40.0  | 56.25   | 103.125  |
|     | 8.0  | 16.0 | 32.0  | 54.54   | 100.0    |
| 8X  | 20.0 | 40.0 | 80.0  | 112.50  | 206.25   |
|     | 16.0 | 32.0 | 64.0  | 109.09  | 200.00   |
| 12X | 30.0 | 60.0 | 120.0 | 168.75  | 309.375  |
|     | 24.0 | 48.0 | 96.0  | 163.63  | 300.00   |

### B. Introduction to IPOIB

InfiniBand provides “verbs” to do low level IOs, but till date, very few applications have been developed with them. Hence, a mechanism is required to run TCP/IP on top of InfiniBand. The role of IPOIB [14][15][16] (IP over InfiniBand) is to provide an IP network emulation layer on top of InfiniBand networks, allowing the numerous existing socket-based applications to run over InfiniBand networks

unmodified. As a drawback, the performance of those applications will be considerably lower than if they were directly written to use RDMA communications natively, since they do not benefit from typical features offered by InfiniBand (kernel bypass, zero copy, splitting and assembly of messages to packets in the CAs, etc). However, for the users, IPoIB is a tradeoff between running their favorite socket-oriented applications without having to wait for the port to verbs and loosing part of the high performance of this emerging technology.

Linux has a module, called “ib\_ipoib”, for implementing IPoIB. This module creates a virtual NIC (ib0, ib1, ib2, etc) for each InfiniBand port on the system, which makes an HCA (Host Control Adapter) act like an ordinary NIC. IPoIB has two modes of operation: datagram mode [15] and connected mode [16]. In datagram mode the UD transport service is used, while the connected mode is based on the RC transport service. By default, IPoIB on Linux is configured in datagram mode. However, it is easy to switch between modes using the simple commands of Fig. 1. Line 01 shall be used to switch to connected mode, while Line 02 can be entered to switch to datagram mode.

```
01: echo connected > /sys/class/net/ib0/mode
02: echo datagram > /sys/class/net/ib0/mode
```

Fig. 1. Switching between Datagram and Connected Modes

### C. IPoIB in Connected Mode in a Unique Subnet Fabric

In the connected mode of IPoIB, the RC transport service is used. Hence a private connection must be established prior to the exchange of packets. Communication Management encompasses the protocols and mechanisms used to establish, maintain, and release channels for the RC transport service. The connection is established by exchanging three packets: ConnectRequest, ConnectReply, and ReadyToUse. Once the channel is created, the IPoIB packets can be sent. To close the connection, two packets must be sent: DisconnectRequest and DisconnectReply. Fig. 2 shows an IPoIB packet in connected mode in a fabric with a unique subnet. It is composed of three headers, the IPv6 or IPv4 packet per se, and two CRCs (Invariant CRC and Variant CRC).

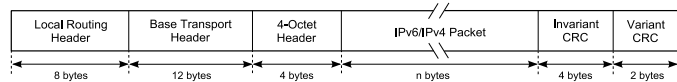


Fig. 2. IPoIB Packet in Connected Mode in a Fabric with a Unique Subnet

The first header, known as LRH (Local Routing Header), is shown in Fig. 3. It corresponds to the data-link layer of the OSI model. LNH (Link Next Header) is a 2-bit field that indicates the next header. It must be (10)<sub>2</sub> in a fabric with a unique subnet to inform that the next header is BTH (Base Transport Header). “Packet Length” is an 11-bit field, and its value shall equal the number of bytes in all the fields starting with the first byte of the LRH header and ending with the last byte of the Invariant CRC, inclusive, divided by 4. The Layer-2 address of the destination port is specified as “Destination Local Identifier” or DLID. The LIDs (Local Identifiers) are unique within a subnet and are assigned by the Subnet Manager during the initial startup or the reconfiguration of InfiniBand devices.

The Layer-2 address of the port that injected the packet into the subnet is specified as “Source Local Identifier” or SLID.

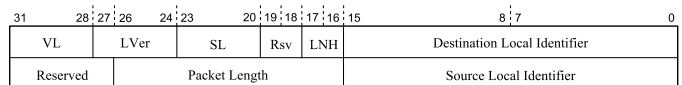


Fig. 3. Local Routing Header

The second header, known as BTH (Base Transport Header), is depicted in Fig. 4. It corresponds to the transport layer of the OSI model. Since RC is reliable, there is an Ack/Nak mechanism. The 1-bit A field of BTH is a request for the responder to schedule an acknowledgment for the packet. PSN (Packet Sequence Number) is a 24-bit field to identify the position of a packet within a sequence of packets. In that way, the responder can verify that all requested packets are received in order, and are only processed once. The 24-bit field called “Destination QP” identifies the receiving QP. Unlike IP, where the source and destination ports are present in all the segments sent by TCP, in InfiniBand just the destination QP is transported by a packet in the RC transport service. The source QP is not required, since RC is connection-oriented and both sides of the communication must keep information of the state of the connection, with includes the remote QP. That is, sending the source QP will be redundant and InfiniBand opts to save bandwidth by not transporting it.

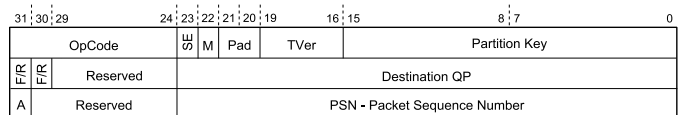


Fig. 4. Base Transport Header

The third header, known as “4-Octet Header”, is shown in Fig. 5. The 16-bit field called “Type” is used to specify the type of payload (0x0800, 0x86DD, 0x0806, 0x8035 for IPv4, IPv6, ARP, and RARP, respectively).



Fig. 5. 4-Octet Header

After these three headers (LRH, BTH, and 4-Octet header), the payload of the IPoIB packet can be either an IPv6 or an IPv4 packet, starting with its respective IPv6 or IPv4 header, and followed by its own payload. Finally, the IPoIB packet is finished with the two CRCs (Invariant CRC and Variant CRC) managed by InfiniBand.

### D. IPoIB in Datagram Mode in a Unique Subnet Fabric

In the datagram mode of IPoIB, the UD transport service is used. Hence, there is no private connection between the requester and the responder. That is, it is not a QP-to-QP connection and no Ack/Nak mechanism is available. Even though each packet contains a sequential PSN (see Fig. 4), it is not meaningful because the entire message is encapsulated in a single packet. Fig. 6 shows an IPoIB packet in datagram mode in a fabric with a unique subnet.

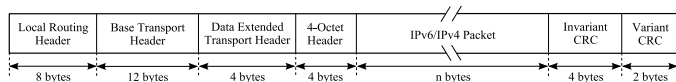


Fig. 6. IPoIB Packet in Datagram Mode in a Fabric with a Unique Subnet

It is similar to the one of the connected mode (see Fig. 2), with an additional header called DETH (Data Extended Transport Header).

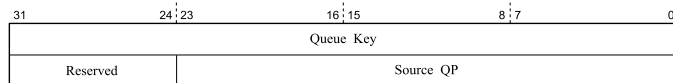


Fig. 7. Datagram Extended Transport Header

Fig. 7 shows the DETH header. Since the service is not oriented to connection, many remote devices can send packets to a local UD queue pair. Due to this, the sending QP is required in a packet and is specified in the 24-bit field called “Source QP”. It is used by the receiver as the destination QP for response packets. The 32-bit field called “Queue Key” should be used for authentication to authorize access to the destination queue. The responder compares this field with the destination’s QP key. Access will be allowed only if they are equal.

### E. IPoIB in a Fabric with Multiple Subnets

In the case of an InfiniBand fabric with several subnets, routers are required to connect the subnets together. In this case, in addition to Layer-2 addresses which are LIDs (SLID and DLID in the LRH header as shown in Fig. 3), Layer-3 addresses are required. In InfiniBand, these addresses are called GIDs (Global Identifiers) and are 128-bit long and similar to IPv6 addresses. They are constructed by concatenating a 64-bit GID prefix with a EUI-64 (64-bit Extended Unique Identifier), where the latter is assigned by the manufacturer. Each subnet must have its own 64-bit GID prefix and is generally set by the network administrator.

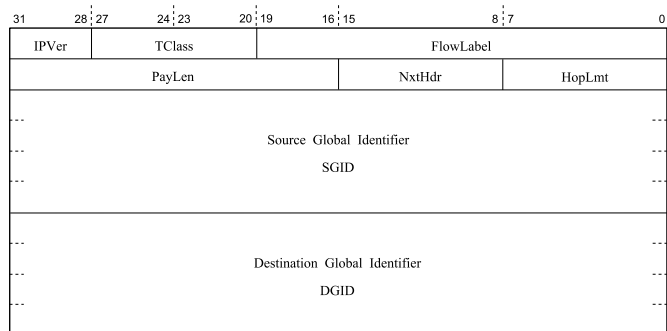


Fig. 8. Global Routing Header

An IPoIB packet traveling a fabric with several subnets is similar to the one of Fig. 2 in connected mode and Fig. 6 in datagram mode, with an additional header, called GRH (Global Routing Header), as shown in Fig. 8. GRH corresponds to the network layer of the OSI model and is placed between the LRH (data-link layer header) and the BTH (transport layer header). The SGID (Source Global Identifier) field corresponds to the GID of the port which injected the packet into the network. The DGID (Destination Global Identifier) identifies the GID for the port which will extract the packet from the network.

### F. InfiniBand MTU

The IBTA (InfiniBand Trade Association) defines the following MTUs: 256, 512, 1024, 2048, or 4096 bytes. Messages must be segmented into packets for transmission according to the PMTU. Segmentation of messages into packets on transmission and reassembly on reception are provided by CAs (Channel Adapters) at the end-nodes.

### IV. TESTBED FOR OUR EXPERIMENTS

For our experiments, the testbed was based on a cluster with end-nodes that were running CentOS v6.6. As shown in Fig. 9, the cluster was made of four end-nodes, one InfiniBand switch (SW1), and one 10 Gigabit Ethernet switch (SW2). The InfiniBand switch was a Mellanox Technologies SX6012, with 12 QSFP ports that support full-duplex signal rate of 56 Gbps (FDR). It is a managed switch that can be administered through the CLI (Command Line Interface) and SNMP, and also offers IPMI (Intelligent Platform Management Interface) support. It was running Mellanox MLNX-OS version 3.4.2008 as operating system. The 10 Gigabit Ethernet switch was a Cisco Catalyst 4500-X with 16 ports (10 Gigabit Ethernet SFP+/SFP ports).

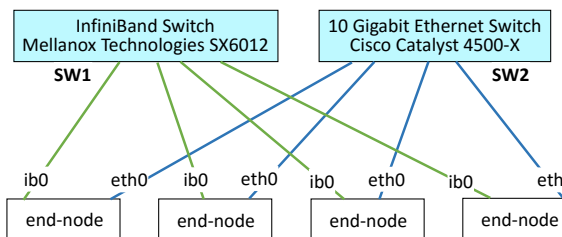


Fig. 9. Testbed for our Experiments

The connection between the end-nodes and the InfiniBand switch was based on 4X-width cables, while we used twinax cables between the end-nodes and the 10 Gigabit Ethernet switch. The InfiniBand fabric was configured with a 2048-byte MTU. The end-nodes had the following characteristics:

- Processors: 2 16-core Intel Xeon E5-2630 v3 at 2.4 GHz
- RAM: 64 GiB – 4 x 16 GiB DIMM (DDR4 2133 MHz)
- HCA: Mellanox Technologies single-port MT27500 ConnectX-3
- NIC: dual port NetXtreme II BCM57810 10 Gigabit Ethernet
- Hard Disk: Seagate ST1000NM0033 (1 TB, 7200 RPM, 128 MB Cache, SATA 6.0 Gb/s) for a local installation of the operating system (CentOS v6.6)
- Remote Management: IPMI.

It is worth clarifying that the InfiniBand network was composed of a single subnet, that is, the IPoIB packets did not have the GRH header (see Fig. 8) and were as shown in Fig. 2 and Fig. 6, for connected and datagram modes, respectively. Moreover, InfiniBand allows the Subnet Manager to be run in an end-node or in a switch. For our experiments, we chose to run it in an end-node.

## V. BENCHMARKING TOOLS USED IN OUR EXPERIMENTS

Many socket-based benchmarking tools have been proposed for network performance evaluation at the level of UDP and TCP. Unfortunately, not all of them support IPv6. Netperf is a benchmarking tool that can be used to measure various aspects of networking performance. It has support for IPv6 and IPv4. Its primary focus is on bulk data transfer (TCP\_STREAM, UDP\_STREAM, etc) and request/response performance (TCP\_RR and UDP\_RR) using either TCP or UDP. It is designed around the basic client/server model. In the TCP\_STREAM test, a constant bitrate of data is transferred from the client (netperf) to the server (netserv), and the actual throughput is reported as the result. It is worth mentioning that the reported throughput is equal to the maximum throughput, since Netperf saturates the communication link. The UDP\_STREAM test is similar to the TCP\_STREAM test, except that UDP is used as the transport protocol rather than TCP. In the TCP\_RR test, a fixed quantity of data is exchanged by TCP between the client (netperf) and the server (netserv) a number of times, and the benchmark reports the transaction rate which is the number of complete round-trip transactions per second. The UDP\_RR is very much the same as the TCP\_RR test, except that UDP is used rather than TCP.

Since Netperf does not report the latency, we developed our own benchmarking tool using the C programming language for IPv6 and IPv4. The benchmark is based on the client/server model. Basically, an UDP datagram or TCP segment with a fixed payload length is exchanged between the client and the server a number of times. We take a timestamp before and after the interchange. The difference of the timestamps is divided by the number of times the message was sent and received, and by 2 to get the average latency.

## VI. RESULTS AND ANALYTICAL COMPARISON

In this section, we do several experiments to measure the performance of IPv6 and IPv4, in our testbed, with 10 Gigabit Ethernet and IPoIB. All the throughput measurements were done with Netperf. Regarding the latency assessments, we used the benchmarking tool that we developed. Also, it is important to clarify that each experiment was repeated several times, and the result that we report is an average, for a better consistency.

### A. Experiments when Changing the IPoIB Mode

The objective of these first experiments is to compare the performance achieved by IPoIB in datagram and connected modes, for IPv6 and IPv4. For these performance tests, we chose FDR for the signal rate of InfiniBand.

Table II shows the results obtained for the UDP throughput when varying the payload size from 4 to 32,768 bytes. We did not take biggest UDP payload sizes since we were limited by

the IPv4 maximum packet size. These experiments indicate that the throughput for the datagram mode is higher than the one of the connected mode. Also, it is noticeable that IPv4 has a better throughput than IPv6.

TABLE II. UDP THROUGHPUT IN MBPS FOR IPV6 AND IPV4 OVER IPoIB/FDR IN DATAGRAM AND CONNECTED MODES

| Payload Size | Datagram Mode |          | Connected Mode |          |
|--------------|---------------|----------|----------------|----------|
|              | IPv6          | IPv4     | IPv6           | IPv4     |
| 4            | 13.21         | 16.41    | 10.15          | 11.43    |
| 8            | 25.22         | 34.63    | 19.46          | 21.09    |
| 16           | 54.51         | 66.10    | 43.37          | 44.21    |
| 32           | 119.04        | 134.78   | 86.10          | 88.78    |
| 64           | 255.12        | 271.18   | 175.48         | 178.67   |
| 128          | 513.77        | 544.76   | 352.92         | 356.77   |
| 256          | 902.85        | 1,064.14 | 429.53         | 432.51   |
| 512          | 2,137.53      | 2,162.18 | 723.49         | 725.36   |
| 1,024        | 3,096.52      | 3,107.23 | 1,145.08       | 1,152.42 |
| 2,048        | 3,805.11      | 3,851.54 | 1,411.72       | 1,429.32 |
| 4,096        | 4,408.75      | 4,583.80 | 1,502.55       | 1,514.37 |
| 8,192        | 6,101.41      | 6,352.89 | 3,402.70       | 3,418.76 |
| 16,384       | 6,414.42      | 7,925.14 | 6,301.15       | 7,643.12 |
| 32,768       | 7,438.32      | 9,721.07 | 7,030.24       | 7,777.30 |

Table III shows the results obtained for the UDP latency when varying the payload size from 4 to 32,768 bytes. We did not take biggest UDP payload sizes since we were limited by the IPv4 maximum packet size. These experiments indicate that the latency for the datagram mode is lower than the one of the connected mode. Also, it is noticeable that IPv4 has a better latency than IPv6.

TABLE III. UDP LATENCY IN MICROSECONDS FOR IPV6 AND IPV4 OVER IPoIB/FDR IN DATAGRAM AND CONNECTED MODES

| Payload Size | Datagram Mode |       | Connected Mode |       |
|--------------|---------------|-------|----------------|-------|
|              | IPv6          | IPv4  | IPv6           | IPv4  |
| 4            | 10.92         | 7.37  | 11.25          | 7.38  |
| 8            | 11.05         | 7.41  | 11.31          | 7.42  |
| 16           | 11.23         | 7.45  | 11.47          | 7.49  |
| 32           | 11.51         | 7.51  | 11.72          | 7.55  |
| 64           | 11.75         | 7.53  | 11.89          | 7.58  |
| 128          | 12.02         | 7.55  | 12.15          | 7.62  |
| 256          | 12.40         | 7.62  | 12.45          | 7.65  |
| 512          | 12.53         | 7.75  | 12.57          | 7.76  |
| 1,024        | 12.72         | 7.83  | 12.82          | 7.89  |
| 2,048        | 15.01         | 11.17 | 15.42          | 11.31 |
| 4,096        | 19.47         | 14.76 | 19.77          | 15.85 |
| 8,192        | 21.32         | 18.37 | 22.63          | 18.47 |
| 16,384       | 31.58         | 23.19 | 34.92          | 31.52 |
| 32,768       | 48.32         | 34.98 | 50.32          | 45.74 |

According to these first experiments, the IPoIB datagram mode seems to have a better performance than the IPoIB connected mode. Hence, the rest of our experiments were done with the datagram mode.

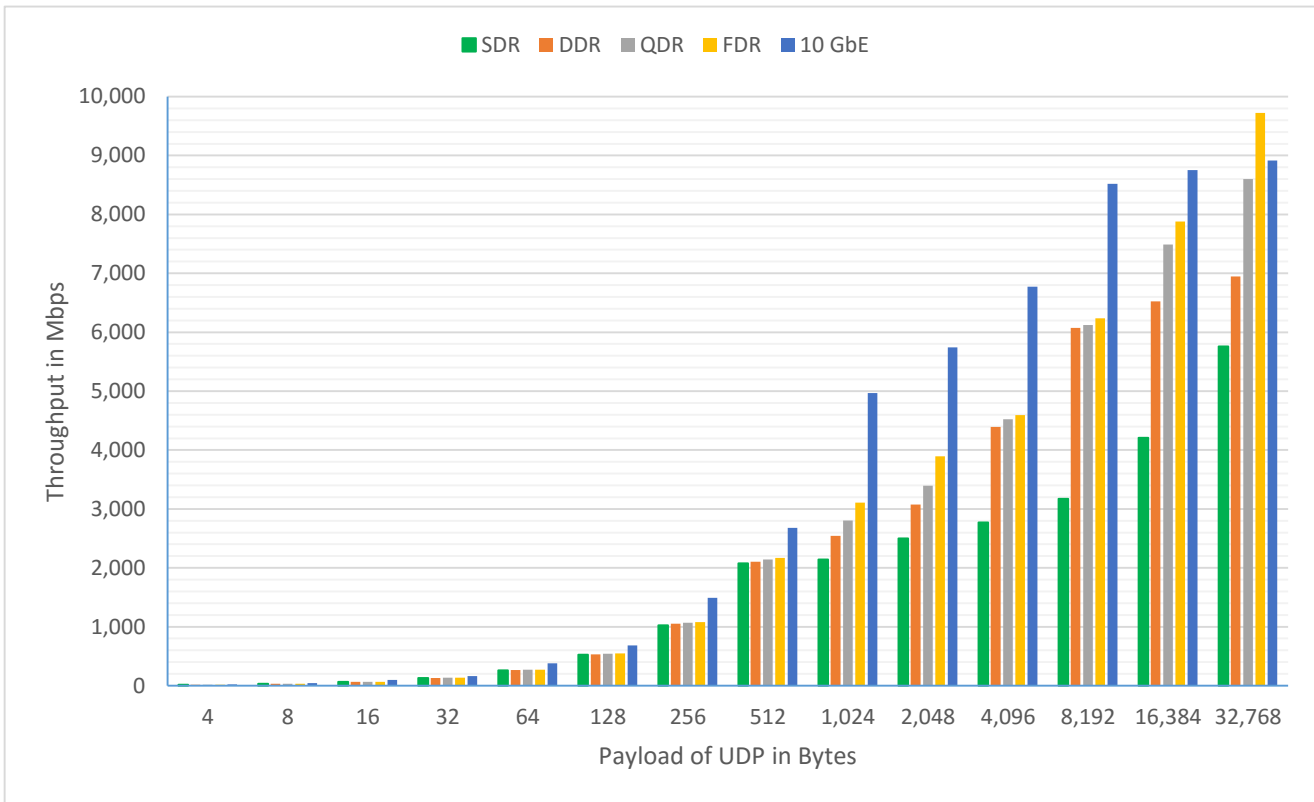


Fig. 10. Throughput for UDP/IPv4 over 10 GbE and IPoIB in Datagram Mode when Varying the Signal Rate of InfiniBand

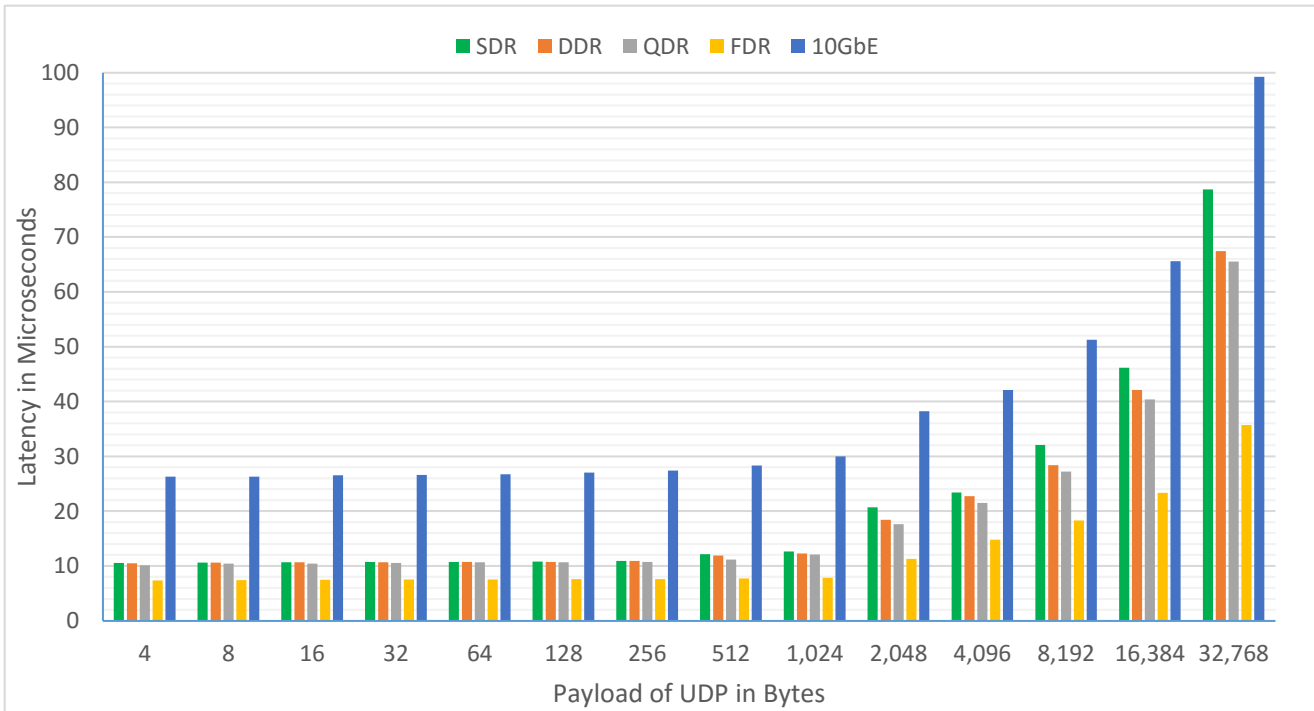


Fig. 11. Latency for UDP/IPv4 over 10 GbE and IPoIB in Datagram Mode when Varying the Signal Rate of InfiniBand

**B. Experiments when Changing the Signal Rate in UDP/IPv4**

In these experiments, we compare the throughput and latency obtaining between two end-nodes, for UDP/IPv4, for both 10 Gigabit Ethernet and IPoIB when changing the signal

rate. In the case of 10 Gigabit Ethernet (10GbE), we took the default configuration. Meanwhile for IPoIB, we chose the datagram mode in the end-nodes (see Fig. 1) and we had to

adjust the signal rate (SDR, DDR, QDR, and FDR) in the interfaces of the InfiniBand switch.

Fig. 10 depicts the throughput obtained when varying the UDP payload size from 4 to 32,768 bytes. For each value of the UDP payload size, there are five bars. The first four bars represent the SDR, DDR, QDR, and FDR throughputs for IPoIB, respectively. The last and fifth bar is for 10GbE. Our experiments indicate that the throughput of 10GbE outperforms the ones of IPoIB, except for very large payload sizes (e.g. 32,768 bytes) where IPoIB in FDR has the best throughput. As far of InfiniBand is concerned, the results of the throughput are as expected, that is SDR has the lowest one, while FDR has the biggest one.

Fig. 11 shows the latency obtained when varying the UDP payload size from 4 to 32,768 bytes. For each value of the UDP payload size, there are five bars. The first four bars represent the SDR, DDR, QDR, and FDR latencies for IPoIB, respectively. The last and fifth bar is for 10GbE. From our experiments, we can see that 10GbE has the biggest latency. Also, it is worth to point out that for each technology, the latency does not vary for small UDP payload sizes, and a difference can be noticed when the size is greater than or equal to 256 bytes. With respects to InfiniBand, the results of the latency are as expected, that is SDR has the biggest one while FDR has the lowest one.

C. Experiments for UDP/IPv6 and UDP/IPv4

In these experiments, we compare the throughput and latency obtaining between two end-nodes for UDP/IPv6 and UDP/IPv4, over 10GbE and IPoIB/FDR. In the case of IPoIB, we chose the datagram mode in the end-nodes (see Fig. 1). Whereas for 10GbE, we took the default configuration.

Table IV shows the results of the throughput when varying the UDP payload size from 4 to 32,768 bytes. We can see that 10GbE has the best throughput for almost all the payload sizes, except for very large payload sizes (e.g. 32,768 bytes) where the performance of IPoIB/FDR is better. Also, IPv4 exceeds IPv6 for both technologies.

TABLE IV. UDP THROUGHPUT IN MBPS FOR IPV6 AND IPV4 OVER 10GBE AND IPOIB/FDR

| Payload Size | 10GbE    |          | IPoIB/FDR |          |
|--------------|----------|----------|-----------|----------|
|              | IPv6     | IPv4     | IPv6      | IPv4     |
| 4            | 14.38    | 20.15    | 13.21     | 16.41    |
| 8            | 26.97    | 45.22    | 25.22     | 34.63    |
| 16           | 57.68    | 100.46   | 54.51     | 66.10    |
| 32           | 112.65   | 164.86   | 109.04    | 134.78   |
| 64           | 272.96   | 383.41   | 255.12    | 271.18   |
| 128          | 531.80   | 703.52   | 513.77    | 544.76   |
| 256          | 910.42   | 1,492.17 | 902.85    | 1,064.14 |
| 512          | 2,254.57 | 2,723.55 | 2,137.53  | 2,162.18 |
| 1,024        | 3,490.73 | 4,967.32 | 3,096.52  | 3,107.23 |
| 2,048        | 4,319.39 | 5,742.73 | 3,805.11  | 3,851.54 |
| 4,096        | 5,107.52 | 6,784.56 | 4,408.75  | 4,583.80 |
| 8,192        | 6,208.20 | 8,522.13 | 6,101.41  | 6,352.89 |
| 16,384       | 6,532.70 | 8,796.20 | 6,414.42  | 7,925.14 |
| 32,768       | 6,754.10 | 8,893.05 | 7,438.32  | 9,721.07 |

Table V gives the results of the latency when varying the UDP payload size from 4 to 32,768 bytes. We can see that IPoIB/FDR has the lowest latency for all the payload sizes.

Also, it is worth pointing out that the latency of IPv4 is under the one of IPv6.

TABLE V. UDP LATENCY IN MICROSECONDS FOR IPV6 AND IPV4 OVER 10GBE AND IPOIB/FDR

| Payload Size | 10GbE  |       | IPoIB/FDR |       |
|--------------|--------|-------|-----------|-------|
|              | IPv6   | IPv4  | IPv6      | IPv4  |
| 4            | 31.17  | 26.28 | 10.92     | 7.37  |
| 8            | 31.32  | 26.30 | 11.05     | 7.41  |
| 16           | 31.56  | 26.57 | 11.23     | 7.45  |
| 32           | 31.71  | 26.59 | 11.51     | 7.51  |
| 64           | 31.93  | 26.70 | 11.75     | 7.53  |
| 128          | 32.46  | 27.01 | 12.02     | 7.55  |
| 256          | 32.82  | 27.42 | 12.40     | 7.62  |
| 512          | 33.41  | 28.30 | 12.53     | 7.75  |
| 1,024        | 35.72  | 30.02 | 12.72     | 7.83  |
| 2,048        | 46.17  | 38.39 | 15.01     | 11.17 |
| 4,096        | 50.62  | 42.08 | 19.47     | 14.76 |
| 8,192        | 60.58  | 51.25 | 21.32     | 18.37 |
| 16,384       | 78.32  | 65.59 | 31.58     | 23.19 |
| 32,768       | 114.41 | 99.23 | 48.32     | 34.98 |

D. Experiments for TCP/IPv6 and TCP/IPv4

In these experiments, we compare the throughput and latency obtaining between two end-nodes for TCP/IPv6 and TCP/IPv4, over 10GbE and IPoIB/FDR. In the case of IPoIB, we chose the datagram mode in the end-nodes (see Fig. 1). Meanwhile for 10GbE, we took the default configuration.

Table VI shows the results of the throughput when varying the TCP payload size from 4 to 32,768 bytes. We can see that 10GbE has the best throughput for almost all the payload sizes, except for very large payload sizes (e.g. 32,768 bytes) where the performance of IPoIB/FDR is better. Also, IPv4 exceeds IPv6 for both technologies.

TABLE VI. TCP THROUGHPUT IN MBPS FOR IPV6 AND IPV4 OVER 10GBE AND IPOIB/FDR

| Payload Size | 10GbE    |          | IPoIB/FDR |          |
|--------------|----------|----------|-----------|----------|
|              | IPv6     | IPv4     | IPv6      | IPv4     |
| 4            | 13.72    | 19.62    | 12.39     | 15.28    |
| 8            | 24.32    | 39.45    | 23.41     | 32.73    |
| 16           | 55.15    | 73.93    | 50.73     | 64.23    |
| 32           | 109.46   | 142.52   | 105.47    | 130.94   |
| 64           | 258.72   | 297.58   | 241.69    | 265.44   |
| 128          | 510.60   | 613.78   | 497.08    | 540.98   |
| 256          | 904.78   | 1,176.34 | 897.43    | 1,061.54 |
| 512          | 2,231.78 | 2,296.75 | 2,005.81  | 2,157.76 |
| 1,024        | 3,482.23 | 3,984.84 | 3,087.36  | 3,102.42 |
| 2,048        | 4,315.17 | 5,654.91 | 3,798.34  | 3,845.72 |
| 4,096        | 5,098.92 | 6,575.67 | 4,401.43  | 4,575.59 |
| 8,192        | 6,201.53 | 8,343.26 | 6,098.52  | 6,345.74 |
| 16,384       | 6,528.38 | 8,576.45 | 6,407.31  | 7,917.27 |
| 32,768       | 6,742.57 | 8,744.21 | 7,429.50  | 9,714.57 |

Table VII gives the results of the latency when varying the TCP payload size from 4 to 32,768 bytes. We can see that IPoIB/FDR has the lowest latency for all the payload sizes. Also, it is worth pointing out that the latency of IPv4 is under the one of IPv6.

TABLE VII. TCP LATENCY IN MICROSECONDS FOR IPV6 AND IPV4 OVER 10GBE AND IPOIB/FDR

| Payload Size | 10GbE |      | IPoIB/FDR |      |
|--------------|-------|------|-----------|------|
|              | IPv6  | IPv4 | IPv6      | IPv4 |

|        |        |        |       |       |
|--------|--------|--------|-------|-------|
| 4      | 32.24  | 30.02  | 17.02 | 14.32 |
| 8      | 32.51  | 30.62  | 17.14 | 14.41 |
| 16     | 32.76  | 31.04  | 17.50 | 14.58 |
| 32     | 32.87  | 31.46  | 17.72 | 14.65 |
| 64     | 33.36  | 31.82  | 18.01 | 14.72 |
| 128    | 33.75  | 32.17  | 18.15 | 14.81 |
| 256    | 34.63  | 32.90  | 18.28 | 14.88 |
| 512    | 35.27  | 33.42  | 18.42 | 14.92 |
| 1,024  | 37.94  | 35.63  | 18.82 | 15.26 |
| 2,048  | 52.47  | 50.79  | 21.18 | 18.41 |
| 4,096  | 53.02  | 51.82  | 26.24 | 23.52 |
| 8,192  | 61.23  | 53.48  | 34.51 | 31.02 |
| 16,384 | 79.17  | 67.97  | 40.26 | 36.41 |
| 32,768 | 114.98 | 103.77 | 55.73 | 53.91 |

## VII. CONCLUSIONS AND FUTURE WORK

In this research work, we analyzed the performance of IPv6 and IPv4 over 10 Gigabit Ethernet and iPoIB. For small and medium IPv6 and IPv4 packets, our experiments showed that the throughput of 10 Gigabit Ethernet is over the one shown by iPoIB/FDR and the differences are significant. However, as the size of the UDP and TCP payload increases, iPoIB/FDR improves its performance and finally outperforms 10 Gigabit Ethernet. Regarding latency, iPoIB/FDR does better than 10 Gigabit Ethernet for all the UDP and TCP payload sizes. Additionally, our experiments showed that the performance of IPv4 is over the performance of IPv6, however, the differences are small and are mostly likely due to the IP headers, 20 bytes in IPv4 and 40 bytes in IPv6, resulting in a higher transmission time for IPv6.

As future work, we are planning to develop some mathematical models to represent the maximum throughput and the minimum latency that can be achieved by different transport services of InfiniBand, in connections between two end-nodes with zero or more intermediate switches between them. Another direction of research that we also want to explore is the performance evaluation of parallel file systems over InfiniBand (e.g. Lustre [32] and NFS over RDMA).

## ACKNOWLEDGMENT

We want to thank the NSF (National Science Foundation) which partially supported this research under grant number 1010094 through the EPSCoR Track 2 program. We also express our gratitude for all the valuable assistance and comments that we received throughout this project from José Bonilla and Ramón Sierra of the High Performance Computer Facility of the University of Puerto Rico, and José Muñoz and Osvaldo Casiano of the Resource Center for Science and Engineering of the University of Puerto Rico.

## REFERENCES

- [1] J. Davies, Understanding IPv6, 3rd edition, Microsoft Press, June 2012.
- [2] J. Pyles, J. Carrell, and E. Tittel, Guide to TCP/IP: IPv6 and IPv4, 5th edition, Cengage Learning, June 2016.
- [3] S. Deering and R. Hinden. Internet Protocol, Version 6 (IPv6) Specification. RFC 2460. December 1998.
- [4] M. Dooley and T. Rooney, IPv6 Deployment and Management, 1st edition, Wiley-IEEE Press, May 2013.
- [5] Google IPv6, <https://www.google.com/intl/en/ipv6>.
- [6] 6lab - The Place to Monitor IPv6 Adoption, <http://6lab.cisco.com>.
- [7] InfiniBand Trade Association, InfiniBand Architecture Specification Volume 1, Release 1.3, March 2015.

- [8] InfiniBand Trade Association, InfiniBand Architecture Specification Volume 2, Release 1.3, March 2015.
- [9] MindShare and T. Shanley, InfiniBand Network Architecture, 1st edition, Addison Wesley, November 2002.
- [10] InfiniBand Trade Association, Supplement to InfiniBand Architecture Specification Volume 1, Release 1.2.1, RDMA over Converged Ethernet (RoCE), Annex A16, April 2010.
- [11] InfiniBand Trade Association, Supplement to InfiniBand Architecture Specification Volume 1, Release 1.2.1, RoCEv2, Annex A17, September 2014.
- [12] Mellanox, RoCE vs. iWARP Competitive Analysis, White Paper, August 2015.
- [13] Chelsio Communications, The Case Against iWARP, 2015.
- [14] V. Kashyap, IP over InfiniBand (iPoIB) Architecture, RFC 4392, April 2006.
- [15] J. Chu and V. Kashyap, Transmission of IP over InfiniBand (iPoIB), RFC 4391, April 2006.
- [16] V. Kashyap, IP over InfiniBand: Connected Mode, RFC 4755, December 2006.
- [17] S. Narayan, P. Shang, and N. Fan, "Performance Evaluation of IPv4 and IPv6 on Windows Vista and Linux Ubuntu," in proceedings of the 2009 International Conference on Networks Security, Wireless Communications and Trusted Computing (NSWCTC'09), Wuhan, China, April 2009.
- [18] S. Narayan, P. Shang, and N. Fan, "Network Performance Evaluation of Internet Protocols IPv4 and IPv6 on Operating Systems," in proceedings of the 6th International Conference on Wireless and Optical Communications Networks (WOCN'09), Cairo, Egypt, April 2009.
- [19] S. S. Kolahi, B. K. Soorty, Z. Qu, and N. Chand, "Performance Analysis of IPv4 and IPv6 on Windows Vista and Windows XP over Fast Ethernet in Peer-peer LAN," in proceedings of the 3rd International Conference on New Technologies, Mobility and Security (NTMS'09). Cairo, Egypt, December 2009.
- [20] J. Balen, G. Martinovic, and Z. Hocenski, "Network Performance Evaluation of Latest Windows Operating Systems," in proceedings of the 20th International Conference on Software, Telecommunications and Computer Networks (SoftCOM), vol. 7, Split, Croatia, September 2012.
- [21] P. Jain, S. Singh, G. Singh, and C. Goel, "Performance Comparison of IPv4 and IPv6 using Windows XP and Windows 7 over Gigabit Ethernet LAN," International Journal of Computer Applications, vol. 43, no. 16, April 2012.
- [22] B. Soorty and N. Sarkar, Evaluating IPv6 in Peer-to-Peer Gigabit Ethernet for UDP using Modern Operating Systems, in proceedings of the 2012 IEEE Symposium on Computers and Communications (ISCC 2012), Cappadocia, Turkey, July 2012.
- [23] B. Soorty and N. Sarkar, "UDP-IPv6 Performance in Peer-to-Peer Gigabit Ethernet using Modern Windows and Linux Systems," International Journal of Computer and Information Technology (IJCIT), vol. 3, no. 3, pp. 496-502, May 2014.
- [24] H. Fahmy and S. Ghoneim, "Performance Comparison of Wireless Networks over IPv6 and IPv4 under Several Operating Systems," in proceedings of the IEEE 20th International Conference on Electronics, Circuits, and Systems (ICECS'13), Abu Dhabi, UAE, December 2013, pp. 670-673.
- [25] E. Gamess and R. Surós, "An Upper Bound Model for TCP and UDP Throughput in IPv4 and IPv6," Journal of Network and Computer Applications, vol. 31, no. 4, pp. 585-602, November 2008.
- [26] E. Gamess and N. Morales, "Modeling IPv4 and IPv6 Performance in Ethernet Networks," International Journal of Computer and Electrical Engineering, vol. 3, no. 2, pp. 282-288, April, 2011.
- [27] A. Cohen, A Performance Analysis of 4X InfiniBand Data Transfer Operations, in proceedings of the 2003 International Parallel and Distributed Processing Symposium (IPDPS 2003), Nice, France, April 2003.
- [28] M. Rashti and A. Afsahi, 10-Gigabit iWARP Ethernet: Comparative Performance Analysis with InfiniBand and Myrinet-10G, in proceedings of the 2007 IEEE International Parallel and Distributed Processing Symposium (IPDPS 2007), Long Beach, CA, USA, March 2007.

- [29] Message Passing Interface Forum, MPI: A Message-Passing Interface Standard, Version 3.1, High Performance Computing Center Stuttgart, June 2015.
- [30] J. Vienne, J. Chen, Md. Wasi-ur-Rahman, N. Islam, H. Subramoni, and D. Panda, Performance Analysis and Evaluation of InfiniBand FDR and 40GigE RoCE on HPC and Cloud Computing Systems, in proceedings of the Symposium on High-Performance Interconnects, Santa Clara, CA, USA, August 2012.
- [31] S. Sur, M. Koop, L. Chai, and D. Panda, Performance Analysis and Evaluation of Mellanox ConnectX InfiniBand Architecture with Multi-Core Platforms, in proceedings of the 15th Annual IEEE Symposium on High-Performance Interconnects (HOTI 2007), Stanford, CA, USA, August 2007.
- [32] Y. Wang, Y. Lu, C. Qiu, P. Gao, and J. Wang, Performance Evaluation of a InfiniBand-based Lustre Parallel File System, in proceedings of the 2011 2nd International Conference on Challenges in Environmental Science and Computer Engineering (CESCE 2011), Haikou, China, December 2011.

# Ontology-based Query Expansion for Arabic Text Retrieval

Waseem Alromima<sup>1</sup>, Ibrahim F. Moawad<sup>2</sup>, Rania Elgohary<sup>3</sup>, Mostafa Aref<sup>4</sup>

Faculty of Computer and Information Science  
Ain Shams University  
Cairo, Egypt

**Abstract**—The semantic resources are important parts in the Information Retrieval (IR) such as search engines, Question Answering (QA), etc., these resources should be available, readable and understandable. In semantic web, the ontology plays a central role for the information retrieval, which use to retrieves more relevant information from unstructured information. This paper presents a semantic-based retrieval system for the Arabic text, which expands the input query semantically using Arabic domain ontology. In the proposed approach, the search engine index is represented using Vector Space Model (VSM), and the Arabic's place nouns domain ontology has been used which constructed and implemented using Web Ontology Language (OWL) from Arabic corpus. The proposed approach has been experimented on the Arabic Quran corpus, and the experiments show that the approach outperforms in terms of both precision and recall the traditional keyword-based methods.

**Keywords**—Information Retrieval; Arabic Ontology; Semantic Search; Arabic Quran Corpus

## I. INTRODUCTION

In the information overloading era, the search engines are the most important applications. The existing search engines still present several problems related to the user's query such as word mismatch or retrieve many irrelevant documents, particularly when the user's queries are not specific enough. Nowadays, the World Wide Web (WWW) has become a library of a huge unstructured data, which is difficult to be understood and processed without representing the web content in machine processable form.

The semantic-based retrieval aims to search with concepts rather than with terms, which retrieves more relevant information. Various semantic based search techniques have been adopted since the evolution of semantic web. Semantic Web (SW) is an extension of the current web in which information provides well-defined meaning, its enable system and people for better understanding. Although, SW enable to work effectively by understanding information from different sources [1]. In general, semantic search is a process use to improve search retrieval by applying data from semantic networks, which is disambiguate the queries and web texts. Hence, the semantic network at the level of ontology expresses a vocabulary that is helpful and can be used for machine processing [2] [3]. Besides, ontologies play a major role in support information search and retrieval processes for the Arabic language [4]. The Arabic WordNet (AWN) is a semantic resource and a free lexical for the Arabic ontologies

[5]. But constructing AWN presents a challenges that are include the scripts and the morphological properties of Semitic languages, which centered on roots [6].

The semantic web contains a meta-data which is a data about data. Moreover, ontology applies major rule in the semantic web, which adds to the Web page to let the machine understanding the document. In this aspect, Tim Berners-Lee-2006 introduced the semantic Web architecture, which contains eight layers, which is the Resource Description Framework (RDF) and Ontology has considered the most important layers [7]. The RDF is a language for creating a data model for objects ('resources') and relations among them. It enables to represent information in the form of graph. The Resource Description Framework Schema (RDFS) provides basic vocabulary for describing properties and classes of RDF resources. The Web Ontology Language (OWL) extends of RDFS by adding more advanced constructs to describe semantics of RDF statements [8], [9].

The Arabic language is one of the Semitic language groups, is the language of the Islamic Holy Quran [4], [10]. Recently, the complexity of Arabic's grammar and ambiguity face a difficult to develop Arabic ontologies. Besides, many researchers are interested in the Islamic research such as the Holy Quran and developed different domain ontologies, which are the most of them are free [11], [12]. There are many tools using for searching on holy Quran, most of these tools are using keyword-based search. These tools face problems related to the meaning of the query terms. Hence, find accurate information directly from the holy Quran is very difficult [7]. Therefore, intelligent methods are required to enhance the current search engines especially for the Arabic holy Quran that is related to the Islamic concepts, because the Muslims need the Quran in all their affairs.

This paper presents a semantic-based system for Arabic information retrieval to improve Arabic retrieval results. The system semantically expands the input query using Arabic domain ontology. In this approach, we used our previous work for domain ontology 'Place Nouns' mention in Arabic Quran [13]. The term index is built using Vector Space Model (VSM) to represent both documents and user query. The proposed approach applied to the Arabic Quran corpus, and found that the query expansion is promising which the experiments shows good results comparing to the traditional Arabic information retrieval systems.

This paper is organized as follows. Section 2 presents the Related Work. The proposed system architecture is described in section 3, while section 4 explains the Ontology-based Query Expansions. Moreover, section 5 presents Experimental Results and Evaluation. Finally, the conclusion has presented in section 6.

## II. RELATED WORK

A Semantic-based approach aims to search with the concepts rather than the words. Semantic Search Engine (SSE) attempts to make sense of the search results based on document context. The specific domain ontology and upper ontology are the main two types of the ontology [14]. In recent times, a lot of researchers interested to devolve Arabic ontologies, the vast majority were in a specific domain and others for usage available ontology to reuse [12]. The semantic-based approaches expand the input query semantically using term co-occurrence or exterior resources such as a lexical thesaurus, domain ontology, etc.. In his work, [15] proposed a web-based multilingual tool for information retrieval including the Arabic language. The authors built domain ontology in the legal Arabic. By applying the Arabic ontology, the authors improved the recall 115 to 1230 and precision from 2 to 7.

The Arabic Quran is the Holy book of Islam, which is undoubtedly an important book, covering many themes and concepts in the all worlds. The Arabic Quran corpus is annotated linguistic resource, which consists of (6,236) verse (Ayah), and a total of (77,430) word [16]. Several studies have presented to facilitate and develop the search process for the Holy Quran and how to build Islamic ontology such as [10][17][18][19], and [13]. Although, most of these studies were directed to the Arab user, on the other hand, it has presented studies investigate in the Quran translations for other languages such as [18] covered limit knowledge for the domain solat (prayers) in the Holy Quran. In the same aspect, research [21] worked in the last Juz' in the Quran (Juz' Amma), which the authors developed the ontology for Juz' Amma.

In the meantime, ISWSE is an "Islamic Semantic Web Search Engine" system presented in [7], which is based on Islamic Ontology, and used Azhary [22] as a lexical ontology for the Arabic language. The experiments have been used in the Quran Prophets stories as the most detailed part of the Islamic Ontology, which contains 1153 concepts. The system improves 98.5% and 97% for precision and recall respectively for 30 executed queries. The system retrieval is based on the classify concepts in the ontology.

Dukes K. [23] presented in his PhD thesis the Arabic corpus ontology based on the Tafsir by Ibn-Kathir book, which defines 300 concepts in the Quran, and the number of relations is 350 based on Part-of or IS-A relation between concepts. In same corpus works, [2] presented a QurSim as a language resource for Quran scholar and researchers. They create a dataset called QurSim, which consists of 7600 pairs of related verses for evaluating the relatedness of short texts. Also research [24] developed a tool "Quran Search for a Concept" for searching in the Quran topics index from an academic source: Tafsir Ibn-Kathir and book of Mushaf Altajweed topics, which consists of 1100 concepts.

In the meantime, the researches [6], [21] proposed a model for detect the concepts in the Quran by using knowledge representation and shows the relationship between the concepts by Description Logic (Predicate logic). This research attempts to reuse and improve exist Arabic Quran corpus ontology by [23], which extend and add more than 650 relationships depends on the Quran, Hadith, and Islamic websites. Also, the authors proposed a semantic search system for the Quran domain, a top-down approach was followed, which consist of 15 abstract concepts.

Figure 1 display ontology base system for the Arabic ontologies developed, which is classify in to Arabic ontologies and holy Quran ontologies.

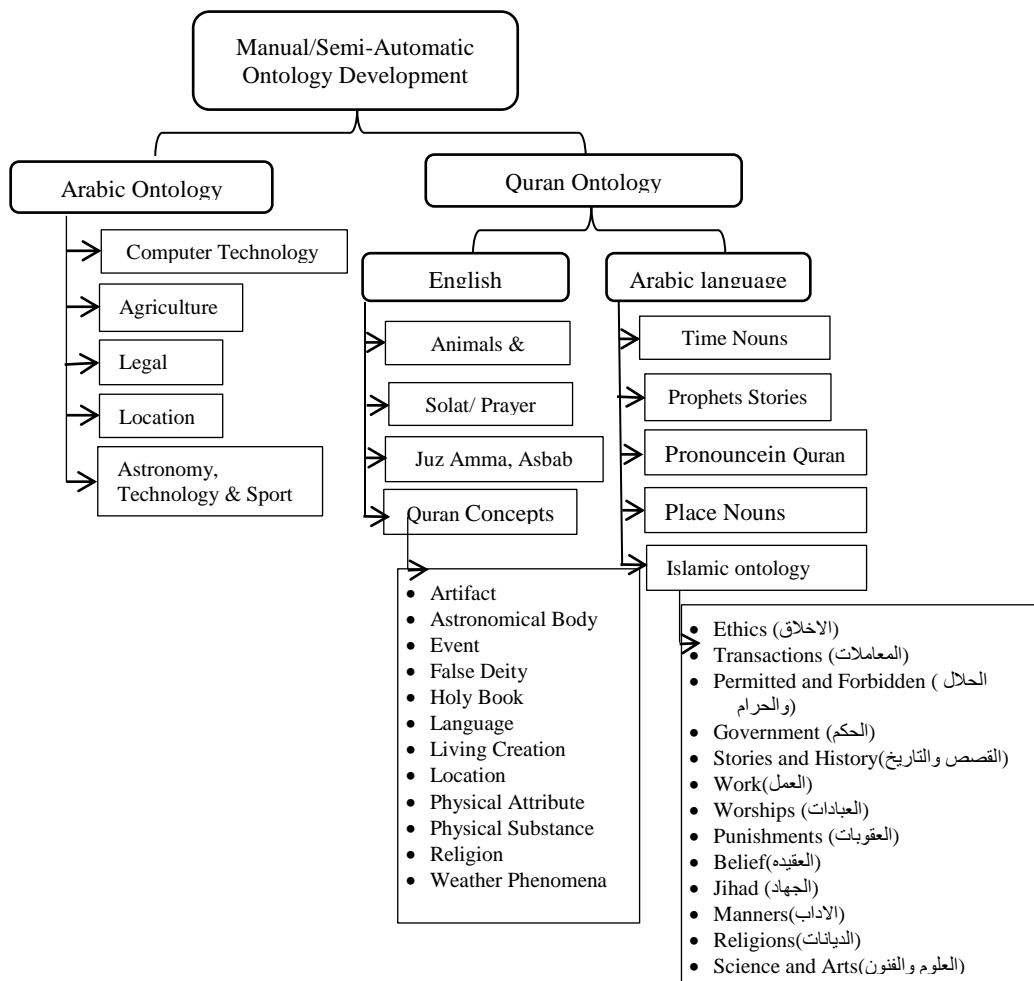


Fig. 1. Ontology Base System for Arabic Ontology Developed

The papers [10], [25] are proposed a methodology for automatic extraction the concept from the Holy Quran, which is for the format of English translation, and used these concepts to build domain ontology. The ontology is based on the information toked from the domain experts. The authors does not cover all subjects in the Quran only 63 verses, and don't talk about the format or ontology technologies used. In other his work, [18] the framework recognizes into account the sciences of the Quran, such as the reason of revelation (Asbab Al Nuzul). The ontology consists of 374 extracted cases cover for the verses that have the word salat/prayer.

In the same vein, the research [17] developed a simple ontology for the domain animals and birds that are mentioned in Holy Quran, and applied a semantic web search for the Quran in semantic search. The Pickthall used to English

translation the Quran in this paper, the ontology consist of 167 references for animals mentioned in direct or indirect in the Holy Quran based in the book entitle "Hewanat-El-Qurani".

### III. THE PROPOSED SYSTEM ARCHITECTURE

The architecture of the system has shown in Figure 2. It consists of two phases: offline and online phases. In the offline phase, the index of the Arabic information retrieval system is created and maintained for the Arabic corpus based on vector space model. In addition, the Arabic domain ontology has designed and implemented from the Arabic corpus. In the online phase, the user query has expanded using ontology and then the search results are retrieved and ranked. These phases can be described as follow.

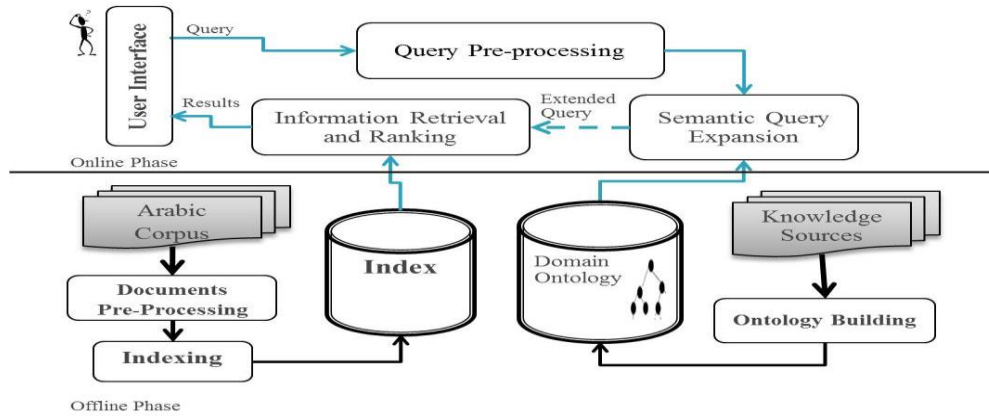


Fig. 2. The proposed System Architecture

The first phase is offline phase, which consists of three modules: Documents-Pre-processing, Indexing, and Ontology Building modules. Those modules can describe briefly as follow.

1) *Documents Pre-Processing Module*: This module consists of three processes: words-tokenization, stop-words-Removal, and words-weights. The words-tokenization response to break Arabic sentences into tokens each document for the Arabic corpus. Stop-words-Removal removes the useless words like “من” (from), “على” (on), etc. Finally, words-weighting this process computes the terms’ weights based on Term Frequency-Inverse Document Frequency (TF-IDF) statistical measures by using equation (1), which shows computation of the term frequency, equation (2), which calculates the inverse of the number of documents in which the term occurs, and equation (3), shows how the term weight is computed [26]:

$$TF_{i,j} = \begin{cases} 1 + \log_2 f_{i,j} & \text{if } f_{i,j} > 0 \\ 0 & \text{otherwise} \end{cases} \quad (1)$$

where  $TF_{i,j}$  denotes the normalized term frequency for term  $i$  in document  $j$ , and  $f_{i,j}$  is the number of occurrence for term  $i$

$$IDF_i = \log_2 \frac{N}{n_i} \quad (2)$$

where  $N$  denotes the number of the documents in the corpus, and  $n_i$  is the total number of occurrence term  $i$  in all documents.

$$w_{i,j} = \begin{cases} TF_{i,j} \times IDF_i & \text{if } f_{i,j} > 0 \\ 0 & \text{otherwise} \end{cases} \quad (3)$$

where  $w_{i,j}$  denotes the weight of term  $i$  in document  $j$ .

2) *Indexing Module*: For the terms’ weights generated by the word-weighting process, this module indexes the document terms, where the index contains the term weights of

words using Vector Space Model (VSM) [26]. VSM is an algebraic model that represents both documents and queries as vectors. For example, the vector  $d_j = (\omega_{1j}, \omega_{2j}, \omega_{3j}, \dots, \omega_{nj})$  represents the vector weights of document  $j$ , where  $\omega_{ij}$  is the weight for term  $i$  in document  $j$ .

3) *Ontology Building Module*: This module responses to build the domain ontology, and represents the domain ontology for Arabic language. This ontology is represents by the Web Ontology Language (OWL), which is the standard language for the semantic web. In this paper, the proposed system is an Islamic semantic search engine searching in the Holy Quran. It is ontology-based search and uses Arabic language vocabulary associated with the “Place Noun” mentioned in the Arabic Quran [13].

The second phase is online phase, which consists of four modules, User-Interface, Query-Pre-processing, Semantic Query Expansion, and Information Retrieval based VSM and Results Ranking. Those models can describe briefly as follow.

1) *User-Interface Module*: the module is facilities the query input from the end user and displays the results retrieved.

2) *Query-Pre-processing module*: this module pre-processes the input query for tokenization, stop words removal, etc.

3) *Semantic Query Expansion Module*: This module expands the input query based on the domain ontology. For each query words related to the concepts in the domain ontology, the relations between concepts including that individuals is retrieved, and hence to enrich the expanded query. In this paper the OWL API[27] package have been used in the proposed system in the loading the ontology, extract the concepts and the relations.

4) *Information Retrieval based VSM and Ranking Module*: this module matches the expanded query vector versus the document vectors to compute the similarity between them. In this paper, the cosine similarity is used as

shown in equation (4) [26]. Then the documents retrieves will rank according to the similarity to the user query.

$$sim(d_j, q) = \frac{\sum_{i=1}^t \omega_{i,j} \times \omega_{i,q}}{\sqrt{\sum_{i=1}^t \omega_{i,j}^2} \times \sqrt{\sum_{i=1}^t \omega_{i,q}^2}} \quad (4)$$

where  $sim(d_j, q_i)$  is the similarity between document  $j$  and query  $q_i$ ,  $w_{i,j}$  denote the weight of term  $i$  in document  $j$ , and  $w_{i,q}$  is the weight of term  $i$  in query  $q$ .

#### IV. THE ONTOLOGY-BASED QUERY EXPANSION

The main contribution of this paper is semantic-based retrieval, which automatically expands the input query based on Arabic domain ontology. Both Arabic domain ontology and query expansion process are described in details as follow.

##### A. The Arabic Domain Ontology

In this paper, we used our previous Arabic domain ontology, it is completely manually built using protégé [13]. Protégé-OWL editor has been used to implement the ontology by covering the knowledge on the Arabic language vocabulary associated with Place Noun mentioned in the Holy Quran. The output of this process is the Islamic ontology that includes the Islamic concepts in a hierarchal classes form.

The domain ontology consists of three main classes ‘مكان جغرافي’ (Geographic place), ‘مكان عباده’ (Devotional place), and ‘اماكن ما بعد الحياة’ (After Life place), which contain two main sub-classes: ‘الجنة’ (Paradise) and ‘الجحيم’ (Hell). The vocabulary contains a total of 99 words. Words in hierarchy are linked with components via ontological semantic relations. Semantic relationship synonyms have been used (in the protégé is named ‘same individual as’ such as the individual ‘مكة’ (Makka) has a lot of synonyms names in the Holy Quran such as ‘ام القرى’ (mother of cities), ‘البلد الامين’ (city of security), ‘البلد’ (city), ‘بكه’ (Bakka), etc.), Figure 3 show the sample RDF which represents the synonyms of the term, and Figure 4 displays the graph ontology of the classes with the individuals.

```

<SameIndividual>
<NamedIndividual IRI="http://www.Ain-Shams.org/ont.owl#بكه"/>
<NamedIndividual IRI="http://www.Ain-Shams.org/ont.owl#مكة"/>
</SameIndividual>
<SameIndividual>
<NamedIndividual IRI="http://www.Ain-Shams.org/ont.owl#ام_القرى"/>
<NamedIndividual IRI="http://www.Ain-Shams.org/ont.owl#مكة"/>
</SameIndividual>

```

Fig. 3. Sample RDF represent synonym in ontology

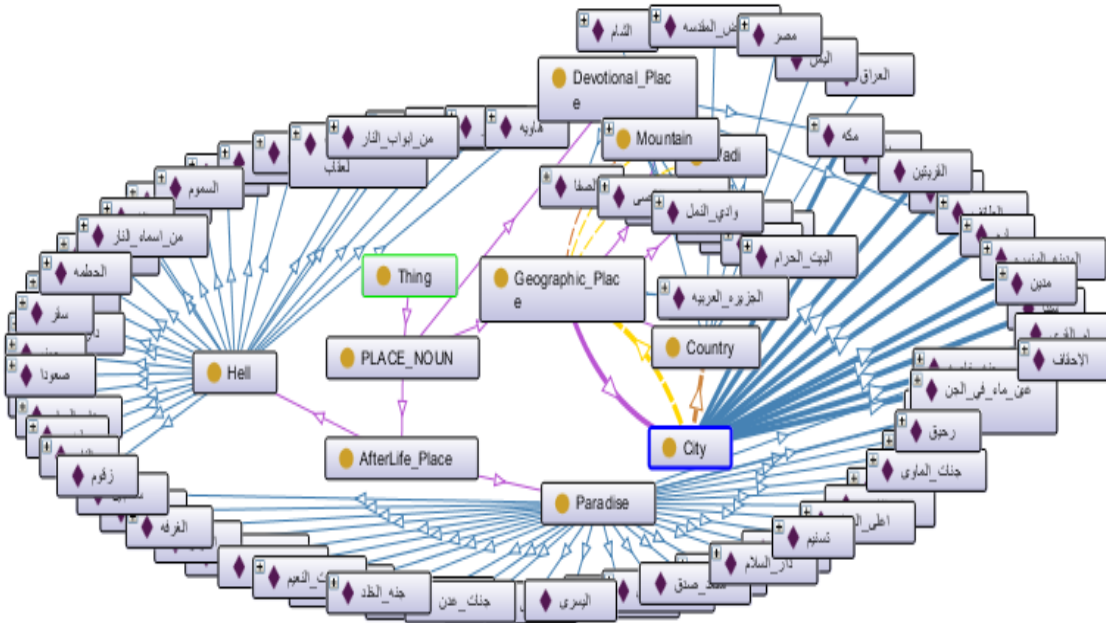


Fig. 4. Sample of Graph ontology classes with individual

##### B. The Query Expansion using Arabic Domain Ontology

This section describe how to expand the input query based on the ontology, the query preparing module improves the system retrieves for relevant information to the user. It is converting the RDF triples to hash map, and extracts the

equivalents terms from the relations between concepts such as ‘الكعبة’ (alkaba) same-as ‘البيت الحرام’ (the scaret house), which have the same Arabic meaning. For Example, Figure 5 shows the concept ‘الكعبة’ in the ontology as OWL with the relations and object property. These relations and object property of the terms will be used in the expanded query process.

```
<ClassAssertion>
 <Class IRI="http://www.Ain-Shams.org/ont.owl#PLACE_NOUN"/>
 <NamedIndividual IRI="http://www.Ain-Shams.org/ont.owl#الكعبة"/>
</ClassAssertion>
<ClassAssertion>
 <Class IRI="http://www.Ain-Shams.org/ont.owl#Devotional_Place"/>
 <NamedIndividual IRI="http://www.Ain-Shams.org/ont.owl#الكعبة"/>
</ClassAssertion>
<SameIndividual>
 <NamedIndividual IRI="http://www.Ain-Shams.org/ont.owl#البيت_الحرام"/>
 <NamedIndividual IRI="http://www.Ain-Shams.org/ont.owl#الكعبة"/>
</SameIndividual>
<ObjectPropertyAssertion>
 <ObjectProperty IRI="http://www.Ain-Shams.org/ont.owl#is_partOf"/>
 <NamedIndividual IRI="http://www.Ain-Shams.org/ont.owl#الكعبة"/>
 <NamedIndividual IRI="http://www.Ain-Shams.org/ont.owl#مكة"/>
</ObjectPropertyAssertion>
<ObjectPropertyAssertion>
 <ObjectProperty IRI="http://www.Ain-Shams.org/ont.owl#isLocated_in"/>
 <NamedIndividual IRI="http://www.Ain-Shams.org/ont.owl#الكعبة"/>
 <NamedIndividual IRI="http://www.Ain-Shams.org/ont.owl#الجزيره_العربية"/>
</ObjectPropertyAssertion>
```

Fig. 5. Sample of relations and property of concept “الكعبة”

### V. EXPERIMENTAL RESULTS AND EVALUATION

The proposed semantic-based Arabic information retrieval has designed and implemented using the Java language and the SQLite database. Figure 6 shows the system user interface, which enables the user to input the query and set the search

methods mode (with query expansion or without query expansion). The proposed system shows a set of retrieved and ranked documents for the input query with or without expansion as shown in Figure 6, which presents the search results for the input query “مكة” (Makka) using the ontology-based expansion.

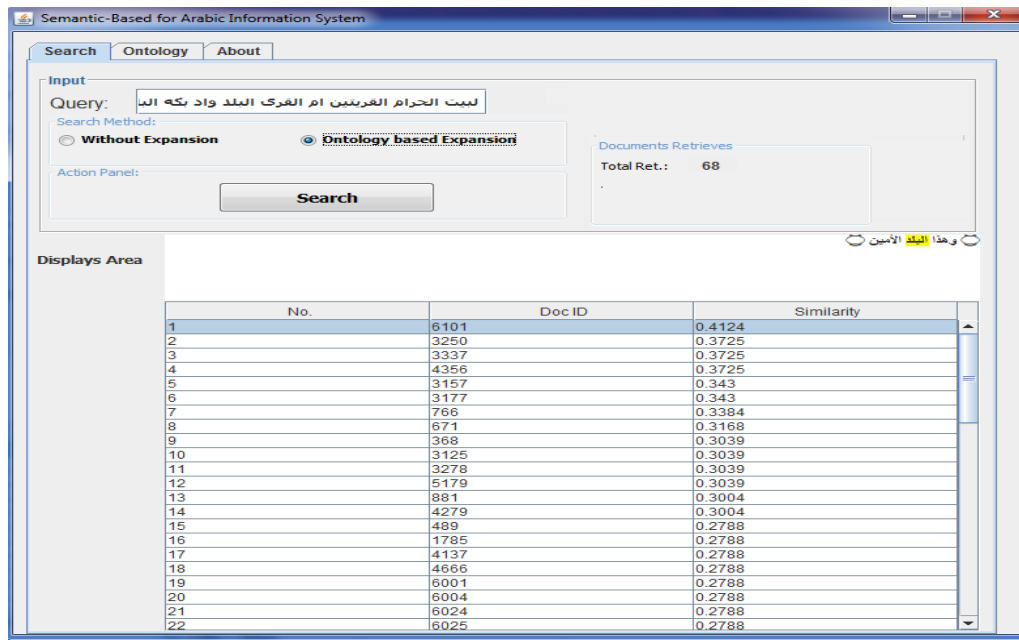


Fig. 6. The user interface with sample results query

#### A. Dataset and Arabic Domain Ontology

The system has been experimented on the corpus of the Holy Quran scripts. The number of documents (verses) is 6236, the number of words in the corpus is 77430, and the number of unique tokens is 14662 [28]. The Arabic domain ontology

implemented using protégé as discussed in the previous section (IV-A). The ontology has been tested on the place nouns vocabulary and on new terms from the new semantic filed in the Quran. While protégé editor has been used to build the domain ontology, which the syntactic and semantic qualities are both verifies by this tool. Therefore, proposed approach

extracted more relevant concepts for the input query, which are used in expansion as shown in Table 1.

There are two experiments have conducted to test our system: word-based and ontology-based query expansion. Word-based is use full-form terms without modification the input query. Ontology-based expansion is expands the query terms automatically using place nouns domain ontology. As well as, to depict the accuracy and functionality of the ontology for checking that the concepts from relationship and its characteristics, also we have used the DL query language in the protégé tool [20].

For example: If we have a query 'الكعبة' (AlKaba), the query expansion process expands the query using place nouns domain ontology by extract the concepts based on the relations. The proposed system is search in the ontology for the concept 'الكعبة' (AlKaba), and then all synonyms and relative derivatives attached to the concept are extracted as shown in Table 1. Then the extended query becomes: { البيت الحرام, البيت الكعبة, مكة, بكة, البيت العتيق, (Ka'aba),(Makka),( the sacred house),(the Ancient house ),(Bakka )}, the translation by Yousf Ali [29].

TABLE I. SAMPLE OF THE OBJECT PROPERTY FOR CONCEPT "الكعبة"

Concept	Relation	Concept	Concept Translation
الكعبة (Alka'aba)	is_PartOf جزء من	مكة	Maka'a
	is_a	مكان عبادة	Devotional place
	is_Located_in توجد في	الجزيرة العربية	Algezeera_Alarabia
	Same_as (Synonym) مرادف لها	البيت الحرام	The sacred house

Table 2 shows the total of relevant documents retrieved versus a simple query for the word-based and proposed approach using the domain ontology for the place nouns domain. The word-based search method retrieved only 2 documents from the corpus. The proposed approach using ontology-based method is retrieved a total of 54 documents, which are semantically related to the input query. The preliminary results are quite promising and show that there is a significant improvement in the precision and recall.

TABLE II. RELEVANT DOCUMENTS RETRIEVED FOR THE QUERY "الكعبة"

Query	word-based	Ontology-based	
الكعبة (Alka'aba)	2	By-Same_as Individual	29
		By-Class & Object-property	25
			54

In additions, the proposed approach has experimented using five queries as shows in Table 3. The results of the proposed system have been compared with word-based and stem-based methods. Therefore, the results of the proposed system are evaluated versus the results of this method. Figure 7 shows the proposed system has better precision comparing in to both the word-based and stem-based methods.

TABLE III. LIST OF QUERIES

Query #	Query	Query-Translation
1	الكعبة المشرفة	Alka'ba Almusharfa

2	طور سينا	Mount Sinai
3	جنان عدن	Garden of Eternity
4	مقام ابراهيم	Station of Abraham
5	تسنيم	Tasnim

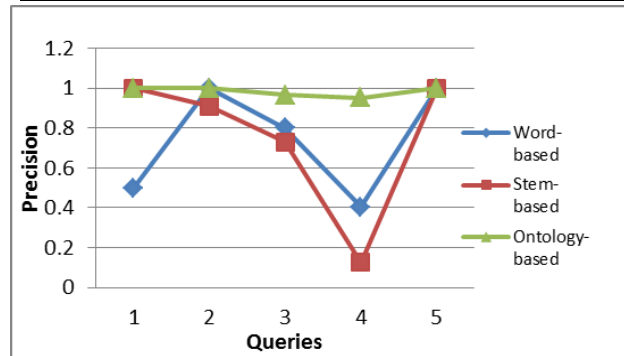


Fig. 7. Precision for word-based, stem-based, and ontology based

The SPARQL query language is used [30]. Thus ensures that use ontology can do semantics manipulation and inference, among many following sample queries were used, such as the following example:

Query: "ماهي اماكن العبادة في مكة" (what is the devotional places in Mekka)?

Answer: "الكعبة", "الصفاء", "المروه", "جبل عرفات", (alka'aba), (Arafat Mount), (Safa), (Marwa).

SELECT? Place\_Nounc\_Class

WHERE {? Devotional\_Palce: مكة .

:مكة rdf: type: City.

? Devotional\_Palce rdf: type? Devotional\_Palce\_subClass

? Devotional\_Palce rdfs: subclass Of: Place\_Nounc\_Class.

? "الصفاء", "المروه", "الكعبة", "جبل عرفات", hasPart, :مكة }

## VI. CONCLUSION

In this paper, we present a semantic-based Arabic information retrieval system, which semantically expands the input query using domain ontology. The search engine index is represents using Vector Space model (VSM), and the place nouns domain ontology is used, which constructed from Arabic corpus and implemented using Web Ontology Language (OWL). Many researches have been done in information retrieval domain of knowledge but no work has been done for efficient topic search from Arabic Holy Quran. In addition, trials to develop the Arabic ontologies are present but with low usefulness, because the complexity of Arabic's grammar and ambiguity, therefore several of the ontology developed in specific domain. The proposed approach improves retrieval for Arabic query through place nouns domain ontology. The proposed approach outperforms results in term precision and recall obtained from term-based method. Moreover, it is useful in the knowledge of the Islamic learning, linguistics researches, and semantic Web applications. In the future work we plan to merge and integrate the Place-Noun ontology with the Time-Nouns ontology (Al-khalefa .H et. al, 2010) and apply the proposed approach for the semantic retrieval.

## REFERENCES

- [1] S. M. R and P. S. Bala, "Ontology Based Information Retrieval - An Analysis," vol. 3, no. 10, pp. 486-493, 2013.
- [2] M. Sharaf and E. S. Atwell, "QurSim: A corpus for evaluation of relatedness in short texts," Lr., pp. 2295-2302, 2012.

- [3] M. Hazman, S. R. El-Beltagy, and A. Rafea, "Ontology learning from domain specific web documents," *Int. J. Metadata, Semant. Ontol.*, vol. 4, no. 1–2, pp. 24–33, 2009.
- [4] H. Ai-khalifa and M. M. Ai-yahya, "SemQ : A Proposed Framework for Representing Semantic Opposition in the Holy Quran using," *Curr. Trends Inf. Technol. (CTIT)*, 2009 Int. Conf. the. IEEE, pp. 0–3, 2009.
- [5] R. Amaro, R. P. Chaves, P. Marrafa, and S. Mendes, "Enriching wordnets with new relations and with event and argument structures," in *Computational Linguistics and Intelligent Text Processing*, Springer, 2006, pp. 28–40.
- [6] R. Yauri, R. A. Kadir, A. Azman, and M. A. A. Murad, "Quranic-based concepts: Verse relations extraction using Manchester OWL syntax," in *Information Retrieval & Knowledge Management (CAMP)*, 2012 International Conference on, 2012, pp. 317–321.
- [7] H. M. Harb and H. Ishkewy, "ISWSE : Islamic Semantic Web Search Engine ISWSE : Islamic Semantic Web Search Engine," *Int. J. Comput. Appl.* 112.5, no. APRIL, pp. 1–8, 2015.
- [8] M. Beseiso, A. R. Ahmad, and R. Ismail, "An Arabic Language Framework for Semantic Web," *Semant. Technol. Inf. Retr. (STAIR)*, 2011 Int. Conf. on. IEEE, no. June, pp. 7–11, 2011.
- [9] J. M. Kassim and M. Rahmany, "Introduction to Semantic Search Engine," 2009 Int. Conf. Electr. Eng. Informatics, vol. 02, no. August, pp. 380–386, 2009.
- [10] S. Saad, N. Salim, and H. Zainal, "Islamic Knowledge Ontology Creation," *Inst. Electr. Electron. Eng.*, 2009.
- [11] F. Harrag, A. Al-nasser, A. Al-musnad, R. Al-shaya, and A. S. Al-salman, "Intelligent Construction Approach of Quran Ontology Using Association Rules Mining," *Int. J. Islam. Appl. Comput. Sci. Technol.* ISSN. 2289-4012, Vol. 1, N. 2, pp. 41–48, 2013.
- [12] W. Alromima, R. Elgohary, I. F. Moawad, and M. Aref, "Applying Ontological Engineering Approach for Arabic Quran Corpus : A comprehensive Survey," 2015 IEEE Seventh Int. Conf. Intelligent Comput. Inf. Syst. Appl., 2015.
- [13] W. Alromima, I. F. Moawad, R. Elgohary, and M. Aref, "Ontology-Based Model for Arabic Lexicons : An Application of the Place Nouns in the Holy Quran," 11th Int. Comput. Eng. Conf. (ICENCO), IEEE, pp. 137–143, 2015.
- [14] K. S. Esmaili and H. Abolhassani, "A Categorization Scheme for Semantic Web Search Engines.," in *AICCSA*, 2006, pp. 171–178.
- [15] S. Zaidi, "A Cross-language Information Retrieval Based on an Arabic Ontology in the Legal Domain," *roceedings Int. Conf. Signal-Image Technol. Internet-Based Syst.*, pp. 86–91, 2005.
- [16] K. Dukes, E. Atwell, and N. Habash, "Supervised Collaboration for Syntactic Annotation of Quranic Arabic," *Lang. Resour. Eval.* 47.1 33-62., pp. 1–30, 2013.
- [17] H. U. Khan, S. M. Saqlain, M. Shoaib, and M. Sher, "Ontology Based Semantic Search in Holy Quran," *Int. J. Futur. Comput. Commun.*, vol. 2, no. 6, 2013.
- [18] S. Saad, N. Salim, H. Zainal, and Z. Muda, "A process for building domain ontology: An experience in developing Solat ontology . A process for building domain ontology : an experience in developing Solat ontology," *Int. Conf. Electr. Eng. Informatics (ICEEI)*, 2011 . IEEE, 2011.
- [19] R. Iqbal and A. Mustapha, "An experience of developing Quran ontology with contextual information support," *Multicult. Educ. Technol. J.*, vol. 7, no. 4, pp. 333–343, 2013.
- [20] ProtegeWeb, "Protege." [Online]. Available: <http://protege.stanford.edu/>. [Accessed: 11-Feb-2015].
- [21] R. Yauri, R. A. Kadir, A. Azman, M. Azrifah, and A. Murad, "Quranic Verse Extraction base on Concepts using OWL-DL Ontology," *Res. J. Appl. Sci. Eng. Technol.*, vol. 6, no. 23, pp. 4492–4498, 2013.
- [22] H. Ishkewy, H. Harb, and H. Farahat, "Azhary : An Arabic Lexical Ontology," *Int. J. Web Semant. Technol.*, vol. 5, no. 4, 2014.
- [23] K. Dukes, "Ontology of Quranic Concepts," Leeds University, 2010. [Online]. Available: <http://corpus.quran.com/ontology.jsp>.
- [24] N. H. Abbas, "Quran 'Search for a Concept' Tool and Website," *Msc , Univ. Leeds (School Comput.*, 2009.
- [25] S. Saad, N. Salim, U. Teknologi, and H. Zainal, "Towards Context-Sensitive Domain of Islamic Knowledge Ontology Extraction," *Int. J. Infonomics (IJ)*, vol. 3, no. 1, pp. 197–206, 2010.
- [26] de A. N. Ribeiro and R. Baeza-Yates, *Modern information retrieval*. Pearson Higher Education, 2010.
- [27] OwlApi, "OWLAPI," 2015. [Online]. Available: <http://owlapi.sourceforge.net/>.
- [28] K. Dukes, "Quran Project," Leeds University, 2010. [Online]. Available: [www.corpus.quran.com](http://www.corpus.quran.com/). [Accessed: 02-Feb-2016]. Y. Ali and T. Abdullah, "The Qur'an: Translation, Tahrike Tarsile Qur'an," Inc Elmhurst NY, 2003.
- [29] S. Eric and S. Andy, "SPARQL Query Language for RDF." [Online]. Available: <http://www.w3.org/TR/rdf-sparql-query>.
- [30] M. Al-yahya and H. Al-khalifa, "AN ONTOLOGICAL MODEL FOR REPRESENTING SEMANTIC LEXICONS : AN APPLICATION ON TIME NOUNS IN THE HOLY QURAN," *Arab. J. Sci. Eng.*, vol. 35, no. 2, pp. 21–35, 2010.

# A Hybrid Approach for Measuring Semantic Similarity between Documents and its Application in Mining the Knowledge Repositories

Ms. K. L. Sumathy,

Research and Development center, Bhararthyiar University,  
Coimbatore,  
Tamil Nadu

Dr. Chidambaram,

Asst prof, Rajah serofiji College,  
Thanjavur,  
Tamil Nadu

**Abstract**—This paper explains about similarity measure and the relationship between the knowledge repositories. This paper also describes the significance of document similarity measures, algorithms and to which type of text it can be applied. Document similarity measures are of full text similarity, paragraph similarity, sentence similarity, semantic similarity, structural similarity and statistical measures. Two different frameworks had been proposed in this paper, one for measuring document to document similarity and the other model which measures similarity between documents to multiple documents. These two proposed models can use any one of the similarity measures in implementation aspect, which is been put forth for further research.

**Keywords**—dataset documents; research similarity documents; ontology and corpus

## I. INTRODUCTION

### Objectives:

Now-a-days information on the web is increasing rapidly day-by-day. The increase of web based information and number of internet users', difficult to find the relevant documents for users to particular needs. In order to resolve this issue this paper proposes semantic similarity based document retrieval.

### Methods/Statistical Analysis:

The dataset documents are stored in the knowledge repositories. To get the relevant documents mining approach is used. The number of repeated words in a document considers as a keyword. Through preprocessing technique the repeated words in the documents will be removing. The term frequency mechanism proposes to identify important keywords in the documents. Term frequency determines the frequently occurring words in a document as keywords. The Jaccard similarity coefficient estimates the similarity between the documents and the ontology plays an important role in retrieval of similarity document.

### Findings:

In retrieval process the pos tagger applied to the document and obtains noun, verb and adverb. This fed in to word net. Through word net the related keyword like synonyms, antonyms, and hypernyms are obtained. The SWETO

technique provides similar documents from the knowledge repositories.

Accurately measuring semantic similarity between text documents presents a significant challenge due to the complexity and ambiguity of natural language semantics. Several natural language applications such as information retrieval, information recommendation, and machine translation require the similarity between sentences or documents. Generally, a pair of sentences or documents are said to be similar if they are predicted to have same meaning or conveys the same idea or subject. In natural language, there are different meanings in granularities such as word, phrase, sentence, and document. Word is the minimum mining unit, whereas sentence is the minimum unit to communicate some complete meaning. Moreover, there are various levels of similarities in natural languages. Words are generally categorized into synonyms and antonyms depending on the similarity between words and phrases. The calculation of similarities between documents is the basis for text classification and clustering. The techniques for similarity calculation vary in different levels. The word level similarity can be calculated from the spelling of words or the meaning of words. Word similarity is of two types such as symbolic similarity and semantic similarity. The symbolic similarity of words can be measured using the edit distance measure. The semantic similarity of words can be measured using WordNet.

The similarities between words in different sentences have a great impact on the similarity between two sentences. Words and their orders in the sentences are two chief factors to calculate sentence similarity. Sentence similarity is similar to the word similarity and document similarity. If words in two sentences are similar, the two sentences are said to be similar. Similarly, if sentences in two documents are similar, then the two documents are said to be similar. The sentence similarity measure considers the relation between words. The word similarity measures cannot calculate the sentence similarity as the word similarity reflects the closeness of two discrete words or concepts while the sentence similarity reflects the closeness of two sequences of words.

The similarities between sentences have a great impact on the similarity between documents. Most of the existing approaches calculate the document similarity based on the similarity between the keyword sets or the vectors of

keywords. Generally documents are represented in the form of bag-of-words while the meanings of documents are represented as vectors. The document similarity can be calculated using the cosine of the vectors. If the weight of the words is ignored, the document similarity can be measured based on the keywords set using Dice similarity or Jaccard Coefficient similarity.

#### A. Significance of Sentence/Document Semantic Similarity

Several recent applications of natural language processing demand an effective approach to calculating the similarity between sentences as in [1]. The deployment of sentence similarity can simplify the agent's knowledge base using natural sentences instead of using structural patterns of sentences. Semantic Similarity evaluates the similarity between concepts that are not lexicographically similar. The deep understanding of these concepts is necessary for computing semantic measures and for web mining. Similarity and relatedness measure can be applied to solve many problems in different applications. The measure of similarity and relatedness can be extended to many types of entities, such as words, sentences, texts, concepts, or Ontologies depending on the requirement. Lexical Semantics extracts semantic relations. Tasks such as document classification and clustering, information retrieval, and synonym extraction require precise measurement of semantic similarity between words. As the several applications and domains require semantic similarity, the measurement of sentence / document similarity has greater significance.

#### B. Potential Applications of Sentence/Document Semantic Similarity

Calculating semantic similarity among entities has application in several areas such as recommendation systems, e-commerce, search engines, biomedical informatics and in natural language processing tasks such as word sense disambiguation. In particular, user-based collaborative filtering tries to find people with similar tastes and recommend items to their peers liked by most of the people. The content-based recommender systems and search engines find items that are more similar to user queries. The sentence similarity has proven to be one of the effective techniques for enhancing retrieval performances as in [2]. The use of sentence representing the images can achieve a higher retrieval precision during the image retrieval from the web as in [3]. In text mining, sentence similarity act as an important factor to discover unseen knowledge from textual databases as in [4]. Semantic similarity efficiently evaluates the web search method of finding and ranking results. Hence, semantic similarity becomes vital in search engines as in [5]. Moreover, the short text similarity is important in applications like text summarization as in [6], text categorization as in [7], and machine translation as in [8].

## II. RELATED WORK

This section divides the related works into three parts such as sentence/document similarity based on metrics, sentence/document similarity based on methodologies, and hybrid approaches.

#### A. Sentence/Document Similarity Based on Metrics

There are several metrics for identifying the similarity between sentences as shown in table 1. The Jaccard similarity coefficient is measured by comparing the size of the intersection of words in two sentences with the size of the union of the words in two sentences as in [9]. The proportion of words that appear in both sentences normalized by the length of the sentence provides simple word overlap fraction as in [10]. The proportion of words that appear in two sentences weighted by their inverse document frequency is the value of IDF overlap [10]. The Zipfian overlap represents the Zipfian relationship between the length of words and their frequencies in a text collection as in [11]. IDF overlap is measured based on the sum of the product of term frequency and IDF of words that appear in both sentences as in [12]. The sums of IDF in the words that appear in both sentences are normalized by the overall lengths of the sentences and the relative frequency of words between two sentences as in [13].

TABLE I. SENTENCE/DOCUMENT SIMILARITY BASED ON METRICS

Title	Similarity level	Metrics	Pros	Cons
Jacob B, et. al (2008) [9]	Sentence similarity	Jaccard similarity coefficient	Calculation of sentence similarity involves fewer computations	Word co-occurrence may be null. Considers only the surface similarity which is not reliable
Metzler. D et. al (2005) [10]		Simple word overlap fraction		
Metzler. D et. al (2005) [10]		IDF overlap		
Banerjee, S (2003) [11]		Zipfian overlap		
Allan. J et. al (2003) [12]		TF-IDF measure	Better performance	It requires a large text corpus for statistics computation
Hoad. T et. al (2003) [13]		Identity measure		
Chukfong H et.al (2003) [14]		WSD based measure		
Tversky, A (1977) [15]	Document similarity	Tversky's Contrast Model	These models are relatively simple	Natural language allows users to express the same meaning using different words and hence, calculating text similarity by word's surface similarity is implausible
Shepard. R et.al (1979) [16]		Common Features Model		
Rohde. D et.al (2002) [17]		Distinctive Features based contrast Model		
Lee. M et.al (2002) [18]		Local and global weighting functions	Weighted corpus representation improves the performance	It is hard to obtain large text corpus for a specific domain

Yun.M et.al (2013) [19] and Rushdi S et.al (2010) [20]		Conceptual tree similarity measure (WordNet Based)	Simple computation	This kind of similarity computation is based on literal similarity which is not highly accurate
--------------------------------------------------------	--	----------------------------------------------------	--------------------	-------------------------------------------------------------------------------------------------

**B. Sentence/Document Similarity Based On Methodologies**

The measurement of sentence/document similarity based on methodologies are classified into corpus-based statistical approaches, lexical based semantic similarity approaches, lexical based semantic similarity, ontologies based semantic similarity, relational based semantic similarity. Corpus-based Statistical Approaches are used to find the similarity between terms based on the corpus. Ontology is a significant resource for measuring the semantic similarity and relatedness. OWL represents the domain knowledge and plays a vital role in the application area of Artificial Intelligence (AI). The Relational based approaches compute the similarity based on the relation between the words.

**C. Hybrid Approaches**

The hybrid approach combines the semantic, corpus, ontology and relational based approaches. A novel hybrid approach extracts semantic knowledge from the structural representation of Wordnet and the statistic information on the Internet [32]. Internet based semantic knowledge estimates the semantic similarity between the two concepts in Wordnet. A useful measure called Normalized Google Distance (NGD) computes the semantic distance between the adjacent concepts, along the shortest path in WordNet using Internet semantic knowledge. It is one of the best approaches due to the deployment of Internet knowledge in WordNet based semantic relatedness measure.

TABLE II. HYBRID APPROACHES

Title	Features combination	Pros	Cons
Emiliano Giovannetti et.al (2008) [31]	Statistical methods and lexico-syntactic patterns	Improved accuracy	Data sparseness of the corpus
Liu et.al (2011) [32]	Structural, semantic network (Wordnet) and the Internet	Deployment of Internet knowledge improves overall system performance	
Jay J. Jiang and David W. Conrath (1997) [33]	Corpus statistics and lexical taxonomy	Useful in word sense disambiguation	

**III. PROPOSED WORK**

**A. Combining Ontology Based And Count Based Similarity Model For Measuring Document Similarity**

This work proposes a hybrid approach for measuring semantic similarity between documents. There is an extensive literature on measuring the similarity between the words, but there is less work related to the measurement of similarity

between sentences and documents. This work measures the similarity between the documents using both ontology-based similarity model and counts based similarity model. Figure 1 shows the components used in this methodology. Initially, the proposed system represents the input documents as a bag of words, and it avoids the repeated terms. The pre-processing step removes stop words from the representation. The important keywords in the documents are identified using the term frequency mechanism. Term frequency determines the frequently occurring words in a document as keywords. The derived keywords are given to the ontology to obtain related keywords. The related keywords are given to the Jaccard similarity coefficient to decide the documents are similar or not. The Jaccard similarity coefficient is the count based similarity measure estimates the similarity between the documents by dividing the number of commonly related keywords by the total number of total keywords. In Jaccard coefficient result a value of “0” indicates the documents are completely dissimilar, “1” indicates that they are identical, and values between 0 and 1 represent a degree of similarity.

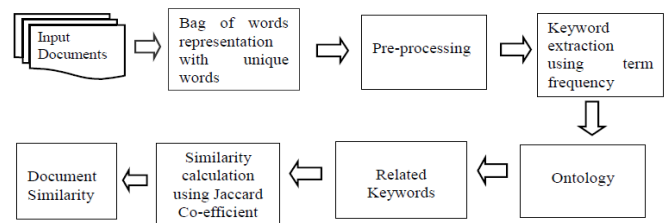


Fig. 1. Hybrid approach for measuring document similarity using ontology based and count based similarity model

**B. Preprocessing**

There is uncertainty of spelling convention in the language of Vietnamese. The majority typical ones contain “y” or “i” and situate marks on the syllables. Thus, preprocessing step intends to normalize information for additional investigation by one standard. Furthermore, this step intends to discover original words in named entities form like company’s names, factoids, people, etc. We utilize usual expression as major technique to distinguish named entities.

**C. Term Frequency Computation**

Term frequency (TF) signifies number of concept occurrence in documents. Through text processing the concepts are extracted that characterized as vectors, the vectors calculated with Term Frequency. TF count up for documents facilitates to obtain elevated accuracy rate.

**D. Ontology Construction**

Ontology signifies the knowledge as set of concept. The Swoogle web search engine is also known as semantic engine. From the Swoogle OWL file (knowledge source) is extracted for ontology construction in Ontograph form by protégé to determine semantic weight is considered by discovering minimum distance for every concept in constructed ontograph. The automobile fragmentation ontograph is exposed below.

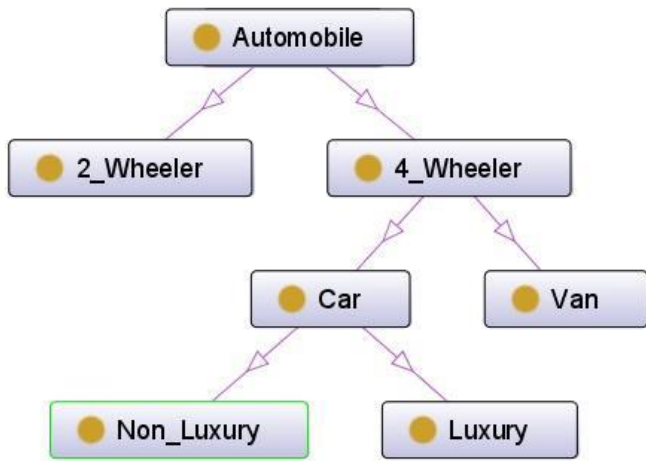


Fig. 2. Construction of Onto Graph

E. Jaccard Similarity Coefficient

Jaccard similarity is statistical measurement of the similarity among sample sets. Jaccard similarity coefficient is also known as Jaccard index. For both sets, it is defined as intersection of the cardinality divided by their cardinality union. Mathematically,

$$J(X, Y) = \frac{|X \cap Y|}{|X \cup Y|}$$

For Wikipedia data, slightly various approach required. For entities pair, computation is achieved on entities set with which pair elements occurred. For instance, in manipulating the pages similarity pairs, numerator is no. of users that reduced both pages, no. of users who have reduced both or either in the denominator. Mathematically,

$$J(X, Y) = \frac{|A \cap B|}{|A \cup B|}$$

Where A and B match to the entities sets that take place with X and Y, correspondingly.

F. Hybrid Approach For Measuring Document Similarity Using Ontology And Corpus

The proposed system presents the hybrid framework to measure the similarity between the documents using WordNet ontology and Wikipedia corpus. Figure 3 explains the procedure involved in the proposed stem. Most of the existing approaches does not consider the document context in semantic similarity. It may lead to the inaccurate similarity measurement. Due to overcome this limitation the proposed approach exploits the Wikipedia and WordNet to identify the context of the document since, it has been extensively and effectively exploited to facilitate better understanding of documents. Moreover, both Wikipedia and WordNet are domain independent while they provide extensive coverage of almost every branch of knowledge. Initially, the input documents are applied to the POS tagger to obtain only nouns, verbs and adjectives from the input documents. The resultant terms of the POS tagger are fed into the WordNet ontology. It gives all the related keywords such as synonyms, antonyms, and hypernyms for a given input terms. The context of the each input documents is identified through the Wikipedia related articles for the related keywords. If the identified

concepts from the Wikipedia for connecting document D1 with D2 are related then, the documents are considered as similar documents otherwise the documents are dissimilar.

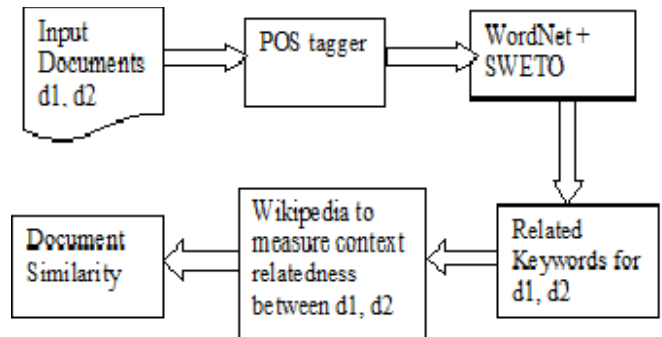


Fig. 3. Hybrid approach for measuring document similarity using ontology and corpus

G. POS Tagger Using Hidden Markov Model

HMM (Hidden Markov Model) is the statistical representation that is utilized to establish hidden parameter derived from observed parameters. It's extensively used, particularly in POS tagging for the input sequence.

- Hidden part: T sequence tag
- observed part: Word sequence
- Transition probability:
  - $a_{j-1,j} = P(ts_j|ts_{j-1})$  by hypothesis Markov-1, or  $a_{j-1,j} = P(ts_j|ts_{j-1}, ts_{j-2})$  by hypothesis Markov-2
- Output probability:  $b_j = P(w_j|ts_j)$

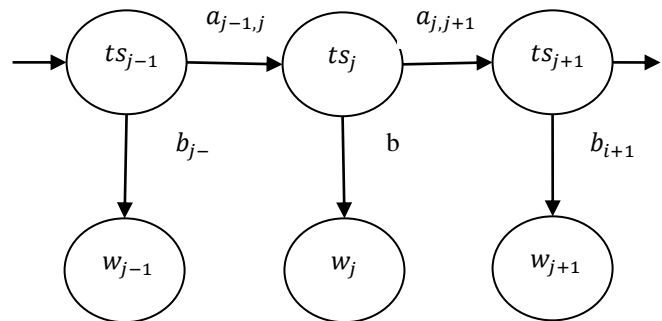


Fig. 4. POS tagging for HMM

The tagged sequence  $\hat{T} = ts_1, ts_2, \dots, ts_n$  suits

$$\hat{T} = \underset{T}{\operatorname{argmax}} P(w_1, w_2, \dots, w_n | ts_1, ts_2, \dots, ts_n) * P(ts_1, ts_2, \dots, ts_n)$$

If we identify parts of speech of the word easily can determine word. The probability P(W/T) depends only basic probability  $P(W_j|ts_j)$

$$P(W|T) \approx \prod_{j=1}^n P(W_j|ts_j)$$

Further computation for P(T)

$$P(T) = P(ts_1) * P(ts_2 | ts_1) * \dots * P(ts_n | ts_1, ts_2, \dots, ts_n)$$

When we know previous POS probability we can predict POS probability appearing in sequence by Concern Markov-1 hypothesis. That means

$$P(T) = \prod_{j=1}^n P(ts_j|ts_{j-1})$$

Finally we obtain

$$\hat{T} = \underset{T}{\operatorname{argmax}} \prod_{j=1}^n P(W_j|ts_j) * P(ts_j|ts_{j-1})$$

Where probabilities  $P(W_j|ts_j)$  and  $P(ts_j|ts_{j-1})$  can be calculate by annotated corpus which is based on Maximum likelihood technique.

In similar manner, when concern Markov-2 hypothesis we obtain

$$\hat{T} = \underset{T}{\operatorname{argmax}} \prod_{j=1}^n P(W_j|ts_j) * P(ts_j|ts_{j-2}, ts_{j-1})$$

Therefore, we can apply dynamic programming method Viterbi to resolve POS tagging.

#### H. Wordnet Ontology

Model descriptions of the word “country” on the WordNet seem like the subsequent. “people who be alive in the country or nation”. Here Synset is a country and Hypernym is the nation. Hyponym is the people.

#### I. Sweto Ontology

SWETO Ontology is introduced by Large Scale Distributed Information Systems (LSDIS). Three SWETO versions are there namely small, medium and large.

Similarity among diverse ontologies concepts in following equations,

$c_j, c_k$  are refer to the concepts

$P() \rightarrow$  probability function.

$$\text{Mutual Similarity} = \frac{\log(p(c_j)p(c_k))}{P(c_j, c_k)}$$

$$P(c_j) = \frac{W_c}{W}$$

$P(c_j, c_k)$  is a common terms joint probability distribution incident on same window and  $P(c_j)$  is particular keyword ki probability appears in text window. The text window is text sequences frame in the web documents. To determine obscure concepts ambiguity we require membership of fuzzy which is related to mutual similarity. Let the function of fuzzy membership  $\mu_i$  be in  $j^{\text{th}}$  concept and constant  $\alpha$  and their value is being set at 0.5.

$$\mu_i(c_k) = \alpha \times P(c_i, c_k) \log_2 \left( \frac{P(c_j)P(c_k)}{P(c_j, c_k)} \right)$$

#### J. Information Content Based Measure

Both depth and path length relative measure utilize the information exclusively incarcerate with ontology to additionally establish the similarity among concept. In this sector the knowledge discovered with corpus is utilized to enhance information already currently in the taxonomy or ontologies. The approach of content based information is being referred the approach based on theory and corpus approach.

## IV. RESULT AND DISCUSSION

### A. Experimental Requirements

This section explains the materials required to evaluate the effectiveness of the proposed methodology.

### B. Dataset

For document similarity, the dataset used is the Michael D.Lee document dataset, a collection of 50 documents from the Australian Broadcasting Corporation’s news mail service. These documents were paired in all possible ways, and each of the 1,225 pairs has 8-12 human judgments.

### C. Software Requirements

- Platform: Java
- IDE: Netbeans
- Database: MySQL Server
- Tool: Weka

### D. Performance Metrics

- **Precision:** It is a ratio of correctly predicted similar documents to the total input documents.

#### Precision

$$= \frac{\text{Correctly predicted similar documents (TP)}}{\text{Total input documents (TP + FP)}}$$

- **Recall:** It is a ratio of correctly predicted similar documents to all similar sentences.

$$\text{Recall} = \frac{\text{Correctly predicted similar documents (TP)}}{\text{Total input documents (TP + FN)}}$$

**F-measure:** It is a uniform harmonic mean of precision and recall.

$$\text{Recall} = (1 + \beta)PR / (\beta P + R) = 2PR / (P + R)$$

( $\beta=1$ , when precision and recall have the same weight)

Where,

TP: Number of documents predicted to be similar documents that actually are similar.

TN: Number of documents predicted to be dissimilar documents that actually are dissimilar

FP: Number of documents predicted to be similar that are actually dissimilar

FN: Number of documents predicted to be dissimilar that are actually similar

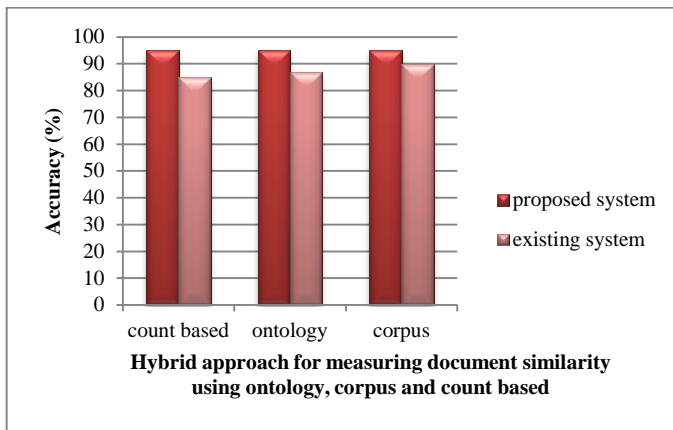


Fig. 5. Hybrid Approach for measuring document similarity using ontology, corpus and count based

The figure 5 shows Hybrid Approach for measuring document similarity using ontology, corpus and count based accuracy. When compare to existing and proposed the proposed approach has better accuracy.

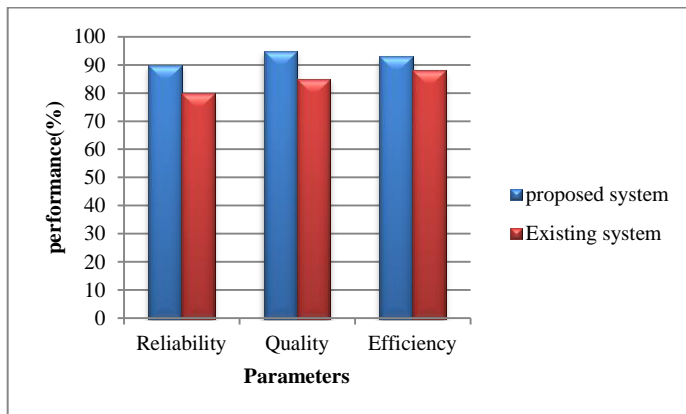


Fig. 6. Performance comparison

The figure 6 shows comparison of existing and proposed parameters performance. Here the parameters like reliability, quality and efficiency performance.

## V. CONCLUSION

This work presented a hybrid approach for measuring semantic similarity between documents. Semantic similarity plays a crucial role in information retrieval and text processing. This work provided an overview of semantic similarity and its existing approaches. Semantic similarity measure determines the similarity between words, sentence, and documents. The proposed approaches are divided into two folds: In a first fold the proposed system exploits ontology-based similarity model and count based similarity model for measuring document similarity. In a second fold, the proposed system exploits ontology and corpus to estimate the document similarity. Due to the hybrid approach the proposed system achieves high accuracy in document similarity estimation.

## REFERENCES

[1] D. Michie, "Return of the Imitation Game," *Electronic Trans. Artificial Intelligence*, Vol. 6, No. 2, pp. 203-221, 2001.

[2] E.K. Park, D.Y. Ra, and M.G. Jang, "Techniques for Improving Web Retrieval Effectiveness," *Information Processing and Management*, Vol. 41, No. 5, pp. 1207-1223, 2005.

[3] T.A.S. Coelho, P.P. Calado, L.V. Souza, B. Ribeiro-Neto, and R. Muntz, "Image Retrieval Using Multiple Evidence Ranking," *IEEE Trans. Knowledge and Data Eng.*, Vol. 16, No. 4, pp. 408-417, 2004.

[4] J. Atkinson-Abutridy, C. Mellish, and S. Aitken, "Combining Information Extraction with Genetic Algorithms for Text Mining," *IEEE Intelligent Systems*, Vol. 19, No. 3, 2004.

[5] Moldovan, Dan I., and Rada Mihalcea. "A WordNet-Based Interface to Internet Search Engines", *Proceedings of the Eleventh International FLAIRS Conference*, pp. 275-279, 1998

[6] G. Erkan and D.R. Radev, "LexRank: Graph-Based Lexical Centrality As Saliency in Text Summarization," *J. Artificial Intelligence Research*, Vol. 22, pp. 457-479, 2004.

[7] Y. Ko, J. Park, and J. Seo, "Improving Text Categorization Using the Importance of Sentences," *Information Processing and Management*, Vol. 40, pp. 65-79, 2004.

[8] Y. Liu and C.Q. Zong, "Example Based Chinese English MT," *IEEE Proceedings IEEE Int'l Conf. Systems, Man, and Cybernetics*, Vol. 1-7, pp. 6093-6096, 2004.

[9] Jacob B, Benjamin C(2008) "Calculating the Jaccard Similarity Coefficient with Map Reduce for Entity Pairs in Wikipedia", <http://www.infosci.cornell.edu/weblab/papers/Bank2008.pdf>

[10] Metzler, D., Bernstein, Y., Croft, W., Moffat, A., and Zobel, J. "Similarity measures for tracking information flow" *Proceedings of CIKM*, 517- 524, 2005.

[11] Dolan, W., Quirk, C., and Brockett, C. Unsupervised construction of large paraphrase corpora: Exploiting massively parallel new sources" In *Proceedings of the 20th International Conference on Computational Linguistics*, pp. 350- 356, 2004

[12] Allan, J., Bolivar, A., and Wade, C. "Retrieval and novelty detection at the sentence level" In *Proceedings of SIGIR'03*, 314-321, 2003.

[13] Hoad, T. and Zobel, J. "Methods for identifying versioned and plagiarized documents" *Journal of the American Society of Information Science and Technology*, Vol. 54, No. 3, pp. 203-215, 2003

[14] Chukfong H., Masrah A. Azmi M., Rabiah A. K, Shyamala C. Doraisamy. "Word sense disambiguation based sentence similarity", *Proceedings of the 23<sup>rd</sup> International Conference on Computational Linguistics*, pp. 418-426, 2003

[15] Tversky, A. "Features of similarity Psychological Review", Vol. 84, No. 4, pp. 327-352, 1977

[16] Shepard, R. N. and Arabie, P. "Additive clustering representations of similarities as combinations of discrete overlapping properties" *Psychological Review*, Vol. 86, No. 2, pp. 87-123, 1979

[17] Rohde, D. L. T. "Methods for binary multidimensional scaling" *Neural Computation*, Vol. 14, No. 5, pp. 1195- 1232, 2002.

[18] Lee, M. D. and Navarro, D. J. "An Empirical Evaluation of Models of Text Document Similarity" *The annual conference of the Cognitive Science Society*, pp. 1254- 1259, 2002.

[19] Yun .M, Jie L, and Zhengtao Y. "Concept Name Similarity Calculation Based on Wordnet and Ontology", *Journal of software*, Vol. 8, No.3, pp.746- 753, 2013.

[20] Rushdi S, and Adel E. "A Corpus-based Evaluation of a Domain-specific Text to Knowledge Mapping Prototype", *Journal of computers*, Vol. 5, No.1, pp. 69- 80, 2010.

[21] Deerwester, Scott C., et al., "Indexing by latent semantic analysis" *Journal of the American Society for Information Science*, Vol.41, No.6, pp. 391-407, 1990

[22] Royer, and Christiaan, "Term representation with generalized latent semantic analysis" *proceedings in Recent Advances in Natural Language Processing*, Vol.292, No. 45, 2005

[23] Gabrilovich, Evgeniy, and Shaul Markovitch. "Computing Semantic Relatedness Using Wikipedia-based Explicit Semantic Analysis", *Proceedings of the 20th International Joint Conference on Artificial Intelligence*, Vol. 7, pp. 1606-1611, 2007.

- [24] Qin, P., Lu, Z., Yan, Y., et al., "A new measure of word semantic similarity based on WordNet hierarchy and DAG theory", *International Conference on IEEE Web Information Systems and Mining*, pp. 181-185, 2009.
- [25] May Sabai Han, "Semantic Information Retrieval based on Wikipedia Taxonomy", *International Journal of Computer Applications Technology and Research*, Vol. 2, No.1, pp 77-80, 2013
- [26] Sanchez, David, Montserrat Batet, et al., "Ontology-based semantic similarity: A new feature-based approach", *Expert Systems with Applications*, Vol. 39, No. 9, pp.7718- 7728, 2012.
- [27] Zhang, Ce, et al., "Semantic similarity based on compact concept ontology" *Proceedings of the 17<sup>th</sup> international conference on World Wide Web*, ACM, pp. 1125-1126, 2008.
- [28] Oleshchuk, Vladimir, and Asle Pedersen. "Ontology based semantic similarity comparison of documents", *IEEE proceedings of 14th International Workshop on Database and Expert Systems Applications*, 2003.
- [29] Tous, Rubén, and Jaime Delgado, "A vector space model for semantic similarity calculation and OWL ontology alignment" In *Database and Expert Systems Applications*, Springer Berlin Heidelberg, Vol.4080, pp. 307-316, 2006.
- [30] Peter D. Turney, "Measuring Semantic Similarity by Latent Relational Analysis", *Proceedings of the 19th international joint conference on Artificial intelligence*, pp. 1136-1141, 2005.
- [31] Emiliano Giovannetti, Simone Marchi, and Simonetta Montemagni, "Combining Statistical Techniques and Lexico -syntactic Patterns for Semantic Relations Extraction from Text", *SWAP 2008*
- [32] Liu, Gang, Ruili Wang, Jeremy Buckley, et al., "A WordNet-based Semantic Similarity Measure Enhanced by Internet-based Knowledge", In *SEKE*, pp. 175-178, 2011.
- [33] Jiang, Jay J., and David W. Conrath. "Semantic similarity based on corpus statistics and lexical taxonomy", *arXiv preprint cmp-lg/9709008*, 1997.

# A Novel Approach for Submission of Tasks to a Data Center in a Virtualized Cloud Computing Environment

B.Santhosh Kumar

Dept. of Computer Science and Engineering  
G. Pulla Reddy Engineering College  
Kurnool, India

Dr. Latha Parthiban

Dept. of Computer Science  
Community College, Pondicherry University  
Pondicherry, India

**Abstract**—The submission of tasks to a data center plays a crucial role to achieve the services like scheduling, processing in a cloud computing environment. Energy consumption of a data center must be considered for task processing as it results in high operational expenditures and bad environmental impact. Unfortunately, none of the current research works focus on energy factor while submitting tasks to a cloud. In this paper a framework is proposed to select a data center with minimum energy consumption. The service provider has to register all the data centers in a registry. The energy consumed by task processing using virtualization and energy of IT equipments like routers, switches is calculated. The data center selection framework finally selects the data center with minimum energy consumption for task processing. The experimental results indicate that the proposed idea results in a less energy when compared to the existing algorithms for selection of data centers.

**Keywords**—Energy consumption; Virtualization; Data Center Selection Framework

## I. INTRODUCTION

Cloud computing is growing predominantly because of the pay-as-you go model [1]. According to Gartner Report the cloud services expanded in to a \$210 billion market by the year 2016 [2]. Infrastructure maintenance is done by service providers while the actual development can be concentrated by the companies [3]. Data centers consume a lot of energy for storage and processing of data. The energy consumption of cloud infrastructure has been growing extensively and by the year 2020 it is expected to reach 1,963.74 terawatt-hours (TWh) [3]. The data centers growth rate is around 9 percent every year and hence the energy demands are also doubled in the last five years [4]. The heavy energy consumption of data Centers result in growth of operational expenses and also result in environment pollution due to excess of carbon emissions.

The tasks submission can be done in such a way that the data center with minimum energy consumption can be preferred over others for processing. To the best of our knowledge the existing algorithms don't concentrate on energy consumption. The algorithms often used in literature are outlined below:

1) **Spot electricity prices:** In this procedure the current electricity consumed by the data centers are taken in to

account and the tasks submission is done by predicting the future variations in the electricity prices. The data center with minimum electricity consumption is preferred. The drawback of this approach is it considers various non processing elements like lights, air conditioning units .., for selection of data centers.

2) **Shortest Distance First:** This algorithm forwards the request to the closest data center from the point of origin. The disadvantage is it does not take in to account the energy consumption which is relatively expensive when compared to the network elements like routers, bridges.., required to expedite the process of forwarding requests to the data centers.

3) **Round Robin Technique:** This algorithm chooses a data center randomly within a region where the request is originated. It might lead to a delay factor and the energy factor is also not considered.

To overcome the shortcomings in the existing approaches a data center selection framework (DCSF) is proposed which will calculate the energy used for processing of tasks. The execution time of the tasks and the energy consumed by the virtual machines are considered for calculation. The tasks are forwarded to the data center with minimum energy consumption. The procedure is simulated and compared with the existing algorithms. The results indicate that the proposed approach consumes less energy when compared to the others.

## II. RELATED WORK

Many algorithms have been proposed for data center selection for task processing. Service broker routing policy is proposed in [5], [6] where the cloud analyst tool has been used. A probability based approach has been suggested in [7]. The research works in [8],[9] mainly focused on cost effective data center selection which take in to account the equipments needed to setup the data centers. A matrix based approach including the resources needed for data centers is discussed in [10]. The work in [11] signifies the expenditure spent on energy consumption for selection of data centers. A general data center selection approach based on factors like location, proximity is implemented in [12]. The algorithms in [13], [14] mainly concentrates on round robin and shortest job first approaches to select the data centers for processing. The virtualization technology which improves the task processing

capability is not given much importance in all these proposed works.

The importance of virtualization in cloud environment has been highlighted in [15]. Effective resource utilization using virtualization is discussed in [16], [17], [18] which focused on optimal allocation of resources to virtual machines. The scheduling of virtual machines for efficient energy consumption is formulated in [19] but it does not take into account the current energy being consumed by virtual machines. All the existing works concentrated on data center selection based on either random allocation or proximity and the energy consumption was given least importance. In the current work a framework is developed which focuses on the virtual machines consuming energy for processing of tasks.

### III. PROPOSED WORK

In General the tasks generated by the users are transferred to the web servers situated at different locations which in turn route them to the data centers for processing. The current work forwards the tasks to a data center selection framework (DCSF) which calculates the energy consumed by different data centers and decides the one for which the tasks must be submitted for processing. The general depiction of the scenario is illustrated using Fig. 1.

TABLE I. DATA CENTER REGISTRY CONTENTS

Data Center ID (DCID)	No. Of Servers (NS)	No. Of Routers (NR)	No. Of Switches (NSW)	Total Energy Consumed (E <sub>Tot</sub> )

A user base (UB) is a region situated around the globe where a lot of users are submitting the tasks to the service provider.

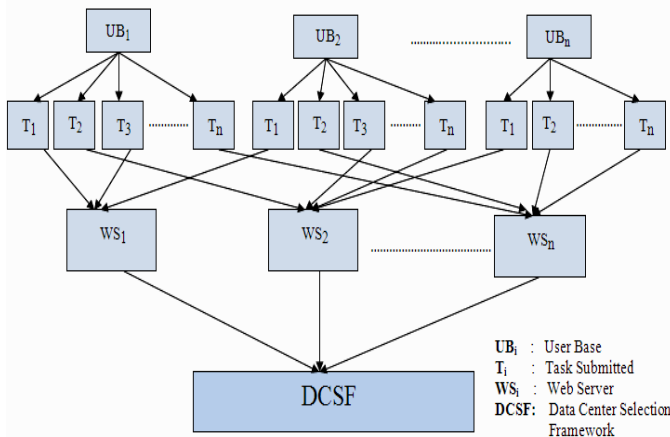


Fig. 1. Tasks Submission Process

Each data center is registered by the service provider in data center registry (DCR) as illustrated in Table I. A Data Center Id (DCID) is stored as a 16 bit number in which the first 4 bits represents service provider Id and the remaining 12 bits are allotted to data center id which should be a unique

number generated by the service provider. The information regarding number of servers, routers, switches..., in a data center has to be updated by the service provider. The total energy consumption is calculated and corresponding value is stored in DCR for further processing.

#### A. Data Center Selection Framework

The selection of data center is done by the Data Centre Selection Framework (DCSF) which is depicted in Fig. 2. Initially the tasks submitted to DCSF are stored in a Wait Queue. As soon as the tasks are removed from Ready Queue for processing then the tasks are allotted from Wait Queue into Ready Queue. A threshold value (Th) is considered depending upon the traffic received by the DCSF.

If the no. of tasks ( $\lambda$ ) in Ready Queue > Th or the Time > 60s whichever condition is met earlier then the tasks are assigned to Task Allocator (TA). Then TA sends a request to Energy calculator Module (EC) where the total energy consumed by the data centers is calculated and the data center with minimum energy consumption is given the tasks for processing. The required information such as data center Id, no. of servers... is obtained from DCR. The server energy module (SEM) calculates the total energy consumed by the servers of data centers while the energy consumed by IT equipment is calculated by IT energy consumption (ITE) module.

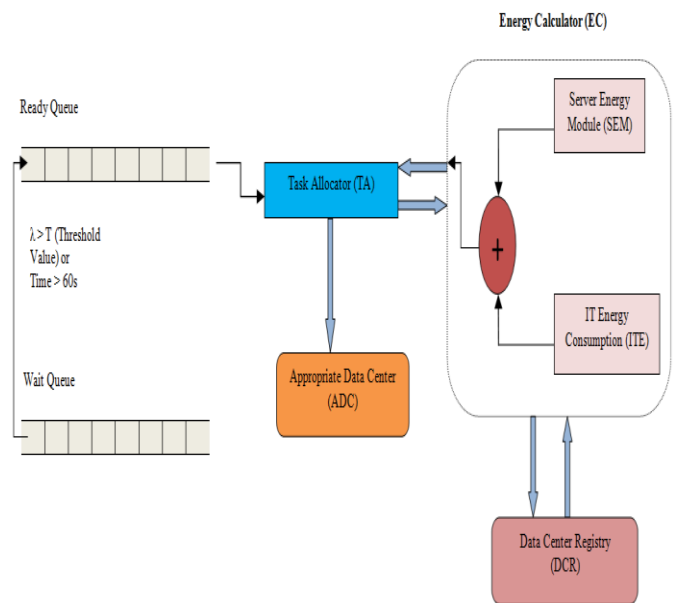


Fig. 2. Data Center Selection Framework

Finally the data center with minimum energy consumption is selected for task processing and the tasks are forwarded by TA to the appropriate Data center (ADC) depending upon its DCID.

#### a) Server Energy Module

In order to process the tasks efficiently and rapidly virtualization technique is employed in the servers of data centers. It also reduces the energy consumption of servers and increases the resource utilization. Multiple virtual machines are created on the same physical host thus increasing the

processing power of a server. Hence the energy consumption of the servers is obtained by the total energy consumed by execution of the tasks on virtual machines.

Let  $S = \{S_1, S_2, S_3 \dots S_n\}$  be the set of servers located in a data centre  $DC_i$ . For each server  $S_k$  Let  $VM_k = \{VM_{1k}, VM_{2k} \dots VM_{nk}\}$  be the set of virtual machines created. A decision variable  $x_{ijk}$  is set to 1 if task  $T_i$  is allotted to virtual machine  $VM_{jk}$  for processing. Let  $EC_{ijk}$  be the energy consumed by task  $T_i$  running on VM  $VM_{jk}$  and let  $ET_{ijk}$  be the execution time. The energy consumption rate of the VM is denoted by  $ECR_{ijk}$  and energy consumption  $EC_{ijk}$  can be calculated as follows:

$$EC_{ijk} = ECR_{ijk} \times ET_{ijk} \quad (1)$$

Where  $ET_{ijk} = ft_{ijk} - st_{ijk}$  (finish time – start time)

Hence using (1) the total energy consumption can be calculated as follows:

$$TE_1 = \sum_{k=1}^{|S|} \sum_{j=1}^{|VM_k|} \sum_{i=1}^{|T|} x_{ijk} \times EC_{ijk} \quad (2)$$

Where  $|T|$  Indicates Total no. of tasks submitted to  $VM_k$

#### b) IT Energy Consumption Module

The no. of switches (NSW) and routers (NR) is obtained from DCR and the energy consumption is obtained by utility meter. The total energy consumed by IT equipments is given by  $TE_2$  by equation (3)

$$TE_2 = NSW \times E_{SW} + NRT \times E_{RT} \quad (3)$$

Where  $E_{SW}$  is the avg. energy consumed by a switch and  $E_{RT}$  is the avg. energy consumed by a router of the data center. The output obtained by the two modules is combined to get the total energy ( $E_{Tot}$ ) of the data center.

$$E_{Tot} = TE_1 + TE_2 \quad (4)$$

The total energy consumed ( $E_{Tot}$ ) is updated in the DCR and the data center with the minimum  $E_{Tot}$  is selected as the appropriate data center (ADC) for tasks submission. The entire procedure can be illustrated in the following algorithm.

#### B. Data Center Selection Algorithm

```

START
 For Each Service Provider SP
 Register Each Data Centre DC_i in Data Centre Registry
 Registry DCR as in Table 1
 End For
 Initialize Ready Queue $RQ \leftarrow Null$,
 Size $(RQ) \leftarrow$ Threshold Value (Th) ,
 Wait Queue $WQ \leftarrow Null$
 For Each Task T_i submitted by User Base UB_i
 Assign $WQ \leftarrow T_i$

```

**If**  $RQ$  is Null **Then** Assign  $RQ \leftarrow WQ$

Until no. of tasks  $(\lambda) > \text{Size}(RQ)$

**End If**

End For

**If**  $\lambda > \text{Size}(RQ)$  or Time  $> 60s$

Request Task Allocator  $TA$  to find Data Centre (ADC).  $TA$  assigns the request to Energy Calculator (EC) which retrieves each  $T_i$  from  $R$  and Perform the following computations:

$$|S| \quad |VM_k| \quad |T|$$

$$TE_1 = \sum_{k=1}^{|S|} \sum_{j=1}^{|VM_k|} \sum_{i=1}^{|T|} x_{ijk} \times ECR_{ijk} \times ET_{ijk}$$

$$TE_2 = NSW \times E_{SW} + NRT \times E_{RT}$$

$$E_{Tot} = TE_1 + TE_2$$

$$ADC \leftarrow DCID(\min(E_{Tot}))$$

**End If**

**For** Each Task  $T_i$ ,  $TA$  does

Assign  $ADC \leftarrow T_i$  for Processing

End For

END

#### IV. PERFORMANCE ANALYSIS

##### A. Analysis using real world trace logs

The proposed algorithm is evaluated by using the real world trace obtained from Google cloud trace logs [20]. The log contains information regarding 25 million tasks that were submitted for a period of 29 days. The analysis is done only by considering the tasks submitted to the cloud system in the first 5 hours of the day number 18. Fig. 3 illustrates the count of tasks submitted in every 60 seconds in those 5 hours. The count of the tasks is over 200 thousand.

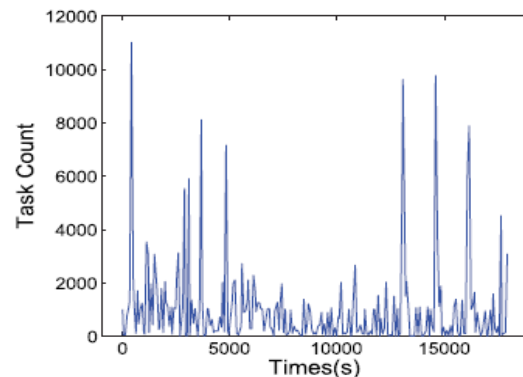


Fig. 3. Tasks Submitted to Cloud

The execution times of the tasks have been calculated by obtaining the start time and finish time from the logs. The sample data for our analysis is depicted in Table II. In order to understand easily the data center Ids are assumed as  $DC1 \dots DC5$ , instead of binary format. The units of energy consumption are in KWh. The metrics considered for analysis

of the algorithms are Total Energy Consumption (TOT) and Energy Consumption per Task (ECT).

TABLE II. DATA FOR SIMULATION

Data Center ID (DCID)	No. Of Servers (NS)	No. Of Routers (NR)	Energy Consumed per Router ( $E_{Rt}$ )	No. Of Switches (NSW)	Energy Consumed per Switch ( $E_{Sw}$ )
DC1	45	35	1.5	300	2.5
DC2	32	23	1.75	225	2.2
DC3	48	28	1.9	143	2.7
DC4	38	32	2.1	345	2.1
DC5	40	27	2.3	173	2.9

The proposed work Data center selection framework (DCSF) is compared with the Shortest Distance First (SDF) and Round Robin (RR) algorithms and the results are depicted in Fig. 4 and Fig. 5. When compared with the existing algorithms the total energy consumption is far less in the proposed approach. The data center DC4 is assumed to be shortest distance data center when compared to the others.

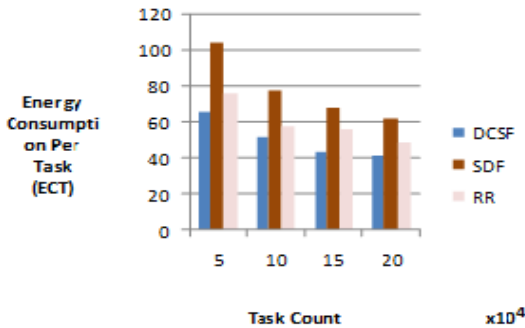


Fig. 4. Analysis using ECT metric

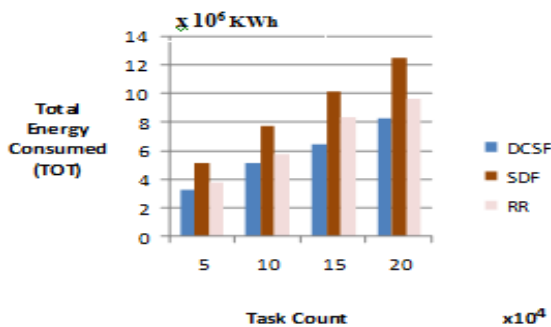


Fig. 5. Analysis using TOT metric

B. Analysis Using Node Red

The requests are generated as shown in Fig. 3 using Apache JMeter tool. All the threads generated by JMeter are created using algorithms of computer science like graph theory, data structures..., and submitted to three data centers.

```
[{"id": "5dd2be7.f22d4", "type": "serial-port", "z": "", "serialport": "/dev
/ttyUSB0", "serialbaud": "57600", "databits": "8", "parity": "none", "stopbits": "1", "newline": "\n
", "bin": "false", "out": "char", "addchar": "false", {"id": "5d9f1647.8da548", "type": "serial
in", "z": "d1767f1.cc1968", "name": "CurrentCost
Envir", "serial": "5dd2be7.f22d4", "x": 298, "y": 161, "wires": [{"2e38cccb.02c6b4"}]},
{"id": "1656c54c.43f1eb", "type": "function", "z": "d1767f1.cc1968", "name": "extract
watts", "func": "/* sample message\n(Object) {\n \"msg\": {\n \"src\": [\"CC128-
v0.11\"]\n, \"deb\": [\"00600\"]\n, \"time\": [\"19:04:49\"]\n, \"tmpr\": [\"18.3
\"]\n, \"sensor\": [\"0\"]\n, \"id\": [\"02902\"]\n, \"type\": [\"1\"]\n, \"ch1\":
[\"watts\": [\"00023\"]]\n}\n}\n*\n\nvar reading = msg.payload\n\n//ignore if history
packet\nif (reading.msg.hist) (return null;)\n\nmsg.payload = {};\n\nmsg.payload.sensor =
reading.msg.sensor[0]*1;\n\n// This is the temperature of the Envir base station, not the
sensor.\n\nmsg.payload.temperature = reading.msg.tmpr[0]*1;\n\nmsg.payload.watts =
reading.msg.ch1[0].watts[0]*1;\n\nreturn msg;
\", \"outputs\": 1, \"noerr\": 0, \"x\": 625, \"y\": 161, \"wires\": [{"d8e625b9.46a778"}]},
{"id": "d8e625b9.46a778", "type": "debug", "z": "d1767f1.cc1968", "name": "", "active": "false", "compl
ete": "false", "x": 805.5, "y": 161, "wires":
[[]], {"id": "2e38cccb.02c6b4", "type": "xml", "z": "d1767f1.cc1968", "name": "", "x": 466.5, "y": 161, "
wires": [{"1656c54c.43f1eb"}]}}
```

Fig. 6. Node Red flow to read energy from a Server

The data centers are implemented using three Dell Power Edge C5220 Micro servers represented as DC1, DC2, and DC3. The data center capabilities such as virtualization, storage management are implemented using Windows Server 2012 R2 data center Operating System which is installed in the data centers. The Raspberry Pi chips are incorporated in each of the servers in the data centers so as to read the energy consumption.

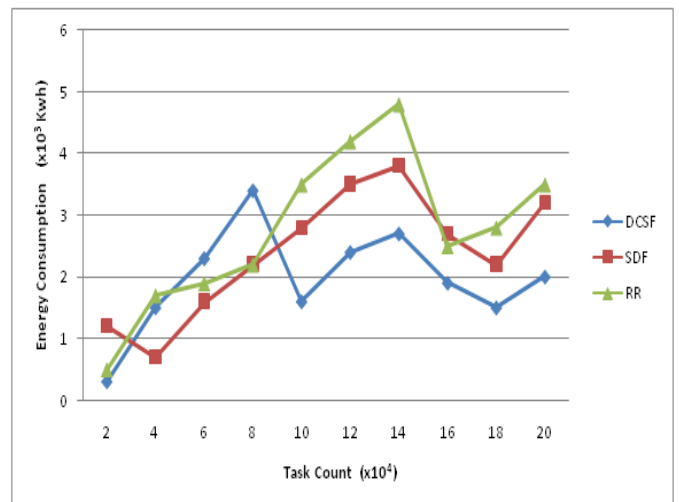


Fig. 7. Analysis using Node Red

The results obtained are illustrated in Fig. 7 which shows that the total energy consumed by the proposed framework is less than the energy consumption of the remaining algorithms. While the remaining algorithms like Shortest Distance First (SDF), Round Robin (RR) consume less energy at some instances, on an average the proposed framework DCSF results in low energy consumption.

V. CONCLUSION

In this paper a framework is implemented for selection of data centers based on minimum energy consumption of data centers for task processing. The total energy is calculated by summation of the server energy consumption and IT equipment energy calculation. The server energy is obtained by combining the energy consumed by virtual machines for task processing. The results are obtained by simulation of real

world cloud trace logs and Node-red tool. The obtained results indicate that the proposed framework outperforms the already existing algorithms for selection of data centers. This work can be further extended by implementing the concept of Internet of Things using the IBM Bluemix tool.

#### REFERENCES

- [1] R. Buyya, C.S. Yeo, S. Venugopal, J. Broberg and I. Brandic, "Cloud Computing and Emerging IT Platforms: Vision, Hype, and Reality for Delivering Computing as the Fifth Utility," *Future Generation Computer Systems*, Vol.25, 2009, pp. 599-616.
- [2] "Gartner. Forecast overview: Public cloud services," Worldwide 2013-2019, 1Q15 update.
- [3] Greenpeace international, "Make IT Green, cloud computing and its contribution to climate change," 2010.
- [4] IBM, "IBM and Cisco: Together for a World Class Data Centre," 2013.
- [5] A.M. Manasrah, T.Smadi and A.ALmomanA, "A variable service broker routing policy for data centre selection in Cloud Analyst," *Journal of King Saud University*, Vol.28, 2016, pp.1-13
- [6] D.Kapgate, "Efficient Service Broker Algorithm for Data Centre Selection in Cloud Computing," *International Journal of Computer Science and Mobile Computing*, Vol.3, 2014, pp.355-365.
- [7] S.Yan, X.Wang, M.Razo, M.Tacca and A.Fumagalli, "Data centre selection: A probability based approach," in proceedings of 16<sup>th</sup> International Conference on Transparent Optical Networks, 2014, pp.1-5.
- [8] H.Xu and B. Li, "Cost Efficient Data Centre Selection for Cloud Services", in proceedings of 1<sup>st</sup> IEEE International Conference on Communications in China, 2012, pp.51-56.
- [9] P.M.Rekha and M.Dakshayini, "Cost Based Data Centre Selection Policy for Large Scale Networks," in proceedings of International Conference on Computation of Power, Energy, Information and Communication, 2014, pp.18-23.
- [10] A.Jaikar, G.Ryoon Kim and S.Young Noh, "Matrix-based Data Centre Selection Algorithm for a Federated Cloud," *International Journal of Multimedia and Ubiquitous Engineering*, Vol.9, 2014, pp.143-148.
- [11] K.S.Swe Myint and T.Thein, "Energy and Cost Efficient Data Centre Selection for Cloud Services," in proceedings of 3rd International Conference on Computational Techniques and Artificial Intelligence, 2014, pp.35-38.
- [12] H. Xu and B.Li, "A General and Practical Data Centre Selection Framework for Cloud Services," in proceedings of IEEE 5<sup>th</sup> International Conference on Cloud Computing, 2012, pp.9-16.
- [13] V.Sharma, Dr. Rakesh and S.Bol, "Round-Robin Data Centre Selection in Single Region for Service Proximity Service Broker in Cloud Analyst," *International Journal of Computers and Technology*, Vol.4, 2013, pp.254-260.
- [14] D.Chudasama, N.Trivedi and R.Sinha, "Cost effective selection of Data centre by Proximity-Based Routing Policy for Service Brokering in Cloud Environment," *International Journal of Computer Technology and Applications*, Vol.3, 2012, pp.2057-2059.
- [15] K.Shyamala and R.T.Sunitha, "An analysis on efficient resource allocation mechanisms in cloud computing," *Indian Journal of Science and Technology*. Vol.8, 2015, pp.814-821.
- [16] I. Goiri, J.L. Berral, J.O. Fit\_o, F. Juli\_a, R. Nou, J. Guitart, R. Gavalda and J. Torres, "Energy-Efficient and Multifaceted Resource Management for Profit-Driven Virtualized Data Centres," *Future Generation Computer Systems*, Vol.8, 2012, pp.718-731.
- [17] Z.Xiao, W.Song and Q.Chen, "Dynamic Resource allocation using virtual machines for cloud computing environment," *IEEE Transactions on Parallel and Distributed Systems*, Vol.24, 2013, pp.1107-1117.
- [18] C.Papagianni, A.Leivadreas, S.Papavassiliou, V. Maglaris, C.Cervello and A.Monje, "On the optimal allocation of resources in cloud computing Networks," *IEEE Transactions on Computers*, Vol.62, 2013, pp.1060-1071.
- [19] D.Jiankang, W.Hongbo, L.Yangyang and C.Shiduan, "Virtual machine scheduling for improving energy efficiency in IaaS cloud", *China communications*, Vol.11, 2014, pp.1-12.
- [20] GoogleClusterDataV2[Internet], 2011 Available from: [http://code.google.com/p/googleclusterdata/Wiki/ClusterData2011\\_1](http://code.google.com/p/googleclusterdata/Wiki/ClusterData2011_1)

# Evaluation of Wellness Detection Techniques using Complex Activities Association for Smart Home Ambient

<sup>1</sup>Farhan Sabir Ujager, <sup>\*1</sup>Azhar Mahmood, <sup>2</sup>Shaheen Khatoun, <sup>1</sup>Muhammad Imran, <sup>1</sup>Umair Abdullah

<sup>1</sup>Department of Computer Science, SZABIST, Islamabad, Pakistan

<sup>2</sup>College of Computer Science, King Faisal University, Al Hassa, Saudi Arabia

**Abstract**—Wireless Sensor Network based smart homes have the potential to meet the growing challenges of independent living of elderly people in smart homes. However, wellness detection of elderly people in smart homes is still a challenging research domain. Many researchers have proposed several techniques; however, majority of these techniques does not provide a comprehensive solution because complex activities cannot be determined easily and comprehensive wellness is difficult to diagnose. In this study's critical review, it has been observed that strong association lies among the vital wellness determination parameters. In this paper, an association rules based model is proposed for the simple and complex (overlapped) activities recognition and comprehensive wellness detection mechanism after analyzing existing techniques. It considers vital wellness detection parameters (temporal association of sub activity location and sub activity, time gaps between two adjacent activities, temporal association of inter and intra activities). Activity recognition and wellness detection will be performed on the basis of extracted temporal association rules and expert knowledgebase. Learning component is an important module of our proposed model to accommodate the changing trends in the frequent pattern behavior of an elderly person and recommend a caregiver/expert to adjust the expert knowledgebase according to the found abnormalities.

**Keywords**—Wellness detection; Elderly people; WSN Smart homes; Activity recognition

## I. INTRODUCTION

World population is increasing and according to the World Health Organization (WHO) elderly people population will also increase drastically in the near future [1]. Independent living is a concept that defines a person can live alone without any assistance of any other human being (care giver). Automated mechanisms for the monitoring of an individual are required to ensure the wellness of the elderly person. This monitoring should be accurate, error free and automated (without any human involvement) for an independent living ambient.

Elderly people have health related issues with the age such as limitations in physical functions, different diseases such as Alzheimer's disease, diabetes, cardio vascular disease. Smart homes technologies have potential to meet the emerging challenges of elderly people independent livings with enhance quality of life.

Wireless sensor network is a vital component of smart home for monitoring of the elderly persons. Variety of sensors deployed all over the house for monitoring purpose such as in electric appliances, gadgets and objects of daily usage for the monitoring of elderly persons as reported in [2].

Activity recognition is one of the active areas of research domain. The aim is to recognize the actions an individual takes to conduct an act of daily living. Most of the researcher have divided these actions into a set of defined activities and termed them "Activities of daily living". This concept was originally proposed in 1950 [3]. There are broadly three categories of activities. These categories are concurrent activities, interleaved and simple atomic activities as reported in [4]. However, most of the literature does not consider all type of activities for their activity recognition and wellness detection of elderly people in smart homes ambient.

Frequent pattern of an individual exists while conducting a specific activity, resulting in sequential frequent pattern as reported [1, 5, 6]. There is a strong association among sub-activities and locations where the sub activity is being performed, time duration taken to perform a specific sub activity and specific day of time [7-9]. Wellness detection is determined, when an individual deviates from its sequential frequent pattern among sub activities, individual is not conducting a specific activity on a specific location.

Accurate wellness detection is a challenging research area, several researchers have employed artificial intelligence and machine learning techniques (such as artificial neural networks, support vector machines, Naïve Bayes) as a classifier for the determination of wellness of elderly people in [9, 10]. Few researchers have also proposed fuzzy rules based classifiers for the activity detection and wellness determination of elderly people in smart home environments [11]. In probabilistic approaches, Markov and Hidden Markov models, where each sub activity is considered as a component of main activity for the activity recognition. Human activities pattern rely on temporal sequence as reported in [10, 12, 13]. Similarly data mining techniques also attracted many researchers to explore for the activity recognition and wellness detection, such as classification techniques, association rule mining techniques and clustering techniques, as reported in [1, 5, 10]. However, wellness detection is a complex research problem; many researchers proposed hybrid models to achieve the said

objective. There are few hierarchal models proposed for wellness and activity detection [6, 14].

In this paper, we have proposed an association rules based model with the following contribution:

- Temporal association of sub activity and their location
- Time gaps between two adjacent activities consideration
- Temporal association of inter and intra activities
- Learning module
- Recommendations to the caregiver or expert

Rest of the paper is organized as follow: Section II summarizes literature review and highlighting strength and weakness of existing technique by critically analyzing them in tabular formats. In section III a new model is proposed to address the limitation of existing techniques. Finally, paper is concluded and future work is presented in section IV.

## II. RELATED WORK

Wellness detection is a complex and challenging research domain. Majority of proposed models does not provide a comprehensive solution from different perceptive of wellness and activity detection.

J. Wen., et al [15], proposed a model based on weighted frequent pattern (association mining). The objectives of this model is to find the association rules of activities performed by the elderly person, and build a classifier which is based on these extracted association rules. However, time series analysis of activities with the location of activities is not considered. M.T Moutacalli., et al [5], have employed frequent pattern mining for the determination of activity recognition and wellness detection. In proposed model, association mining is performed for extraction of homogenous frequent pattern activity model. The strength of this work is that this model considers event duration and time gap between adjacent activities. However, this model cannot recognize complex activities. S.T.Bourbou., et al [10] proposed a hybrid model based of association mining and AAN. The proposed model consists of two steps of repeated activity discovery by using FP growth algorithm and clustered these patterns into activities using K-pattern algorithm. ANN based classifier is used for the classification of the activities. However, integration of multiple techniques into a single model makes the whole process difficult and complex to implement. L.G. Fahad., et al [6] proposed a hybrid hierarchal model based on frequent patterns and probabilistic approach to find the activity tasks. Frequent pattern mining is being conducted to extract the inhabitant behavior pattern. However, it is a tedious task to create routine tasks lists manually. This model does not follow temporal analysis for wellness determination. S.Nasreen., et al [16], a hybrid model is proposed based on Association rules for inhabitant pattern. These association rules are used for the assignment of activity category when new activity arrives as an input. Binary support vector machine is used to detect correct or incorrect assignment. However, inter and intra relationship of activities has not been considered. L.G. J. Saives., et al [17] have proposed a hybrid model based on association rule mining

and extended finite automata for the mapping of activities found from the association rule mining. However, prior knowledge is required and temporal deviations are not considered for wellness detection. Similarly repeated activities might not represent the same sequence of events.

A. Forkan., et al [11] proposed a probabilistic model to detect the abnormality in the activity build model, to identify the wellness of an elderly person. Hidden Markov Model (HMM) is used for the change detection in the activities of daily living along with identification of change in daily routine using statistical history and expert knowledgebase for abnormality detection. This model does not follow single wellness detection criteria which is the major contribution of this study. The outcome of each module is then serves as an input to fuzzy rules based classifier for the classification of activities and detection of abnormality. However, this model might have less acceptability for elderly as wearable sensors must be used for expert knowledgebase. Similarly, different modules working together making the process complex and prior knowledge is required as a statistical histories for the prediction and abnormality detection. Similarly N.K. Suryadevara [8], proposed another probabilistic model is for the prediction wellness in the smart home environment based on appliance usage. Two wellness functions been used. Irregular patterns will lead to the abnormality which helps to identify whether an elderly person is well or unwell. However, activities are presented in simple manner and appliance usage monitoring might not be suitable when the person is not using any specific appliance. F.Ordonez., et al [2], proposed a hybrid model which is based on training phase and classification phase. For temporal and sequential activities analysis Hidden Markov model is used. The objective of this study is to validate hybrid model performs better than single technique based model. It used Hidden Markov Model for training and for classification phase SVM reported better results. However, while validating the results for temporal and sequential activities, other sequential and association mining techniques were not considered. L.Kalra., et al [13], proposed two stage probabilistic model based on Markov model. The proposed model process the sensor data in two stages, in the first stage sensor data is analyzed for the patterns of activity events by using Markov Model. However, time gap between adjacent activities are not considered for the determination of wellness of elderly person. K. Gayathri., et al [14] proposed a probabilistic hierarchal model for abnormality detection to determine the wellness. This model combines the data and knowledge driven parameters by employing Markov logic networks for abnormality detection. This model considers location, object usage, time of usage for the abnormality detection. However, manual rules based systems requires effort to create knowledgebase. Sensor and data relationship is ignored.

E. Kim., et al [4] have discussed the uncertainty parameters in the wellness determination. This study serves as groundwork to develop diagnostic system. In [7], tree based regression algorithm is being proposed for the classification of activities in the training phase and in the later phase when new activity can be predicted as future activity. However, this model does not consider complex activities.

E. Nazerfard., et al [9] proposed an activity classification model based on Bayesian network. This proposed model proposes two steps of inference for the prediction of upcoming activity and its label. This model considers time analysis and activity features. However, complex activities are not considered for the prediction.

X. Hong., et al [18] proposed model based on time segmentation. The model extracts events that are associated with a complete activity. The first segmentation is location based, second segmentation is model-based, and third is based on modeling of each activity in terms of sensor activation to determine. The third proposed algorithm identifies the most predominate sensor in the activity to identify the event which that sensor exhibits. However in this approach, rules need to be defined manually for the activity discovery.

#### A. Critical Evaluation

In this sub section of literature review, critical evaluation is being conducted. Fifteen papers are represented in three different tables for the cumulative review of each literature under the set of predefined vital parameters.

Table.I represents the methodology of the proposed techniques for wellness and activity detection for smart home. Majority of the existing techniques aimed to extract elderly persons frequent behavior patterns, whether they have employed Hidden Markov model [2, 9, 10], [7] tree based regression analysis association rules or frequent pattern mining [5, 6, 15, 16] and deviation from this pattern leads to the abnormality. A proven technique should be employed for the extraction of frequent patterns of an elderly person, like frequent pattern or association mining.

Table.II represents the implementation details of existing techniques which helps to explain the implementation details, environment and validation. Majority of the proposed models have not validated and compared their results with the existing models and methods.

Table.III represents the vital parameters which are necessary for the wellness detection. These parameters have strong impact of elderly person's activities and wellness detection. In table.III, type of the activities which different proposed models have used in activity detection, similarly the association of intra and inter activities is necessary to understand pattern of elderly person behaviors. Time gap between adjacent activities is important criteria to measure the wellness of elderly person. Association of time with location is a necessary parameter to understand pattern where an individual will perform a specific activity. Temporal analysis is important criteria to understand the elderly person is also one of the most vital criteria to understand elderly person activity pattern.

### III. PROPOSED MODEL

In this section, a model is proposed for the wellness detection based on association rules mining and frequent patterns of the behavior of the elderly people. From the critical evaluation section it is evident that association exists among different parameters of activity recognition and wellness detection. Association rules between sub activities and location

of sub activities have been extracted from the sensor data, correlation among sub activities for as inter temporal association among sub activities rules are extracted and time gap between adjacent activities have proposed to be found to determine the wellness of elderly people. Model is proposed by considering all those parameter which were mainly ignored in existing literature such as detection of overlapped activities; location based association, intra and inters activities associations.

The proposed model consists of 9 modules, namely, data transformation module, sub activity (location and time) correlation module, time gap between two adjacent activities module, sub activity (sequence of sub activities and time) correlation module, sub activity (location and sequence of activities) correlation w.r.t time module, expert knowledgebase module, contextual database module, learning component and activity recognition module as shown in the Fig.1.

#### A. Data Transformation module

In smart home data is generated from the WSN's network. To make the sensor data suitable for processing, sensor data is transformed with labels (for example, if a person is sleeping, bed sensor is active, the activity will be marked as 'sleeping', time duration of this active sensor will be the duration of the activity and location of the sensor will be the location of activity). For example, an elderly person of a smart home wants to make coffee, he/she will achieve the said task in a series of sub activities for example: 1. Staring of stove, 2. Filling the pan with water, 3. Opening coffee jar and 4. Mixing coffee & water etc.

These steps are considered as sub activities and while making of coffee are considered as an activity. Similarly it is also important to consider time gap between two adjacent sub activities for the determination of wellness of an elderly person.

#### B. Temporal Association of sub activity's location and sub activities

For activity recognition and wellness detection it is important to determine and extract the association of each sub activity time duration with the location where that sub activity has been performed along with the day of time. Most frequent association rules are extracted by using FP-Growth. For example, the normal pattern of an individual sleeping routine at around 2200hrs in 'bedroom' for approximately 8 hours. If a person is in 'dining room' at around 2200hrs and duration of the activity is more than it should spend in the 'dining room' so the violation of rule will indicate that person is not well.

#### C. Sub activity (sequence of sub activities and time) correlation module:

For activity recognition the correlation of sequence of sub activities with their time duration is required to handle complex activities. As discussed earlier an activity consists of sequence of sub activities. An example is discussed earlier of coffee making. The correlation among the sub activities and time in 24hrs is determined by using Generalized Sequential Pattern mining (GSP) [19].The outcome of this process will be association rules (correlation among sub activities and time).

*D. Time gap determination of two adjacent activities over a specific time:*

The input of this process is sub activities labels and time duration to perform each sub activity to determine the time gap between two adjacent sub activities over a specific day of time. The benefit of this outcome is the determination of the wellness of an elderly person most of the literature surveyed has ignored this important wellness parameter. For example, a healthy person will perform sub activities in normal routine with a normal time gap between two adjacent activities, while an unhealthy elderly person might not execute the sub activities with the normal time gap.

*E. Sub activity (location, time gap and sequence of activities) correlation w.r.t time module:*

This module servers as global perceptive of activity, in this module activities rules are formulated from vital parameters of complete activity detection rules. In this module association rules of (location + time duration), association rules of sub activities and time gap between adjacent sub activities with respect to time of day respectively are correlated using association rule mining (using FP- Growth) to extract pattern of these vital parameter over a specific time of day. The outcome of this module will be association rules of the required parameters (location, time gap and sequence of sub activities) over a specific time of day to accurately determine the wellness of an elderly person. For example, a healthy person has a routine to wake up (S1) around (0700 – 0715hrs).

(T) in (location = bed room) (L1) , time gap from bed to washroom(L2) (45- 50s)(G1) and to the washroom (use of toilet (2 mins)(S2), use of tap (3 mins) (S3) time duration between these two adjacent activities is usually (30-45s) (G2) and then go the kitchen. In this brief example, the generated rule:

$$(S1, S2, S3) \wedge (L1, L2, L3) \wedge (G1, G2, G3) \wedge T \rightarrow \text{Activity}$$

For overlapped activities, a set of rules have same location and temporal association (location of sub activities and time of day) but different sequence of sub activities and different time duration between adjacent activities.

*F. Expert (medical) knowledgebase:*

This module will have hard rules for an individual from medical history perspective. This rules are the recommendation for an individual like walk time, sleep time (recommended).

*G. Database module*

In this module association rules which are extracted from above mentioned model will be saved in this module. Expert (medical) knowledgebase rules will also be saved. This module will serve as a rules repository for the online activity recognition module.

*H. Learning module:*

The learning module updates the existing set of rules by monitoring the sensor data streams and extracting the contextual spatial-temporal association of the changing trends in the behavior pattern of an elderly person. The learning component also monitors of the outcome of the online activity recognition and wellness detection module, on correct diagnoses the weight of the rule will increase and will have high priority. Similarly to accommodate the changing trends in the behavior pattern, rules will be updated in the database repository.

The second novel function of the learning module is to recommend the caregiver the abnormalities found in the inhabitant behavior to make necessary changes in the expert knowledgebase according to the recommendation.

*I. Online activity recognition and wellness detection module:*

In this module have the association rules generated and the hard rules of expert knowledge base will be mapped with sensor data. Data from the sensor network is coming to this module and data is being compared with knowledge base and association rules. If the rules are met for the input data the activities are considered normal and the elderly person is considered well. Incase rules are violated the elderly person is considered unwell.

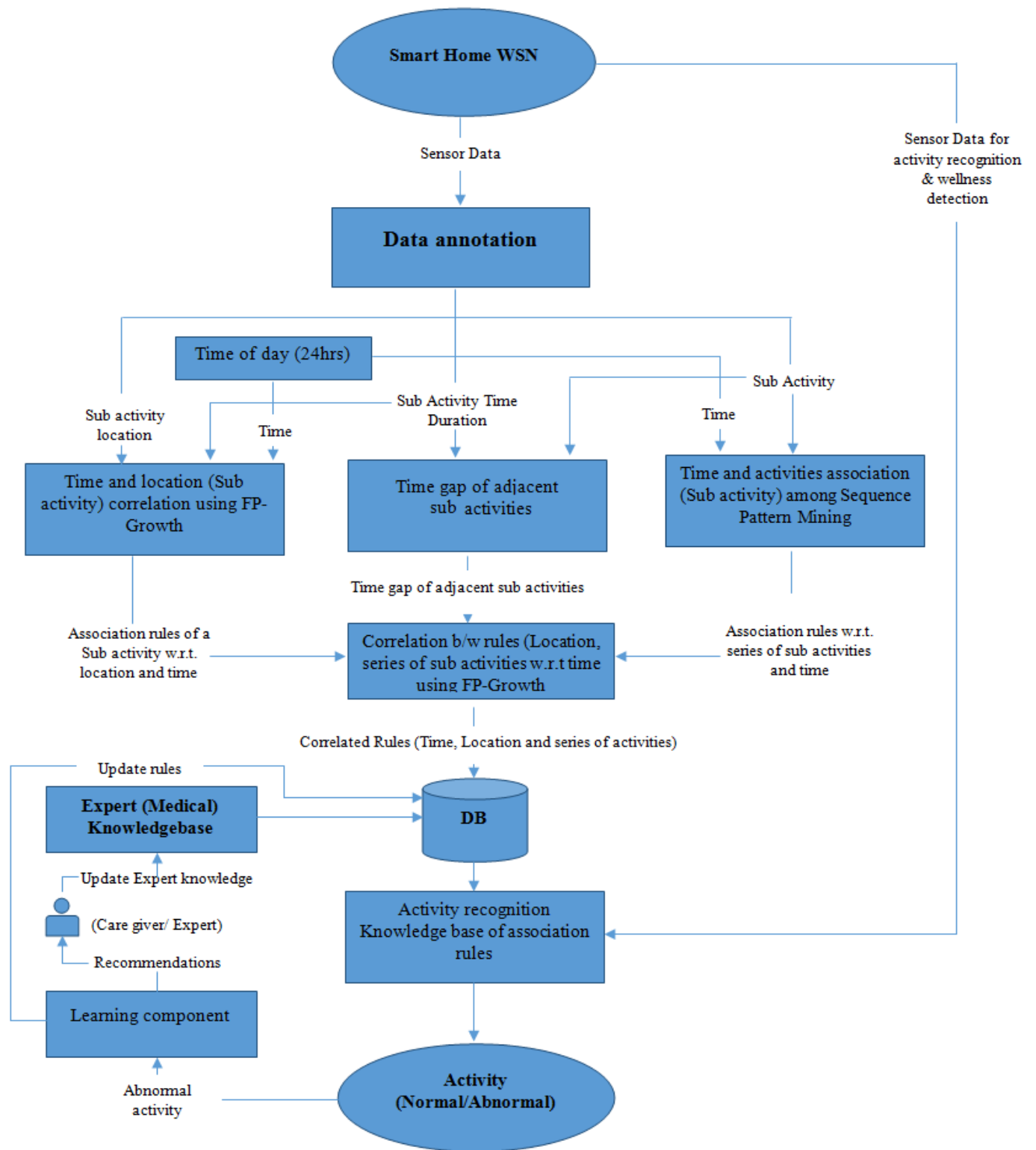


Fig. 1. Proposed Model View

TABLE I. CRITICAL EVALUATION OF RELATED WORK

Ref	Wellness determination Criteria	Approach\Algorithm	Study Characteristics	Main Outcomes	Strengths	Limitations	Suggestions
[15]	Detecting ADL activities	-Association rules btw activities -Build activity classifier over association rules -Classification of overlapped activities	Identification of frequent patterns based on Association rules.	- Use of global weight & local weight of the sensor events to differentiate the activities for overlapped activities. -The activities that have overlapped frequent patterns or even share the same frequent patterns can still be differentiated	- Overlapped ADLs are considered. - Results validated & Compared with existing techniques such as Decision Tree, Naïve Bayesian & HMM	- Hidden variables (such as interleaved activities) of ADLs are ignored -Time series analysis missing - Unable to detect complex activities	Association rules integration with HMM may produce better results in activity recognition. Fuzzy rules based classifier along with temporal mining helpful in determining complex activity recognition.
[5]	Detecting ADL activities (Alzheimer's disease)	-Frequent pattern Mining (time series analysis) -Wellness functions -Classification	(1) Transforming the temporal Db to non-temporal (2) Finding homogenous subsequence activities (3) Activity model: Classification of activities	-Present the various stages of Technological assistance & propose a new algorithm for the step of activities models detection	-Test bed implementation -Each concept is properly defined	- Activity time gap - Results are not compared & validated. - Dataset is not being discussed	Association rule mining along with the time series analysis should be considered while keep the event duration & gap among events.
[11]	Detecting abnormalities in ADLs	-Hidden Markov Model -Statistical estimations (Mean & standard deviations) - Fuzzy rule classifier	Learning techniques for predicting abnormalities & behavioral trends Hidden Markov Model based approach for detecting abnormalities (trained by Machine learning techniques) Fuzzy rule-based model for making the final guess	-HMM used to detect the anomalies in the ADLs -Fuzzy rule-based system gives output as whether the anomaly is true.	- Comprehensive ADLs monitoring - Different medical aspects are considering along ADLs	- Fuzzy rules are generated manually -Target user with many wearable sensors which periodically send different vital signs data of the user -Model is expensive & complex	Self-generated association fuzzy rule system can be a major improvement
[4]	Identification of activity recognition parameters & their impact of accuracy	-Fault tree analysis (FTA)	Uncertainty parameters & measures are discussed. Different models are taken into consideration TAM, GAM & SGAM for the analysis.	- Diagnostic accuracy measures of AR systems capable of pinpointing the sources of accuracy loss	- Introduced a method for uncertainty impact analysis, which for a given AR system, measures the impact of each uncertainty source on AR performance	Different datasets should be used for analysis Hybrid models are not considered for the analysis	Different datasets should have been used for the evaluation of identified measures & hybrid models are ignored while evaluating.
[7]	Activity forecasting & predicting the occurrence of future activities	-Regression-tree-based (Machine Learning technique)	Algorithm extracts high-level features from sensor events & inputs these features to a machine learning algorithm which forecasts when a target activity will next occur	-The proposed algorithm does not rely on a separate AR component, but rather derives feature attributes directly from sensor event data within the smart home	Well defined time boundaries of the activities & gap between activities are important to discover	- Complex ADLs are not considered -Activities time boundaries -Complex activities not considered	Hybrid approach, especially for the data preparation for the classifier & for the consideration of temporal element.
[8]	Abnormality identification	-Activity annotated via conditional probability method -Probabilistic method wellness determination	Behavior detection process based on the observed sensor data in performing essential daily activities	-A proposed framework to verifies the behavior of elderly at three different stages of daily living (usage of appliances, activity recognition & forecast levels)	-Trivial process -Experimental details are clear -Experimentation are conducted on five different dataset for validation -Prototype is developed	-Prior knowledge is required -Activities boundaries undefined - Energy inefficient - Simple activities	For efficient training period fixed rules & training should be implemented side by side & remove fixed rules by their application in the process.
[9]	Predicting future ADLs	- Bayesian network	An activity prediction model using Bayesian networks together with a novel two-step	- Predicting the start time of next activity -Activity label prediction based on features	-Physical implementation -Tested on three different elderly	-Prior knowledge is required -Different types	Association between sequences are necessary to find complex ADLs along

			inference process to predict both the next activity features & the next activity label		people -Results validated against existing approaches	of ADLs are not considered.	statistical methods such as Hidden Markov Method (HMM) is helpful in finding the hidden variables
[10]	User activity detection	-Pattern Clustering (K- Pattern clustering algo) along frequent pattern by FP growth & activity decision (ANN)	1. Frequent pattern are extracted using FP growth 2. Frequent pattern are clustered by using K-Pattern algo (for overlapping patterns in multiple clusters) 3. ANN for classification	-Activity recognition -Noisy data handling in datasets	-Considering both concepts of activity clustering & activity decisions	- For Learning part (ANN) will be expensive - Expensive processing as integrating multiple techniques together	To reduce the complexity, efficient classifiers can be used
[2]	Detecting ADLs	-Recognition of ADLs by using Hybrid approach -HMM is used as trainer of different ML techniques	HMM is used for dealing with temporal characteristics of sequential data. HMM is trained with the probabilistic classifier which is able to predict the given sample as a classifier	-Recognition of ADLs by using Hybrid approach -Hidden Markov model is hybrid & tested with different machine learning techniques	-Discussed in detail on ANN & SVM. -Raw data is represented in Raw, Change point, Last Sensor -Results validated with five different models	Prior expert knowledge is required for the system at the initial stage.	For efficient training period fixed rules & training should be implemented side by side & remove fixed rules by their application in the process
[13]	Detecting ADLs	- Markov Model - Hidden Markov Model	This study deals with learning user's daily behavior by markov model; it applies markov model in two level to first learn user's habits & then correct any misclassification of activity.	- To model each activity separately where sensors correspond to states (Markov Model) - To enhance accuracy & find inter-activity transition wrt time-dependent relationships between two contiguous activities (Hidden Markov Model)	- Temporal associations of ADLs are considered - Use of concurrent active sensors to train the activity model by considering sensor activations as the states for that model. - Evaluation perform over multiple datasets	-Time gap between two activities are not considered. -Different medical aspects are missing -Overlapped activities are not considered	Association rule mining can be helpful for finding the inter activities temporal association along HMM.
[18]	ADLs Detection	Evidential Activity Monitoring (Evidence Theory)	The architecture consists of two main processes, the detection process & the recognition process	-The detection process is responsible for the segmentation of sensor streams to detect activity occurrences (Evidence) - The segmented sensor streams are then used as inputs to the recognition process	-Sensor data as an evidence for an activity monitoring -Time series segment correlation with a complete activity -Considering correlations of locations, objects & sensors	-Single occupancy environment - Simple activities -The current study focuses only on the environmental activities	Correlations of locations, objects & sensors with activities can be found out using association rules & later used as evidence for evidential ontology network of activity
[17]	Detecting ADLs	Sequence pattern mining, Apriori Algo (discovery of habits) Extended Finite Automata (Map event to an activity model)	The proposed approach is used for over watching the disease evolution that can be characterized by behavior changes, to be helped by detecting the activities the inhabitant performs.	- Activity recognition by sequence pattern mining - Activity model by EFA - A method to build a model representing recommendations from the medical staff, so that the recognized activities & behavior deviations of the inhabitant can be detected	-Claims to have no prior knowledge for activity discovery -Real time activity recognition -Case studies discussion w.r.t to proposed approach	-No temporal deviations -Repeated activities might not be presented by the same series of events -Healthcare contextual features	Time series analysis along with the proposed solution might give better results & association among sub activities consideration will help in better activity recognition
[14]	Detecting ADLs	Markov Logic Network (MLN) (Discovery of Activity & abnormality detection)	Hierarchical activity recognition concept, any abnormality in the occupant's activity is recognized & decision is at each layer. Factors (objects, time, location & duration of activity)	-Use a hierarchical approach to detect abnormality in occupant behavior -Identification of factors associated with the activity such as objects, location, time & duration -Knowledgebase consist of	-Hybrid approach (spatio-temporal & context-based reasoning) -Distributed decision making -Concurrent activities consideration	-Self-generation of knowledgebase for activity recognition -No Sensor data relationships - Simple	In hierarchal model if at each level the best approach with respect to the factor is applied could yield better results. Fuzzy association rules generation could be helpful for automated

				hard & soft rules for activity recognition	- Quick decision response	activities - Time gaps not considered	rules generation
[6]	Abnormality detection in ADLs	Finding activity patterns using Frequent pattern Mining, tasks set by conditional probabilities & Self defined rules to find abnormalities	Pattern mining algorithm to detect the abnormality in inhabitant behaviors. System learns & update from new stream. GATS algorithm compute task sequences. Tasks used for activity recognition	- Activities Pattern - Activities Tasks - Activities Recognitions & abnormality detection	- Hierarchal structure - Activities & sub activities are considered - Quick decision response	- Hierarchal structures are complex - Self-generation of routine plans - Temporal analysis needs to be done efficiently	In hierarchal model if at each level the best approach with respect to the factor is applied could yield better results. Fuzzy association rules generation could be helpful for automated rules generation
[16]	Activities recognition	- Category assignment to incoming activity (Association rules) - reduces the false assignments - Multi-class activity classification	The proposed activity assigns a category to the incoming activity, confidence score of the assigned category to reduce false assignments. A binary solution is proposed using SVM, which simplifies the problem to correct/incorrect	- Assign a category to the incoming activity - Reduces the false positives in the assignments - Multi-class activity classification	- Activities and sub activities are considered - Quick decision response	- Prior patterns needs to be extracted to identify abnormal - Manual rule based system for recognizing discrepancies Temporal analysis needs to be efficient	In hybrid model Association rules can be merged with other classification techniques such as ANN for better results as ANN well suits for temporal associations.

TABLE II. CRITICAL EVALUATION OF RELATED WORK - IMPLEMENTATION AND VALIDATION

Ref	Dataset	Environment	WSN Size	Types of Sensors	ADL Attributes	Major Parameter improvement	Compared and Validated against	Implementation Complexity
[15]	Dataset from "CASAS: A smart home in a box." [10]	4 rooms apartment with one person in monitoring	26 sensors	Motion, door closure and temperature (Binary Sensors)	Bed_to_toilet, Eating, Enter/Leave_home, Housekeeping, Meal_preparation, Relaxing, Sleeping, Working	Activity Recognition Accuracy (99.10%)	Decision Tree (96%), Naïve Bayesian (88%) and HMM (95.47%)	Average
[5]	Synthetic and real data	LIARA Lab setup of WSN smart home.	More than 100 but no exact numbers	Binary and numerical value sensor: Infrared sensors, Pressure, electromagnetic contacts, temperature sensors, light sensors and eight RFID antennas	Wake up, Use toilet, Wash hands, Take shower, Prepare coffee, Leave house	Performance measure: Execution time	Not compared with any existing approaches	Average
[11]	Synthetic and real dataset [9]	Single elderly person four locations are considered: Bedroom, toilet, dining and kitchen	Wearable sensors And no details of ambient sensors	Wearable sensors And no details of ambient sensors	Resting, Sleeping, Waking up, Walking, Eating, Toileting, Exercise, House hold	Accuracy of the abnormality in daily routine (95%)	Fuzzy classification mode (90%) Asthma attack classification (93.8%) Stress classification model (80%)	Complex systems as multiple models are combined together
[4]	Dataset of SERG laboratory at Ulster University performed the activities over a period of 1 week	A 27-year-old man in the smart home environment.	No description provided	Accelerometer sensors, light sensor and contact sensors were utilized	Entering/ Leaving home, Watching TV, Phone call, Cooking, Eating, Drinking, Washing dishes	Identifying the uncertainties w.r.t precision and accuracy	Traditional Activity Model (TAM) Generic Activity Model (GAM) Semantic Generic Activity Model (SGAM)	Average
[7]	Dataset from "CASAS: A	Datasets represent sensor data collected from	26 sensors	Binary sensors and temperature sensors	Bathing, Eating, Enter Home, Housekeeping, Leave	Error rates	Baseline linear regression classification	Average

	smart home in a box." [10]	three apartment testbeds, each housing has one older adult			Home, Meal Preparation , Personal Hygiene		Win Size p-val 1000 0.042 2000 0.0006 5000 0.0059	
[8]	Physical implementation	8 weeks Appliance usage. Ninth and 10th week prediction of appliances usages are derived and compared with the actual durations	Not discussed (communication standard is IEEE 802.15.4)	Electrical, Force and contact(appliance usage) , Flexi force sensors (Data Acquisition, Activity Recognition	Sleeping, Dinning, Watching TV Relaxing , Toilet	Accuracy in activity recognition and forecasting in the given period of time (95% improvement )	With (Das and Cook (2005)	Complex
[9]	Physical implementation	Three one-bedroom single resident smart home apartments for experiments, referred to as Apt1, Apt2 and Apt3.	12 door/cabinet sensors Rest of 20 sensors are motion and temperature sensors	motion sensors, door closure sensors and temperature sensors (Binary Sensors)	Bathing, Eating, Enter Home, Housekeeping, Leave Home, Meal Preparation, Personal Hygiene, Resting on Couch, Sleeping in Bed, Taking Medication	Activity prediction (90%) and forecasting	Decision Tree (DT) (64%) Support Vector Machines (SVMs) (60%) Multi-layer Perceptron (MLP) algorithms (62%)	Complex
[10]	Data set from CASAS smart home project [10]	Datasets represent sensor data collected from 3 apartment testbeds, each apt has one older adult	26 sensors	Binary Sensors and temperature sensors	Taking bath , Preparing breakfast , Listening to music , Playing game, Preparing lunch	Activity recognition accuracy (ANN 98%)	HMM (hidden Markov model) (92%) NB (Naïve Bayes) (92%) C4.5 (93%)	Average
[2]	Data set from [11]	5 residents in smart home environment, no description is given.	No description related to WSN implementation	Binary sensors	Leaving, Toileting , Showering, Sleeping, Breakfast, Lunch , Snack , Spare time/TV , Grooming	Accuracy of Activity recognition (Hybrid SVM/HMM approach) (68%)	Hybrid MLP/HMM approach (69%), HMM (52%), SVM (65%)	Average
[13]	Datasets [12] [13]	57 years old resident in double story building with sensors installed in doors, bed, chair etc	21 Sensors	Motion, door closure and temperature (Binary Sensors)	Resting , Sleeping, Waking up, Walking , Eating, Toileting , Exercise , House hold	Activity identification accuracy (61%) and Window (time slice) (89%) for accuracy	HMM (A.ID=55%, T.S=87%)	Average
[18]	Dataset [12]	Single 26-year-old male is considered in three room Apartments. The data set consisted of 28 days.	14 state-change sensors were installed throughout the apartment.	Binary sensors	Leave house , Use toilet, Take shower, Go to bed , Prepare breakfast, Prepare dinner, Get drink Idle	Activity identification accuracy ( 81.6, 81.6 and 82.9%) are achieved by three proposed algorithms respectively	Not validated with any other	Average
[17]	The Domus Smart home [14]	Single room apartment where each user performed the routine ten times, thus ten sequences of events to find frequent patterns	The smart home equipped by 36 sensors	Binary sensors (IR, Pressure detector, Lamps, door contacts, switch contacts, flow meter	Waking up, Use Toilet, Preparing Breakfast, Having Breakfast, Washing Dishes	Activities Pattern and Deviation	Not validated	Average
[14]	Data set [9]	Analysis conducted on two humans in separate 4 rooms and 5 rooms apartments for 14 and 21 days respectively	12 sensors (for both apartments )	Binary Sensors PIR: shower, basin, cooktop Magnetic: main door, fridge, cabinet, cupboard Flush: toilet Pressure: seat, bed electric: microwave, toaster	Leaving, Toileting, Showering, Sleeping, Breakfast, Lunch, Snack/ SparetimeTV, Grooming	Response time (11.3 ms) and F-measure (0.91)	Hidden Markov Model Response time (17 ms) , F-measure (0.83)	Complex

[6]	Data set (No information)	Five individuals were asked to carry out a series of typical daily activities. These activities were performed in a house	Multiple sensors as RFID	RFID	Brush teeth , Wash face , Make tea Wash dishes , Read newspaper , Read book , Make curry , Phone call	Activity recognition (100%) ***	Not validated	Complex
[16]	Nine datasets	Different datasets with different experiment environments	Sensors	Different sensors	Bed_to_toilet, Eating , Enter/Leave_home, Housekeeping , Meal_preparation, Relaxing, Sleeping , Working	Precision (94.57), Recall (94.57), Specificity (90.39) , False Positive Rate (FPR) (99.36), Matthews Correlation Coefficient (0.64)	Different proposed works	Complex

TABLE III. CRITICAL EVALUATION OF RELATED WORK BASED ON WELLNESS AND ACTIVITY RECOGNITION PARAMETERS

Ref	Type of activity			Activities association		Time gap between adjacent activities	Activities time boundaries	Correlation of activity and location	Temporal correlation with the activities	Expert knowledgebase (Healthcare rules)
	Simple	Overlapped	Interleaved	Inter	Intra					
[15]	-	✓	-	✓	✓	-	-	-	-	✓
[5]	✓	-	-	-	-	✓	✓	-	✓	-
[11]	✓	-	-	-	-	-	-	✓	✓	-
[7]	✓	-	-	✓	-	-	-	✓	✓	-
[8]	✓	-	-	✓	-	-	-	✓	✓	-
[9]	✓	-	-	-	-	-	✓	-	✓	-
[10]	-	✓	-	✓	-	-	-	-	✓	-
[2]	✓	-	-	✓	-	-	-	-	✓	-
[13]	✓	-	-	✓	✓	-	-	-	✓	-
[18]	✓	-	-	✓	-	-	-	✓	✓	✓
[17]	✓	-	-	✓	-	-	-	-	✓	-
[14]	✓	-	-	-	-	-	-	✓	✓	✓
[6]	✓	-	-	-	-	-	-	-	-	✓
[16]	✓	-	-	-	-	-	-	-	✓	-

IV. CONCLUSION

This study includes literature survey and critical evaluation of existing techniques for wellness detection of elderly people in WSN based smart homes. There are certain vital parameters such as sub activity, location of sub activity, time gap between adjacent sub activities and their temporal associations are identified for the activity detection and wellness detection. Similarly existing literature used different methods for the identification of frequent patterns of elderly people behaviors and finding correlation and association among different parameters. On the basis of the critical evaluation, a model is proposed which is based on association rule mining. The proposed model is based on temporal association of location and sub activities, time gap and temporal association among sequence of sub activities been extracted for the determination of complex activities such as overlapped activities. Association rules and expert knowledge base classifier is proposed for the wellness detection of online data stream from sensor data of smart homes. Learning component is proposed to accommodate the changing trends in the activities pattern of the behavior of the elderly people. In future proposed model will be implemented and tested for 50 elderly people.

Furthermore, result will be compared to existing techniques to evaluate its performance.

REFERENCES

- [1] C. Lindmeier, "'Ageing well" must be a global priority, <http://www.who.int/mediacentre/news/releases/2014/lancet-ageing-series/en/>," 6 NOVEMBER 2014.
- [2] F. J. Ordóñez, P. d. Toledo, and A. Sanchis, "Activity recognition using hybrid generative/discriminative models on home environments using binary sensors," *Sensors*, vol. 13, pp. 5460-5477, 2013.
- [3] Y. Yao, Q. Cao, and A. V. Vasilakos, "EDAL: An energy-efficient, delay-aware, and lifetime-balancing data collection protocol for heterogeneous wireless sensor networks," *IEEE/ACM Transactions on Networking*, vol. 23, pp. 810-823, 2015.
- [4] E. Kim, S. Helal, C. Nugent, and M. Beattie, "Analyzing activity recognition uncertainties in smart home environments," *ACM Transactions on Intelligent Systems and Technology (TIST)*, vol. 6, p. 52, 2015.
- [5] M. T. Moutacalli, A. Bouzouane, and B. Bouchard, "The behavioral profiling based on times series forecasting for smart homes assistance," *Journal of Ambient Intelligence and Humanized Computing*, vol. 6, pp. 647-659, 2015.
- [6] L. G. Fahad, A. Khan, and M. Rajarajan, "Activity recognition in smart homes with self verification of assignments," *Neurocomputing*, vol. 149, pp. 1286-1298, 2015.
- [7] B. Minor and D. J. Cook, "Regression tree classification for activity prediction in smart homes," in *Proceedings of the 2014 ACM*

- International Joint Conference on Pervasive and Ubiquitous Computing: Adjunct Publication, 2014, pp. 441-450.
- [8] N. K. Suryadevara, S. C. Mukhopadhyay, R. Wang, and R. Rayudu, "Forecasting the behavior of an elderly using wireless sensors data in a smart home," *Engineering Applications of Artificial Intelligence*, vol. 26, pp. 2641-2652, 2013.
- [9] E. Nazerfard and D. J. Cook, "CRAFFT: an activity prediction model based on Bayesian networks," *Journal of Ambient Intelligence and Humanized Computing*, vol. 6, pp. 193-205, 2015.
- [10] S. T. M. Bourobou and Y. Yoo, "User activity recognition in smart homes using pattern clustering applied to temporal ann algorithm," *Sensors*, vol. 15, pp. 11953-11971, 2015.
- [11] R. M. Forkan, I. Khalil, Z. Tari, S. Fofou, and A. Bouras, "A context-aware approach for long-term behavioural change detection and abnormality prediction in ambient assisted living," *Pattern Recognition*, vol. 48, pp. 628-641, 2015.
- [12] F. J. OrdÃ±ez, P. de Toledo, and A. Sanchis, "Activity recognition using hybrid generative/discriminative models on home environments using binary sensors," *Sensors*, vol. 13, pp. 5460-5477, 2013.
- [13] L. Kalra, X. Zhao, A. J. Soto, and E. Milios, "Detection of daily living activities using a two-stage Markov model," *Journal of Ambient Intelligence and Smart Environments*, vol. 5, pp. 273-285, 2013.
- [14] K. Gayathri, S. Elias, and B. Ravindran, "Hierarchical activity recognition for dementia care using Markov Logic Network," *Personal and Ubiquitous Computing*, vol. 19, pp. 271-285, 2015.
- [15] J. Wen, M. Zhong, and Z. Wang, "Activity recognition with weighted frequent patterns mining in smart environments," *Expert Systems with Applications*, vol. 42, pp. 6423-6432, 2015.
- [16] S. Nasreen, M. A. Azam, U. Naeem, M. A. Ghazanfar, and A. Khalid, "Recognition Framework for Inferring Activities of Daily Living Based on Pattern Mining," *Arabian Journal for Science and Engineering*, pp. 1-14, 2016.
- [17] J. r. m. Saives, C. m. Pianon, and G. Faraut, "Activity discovery and detection of behavioral deviations of an inhabitant from binary sensors," *IEEE Transactions on Automation Science and Engineering*, vol. 12, pp. 1211-1224, 2015.
- [18] X. Hong and C. D. Nugent, "Segmenting sensor data for activity monitoring in smart environments," *Personal and Ubiquitous Computing*, vol. 17, pp. 545-559, 2013.
- [19] R. Srikant and R. Agrawal, "Mining sequential patterns: Generalizations and performance improvements," in *International Conference on Extending Database Technology*, 1996, pp. 1-17

# A Study of Resilient Architecture for Critical Software-Intensive System-of-Systems (Sisos)

Nadeem Akhtar  
Department of Computer Science &  
IT  
The Islamia Univ. of Bahawalpur,  
Pakistan

Malik Muhammad Saad Missen  
Department of Computer Science &  
IT  
The Islamia Univ. of Bahawalpur,  
Pakistan

Nadeem Salamat  
Department of Basic Science and  
Humanities  
Khawaja Fareed Univ. of  
Engineering and Technology, RYK,  
Pakistan

Amnah Firdous  
Department of Computer Science  
COMSATS Institute of Information Technology, Pakistan

Mujtaba Husnain  
Department of Computer Science & IT  
The Islamia Univ. of Bahawalpur, Pakistan

**Abstract**—The role of critical system-of-systems have become considerably software-intensive. A critical system-of-system has to satisfy correctness properties of liveness and safety. As critical system-of-systems have to operate in open environments in which they interact and collaborate with other systems, satisfy action of the requirements through traditional offline top-down engineering no longer suffice. Most of the critical software-intensive system-of-systems have no fixed boundaries and services provided by other systems will come and go in unpredictable ways; in these systems assuring correctness is a challenging issue. These systems need to tolerate faults in the face of change; they need a resilient architecture. An approach has been proposed for the analysis, design, formal specification and verification of critical Software-intensive System-of-Systems.

**Keywords**—Resilient architecture; Critical systems; System-of-System (SoS); Software-intensive SoS (SiSoS); Emergent behavior; Correctness; Safety

## I. INTRODUCTION

Most of the critical Software-intensive System-of-Systems (SiSoS) have no fixed boundaries (i.e. they have open environment); and services provided by other systems come and go in unpredictable ways. In such system-of-systems assuring correctness by construction is not possible. Such system-of-systems need to tolerate faults in the face of change; in short they need to be resilient.

Nowadays, software systems are performing critical tasks, thus more and more software systems are becoming critical. Defects in a critical system can cause human life loss, and can also have a dramatic impact on the environment. The functions performed by these systems have become considerably software-intensive. The software of critical systems has to satisfy correctness properties of *liveness* and *safety*.

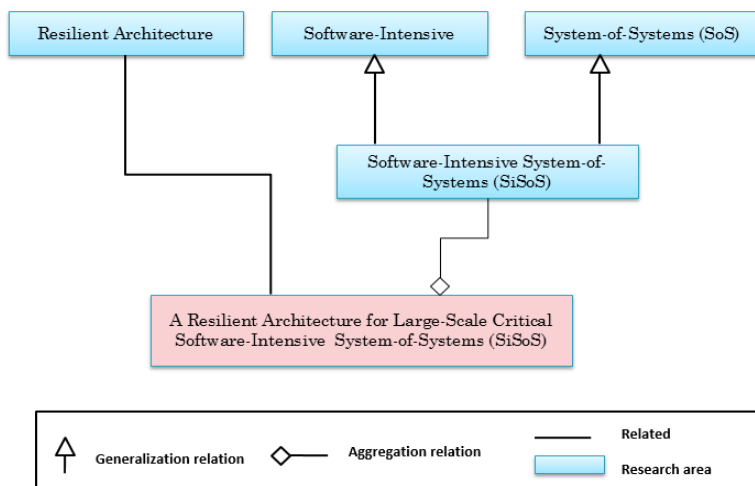


Fig. 1. Study domain

As critical systems increasingly have to operate in open environments in which they interact and collaborate with other

systems, satisfaction of the requirements through traditional offline top-down engineering no longer suffice

#### A. Software-Intensive System-of-Systems (SiSoS)

A system is a collection of elements that work together and produce results that cannot be obtained by the elements operating individually. An individual element of a system may itself be large and complex, and comprised of sub-elements acting in concert with one another.

A System-of-System (SoS) integrates independently useful systems into a larger system, delivering new unique functions to users that emerge from the combination of the individual parts. Examples are *intelligent traffic systems, integrated surveillance systems, and networked smart homes*. Engineering SoS and guaranteeing runtime qualities (i.e. *performance, reliability* etc.) is complex due to a variety of uncertainties. Examples of such uncertainties are *systems that attach and detach at will, dynamically changing availability of resources, and faults and intrusions that are difficult to predict*.

SoS are formed by the integration of autonomous and heterogeneous systems. The SoS were first applied in the analysis and design of military systems of the American Department of Defense. [3]

SoS is used as a method to reach goals or provide unique capabilities for the collaborative work between existing systems. [4][5]

The first definitions and taxonomies for SoS were introduced by Maier [4] in 1990's in which three SoS basic types (*virtual, collaborative, and directed*) are proposed. He also specified the five characteristics (*operational independence, managerial independence, evolutionary development, emergent behavior and geographic distribution*) of SoS. Based on this characterization, Maier identifies a set of guiding design principles for SoS:

- *Stable intermediate forms*: The individual systems or subsets of systems of a SoS should be capable of operating and fulfilling useful purposes, before full deployment and during operation.
- *Policy triage*: SoS design team should carefully choose what to control; over-control will fail for lack of authority, under-control will eliminate the integrated nature of the SoS.
- *Leverage at the interfaces*: The architecture of SoS is essentially defined by its interfaces, which are the primary points at which designers can exert control.
- *Ensuring collaboration*: Mechanisms should be exploited that create joint utility, which is known to be a basis for consistent behavior.

[6] refers to SoS or Federations Of Systems (FOS) or Federated Systems Of Systems (F-SOS) as systems that possess characteristics of complex adaptive systems. [7] focuses on the nature of the composition to define the distinguishing characteristics of SoS, including *autonomy, connectivity, diversity and emergence*. [8] stresses scale and complexity as central properties of ultra-large scale systems, phrased by the slogan "*scale changes everything*". [9] describes SoS as a combined arrangement of managerially

independent and geographically distributed elements (i.e. already fulfilling some purposes) put together to work and provide a functionality that is not possible otherwise.

Energy systems, healthcare systems, logistic systems, and transportations systems can be designed and developed based on SoS concept. [10]

SoS are complex and large-scale systems and are software-dependent, therefore they become Software-Intensive SoS (SiSoS). [11]

SoS facilitates development of complex systems. It is a composition of systems in which its constituents are themselves systems. These constituent systems are separately discovered, selected and composed at run-time or design-time to form a more complex system to fulfill a specific mission. It is an integration of autonomous systems that are geographically distributed and support continuous evolution. These systems are functionally and managerially independent. These systems on integration, share their resources and services to serve a larger, complex and unique functionality that is not possible to achieve otherwise.

SoS is a larger system that performs a function not performable by one of the constituent systems alone, thus it creates emergent behavior. Constituent systems fulfill their own objectives. If they are disassembled from the encompassing SoS they continue to operate to fulfill their own objectives and tasks. They are managed for their own objectives rather than the objectives of the whole SoS. Intrinsic characteristics of SoS are: (1) *Operational independence of systems*: If the SoS is disassembled into its component systems these systems must be able to usefully operate independently; (2) *Managerial independence of systems*: The component systems are separately acquired and integrated but maintain a continuing operational existence independent of the SoS; (3) *Geographical distribution of systems*: (4) *Evolutionary development of SoS*: (5) *Emergent behavior of SoS*: In addition, characteristics of Open-World SoS are the *unpredictable environment and unpredictable constituents*.

ISO/IEC/IEEE 42010 International Standard [1] defines a software-intensive system as any system in which software influences the *design, implementation, deployment, and evolution* of the system as a whole to encompass individual applications, subsystems, systems-of-systems, product lines, product families, whole enterprises and other aggregations of interest.

Self-adaptation enables a software system to reason about itself and adapt autonomously to achieve particular quality objectives in the face of uncertainties and change. Central to the realization of self-adaptation are feedback loops that monitor and adapt managed parts of a system when needed. Studies conducted in the field of self-adaptation have primarily focused on centralized and hierarchical control in self-adaptation, which is not applicable to systems that are inherently decentralized. Realizing self-adaptation in a SoS where no single entity has the knowledge and authority to supervise and adapt the constituent parts raises fundamental engineering challenges. [2]

In Software-intensive SoS, software essentially influences the analysis, design, architecture, implementation, deployment, and evolution of the system in itself. Software is essential to enable the behavior of these systems. It encompasses single systems and aggregations of interest, i.e. Systems-of-systems. Software-intensive system-of-systems constituents are themselves systems

### B. Formal methods

Formal methods have a mathematical foundation. They provide a formal foundation in requirement specification, architecture definition, implementation, testing, maintenance and evolution of large-scale software. In industrial projects, multiple levels of formal methods are applied at different stages of software development life cycle depending upon the degree of criticality of the software project. The major emphasis is on the application of formal methods at the earlier stage of software development life cycle (i.e. specification and design).

At software design level formal methods are used to refine data using state machines, abstraction functions and simulation proofs while at implementation level code verification may be done by *theorem proving* or *inductive assertions*. The major emphasis will be the application of formal methods at the earlier stage of software specification and design. A number of researchers have conducted research surveys for the industrial use of formal methods. Formal methods are useful in the development and certification of critical systems. [12]

### C. Correctness properties

Correctness properties play important role in system verification. Correctness properties of safety and liveness complement each other. Safety alone or liveness alone is not sufficient to ensure system correctness. The safety property is an invariant which asserts that “*something bad never happen*”, that an acceptable state of affairs is maintained. For example consider a power reactor generating electricity; the reactor temperature should never exceed 100 degrees Centigrade to assure safe and efficient working. The property which assures that a power reactor temperature would never exceed 100 degrees Centigrade is a safety property.

[13] have defined safety property  $S = \{a1, a2 \dots an\}$  as “*a deterministic process that asserts that any trace including actions in the alphabet of S, is accepted by S*”. ERROR conditions are like exceptions which state what is not required. In complex systems, safety properties are specified by directly stating what is required.

The liveness property asserts that “*something good happens*”. It describes the states of a system that an agent must bring about given certain conditions. One of the most significant methods to ensure correctness of large-scale system is to use formal methods.

## II. MOTIVATION

The functions performed by a critical system have become considerably software-intensive. A critical system has to satisfy specific quality attributes like *liveness* and *safety*. As a critical system has to operate in open environment in which it

interact and elaborate with other systems, satisfaction of the requirements through traditional offline top-down engineering no longer suffice. Guaranteeing correctness by construction is not possible for large-scale critical systems in which boundaries are no longer fixed and services provided by other systems will come and go in unpredictable ways. Such systems need to tolerate faults in the face of change; in short they need to be *resilient*. Building and managing resilient large-scale critical systems call for a fundamental shift in engineering vision in which satisfaction of requirements has to be realized via online collaboration among autonomous components.

## III. MATERIAL AND METHODS

### A. Objectives

The major objective of resilient architecture for software intensive system-of-systems is to develop efficient and robust approach for building resilient large-scale critical system-of-systems. Resilient Architecture is centered on four pillars:

1) *Self-adaptation as a technique to achieve resilience*: As large-scale critical system-of-systems are long-lived systems, they have to be prepared for openness. In an open environment, the context of the system can change at any time, availability of resources may change, services may evolve, services may disappear or new services may become available. To enable a system to deal with these dynamics it must be self-adaptive. A self-adaptive system is goal-oriented, it is aware of its context and reasons upon it, it coordinates with other systems in its environment and adapts itself with changing operating conditions.

2) *Executable language for architecture*: Designing and realizing self-adaptive large-scale critical systems requires suitable models at appropriate levels of abstraction. This calls for an innovative description and executable language for architecture which seamlessly integrates multi-view modeling with runtime model evolution. Support for multi-view modeling is crucial for two reasons. On the one hand, it enables the specification of different perspectives on the system and its environment according to the interests of the variety of system stakeholders. On the other hand, it enables the specification of the appropriate models of critical systems that are needed for automatic adaptation. Support for runtime model evolution is crucial to enable model adaptation to changes in the environment, possibly in unpredicted ways.

3) *Formal foundation*: Since large-scale critical systems have a number of mandatory requirements, a sound formal foundation is a prerequisite for the engineering approach. Assuring the qualities requires a rigorous specification of semantics of models and a formal understanding to enable automatic verification of model adaptations. For example, guaranteeing a safe adaptation in a decentralized system requires safety along the path of subsequent local adaptations, which demands formally founded methods and techniques.

4) *Runtime execution platform*: Automatic adaptation and evolution of critical systems requires a suitable runtime execution platform. Key aspects of this platform are automatic

and decentralized discovery of components services in large-scale open systems, goal-oriented decision making and coordination for adaptation, verification of fragments of the specification assuring the required qualities under adaptation, and automatic execution of system adaptation, based on the connection of the runtime models with the underlying implementation. A key quality aspect of the platform is scalability. In particular, the platform should support the

realization of the applications' quality of service requirements in large-scale distributed settings.

### B. Scope of Study

1) Security is not considered as a primary concern for the analysis and design of the resilient architecture for critical Software-intensive System-of-Systems (SiSoS).

2) Semantic interoperability (i.e. information exchange among systems) should be unambiguously defined.

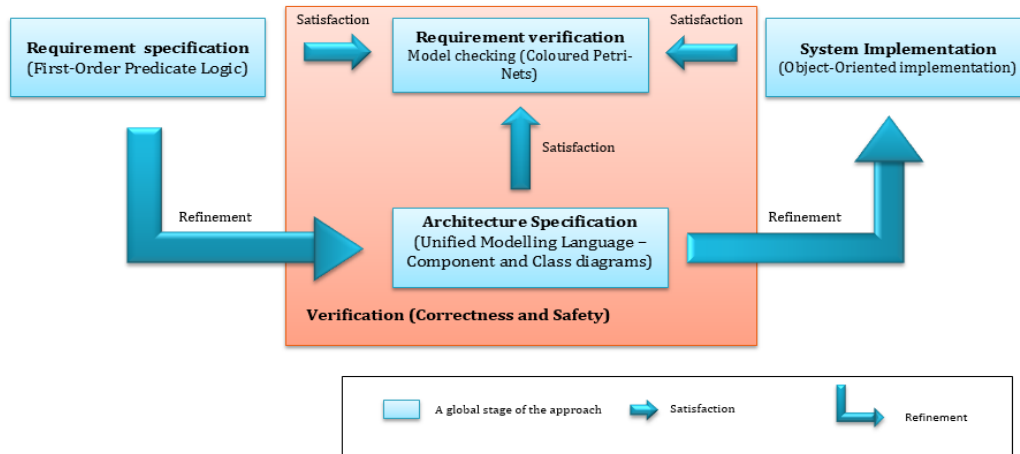


Fig. 2. The four phases of resilient architecture for critical Software-intensive System-of-Systems (SiSoS)

3) The degree of automation depends on the context from human designed to human-in-the-loop to fully automatic.

4) The scope of automatic verification depends on the support present in the formal method or language chosen.

### C. Formal verification and Architecture definition

The formal foundation for specifying and verifying behavior-oriented software architecture developed in the European ArchWare [11] project offers a sound basis upon which the envisioned next generation description and executable language for architecture can be built. In addition, the lessons learned in ArchWare [11] with defining and designing architectural languages and supporting tools are highly valuable for Resilient Architectures.

The proposed approach has four major phases of requirement specification, requirement verification, architecture specification, and system implementation.

The architecture of an Information Management System has been specified, verified, and designed to validate the approach. The first phase is of requirement specification. The requirements are specified in *First-Order Predicate Logic*. There is a satisfaction relation between requirement specification and requirement verification.

Requirements are modeled and verified by Coloured Petri-Nets. The structural architecture is specified by using UML Component and Class diagrams, the behavioral architecture is modeled and verified by Coloured-Petri Nets. This architecture is refined into object-oriented implementation.

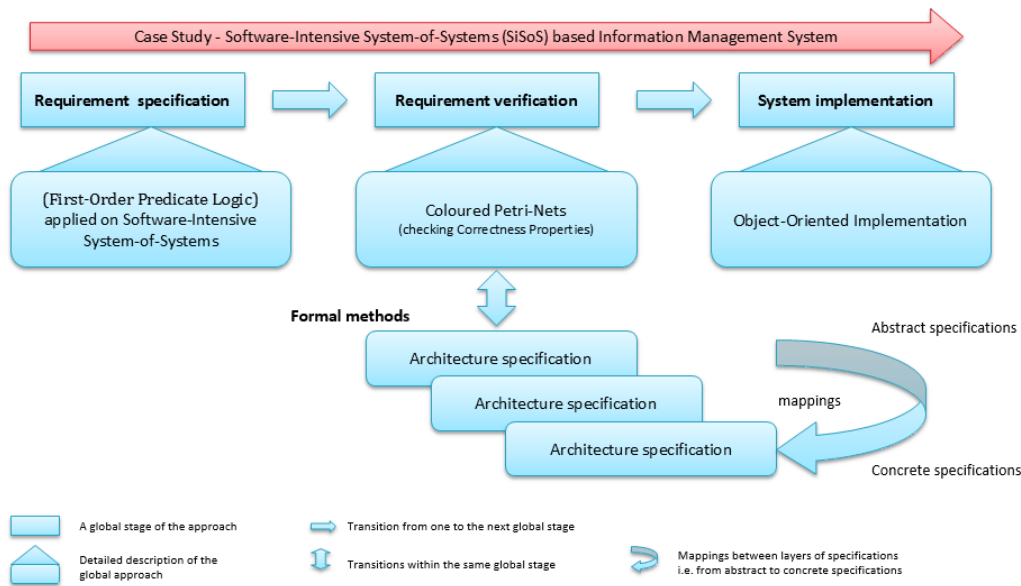


Fig. 3. The four phases of resilient architecture for critical Software-intensive System-of-Systems (SiSoS)

There is a satisfaction relation between system implementation and requirement verification. The system is implemented by using object-oriented implementation. The implementation satisfies the verification specifications.

#### IV. RESULTS AND DISCUSSION

The expertise acquired during the proposition of decentralized control for autonomous robotic transport agents [14][15] proved to be valuable for the design of resilient architecture for SiSoS. In this research project, multi-agent system architecture is formally verified and developed to endow an automatic transportation system with advanced self-managing capabilities. Although this control system has fixed boundaries, the knowledge and expertise acquired from decentralizing control in this complex domain provides a substantial basis upon which resilient architecture can be built on.

As a result of this work, a resilient architecture for SiSoS has been proposed. The proposed approach is centered on formal verification of correctness properties. This approach is based on a combination of formal methods and techniques. By following this approach a resilient architecture for Software-intensive System-of-Systems can be specified, formally verified and implemented. As our previous expertise and experience is on decentralized control of autonomous robotic transport agents [14][15], our future goal is to use resilient architecture for Software-intensive System-of-Systems.

#### REFERENCES

- [1] ISO/IEC/IEEE 42010:2011(E), "ISO/IEC/IEEE International Standard for Systems and Software Engineering – Architectural description," 2011.
- [2] Danny Weyns and Jesper Andersson. "On the challenges of self-adaptation in systems of systems". In *Proceedings of the First International Workshop on Software Engineering for Systems-of-Systems (SESOS '13)*, Paris Avgeriou, 2013, Carlos E. Cuesta, José Carlos Maldonado, Elisa Y. Nakagawa, Khalil Drira, and Andrea Zisman (Eds.). ACM, New York, NY, USA, 47-51, 2013. DOI=http://dx.doi.org/10.1145/2489850.2489860
- [3] Office of the Deputy Under Secretary of Defense for Acquisition and Technology, *Systems and Software Engineering, System engineering guide for systems of systems*, ODUSD (A&T), 2008, version 1.0.
- [4] M. W. Maier, "Architecting principles for systems-of-systems," *Systems Engineering*, vol. 1, no. 4, pp. 267–284, 1998.
- [5] D. Firesmith, "Profiling systems using the defining characteristics of systems (SoS)," *Software Engineering Institute*, Carnegie Mellon University, Pittsburgh, PA, USA, Tech. Rep. TN-001, 2010.
- [6] A. P. Sage and C. D. Cuppan. "On the systems engineering and management of systems of systems and federations of systems". *Information Knowledge Systems Management*, 2(4):325-345, Dec. 2001.
- [7] J. Boardman and B. Sauser. "System of systems-the meaning of of". In *International Conference on System of Systems Engineering*. IEEE, 2006.
- [8] L. Northrop, P. Feiler, R. P. Gabriel, J. Goodenough, R. Linger, T. Longsta\_, R. Kazman, M. Klein, D. Schmidt, K. Sullivan, and K. Wallnau. "Ultra-Large-Scale Systems - the software challenge of the future". *Technical report*, SEI, Carnegie Mellon, 2006.
- [9] B. Blanchard and W. Fabrycky, *Systems Engineering and Analysis*, 3<sup>rd</sup> Edition. Prentice Hall, pp. 2, 1998.
- [10] D. A. DeLaurentis and W. A. Crossley, "A taxonomy-based perspective for systems of systems design methods," In *Proceedings of the 2005 IEEE International Conference on Systems, Man and Cybernetics*, vol. 1. USA: IEEE, 2005, pp. 86–91.
- [11] F. Oquendo, B. Warboys, R. Morrison, R. Dindeleux, F. Gallo, H. Garavel, C. Occhipinti, "ArchWare: Architecting Evolvable Software," *Proc. 1st European Workshop Software Architecture (EWSA 2004)*, LNCS 3047, Springer-Verlag, 2004, pp. 257-277.
- [12] J. Woodcock, P. G. Larsen, J. Bicarregui and J. Fitzgerald, "Formal Methods and Experience", *ACM Computing Surveys*, Vol 16, No. 4, Article 19, October 2009.
- [13] J. Magee, and J. Kramer, *Concurrency: State Models and Java Programs*. John Wiley and Sons, 2<sup>nd</sup> edition, 2006.
- [14] N. Akhtar, "Contribution to the formal specification and verification of multi-agent robotic systems". *PhD thesis*, Ecole Doctorale, Laboratory VALORIA, University of South Brittany, 2010.
- [15] N. Akhtar, Y. L. Guyadec, and F. Oquendo, "FORMAL SPECIFICATION AND VERIFICATION OF MULTI-AGENT ROBOTICS SOFTWARE SYSTEMS: A Case Study". *Proceedings of the International Conference on Agents and Artificial Intelligence (ICAART 09)*. Porto, Portugal, January 19-21. INSTICC Press, 2009.

# Speech Impairments in Intellectual Disability: An Acoustic Study

Sumanlata Gautam

Computer Science and Engineering Department  
The NorthCap University  
Gurgaon, India

Latika Singh

Computer Science and Engineering Department  
The NorthCap University  
Gurgaon, India

**Abstract**—Speech is the primary means of human communication. Speech production starts in early ages and matures as children grow. People with intellectual or learning disabilities have deficit in speech production and faces difficulties in communication. These people need tailor-made therapies or trainings for rehabilitation to lead their lives independently. To provide these special trainings, it is important to know the exact nature of impairment in the speech through acoustic analysis. This study calculated the spectro-temporal features relevant to brain structures, encoded at short and long timescales in the speech of 82 subjects including 32 typically developing children, 20 adults and 30 participants with intellectual disabilities (severity ranges from mild to moderate). The results revealed that short timescales, which encoded information like formant transition in typically developing group were significantly different from intellectually disabled group, whereas long timescales were similar amongst groups. The short timescales were significantly different even within typically developing group but not within intellectually disabled group. The findings suggest that the features encoded at short timescales and ratio (short/long) play a significant role in classifying the group. It is shown that the classifier models with good accuracy can be constructed using acoustic features under investigation. This indicates that these features are relevant in differentiating normal and disordered speech. These classification models can help in early diagnostics of intellectual or learning disabilities.

**Keywords**—*speech development; spectro-temporal; intellectual disabilities; timescales; learning disability; classification model*

## I. INTRODUCTION

Humans use speech, the vocalized form of communication, to express their thoughts, emotions, necessities etc. In speech research, psycholinguistics, auditory cognitive neurosciences and psychoacoustics focused on cues essential for production and perception of speech sound along with processing done by the brain. Language acquisition process [1], requires to perceive sound, produce sound and relate both of them. Speech perception starts at very early stage, when child is in mother's womb but speech production starts with cooing and babbling in infants and children take several years to become fluent speakers. Speech is a primary key, used by the children at the age of 2-3 years to express their thoughts, necessities, feelings and in creating and maintaining social relationships. While growing children master this skill to intervene higher level complex cognitive tasks. Children [10] take years to learn these complex patterns. Communication is rated as abnormal in children with learning and intellectual disabilities [11-13]. It is beneficial to investigate the nature of speech impairment in

these special children that will aid in developing tailor made therapies for their rehabilitation. Also, spotting a common speech features deficit pattern in disorders can help in classifying the group and aid in early stage diagnosis of the disease. In this study, we have examined acoustical differences between normal and group of people with mild to moderate intellectual disability to determine a pattern of speech impairments in the given disability.

Intellectual disability is the state in which deficits in the basic intelligence, social and practical skills to execute day to day necessities occur. According to American Association on Intellectual and Developmental Disabilities (AAIDD)[14], Intellectually disability can be characterized by limitation in both intellectual functioning (mental capacity : Intellectual Quotient (IQ)  $\leq 70$  (approx)) and adaptive behaviour (conceptual, social and practical skill) originate before the age of 18 years. In DSM-5 [15], the severity of intellectual disability is measured by comparing the functional ability with age matched norms. It involves impairment in general mental abilities in three domains, the first is conceptual domain ( language, reading, writing, reasoning, math, memory, and knowledge), the second is social domain which includes lack of interpersonal communication skills, friendship, social judgments and empathy. The third practical domain includes deficit in personal care, responsibilities, money management, job duties and organizing school and tasks. To enhance the quality of life of these special people, many rehabilitation methods/techniques which were specific to these skills have been evolved [16,17]. One of the crucial adaptive skill i.e. lack of communication ability is most salient hurdle in rehabilitation of intellectually disabled population.

The children with mental retardation (including mild and moderate impaired population) lack in phonological development [18-20] in their speech. These children also exhibit many articulatory deficit, delays in expressive language [21,22] and show significant limitations in grammar and syntax development[23,24] as compared to age matched control. Several neuro-anatomical and neuro-imaging studies [25] have tried to correlate the disorder with impairments in different parts of the brain. All of these research studies look at the phonological and linguistic aspect of speech of normally developing children, normal adults and subjects with intellectual disabilities. There is a shortfall in bringing quantitative base for finding a common pattern of speech impairments in the subjects with intellectual disabilities. In speech perception, auditory mechanism act as frequency

analyzer. Numerous studies [2-6] analyse speech production development using spectral acoustic measures. One of the Study [5] estimated pitch and intensity in the speech of children and adults for differentiating normal and intellectually disabled population. However, a different line of thought have shown that temporal structure of speech plays a crucial role [7-9] in speech perception and production. These studies [26, 27] have proposed that amplitude envelope of speech between 20msec-500msec carry information representing phonetic segment duration, formant transition, place of articulation, stress and syllabicity. The spectro-temporal features [28- 33] at these timescales highly correlated speech intelligibly and ability to understand or comprehend. Studies reported impairments in short time scales [34- 36] and long time scales [37, 38, 40] on the speech signal of children with neuro-developmental disorders. Most of these studies focused on the impairments in the spectro-temporal features in the speech of subjects with intellectual disabilities but none has developed the classification model for these groups based on features encoded at multiple timescales. The present study has partially filled this gap by extracting spectro-temporal features at two timescales followed by building a classification model based on these features. It focuses on spectro-temporal features encoded at two timescales: short (25-50msec) and long (100-500msec).

The study was completed in two phases. During the first phase, the statistics of short and long timescales for all speech samples in each group were calculated. In the second phase different classification models to classify normal and intellectually disabled group based on the statistics obtained in first phase were made. All the models showed good accuracy which demonstrates the differentiating power of the features that are investigated in the present study. This indicates that these features can be used for designing diagnostic and therapeutic tools for children with mild to moderate intellectual disabilities.

## II. METHODS AND MATERIAL

### A. Subjects

The speech database included two groups, TD (Typically developing) and ID (Intellectually disabled) with ages between 5 to 20 years. TD group was further divided into three subgroups TD1, TD2 and TD3. Detailed description is provided in Table I.

### B. Experimental settings and procedure

The 3 minutes (approx) speech recording was done at the sampling rate of 22.5 kHz and 16 bit PCM (Pulse Code Modulation) using head fitted microphone of Sony recorder (ICD-UX533F). The recording procedure consisted of picture naming and reading task. Picture naming task included the pictures of common animals, birds, vegetables, fruits and objects. The participant has to speak the name of the picture presented before them. Reading task compromised reading of the phonetically rich article from a book. Children ages (4-5 years) from TD1 group and all participants of ID group could perform picture naming only. As children in TD1 group were too young to read the book and similarly, participants from ID group could not read the book but could perform picture

naming as they were familiar with these pictures. Participants of TD2 and TD3 group have performed both the tasks. The tasks were explained to all the participants before taking their recordings. The low quality speech recordings were checked and poor quality samples were excluded from the experiment

TABLE I. SPEECH SAMPLES DATABASE

S/No	Data Acquisition		
	Group	Age	No of Subjects
1.	TD	5-20 years	52 (25 male + 27 female)
	1.TD1	4.8 years $\pm$ 0.8	10 (6 male + 4 female)
	2.TD2	7.5 years $\pm$ 0.7	22 (10 male + 12 female)
	3.TD3	19.5 years $\pm$ 0.8	20 (9 males + 11 female)
2.	ID	5-20 years	30 (22 male + 8 female)

TD :Typically Developing  
ID: Intellectually disabled

## III. DATA ANALYSIS

### A. Spectro-temporal feature extraction

Speech is a complex signal that fluctuates rhythmically in time and timbrally in frequency. As mentioned earlier (section I: Introduction), the speech signals can be effectively analysed by investigating spectro-temporal features that are encoded at different timescales. In the present study, we have extracted spectro-temporal features encoded at two different time-scales (short timescales: 25- 50 msec and long time scales: 100-500 msec) and developed a classification model to differentiate the speech of the normal children and children with mild to moderate intellectual disabilities. The block diagram and workflow of the proposed system is mentioned in Fig. 1. Each speech sample was pre-processed for the removal of background noise. Spectrogram was then generated for each speech sample using 512 point FFT (Fast Fourier Transform) and 22 msec time windowing. The resultant spectrogram image was pre-processed by applying filtering and thresholding for removing noise and extracting spectro-temporal from the converted binary image. The resultant binary image holds spectro-temporal features separated from its surrounding. These features can be extracted using 8-connected component algorithms[39]. These spectro-temporal features were encoded at different timescales (for detail section I: Introduction). Speech signal carries acoustic and linguistic information at multiple timescales [ 26 , 37, 40]. For each speech sample, the spectro-temporal features were classified into two time-scales short time-scales (25-50 msec) which carries information such as stress, intonation, voicing and formant transition and long time scales (100-500 msec) which include features representing tempo, syllabicity and rhythm. As discussed earlier, both timescales altogether define the prosodic information in the sample, hence it is meaningful to calculate the ratio of short versus long timescales and consider it as one of the important attribute. The statistics of short timescales, long timescales and their ratios were taken as the prime input attributes to design the feature vector for classification. To analyse the developmental pattern of these spectro-temporal features encoded in different timescales with age and compare these

patterns with intellectually disabled population, different classification algorithms were constructed.

**B. Classification techniques**

The spectro-temporal features measured during phase-I (mentioned in Fig. 1) served as input to the classifier. The count of spectro-temporal features at short timescales, long timescales and their ratios were calculated for each speech sample in both the groups. The created feature vector is shown in Table II. and it represents the number features in short timescales range, the number of features in long timescales, their ratios and the age of the subjects as attributes. These input attributes were used to train five different types of classifiers to develop a predictive model for distinguishing speech of normal and intellectually disabled subject. We have applied k-Nearest Neighbour, Naive Bayes, SVM (Support Vector Machine), Decision tree and Neural Network approaches. The statistical performance of learning in the dataset was estimated by applying 10 fold cross-validation. In this process, model was first trained and then trained model was used to measure the performance. The present model used 70% cases for training and rest 30% for testing. k-NN is an instance based learning that takes the input of k closest training examples in the feature vector and assign the unknown example to the class of single nearest neighbour if k is 1. Gain ratio was used as a criteria to predict the output attribute based on input attributes in decision tree. Naive Bayes is a conditional probabilistic model assumes that the contributions of the attributes are independent to the probabilistic label. Lib-SVM (Support Vector Machine) used with C-SVC and rbf kernel for two class classification, it maps samples nonlinearly into higher dimensions. Neural Network learns with feed forward neural network trained by a back propagation algorithm. Neural network is based on adaptive system that changes the structure based on the information passes in learning phase with propagation and weight update provided in supervised learning. The objective of the current study is to classify the speech of typically developing and intellectually disabled population. The results are discussed in next section

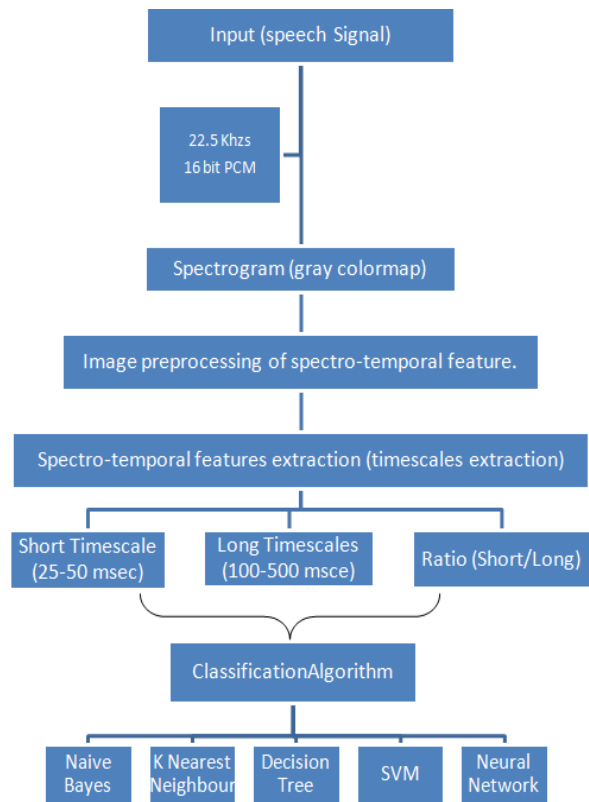


Fig. 1. Block diagram of the proposed work

TABLE II. CLASSES AND ATTRIBUTES USED IN CLASSIFICATION

S/No.	Attribute	Type	Mean ± SD
1	Number of short timescales	Numeric	6269.1 ± 2492.3
2	Number of long timescales	Numeric	407.7 ± 107.3
3	Ratio (short/long timescales)	Numeric	16.6 ± 6.7
4	Age	Numeric	11.7 ± 6.4
Output Classes : Typically Developing (TD) Intellectually Disable (ID)			

IV. RESULTS

Fig. 2 shows the number of spectro-temporal features at short and long timescales for two children (ages:4-5 years) representative from TD1 and ID group and two adults(male) representative from TD3 and ID group. The Fig 2. inspection reveals that the number of short timescales is more in number than long timescales. Table 3. represents the statistics of short and long timescales in TD1,TD2 ,TD3 and ID groups. In order to examine the validity of these stats significance testing was done. The unpaired t-test for features encoded at short timescales between age matched peers in TD and ID found to be significantly different ( $p=0.005521$ ), where as long timescales measure ( $p=0.120905$ ) did not show any significant effect on groups. To check whether the short and long timescales were affected by gender of the participant, unpaired t-test between male and female subjects for TD1, TD2 and TD3 were performed and no significant difference was found amongst genders in these groups. These findings suggest that the short and long timescales in the speech were not influenced by the gender of the speaker. A one-way ANOVA between children of ages 4-5 years, 7-8 years and adult for short timescales was performed in Intellectually disabled group and no significant difference was found ( $F=0.472523$ ,  $df=2$ ,  $p=0.629$ ). However, in case of Typically developing (TD) group, the short timescales measures were significantly different ( $F=10.04$ ,  $df=2$ ,  $p=0.000677$ ). The similar pattern was present for the ratio (short/long) of timescales. Hence, it can be concluded that the short timescales are changes with age in typically developing children but this growth is not happening in intellectually disabled subjects. The changes in long timescales were not significant in typically developing ( $F=3.43$ ,  $df=2$ ,  $p=0.048$ ). On the other hand, the long timescales are developing relatively well in subjects with intellectual disabilities ( $F=9.176132$ ,  $df=2$ ,  $p=0.001368$ ).

From these findings, we can conclude that features belonging to long-timescales (100 - 500 msec) develop earlier than those belonging to short timescales (25-50 msec). Whereas in intellectually disable population, spectro-temporal features at short timescales were not matured even in adults. It is important to understand the relationship of these timescales so, ratio (short/long timescales) was calculated and considered as one of the attribute. This differentiation of groups can be quantified further by classifying them into two classes, typically developing (TD) and Intellectually disabled (ID). The feature vector for classification consisted of short timescales, long timescales, their ratios and age. Table II. represents the feature vector for classification using k-NN, Naive Bayes, SVM, Decision tree, SVM and Neural Network respectively. The statistical distribution of attributes is shown in Table III.

A. Classification

The accuracy, class recall and class precision for classification of typically developing (TD) and Intellectually disabled (ID) using different classification techniques listed in Table IV. (a), (b), (c), (d) and (e). A good accuracy results were obtained by all five classification techniques. Neural Network and decision tree approach showed better accuracy than other four techniques. Neural Network showed highest accuracy of 95.28% as shown in Table IV (E) where as k-NN

model was least accurate for this dataset amongst all five classification techniques. The decision tree approach gave better results than Naive Bayes, k-NN and SVM with the accuracy of 91.39%. In Fig. 3, the Receiver Operating Characteristics(ROCs) for visualizing the performance of different classification techniques are provided. An optimistic ROC curve was calculated which consider correct classified examples before false. From Fig. 3 , it is clear that the decision tree approach has more area under the curve (AUC) than neural network and other three classification techniques. In the next section, conclusion and future scopes are provided.

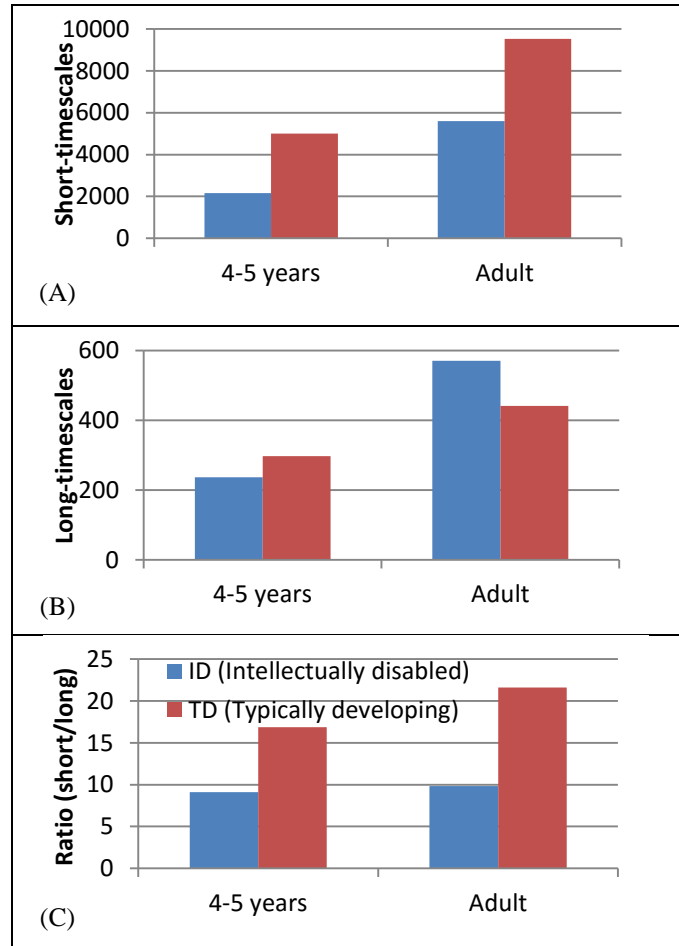


Fig. 2. Comparative graph representation of randomly selected representative from children and adult from Typically Developing(TD) and Intellectually Disabled (ID) (A) Short-timescales, (B) Long-timescales, (C) Ratio (Short/Long)

TABLE III. STATISTICAL DISTRIBUTION OF SHORT AND LONG TIMESCALES

Number of Timescales						
Groups	Short Timescale		Long Timescale		Ratio (Short /Long Timescale)	
	M	SD	M	SD	M	SD
		SEM		SEM		SEM
TD1 (n=10)	4123.75	711.77	406.31	83.01	10.2	1.82
		165.44		21.73		0.44
TD2	7047.81	1096.03	406.44	92.85	17.8	3.05

(n=22)		274.00		27.0		0.76
TD3 (n=20)	8194.56	1038.79	378.19	55.84	22.1	3.68
		259.07		25.20		0.88
MD (n= 30)	4535.66	2119.68	373.33	189.76	13.1	4.13
		387.00		34.64		0.75

SD: Standard Deviation, SEM: Standard Error of the mean.

TABLE IV. CLASSIFICATION RESULT: PERFORMANCE VECTOR AND CONFUSION MATRIX FOR NORMAL AND INTELLECTUALLY DISABLED POPULATION (A) K-NEAREST NEIGHBOUR (B) NAIVE BAYES, (C) SVM (SUPPORT VECTOR MACHINE), (D) DECISION TREE METHOD, (E) NEURAL NETWORK

(a) k-NN Accuracy: 70.28% ± 15.33%			
	True TD	True ID	Class precision
Pred. TD	39	11	78.00%
Pred. ID	13	19	59.38%
Class recall	86.54%	66.67%	
(b) Naive Bayes Accuracy: 86.67% ± 8.45%			
	True TD	True ID	Class precision
Pred. TD	46	5	90.20%
Pred. ID	6	25	80.65%
Class recall	88.46%	83.33%	
(c) Support Vector Machine Accuracy: 80.42% ± 6.13%			
	True TD	True ID	Class precision
Pred. TD	52	16	76.47%
Pred. ID	0	14	100%
Class recall	100%	46.67%	
(d) Decision Tree Method Accuracy: 91.39% ± 7.95%			
	True TD	True ID	Class precision
Pred. TD	48	3	94.12%
Pred. ID	4	27	87.10%
Class recall	92.31%	90.0%	
(e) Neural Network Accuracy: 95.28% ± 7.64%			
	True TD	True MD	Class precision
Pred. TD	50	2	96.15%
Pred. ID	2	28	93.33%
Class recall	96.15%	93.33%	

### V. CONCLUSION AND FUTURE SCOPE

In the present study, statistical properties of spectro-temporal features encoded at two different timescales were examined in the speech of normal and intellectually-disabled groups. The spectro-temporal features encoded at short timescales were developing well in normal developing children but this development was inadequate in the speech of age matched children with intellectual disabilities. The spectro-temporal features encoded at short and long timescales were tested on 52 normal and 30 participants with mild to moderate intellectual disabilities. The results revealed that features of short timescales, long timescales and their ratio were significantly different in intellectually disabled and age match control. These features were used to classify intellectually disabled and normal population by developing different classification models. A good accuracy of range of 90% was achieved through decision tree and neural networks. The above

system can be used as an early assessment aid for speech disorders and intellectual disabilities. In Future, we wish to apply this system for specific disorders like autism, ADHD, SLI etc . The study can be made more robust by further classifying the intellectually disabled in to mild and moderate level.

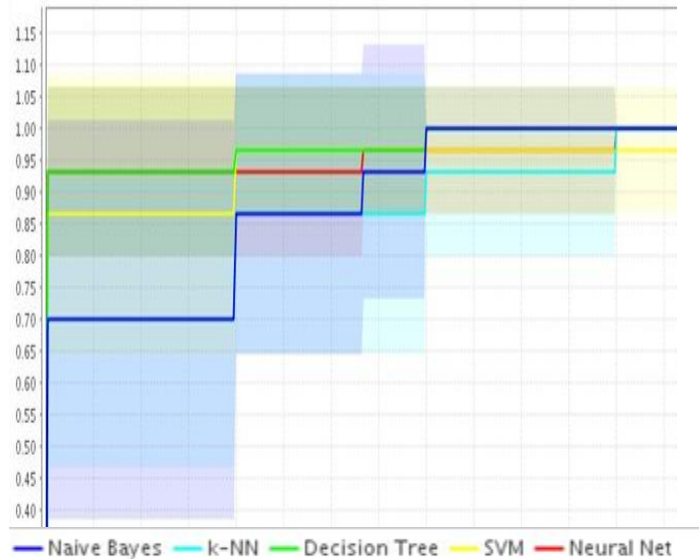


Fig. 3. Basic ROCs (Receiver Operating Characteristics) graph showing five classifier: K-Nearest Neighbour, Naive Bayes, Decision Tree Method, SVM and Neural Network

### REFERENCES

- [1] Doupe, Allison J., and Patricia K. Kuhl. "Birdsong and human speech: common themes and mechanisms." *Annual review of neuroscience* 22.1 (1999): 567-631.
- [2] P. F.Assmann, Peter F., Terrance M. Nearey, and Sneha V. Bharadwaj. "Developmental patterns in children's speech: patterns of spectral change in vowels." *Vowel inherent spectral change*. Springer Berlin Heidelberg, 2013. 199-230.
- [3] Ballard, Kirrie J., et al. "Developmental trajectory for production of prosody: lexical stress contrastivity in children ages 3 to 7 years and in adults." *Journal of Speech, Language, and Hearing Research* 55.6 (2012): 1822-1835.
- [4] Traunmüller, Hartmut, and Anders Eriksson. "Acoustic effects of variation in vocal effort by men, women, and children." *The Journal of the Acoustical Society of America* 107.6 (2000): 3438-3451.
- [5] Gautam, Sumanlata, and Latika Singh. "Classification of the Speech of Normally Developing and Intellectually Disabled Children." *International Journal of Data Mining And Emerging Technologies* 6.1 (2016): 28-37.
- [6] Gautam, Sumanlata, and Latika Singh. "Developmental pattern analysis and age prediction by extracting speech features and applying various classification techniques." *Computing, Communication & Automation (ICCCA), 2015 International Conference on*. IEEE, 2015.
- [7] Rosen, S. "Temporal information in speech and its relevance for cochlear implants." *Cochlear Implant: Acquisitions and Controversies, ed. B. Frayssse, N. Couchard* (1989): 3-26.
- [8] Moon, Il Joon, and Sung Hwa Hong. "What is temporal fine structure and why is it important?." *Korean journal of audiology* 18.1 (2014): 1-7.
- [9] Chait, Maria, et al. "Multi-time resolution analysis of speech: evidence from psychophysics." *Frontiers in neuroscience* 9 (2015).
- [10] Nittrouer S, Estee S, Lowenstein JH, Smith J. The emergence of mature gestural patterns in the production of voiceless and voiced word-final stops. *The Journal of the Acoustical Society of America*. 2005 Jan 1;117(1):351-64.

- [11] Tallal P, Gaab N. Dynamic auditory processing, musical experience and language development. *Trends in neurosciences*. 2006 Jul 31;29(7):382-90.
- [12] Tallal P, Stark RE, Mellits ED. Identification of language-impaired children on the basis of rapid perception and production skills. *Brain and language*. 1985 Jul 31;25(2):314-22.
- [13] Goswami U, Thomson J, Richardson U, Stainthorp R, Hughes D, Rosen S, Scott SK. Amplitude envelope onsets and developmental dyslexia: A new hypothesis. *Proceedings of the National Academy of Sciences*. 2002 Aug 6;99(16):10911-6.
- [14] Schalock RL, Borthwick-Duffy SA, Bradley VJ, Buntinx WH, Coulter DL, Craig EM, et al. Intellectual disability: Definition, classification, and systems of supports. American Association on Intellectual and Developmental Disabilities. 444 North Capitol Street NW Suite 846, Washington, DC 20001; 2010.
- [15] DSM-5 American Psychiatric Association. Diagnostic and statistical manual of mental disorders. Arlington: American Psychiatric Publishing. 2013.
- [16] Maber-Aleksandrowicz S, Avent C, Hassiotis A. A Systematic Review of Animal-Assisted Therapy on Psychosocial Outcomes in People with Intellectual Disability. *Research in Developmental Disabilities*. 2016 Mar 31;49:322-38.
- [17] Cabanas R. Some findings in speech and voice therapy among mentally deficient children. *Folia Phoniatria et Logopaedica*. 1954 Jul 1;6(1):34-7.
- [18] Cardoso-Martins C, Mervis CB. Maternal speech to prelinguistic children with Down syndrome. *American Journal of Mental Deficiency*. 1985 Mar.
- [19] Mervis CB. Early conceptual development of children with Down syndrome. *Children with Down syndrome: A developmental perspective*. 1990 Mar 30:252-301.
- [20] Mervis CB, Bertrand J. Developmental relations between cognition and language: Evidence from Williams syndrome. *Research on communication and language disorders: Contributions to theories of language development*. 1997:75-106.
- [21] Ingram D. First language acquisition: Method, description and explanation. Cambridge University Press; 1989 Sep 7.
- [22] Stoel-Gammon C. Down syndrome phonology: Developmental patterns and intervention strategies. *Down Syndrome Research and Practice*. 2001 Jan 1;7(3):93-100.
- [23] Singer Harris NG, Bellugi U, Bates E, Jones W, Rossen M. Contrasting profiles of language development in children with Williams and Down syndromes. *Developmental Neuropsychology*. 1997 Jan 1;13(3):345-70.
- [24] Tager-Flusberg H, Calkins S, Nolin T, Baumberger T, Anderson M, Chadwick-Dias A. A longitudinal study of language acquisition in autistic and Down syndrome children. *Journal of autism and developmental disorders*. 1990 Mar 1;20(1):1-21.
- [25] Fowler AE. Language abilities in children with Down syndrome: Evidence for a specific syntactic delay. *Children with Down syndrome: A developmental perspective*. 1990 Mar 30;9:302-28.
- [26] Rosen, Stuart. "Temporal information in speech: acoustic, auditory and linguistic aspects." *Philosophical Transactions of the Royal Society B: Biological Sciences* 336.1278 (1992): 367-373.
- [27] Greenberg, Joseph H. *Language universals: With special reference to feature hierarchies*. Walter de Gruyter, 2005.
- [28] Greenberg, Steven, and A. R. A. I. Takayuki. "What are the essential cues for understanding spoken language?." *IEICE transactions on information and systems* 87.5 (2004): 1059-1070.
- [29] Obleser, Jonas, Frank Eisner, and Sonja A. Kotz. "Bilateral speech comprehension reflects differential sensitivity to spectral and temporal features." *The Journal of Neuroscience* 28.32 (2008): 8116-8123.
- [30] Elliott, Taffeta M., and Frédéric E. Theunissen. "The modulation transfer function for speech intelligibility." *PLoS comput biol* 5.3 (2009): e1000302.
- [31] Ghitza, Oded. "On the role of theta-driven syllabic parsing in decoding speech: intelligibility of speech with a manipulated modulation spectrum." *Frontiers in psychology* 3 (2012): 238.
- [32] Peelle, Jonathan E., Joachim Gross, and Matthew H. Davis. "Phase-locked responses to speech in human auditory cortex are enhanced during comprehension." *Cerebral Cortex* 23.6 (2013): 1378-1387.
- [33] Doelling, Keith B., Luc H. Arnal, Oded Ghitza, and David Poeppel. "Acoustic landmarks drive delta-theta oscillations to enable speech comprehension by facilitating perceptual parsing." *Neuroimage* 85 (2014): 761-768.
- [34] Tallal, Paula, Steve L. Miller, Gail Bedi, Gary Byrna, Xiaojin Wang, Srikantan S. Nagarajan, Christoph Schreiner, William M. Jenkins, and Michael M. Merzenich. "Language comprehension in language-learning impaired children improved with acoustically modified speech." *Annual progress in child psychiatry and child development* (1997): 193-200.
- [35] Rocheron, Isabelle, Christian Lorenzi, Christian Füllgrabe, and Annie Dumont. "Temporal envelope perception in dyslexic children." *Neuroreport* 13, no. 13 (2002): 1683-1687.
- [36] Lehongre, Katia, Franck Ramus, Nadège Villiermet, Denis Schwartz, and Anne-Lise Giraud. "Altered low-gamma sampling in auditory cortex accounts for the three main facets of dyslexia." *Neuron* 72, no. 6 (2011): 1080-1090.
- [37] Goswami, Usha. "A temporal sampling framework for developmental dyslexia." *Trends in cognitive sciences* 15.1 (2011): 3-10.
- [38] Leong, Victoria, and Usha Goswami. "Acoustic-emergent phonology in the amplitude envelope of child-directed speech." *PloS one* 10.12 (2015): e0144411.
- [39] Di Stefano, Luigi, and Andrea Bulgarelli. "A simple and efficient connected components labeling algorithm." *Image Analysis and Processing, 1999. Proceedings. International Conference on*. IEEE, 1999.
- [40] Singh, Latika, and Nandini C. Singh. "The development of articulatory signatures in children." *Developmental science* 11.4 (2008): 467-473.

# Urdu Text Classification using Majority Voting

Muhammad Usman

Punjab University College of Information Technology  
University of the Punjab  
Lahore, Pakistan

Saba Ayub

Punjab University College of Information Technology  
University of the Punjab  
Lahore, Pakistan

Zunaira Shafique

Punjab University College of Information Technology  
University of the Punjab  
Lahore, Pakistan

Kamran Malik

Punjab University College of Information Technology  
University of the Punjab  
Lahore, Pakistan

**Abstract**—Text classification is a tool to assign the predefined categories to the text documents using supervised machine learning algorithms. It has various practical applications like spam detection, sentiment detection, and detection of a natural language. Based on the idea we applied five well-known classification techniques on Urdu language corpus and assigned a class to the documents using majority voting. The corpus contains 21769 news documents of seven categories (Business, Entertainment, Culture, Health, Sports, and Weird). The algorithms were not able to work directly on the data, so we applied the preprocessing techniques like tokenization, stop words removal and a rule-based stemmer. After preprocessing 93400 features are extracted from the data to apply machine learning algorithms. Furthermore, we achieved up to 94% precision and recall using majority voting.

**Keywords**—Text Classification; Tokenization; Stemming; Naïve Bayes; SVM; Random Forest; Bernoulli NB; Multinomial NB; SGD; Classifier; Majority Voting

## I. INTRODUCTION

Urdu is a well-known language in Indo-Pak regions. There are more than 100 million speakers of Urdu around the globe. It is a national language of Pakistan, one of the twenty-three official languages of India and is a 21st most spoken language in the world.

Due to the increasing use of Internet, electronic data is increasing tremendously. Users nowadays are interested in to find the information from large data sets quickly and efficiently. Therefore, Text Classification is vital and has numerous applications, including identification of text genre, filtration of news according to user's interest, recognition of email whether it is spam or not. Text classification can be helpful in article tagging where we want to assign particular category tag to the articles. There is a lot of work still required in the Urdu language in this area.

The purpose of this paper is to address the challenges in Urdu Text Classification and to introduce a method to achieve maximum accuracy using Machine Learning algorithms along with the max voting system. We used five different machine learning techniques to classify news into seven pre-defined classes which are sports, health, business, entertainment, science, culture and weird. Our method contains five primary

processes: tokenization, stop words removal, stemming, applying the machine learning algorithms and assign the class to the document by majority voting.

This paper is structured as follows: Section II explains literature review in which we described some of the work previously done regarding text classification. Section III explains the methodology that describes the complete process that we followed. It includes the details of collecting corpus through crawler, tokenization of the collected data, stop words removal, to convert each word into its stem or root form and then the application of classification algorithms on the preprocessed data. The algorithms are Naïve Bayes, Linear SGD, Multinomial Naïve Bayes, Bernoulli Naïve Bayes, Linear SVM and random forest classifier. Section IV explains results and the last section concludes the summary of all of the work.

## II. LITERATURE REVIEW

(Duwairi et al. 2009) compared the performance of three different classifiers Naïve Bayes, k-nearest-neighbor (KNN) and distance based classifier to the Arabic language. They selected ten categories and collected 1000 document corpus. Data cleaning is performed by removing punctuation marks, and the stop words and by formatting tags. The documents were classified using above mentioned three algorithms. Results showed that performance of Naïve Bayes classifier outperformed the other two classifiers.

(Ali et al. 2009) applied Text Classification on the Urdu Language. Tokenization is performed to convert the words normalization. Two algorithms, Naïve Bayes and SVM are used to measure the accuracy by eliminating the features like stop words, stemming and normalizing one by one from the corpus. The result showed 71.31 % accuracy on the baseline, 76.79% after eliminating stop words and 70.08% after stemming. SVM algorithm is applied for the lexicon with maximum accuracy in Naïve Bayes. Their accuracy with the baseline is 78.60%.

(S. Dumais et al. 1998) compared effectiveness of five different classification algorithms (Find Similar, Naïve Bayes, Decision Trees, Bayes Nets, and SVM) in term of accuracy and speed of learning and classification are compared. The dataset is divided into 75% and 25% parts which are used as training

set and development set respectively. The classifier is trained on the training set, and its accuracy is calculated using development set. Find similar has minimum learning time as this algorithm does not have any error minimization procedure and SVM is a second fastest method. The classification speed of all algorithms is almost same. The results showed that SVM is a useful and most accurate algorithm for classification purpose.

(Joachims 1998) expressed the multiple reasons to choose SVM as a classifier for his experiments. SVM does not depend on the number of input features. Furthermore, the document vectors used in this algorithm has very few non-zero entries, and SVM can find out a linear boundary in text categorization. They used two different types of datasets with ten predefined categories for the experiments. They compared the results of SVM with four conventional methods which are Naïve Bayes, Rocchio algorithm, C4.5, and KNN. SVM gives 86.4% results.

(Ahmed, Kashif et al. 2016) used only the SVM for text classification of Urdu headlines. Term frequency was computed for each word in the vocabulary, and inverse document frequency was computed after preprocessing on the corpus (normalization, stop words removal and stemming). They applied fixed value threshold for the unseen words on a list of words developed by calculating TF-IDF. Model is experimented with and without using stemming approach and got improved results with stemming with an accuracy increased by 3.5 %.

(Nidhi and Gupta 2012) performed Text Classification for Punjabi news articles; the results are computed using Naïve Bayes classification, ontology-based classification, and hybrid approach algorithms. They selected seven different categories on sports. Processing phases include stop words removal, stemming, punctuation marks and symbols removal. After feature extraction, the algorithms mentioned above were performed and classes assigned. They showed that the hybrid approach has better results over the other two.

(Odeh et al. 2015) purposed a new method for Arabic Text Classification using vector classification. The proposed approach uses a categorized Arabic documents corpus. The words are calculated to determine the documents keywords. The keywords of the training data categories were compared with the test documents keyword to find out the document's category. After testing, the accuracy of the proposed document was 98% in one category, and the other category has 93%.

(Wajeed et al. 2009) performed experiments on a large number of documents. He focused on hierarchical classification and worked on to extract the Lexicons from the data. The documents vectors are built by those lexicons and applied the Machine learning techniques to these vectors.

(Jain et al. 2015) performs text classification for the Punjabi language. Model is trained on Naïve Bayes and performed testing on four categories from news domain. They faced the issues in corpus collection, so the model is trained on limited data, but their model gives the satisfactory results based on four categories.

(Purohit et al. 2015) formed a word set to get probabilities by using Apriori algorithm and Naive Bayes. They used

Porter's stemmer algorithm for tokenization and the two classifiers, Parallel Formulation of Decision Tree and Sequential Decision Tree for Text Classification. By applying the algorithms, 75% accuracy is achieved.

(Dalal et al. 2011) used the pre-processing strategies and text classification algorithms like Naïve Bayes, decision trees to compare with Neural Networks. Additionally, some major issues involved in automatic text classification such as dealing with unstructured text, handling a large number of attributes and choice of suitable machine learning techniques are described. It was concluded that the performance of a classifier that based on Neural Networks is comparably better than Naïve Bayesian method.

(E. Han et al. 2001) used weight-adjusted k-Nearest Neighbor (WAKNN) for text classification. In WAKNN, the whole training set is converted into a matrix where each entry shows frequency of a word in a document which is called term frequency (TF). This matrix is normalized to get all values between 0 and 1. They used cosine similarity to find between documents. That takes documents and weights vector as input. These weight vectors are adjusted to get the best output. In the experiment, different algorithms like WAKNN, K-nearest neighbor and C4.5 are used. It is found by these experiments that WAKNN has the best accuracy as compared to other techniques.

(S. Al-Harbi et al. 2008) evaluated performance of two famous text classification algorithms (SVM and C5.0) on Arabic text. First, the words from the documents converted into a vector of features. To reduce input space of vector, Chi-Squared statistics ( $\chi^2$ ) are used. Chi-Squared statistics is applied on documents frequency, and top 30 features regarding class are selected. Data is divided into 70% and 30% parts which are used as the training and test data. The algorithms mentioned above were used for Text Classification the basis of the selected terms. C5.0 (78.42% accuracy) perform better than SVM (68.65% accuracy) in all categories of the data.

(Dennis et al. 2009) worked on the data of MIT newspaper "The Tech". They classified the historically archived data into six categories, as the data was already labeled; they used supervised learning for their experiments. Five hundred articles were selected from each category and randomly divided into training and testing data and applied three different classifier models on the data: Naïve Bayes, Maximum Entropy, and Probabilistic Grammar classification. Naïve Bayes classifier with Multi-Variate Bernoulli feature set gave 77% accuracy in their experiments.

(Maneka, S. and Radha N. 2013) introduced a technique to classify the text using keywords extraction. TF-IDF and WordNet are used to extract keywords. TF-IDF gives the words that can be possible keywords and WordNet is a lexical database for English words, and it calculates the similarity between the provided words. Naïve Bays, Decision tree, and KNN are the algorithms that are used to classify the text. To evaluate the algorithms on training and test data 10 folds cross-validation technique was used. From the results, Naïve Bayes gives the efficient result among all with 0.3 Root Mean Square error.

(Kamruzzaman et al. 2010) proposed a new algorithm that uses association rule mining along with Naïve Bayes. Although, the accuracy of this algorithm is acceptable, but this classification method requires time-consuming steps.

(Nidhi and Gupta 2012) applied text classification on Indian Punjabi language. Pre-processing includes special character removal, stop words removal and stemming. The Corpus is collected contains 150 Punjabi documents, which is extracted from Punjabi news websites and trained model for seven categories. The ontology-based classification algorithm is applied as it did not require training data. The result is 85%.

(Li et al. 2015) performed the experiment by using the text categorization method to predict the trend of Chinese stock. Text process was divided into three steps: Text representation, features selection, and Text categorization. KNN and SVM algorithms are performed for text classification. 1000 Poly Real Estate news are collected for the model. By applying process and techniques, SVM model shows better results with 83% precision.

(Jain et al. 2015) reviewed different techniques proposed by various authors for Punjabi text classification. The techniques used for Punjabi Text Classification are Rocchio's algorithms, K-nearest neighbors, Naïve Bayes, decision tree and neural networks. There is not much work has been done in the Punjabi language. So it is the very challenging task to perform classification on Punjabi data.

(Bhumika et al. 2013) performed research to get what is known about text classification so that it will make easy to decide what next steps should be made. For this purpose, Text Classification process is described which contains documentation collection, pre-processing, indexing, features extraction, classification and then evaluation to get fallout and accuracy. Types of text mining algorithms are text classification, discovering association and clustering algorithm. Further algorithms are discussed in each of the mentioned algorithms, and their advantages and disadvantages are discussed. It will make the decision easy which approach should be followed with which algorithm.

### III. METHODOLOGY

Our methodology contains a step-wise procedure; we started from the Urdu language corpus collection and then used some preprocessing techniques for features selection to apply actual classification algorithms. The flow chart in Fig-1 summarizes the process which we followed for our technique.

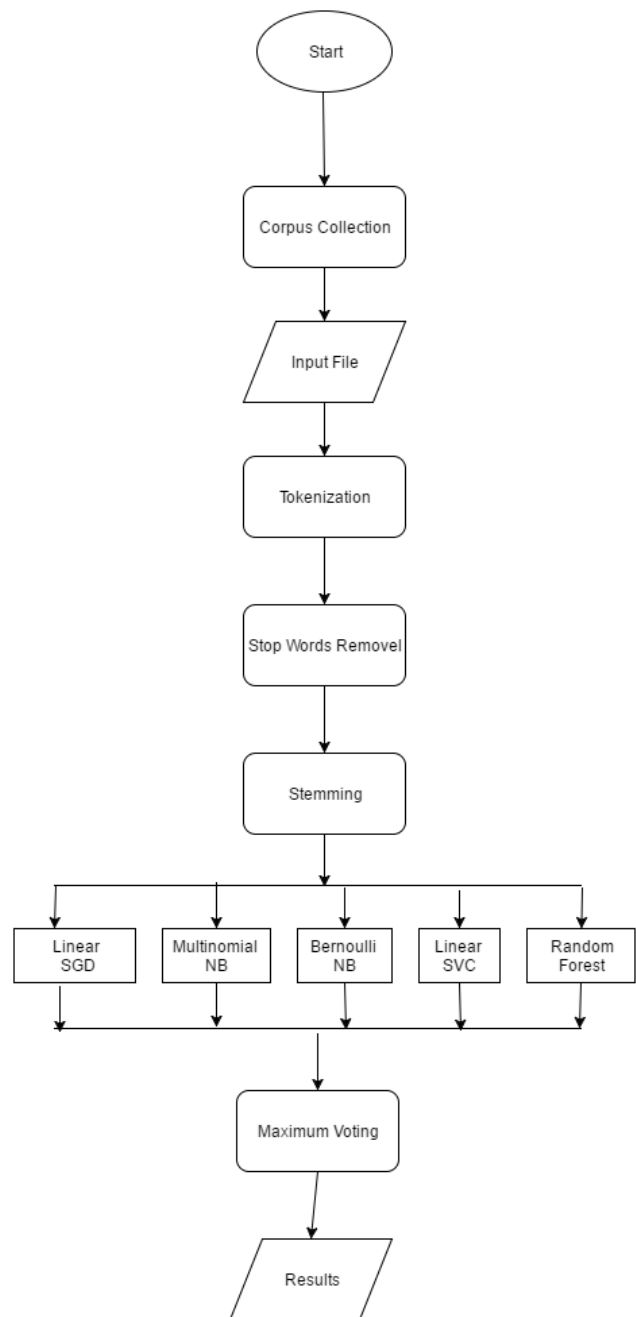


Fig. 1. Flow chart of Urdu News Classification

### A. CorpusCollection

Extensive training data plays a vital role in the development of a model that uses supervised learning algorithm. For this purpose, we write multiple crawlers to collect data from different news websites, e.g., express.pk, urdutimes.com, cricnama.com, bbc Urdu.com, dawnnews.tv. In total, we collected 21769 documents, and there are more than five million tokens and 120166 vocabularies. Data is collected category-wise in the text files, and categories are as follow: Business, Entertainment, Health, Science, Sports, Culture, and Weird. These categories are the classes used to classify our news data. After data collection, we performed preprocessing techniques like data cleaning, tokenization and stemming to convert the data in a required form on which we need to run algorithms. Details of the collected data are as following:

TABLE I. CORPUS DETAILS

Category	Total Documents	Total Tokens	Total Vocabulary
Sports	5288	1879731	34620
Culture	5285	1142748	48967
Entertainment	4395	652137	33252
Business	2683	560112	23154
Weird	1688	303815	23496
Science	1470	327176	21571
Health	960	212293	15377
Total Dataset	21769	5078012	120166

The sum of total vocabulary in all seven categories is 222008, but the vocabulary of the complete data set is 120166.

### B. Tokenization

While processing any natural language, tokenization is often considered as a very first step. Languages usually use white spaces, periods, punctuation marks as a word boundary. In our process, we tokenized the data set into words by space and by removing sentence boundary identifiers (i.e., '.', ',', '?', '!').

#### Example of Tokenization

پاکستان کی سرٹیفیکیشنز کافی بہتر ہیں

The above mention sentence will be tokenized as:

پاکستان	کی	سرٹیفیکیشنز	کافی	بہتر	ہیں
---------	----	-------------	------	------	-----

### C. Stop Words Removal

The words which are either not useful for the proposed classification models or used as prepositions are included in the stop words list. In our case, we maintained a list of stop words to omit from our text to extract meaningful data for the classifiers. We built the stop words list manually, which also includes the Arabic I'rāb and has more than 1000 entries. We used a look-up based approach to remove the stop words. Some examples of stop words are given below:

پوچھتی	لگیں	گی	انہوں	لوجی
تب	کیوں	تھے	اُنے	کھولیں
رکھی	چلو	معلوم	برائے	کہاں
والے	لگی	چلا	کریں	ہوچکے

Example of stop words

The same example which was used in tokenization, a dictionary list is generated after stop words removal is:

پاکستان	سرٹیفیکیشنز	کافی	بہتر
---------	-------------	------	------

### D. Stemming

In Urdu language word stemming is critical for Information Retrieval (IR). The stem is considered as the base word or a root word. Stemming is an iterative approach to reducing the words into their root form e.g. (منتظمین, Organizers) into (منتظم, Organizer). Urdu stemming rules are entirely different from English, and there is not very much work done in this language. There are many challenges we have faced while stemming. We are using two different approaches in our paper, lookup based and rule based approach. Lookup based method is fast, but it requires a significant amount of memory for words, and rule based approach requires a keen knowledge of literature. After some analysis of literature and study of Urdu grammar, 23 rules are used in this paper to get the stem of an Urdu word. We developed a stemmer which stems words into their base form by using the approaches mentioned above.

#### Approaches for Stemmer

Following are two approaches for stemming:

- 1) Look Up based Approach
- 2) Rule-based Approach

#### Look Up based Approach

After extracting stop words, we get the list of words vocabulary. The words in the vocabulary can be in their different forms; the words can be in singular, plural, past tense, or having affixes attached. So we need to get their base form to classify in a particular class. We maintain a dictionary of about 120000 unique Urdu words which are used in look-up approach to validate the word formed after applying stemming rules. We maintain a dictionary of about 120000 manually verified Urdu words which are used in look-up method to validate the word formed after applying stemming rules. For all words in the list, we go through the dictionary and check whether that word exists in the dictionary. If we find the word, we consider it a stemmed word. Our model will always return a legitimate word.

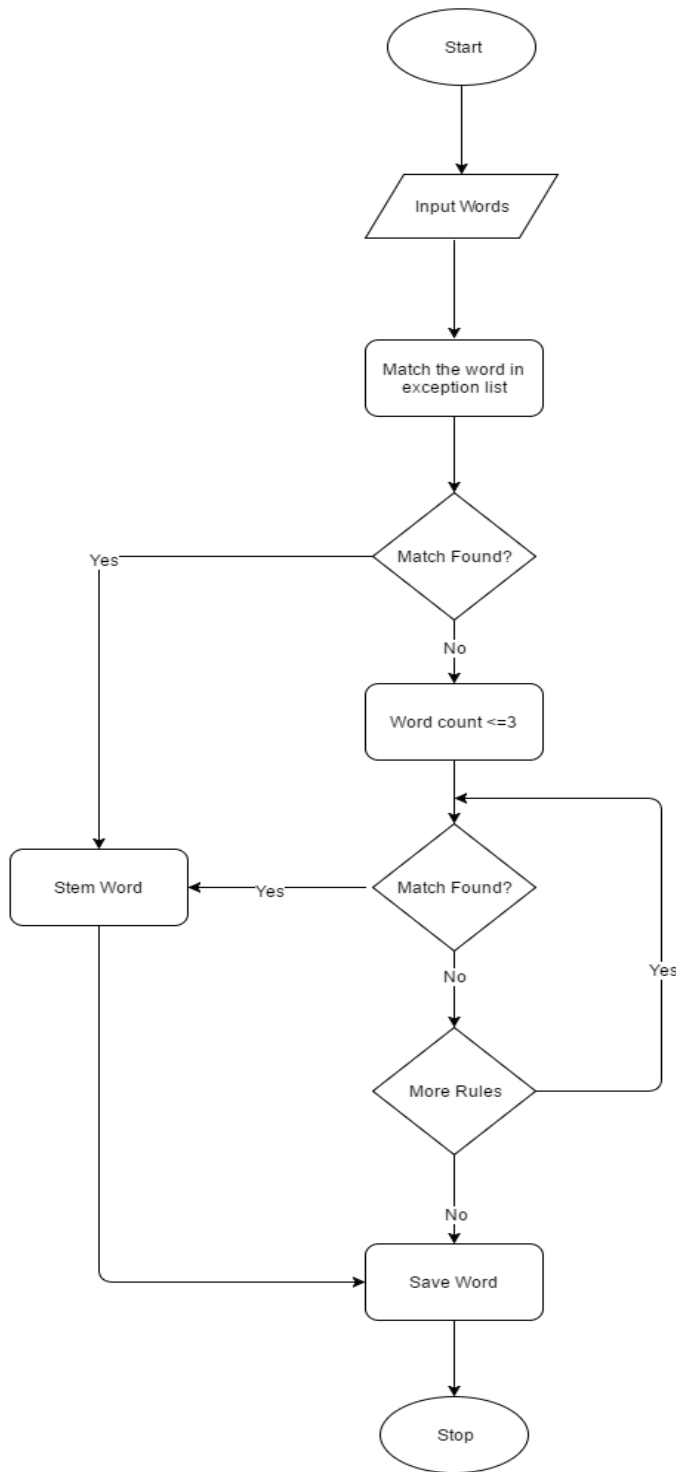


Fig. 2. Flow Chart for Stemmer

### Rule-based Approach

In this approach, we implemented 23 rules to convert word tokens into their stem form.

#### Exception List

Some words cannot stem by the stemming rules, and they are unique words, such words are exceptions. We have an exception list and at the very first step, our algorithm tries to

find out the word within the exception list and does not apply any further rule if it finds the word in the list.

#### 1) Length Based Decision

Domain experts suggest that if a word length is less than or equal to three, then the word is already in its root/stem form. So accept that word in the same form.

مات	رات	دین
ایر	چھت	مان

#### 2) Affixes Removal

Affixes are the addition to the base form of a word to modify its meaning or create a new word. Affixes are of two types: prefix and suffix.

- The prefix is a morpheme that can either be of a single, two or more than two letters attached at the beginning of a word.

Word	Rule	Stem
بالتر	Remove → با	التر
پر اعتماد	Remove → پر	اعتماد

- The suffix attaches at the end of a word. It may also have a single, two or more than two characters.

Word	Rule	Stem
دغلیاز	Remove → باز	دغا
خوددار	Remove → دار	خود

#### 3) Word ends with ء (Rule 1)

If a word ends with ء (hamza, bari-yay), remove ء (hamza, bari-yay) and add ا (Alif).

Word	Rule	Stem
چاہئے	ا → ء	چاہا
جوئے	ا → ء	جوا

#### 4) Word ends with ئ (Rule 2)

If a word ends with ئ (hamza, bari-yay), remove ئ (hamza,) and add ا (Alif) at the end of the word.

Word	Rule	Stem
گزرگئے	Remove → ئ Add → ا	گزرگیا
کمائے	Remove → ئ Add → ا	کمایا

#### 5) Word ends with ئے (Rule 3)

If a word ends with ئے (hamza, bari-yay), remove ئے (hamza, bari-yay).

Word	Rule	Stem
چڑھائے	Remove → ئے	چڑھا
اٹھائے	Remove → ئے	اٹھا

#### 6) Word ends with ے (Rule 4)

If a word ends with ے (bari-yay), remove ے (bari-yay) and add ا (Alif) at the end of the word.

Word	Rule	Stem
گزرئے	Remove → ے Add → ا	گزرنا

دھرنے	Remove → ے Add → ا	دھرنا
-------	-----------------------	-------

7) Word ends with ے (Rule 5)

If a word ends with ے (bari-yay), remove ے (bari-yay) and add ۰ (Hey) at the end of the word.

Word	Rule	Stem
علاقے	Remove → ے Add → ۰	علاقہ
پیمانے	Remove → ے Add → ۰	پیمانہ

8) Word ends with ے (Rule 6)

If a word ends with ے (bari-yay), remove ے (bari-yay).

Word	Rule	Stem
ضلعے	Remove → ے	ضلع
درمیانے	Remove → ے	درمیان

9) Word ends with وں (Rule 7)

If a word ends with وں (wao-non guna), remove وں (wao-non guna).

Word	Rule	Stem
سرخیوں	Remove → وں	سرخی
باغیوں	Remove → وں	باغی

10) Word ends with وں (Rule 8)

If a word ends with وں (wao-non guna), remove وں (wao-non guna) and add ۰ (Hey) at the end of the word.

Word	Rule	Stem
حملوں	Remove → وں Add → ۰	حملہ
چھاپوں	Remove → وں Add → ۰	چھاپہ

11) Word ends with وں (Rule 9)

If a word ends with وں (wao-non guna), remove وں (wao-non guna) and add ا (alif) at the end of the word.

Word	Rule	Stem
اندھیروں	Remove → وں Add → ا	اندھیرا
کپڑوں	Remove → وں Add → ا	کپڑا

12) Word ends with یں (Rule 10)

If a word ends with یں ('yay' and non-guna) remove یں ('yay' and non-guna)

Word	Rule	Stem
خیریں	Remove → یں	خیر
ٹیمیں	Remove → یں	ٹیم

13) Word ends with ۓں (Rule 11)

If a word ends with ۓں (Hamza-wao , non-guna), remove ۓں (Hamza-wao , non-guna).

Word	Rule	Stem
رینماوں	Remove → ۓں	رینما
بندوؤں	Remove → ۓں	بندو

14) Word ends with یان (Rule 12)

If a word ends with یان (yay ,alif , non-guna), remove یان (yay , alif , non-guna) and add ی (choti-yay) at the end.

Word	Rule	Stem
گرفتاریاں	Remove → یان Add → ی	گرفتاری
کہانیاں	Remove → یان Add → ی	کہانی

15) Word ends with یات (Rule 13)

If a word ends with یات (yay ,alif , te), remove یا (yay , alif ).

Word	Rule	Stem
ضروریات	Remove → یا	ضرورت
سہولیات	Remove → یا	سہولت

16) Word ends with یات (Rule 14)

If a word ends with یات (yay ,alif , te), remove last ا ( alif ).

Word	Rule	Stem
بدایات	Remove → ا	بدایت
شکایات	Remove → ا	شکایت

17) Word ends with یات (Rule 15)

If a word ends with یات (yay ,alif , te), remove یات (yay ,alif , te).

Word	Rule	Stem
جنگلیات	Remove → یات	جنگل
نمکیات	Remove → یات	نمک

18) Word ends with ات (Rule 16)

If a word ends with ات (alif ,te), remove ات (alif ,te).

Word	Rule	Stem
خواہشات	Remove → ات	خواہش
بخارات	Remove → ات	بخارا

19) Word ends with ات (Rule 17)

If a word ends with ات (alif ,te), remove ات (alif ,te) and add ۰ (Hey) at the end of the word.

Word	Rule	Stem
جذبات	Remove → ات Add → ۰	جذبہ
مقدمات	Remove → ات Add → ۰	مقدمہ

20) Word ends with یں (Rule 18)

If a word ends with یں (yay, non-guna), remove یں (yay, non-guna).

Word	Rule	Stem
ماہرین	Remove → یں	ماہر
صارفین	Remove → یں	صارف

21) Word ends with ی (Rule 19)

If a word ends with ی (choti-yay), remove ی (choti-yay) from end. If legit then accept.

Word	Rule	Stem
پاکستانی	Remove → ی	پاکستان
غلطی	Remove → ی	غلط

22) Word ends with ی (Rule 20)

If a word ends with ی (choti-yay), replace ی (choti-yay) with ا (Alif).

Word	Rule	Stem
کتنی	Remove → ی Add → ا	کتنا

چاپتی	Remove → ی Add → ا	چاپتا
-------	-----------------------	-------

23) Word ends with وں (Rule 21)

If a word ends with وں (wao-non guna), remove وں (wao-nonguna).

Word	Rule	Stem
کسانوں	Remove → وں	کسان
مرغیوں	Remove → وں	مرغی

24) Word ends with نگ (Rule 22)

If a word ends with نگ (non ,gaf), remove نگ (non , gaf).

Word	Rule	Stem
انجینئرنگ	Remove → نگ	انجینئر
مارکیٹنگ	Remove → نگ	مارکیٹ

25) Word ends with ز (Rule 23)

If a word ends with ز (zae), remove ز (zae).

Word	Rule	Stem
فانڈرز	Remove → ز	فانڈر
سسٹرز	Remove → ز	سسٹر

E. Stemmer Accuracy

The following strategy computes the accuracy:

- Split whole corpus in training, development and testing data by 60, 20 and 20 ratios respectively.
- Apply all approaches mentioned in 3.4.2 section on training data and trained our model.
- Using trained model and manually stemmed dataset, calculated accuracy on development data.
- Identify new rules and exceptional words by analysis on stemmed words generated using development data and manually stemmed dataset.
- Add newly identified rules in rules list and new exceptional words in the exceptions list.
- Run updated model on test data and obtained accuracy.
- Repeat all steps three times.

TABLE II. STEMMER ACCURACY TABLE

Iterations	Development Data Accuracy	Test Data Accuracy
First	0.89	0.91
Second	0.93	0.94
Third	0.94	0.95

F. Classification Algorithms

After applying all preprocessing, we have a list of features to apply classification algorithm. Data is divided into two parts: training data and testing data. Out of 21769 documents, 70% of the documents are considered as training dataset and 30% as a testing dataset. Following are the details of the algorithms we have applied. Each classifier gives different accuracy score, and can suggest a different class to a document as compared to the other algorithms. We assigned a class to a document by majority voting from each algorithm. We discuss the detailed results from each classifier in this section.

1) Multinomial Naïve Bayes classifier

Naïve Bayes technique is a set of supervised learning algorithms. Naïve Bayes techniques are very common in text classification.

As name proposes, Multinomial Naïve Bayes works on the data that is distributed among multiple features. We consider vocabulary V as features (N total features) so we can define a document as an occurrence of features in an ordered sequence.

We compute a vector  $\theta_y = (\theta_{y1}, \dots, \theta_{yn})$  for each category y. We can calculate the probability of occurrence of each feature i in a category y as  $P(x_i | y)$ .

So we can estimate the category by the following calculation.

$$\theta = \frac{\alpha + N_{yi}}{an + N_y}$$

Where  $\alpha = 1$  is to add Laplace smoothing for unseen features. The precision of this model is 87%.

TABLE III. MULTINOMIAL NAÏVE BAYES RESULTS

Classes	Precision	Recall	F1-Score
Business	0.979	0.988	0.983
Entertainment	0.978	0.938	0.957
Health	0.924	0.967	0.945
Science	0.659	0.895	0.759
Sports	0.738	0.595	0.659
Weird	0.999	0.978	0.988
Culture	0.800	0.822	0.811
Average / Total	0.868	0.883	0.872

2) Bernoulli Naïve Bayes Classifier

Bernoulli is also similar to Multinomial technique. It also works on the data that is discrete and distributed among N features. The only difference is Multinomial computes the frequency of each feature in a particular category whereas the Bernoulli is more like binary distributed and assign 1/0 if the feature is seen or not in a category.

$$P(x_i|y) = P(I|y) x_i + (1 - P(I|y)) (1 - x_i)$$

As the above equation shows Bernoulli's is interested only in the occurrence of a word and penalizes if a feature does not be seen in a category. So it gives the better results on small data sets. Once the model is trained, we test it using testing data (McCallum and Nigam 2002). The precision of this model is 84%.

TABLE IV. BERNOULLI NAÏVE BAYES RESULTS

Classes	Precision	Recall	F1-Score
Business	0.949	0.987	0.968
Culture	0.981	0.597	0.742
Entertainment	0.647	0.979	0.779
Health	0.804	0.885	0.842
Science	0.760	0.625	0.686
Sports	1.000	0.935	0.966
Weird	0.742	0.842	0.789
Average / Total	0.840	0.836	0.825

3) Linear SVM

Another algorithm which we are using in our classification system is Linear SVM. In SVM we treat features as 2D space and try to find the closest point which we call support vector

because features are treated as vectors in space, once we find the closest point then draw a line connecting them. We have already made a line that separates these two points as far as possible, and the SVM says the best separated line is, that bisects the two points and is perpendicular to the line that connects them. We are making some connection between documents and classes by connecting them as well as separating them to the particular distance. Whenever a document appears, we map it to a point and check the point on the other end of the separating line, to predict its class. By applying this algorithm, we get the precision up to 89%.

TABLE V. LINEAR SVM RESULTS

Classes	Precision	Recall	F1-Score
Business	0.980	0.993	0.986
Culture	0.962	0.963	0.962
Entertainment	0.955	0.945	0.950
Health	0.739	0.920	0.820
Science	0.785	0.689	0.734
Sports	0.995	0.994	0.994
Weird	0.831	0.808	0.820
Average / Total	0.892	0.902	0.895

4) Random Forest Algorithm

The fourth classification algorithm in our classifier system to get accuracies is Random Forest Classifier. In this model, we make decision trees by selecting a random sample from our training set using tree bagging and random subspace technique. We generate different trees in the forest by choosing random samples. Each tree gives us a classification. Then we choose the output of most correlated trees from the forest.

Once all of the trees assembled in the forest, the labeled data get pass through the trees. Here come the proximities, the proximity of two events get increased by one if both events lie on the same leaf node.

In the end, proximities get normalized with the Total number of trees in the forest. The precision of Random Forest Algorithm on our data set is 83%.

TABLE VI. RANDOM FOREST

Classes	Precision	Recall	F1-Score
Business	0.887	0.995	0.938
Culture	0.847	0.975	0.906
Entertainment	0.926	0.891	0.908
Health	0.645	0.784	0.708
Science	0.675	0.443	0.535
Sports	0.998	0.982	0.990
Weird	0.825	0.542	0.654
Average / Total	0.829	0.802	0.805

5) Linear SGD Classifier

Linear SGD is the simplest algorithm for classification. In this algorithm, we use the gradient descent approach of gradually increasing or decreasing parameters to achieve our goal. With the combination of linear regression, we randomly initialize our parameters and compute accuracy through error function.

In this method, we learn the weights for our data that help to minimize the error of the model. In each cycle, the weights get updated until the error reaches to its minimum threshold. The equation is

$$\omega = \omega - \alpha * \Delta$$

Where  $\omega$  is a learned weight, and  $\alpha$  is learning rate. The precision of this algorithm is 90%.

TABLE VII. LINEAR SGD RESULTS

Classes	Precision	Recall	F1-Score
Business	0.978	0.991	0.985
Entertainment	0.963	0.962	0.963
Health	0.948	0.946	0.947
Science	0.796	0.913	0.851
Sports	0.790	0.734	0.761
Weird	0.995	0.994	0.995
Culture	0.826	0.798	0.812
Average / Total	0.899	0.906	0.902

6) Max Voting:

The maximum voting technique is quite famous in decision making that is implemented to get best voted predicted class by all the algorithms. For this technique, all of the results generated by above five algorithms is gathered and then take mod of the predicted class of each document. Below table shows the accuracy of the maximum voting technique for every class.

TABLE VIII. MAX VOTING RESULTS

Classes	Precision	Recall	F1-Score
Business	0.980	0.994	0.987
Culture	0.978	0.966	0.972
Entertainment	0.953	0.974	0.963
Health	0.876	0.913	0.894
Science	0.911	0.880	0.895
Sports	0.998	0.987	0.993
Weird	0.898	0.893	0.896
Average / Total	0.942	0.944	0.943

IV. RESULTS

We applied five algorithms on the data and got different accuracies. We also applied some preprocessing techniques like tokenization, stop words removal and stemming before the application of classifiers. Does the preprocessing help to maximize the classifier's accuracy? To check the difference between preprocessed data and raw data we run our algorithms on the tokenized data and data after stemming has been applied. The following table describes the brief summary of all the applied algorithms.

TABLE IX. ACCURACY OF ALGORITHMS BEFORE STEMMING

Algorithms	Precision	Recall	F1-score
Multinomial NB	0.671	0.683	0.638
Bernoulli NB	0.713	0.714	0.711
Linear SVM	0.772	0.795	0.774
Random Forest	0.771	0.772	0.756
Linear SGD	0.763	0.781	0.764
Max Voting	0.825	0.815	0.811

TABLE X. ACCURACY OF ALGORITHMS AFTER STEMMING

Algorithms	Precision	Recall	F1-score
Multinomial NB	0.868	0.883	0.872
Bernoulli NB	0.742	0.842	0.789
Linear SVM	0.892	0.902	0.895
Random Forest	0.825	0.542	0.654
Linear SGD	0.899	0.906	0.902
Max Voting	0.942	0.944	0.943

Clearly, from the table, Maximum Voting technique gives better precision, recall, and f1-score. Regarding the algorithm used, SVM gives us better precision where linear SGD have better recall and f1-score.

The purpose of this experiment is to develop Urdu Text Classifier using the best approach which is used in previous experiments. The main parts of this experiment are to stem data and to classify that data into classes. For stemming we follow two papers; Urdu based stemmer by (Akram et al. 2009) and stemmer for multi Urdu text by (Ali et al. 2016). Our stemming accuracy is 95% which is more than Asma's experiment (91%) and Waheed's experiment (85.02%).

For text classification, we have applied five different algorithms and their accuracies are compared with each other. Best accuracy we find by applying Linear SVM and Linear SGD algorithms on our data set. To get the maximum accuracy Max voting technique is also being implemented in this paper and gives 94% accuracy.

## V. CONCLUSION

The paper presents the work performed to develop a text classifier for Urdu. The process we followed is stepwise, In the first step it tokenizes the data, applies pre-processing techniques including stop words removal and stemming using different algorithms, on the tokenized data. The experimental evaluation using seven different news classes are showing good accuracies by using five different algorithms, and max voting technique. Authors believe that the trained models will also work well on all type of Urdu text data, and their research will be used and help to develop innovative solutions using Urdu text.

## VI. FUTURE WORK

Urdu Text classification has much room for improvement. Currently, we are using space-based tokenization, we can use the techniques of text segmentations, POS tagging to get better information from data and we can also use lemmatization instead of stemmer to get more improved results of text classification.

## REFERENCES

- [1] Duwairi, Rehab, Mohammad Nayef Al-Refai, and Natheer Khasawneh. "Feature reduction techniques for Arabic text categorization." *Journal of the American society for information science and technology* 60.11 (2009): 2347-2352.
- [2] Ali, Abbas Raza, and Maliha Ijaz. "Urdu text classification." *Proceedings of the 7th international conference on frontiers of information technology*. ACM, 2009..
- [3] Dumais, Susan, et al. "Inductive learning algorithms and representations for text categorization." *Proceedings of the seventh international conference on Information and knowledge management*. ACM, 1998..
- [4] Joachims, Thorsten. "Text categorization with support vector machines: Learning with many relevant features." *European conference on machine learning*. Springer Berlin Heidelberg, 1998.
- [5] AHMED, Kashif, et al. "Framework for Urdu News Headlines Classification." *Journal of Applied Computer Science & Mathematics* 21 (2016).
- [6] Nidhi, Vishal Gupta. "Domain Based Classification of Punjabi Text Documents using Ontology and Hybrid Based Approach." *24th International Conference on Computational Linguistics*. 2012.
- [7] Odeh, Ashraf, et al. "Arabic Text Categorization Algorithm using Vector Evaluation Method." *arXiv preprint arXiv:1501.01318* (2015).
- [8] Wajeed, Mohammed Abdul, and T. Adilakshmi. "Text classification using machine learning." *Journal of Theoretical and Applied Information Technology* 7.2 (2009): 119-123.
- [9] Jain, Ubeeka, and Kavita Saini. "A Review on the Punjabi Text Classification using Natural Language Processing.", 2015.
- [10] Purohit, Anuradha, et al. "Text Classification in Data Mining.", 2015.
- [11] Dalal, Mita K., and Mukesh A. Zaveri. "Automatic text classification: a technical review." *International Journal of Computer Applications* 28.2 (2011): 37-40.
- [12] Han, Eui-Hong Sam, George Karypis, and Vipin Kumar. "Text categorization using weight adjusted k-nearest neighbor classification." *Pacific-asia conference on knowledge discovery and data mining*. Springer Berlin Heidelberg, 2001.
- [13] Al-Harbi, S., et al. "Automatic Arabic text classification." (2008).
- [14] Ramdass, Dennis, and Shreyes Seshasai. "Document classification for newspaper articles." (2009).
- [15] Menaka, S., and N. Radha. "Text classification using keyword extraction technique." *International Journal of Advanced Research in Computer Science and Software Engineering* 3.12 (2013).
- [16] Kamruzzaman, S. M., Farhana Haider, and Ahmed Ryadh Hasan. "Text classification using data mining." *arXiv preprint arXiv:1009.4987* (2010).
- [17] Nidhi, Vishal Gupta. "Domain Based Classification of Punjabi Text Documents using Ontology and Hybrid Based Approach." *24th International Conference on Computational Linguistics*. 2012.
- [18] Li, Bozhao, et al. "Text Categorization System for Stock Prediction." *International Journal of u-and e-Service, Science and Technology* 8.2 (2015): 35-44.
- [19] Jain, Ubeeka, and Kavita Saini. "A Review on the Punjabi Text Classification using Natural Language Processing.", 2015.
- [20] Bhumika, Prof Sukhjot Singh Sehra, and Prof Anand Nayyar. "A review paper on algorithms used for text classification." *International Journal of Application or Innovation in Engineering & Management* 3.2 (2013): 90-99.
- [21] McCallum, Andrew, and Kamal Nigam. "A comparison of event models for naive bayes text classification." *AAAI-98 workshop on learning for text categorization*. Vol. 752. 1998.
- [22] Akram, Qurat-ul-Ain, Asma Naseer, and Sarmad Hussain. "Assas-Band, an affix-exception-list based Urdu stemmer." *Proceedings of the 7th workshop on Asian language resources*. Association for Computational Linguistics, 2009.
- [23] Ali, Mubashir, et al. "A Rule based Stemming Method for Multilingual Urdu Text." *International Journal of Computer Applications* 134.8 (2016): 10-18.

# An Item-based Multi-Criteria Collaborative Filtering Algorithm for Personalized Recommender Systems

Qusai Shambour, Mou'ath Hourani, Salam Fraihat

Department of Software Engineering, Faculty of Information Technology  
Al-Ahliyya Amman University  
Amman, Jordan

**Abstract**—Recommender Systems are used to mitigate the information overload problem in different domains by providing personalized recommendations for particular users based on their implicit and explicit preferences. However, Item-based Collaborative Filtering (CF) techniques, as the most popular techniques of recommender systems, suffer from sparsity and new item limitations which result in producing inaccurate recommendations. The use of items' semantic information besides the inclusion of multi-criteria ratings can successfully alleviate such problems and generate more accurate recommendations. This paper proposes an Item-based Multi-Criteria Collaborative Filtering algorithm that integrates the items' semantic information and multi-criteria ratings of items to lessen known limitations of the item-based CF techniques. According to the experimental results, the proposed algorithm prove to be very effective in terms of dealing with both of the sparsity and new item problems and therefore produce more accurate recommendations when compared to standard item-based CF techniques.

**Keywords**—Collaborative Filtering; Recommender Systems; Multi-Criteria; Sparsity; New Item

## I. INTRODUCTION

The information overload problem occurs due to the increasing growth of web information, which makes it difficult for web users to locate relevant information, products or services according to their needs and preferences. Recommender systems have been broadly utilized to address the information overload problem by helping web users in finding the most related information, products or services in diverse application domains such as e-commerce, e-learning, e-government and e-tourism [1-6]. Recommender systems are personalized decision support tools employed to exploit the users' explicit and implicit preferences to recommend to them the most relevant information, products or services. Collaborative filtering (CF) is one of the most known techniques in recommender systems to generate personalized recommendations. The CF technique can be further classified into user-based and item-based CF techniques. In user-based CF, recommendations for users are generated based on items that are liked by other similar users. In item-based CF, recommendations for users are generated based on items that are similar to those they have liked in the past [1, 7].

However, the item-based CF technique is proved to be more successful in terms of the prediction accuracy than the user-based CF technique [8, 9]. Regardless of its efficiency, the item-based CF does not perform well and may produce

inaccurate recommendations when there is a lack of users' ratings due to two key obstacles: the sparsity and the new item problems [8, 9]. To solve such problems, recent recommender systems have focused on the integration of additional information, thus, allowing recommender systems to exploit the added information as a supplementary to the insufficient users' ratings to generate more accurate recommendations. Examples of such additional information are: the semantic relationships that exist among users or items [10-14]; and the multi-criteria ratings which can imply more complex users' preferences [7, 15-17].

Semantic information associated with users or items can be represented by taxonomies or ontologies and has an important task, by including concepts and their relationships, in accurately representing the item information and the user model [10-14]. In addition, recent studies acknowledge that multi-criteria ratings of users can be utilized to find the actual correlations between users as it based on more than one criterion [18-25]. To sum up, the additional information of users and items would assist in precisely model users' preferences and items' relations, and accordingly can result in more accurate recommendations.

This paper proposes an Item-Based Multi-Criteria CF (IMCCF) algorithm for personalized recommender systems. The proposed algorithm is a hybrid of MC item-based CF and an item-based semantic filtering techniques. The proposed algorithm exploits the additional information provided by both the semantic relationships among items and the multi-criteria ratings of users to address the sparsity and new item problems. The proposed algorithm proved to be more effective in dealing with the above limitations and therefore produce more accurate recommendations when compared to standard item-based CF techniques. The rest of this paper is ordered as follows. Section 2 describes the related work of the research. Section 3 demonstrates the proposed Item-Based Multi-Criteria CF algorithm. Section 4 shows the experimental setup and results. The conclusion and future work are revealed in Section 5.

## II. RELATED WORK

In general, most of current recommender systems use single-criterion CF recommendation approaches, which have been deployed highly successfully for many years. Recently, a number of research studies [18-25] have employed multi-criteria ratings in their recommender systems taking into account that multi-criteria ratings would facilitate the accurate modeling of users' preferences, and thus provide more precise

recommendations. Examples of recent studies on Multi-Criteria Recommender Systems are:

Ebadi & Krzyzak [18] develop an intelligent hybrid multi-criteria hotel recommender system that suggests a number of hotels that are tailored for the preferences of a given user. To enhance the recommendation accuracy, the proposed system utilizes a multi-criteria rating technique to better capture and learn the preferences of users. TripAdvisor data is used to train the proposed system. Experimental results based on different settings and scenarios confirm the outstanding performance of recommendation accuracy of the system.

Jhalani et al. [19] propose the employment of multi linear regression approach for determining the weights for each criterion and calculating the overall ratings predictions of each item. Experimental results on Yahoo movie dataset show the effectiveness of the proposed method in generating quality recommendation compared with single criterion and multi-criteria CF benchmark algorithms.

Nilashi et al. [20] propose a novel recommendation algorithm using expectation maximization (EM) and classification and regression tree (CART) in order to improve the recommendation accuracy of multi-criteria recommender systems. The authors also employ the principal component analysis as a dimensionality reduction technique to alleviate the multi-collinearity limitation due to the interdependencies between different criteria in multi-criteria CF datasets. TripAdvisor and Yahoo! Movies datasets are used to validate the performance of the proposed algorithm. Experimental results show that the proposed algorithm extensively enhances the accuracy of recommendations in multi-criteria CF.

Farokhi et al. [21] propose a tourism recommender system that employs a recommendation method that integrates both multi criteria user-based and multi criteria item-based CF approaches. Fuzzy C-means algorithms beside k-means algorithms have been used to improve the recommendation accuracy of user-based and item-based CF approaches. The authors acknowledge that the use of multi-criteria rating in producing recommendations can improve the recommendation accuracy by providing more realistic recommendation that are very close to users' interests. Experimental results on the TripAdvisor dataset confirm the high performance in accuracy of the proposed method.

Nilashi et al.[22] incorporate the multi-criteria ratings in a new hybrid method for hotel recommendation using prediction and dimensionality reduction techniques to improve the predictive accuracy. The proposed method is a hybrid of the expectation maximization (EM) clustering, adaptive neuro-fuzzy inference system (ANFIS) and the principal component analysis (PCA) techniques. These techniques are combined to boost the predictive accuracy of the multi-criteria CF in tourism domain by exploiting the extra knowledge hidden in the multi-criteria ratings and reducing the dimensionality of a dataset to deal with the multi-collinearity problem presents in the multi-criteria ratings. Experimental results on TripAdvisor dataset show that the proposed method achieved high recommendation accuracy in the tourism sector.

Bokde et al.[23] propose a university recommendation system that provides students, of the Engineering College, with recommendations derived from their past preferences. The proposed system employ a hybrid method of multi-criteria item-based CF and dimensionality reduction approaches to produce high quality recommendations. The hybrid method decreases the computational cost and increases the prediction accuracy, thus overcoming the scalability and sparsity limitations.

Bilge & Kaleli [24] propose a multi-criteria item-based CF framework that extends the conventional item-based CF algorithm to make use of the benefits of multi-criteria rating systems. The authors determine the most suitable neighborhood selection approach and examine the performance of accuracy of statistical regression-based predictions. Experimental results on Yahoo Movies dataset affirm the assumption that multi-criteria item-based CF algorithms can accurately generate more reliable recommendations than single criterion rating item-based CF algorithms.

Shambour & Lu [25] propose a hybrid multi-criteria trust-enhanced CF (MC-TeCF) method that addresses the limitations of single criterion user-based CF techniques by integrating the MC user-based CF and the MC user-based Trust filtering techniques. Empirical results of the proposed MC-TeCF method prove its significance over single criterion user-based CF techniques, in improving the accuracy and coverage of recommendations, when faced with extreme sparse data sets or new users.

However, compared to the huge amount of research carried on in the last years on single-criteria recommender systems, the adoption and employment of multi-criteria ratings in recommender systems has received limited attention [15, 22]. Thus, the need of more research in the area of multi-criteria recommender systems has provoked our interest toward the development of an Item-Based Multi-Criteria CF algorithm in this study.

### III. THE ITEM-BASED MULTI-CRITERIA CF (IMCCF) ALGORITHM

The proposed IMCCF algorithm takes a raw matrix of user-item MC ratings, as input, which consists of multi-criteria ratings of  $M$  users on  $N$  items, and a hierarchical tree structured item taxonomy. The item taxonomy, given by the domain experts, has a set of main items' categories where items should belong to as leaf nodes. It should be noted that each item can be a member of one or more items' categories. The process of recommendation of the proposed IMCCF algorithm is demonstrated by the subsequent three main tasks:

#### A. The Computation of MC Item-based CF Similarity

The MC item-based CF similarity between a given target item  $i$  and an item neighbor  $j$  is computed in this step through: 1) the calculation of the partial similarities between each of the rating criteria  $c$ , then 2) the use of an aggregation function to get the overall similarity value. According to [24], the use of Euclidean distance as similarity measure proved to be an excellent choice for item-item similarity computation in comparison with the traditional item-based CF similarity techniques. Thus, the *Euclidean Distance* similarity measure

[16, 24] is used here to calculate the MC item-based CF similarity values between the target item  $i$  and the item neighbor  $j$  based on each individual criterion as shown below:

$$Dis_{i,j}^c = \sqrt{\sum_{u=1}^n abs(r_{u,i}^c - r_{u,j}^c)^2} \quad (1)$$

where  $r_{u,i}^c$  and  $r_{u,j}^c$  denote the user  $u$  ratings on items  $i$  and  $j$  with regard to criteria  $c$  correspondingly.  $n$  is the number of users who commonly rated items  $i$  and  $j$ . The smaller is the distance between two items are, the larger the similarity value between them is. Therefore, the following metric is needed to convert the resultant distance into the similarity value based on each individual criterion:

$$Sim_{i,j}^c = \frac{1}{1 + Dis_{i,j}^c} \quad (2)$$

Then, we use the worst-case (i.e., smallest) similarity [16, 24] as an aggregation approach on the partial similarities to find out the overall similarity value between a given target item  $i$  and an item neighbor  $j$  as follows:

$$Sim_{i,j} = \min_{c=1,\dots,x} sim_{i,j}^c \quad (3)$$

where  $Sim_{i,j}^c$  is the value of partial similarity based on criteria  $c$ ,  $x$  is the number of individual criterion.

Nevertheless, the Euclidean Distance similarity measure that is used to calculate the similarity values between items based on each individual criterion considers only the absolute value of ratings between users who have commonly rated items  $i$  and  $j$ . This could produce unreasonable similarity values between items since two items can have a high similarity value even though they have obtained an extremely limited amount of ratings. This issue can be improved by taking into account the amount of the users who have rated both items while computing the similarity between them. To solve this issue, we employ the *Dice* coefficient [26], as shown in (4), as a weighting factor to consider the percentage of users who have commonly co-rated both items  $i$  and  $j$  to the total number of users who have rated items  $i$  and  $j$  separately. Thus, the final MC item-based CF similarity is given by (5).

$$Dice_{i,j} = \frac{2 \times |U_i \cap U_j|}{|U_i| + |U_j|} \quad (4)$$

$$CFSim_{i,j} = Sim_{i,j} \times Dice_{i,j} \quad (5)$$

### B. The Computation of Item-based Semantic Similarity

The item taxonomy is used to exploit the semantic relationships among items. To form such taxonomy in a particular domain: 1) The total number of main items' categories should be identified ; 2) The main items' categories should be created; 3) each item should be assigned to one or more appropriate main category. Formally, every item is modeled as a vector of binary values [0,1], as depict by (6).

$$\vec{V}^{(i)} = (y_{i,1}, y_{i,2}, \dots, y_{i,t}), \text{ where} \quad (6)$$

$$y_{i,t} = \begin{cases} 1 & \text{Indicates that Item } i \text{ is attached to a Category } t \\ 0 & \text{Indicates that Item } i \text{ doesn't attached to a Category } t \end{cases}$$

Where  $\vec{V}^{(i)}$  is the binary vector representation of item  $i$ ,  $t$  is the overall number of the major items' categories. The value of item-based semantic similarity among two items  $i$  and  $j$  is computed using the standard vector-based cosine similarity [8], as shown in (7).

$$SemSim_{i,j} = \frac{\sum_{u=1}^n v_i \times v_j}{\sqrt{\sum_{u=1}^n (v_i)^2} \times \sqrt{\sum_{u=1}^n (v_j)^2}} \quad (7)$$

### C. The Computation of Rating Predictions

The prediction process of unrated item  $x$  by an active user  $a$  consists of two major steps. First, we use the weighted sum of deviations from the mean approach [27] to compute the rating predictions for each unrated item twice: 1) using the MC item-based CF similarity as specified by (8); and 2) using the item-based semantic similarity as specified by (9).

$$P_{a,x}^{CFSim} = \bar{r}_x + \frac{\sum_{n=1}^{NN^{CFSim}} (CFSim_{x,n} \times (\bar{r}_{a,n} - \bar{r}_n))}{\sum_{n=1}^{NN^{CFSim}} CFSim_{x,n}} \quad (8)$$

$$P_{a,x}^{SemSim} = \bar{r}_x + \frac{\sum_{n=1}^{NN^{SemSim}} (SemSim_{x,n} \times (\bar{r}_{a,n} - \bar{r}_n))}{\sum_{n=1}^{NN^{SemSim}} SemSim_{x,n}} \quad (9)$$

where,  $\bar{r}_x$  and  $\bar{r}_n$  denote the mean values of ratings of items  $x$  and  $n$  respectively.  $CFSim_{x,n}$  and  $SemSim_{x,n}$  represent the CF-based and semantic similarities between the items  $x$  and  $n$  respectively. The most Nearest Neighbors of items to the target item  $x$  identified according to the MC item-based CF and item-based semantic similarity weights denoted by  $_{NN}^{CFSim}$  and  $_{NN}^{SemSim}$  respectively.  $\bar{r}_{a,n}$  denotes the mean rating value based on all rating criteria of item  $n$  by the active user  $a$ .

Finally, the above rating predictions is merged using the weighted harmonic mean aggregation method as revealed by (10) to guarantee that a high rating value of the  $P_{a,x}$  will be attained only if both  $P_{a,x}^{CFSim}$  and  $P_{a,x}^{SemSim}$  have high prediction values.

$$P_{a,x} = \frac{2 \times P_{a,x}^{CFSim} \times P_{a,x}^{SemSim}}{P_{a,x}^{CFSim} + P_{a,x}^{SemSim}} \quad (10)$$

#### IV. EXPERIMENTAL SETUP AND RESULTS

##### A. Dataset and Evaluation metrics

To validate the performance of the proposed IMCCF recommendation algorithm, we use the Yahoo! Movies MC dataset [28] which was collected from the Yahoo! movies website (<http://movies.yahoo.com>). Each record of the rating data includes ratings for four criteria: story, acting, direction and visuals, in addition to an overall rating, user ID, and movie ID. The Yahoo! Movies MC dataset consists of 34,800 ratings from 1,716 users on 965 movies. The ratings are on the scale from 1 to 5. We built a movie taxonomy hierarchical tree structure with two levels. The main categories of items, referred to as movie genres, in which every item should be attached to are included in the first level. Whereas, the second level includes the items, referred to as movies, as leaf nodes. The movie genres has 32 attributes such as Action, Drama, Fantasy, ... etc.

To evaluate the quality of the proposed algorithm, the recommendations produced were evaluated using: 1) the Mean Absolute Error (MAE) metric to measure the prediction accuracy (Note that the lower MAE is, the higher is the prediction accuracy), and 2) the Coverage metric to evaluate the capability of a given recommendation algorithm to produce recommendations (refer to [29] for more details on the metrics).

##### B. Benchmark algorithms

For benchmark purposes, we compare the results of the proposed IMCCF algorithm with the results of two widely used item-based CF algorithms: 1) The item-based CF based on cosine similarity proposed by [8] (denoted as VC-ICF); and 2) The item-based CF based on adjusted cosine similarity (denoted as AVC-ICF) proposed by [30].

##### C. Experimental results

Two main experiments have been performed to prove the improvement of the proposed IMCCF recommendation algorithm with respect to the prediction accuracy and recommendation coverage when faced with the challenges of sparsity and new item.

1) *Evaluating the Prediction Accuracy and Recommendation Coverage of the IMCCF on the Sparsity problem.* On this experiment, we verify the efficiency of the proposed IMCCF algorithm compared with the benchmark algorithms in reducing the impact of the sparsity problem. As shown in Fig. 1 and Fig. 2, the proposed IMCCF algorithm has proven its superiority over other benchmark algorithms by obtaining the highest prediction accuracy (i.e., lowest MAE) and the maximum recommendation coverage at all sparsity levels.

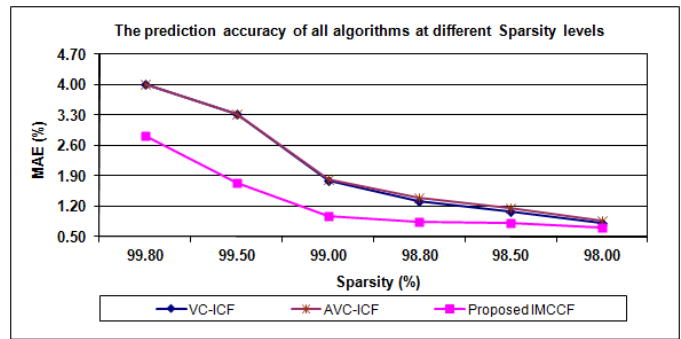


Fig. 1. Comparing the prediction accuracy of each algorithm on different levels of sparsity

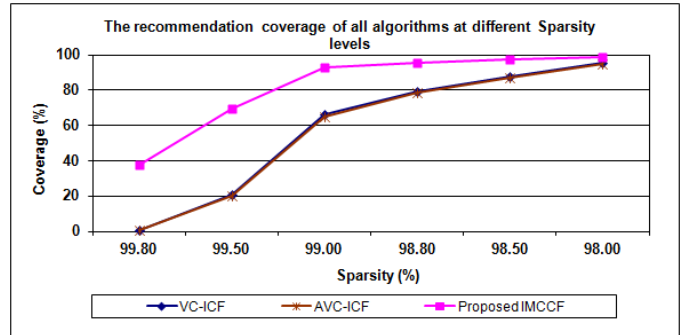


Fig. 2. Comparing the coverage of recommendation of each algorithm on specific levels of sparsity

2) *Evaluating the Prediction Accuracy and Recommendation Coverage of the IMCCF on the new item problem.* The aim of this experiment is to verify the efficiency of the proposed IMCCF algorithm compared with the benchmark algorithms in reducing the impact of the new item problem. As shown in Fig. 3 and Fig. 4, the proposed IMCCF algorithm has proven its superiority over other benchmark algorithms by obtaining the highest prediction accuracy (i.e., lowest MAE) and the maximum recommendation coverage at every specified amount of ratings of new items.

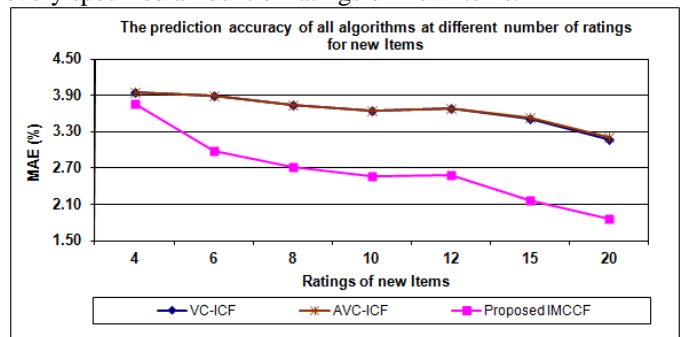


Fig. 3. Comparing the prediction accuracy of each algorithm on specific number of ratings of new items

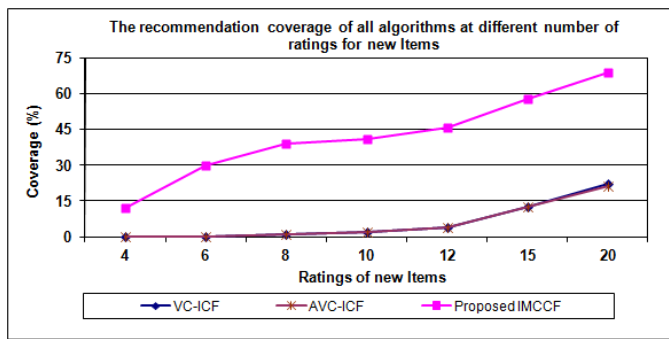


Fig. 4. Comparing the recommendation coverage of each algorithm on different number of ratings for new items

To conclude, it can be proven that the proposed IMCCF algorithm has a considerable improvement in lessen the effect of the sparsity and new item problems in comparison to the benchmark algorithms.

## V. CONCLUSION AND FUTURE WORK

This paper proposes an Item-based Multi-Criteria Collaborative Filtering algorithm that integrates the items' semantic information and multi-criteria ratings of items to lessen known obstacles of the item-based CF techniques. The experimental results of the proposed algorithm, in comparison to the benchmark item-based CF algorithms, prove that the proposed IMCCF algorithm is very effective in dealing with both of the sparsity and new item problems with respect to the prediction accuracy and recommendation coverage. The proposed IMCCF algorithm enhances the quality of produced recommendations by exploiting the added information obtained from both the multi-criteria ratings of users and the semantic relationships among items to address the sparsity and new item limitations. In future, we will focus on further validating the performance of the proposed algorithm against more benchmark CF-based algorithms on larger data sets.

### REFERENCES

- [1] J. Lu, D. Wu, M. Mao et al., "Recommender system application developments: A survey," *Decision Support Systems*, vol. 74, pp. 12-32, 2015.
- [2] Q. Shambour, and J. Lu, "A trust-semantic fusion-based recommendation approach for e-business applications," *Decision Support Systems*, vol. 54, no. 1, pp. 768-780, 2012.
- [3] Q. Shambour, and J. Lu, "An effective recommender system by unifying user and item trust information for B2B applications," *Journal of Computer and System Sciences*, vol. 81, no. 7, pp. 1110-1126, 2015.
- [4] S. Fraihat, and Q. Shambour, "A Framework of Semantic Recommender System for e-Learning," *Journal of Software*, vol. 10, no. 3, pp. 317-330, 2015.
- [5] Q. Shambour, and J. Lu, "A framework of hybrid recommendation system for government-to-business personalized e-services," in *Proceedings of the 7th International Conference on Information Technology: New Generations (ITNG 2010)*, Las Vegas, Nevada, USA, 2010, pp. 592-597.
- [6] J. Lu, Q. Shambour, and G. Zhang, "Recommendation technique-based government-to-business personalized e-services," in *Proceedings of the Annual Meeting of the North American Fuzzy Information Processing Society (NAFIPS 2009)*, Cincinnati, OH, 2009, pp. 1-6.
- [7] C. C. Aggarwal, "An Introduction to Recommender Systems," *Recommender Systems: The Textbook*, pp. 1-28, Cham: Springer International Publishing, 2016.

- [8] B. Sarwar, G. Karypis, J. Konstan et al., "Item-based collaborative filtering recommendation algorithms," in *Proceedings of the 10th International Conference on World Wide Web*, Hong Kong, China, 2001, pp. 285-295.
- [9] C. C. Aggarwal, "Neighborhood-Based Collaborative Filtering," *Recommender Systems: The Textbook*, pp. 29-70, Cham: Springer International Publishing, 2016.
- [10] E. Peis, J. M. del Castillo, and J. A. Delgado-López, "Semantic recommender systems. analysis of the state of the topic," *Hipertext. net*, vol. 6, no. 2008, pp. 1-5, 2008.
- [11] M. Pozo, R. Chiky, and E. Métais, "Enhancing Collaborative Filtering Using Implicit Relations in Data," *Transactions on Computational Collective Intelligence XXII*, pp. 125-146: Springer, 2016.
- [12] M. I. Martín-Vicente, A. Gil-Solla, M. Ramos-Cabrer et al., "A semantic approach to improve neighborhood formation in collaborative recommender systems," *Expert Systems with Applications*, vol. 41, no. 17, pp. 7776-7788, 2014.
- [13] F. S. Gohari, and M. J. Tarokh, "New Recommender Framework: Combining Semantic Similarity Fusion and Bicluster Collaborative Filtering," *Computational Intelligence*, pp. 1-26, 2015.
- [14] Q. Shambour, and J. Lu, "Government-to-business personalized e-services using semantic-enhanced recommender system," *EGOVIS 2011*, LNCS, K. Andersen, E. Francesconi, Å. Grönlund et al., eds., pp. 197-211, Heidelberg: Springer, 2011.
- [15] G. Adomavicius, N. Manouselis, and Y. Kwon, "Multi-Criteria Recommender Systems," *Recommender Systems Handbook*, pp. 769-803, , US: Springer, 2010.
- [16] G. Adomavicius, and Y. O. Kwon, "New recommendation techniques for multicriteria rating systems," *IEEE Intelligent Systems*, vol. 22, no. 3, pp. 48-55, 2007.
- [17] Q. Shambour, and J. Lu, "A hybrid multi-criteria semantic-enhanced collaborative filtering approach for personalized recommendations," in *Proceedings of the 2011 IEEE/WIC/ACM International Conference on Web Intelligence (WI'11)*, Lyon, France, 2011, pp. 71-78.
- [18] Ebadi, and A. Krzyzak, "A Hybrid Multi-Criteria Hotel Recommender System Using Explicit and Implicit Feedbacks," *International Journal of Computer, Electrical, Automation, Control and Information Engineering*, vol. 10, no. 8, pp. 1237-1245, 2016.
- [19] T. Jhalani, V. Kant, and P. Dwivedi, "A Linear Regression Approach to Multi-criteria Recommender System," *Data Mining and Big Data: First International Conference, DMBD 2016*, Bali, Indonesia, June 25-30, 2016. *Proceedings*, Y. Tan and Y. Shi, eds., pp. 235-243, Cham: Springer International Publishing, 2016.
- [20] M. Nilashi, M. D. Esfahani, M. Z. Roudbaraki et al., "A Multi-Criteria Collaborative Filtering Recommender System Using Clustering and Regression Techniques," *Journal of Soft Computing and Decision Support Systems*, vol. 3, no. 5, pp. 24-30, 2016.
- [21] N. Farokhi, M. Vahid, M. Nilashi et al., "A Multi-Criteria Recommender System for Tourism Using Fuzzy Approach," *Journal of Soft Computing and Decision Support Systems*, vol. 3, no. 4, pp. 19-29, 2016.
- [22] M. Nilashi, O. bin Ibrahim, N. Ithnin et al., "A multi-criteria collaborative filtering recommender system for the tourism domain using Expectation Maximization (EM) and PCA-ANFIS," *Electronic Commerce Research and Applications*, vol. 14, no. 6, pp. 542-562, 2015.
- [23] D. K. Bokde, S. Girase, and D. Mukhopadhyay, "An Approach to a University Recommendation by Multi-criteria Collaborative Filtering and Dimensionality Reduction Techniques," in *Proceedings of 2015 IEEE International Symposium on Nanoelectronic and Information Systems*, 2015, pp. 231-236.
- [24] Bilge, and C. Kaleli, "A multi-criteria item-based collaborative filtering framework," in *Proceedings of the 11th International Joint Conference on Computer Science and Software Engineering (JCSSE)*, Chon Buri, 2014, pp. 18-22.
- [25] Q. Shambour, and J. Lu, "Integrating multi-criteria collaborative filtering and trust filtering for personalized recommender systems," in *Proceedings of the 2011 IEEE Symposium on Computational Intelligence in Multicriteria Decision-Making (MCDM 2011)*, Paris, France, 2011, pp. 44-51.

- [26] W. B. Frakes, and R. Baeza-Yates, *Information retrieval: data structures and algorithms*: Prentice Hall, 1992.
- [27] J. Herlocker, J. A. Konstan, and J. Riedl, "An empirical analysis of design choices in neighborhood-based collaborative filtering algorithms," *Information Retrieval*, vol. 5, no. 4, pp. 287-310, 2002.
- [28] K. Alodhaibi, "Decision-guided recommenders with composite alternatives," *Information Technology*, George Mason University, Virginia, 2011.
- [29] C. Aggarwal, "Evaluating Recommender Systems," *Recommender Systems: The Textbook*, pp. 225-254, Cham: Springer International Publishing, 2016.
- [30] M. Deshpande, and G. Karypis, "Item-based top-N recommendation algorithms," *ACM Transactions on Information Systems*, vol. 22, no. 1, pp. 143-177, 2004.

# Pattern Recognition Approach in Multidimensional Databases: Application to the Global Terrorism Database

Semeh BEN SALEM<sup>1</sup>, Sami NAOUALI<sup>2</sup>

<sup>1</sup>Polytechnic School of Tunisia, Rue El-Khawarizmi, B.P 743, La Marsa, 2078, TUNISIA

<sup>2</sup>Military Academy of Fondouk Jedid, Virtual Reality and Information Technologies lab  
8012 Fondouk Jedid, Nabeul -TUNISIA

**Abstract**—This paper presents a pattern recognition approach in multidimensional databases. The approach is based on a clustering method using the distance measurement between a reference profile and the database observations. Two distance measurements will be proposed: an adaptation of the  $Khi^2$  formula to the multidimensional context, extracted from the Multiple Correspondence Analysis (MCA), and the Euclidean distance. A comparison between the two distances will be provided to retain the most efficient one for the multidimensional clustering context. The proposed approach will be applied to a real case study representing armed attacks worldwide stored in the Global Terrorism Database (GTD).

**Keywords**—clustering; pattern recognition; multidimensional databases; distance measurement;  $Khi^2$  formula; Euclidean distance; Multiple Correspondence Analysis

## I. INTRODUCTION

Data Warehouses (DW) [1] are centralized huge databases used to store heterogeneous data collected from disparate sources. Specific Data Mining techniques, such as clustering, are applied to analyze these structures for patterns recognition. Graphically, these data sets can be represented by cubic multidimensional data structures called OLAP (OnLine Analytical Processing) cubes [2]. Given a population of  $N$  observations described by a set of  $m$  attributes, clustering them into distinct groups allows identifying interesting patterns. In machine learning and Data Mining applications, data sets arise in huge matrix format [3] composed of a large number of rows and columns which processing requires effective techniques such as clustering and robust knowledge discovery algorithms.

This paper proposes a clustering approach using the  $Khi^2$  formula adapted to the multidimensional context, and the Euclidean metric. The  $KHP^2$  formula is commonly used to reduce the number of columns and lines in a dataset by evaluating similarities between observations and attributes. Reducing the lines or columns of a data table helps decreasing the amount of data in the data table and consequently computation costs and resources consumption. However, the Euclidean distance, specially used for geometric computations, allows calculating the distance between two distinct points.

This article is organized as follows: the next section presents previous related works in the field of pattern recognition and clustering techniques. The third section details

the proposed approach to be applied to multidimensional databases and introduces the corresponding algorithm. The corresponding case study of terrorist attacks in the year 1993 is presented in section four and finally results interpretation, conclusion and perspectives are given.

## II. RELATED WORKS AND MOTIVATIONS

### A. Clustering large dataset: state of the art

Clustering is an analytical exploratory *unsupervised* method to classify a data set observations into a finite and a small number of groups based upon two or more variables. The clustering process finds most similar observations among a set of untagged data according to the specified patterns. A clustering  $\mathcal{C}$ , is a partition of a *data set*  $\mathcal{D}$  containing  $n$  elements, into different subsets  $\mathcal{C}_1, \mathcal{C}_2, \dots, \mathcal{C}_K$  with respectively  $n_1, n_2, \dots, n_k$  elements called *clusters*. Formally we have the following findings:

- $\mathcal{C} = \{\mathcal{C}_1, \mathcal{C}_2, \dots, \mathcal{C}_K\}$  where  $\mathcal{C}_k \cap \mathcal{C}_l = \emptyset$  and  $\bigcup_{k=1}^K \mathcal{C}_k = \mathcal{D}$
- $n = \sum_{k=1}^K n_k$

However, two clusterings  $\mathcal{C}$  and  $\mathcal{C}'$  of the same data set  $\mathcal{D}$  can lead to different clustering results  $\mathcal{C}_1, \mathcal{C}_2, \dots, \mathcal{C}_K$  and  $\mathcal{C}'_1, \mathcal{C}'_2, \dots, \mathcal{C}'_K$  depending on the technique and algorithms used. An evaluation of the clusterings obtained is then required in order to identify the most appropriate clustering technique proposed. In a clustering process, elements belonging to the same group are given the same label and are similar but are dissimilar to elements belonging to other groups. In the literature, many clustering methods were proposed and developed [4]. These approaches are either:

- Hierarchical: A hierarchical algorithm uses a *dendrogram* representing the grouping of patterns and similarity levels at which groupings change. Most hierarchical clustering algorithms are variants of the *single-link* [5] (*minimum* distances between pairs), and *complete-link* [6] (*maximum* distances between pairs).
- Partitional: A partitional clustering algorithm obtains a single partition of the data instead of a clustering structure, such as the dendrogram produced by a hierarchical technique. For this method, the choice of the number of desired output clusters is problematic [7].

- Polythetic: Most algorithms are polythetic which means that all the features enter into the computation of distances between the patterns.
- Monothetic : A simple monothetic algorithm reported in [8] considers features successively to divide the given collection of patterns. The limitation of such an approach is the number of clusters generated ( $2^d$  clusters where  $d$  is the dimensionality of the patterns). The number of clusters obtained may be so large that the data set is divided into uninterestingly small and fragmented clusters.

In [9], the authors describe the limits of K-means algorithm, which is a well known clustering algorithm proposed for *numeric* (quantitative) data. The algorithm optimizes an objective function defined on the Euclidean distance measure. Although this algorithm gives promising results, the quality of clusters produced depends on the initialization of clusters and the order in which data elements are processed in the iteration.

In [10], the author proposes four clustering distances: Russel/Rao, Jaccard, Matching and Dice. The results show that over 90% of the cases were correctly grouped together.

In [11, 12], the authors conduct a clustering analysis with binary data. Two individuals should be viewed as similar to the degree that they share a common pattern of attributes among the binary variables. Observations with more similar patterns of response on the variables of interest are seen as closer to one another than are those with more disparate response patterns.

### B. Similarity measures

Distance measurement is used in many clustering algorithms to evaluate the similarity between two observations. The most known distance measurement is the Euclidean distance defined as follows:

$$d^2(x_i, x_j) = \sum_{k=1}^d (x_{ik} - x_{jk})^2$$

$x_i, x_j$  are two individuals (observations) with  $d$  attributes. The total number of modalities is  $k$  and each observation is defined by a vector as follows:  $x_{ik}(x_{i1}, x_{i2}, \dots, x_{i(k-1)}, x_{ik})$  where  $x_{ik}$  corresponds to the modality  $k$  of the individual  $i$ . The Euclidean distance is usually used for quantitative variables with varied values and wasn't previously used in a binary computation context and produces compact or isolated clusters [13].

The use of metrics to measure the distance is reduced to the computation of a symmetric matrix of  $\frac{n(n-1)}{2}$  pairwise distances values for the  $n$  patterns to simplify the computation process and complexity. However, major clustering approaches are provided for quantitative (numerical) data and fewer techniques are proposed for qualitative (continuous) data. Some methods were developed to measure the proximity for heterogeneous type patterns: [14] proposes a combination of a modified Minkowski metric for continuous features and a distance for nominal attributes. A variety of other metrics have been reported in [15, 16] for computing the similarity between

patterns represented using quantitative as well as qualitative features.

### C. Multiple Correspondence Analysis (MCA)

Multiple Correspondence Analysis (MCA) is a statistical method initially used to reduce either the number of columns or lines of a huge data set table by measuring the similarity between the profiles. It is used in this approach to evaluate the similarity between the observations in the data of our case study for clustering purposes using the  $\text{Khi}^2$  distance. This method was also used in [17] to reduce the dimensions of a DW and has provided remarkable results.

A DW, which can then be considered as a large data table, containing  $I$  observations (facts) and  $J$  variables (dimensions) and represented by a matrix  $I \times J$ , called the *Complete Disjunctive Table (CDT)* [18] where  $x_{ij}$  represents the modality of the variable  $j$  possessed by the individual  $i$ . If  $k_j$  is the number of modalities of the variable  $j$ , and  $K$  the total number of modalities, then we have  $K = \sum_j k_j$ . This table permits transforming the initially discrete (qualitative) data of the DW into a binary data table. If the patterns contains the considered modality, we will affect 1 in the corresponding  $k_{ij}$  of the CDT else we affect the value 0. The form of the CDT is presented in the following Table 1:

TABLE I. MATRIX OF THE CDT TABLE DATA

	1	...	J	...	$k_j$
1					$\vdots$
$\vdots$					$\vdots$
$i$	...	...	$k_{ij}$	...	...
$\vdots$					$\vdots$
$n$					$\vdots$

The  $\text{Khi}^2$  formula is given by the following Equation 1:

$$D^2(s, s') = \sum_{i=1}^n \frac{1}{f_i} \left( \frac{k_{is}}{n_s} - \frac{k_{is'}}{n_{s'}} \right)^2 = n \sum_{i=1}^n \left( \frac{n_{is}}{n_s} - \frac{n_{is'}}{n_{s'}} \right)^2 \quad (1)$$

However, in this study, another adapted formula derived from the Equation 1 will be presented and considered for the computation in the approach.

## III. PROPOSED APPROACH FOR MULTIDIMENSIONAL DATABASE CLUSTERING

### A. The adapted $\text{KHI}^2$ formula

In this paper, a clustering qualitative data approach is proposed using both: the  $\text{Khi}^2$  and the Euclidean distance formula. An experimental comparison between the two distances is also provided. The adapted  $\text{Khi}^2$  formula is given in the following Equation 2:

$$D^2(x, x') = \frac{1}{p} \sum_{\mu=1}^{\alpha} \frac{(x_{\mu} - x'_{\mu})^2}{m_{\mu}} = \frac{n}{p} \sum_{\mu=1}^{\alpha} \frac{(x_{\mu} - x'_{\mu})^2}{m_{\mu}} \quad (2)$$

- $x$  and  $x'$  are two observations (elements);
- $p$  is the *number* of dimensions;
- $n$  is the *number* of observations in the dataset (lines);
- $m_{\mu}$  is the number of occurrence of a modality  $\mu$ ;
- $\alpha$  the number of modalities in a dimension.

**B. Data pretreatment: data cleaning and multidimensional structure extraction**

A transformation process from the initial qualitative data to binary values is required in this approach. Each observation in the data table (row) represents a K-dimensional vector profile, where K represents the total number of modalities. Each observation is will then represented by the following vector:

$obs_i(x_{i1}, \dots, x_{ik}, \dots, x_{iK}), \forall i \in \{1, \dots, I\}, \forall k \in \{1, \dots, K\}$ , where I is the number of observations and K the number of modalities,  $x_{ik} = 1$ , if the corresponding modality exists for the observation and 0 otherwise. On the other hand, J represents the total number of dimensions in the DW and we should verify the following findings;

- $\forall j \in J, \mathcal{D}_j$  represents the dimension j of the DW and  $\mathcal{U}_{\mathcal{D}}$  the universe of dimensions, i.e the set of values taken by the dimensions and  $card(\mathcal{U}_{\mathcal{D}}) = J$  its cardinality.
- Each dimension  $\mathcal{D}_j$  contains a set of modalities  $\mathcal{M}$ ,  $\mathcal{U}_{\mathcal{M}}$  is the universe of the modalities and  $card(\mathcal{U}_{\mathcal{M}}) = K$  and  $\mathcal{M}(\mathcal{D}_j)$  represents the modalities taken by the dimension  $\mathcal{D}_j$ ;

$$\mathcal{U}_{\mathcal{M}} = \bigcup_{j \in J, k \in K} \mathcal{U}_{\mathcal{M}_k(\mathcal{D}_j)}$$

- $\forall i \in \{1, \dots, I\}, \sum_{k=1}^K card(x_{ik} \setminus x_{ik} = 1) = J$

The algorithm corresponding to such a process is given by the following Table 2:

TABLE II. KHI<sup>2</sup> CLUSTERING ALGORITHM

Algorithm <b>DIST_COMPUTE</b>
<b>FUNCTION GEN_CDT</b>
1. for each fact <sub>ij</sub> (1 ≤ i ≤ I, 1 ≤ j ≤ J) do
2. if fact <sub>ij</sub> = aux <sub>k</sub> (1 ≤ k ≤ K) then CDT <sub>i,k</sub> ← 1
3. else CDT <sub>i,k</sub> ← 0
4. end for
<b>END GEN_CDT</b>
<b>FUNCTION COMPUTE</b>
5. occ ← 0, som ← 0
6. for each CDT <sub>k,i; 1 ≤ k ≤ K, 1 ≤ i ≤ I</sub> do
7. if CDT <sub>i,j</sub> = 1 then occ++
8. end if
9. end for
10. for each CDT <sub>i,k; 1 ≤ i ≤ I, 1 ≤ k ≤ K</sub> do
11. A = math.pow((TDC <sub>k,i</sub> - ref), 2) / occ
12. som ← som + A
13. end for
<b>END-COMPUTE</b>

**IV. CASE STUDY: GLOBAL ARMED ATTACKS IN THE YEAR 1993**

In this section, a real case study is presented based on publicly available information collected on terrorist attacks that occurred worldwide in the year 1993. The objective is to apply the proposed clustering approach to recognize interesting groups and their associated patterns. Data Mining application deal with data sets containing a large amount of qualitative and quantitative data. This approach is proposed for qualitative

data. The initial dataset is filtered in order to keep only the most relevant attributes for the considered analyzing objectives.

**A. The Global Terrorism Database (GTD)**

The Global Terrorism Database (GTD) [19, 20, 21] is a vast collection of terrorist activities reported around the globe that incorporates more than 27.000 terrorist incidents, provided by the National Consortium for the Study of Terrorism and Response to Terrorism (START), a United States department of Homeland Security of Excellence based at the University of Maryland. The data set is assembled from public sources including media, articles, electronic news, books, journals and legal documents. Using clustering techniques would provide interesting results in order to identify terrorist activities patterns correlated with each other.

**B. Multidimensional structure extraction**

The considered data table of the case study contains 748 observations associated with 123 qualitative and quantitative variables to characterize armed attacks that took place worldwide in 1993. These data are presented in a MS EXCEL table without any specific structure. As already defined, the pretreatment step also identifies a multidimensional structure to be extracted from the table. Only three dimensions will be retained in the computational process later which could be easier than considering all the identified dimensions. The following seven dimensions with the associated attributes are then identified:

- TIME (year, moth, approxdate, extended, resolution);
- LOCATION (country, region, provstate, city, latitude, longitude, specificity, vicinity, location);
- FEATURES (summary, crit1, crit2, crit3, doubter, alternative, multiple, succeed, suicide);
- ATTACK\_TYPE (attack\_type1, attack\_type2, attack\_type3, nbpers );
- TARGET (target\_type1, corp1, target1, nationality, target\_type2, corp2, target2, nbkills, nbwounded );
- WEAPON (weapon\_type1, weapon1, weapon\_subtype, weapon\_details, target\_type2, corp2, target2 );
- TERRORIST\_GROUP (group\_name, group\_subname, motivation, claimed);

The following Figure1 represents the three dimensions to be retained for the study:

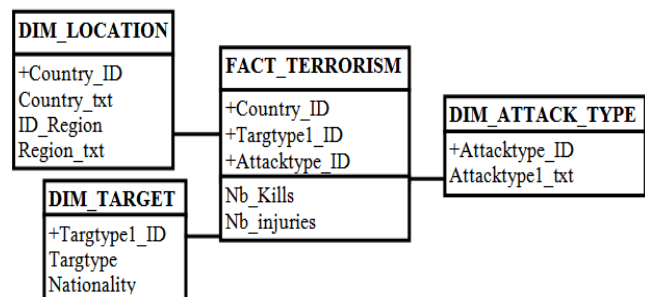


Fig. 1. Fact table and retained dimensions of the DW

The three retained dimensions are {LOCATION, ATTACK\_TYPE, TARGET}. The DW contains qualitative data where each dimension has a limited and fixed number of possible values. The dimensions and the measures are presented as follows:

- LOCATION{ Europe, Middle East & North Africa, Asia, America, Russia };
- ATTACK\_TYPE{ Assassination, Armed Assault, Bombing, Hostage Taking, Facility};
- TARGET{ Civilians, Government, Military, Business, Other };
- Total number of fatalities NB-KILLS;
- Total number of injuries NB-INJURIES;

Each observation in the CDT table is represented by a profile containing five information: three dimensions and two measures. An example of two observations is given by the following Table 3:

TABLE III. INDIVIDUAL REPRESENTATION IN THE DW FACT TABLE

	IND 1	IND 2
LOCATION	ME & NA	AMERICA
ATTACK_TYPE	ARMED ASSAULT	BOMBING
TARGET	MILITARY	CIVILIANS
NB_KILLS	$x_{11}$	$x_{12}$
NB-INJURIES	$x_{21}$	$x_{22}$

The transformation of the previous qualitative profile in Table 3 to binary representation is given by the following Table 4:

TABLE IV. BINARY FACT TABLE REPRESENTATION: CDT

	LOCATION			ATTACK_TYPE					TARGET						
	EUROPE	ME & NA	ASIA	AMERICA	RUSSIA	ASSAS	ARM_ASS	BOMBING	HOSTAGE	FACILITY	CIVILIANS	GOV	MILITARY	BUSINESS	OTHER
OBS 1	0	1	0	0	0	0	1	0	0	0	0	0	1	0	0
OBS 2	0	0	0	1	0	0	0	1	0	0	1	0	0	0	0

In the CDT, each individual has an encoding of 15-bit representing its whole characteristic profile. This encoding is not random; it should respect the following findings to preserve the integrity of the table:

- The number of bits encoded 1 in a line is equal to the number of dimensions;
- The total number of occurrences  $m$  of all modalities in a dimension is equal to the total number of observations;

V. RESULTS INTERPRETATION

A. Clustering using the KHI<sup>2</sup> distance

The clustering results performed in this approach are shown in Figures 2 and 3 below: clusters are represented according to the computed distances (D<sup>2</sup>) and the number of items in each

cluster. Each point in the Figure 2 and 3 represents a cluster. The computation was performed according to two reference profiles represented in the following Table 5.

TABLE V. REFERENCE PROFILES REPRESENTATION

	LOCATION			ATTACK_TYPE					TARGET						
	EUROPE	ME & NA	ASIA	AMERICA	RUSSIA	ASSAS	ARM_ASS	BOMBING	HOSTAGE	FACILITY	CIVILIANS	GOV	MILITARY	BUSINESS	OTHER
$x_{ref1}$	0	1	0	0	0	0	1	0	0	0	0	0	1	0	0
$x_{ref2}$	0	0	0	0	0	0	0	0	0	0	0	0	0	0	0

The distance would be measured between the reference profile  $x_{ref}$  and all the other individuals  $x_i$  of the dataset.

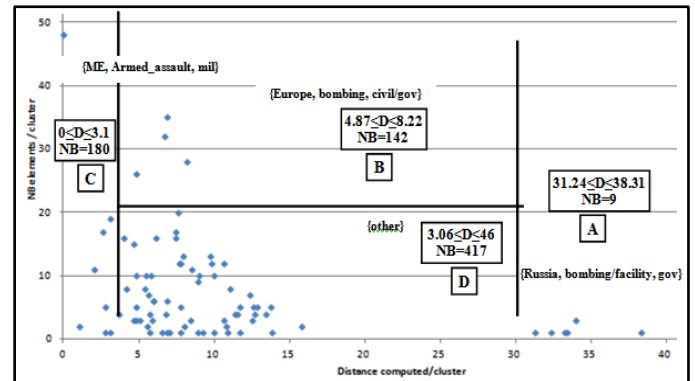


Fig. 2. Clustering results with profile 1

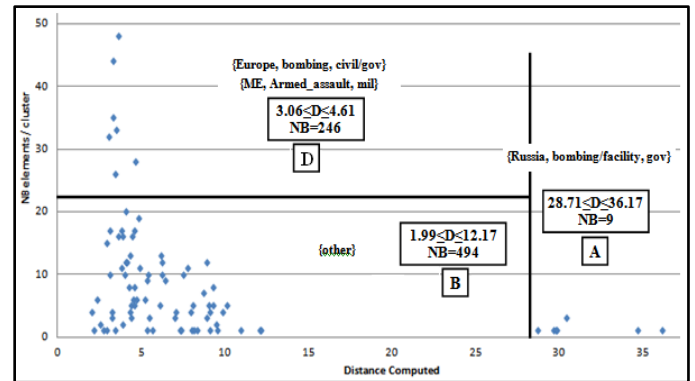


Fig. 3. Clustering results with profile 2

According to the experimental results, 86 distinct groups were identified ( $0 < D < 38.3$ ). The following Table 6 represents statistical results concerning the number of clusters and elements obtained according to each profile.

TABLE VI. PROFILE 1 AND PROFILE 2 COMPARISON

	NB clusters	NB super groups	NB elements / super cluster			
			A	B	C	D
Profile1	86	4	9	141	180	418
%			1.2	18.85	20.06	55.88
Profile2	85	3	9	246	494	
%			1.2	32.88	66.04	

In the previous Figure 2, we identify four main groups containing all the clusters (and therefore the corresponding elements) and having similar profiles. It is also proposed to introduce another parameter representing the number of common modalities between each individual and the reference. If the distance computed increases, the number of common modalities decreases, which explains that the elements become more and more dissimilar as shown in the following Table 7.

TABLE VII. DISTANCES COMPUTED WITH THE NUMBER OF RETAINED MODALITIES

$D^2(x_{ref}, x_i)$	0	1,08	2	2,03	2,63	2,76	2,82	2,83	3,10
NB (same modalities)	3	2	2	2	2	2	2	2	2

The following Table 8 presents the characteristics of the groups identified in relation with the distance computed and the number of elements in the groups.

TABLE VIII. CLUSTERS IDENTIFICATION

		A	B	C	D
Distance computed ( $D^2$ )	$x_{ref1}$	High	Low	Low	Medium
	$x_{ref2}$	High	Low	Low	
NB elements	$x_{ref1}$	Low	High	High	Low/Medium
	$x_{ref2}$	Low	High	High	

The four groups identified in Figures 2 and 3 can be interpreted as follows:

- *Group A* contains only five clusters (1.09% of the total number of clusters) with the highest computed distances from the reference. The associated profile to this group is {RUSSIA, BOMBING, FACILITY / GOV}. It concerns armed attacks that occurred in Russia against either governmental or facility targets using bombs. These clusters, given their small number, are not representative of a specific behavior of armed group attacks in the country. The attacks mainly targeted the state and not the military or civilians which can be explained by the policy of the country and clarify the claims of the attacks that may have political backgrounds.
- *Group C* is the most interesting super cluster; it contains clusters with minimum distances to the reference and consequently most similar to the initial profiles defined. Further information extraction and analysis from the database could provide more remarkable information : the most active armed groups in the region, the relation between these groups.
- *Group B* contains elements with medium distances (< 10) with relatively high cardinality (> 25 elements) by the maximum cluster distance to our reference, this is a result of groups containing more dissimilar elements.
- *Group D* represents various clusters that are compact and even close. The distance between clusters is sometimes reduced which means that the results and profiles are quite similar.

The following Table 9 represents the different labels that could be assigned to each cluster with the corresponding groups:

TABLE IX. CLUSTER LABELS

CLUSTER	Label	Nb clusters	Nb elements
A	RUSSIA, BOMBING/FACILITY, GOV	7	9
B	EUROPE, BOMBING, CIVIL/GOV	5	142
C	ME, ARMED_ASSAULT, MIL	9	181
D	OTHER	62	416
		TOTAL= 748	

We note that during the year 1993, Europe and ME & NA are the most concerned regions by the armed attacks. These results indicate that criminal activities are very relevant in these regions. The total number of observations corresponding to the profile {MIDDLE EAST & NORTH AFRICA, ARMED ASSAULT, MILITARY} is 181, the total number of observations corresponding to the profile {EUROPE, BOMBING, GOVERNMENT} is 142. These results can have great importance for specialists in the counter-terrorist or criminal investigation services. Besides, according to Figures 2 and 3, we notice that the corresponding clusters are easily identifiable. Additional efforts should be led in order to strengthen the military intelligence services in the ME & NA countries while general intelligence for private government representatives should be considered in the European countries. Besides, attacking the governments and an official representative can be explained by the political issues declared by the government and these attacks may have political reasons. However, targeting the army and law enforcement agencies can be seen as an attempt to weaken the government capabilities in facing terrorism for more reasons not essentially political issues: we can mention the case of Islamic groups that are targeting military and police in order to widespread their jihadist beliefs.

B. Clustering using the Euclidean distance

The objective of this study is to conduct a clustering using both: the Euclidean and KHI<sup>2</sup> distances. The Figure 4 below shows the clustering results obtained by the Euclidean distance.

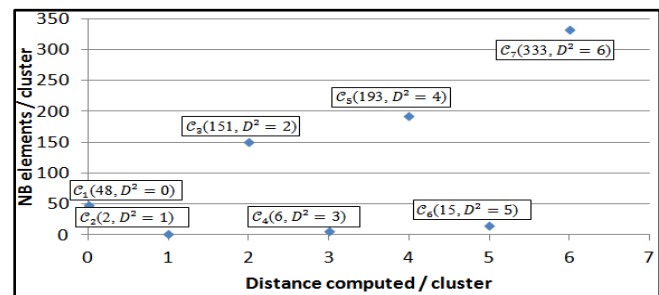


Fig. 4. Clustering results with the Euclidean Distance

The total number of clusters obtained using the Euclidean distance represents 8.13% (7/86) groups compared to those obtained with the KHI<sup>2</sup> distance. This indicates that some distinct groups, initially identified with the KHI<sup>2</sup> formula, were assembled with the Euclidean distance. The KHI<sup>2</sup> distance

provides better clustering results compared to the Euclidean distance: The clusters are more visible and the results are better exposed. These results are due to the fact that the  $KHI^2$  formula takes into consideration additional parameters that are not identified with the Euclidean distance, including the occurrence  $m$  of each modality, the total number of observations  $N$  and the number of dimensions  $P$ .

Lets consider the cluster computed with the Euclidean distance where  $D^2 = 2$ . The cluster contains all other groups previously identified with the  $KHI^2$  formula (11 groups) and having the distances around  $D^2 = 2$ . This result presents one of the limits of the Euclidean distance: it is possible to group many observations that may have different profiles in the same cluster while they are distinguished with the  $KHI^2$  distance.

C. Further data analysis: armed groups identification

According to the following Table 10, most of the armed attacks in the year 1993 occurred in Europe and ME& NA with a total of 492 attacks (65.77%). Given their geographical proximity, it would be possible to conclude that links may exist between these attacks especially if the same armed group conducts attacks on both territories. Investigations has shown that many armed attacks happening in Europe were planned by terrorist groups adherents from the Middle East and North Africa. Thus more and more attention should be given to these groups and additional bilateral collaboration between these two continents should be taken into consideration. In Table 10, we represent the number of occurrence  $m$  of each modality. The  $m$  parameter is part of the  $KHI^2$  formula used to characterize the most frequent modalities. Data integrity is verified because the total number of observations for each dimension is the same:

TABLE X. NUMBER OF OCCURRENCE OF THE MODALITIES IN THE DW

	LOCATION					ATTACK_TYPE					TARGET				
	EUROPE	ME & NA	ASIA	AMERICA	RUSSIA	ASSAS	ARM_ASS	BOMBING	HOSTAGE	FACILITY	CIVILIANS	GOV	MILITARY	BUSINESS	OTHER
Occ (M)	227	265	115	132	9	36	230	270	43	148	199	237	157	97	59
%	30	36	15	18	1	5	32	37	6	20	26	32	21	13	8
Total	748					748					748				
Nb_Kills	2668														
Nb_Wounds	5599														

The most frequent modalities previously identified are {ME & NA, BOMBING, GOV}. The number of corresponding observations is only 17 which doesn't represent an interesting profile to study despite it contains the most frequent modalities. Furthermore, the results provided by the approach, do not identify the profile {ME & NA, BOMBING, GOV} as an interesting profile with a great number of elements. This highlights the value of using reliable analytical techniques such as clustering for discovering interesting patterns and extracting relations between patterns.

There are various armed organizations identified in the GTD dataset where more than two thousand different groups of terrorists have been recorded. The following Figure 5 presents

the most common identified groups according to the number of attacks, the number of kills and injuries.

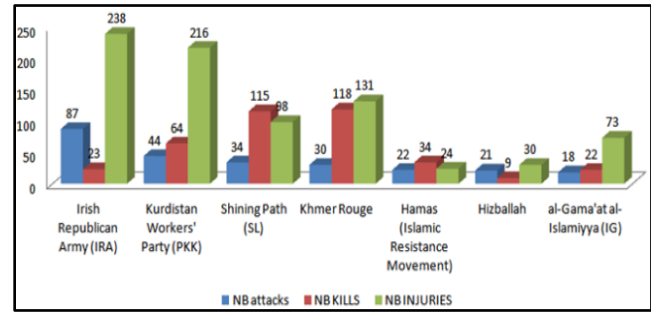


Fig. 5. Statistics of damages caused by armed groups

The following Table 11 presents the countries where the attacks happened according to each group:

TABLE XI. ACTIONS OF GROUPS BY COUNTRY

Groups	NB attacks	Region	Place of attacks
IRA <sup>1</sup>	87	Europe	Great Britain / Northern Ireland
PKK <sup>2</sup>	26		Germany / Great Britain/Switzerland / France/Denmark / Austria
Hamas <sup>3</sup>	22	The Middle East & North Africa	West Bank and Gaza Strip Israel
Hezbollah	21		Lebanon / Israel
IG <sup>4</sup>	18		Egypt
PKK	18		Turkey

According to the previous Table 11, we identify the number of attacks by region and by country associated with the most identified armed groups. Seeing the results provided, two categories of the most active groups are distinguished:

- Groups operating in one geographical area such as (IRA) in Europe and "Hamas (Islamic Resistance Movement)", "Hizballah", (IG) in the Middle East & North Africa.
- Groups that act on two different continents including (PKK) in Europe (26 attacks) and Turkey (18 attacks).

The results obtained are with a great importance for intelligence services and law enforcement agencies. These results help giving more intelligence about the behavior of these groups to understand the motives and reasons for their actions: Generally, an attack to foreign boundary includes locals from the same country. Similarly, the domestic attacks involve a national or a group of nationals who attack their own homeland.

While the world may confront extraordinary terrorist threats today, experts can explore a lot of things about today's dangers by investigating the practices of terrorist groups in the recent past and the effects that these terrorist actors, and the terrorist vents they executed, have had.

<sup>1</sup> Irish Republican Army.

<sup>2</sup> Kurdistan Workers' Party

<sup>3</sup> Islamic Resistance Movement

<sup>4</sup> al-Gama'at al-Islamiyya

## VI. CONCLUSIONS AND PERSPECTIVES

Data mining is a fundamental tool that has been widely used to model crime detection problems, detect unusual patterns, terrorist activities and fraudulent behaviors. It has great effectiveness and high influence in law enforcement studies or crime prevention, detection and analysis. Our approach is based on clustering armed attacks events to identify interesting patterns such as the main regions and countries concerned, targets and kind of attacks. The approach is based on the use of the KHI<sup>2</sup> distance extracted from the MCA and the Euclidean distance, to express the similarity between the observations. According to the study, the KHI<sup>2</sup> distance measurement is more effective than the Euclidean distance and can provide better discernible results. However, the approach is proposed for qualitative data and a pretreatment procedure is required to switch from the qualitative data to the binary one. Experimental results with quantitative data should also be presented to compare the effectiveness of the approach. Evaluating the effectiveness of the approach based on a specific method is also required especially when using different clustering methods providing almost comparable data. This issue will be taken into consideration in the following publications.

### REFERENCES

- [1] W. H. INMON. (1994). "Building the Data Warehouse Toolkit". Wiley Computer Publishing, ISBN 0-471-56960-7.
- [2] L. Lebart, A. Morineau, M. Piron (2006). "Statistique exploratoire multidimensionnelle". Dunod, Paris.
- [3] D. Agarwal and S. Merugu, "Predictive discrete latent factor models for large scale dyadic data", In proceedings of the 13<sup>th</sup> ACM SIGKDD international conference on Knowledge Discovery and Data Mining (KDD'07), 2007, pp:26-35.
- [4] Dillon, W.R and Goldstein, M.(1984), "Multivariate Analysis: Methods and applications", John Wiley and Sons.
- [5] Snijders, T. A., Dormar, M. van Schurr, W.H, Dijkman Caes, C and Driessen, G (1990), "Distribution of some similarity coefficients for dyadic binary data in the case of associated attributes", Journal of classification 7, 1409-1438.
- [6] A.K. JAIN, M.N. MURTY, P.J. FLYNN, "Data Clustering: A Review", ACM Computing Surveys, Vol. 31, No. 3, September 1999.] [S NEATH, P.H.A. AND SOKAL, R. R., "Numerical Taxonomy", Freeman, London, UK, 1973.
- [7] KING, B. 1967 "Step-wise clustering procedures". J. Am. Stat. Assoc. 69, 86-101.
- [8] A. NDERBERG, M. R. 1973. Cluster Analysis for Applications. Academic Press, Inc., New York, NY.
- [9] J.A. Hartigan, "Clustering Algorithms", Wiley, New York, 1991.
- [10] A.K. Jain, R.C. Dubes, "Algorithms for clustering data", Prentice Hall, Englewood Cliffs, NJ, 1998.
- [11] S K Gupta, K Sambasiva Rao, Vasudha Bhatnagar, "K-means clustering Algorithm for categorical attributes".
- [12] Holmes Finch, "Comparison of distance Measures in Cluster Analysis with Dichotomous Data", Ball State University, Journal of Data Science 3(2005), 85-100.
- [13] MAO, J. AND JAIN, A. K. 1996. "A self-organizing network for hyperellipsoidal clustering", (HEC). IEEE Trans. Neural Network. 7, 16-29.
- [14] WILSON, D.R. AND MARTINEZ, T. R. 1997. Improved heterogeneous distance functions. J. Artif. Intell. Res. 6, 1-34.
- [15] D IDAY, E. AND SIMON, J. C. 1976. Clustering analysis. In Digital Pattern Recognition, K. S. Fu, Ed. Springer-Verlag, Secaucus, NJ, 47-94.
- [16] I CHINO, M. AND YAGUCHI, H. 1994. Generalized Minkowski metrics for mixed feature-type data analysis. IEEE Trans. Syst. Man Cybern. 24, 698-708.
- [17] S. Naouali, S. Ben Salem, "Towards reducing the multidimensionality of OLAP cubes using the Evolutionary Algorithms and Factor Analysis Methods", International Journal of Data Mining & Knowledge Management Process (IJDKP) Vol.6, No.1, January 2016
- [18] Jérôme Pagès, "Analyse des Correspondances Multiples ACM, introduction à l'aide d'un exemple" Laboratoire de mathématiques appliqués Agrocampus, Rennes.
- [19] Gary LaFree and Laura Dugan. (2007), "Introducing the Global Terrorism Database", Political violence and terrorism 19:181-204. G.P. Zarri. Semantic web and knowledge Representation, Proc. Of the 13<sup>th</sup> International Workshop on Database and Expert System applications (DEXA'02), 2002, pp. 1529-4188.
- [20] G. LaFree, "the Global Terrorism Database: Accomplishments and Challenges", Perspectives on Terrorism, vol. 4, no.1, 2010.
- [21] G. LaFree and L. Dugan, "Introducing the Global Terrorism Database", Terrorism and political Violence, vol.19, no.2, pp:181-204, 2007.
- [22] D. Guo, K. Liao and M. Morgar, "Visualizing patterns in a global terrorism database", Environment and Planning B: Planning and Design, vol.34, pp:767-784, 2007.

# An Improved Pulmonary Nodule Detection Scheme based on Multi-Layered Filtering and 3d Distance Metrics

Baber Jahangir

International Islamic University  
Islamabad Pakistan

Muhammad Imran

<sup>2</sup>Shaheed Zulfikar Ali Bhutto  
Institute of Science and Technology

Qamar Abbas

Iqra university Islamabad

Shahina Rabeel

International Islamic University Islamabad Pakistan

Ayyaz Hussain

International Islamic University Islamabad Pakistan

**Abstract**—This paper proposed a computer-aided detection (CAD) system to automatically detect pulmonary nodules from thoracic computed tomography (CT) images. Automatically detect pulmonary nodules is a difficult job because of the large deviation in size, shape, location and density of nodules. The proposed CAD scheme applies multiple 3D disk-shaped laplacian filters to enhance the shape of spherical regions. Optimal multiple thresholding and 3D distance mapping is used to extract regions of interest and separate nodules. Finally, rule-based pruning removes easily dismissible false positive structures. The proposed system provides an overall nodule detection rate of 80% with an average of 12.2 false positives per scan. The experimental results reveals that the proposed CAD can attain a comparatively high performance.

**Keywords**—computer-aided detection system; nodule detection lung nodule

## I. INTRODUCTION

Among all types of cancer, lung cancer presents the leading rates of mortality around the world [1]. To detection the lung cancer at the earliest stages, computed tomography is known to be the most accurate, non-invasive imaging technique, which motivate the researchers to use computer for the early detection of lung cancer [2–3]. Lung cancer manifests itself in the form of pulmonary nodules which are visible as anatomic structures having a radio density greater than the lung parenchyma. Due to the large number of images per scan, radiologists can make errors while evaluating them. To aid the radiologists, there has been a growing interest in developing automatic computer-aided detection (CAD) methods [4,5]. Sahiner et al. [6] proved through experimental study that a medical physician with the help of CAD system can easily diagnose cancer rather than without CAD system. similarly a CAD system alone cannot perform well without the help of medical physician. The automatic detection of lung nodules, however, is a challenging task due to the variance in shape, size, location and density of the nodules Various researchers proposed different techniques for computer-aided nodule detection system. Because lung nodules have higher intensity values than those of the surrounding lung parenchyma, intensity based schemes provide the advantage of simplicity. Armato et al. [4] and Messay et al.

[5] used multiple gray-level thresholds to extract the nodule candidates from the segmented lung volume. Kostis et al. [6] applied morphological opening along with iterative dilation procedure to separate small nodules from the attached vessels. The study by Brown et al. [7] involved intensity thresholding, region growing and mathematical morphology to identify regions of interest. Similarly, the technique by Choi et al. [8] uses optimal multiple thresholding and rule-based pruning that uses local shape features to extract potential nodules from the lung region. Upon analysis, it was observed that the algorithm provides good performance in the detection of high-contrast, well shaped nodules but has low sensitivity for irregularly shaped non-solid nodules. In addition, the number of omissions for nodules that touched or infiltrated vascular structures was high. The objective of the proposed study is to improve upon this technique by adding filtering-based method and distance measures to improve the detection of such nodules.

Studies have demonstrated the advantages of using such techniques. Li et al. [9] obtained high sensitivity with low false positive detections per scan by using selective rule based segmentation based and enhancement. Suzuki et al. [10] enhanced the nodule intensity and remove non-nodules through a machine learning technique which is based on based filter. Retico et al. [11] proposed an automatic filter to enhance the shape of spherical structures. Additionally, using a signed distance field, Pu et al. [12] detected maximums found as nodule candidates. Ozekes et al. [13], presented a rule based segmentation technique with the help genetic algorithm. the proposed system achieved good results i.e. 93.4% sensitivity and 0.594 false positives on each examined. Similarly, Netto et al. [14] applied 3D distance transform and region growing to separate the lung nodules from vessels and bronchi. Ye et al. [15] extract five features such as "containing intensity information, shape index, and 3D spatial location".

Model based methods also provide promising results for nodule detection. Cascio et al. [16] use a stable 3D mass-spring model combined with a spline curve reconstruction process in order to segment and extract the nodular candidate regions. Lee et al. [17] presented a novel template-matching technique with the help of genetic algorithm template-matching technique for nodule detection. Dehmeshki et al. [18] enhanced this method

by adding a shape-based methodology for nodule detection from spherical elements. Tan et al. [19] utilized the three classifiers such as artificial neural network and genetic algorithm for lung nodule detection. To validate the proposed model, results were compared with SVM and fixed-topology neural networks based models.

The CAD system proposed by Tan et al. [19] utilized three classifier; two of them were artificial neural network and genetic algorithms and compared the results of these classifier with SVM and fixed-topology neural networks. Sua´ rez-Cuenca et al. [20] have explored discriminant analysis (LDA), three types of support vector machines (SVM), artificial neural network (ANN) and quadratic discriminant analysis (QDA). These all six classifiers were tested combined and separately as well on LIDC base having 85 samples.

The objective of this research work is to present a new and improved pulmonary nodule detection system that uses multiple sharpening filters along with intensity thresholding and 3D shape-based metrics to improve accuracy of nodule detections while reducing the number of false positives.

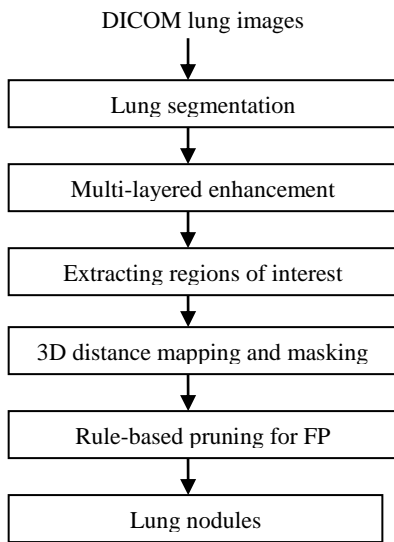


Fig. 1. Overview of proposed CAD system

## II. METHODOLOGY

The research work conducted by Choi et al. [8], is closely related to this research work in which automatic detection of lung nodules is performed by using multiple intensity thresholds and rule-based pruning based on shape-based features of the nodule candidates. However, our work has some major differences. First, structures in the lung image that have a spherical appearance are enhanced by using 3D circular laplacian filters of varying sizes. This highlights nodular regions and de-emphasizes non-nodule objects in the segmented lung volume. Second, apart from using multiple thresholding to extract initial possible nodule, the 3D distance map is computed in each of the segmented structures. The distance map gives a measure of the radius of objects, which is the distance from the boundary to the centroid. Masking the 3D image to extract the inner most layers of each structure separates the lung nodules from vessels and bronchi. Finally,

easily dismissible false positive objects are removed using rule-based pruning based on local shape-based features.

### A. Lung segmentation

The algorithm for lung volume segmentation has three stages. In order to separate low density non-body voxels (nodule candidate) from the high density body voxels (non-nodule candidate) a fixed threshold value is used first. Second, 3D connected component labeling is used to extract the lung regions from non-body voxels. To make sure that the extracted lung mask volume includes the juxtapleural nodules, a third step of contour correction is applied. Critical section is removed by using chain code representation in this step. Fig.2 shows the various stages of the lung segmentation process.

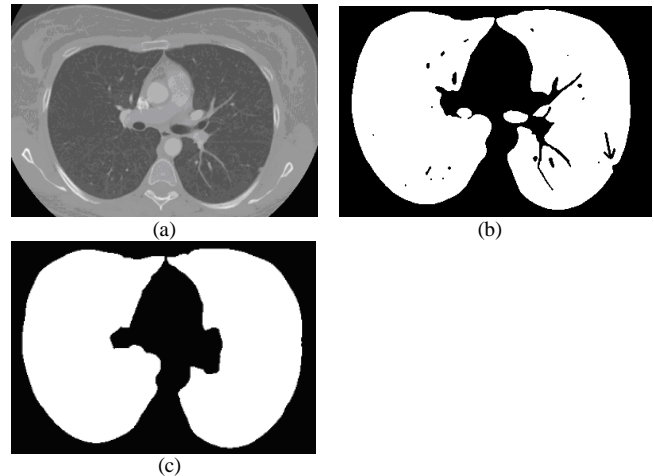


Fig. 2. Stages of lung segmentation process. (a) Original CT lung image; (b) Extracted lung volume (with concave region on the pleural boundary); (c) Final segmented lung mask with refined boundary

### B. Multi-layered enhancement of disk-shaped regions

Before beginning with nodule detection, multiple linear 3D spatial filters of varying sizes are used to convolve the original 3D image. The result of displacing the convolution filter over the image is a new 3D image in which the contrast of structures that match the size of the disk-shaped kernel is increased. The enhanced image for kernel size 3 x 3 x 3 is obtained by:

$$g(x, y, z) = f(x, y, z) + c[\nabla^2 f(x, y, z)] \quad (1)$$

where  $f(x,y,z)$  and  $g(x,y,z)$  are the input and sharpened images, respectively. The value of constant  $c = 1$ , and  $\nabla^2 f(x, y, z)$  is the discrete laplacian of three variables:

$$\begin{aligned} \nabla^2 f(x, y, z) = & -[f(x+q, y, z) + f(x-q, y, z) + \\ & f(x, y+q, z) + f(x, y-q, z) + \\ & f(x, y, z+q) + f(x, y, z-q) - \\ & f(x, y, z)] \end{aligned} \quad (2)$$

where  $q = 1, 2, 3, \dots, n$  ( $n =$  number of kernels). Similar enhanced images as in (1) are obtained by progressively increasing the kernel size in odd increments. The coefficient values are determined by varying the value of  $q$  and inserting respective terms in (2).

In the next step, all sharpened images are compared and only the highest intensity value between corresponding voxels is retained to obtain a final enhanced image. This preprocessing step provides two-fold advantage of making the system more sensitive to detection of non-solid nodules and decreasing the likelihood of oblong shapes passing the gray-value thresholds. Fig.3 shows an example of a non-solid, juxtapleural nodule that was successfully detected as a true positive structure.

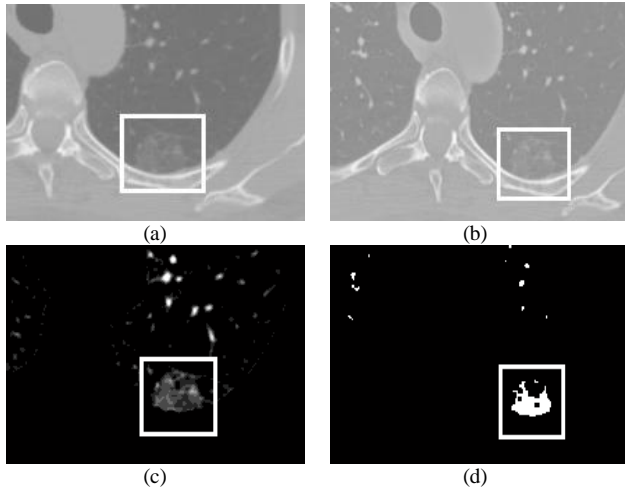


Fig. 3. An example of a non-solid nodule successfully detected by the proposed system. (a) Original CT lung image; (b) Corresponding enhanced lung image; (c) Separated regions of interest; (d) Potential nodule candidates

### C. Extracting regions of interest

multiple threshold is used to extract regions of interest from the segmented lung volume, which uses an optimal threshold as the base threshold. The optimal threshold is calculated by using an iterative approach. The average intensity value of 3D image is selected as the primary threshold  $T$ . Applying this threshold to the image segments the image into two groups of voxels: voxels with intensity values higher than the threshold, and voxels with grayscale values less than or equal to the threshold. Let  $\mu_a$  and  $\mu_b$  represent the mean intensity of the first and second group, respectively. The new threshold is calculated by:

$$T = \frac{\mu_a + \mu_b}{2} \quad (3)$$

The above process is repeated until the threshold converges.

The final obtained threshold becomes the base threshold  $T_{base}$  for multiple thresholding. Instead of using a fixed value threshold as the base threshold, the use of optimal threshold is more suitable as it adapts the input CT image, taking into consideration the wide intensity range of nodules. A total of seven thresholds are used to obtain one image containing regions of interest. The threshold values are listed as follows:  $T_{base}-200$ ,  $T_{base}-100$ ,  $T_{base}$ ,  $T_{base}+100$ ,  $T_{base}+200$ ,  $T_{base}+300$ , and  $T_{base}+400$ . The resultant image preserves nodule opacity information. The separated regions of interest are shown in Fig.4.

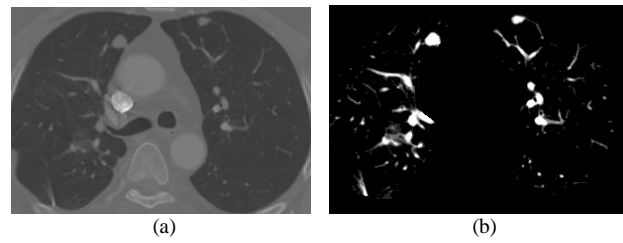


Fig. 4. An example of nodule candidates extraction. (a) Original lung image; (b) Segmented regions of interest

### D. Segmentation of nodular structures

The structures that are segmented from the lung volume through multiple thresholding include nodules, vessels, and the bronchi. For a CAD system to give efficient results, it is important that the nodules are correctly separated from tubular, elongated structures.

For each of the segmented regions, a 3D distance map is calculated. This map assigns ascending weighted values to voxels from the boundary of the region to the centroid giving a measure of the radius of both spherical and cylindrical structures. Spherical structures have a higher distance value at their innermost layer, as compared to oblong structures. The separation is performed by removing the outermost layer of each region. Fig.5 shows a 3D image of a large juxtavascular nodule that was correctly separated from the attached vascular tree. Finally, shape based features of the nodule candidates, namely, "diameter, area, volume, elongation, and circularity" are computed to prune nodules from the non-nodules.

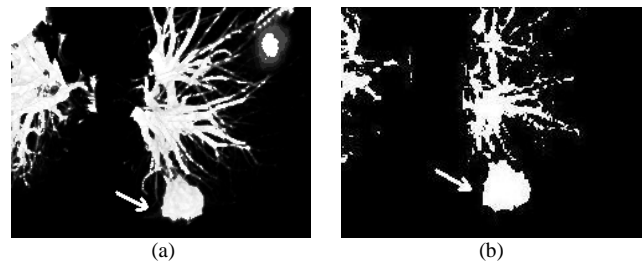


Fig. 5. Nodule segmentation from the attached anatomical structure (a) Nodule and the attached vascular tree; (b) Separated nodule

## III. EXPERIMENTAL RESULTS

The proposed CAD system is tested using the CT scans from the Lung Image Database Consortium (LIDC). LIDC is a publicly available database from the National Biomedical Imaging Archive (NBIA). The nodules in this database are annotated by four radiologists. For nodules that are smaller than 3mm in size, only the approximate centroid location that identifies the nodule is given. But for nodules that are more than or equal to 3mm, the complete boundary outline of the nodule is drawn by each radiologist. In addition, each radiologist classifies the nodule as either benign or malignant. Benign nodules appear solid in the CT images, whereas malignant nodules are manifested as semi-solid and non-solid structures.

To evaluate and compare performance, the algorithm presented by Choi et al. [8] is applied to the CT images. Only the performance of the nodule detection stage was evaluated,

and the classification step is not considered for comparison. The technique provided a nodule detection rate of 60% with a false positive rate of 12.6 per scan. The low detection rate is due to the fact that the CT images contained a large number of non-solid nodules, which were not successfully detected by the system. In addition, juxtavascular nodules presented a greater challenge because they get wrongly classified as part of the vessel. However, the system provided very good detection results for high intensity solid nodules of varying sizes.

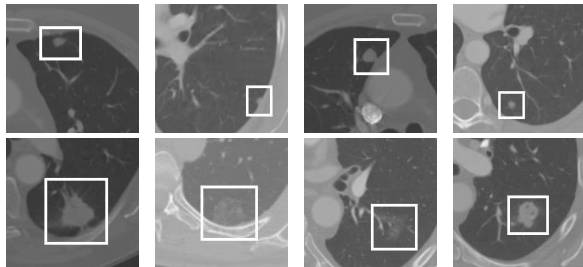


Fig. 6. Examples of detected nodules. Top Row: Nodules detected by both systems. Bottom Row: Previously missed nodules detected by the proposed method

In comparison, the nodule detection method proposed in this paper provides a higher nodule detection rate of 80% and a relatively lower false positive rate of 12.2 per scan. It was observed that the increase in nodule detection rate is a result of successful detection of a higher number of non-solid nodules. In addition, a few juxtavascular nodules that were missed previously by Choi et al. [8] and Suzuki et al [10] techniques were also detected by the proposed system. The detection performance on high intensity and well-shaped, dense nodules was unchanged. Fig.6 shows examples of detected nodules.

TABLE I. COMPARISON OF OVERALL NODULE DETECTION PERFORMANCE

Methods	Nodule detection rate (%)	Average FPs per scan
Suzuki et al. [10]	80	16.1
Choi et al. [8]	60	12.6
Proposed method	80	12.2

#### IV. CONCLUSIONS

In this paper, a filtering-based method is proposed for the automatic detection of pulmonary nodules. A multi-layered enhancement scheme is applied before extracting potential nodule candidates. 3D disk-shaped kernels of varying sizes sharpen spherical nodules, irregularly shaped nodules with spherical elements, and non-solid nodules. Optimal multiple thresholding segments regions of interest and masking the 3D distance map separates spherical nodules from the attached vessels. Further, rule-based pruning removes false positive regions.

Non-solid nodules can be an indication of malignancy. Therefore, it is important for a nodule detection system to provide good detection results for these nodules. Sharpening non-solid regions provide better detection rate. Another advantage of enhancement is that it de-emphasizes vascular structures. Hence, a decrease in the overall rate of false positives per scan is observed. In addition, juxtavascular nodules get omitted because they are erroneously classified as

part of the vessel. Masking a 3D distance map successfully separates spherical structures from the attached vessels. The proposed method provides a nodule detection rate Of 80% and an average rate of 12.2 false positives per scan. A higher detection performance for non-solid and juxtavascular nodules is observed.

#### REFERENCES

- [1] A. Jemal, R. Siegel, E. Ward, Y. Hao, J. Xu, M.J. Thun, "Cancer statistics, 2009," *CA: A Cancer Journal for Clinicians*, vol. 59, pp. 225-249, 2009.
- [2] S. Matsuoka, Y. Kurihara, K. Yagihashi, H. Niimi, Y. Nakajima, Peripheral solitary pulmonary nodule: CT findings in patients with pulmonary emphysema1, *Radiology* 235 (1) (2005) 266-273, <http://dx.doi.org/10.1148/radiol.2351040674>. URL <http://radiology.rsna.org/content/235/1/266.abstract> .
- [3] K. Awai, K. Murao, A. Ozawa, M. Komi, H. Hayakawa, S. Hori, Y. Nishimura, Pulmonary nodules at chest CT: effect of computer-aided diagnosis on radiologists' detection performance, *Radiology* 230 (2) (2004) 347-352, <http://dx.doi.org/10.1148/radiol.2302030049>. URL <http://radiology.rsna.org/content/230/2/347.abstract> .
- [4] S.G. Armato, M.L. Giger, C.J. Moran, J.T. Blackburn, K. Doi, H. MacMahon, "Computerized detection of pulmonary nodules on CT scans," *Radiographics*, vol. 19, pp. 1303-1311, 1999.
- [5] T. Messay, R. Hardie, S. Rogers, "A new computationally efficient CAD system for pulmonary nodule detection in CT imagery," *Medical Image Analysis*, vol. 14, pp. 390-406, 2010.
- [6] W. Kostis, A. Reeves, D. Yankelevitz, C. Henschke, "Three dimensional segmentation and growth-rate estimation of small pulmonary nodules in helical CT images," *IEEE Trans. Med. Imaging*, vol. 22, no. 10, pp. 1259-1274, 2003.
- [7] M.S. Brown, J.G. Goldin, S. Rogers, H.J. Kim, R.D. Suh, M.F. McNitt-Gray, S.K. Shah, D. Truong, K. Brown, J.W. Sayre, D.W. Gjertson, P. Batra, D.R. Aberle, "Computer-aided lung nodule detection in ct: results of large-scale observer test," *Academic Radiology*, vol. 12, pp. 681-686, 2005.
- [8] W.-J. Choi, T.-S. Choi, "Genetic programming-based feature transform and classification for the automatic detection of pulmonary nodules on computed tomography images," *Information Sciences*, vol. 212, pp. 57-78, 2012.
- [9] Q. Li, F. Li, K. Doi, "Computerized detection of lung nodules in thin-section CT images by use of selective enhancement filters and an automated rule-based classifier," *Academic Radiology*, vol. 15, no. 2, pp. 165-175, 2008.
- [10] K. Suzuki, S.A. ArmatoIII, F. Li, S. Sone, K. Doi, "Massive training artificial neural network (MTANN) for reduction of false positives in computerized detection of lung nodules in low-dose computed tomography," *Medical Physics*, vol. 30, pp. 1602-1617, 2003.
- [11] A. Retico, P. Delogu, M. Fantacci, I. Gori, A. Preite Martinez, "Lung nodule detection in low-dose and thin-slice computed tomography," *Computers in Biology and Medicine*, vol. 38, pp. 525-534, 2008.
- [12] J. Pu, B. Zheng, J.K. Leader, X.-H. Wang, D. Gur, "An automated CT based lung nodule detection scheme using geometric analysis of signed distance field," *Medical Physics*, vol. 35, no. 8, pp. 3453-3461, 2008.
- [13] S. Ozekes, Rule based lung region segmentation and nodule detection via genetic algorithm trained template matching, *Istanbul Commer. Univ. J. Sci.* 6 (11) (2007) 17-30.
- [14] S.M.B. Netto, A.C. Silva, R.A. Nunes, M. Gattass, "Automatic segmentation of lung nodules with growing neural gas and support vector machine," *Computers in Biology and Medicine*, vol. 42, pp. 1110-1121, 2012.
- [15] X. Ye, G. Beddoe, G. Slabaugh, Graph cut-based automatic segmentation of lung nodules using shape, intensity, and spatial features, in: *The Second International Workshop on Pulmonary Image Analysis*, 2009, pp. 103-113.
- [16] D. Cascio, R. Magro, F. Fauci, M. Iacomi, G. Raso, "Automatic detection of lung nodules in CT datasets based on stable 3D mass-spring

- models,” *Computers in Biology and Medicine*, vol. 42, pp. 1098-1109, 2012.
- [17] Y. Lee, T. Hara, H. Fujita, S. Itoh, T. Ishigaki, “Automated detection of pulmonary nodules in helical CT images based on an improved template matching technique,” *IEEE Transactions on Medical Imaging*, vol. 20, pp. 595-604, 2001.
- [18] J. Dehmeshki, X. Ye, X. Lin, M. Valdivieso, H. Amin, “Automated detection of lung nodules in CT images using shape-based genetic algorithm,” *Computerized Medical Imaging and Graphics*, vol. 31, pp. 408-417, 2007.
- [19] M. Tan, R. Deklerck, B. Jansen, M. Bister, J. Cornelis, A novel computer-aided lung nodule detection system for CT images, *Med. Phys.* 38 (10) (2011) 5630–5645, <http://dx.doi.org/10.1118/1.3633941>. ISSN: 0094-2405. URL <http://www.ncbi.nlm.nih.gov/pubmed/21992380>.
- [20] Sua ´ rez-Cuenca, W. Guo, Q. Li, Automated detection of pulmonary nodules in CT: false positive reduction by combining multiple classifiers, in: *Proceedings of the SPIE*, vol. 7963, 2011, pp. 796338–796338-6. URL <http://dx.doi.org/10.1117/12.878793> .

# Autonomous Vehicle-to-Vehicle (V2V) Decision Making in Roundabout using Game Theory

Lejla Banjanovic-Mehmedovic  
Faculty of Electrical Engineering  
University of Tuzla,  
Tuzla, Bosnia and Herzegovina

Edin Halilovic  
CA Design  
Tuzla, Bosnia and Herzegovina

Ivan Bosankic  
IVL  
Tuzla, Bosnia and Herzegovina

Mehmed Kantardzic  
Speed School of Engineering  
University of Louisville  
Louisville, USA

Suad Kasapovic  
Faculty of Electrical Engineering  
University of Tuzla,  
Tuzla, Bosnia and Herzegovina

**Abstract**—Roundabout intersections promote a continuous flow of traffic. Roundabouts entry move traffic through an intersection more quickly, and with less congestion on approaching roads. With the introduction of smart vehicles and cooperative decision-making, roundabout management shortens the waiting time and leads to a more efficient traffic without breaking the traffic laws and earning penalties. This paper proposes a novel approach of cooperative behavior strategy in conflict situations between the autonomous vehicles in roundabout using game theory. The game theory presents a strategic decision-making technique between independent agents - players. Each individual player tends to achieve best payoff, by analyzing possible actions of other players and their influence on game outcome. The Prisoner's Dilemma game strategy is selected as approach to autonomous vehicle-to-vehicle (V2V) decision making at roundabout test-bed, because the commonly known traffic laws dictate certain rules of vehicle's behavior at roundabout. It is shown that, by integrating non-zero-sum game theory in autonomous vehicle-to-vehicle (V2V) decision making capabilities, the roundabout entry problem can be solved efficiently with shortened waiting times for individual autonomous vehicles.

**Keywords**—autonomous vehicles; decision making; non-zero-sum game theory; mobile robots; roundabout; vehicle-to-vehicle cooperation (V2V); wireless communication

## I. INTRODUCTION

Roundabout intersections have recently become very popular, since they reduce the number of conflict points, which are characteristic for classic intersections, reduce driving speeds and increase driver attention [1]. When traffic is heavy, waiting time is a significant problem [2]. Possible solutions include installation of traffic lights at a roundabout entry, which can decrease waiting times during increased traffic flow times [3], especially if it is optimized [4]. Modern approaches, such as flower and turbo roundabouts, present recent solutions that improve road safety and reduce number of collisions [5]. Increased capacity also increases pollutant emissions [6].

With the introduction of smart vehicles, an alternative method for roundabout management has emerged. In the paper

[7], a new concept for lateral control on roundabouts is introduced, taking into account entrances, exits and lane changes inside the roundabouts. The experiments have been tested in a 3D simulator that emulates the behaviour of driverless vehicle from the real world - Cybercars. Using vehicle-to vehicle communication (V2V) and vehicle-to-infrastructure (V2I), vehicle gaps can be reduced, thus increasing roundabout traffic flow [8]. Besides that, non communicating vehicles should be identified and reported by the road-side infrastructure [9]. In [10], a microscopic traffic simulator was developed to study intelligent traffic management techniques and evaluate their performance at roundabouts and crossroads. In the paper [11], the fuzzy-behavior-based algorithm for roundabout intersection management is presented. The various different vehicle communication types – combinations of cooperative and non-cooperative vehicles as well as possibility of faulty or missing infrastructure controller were examined.

It is found in [12] that by applying game theory in VANETs and fuzzy logic control for simulation, minimizing traffic congestion and reduced wait time can be achieved quite well. The approach makes traffic regularized not only in the mountainous areas after the occurrence of landslides, but in urban and rural areas as well, upon facing road hurdles. One example of using Game Theory (GT) in Intelligent Transport systems is seen in Vehicle Platoon [13].

In deciding an action of the robot in the coordination for the target tracking, [14] presents a method using the “Nash equilibrium” based on the noncooperative game theory. On the other hand, [15] proposes the “Stackelberg equilibrium”, based on a type of cooperative game. In [16], the switching method is proposed in order to coordinate the Nash equilibrium with the Stackelberg equilibrium, which needs communication in the situation that only the Nash equilibrium that needs no communication, is a difficult task to achieve.

The key contribution of this work is twofold. First, we propose a novel approach of cooperative behavior strategy in conflict situations between the two robot vehicles in a roundabout model, based on game theory. Second, this

autonomous vehicle-to-vehicle (V2V) decision making framework was implemented as cyber-physical system, through wireless connected mobile robot platforms, in order to demonstrate real-life situations in a roundabout.

The rest of this paper is organized as follows. Section II describes the basics of game theory. Section III proposes the non-zero-sum game structure in roundabout. In Section IV, the results of game theory in autonomous V2V decision making are presented to demonstrate the effectiveness of the proposed approach in cyber-physical system framework. In the last section, conclusions and directions for future work are presented.

## II. GAME THEORY

Game theory is a formal study of decision-making where several players must make choices that potentially affect the interests of other players [17]. The sequence of optimal decisions chosen by the players is closely related to optimal control problem. Game theory applies in many studies of competitive scenarios, therefore, the problems are called games and the participants are called players or agents of the game [18]. A player is defined as an individual or group of individuals making a decision [19]. Each player of the game has an associated amount of benefit or gain, which he receives at the end of the game, and this, is called payoff or utility, which measures the degree of satisfaction an individual player derives from the conflicting situation [20]. For each player of the game, the choices available to them are called strategies [21]. The game presents the description of strategic interactions that include the constraints on the action that a player can take and also the player's interests but does not specify the actions that the players do take [19].

Game theory is generally divided into two branches, and these are the non-cooperative and cooperative game theory [19]. Whether a game is cooperative or non-cooperative would depend on whether the players can communicate with one another. The non-cooperative game theory is concerned with the analysis of strategic choices [17]. While the non-cooperative game theory focuses on competitive scenarios, the cooperative game theory provides analytical tools to study the behavior of rational players when they cooperate [19].

Formally, n-player normal form game is defined as the  $(2n + 1)$ -tuple:

$$(Q; S_1, \dots, S_n; u_1(s_1, \dots, s_n), u_2(s_1, \dots, s_n), \dots, u_n(s_1, \dots, s_n)) \quad (1)$$

where  $n \geq 2$  is a natural number,  $Q = \{1, 2, \dots, n\}$  is a given finite set, so-called *set of players*, its elements are called *players*; for every  $i = \{1, 2, \dots, n\}$ ,  $S_i$  is an arbitrary set, so-called *set of strategies of the player i*, and

$$u_i: S_1 \times S_2 \times \dots \times S_n \rightarrow \mathbb{R} \quad (2)$$

is a real function called *payoff function (utility function)* of the player  $i$ . A set of all strategies space of all players is represented by the matrix  $S = S_1 \times S_2 \times \dots \times S_n$  [21]. In such a case, we denote the game by  $\langle N, (S_i), (u_i) \rangle$ .

The *Nash equilibrium*, also called the *strategic*

*equilibrium*, is a list of strategies, one for each player, which has the property that no player can unilaterally change his strategy and get a better payoff. In other words, no player in the game would take a different action as long as every other player remains the same [22].

An n-tuple of strategies  $s^* = \{s_1^*, \dots, s_n^*\}$  is called an equilibrium point or Nash equilibrium of the game, if and only if for every  $i \in \{1, 2, \dots, n\}$  and every  $s_i \in S_i$  the following condition holds:

$$u_i(s_1^*, \dots, s_{i-1}^*, s_i, s_{i+1}^*, \dots, s_n^*) \leq u_i(s_1^*, \dots, s_{i-1}^*, s_i^*, s_{i+1}^*, \dots, s_n^*) \quad (3)$$

Depending upon the number of players, a game can be classified as 2-player game or N-players where  $N > 2$  [21]. Bimatrix game is a two-player finite normal form game where

- player 1 has a finite strategy set  $S = \{s_1, s_2, \dots, s_m\}$
- player 2 has a finite strategy set  $T = \{t_1, t_2, \dots, t_n\}$
- when the pair of strategies  $(s_i, t_j)$  is chosen, the payoff to the first player is  $a_{ij} = u_1(s_i, t_j)$  and the payoff to the second player is  $b_{ij} = u_2(s_i, t_j)$ ;  $u_1, u_2$  are payoff functions.

The values of payoff functions can be given separately for particular players:

$$A = \begin{bmatrix} a_{11} & \dots & a_{1n} \\ \vdots & \ddots & \vdots \\ a_{m1} & \dots & a_{mn} \end{bmatrix} \quad B = \begin{bmatrix} b_{11} & \dots & b_{1n} \\ \vdots & \ddots & \vdots \\ b_{m1} & \dots & b_{mn} \end{bmatrix} \quad (4)$$

Matrix A is called a payoff matrix for player 1, matrix B is called a payoff matrix for player 2.

TABLE I. THE BIMATRIX FOR TWO PLAYERS

		Player 2			
		Strategy	$t_1$	$t_2$	..
Player 1	$s_1$	$(a_{11}, b_{11})$	$(a_{12}, b_{12})$		$(a_{1n}, b_{1n})$
	$s_2$	$(a_{21}, b_{21})$	$(a_{22}, b_{22})$		$(a_{2n}, b_{2n})$
	...				
	$s_m$	$(a_{m1}, b_{m1})$	$(a_{m2}, b_{m2})$		$(a_{mn}, b_{mn})$

There are a number of possible strategies that a player can choose to follow: Dominating, Extensive game, Mixed strategy, Zero-sum game and Non-zero-sum games Evolutionary interpretation, etc [17].

The *dominant strategy* presents the best choice for a player for every possible choice by the other player. A dominant strategy has such payoffs that, regardless of the choices of other players, no other strategy would result in a higher payoff. An *extensive game* (or extensive form game) describes with a tree how a game is played. It depicts the order in which players make moves, and the information each player has at each decision point. A *mixed strategy* is an active randomization, with given probabilities, which determine the player's decision. As a special case, a mixed strategy can be the deterministic choice of one of the given pure strategies. A game has *perfect information* when at any point in time only one player makes a move, and knows all the actions that have

been made until then. In the *evolutionary interpretation*, there is a large population of individuals, each of whom can adopt one of the strategies. The game describes the payoffs that result when two of these individuals meet. The dynamics of this game are based on assuming that each strategy is played by a certain fraction of individuals. Then, given this distribution of strategies, individuals with better average payoff will be more successful than others, so that their proportion in the population increases over time.

A game is said to be *zero-sum* if for any outcome, the sum of the payoffs to all players is zero. In a two-player zero-sum game, one player's gain is the other player's loss, so their interests are diametrically opposed. The theory of zero-sum games is vastly different from that of non-zero-sum games because an optimal solution can always be found. Non-zero-sum games differ from zero-sum games in that there is no universally accepted solution. That is, there is no single optimal strategy that is preferable to all others, nor is there a predictable outcome. Non-zero-sum games are also non-strictly competitive, as opposed to the completely competitive zero-sum games, because such games generally have both competitive and cooperative elements. Players engaged in a non-zero sum conflict have some complementary interests and some interests that are completely opposed. The examples of non-zero-sum games are the Prisoner's Dilemma game, the Battle of the Sexes, the symmetric games, etc.

The Prisoner's Dilemma game can be generalized to any situation when two players are in a non-cooperative situation where the best all-around situation is for both to cooperate, but the worst individual outcome is to be the cooperating player while the other player defects.

The Prisoner's Dilemma game strategy is selected as an approach to autonomous vehicle-to-vehicle (V2V) decision making at roundabout test-bed, because the commonly known traffic laws dictate the certain rules of vehicle's behavior at roundabout.

### III. GAME STRATEGY IN ROUNDABOUT

#### A. Roundabout Model

The basic idea for the application of game theory and appropriate structures in roundabout will be illustrated through the Roundabout model as shown in "Fig. 1". The mobile robot was considered as autonomous vehicles - players. Regarding the position of the autonomous vehicles toward to roundabout, players could be in next states: "*normal (NS)*", "*including (RI)*" and "*circulating (RC)*".

Each autonomous vehicle player has two statuses: Entering Vehicle (EV) and Circulating Vehicle (CV, roundabout inside). The Entering vehicle, while entering the roundabout, can detect the Circulating vehicle. Both autonomous vehicles must have certain information about one another. The Entering vehicle can calculate and send an angle at which it saw the Circulating vehicle, its own traveled distance and current speed. The circulating vehicle sends information to the Entering vehicle about the circulating continuing or not in order that the Entering vehicle decides to smoothly include or slow down.

Common known traffic laws in a roundabout dictate that the Circulating vehicle always has the advantage over the Entering vehicle, i.e. the Entering vehicle must slow down and ultimately stop if the Circulating vehicle has not passed the specific roundabout intersection.

#### B. Vehicle-to-Vehicle Cooperation

Let the autonomous vehicle R1 be in status Entering vehicle, and the autonomous vehicle R2 in the status of Circulating vehicle. The cooperation of autonomous vehicles in the roundabout is done through the following steps:

a) When the autonomous vehicle R1 goes from "normal" state to "including", then the autonomous vehicle R1 can start to move constant speed  $v_1$  towards the point of inclusion and parallel scanning on the R2 autonomous vehicle from the left side. If the autonomous vehicle R1 notices the autonomous vehicle R2 from the left side, it calculates the angle at which the autonomous vehicle R2 was noticed and its distance  $D_2$ . Value  $D_{10}-D_1$  is the distance travelled by the autonomous vehicles R1 from the point where it went from the "normal" state to "including" until the moment when it noticed the autonomous vehicle R2 on the left side. Once it notices the autonomous vehicle R2, the autonomous vehicle R1 stops the scanning.

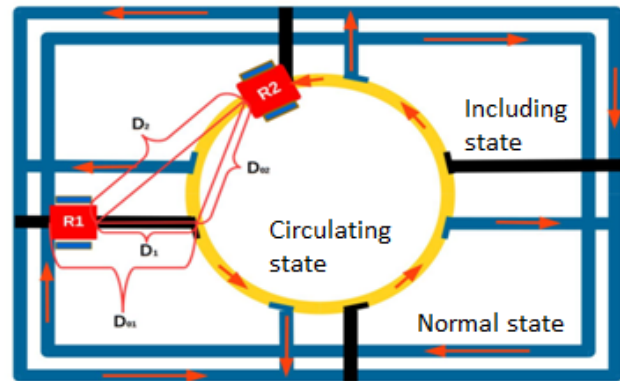


Fig. 1. Roundabout Model with states regarding the position

b) The autonomous vehicle R1 sends a request for communication with the autonomous vehicle R2, noticed earlier in the first stage. The autonomous vehicle R1 sends the angle and the distance  $D_2$  under which it noticed the autonomous vehicle R2, its own moving speed  $v_1$  and distance  $D_{10}-D_1$  from the point when it turns from "normal" state to "including", to the moment when it notices the autonomous vehicle R2 on the left side.

c) After the autonomous vehicle R2 received the necessary information from the autonomous vehicle R1, the autonomous vehicle R2 performs the action of coordination. Autonomous vehicle R2 reads its own uniform speed  $v_2$ .

"Fig. 2" shows the important parameters of positioning of autonomous vehicles in the roundabout.

The  $\alpha$  is the angle between  $D_1$  i  $D_2$ , and, based on the cosines theorem, it is:

$$D_{02} = \sqrt{D_1^2 + D_2^2 - 2 \cdot D_1 \cdot D_2 \cdot \cos \alpha} \quad (5)$$

The  $\beta$  is the angle between values  $R_1$  i  $R_2$ , so, based on the cosines theorem, it is:

$$\beta = \arccos \left( \frac{R_1^2 + R_2^2 - D_{02}^2}{2 \cdot R_1 \cdot R_2} \right) \quad (6)$$

The length of  $L$  represents the distance travelled by the autonomous vehicle  $R_2$ , that is, the time needed to reach the point of inclusion / exclusion.

$$L = \frac{r \cdot \pi \cdot \beta}{180^\circ} \quad (7)$$

In minimizing roundabout congestions, travel time is the most important factor that needs to be considered. The times  $t_1$  and  $t_2$  are the times that are necessary for the autonomous vehicles  $R_1$  and  $R_2$  respectively, to reach the point of inclusion in the roundabout, from the moment when the autonomous vehicle  $R_1$  notices the autonomous vehicle  $R_2$ .

The time required for the autonomous vehicle  $R_1$  to travel the part  $D_1$  up until inclusion with speed  $v_1$  is  $t_1 = D_1/v_1$ .

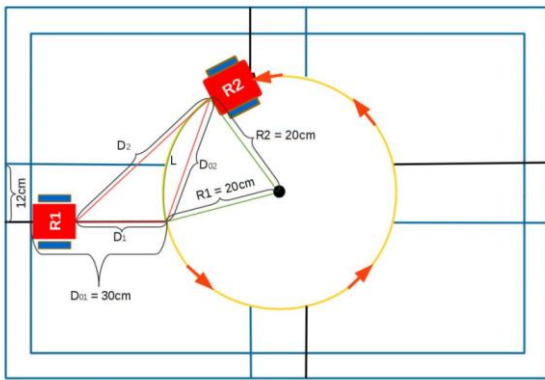


Fig. 2. Roundabout Model geometry

The time required for the autonomous vehicle  $R_2$  to cross the section  $L$  with speed  $v_2$  is  $t_2 = L/v_2$ . Time  $\Delta t$  represents the passing of an autonomous vehicle  $R_2$  through the point of inclusion / exclusion inside the roundabout, in order to avoid a collision between the autonomous vehicles  $R_1$  and  $R_2$ . Time  $\Delta t$  only relates to the speed of autonomous vehicle  $R_2$  and its dimension  $d_2$  and it is  $\Delta t = d_2/v_2$ .

During the V2V cooperation, the following specific cases are possible, to which we apply game theory:

- If  $t_1 < t_2 - \Delta t$ , the autonomous vehicle  $R_1$  includes freely and moves into the "circulating" state. If the autonomous vehicle  $R_2$  decides to continue to circulate, the autonomous vehicle  $R_2$  remains in the state of "circulating". If the autonomous vehicle  $R_2$  decides to exclude from the roundabout, then, it moves into the "normal" state, and freely excludes itself from the roundabout. The waiting time for both autonomous vehicles  $R_1$  and  $R_2$  are zero.
- If  $t_1 > t_2 - \Delta t$  AND  $t_1 < t_2 + \Delta t$  and if the autonomous vehicle  $R_2$  decides to exclude itself from the roundabout, then, the autonomous vehicles move freely. The autonomous vehicle  $R_1$  moves into the "circulating" state, and the autonomous vehicle  $R_2$

moves into the "normal" state. The waiting time for both autonomous vehicles  $R_1$  and  $R_2$  are zero.

- If  $t_1 > t_2 - \Delta t$  AND  $t_1 < t_2 + \Delta t$  and if the autonomous vehicle  $R_2$  decides to remain in the "circulating" state, conflicts are possible. The autonomous vehicle  $R_2$  has the advantage and continues to circulate freely, while the autonomous vehicle  $R_1$  adjusts its speed to avoid conflicts. The autonomous vehicle  $R_1$  must come to a point of inclusion for  $t_2 + \Delta t$ . Then the waiting time of autonomous vehicle  $R_2$  is zero, and for the autonomous vehicle  $R_1$  is  $t_1 - (t_2 + \Delta t)$ . (Autonomous vehicle  $R_1$  will slow down linearly, to the point of inclusion, in order to reach that point for the time  $t_2 + \Delta t$ . Once the autonomous vehicle  $R_1$  gets included, it goes into the "circulating" state.
- If  $t_1 > t_2 - \Delta t$ , the autonomous vehicle  $R_1$  includes freely and moves into the "circulating" state. If the autonomous vehicle  $R_2$  decides to continue to circulate, it remains in the state of "circulating". If the autonomous vehicle  $R_2$  decides to exclude from the roundabout, then the autonomous vehicle  $R_2$  moves into the "normal" state and freely excludes from the roundabout. The waiting time for both autonomous vehicles  $R_1$  and  $R_2$  are zero.

### C. Localisation of Autonomous Vehicle in Roundabout

In case of turning detection, the localisation algorithm in roundabout for each autonomous vehicle is based on combination of previous state and current state in which the vehicle was or can be and random moving as action through the space. The next sequence describe the condition, action and localisation state after moving action:

(new previous state, new current state) =  $f(\text{previous state, current state, action})$ .

For different situation in a roundabout, there exist the next sequences:

(normal, including) =  $f(\text{normal, normal, Turn right})$

(normal, normal) =  $f(\text{normal, normal, Move ahead})$

(including, circulating) =  $f(\text{normal, including, Including\_in Roundabout})$

(circulating, circulating) =  $f(\text{including\_OR\_circulating, circulating, Circulate continuing})$

(circulating, normal) =  $f(\text{including\_OR\_circulating, circulating, Excluding})$

(normal, normal) =  $f(\text{circulating, normal, Turn right or left})$

(normal, normal) =  $f(\text{circulating, normal, Turn right or left})$

For example, if current state is "normal" and previous state is "normal" and the vehicle random turns right then new values are current state = "including" and previous state = "normal".

### D. Game Strategy in autonomous V2V Decision making

Based on the "Prisoner's dilemma" and the predefined

algorithm, we can create a table that shows the waiting time for the autonomous vehicles R1 and R2 according to the situation in which they find themselves within the roundabout.

Each player has two strategies. The autonomous vehicle R1 is Entering vehicle and the autonomous vehicle R2 is the Circulating vehicle. For the Entering vehicle, those strategies are "smoothly inclusion (SI)" and "adjusting speed (AS)". For Circulating vehicle, those strategies are "smoothly exclusion (SE)" and "smoothly circulate (SC)". Game Strategies for Entering and Circulating vehicles and their payoffs are shown in Table II. Autonomous vehicle R1 is trying out all possible actions starting with the one that is best:  $(SI, SE) = (SI, SC) = (AS, SE) < (t_1 - (t_2 + \Delta t), 0)$ . For the autonomous vehicle R2, all actions lead to zero waiting time. For the autonomous vehicle R1, the greatest waiting time, also the only waiting time is in case it chooses a strategy (AS), and the autonomous vehicle R2 chooses (SC). All other actions by the autonomous vehicles R1, lead to zero waiting time.

Based on the Nash equilibrium in the Prisoner's dilemma, if the prisoners are not "selfish", we can conclude that the Nash equilibrium actions are  $(SI, SE) = (SI, SC) = (AS, SE) = (0,0)$ . In case of two interacting vehicles, Entering vehicle loses some minimal amount of time, but overall time loss is avoided.

TABLE II. POSSIBLE STRATEGIES AND PAYOFFS FOR VEHICLES

	Strategies	Circulating vehicle	
		SE	SC
Entering vehicle	SI	(0,0)	(0,0)
	AS	(0,0)	$(t_1 - (t_2 + \Delta t), 0)$

#### IV. EXPERIMENTAL RESULTS

##### A. Autonomous Mobile Robot Structure

The modified Parallax Boe-Bot mobile robots are used as autonomous vehicles, and used for demonstration scenarios in roundabout. This mobile robot consists of the two geared motors mounted on aluminum chassis, batteries and control electronics. In order to achieve advanced performance and utilize Arduino libraries, BasicStamp was replaced by Arduino Uno microcontroller board, which is based on ATmega328 microcontroller. Each autonomous vehicle has QTI sensors for line following (as road detection). In order to detect obstacles and other vehicles, the robot was also equipped with Parallax Ping))) ultrasonic sensors distances.

The communication between the robots is established through a wireless communication using XBee modules and ZigBee protocol.

##### B. Example of Conflict Scenario

Consider a scenario, where conflict situation between autonomous vehicles R1 and R2 are possible. In "Fig. 3", the autonomous vehicle R2 is in "circulate" state and autonomous vehicle R1 is in "including" state. Autonomous vehicle R1 scans whether the autonomous vehicle R2 comes from the left. In that case, the autonomous vehicle R1 sends the message that it wants to include itself in the roundabout and asks

whether the autonomous vehicle R2 will continue to circulate or exclude from the roundabout. In this case, the autonomous vehicle R2 decided to continue to circulate in the roundabout and the autonomous vehicle R1 adjusts its speed and waits until another autonomous vehicle R2 passes the point of inclusion in the roundabout, "Fig. 4".

"Fig. 5" presents time responses of left and right servo motors for autonomous vehicle R1 and "Fig. 6" presents states of autonomous vehicle R1.



Fig. 3. Vehicle R1 waits to include in roundabout



Fig. 4. R1 includes in roundabout

"Fig. 7" presents time responses of left and right servo motors for autonomous vehicle R2 and "Fig. 8" presents states of autonomous vehicle R2. In start position  $t=0[s]$ , autonomous vehicle R1 is in "normal" state.

When the vehicle is accelerating from  $0[s]$  to  $2[s]$ , the left and right servomotors are linearly accelerating, and from the time  $t = 2[s]$  to time  $t = 6[s]$  the autonomous vehicle R1 is

moving at maximum speed. From the time  $t = 6[s]$  the right servomotor's speed linearly decreases and the autonomous vehicle R1 goes from the "normal" state to "including (RI)" and turns right.

At the time  $t = 12[s]$ , the left and right servomotors are moving at maximum speed, the autonomous vehicle R1 moves straight ahead and scans the environment at a distance of up to 40[cm] in the range of  $90^{\circ}$ - $135^{\circ}$ . If it notices another vehicle, this means that it is in "circulating (RC)" and that it can eventually cause a crash if another autonomous vehicle decides to continue circulating. Therefore, when the autonomous vehicle R1 notices another vehicle R2, it asks whether it will continue to circulate (possible conflict) or exclude from the roundabout. In this experiment, the autonomous vehicle R2 decided to continue to circulate, and the autonomous vehicle R1 stops its movement and waits until another autonomous vehicle R2 passes the point of inclusion in the roundabout. This waiting time lasts from  $t = 12[s]$  to  $t = 15[s]$ , when another autonomous vehicle R2 leaves the point of inclusion in the roundabout, and the autonomous vehicle R1 can continue its movement.

At the time  $t = 17[s]$ , the autonomous vehicle R1 is included in the roundabout, a new state status of autonomous vehicles R1 is "circulating (RC)", and for the autonomous vehicle R2, it is "normal" state. The autonomous vehicle R1 circulates until the time  $t = 21[s]$ , when it excludes from the roundabout and passes to "normal (NS)" state.

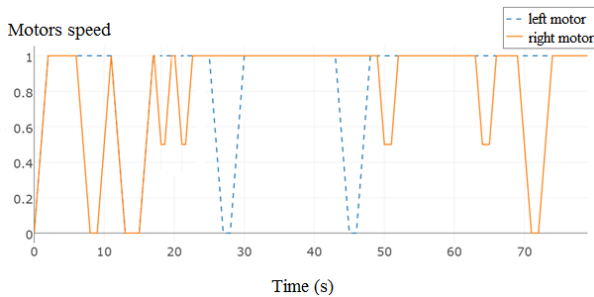


Fig. 5. Time response of left and right servo motors for vehicle R1

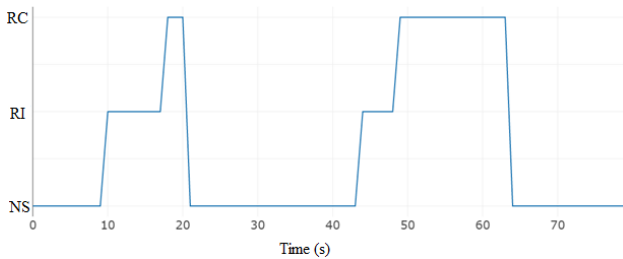


Fig. 6. States of vehicle R1

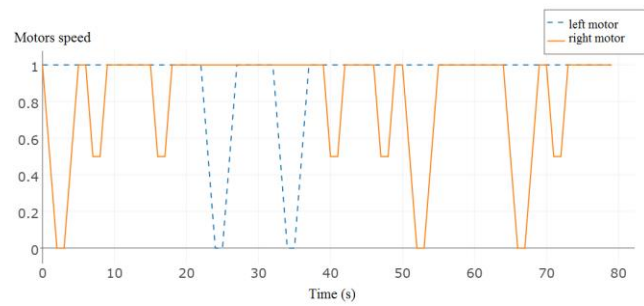


Fig. 7. Time response of left and right servo motors for vehicle R2

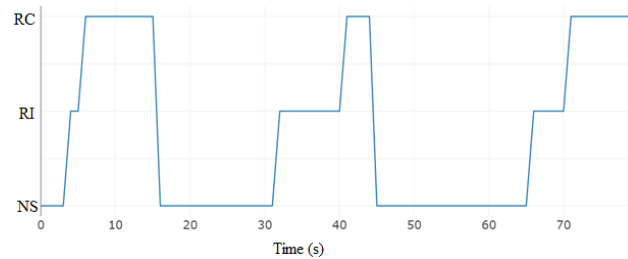


Fig. 8. States of vehicle R2

## V. CONCLUSION

In our paper, the non-zero-sum game is proposed for the autonomous vehicle-to-vehicle (V2V) decision making in conflict situations at roundabout test-bed. With the introduction of smart vehicles and Prisoner's Dilemma game based cooperative decision-making for two players, the method for roundabout management has emerged.

It is found that by applying Game theory in autonomous vehicle-to-vehicle (V2V) decision making, results can be achieved quite well in the form of management in critical section and reduced waiting time for individual autonomous vehicles. Our approach is verified in cyber-physical framework of wireless connected mobile robots.

In real life traffic scenarios, additional factors may shape the cooperate model between more vehicles. For the future work, we plan to investigate a more advanced decision making model with multiple vehicles inside roundabout, so different congestion scenarios can be analyzed.

## ACKNOWLEDGMENT

The authors express their sincere thanks for the funding support they received from Ministry of Civil Affairs of Bosnia and Herzegovina.

## REFERENCES

- [1] P. Lipar and J. Kostjansk, "Traffic Calming in Slovenia", in *3rd Urban Street Symposium*, Seattle, Washington, 2007.
- [2] I. Legac, H. Pilko, N. Subic, "Analysis of traffic safety on roundabout Jadranska Avenue - Avenue Dubrovnik in Zagreb", in *Conference proceedings Transport, Maritime and Logistics Science, 14th ICTS 2011, Slovenia*, 2014.
- [3] J. Ben-Edigbe, A. Abdelgalil and I. Abbaszadehfallah, "Extent of Delay and Level of Service at Signalised Roundabout", *International Journal of Engineering and Technology*, Volume 2, No. 3, pp. 419-424, 2012.
- [4] Y.-J. Gong and J. Zhang, "Real-Time Traffic Signal Control for Modern Roundabouts by Using Particle Swarm Optimization-Based Fuzzy Controller", *Publisher Cornell University Library*, 2014.

- [5] T. Tollazzi and M. Rencelj, "Comparative analyse of the two new alternative types of roundabout - turbo and flower roundabout", *The Baltic Journal of Road and Bridge Engineering*, Volume 9(3), pp. 164–170, 2014.
- [6] F. Corriere, M. Guerrieri, D. Ticali and A. Messineo, "Estimation of air pollutant emissions in flower roundabouts and in conventional roundabouts archives of civil engineering", *Archives of Civil Engineering*, LIX, 2, 2013.
- [7] J. P. Rastelli, V. Milan'és, T. De Pedro and Lj. Vlacic, "Autonomous driving manoeuvres in urban road traffic environment: a study on roundabouts", in *Proceedings of the 18th World Congress The International Federation of Automatic Control*, Milan, Italy, 2011.
- [8] H.K. Kim, Y.B. Lee, C.Y. and Y.P. Oh, "Development and Evaluation of Smart Roundabout Using Connected Vehicle", *Journal of the Korean Society of Civil Engineers*, Vol. 34, No. 1, pp. 243-250, 2014.
- [9] V. Rajeev, and D. Vecchio, "Semiautonomous Multivehicle Safety" *IEEE Robotics & Automation Magazine*, Vol. 18, No. 3 pp.44–54, 2011.
- [10] L. C. Bento and U. Nunes, "Intelligent traffic management at intersections supported by V2V and V2I communications", in *IEEE Conference on Intelligent Transportation Systems*, 2012.
- [11] I. Bosankic and L. Banjanovic-Mehmedovic: "Cooperative intelligence in roundabout intersections using hierarchical fuzzy behavior calculation of vehicle speed profile", *5th International Conference on Transportation and Traffic Engineering (ICTTE 2016)*, pp. 319-324, Switzerland, 2016.
- [12] Y. Saeed, S. A. Lodhi and K. Ahmed, "Obstacle Management in VANET using Game Theory and Fuzzy Logic", *Control International Journal of Scientific & Engineering Research*, Volume 4, Issue 1, 2013.
- [13] A. A. Alam, A. Gattami, K. H. Johansson and C. J. Tomlin, "Establishing Safety for Heavy Duty Vehicle Platooning: A Game Theoretical Approach", in *Proceedings of the 18th World Congress The International Federation of Automatic Control*, Italy, 2011.
- [14] K. Skrzypczyk, "Game theory based target following by a team of robots", in *Proceedings of Forth International Workshop on Robot Motion and Control*, pp.91-96, 2004.
- [15] I. Harmati, "Multiple robot coordination for target tracking using semi-cooperative Stackelberg equilibrium", in *IEE International Control Conference*, 2006.
- [16] W. Inujima, K. Nakano and S. Hosokawa, "Multi-Robot Coordination Using Switching of Methods for Deriving Equilibrium in Game Theory", *Ecti Transactions on Computer and Information Technology*, Vol.8, No.2, 2014.
- [17] T. Turocy and B. von Stengel, *Game Theory*, London: Academic Press, London School of Economics, 2001.
- [18] S. Wandile, "A review of Game Theory", *University of Stellenbosch*, 2012.
- [19] M. Osborne, *An introduction to Game Theory*, Oxford University Press, 2003.
- [20] C. F. Camerer, T-H. Hua and J. T., *Behavioral Game Theory: Thinking, Learning, and Teaching*, Pasadena: California Institute of Technology California Institute of Technology, 2001.
- [21] A. Shah, S. Jan, I. Khan and S. Qamar, "An Overview of Game Theory and its Applications in Communication Networks", *International Journal of Multidisciplinary Sciences and Engineering*, Vol. 3, No. 4, 2012.
- [22] K. Leyton-Brown and Y. Shoham, *Essentials of Game Theory: A Concise, Multidisciplinary Indtroduction*, Morgan & Claypool Publishers. 2008.

# Analytical and Numerical Study of the Onset of Electroconvection in a Dielectric Nanofluid Saturated a Rotating Darcy Porous Medium

Abderrahim Wakif

Hassan II University, Faculty of  
Sciences Ain Chock,  
Laboratory of Mechanics,  
B.P.5366 Maarif, Casablanca,  
Morocco

Zoubair Boulahia

Hassan II University, Faculty of  
Sciences Ain Chock,  
Laboratory of Mechanics,  
B.P.5366 Maarif, Casablanca,  
Morocco

Rachid Sehaqui

Hassan II University, Faculty of  
Sciences Ain Chock,  
Laboratory of Mechanics,  
B.P.5366 Maarif, Casablanca,  
Morocco

**Abstract** — The simultaneous effect of rotation and a vertical AC electric field on the onset of electroconvection in a horizontal dielectric nanofluid layer saturated a Darcy porous medium is investigated. The boundaries of the dielectric nanofluid layer are considered isothermal, where the vertical nanoparticle flux is zero. The resulting eigenvalue problem is solved analytically by the Galerkin weighted residuals technique (GWRT) and numerically using the power series method (PSM). The results show that the onset of electroconvection in dielectric nanofluids can be accelerated when we increase the AC electric Rayleigh-Darcy number, the Lewis number, the nanoparticle Rayleigh-Darcy number or the modified diffusivity ratio. On the contrary, it can be delayed when we increase the Taylor-Darcy number or the porosity of the medium.

**Keywords** — Linear Stability; Electroconvection; Dielectric Nanofluid; Rotation; Porous Medium; Power Series Method

## I. INTRODUCTION

The electro-thermo-hydrodynamics (ETHD) is an interdisciplinary area dealing simultaneous complex interactions among the thermal gradient and electric field applied to a horizontal dielectric liquid (fluid or nanofluid) layer. These interactions, can be studied by performing experiments aimed to control the improvement of heat transfer by applying an electric field across a dielectric fluid, this active method has some advantages for heat transfer enhancement due the electrical effects, such as the low operational costs, rapid and smart control of enhancement, low power consumption, and so on.

In the interest to obtain a high thermal efficiency, the application of the electro-thermo-hydrodynamics transport phenomena received extensive attentions, it may be found in different areas of physics like engineering, heat exchangers, steam pipes, optical and bio-engineering devices, waste heat

recovery and many others. Hence, due to the importance of the electro-thermo-hydrodynamics in practice, several studies have been carried out to assess the effect of electric field on natural convection. A temperature gradient applied to a dielectric fluid produces a gradient in the dielectric constant and electrical conductivity. Keeping this fact in mind, several problems of the onset of convection instability in a horizontal layer of dielectric fluid under the action of a vertical electric field and a vertical temperature gradient have been investigated in the past. Notable among them, we find P.H.Roberts [1] which was the first one who made an individual study on electrohydrodynamic convection by considering the dielectric constant as well as electrical conductivity as a linear function of temperature. Takashima and Aldridge [2], Peter J.Stiles [3] and Mohamed I.A Othman [4] have studied the natural convection in the presence of an applied electric field. M.Takashima [5] was the first one who studied the simultaneous effect of a vertical temperature gradient and a vertical electric field on the onset of convection in a horizontal dielectric fluid saturated a rotating layer. S. Shivakumara et al. [6-7] have investigated the onset of electrothermoconvection in a dielectric fluid saturated a rotating or non-rotating porous layer using the Galerkin technique. P.G.Siddheshwar and D.Radhakrishna [8] have performed a linear and nonlinear studies on the convective instability in dielectric fluids under a vertical temperature gradient and an AC electric field using the normal mode method and truncated representation of Fourier series.

The dielectric nanofluid may be used in an electrical apparatus and other electrical equipments such as distribution transformers, regulating transformers, shunt reactors, converter transformers, generating station units, and power transformers [9-11]. Given the importance of these types of dielectric liquids, we will examine theoretically and

numerically the effect of a vertical AC electric field on the onset of convection in a dielectric nanofluid saturated a rotating Darcy porous medium , which is subjected to a temperature gradient, where the vertical nanoparticle flux is taken zero on the horizontal boundaries.

## II. MATHEMATICAL FORMULATION

We consider an infinite horizontal layer of incompressible dielectric nanofluid saturated a rotating Darcy porous medium with a uniform angular velocity  $\vec{\Omega} = \Omega \vec{e}_z$ , this layer is confined between two parallel impermeable boundaries ( $z^* = 0, z^* = L$ ) and heated from below , where the temperatures at the lower and upper boundaries are taken to be  $T_h^*$  and  $T_c^*$  respectively ( $T_h^* > T_c^*$ ), and the vertical nanoparticle flux  $J_z^*$  is zero on the boundaries. The nanofluid layer is Newtonian , subjected to the gravitational field  $\vec{g} = -g \vec{e}_z$  and also to a vertical AC electric field applied across the layer , such that the lower surface is grounded and the upper surface is kept at an alternating potential whose root mean square is  $\psi_1^*$  (Fig. 1).The thermo-physical properties of nanofluid (viscosity, thermal conductivity, specific heat) are assumed constant in the vicinity of the reference temperature  $T_c^*$  , except for the dielectric constant and the density in the Maxwell equations and the momentum equation respectively , which are based on the Oberbeck-Boussinesq approximation .The asterisks are used to distinguish the dimensional variables from the non-dimensional variables (without asterisks).

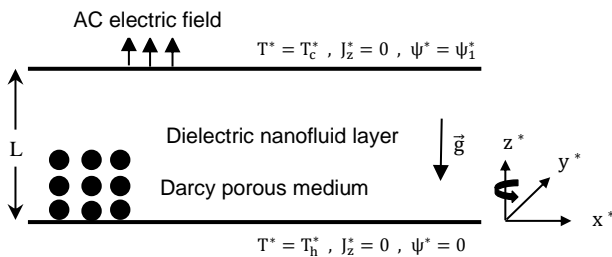


Fig. 1. Physical configuration of the problem

### A. Governing equations

In the case where the centrifugal acceleration is negligible compared to the buoyancy and the electrical forces, the relevant basic equations are [10-15]:

$$\vec{\nabla}^* \cdot \vec{V}^* = 0 \quad (1)$$

$$-\vec{\nabla}^* P^* - K^{-1} \mu \vec{\nabla}^* - 2\gamma^{-1} \rho_0 \vec{\Omega} \times \vec{V}^* + \vec{f}_e + \rho \vec{g} = 0 \quad (2)$$

$$\rho = \rho_0 [1 - \beta(T^* - T_c^*)] (1 - \chi^*) + \rho_p \chi^* \quad (3)$$

$$(\rho c)_m \frac{\partial T^*}{\partial t^*} + (\rho c)_f (\vec{V}^* \cdot \vec{\nabla}^*) T^* = k_m \vec{\nabla}^{*2} T^* + \gamma (\rho c)_p \left( D_B \vec{\nabla}^* \chi^* \cdot \vec{\nabla}^* T^* + \left( \frac{D_T}{T_c^*} \right) \vec{\nabla}^* T^* \cdot \vec{\nabla}^* T^* \right) \quad (4)$$

$$\frac{\partial \chi^*}{\partial t^*} + \gamma^{-1} (\vec{V}^* \cdot \vec{\nabla}^*) \chi^* = D_B \vec{\nabla}^{*2} \chi^* + \left( \frac{D_T}{T_c^*} \right) \vec{\nabla}^* T^* \quad (5)$$

Where  $\vec{V}^*(u^*, v^*, w^*)$  is the Darcy's velocity,  $t^*$  is the time,  $\rho_0$  is the nanofluid density at reference temperature  $T_c^*$ ,  $P^*$  is the pressure ,  $K$  ,  $\gamma$  ,  $\mu$  ,  $\rho$  and  $k_m$  are the permeability , the

porosity of the medium , the viscosity, the density and the effective thermal conductivity of nanofluid respectively ,  $\rho_p$  is the density of nanoparticles,  $\beta$  is the thermal expansion coefficient,  $\chi^*$  is the volumetric fraction of nanoparticles,  $(\rho c)_p$  and  $(\rho c)_f$  are the heat capacity of nanoparticles and base fluid respectively,  $(\rho c)_m$  is the effective heat capacity of nanofluid,  $D_B$  is the Brownian diffusion coefficient ,  $D_T$  is the thermophoretic diffusion coefficient ,  $\vec{\nabla}^*$  is the vector differential operator and  $\vec{f}_e$  is the force of electrical origin which can be expressed by Landau and Lifshitz [16] as follows:

$$\vec{f}_e = \rho_e \vec{E}^* - \frac{1}{2} (\vec{E}^* \cdot \vec{E}^*) \vec{\nabla}^* \epsilon^* + \frac{1}{2} \vec{\nabla}^* \left[ \rho \frac{\partial \epsilon^*}{\partial \rho} (\vec{E}^* \cdot \vec{E}^*) \right] \quad (6)$$

Where  $\vec{E}^*$  is the root mean square value of the electric field,  $\rho_e$  is the charge density and  $\epsilon^*$  is the dielectric constant.

In the equation (6), the last electrostriction term can be grouped with the pressure  $P^*$  in the equation (2) and it has no effect on an incompressible nanofluid. The first term on the right hand side is the Coulomb force due to a free charge and the second term depends on the gradient of  $\epsilon^*$ . If an AC electric field is applied at a frequency much higher than the reciprocal of the electrical relaxation time, the free charge doesn't have time to accumulate. Moreover, the electrical relaxation times of most dielectric liquids appear to be sufficiently long to prevent the buildup of free charge at standard power line frequencies. At the same time, the dielectric loss at these frequencies is so low that it makes no significant contribution to the temperature field. Under the circumstances, only the force induced by non-uniformity of the dielectric constant is considered. Furthermore, since the second term in the above equation depends on  $\vec{E}^* \cdot \vec{E}^*$  rather than  $\vec{E}^*$  and the variation of  $\vec{E}^*$  is very rapid, the root mean square value of  $\vec{E}^*$  can be assumed as the effective value. In other words, we can treat the AC electric field as the DC electric field whose strength is equal to the root mean square value of the AC electric field [10,11,17].

Since there is no free charge, the relevant Maxwell equations are:

$$\vec{\nabla}^* \times \vec{E}^* = \vec{0} \quad (7)$$

$$\vec{\nabla}^* \cdot (\epsilon^* \vec{E}^*) = 0 \quad (8)$$

In view of the equation (7),  $\vec{E}^*$  can be expressed as:

$$\vec{E}^* = -\vec{\nabla}^* \psi^* \quad (9)$$

Where  $\psi^*$  is the root mean square value of the electric potential, such that the dielectric constant  $\epsilon^*$  is assumed to be in the form:

$$\epsilon^* = \epsilon_0 [1 - e(T^* - T_c^*)] \quad (10)$$

Here  $e$  is the thermal expansion coefficient of dielectric constant, it's assumed to be very small ( $0 < e \Delta T^* \ll 1$ ). If we consider that the temperature is constant and the vertical nanoparticle flux  $J_z^*$  is zero on the boundaries, we can write the boundary conditions under the Darcy's model as follows:

$$\begin{aligned} w^* = 0 & ; T^* = T_h^* ; J_z^* = 0 & \text{at } z^* = 0 \\ w^* = 0 & ; T^* = T_c^* ; J_z^* = 0 & \text{at } z^* = L \end{aligned} \quad (11)$$

Such that:

$$J_z^* = -\rho_p \left[ D_B \frac{\partial \chi^*}{\partial z^*} + \left( \frac{D_T}{T_c^*} \right) \frac{\partial T^*}{\partial z^*} \right]$$

If we consider the following dimensionless variables:

$$(x^*, y^*, z^*) = L(x, y, z) ; t^* = \frac{\sigma L^2}{\alpha_m} t ; \vec{V}^* = \frac{\alpha_m}{L} \vec{V} ; P^* = \frac{\mu \alpha_m}{K} P$$

$$T^* - T_c^* = \Delta T^* T ; \chi^* - \chi_0^* = \chi_0^* \chi ; J_z = -\frac{L}{\rho_p D_B \chi_0^*} J_z^*$$

$$\vec{E}^* = e \Delta T^* E_0^* \vec{E} ; \psi^* = e \Delta T^* L E_0^* \psi ; \epsilon^* = \epsilon_0 \epsilon$$

Then, we can get for a nanofluid at low concentration of nanoparticles, the following non-dimensional equations:

$$\vec{\nabla} \cdot \vec{V} = 0 \quad (12)$$

$$-\vec{\nabla} \left( P + R_M z - \frac{1}{2} R_{ae} \rho \frac{\partial \epsilon}{\partial \rho} (\vec{E} \cdot \vec{E}) \right) - \vec{V} + \sqrt{T_A} (v \vec{e}_x - u \vec{e}_y) - \frac{1}{2} R_{ae} (\vec{E} \cdot \vec{E}) \vec{\nabla} \epsilon + (R_a T - R_N \chi) \vec{e}_z = 0 \quad (13)$$

$$\frac{\partial T}{\partial t} + (\vec{V} \cdot \vec{\nabla}) T = \bar{\nabla}^2 T + N_B L_e^{-1} \bar{\nabla} \chi \cdot \vec{\nabla} T + N_A N_B L_e^{-1} \bar{\nabla} T \cdot \vec{\nabla} T \quad (14)$$

$$\sigma^{-1} \frac{\partial \chi}{\partial t} + \gamma^{-1} (\vec{V} \cdot \vec{\nabla}) \chi = L_e^{-1} \bar{\nabla}^2 \chi + N_A L_e^{-1} \bar{\nabla}^2 T \quad (15)$$

$$\vec{\nabla} \times \vec{E} = \vec{0} \quad (16)$$

$$\vec{\nabla} \cdot (\epsilon \vec{E}) = 0 \quad (17)$$

$$\vec{E} = -\vec{\nabla} \psi \quad (18)$$

$$\epsilon = (1 - e \Delta T^* T) \quad (19)$$

Where  $E_0^*$  is the root mean square value of the electric field at  $z^* = 0$ ,  $\Delta T^*$  is the temperature difference between the horizontal plates,  $\epsilon_0$  is the dielectric constant at reference temperature  $T_c^*$  and  $\chi_0^*$  is a reference value for the nanoparticle volume fraction.

In the above equations the non-dimensional parameters are given as follows:

$$R_M = \frac{[\rho_0(1 - \chi_0) + \rho_p \chi_0] L K g}{\mu \alpha_m} ; R_{ae} = \frac{\epsilon_0 (e \Delta T^* E_0^*)^2 K}{\mu \alpha_m} ; \sqrt{T_A} = \frac{2 \rho_0 \Omega K}{\gamma \mu}$$

$$R_a = \frac{\rho_0 g \beta \Delta T^* L K}{\mu \alpha_m} ; R_N = \frac{(\rho_p - \rho_0) g L K \chi_0}{\mu \alpha_m} ; N_A = \frac{D_T}{D_B T_c^*} \frac{\Delta T^*}{\chi_0^*}$$

$$N_B = \frac{\gamma (\rho c)_p \chi_0^*}{(\rho c)_f} ; L_e = \frac{\alpha_m}{D_B} ; \alpha_m = \frac{k_m}{(\rho c)_f}$$

Such that:

$$\sigma = \frac{(\rho c)_m}{(\rho c)_f} ; \Delta T^* = T_h^* - T_c^* ; J_z = \frac{\partial \chi}{\partial z} + N_A \frac{\partial T}{\partial z}$$

Where  $R_M$  is the density Rayleigh-Darcy number,  $R_{ae}$  is the AC electric Rayleigh - Darcy number,  $T_A$  is the Taylor - Darcy number,  $R_a$  is the thermal Rayleigh-Darcy number,  $R_N$  is the nanoparticle Rayleigh - Darcy number,  $N_A$  is the modified diffusivity ratio,  $N_B$  is the modified particle - density increment,  $L_e$  is the Lewis number and  $\alpha_m$  is the effective thermal diffusivity of the nanofluid.

### B. Basic solutions

The basic state is quiescent, such that:

$$\vec{\nabla}_b = \vec{0} ; T_b = T_b(z) ; P_b = P_b(z) ; \chi_b = \chi_b(z) ; \epsilon_b = \epsilon_b(z) \quad (20)$$

$$\vec{E}_b = E_b(z) \vec{e}_z ; \psi_b = \psi_b(z)$$

The solutions of the basic state are:

$$\chi_b = N_A z + \chi_0 ; T_b = 1 - z ; \epsilon_b = 1 + e \Delta T^* z$$

$$E_b = \frac{1}{e \Delta T^* (1 + e \Delta T^* z)} ; \psi_b = -\frac{1}{(e \Delta T^*)^2} \log(1 + e \Delta T^* z)$$

Such that:

$$\vec{\nabla}_{P_b} = -\frac{1}{2} R_{ae} (\vec{E}_b \cdot \vec{E}_b) \vec{\nabla} \epsilon_b + (R_a T_b - R_N \chi_b) \vec{e}_z$$

$$P_b = P_b + R_M z - \frac{1}{2} R_{ae} \rho \frac{\partial \epsilon_b}{\partial \rho} (\vec{E}_b \cdot \vec{E}_b)$$

$$E_0^* = \frac{-e \Delta T^* \psi_1^*}{L \log(1 + e \Delta T^*)}$$

Where  $\chi_0 = (\chi_b^*(0) - \chi_0^*)/\chi_0^*$  is the relative nanoparticle volume fraction at  $z = 0$

### C. Perturbation equations

To study the stability of the steady state, we superimpose infinitesimally small perturbations on the basic solutions in the form:

$$\vec{V} = \vec{V}' ; P = P_b + P' ; T = T_b + T' ; \chi = \chi_b + \chi' \quad (21)$$

$$\epsilon = \epsilon_b + \epsilon' ; \vec{E} = \vec{E}_b + \vec{E}' ; \psi = \psi_b + \psi'$$

Where  $\vec{V}', P', T', \chi', \epsilon', \vec{E}'$  and  $\psi'$  are the perturbed quantities over their equilibrium counterparts.

Substituting the expressions (21) into equations (12)-(19), linearizing the equations, eliminating the pressure from the momentum equation (13) by operating curl twice and retaining the vertical component, we obtain the linear stability equations in the form:

$$\vec{\nabla} \cdot \vec{V}' = 0 \quad (22)$$

$$\left( \bar{\nabla}^2 + T_A \frac{\partial^2}{\partial z^2} \right) w' - (R_{ae} + R_a) \bar{\nabla}^2 T' + R_N \bar{\nabla}^2 \chi' - R_{ae} \bar{\nabla}^2 \left( \frac{\partial \psi'}{\partial z} \right) = 0 \quad (23)$$

$$w' + \left( \bar{\nabla}^2 - N_A N_B L_e^{-1} \frac{\partial}{\partial z} - \frac{\partial}{\partial t} \right) T' - N_B L_e^{-1} \frac{\partial \chi'}{\partial z} = 0 \quad (24)$$

$$N_A \gamma^{-1} w' - N_A L_e^{-1} \bar{\nabla}^2 T' - \left( L_e^{-1} \bar{\nabla}^2 - \sigma^{-1} \frac{\partial}{\partial t} \right) \chi' = 0 \quad (25)$$

$$\frac{\partial T'}{\partial z} + \bar{\nabla}^2 \psi' = 0 \quad (26)$$

$$\epsilon' = -e \Delta T^* T' \quad (27)$$

Where  $\bar{\nabla}^2 = \partial^2/\partial x^2 + \partial^2/\partial y^2$  is the horizontal Laplacian operator.

In non-dimensional form, the boundary conditions become:

$$w' = T' = \frac{\partial}{\partial z} (\chi' + N_A T') = \frac{\partial \psi'}{\partial z} = 0 \text{ at } z = 0; 1 \quad (28)$$

### III. LINEAR STABILITY ANALYSIS

For simplicity, we restrict our analysis to two dimensional rolls, so that all physical quantities are independent of  $y$  which allows us to define a stream function  $F'$ , such that:

$$u' = -\frac{\partial F'}{\partial z} ; w' = \frac{\partial F'}{\partial x}$$

Using the definition of stream function, the governing equations (23) - (26) become:

$$\left[ \left( \frac{\partial^2}{\partial x^2} + \frac{\partial^2}{\partial z^2} \right) + T_A \frac{\partial^2}{\partial z^2} \right] \frac{\partial F'}{\partial x} - (R_{ae} + R_a) \frac{\partial^2 T'}{\partial x^2} + R_N \frac{\partial^2 \chi'}{\partial x^2} - R_{ae} \frac{\partial^2}{\partial x^2} \left( \frac{\partial \psi'}{\partial z} \right) = 0 \quad (29)$$

$$\frac{\partial F'}{\partial x} + \left[ \left( \frac{\partial^2}{\partial x^2} + \frac{\partial^2}{\partial z^2} \right) - N_A N_B L_e^{-1} \frac{\partial}{\partial z} - \frac{\partial}{\partial t} \right] T' - N_B L_e^{-1} \frac{\partial \chi'}{\partial z} = 0 \quad (30)$$

$$N_A \gamma^{-1} \frac{\partial F'}{\partial x} - N_A L_e^{-1} \left( \frac{\partial^2}{\partial x^2} + \frac{\partial^2}{\partial z^2} \right) T' - \left[ L_e^{-1} \left( \frac{\partial^2}{\partial x^2} + \frac{\partial^2}{\partial z^2} \right) - \sigma^{-1} \frac{\partial}{\partial t} \right] \chi' = 0 \quad (31)$$

$$\frac{\partial T'}{\partial z} + \left( \frac{\partial^2}{\partial x^2} + \frac{\partial^2}{\partial z^2} \right) \psi' = 0 \quad (32)$$

The equations (29)-(32) are simplified in the usual manner by decomposing the solution in terms of normal modes. According to Borujerdi et al. [18], we can take the perturbation quantities in the form:

$$F' = \mathcal{F}(z) \cos(ax) \exp(nt) ; T' = \mathcal{T}(z) \sin(ax) \exp(nt) \\ \chi' = \mathcal{X}(z) \sin(ax) \exp(nt) ; \psi' = \Psi(z) \sin(ax) \exp(nt) \quad (33)$$

Where  $a$  is the horizontal wave number and  $n$  is the growth rate of the disturbances.

Substituting the expressions (33) into the differential equations (29) - (32), the linearized equations become:

$$-a[(D^2 - a^2) + T_A D^2] \mathcal{F} + a^2(R_{ae} + R_a) \mathcal{T} - a^2 R_N \mathcal{X} + a^2 R_{ae} D \Psi = 0 \quad (34)$$

$$-a \mathcal{F} + [(D^2 - a^2) - N_A N_B L_e^{-1} D - n] \mathcal{T} - N_B L_e^{-1} D \mathcal{X} = 0 \quad (35)$$

$$-a N_A \gamma^{-1} \mathcal{F} - N_A L_e^{-1} (D^2 - a^2) \mathcal{T} - [L_e^{-1} (D^2 - a^2) - \sigma^{-1} n] \mathcal{X} = 0 \quad (36)$$

$$D \mathcal{T} + (D^2 - a^2) \Psi = 0 \quad (37)$$

Here  $D = \partial/\partial z$  and  $D^2 = \partial^2/\partial z^2$ .

The boundary conditions of the problem in view of normal mode analysis are:

$$\mathcal{F} = \mathcal{T} = D(\mathcal{X} + N_A \mathcal{T}) = D \Psi = 0 \text{ at } z = 0; 1 \quad (38)$$

### A. Analytical solution

The Galerkin weighted residuals technique (GWRT) is used to obtain an analytical solution to the system of equations (34)-(37). Accordingly, the base functions  $\mathcal{F}$ ,  $\mathcal{T}$ ,  $\mathcal{X}$  and  $\Psi$  are taken in the following way:

$$\mathcal{F} = \sum_{s=1}^{s=N} A_s \mathcal{F}_s ; \mathcal{T} = \sum_{s=1}^{s=N} B_s \mathcal{T}_s ; \mathcal{X} = \sum_{s=1}^{s=N} C_s \mathcal{X}_s ; \Psi = \sum_{s=1}^{s=N} D_s \Psi_s \quad (39)$$

The previous base functions must satisfy the boundary conditions (38). For this purpose, we take the solutions in the form:

$$\mathcal{F}_s = \mathcal{F}_s = \sin(s\pi z) ; \mathcal{X}_s = -N_A \mathcal{T}_s ; \Psi_s = \cos(s\pi z) \quad (40)$$

Where  $A_s, B_s, C_s$  and  $D_s$  are unknown coefficients, such that the index  $s$  varies between 1 and  $N$  ( $s = 1, 2, 3 \dots, N$ ).

Substituting the expressions (39) and (40) in the equations (34) - (37) and multiplying the first equation by  $\mathcal{F}_p$ , second equation by  $\mathcal{T}_p$ , third equation by  $\mathcal{X}_p$  and fourth equation by  $\Psi_p$ , and then integrating in the limits from zero to unity for obtaining a set of  $4N$  linear homogeneous equations with  $4N$  unknowns  $A_s, B_s, C_s$  and  $D_s$ , such that  $p = 1, 2, 3 \dots, N$ . For the existence of nontrivial solution, the determinant of coefficients matrix must vanish which gives the characteristic equation for the system with the thermal Rayleigh-Darcy number  $R_a$  as the eigenvalue of the characteristic equation. The resulting eigenvalue problem is solved analytically by the Galerkin method of first order ( $N = 1$ ) which is given by the following condition:

$$\det(M) = 0 \quad (41)$$

Where:

$$M = \begin{pmatrix} a(J + \pi^2 T_A) & a^2(R_{ae} + R_a) & a^2 R_N N_A & -\pi a^2 R_{ae} \\ -a & -(J + n) & 0 & 0 \\ a\gamma^{-1} & -L_e^{-1} J & (L_e^{-1} J + \sigma^{-1} n) & 0 \\ 0 & \pi & 0 & -J \end{pmatrix} \\ J = \pi^2 + a^2$$

The previous condition (41) allows to give an expression for the dispersion relation in the form:

$$pn^2 + qn + s = 0 \quad (42)$$

Such that:

$$n = r + i\omega$$

$$p = \sigma^{-1} (J + \pi^2 T_A) J$$

$$q = (\sigma^{-1} + L_e^{-1}) (J + \pi^2 T_A) J^2 - \sigma^{-1} R_{ae} a^4 - R_N N_A \gamma^{-1} a^2 J - \sigma^{-1} R_a a^2 J$$

$$s = L_e^{-1} [(J + \pi^2 T_A) J^2 - R_{ae} a^4 J] - R_N N_A (\gamma^{-1} + L_e^{-1}) a^2 J^2 - L_e^{-1} R_a a^2 J^2$$

For the stationary convection, the real and imaginary parts of  $n$  are zero. Hence the relation (42) allows us to give the expression of the thermal Rayleigh - Darcy number  $R_a$  as follows:

$$R_a = \frac{J^2 + \pi^2 T_A J}{a^2} - R_{ae} \frac{a^2}{J} - R_N N_A (1 + L_e \gamma^{-1}) \quad (43)$$

To find the critical value of  $R_a$ , the equation (43) is differentiated with respect to  $a^2$ , and then equated to zero. A polynomial in  $a_c$ , whose coefficients are functions of the physical parameters  $T_A$  and  $R_{ae}$  is obtained in the form:

$$a_c^8 + 2\pi^2 a_c^6 - \pi^2 (\pi^2 T_A + R_{ae}) a_c^4 - 2\pi^6 (T_A + 1) a_c^2 - \pi^8 (T_A + 1) = 0 \quad (44)$$

The equation (44) is solved numerically for various values of  $T_A$  and  $R_{ae}$  and the critical value  $a_c$  is obtained each time using the Newton-Raphson method. The above results coincide with that of P.H.Roberts [1] in the absence of nanoparticles and rotation ( $R_N = T_A = 0$ ), Dhananjay Yadav et al. [10] in the absence of rotation ( $T_A = 0$ ) and Ramesh Chand [11] for a thermal equilibrium case in a non-rotating Darcy porous medium ( $T_A = \overline{D}_a = 0$ ).

For the oscillatory convection, the real part of  $n$  is zero and hence the relation (42) yields the following expressions for the frequency of oscillations  $\omega$  and the thermal Rayleigh-Darcy number  $R_a^{osc}$  :

$$q = 0 ; \quad \omega^2 = \frac{S}{p} \quad (45)$$

From the above results (45), we can write:

$$(\sigma^{-1} + L_e^{-1})(J + \pi^2 T_A)^2 - \sigma^{-1} R_{ae} a^4 - R_N N_A \gamma^{-1} a^2 J - \sigma^{-1} R_a^{osc} a^2 J = 0$$

$$\omega^2 = \frac{(J + \pi^2 T_A)^2 - R_{ae} a^4 - R_N N_A (1 + L_e \gamma^{-1}) a^2 J - R_a^{osc} a^2 J}{L_e \sigma^{-1} (J + \pi^2 T_A)}$$

Therefore:

$$R_a^{osc} = \frac{(1 + \sigma L_e^{-1})(J + \pi^2 T_A)^2 - R_{ae} a^4 - R_N N_A \sigma \gamma^{-1} a^2 J}{a^2 J} \quad (46)$$

$$\omega^2 = - \left\{ \left( \frac{\sigma}{L_e} \right)^2 J^2 + \frac{R_N N_A \sigma (L_e + \gamma - \sigma) a^2 J}{\gamma L_e (J + \pi^2 T_A)} \right\} \quad (47)$$

If we take  $T_A = 0$  in the above expressions, we find the same results, which are already shown by Dhananjay Yadav et al. [10], when they have studied the electrothermal instability in a Darcy porous medium saturated by a dielectric nanofluid.

From equation (47), it is interesting to note that the vertical AC electric field doesn't influence the existence of oscillatory convection.

According to Yadav et al. [10], Ramesh Chand [11] and Shivakumara et al. [19] the Lewis number  $L_e$  is on the order of  $10^1 - 10^3$ , the nanoparticle Rayleigh-Darcy number  $R_N$  is on the order of  $10^0 - 10^1$ , the modified diffusivity ratio  $N_A$  and the ratio  $\sigma$  aren't more than 10, the porosity  $\gamma$  is not more than the unity. Hence, the value of  $\omega^2$  in the expression (47) will be always negative, which implies that the oscillatory convection is not possible for the studied problem. Therefore, the vertical AC electric field and the uniform rotation have no effect on the existence of the oscillatory convection.

The modified particle-density increment  $N_B$  doesn't appear in the expression (43) of the thermal Rayleigh-Darcy number  $R_a$  characterizing the onset of stationary convection, because of an orthogonal property of the first-order trial functions and their first derivatives. Fortunately, this approximation is valid because this term ( $N_B \sim 10^{-3} - 10^{-1}$  Shivakumara et al. [19]) appears only in the energy equation (14) as a product with the inverse of the Lewis number ( $L_e \sim 10^1 - 10^3$  Yadav et al. [10]) near the temperature gradient and the volume fraction gradient of nanoparticles. So, it makes sense to neglect the effect of the modified particle-density increment  $N_B$  on the onset of stationary convection.

### B. Numerical solution

The analytical study shows that the oscillatory convection is ruled out for the dielectric nanofluids, so the stationary convection ( $n = 0$ ) is the predominant mode.

Using the power series method (PSM) [20-24], we can solve numerically the equations (34) - (37) in their stationary forms ( $n = 0$ ) by choosing a suitable change of variables that

makes the number of variables equal to the number of boundary conditions, after this step we obtain a set of eight first order ordinary differential equations which we can write it in the following form:

$$\frac{d}{dz} u_i(z) = a_{ij} u_j(z); \quad 1 \leq i, j \leq 8 \quad (48)$$

Such that:

$$u_1 = u_3 = u_6 = u_8 = 0 \quad \text{at} \quad z = 0; 1 \quad (49)$$

Where:

$$u_1 = \mathcal{F}; \quad u_2 = D\mathcal{F}; \quad u_3 = \mathcal{T}; \quad u_4 = D\mathcal{T}; \quad u_5 = \mathcal{X}$$

$$u_6 = D(\mathcal{X} + N_A \mathcal{T}); \quad u_7 = \Psi; \quad u_8 = D\Psi$$

The solution of the system (48) in matrix notation can be written as follows:

$$U = BC \quad (50)$$

Where:

$$B = \left( (u_i^j(z))_{\substack{1 \leq i \leq 8 \\ 1 \leq j \leq 8}} \right); \quad U = \left( (u_i(z))_{1 \leq i \leq 8} \right)^T; \quad C = \left( (c_j)_{1 \leq j \leq 8} \right)^T$$

The use of the boundary conditions (49) at  $z = 0$  allows us to write each variable  $u_i(z)$  as a linear combination for four functions  $u_i^j(z)$ , such that:

$$u_i^j(0) = \delta_{ij} \quad (51)$$

$$c_1 = c_3 = c_6 = c_8 = 0 \quad (52)$$

Where  $\delta_{ij}$  is the Kronecker delta symbol.

After introducing the new expressions of the variables  $u_i(z)$  in the system (48), we will obtain the following equations:

$$\frac{d}{dz} u_i^j(z) = a_{ij} u_i^j(z); \quad 1 \leq i, j \leq 8 \quad (53)$$

For each value of  $j$ , we must solve a set of eight first order ordinary differential equations which are subjected to the initial conditions (51) by approaching the variables  $u_i^j(z)$  with power series defined in the interval  $[0,1]$  and truncated at the order  $N$ , such that:

$$u_i^j(z) = \sum_{p=0}^{p=N} d_p^{i,j} z^p \quad (54)$$

A linear combination of the functions  $u_i^j(z)$  satisfying the boundary conditions (49) at  $z = 1$  leads to a homogeneous algebraic system for the coefficients of the combination, which is written as:

$$M'C' = Z \quad (55)$$

Where:

$$M' = \begin{pmatrix} u_1^2(1) & u_1^4(1) & u_1^5(1) & u_1^7(1) \\ u_3^2(1) & u_3^4(1) & u_3^5(1) & u_3^7(1) \\ u_6^2(1) & u_6^4(1) & u_6^5(1) & u_6^7(1) \\ u_8^2(1) & u_8^4(1) & u_8^5(1) & u_8^7(1) \end{pmatrix}; \quad C' = \begin{pmatrix} c_2 \\ c_4 \\ c_5 \\ c_7 \end{pmatrix}; \quad Z = \begin{pmatrix} 0 \\ 0 \\ 0 \\ 0 \end{pmatrix}$$

A necessary condition for the existence of nontrivial solution is the vanishing the determinant of the matrix  $M'$  for obtaining the following dispersion relation:

$$f(R_a, a, T_A, R_{ae}, N_B, L_e, R_N, N_A, \gamma) = \det(M') = 0 \quad (56)$$

If we give to each control parameter  $(T_A, R_{ae}, N_B, L_e, R_N, N_A, \gamma)$  its value, we can plot the neutral curve of the stationary convection by the numerical research of the smallest real positive value of the thermal Rayleigh - Darcy number  $R_a$  which corresponds to a fixed wave number  $a$  and verifies the dispersion relation (56). After that, we will find a set of points  $(a, R_a)$  which help us to plot our curve, and find the critical value  $(a_c, R_{ac})$  which characterizes the onset of the stationary instability, this critical value represents the minimum value of the obtained curve.

#### IV. RESULTS AND DISCUSSION

To have a check on the accuracy of the numerical procedure used (PSM) in this study compared to the analytical results (GWRT), the first test computations are carried out for the dielectric fluids in the tables I and II ( $R_N = 0$ ) and the second tests are reserved to a dielectric nanofluid characterized by  $N_B = 0, L_e = 40, R_N = 0.3, N_A = 2$  and  $\gamma = 0.9$  in the tables III and IV by varying every time the Taylor-Darcy number  $T_A$  and the AC electric Rayleigh-Darcy number  $R_{ae}$ .

TABLE I. CRITICAL THERMAL RAYLEIGH-DARCY NUMBER AND CRITICAL WAVE NUMBER FOR DIFFERENT VALUES OF  $T_A$  IN THE CASE WHERE  $R_N = R_{ac} = 0$

**The dielectric fluids case**

$T_A$	Numerical method			Analytical method	
	N	$a_c$	$R_{ac}$	$a_c$	$R_{ac}$
10	17	5.7213	183.9028	5.7213	183.9028
20	17	6.7251	307.5877	6.7251	307.5877
40	17	7.9496	540.9159	7.9496	540.9159

TABLE II. CRITICAL THERMAL RAYLEIGH-DARCY NUMBER AND CRITICAL WAVE NUMBER FOR DIFFERENT VALUES OF  $R_{ae}$  IN THE CASE WHERE  $T_A = 40$  AND  $R_N = 0$

**The dielectric fluids case**

$R_{ae}$	Numerical method			Analytical method	
	N	$a_c$	$R_{ac}$	$a_c$	$R_{ac}$
0	17	7.9496	540.9159	7.9496	540.9159
50	17	8.1293	497.5393	8.1293	497.5393
100	17	8.3013	453.9178	8.3013	453.9178

TABLE III. CRITICAL THERMAL RAYLEIGH-DARCY NUMBER AND CRITICAL WAVE NUMBER FOR DIFFERENT VALUES OF  $T_A$  IN THE CASE WHERE  $R_{ae} = 0, N_B = 0, L_e = 40, R_N = 0.3, N_A = 2$  AND  $\gamma = 0.9$

**The dielectric nanofluids case**

$T_A$	Numerical method			Analytical method	
	N	$a_c$	$R_{ac}$	$a_c$	$R_{ac}$
10	23	5.4532	151.9976	5.7213	156.6361
20	26	6.5778	277.3816	6.7251	280.3210
40	29	7.8698	511.8082	7.9496	513.6493

TABLE IV. CRITICAL THERMAL RAYLEIGH-DARCY NUMBER AND CRITICAL WAVE NUMBER FOR DIFFERENT VALUES OF  $R_{ae}$  IN THE CASE WHERE  $T_A = 40, N_B = 0, L_e = 40, R_N = 0.3, N_A = 2$  AND  $\gamma = 0.9$

**The dielectric nanofluids case**

$R_{ae}$	Numerical method			Analytical method	
	N	$a_c$	$R_{ac}$	$a_c$	$R_{ac}$
0	29	7.8698	511.8082	7.9496	513.6493
50	28	8.0549	468.5429	8.1293	470.2726
100	30	8.2318	425.0199	8.3013	426.6511

The above tables show that the numerical stationary instability threshold of dielectric fluids and dielectric nanofluids depend implicitly of the truncation order  $N$ , the Taylor-Darcy number  $T_A$  and the AC electric Rayleigh-Darcy number  $R_{ae}$ , such that the truncation order  $N_c$  which corresponds to the convergence of the numerical method (PSM) is determined, when the absolute value of the difference between the critical thermal Rayleigh-Darcy numbers  $R_{ac}(N_c + 1)$  and  $R_{ac}(N_c)$  is of the order of  $10^{-5}$ .

Where  $R_{ac}(N_c)$  and  $R_{ac}(N_c + 1)$  are the critical thermal Rayleigh-Darcy numbers which correspond to the truncation orders  $N_c$  and  $N_c + 1$  respectively, such that:

$$R_{ac} = R_{ac}(N_c)$$

A quantitative comparison between the numerical procedure (PSM) and the analytical method (GWRT) shows that there is an excellent agreement between these two methods when we studied the dielectric fluids, but on the contrary we found a remarkable difference between these methods when we treated the dielectric nanofluids, such that  $a_c(GWRT) > a_c(PSM)$  and  $R_{ac}(GWRT) > R_{ac}(PSM)$ . The observed difference is due principally to the wrong choice of the test function  $\chi_s$  characterizing the presence of the nanoparticles in a dielectric base fluid in the case where the nanoparticle flux is taken zero on the horizontal boundaries with  $\chi_s = -N_A \mathcal{T}_s$ . It's important to note that the previous problem doesn't arise if we impose a constant nanoparticle volume fraction at the boundaries of the layer instead to consider a zero nanoparticle flux (A.Wakif et al. [23]).

To give an additional credibility to the trueness of the results obtained by the power series method (PSM) in this investigation, we can compare this numerical procedure with another known numerical method. For this reason, we solve again the system of sixty-four differential equations (53) with the initial conditions (51) using the fourth-order explicit Runge-Kutta method (RKM) on the one hand with a fixed step size ( $h = 0.01$ ); and on the other hand with a variable step size. The results obtained for a dielectric fluid and a dielectric nanofluid are tabulated in the tables V and VI, respectively. The comparison between the results obtained with the power series method (PSM) and those found with the Runge-Kutta methods (RKM) shows the existence of an excellent agreement between the power series method (PSM) and the adaptive step-size control.

TABLE V. COMPARISON BETWEEN THE POWER SERIES METHOD (PSM) AND THE RUNGE-KUTTA METHODS (RKM) FOR A DIELECTRIC FLUID

$R_{ae}$	$T_A$	PSM			RKM with a fixed step size		RKM with a variable step size	
		N	$a_c$	$R_{ac}$	$a_c$	$R_{ac}$	$a_c$	$R_{ac}$
0	0	17	3.1415	39.4784	3.1415	39.4783	3.1415	39.4784
	10		5.7213	183.9028	5.7213	183.9026	5.7213	183.9027
	20		6.7251	307.5877	6.7251	307.5874	6.7251	307.5877
	30		7.4129	425.7306	7.4129	425.7303	7.4129	425.7305
	40		7.9496	540.9159	7.9496	540.9156	7.9496	540.9159
	50		8.3954	654.1855	8.3954	654.1851	8.3954	654.1855
20			8.0224	523.5962	8.0224	523.5959	8.0224	523.5962
40			8.0940	506.2349	8.0940	506.2346	8.0940	506.2349
60	40	17	8.1643	488.8338	8.1643	488.8335	8.1643	488.8338
80			8.2334	471.3943	8.2334	471.3939	8.2334	471.3943
100			8.3013	453.9178	8.3013	453.9175	8.3013	453.9178

TABLE VI. COMPARISON BETWEEN THE POWER SERIES METHOD (PSM) AND THE RUNGE-KUTTA METHODS (RKM) FOR A DIELECTRIC NANOFUID CHARACTERIZED BY  $N_B = 0.01$ ,  $L_e = 10$ ,  $R_N = 0.1$ ,  $N_A = 0.5$  AND  $\gamma = 0.3$

$R_{ae}$	$T_A$	PSM			RKM with a fixed step size		RKM with a variable step size	
		N	$a_c$	$R_{ac}$	$a_c$	$R_{ac}$	$a_c$	$R_{ac}$
0	0	30	3.0307	36.5544	3.0307	36.5544	3.0307	36.5544
	10		5.7059	181.9134	5.7059	181.9133	5.7059	181.9134
	20		6.7163	305.6927	6.7163	305.6925	6.7163	305.6927
	30		7.4066	423.8767	7.4066	423.8764	7.4066	423.8767
	40		7.9447	539.0858	7.9447	539.0855	7.9447	539.0858
	50		8.3914	652.3712	8.3914	652.3709	8.3914	652.3712
20			8.0176	521.7689	8.0177	521.7685	8.0177	521.7689
40			8.0893	504.4103	8.0894	504.4099	8.0893	504.4103
60	40	30	8.1598	487.0117	8.1598	487.0114	8.1598	487.0117
80			8.2290	469.5746	8.2290	469.5743	8.2290	469.5746
100			8.2970	452.1004	8.2970	452.1001	8.2970	452.1004

The combined effects of Coriolis forces due to rotation and vertical AC electric field on the criterion for the onset of thermal convection in a dielectric nanofluid saturated a Darcy porous layer are investigated. The bounding surfaces of the dielectric nanofluid are isothermal and subjected to a zero nanoparticle flux. If we neglect the modified particle-density increment  $N_B$ , the numerical procedure and the analytical method carried out for the dielectric nanofluids reveal that the thermal stability of this type of nanofluids depends on six parameters:  $T_A, R_{ae}, L_e, R_N, N_A$  and  $\gamma$ .

To study numerically and analytically the effect of a parameter ( $T_A, R_{ae}, N_B, L_e, R_N, N_A, \gamma$ ) on the onset of the electroconvection in a rotating Darcy porous medium filled of a Newtonian dielectric nanofluid with a zero vertical flux of nanoparticles on the isothermal boundaries ( $z^* = 0, z^* = L$ ), we must fix the others and determine the variations of the critical wave number  $a_c$  and the critical thermal Rayleigh - Darcy number  $R_{ac}$  as a function of the AC electric Rayleigh - Darcy number  $R_{ae}$  in the interval [0,50] for different values of this parameter and then compare the numerical and analytical results through the curves obtained in Fig. 2 and Fig. 3. To ensure the accuracy in this study, we will take as truncation order  $N_c = 30$  in all subsequent computations.

The zero boundary conditions for the variables  $u_1, u_3, u_6, u_8$  at  $z = 0$  and  $z = 1$  provide a sufficient number of boundary conditions for the system of differential equations (48) to find exactly the thermal Rayleigh-Darcy number  $R_a$  and the wave number  $a$ , and also to conclude the critical couple ( $a_c, R_{ac}$ ) which characterizes the onset of the stationary instability. However, it's difficult to obtain some typical streamlines and isonanoluxes in z-direction (for the nanoparticles) at the onset of convection for a dielectric nanofluid, because this problem requires one more condition named the normalization condition [18] which simply fixes the coefficients  $c_2, c_4, c_5, c_7$  and allows to find the expressions of the stream function  $F$  and the vertical flux of nanoparticles  $J_z$ , and hence to plot the streamlines and the isonanoluxes in Fig. 4 for a dielectric nanofluid. The normalization condition is written as:

$$u_4 = 1 \text{ at } z = 1 \tag{57}$$

We point out that, the determination of the threshold ( $a_c, R_{ac}$ ) by the power series method (PSM) and the use of the condition (57), allow us to find the expressions of the stream function  $F$  and the vertical flux of nanoparticles  $J_z$  at the onset of convection with a good accuracy, these expressions are written as follows:

$$F = F_b + F' \tag{58}$$

$$J_z = J_{z_b} + J_z' \tag{59}$$

In the expressions (58) and (59), we take:

$$a = a_c ; R_a = R_{ac} ; F_b = J_{zb} = 0 ; F' = u_1 \cos(ax) ; J_z' = u_6 \sin(ax)$$

$$u_1 = c_2 u_1^2(z) + c_4 u_1^4(z) + c_5 u_1^5(z) + c_7 u_1^7(z)$$

$$u_6 = c_2 u_6^2(z) + c_4 u_6^4(z) + c_5 u_6^5(z) + c_7 u_6^7(z)$$

Where  $J_{zb}$  and  $F_b$  are the basic states of the vertical flux of nanoparticles and the stream function, respectively.

From the expressions (58) and (59), we can conclude the expressions of the Darcy's velocity  $V$  and the vertical flux of nanoparticles  $J_z$ , and hence we can plot the variation of  $V$  and  $J_z$  as a function of  $z$  in Fig. 5 and Fig. 6 respectively at different positions of  $x$ , such that:

$$V = \sqrt{\left(-\frac{\partial F}{\partial z}\right)^2 + \left(\frac{\partial F}{\partial x}\right)^2} \quad (60)$$

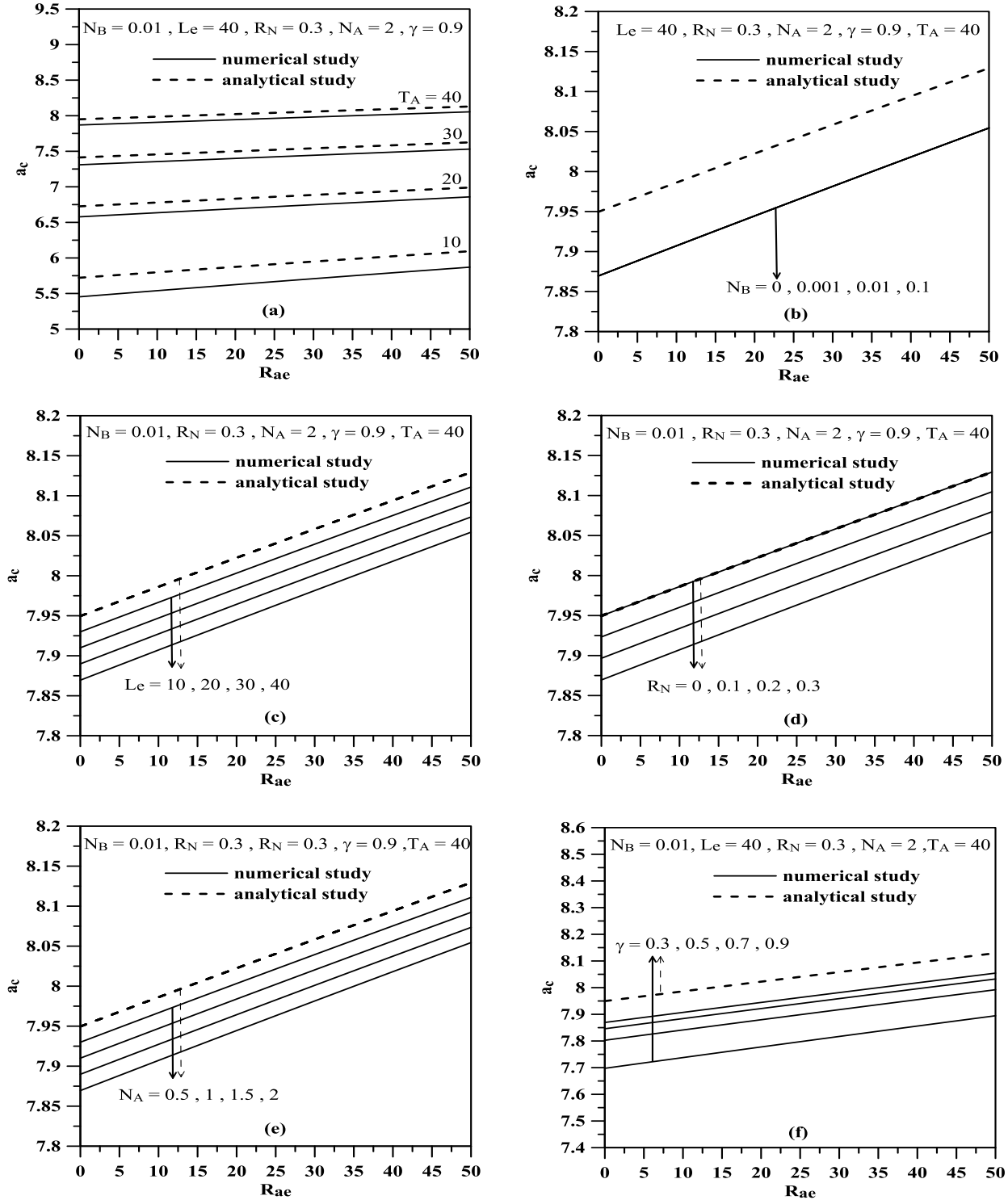


Fig. 2. Plot of  $a_c$  as a function of  $R_{ae}$  for different values of (a)  $T_A$ , (b)  $N_B$ , (c)  $L_e$ , (d)  $R_N$ , (e)  $N_A$  and (f)  $\gamma$  for a dielectric nanofluid

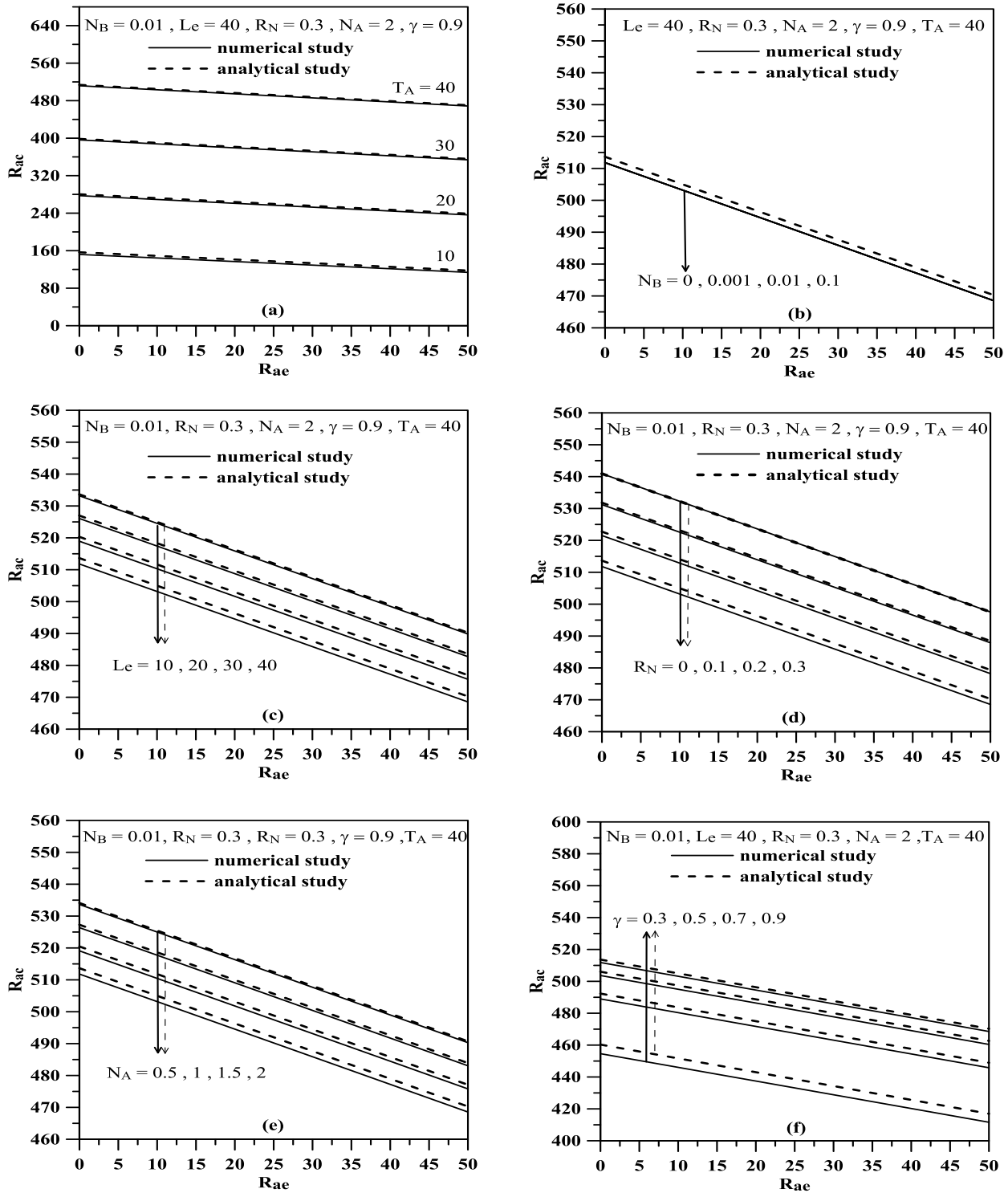


Fig. 3. Plot of  $R_{ac}$  as a function of  $R_{ae}$  for different values of (a)  $T_A$ , (b)  $N_B$ , (c)  $Le$ , (d)  $R_N$ , (e)  $N_A$  and (f)  $\gamma$  for a dielectric nanofluid

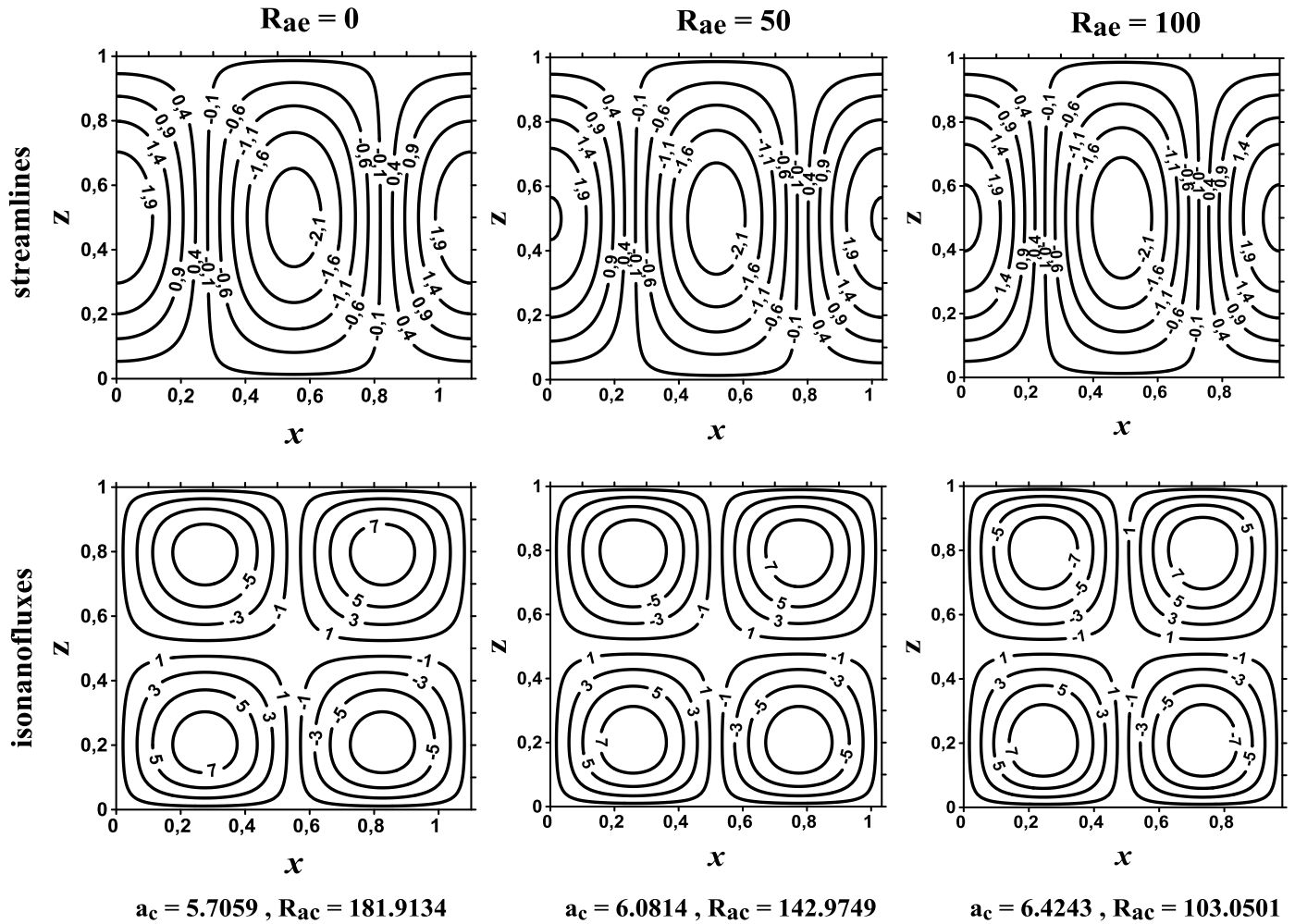


Fig. 4. Variation in streamlines and isonofluxes at different values of  $R_{ae}$  for a dielectric nanofluid characterized by  $N_B = 0.01, L_e = 10, R_N = 0.1, N_A = 0.5, \gamma = 0.3$  and  $T_A = 10$

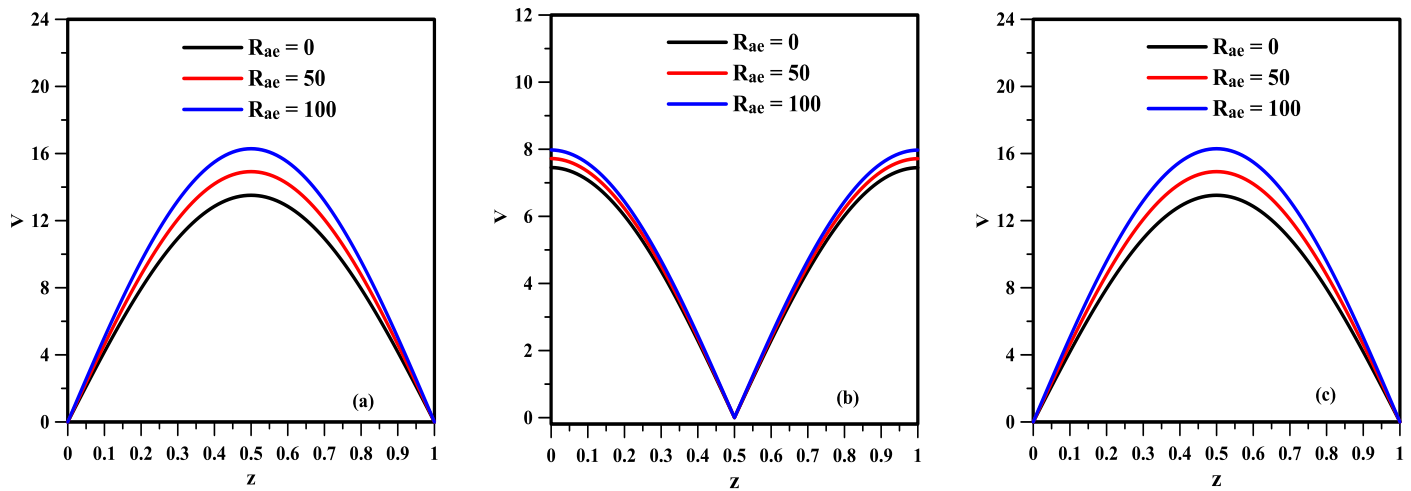


Fig. 5. Plot of  $V$  as a function of  $z$  for different values of  $R_{ae}$  at (a)  $x = \pi/2a_c$ , (b)  $x = \pi/a_c$  and (c)  $x = 3\pi/2a_c$  for a dielectric nanofluid characterized by  $N_B = 0.01, L_e = 10, R_N = 0.1, N_A = 0.5, \gamma = 0.3$  and  $T_A = 10$

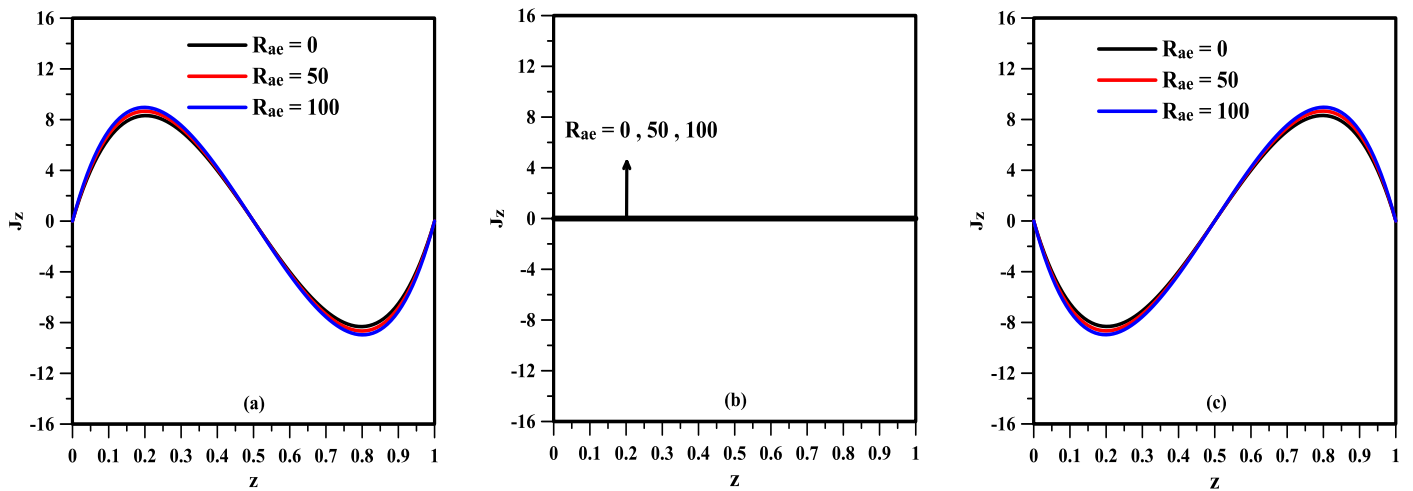


Fig. 6. Plot of  $J_z$  as a function of  $z$  for different values of  $R_{ae}$  at (a)  $x = \pi/2a_c$ , (b)  $x = \pi/a_c$  and (c)  $x = 3\pi/2a_c$  for a dielectric nanofluid characterized by  $N_B = 0.01$ ,  $L_e = 10$ ,  $R_N = 0.1$ ,  $N_A = 0.5$ ,  $\gamma = 0.3$  and  $T_A = 10$

For the numerical study, we find from Fig.2 that the critical wave number  $a_{ac}$  increases with an increase either in the Taylor-Darcy number  $T_A$ , in the AC electric Rayleigh-Darcy number  $R_{ae}$  or in the porosity of the medium  $\gamma$ . However, it decreases when the Lewis number  $L_e$ , the nanoparticles Rayleigh-Darcy number  $R_N$  or the modified diffusivity ratio  $N_A$  increases. Hence, an increase in the parameters  $T_A$ ,  $R_{ae}$  or  $\gamma$  allows to reduce the size of convection cells (see Fig.4) and an increase in the parameters  $L_e$ ,  $R_N$  or  $N_A$  allows to increase also the size of convection cells. On the contrary, we find that the modified particle-density increment  $N_B$  has no significant effect on the critical wave number  $a_c$ .

Fig.3 (a) shows the variation of the critical thermal Rayleigh-Darcy number  $R_{ac}$  as a function of AC electric Rayleigh-Darcy number  $R_{ae}$  for different values of the Taylor-Darcy number  $T_A$ , indicating that the variation in the critical thermal Rayleigh-Darcy number  $R_{ac}$  with the Taylor-Darcy number  $T_A$  is an increasing function in both studied cases (numerical and analytical), this result shows that the presence of the Coriolis forces allows to minimize the effect of the buoyancy forces on the onset of electroconvection in dielectric nanofluids, and hence the Taylor-Darcy number  $T_A$  has a stabilizing effect for the dielectric nanofluids.

Fig.3 (b) shows the effect of the modified particle-density increment  $N_B$  on the onset of electroconvection in dielectric nanofluids. From Fig.3 (b), it's observed that the modified particle-density increment  $N_B$  has no significant effect on the onset of electroconvection in a dielectric nanofluid. This is happened due to the weak value of the term  $N_B L_e^{-1}$  in the energy equation (14). The product  $N_B L_e^{-1}$  is on the order of  $10^{-6} - 10^{-2}$ , such that the effect of this parameter on the thermal stability of dielectric nanofluids is very small which we can neglect it in the equation (14), this remark is in good

agreement with the obtained analytical results, such that the parameter  $N_B$  doesn't appear in the expression (43) of the thermal Rayleigh-Darcy number  $R_a$ .

Fig.3 (c) shows the variation of the critical thermal Rayleigh-Darcy number  $R_{ac}$  as a function of AC electric Rayleigh-Darcy number  $R_{ae}$  for different values of the Lewis number  $L_e$ . It is found that the critical thermal Rayleigh-Darcy number  $R_{ac}$  decreases analytically and numerically when the value of Lewis number  $L_e$  increases, indicating that the Lewis number has a destabilizing effect on the dielectric nanofluids. Hence, to ensure the stability of the system, we can use a dielectric nanofluid characterized by a less effective thermal diffusivity.

The variation of the critical thermal Rayleigh-Darcy number  $R_{ac}$  as a function of AC electric Rayleigh-Darcy number  $R_{ae}$  for different values of the nanoparticles Rayleigh-Darcy number  $R_N$  is shown in Fig.3 (d). It's observed that the critical thermal Rayleigh-Darcy number  $R_{ac}$  decreases analytically and numerically when the nanoparticles Rayleigh-Darcy number  $R_N$  increases, This is because as an increase in the volumetric fraction of nanoparticles allows to increase both the Brownian motion and the thermophoresis of nanoparticles which cause a destabilizing effect on the stability of the system. Hence, we can consider that the thermophoresis and the Brownian motion as driving forces favoring the motion of the nanoparticles.

Fig.3 (e) shows the variation of the critical thermal Rayleigh-Darcy number  $R_{ac}$  as a function of AC electric Rayleigh-Darcy number  $R_{ae}$  for different values of the modified diffusivity ratio  $N_A$ , this figure indicates that an increase in the modified diffusivity ratio  $N_A$  allows to accelerate the onset of electroconvection in the dielectric nanofluids in both studied cases (numerical and analytical).

Therefore an increase in the temperature difference between the horizontal plates increases also the buoyancy forces which destabilize the system.

Fig.3 (f) shows the variation of the critical thermal Rayleigh-Darcy number  $R_{ac}$  as a function of AC electric Rayleigh-Darcy number  $R_{ae}$  for different values of the porosity of the medium  $\gamma$ . It's found that the porosity parameter  $\gamma$  delays the onset of electroconvection in the dielectric nanofluids for both studied cases (numerical and analytical). Hence, it has a stabilizing effect. This result shows that the space occupied by a dielectric nanofluid in a porous medium has an important role on the thermal stability of dielectric nanofluids.

From Fig.2 - Fig.6, we find generally that the critical thermal Rayleigh-Darcy number  $R_{ac}$  decreases with an increase in the value of the AC electric Rayleigh-Darcy number  $R_{ae}$ , this result can be explained by the increase in the electrostatic energy which allows to increase both the velocity of the dielectric nanofluid  $V$  and the vertical flux of nanoparticles  $J_z$  at the onset of electroconvection (Fig.5 and Fig.6), and hence the AC electric Rayleigh-Darcy number  $R_{ae}$  has a destabilizing effect for the dielectric nanofluids.

## V. CONCLUSION

In this paper, we have examined the simultaneous effect of rotation and a vertical AC electric field on the onset of electroconvection in a horizontal dielectric nanofluid layer saturated a Darcy porous medium. The analysis has been performed for zero flux nanoparticles condition at horizontal boundaries, such that these latter are taken as isothermal where  $T_h^* > T_c^*$ . The resulting eigenvalue problem is solved analytically and numerically using the Galerkin weighted residuals technique and the power series method, respectively. The behavior of various parameters like the Taylor - Darcy number  $T_A$ , the modified particle-density increment  $N_B$ , the Lewis number  $L_e$ , the nanoparticle Rayleigh - Darcy number  $R_N$ , the modified diffusivity ratio  $N_A$ , the porosity of the porous medium  $\gamma$  and the AC electric Rayleigh - Darcy number  $R_{ae}$  on the onset of electroconvection has been analysed and presented graphically.

The principal results derived from the present analysis can be summarized as follows:

- The increase in the porosity of the medium  $\gamma$  and the presence of the Coriolis forces allow to stabilize the dielectric nanofluids.
- The Lewis number  $L_e$ , the nanoparticle Rayleigh-Darcy number  $R_N$ , the modified diffusivity ratio  $N_A$  and the AC electric Rayleigh-Darcy number  $R_{ae}$  have a destabilizing effect on the stationary convection.

- The presence of an AC electric field allows to reduce the size of convection cells in the dielectric nanofluids.
- The modified particle-density increment  $N_B$  has no significant effect on the convective instability for the nanofluids. Hence, we can neglect the contribution of this parameter in the energy equation.
- The oscillatory convection has been ruled out in this problem.
- Qualitatively, there is a good agreement between the analytical and numerical method. Contrariwise, we find a difference in the results between these two methods when we treated the dielectric nanofluids with a zero nanoparticle flux on the horizontal boundaries, this difference will disappear when we consider the case of dielectric fluids.

## ACKNOWLEDGEMENTS

The authors wish to express their very sincerely thanks to the reviewers for their valuable and lucid comments which have improved the paper appreciably.

## REFERENCES

- [1] P.H. Roberts, Electrohydrodynamic convection, *Quarterly Journal of Mechanics and Applied Mathematics*, vol.22, pp.211-220, 1969.
- [2] M. Takashima, K.D. Aldridge, The stability of a horizontal layer of dielectric fluid under the simultaneous action of a vertical DC electric field and vertical temperature gradient, *Quarterly Journal of Mechanics and Applied Mathematics*, vol. 29, pp.71-87,1976.
- [3] Peter J. Stiles, Electro-thermal convection in dielectric liquids, *Chemical Physics Letters*, vol. 179, n. 3, pp.311-315, 1991.
- [4] Mohamed I.A Othman, Electrohydrodynamic stability in a horizontal viscoelastic fluid layer in the presence of a vertical temperature gradient, *International Journal of Engineering Science*, vol. 39, pp.1217-1232, 2001.
- [5] M. Takashima, The effect of rotation on electrohydrodynamic instability, *Can.J.Phys.* vol. 54, pp.342-347, 1976.
- [6] I. S. Shivakumara, N. Rudraiah, Jinho Lee, K. Hemalatha, The Onset of Darcy-Brinkman Electroconvection in a Dielectric Fluid Saturated Porous Layer, *Transp. Porous Med.*, vol. 90, pp.509-528, 2011.
- [7] I. S. Shivakumara, Chiu-On Ng, M.S. Nagashree, The onset of electrothermoconvection in a rotating Brinkman porous layer, *International Journal of Engineering Science*, vol. 49, n. 7, pp.646-663, 2011.
- [8] P.G.Siddheshwar, D.Radhakrishna, Linear and nonlinear electroconvection instability under AC electric field, *Communications in Nonlinear Science and Numerical Simulation*, vol. 17, pp.2883-2895, 2012.
- [9] F.Asadzadeh, M.Nasr Esfahany, N. Etesami, Natural convective heat transfer of Fe<sub>3</sub>O<sub>4</sub>/ethylene glycol nanofluid in electric field, *International Journal of Thermal Sciences*, vol. 62, pp. 114-119, 2012.
- [10] Dhananjay Yadav, Jinho Lee, Hyung Hee Cho, Electrothermal instability in a porous medium layer saturated by a dielectric nanofluid, *Journal of Applied Fluid Mechanics*, vol. 9, in press,2015.
- [11] Ramesh Chand, Electro-thermal convection in a Brinkman porous medium saturated by nanofluid, *Ain Shams Engineering Journal*, 2015. <http://dx.doi.org/10.1016/j.asej.2015.10.008>
- [12] J. Buongiorno, Convective transport in nanofluids, *Journal of Heat Transfer*, vol.128, pp.240-250, 2006.

- [13] D.Y. Tzou, Thermal instability of nanofluids in natural convection, *International Journal of Heat and Mass Transfer*, vol.51, pp.2967-2979, 2008.
- [14] D.Y. Tzou, Instability of nanofluids in natural convection, *ASME Journal of Heat Transfer*, 130, 2008, 372-401.
- [15] D.A. Nield and A.V. Kuznetsov, Thermal instability in a porous medium layer saturated by a nanofluid: a revised model, *International Journal of Heat and Mass Transfer*, vol.68, pp.211-214, 2014.
- [16] L.D.Landau, E.M. Lifshitz, *Electrodynamics of Continuous Media* (Pergamon Press, London, 1960).
- [17] I.S.Shivakumara, M.Akkanagamma, Chiu-On Ng, Electrohydrodynamic instability of a rotating couple stress dielectric fluid layer, *International Journal of Heat and Mass Transfer*, vol. 62, pp.761-771, 2013.
- [18] A.N.Borujerdi, A.R.Noghrehabadi, D.A.S. Rees, Influence of Darcy number on the onset of convection in a porous layer with a uniform heat source, *International Journal of Thermal Sciences*, vol. 47, pp.1020-1025, 2008.
- [19] I.S. Shivakumara, M. Dhananjaya and Chiu-On Ng, Thermal convective instability in an Oldroyd-B nanofluid saturated porous layer, *International Journal of Heat and Mass Transfer*, vol.84, pp.167-177, 2015.
- [20] A.Wakif , Z.Boualahia , R.Sehaqui , A Realistic Approach for Studying the Effect of an Internal Heat Source on the Onset of Convection in a Newtonian Nanofluid Layer: rigid-rigid case , *IOSR-Journal of Mathematics*,vol.11, pp.21-30, 2015.
- [21] A.Wakif, R.Sehaqui, A Realistic Study of the Rayleigh-Bénard Problem in the Newtonian Nanofluids with a Uniform Heat Source: Free-Free Case, *International journal of science and research*, vol.4, pp. 611-615, 2015.
- [22] A.Wakif , Z.Boualahia , R.Sehaqui, An accurate method to Study the Rayleigh-Bénard Problem in a Rotating Layer Saturated by a Newtonian Nanofluid , *International Journal of Innovation and Scientific Research*,vol.20,n.1, pp.25-37, 2016.
- [23] A. Wakif , Z. Boualahia , M. Zaydan , N.Yadil and R.Sehaqui , The Power Series Method to Solve a Magneto-Convection Problem in a Darcy-Brinkman Porous Medium Saturated by an Electrically Conducting Nanofluid Layer , *International Journal of Innovation and Applied Studies*,vol.14, n.4, pp.1048-1065,2016.
- [24] A.Wakif , Z.Boualahia , R.Sehaqui , Numerical Study of a Thermal Convection Induced by a Purely Internal Heating in a Rotating Medium Saturated by a Radiating Nanofluid, *International Journal of Computer Applications*,vol.135,n.10, pp.33-42, 2016.

# BRIQA: Framework for the Blind and Referenced Visual Image Quality Assessment

Jaime Moreno<sup>\*†</sup>, Oswaldo Morales<sup>\*</sup>, Ricardo Tejeida<sup>\*</sup>, Eduardo García<sup>†</sup>, and Yasser Sánchez<sup>†</sup>.

Escuela Superior de Ingeniería Mecánica y Eléctrica, Campus Zacatenco  
Instituto Politécnico Nacional  
07738, Mexico.

<sup>\*</sup>Research professors (Docente Investigador).

<sup>†</sup>Thesis students of degree level (Tesis de Nivel Licenciatura).

**Abstract**—Our proposal is to present a Blind and Referenced Image Quality Assessment or BRIQA. Thus, the main proposal of this paper is to propose an Interface, which contains not only a Full-Referenced Image Quality Assessment (IQA) but also a No-Referenced or Blind IQA applying perceptual concepts by means of Contrast Band-Pass Filtering (CBPF). Then, this proposal consists in contrast a degraded input image with the filtered versions of several distances by a CBPF, which computes some of the Human Visual System (HVS) variables. If BRIQA detects only one input, it performs a Blind Image Quality Assessment, on the contrary if BRIQA detects two inputs, it considers that a Referenced Image Quality Assessment will be computed. Thus, we first define a Full-Reference IQA and then a No-Reference IQA, which correlation is important when is contrasted with the psychophysical results performed by several observers. BRIQA weights the Peak Signal-to-Noise Ratio by using an algorithm that estimates some properties of the Human Visual System. Then, we compare BRIQA algorithm not only with the mainstream estimator in IQA, PSNR, but also state-of-the-art IQA algorithms, such as Structural SIMilarity (SSIM), Mean Structural SIMilarity (MSSIM), Visual Information Fidelity (VIF), etc. Our experiments show that the correlation of BRIQA correlated with PSNR is important, but this proposal does not need imperatively the reference image in order to estimate the quality of the recovered image.

**Keywords**—Image Quality Assessment; Contrast Band-Pass Filtering; Peak Signal-to-Noise Ratio.

## I. INTRODUCTION

The evolution of sophisticated Models and applications of Processing of Digital Images gives as a result of extensive literature describing these models. A significant number of this research is dedicated to Algorithms for improving only the image appearance. However, we consider that the digital image quality is distantly perfect. Images are presumably distorted during the whole process of compression or representation. Thus, it is important in the coding process of any image to improve image quality in order to identify and quantify the degree of degradation of a digital image.

Today, MSE or Mean Square Error is yet the most used quantitative metrics, since many other algorithms which evaluate image quality are based on it, Peak Signal-to-Noise Ratio (PSNR), for instance. Some authors as Wang and Bovik in [1], [2] mention that MSE is a poor assessment to be used in systems that predict image quality or fidelity. So, we want

to expose what is wrong regarding MSE estimations, in order to propose new algorithm that makes use of some properties of the human eye, also our proposal tries to maintain the best properties of the MSE.

By one hand, let us define  $f(i, j)$  and  $\hat{f}(i, j)$  as the couple of images compared, which size is the amount of pixels inside them. Being  $f(i, j)$  the original image, considered with best possible quality or fidelity, and  $\hat{f}(i, j)$  a possible degraded version of  $f(i, j)$ , whose quality we want to estimate. By the other hand, let us define the of the MSE and the PSNR in Equations 1 and 2, respectively.

$$MSE = \frac{1}{l \times m} \sum_{i=1}^l \sum_{j=1}^m [f(i, j) - \hat{f}(i, j)]^2 \quad (1)$$

and

$$PSNR = 10 \log_{10} \left( \frac{\alpha^2}{MSE} \right) \quad (2)$$

where  $\alpha$  is the high value in terms of intensity inside  $f(i, j)$ , size= $l \times m$ . Thus, for images witch contains only one channel, namely 8 bits per pixel (bpp)  $\alpha = 2^8 - 1 = 255$ . For chromatic images, Equation 2 also defines the estimation of PSNR, but for color images the MSE is separately computed of every component and then individual results are averaged.

Both MSE and PSNR are widely used in the field of image processing, as these algorithms have favorable features:

- 1) Convenient for the purpose of optimizing a certain algorithm that needs to improve quality. For instance in JPEG2000, MSE is employed both in *Optimal Rate Allocation Methodology* [3], [4] and *Region of Interest Algorithms*[5], [4]. Also, MSE is differentiable and integrable, so its employment could solve these kind of problems in terms of optimization, when it is use along with linear algebra, for instance.
- 2) By definition MSE compares the square difference of two images, giving as a result a clear meaning of leak of energy.

However, in some cases MSE estimates image quality with a low relation with quality given by an observer. A clear example is depicted by Figure 1, where both (a) *Baboon* and (b) *Splash* are coded and decoded by JPEG2000 compression

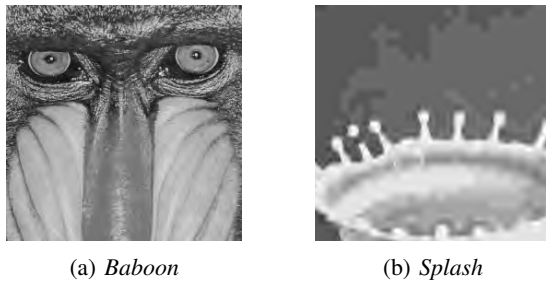


Figure 1: Patches with size= $256 \times 256$  of recovered images compressed by JPEG2000, PSNR=32dB.

with PSNR=32 dB. Figures 1(a) and 1(b) have very different visual quality. Then, either MSE or PSNR do not correlate with Human Visual System (HVS).

## II. DEFINITION OF IMAGE QUALITY ASSESSMENT

In this section we outline of IQA definition, thus, we divide the IQA algorithms in two: Referenced and Non-Referenced approaches, the latter is known as Blind IQA. Thus, Referenced IQA Metrics can be divided in Bottom-Up and Top-Down Approaches.

Bottom-up approaches for evaluating image quality are methods that try to simulate well modeled features of HVS, and integrate them into the design of algorithms quality evaluation, hopefully, perform similar to HVS in the evaluation of the image quality.

Moreover, the bottom-up attempt to simulate functional features in HVS that are important for the evaluation of image quality approaching. The main objective is to build algorithms that work alike HVS, at least for assessing of image quality evaluation.

On the contrary, the top-down systems simulate HVS differently. Top-down algorithms see HVS as a black box, and only the input-output task is cause for concern. A system for evaluating image quality from top to bottom can operate quite differently, since it predicts the behavior evaluation of image quality of an average human observer correctly.

An obvious task for the construction of a methodology of this type top-down approach is to formulate the problem of automatic supervised learning, as illustrated in Figure 2. Thus, HVS is blindly treated in order to learn its behavior. Training data is obtained through subjective experiments, where are viewed and evaluated by human subjects a large number of test images. The main objective is to model the system algorithm, so as to minimize the error between the desired output (subjective assessment) and the model prediction. This is generally a problem of regression or an approximation function.

By the other hand, No-reference or Blind image quality evaluation is a very difficult task in this field of image coding, but the conceptualization of the problem is very simple.

Somehow, an objective model should assess the quality of any real-world image, without reference to an original image. Thus, this looks like very difficult mission. The quality of an

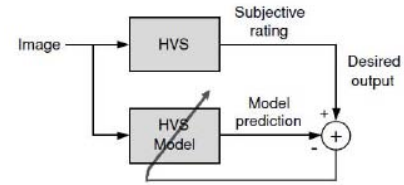


Figure 2: Learning Human Visual System.

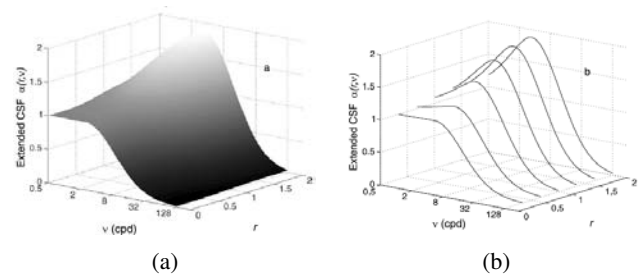


Figure 3: (a) Representation of the CSF ( $\beta_{s,o,i}(r, \nu)$ ) for Y channel of illuminate component.

image can be judged quantitatively without having an objective algorithm of what a good/poor image quality is supposed to be similar. Then, surprisingly, this is a fairly easy assignment for human observers. HVS can easily recognize images with high quality when they are contrasted with low-quality images, and also our eye can identify what of these two images is good or bad without watching the reference image. In addition, humans observers tend to agree with each other to a very high degree. Example of this behavior when the human eye assesses image quality without seeing the reference image, it is very probable that says that the image is noisy, fuzzy, or compressed by any image coder. In this way, Figure 1 shows an example of JPEG2000 compression, where the recovered images have lower quality than moved and stretched luminance contrast images.

## III. BRIQA ALGORITHM

### A. Contrast Band-Pass Filtering

The Contrast Band-Pass Filtering (CBPF) approximately estimates the image seen by a human observer with a  $\delta$  separation by filtering some frequencies which are important or irrelevant for HVS. So, first of all let us define  $f(i, j)$  as the mathematical representation of the reference image and  $\delta$  as the separation between observer and the screen. Then CBPF estimates a filtered image  $\check{f}(i, j)$ , when  $f(i, j)$  is seen from  $\delta$  centimeters. CBPF is founded on three main features: frequency of the pixel, spatial scales and surround filtering.

The CBPF methodology decomposes reference image  $f(i, j)$  into a set of wavelet planes  $\omega(s, o)$  of different spatial scales  $s$  (i.e., frequency of the pixel  $\nu$ ) and spatial scales as:

$$f(i, j) = \int_{s=1}^n \omega(s, o) + c_n \quad (3)$$



Figure 4: (a) Reference image *Lenna* . (b)-(d) Filtered images obtained by CBPF at three distances.

where  $n$  is the amount of wavelet decompositions,  $c_n$  is the plane in the pixel domain and  $o$  spatial scale either vertical, horizontal or diagonal.

The filtered image  $\check{f}(i, j)$  is recovered by scaling these  $\omega(s, o)$  wavelet coefficients employing *Contrast Band-Pass Filtering* function, which is at the same time an approximation Contrast Sensitivity Function(CSF, Figure 3). The CSF tries to approximate some psychophysical features [6], considering surround filtering information (denoted by  $r$ ), perceptual frequency denoted by  $\nu$ , which is the gain of frequency either positive or negative depending on  $\delta$ . Filtered image  $\check{f}(i, j)$  is defined by Equation 4.

$$\check{f}(i, j) = \int_{s=1}^n \beta(\nu, r) \omega(s, o) + c_n \quad (4)$$

where  $\beta(\nu, r)$  is the CBPF weighting function reproduce some properties of the HVS. The term  $\beta(\nu, r) \omega(s, o) \equiv \omega_{s,o,p,\delta}$  is the *filtered wavelet coefficients* of image  $f(i, j)$  when it is watch at  $\delta$  centimeters and is written as:

$$\beta(\nu, r) = z_{ctr} \cdot C_{\delta}(\dot{s}) + C_{min}(\dot{s}) \quad (5)$$

Figure 4 depicts some examples of filtered images of *Lenna*, estimated by Equation 4 for a 19 inch monitor in the diagonal and 1280 pixels in columns, at  $\delta = \{30, 100, 200\}$  cm.

## B. General Methodology

Algorithm 1 shows the main methodology of this work. Thus, BRIQA Algorithm estimates the referenced visual quality of the distorted image  $\hat{f}(i, j)$  regarding  $f(i, j)$  the original reference image, if it exists, otherwise BRIQA estimates a blind visual image quality. Both algorithms need the definition of the Observational Distance  $d$  given by the observer, so if  $d$  is not defined, we estimate the distance  $d$  from the actual observer by means of 3D/stereoscopic methodology, Algorithm 3.

---

### Algorithm 1: BRIQA: Framework to assess the quality of a digital image.

---

**Input:**  $f(i, j)$ ,  $\hat{f}(i, j)$ , and  $\delta$   
**Output:** *ImageQuality*

- 1 **if**  $d$  does not exist **then**
- 2      $d$ =Compute Observational Distance by means of 3D/stereoscopic approach  
    in Algorithm 3.
- 3 **if**  $f(i, j)$  exists **then**
- 4     ImageQuality = Algorithm 2( $f(i, j)$ ,  $\hat{f}(i, j)$ ,  $\delta$ ), Referenced-IQA
- 5 **else**
- 6     Estimate  $f(i, j)$  from a pattern of the same size of  $\hat{f}(i, j)$ , Figure 5
- 7     ImageQuality = Algorithm 2( $f(i, j)$ ,  $\hat{f}(i, j)$ ,  $\delta$ ), Blind-IQA

---

Then a Full-reference image quality metric is performed, there is an reference image  $f(i, j)$  and a recovered presumably distorted version  $\hat{f}(i, j) = \theta[f(i, j)]$  that is contrasted against  $f(i, j)$ . It is important to mention  $\theta$  is the algorithm that distorts the reference image and henceforth we refer the Full-reference image quality algorithm in BRIQA as RIQA. Otherwise, in the no-referenced image quality issue we refer BRIQA as BIQA. Furthermore, it is important to mention that BIQA only processes a degraded version of  $\hat{f}(i, j)$ . Thus from Figures 5(a) and 5(b), we compare  $\hat{f}(i, j)$  against a repetitive pattern  $\Upsilon([0,1;1,0])$ . Then, we perform the same algorithm in RIQA.

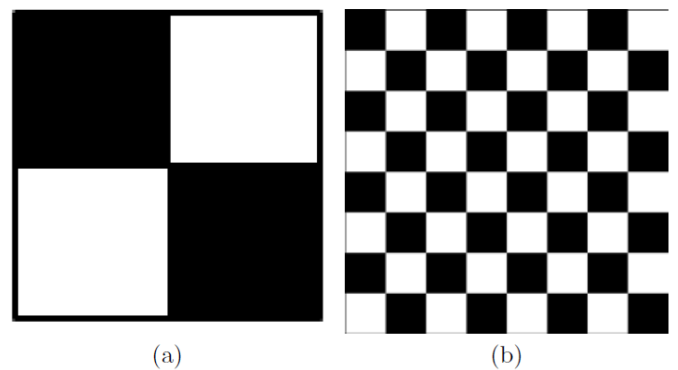


Figure 5: (a) Primary Pattern [0,1;1,0] or  $\Upsilon$ . (b) Sixteenth Pattern or  $\Upsilon^{16}$ .

Since both  $f(i, j)$  and  $\hat{f}(i, j)$  are observed at the same time at an observational distance  $\delta$ , if the similarity between  $f(i, j)$  and  $\hat{f}(i, j)$  appears to be better perceived is because  $\delta$  tends to 0. In contrast, if the observer judges  $f(i, j)$  and  $\hat{f}(i, j)$  when  $\delta$  tends to  $\infty$  the correlation between reference and distorted image would be the same. As any algorithm we

need to approximate the  $\delta = \infty$ , namely where similarity is so big that the observer confuse both images, we propose a no-linear regression for approximating  $\infty$  to  $\delta = \Delta$ .

Either Reference Assessment or Blind Assessment, our proposal is based on Algorithm 2.

---

**Algorithm 2:** Algorithm for estimating Visual Image Quality Assessment.

---

- Input:**  $f(i, j)$ ,  $\hat{f}(i, j)$ , and  $\delta$   
**Output:** *ImageQuality*
- 1 Direct Wavelet Transformation of images  $f(i, j)$  and  $\hat{f}(i, j)$
  - 2 Estimation of Distance  $\Delta$  (Equation 6), The distance where the observer cannot distinguish any difference in terms of quality between  $f(i, j)$  and  $\hat{f}(i, j)$
  - 3 Compute  $f_p(i, j)$  and  $\hat{f}_p(i, j)$ , namely, contrast band-pass filtered wavelet coefficients at a distance  $\Delta$ . Where  $\omega_{(s,o;\rho,\Delta)} = \text{CBPF}(f(i, j), \Delta)$  and  $\hat{\omega}_{(s,o;\rho,\Delta)} = \text{CBPF}(\hat{f}(i, j), \Delta)$
  - 4 Inverse Wavelet Transformation of  $\omega_{(s,o;\rho,\Delta)}$  and  $\hat{\omega}_{(s,o;\rho,\Delta)}$  obtaining the contrast band-pass filtered images  $f_p(i, j)$  and  $\hat{f}_p(i, j)$ , respectively.
  - 5 *ImageQuality* =PSNR between contrast band-pass filtered images  $f_p(i, j)$  and  $\hat{f}_p(i, j)$ .
- 

$n\mathcal{P}$  and  $\varepsilon m\mathcal{L}$  are two features involved in the evaluation of Distance  $\Delta$ . Equation 6 show the estimation of  $\Delta$ , besides these two parameters it is important to know or estimate also  $\delta$  in order to figure out the  $n\mathcal{P}$  and  $\varepsilon m\mathcal{L}$  distances. Furthermore Figure 6 depicts the Wavelet Energy Loss or  $\varepsilon\mathcal{R}$  (b), which shows not only the behavior of the relative energy but also the significance of  $\Delta$ ,  $n\mathcal{P}$  and  $\varepsilon m\mathcal{L}$  inside an  $\varepsilon\mathcal{R}$  chart (a).

$$D = n\mathcal{P} + \varepsilon m\mathcal{L} \quad (6)$$

Furthermore Figure 6(b) also show that the pinnacle inside the function is  $n\mathcal{P}$ , which is describe for the eye specialist as Near Point, which is between 15 to 20 centimeters for an adult. Thereby,  $n\mathcal{P}$  also can be defined as the distance where human eye can evaluate a pair of images  $f(i, j)$  and  $\hat{f}(i, j)$ . From this point  $n\mathcal{P}$ , fewer the differences are perceived by the observer, until these differences disappear in the  $\infty$ . We find  $\Delta$  by projecting the points  $(n\mathcal{P}, \varepsilon\mathcal{R}(n\mathcal{P}))$  and  $(d, \varepsilon\mathcal{R}(d))$  to  $(\Delta, 0)$ .

### C. Estimation of the Observational Distance $\delta$

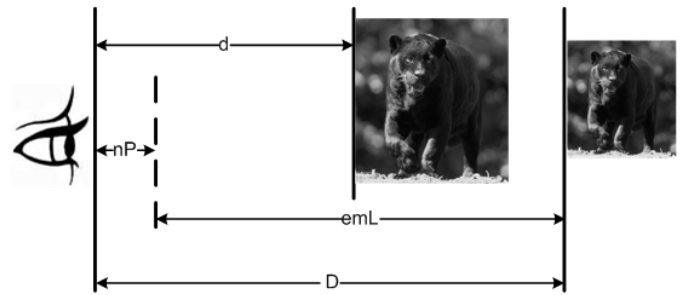
Estimation of the Observational Distance  $\delta$  is based on Algorithm 3, which divided in six steps and is described as follows:

*Step 1:* Camera calibration by means of Function *Stereo Calibration*. Calibration Results are stored in a structure, which is defined as *stereoParams*.

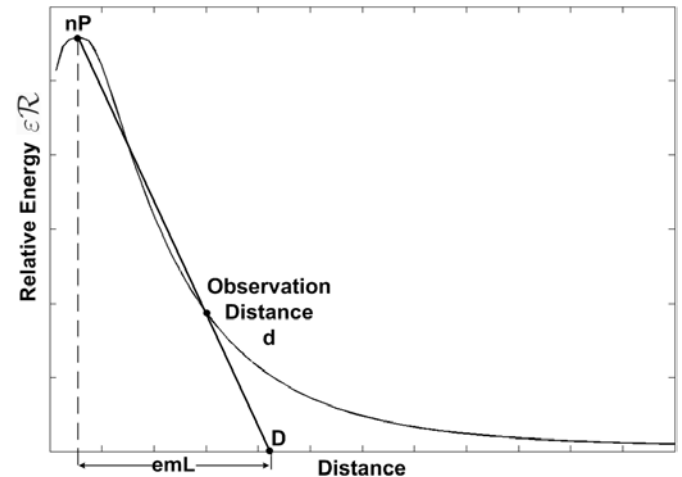
*Step 2:* Ones both left and right cameras are calibrated, we take two images  $I_l$  and  $I_r$ .

*Step 3:* With the parameters defined in *stereoParams*, we calibrate both  $I_l$  and  $I_r$  images using *undistortImage* function, giving as a result  $I_{c_l}$  and  $I_{c_r}$ .

*Step 4:* In both  $I_{c_l}$  and  $I_{c_r}$  images we estimate two human characteristics: face and eyes detection. This detection is made by means of the function *vision.CascadeObjectDetector*. If in both  $I_{c_l}$  and  $I_{c_r}$  images are detected faces, then we detect eyes. This procedure increases the probability to find the head of the observer in the stereo-pair.



(a) Portrayal of distances employed by the BRIQA algorithm.



(b)  $\varepsilon\mathcal{R}$  Chart.

Figure 6:  $D$ ,  $n\mathcal{P}$  and  $\varepsilon m\mathcal{L}$  depicted by (a) a graphical representation and (b) inside an  $\varepsilon\mathcal{R}$  Chart.

*Step 5:* We estimate the center of the heads located both in  $I_{c_l}$  and  $I_{c_r}$  images.

*Step 6:* Finally, we estimated the distance  $\delta$  in centimeters between cameras and the observer, using the function *triangulate*.

It is important to mention that all functions employed in this methodology are toolboxes of MatLab R2015a.

---

**Algorithm 3:** Estimation of the Observational Distance  $\delta$ .

---

- Input:** void  
**Output:**  $\delta$
- 1 Camera Calibration
  - 2 Taking stereo-pair  $I_l$  and  $I_r$
  - 3 Calibration of the stereo-pair,  $I_{c_l}$  and  $I_{c_r}$
  - 4 Head detection in the stereo-pair
  - 5 Center of detected Heads in original stereo-pair
  - 6 Estimation of distance  $\delta$  between cameras and the observer
- 

## IV. EXPERIMENTAL RESULTS

### A. Referenced Image Quality Assessment

MSE[7], PSNR[7], SSIM[8], MSSIM[9], VSNR[10], VIF[11], VIFP[8], UQI[12], IFC[13], NQM[14], WSNR[15] and SNR are compared against the performance of BRIQA

for JPEG2000 compression distortion. We chose for evaluating these assessments the implementation provided in [16], since it is based on the parameters proposed by the author of each indicator.

Table I shows the performance of RIQA and the other twelve image quality assessments across the set of images from TID2008, LIVE, CSIQ and IVC image databases employing Kendall Rank-Order Correlation Coefficient (KROCC) for testing the distortion produced by a JPEG2000 compression.

Table I: KROCC of BRIQA and other quality assessment algorithms on multiple image databases using JPEG2000 distortion. The higher the KROCC the more accurate image assessment. Bold and italicized entries represent the best and the second-best performers in the database, respectively. The last column shows the KROCC average of all image databases.

Metrics	Image Database				
	TID2008	LIVE	CSIQ	IVC	All
Images	100	228	150	50	528
IFC	0.7905	0.7936	0.7667	0.7788	0.7824
MSE	0.6382	0.8249	0.7708	0.7262	0.7400
MSSIM	0.8656	0.8818	0.8335	0.7821	0.8408
NQM	0.8034	0.8574	0.8242	0.6801	0.7913
PSNR	0.6382	0.8249	0.7708	0.7262	0.7400
SNR	0.5767	0.8055	0.7665	0.6538	0.7006
SSIM	0.8573	0.8597	0.7592	0.6916	0.7919
UQI	0.7415	0.7893	0.6995	0.6061	0.6602
VIF	0.8515	0.8590	0.8301	0.7903	0.8327
VIFP	0.8215	0.8547	0.8447	0.7229	0.8110
VSNR	0.8042	0.8472	0.7117	0.6949	0.7645
WSNR	0.8152	0.8402	0.8362	0.7656	0.8143
<b>RIQA</b>	<b>0.8718</b>	<b>0.8837</b>	<b>0.8682</b>	<b>0.7981</b>	<b>0.8555</b>

Thus, for JPEG2000 compression distortion, RIQA is getting the best results in all databases. RIQA correlates in 0.8837 for a database of 228 images of the LIVE database. On the average, RIQA algorithm is also correlates in 0.8555, using KROCC. Furthermore, JPEG2000 compression distortion, MSSIM is the second best indicator not only for TID2008, LIVE and IVC image databases but also on the average, since VIFP occupies second place for CSIQ image database. Thus, the correlation between the opinion of observers and the results of MSSIM is 0.0143 less than the ones of RIQA. So in general, we can conclude that PSNR can be improved its performance in 11.5% if it includes four steps of filtering, RIQA.

### B. Blind Image Quality Assessment

Some metrics estimate Quality as PSNR does, but some metrics estimates degradation, MSE, for instance. It is important to mention that BIQA estimates the degradation when this degradation tends to zero means that the overall quality is getting better. We already check the behavior of RIQA, so in this section we develop comparisons for verifying the performance BIQA by comparing significance performance of different compress versions of the image *Baboon*. BIQA is a metric that gives decibels as PSNR does, so instead of employing a Non-Parametric Correlation, we use a parametric correlation coefficient, i.e. Pearson correlation coefficient in order to better compare the results between BIQA and PSNR.

Figures 7(a), 7(b), and 7(c) depict three JPEG2000 compression of the image *Baboon* with 0.05, 0.50, and 1.00 bits per pixel, respectively. Thereby PSNR estimates 18.55dB for Figure 7(a), 23.05dB for Figure 7(b), and 25.11dB Figure 7(c). While BIQA computes 43.49, 30.07 and 28.71 dB, respectively. Thus for the 0.05 bpp (Figure 7(a)), higher distortion is estimated both PSNR and BIQA.

Figure 8) depicts multiple JPEG2000 decoded images from 0.05 bpp to 3.00bpp, the increments of varies every 0.05 bpp. With the later data we can found that PSNR and BIQA between them is 0.9695, namely, for image *Baboon* for every 1,000 tests BIQA estimates in a wrong way only 30 assessments.

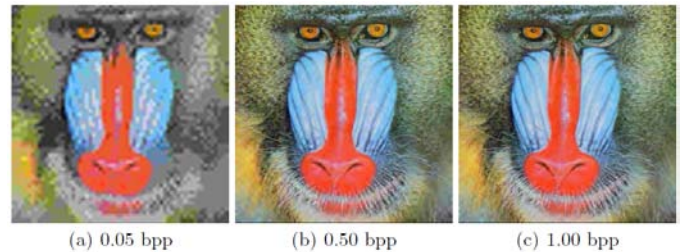


Figure 7: JPEG2000 Distorted versions of color image *Baboon* at different bit rates expressed in bits per pixel (bpp). (a) High Distortion, (b) Medium Distortion and (c) Low Distortion.

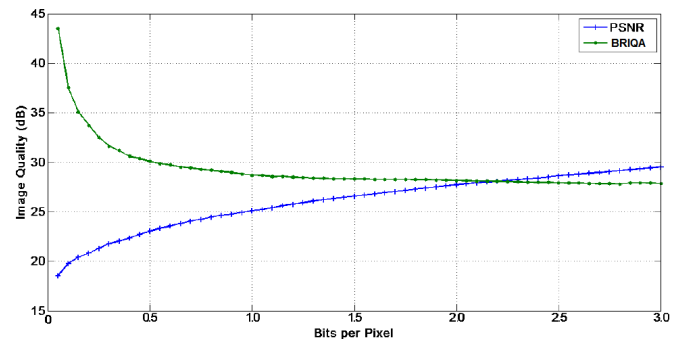
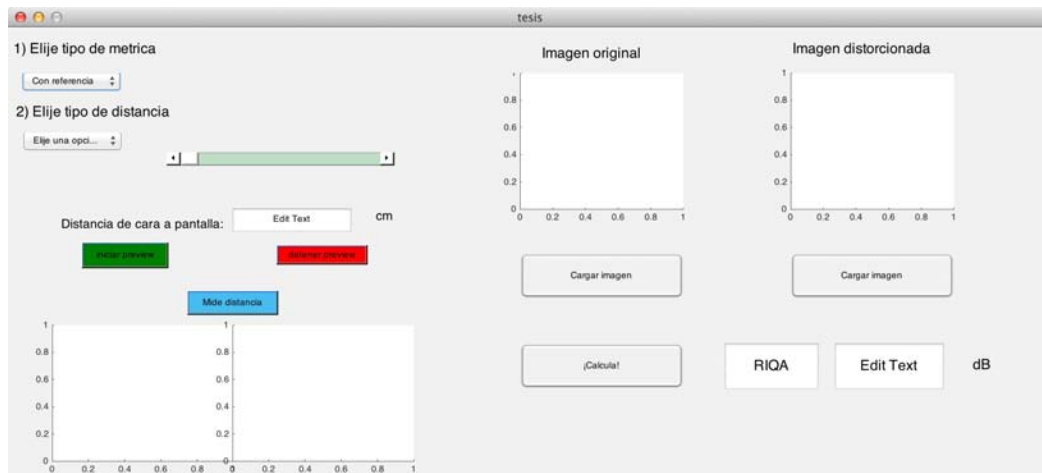


Figure 8: Comparison of PSNR and BRIQA for the JPEG2000 distorted versions of image *Baboon*.

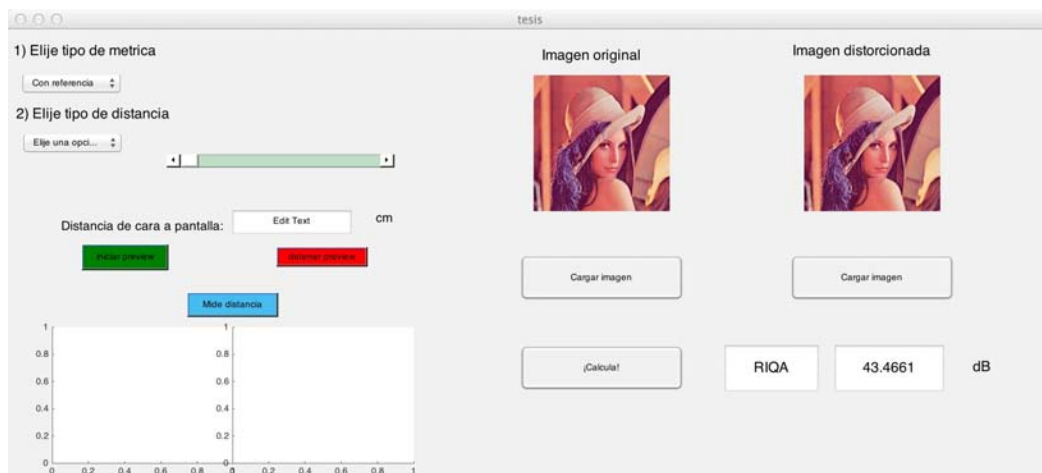
### C. BRIQA Interface

In Figure 9(a) the graphic interface is shown that allows upload pictures and calculate their quality by using methods with and without reference which are selectable via a drop-down menu. The observer can also select the type of distance  $\delta$  used the code which is the distance from the screen to the face of the observer.

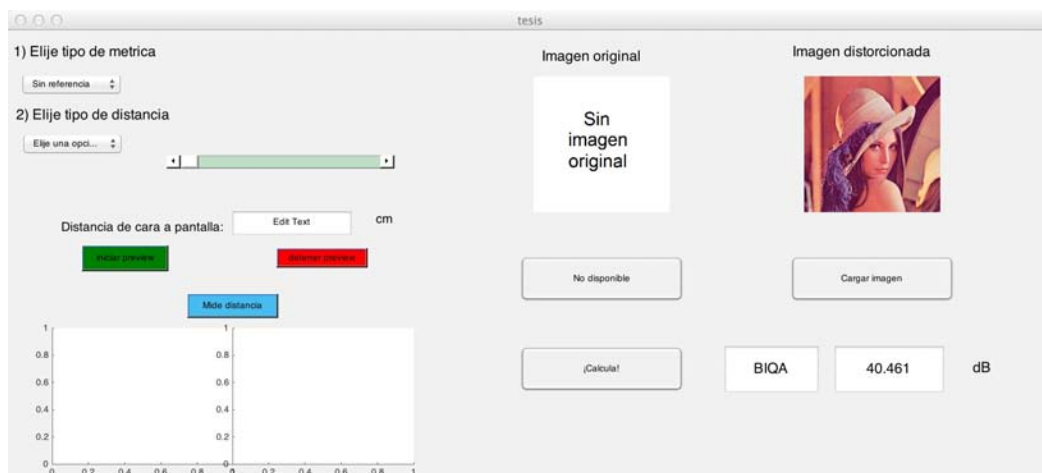
In the Figure 9(b), it shows that selecting the metric referenced by the drop-down menu, you can load the original images (without compression) and distorted (noisy) using the buttons to load image which display a window that lets you explore folders and select the image. Pressing the button Calculate the Legend RIQA method allowing the return a numeric result associated with the image quality is applied.



(a) BRIQA Graphic Interface



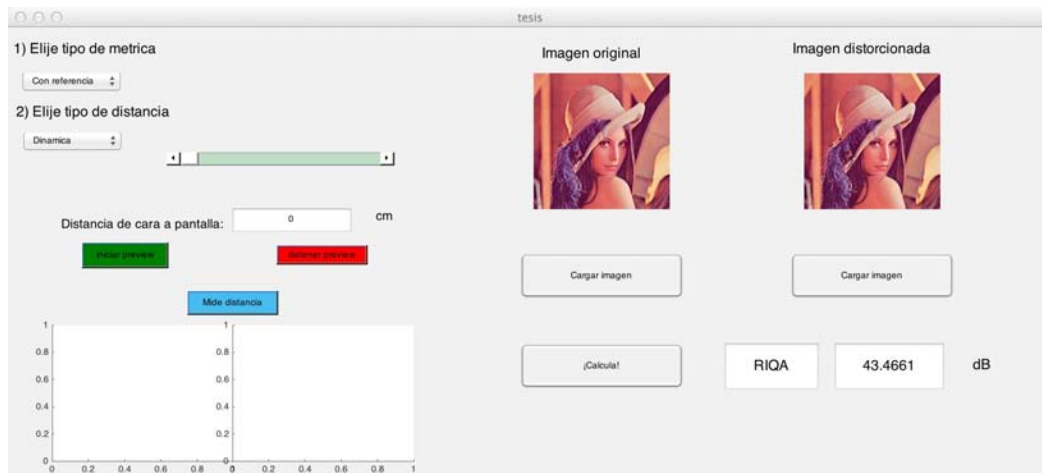
(b) Referenced Image Quality Assessment



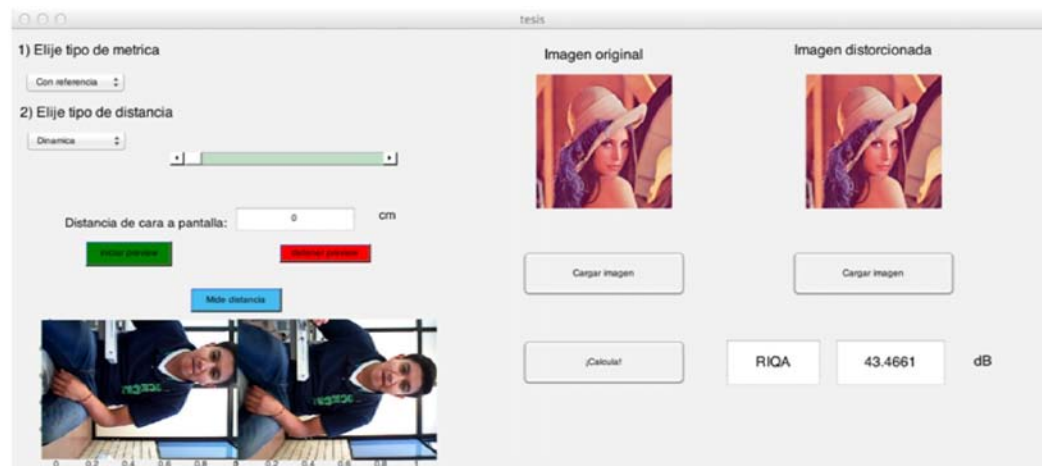
(c) Blind Image Quality Assessment

Figure 9: Estimation of distance: Static Distance

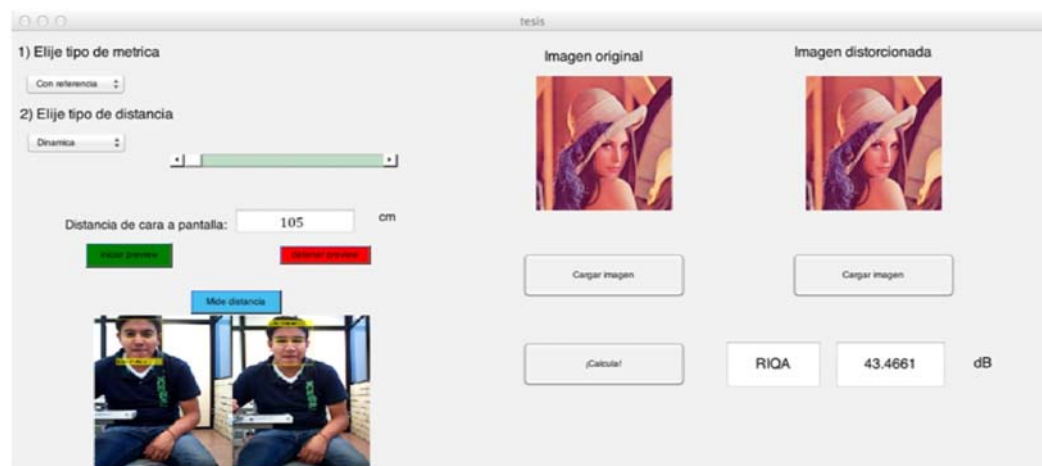
Figure 9(c) shows that selecting the metric without reference automatically displays a window with the caption: *No original image* and the button to load the original image now is disabled.



(a) Selecting the distance: Dynamic type



(b) Taking stereo-pair  $I(r, l)$ , i.e.  $I_r$  and  $I_l$  images



(c) Dynamic Estimation of Distance  $\delta$

Figure 10: Estimation of distance: Dynamic Distance.

By selecting the metric without reference *Calculate* button, the algorithm automatically switches to a method without reference to return a numeric value associated with the image

quality, namely BIQA.

When selecting the type of distance in static mode, it is possible to move the slider that lets you change the value

of the distance used in the algorithms metrics with and without reference. By selecting the distance of dynamic type green buttons (enabled *preview*), show preview (blue) stop preview (red) are enabled allowing handling. Otherwise slider is disabled, Figure 10(a).

When the *Preview button* is pressed stereo cameras transmit the images to the computer and it is displayed on the screen, Figure 10(b).

Thus, When *Measure distance button* is pressed, it takes an arrangement of pictures from stereo-cameras. With this arrangement our algorithm automatically tries to detect the face and eyes of the observer if BRIQA finds them it estimates the observational distance  $\delta$ , Figure 10(c).

## V. CONCLUSIONS AND FUTURE WORK

BRIQA is a metric divided in two algorithms full-reference (RIQA) and non-reference (BIQA) image quality assessments based on filtered weighting of PSNR by using a model that tries to simulate some features of the Human Visual System (CBPF model). Both proposed metrics in BRIQA are based on five steps.

When we compared RIQA Image Quality Assessment against several state-of-the-art metrics our experiments gave us as a result that RIQA was the best-ranked image quality algorithm in the well-know image databases such as TID2008, LIVE, CSIQ and IVC, JPEG2000 compression algorithm is used as a method of distorting the cited image databases. Thus, it is 2.5% and 1.5% better than the second best performing method, MSSIM. On average, RIQA improves the results of PSNR in 14% and 11.5% for MSE.

In the Blind Image Quality Assessment, BIQA assessment correlates almost perfect for JPEG2000 distortions, since difference between BIQA and PSNR, on the average is only 0.0187.

Combine both RIQA and BIQA in the same interface was the main contribution of this work. Thus, a expert or non-expert in the quality images assessment field can perform its own experiments. These experiments could include dynamic quality estimations or static ones. As a future work of this paper could be to include a set of quality images estimators including RIQA and BIQA.

## ACKNOWLEDGMENT

This work is supported by National Polytechnic Institute of Mexico (Instituto Politécnico Nacional, México) by means of Project No. SIP-20160786, the Academic Secretary and the Committee of Operation and Promotion of Academic Activities (COFAA) and National Council of Science and Technology of Mexico (CONACyT) by means of grant No. 204151/2013.

It is important to mention that Sections III and IV are part of the degree thesis supported by Eduardo García and Yasser Sánchez.

## REFERENCES

- [1] Z. Wang and A. Bovik, "Mean squared error: Love it or leave it? a new look at signal fidelity measures," *Signal Processing Magazine, IEEE*, vol. 26, no. 1, pp. 98–117, jan. 2009.
- [2] Z. Wang and A. C. Bovik, *Modern Image Quality Assessment*, 1st ed. Morgan & Claypool Publishers: Synthesis Lectures on Image, Video, & Multimedia Processing, February 2006.
- [3] F. Auli-Llinas and J. Serra-Sagrasta, "Low complexity JPEG2000 rate control through reverse subband scanning order and coding passes concatenation," *IEEE Signal Processing Letters*, vol. 14, no. 4, pp. 251–254, april 2007.
- [4] D. S. Taubman and M. W. Marcellin, *JPEG2000: Image Compression Fundamentals, Standards and Practice*, ser. ISBN: 0-7923-7519-X. Kluwer Academic Publishers, 2002.
- [5] J. Bartrina-Rapesta, F. Auli-Llinas, J. Serra-Sagrasta, and J. Monteagudo-Pereira, "JPEG2000 Arbitrary ROI coding through rate-distortion optimization techniques," in *Data Compression Conference*, 25-27 2008, pp. 292–301.
- [6] K. Mullen, "The contrast sensitivity of human color vision to red-green and blue-yellow chromatic gratings," *Journal of Physiology*, vol. 359, pp. 381–400, 1985.
- [7] Q. Huynh-Thu and M. Ghanbari, "Scope of validity of PSNR in image/video quality assessment," *Electronics Letters*, vol. 44, no. 13, pp. 800–801, 2008.
- [8] H. Sheikh and A. Bovik, "Image information and visual quality," *IEEE Transactions on Image Processing*, vol. 15, no. 2, pp. 430–444, feb. 2006.
- [9] Z. Wang, E. Simoncelli, and A. Bovik, "Multiscale structural similarity for image quality assessment," in *Conference Record of the Thirty-Seventh Asilomar Conference on Signals, Systems and Computers*, vol. 2, 2003, pp. 1398–1402 Vol.2.
- [10] D. Chandler and S. Hemami, "Vsnr: A wavelet-based visual signal-to-noise ratio for natural images," *IEEE Transactions on Image Processing*, vol. 16, no. 9, pp. 2284–2298, 2007.
- [11] Z. Wang, A. Bovik, H. Sheikh, and E. Simoncelli, "Image quality assessment: from error visibility to structural similarity," *IEEE Transactions on Image Processing*, vol. 13, no. 4, pp. 600–612, april 2004.
- [12] Z. Wang and A. Bovik, "A universal image quality index," *IEEE Signal Processing Letters*, vol. 9, pp. 81–84, 2002.
- [13] R. Sheikh, A. Bovik, and G. de Veciana, "An information fidelity criterion for image quality assessment using natural scene statistics," *IEEE Transactions on Image Processing*, vol. 14, pp. 2117–2128, 2005.
- [14] N. Damera-Venkata, T. Kite, W. Geisler, B. Evans, and A. Bovik, "Image quality assessment based on a degradation model," *IEEE Transactions on Image Processing*, vol. 9, pp. 636–650, 2000.
- [15] T. Mitsa and K. Varkur, "Evaluation of contrast sensitivity functions for formulation of quality measures incorporated in halftoning algorithms," *IEEE International Conference on Acoustics, Speech and Signal Processing*, vol. 5, pp. 301–304, 1993.
- [16] C. U. V. C. Laboratory. (2010) MeTriX MuX visual quality assessment package, available at [http://foulard.ece.cornell.edu/gaubatz/metrix\\_mux/](http://foulard.ece.cornell.edu/gaubatz/metrix_mux/). Cornell University Visual Communications Laboratory.

# Cohesion Based Personalized Community Recommendation System

Md Mamunur Rashid\*, Kazi Wasif Ahmed<sup>†</sup>, Hasan Mahmud<sup>‡</sup>, Md. Kamrul Hasan<sup>§</sup> and Husne Ara Rubaiyeat<sup>¶</sup>

Systems and Software Lab (SSL), Department of Computer Science and Engineering (CSE),  
Islamic University of Technology (IUT), Gazipur, Bangladesh

<sup>¶</sup>Department of Computer Science, Natural Science Faculty, National University, Bangladesh

**Abstract**—Our life is totally engaged by the progressive growth of online social networking. Because, millions of users are interconnecting with each other using different social media sites like Facebook, Twitter, LinkedIn, Google+, Pinterest, Instagram etc. Most of the social sites like Facebook, Google+ allow users to join different groups or communities where people can share their common interests and express opinions around a common cause, problem or activity. However, an information overloading issue has disturbed users as thousands of communities or groups are creating each day. To resolve this problem, we have presented a community or group recommendation system centered on cohesion where cohesion represents high degree of connectedness among users in social network. In this paper, we emphasis on suggesting useful communities (or groups in term of Facebook) that users personally attracted in to join; reducing the effort to find useful information based on cohesion. Our projected framework contains of the steps like: extracting sub-network from a social networking site (SNS), computing the impact of amity(both real-life or social and SNS connected), measuring user proclivity factor, calculating threshold from existing communities or groups of a user and lastly recommending community or group based on derived threshold. In result analysis part, we consider the precision-recall values by discarding community or group one at a time from the list of communities or groups of a certain user and checking whether the removed community or group is recommended by our proposed system. We have evaluated our system with 20 users and found 76%  $F_1$  accuracy measure.

**Keywords**—Social network, Community or Group recommendation, Cohesion, Amity factor, User Preferences or proclivity

## I. INTRODUCTION

With the advent of Web 2.0, social networking sites are becoming more widespread and interactive. Face-to-face, voice, email, video communications are traditional medium of interaction between friends, family and relatives [15]. Although, in online social network, two parties initiate communication without any common value between them. They can freely share their personal information with each other without any precondition [13]. In the virtual world, joining or creating communities or groups with common interests and becoming friends are simply clicking of a button [9]. Recommending useful communities or groups to a particular user is a challenge as it is dependent on a lot of factors. If a community or group is worthwhile to a user then the user might be interested to join that community or group. However, profiling user's personal interests is very difficult task as it is influenced by many factors or parameters. We offer a technique of recommending communities or groups based on

cohesion which is affiliated by collaborative ranking strategy. It works by determining correlation between communities or groups and user observing user preferences. The overlooked user preferences are inferred from the detected ones. The more cohesive group of community or group has higher linked strength measured in terms of three factors: amity factors, user proclivity rank, community preferences. We have defined these terms in our proposed recommendation system to suggest the user effective communities or groups to join rather than the irrelevant ones. An previous group of study in this field focused on recommending groups or communities or groups on basis of user profile contents or Homophily [21] (user similarity). However, they do not ponder over degree of interaction among users or combinational impact of various factors like user preference and amity impact. The major contributions of the paper are as follows:

- (1) We apply user proclivity factor to approximate user's personal interest over groups or communities or groups in social network.
- (2) We introduce friendliness or impact of SNS connected and real-life amity to construct users' social associations which greatly affect their choices in social sites. From the research activities [19] concentrating on personalized tweet recommendation, it is vividly noticeable that "including social relationship factors" escalates the correctness of recommendation.
- (3) Our model integrates content based statistics as user proclivity choice or factor, social connection and friendliness impact to appropriately ratify user behavior and personality. The investigational result displays refining community or group recommendation performance and the incorporation of all the factors creates an ultimate model dubbed as cohesion impressively outperforming several baseline approaches.
- (4) Our suggested recommendation system executes based on automatically derived threshold which is determined based on user profile and distinct factors. As the threshold value is not constant and differs from user to user according to defined factors it can effectively recommend relevant and useful communities or groups to user.

The remainder of this paper is structured as follows. Related work is discussed in Section 2. In section 3, we describe our proposed model for community or group recommendation. Experimental evaluations are presented in Section 4. Finally, we conclude this paper in Section 5. The initial research of this paper was published in the 18th International Conference

on Computer and Information Technology (ICCIT), Dhaka, Bangladesh, held on 21-23 December, 2015 [1].

## II. RELATED WORKS

In this chapter, we define the state-of-the-art of social networking terminologies and insights essential to perceive our suggested approach. Social Network Analysis has its origins in both social science and in the broader fields of network analysis and graph theory [21]. From the concept of online social networking, we emphasize on the importance of connectedness (cohesion) among social network users, community or group recommendation systems and their implications.

### A. Community Recommendation System

Community (i.e. Groups in term of Facebook) recommendation is proposing communities or groups for users they might like to join; however, not joined yet. There are some preceding research like anticipating communities or groups for user based on interaction in social networking site. Social graph is engendered on basis of social bonding of user in a social networking site [3]. Several works are motivated by bi-directional communication between users and activeness of friends in the community or group [5]. There are also some effort like recommending friends in social networking sites based on cohesion [2]. Some works endorse groups based on decision trees and feature extraction from user profile [13]. Certain recommendation systems use collaborative filtering methodology for recommending communities or groups [17]. However, current community or group detection techniques either depend on the content study or only cogitate the underlying configuration of the social network graph while detecting communities or groups. As a consequence, these methods fail to find pertinent communities or groups. In a nutshell, there are several limitations in contemporary techniques as follows:

In [3], [5] and [6], they did not ponder over personalization but only the friendliness strength to find communities or groups for a user to connect. User affinity to particular type of community or group was overlooked and the used parameters for calculation were not appropriate enough to validate user behavior. User proclivity rank is the summation of resemblance among list of communities or groups that user has already joined and the groups to join. In our work we consider user's social relation termed as amity factor which is degree of interaction between user and his friends and user proclivity rank. Our experimental results show that it provides better user experience recommending related community or group for individual.

### B. Limitation of present Approach

- 1) In the first two research works, only the amity factor is used for recommending communities or groups for a user; however, the user proclivity is unnoticed.
- 2) Collaborative approach for community or group detection is suitable to some extent but doesn't consider the amity strength. Therefore, the collaborative approach lacks intuition in judging rational behavior of user.
- 3) The constraints used are not suitable enough to ratify users ordinary behavior. In our work, we are considering both amity and users sense of proclivity. We believe that it provides better user experience recommending associated community or group for

individual. Business perspective behind our work is to successfully recommend community or group for a user where it is also possible to identify user's taste and to recommend business products for the user.

## III. PROPOSED APPROACH

In the preceding chapter, we have comprehensively discussed about the prevailing community or group recommendation systems. After evaluating those, we also attempt to prepare a new system for advising communities or groups. In this section, we describe our proposed algorithm based on cohesion.

### A. Cohesion in Social Community

Cohesion is an abstract term that is straightforward to comprehend by intuition but unexpectedly tough to delineate in exact definition. Offhandedly, cohesion is the quantity of all the factors that generates interest in people to join or to be part of a group. [2]. In Social Networking, Cohesion is defined as a connected network and it is considered that network with high degree of connectedness is more cohesive [12]. Cohesion is an essential part of community or group and it is presumed that cohesion would have the same influence on social networking. It is expected that similar individuals interact greatly, at least more often than with divergent people. So, the impact of the cohesion cannot be overlooked in social network and it an effective term to recommend groups or communities or groups for an individual in social networking sites. Our proposed methodology is outlined on the basis of cohesion which is affected by collaborative ranking approach assimilating user's social bonding and activeness in the network. One significant supposition underlying collaborative ranking is that users who accorded in the past are expected to agree again in the future [20]. This assumption allows us to consider past user preferences and forecast communities or groups they might join by checking similar users. In personalized community or group recommendation we can have assumption like below: Assume a user's propensity to join communities or groups depends on user's taste or proclivity and it is impacted by social bonding and correlations. For example, User might be attracted towards particular class of groups or communities providing informative records about different eatery locations and reviews on diverse food items. Therefore, a restaurant related group or community can be a worthy recommendation for that user which is inclined to his own proclivity factor as well as the total number of his/her friends in the same community or group. Amity is an imperative issue here as because user's friends review will be more trustworthy or interesting for him rather than considering review of some unknown individuals. So, user proclivity rank and social connections have great influence on personalized community or group recommendation. In this paper, the cohesiveness or the connectedness among users is recognized on the basis of interaction where we measure amity factor based on carefully chosen parameters. We joined the user proclivity rank with the connectedness among users which attract individual to join a community or group communally termed as cohesion.

### B. Framework of proposed approach

We have outlined a framework of community or group recommendation system centered on cohesion consisting of six functional steps.

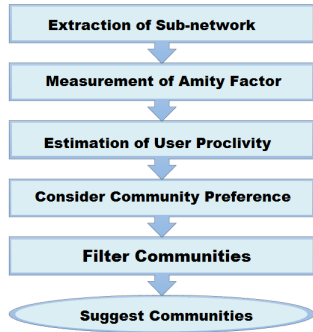


Fig. 1: Outline of Community Recommendation System

### C. Detailed explanation of proposed system

An essential property of social networks is that people tend to have attributes similar to those of their friends. There are two underlying reasons. Firstly, the process of social influence leads people to embrace behaviors exhibited by those they interact with; this effect at work in many settings where new ideas are diffused by word-of-mouth or imitation through a network of people. A second, distinct reason is that people tend to form relationships with others who are already alike to them [8]. This phenomenon, which is often called selection, has a long history of study in sociology. These factors are utilized by us as because they show a vital role defining amity, bonding or strength, which is obligatory for community or group finding. We are also keeping track of homologous communities or groups as user is already member termed as user proclivity. These factors together provide vivid idea about an individual's mentality and the kind of community or group he/she prefer to join in term of cohesion in this paper.

1) *Extraction of sub-network*: For the experimental purpose of our proposed system, we take network of a random individual. We collect the available data for our defined factors for a target user.

2) *Measurement of amity factor*: Amity Factor specifies the numerical quantity of strength of amity between two nodes (friends). In social network, a user has both SNS connected and real-life or social friends. Both types of relationships are significant for assessing amity strength. We compute both SNS connected and social amity factor and they are dubbed as *Amity* rank or strength *Fr*. Considering two users  $t$  and  $t_1$ , the measurement of amity is dependent on the factors as defined below:

$$Amity\ Fr(t, t_1) = \frac{SNSAmity_{factor}(t, t_1)}{2} + \frac{SocialAmity_{factor}(t, t_1)}{2} \quad (1)$$

a) *Measuring SNS amity factors*: We approximate the connectivity strength among the SNS connected friends on the basis of amity factors as declared previously. To find the degree of strength between two nodes  $T$  and  $t_1$ , the factors are defined below:

$$SNSAmity_{factor}(t, t_1) = \frac{\sum_{i=1}^n F_n(t, t_1)}{n} \quad (2)$$

Where,  $n$  = number of factors for computing SNS amity strength, To identify the amity factors, a survey [18] was performed which ascertained the parameters having impact on

TABLE I: Parameters to calculate SNS connected amity

Factors	Formula
$F_1(t, t_1)$	Number of mutual friends of $t$ and $t_1$ / Total friends of $t$
$F_2(t, t_1)$	Number of applications used by both $t$ and $t_1$ / Total number of applications used by $t$
$F_3(t, t_1)$	Number of photos tagged in common between $t$ and $t_1$ / Total photos of $t$
$F_4(t, t_1)$	Number of post on each others wall / Total post by $t$
$F_5(t, t_1)$	Number of common events of $t$ and $t_1$ / Total number of events by $t$
$F_6(t, t_1)$	Number of messages between $t$ and $t_1$ / Total number of messages by $t$
$F_7(t, t_1)$	Number of common likes between $t$ and $t_1$ / Total number of likes by $t$
$F_8(t, t_1)$	Number of common communities or groups between $t$ and $t_1$ / Total number of communities or groups by $t$

social relationship. We define eight factors to measure SNS amity strength as shown below on the basis of observation and intuition. Therefore,  $SNSAmity_{factor}(t, t_1)$  between users  $t$  and  $t_1$  can be defined as,  $SNSAmity_{factor}(t, t_1) =$

$$\frac{F_1 + F_2 + F_3 + F_4 + F_5 + F_6 + F_7 + F_8}{8}$$

b) *Measuring social amity factors*: There exist specific class of friends who do not have much online mutual interactions among them in cyber space via social networking sites. However, they belong to common background like same school, college, or same work place, which can be considered as real-life or social friends. To measure the strength between two users  $t$  and  $t_1$ , the factors are defined below:

$$SocialAmity_{factor}(t, t_1) = \frac{\sum_{j=1}^m P_m(t, t_1)}{m} \quad (3)$$

Where,  $m$  = Number of parameters or factors for calculating social amity;  $P_m(t, t_1)$  = Parameter value of  $m$  for link from  $t$  to  $t_1$  Accordingly,

$P_1(t, t_1)$  = Number of common educational institutions for  $t$  and  $t_1$  / Total number educational institutes of  $t$ .

$P_2(t, t_1)$  = Number of common workplaces for  $t$  and  $t_1$  / Total number of workplaces for  $t$ .

We make an assumption for evaluating social amity. Users who have common background or environment tends to have akin interest or mentality. Those users are termed as real-life or social friends who share the defined common factors and also friends in Facebook. Educational background means from where and what school someone came from. Basically it refers all the schools that someone has been. Generally persons with such common backgrounds can be called as old friends.

$$SocialAmity_{factor}(t, t_1) = \frac{P_1(t, t_1) + P_2(t, t_1)}{2}$$

Combining  $SNSAmity_{factor}(t, t_1)$  and  $SocialAmity_{factor}(t, t_1)$  we can get the  $amityFr(t, t_1)$  which is termed as *Amity Factor* indicating the connectedness between two friends. Maximum value of amity  $Fr(t, t_1)$  is 1.

3) *Measurement of user proclivity rank*: Certain user activities passively redirect users judgments of the usefulness [19]. Assume a user's extra contribution to particular type of communities or groups which reflects their personal judgment of informativeness and efficacy. The user proclivity rank is computed on the basis of user attraction to the certain sort of community or group. All the communities or groups are

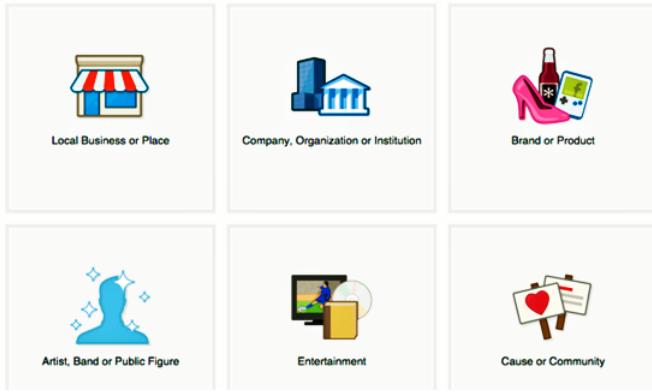


Fig. 2: Types of communities or groups (or groups) in Facebook

TABLE II: Division of user communities or groups into clusters

Cluster no.	1st	2nd	3rd	4th	5th	6th
Number of Community	11	5	9	4	7	2

classified into six categories: local business, organization or institution, Brand or product, public figure, entertainment and cause based on intuitive observation in Facebook social network as below figure. The user proclivity rank for a particular community or group is calculated in terms of category of the community or group and number of user community or group present in that category which determines the user preference to that category of community or group. For example: Select a community or group and detect if the community or group belongs to any cluster. User factor of a group for a target user can be defined as: *User Proclivity Rank* ( $U_n$ ) =

$$\frac{\text{Number of Communities in the cluster of selected group}}{\text{Summation of communities or groups of target user}} \quad (4)$$

Suppose, the user belongs to 38 communities or groups which are divided into 6 classes or clusters shown in Table 2. If the community or group to be recommended is  $C_3$  and it is belonged to cluster no. 3 then User Proclivity Rank ( $U_3$ ) =

$$\frac{\text{Number of communities or groups in 3rd cluster/cluster no. 3}}{\text{Total number of communities or groups of target user}} = \frac{9}{38} = .237$$

4) *Measurement of community preference*: Suppose, we want to recommend communities or groups for a user  $t_x$ .  $t$  is assumed to be the set of users including user  $t_x$  and his/her friends. Accordingly,  $C$  is the list of communities or groups of which the user  $t_x$  and his/her friends are members. We make an adjacency matrix to represent the belongingness of  $t$  to communities or groups  $C$  which is defined as  $A$ . Therefore,

$$T = \{t_x \text{ and his / her friends}\} \subseteq \text{All groups in social network}$$

$$C = \{\text{Communities where the user } t_x \text{ and his / her friends belong}\} \subseteq \text{All the communities or groups in social network}$$

Visually we can present this relationship in a bipartite graph  $K_{t,C}$ . For user  $t_x$ , where  $t_0$  is the target user having friends

$$A_{t_x} = A_{i,j} = \begin{matrix} & C_0 & C_1 & \cdots & C_j \\ \begin{matrix} t_0 \\ t_1 \\ \vdots \\ t_i \end{matrix} & \begin{pmatrix} a_{0,0} & a_{0,1} & \cdots & a_{0,j} \\ a_{1,0} & a_{1,1} & \cdots & a_{1,j} \\ \vdots & \vdots & \ddots & \vdots \\ a_{i,0} & a_{i,1} & \cdots & a_{i,j} \end{pmatrix} \end{matrix}$$

Fig. 3: Adjacency matrix of user to community or group relationship

$$A_{t_0} = \begin{matrix} & C_0 & C_1 & C_2 & C_3 \\ \begin{matrix} t_0 \\ t_1 \\ t_2 \\ t_3 \\ t_4 \end{matrix} & \begin{pmatrix} 1 & 1 & 1 & 0 \\ 0 & 1 & 0 & 1 \\ 0 & 0 & 1 & 0 \\ 0 & 0 & 0 & 1 \\ 1 & 0 & 0 & 1 \end{pmatrix} \end{matrix}$$

Fig. 4: Finding out possible communities or groups for recommendation

$$A_{t_0} = \begin{matrix} & C_0 & C_1 & C_2 & C_3 \\ \begin{matrix} t_0 \\ t_1 \\ t_2 \\ t_3 \\ t_4 \end{matrix} & \begin{pmatrix} 0 & Fr(t_0, t_1) & 0 & Fr(t_0, t_1) \\ 0 & 0 & Fr(t_0, t_2) & 0 \\ 0 & 0 & 0 & Fr(t_0, t_3) \\ Fr(t_0, t_4) & 0 & 0 & Fr(t_0, t_4) \end{pmatrix} \end{matrix}$$

Fig. 5: Calculation of weight factor ( $C_3$ )

$t_1 \dots t_i$ . So the total no. of friends of  $t_0$  is  $i$ . And,  $C_0 \dots C_n$  are collection of communities or groups of which the target user  $t_0$  and his/her friends  $t_1 \dots t_m$  are members. the corresponding adjacent matrix can be illustrated below: Here,

$$a_{i,j} = \begin{cases} 1, & \text{if } t_i \text{ is a member of } C_j \\ 0, & \text{otherwise} \end{cases}$$

For a user  $t_x$ , the recommendable set of communities or groups is the set of communities or groups that user  $t_x$  does not belongs. In effective community or group recommendation system, a subset of these communities or groups should be recommended. Following figure depicts the possible recommendable set community or group is  $\{C_3\}$  for user  $t_0$ . Following step is to calculate the community preference ( $Cf_n$ ) of a community or group  $n$ . Firstly, we determine weight factor ( $W_n$ ) derived from the amity factors of all the users belonging to a particular community or group  $C_n$  and multiply it with the User Proclivity Rank ( $U_n$ ). We replace the elements of  $A_x$  with corresponding amity factor  $Fr(t_x, t_i)$  where  $a_{i,j} = 1$ . As we are recommending for user  $t_x$ , row of that user is omitted from  $A_x$ . Following figure explains the above operation for community or group  $C_3$ .

$$\text{Weight factor } W_n = \sum_{\forall y \neq x \in T} Fr(t_x, t_y) \times A_{y,n} \quad (5)$$

So the *Weight factor* of community or group  $C_3$  could be

$$W_3 = Fr(t_0, t_1) + Fr(t_0, t_3) + Fr(t_0, t_4)$$

Combining the weight factor and user proclivity rank, community preference is calculated for each community or group. The equation for community preference of a particular community or group  $C_n$  is given below:

$$Community\ Preference\ (Cf_n) = User\ Proclivity\ Rank\ (U_n) \times Weight\ factor\ (W_n) \quad (6)$$

If Community Preference ( $Cf_n$ ) is greater than the  $Threshold_x$  (calculated for the user  $t_x$ ) then this community or group is to be processed for further filtering. Threshold can be found by summing up the community preference of present communities or groups of user and then divide it by total number of present communities or groups.

$$Threshold_x = \frac{\sum_{i=0}^n CommunityPreference(Cf_i)}{n} \quad (7)$$

Here, Community Preference ( $Cf_i$ ) are the Community Preferences of present communities or groups of user  $t_x$  and  $n$  is the total number of communities or groups of user  $t_x$ . As we can see, the value of the threshold varies for user to user is automatically determined.

5) *Filter and Suggest Communities*: After performing the all steps of our proposed method and filtering based on gender and location, a list of community or group for user is generated. Then finally, we recommend the communities or groups to the user.

#### D. Challenges

There are some challenges we have to face during our research like:

- 1) Attempting to second-guess a mysterious, perverse and profoundly human form of behavior: the personal response to a work of art is a challenge task for a recommendation system.
- 2) There are some limitations for determining the factor of amity strength as there are so many things to consider and recommending community or group for a new user will be the most challenging task.
- 3) The major problem in collecting the Facebook data was privacy concerns. At the same time, the format of the Facebook data was the most congenial to our research method. So, we have collected our data using roster method within a small network of user in Facebook.
- 4) Our proposed model doesn't solve the fresh start problem. So, user must be member of at least one community or group and user should have some friends because we recommending based on cohesion and user preference.
- 5) If the target user has no friend or friends do not belong to any community or group then our recommended system fails to calculate the threshold value.

### IV. EXPERIMENTAL EVALUATION

#### A. Dataset

There is no API to get user's profile information from Facebook without authorization because of privacy concerns. At the same time, the format of Facebook data is the more congenial to our research. We collected 200 users' data based on their permission and listed the required factors as sample in our database for experimental evaluation. Using the data

TABLE III: Profile Information of user  $t$

Total Friends	976
Total Apps use	28
Total photos	470
Total posts	212
Total messages	12203
Total events	68
Total Likes	218
Total Communities	38
Total educational institutions	3
Total work place	2

TABLE IV: SNS amity related information of target user  $t$

amity	$t_1 - t_2$	$t_1 - t_3$	$t_1 - t_3$	$t_1 - t_4$
Mutual Friends	37	22	48	10
Common Apps use	6	10	12	2
Common photos	54	28	66	18
Common posts	31	10	28	8
Common messages	1030	2203	1240	860
Common events	8	12	09	3
Common likes	33	28	36	18
Common communities or groups	6	8	6	3

TABLE V: Social amity connection information of target user  $t$

Amity connection	$t_1 - t_2$	$t_1 - t_3$	$t_1 - t_3$	$t_1 - t_4$
Common educational institutions	2	1	0	1
Common work place	1	0	1	0

TABLE VI: User proclivity information of target user  $t$

Community Type	Number of communities or groups
Local business	11
Organization/Institutions	5
Brand or product	9
Entertainment	4
Public Figure	7
Cause based	2

sets we calculate list of possible communities or groups for recommendation using our proposed approach. Below tables display sample data sets for a Facebook target user  $t$ .

Using the data sets we calculate list of possible communities or groups for recommendation using our proposed approach.

#### B. Evaluation Metrics

We corroborate our idea on small network in Facebook. List of present community or group of user is considered. Then a number of communities or groups from the present list of user is eliminated and checked if the community or group is suggested using our offered model. The result is ratified in terms of precision, recall and final score. As we are not using any global threshold value. The value of threshold changes based on users present community or group list according to user proclivity rank and amity factor.

*Precision* is the ratio of the number of relevant records retrieved to the total number of irrelevant and relevant records retrieved. It is usually expressed as a percentage.

*Recall* is the ratio of the number of relevant records retrieved to the total number of relevant records in the database. It is generally expressed as a percentage.

$F_1$  score(also F-score or F-measure) is a measure of a test's

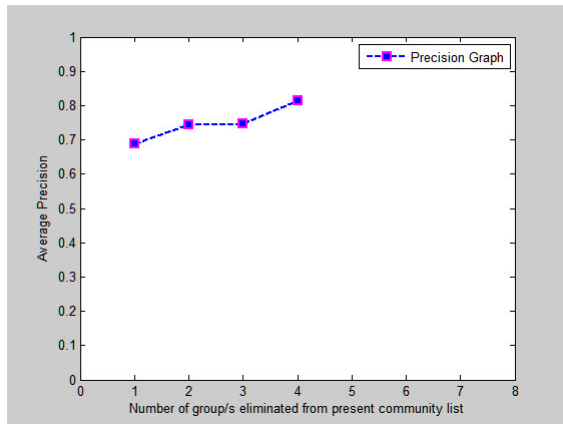


Fig. 6: Average precision graph eliminating half of the communities or groups

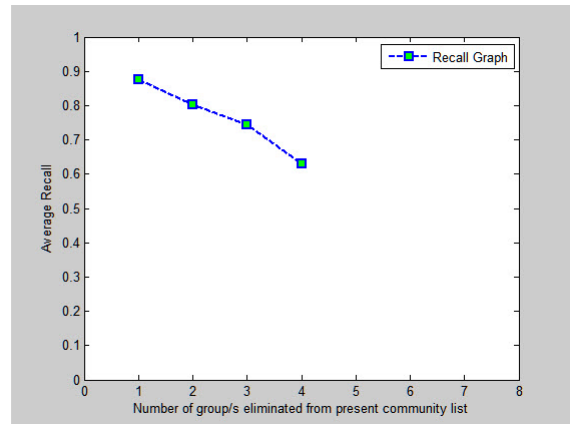


Fig. 7: Average recall graph eliminating half of the communities or groups

accuracy. It considers both the precision and recall of the test to compute the score.

$$F_1 = 2 \times \frac{\text{precision} \times \text{recall}}{\text{precision} + \text{recall}} \quad (8)$$

Firstly, we take one target user and eliminate one random community or group from his/her existing communities or groups and calculate the precision and recall. Then we estimate the average of that and then we eliminate any two communities or groups from his/her community or group list randomly and calculate the mean or average of precision and recall. We do the similar execution until we delete half of the existing communities or groups from the user. Because removing more than half of present community or group from the list increases the possibilities of incorrect suggestion as enough information is already lost. Let us illustrate an example regarding the estimation of precision and recall for better perception. Our target user has 8 communities or groups in his/her present community or group list. We can remove maximum 4 communities or groups from the list to check our recommendation system can identify the relevant communities or groups or not. Following table is displayed as reference. From the table, average precision = 0.7486 and average recall = 0.7629. In our case, present communities or groups in the

table[!t]

TABLE VII: Calculation of precision and recall by eliminating user communities or groups

No. of communities or groups eliminated	Precision	Recall
1	0.6876	0.8750
2	0.7442	0.8036
3	0.7473	0.7440
4	0.8154	0.6289

present community or group list are the relevant (true) records for the user. The newly recommended communities or groups from the universal set which were absent in the present community or group list would be considered as irrelevant record. Suppose, 3 communities or groups are selected from the present community or group list at random and removed. As a consequence, our recommendation system recommended 5 communities or groups in which 3 communities or groups

are newly recommended (previously not existed in the list) and the last 2 communities or groups are from the removed three (which are considered to be relevant records for user). Here, records retrieved = relevant record retrieved (A) + irrelevant records retrieved (C) = 2 + 3

$$\text{Hence, Precision} = \frac{2}{2+3} \times 100\%$$

On the other hand, *RECALL* is the ratio of the number of relevant records retrieved to the total number of relevant records in the database. Here, the number of relevant record = relevant record retrieved (A) + relevant records not retrieved (B) = 2 + 1

$$\text{Hence, Recall} = \frac{2}{2+1} \times 100\%$$

Finally, we calculated  $F_1$  score from the precision and recall value that we got from our experiment to measure the accuracy of our proposed approach.

### C. Method Comparison

Our works key contribution is to plan and formulate an efficient personalized community or group recommendation system. We compare the proposed model with the prevailing ones intuitively. To the best of our knowledge, we are the first to experiment on real data sets of Facebook users to recommend communities or groups on Facebook using defined parameters. For a target of 20 users, our proposed model successfully recommends correct communities or groups with around 76% of  $F_1$  measure accuracy. The average  $F_1$  score graph for 20 target users is displayed in the following figure. The prevailing approaches do not cogitate the combination of content features which is termed as user preference in our approach and social relationship factors. It is clearly visible from the work of Chen at [19], consideration of social relationship factors increase the accuracy of recommendation to a great extent. Our cohesion based approach considers both the factors of user preference and social relationship providing better recommendation of communities or groups.

The existing approaches using social graph generation in [5], [6] do not give any idea about accuracy of recommendation. Our proposed approach out performs methods proposed in [15] based feature selection strategy by better 3% of accuracy. From

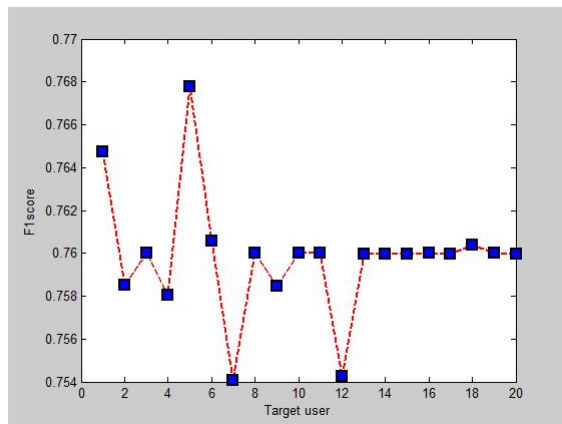


Fig. 8: Average  $F_1$  score graph for 20 target user

the above results, we conclude that our proposed approach gives better recommendation performance based on cohesion.

## V. CONCLUSION

Apposite groups or communities are suggested by an efficacious community or group recommendation system to a particular user so that user feels confident enough to join those suggested communities or groups. However, it involves special concern as the psychology of human being fluctuates from person to person in terms of collaboration and interactions. In this paper, we attempt to estimate these bonding and corroboration by defining several parameters to determine most cohesive community or group to be suggested. Our proposed community or group recommendation system is based on user proclivity and also user actives, liveliness or interaction in social networking sites.

This research will assist users to become a member of group or community of their own interest. However, still, there are some boundaries for determining the parameters of amity strength as there are so many things to cogitate and recommending community or group for a new user (a fresh user who has no information in internet). The foremost difficulty while accumulating the Facebook data is privacy concerns. At the same time, the format of the Facebook data is the most congenial to our research necessity. So, we have to collect our data using roster method within a small network of user in Facebook. Our proposed model does not resolve the fresh start problem. So, user must be member of at least one community or group and user should have some friends because we are recommending based on cohesion and user proclivity.

## REFERENCES

[1] K. W. Ahmed, M. M. Rashid, M. K. Hasan, and H. Mahmud, "Cohesion based personalized community recommendation system." IEEE,

2015. [Online]. Available: [http://ieeexplore.ieee.org/xpl/articleDetails.jsp?tp=&arnumber=7488038&url=http%3A%2F%2Fieeexplore.ieee.org%2Fxppls%2Fabs\\_all.jsp%3Farnumber%3D7488038](http://ieeexplore.ieee.org/xpl/articleDetails.jsp?tp=&arnumber=7488038&url=http%3A%2F%2Fieeexplore.ieee.org%2Fxppls%2Fabs_all.jsp%3Farnumber%3D7488038)

[2] M. N. Hamid, A. Naser, M. K. Hasan, and H. Mahmud, "A cohesion based friend recommendation system," *Springer Journal, Social networking and Mining*, Feb. 2014.

[3] S. Kadge and G. Bhatia, "Graph based forecasting for social networking site," *International Conference on Communication, Information and Computing Technology (ICCICT), India*, Oct. 2012.

[4] B. Krulwich and C. Burkey, "Learning user information interests through the extraction of semantically significant phrases," Mar. 1996.

[5] M. Safaei, M. Sahan, and M. Ilkan, "Social graph generation and forecasting using social network mining." 33rd Annual IEEE International Computer Software and Applications Conference, 2009.

[6] N. Silva, I. R. Tsang, G. Cavalcanti, and I. J. Tsang, "A graph-based friend recommendation system using genetic algorithm," Jul. 2010.

[7] J. Yang, J. McAuley, and J. Leskovec, "Community detection in networks with node attributes," 2013.

[8] D. Crandall, D. Cosley, D. Huttenlocher, and J. Kleinberg, "Feedback effects between similarity and social influence in online communities," 2008.

[9] Wellman, Boase, and Chen, "The networked nature of community," *ITandSociety*, 2002.

[10] G. Adomavicius and A. Tuzhilin, "Towards the next generation of recommender systems: A survey of the state-of-the-art and possible extensions," *Journal IEEE Transactions on Knowledge and Data Engineering archive*, 2005.

[11] C. K. John Breese, David Heckerman, "Empirical analysis of predictive algorithms for collaborative filtering," 1998.

[12] Chin and Chignell, "Automatic detection of cohesive subgroups within social hypertext: A heuristic approach," *New Review of Hypermedia and Multimedia*, 2008.

[13] J. M. Vitak, "Facebook friends: How online identities impact offline relationships, a thesis submitted to the faculty of the graduate school of arts and sciences of georgetown university in partial fulfillment of the requirements for the degree of master of arts in communication," *Culture and Technology*, 2008.

[14] P. Melville, R. J. Mooney, and R. Nagarajan, "Content-boosted collaborative filtering for improved recommendations," 2002.

[15] *Group Recommendation system for Facebook. On the Move to Meaningful Internet Systems: OTM 2008 Workshops Lecture Notes in Computer Science*, 2008.

[16] Gartrell, Xing, and Qin, "Enhancing group recommendation by incorporating social relationship interactions."

[17] W. Y. Chen, D. Zhang, and E. Chang, "Combinational collaborative filtering for personalized community recommendation."

[18] E. carolinllins, "Success factors of online social networks."

[19] K. Chen, T. Chen, and G. Zheng, "Collaborative personalized tweet recommendation," *SIGIR*, 2012.

[20] Resnick, Iacovau, and Suchak, "An open architecture for collaborative filtering of newnews."

[21] D. G. Cheliotis, "Social network analysis (sna) including a tutorial on concepts and methods."

# Face Recognition in Uncontrolled Environment

Radhey Shyam and Yogendra Narain Singh

Department of Computer Science & Engineering  
Institute of Engineering and Technology  
Lucknow - 226 021, India

**Abstract**—This paper presents a novel method of facial image representation for face recognition in uncontrolled environment. It is named as augmented local binary patterns (A-LBP) that works on both, uniform and non-uniform patterns. It replaces the central non-uniform pattern with a majority value of the neighbouring uniform patterns obtained after processing all neighbouring non-uniform patterns. These patterns are finally combined with the neighbouring uniform patterns, in order to extract discriminatory information from the local descriptors. The experimental results indicate the vitality of the proposed method on particular face datasets, where the images are prone to extreme variations of illumination.

**Keywords**—Face recognition, A-LBP, descriptor, distance metrics, area under curve, decidability index

## I. INTRODUCTION

Face recognition is one of the popular biological characteristic that is universally accepted for personal identification. In order to automate face recognition process, the biometric researchers have devised numerous methods [1]–[4]. Typically, a face recognition system consists of facial image acquisition and its processing, that includes image normalization, face detection and their alignment, data representation for extraction of relevant features. Extracted facial features finally classify the facial images of the individuals. The automated process of face image is shown in Figure 1.

The applications of automatic face recognition are diverse, in a variety of civil spheres ranging from public checking systems to stringent border crossing. In these domain of applications, the face recognition challenges are partially addressed. The face recognition methods that are performing strictly in controlled environments are principal component analysis [1], linear discriminant analysis [2], Fisherfaces [3], independent component analysis [5], and many more. In some other application areas including visual inspection, remote sensing, biometrics and motion analysis, the environments are not controlled. Therefore, there is a need to devise an efficient method that is correctly recognising the individuals from their uncontrolled facial images.

In literature, the methods that work in uncontrolled environments are mainly based on texture representations. The local features-based and multi-biometric based frameworks for the face recognition have achieved much greater attention in the biometric field [7]–[9]. The local features-based and multi-biometric based frameworks are less sensitive to variations, such as pose and illumination than the traditional techniques. In uncontrolled environments, the local binary pattern (LBP) is one of the most popular approaches for face recognition. The intention behind using the LBP operator for facial image

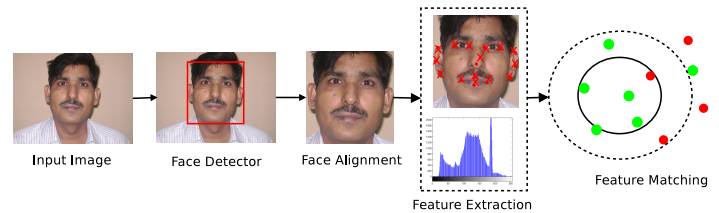


Fig. 1. Example of a typical face recognition system [6].

representation is that: (i) The faces can be visualised as a composition of various micro-patterns and (ii) Because of its insensitiveness to variations of pose and illumination too. The final description of a face image is obtained by combining these micro-patterns [10].

The major challenges of LBP approaches are insensitiveness to monotonic transformation of gray-scale, while they are still susceptible by the variation of illumination that generate the non-monotonic gray-scale changes. LBP may not work properly on the areas of the constant gray-levels because of the thresholding schemes of the operator [11].

The remainder of the paper is structured as follows: Section II describes the review works. Section III describes the technique of facial image representation for face recognition framework. Section IV presents the experimental setup requires for computation. Evaluation of the proposed method and their comparison with LBP method are presented in Section V. Finally, the conclusions are outlined in the last Section.

## II. REVIEW WORKS

### A. Frameworks of Local Binary Patterns

Ojala *et al.* have introduced LBP operator for the study of texture of gray-scale images. It is an efficient technique for texture representation [4]. It was encouraged by Ahonen *et al.* in recognition of human faces [11], [12]. The intention behind using the LBP operator for facial description is that the faces can be considered as a composition of the various micro-patterns. And, it is also found that the LBP is insensitive to the variation of (e.g., small changes of illumination and rotation). The description of the facial image is obtained by combining these micro-patterns [6].

A LBP operator which labels the pixels of an image with decimal numbers and also encodes the local structure around each pixels as illustrated in Figure 2. Each pixel is compared with its eight neighbours in a  $3 \times 3$  neighbourhood by subtracting the central pixel's value as a threshold. The

resulting non-negative values are encoded with 1 and the others with 0, as mentioned in Equation (1). A binary number is obtained by concatenating all these binary codes in a clockwise direction starting from the top-left corner and placed from left to right. Its decimal value is then computed, and used for the labelling perspective. The derived binary numbers are called LBP. The working framework of LBP operator is illustrated as follows:

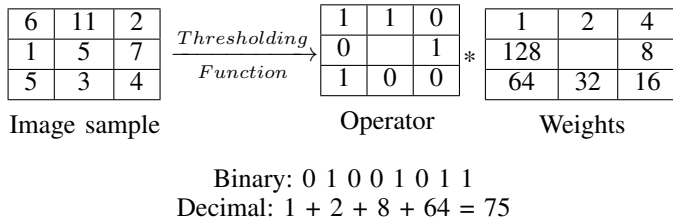


Fig. 2. Basic principles of LBP operator.

$$LBP_{(P,R)} = \sum_{p=0}^{p-1} s(g_p - g_c) 2^p, s(z) = \begin{cases} 1, & z \geq 0 \\ 0, & z < 0 \end{cases} \quad (1)$$

where  $P$  runs over 8 neighbours of the central pixel and  $R$  is the radius of the neighbourhood,  $g_c$  and  $g_p$  are the gray values of the central pixel and its neighbour pixels, the function  $s(z)$  is defined as thresholding function. After the LBP pattern of each pixel is identified, a histogram is computed to represent the texture image:

$$H(k) = \sum_{i=0}^I \sum_{j=0}^J f(LBP_{P,R}(i, j), k), k \in [0, K], \quad (2)$$

$$f(x, y) = \begin{cases} 1, & x = y \\ 0, & \text{otherwise} \end{cases}$$

where  $K$  is the maximal LBP pattern. The value  $U$  of a LBP pattern is defined as the number of spatial transitions in a pattern

$$U(LBP_{P,R}) = |z(g_{p-1} - g_c) - z(g_0 - g_c)| + \sum_{p=1}^{p-1} |z(g_p - g_c) - z(g_{p-1} - g_c)| \quad (3)$$

A pattern is called uniform pattern, if it has at most two bit wise transitions from 0 to 1 or vice-versa when traversed circularly. For instance, strings 00000000 (0 transition), 11000011 (2 transitions) and 11000001 (2 transitions) are uniform patterns, whereas the strings 10100001 (4 transitions) and 01010100 (6 transitions) are non-uniform patterns. Ojala *et al.* observed that the only 90% patterns are viable from the entire patterns when traversed in (8, 1) neighbourhood, whereas 70% are viable in the (16, 2) neighbourhood [11]. Therefore, some of the information is lost by assigning all non-uniform patterns to a single bin in histogram computation. Since, there is only 58 patterns that are uniform among 256 possible patterns of size 8-bits each. This leads towards space saving while computing the LBP histograms, e.g., there are total  $p(p - 1) + 2$  uniform patterns for  $p$  bits of sampling point. A final histogram is computed by concatenating all these sub

histograms that to be compared with the template histograms thereafter.

### B. Variants of Local Binary patterns

In order to improve the performance of a LBP operator in the sphere of uncontrolled environments, the numerous LBP variants have been proposed in the literature are as follows: Zhang *et al.* proposed multi-block LBP that uses the mean pixel value of the image block to replace the other pixel values and that are finally used in creation of LBP operator [13]. Hong and Wang computed Hamming distance based LBP for noise reduction from the facial images [14]. Shu and Shing, developed an elongated LBP that considered the elliptical sampling for capturing anisotropic structures of the facial images [15]. Ahonen and Pietikäinen developed two fuzzy membership functions rather than a single threshold to achieve the robustness in local descriptors i.e., soft local binary patterns [16]. The combination of information that is received from LBP and Gabor methods has been proposed by Tan and Triggs to improve the performance [17]. In addition to that, the local ternary patterns (LTP) was initiated by Tan and Triggs, to strengthen the insignificant information [18]. LTP requires a parameter called a threshold constant, which defines a tolerance for similarity between different gray-levels allowing robustness to noise. However, LTP and LBP representations are still limited because of its non variable quantization.

Wolf *et al.* developed the three-patch LBP approach that obtained by comparing the values of the three patches resulting a single bit value in the code assigned to each pixels. Furthermore, the four-patch LBP has also been suggested to compare two center symmetric patches in the inner ring with two other center symmetric patches presented in the outer ring [19]. Liao *et al.* proposed dominant LBP (DLBP) which makes use of the most frequently occurred patterns of LBP to improve the recognition results. In addition to that, the Gabor-based features is used to supplement to the features of the DLBP [20]. Heikkila *et al.* proposed center-symmetric local binary pattern that replaces the gradient operator which is based on fusion of strengths of SIFT and LBP operators [21]. Werghi *et al.* has proposed a framework called mesh-LBP that is used to extract local binary patterns from a 2D mesh-manifold [22]. They utilize advantages of mesh-LBP for the task of 3D texture classification of triangular-mesh surfaces collected from public datasets [23]. Their results have shown an improved performance over LBP.

Some of the above approaches have focused on how to make accountable the non uniform patterns for facial representations up to certain extent. Therefore, it inspires us to visualise on the non-uniform patterns too. The article concern is to make them accountable (transformed form of non uniform patterns) and combined with the existing uniform patterns thereafter, so that the discerning information can be extracted from image texture. This effort may contribute a significant role in texture classification. In order to improve performance towards uncontrolled environments, the paper proposes a new approach for facial image representations.

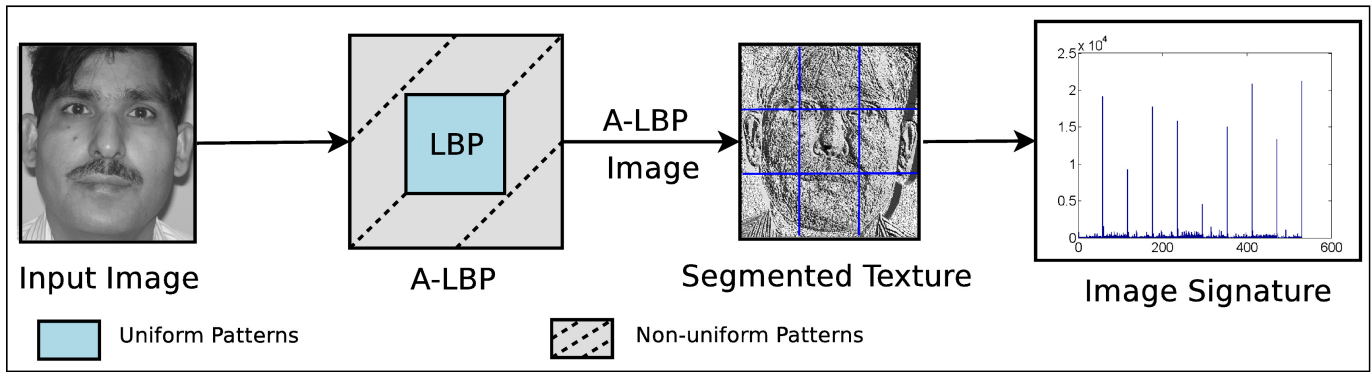


Fig. 3. A typical schematic diagram of A-LBP face recognition system.

### III. FRAMEWORKS OF AUGMENTED LOCAL BINARY PATTERNS

This section proposes a novel method of face recognition under variable conditions is called augmented local binary patterns (A-LBP). Earlier works on LBP method have not much focused on the utilization of non-uniform patterns. Some work already have treated them as an unwanted information that are discarded during the texture representation whereas very few work used them in integration with uniform patterns as a separate bin [11], [12]. The proposed approach considers the non-uniform patterns along with uniform patterns and extract the discriminatory information available to them. Thus, they prove their usefulness in distinguishing the facial patterns. The non-uniform patterns are used in combination with the neighbouring uniform patterns and extract the discriminatory information from the local descriptors. A typical schematic diagram of a proposed A-LBP face recognition method is illustrated in Figure 3.

The proposed approach uses a segment-based texture to compute the histogram that results a image signature. More formally, it replaces all non-uniform patterns with the majority value of neighbouring uniform patterns instead of putting non-uniform patterns into 59<sup>th</sup> bin as in LBP. To do this, a kernel of size  $3 \times 3$  is taken and moved on the entire image (e.g., a kernel of  $3 \times 3$  consists a set of 9-elements and can be represented as  $p = \{p_c, p_0, p_1, p_2, p_3, p_4, p_5, p_6, p_7\}$ , where  $p_c$  represents the intensity value of the central pixel and  $p_i (0 \leq i \leq 7)$  represents the intensity value of the neighbouring pixels). In this process, the central pixel value, ( $p_c$ ) is replaced with a majority value (i.e.,  $m = majority(p_i)$ ) of a set in case of non-uniformity (i.e.,  $p_c \notin U$ ) of central pixel. This set contains 8-closet neighbours of the central pixel, wherein all non-uniform patterns are replaced with a value of 255 i.e.,  $p_i = 255$ . Here, 255 is a highest uniform value. Working framework of the proposed approach is illustrated as in Algorithm.

The look-up table containing decimal values of 8-bit uniform patterns are  $U = \{0, 1, 2, 3, 4, 6, 7, 8, 12, 14, 15, 16, 24, 28, 30, 31, 32, 48, 56, 60, 62, 63, 64, 96, 112, 120, 124, 126, 127, 128, 129, 131, 135, 143, 159, 191, 192, 193, 195, 199, 207, 223, 224, 225, 227, 231, 239, 240, 241, 243, 247, 248, 249, 251, 252, 253, 254, 255\}$  [24]. The uniformity and non-uniformity of the patterns are verified from constructed look-up table which contains only a set of uniform patterns. During computations it has been found that, there are only 58

uniform patterns out of 256 patterns in 8-bit image. The values of uniform patterns in look-up table are computed, harnessing the stated principle's of the uniformity and the non-uniformity patterns (as described in Section II-A). The filtering process of non-uniform pattern to uniform pattern used in the proposed approach is demonstrated in Figure 4.

**Algorithm** : Computing steps of the A-LBP approach

**Input:** Original image

**Filtering procedure:**

- 1) Check the uniformity of the central pixel's value  $p_c$ .
- 2) If  $p_c$  is uniform, then go to step 1 with next  $p_c$ .
- 3) Otherwise, construct a set  $N_8$  containing 8-closet neighbours of  $p_c$ .
- 4) Replace all non-uniform patterns in  $N_8$  with a uniform pattern, i.e., 255.
- 5) Assign majority value of  $N_8$  to  $p_c$ .

**Output:** Augmented local binary patterns (A-LBP) based image texture

#### A. Complexity Analysis

For analysing the complexity of the proposed method, an image is of size  $n \times n$  and the kernel size is  $m \times m$ . There are  $k$  distinct elements that has to be compared  $\{1, 2, \dots, k\}$  e.g., in this case the value of  $k$  is 58. Since, it has to processed each and every pixel of the image as a central pixel of the kernel, hence total number of comparisons is  $n \times n$  i.e.,  $n^2$ . The complexity has been analysed in two different ways: (a) If the central pixel value matches to any value of look-up table, then it is  $k.n^2.O(1)$ , where  $O(1)$  time is required to compare the central pixel,  $k$ , the total no of times comparison happens for an element and  $n^2$ , the total no of elements. Thus, time complexity of A-LBP method in best case is  $O(k.n^2)$ . (b) If central pixel does not find any match with the values of the look-up table, then the following operations are taken place: (i) Process the remaining  $(m^2 - 1)$  elements by matching them with the  $k$  elements. Thus, time requires =  $O(m^2 - 1).k$ , (ii) For finding the maximum occurrence in the  $(m^2 - 1)$  elements, time requires =  $O(m^2 - 1)$ , and (iii) Now, replace the element with maximum occurrence with the central pixel, the time requires =  $O(1)$ . Thus, time required in worst case by A-LBP method which is  $[O(1).k + O(m^2 - 1).k + O(m^2 - 1) + O(1)]n^2$

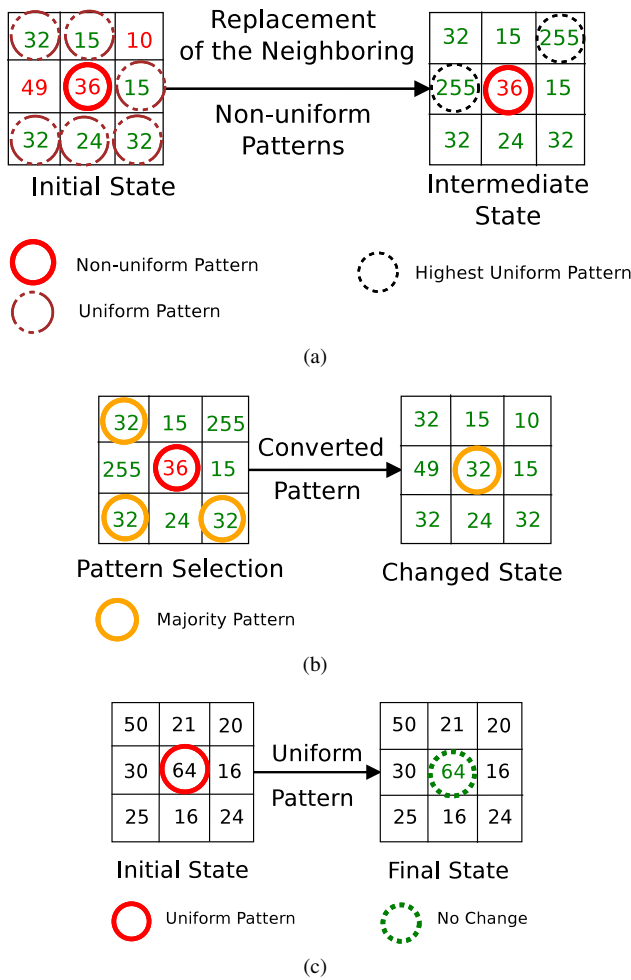


Fig. 4. (a) Neighbouring non-uniform patterns are replaced with highest uniform pattern i.e., 255, (b) Central non-uniform pattern 36 is replaced with majority value of 32, and (c) The next central pattern 64 is found to be uniform, so, it remains unchanged.

$\Rightarrow O(km^2.n^2)$ . If  $m \ll n$ , then worst case time can be reduced to best case time i.e.,  $O(kn^2)$ .

Similarly, space requirement of the proposed method is given as follows: (i) Space requires for storing  $k$  elements is  $O(k)$ , (ii) Space requires for storing the  $n \times n$  image,  $O(n^2)$ , (iii) Space requires for storing the kernel size of  $m \times m$ ,  $O(m^2)$ , and (iv) The space requires to store  $[0, 255]$  value of gray-scale image is  $O(256) = O(1)$ . Therefore, total worst case space complexity of A-LBP method is  $O(k + n^2 + m^2)$ .

#### IV. EXPERIMENTAL SETUP

##### A. Face Datasets

This section briefs the characteristics of the challenging face datasets used in this experiment. Different face datasets available publicly are used for testing of LBP and the proposed face recognition (A-LBP) methods. These face datasets are, AT & T-ORL (ORL) [25], extended Yale B (EYB) [26], Yale A (YA) [27], and Labeled Faces in the Wild (LFW) [28]. The concern of selecting these face datasets is to test the robustness of the proposed method for recognizing individuals on the presence of the different variations in the dimensions e.g.,

pose (p), illumination (i), facial expression (e), eye glasses and occlusion (o), in their facial images. A total of 3435 images are used to recognize 133 distinct individuals from these face datasets. During processing, image samples of each face datasets are down sized by some heuristic to reduced the computational complexity. The new sample size is represented in Table I. The system is trained for each face datasets separately, whereas the test image is selected randomly from the sample set of each individual, and then the performance is measured.

##### B. Performance Measures

In this experiment, the paper computes the performance of the identification systems using following metrics that include—decidability index, receiver operating characteristic (ROC) curve, and area under curve (AUC).

Decidability index is a metric used to define the separation between genuine and impostor scores distributions [29]. The decidability index  $DI$  can be computed as follows:

$$DI = \frac{|\mu_G - \mu_I|}{\sqrt{(\sigma_G^2 + \sigma_I^2)/2}} \quad (4)$$

where  $\mu_G$  and  $\mu_I$  be the mean of the genuine and impostor distributions respectively, whereas  $\sigma_G$  and  $\sigma_I$  be the standard deviations of the above scores.

The ROC curve is a measure of performance of classification that plots the genuine positive rate (GPR) against the false positive rate (FPR), which is shown in Figure 5. The area under the ROC curve (AUC) is used to compare the performance of different methods. It is a two-dimensional visualisation of ROC curve set to assess classifiers performance. The simplest way is to compute the area under the ROC curve which is part of the area of the unit square. Consequently the value of AUC will always satisfies the following inequalities  $0 \leq AUC \leq 1$ , if it computes it on *normalized* match scores [30]. It is assume that, if the AUC is close to 1, then it can be indicated that the system performance is better; otherwise, the system performance may or may not be better.

Classification performance of the proposed face recognition method is evaluated using the chi-square (CS) distance measure. Whose description is illustrated in [24]. It is also been evaluated using the new suggested distance metric i.e., Bray Curtis dissimilarity (BCD) metric for the computation of distance of peer face images, for the soundness of the A-LBP face recognition method, [31]–[33].

#### V. EXPERIMENTAL RESULTS

The face recognition accuracy of the proposed method, A-LBP is compared with LBP using CS distance and BCD distance metrics too, under different face datasets. The experimental results indicate that A-LBP performs better than the LBP on most of the face datasets. For ORL dataset, A-LBP achieved 95% recognition accuracy in both distance metrics, whereas LBP reports an accuracy of 92.50% and 94.52%, respectively. Similar trends are also observed for EYB, YA and LFW datasets. For EYB dataset, proposed method performs better than LBP, such as the accuracy values are reported to 81.22% and 86.45%, respectively; whereas the LBP reports to

TABLE I. CHALLENGING FACE DATASETS USED IN THIS EXPERIMENT.

Datasets	#Subjects	#Samples/ Subject	#Images (size)	Dimension
ORL [25]	40	10	400 (49×60)	p, e, eye glasses
EYB [26]	38	65	2470 (53×60)	i
YA [27]	15	11	165 (79×60)	e, eye glasses, i
LFW [28]	40	10	400 (58×64)	p, e, o, eye glasses, i

TABLE II. A COMPARISON OF RECOGNITION PERFORMANCE BETWEEN LBP AND A-LBP FACE RECOGNITION METHODS ON DIFFERENT FACE DATASETS UNDER VARIOUS DISTANCE MEASURES.

Datasets	Accuracy (%) on CS (BCD)		Area under Curve (AUC)		Decidability Index (DI)	
	LBP	A-LBP	LBP	A-LBP	LBP	A-LBP
ORL	92.50 (94.52)	95.00 (95.00)	0.962654	0.962782	3.0752	3.1501
EYB	74.11 (81.83)	81.22 (86.45)	0.840937	0.884814	1.9643	2.1048
YA	61.19 (60.00)	73.33 (71.90)	0.694004	0.736571	0.6942	0.9323
LFW	65.00 (65.29)	65.00 (67.37)	0.728369	0.743165	0.8463	0.8712

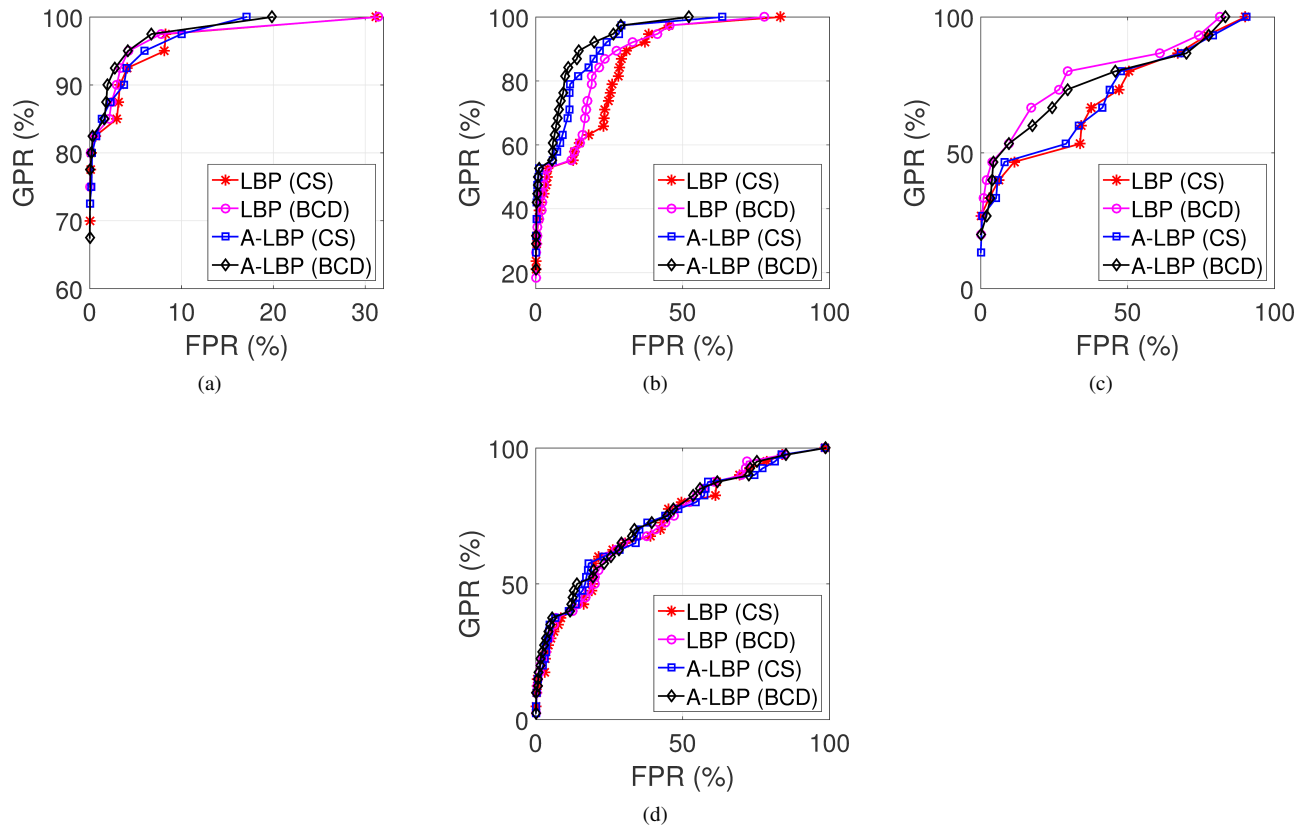


Fig. 5. Receiver operating characteristic curves showing the comparative performance of LBP and A-LBP face recognition methods under chi square distance and Bray Curtis dissimilarity metrics on various publicly available face datasets: (a) ORL, (b) EYB, (c) YA, and (d) LFW.

74.11% and 81.83%, respectively. For YA dataset, proposed method reported better accuracy value of 73.33% and 71.90%, respectively in comparison to LBP accuracy value of 61.19% and 60.00%, respectively.

Similarly, in case of LFW face dataset, the reported values of A-LBP are 65.00% and 67.37%, whereas LBP reports 65.00% and 65.29%, respectively for CS and BCD distance metrics. This proves that the A-LBP face recognition method is robust against the severe illumination variation, and certain extent to p, eye glasses, and o which can be seen from

the Table I. Similarly, the comparative performance of each dataset using two different distance measures are illustrated in Table II. That is an alternative way to visualise the comparative performance of the proposed approach.

The ROC curve for ORL dataset is plotted and shown in Figure 5(a). It indicates that the GPR is found highest for the proposed A-LBP method and reported value 78%; when FPR is actually zero. As FPR value increases, the GPR value also increases. For example, the GPR value is found 93% for LBP and 96% for A-LBP at the value of 5% FPR. The GPR value

is found maximum 100% at 32% of FPR.

Similarly, the results of EYB dataset is visualised in Figure 5(b). It indicates that the GPR is found highest for A-LBP method and reported value of 32%; when the FPR is actually zero. As FPR value increases, the GPR value also increases for all methods. For example, the GPR is found 62% for LBP and 82% for A-LBP at 20% FPR. The GPR is found maximum 100% at 83% of FPR for LBP and 78% of FPR for A-LBP. The A-LBP method achieves better recognition accuracy, because it is insensitive to changes such as illumination.

The ROC curve for YA dataset is plotted and shown in Figure 5(c). It indicates that the GPR is found highest for A-LBP method and reported value of 20%; when the FPR is actually zero. As FPR value increases, the GPR value also increases for all methods. For example, the GPR is found 50% for LBP and 69% for A-LBP at 20% of the FPR. The GPR is found maximum 100% at 90% of FPR for LBP and 82% of FPR for A-LBP. The A-LBP method achieves better recognition accuracy, due to its insensitiveness to the changes of illumination.

Similarly, the results of LFW face dataset is also visualised in Figure 5(d), which indicates that the GPR is found higher in A-LBP method and reported value of 15% at zero FPR. As FPR increases, the GPR value will also increase, for both methods, respectively. For example, the GPR found 35% and 41% for LBP, 39% and 50% for A-LBP at 6% and 16% of the FPR, respectively. The GPR is found maximum 100% for both methods at 98% of FPR. A-LBP method shows the marginal recognition accuracy over the LBP on LFW dataset. It shows a moderate improvement over LBP method. It is because of the proportion of non-uniform patterns is comparatively larger than the uniform patterns. As an effect, the feature descriptor of A-LBP becomes brighter that may lose some discriminatory information.

In order to evaluate the performance of reported results for ORL dataset, AUC of A-LBP and LBP are resulted as 0.962782 and 0.962654, respectively. These values for extended Yale B dataset are achieved 0.884814 and 0.840937, respectively; while on Yale A dataset the computed values are 0.736571 and 0.694004, respectively. Finally, on LFW dataset AUC of A-LBP and LBP are resulted as 0.743165 and 0.728369, respectively. In most of the cases, A-LBP shows better AUC than LBP. Performance of A-LBP and LBP are given in Table II.

$DI$  is a critical metric that is used to find out separation between genuine and impostor scores distributions. The  $DI$  of A-LBP and LBP on ORL dataset are found 3.1501 and 3.0752, respectively. The  $DI$  on extended Yale B dataset are found 2.1048 and 1.9643, respectively; while on Yale A dataset it has achieved values are 0.9323 and 0.6942, respectively. Finally on the LFW dataset, the reported values of  $DI$  for A-LBP and LBP are 0.8712 and 0.8463, respectively. In all the cases, on the basis of  $DI$  values, it can be concluded that the A-LBP face recognition method perform better than LBP, which can be verified from the results depicted in Table II.

## VI. CONCLUSION

The paper has presented a novel method of facial image representation for face recognition in uncontrolled environ-

ments. This method is called as augmented local binary pattern (A-LBP). It works on the combination of principles of locality of uniform and non-uniform patterns. It can be used with combination of neighbouring uniform patterns to extract discriminatory information from the local descriptor.

Comparative results analysis of face recognition methods has been performed, using following publicly available face datasets, such as AT & T-ORL, extended Yale B, Yale A, and Labeled Faces in the Wild. It has been computed using chi-square distance and Bray Curtis dissimilarity measures too. Proposed A-LBP method has efficiently recognised faces from their wild face datasets. The experimental results have indicated that the performance of the A-LBP method has improved substantially with respect to LBP on different experimented datasets, particularly when there is extreme variations in the illumination of facial images in the dataset (e.g., extended Yale B and Yale A).

In future, more exploration can be made to use the non-uniform patterns in addition to uniform patterns. The majority criterion to be experimented on the values of (8, 2) and (16, 2) neighbourhoods in the direction of the robustness of the A-LBP frameworks. It could be further extended to include region-wise weights based on the probability of occurrences of the non-uniform patterns in particular regions.

## ACKNOWLEDGMENT

The authors acknowledge the Institute of Engineering and Technology (IET), Lucknow, Dr. A.P.J. Abdul Kalam Technical University, Uttar Pradesh, Lucknow for their partial financial support to carry out this research under the Technical Education Quality Improvement Programme (TEQIP-II) grant.

## REFERENCES

- [1] M. A. Turk and A. P. Pentland, "Eigenfaces for Recognition," *J. of Cogn. Neurosci.*, vol. 3, no. 1, pp. 71–86, 1991.
- [2] J. Lu, N. P. Kostantinos, and N. V. Anastasios, "Face Recognition using LDA-based Algorithms," *IEEE Trans. on Neural Networks*, vol. 14, no. 1, pp. 195–200, 2003.
- [3] P. N. Belhumeur, J. P. Hespanha, and D. J. Kriegman, "Eigenfaces vs. Fisherfaces: Recognition Using Class Specific Linear Projection," *IEEE Trans. Pattern Anal. Mach. Intell.*, vol. 19, no. 7, pp. 711–720, July 1997.
- [4] T. Ojala, M. Pietikäinen, and D. Harwood, "A Comparative Study of Texture Measures with Classification Based on Feature Distributions," *Pattern Recogn.*, vol. 29, no. 1, pp. 51–59, 1996.
- [5] M. S. Bartlett, J. R. Movellan, and T. J. Sejnowski, "Face Recognition by Independent Component Analysis," *IEEE Trans. on Neural Networks*, vol. 13, no. 6, pp. 1450–1464, Nov 2002.
- [6] R. Shyam and Y. N. Singh, "A Taxonomy of 2D and 3D Face Recognition Methods," in *Proc. of 1<sup>st</sup> Int'l Conf. on Signal Processing and Integrated Networks (SPIN 2014)*. IEEE, Feb. 2014, pp. 749–754.
- [7] R. Shyam and Y. N. Singh, "Identifying Individuals Using Multimodal Face Recognition Techniques," *Procedia Computer Science, Elsevier*, vol. 48, pp. 666–672, 2015. [Online]. Available: <http://www.sciencedirect.com/science/article/pii/S1877050915006596>
- [8] R. Shyam and Y. N. Singh, "Robustness of Score Normalization in Multi-biometric Systems," in *Proc. of Lect. Notes in Computer Science(LNCS)*, Springer, vol. 9478, Switzerland, 2015, pp. 542–550.
- [9] R. Shyam and Y. N. Singh, "Multialgorithmic Frameworks for Human Face Recognition," *J. Electrical and Computer Engineering*, vol. 2016, pp. 1–9, 2016. [Online]. Available: <http://dx.doi.org/10.1155/2016/4645971>

- [10] R. Shyam and Y. N. Singh, "Automatic Face Recognition in Digital World," *Int'l J. of Advances in Computer Science and Information Technology (ACSIT)*, vol. 2, no. 1, pp. 64–70, 2015.
- [11] M. Pietikainen, A. Hadid, G. Zaho, and T. Ahonen, "Computer Vision Using Local Binary Patterns," in *Proc. of Computational Imaging and Vision*, vol. 40, Springer-Verlag, 2011, pp. 13–43.
- [12] T. Ahonen, A. Hadid, and M. Pietikainen, "Face Description with Local Binary Patterns: Application to Face Recognition," *IEEE Trans. Pattern Anal. Mach. Intell.*, vol. 28, no. 12, pp. 2037–2041, Dec. 2006.
- [13] L. Zhang, R. Chu, S. Xiang, S. Liao, and S. Li, "Face detection based on multi-block LBP representation," in *Proc. of Int'l Conf. on Biometrics*, 2007.
- [14] H. Yang and Y. Wang, "A LBP-based Face Recognition Method with Hamming Distance Constraint," in *Proc. of 4<sup>th</sup> Int'l Conf. on Image and Graphics*, ser. ICIG '07. Washington, DC, USA: IEEE Computer Society, 2007, pp. 645–649.
- [15] L. Shu and C. A. C. Shing, "Face Recognition by using Elongated Local Binary Patterns with Average Maximum Distance Gradient Magnitude," in *Proc. of 8<sup>th</sup> Asian Conference on Computer Vision - Volume Part II*, ser. ACCV'07. Berlin, Heidelberg: Springer-Verlag, 2007, pp. 672–679.
- [16] T. Ahonen and M. Pietikainen, "Soft histograms for local binary patterns," in *Proc. Finnish Signal Processing Symposium (FINSIG 2007)*, Oulu, Finland, 2007.
- [17] X. Tan and B. Triggs, "Fusing Gabor and LBP feature Sets for Kernel-based Face Recognition," in *Proc. of IEEE Int'l Workshop on Analysis and Modeling of Face and Gesture*, 2007, pp. 235–249.
- [18] X. Tan and B. Triggs, "Enhanced Local Texture Feature Sets for Face Recognition under Difficult Lighting Conditions," ser. Lect. Notes in Computer Science(LNCS), vol. 4778. Springer-Verlag, 2007, pp. 168–182.
- [19] L. Wolf, T. Hassner, and Y. Taigman, "Descriptor Based Methods in the Wild," in *Proc. of Workshop Faces in Real-Life Images: Detection, Alignment, and Recogn.*, Marseille, France, Oct. 2008, <https://hal.inria.fr/inria-00326729>.
- [20] S. Liao, M. W. K. Law, and A. C. S. Chung, "Dominant Local Binary Patterns for Texture Classification," *IEEE Trans. on Image Processing*, vol. 18, no. 5, pp. 1107–1118, 2009.
- [21] M. Heikkila, M. Pietikainen, and C. Schmid, "Description of Interest Regions with Local Binary Patterns," *Pattern Recogn.*, vol. 42, no. 3, pp. 425–436, 2009.
- [22] N. Werghi, S. Berretti, A. D. Bimbo, and P. Pala, "The Mesh-LBP: Computing Local Binary Patterns on Discrete Manifolds," in *Proc. of IEEE Int'l Conf. on Computer Vision (ICCV) Workshops*, December 2013, pp. 562–569.
- [23] N. Werghi, S. Berretti, and A. D. Bimbo, "The mesh-LBP: a framework for extracting local binary patterns from discrete manifolds," *IEEE Trans. on Image Processing*, vol. 24, no. 1, pp. 220–235, Jan. 2015.
- [24] R. Shyam and Y. N. Singh, "Analysis of Local Descriptors for Human Face Recognition," in *Proc. of Smart Innovation, Systems and Technologies (SIST)*, Springer-Verlag, vol. 43, India, Oct. 2015, pp. 263–269.
- [25] F. Samaria and A. Harter, "Parameterisation of a Stochastic Model for Human Face Identification," in *Proc. of 2<sup>nd</sup> IEEE Workshop on Applications of Computer Vision*, Sarasota, FL, Dec. 1994.
- [26] K. C. Lee, J. Ho, and D. Kriegman, "Acquiring Linear Subspaces for Face Recognition under Variable Lighting," *IEEE Trans. Pattern Anal. Mach. Intell.*, vol. 27, no. 5, pp. 684–698, 2005.
- [27] UCSD, "YALE ,", 2007, <http://vision.ucsd.edu/content/yale-face-database>.
- [28] G. B. Huang, M. Ramesh, T. Berg, and E. Learned-Miller, "Labeled Faces in the Wild: A Database for Studying Face Recognition in Unconstrained Environments," in *Tec. Report*, University of Massachusetts, Amherst, 2007, pp. 07–49.
- [29] C. H. Park, J. J. Lee, M. J. T. Smith, and K. H. Park, "Iris-Based Personal Authentication using a Normalized Direction Energy Feature," in *AVBPA 2003*, ser. Lect. Notes in Computer Science(LNCS), vol. 2688, Berlin Heidelberg, 2003, pp. 224–232.
- [30] A. E. Bradley, "The use of the area the ROC curve in the evaluation of machine learning algorithms," *Pattern Recognition*, vol. 30, no. 7, pp. 1145–1159, 1997.
- [31] R. Shyam and Y. N. Singh, "Evaluation of Eigenfaces and Fisherfaces using Bray Curtis Dissimilarity Metric," in *Proc. of 9<sup>th</sup> IEEE Int'l Conf. on Industrial and Information Systems (ICIIS 2014)*. Gwalior, India: IEEE, Dec. 2014, pp. 1–6.
- [32] R. Shyam and Y. N. Singh, "Face Recognition using Augmented Local Binary Patterns and Bray Curtis Dissimilarity Metric," in *Proc. of 2<sup>nd</sup> Int'l Conf. on Signal Processing and Integrated Networks (SPIN 2015)*. IEEE, Feb. 2015, pp. 779–784.
- [33] R. Shyam and Y. N. Singh, "Recognizing Individuals from Unconstrained Facial Images," in *Proc. of Advances in Intelligent Systems and Computing Series (AISC)*, Springer, vol. 384, Switzerland, Aug. 2015, pp. 383–392.

# Architecture Considerations for Big Data Management

Khalim Amjad Meerja  
Western University, London Ontario,  
Canada  
Email: kmeerja2@uwo.ca

Khaled Almustafa  
Prince Sultan University,  
Riyadh, K.S.A.  
Email: kalmustafa@psu.edu.sa

**Abstract**—A network architecture is concerned with holistic view of interconnection of different nodes with each other. This refers to both physical and logical ways of interconnection of all nodes in the network. The way in which they are connected influences the strategies adopted for Big Data Management. In this present day of Internet of Things (IoT), each kind of device is required and made possible for communicating with other completely different kinds of devices. The heterogeneous nature of devices in the network needs a completely new architecture to efficiently handle Big Data which is generated continually, either for providing services to end users or for study and analysis in a research process. It is thus very essential to visit various kinds of devices that are available on the Internet, their characteristics and requirements, how they communicate and process data, and eventually how the human society embraces the Big Data generation for their daily consumption. This paper is dedicated to bringing all these aspects together in one place, bringing different technologies into one single network architecture.

**Keywords**—Internet of Things (IoT), Big Data, Cloud network, RFID, Sensor Networks, 5G.

## I. INTRODUCTION

A notable feature of our present day network communications is new ways in which different kinds of devices talk to each other over the Internet. Devices vary in shapes and sizes. Some are from very tiny to small, operating autonomously while others are comparatively large and more complex. They are highly heterogeneous in many aspects, having different functionalities, computational capabilities, and storage. With regards to mobility, some are highly mobile, while others are either portable or fixed in their locations. They work in master slave relation or as peers. They transmit multimedia such as voice, video, images, and text. All these various functionalities need different network conditions and communication practices to operate better and serve.

For instance, tiny devices have constrained energy resources. Their operations are based on energy conservation mechanisms and needs completely different practices such as network protocols, architectures, energy harvesting mechanisms, robustness to failures in adverse conditions, system security measures, to name a few. Data has to be periodically collected and forwarded to more stable and powerful system for manipulation and analysis. Larger devices such as smart computational devices have higher expectations in terms of services offered. So, their underlying network conditions have to be more powerful and robust. It is therefore important to look into the available types of devices and their network

requirements. From studying all these network requirements, it is possible to come up with a unified architecture as a solution to efficiently handle Big Data evolving from trillions of such devices connected to the Internet.

### A. Wireless Sensor Networks

Wireless sensor networks are predominantly used for environmental, industrial, agricultural, health, and habitat monitoring purposes [1]. These are mostly ad hoc networks that were originally developed for communication in military operations. Later they are found in many useful applications in domestic environment [2]. Sensor devices are generally placed in harsh environmental conditions. Therefore node failures are common in sensor networks. Network routing and media access control protocols should deal with node failures and still maintain communication links with their destination sink nodes. While doing so, they have to conserve their energy as it is difficult to replenish them with power sources. In some cases, it is possible that these sensor devices derive energy from solar cells or from some sort of mechanical stress induced by onboard piezoelectric material.

Network architecture should consider all these issues. More importantly, fault tolerant mechanisms are essential to keep up with node failures. Some node failures are intermittent and short lived while some are permanent. The path between the network nodes will constantly be changing due to these reasons and also because of another important reason, which is the unreliable nature of wireless channels. The sink nodes have to maintain a simultaneous connection with a group of sensor nodes in a particular region that are performing monitoring. At the same time, it is essential that only a single node out of all available nodes in the region should forward the data to the sink node. Otherwise, there would be redundancy in the data that wastes channel and energy resources. Appropriate data aggregation mechanisms should be developed for forwarding the required information to the sink node.

The next important aspect is the availability of sink node. The architecture should consider forwarding to multiple sink nodes simultaneously to protect data against sink node failures. It is possible that the communication link to a particular sink node for certain duration is highly noisy because of some nearby activity or the link is in deep fade due to surrounding weather conditions. Also the sink node storage capacity must be taken into consideration. It is very common now that the number of sensor devices are increasing enormously and each sensor device is pumping huge amount of data into the

network. For example consider the case of connected cars. The sensors in a car will be sending gigabytes of data during every hour of its running to the edge network. The edge network with destined sink nodes must have adequate capacity to collect data from the oncoming cars. Also due to high mobility, a particular car will be changing its sink node destination along this path of travel. So, the kind of application plays a key role in coming up with the right kind of architecture. All such varied degree of requirements must be considered in coming up with a single unified architecture.

Besides simple storage, are the sink nodes able to process and manipulate data appropriate for analysis? A better scalable architecture may or may not allow this. It is also possible that the sink nodes are not better equipped with tools and resources for processing the data. They are better equipped to efficiently store and simply forward to the right kind of servers in the core network. For high availability of data and that too in realtime is making the service providers push data to edge networks by placing servers close to the routers in these edge networks that are providing network access to end users. Such kind of architecture will profoundly improve latency issues in the network.

### B. Cellular Networks

Cellular networks have emerged predominantly as single hop infrastructure based service networks to initially provide voice communication. Their main concern is reliable connectivity along with mobility. With the proliferation of wireless devices such as smartphones, tablets, and laptops, wireless communication have evolved into multimedia provisioning networks [3]. Users are now accessing videos, mobile TV, voice over IP, multimedia streaming, video chatting, e-commerce, banking, and many killer applications in social networking. The demand for higher bandwidth is therefore constantly raising. People are relying more on their smartphones and other devices for monitoring their homes and for other remote operations. People are spending more time online now than before and this trend is growing tremendously. New users are constantly added to the networks and so as new bandwidth intensive applications. Data movement in these networks is humongous and to keep with such growth HetNets are evolving [4]. HetNets have multi-sized cells such as macro, micro, pico, and femto cells. This is mainly because, smaller cells can provide higher bandwidths and reliable connections in highly dense locations where there is low mobility. Macro and micro cells on the other hand provide overlay coverage as an umbrella network for mobile users. Large cells reduce the number of handovers and as a result are effective in reducing the call drops.

Now the new requirement along with connectivity and mobility is bandwidth and affordability. The demand for data bandwidth is growing but the revenues generation for service providers is not growing proportionally. The network costs are constantly raising with newly adopted technologies, and if this trend is not changed, the upcoming 5G networks will be prohibitively expensive to do business for service providers. So, the prime concern of the next upcoming 5G network architecture is affordability of the new technology, how this new technology can be rolled out to the common users. The major portion of this expenditure is the energy required to

keep the networks up and running and the operations and maintenance of the networks. New network consolidation models are required to reduce the operations cost and energy bills. The networks have to be self organizing to eliminate expensive manual interventions [5]. The new considerations of service providers is to reduce the energy consumption of their base stations [6].

Deploying smaller cells like pico and femto cells will profoundly reduce energy consumption in their base stations [7], [8]. For instance, femto cells can be user deployed which eliminates the burden on service providers to power and maintain them [9], [10]. It is expected that these femto base stations would be plug and play devices that are easy to install and operate. However this puts a much greater onus on service providers to synchronize transmissions between various femto base stations and other nearby pico, micro, and macro cells. Interference is a major issue between adjacent cells which are sometimes overlapping in coverage regions. The networks become highly complex as resource block scheduling MAC protocols and interference mitigation schemes have to work under very tight constraints.

While the new 5G architecture has to take all these factors into account, one more important factor that is our main focus is the generation and handling of Big Data in these networks. It is expected that data has to be available to users in realtime while they are moving between locations. Networks have to ensure that the data stored and retrieved is less expensive and less complicated. The data manipulation for analysis requires suitable architecture for display of results to right users within the right time frame. It is important to know that user devices such as smartphones, tablets, and laptops are the sources of data. Millions of users are always on the service providers network constantly generating data such as location information, services accessed, and other critical data. For instance, a safety application can use such data to provide rescue operations and alert the nearest fire and police department for immediate help.

Another major instance from where data is generated is the large and growing number of social networks. Data is shared between users in form of pictures, videos, files, information on certain activities, concerts, shows, and fashion. Like minded people will be discussing on a particular topic may it be of social nature, hobby, technology, or scientific. Conversations from all these sort of activities generate data on the network. Smart homes and smart cities generate data every single instant of time. Telemedicine, health monitoring, and reporting applications are gaining a lot more importance in old age people preferring to lead independent life. On the other hand, the news is constantly shared among people in communities on various political, technical, health, and entertainment issues. A unified architecture should also accommodate various technologies into a solution and promote applications working on cross platforms and multiple technologies simultaneously.

### C. RFID Networks

Radio frequency identification (RFID) tags [11] are attached to every imaginable thing that is monitored such as any inventory, commercial goods and merchandize, home and business equipment, industrial production cycle for automation, citywide as well as countrywide infrastructure including

buildings and roadways, domestic and wild life animals, bird species migration habits, natural habitat, old age people and patients, etc., to name a few. RFID tags are sleeker than sensor devices and are less complex. They only store certain amount of data which will be read by a RFID reader. Sensor devices on the other hand have some sort of sensing functionality, which they use to produce data and forward it to their sink nodes. Sensor nodes can initiate communication with their sink nodes and have a MAC module built in them whereas RFID tags are not equipped with such MAC module. MAC intelligence in RFID networks is incorporated only in RFID readers, which read data from RFID tags and forward them to gateway node attached to central network [12]. These RFID readers can be sensors placed in ad hoc manner in between the gateway on the wired network and RFID tags attached to the monitored devices. In this manner both RFID networks and sensor networks work together to complete the required job [13].

RFID tags are either active or passive. Active RFID tags are considerably bulky as they are equipped with battery source and protective gear for the onboard battery. Passive RFID tags on the other hand do not have any battery onboard as they harvest power from the electromagnetic energy of the RFID reader communication. The main challenge with these RFID networks is the communication range. Though active RFID tags can communicate with longer range than passive RFID tags, still the communication range is only around 5 to 10 meters for active tags. Passive tags communicate only up to 1 to 2 meters. Further the amount of data they can store is very low due to size limitations. For instance the tags attached to many bird species should be less than 1 gram, which is less than 5% of the body weight as recommended by a standard norm. Further the data rate in these RFID is very low and is often one way communication, from the tags to the reader. However it is possible to have two-way communication in some active tags, but will increase the size and complexity. This is also because, the two-way communication may require a simple onboard MAC module on these active RFID tags. Another drawback with active RFID tags is that their lifetime is limited unlike passive RFID tags (which is unlimited).

RFID tags are also suitable for near field communications (NFC). These tags can be used in credit cards for transactions in stores, in passports to scan information on identity in airports, patient identification in hospitals, and many such applications. Though the data that is generated by each individual RFID tag is very less, the total data of collective millions of such tags in a certain location is huge. The data is very critical in offering services to the end users. The authenticity of the transactions is very critical as people rely on the technology in their daily lives. The system of RFID networks has to be reliable as business transactions are performed. Secondary nature data and analysis for research and study purposes for improving the business performance and any other such tasks is also highly essential. A proper combination of RFID networks and sensor networks can be designed for efficiently conducting daily business and operations. The unified network architecture has to consider all these factors in designing a robust monitoring system. It is particularly important to know that the information is not only used by the main business owners but also by general public over the Internet. Take for instance a certain consumer is going online on the Internet to

look for available stock in a particular Walmart or Canadian Tire store. The data available on the stores website can be realtime data acquired from the the RFID tags on the available inventory.

#### D. Device-to-Device (D2D) Networks

A major challenge for the emerging 5G networks is to accommodate tremendously huge number of users, increased by many folds compared to the current number of users. The current number of users in cellular networks is already significantly high. The density of users is going to increase exponentially, which makes it very difficult for the base stations to provide service to all these users. Keeping this in mind, the service providers have already decided to reduce the cell sizes leading to HetNets. But the problem with handling these increased number of smaller cells leads to complex signalling. Further, the traffic has to be passed through the base stations of this cellular networks. Given the increased amount of social activity and proximal communications for applications involving photo sharing, games, chatting, etc., the traffic puts an enormous burden on the cellular network. It is possible to offload some of the traffic from cellular network by initiating direct communication between the parties that are proximally located and involved in some sort of communication. Such cases of proximal communications are predicted to be significantly high. It is, therefore, beneficial to develop a robust technological solution in this direction for offloading cellular network traffic in case of proximal communications. Keeping this in mind device-to-device (D2D) networks that provide direct communication between devices participating in communications is being developed [14], [15].

There are many benefits in D2D network communications because of their close physical proximity [16]. Better channel conditions prevail when devices are much closer. Higher throughput is possible under low signal to interference noise (SINR) ratios, leading to the possibility of having energy efficient communications [17]. D2D networks can be monitored by cellular base station through out the session by controlling it from initiation to termination [18]. This is defined as network controlled D2D communications. Network controlled D2D communications can be robust due to continuous control of the cellular base station. The advantage with this kind of D2D communications is that, they will not interfere with cellular communications or at least the observed interference will be low. Highly secure communications are possible through this scenario. It is also advantageous when devices are moving frequently. During high mobility, D2D sessions can switch to their communications through base station almost instantaneously and more seamlessly. The disadvantage of this kind of scenario is however that though data is transferred directly between communicating devices without passing through the cellular base station, still the control channel for these sessions is maintained through this base station. Due to this reason, not many simultaneous D2D network communications can be initiated within the cell region of a particular base station. This scenario is not highly scalable and not appropriate for dense D2D networks.

A more scalable solution for low mobility scenarios is partial assistance of base station during D2D communication initiation. Through this approach, it is possible to authenticate

the parties that are willing to participate in D2D communication. Since there is no further involvement of Cellular base station, no control channel is maintained for the ongoing D2D communication sessions which may last for very long durations. The resources of the cellular base stations are not tied up with the current ongoing, already established D2D network communications. This scenario is better scalable compared to the previous one and is also secure. As mentioned, this is a very good solution for low mobility situations where the devices are not expected to move from their positions. In practical situations, such conditions exist on a more frequent basis. Since the cellular base station is involved in setting up the D2D communication sessions, it can control and lower inference to the cellular communication network. This scenario can be regarded as network assisted D2D communications [19], [20].

It is possible to have autonomous operations for D2D communications [21]. These communications are established, maintained, and terminated without the need of a cellular base station. This is called assistance-free D2D communication, where cellular base stations are relieved from operations of D2D communications. Since cellular base stations are not involved in assistance-free D2D communications, there can be many D2D sessions, which is particularly suitable for dense environments. However, there is a growing concern of interference between D2D communications and cellular communications. There is no central authority controlling interference in the entire cell area. To overcome interference issues, D2D networks are using cognitive radio (CR) technology. It is possible to have either underlay or overlay CR communications in licensed frequency spectrum without interrupting primary users in cellular communications [22], [23]. D2D network users will be considered as secondary users to spatiotemporally available spectral resources. The secondary users ensure that their communications do not interfere with the primary users. They ensure that the total interference from their communications is below the tolerable level for primary users. In order to completely eliminate interference in the licensed bands used by cellular communications, D2D communications can use unlicensed bands. However, quality of service (QoS) in unlicensed bands is not guaranteed. As a result D2D communications will face more interference. For this reason, millimeter waves are being explored for D2D communications in upcoming 5G networks [24].

Due to varied degree of involvement of cellular base stations in the above three different scenarios, it best to leave it to the end users requesting the kind of service for their D2D network communications. Depending on the required QoS for D2D communications, based on their degree of mobility, security level requirement, and device capabilities, there would be an option to choose network controlled, network assisted, or assistance-free D2D service. The network architecture should embrace all these three types of service configurations and maintain statistics of the entire data communicated along with the level of data management and analysis required for the end Big Data applications.

## II. BIG DATA MANAGEMENT ISSUES

Having glanced at various types of networks available around us that specialize in their services to diverse users, its time to move on to a more important issues surrounding the

data generated in these networks. All of us will be interested in the answers to the following questions:

- What to do with the data generated in these networks on daily basis?
- Do we simply discard data or store it for later retrieval?
- What are the benefits of storing the data?
- How important is the data?
- Is the information derived from the data reliable to take action on it?
- Who will access the data and what are its implications?
- Who does it benefit?
- Are you comfortable in sharing your data and what are the consequences?
- How do you guarantee privacy and confidentiality?
- What kind of technology is needed for the job and how you compare with the current available technology?
- Is the available technology scalable according to our growing needs?
- Is the technology affordable and energy efficient to meet green objectives?

These are some very general questions pertaining to the data that is being produced daily by user activities in cities, countries, and around the planet. In addition to the surveillance activities, much information can be gathered from the daily generated data to know the preferences of users, their requirements, and problems faced. The data can be used to systematically tackle issues that are faced by general public in a more comprehensive and economical manner. Data will be useful while making meaningful analysis to improve technology and services for users. Social networks provide most of this information [25], [26], [27]. For instance, traffic pattern on a particular highway can be known from using communications infrastructure [28], [29]. From this information, the province can plan gas stations, motels, and other services needed during traveling. Expansion of highways and other planning activities need information on the kind of activity on the highway. Emergency response teams need timely data to deliver their services within time.

While taking appropriate measures in preserving sensitive private information from public disclose, it is highly beneficial to share data with right institutions and companies to enhance services and technology. Data sharing becomes vital during catastrophic situations such as an earthquake, fire, political and social disturbance, road accidents, construction, traffic congestion, and when any other unusual phenomena happen. Proper use of data will improve living and save lives during disasters [30]. People will be updated with knowledge and information upon access to required data. There are many other benefits such as gaining insights and relations to the surrounding activities related to human, nature, and technological interactions. It is possible to gain new grounds, and

avoid disasters before hand with the available data gathered from various sources.

To gain any of such new insights, huge unstructured data from many sources is needed. This huge data is available from surrounding activities and needs powerful computing platform and huge but compact storage space [31]. The technology should be scalable with the growing size of data and also be economical. Along with being affordable, the technology should be green using as little energy as possible. The technology should provide results in realtime or within the required time constraints. The results have to be reliable and verifiable. The rest of the paper will look into the technological requirements to handle data and in particular answer the last three of the questions listed above.

A network architecture should address all these issues such as scalability, energy efficiency, time and space constraints [32]. At the same time, the architecture has to deal with heterogeneous networks and the various kinds of devices connected to these networks. The data generated on these devices are from various applications and services leading to the handling of highly unstructured data. The devices have varied capabilities, various network topologies exist, different protocols, and conflicting objectives. All these factors have to be taken into consideration for handling Big Data generated from IoT devices.

#### A. IP Device Capabilities

The main characteristic of IoT devices is that they have varied device capabilities. These capabilities are in terms of computational power, storage capacity, energy constraints, and network connectivity. For instance, sensor devices have very limited battery capacity and most of the time it is hard and almost impossible to recharge the batteries. In such cases, the main focus will be to increase the lifetime of the sensor devices as much as possible. So they use the concept of duty cycle in their transmission operations. This is because, most of the battery energy is consumed by transmission and reception activities. In a duty cycle, there will be a sleep period and wake-up period. During sleep period, the devices turn off their transceivers and enter sleep mode. They wake up after the end of their sleep duration. They can transmit and receive only during the wake up period. It is typical to have 50% or less duty cycle to ensure longer sleep periods to enhance battery life.

Sensor devices constantly gather environmental data and need onboard storage to store data and transmit during the wake up period. Since these devices are not equipped with large storage capacity, the duty cycle should be adjusted accordingly. If the sensing activity is not very intense or frequent, then the devices can have very large sleep durations. The MAC operations have to be turned optimally to the sensing activity carried out by the devices. The MAC layer, therefore, has to ensure that battery life is elongated along with efficient transmission of the sensing data to its sink node. The network architecture has to consider these aspects and may need to provide multi-hop communications to conserve battery life in sensor devices. It is important to synchronize transmissions among sensor devices such that the relevant communicating partners are awake at the same time and go to sleep mode in a synchronized fashion.

Sensor devices are not meant for complex processing of the data onboard. So, they do not have processors on board. Most of the time they are transducers that convert one form of energy into another and send the raw data over the sensing activity to their central processing and storage sink nodes which are considered more powerful than these sensor devices. The sink nodes will preprocess the data and later forward the central network for complex analysis and permanent storage of the data in appropriate form.

Cellular network devices are more powerful. They are mainly smartphones, tablets, and PDAs that transmit data, voice, and multimedia containing audio and video communications. They have powerful onboard processors but rely heavily on central base station for complex network scheduling operations. Communications in these networks are two-way, although these communications are asymmetrical in uplink and downlink bandwidth occupancies. The download communications from central base station to the mobile terminals are bandwidth intensive compared to the uplink communications going from mobile terminals to the central base station. This is particularly true with data communications where the mobile terminal will be constantly downloading data from the central servers on the Infrastructure based network through the base station. Compared to sensor devices, these devices are easily rechargeable. However, energy considerations are still vital due to limited battery capacity. These devices also use some sort of sleep cycle to conserve energy in their batteries. MAC operations in these devices are more power hungry due to advanced applications that are built for these type of devices.

RFID tags are passive devices which harvest energy from RF communications of their RFID readers. They have no onboard processing and are suitable for very short range communications. They may not have MAC module and are reactive to the communications from the RFID reader. The communication will be mainly one way from RFID tags to the central reader. The RFID readers will be connected to the main central server in the Infrastructure based network. The RFID readers are simply bridges from the RFID networks to the central core data networks. Data will be processed and stored in the central core data networks.

Multihop D2D communications are being incorporated in cellular networks to conserve energy in mobile devices. When devices are in close proximity with each other, direct communications are possible between these devices without any need of services from the central base station. Thus central base station can be relieved from providing services to such directly possible communications between close vicinity mobile terminals. D2D communication networks are being developed to take advantage of such network communications. The devices will be able to setup, manage, and tear down communication sessions among them, thus offloading some of the traffic from the central base station. D2D devices have to be more complex to avoid interference with the cellular communications that are present overlapping with the regions of D2D communications.

#### B. Network Considerations

Network topology has to be robust to maintain both physical and logical links all the time. Network redundancy must

be maintained to overcome intermittent failures, which are commonly known as backup and restoration mechanisms. The network redundancy can also be used to provide load balancing features into the network. For instance, it is critical in sensor networks to have such type of network redundancy. If a sensor node failure occurs due to adverse environmental conditions or due to battery failure, it may bring the whole network down depending on its location in the network. Such bottlenecks have to be eliminated by maintaining alternative routes in the network. It is very challenging to have such mechanism particularly when the network is setup in ad hoc manner. Generally, most of the sensor networks are ad hoc networks. Take for instance the case of monitoring a forest area. The sensor nodes are sprayed using a means of air transport such as a helicopter. As the sensor nodes are sprayed over the area, their locations in the overall sensor network are completely random. To avoid frequent node failures, it is best to increase the density of the nodes to have both backup paths and provide load balancing in the network.

The nature of communication in sensor networks is quite the opposite to that of the communications in cellular networks. The communications in sensor networks is always from many leaf sensor nodes to the single central sink node. Whereas in cellular networks, most of the data is downloaded by the mobile terminals from the central base station. Due to this stark contrast, the design of MAC protocols and the network topology design will be completely different. Sensor nodes are seldom mobile. However, there are upcoming sensor network applications that involve high mobility of sensor nodes, such as sensors in connected cars. Varied mobility ranges have to be taken into consideration depending on the type of application at hand. However, in both sensor and cellular networks, critical data is maintained in the central servers which receive data from the base stations or sink nodes. The network topology should ensure that these nodes do not become single point of failures. Communication has to be maintained always through more than one sink node in sensor networks to overcome network and link failures. When there is mobility, sensor nodes need proper handoff mechanism to relay their communications with the next neighboring sink node along the path of travel.

Besides mobility, there has to be enough bandwidth for data to be transferred over wireless media to servers located in the central infrastructure based network connected to the Internet. This is how the data is made available for global access. This is how the data is made available for global access. The time delay is highly critical for realtime applications. The data that is fetched by the mobile terminals should be available readily and on demand. The accessed data will be critical for maintaining the safety and proper operation of the devices attached to the Internet through onboard sensors. Take for instance the highway patrol team using technology attached to the sensor networks. The data carried over these sensor networks is critical for the operations of the highway patrol team to provide emergency services, redirect traffic, and provide warnings for the safety of the travelers on the road. Network congestion should be avoided for proper operation of such network. Adequate network bandwidth has to be provisioned. In addition to the bandwidth, network security is very important. The transmissions have to be highly secure to avoid eavesdropping on the critical communications. Security is needed for protecting the identity of the individuals and any

unauthorized access to the personal information.

Providing high bandwidth over wireless media is highly challenging. This is due to the fact that the available bandwidth over wireless channels is very low compared to the existing wired media such as fiber optics. Wireless links are also challenged with link fading conditions due to multipath transmission, obstructions, weather changes and many other varying surrounding conditions. Because of this kind of fading phenomenon, constant channel bandwidth cannot be guaranteed for wireless links. Wireless links are also subjected to interference from surrounding activities. Due to all these reasons, the signal to interference noise (SINR) ratio of wireless links constantly varies. Mobility creates Doppler effect and the distance between the transmitter and the receiver is not always the same. As a result, communication links have to be constantly changed between the mobile terminals and the closely available base station. This is commonly known as handoff mechanism. The handoff should be seamless to the ongoing transmissions to maintain good quality of service (QoS) and quality of experience (QoE).

One way to increase the bandwidth is to reduce distance between transmitters and receivers involved in wireless communication. Higher SINR is possible over shorter distances, which can be useful for adopting high modulation and coding rates (MCR) to improve spectral efficiency measured in terms of (Bits/s)/Hz. High MCR will increase the transmission data rate on the wireless channel. Further, reducing the link distance between the transmitter and receiver will improve line-of-sight communication between the two transceivers involved in wireless communication. The next advantage is, it is possible to use higher frequency spectrum over shorter distances. Higher frequency spectrum provides higher bandwidths that can be useful for multimedia transmissions. The link distances have to be shorter because fading is heavy over higher frequency ranges compared to the lower frequency range. Higher frequency ranges need line of sight communications. It is possible to reduce SINR of the transmissions to conserve energy that is critical to extending the battery life.

Because of this reason, cellular communications are adopting smaller size cells to improve data rates. Smaller cells will improve frequency reuse over space and time. More number of users can be supported with many smaller cells instead of a single large cell. This is a dire necessity for today's communication requirements as more users are being added to these cellular networks every day. The number of users is not only increasing but also all these users are demanding higher bandwidths at higher mobility speeds. As a result the networks have become complex in terms of signalling. Maintaining many smaller cells increases scheduling complexity because of high level of cross-tier and inter-tier interferences due to transmissions between the cell base stations and its associated users. High mobility and smaller cells means increased number of handoffs for mobile users. This is an additional load on the cellular infrastructure. Traditional cellular communication requires all transmissions passing through the base station. This is required to maintain adequate quality of service and better control of the ongoing communication sessions.

In order to maintain short link distances, and improve QoE, cellular networks are offloading some of the traffic to direct D2D communications in cases where the transceivers are in

close proximity of each other. These D2D transmissions need not pass through the base station thus relieving the cellular network from some of this kind of traffic. Multihop D2D communications are not only energy efficient but also are required for the large data transfers between closely located users. Such kind of communication scenarios are quite common where users that are close by are sharing photos, videos and other personal data files with each other. This type of network topology will substantially enhance the spectral efficiency over space and time. The network topology empowers the mobile terminals to take routing decisions for multihop transmissions and relaying to the base station to conserve energy and improve communication range. This type of communication can also be used to improve QoE for the users located at the cell edges.

### C. Energy and Cost Considerations

Trillions of IoT devices around the world, which are connected to the Internet, consume a significant amount of energy. Higher data rates and increased processing powers make these devices power hungry, consuming more power. As the number of these devices continue to increase exponentially, there is a risk of consuming significant portion of the global energy resources. New initiatives for greener communications are taken to reduce global energy consumption footprint. In existing cellular mobile networks, significant portion of energy is consumed by base stations. In addition to that, backend servers providing services to users and application servers in data centers also consume a lot of energy. Until now, the power saving considerations were made for mobile terminals and sensor devices that are difficult to recharge. While, this is very important and required for satisfying operating constraints, it is now being looked in for saving energy in the network infrastructure as well.

The other important consideration is the involved cost. Lowering infrastructure and operational cost are essential for businesses in communication sector to remain profitable. Communication networks are constantly evolving, and new technologies are developed each year. It is very difficult for the business enterprises to embrace all these new powerful technologies and remain updated for offering better services. Higher bandwidth offerings and the addition of new value added services to its users is not leading to a proportional increase in the revenue generated. Investment costs are skyrocketing, and profit margins are becoming tight. Now the point has come to revolutionize the adopted technology with new architectures to substantially lower investment and operational costs. This also includes changing the business model and ownership of the network infrastructure.

There is a huge cost to manage Big Data across different networks. As the size of the data grows, the cost for handling the data also grows. This growth in cost has to be reduced by innovative strategies that involve optimizing the utilization of hardware resources. Moving the data around the network involves communication costs. However, keeping the data available at fingertips needs a constant movement of data around different parts of the network and keep the frequently accessed chunk of data close to the users to avoid excessive delays. While redundancy in storing data is a favorable feature against network failures, it increases the cost of storage per unit of data. Therefore judicious strategies must be implanted

to reduce the cost of storage. An optimized strategy should be adopted that balances storage cost and availability. It must not be forgotten that more required storage leads to higher energy consumption.

### III. ARCHITECTURE FOR HETEROGENEOUS DEVICES AND NETWORK TYPES

Based on all the considerations that are discussed, that includes the different network types and heterogeneous devices attached to these networks, a single unified architecture for central management is an ambitious goal to achieve. However, that is the trend which is being adopted for reducing the operational costs. The ease of network management is the prime objective to reduce the burden of hiring and retaining network specialists. Network automation minimizes the delays that requires human intervention, and improve service quality. With automation, the network resources are efficiently managed. It is possible to operate networks in their optimized regions, leading to achieve better price versus performance results. More users can be accommodated and managed with less effort.

Starting with this simple objective of reducing operational costs, the solutions that were seem feasible to deploy have more potential benefits. Those benefits are reduced amounts of complex and specialized hardware through replacement with software based systems. Software systems can be better programmed according to the needed requirements, which configuring specialized hardware will do exactly the same operation. A solution in hardware is expensive than performing the same job through software programming on a general purpose device. It is easy to test new things and reprogram software systems. This philosophy is being adopted by business enterprises comprising network operators. They are replacing specialized network hardware equipment with general COTS based servers. The entire network functionality is realized in software implementation on these COTS servers. The other derived benefit of COTS servers is that they are more power efficient and consume less energy than the specialized network hardware.

The next highly preferred feature is a network solution that is scalable and easy to upgrade. Hardware solutions have many limitations to the scalability. Just adding new specialized servers to the rack is not always possible. After a certain stage, the entire hardware need to be replaced causing the solution to be expensive. The network operator will have to decide to move to the new solution or keep the old one due to space limitations in the server room. It is hard to revert back to the previous working scenario in hardware solutions if there is any problem with the new technology. Changes to the hardware equipment will cause network downtime. All these can be easily addressed in software configurable systems. New COTS servers can be added to the server farm as need arise to increase the computational power and storage space.

New solutions need to handle and manage Big Data with ease. Further, these new network solutions have to be cheap to store and process mammoth data. The costs and energy consumption can easily spiral without the right technology and the right solution. Any solution to keep Big Data at bay will be in large scale. This has to be kept in mind. The solution needs

hundreds of thousands of servers for processing and storing Big Data. Where to place these number of servers and how to power them and manage the heat generated by them is a big issue. Besides huge sized server farms, the management complexity should be minimal. Typically these data networks will be clusters of distributed server farms connected through high bandwidth links such as fiber optics. Latency is an issue when these server farms are far located. The data usage should be predicted and kept at optimal locations across the globe for instant access.

#### IV. BIG DATA DELIVERY AND INFORMATION PROCESSING

The main function of future IoT network infrastructure is to be able to deliver Big Data. Data from bits and pieces are amalgamated to form huge unstructured data providing many insightful ways of information for human needs and development. It is not just the infrastructure that is important, it is also important to know what we do with the existing infrastructure. How we build powerful applications that manage and harvest much needed information for our daily business. IoT infrastructure is the backbone for Big Data generation. On demand resources have to be provisioned by the network infrastructure to deliver Big Data to the right places at the right time. Many challenges remain in handling Big Data and one of this is how to efficiently deliver data. Data communication is not cheap as it requires tremendous resources and requires proper network setup and maintenance. Huge energy resources have to be allocated for data transmission. Servers that act as network routers consume power in the order of Mega watts per each day. It is, therefore, essential to know the power consumption per unit of data transfer.

Along with data transfer, is the storage and processing resources for the Big Data. New technologies are needed to reduce the storage cost by increasing the memory size per unit area. High density storage equipment will, in turn, reduce the amount of building space needed for the storage servers. The running costs for storing data is the power consumption of these servers, the airconditioning of the premises, and other wear and tear costs that are incurred on a daily basis. In addition to this is the manpower needed for maintaining the server farm. The computational power of today's available GPUs is high but consume a tremendous amount of power. Efficient data manipulation softwares are needed to intelligently compute data and derive results. These intelligent softwares must use lesser CPU cycles to achieve energy savings. Data analysis and information processing are critical to handle and maintain data. During computation, analysis, and storage, communication protocols in the network play a vital role.

#### V. CONCLUSION

Different kinds of communicating devices that are made for completely different objectives are communicating with each other over the IoT infrastructure. Different types of networks exist today giving connectivity to heterogenous devices which are both mobile and static. Trillions of such devices exist today giving rise to Big Data. New applications are being developed to harness information from proper handling of Big Data. At the same time network operators are faced with the dilemma whether or not to embrace new technologies because of tighter profit margins. Technology is changing and new innovations

are changing the way network communications take place, and that too at a fast pace. For all these reasons, new architecture of IoT is needed to address the concerns of profitability, better services, technology adaption, user growth, and energy conservation. For this reason, we have thoroughly discussed the various issues involved in building an architecture for IoT networks that requires Big Data Management.

#### REFERENCES

- [1] A. Mahapatro and P. M. Khilar, "Fault diagnosis in wireless sensor networks: A survey," *IEEE Communications Surveys & Tutorials*, vol. 15, no. 4, pp. 2000–2026, Fourth Quarter 2013.
- [2] I. Demirkol, C. Ersoy, and F. Alagöz, "Mac protocols for wireless sensor networks: A survey," *IEEE Communications Magazine*, vol. 44, no. 4, pp. 115–121, April 2006.
- [3] K. Hamad, S. Primak, M. Kalil, and A. Shami, "Qos-aware energy-efficient downlink predictive scheduler for ofdma-based cellular devices," to appear in *IEEE Transactions on Vehicular Technologies*, 2016.
- [4] H. Boostanimehr and V. K. Bhargava, "Unified and distributed qos-driven cell association algorithms in heterogeneous networks," *IEEE Transactions On Wireless Communications*, vol. 14, no. 3, pp. 1650–1662, March 2015.
- [5] O. G. Aliu, A. Imran, M. A. Imran, and B. Evans, "A survey of self organisation in future cellular networks," *IEEE Communications Surveys & Tutorials*, vol. 15, no. 1, pp. 336–361, First Quarter 2013.
- [6] Z. Hasan, H. Boostanimehr, and V. K. Bhargava, "Green cellular networks: A survey, some research issues and challenges," *IEEE Communications Surveys & Tutorials*, vol. 13, no. 4, pp. 524–540, Fourth Quarter 2011.
- [7] M. Kalil, A. Shami, A. Al-Dweik, and S. Muhaidat, "Low-complexity power-efficient schedulers for lte uplink with delay-sensitive traffic," *IEEE Transactions on Vehicular Technologies*, vol. 64, no. 10, pp. 4551–4564, October 2015.
- [8] M. Kalil, A. Shami, and A. Al-Dweik, "Qos-aware power-efficient scheduler for lte uplink," *IEEE Transactions on Mobile Computing*, vol. 14, no. 8, pp. 1672–1685, August 2015.
- [9] K. A. Meerja, P.-H. Ho, and B. Wu, "A novel approach for co-channel interference mitigation in femtocell networks," in *proceedings of IEEE Globecom 2011*, December 2011.
- [10] K. A. Meerja, P.-H. Ho, B. Wu, and H.-F. Yu, "Media access protocol for a coexisting cognitive femtocell network," *Computer Networks*, vol. 57, no. 15, pp. 2961–2975, October 2013.
- [11] Z. Yang, T. Ning, and H. Wu, "Distributed data query in intermittently connected passive rfid networks," *IEEE Transactions On Parallel And Distributed Systems*, vol. 24, no. 10, pp. 1972–1982, October 2013.
- [12] M. Shahzad and A. X. Liu, "Fast and accurate estimation of rfid tags," *IEEE/ACM Transactions On Networking*, vol. 23, no. 1, pp. 241–254, February 2015.
- [13] J. Cho, Y. Shim, T. Kwon, and Y. Choi, "Sarif: A novel framework for integrating wireless sensor and rfid networks," *IEEE Wireless Communications*, vol. 14, no. 6, pp. 50–56, December 2007.
- [14] L. Wang, L. Liu, X. Cao, X. Tian, and Y. Cheng, "Sociality-aware resource allocation for device-to-device communications in cellular networks," *IET Communications*, vol. 9, no. 3, pp. 342–349, February 2015.
- [15] S. Sun, Q. Gao, W. Chen, R. Zhao, and Y. Peng, "Recent progress of long-term evolution device-to-device in third-generation partnership project standardisation," *IET Communications*, vol. 9, no. 3, pp. 412–420, February 2015.
- [16] K. W. Choi and Z. Han, "Device-to-device discovery for proximity-based service in lte-advanced system," *IEEE Journal On Selected Areas In Communications*, vol. 33, no. 1, pp. 55–66, January 2015.
- [17] G. Wu, C. Yang, S. Li, and G. Y. Li, "Recent advances in energy-efficient networks and their application in 5g systems," *IEEE Wireless Communications*, vol. 22, no. 2, pp. 145–151, April 2015.

- [18] A. Moubayed, A. Shami, and H. Lutfiyya, "Wireless resource virtualization with device-to-device communication underlaying lte network," *IEEE Transactions on Broadcasting*, vol. 61, no. 4, pp. 734–740, December 2015.
- [19] S. Andreev, O. Galinina, A. Pyattaev, K. Johnsson, and Y. Koucheryavy, "Analyzing assisted offloading of cellular user sessions onto d2d links in unlicensed bands," *IEEE Journal On Selected Areas In Communications*, vol. 33, no. 1, pp. 67–80, January 2015.
- [20] Y. Ni, X. Wang, S. Jin, K.-K. Wong, H. Zhu, and N. Zhang, "Outage probability of device-to-device communication assisted by one-way amplify-and-forward relaying," *IET Communications*, vol. 9, no. 2, pp. 271–282, January 2015.
- [21] Q. Ye, M. Al-Shalash, C. Caramanis, and J. G. Andrews, "Distributed resource allocation in device-to-device enhanced cellular networks," *IEEE Transactions On Communications*, vol. 63, no. 2, pp. 441–454, February 2015.
- [22] M. G. Khoshkholgh, Y. Zhang, K.-C. Chen, K. G. Shin, and S. Gjessing, "Connectivity of cognitive device-to-device communications underlying cellular networks," *IEEE Journal On Selected Areas In Communications*, vol. 33, no. 1, pp. 81–99, January 2015.
- [23] Z. Zhou, M. Dong, K. Ota, R. Shi, Z. Liu, and T. Sato, "Game-theoretic approach to energy-efficient resource allocation in device-to-device underlay communications," *IET Communications*, vol. 9, no. 3, pp. 375–385, February 2015.
- [24] J. Qiao, X. S. Shen, J. W. Mark, Q. Shen, Y. He, and L. Lei, "Enabling device-to-device communications in millimeter-wave 5g cellular networks," *IEEE Communications Magazine*, vol. 53, no. 1, pp. 209–215, January 2015.
- [25] M. Jammal, T. Singh, A. Shami, R. Asal, and Y. Li, "Software-defined networking: State of the art and research challenges," *Computer Networks*, vol. 72, no. 0, pp. 74 – 98, October 2014.
- [26] M. Jammal, A. Kanso, and A. Shami, "Chase: Component high availability-aware scheduler in cloud computing environment," in *Cloud Computing (CLOUD), IEEE 8th International Conference on*, June-July 2015, pp. 477–484.
- [27] —, "High availability-aware optimization digest for applications deployment in cloud," in *IEEE International Conference on Communications (IEEE ICC)*, June 2015.
- [28] H. Hawilo, A. Shami, M. Mirahmadi, and A. Asal, "Nfv: State of the art, challenges and implementation in next generation mobile networks (vepc)," *IEEE Network*, vol. 28, no. 6, pp. 18–26, November-December 2014.
- [29] H. Hawilo, A. Kanso, and A. Shami, "Towards an elasticity framework for legacy highly available applications in the cloud," in *Services (SERVICES), 2015 IEEE World Congress on*, June-July 2015, pp. 253–260.
- [30] K. Alhazmi, M. A. Sharkh, and A. Shami, "Drawing the cloud map: Virtual network provisioning in distributed cloud computing data centers," *to appear in IEEE Systems Journal*, 2016.
- [31] K. A. Meerja, A. Shami, and A. Refaey, "Hailing cloud empowered radio access networks," *IEEE Wireless Communications*, February 2015.
- [32] M. A. Sharkh, A. Kanso, A. Shami, and P. Öhlén, "Building a cloud on earth: A study of cloud computing data center simulators," *Computer Networks*, vol. 108, pp. 78–96, October 2016.

# An Improved Approach for Text-Independent Speaker Recognition

Rania Chakroun<sup>1,4</sup>, Leila Beltaïfa Zouari<sup>1,3</sup>, Mondher Frikha<sup>1,2</sup>

<sup>1</sup>Advanced Technologies for Medicine and Signals (ATMS) Research Unit

<sup>2</sup>National School of Electronics and Telecommunications of Sfax, Sfax, Tunisia

<sup>3</sup>National School of Engineering of Sousse, Sousse, Tunisia

<sup>4</sup>National School of Engineering of Sfax, Sfax, Tunisia

**Abstract**—This paper presents new Speaker Identification and Speaker Verification systems based on the use of new feature vectors extracted from the speech signal. The proposed structure combine between the most successful Mel Frequency Cepstral Coefficients and new features which are the Short Time Zero Crossing Rate of the signal. A comparison between speaker recognition systems based on Gaussian mixture models using the well known Mel Frequency Cepstral Coefficients and the novel systems based on the use of a combination between both reduced Mel Frequency Cepstral Coefficients features vectors and Short Time Zero Crossing Rate features is given. This comparison proves that the use of the new reduced feature vectors help to improve the system's performance and also help to reduce the time and memory complexity of the system which is required for realistic applications that suffer from computational resource limitation. The experiments were performed on speakers from TIMIT database for different training durations. The suggested systems performances are evaluated against the baseline systems. The increase of the proposed systems performances are well observed for identification experiments and the decrease of Equal Error Rates are also remarkable for verification experiments. Experimental results demonstrate the effectiveness of the new approach which avoids the use of more complex algorithms or the combination of different approaches requiring lengthy calculation.

**Keywords**—GMM; speaker verification; speaker recognition; speaker identification

## I. INTRODUCTION

The speech signal is an information rich signal that conveys various data to the listener. In addition to the message and words being spoken, the speech conveys much other information such as the language used, the emotion of the speaker, the gender and also the identity of the speaker.

Based on the speech signal, the main goal of automatic speaker recognition is to extract and characterize the information in the speech signal conveying the identity of the speaker.

The broad area of speaker recognition comprehends two fundamental tasks which are speaker identification and speaker verification.

For speaker identification, the system aims at determining who is talking from a set of known voices. The system looks then for the voice which best matches the unknown speaker which makes no identity claim. Speaker identification can be

also divided into closed set or open set speaker identification. For the closed set problem, the unknown voice must be among a fixed set of known speakers. However, for the open set speaker identification, the unknown speaker may not exist among the set of known speakers. So, unknown voices are referred to as unknown speakers.

For the task of speaker verification, the system tries to determine whether the unknown person is who he/she claims to be or not. The system makes then a binary decision. Even it accepts the pretended speaker or it reject this unknown speaker.

Depending on the message being spoken by the speaker, the speech used for speaker recognition applications can be either text dependent or text-independent. For text-dependent speaker recognition application, the recognition system has prior knowledge of the text that must be spoken and the system requires that the speaker says exactly the given text. However, for text-independent speaker recognition application, there is no prior knowledge about the text to be spoken, and the speaker is free to say any message he want. Text independent speaker recognition applications are then more difficult but also more flexible.

In this context, this work aims to propose a new approach for Text independent speaker recognition applications based on the use of new information extracted from the speech signal. The proposed system use the Short Time Zero Crossing Rate (STZCR) [14] information with reduced cepstral features to ensure higher performance for the system and also guarantee a reduction of the time and memory complexity of the system. The results are compared to state-of-the-art systems.

This paper is organized as follows: First, related works are summarized. Then, the approach used for the speaker recognition systems is explained. After that, a description of the database used during the experiments is given, followed by a description of the experimental protocol and their results. These results are compared with the state-of-the-art speaker recognition systems. Finally, a conclusion illustrating the main matter of the proposed system for speaker recognition is provided.

## II. RELATED WORKS

Research and development on speaker recognition field have lead to powerful methods and techniques permitting high performing applications. The most successful approaches are modern statistical approaches [20] where the Gaussian Mixture

Models (GMM) [3] is considered as the most popular approach for current speaker recognition systems [21].

It is also interesting to note that, the process of extracting features from the speech signal is a fundamental process on which the system depends to capture the speaker specific characteristics. For that, many features have been investigated in the literature [2], [11] where the cepstral features [6] are the most appropriate ones for speaker recognition tasks. Up today, the most popular and successful cepstral features are Mel frequency cepstral coefficients (MFCC) [3], [10], [22].

Since speaker recognition application succeed to achieve good performances with appropriate conditions [19], current speaker recognition applications looks for more realistic and challenging conditions. In fact, current speaker recognition systems require a quality recording environment with as large as possible of a set of training and testing data. A more extensive speech database increases the chance of matching during the test phase. There are also some other technical parameters that can be take into account, which alter the system's effectiveness. The main factors are related to the approach used and the features to be extracted from the speech signal. The systems used in this article have been developed using the well-known state-of-the art approach which is the GMM. Most of the works in this area focus on the use of cepstral coefficients. However, this work focuses on determining whether the Short Time Zero Crossing Rate [14] information is useful for improving current state-of-the-art automatic speaker recognition systems.

### III. PROPOSED APPROACH

The proposed system for speaker recognition task is shown in Figure 1. The learning phase serves to acquire the characteristics of every speaker from the extracted parameters. A test utterance is input to the system and the recognition task is realized with Gaussian Mixture Models (GMM).

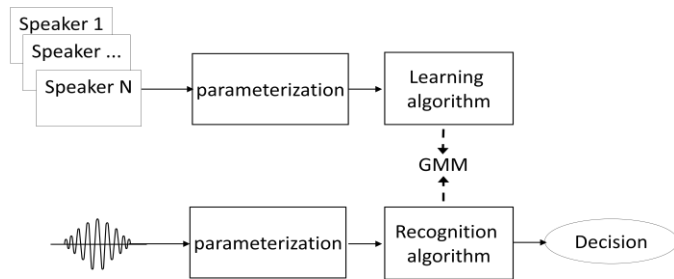


Fig. 1. The architecture of the Automatic Speaker Recognition system

#### A. GMM approach

The GMM approach can be considered as a model reference for speaker recognition systems [3], [4], [15].

For an utterance of length T frames belonging to a speaker j and D-dimensional feature vector extracted for each frame, so for each utterance:  $\{x_t \in \mathbb{R}^D : 1 \leq t \leq T\}$ , A Gaussian model for a speaker j for any utterance from that same speaker assumes that feature vectors follow a Gaussian distribution,

characterized by a mean and a deviation about the mean. Indeed, The Gaussian mixture model for speaker j,  $\lambda_j$  is a weighted sum of M component densities calculated as follows [3]:

$$p(x_t | \lambda_j) = \sum_{i=1}^M g_i N(x_t; \mu_i, \Sigma_i) \quad (1)$$

Where  $g_i$  are mixtures weights having  $\sum_{i=1}^M g_i = 1$ . The

individual component densities  $N(x_t; \mu_i, \Sigma_i)$  represent:

$$N(x_t; \mu_i, \Sigma_i) = \frac{1}{(2\pi)^{D/2} |\Sigma_i|^{1/2}} \times \exp\left[-\frac{1}{2} (x_t - \mu_i)' \Sigma_i^{-1} (x_t - \mu_i)\right] \quad (2)$$

Where  $\mu_i$  is the mean vector and  $\Sigma_i$  is the covariance matrix.

The GMM model for the speaker j, presented by  $\lambda_j$ , is parameterized by the mean vectors, covariance matrices and mixture weights from all M component densities:

$$\lambda_j = \{ \mu_i, \Sigma_i, g_i \}_{i=1, 2, \dots, M} \quad (3)$$

#### a) GMM for speaker identification

In the test phase, an utterance having T feature vectors

$$X = \{x_1, x_2, \dots, x_T\}$$

is presented to the system. The main objective of an identification system is to find from N GMM speaker models, the model of the speaker which has the maximum a posteriori probability [9] for that input feature vector sequence:

$$\hat{j} = \arg \max_{1 \leq j \leq N} P(\lambda_j | X) \quad (4)$$

Where  $\hat{j}$  is the identified speaker.

With the use of logarithms and the assumed independence between the observations, the decision can be shown with Maximum-Likelihood (ML) scoring of the log likelihoods:

$$\hat{j} = \arg \max_{1 \leq j \leq N} \sum_{t=1}^T \log P(x_t | \lambda_j) \quad (5)$$

Where  $P(x_i | \lambda_j)$  is given above in equation 1.

b) *GMM for speaker verification*

The speaker verification system need to make a binary decision, even it accepts or rejects the pretence speaker. The verification system uses a likelihood ratio test to an input speech sequence in order to detect if the claimed speaker is true

or false. Indeed, for an input vector  $X = \left\{ \overset{\rightarrow}{x_1}, \overset{\rightarrow}{x_2}, \dots, \overset{\rightarrow}{x_T} \right\}$ , and a claimed speaker having a model  $\lambda_c$ , the likelihood ratio is as follows[7]:

$$\frac{p(X \text{ is from the claimed speaker})}{p(X \text{ is not from the claimed speaker})} = \frac{p(\lambda_c | X)}{p(\lambda_{\bar{c}} | X)} \quad (6)$$

With the application of Bayes' rule, the likelihood ratio becomes

$$\Lambda(X) = \log p(X | \lambda_c) - p(X | \lambda_{\bar{c}}) \quad (7)$$

The likelihood ratio between the pretence speaker model and other models (back ground models) is compared to a given threshold  $\theta$  [9]. The claimed speaker is accepted only if  $\Lambda(X) > \theta$ .

B. *Short Time Zero Crossing Rate (STZCR)*

Speech is a signal produced from a time varying vocal tract system with a time varying excitation. That's why, the speech signal is considered as non-stationary in nature. This signal is stationary when it is viewed in blocks of 10-30 msec [16]. Short Time processing divides the input speech signal into short analysis segments that have realatively fixed (non-time varying) properties. These short analysis segments called as analysis frames almost overlap one another.

Zero Crossing Rate is defined as the number of times the zero axes is crossed by the signal per frame. If the number of zero crossings is more in a given signal, then the signal is changing rapidly and accordingly the signal may contain high frequency information which is termed as unvoiced speech. On the other hand, if the number of zero crossing is less, then the signal is changing slowly and accordingly the signal may contain low frequency information which is termed as voiced speech [17]. That's why the Zero Crossing Rate can gives information about the frequency content of the signal, which can be considered as a good indicator about the speaker itself. Short Time Zero Crossing Rate is defined as the weighted average of number of times the speech signal changes sign within the time window [18]. The STZCR for a signal having the window  $\omega(n)$  with length  $n$  is defined as [18]:

$$Z_n = \frac{1}{2} \sum_m |\text{sgn}[x(m)] - \text{sgn}[x(m-1)]| \cdot \omega(n-m) \quad (8)$$

with:

$$\begin{aligned} \text{sgn}[x(n)] &= 1 \text{ if } x(n) \geq 0 \\ &= -1 \text{ if } x(n) < 0 \end{aligned}$$

IV. EXPERIMENTAL RESULTS

A. *TIMIT corpus*

In this paper, speaker verification and identification tasks are evaluated with TIMIT (Texas Instruments Massachusetts Institute of Technology) database. The TIMIT corpus has been designed to provide speaker data for the acquisition of acoustic-phonetic knowledge and also for the development and evaluation of automatic speaker recognition systems [12]. TIMIT contains in totality 6300 sentences with 10 sentences spoken by each one of the 630 speakers. The speakers are from the 8 major dialect regions of the United States. The speech signal was sampled at 16 kHz sampling frequency.

B. *Experiments*

All evaluations are dealt with 64 speakers selected from all the regions of TIMIT database. Following the protocol suggested in [3], the sentences recorded from each speaker are divided into 8 utterances for training task (two SA, three SX and three SI sentences) and the remaining 2 utterances (two SX sentences) for the test task.

Mel frequency cepstral coefficients (MFCC) features have been used for extracting features from the speech signal. Since many years, these features proved their success in speaker recognition domain [1], [3], [5]. In this work, MFCC features are used, since they are the most popular choice for any speaker recognition system [3]. The experiments operate on cepstral features extracted from the speech signal with a 25-ms Hamming window. Every 10 ms, 12 MFCC together with log energy were calculated. Then Delta and delta-delta coefficients are calculated to produce 39-dimensional feature vectors. Indeed, this MFCC feature vector constitutes one of the most broadly used vectors to this day [3], [5]. The features were extracted using the Hidden Markov Model ToolKit (HTK) [8].

Since realistic applications suffer from some constraints like computational resource limitation or reduced memory space, this work looks for an improved approach using more reduced feature vectors and ameliorating the system's performance. In this context, the inclusion of new information extracted from the speech signal which is STZCR of the signal [14] with reduced MFCC feature vectors can improve the system's performance and give significant results. For that, MFCC vector are combined with STZCR features. The new structure of the vectors is evaluated and compared with traditional MFCC vectors.

a) *Speaker identification systems*

For speaker identification experiments, the number of mixture components is varied from 1 to 256 mixtures and the correct Identification Rates (IR) given with the different feature vectors are plotted in Figure 2.

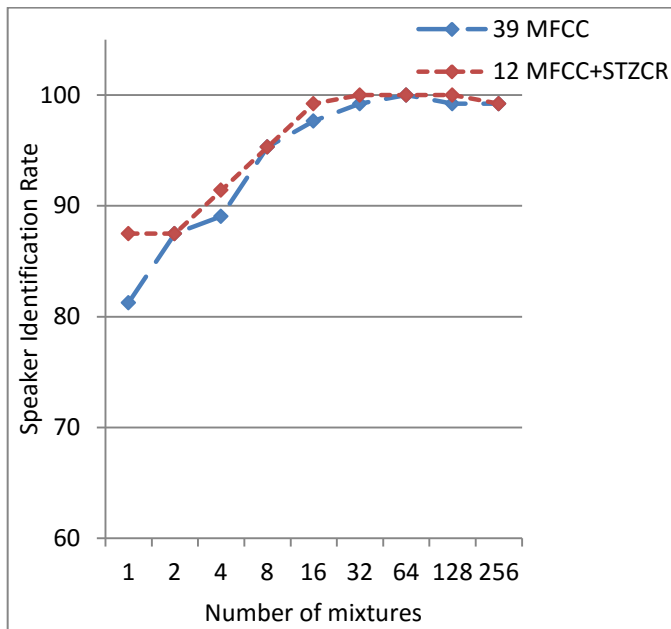


Fig. 2. Speaker IR with different feature vectors for 8 utterances for the training task and 2 utterances for the test task for various number of mixtures of GMM

In this study, identification experiments are done to demonstrate the feasibility of using STZCR of the signal to improve the system's performance. The results obtained with different feature vectors show that the use of MFCC coefficients together with STZCR can give more significant results. In fact, the proposed system succeeded to improve the performance of the system and achieved the best result of 100% of correct Identification Rate with the number of 32 mixtures components with only 12 MFCC together with STZCR for 8 utterances for training and 2 utterances for the test task. However, with 39 MFCC feature vectors, the system achieved 100% of correct Identification Rate only with 64 mixtures components with deterioration of the system performance when more components are added.

To further examine the effectiveness of the proposed parameterization, the system's performance is evaluated for more reduced training data. Experimental results were then evaluated for 3 utterances for training and 2 utterances for the test task. The curves given in figure 3 present the results obtained by using 39-dimensional MFCC feature vectors and 12-MFCC coefficients together with STZCR on speakers from TIMIT database.

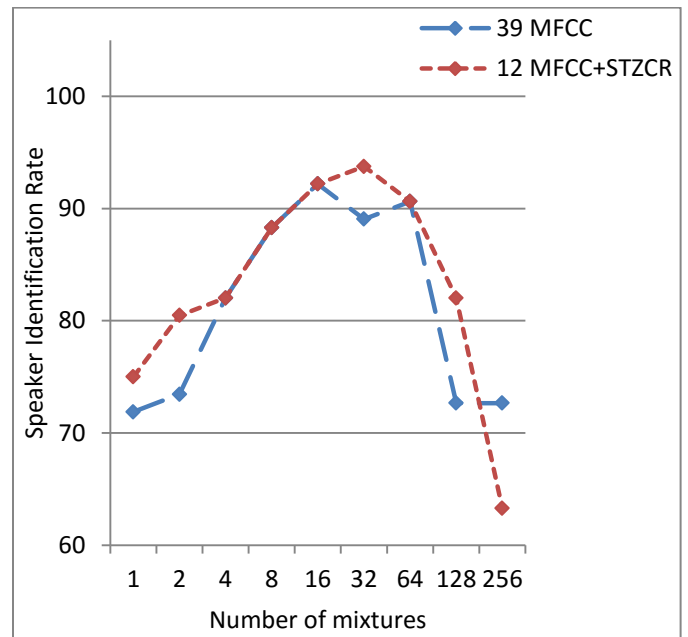


Fig. 3. Speaker IR with different feature vectors for 3 utterances for the training task and 2 utterances for the test task for various number of mixtures of GMM

From the curves presented above, it can be seen that the use of the proposed feature vector composed of MFCC coefficients together with STZCR gives more significant results than the standard MFCC coefficients. In fact, the performance of the system is improved and achieved the best result of 93.75 % of correct Identification Rate with 32 mixtures components with only 12 MFCC together with STZCR for 3 utterances for training and 2 utterances for the test task. However, the system achieved only 92.19 % of correct Identification Rate with 16 mixtures components with 39 MFCC feature vectors. These results explained the superiority of the proposed approach towards the state of the art applications.

#### b) Speaker verification systems

Speaker verification experiments for the different speakers are dealt for the different feature vectors with 8 utterances for the training task and 2 utterances for the test task. The Equal Error Rates (EER) given with each of the feature vectors are plotted in Figure 4.

Figure 4 shows the results obtained by using the two kinds of feature vectors for 8 utterances for training and 2 utterances for the test task. As can be seen from the graph, the new feature vector succeeded to reduce the EER of the system and gives the best result of 2.26% of EER for 128 mixtures components. However, for the state-of-the-art system based on 39-dimensional feature vectors, the best result realized was only 13.28 % of EER for 64 mixtures components.

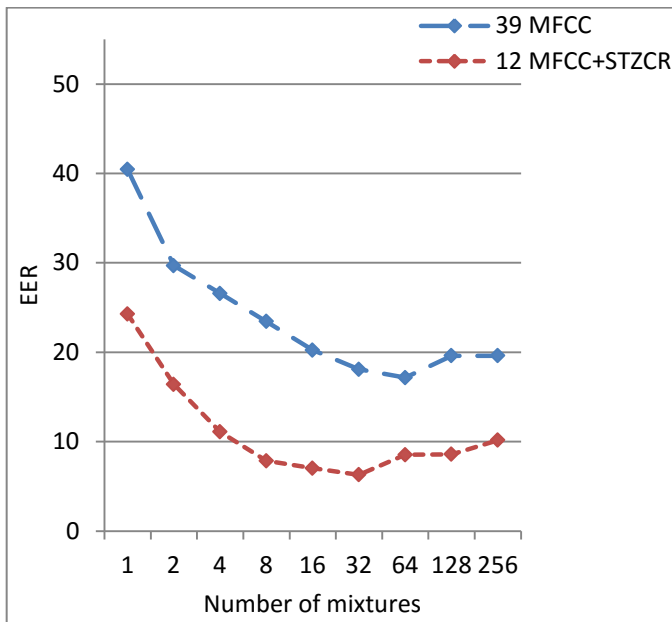


Fig. 4. EER with different feature vectors for 8 utterances for the training task and 2 utterances for the test task for various number of mixtures of GMM

Comparative results between best verification results obtained with the different verification systems evaluated with 39-MFCC feature vectors and 12-MFCC coefficients together with STZCR are given with The DET curves [13] plotted in Figure 5.

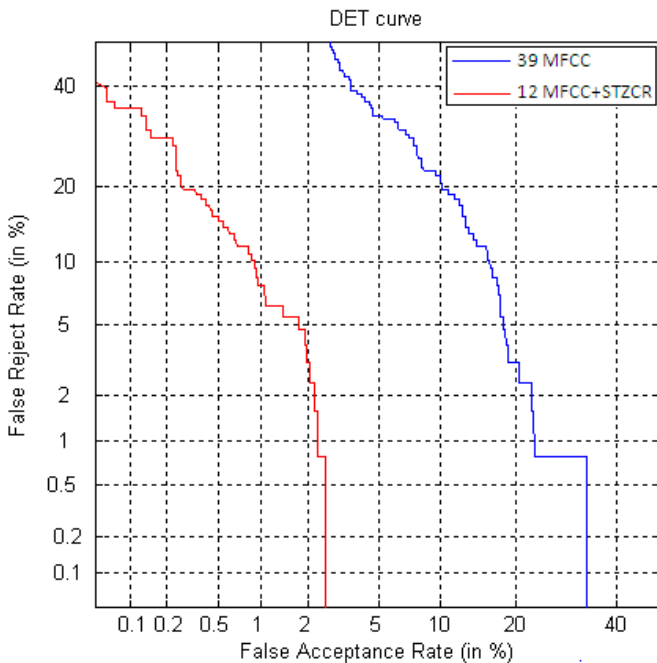


Fig. 5. Detcurves comparison between the different feature vectors with 8 utterances for the training task and 2 utterances for the test task

By examining the results given above with DET curves, it is clear to conclude that the proposed methods yield to more significant results. The use of the combination between reduced MFCC features and STZCR is more appropriate

because it avoids the use of high dimensional feature vectors and it gives more efficient system.

In addition to the reduction of the dimension of feature vectors to resolve the problems related to computational resource limitation for realistic applications, the need of limited speakers data is also essential to diminish the system's complexity. That's why, the performance of the system with more reduced training data. The Equal Error Rates (EER) given with each of the feature vectors for 3 utterances for the training task and 2 utterances for the test task are plotted in Figure 6.

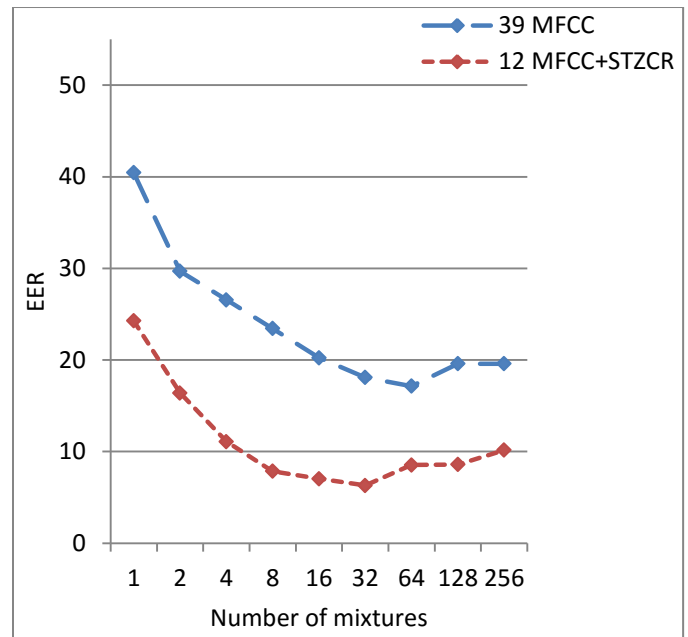


Fig. 6. EER with different feature vectors for 3 utterances for the training task and 2 utterances for the test task for various number of mixtures of GMM

The results presented above highlight the influence of the amount of training data on the system performance. Indeed, experimental results show that the performance of the GMM-based speaker recognition system decreases when the speech utterance duration becomes shorter.

The results obtained clearly demonstrate that the inclusion of the new information extracted from the speech signal which is the STZCR of the signal with reduced MFCC feature vectors dimension can improve the system's performance and give more significant results. In fact, the proposed system achieved a reduction of nearly 11 % of EER with regard to EER obtained with the state-of-the-art systems based on 39-dimensional feature vectors with a reduced training time. Indeed, the best result achieved with the proposed system achieved 6.30 % of EER with 32 mixtures components. However, the state-of-the-art system achieved the best result of 17.15% of EER for 64 mixtures components.

The DET curves given in Figure 7 present comparative results between best verification EER obtained with verification systems evaluated with the different feature vectors.

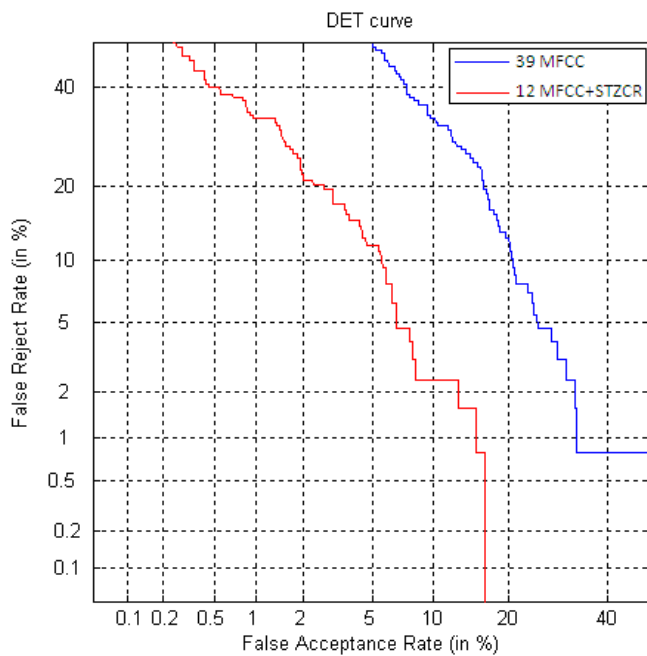


Fig. 7. Detcurves comparison between the different feature vectors with 3 utterances for the training task and 2 utterances for the test task

Throughout this study, it can be seen that the proposed approach gives better results than the results obtained by the state-of-the-art speaker identification and verification systems. The use of the new approach seems to be quite favorable to realistic speaker recognition systems since it avoids the use of high dimensional feature vectors or the combination of complex algorithms requiring more computational and memory costs.

## V. CONCLUSIONS AND PERSPECTIVES

This paper identifies the importance of using Short Time Zero Crossing Rate of the signal to improve speaker recognition. It presents a new approach based on low dimensional feature vectors composed by reduced MFCC feature vector together with STZCR of the signal. This new approach gives better results than those obtained by the baseline systems with Gaussian mixture models. The proposed method substantially improves the system performance and avoids the use of additional, lengthy and complicated calculations.

Future work will also investigate the performance of the proposed system with other features or applications.

### REFERENCES

[1] N. Dehak, Z. Karam, D. Reynolds, R. Dehak, W. Campbell, and J. Glass, "A Channel-Blind System for Speaker Verification", Proc. ICASSP, pp. 4536-4539, Prague, Czech Republic, May 2011.  
[2] N R. Mammone, X. Zhang, and R. Ramachandran, "Robust speaker recognition: A feature-based approach," IEEE Signal Processing Mag., vol. 13, no. 5, pp. 58-71, 1996.

[3] R. Togneri and D. Pullella, "An Overview of Speaker Identification: Accuracy and Robustness Issues", In: IEEE Circuits And Systems Magazine, Vol. 11, No. 2 , pp. 23-61, ISSN : 1531-636X, 2011.  
[4] D. A. Reynolds, "A Gaussian Mixture Modeling Approach to Text Independent Speaker Identification", PhD Thesis. Georgia Institute of Technology, August 1992.  
[5] T. Kinnunen and H. Li, "An overview of text-independent speaker recognition: From features to supervectors", Speech Communication 52(1): 12-40, 2010.  
[6] D. Reynolds, "Experimental evaluation of features for robust speaker identification," IEEE Trans. Speech Audio Process., vol. 2, no. 4, pp. 639-643, 1994.  
[7] D. A. Reynolds, T. F. Quatieri, and R. B. Dunn, "Speaker verification using adapted Gaussian mixture models", Digital Signal Process., vol. 10, no. 1-3, pp. 19-41, 2000.  
[8] S. Young, D. Kershaw, J. Odell, D. Ollason, V. Valtchev, and P. Woodland, "Hidden Markov model toolkit (htk) version 3.4 user's guide", 2002.  
[9] D. A. Reynolds, "Speaker identification and verification using Gaussian mixture speaker models," Speech Commun., vol. 17, no. 1-2, pp.91-108, 1995.  
[10] Ramaligeswararao, N. M., V. Sailaja, and K. Srinivasa Rao. "Text Independent Speaker Identification using Integrated Independent Component Analysis with Generalized Gaussian Mixture Model." THE SCIENCE AND INFORMATION ORGANIZATION (2011): 85.  
[11] Kekre, H. B., and Vaishali Kulkarni. "Speaker Identification using Frequency Distribution in the Transform Domain." www.thesai.org/info@thesai.org (2012).  
[12] Garofolo, J. S., Lamel, L. F., Fisher, W. M., Fiscus, J.G., Pallett, D. S., and Dahlgren, N. L., "DARPA TIMIT Acoustic Phonetic Continuous Speech Corpus CDROM, "NIST, 1993.  
[13] A. Martin, G. Doddington, T. Kamm, M. Ordowski, and M. Przybocki, "The DET Curve in Assessment of Detection Task Performance", in EUROSPEECH, vol. 4, pp. 1895-1898, 1997.  
[14] L.R. Rabiner, and R.W. Schafer, Digital speech processing. The Froehlich/Kent Encyclopedia of Telecommunications, 6, pp.237-258, 2011.  
[15] C. Barras & J. Gauvain, "Feature and score normalisation for speaker verification of cellular data", International Conference on Acoustics, Speech, and Signal Processing(ICASSP), in Hong Kong SAR, China, April 6-10, 2003.  
[16] Ronald W.Schafer and Lawrence R.Rabiner, "Digital Representations of Speech Signals", Proceedings of the IEEE, Vol.63, No.4, April 1975.  
[17] R.G.Bachu, S.Kopparthi, B.Adapa and B.D.Barkana, "Voiced/Unvoiced Decision for Speech Signals Based on Zero-Crossing Rate and Energy", Advanced Techniques in Computing Sciences and Software Engineering, pp.279-282, 2010.  
[18] Lawrence R.Rabiner and Ronald W.Schafer, "Introduction to Digital Speech Processing", Foundations and Trends in Signal Processing, Vol.1, No.33-53, 2007.  
[19] Reynolds, D. An overview of automatic speaker recognition Technology. In Proceedings of the International Conference on Acoustics, Speech and Signal Processing (ICASSP)(S. 4072-4075). (2002).  
[20] N. Fatima and T. F. Zheng, "Short Utterance Speaker Recognition A research Agenda", In International Conference on Systems and Informatics (ICSAD), 2012.  
[21] P. Motlicek, S. Dey, S. Madikeri, and L. Burget, "Employment of Subspace Gaussian Mixture Models in speaker recognition." Acoustics, Speech and Signal Processing (ICASSP), 2015 IEEE International Conference on. IEEE, 2015.  
[22] Almaadeed, Noor, Amar Aggoun, and Abbes Amira. "Text-Independent Speaker Identification Using Vowel Formants." Journal of Signal Processing Systems 82.3: 345-356, 2016.

# Using Persuasive Recommendations in Wellness Applications based upon User Activities

Hamid Mukhtar

Department of Computer Science, College of CIT Taif  
University, Taif, 21974, Kingdom of Saudi Arabia

**Abstract**—Recently, a large number of mobile wellness applications have emerged for assisting users in self-monitoring of daily food intake and physical activities. While such applications are in abundance, many research surveys have found that the users soon give them up after giving some initial try. This article presents our application for healthcare self-management that monitors users' activities but –unlike the existing applications– it focuses on keeping the users engaged for self-management. The distinguishing feature of our application is that it uses persuasive mechanisms to help users adopt healthy behavior. For this purpose, users' various activities are monitored and then they are persuaded using different persuasion strategies that are adaptive and are according to their behavior.

For each user, a behavior model is created that is based on Fogg's behavior model but, in addition, it also holds within it user preferences, and user health profile. The behavior model is then used to create a persuasion profile of the user that allows us to propose personalized suggestions targeted to overcome his lacking behavior. We also describe a case study that describes the actual application.

**Keywords**—user goal; modeling; user feedback; context; preferences

## I. INTRODUCTION

To promote a behavioral change can be a challenge for most people as changing a lifestyle habit often means trying something new and different from the ordinary, and this has proven difficult. Karapanos [1] argues that contrary to the common belief that behavior change is the result of deep knowledge about one's own behaviors, they found that people rarely look back at their past performance data and may not have deep knowledge about their own behaviors. Rather, a glance of a brief, 5-second session make them knowledgeable about their behavior where users check how much they have walked so far without any further interaction.

As the healthcare costs have risen significantly, much of the recent healthcare research focuses on self-management of health. Systems have been developed that monitor users for their health-related behavior and make informed decisions to help them in attaining better health. Future environments are envisioned to be populated with such computational technologies that adapt to meet the needs of individual users. However, such technologies will be effective only if the users feel comfortable in adopting them. Unfortunately, while the existing solutions for healthcare self-management focus on the improvement of data acquisition and analysis methods, they have not achieved the desired outcome because of the resistance by the users to adopt them.

There are several reasons for them. First, as human beings, we are not interested to perform a task unless we associate

it with some sort of outcome that is beneficial. Thus, it is unrealistic to expect that users will use some system without knowing or receiving any benefits from the system. That is why, when designing applications and systems for healthcare self-management, we should take extra measures and consider additional requirements as well. Second, usually such systems require the users to wear or carry-on additional accessories, usually electronic equipment, to keep track of their health. But people usually feel about them as an overhead that should be avoided. Third, self-management requires the user to be determined and undertake certain activities which may have compromising effects on their personal life-style. Since nobody likes such changes, people resist to adopt such systems which change the normal *status quo* of the users.

To address such issues, researchers have suggested the use of technology for persuading people for changing their behavior. Persuasive technology is defined as, "any interactive computing system designed to change people's attitudes or behaviors" [2]. Two of the most widely used persuasive technologies are mobile devices and websites. Mobile devices have added advantage for supporting behavior change because they are always in the ON state can intervene at the right time, in the right context, in a convenient way [2]. Moreover, virtually everyone has got a mobile phone so they are suitable for the development of persuasive applications. That is why most of the recent research work focuses on mobile phone based health intervention systems and applications.

However, everyone cannot be persuaded using the same approach. Different people are persuaded differently for different reasons related to their behavior, attitude, lifestyle, social setup, etc. For example, let's consider the health-related goal of *Going for a 30 minute walk daily early morning*. Although the goal is very clear and it should be achievable. However, most of the people fail to do so. Some people simply do not have the motivation to wake up early from the bed. Others may be motivated and would wake up early but they may not find the time for a walk. Similarly, some people will be both motivated and have time but they simply forget about it. For this purpose, various persuasion strategies can be used to persuade users and help them in changing their behavior. Each user can be persuaded by different strategies at different times. Previously, we developed a mobile phone application called Sedentaware whose purpose was to promote activeness in adults by monitoring their physical activities and providing them with appropriate feedback to adjust their behavior accordingly [3]. To make the application engaging for the users, we used several design techniques that would

persuade the users to take preventive actions. The current work addresses some limitations of that work as well as proposes some enhancements to it.

One of the foremost motivating aspects used in our app is that of goal setting whereby the user is empowered to define their own means for achieving the desired level of fitness. In our case, the goal is set in terms of number of minutes of daily walk. Users feel more engaged when they have the ability to manage set their goals. Moreover, from persuasion point of view, this also means they abide by keeping to their goal more often. In case the users do not follow the goal, the persuasive messages try to get them back on track. As found by Karapanos [1], individuals who have the intention but not yet the means (i.e. motivation) to change, had an adoption rate of 56%, whereas individuals in pre-contemplation, action or maintenance stages had an adoption rate of only 20%.

In this article, we extend on our previous work and present our approach for healthcare self-management considering the above mentioned aspects. Our focus is more towards developing an intelligent system for recommending the users rather than solely following other users or doctors as done by various existing systems. As discussed in [3], users are monitored for activities using the sensors on their mobile phones and recommendations are provided according to their profile, health level, and preferences. In the current approach, the objective is to describe how to persuade users for behavior change using the appropriate strategies designed for this purpose. The persuasion strategies have been designed using a formal behavior model.

In addition to monitoring the users, the application also provides analysis using a rule-based system. On the basis of analysis outcomes, the user is suggested activities according to their past behavior and their current preferences. The activities are then assessed and compared with the user's health-related variables. In case of any conflict, a precisely defined goal is set for the user in the form of a target behavior to be adopted. Thereafter, the user is monitored for the new goal.

The remainder of the article is organized in the following manner. In the next section, we describe related work and advances in healthcare self-management as well as use of persuasive technology for that purpose. Section III explains the steps carried out in our design based upon the guidelines set forth by BJ Fogg. In Section IV, we explain the underlying model behind our approach and the developed mobile application on top of it. Section V, we explain how different persuasion strategies can be applied for behavior change based on Fogg's behavior model. Finally, in Section VI we describe the prototype implementation of our application considering diabetes self-management as a case study. We then conclude this article with a brief discussion of future work in Section VII.

## II. RELATED RESEARCH IN PERSUASIVE HEALTHCARE

Mobile apps have been one of the most adapted mechanism persuasion, whether in healthcare, education, e-government, politics, etc. It is mainly because of the added value and benefit of mobile phones' ability to adapt day-to-day interactions based on previous usage patterns [4]. Moreover, mobile service benefits include extensive data capturing throughout the day to

enable more participant empowerment, improved data quality for the health management process, improved feedback options based on improved data in different types of visualizations suited for the type of data, stimulating the ownership of their health by the users, more health data integration at the level of the person involved, etc. [5].

Persuasive technologies have been used in healthcare domain for: motivating healthier behavior using smartphones [6], motivating elderly individuals to walk [7] encouraging social and physical activities [8], self-management of chronic diseases such as diabetes, stroke, Alzheimers, obesity, etc. [9], promoting health education in children [10], and for changing existing social beliefs and health practices of rural women in a positive manner [11].

More relevant to our work is the UbiFit Garden system that was designed to encourage regular physical activity using persuasion [12]. The system mainly comprises of wearable sensors for detecting and tracking people's physical activities and displaying them through an aesthetic image in the form of a flower garden. When the sensors detect that user has performed some physical activity, the appearance of the garden improves by adding new elements, such as butterflies, flowers and plants. If no physical activity is detected from the user, the flowers in the garden perish slowly. This induces a sense of motivation in the users and they continue with their physical activities.

The Chinese Aged Diabetes Assistant (CADA) project<sup>1</sup> is using mobile device for healthcare management to enable multiple forms of input to accommodate users with very basic computer skills. It supports a range of self-management and educational activities needed for self-care. The data obtained can be readily shared with physicians given the existing infrastructure. To help users in adopting the system, this project is using the users' own cultural (Chinese) icons for eliciting and gathering user requirements and goals and also for the sake of education.

Lin et al. [13] have developed a Web 2.0 based diabetes support system with care provider perspectives. The system supports care managers in a health service center to conduct patient management through collecting patients daily physiological information, sharing care information, and maintaining patient-provider relationships. However, there is no support for other media including mobile phones. Moreover, it does neither consider patients' perspective nor it outlines how the social capabilities of Web 2.0 can be utilized to support patients.

After looking at all these efforts of assisting users for healthcare self-management, we find focus on monitoring the user's data and then giving feedback to them. A user is advised in some traditional way and then it is left to them how to bring in these changes for self-improvement. In our opinion, any system designed for wellness of users should be able to identify the lacking aspects and then it should include not only assistance but help users in motivating in that particular aspect.

Tatara et al. [14] conducted a survey regarding feasibility of using mobile phone based terminal for acceptability or effectiveness of self-management of diabetes. The finding was that acceptability factors depend on variables like motivation in

<sup>1</sup><http://www.cadaproject.com/>

self-management, long-term adherence, relationship between patients, and long term application use among others. The research concludes that various factors such as lifestyles, skills, and cognitive abilities of patients need to be considered when using mobile-based healthcare applications.

Based on the analysis of above mentioned limitations and problems in the existing solutions, we now describe our application in detail.

### III. DESIGN RATIONALE

B.J. Fogg proposed eight steps to outline a path to follow in designing persuasive technologies [15]. Considering these 8 steps as guidelines, we explain here our design methodology.

Step 1: Choose a simple behavior to target for change: In our work we have chosen the exercise habit (particularly walk for a specific duration) as our behavior target.

Step 2: Choose a receptive audience: During our research phase, we preferred to rely on the research team consisting of two Master students (aged 22 and 23), a PhD researcher (aged 29) and the supervisor (aged 54). Once a working prototype was developed, we chose three more participants (ages 24, 27, and 56) to test our application. Two of these were females while remaining five were male participants.

Step 3: Find what is preventing the audience from performing the target behavior: As explained later, it was about identification of motivation, ability and trigger factors that we designed for. The detail is given in later sections.

Step 4: Choose a familiar technology channel: We chose mobile phone technology channel.

Step 5: Find relevant examples of persuasive technology: There is quite a lot of work considered as examples from which we learnt. Some of them have been described in the related work.

Step 6: Imitate successful examples: As identified in the related work, we have incorporated different aspects of our own work as well as some from the notable peer-reviewed work of others.

Step 7: Test and iterate quickly: The application was testing constantly during development phase and issues were resolved on regular basis. The prototype was then tested on additional users.

Step 8: Expand on success: The last step has yet to be carried out as we have not yet done extensive experiments on a large group of users.

Having outlined our steps, we now go into the technical details of our scientific approach.

### IV. APPLICATION ARCHITECTURE FOR PERSUASIVE HEALTHCARE RECOMMENDATIONS

Persuasive technology is centered on the concept that persuasion can be carried out by machines instead of human with the objective to induce some change in their behavior. Persuasion is a complicated process and cannot be carried out using an automated set of certain steps thanks to the complex behavior of human being. One of the important findings from

studies on extensive lifestyle interventions is that to maximize health benefits, large lifestyle changes are needed. The changes cannot be achieved unless they are being monitored by some entity. In addition, the monitoring must also contain aspect of assessment to determine the progress. That is why a good system should include both the aspects of monitoring and assessment.

#### A. The Monitoring-Assessment Model

The foundation of our persuasive healthcare application is the monitoring-assessment model that has seven stages as shown in figure 1. Its different components have been identified in the conceptual framework of the application. Each one roughly correspond to some stage of the model as depicted in figure 2. Each of the seven stages is described next in some detail.

1) *User Profiling*: This is the preparatory stage and is used to get user information for creating user profile. This is only a onetime process required. User profile is any predefined or existing information related to the user. As shown in figure 2, profiling comprises preferences of the user, their health profile and building the user model from both of them collectively.

The health profile contains basic information about their demographics (name, age, gender, etc.) as well as medical history, chronic conditions, disabilities, and other health-related parameters. Preferences include user's choices about exercise type and routine, their diet, and social interests that are used in the later stages. For profiling, we mainly rely on monitoring of user behavior using automatic means of data gathering by the mobile phones.

2) *Target Behavior*: Our objective is to overcome the weaker aspects of a user's behavior which are affecting his health by persuading them to perform some activities. In this regard, the system identifies a target behavior to be changed, which can be inferred by the user profile or as recommended by the experts. From user profile we can determine the lacking aspects (or weak points) of the user with respect to their activities or behavior, e.g., lack or need of exercise, irregularities in taking medicine or moderation in the intake of particular food; all these are some form of behavior that require an improvement and are candidates for target behavior.

a) *Behavior Modeling*: The user's behavior model allows understanding the user and in proposing them personalized recommendations and persuasion strategies for behavior change. Such a model is built using user's preferences and from their health profile (including history of diet, exercise and physical activities). In the literature, a number of behavior models and theories have been defined [16][17][18][19]. Of all these, Fogg's behavior model [18] has been primarily developed for persuasive behavior design and, being a generic model, we also adopted it for behavior change in our application.

BJ Fogg has identified three factors [18] that are necessary for invoking a behavior change. They are: motivation, ability and triggers. Our proposed behavior model uses these factors to devise the appropriate persuasion strategies for behavior change.



Fig. 1. The monitoring-assessment model

Existing literature differentiates between two types of motivation: extrinsic and intrinsic. Also, research suggests that it's the intrinsic (or internally driven) motivation that lasts longer and is helpful in bringing about a change in one's behavior. Although any external factor (e.g., mobile phones in our case) that persuades a user for motivation will be necessarily an extrinsic motivation factor, we believe that if a user observes even a small, possible change in behavior, they may be intrinsically motivated to promote and enforce the behavior. Thus, while we model the human behavior with respect to mobile phone technology, it will be ultimately part of one's daily activities.

Keeping a user in the loop is an important aspect of the persuasion process. Many studies have indicated that participants fall back into less healthy or the previously held states once the intervention is over [20][21]. But it all starts with the monitoring of activities.

3) *Activities Monitoring*: The user's daily activities are observed to gather data related to physical activities, exercise, food consumption, and medication. The gathered data is used along with the information about the context of the user in the later stages of the model.

a) *Context Gathering*: Human behavior identification is a complex problem and consists of multiple factors. In addition to the state of the users such as posture and position of the body, there are a number of other factors outside the human body that are to be considered to infer the human behavior. To learn about the user behavior and to reason on them, we need to know the context in which an activity is performed. Context is any relevant information that helps us in determining the type of activity, the state of the user and their surrounding environment at that time. Some of the context variables have been identified in figure 2. These variables can be obtained from user's device.

To monitor user activities, we collect data related to the activities and behavior from the user on a regular basis. We can monitor user for activities such as walk, stairs or cycling, still position and in vehicle (reader is referred to [3] for details on this aspect.) Although not implemented in our system, additional activities like eating, exercising, sleeping, and watching television can be carried out using previously developed approaches [22][23][24][25]; however, this discussion is beyond the scope of this article. Moreover, the users are able to enter information about their diet and medication into the application manually.

The identified activities relevant to our need are recorded in user's history and become part of the user's profile. It is used together with user's preferences and their behavior model and is used for persuasion.

4) *Analysis*: This stage is the intelligent processing part of our application. Here, the volume of data from monitoring stage together with various profile elements is analyzed using previously defined rules. The aggregator consolidates the data obtained from various sources (mobile sensors and user input) while the analyzer performs analysis on the gathered data and compares it with the available guidelines for validation. Finally, the assessor evaluates the data for inconsistencies. For analysis, we used rule-based inferencing. It is used to represent knowledge of a particular domain and deduce results on top of it. The knowledge base maintains the required knowledge for the particular domain and is populated from various clinical guidelines for healthcare such as found in both classical and modern findings in research [26][27][28][29]. If the knowledge base has enough data, rules can be constructed out of it and then the current working knowledge will be evaluated against it by chaining rules together until a conclusion is reached. A rule-based system makes the storage of a large amount of information easier, and coming up with the rules help in clarifying the logic used in the decision-making process. Here we are not concerned with the rule-based analysis and this will be described in a future article.

5) *Persuasion*: If it is found that the user's behavior is lacking in some of the aspects (e.g., diet, exercise, or medication), then they should be persuaded to improve on the lacking behavior. The user can be persuaded through various strategies for behavior change. These strategies have been adopted from the literature. Each strategy is relevant in a particular context. That is why we have defined rules that are used to match what is required with what is to be done in that context. Some of the strategies are discussed in Section V.

One of the important aspects of persuasion is to generate fast results to the users so the users can assess the difference, or no difference, or acting on the persuasion. This has to be achieved using frequent reminders and recommendations to the users [30].

6) *Action*: The purpose of a persuasion strategy is to induce some desirable, positive behavior change in the user. If the strategy is successful, it will influence the user who will take some measures or corrective actions. Such actions will contribute toward the self-management of healthcare. Both the actions and inactions of the users are recorded by the system (devices or sensors) as explained previously in the monitoring stage. In the future, we tend to consider the failure of a strategy when it does not influence the user. This will require a pipeline of strategies and adaptivity in the system with respect to different contexts.

a) *End-User Adaptation*: A user is persuaded to change behavior by applying an appropriate persuasion strategy that is designed for a particular action. An important part of our application is that persuasion strategies vary from one

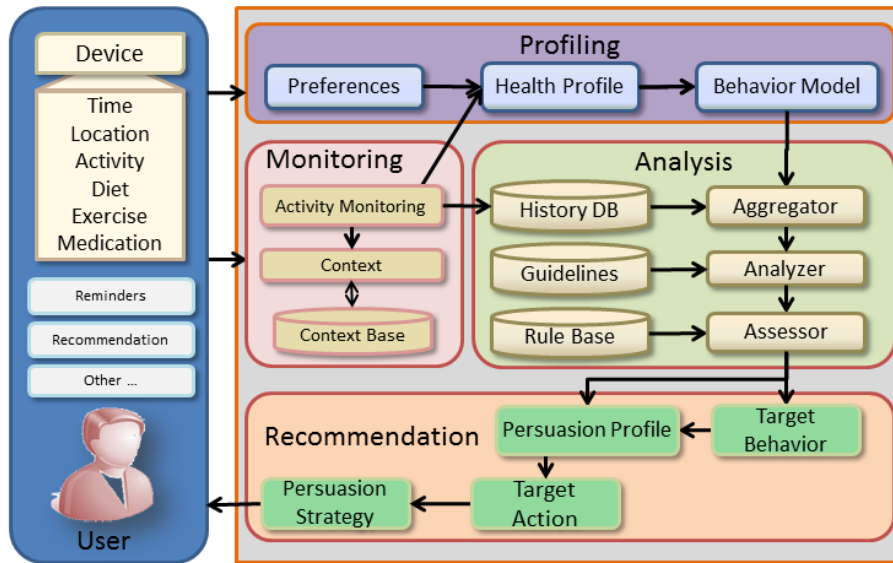


Fig. 2. The various components of mobile based persuasive application

context to another. For example, to persuade a user to exercise regularly, mobile devices will use reminders but to increase the intensity of activities, the strategy will be to show the user their achievement using physical activity data. Thus, the application interface with which the user interacts will be different in both cases. In other words, the user interface of the end application adapts itself according to the target user action. We will discuss example strategies in the case study in Section VI.

One aspect of end-user adaptation is to make the user interface fun and enjoyable. It should also support the users in the reconstruction of recent past actions either for comparison purposes, reflection, or for the satisfaction of the user.

7) *Assessment*: During assessment, a conclusion is drawn whether the analysis has been successfully applied through some persuasion strategies to materialize any behavior change in the user and, if it is, then any action was performed by the user as a result. This is done both quantitatively (yes/no) and qualitatively (how much time, amount, etc.) Based on the outcome of the assessment, either an improved target behavior is identified, such as more duration for exercise, or the previously targeted behavior is strengthened by applying additional persuasion strategies.

An important aspect of assessment is that it should help the user build self-esteem and healthy attitudes and habits. In addition, it should also foster the attitude of care and love for oneself [31].

In the next section, we describe our persuasion strategies and how they can be used for behavior changes.

## V. PERSUASION STRATEGIES AND THEIR USE IN BEHAVIOR CHANGE

A number of generic persuasion strategies have been described in the literature, e.g., in [32][33][34]. Similarly, various specific persuasion strategies have been designed by researchers and they have reported positive results in areas

such as obesity, management of smoking cessation, asthma, stress and insomnia [35], directing users towards proper exercise behaviors [36], and healthier eating [37] among others. All of these approaches target behavioral changes in the end-users through some persuasion strategies. Before outlining how these strategies are used in our system under different contexts, let us briefly describe Fogg's behavior model, which forms the foundation of persuasive technology [2][18][17] as well as the basis for use of persuasion strategies in our application.

### A. Fogg's Behavior Model

Fogg's behavior model [18] has three important factors or dimensions: motivation, ability and trigger. The model asserts that for a target behavior to happen, a person must have sufficient motivation, sufficient ability, and an effective trigger. All three factors must be present at the same instant for the behavior to occur.

*a) Motivation*: A person who has high motivation for performing the target behavior would be more likely to perform the target action. For a low-motivation person, one or more strategies pertinent to motivation should be used to increase the motivation. Users can be motivated by persuading them to do something for pleasure, to achieve some status or to expect some reward upon performing some activity.

*b) Ability*: A person having the required ability to perform a target behavior would be highly likely to perform the target action as compared to a person who is weak or lacks such an ability. To improve one's ability, one or more strategies relevant to ability should be used to enable the person. Examples of ability are: giving additional time to perform an activity, reducing the effort to do some activity, etc.

*c) Trigger*: A trigger is a signal, an event or its associated action that can be used to increase motivation or ability or both. In most cases, without an appropriate trigger, behavior will not occur even if both motivation and ability are

Strategy	Dimension	Meaning	Example Use
Commitment	Motivation	Once a user agrees for taking action, he will commit to carry it out	Accepting a recommendation by the application
Reward	Motivation	Offer the user reward on tasks accomplishment	Every action is logged and taken into account
Effort	Motivation/Ability	Make it easy for users to take actions	Generate reminders at opportune moments when it is easier to walk or exercise
Achievement	Motivation	Keep the user updated about their progress	Provide daily, weekly, monthly statistics on how the user performs
Personalization	Ability	Provide the information that makes it easy to understand and act	User can set his medication/exercise information
Recommendation	Trigger/Motivation	Suggest a user an action to take	End-of-day or end-of-week recommendation to compensate for exercise deficiency
Loss Aversion	Trigger	Help the user avoid any mistake/loss	Appropriate reminder if user misses to take an action (e.g., medication)

TABLE I. DIFFERENT PERSUASION STRATEGIES AND THEIR CONTEXT OF USE IN SEDENTWARE APPLICATION FOR WELLNESS

high. We used reminders, alarms, and notifications as well as recommendations to trigger user action.

Table I shows a list of persuasion strategies, the dimension related to each strategy, their meanings and the context in which they can be applied. For example, the "effort" strategy can be applied to both ability and motivation of a person as it is useful to either increase the ability or the motivation levels of the user. On the other hand, the "reward" strategy will only increase the motivation of a person but not the ability. Using these three factors as guides, in the next few sections, we describe how various persuasion strategies can be used to design for behavior changes. It is worth noting that a single strategy can be applied in different contexts. For example, "reward" is equally applicable for rewarding the user on successful exercise but also on taking appropriate amount of diet and taking medicines regularly, etc.

The system can persuade the users in more than one ways for the same desirable target behavior change. Let's consider, once again, the example of the *commitment* strategy, which states that when a user commits to achieve a certain objective or goal, they are motivated to carry out the required activities. The application initiates commitment strategy by helping the user to set relevant goals. Similarly, the user is also persuaded through *reminders* and context-based suggestions so activities can be performed with reduced *effort*. In such cases, mobile phones come handy to remind the users about proposed recommended activities based on scheduled alarms or appropriate notifications. Similarly, they keep the users updated about their health status and generate notifications in case of divergence from the specified goal.

To propose strategies according to user's activity and history, the persuasion profile of the user is used in addition to considering their preferences and health data. We combine the persuasion profile with the context information and rules to determine the target behavior. User's previous actions are assessed and taken into account before suggesting a target behavior. This is depicted in figure 2, where we translated a target behavior into a target action for the user. A persuasion strategy is then designed that adapts the user interface accordingly.

### B. The Role of Design in Persuasion

According to Change et al., wearable technologies provided more awareness than motivation in physical activities with goal-setting and progress monitoring [38]. Thus, they are not sufficient to induce the required level of motivation that will let a user exercise more regularly. As concluded by the study, the use of wearable devices was not sufficient to rely on for

regularity in physical activities. According to the study, the participants cited various reasons such as being too busy to exercise, finding exercise boring, poor self-management, fear of injury, lack of skills, and lack of encouragement, support, or companionship from family and friends [38].

## VI. DIABETES SELF-MANAGEMENT: A CASE STUDY

Diabetes is a chronic disease that is associated with a metabolic disorder in the human body. Managing diabetes is not an easy task as it needs serious attention by the user. Successful management of diabetes can have dramatic improvements in one's life as it relates to the overall user's life style and affects most of the user's activity. Healthy life style that includes regular physical activity and eating in moderation plays key role in slowing down diabetes related complications. Typically, diabetes has three main behavioral aspects that include diet, medication, and exercise [39]. For successful management of diabetes, all these aspects should be controlled simultaneously. This means taking help from trained healthcare professionals, coordinated care, user education and self-management training [27].

A user's complete and precise data regarding medication, diet, and exercise play an important role in managing their glucose level. This data is used by the experts to advise and suggest the users accordingly. However, since the amount of data recorded on daily basis is of different variety and huge in size, it is not feasible to rely on manual data maintenance mechanisms. This also makes it difficult for doctors to advise a user better.

Considering these complexities in diabetes self-management, we were interested in it as a case study for our research approach. In this section, we explain how our proposed approach for user persuasion is applied practically. We then describe the implementation of the proposed system in the context of persuasion.

We have implemented a smartphone application for the Android platform. As part of the persuasion in the application design, the application has been created as a service that runs inside an Android widget. Being a widget means that the user does not need to explicitly start the application to use it nor the user needs to remember to use the application. The application always remains in active state on the home screen of the smartphone. It starts automatically with the Android boot process and is brought onto the screen whenever the user unlocks the phone for any activity. Being a service means that the application continuously monitors user activities and

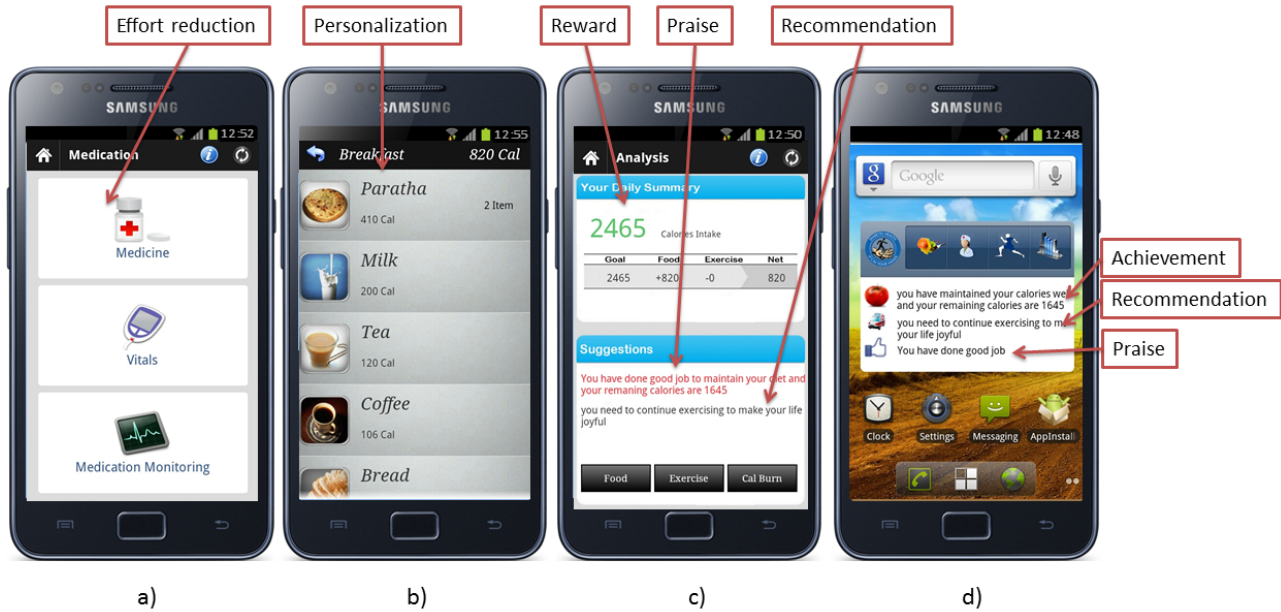


Fig. 3. Mobile screens showing various persuasion strategies applied in different contexts: a) medication activity b) diet activity for breakfast c) summary of food intake as well as recommendation for improving exercise, and d) dashboard on user's home screen showing different persuasion strategies for motivation at a glance

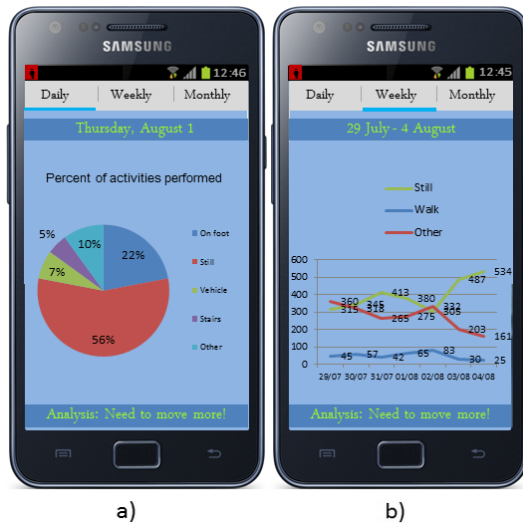


Fig. 4. Mobile views showing user's daily and weekly progress as persuasive graphs to increase user's motivation

updates the user on regular basis about any notifications or events from the social network or experts.

Users record their health-related activities either in their mobile phone where each user maintains a distinct profile. In this prototype implementation, different types of activities entered by users include 1) information about the exercise done, its type, duration, and difficulty level; 2) the medications taken by the user; 3) various parameters related to the type of diet taken including any food taken other than the usual timings. Figure 3 shows different snapshots of our application showing medication and diet-related activities as well as

recommendation given to the user based upon these activities. Figure 3 shows the various persuasion strategies used by the application. Figure 3 d) also shows the home screen widget containing various updates for the user in the form of different persuasion strategies.

In addition, figure 4 depicts the graphical view of daily and weekly activities as persuasion to the users. High achievers may view these graphs as strengthening while a user performing poorly may see it as a need for improving the physical activities due to the persuasion strategy of "loss aversion."

## VII. CONCLUSIONS AND FUTURE WORK

This paper focuses on the usage of persuasion strategies on smartphones as an application for personalized healthcare management; particularly, we considered the case for diabetic users. Our application combines the activity recognition capabilities of mobile phones with analytics to help users in healthcare management.

This paper briefly described a prototype implementation. Currently, we are enriching our system with existing rules available in different clinical guidelines. Once that is done, we will have a fully deployable system. We will then be able to analyze the usability of our system in a real setup. This will also allow us to evaluate the outcome of various persuasion strategies for better self-management of healthcare. In addition, we are looking for a comparison of different persuasive features in our system with recently developed apps for healthcare.

## REFERENCES

- [1] E. Karapanos, "Designing for different stages in behavior change," in *Proceedings of the workshop 'Personalization in Persuasive Technology', Persuasive Technology 2016*, 2016.

- [2] B. Fogg, "Persuasive technology: using computers to change what we think and do," *Ubiquity*, vol. 2002, no. December, p. 5, 2002.
- [3] H. Mukhtar and D. Belaïd, "Using adaptive feedback for promoting awareness about physical activeness in adults," in *In proceedings of the 10th IEEE International Conference on Ubiquitous and Intelligent Computing (UIC) 2013*, 2013.
- [4] S. Sultan and P. Mohan, "Transforming usage data into a sustainable mobile health solution," *Electronic Markets*, vol. 23, no. 1, pp. 63–72, 2013.
- [5] L. P. Simons and J. F. Hampe, "Exploring e/mhealth potential for health improvement; a design analysis for future e/mhealth impact," *23rd Bled eConference. from www.bledconference.org*, vol. 2, 2010.
- [6] H. Kimura, J. Ebisui, Y. Funabashi, A. Yoshii, and T. Nakajima, "idetective: a persuasive application to motivate healthier behavior using smart phone," in *Proceedings of the 2011 ACM Symposium on Applied Computing*, ser. SAC '11. New York, NY, USA: ACM, 2011, pp. 399–404. [Online]. Available: <http://doi.acm.org/10.1145/1982185.1982273>
- [7] I. Albaina, T. Visser, C. van der Mast, and M. Vastenburg, "Flowie: A persuasive virtual coach to motivate elderly individuals to walk," in *Pervasive Computing Technologies for Healthcare, 2009. PervasiveHealth 2009. 3rd International Conference on*. IEEE, 2009, pp. 1–7.
- [8] N. Romero, J. Sturm, T. Bekker, L. De Valk, and S. Kruitwagen, "Playful persuasion to support older adults' social and physical activities," *Interacting with Computers*, vol. 22, no. 6, pp. 485–495, 2010.
- [9] S. Torsi, P. Wright, S. Mawson, G. Mountain, N. Nasr, and B. Rosser, "The self-management of chronic illnesses: Theories and technologies," in *Pervasive Computing Technologies for Healthcare (PervasiveHealth), 2010 4th International Conference on-NO PERMISSIONS*. IEEE, 2010, pp. 1–4.
- [10] S. Ananthanarayan and K. Siek, "Health sense: a gedanken experiment on persuasive wearable technology for health awareness," in *Proceedings of the 1st ACM International Health Informatics Symposium*. ACM, 2010, pp. 400–404.
- [11] V. Parmar, D. Keyson, and C. de Bont, "Persuasive technology to shape social beliefs: A case of persuasive health information systems for rural women in india," *Communications of the Association for Information Systems*, vol. 24, no. 1, 2009.
- [12] S. Consolvo, J. Landay, and D. McDonald, "Designing for behavior change in everyday life," *IEEE Computer*, vol. 405, pp. 100–103, 2009.
- [13] Y. Lin, R. Chen, S. Guo, H. Chang, and H. Chang, "Developing a web 2.0 diabetes care support system with evaluation from care provider perspectives," *Journal of Medical Systems*, pp. 1–11, 2011.
- [14] N. Tatara, E. Arsand, H. Nilsen, and G. Hartvigsen, "A review of mobile terminal-based applications for self-management of patients with diabetes," in *eHealth, Telemedicine, and Social Medicine, 2009. eTELEMED'09. International Conference on*. IEEE, 2009, pp. 166–175.
- [15] B. Fogg, "Creating persuasive technologies: An eight-step design process," in *Proceedings of the 4th International Conference on Persuasive Technology*, April 2009.
- [16] I. Ajzen, "The theory of planned behavior," *Organizational behavior and human decision processes*, vol. 50, no. 2, pp. 179–211, 1991.
- [17] B. Fogg and J. Hreha, "Behavior wizard: a method for matching target behaviors with solutions," *Persuasive Technology*, pp. 117–131, 2010.
- [18] B. Fogg, "A behavior model for persuasive design," in *Proceedings of the 4th international Conference on Persuasive Technology*. ACM, 2009, p. 40.
- [19] B. Sheppard, J. Hartwick, and P. Warshaw, "The theory of reasoned action: A meta-analysis of past research with recommendations for modifications and future research," *Journal of consumer research*, pp. 325–343, 1988.
- [20] W. Demark-Wahnefried, E. C. Clipp, I. M. Lipkus, D. Lobach, D. C. Snyder, R. Sloane, B. Peterson, J. M. Macri, C. L. Rock, C. M. McBride *et al.*, "Main outcomes of the fresh start trial: a sequentially tailored, diet and exercise mailed print intervention among breast and prostate cancer survivors," *Journal of Clinical Oncology*, vol. 25, no. 19, pp. 2709–2718, 2007.
- [21] V. B. Stull, D. C. Snyder, and W. Demark-Wahnefried, "Lifestyle interventions in cancer survivors: designing programs that meet the needs of this vulnerable and growing population," *The Journal of nutrition*, vol. 137, no. 1, pp. 243S–248S, 2007.
- [22] A. Khattak, D. Hung, P. Truc, D. Guan, Z. Pervez, M. Han, S. Lee, Y. Lee *et al.*, "Context-aware human activity recognition and decision making," in *e-Health Networking Applications and Services (Healthcom), 2010 12th IEEE International Conference on*. IEEE, 2010, pp. 112–118.
- [23] A. Khattak, Z. Pervez, K. Ho, S. Lee, and Y. Lee, "Intelligent manipulation of human activities using cloud computing for u-life care," in *2010 10th Annual International Symposium on Applications and the Internet*. IEEE, 2010, pp. 141–144.
- [24] X. Le, S. Lee, P. Truc, A. Khattak, M. Han, D. Hung *et al.*, "Secured wsn-integrated cloud computing for u-life care," in *Consumer Communications and Networking Conference (CCNC), 2010 7th IEEE*. IEEE, 2010, pp. 1–2.
- [25] J. García-Vázquez, M. Rodríguez, M. Tentori, D. Saldaña, Á. Andrade, and A. Espinoza, "An agent-based architecture for developing activity-aware systems for assisting elderly," *Journal of Universal Computer Science (JUCS)*, vol. 16, no. 12, pp. 1500–1520, 2010.
- [26] I. IDF, "Global guidelines for type2 diabetes. available online: <http://www.idf.org/webdata/docs/idf%20ggt2d.pdf>, last accessed on 20th mar 2012," 2005.
- [27] M. Funnell, T. Brown, B. Childs, L. Haas, G. Hosey, B. Jensen, M. Maryniuk, M. Peyrot, J. Piette, D. Reader *et al.*, "National standards for diabetes self-management education," *Diabetes care*, vol. 32, no. Supplement 1, p. S87, 2009.
- [28] B. Elsayy and K. Higgins, "Physical activity guidelines for older adults," *American Family Physician*, vol. 81, no. 1, pp. 55–9, 2010.
- [29] A. Misra, R. Sharma, S. Gulati, S. Joshi, V. Sharma, A. Ibrahim, S. Joshi, A. Laxmaiah, A. Kurpad, R. Raj *et al.*, "Consensus dietary guidelines for healthy living and prevention of obesity, the metabolic syndrome, diabetes, and related disorders in asian indians," *Diabetes Technology & Therapeutics*, vol. 13, no. 6, pp. 683–694, 2011.
- [30] T. M. Campbell II, *The China study: the most comprehensive study of nutrition ever conducted and the startling implications for diet, weight loss and long-term health*. BenBella Books, Inc., 2004.
- [31] D. Ornish, *The spectrum: a scientifically proven program to feel better, live longer, lose weight, and gain health*. Random House Digital, Inc., 2008.
- [32] H. Oinas-Kukkonen and M. Harjumaa, "Persuasive systems design: Key issues, process model, and system features," *Communications of the Association for Information Systems*, vol. 24, no. 1, p. 28, 2009.
- [33] J. Whalen, "Persuasive design: Putting it to use," *Bulletin of the American Society for Information Science and Technology*, vol. 37, no. 6, pp. 16–21, 2011.
- [34] R. Cialdini, "The science of persuasion," *Scientific American Mind*, 2004.
- [35] V. Strecher, "Internet methods for delivering behavioral and health-related interventions (ehealth)," *Annu. Rev. Clin. Psychol.*, vol. 3, pp. 53–76, 2007.
- [36] M. Harjumaa, K. Segerståhl, and H. Oinas-Kukkonen, "Understanding persuasive software functionality in practice: a field trial of polar ft60," in *Proceedings of the 4th international Conference on Persuasive Technology*. ACM, 2009, p. 2.
- [37] P. Chi, J. Chen, H. Chu, and J. Lo, "Enabling calorie-aware cooking in a smart kitchen," *Persuasive Technology*, pp. 116–127, 2008.
- [38] R. C.-S. Chang, H.-P. Lu, P. Yang, and P. Luarn, "Reciprocal reinforcement between wearable activity trackers and social network services in influencing physical activity behaviors," *JMIR mHealth and uHealth*, vol. 4, no. 3, p. e84, 2016.
- [39] HHS, "U.s. department of health and human services. new survey results show huge burden of diabetes," 2009, <http://www.nih.gov/news/health/jan2009/middk-26.htm>.

# Towards Securing Medical Documents from Insider Attacks

Maaz Bin Ahmad  
Dept. of COCIS  
PAF-KIET  
Karachi, Pakistan

Abdul Wahab Khan  
Dept. of COCIS  
PAF-KIET  
Karachi, Pakistan

Muhammad Fahad  
Dept. of COCIS  
PAF-KIET  
Karachi, Pakistan

Muhammad Asif  
Dept. of Electrical Engineering  
CUST  
Islamabad, Pakistan

**Abstract**—Medical organizations have sensitive health related documents. Unauthorized access attempts for these should not only be prevented but also detected in order to ensure correct treatment of the patients and to capture the malicious intent users. Such organizations normally rely on the principle of least privileges together with the deployment of some commercial available software to cope up this issue. But such methods can't be helpful in some of the misuse methods e.g. covert channels. As insiders may be the part of the team which developed such software, he may have deliberately inserted such channels in the source code of that software. The results may be catastrophic not only to that organization but for the patients too. This paper presents an application for securely exchange of documents in medical organizations of our country. The induction of water marking and hash protected documents enhances its security and make it fit to deploy in medical related organizations. The deployment is done in such a way that only higher management has access to the source code for reviewing. Results demonstrate its effectiveness in preventing and detecting majority of the information misuse channels.

**Keywords**—*covert channels; misuse; insider; medical; documents*

## I. INTRODUCTION

Insider [1-4] may be one of your employee, supplier, contractor, consultant or outsourced organization. The problem of insider threats detection/prevention is not a simple one to deal with, since it involves people following best practices and technology means to tackle it [5]. It looks simple to deploy principle of least privileges in medical related organizations. But this damages the organization a lot in terms of de-shaping the working environment of the organization. As there may exist a few insiders, it is not a good approach to monitor all the time other employees who are working hardly for the organization. This not only becomes a processing overhead but also creates dissatisfaction among your loyal employees. So this is not a feasible solution.

Medical related organizations also are sensitive towards insider threats. Blindly trust on user and on any commercial software may create difficulty for such organizations. Using some open source tool in this scenario may be a better choice

but open source software has its own security issues. Also code revision itself is a very hectic job on someone else's code. So an application developed by trusted experts should be built for such organization which is to be reviewed only by higher expert management persons.

This paper presents an application to provide security to the viewing and exchange mechanisms of documents within the medical organizations. An application built in C# is being used to serve this purpose. Different scenarios are crafted and validated in a testing environment. Results show the usefulness of this application. In section II of the paper, the related work is presented. Section III provides the detail of the application. Section IV and V comprises of the implementation & conclusion respectively.

## II. RELATED WORK

Natarajan and hossain [6] utilized action based methodology and social network to detect the insider threats. In it the roles are assigned to the analysts. A social network is pre established for analyst and related system around him. The actions performed by analyst in each role are separately logged. Then these are compared with the expected behavior and results are collected. In this scheme there were few limitations like parameters need to be established prior and it performs slow convergence. Zhang [7] model is an active model for defense against insider threat. The model detects the insider threats in real time effectively. Artificial intelligence, graph theory and access control are used to create the model. Its plus point is that no human supervision is required. The model has several components which work differently from each other to handle the insider threats in different ways. Active defense approach manages all of these components. Information collection module comprises of sensors spread in the system. Information is gathered with the help of collection rules made by responsency module. Audit and application logs, application calling sequence, network data packets etc. are used to gather the information. Then with the help of these rules the necessary information is filtered. The information collection module then gives this information to detection module where orthodox detection tools are used in

combination with detection rules. Due to their unique characters the low level insider threats are handled here properly. Then there comes sense module which analyzes abnormal events. The detection module sends those events which it thinks are suspicious but don't have unique characters to the sense module, where these events are further analyzed with the help of sense rules. So problem of false alarm is reduced here. Then there comes the responsiveness module which is the heart of active detection model. It may perform prediction of insider threats which would occur in the future. Intelligent techniques and insider threat previous history data helps in the prediction process. This module is also responsible for redefining the rules for detection, sensing and information collection. This change of rules and prediction makes this model work actively against insider threat. Wang [8] security model was for sensitive nature organizations. The model was designed to stop the information theft due to insider. Encryption mechanism is the basis of this model. Trusted computing technologies work to achieve the goal. It has a core component named TPM (Trusted Platform Module) which gives the protected data like cryptographic keys and doesn't disclose the root key. Cryptographic functions like generating the random numbers, key generation of RSA (Rivest Shamir Adleman), integrity measurements etc. are also provided by TPM. Protection strength of TPM makes it impossible for someone to get wrapping keys from secured trusted platform. So the system is very secure. Wang and Puleo [9, 10] worked on the behavioral aspect of insiders. According to the research conducted, it was found that most of the insiders have one or more of the following observable behavior. These are: they have a wide range of skills, attack during their duty hours, don't share a common profile, have different motives, share their plan with co-workers, are caught by people manually and not by software or security staff etc. Profiling techniques help to detect attacks but it does work after an attack is completed. CERT (Computer Emergency Response Team) [11] discussed the organized crime approach of malicious insiders. The material for this research was collected from court documents, press releases of department of justice USA, reports of media and from interviews. They highlighted the issue of collaborative attacks where a group of insiders cooperate with each other in launching attacks. Such attacks can easily bypass the existing security measures. So some recommendations were proposed in it to reduce chances of these kinds of attacks. E.g. detailed pre-employment screening, auditing of critical processes regularly, auditing of the database in which auditing information is stored and prefer external audits of process and system. So this methodology is policy based and emphasizes the need of having a strong security policy inside the organization. Eom et al [12] presented a document control system for military environment. This system consists of three sub-modules i.e. authentication access control and water marking. The first two modules are common to many models. The difference here is the watermarking technique. In water marking we add some information to the documents we want to protect. The document can be checked easily whether it is marked or not and accordingly its transmission is controlled. This model is very basic one and doesn't cover several illegal means related

to document contents leakage e.g. copying contents of a marked document to another file, saving the water marked document on our system and later reproduce it etc. A research was conducted in order to see the insider activity in the banking and finance sector [13]. A detailed finding was described in this study. Research says that in most of the incidents observed, insiders required very little technical sophistications. Also it was observed that in most of these cases insiders planned their actions. Financial gain was the motive behind launching these attacks in most of the cases. Another interesting finding was that in all cases insiders didn't share a common profile. Several different methods and persons identified the attacks in all these cases. In these entire cases studied, victim organizations received heavy financial loss. So these were the findings obtained by studying insider threats cases in financial sector. This is a form of survey about attacks in this sector and doesn't give sufficient methodology to prevent or detect these attacks. CERT [14] studied the 123 cases of I.T sabotage and found that in all cases insider showed some suspicious behavior indicators prior to launching an attack. They developed a technical signature approach which can be applied only to a particular group of users inside the organization. In the beginning information like remote access time, protocol used in remote access is collected along with username/I.P and stored in a database. Having this information, they developed a signature. To monitor remote login these signatures are efficient but their limitation is that these cannot be applied to privileged users. Also these can only be applied to particular groups of users not to all population of users. Lihong [15] developed a new framework in order to get and exchange only the essential information and discard the rest of information. The idea is based on the fact that normally special feature of a dataset is required rather than entire information. The proposed algorithm has the capability to process different kinds of data whether digital or continuous. Paal et al [16] targeted cross domain information exchange. As cross domain information exchange requires some kind of information flow between two domains, so it requires placing a guard between both domains which monitors and controls the flow between two domain. The main function of the guard is to provide confidentiality so they proposed a two way guard which also provides integrity.

Fisk et al [17] discussed some methods to send data between different organizations so that the overall risk of information stealing can be minimized by following these.

In short, none of these schemes targeted specifically to the medical related organizations. In medical organizations, the major requirements are to maintain up to date information about all patients, no tempering should be allowed with the prescriptions, treatment methodology should be kept confidential and fake reports and prescriptions shouldn't be generated. In order to cope up with these requirements we modified the document viewing application [19], added certain new features to it and at the end validated it with more scenarios according to the business processes of such organizations.

### III. METHODOLOGY

The sensitive reports and documents are present on server

in encrypted form and the other arrangements are same as mentioned in [19]. In addition to all the previous benefits of document viewing application, some more functionality is introduced in it. First of all, the confidential reports and prescriptions are hash protected. Whenever such a document is viewed, its hash value is computed and matched against the stored value at the server. If both values are same then the access is normal, otherwise the document is marked as suspicious.

As a second line of defense, all the stored medical documents are water marked. So in case of any possibility of illegal view, the user name is appended in the document who illegally viewed it. The induction of water marking also helps in the detection of forged prescription/report created by some unauthorized person.

So the proposed scheme gives the following benefits:

- User cannot copy confidential document to his/her USB
- User cannot forge any fake medical document without being noticed
- User cannot copy contents of confidential document to some other file and cannot make unauthorized changes
- Since it is our own created module, so code is available for techniques like code-analysis in order to detect covert channels
- Even if a user manages to copy some critical document from server, it cannot be decrypted on any other machine
- If any user tries to copy the contents of confidential document from his machine, he will be detected too (detection + protection)
- Supports a variety of file types like .doc/docx, .jpeg, .txt, .ppt/.pptx, .pdf and .xls/.xlsx
- Also provides Logs if any user tries to misuse the unauthorized information

As the medical documents belong to different applications e.g. MS WORD, EXCEL, POWERPOINT, TXT, PDF, JPG etc. and there may be multiple instances of the scenarios of same application. So we created different scenarios keeping in mind the business processes of medical organizations. The naming scheme is same as was discussed in [18]. These scenarios are presented for MS WORD as an example as follows:

CONF [1][1][1]:

*User tries to access un-authorized Word document report of patient.*

In this case, user tries to access an un-authorized MS WORD report of patient present on the server through his/her machine. If s/he manages to do so than it may result in leaking of patient secrets or may damage the security of a treatment process. Access right management and log management in the application help to prevent from it

CONF [1][1][2]:

*User has read only access to a report and tries to copy its contents by selecting contents.*

As the report can only be open in document viewing application, so user will not be able to do so because all such attempts are not only prevented by this application but also detected. Logs are also obtained as a result of these attempts.

CONF [1][1][3]:

*User presses "prts" key to capture screenshot of contents of a confidential patient report.*

The application has different built in checks, so it prevents the user from such kind of misuse. All of these activities are also properly logged in order to identify the intents of the users.

CONF [1][1][4]:

*User tries to save read-only report to his/her machine or USB.*

This scenario when simulated showed that user cannot do so because document viewing application would not allow to save confidential document to some external media.

CONF [1][1][5]:

*User tries to take print of the patient confidential Report*

This kind of action is also protected in the application which doesn't allow printing for such reports. So user would not be able to attack in this manner without being detected.

CONF [1][1][6]:

*User tries to sniff the confidential medical documents*

As the secret documents are decrypted at runtime, so if a user gets it by sniffing, he wouldn't be able to decrypt it because he doesn't know the decryption key.

CONF [1][1][7]:

*User technically tries to change the code of the application or insert code with the application interface*

Accessibility of source code of the application is not given to the users. Only highly privileged user have access to it. The source code is also hash protected so they also cannot make changes without being detected. Frequent code reviews also are helpful to detect such type of misuse.

CONF [1][1][8]:

*User creates a forged medical prescription in order to adjust bills of misused medicines*

Such kind of forgery cannot be done in the presence of this application as hash values of such documents needs to be matched from stored values on server. So such document would be detected as a fake one by this application.

CONF [1][1][9]:

*User manages to open an unauthorized document and only reads it*

Even only reading/opening such document doesn't go unnoticed by this application. The water marking technique introduced in the application captures the user detail that opens such a document. So it enhanced the security of the proposed application.

TABLE I. MISUSE SCENARIOS ALONGWITH DETECTION TIME & FALSE ALARMS

Scenario Application/Category	Scenario #	Detection Result	Detection Time (sec)	False Alarms (%)
MS WORD	[1][1][1]-[150][1][4]	Detected	< 1	0-2
	[1][1][5]-[150][1][5]	Prevented	-	0-1
	[1][1][6]-[150][1][6]	Prevented	-	0-1
	[1][1][7]-[150][1][9]	Detected	< 1	0-2
MS PowerPoint	[1][2][1]-[150][2][4]	Detected	< 1	0-2
	[1][2][5]-[150][2][5]	Prevented	-	0-1
	[1][2][6]-[150][2][6]	Prevented	-	0-1
	[1][2][7]-[150][2][9]	Detected	< 1	0-2
PDF	[1][3][1]-[150][3][4]	Detected	< 1	0-2
	[1][3][5]-[150][3][5]	Prevented	-	0-1
	[1][3][6]-[150][3][6]	Prevented	-	0-1
	[1][3][7]-[150][3][9]	Detected	< 1	0-2
MS Excel	[1][4][1]-[150][4][4]	Detected	< 1	0-2
	[1][4][5]-[150][4][5]	Prevented	-	0-1
	[1][4][6]-[150][4][6]	Prevented	-	0-1
	[1][4][7]-[150][4][9]	Detected	< 1	0-2
JPG	[1][5][1]-[150][5][4]	Detected	< 1	0-2
	[1][5][5]-[150][5][5]	Prevented	-	0-1
	[1][5][6]-[150][5][6]	Prevented	-	0-1
	[1][5][7]-[150][5][9]	Detected	< 1	0-2
TXT	[1][6][1]-[150][6][4]	Detected	< 1	0-2
	[1][6][5]-[150][6][5]	Prevented	-	0-1
	[1][6][6]-[150][6][6]	Prevented	-	0-1
	[1][6][7]-[150][6][9]	Detected	< 1	0-2

#### IV. CONCLUSION & FUTURE DIRECTIONS

Medical organizations have sensitive information and cannot rely solely on documents misuse protective tools due to covert channel presence. The proposed application modified specifically for medical organizations solved that problem while keeping false alarms as minimum as possible. The false alarms can further be minimized by placing a module for

offline analysis to refine the detections of misuse. Different kinds of organizations may adopt this application by modifying it according to their business processes.

#### REFERENCES

- [1] Blackwell C. "A Security Architecture to Protect against the Insider Threat from Damage, Fraud and Theft", CSIIRW April 13-15, Oak Ridge, Tennessee, USA 2009
- [2] Bishop M, Gollmann D, Hunker J and Probst. C W. "Countering Insider Threats". Dagstuhl Seminar Proceedings 2008
- [3] Phyo A H and Furnell S M. "A Detection-Oriented Classification of Insider IT Misuse". Computers & Security journal, Vol. 21, No 1. 2002
- [4] "Research and Development Initiatives Focused on Preventing, Detecting, and Responding to Insider Misuse of Critical Defense Information Systems". Results of a Three-Day Workshop. Santa Monica CA, 2000
- [5] Prasad R S. "Insider Threat to Organizations in the Digital Era and Combat Strategies". Proceedings of workshop icfcf09, 2009
- [6] Natarajan, A., Hossain, L. "Towards A Social Network Approach For Monitoring Insider Threats To Information Security". In Not known (Eds.), Intelligence and Security Informatics : Second Symposium on Intelligence and Security Informatics, ISI 2004, Tucson, AZ, USA, Proceedings [Lecture Notes in Computer Science 3073, (pp.501-507). Nicholson Museum, University of Sydney. 2004
- [7] Hongbin Zhang, Jianfeng Ma, Yinchuan Wang and Qingqi Pei. "An Active Defense Model and Framework of Insider Threats Detection and Sense". Fifth International Conference on Information Assurance and Security. 2009
- [8] Wang, S.H and Li, X.Y. "A Security Model to Protect Sensitive Information Flows Based on Trusted Computing Technologies". Proceedings of the Seventh International Conference on Machine Learning and Cybernetics, Kunming, 12-15 July 2008
- [9] Liu, D., Wang, X.F and Camp, L.J. "Mitigating Inadvertent Insider Threats with Incentives". School of Informatics, Indiana University 2007
- [10] Anthony J. Puleo, Captain, USAF. Thesis. "Mitigating insider Threat Using Human Behavior Influence Models". June 2006
- [11] "Spotlight On: Malicious Insiders and Organized Crime Activity". A technical report: CERT insider threat centre, Jan, 2012.
- [12] Eom, J.H., Kim, N.U., Kim, S.H and Chung, T.M. "An Architecture of Document Control System for Blocking Information Leakage in Military Information System". International Journal of Security and Its Applications Vol. 6, No. 2, April, 2012
- [13] CERT. Insider Threat Study: "Illicit Cyber Activity in the Banking and Finance Sector". Aug., 2004
- [14] Insider Threat Control: "Using a SIEM signature to detect potential precursors to IT Sabotage". CERT insider threat centre, April, 2011.
- [15] Lizhong Zheng. "Lossy Information Exchange and Instantaneous Communication". MIT, Final report , 09/17/2015
- [16] Paal E. Engelstad. "Security Challenges with Cross-Domain Information Exchange: Integrity and Guessing Attacks". IEEE 2015.
- [17] Gina Fisk, Calvin Ardi, Neale Pickett, John Heidemann, Mike Fisk, Christos Papadopoulos." Privacy Principles for Sharing Cyber Security Data ".Department of Homeland Security Science and Technology Directorate, Cyber Security Division, via SPAWAR Systems Center Pacific under Contract No. N66001-13-C-3001, 2015.
- [18] Maaz Bin Ahmad, Adeel Akram, Saeed-ur-Rehman and Hasan Islam. "Implementation of a Behavior Driven Methodology for Insider Threats Detection of Misuse of Information in Windows Environment". Information- An International Interdisciplinary journal. ISSN 1343-4500. Vol.16 No.11 Nov.2013
- [19] Maaz Bin Ahmad, Muhammad Asif, SyedMashhad Mustuzhar Gilani, M. Hasan Islam, and Saeed-ur-Rehman. "A novel application to secure misuse of information in critical organizations for windows environment", Fifth International Conference on Computing Communications and Networking Technologies (ICCCNT), 2014